REYKJAVIK, ICELAND, APRIL 9-11, 2025

Proceedings from the 11th International Symposium on Tunnel Safety and Security

Edited by

Ying Zhen Li
Anders Lönnermark
Jonatan Gehandler
Haukur Ingason

Abstract

This publication includes the Proceedings of the 11th International Symposium on Tunnel Safety and Security (ISTSS) held in Reykjavik, Iceland, April 9-11, 2025. The Proceedings include 43 papers and 17 posters. They were presented in 16 different sessions, i.e., 3 Keynote sessions, Fire Dynamics 1&2, Fixed Fire Fighting Systems, Alternative Fuel Vehicles, Poster session, Evacuation 1&2, Ventilation, Engineering Case Studies 1&2, Risk 1&2, and Emergency Management.

Each day was opened by invited Keynote Speakers (in total six) addressing broad topics of pressing interest. The Keynote Speakers, selected as leaders in their field, consisted of Daniel Joyeux (Efectis Group, France), Haukur Ingason (RISE Research Institutes of Sweden, Sweden), Håkan Frantzich (Lund University, Sweden), Igor Maevski (Jacob, USA), Jie Ji (University of Science and Technology of China, China) and Jennifer Wen (University of Surrey, UK). We are grateful that the keynote speakers were able to share their knowledge and expertise with the participants of the symposium.

RISE Research Institutes of Sweden AB
ISBN 978-91-90036-19-8
Borås, Sweden

Preface

The proceedings include papers presented at the 11th International Symposium on Tunnel Safety and Security (ISTSS) held in Reykjavik on 9-11 April 2025. The symposium is well established in the tunnel fire community and the success of ISTSS is a tribute to the pressing need for continued international research and dialogue on these issues. The proceedings provide state-of-the-art knowledge in the field of fire safety and security in tunnels and other underground structures.

ISTSS usually attracts around 200 delegates from all parts of the world and represents an arena for researchers and engineers to discuss safety and security issues associated with complex underground transportation systems. We clearly see that fire dynamics is a major area of concern with a focus on smoke spread and smoke stratification especially for tunnels with natural ventilation, while fire and explosion hazards of alternative fuel vehicles and the use of water-based fixed firefighting systems continue to attract interests. Furthermore, evacuation, engineering design and risk assessment remain focused areas of many papers. This year there are also specific focuses on ventilation and emergency management. Numerous renowned researchers and engineers have contributed to these topics at this symposium for which we are grateful.

We received over 70 extended abstracts in response to our Call for Papers (not including our six invited Keynote Speakers) and believe that the quality of the accepted papers is a testament to the calibre of research that is on-going around the world. Of these, 37 were selected, based on their high scientific quality, for paper (oral) presentations and inclusion in the proceedings. Besides, the poster session contains 17 posters to canvas interesting emerging research. The selection of paper presentations was based on two-step reviews (extended abstract review and full paper review) conducted by the 19 members of the Scientific Committee. The Scientific Committee consists of many of the most well-known researchers in this field (a list can be found on the Symposium website, www.ri.se/en/istss/, below “About ISTSS”). We are grateful for their contribution to making this symposium the leading one on fire and safety science in tunnels. ISTSS has long-term cooperation with Fire Safety Journal (FSJ) for publishing special issues on tunnel fire safety. Ten papers from the 10th ISTSS were selected as candidates, and after peer reviews the special issue containing nine papers has been published at FSJ. We hope to continue this process in the future to raise the level of the scientific part of the symposium. During the symposium there is also an exhibit where businesses present their expertise, products and services.

Finally, we would like to thank the other members of our organisation committee: Prof. Haukur Ingason (scientific advisor), Jonatan Gehandler (program coordinator), Linnéa Hemmarö (symposium coordinator), Kaisa Kaukoranta, and Jonas Brandt for their help. We would also like to thank our event partners Slökkvilið höfuðborgarsvæðisins and Vegagerðin, The Iceland Road and Costal Administration (IRCA) in Iceland for their cooperation and help, and thank also our sponsors who contributed with their support and engagement.

Ying Zhen Li — Chair of Scientific Committee

Anders Lönnermark — Chair of Organisation Committee

Table of contents

Keynote speakers

State of the Art of Tunnel Fire Research at RISE (SP) 11
Haukur Ingason, Ying Zhen Li
RISE Research Institutes of Sweden, Sweden

Fire and explosion hazards of new energy vehicles in tunnels and underground spaces 28
Jennifer X Wen
Fire and Explosion Modelling Group, School of Engineering, University of Surrey, UK

Evacuation and human behaviours in tunnel fires 37
Håkan Frantzich
Lund University, Lund, Sweden

Overview of confined fire plume behavior and smoke exhausting methods by natural and mechanical ways in tunnels 51
Jie Ji
State Key Laboratory of Fire Science, University of Science and Technology of China, China

Engineering Practice of Tunnel Fire Safety 66
Igor Maevski, PhD, PE
Jacobs, USA, ASHRAE Fellow

Review of the structural fire resistance in Tunnels 83
Daniel Joyeux
EFECTIS Group, France

Fire Dynamics I

Numerical study of the influence of wind on the smoke 99
Matteo Pachera
Sweco, Belgium

An improved model of smoke layer thickness in naturally ventilated tunnel fires considering the effects of aspect ratio 115
Liliang Yang[1], Mingjian Yin[2], Chuangang Fan[3], Jianda Xu[4], Ke Wu[1] & Tianhang Zhang[1]
[1]Research Center for Urban Fire Safety Engineering, Zhejiang University, China
[2]College of Energy, Environment and Safety Engineering, China Jiliang University, China
[3]School of Civil Engineering, Central South University, China
[4]Zhejiang Communications Investment Expressway Operation Management Co.Ltd.

Study on the indoor-outdoor temperature difference-induced smoke re-stratification in naturally ventilated tunnel fires 131
Jiangdong Li[1,2], Ke Wu[1,2], Tianhang Zhang[1,2] & Lizhong Wang[1]
[1]Key Laboratory of Offshore Geotechnics and Material of Zhejiang Province, Zhejiang University,

China
[2]Research Center for Urban Fire Safety Engineering, Zhejiang University, China

Vehicles impact on smoke stratification 144
Benjamin TRUCHOT, Guillaume LEROY and Thierry DURUSSEL
Ineris, France

Fixed Fire Fighting Systems

Laboratory Scale Tests Investigating Fixed Fire Fighting Systems and Emergency Ventilation Interaction for Highway Tunnels 158
Matt Bilson[1], Hasan Raza[1], Alexander Schmidt[2] & Max Lakkonen[2]
[1]WSP USA, USA
[2]IFAB, Germany

Comparison of Fixed Water-Based Fire-fighting Systems for Road Tunnel Application 174
M.K Cheong, L.W Lim, C Tan, A Chong, H Wijaya, M Thong, K.W Leong
Land Transport Authority of Singapore, Singapore

Key findings from fire testing of water-based fixed fire fighting systems in a medium scale tunnel 190
Ying Zhen Li, Haukur Ingason, Joel Blom, Magnus Arvidson & Michael Försth
RISE Research Institutes of Sweden, Sweden

Alternative Fuel Vehicles

Preventing and managing NEC incidents in tunnels: Safety concepts 206
Christophe Willmann &Pascal Blanc & Laurence Champin & Jean Marc Couvert &Yves Fleurial & David Giuliani & Daniel Lamarche & Christophe Lemierre & Olivier Peronne & Christophe Banos &Antoine Mos
CETU, France & ATMB & DIR MC & SFTRF & Métropole Aix-Marseille Provence & GEIE-TMB & CD73 & DIRIF & SNCF (ex DGSCGC)

Deflagration consequences in a tunnel: Experimental evaluation of hydrogen leaks 222
Benjamin TRUCHOT[a] & Jerome DAUBECH[a,b]
[a]Ineris, France
[b]Sorbonne Universités, France

In-Tunnel LIB Cargo Fire Emergency and Impacts on Tunnel Operational Capability 234
Adam Wood, Miguel Angel Fuentes & Sohail Alizadeh
Mott MacDonald, UK

Evacuation I

Numerical investigation of the effects of ventilation on the tenability of egress paths in a metro tunnel fire 250
Ting-Hsuan Liao & Ricky Carvel
Edinburgh Fire Research Centre, School of Engineering, University of Edinburgh, UK

Ventilation and Fire Life Safety upgrades to an existing rail tunnel facility considering modern requirements 265

Jeffrey Bott, Jackie Chen, Kevin Ficarra, Igor Maevski, & Andrew Page
Jacobs, USA

Evacuation II

Disposal of Emergency Telephones in Swedish Railway Tunnels: Practical application of the CSM RA-regulation 280
Karl Fridolf[a] & Johan Lundin[b]
[a]The Swedish Transport Administration, Sweden
[b]Brandskyddslaget AB, Sweden

Safety Enhancement by Introduction of Evacuation Assisting Light for Long Distance Road Tunnel Fires 296
Yuika Sakamoto[1], Shoichi Kume[1], Yudai Matsunaga[2] & Tomoki Kikumoto[3]
[1]Hanshin Expressway Company Limited, Japan
[2]Hanshin Expressway R&D Company Limited, Japan
[3]Techno Hanshin Company Limited, Japan

Tunnel safety, requirements for self-rescue and evacuation - the (mis)use of traffic volume to define the level of safety 312
Pål Andreas Dahl
COWI AS, Sweden

A modified approach to walking speed within smoke-filled rail tunnels 328
Emil Persson, Niclas Åhnberg & Santiago Nordlund Gendra
Brandskyddslaget AB, Sweden

Ventilation

Cross River Rail – Innovations in Metro Tunnel Ventilation and Fire Life Safety 342
Dr Nick Agnew, Michael Meissner, Dr Michael Beyer, & Ben Tuckwell
Stacey Agnew Pty Ltd, Australia

Smoke Management, Differential Pressures on Egress Doors and Controls during Fire Evacuation in Metros 359
Evangelos Krokos[1] & Marios Kalyvas[1]
[1]Mott MacDonald, Sydney, Australia

Tunnel Ventilation in India: State-of-the-Art and Evolution
Ravi Shankar[1] & Marco Bettelini[2]
[1]Amberg Engineering AG, Gurugram, India 369
[2]Amberg Engineering AG, Regensdorf-Watt, Switzerland

Fire Dynamics II

Experimental study on smoke temperature and carbon monoxide diffusion of channel fires under the synergistic action of air curtain and lateral centralized smoke exhaust 385
Xinyang Fan, Fei Tang*, Xinyu Peng, Nannan Zhu, Xiaolei Zhang, Longhua Hu
State Key Laboratory of Fire Science, University of Science and Technology of China, China

A paramedic study of fire conditions in naturally ventilated road tunnels 396
Imad Obadi, George Hadjisophocleous
Department of Civil and Environmental Engineering, Carleton University, Canada

Impact of external wind with upward and downward angles on smoke layer development in tunnel fires 412
Tzu-Yan Tseng[1], Kuang-Chung Tsai[1]
[1] Dept. of Safety, Health and Environmental Engineering, National Kaohsiung University of Science and Technology, Taiwan

Engineering Case Studies I

When is a Tunnel a Tunnel? 427
Salvatore Marsico, Luis Robles & Alexa Laszlo
WSP USA, USA

Reykjavik's Sæbraut Road Tunnel: Balancing Development and Safety 436
Böðvar Tómasson[1], Johan Lundin[2], Erik Hall Midholm[2] & Birgir Þór Guðbrandsson[1]
[1]ÖRUGG verkfræðistofa, Reykjavík, Iceland
[2]Brandskyddslaget AB, Stockholm, Sweden

The Ferney Cut-and-cover: a project with several specific challenges 449
Raphaël Defert[1], Justine Vivien[1] & Christophe Zing[1]
[1]WSP Ingénieurs Conseils SA, Switzerland

Risk I

Managing Disaster Risks in Underground Transportation Infrastructure - A Comprehensive Analysis of Safety Targets and Practices 460
Johan Lundin
Brandskyddslaget AB, Sweden

Using Deep Learning to Predict Traffic Dynamics in Road Tunnels 476
Naeem Khademi, Vinothini Aravindan, Parvathy Anil Kumar & Erlend Tøssebro
University of Stavanger, Stavanger, Norway

Use of a Risk Model to Evaluate Tunnel Safety Features 492
Sigurjon Ingolfsson[1], Peter Woodburn[2], Frederik Møller Paulsen[3], Rory Turnbull[1]
COWI Arup Joint Venture, Denmark
[2]now Jacobs
[3] now University College London

Emergency Management

Dutch road tunnel firefighting in the future: outlook from a Dutch fire fighter's perspective 509
Nils Rosmuller & Arjen van Barreveld
NIPV, Netherlands Institute for Public Safety, The Netherlands

What fire modelling resolution is needed in AI training data for smart firefighting in tunnels? 522
José A. Morales Mere, Nils Johansson & Enrico Ronchi
Division of Fire Safety Engineering, Lund University, Sweden

Review of emergency egress and rescue challenges in rail tunnels from emergency responder's perspective 537
Gary English
Underground Command and Safety, USA

Risk II

Learning from Disasters 551
Iain Bowman
Mott MacDonald, United Kingdom

Evolution of a risk indexing method for evaluating safety in Swedish railway tunnels 567
Håkan Frantzich[1] & Karl Fridolf[2]
[1]Lund University, Sweden
[2]The Swedish Transport Administration, Sweden

Engineering Case Studies II

Rehabilitation of Fire Life Safety Systems for Existing Tunnels 578
Robert Faddoul, E.I.T; Yuan Li, P.E; Igor Maevski, PhD, P.E.; James Fiscella, E.I.T; & Sharanya Nair, PhD Jacobs, New York, USA

CFD Modeling Of The Memorial Tunnel Fire Tests Using An Autonomous Meshing Approach And Adaptive Mesh Refinement 594
Mathias Vångö[1], Sarah Feher[1], Suresh Nambully[1], Matteo D'Elia[1] and Rainer Rothbauer[1]
[1]Convergent Science GmbH, Linz, Austria

Examining tunnel safety features in sustainability-led design 606
Sigurjon Ingolfsson[1], Peter Woodburn[3], Sven Valdemar Sørensen[1], Fabiano Scarbi[1], Bryan Tamakloe[2], Simone Curletto[2]
[1]COWI Arup Joint Venture, Denmark
[2]Metroselskabet, Denmark
[3]Now Jacobs, Denmark

Implications of Peak Heat Release Rate to Optimize Metro Tunnel Ventilation Systems 616
Robert Till[1], Argun Bagis[2], Bruce Dandie[3]
[1]John Jay College of Criminal Justice (CUNY), USA
[2]Arup, Australia
[3]RRT Pty Ltd, Australia

Posters

Influence of tunnel portal geometry on wind-driven airflow in naturally ventilated tunnels 627
Jakub Bielawski[1,2], Dia Luan[2,3], Xinyan Huang[3], Aleksander Król[4], Małgorzata Król[4], Wojciech Węgrzyński[1]
[1]Building Research Institute, Poland

[2]Hong Kong Polytechnic University, China
[3]Central South University, China
[4]Silesian University of Technology, Gliwice

A PID sensor, for initial fire phase detection, with ppb capabilities 629
Madeleine Martinsen & Erik Dahlquist
Mälardalen University, MDU, Sweden

Statistical Analysis of Highway Tunnel Fire Incidents in Zhejiang Province, China from 2020 to 2024 631
Qian Zhou[1], Kai Zhu[1,*], Haitao Mao[2], Qixin He[1], Wenwen Hua[1], Dong Ye[1], Qiang Wang[1]
[1]College of Energy Environment and Safety Engineering, China
[2]Quzhou Fire and Rescue Detachment, China

Impact of Emergency Exit Separation on Passenger Safe Egress in Longitudinally Ventilated Intercity Train Tunnels 633
Manuel Barros-Daza & Jonathan Hodges & Nishant Nayan
Jensen Hughes, USA

Automate the important stuff of fire safety 636
Ben Wolf & Wolfgang Lahner
Honeywell life safety Austria GmbH, Austria

The Effectiveness of a Smoke Barrier Wall in Controlling Portal to Portal Smoke Recirculation: A Case Study 639
Göran Nygren, Raheleh Omranimanesh, Sofia Lundegårdh and Erik Lundström
WSP Sverige AB, Sweden

Study on the mechanism of bidirectional flow in the natural ventilation shaft of urban tunnel 642
Xiaofeng Chen[1,2,3], Ke Wu[1,2,3], Yachao Li[4], Xin Zhang[5], Fanghong Zhao[4], Tianhang Zhang[1,2,3]
[1]Research Center for Urban Fire Safety Engineering, Zhejiang University., China
[2]Center of Balance Architecture, Zhejiang University., China
[3]Key Laboratory of Offshore Geotechnics and Material of Zhejiang Province, Zhejiang University., China
[4]China Railway Tunnel Stock CO., LTD., China
[5]College of Electronic Engineering, Xi'an Shiyou University., China

Life-safety targets in underground stations, continued 645
Erik Hall Midholm[1], Johan Lundin[1], Bo Wahlström[1], Oskar Jansson[2]
[1] Brandskyddslaget AB, Sweden
[2] RiskTec Projektledning AB, Sweden

Research on the Ceiling Maximum Temperature in Inclined Tunnel Fires Based on a Non-Orthogonal Ventilation Plume Model 647
Lei Liu[1,2,3], Ke Wu[1,2,3]& Tianhang Zhang[1,2,3]
[1]Key Laboratory of Offshore Geotechnics and Material of Zhejiang Province, Zhejiang University, China

[2]Center for Balance Architecture, Zhejiang University, China
[3]Research Center for Urban Fire Safety Engineering, Zhejiang University, China

Multidirectional Pedestrian Flow Dynamics: Impact of Cultural Differences on Individual and Group Movement 649
Nashiru Mumuni Daniel Bilintoh, Jun Zhang, & Rehmat Karim
State Key Laboratory of Fire Science, University of Science and Technology of China, China

Integrating Risk-Based Design into a Decision Support System for Enhancing Fire Resilience in Road Tunnels 651
Marta Galuppi, Davide Berardi & Mara Lombardi
Sapienza University of Rome, Italy

Safety Aspects of the Technical Galleries Consolidation Program 653
Iga Krautsztrung & Sebastien Evrard & Olivier Prouteau
CERN European Organization for Nuclear Research, Switzerland

Optimization of passive fire protection in cut-and-cover concrete tunnels through numerical structural analysis 655
Thomas Thienpont & Ruben Van Coile
Department of Structural Engineering and Building Materials, Ghent University, Belgium

Use of Procedural Content Generation and pixel streaming in VR training of Firefighters 657
Jo Skjermo & Gunnar Deinboll Jennsen
SINTEF Community, Norway

Adaptive Control System for Tunnel Ventilation in the LIAISON Project 660
Jorge González Norniella
ZITRÓN, Spain

Influence of sensor data on fire service operations in road tunnels 662
Nils Johansson
Division of Fire Safety Engineering, Lund University, Sweden

Enhancing Safety in a Long Bidirectional Road Tunnel: A Risk-Based Approach to Ventilation Design 664
Juan Carlos de Rueda, Sorosuh Dabiri & Reinhard Gertl
ILF Consulting Engineers Austria GmbH, Austria

State of the Art of Tunnel Fire Research at RISE (SP)

Haukur Ingason, Ying Zhen Li
RISE Research Institutes of Sweden, Borås, Sweden

ABSTRACT

The paper summarizes the key research activities conducted at RISE and its forerunner SP over the past three decades, and evaluate the contributions to safer tunnel fire design. RISE and SP have played a fundamental role in the development and performance of both large-scale and model-scale tunnel fire testing, resulting in numerous data and engineering correlations, scientific papers and books. The main focus has been on heat release rates, temperatures, smoke control, smoke and gas productions, impact on constructions, influence of water-based fire suppression systems, rescue service actions as well as conducting numerical simulations and educational work. Significant contributions have been made through chapters in various tunnel safety books, especially the publication of the book "Tunnel Fire Dynamics" (1st and 2nd editions). Important achievements include providing data on heat release curves of different types of vehicles, developing correlations for critical and confined velocity for smoke control, gas temperature for assessing heat exposure to tunnel structures, and critical distance for smoke descent, and exploring the mechanisms and performance of different water-based fire suppression systems in tunnels. Standardization has also been a priority for the research team, as it allows to contribute valuable data to ongoing discussions in the field.

KEYWORD: fire dynamics, heat release rate (HRR), gas temperature, smoke control, smoke descent, thermal exposure, fire suppression, fire fighting.

INTRODUCTION

The importance of fire safety in tunnels has grown as tunnel and underground projects become larger and more complex. This presents a significant challenge for engineers, authorities and researchers. It is crucial that research questions arise not only from industry and authorities but also from testing institutes and academia. Testing institutes and academia have resources and competence to conduct systematic research studies. This keynote paper summarises the work done by RISE Research Institutes of Sweden (RISE), formerly known as SP Technical Research Institute of Sweden (SP), the last three decays and try to evaluate the impact it has made.

SP and RISE have been actively collaborating with industry – conducting product testing and acting as a bridge between academia and industry. By supporting research initiatives with real-world needs, SP and RISE has successfully formulated and carried out studies that address critical fire safety challenges. Large-scale and model-scale fire testing has been a major contribution by SP and RISE throughout this period. Below a summary of projects related to large-scale and model-scale testing is presented briefely. In the following writing, either SP or RISE will be used to indicate the period we participated in the actual project and RISE (SP) when considering the entire research period (three decays).

LARGE-SCALE TESTING

RISE (SP) has conducted or been involved in numerous large-scale fire tests to study the fire behavior of vehicles in tunnel settings since 1992. The first significant large-scale tunnel research activity was related to the EUREKA 499 tests [1, 2] in Reppafjord 1991-1992. At that time, Sweden had concerns

regarding the planning of these tests, particularly since no HRR measurements were initially planned. In response, SP applied for research funding and received a grant from Brandforsk (the Swedish Research Board). This funding provided an opportunity to design a detailed test setup focused on measuring HRR from different fuels such as vehicles, pool fires and wood cribs. This EUREKA 499 project was the starting point for SPs involvement in tunnel fire research. The main interest was to use oxygen consumption technique to measure the HRR relatively close to the fire source and on both side of the fire source. Later this technique evolved on using longitudinal flow to measure only on one side of the fire and at a far away distance. Corrections for transportation times of fire gases were developed [3]. In the Eureka 499 tests, SP measured the mass flow rates and gas concentrations inside the tunnel. This was necessary to determine the HRR in real time. The method used was the one developed by Huggett [4] and later applied by Parker [5], which had been used in SPs laboratory calorimeters for decays [6]. This led to comprehensive and detailed HRR data for various types of vehicles, including trains, heavy goods vehicles, and passenger cars. In addition, heptane pool fires and wood crib fires were tested. The method SP used became well established and used in most later model-scale and large-scale testing by SP and others. The results have been published by SP in multiple technical reports and proceedings and gained worldwide distribution [7-11].

Further, SP performed and planned the tests in the Runehamar tunnel 2003 in co-operation with the UPTUN project [12]. These tests provided valuable data on HRR and smoke movement for different fire loads consisting of wood/plastic pallets, furniture and packed commodities configurated as a cargo on a Heavy Goods Vehicle (HGV) as well as a diesel pool fire. This data has been applied, analysed and used worldwide, both by scholars and technical committes. The main scientific contributions were done by the authors and colleagues at SP [13-17]. This was a co-operation project between SP, TNO in the Netherlands, SINTEF in Norway and Promatec International BV and Gerco, in the Netherlands [18-21].

In 2011, the Swedish METRO project was conducted by SP and Mälardalen University in Sweden. Numerous scientific papers and technical reports related to the METRO project have been published [22-31]. In the project, extensive large-scale fire and explosion tests were carried out in the Brunsberg Tunnel near Arvika, Sweden. The tunnel was 276 m long with a cross section of 44 m^2. The primary objective was to enhance safety in underground metro rail systems by studying fire dynamics, evacuation procedures, fire fighting and the impact of explosions within tunnel environments. Overall, the METRO project provided valuable insights into fire dynamics, explosion impacts, and evacuation and rescue strategies in metro and rail tunnel environments. This work contributed to improved safety protocols and design recommendations for underground mass transport systems in Sweden and worldwide.

In collaboration with industry partners and authorities, RISE (SP) has been involved in the development and evaluation of water-based fixed fire fighting systems (FFFS) for road tunnels in 2013 – 2019 [32-36]. These tests have evolved the use of FFFS in Sweden. Ulf Lundström at the Swedish Transport Administration (STA) gave an overview on the development of the Swedish road tunnel safety concept involving the tests carried out by RISE (SP) [37]. Also the concept of automatic sprinklers has been tested in co-operation with the STA [38, 39].

In 2018, a series of large scale fire tests was carried out in the Runehamar tunnel to investigate the performance of a line type heat detection system based on Fiber Bragg Grating (FBG) temperature sensing [40]. Different fire scenarios and tunnel velocities were tested with and without a cover surrounding the fire source. The rates of temperature rise obtained from the detectin system (FBG) were found to be more stable compared to thermocouples. A very interesting finding is that the fire detection cables can be considered as a thermal bulb, and the Response Time Index (RTI) can be used to represent the characteristics of the fire detection cables [40]. Simple correlations to predict the rate of FBG temperature rise were proposed and verified using test data. These tests were then used to validate numerical models in a following study [41].

Due to the costs and limitations on number of tests, large scale fire testing was mostly for validation of results from model scale testing which has served as our main research methodology due to its flexibility and cost-effectiveness. In the following text, a short presentation of model scale tests that has been carried out by RISE (SP) is summarized.

MODEL-SCALE TESTS

In 1995 SP started performing model scale tests in tunnels investigating the influence of ventilation on burning rates [42]. In 1995 – 1999 SP did both model and medium scale smoke and fire spread tests [43-46]. In early 2002 SP did some model scale tests prior to the planning of the Runehamar tests but that was published afterwards in 2005 [47]. The tests grounded the basis for many of the fire dynamic parameters investigated by SP in later years. Parameters such as construction of design fires, influence of ventilation on fire growth rate and peak HRR, backlayering length of smoke, critical velocity, maximum and average gas temperatures and decay correlations, incident heat flux and flame length correlations. All these correlations were improved and modified in a later analysis [48].

This research work started a new era in SPs theoretical and experimental work agenda including the following papers [39, 49-63]. This lead to the writing of the textbook "Tunnel Fire Dynamics" which still is the main textbook giving the basics of tunnel fire dynamics [64]. The second edtion of that book was published in 2024, with numerous updated information, among them models and data on alternative fuel vehicle safety [65]. The main contribution by RISE (SP) has been in fire development, smoke control and fire spread, exposure to constructions as well as active suppression and detection systems using scaling techniques. Besides, RISE (SP) has developed methods for scaling of wood pallet fires [58], internal wall temperatures in compartment fires [66] and response of sprinkler head [39], and investigated the scale effect of pool fires [59].

Conclusively, RISE (SP) was pioneering in using model-scale fire tests as a tool to understand fire dynamics and suppression better in tunnels. In the last one and a half decays, scholars from China and other parts of Asia started to become the main driving research force and using model scale technique has become the main experimental method for new knowledge on tunnel safety.

OVERVIEW PAPERS BY RISE (SP)

Two research overviews have been authored by RISE (SP) at different times, one in 2008 [67] and one in 2018 [68]. Further, three chapters in handbooks [69-72] have been published, in addition to our own textbook "Tunnel Fire Dynamics" [64, 65].

The 2008 paper

A keynote paper from 2008 at IAFFS [67] by one of the authors concluded that the critical velocity (the minimum airflow required to prevent smoke backlayering) was well-understood but needed further refinement. The concept of critical velocity was and is still the most well-studied phenomenon in tunnel fire research. However, models at that time were largely based on steady-state conditions and do not fully account for the dynamic of fire development or heat losses to tunnel walls. The original concept was obtained by Thomas [73] and later he presented the concept of critical velocity [74]. Hinkley also worked on the concept of critical velocity but for a different application [75]. Ota and Atkinson [76] conducted an important work on critical velocity using dimensional analysis. Atkinson and Wu [77] extended this work using dimensional analysis for large fires. Dimensional analysis was used by the authors in 2010 classical paper [49] on critical velocity and backlayering length.

The 2008 paper discussed how fire spread in tunnels is heavily influenced by ventilation, which can significantly accelerate the process through mechanisms such as flame impingement, surface spread, and remote ignition. Large-scale tests, including those in the Runehamar tunnel 2003, demonstrated that fire growth rates can increase dramatically with higher ventilation speeds. The maximum HRRs in tunnel fires were found to be higher than previously estimated. Experimental data from large-scale

tests (e.g., Runehamar, EUREKA 499) revealed that tunnel fires, particularly those involving HGVs, can reach HRRs of 100–200 MW – far exceeding the previously assumed 20–30 MW design values at that time. This led to revisions in fire safety standards for tunnel ventilatin systems in fire safety design. Another aspect explored was the effects of the tunnel geometry on fire behavior. Tunnel width had a significant impact on HRR for small scale pool fires, with narrower tunnels increasing fire intensity due to radiation feedback, which has been confirmed by a later study [59]. The effects of tunnel height were less pronounced but still influence temperature distribution and smoke movement.

Ceiling gastemperatures were found to reach higher levels compared to enclosure fires in buildings, usually about 1000 – 1100ºC. Gas temperatures in tunnel fires were recorded between 1200–1365°C, and consequently increased the interest in the use of high-performance fire-resistant materials in tunnel construction. More large-scale experimental research was although found to be necessary. Despite existing model-scale research already at 2008, there was a shortage of high-quality, large-scale and model-scale experimental data to validate theoretical models. It was concluded that future studies should focus on fire spread mechanisms, heat transfer effects, and improving computational fire models.

Finally, it was concluded that tunnel fire safety had improved significantly in 2008, but continued research was essential to refine design standards, enhance fire protection strategies, and better understand fire dynamics in increasingly complex tunnel environments.

The 2018 paper

A later published overview by the authors summarized the research status until 2018 [68]. The relevant work was also presented as a keynote speech at the 8th ISTSS [78]. The 2018 overview provides a comprehensive collection of available research across different areas, particularly concerning HRR for various types of vehicles. In terms of fire growth and HRR development, passenger car fires tend to develop more slowly than the medium t-squared growth curve, whereas HGV fires progress rapidly, often surpassing the "ultra-fast" growth curve. Metro carriages and buses, on the other hand, demonstrate a more linear fire growth along their length, with factors such as window breakage and openings influencing HRR dynamics (fire development). Furthermore, the influences of tunnel ventilation and structure on the maximum heat release rate, fire growth rate and fire spread to nearby vehicle are investigated.

The authors reviewered smoke control for longitudinally ventilated tunnels, cross passages, railway rescue stations and naturally ventilated tunnels with densely distribted short vertical shafts. It illustrated the state of the art of research on critical velocity and backlayering length. It was pointed out that there is a lack of full scale test data concerning smoke control in cross passages and in rescue stations, and further research is also needed on the performance of point extraction ventilation and natural ventilation with short shafts, and also the smoke control in underground railway and metro stations.

The overview also explores temperature exposure and its effects on tunnel structures. Fires in tunnels can reach very high temperatures, although they rarely exceed 1350°C as was measured in the Runehamar tests. It has been anticipated by the authors that due to the effective insulation in the vincinity of the fire, higher gas temperatures were obtained [79]. With concrete tunnel the gas temperature would have been about 100ºC lower. Prolonged exposure to intense heat weakens concrete, steel reinforcements, and tunnel linings. Key structural risks include concrete spalling, which occurs when surface layers crack and detach due to water vapour pressure; steel deformation, which reduces load-bearing capacity; and, in extreme cases, local tunnel collapse if fire temperatures exceed critical structural limits. As mentioned earlier thermal boards tend to increase the gas temperature which complicate the picture.

Water-based FFFSs are the most commonly used FFFS in tunnels. These include deluge systems (which spray large amounts of water over a fire zone (deluge zone) using different water pressure),

high and low pressure water mist systems (which absorb heat efficiently), automatic sprinklers (which activate based on heat), and foam-based systems (which are particularly useful for liquid fuel fires). Some hybrid systems combine water mist with ventilation controls to enhance fire suppression effectiveness. Studies show that FFFS can reduce HRR by 50-80%, delay fire growth, and limit fire spread, particularly in HGV fires. Pressure losses for ventilation system over open deluge zone for this type of systems is not considered as a problem. Despite their effectiveness, FFFS face challenges such as high installation and maintenance costs and dependency on ventilation conditions. High airflow can disperse small water droplets, reducing suppression efficiency, while some systems must be carefully coordinated with smoke extraction to function optimally. However, their implementation requires careful integration with ventilation systems to maximize efficiency. When introduce FFFS into safety concept one may consier technical trade-offs in order to reduce costs at other places [80].

Through these overview studies we know that fire safety research continues to advance tunnel design, influence risk mitigation strategies, and emergency response planning, ensuring safer underground transportation environments. The amount of scientific journal papers published on fire safety in underground structures such as tunnels, in the last decay, has increased exponentially and will continue to do so in the future.

DISCUSSION

It is evident that RISE (SP) has significantly contributed to the understanding of critical fire safety aspects in tunnels. Tunnel fire dynamics are governed by a complex relationship of physical, chemical, and environmental factors, with certain parameters being particularly crucial in determining fire behavior.

There are five areas which can be regarded as major contribution from RISE (SP) and will be discussed in more detail in the following section.

(1) Heat release rates in tunnels

A comprehensive collection of available HRR data for various types of vehicles, large portion from own experimental activities, has been listed [65]. For example passenger cars typically exhibit peak HRR values between 3 and 5 MW, rarely exceeding 6 MW. Buses, depending on fire growth and ventilation conditions, can reach up to 30 MW. Heavy goods vehicles (HGVs) display significant variability in HRR, with values ranging from 66 MW to 202 MW based on the type of cargo they carry, see Figure 1. Metro and railway carriages generally fall within a peak HRR range of 7 MW to 77 MW for a single carriage, as shown in Figure 2, while fuel tanker fires can be catastrophic, with HRR values reaching up to 300 MW to 400 MW.

A summary of HRR data from large-scale tests has also been normalized based on the exposed fuel surface area [65]. The exposed fuel surface refers to the area where vaporized or gasified fuel is released, allowing for peak HRR comparisons across different fuels and fire conditions. HRR data was categorized into three groups: liquid pool fires, solid materials (e.g., wood pallets), and road/rail vehicles. Tests indicate that peak HRR per unit fuel surface area in fuel-controlled vehicle fires ranges from 0.2 to 0.4 MW/m², increasing to 0.5 MW/m² for HGV trailers. Time to peak HRR varies between 10 and 55 minutes. The total released energy varies by vehicle type: 10–240 GJ for HGVs, 41–44 GJ for buses, and 2.1–8 GJ for passenger cars [65]. All of these data obtained are useful in the design process, especially if it is a performance based design.

In large-scale tanker fires, where fuel spreads across the tunnel width, HRR can range from 0.35 to 2.6 MW/m², depending on ventilation and fuel distribution [65]. Further research on spilled liquid fires in tunnels is needed, particularly for thin fuel layers. Large-scale testing is crucial, as small-scale pool fire experiments cannot always be extrapolated to real-world scenarios [65].

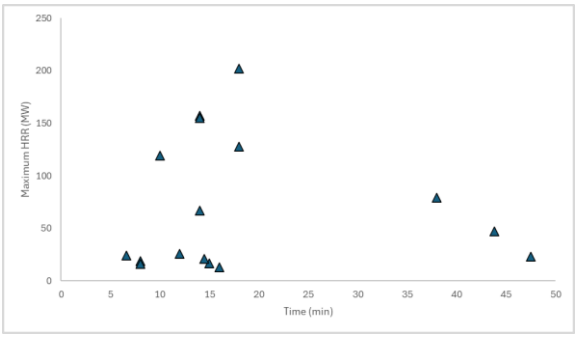

Figure 1 Summary of time to reach peak HRR versus peak HRR for HGV fire loads [65].

The test results for single train carriages show peak HRR ranging from 10 to 77.4 MW, with time to peak HRR varying from 5 to 118 minutes [65], see Figure 2. There is no clear correlation based on this data on time to HRR and maximum HRR. If a fire spreads to multiple carriages, the total HRR and time to peak would increase, but exact estimates require considering various factors, as peak HRR for each coach may not occur simultaneously. The EUREKA 499 tests highlight several factors impacting fire development in train carriages, including body material, window quality, ventilation systems, tunnel geometry, and interior combustion materials. Broken windows can accelerate fire spread, while intact windows may slow the fire's progression. In the METRO project, HRR values were higher compared to previous tests, partly due to luggage contributing to the fuel load and larger openings in metro carriages. Large ignition sources were used to simulate arson fires. Fire development was delayed in one test due to the aluminum roof, and it's known that the combustible linings lead to peak HRR in 10-20 minutes. The flame spread pattern within the carriage is evident. The maximum heat release rate depends on the ventilation conditions, and the type and configuration of the fuels. A theoretical model was proposed for estimating the maximum heat release rate from carriage fires [28, 29].

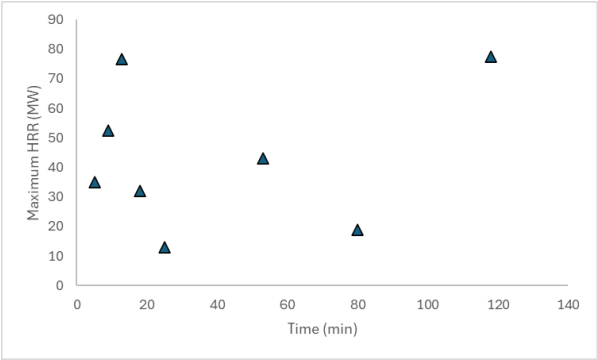

Figure 2 The HRR for rail vehicle tests given in [65].

It was found that tunnel width and ventilation had limited influence on the maximum HRR for well-ventilated (fuel controlled) pool fire and solid fuel fires. The main heat absorbed by the fuels more likely comes from the surrounding flames rather than from the tunnel structure [68]. For well ventilated tunnel fires with vehicle carriages, the influence of tunnel ventilation and structure on the maximum HRR is expected to be insignificant. In most cases, the influence of tunnel ventilation on fire development is also insignificant, but it can have some influence if availability of vehicle openings (e.g. windows, doors or fallen roofs) forms a longitudinal flow inside the carriage which can stimulate the flame spread. For exposed solid fuels (e.g. open truck loads) in a tunnel fire, the maximum HRR could slightly increase (e.g. by around 25%) compared to that in the open, but the fire growth rate increases approximately linearly with the tunnel ventilation velocity. If fire spread to other vehicles or vehicle carriages occurs, the total HRR depends on how fast the fire spread occurs and how many fuels can sustain burning simultaneously. In such cases, higher tunnel ventilation indicates more vehicles or vehicle carriages may be involved in burning simultaneously, i.e. a higher HRR.

One interesting finding is that for well ventilated pool fires, the influence of ventilation and tunnel structure on burning of pool fires is not very significant for large scale pools, but very significant for small pools. The diameter of a pool fire is important for the HRR per unit area of fuel surface. When the diameter is less than 1 meter, the HRR decreases significantly, but it stabilizes at larger diameters. This trend has been observed for fuels such as gasoline, diesel, heptane, and methanol [59]. The burning of pool fires is highly dependent on the scales of the pool pans. Therefore the findings from small scale pool fire tests cannot be directly extrapolated to large scales.

Both spillage and burning behaviours of spilled liquid fires arisen from fuel tank releases in tunnels were studied [81]. Two typical scenarios were identified, i.e., continuous release and instantaneous release. Both experiments and numerical work were conducted [81, 82]. Correlations were established to estimate the spillage area from a continuous release, and test data from instantaneous releases were obtained. The burning of spilled liquid fires were experimentally studied. The thickness of the fuel bed is a critical factor for HRR per unit area; it ranges from 2.4 MW/m² for a thick fuel bed greater than 80 mm to 0.8 MW/m² for a 2-3 mm thick fuel bed [65]. All of these parameters are essential considerations in the design of a spillage fire.

(2) Effects of longitudinal ventilation on smoke control

- Critical velocity and backlayering length with and without blockage

The critical velocity and backlayering length can be obtained by the following equations obtained by RISE (SP) [83]. These equations consider the geometrical form of the cross-section, width and height:

$$u_c^* = \frac{u_c}{\sqrt{gH}} = \begin{cases} 0.81(Q^*\varphi^{-1/4})^{1/3} & Q^*\varphi^{-1/4} \le 0.15 \\ 0.43 & Q^*\varphi^{-1/4} > 0.15 \end{cases} \quad (1)$$

where

$$Q^* = \frac{Q}{\rho_o c_p T_o g^{1/2} H^{5/2}}, \ \varphi = \frac{W}{H}$$

The backlayering length in a tunnel without blockage can be estimated by [49, 60]:

$$L_b^* = \frac{L_b}{H} = 20\ln(\frac{u_c}{u_o}) \quad (2)$$

Recently, it has also been found that influences of upstream blockages can be introduced in these equations [60] as follows:

$$L_b^* = \frac{L_b}{H} = 20\ln(\frac{u_{c,blockage}}{u_o}) \quad (3)$$

where the critical velocity with upstream blockage near the fire source could be estimated by the following equation:

$$u_{c,blockage} = u_c(1-0.88\frac{A_{b,projected}}{A}) \quad (4)$$

It should, however, be noted that when the blockage is attached to the fire source, the correlation factor, *k*, is approximately equal to 1, instead of 0.88.

Eq. (3) and (4) become universal for tunnels with or without blockages. This equation makes it possible to calculate the critical velocity based on information about backlayering distances, and possible blockage ratios in the vicinity of the fire. It is easy to use and has been confirmed recently in an article by RISE (SP) [60]. In Figure 3 experimental results are shown with and without blockages. The preivos model by Li et al. [49] is also shown for comparison.

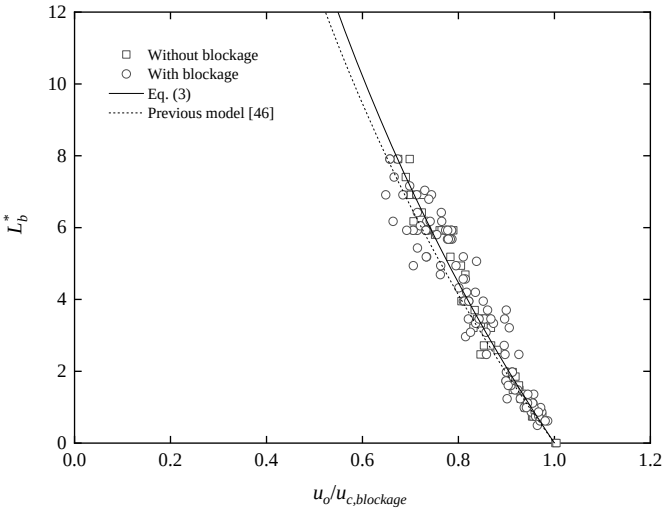

Figure 3 The general equation for backlayering length and critical velocity (L_b=0) and with and without blockage ratio $A_{b,projected}/A$ [60].

There is angoing discussion on backlayering lengths, slope influence, cross-section shape and blockages on critical velocity. Much of the data supporting current calculation models stem from scaled experiments, with only a limited number of full-scale studies, such as the Memorial Tunnel and Runehamar experiments (2003). Between 2018 and 2022, RISE (SP) conducted additional experiments at 1:3 and 1:15 scales to further investigate these issues [60, 84, 85]. There is a new proposal in the NFPA 502 – 2025 edtion that uses a different approach than given in equation (1). The discussion will continue on these different correlations and how well they comply with full-scale and model-scale experiments.

A key criticism of the existing models is their heavy reliance on scaled experiments, resulting in a lack of full-scale data necessary for validation—both for physical models and numerical simulations like the Fire Dynamics Simulator (FDS) [86]. Addressing this gap requires new large-scale experiments, but these demand significant resources. Recently, RISE analyzed full-scale tests, confirming the validity of Equations (1)–(4). However, most of these tests which are the basis for the modesl are conducted without blockages in the tunnel. Since vehicle blockage configurations are unpredictable, the critical velocity for smoke control should be determined without accounting for them.

The Memorial Tunnel tests revealed lower critical velocities and shorter backlayering lengths due to significant blockages due to instrumentation within the tunnel. Furthermore, RISE's recent investigation suggests that the originally assumed blockage of 17% [87] is underestimated and should be revised to at least 30–35%. Consequently, according to Equation (4), the critical velocity must be significantly increased when considering 30–35% blockage compared to 17%. This topic remains under discussion and will continue evolving as new data emerge.

(3) Temperature and thermal loads to constructions

Since the Runehamar tests in 2003, the need for good correlations to estimate the maximum gas temperature and average downstream temperature or gas temperature in the ceiling has increased. Ingason [88] developed an exponential correlation to estimate downstream avergage temperatures, while Hu et al. [89] confirmed that dimensionless excess ceiling temperature follows an exponential decay pattern. Ingason and Li [48] introduced a dimensionless distance variable to correlate test data in different scales, using a sum of two exponential functions. They also identified a virtual origin for large fires, where gas temperatures decrease slowly due to continuous heat introduction from the flame. Li and Ingason [90] later proposed a method to estimate the distance between the virtual origin and the fire source. The calculation models of maximum gas temperature for small fires [53] and large fires [54] as well as the position of maximum ceiling gas temperature [55] have been developed by the authors. These models yield a good estimation of the maximum gas temperature but the effects of heat losses were not explicitly considered more than the embedded heat losses.

Therefore, a new approach was developed by the authors taking into consideration the influences of heat losses on the final max values [79]. The main reason was the discrepancy in the results from the model scale tests and heavily insulated full-scale tunnels. In the 2016 work it was possible to estimate the gas temperatures in model scale, and compare it to scaled full-scale fires yielding similar gas temperatures as the experimental data showed. This was an important discovery as the model scale tests gave consequently lower gas temperatures, although the scaled HRR was correct. The work also showed that correspondeing full-scale tests were also possible to predict, including the lining material on the walls, see Figure 4. The model was validated against both large- and model-scale test data. The correspondence was encouraging, and further development and validation of the model by testing was proposed. It was felt that focus should be placed on parametric study of the effects of lining, ventilation, and geometry in relation to both fuel geometry and tunnel cross-section. The theoretical model considers conduction, convection and radiation, in both scales, explaining the discrepancy between the scales.

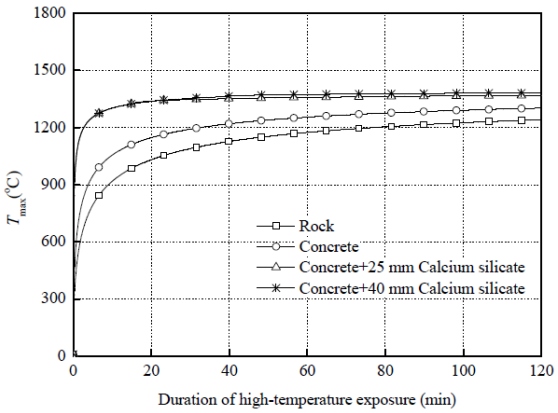

Figure 4 The effect of tunnel structure on gas temperature [79].

In order to verify this, model scale tests were performed with different types of lining material on the surrounding walls [91]. The aim was to further study the theoretical model of maximum gas temperature for structural protection presented by the authors [79]. New correlation for calculation of mass flow rate was introduced into the model [91]. Analysis of the test results showed that the maximum gas temperatures become higher for a more fire-resistant material (with a lower thermal inertia). Also, the maximum gas temperature increases with the increasing HRR, but this increase becomes smaller as the HRR continues to rise. This increase depends on the ventilation velocity, and it is smaller for a lower velocity. It was also found that the maximum gas temperature decreases with the increasing tunnel width due to larger heat losses. Overall, the maximum ceiling gas temperatures increases with the increasing HRR and decreases with the increasing tunnel width and thermal inertia

of the tunnel linings. Comparisons of model scale tests and theoretical models showed that the theoretical models predict the maximum ceiling gas temperature very well, whether it is a fire with a fixed HRR or a time-varying HRR. The effects of tunnel structure, tunnel ventilation, tunnel width and fire size were well considered by the model.

Important contribution by the authors is also the conversion of standardized time-temperature curves such as ISO, HC and RWS, to corresponding HRR, for a given tunnel cross section, tunnel height and longitudinal ventilation velocity. This has been a key question that RISE (SP) has raised throughout participating in infrastructure design, i.e. connecting a determined design fire to corresponding ceiling gas temperatures. It is much easier to discuss within a project if this possibility is available. In [65] there is an example of a tunnel designed for HC curve, with an height of 6 m and 12 m wide. The longitudinal ventilation rate is 3 m/s. In Figure 5 the calculated HRR corresponding to HC time temperature curve for this example is given.

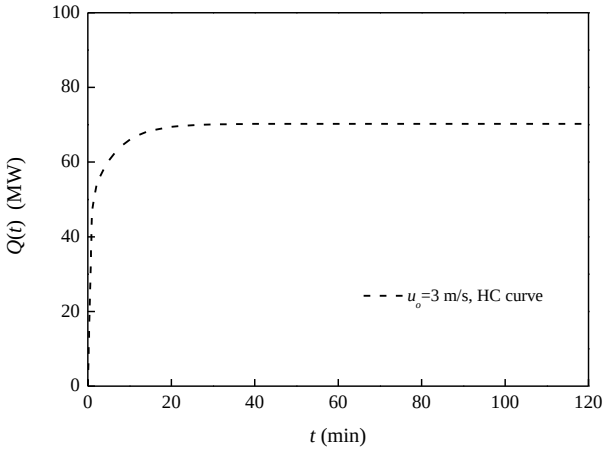

Figure 5 The calculated HRR corresponding to a HC curve in a 6 m high tunnel with ventilation of 3 m/s [65].

The work carried out by the authors indicate that insulating a tunnel with boards may be counterproductive. It may be better to add a concrete layer instead and thereby reduce the gas temperature and thus the tunnel temperature. A more accurate engineering approach would be to use the actual design fire and calculate the temperature based on thermal inertia and cross-section, rather than relying on assumptions unrelated to real traffic conditions, tunnel size, and ventilation. The use of a FFFS also adds another perspective, as it introduces a potential technical trade-off [80]. Additionally, gas temperatures are significantly influenced by water spray systems [92].

(4) Smoke spread and smoke descent

Previous research on smoke flow in tunnel fires usually followed the conclusion that the smoke layer height would be kept as a constant after the smoke travelled for a certain distance, especially for tunnels under natural ventilation. However, this conclusion was usually drawn either from fire tests in small scale tunnels of a limited length, or from fire simulations in short tunnels and within a short period. It is not expected to be valid for long tunnels.

Under natural ventilation or at a very low ventilation rate (non-ventilated tunnels), there may not be a dominating air flow in the tunnel. In such a quiescent tunnel, it may be reasonable to assume that the scenarios are symmetrical to the plane of the fire source, at least in the early stage of a fire. The scenarios are thus simplified and serve as the basis for the scenarios with longitudinal ventilation. In such case, analytical solutions of the ceiling gas temperature distribution and smoke layer thickness were proposed, assuming the convective heat transfer dominates, and the Reynolds analogy and the Boussinesq approximation apply [93]. From the theoretical model, the smoke layer thickness increases

along the distance from the fire. and thus the smoke will finally descend to tunnel floor.
This phenomenon of smoke descent to the floor has been confirmed and investigated recently [94, 95]. It was found that the mass flow rate of outgoing smoke flow increases with the distance to a critical point and then decreases gradually with the distance. At the critical point, the smoke descends to the floor level. The research group at RISE adopted two methodologies to investigate this issue. The entrainment theory [95] explained how the mass flow rate of the outgoing smoke flow increased with the distance before the critical point. The thermodynamics theory [94] showed that the mass flow rate of outgoing smoke flow was controlled by the vertical gas temperature distribution (the buoyancy force), and it explained why the smoke mass flow rate increases with the distance to a critical point and then decreases gradually with the distance. In other word, before the critical point, both the smoke layer thickness and the outgoing mass flow rates increase with the increasing distance from the fire, while after the critical point, both of them decreases with the increasing distance from the fire.This can be regarded as the lowest point of the smoke spread if it does not hit the road surface. A correlation was proposed to estimate the critical smoke spread length. This length increases with the tunnel height and width but decreases with the HRR, and it lies between 23 and 43 times tunnel height for fire sizes between 10 – 30 MW and tunnel heights and widths varying from 5 – 10 m [94].

Under longitudinal ventilation, more smoke will spread towards the downstream side. If the velocity is higher than the critical velocity, there will be no smoke upstream of the fire. A simplified tunnel ventilation model is proposed to account for the effects of fire and tunnel dimensions incl. slope [51] . A special case is the smoke flow in a tunnel with a large slope [96]. When the tunnel flow initially moves downwards, the firefighters may probably access the tunnel from the upper tunnel portal. In such case, the re-direction of smoke flow is very sensitive to the change in the positive pressure and the thermal pressure. A slight decrease in the positive pressure or a slight increase in the HRR (or thermal pressure) can cause the re-direction of smoke flow, thus putting fire and rescue team at a high risk. By contrast, if the firefighters access the tunnel from the lower portal and the smoke moves initially upwards, the re-direction of smoke flow is less sensitive to the changes in positive pressure and thermal pressure. Therefore, the situations are less dangerous when the firefighters access the tunnel from the lower portal, compared to the access from the upper portal. The firefighters are thus recommended to access the tunnel from the lower portal, with the aid of fixed or movable fans to provide a safety margin on the positive pressure at the lower portal to prevent flow re-direction.

For naturally ventilated tunnels with vertical shafts, smoke flow can be exhausted from the shafts mainly by thermal buoyancy. A theoretical model for mass flow rate in the shaft was developed and validated [97]. The smoke flow properties and smoke exhaust efficiency relating to the nearest shaft have been studied [98], showing that the exhaust efficiency of the nearest shaft is a function of the tunnel and shaft dimensions, independent of the HRR. This is consistent with another study [99] showing that a total shaft cross-sectional area of 100 m^2 for complete smoke exhaust even if several shaft pairs are used. It is worth mentioning that it may not be practical to completely prevent the occurrence of plug-holing as smoke control should be the main goal of such natural ventilation systems.

(5) Fixed Fire Fighting Systems (FFFS)

The research RISE (SP) has been involved in historically has shown the benefits of FFFS dealing with large fires. This is mainly related to road tunnel scenarios. As mentioned earlier this work has mainly been focused on large-scale testing [32-34, 36, 100, 101] but also model-scale testing [38, 39, 63, 102-106].

RISE (SP) has investigated the effectiveness of different water spray systems (FFFS) in reducing HRR, total energy released, and fire spread in road tunnels [92]. A 1:3 scale study compared three typical systems—low, medium, and high pressure—using varying water densities, ventilation velocities, and activation criteria across multiple fire scenarios, including wood pallet fires, wood crib fires, wood and plastic crib fires, and heptane pool fires. Results show that the low-pressure system

generally performs best, particularly in early suppression and fire spread prevention, while the high-pressure system is sometime the least effective. For heptane pool fires, low and medium pressure systems reduced HRR by 50%–68%, compared to 20%–36% for the high-pressure system. In covered fires, an optimal pressure likely exists between the low and medium levels, suggesting performance improvements with slight pressure increases. Fire spread prevention was most effective with the low-pressure system, with only minor charring in one test at the lowest water density. The medium-pressure system performed similarly, while the high-pressure system struggled to prevent fire spread in some of the tests. Overall, higher water density and larger droplet size were key factors in reducing fire spread, with system pressure playing a secondary role.

A key issue is the impact of FFFS on design fire. A parametric study has shown that, if the burning vehicle has steel end blocks, 30% of the total HRR without fire suppression could be considered as the design fire for a deluge water spray system operating at a water density of approximately 10 mm/min (or higher). This has been largely validated in the large scale tests [32, 33]. If there is no end blocks, for a deluge water spray system operating at a water density of approximately 10 mm/min (or higher than this value), 50% of the maximum HRR in the free-burn test could be considered as the design fire.

Anoteher key question explored is whether using FFFS affects CO production and deterioriate tunnel tenability [107]. Analysis of various tests show that early activation of the fire suppression system significantly reduces CO concentration, CO production rate, and FED, while also improving visibility. In tests with earlier activation, the tunnel environment is notably better compared to free-burn tests. For wood pallet fires, ensuring that fire suppression leads to better conditions than free-burn tests throughout the entire duration requires limiting fire size to approximately 30% of that observed in free-burn scenarios. Achieving this requires early activation and a high water density. If the fire is not effectively suppressed—due to insufficient water density or delayed activation—CO concentration and visibility could be worse than in free-burn conditions. However, even in such cases, the reduction in HRR and tunnel gas temperature remains evident when using a water spray system. From the perspective of controlling combustion byproducts such as CO and smoke, only fire suppression systems with sufficient capacity and early activation should be used in tunnels.

CONCLUSIONS

Among all the parameters influencing tunnel fire dynamics, three stand out as the most critical: heat release rate (HRR), ventilation (including airflow velocity and direction), and smoke and toxic gas production. HRR defines the severity of a fire and determines how much energy is released, affecting temperature rise and fire growth. Ventilation plays a central role in governing fire development, smoke movement, and oxygen supply. Lastly, smoke and toxic gas production have a direct impact on evacuation safety, as they influence visibility, air quality, and survivability within the tunnel. To ensure effective fire safety in tunnels, these parameters must be carefully balanced. Controlled ventilation systems, use of fire suppression sytems, proper design of tunnel structural protection, and well-planned emergency response strategies (operation, evacuation, fire and rescue service) are all essential to mitigate the risks associated with tunnel fires and protect both infrastructure and human life.

The main contribution of RISE (SP) is in form of large-scale and model-scale experiments with corresponding data. Based on testing data and theoretical analyses, important engineering correlations have been established. This refers to HRR curves, fire growth rates, design fires, maximum ceiling gas temperature, smoke control, fire suppression (FFFS), toxic components from fires, smoke spread and smoke descent. These parameters have been used in many infrastructure projects and the knowledge provided has raised the understanding of fire dynamics. Through technical reports, scientific papers, chapter sections and books this knowledge has been spread worldwide.

REFERENCES

1. Haack, A. *Introduction to the Eureka-EU 499 Firetun Project*. in *Proceedings of the International Conference on Fires in Tunnels, SP Report 1994:54*. 1994. Borås, Sweden.
2. *Fires in Transport Tunnels: Report on Full-Scale Tests*. 1995, edited by Studiensgesellschaft Stahlanwendung e. V.: Düsseldorf, Germany.
3. Ingason, H. and A. Lönnermark. *Large-scale Fire Tests in the Runehamar tunnel - Heat Release Rate (HRR)*. in *International Symposium on Catastrophic Tunnel Fires (CTF)*. 2003. Borås, Sweden: SP Swedish National Testing and Research Institute.
4. Huggett, C., *Estimation of Rate of Heat Release by Means of Oxygen Consumption Measurements.* Fire and Materials, 1980. **4**(2): p. 61-65.
5. Parker, W.J., *Calculations of the Heat Release Rate by Oxygen Consumption for Various Applications*. 1982, National Bureau of Standards: Gaithersburg, USA.
6. Dahlberg, M., *The SP Industry Calorimeter: For rate of heat release measurements up to 10 MW*. 1992, SP Rapport 1992:43: Borås, Sweden.
7. Ingason, H. *Heat Release Rate Measurements in Tunnel Fires*. in *International Conference on Fires in Tunnels*. 1994. Borås, Sweden: SP Swedish National Testing and Research Institute.
8. Ingason, H., S. Gustavsson, and M. Dahlberg, *Heat Release Rate Measurements in Tunnel Fires*. 1994, SP Swedish National Testing and Research Institute: Borås, Sweden.
9. Ingason, H. *Heat Release Rate Measurements in Tunnel Fires*. in *Second International Conference on Safety in Road and Rail Tunnels*. 1995. Granada, Spain: University of Dundee and Independent Technical Conferences Ltd.
10. Ingason, H. *Design Fires in Tunnels*. in *Conference Proceedings of Asiaflam 95*. 1995. Hong Kong: Interscience Communications Ltd.
11. Ingason, H. *An Overview of Vehicle Fires in Tunnels*. in *Fourth International Conference on Safety in Road and Rail Tunnels*. 2001. Madrid, Spain, 2-6 April.
12. *UPTUN - Final Technical Report - Document UPTUN FTR v10 20061204*. 2006.
13. Ingason, H. and A. Lönnermark, *Heat Release Rates from Heavy Goods Vehicle Trailers in Tunnels.* Fire Safety Journal, 2005. **40**: p. 646-668.
14. Lönnermark, A. and H. Ingason, *Gas Temperatures in Heavy Goods Vehicle Fires in Tunnels.* Fire Safety Journal, 2005. **40**: p. 506-527.
15. Lönnermark, A. and H. Ingason, *Fire Spread and Flame Length in Large-Scale Tunnel Fires.* Fire Technology, 2006. **42**(4): p. 283-302.
16. Lönnermark, A., B. Persson, and H. Ingason, *Pulsations during Large-Scale Fire Tests in the Runehamar Tunnel.* Fire Safety Journal, 2006. **41**(5): p. 377-389.
17. Ingason, H., Y.Z. Li, and A. Lönnermark, *Runehamar tunnel fire tests.* Fire Safety Journal, 2015. **71**.
18. Brandt, A.B. *Presentation of test result from large scale fire tests at the Runehamar tunnel*. in *International Symposium on Catastrophic Tunnel Fires (CTF), SP Report 2004:05*. 2003. Borås, Sweden: SP Swedish National Testing and Research Institute.
19. Lemaire, T. *Runehamar Tunnel Fire Tests: Radiation, Fire Spread and Back Layering*. in *International Symposium on Catastrophic Tunnel Fires (CTF), SP Report 2004:05*. 2003. Borås, Sweden: SP Swedish National Testing and Research Institute.
20. Olst, D.v. and R.v.d. Bosch, *Protecting the Runehamar Tunnel in Norway with Promatec®-T against Multiple Fires, as Part of the UPTON Research Programme*, in *International Symposium on Catastrophic Tunnel Fires (CTF), Borås, Sweden, November 20 – 21, 2003*. 2003: Borås.
21. Anton, O. and X. Wu, *Runehamar Tunnel Fire Tests – UPTUN: Fire Protection*, in *International Symposium on Catastrophic Tunnel Fires (CTF), Borås, Sweden, November 20 – 21, 2003*. 2003: Borås.
22. Ingason, H., M. Kumm, D. Nilsson, A. Lönnermark, A. Claesson, Y.Z. Li, K. Fridolf, R. Åkerstedt, H. Nyman, T. Dittmer, R. Forsén, B. Janzon, G. Meyer, A. Bryntse, T. Carlberg, L. Newlove-Eriksson, and A. Palm, *The METRO project - Final Report 2010:08*. 2012, Mälardalen University: Västerås.
23. Lönnermark, A., J. Lindström, and Y.Z. Li. *Model Scale Metro Carriage Fire Tests -*

Influence of Material and Fire Load. in *Second International Conference on Fires in Vehicles*. 2012. Chicago, USA: SP Technical Research Institute of Sweden.
24. Lönnermark, A., J. Lindström, Y.Z. Li, A. Claesson, M. Kumm, and H. Ingason, *Full-scale fire tests with a commuter train in a tunnel*. 2012, SP Technical Research Institute of Sweden: Borås, Sweden.
25. Lönnermark, A., J. Lindström, Y.Z. Li, H. Ingason, and M. Kumm. *Large-scale Commuter Train Tests - Results from the METRO Project*. in *Proceedings from the Fifth International Symposium on Tunnel Safety and Security (ISTSS 2012)*. 2012. New York, USA: SP Technical Research Institute of Sweden.
26. Kumm, M., *Carried Fire Load in Mass Transport Systems - a study of occurrence, allocation and fire behavior of bags and luggage in metro and commuter trains in Stockholm*. 2010, Mälardalen University: Västerås, Sweden.
27. Claesson, A., A. Lönnermark, H. Ingason, J. Lindström, Y.Z. Li, and M. Kumm, *Laboratory fire experiments with a 1/3 train carriage mockup*. 2012, SP Technical Research Institute of Sweden: Borås, Sweden.
28. Li, Y.Z., H. Ingason, and A. Lönnermark, *Correlations between different scales of metro carriage fire tests*. 2013, SP Report 2013:13, SP Technical Research Institute of Sweden: Borås.
29. Li, Y.Z., H. Ingason, and A. Lonnermark, *Fire development in different scales of train carriages.* Fire Safety Science, 2014. **11**: p. 302-315.
30. Li, Y.Z. and H. Ingason, *A new methodology of design fires for train carriages based on exponential curve method.* Fire Technology, 2016. **52**: p. 1449–1464.
31. Lönnermark, A., H. Ingason, Y.Z. Li, and M. Kumm, *Fire development in a 1/3 train carriage mock-up.* Fire Safety Journal, 2017. **91**: p. 432-440.
32. Ingason H., Li Y.Z., Appel G., Lundström U., and Becker C., *Large scale fire tests with a Fixed Fire Fighting System (FFFS) in the Runehamar tunnel.* Fire Technology, 2015: p. 1 - 20.
33. Ingason, H., G. Appel, and Y.Z. Li, *Large scale fire tests with fixed fire fighting system in Runehamar tunnel*. 2014, SP Report 2014:32, SP Technical Research Institute of Sweden: Borås, Sweden.
34. Ingason, H., G. Appel, Y.Z. Li, U. Lundström, and C. Becker. *Large scale fire tests with a Fixed Fire Fighting System (FFFS)*. in *ISTSS 6th International Symposium on Tunnel Safety and Security*. 2014. Marseille.
35. Li, Y.Z., H. Ingason, G. Appel, U. Lundström, and H. Modig, *Influence of fire suppression on combustion products in tunnel fires*, in *7th International Symposium on Tunnel Safety and Security*. 2016, SP Technical Research Institute of Sweden: Montreal, Canada. p. 575-586.
36. Ingason, H. and Y.Z. Li, *Large scale tunnel fire tests with different types of large droplet fixed fire fighting systems.* Fire Safety Journal, 2019. **107**: p. 29-43.
37. Lundström, U. *Development of the Swedish road tunnel safety concept*. in *ISTSS*. 2023. Stavanger.
38. Ingason, H., Y.Z. Li, M. Arvidson, and L. Jiang, *Fire tests with automatic sprinklers in an intermediate scale tunnel.* Fire Safety Journal, 2022. **129**: p. 103567.
39. Li, Y.Z. and H. Ingason, *Model scale tunnel fire tests with automatic sprinkler.* Fire Safety Journal, 2013. **61**: p. 298-313.
40. Li, Y.Z. and X. Du. *Fire tests with a line type heat detection system in the Runehamar tunnel*. in *Proceedings from the ninth International Symposium on Tunnel Safety and Security*. 2020. Munich.
41. Li, Y.Z., J. Lei, and H. Ingason. *Numerical modelling of a line type heat detection system in tunnel fires*. in *ISTSS 2020*. 2020.
42. Ingason, H., *Effects of Ventilation on Heat Release Rate of Pool Fires in a Model Tunnel*. 1995, SP Swedish National Testing and Research Institute: Borås, Sweden.
43. Ingason, H. and P. Werling, *Experimental Study of Smoke Evacuation in a Model Tunnel*. 1999, FOA Defence Research Establishment: Tumba, Sweden.
44. Ingason, H., B. Hägglund, and P. Werling. *Effects of Ventilation on Smoke Spread in Tunnels*. in *International Conference on Tunnel Fires and Escape from Tunnels*. 1999. Lyon, France:

Independent Technical Conferences Ltd.
45. Ingason, H., S. Gustavsson, and P. Werling, *Brandförsök i en bergtunnel - Naturlig ventilation*. 1995, SP Swedish National Testing and Research Institute: Borås.
46. Ingason, H., K. Nireus, and P. Werling, *Fire Tests in a Blasted Rock Tunnel*. 1997, FOA: Sweden.
47. Ingason, H., *Model Scale Tunnel Fire Tests - Longitudinal ventilation*. 2005, SP Swedish National Testing and Research Institute: Borås, Sweden.
48. Ingason, H. and Y.Z. Li, *Model scale tunnel fire tests with longitudinal ventilation.* Fire Safety Journal, 2010. **45**: p. 371-384.
49. Li, Y.Z., B. Lei, and H. Ingason, *Study of critical velocity and backlayering length in longitudinally ventilated tunnel fires.* Fire Safety Journal, 2010. **45**: p. 361 - 370.
50. Ingason, H. and Y.Z. Li, *Model scale tunnel fire tests with point extraction ventilation.* Journal of Fire Protection Engineering, 2011. **21**(1): p. 5-36.
51. Ingason, H., A. Lönnermark, and Y.Z. Li, *Model of ventilation flows during large tunnel fires.* Tunnelling and Underground Space Technology, 2012. **30**: p. 64-73.
52. Li, Y.Z., B. Lei, and H. Ingason, *Scale modeling and numerical simulation of smoke control for rescue stations in long railway tunnels.* Journal of Fire Protection Engineering, 2012. **22**(2): p. 101-131.
53. Li, Y.Z., B. Lei, and H. Ingason, *The maximum temperature of buoyancy-driven smoke flow beneath the ceiling in tunnel fires.* Fire Safety Journal, 2011. **46**(4): p. 204-210.
54. Li, Y.Z. and H. Ingason, *The maximum ceiling gas temperature in a large tunnel fire.* Fire Safety Journal, 2012. **48**: p. 38-48.
55. Li, Y.Z. and H. Ingason, *Position of maximum ceiling temperature in a tunnel fire.* Fire Technology, 2014. **50**: p. 889-905.
56. Li Y.Z., Fan C. G., Ingason H., Lönnermark A., and J. J., *Effect of cross section and ventilation on heat release rates in tunnel fires.* Tunnelling and Underground Space Technology, 2016. **51**: p. 414-423.
57. Fan C. G., Li Y.Z., Ingason H., and A. Lönnermark, *Effect of tunnel cross section on gas temperatures and heat fluxes in case of large heat release rate.* Applied Thermal Engineering, 2016. **93**: p. 405-415.
58. Li, Y.Z. and H. Ingason, *Scaling of wood pallet fires.* Fire safety journal, 2017. **88**: p. 96-103.
59. Yao, Y., Y.Z. Li, H. Ingason, and X. Cheng, *Scale effect of mass loss rates for pool fires in an open environment and in tunnels with wind.* Fire Safety Journal, 2019. **105**: p. 41-50.
60. Li, Y.Z. and H. Ingason, *Influence of upstream blockage on smoke control in tunnel fires.* Fire Safety Journal, 2024. **147**.
61. Li, Y., H. Ingason, M. Arvidson, and M. Försth, *Performance of various water-based fire suppression systems in tunnels with longitudinal ventilation.* Fire Safety Journal, 2024. **146**.
62. Li, Y.Z. and H. Ingason, *Effect of cross section on critical velocity in longitudinally ventilated tunnel fires.* Fire safety journal, 2017. **91**: p. 303-311.
63. Ying Zhen Li, Glenn Appel, Haukur Ingason, and H. Nyman, *Model scale tunnel fire tests with water-based fire suppression systems*, in *SP Report 2014:02*. 2014, SP Technical Research Institute of Sweden.
64. Ingason, H., Y.Z. Li, and A. Lönnermark, *Tunnel Fire Dynamics*. 2015, New York: Springer.
65. Ingason, H., Y.Z. Li, and A. Lönnermark, *Tunnel Fire Dynamics 2nd Edition*, ed. Springer. 2024.
66. Li, Y.Z. and T. Hertzberg, *Scaling of internal wall temperatures in enclosure fires.* Journal of Fire Science, 2015. **33**(2): p. 113-141.
67. Ingason, H. *Keynote Paper - State of the Art of Tunnel Fire Research*. in *9th International Symposium on Fire Safety Science*. 2008. Karlsruhe.
68. Li, Y.Z. and H. Ingason, *Overview of research on fire safety in underground road and railway tunnels.* Tunnelling and Underground Space Technology, 2018. **81**: p. 568-589.
69. Ingason, H., *Fire Dynamics in Tunnels*, in *In The Handbook of Tunnel Fire Safety, 2nd Edtion* A.N. Beard and R.O. Carvel, Editors. 2012, ICE Publishing: London. p. 273-304.
70. Ingason, H. and A. Lönnermark, *Heat Release Rates in Tunnel Fires : A Summary*, in *In The Handbook of Tunnel Fire Safety, 2nd edition*, A. Beard and R. Carvel, Editors. 2012, ICE

Publishing: London.
71. Ingason, H., *Fire testing in road and railway tunnels*, in *2nd Edition Flammability Testing of Materials used in Construction, Transport and Mining*, V. Apte, Editor. 2022, Elsvier. p. 237-279.
72. Carvel, R. and H. Ingason, *Fires in Vehicle Tunnels*, in *SFPE Handbook of Fire Protection Engineering*. 2022.
73. Thomas, P., *The movement of buoyant fluid against a stream and the venting of underground fires*. 1958, Fire Research Station: Boreham Wood.
74. Thomas, P.H., *The Movement of Smoke in Horizontal Passages Against an Air Flow*. 1968, Fire Research Station: Boreham Wood.
75. Hinkley, P.L., *The Flow of Hot Gases Along an Enclosed Shopping Mall - A Tentative Theory*. 1970, Fire Research Station.
76. Oka, Y. and G.T. Atkinson, *Control of Smoke Flow in Tunnel Fires.* Fire Safety Journal, 1995. **25**: p. 305-322.
77. Atkinson, G.T. and Y. Wu, *Smoke Control in Sloping Tunnels.* Fire Safety Journal, 1996. **27**: p. 335-341.
78. Li, Y.Z. *Overview of tunnel fire research*. in *Eighth International Symposium on Tunnel Safety and Security*. 2018. Borås, Sweden.
79. Li, Y.Z. and H. Ingason, *New models for calculating maximum gas temperatures in large tunnel fires*, in *SP Report 2016:95*. 2016.
80. Ingason, H. and Y.Z. Li., *Technical Trade-Offs Using Fixed Fire Fighting Systems*, in *7thInternational Conference 'Tunnel Safety and Ventilation*. 2014: Graz.
81. Ingason, H. and Y.Z. Li, *Spilled Liquid Fires in Tunnels* Fire Safety Journal, 2017. **91**: p. 399-406.
82. Guo, Q., Y.Z. Li, H. Ingason, Z. Yan, and H. Zhu, *Study on spilled liquid from a continuous leakage in sloped tunnels.* Tunnelling and Underground Space Technology, 2022. **120**: p. 104290.
83. !!! INVALID CITATION !!! { Li, 2017 #3035;Li, 2010 #2646}.
84. Li, Y.Z., *Smoke control using point extraction systems in tunnel fires*, in *RISE Report 2018:73*. 2018, RISE Research Institutes of Sweden,.
85. Li, Y.Z., *Influence of slope on smoke control in tunnel fires*, in *RISE Rapport 2020:89*. 2020: RISE Reseach Institute of Sweden.
86. McGrattan, K., S. Hostikka, J. Floyd, R. McDermott, and M. Vanella, *Fire Dynamics Simulator User Guide (Sixth Edition, Nist Publication 1019)* 2020, National Institute of Standards and Technology: USA.
87. Kile, G.W. and J.A. Gonzalez, *The Memorial Tunnel Fire Ventilation Test Program: The Longitudinal and Natural Tests.* ASHRAE Transactions; ProQuest Science Journals, 1997: p. 701 - 713.
88. Ingason, H., *Fire Dynamics in Tunnels*, in *The Handbook of Tunnel Fire Safety*, R.O. Carvel and A.N. Beard, Editors. 2005, Thomas Telford Publishing: London. p. 231-266.
89. Hu, L.H., R. Huo, H.B. Wang, Y.Z. Li, and R.X. Yang, *Experimental studies on fire-induced buoyant smoke temperature distribution along tunnel ceiling.* Building and Environment 2007. **42**: p. 3905–3915.
90. Li, Y.Z. and H. Ingason, *Fire-induced Ceiling Jet Characteristics in Tunnels Under Different Ventilation Conditions*, in *SP Report 2015:23*. 2015, SP Technical Research Institute of Sweden.
91. Li, Y.Z. and H. Ingason, *Model scale tunnel fire tests on maximum ceiling gas temperature for structural protection, RISE Report 2018:58*. 2018.
92. Li, Y.Z., H. Ingason, M. Arvidson, and M. Försth, *Performance of various water-based fire suppression systems in tunnels with longitudinal ventilation* Fire Safety Journal, 2024. **146**.
93. Guo, Q., Y.Z. Li, H. Ingason, Z. Yan, and H. Zhu, *Theoretical studies on buoyancy-driven ceiling jets of tunnel fires with natural ventilation.* Fire Safety Journal, 2021. **119**: p. 103228.
94. Guo, Q., Y.Z. Li, H. Ingason, Z. Yan, and H. Zhu, *Numerical study on thermally driven smoke flow characteristics in long tunnels under natural ventilation.* International Journal of Thermal Sciences, 2023. **192**: p. 108379.

95. Zhao, S., H. Yang, Y.Z. Li, H. Ingason, and F. Liu, *Theoretical and numerical study on smoke descent during tunnel fires under natural ventilation condition.* Tunnelling and Underground Space Technology, 2023. **142**: p. 105414.
96. Zhao, S., Y.Z. Li, M. Kumm, H. Ingason, and F. Liu, *Re-direction of smoke flow in inclined tunnel fires.* Tunnelling and Underground Space Technology, 2019. **86**: p. 113-127.
97. Zhao, S., Y.Z. Li, H. Ingason, and F. Liu, *A theoretical and experimental study on the buoyancy-driven smoke flow in a tunnel with vertical shafts.* International Journal of Thermal Sciences, 2019. **141**: p. 33-46.
98. Guo, Q., Y.Z. Li, H. Ingason, Z. Yan, and H. Zhu, *Theoretical and numerical study on mass flow rates of smoke exhausted from short vertical shafts in naturally ventilated urban road tunnel fires.* Tunnelling and Underground Space Technology, 2021. **111**: p. 103782.
99. Yao, Y., Y.Z. Li, H. Ingason, and X. Cheng, *Numerical study on overall smoke control using naturally ventilated shafts during fires in a road tunnel.* International Journal of Thermal Sciences, 2019. **140**: p. 491-504.
100. Ingason, H., G. Appel, and U. Lundström, *Water spray interaction with liquid spill fire in a road tunnel*, in *SP Report 2015:91*, S.R. 2015:91, Editor. 2015, SP Report 2015:91.
101. Ingason, H., Y.Z. Li, and M. Bobert, *Large scale fire tests with different types of fixed fire fighting system in the Runehamar tunnel*, in *SP Report 2016:76*. 2016.
102. Ingason, H., *Model Scale Tunnel Fire Tests - Sprinkler*. 2006, SP Technical Research Institute of Sweden.
103. Ingason, H., *Model scale tunnel tests with water spray*. Fire Safety Journal, 2008. **43**(7): p. pp 512-528.
104. Li, Y.Z. and H. Ingason, *Model scale tunnel fire tests – Automatic sprinklers* 2011, SP Report 2011:31, SP Technical Research Institute of Sweden: Borås, Sweden.
105. Ingason, H., M. Arvidson, Y.Z. Li, L. Jiang, and J. Blom, *Model scale tests with automatic sprinkler in a tunnel*. 2019, Research Institute of Sweden.
106. Ingason, H., Y.Z. Li, M. Arvidson, and L. Jiang. *Model scale tests with automatic sprinkler in a tunnel*. in *ISTSS2020*. 2020. Stockholm.
107. Li, Y.Z. and H. Ingason, *Influence of fire suppression on combustion products in tunnel fires.* Fire Safety Journal, 2018. **97**: p. 96-110.

Fire and explosion hazards of new energy vehicles in tunnels and underground spaces

Jennifer X Wen

Fire and Explosion Modelling Group, School of Engineering, University of Surrey, Guildford, UK

ABSTRACT

Recent publications concerning fire and explosion safety of new energy vehicles in tunnels are reviewed. While the review covers the fire hazards of both battery and hydrogen powered vehicles, the main content is focused on the explosion hazards of the later, highlighting the potential serious consequences associated with hydrogen explosion in a tunnel. The international efforts so far have included limited experimental and numerical studies with relatively little validation for tunnel configurations. Few of the simulations addressed the flame acceleration and deflagration to detonation transition which are of particular concern to tunnels, which act like shock tubes, as in the conext of gas explosions. Significant knowledge gaps exisit concerning mitigation measures that can be effectively and practically deployed in tunnels for new energy vehicles, especially those powered by hydrogen.

KEYWORD: New energy vehicles, tunnels, fire, explosion, mitigation

INTRODUCTION

The number of new energy vehicles (NEVs) are increasing rapidly. NEVs use clean energy to reduce environmental pollution and resource shortages. Although currently, NEVs are primarily powered by batteries, being either battery electric vehicles (BEVs) or plug-in hybrid electric vehicles (PHEVs), the number of hydrogen fuel cell powered vehicles (HFCVs), either passenger cars or heavy duty trucks, are also set to increase in order to meet the net zero target. There is also ongoing development of trucks powered by hydrogen combustion engines. Such development entails that increasing number of NEVs are entering tunnels and other underground spaces, e.g. underground garages [1].

Comparing with traditional fuel powered vehicles, NEVs incur new/different hazards. While this review includes a sub-section to briefly outline the fire hazards of BEVs and PHEVs as well as hydrogen powered vehicles, the main content will focus on the explosion hazards of the later.

Explosion of accidentally released hydrogen is a safety concern even in open spaces, and even more so in confined spaces like tunnels. The combustion properties of hydrogen are different from other fuels. It requires little energy for ignition and has broad flammability limits (between 4 to 75% by volume in air), compared to conventional fuels (natural gas 5-15% vol.). The flame speed of hydrogen-air mixture is about 8 times greater than that for methane or propane air mixture, particularly at concentrations greater than 10%. Historic data indicated that most of the incidents involving hydrogen releases led to fire and explosions; and accidentally released pressurized hydrogen could ignite in the absence of clearly identifiable ignition sources [2-4]. As shown in Figure 1, the statistics from 426 out of a total of 706 events in "HIAD 2.0 - Hydrogen Incidents and Accidents Database HIAD 2.0 [3] which were considered of statistical value in July 2020 indicated that 84% of the accidental releases resulted in ignition with 56% explosions and 28% fires.

Whilst the high burning velocity of hydrogen reduces heat transfer to the surroundings and the risk of secondary fires, it would lead to higher explosion pressures in the right conditions. In general, the term "explosion" refers to deflagration, which is characterized by a subsonic flame propagation velocity. A

gentle deflagration may be just a flash fire. In contrast, a detonation is characterized by supersonic flame propagation velocities, typically up to 2,000 m/s and substantial overpressures in the range of 20 bar. Under certain conditions, especially in regions of confinement (including semi-confinement) and congestion, a subsonic flame front may accelerate to supersonic speed, resulting in Deflagration to Detonation Transition (DDT).

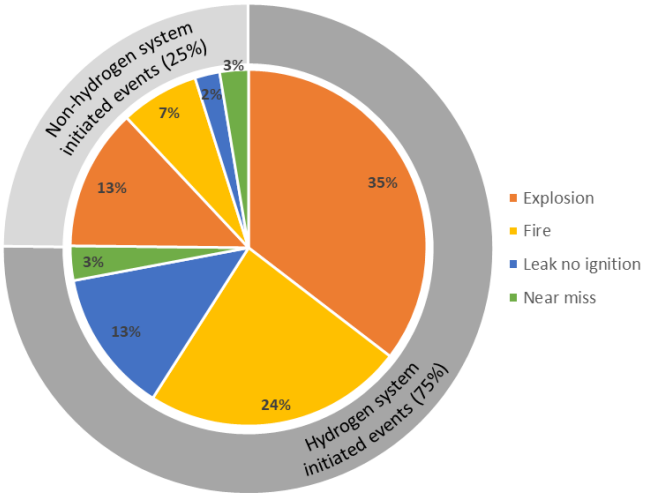

Figure 1 Percentages of the events initiated by hydrogen or non-hydrogen systems (outer circle) and those related to different consequences (the inner circle) (Reproduced from [3]).

EXPLOSION HAZARDS OF HYDROGEN POWERED VEHICLES IN TUNNELS

Li et al. [1] developed a one dimensional (1-D) computational fluid dyanmics (CFD) program to simulate compressible flows in tunnels following tank rupture, boiling liquid expanding vapour explosion (BLEVE) and gas cloud explosions, and validated the predictions against test data for explosion in tunnels [5]. Figure 2 shows the simulated peak overpressure as a function of distance for cloud explosion of hydrogen gas , liquified natural gas (LNG), liquid hdyrogen and liquified petrulum gas (LPG) vehicles in the tunnel. The maximum overpressure was predicted to be located somewhat further from the tank than the edge of the cloud. A growth tendency can be seen before the position with maximum overpressure due to the increasing flame spread speed, and a decay tendency after it. In the far field, the overpressure decays along the distance at a much slower rate.

Kudriakov et al. [6] conducted a number of tests in a full-scale tunnel in France in the frame of pan Euroopean project HyTunnel sponsored by Clean Hydrogen Joint Undertaking (CHJU). These tests were designed to investigate the safety of hydrogen-fuelled vehicles with onboard compressed hydrogen gas storage. The tests included five tests with compressed hydrogen tanks and two tests with compressed helium tanks. Both Type II and Type IV tanks were tested. The hydrogen gas pressure varied between 47 bar and 610 bar. The blast wave overpressures were recorded together with fireball characteristics.

Figure 3 shows the results for maximum overpressure decay along the tunnel corresponding to the group of tests shown in Table 1. The helium-related results for maximum overpressure are lower than the results corresponding to hydrogen-filled tanks. Moreover, the slopes of the best-fit lines corresponding to the helium-filled tanks have lower values than the slopes corresponding to hydrogen-filled tanks. The slopes of the best-fit lines (in log- log scales) corresponding to to the Tests 6, 4 and 7 are 0.077 mbar/m, -0.323 mbar/m and À0.196 mbar/m, respectively. For Test 4 with helium gas, the maximum overpressure levels are lower than 140 mbar, representing the threshold for the first lethal effects while for Test 7 with compressed hydrogen gas, the maximum overpressure levels are higher than 200 mbar, the threshold for significant lethal effects with respect to human health. These results were in line with the predictions of the correlation for for blast wave decay after hydrogen tank rupture in a tunnel fire.

developed by Mokov and Dery [7] that a fraction of chemical energy contributes to the blast wave strength. However, the value of this fraction strongly depends on two factors: the mechanical energy of the compressed hydrogen and the surrounding geometry (tank is isolated or located inside a car, but has yet to be determined. There is potential to use the data geerated in these tests to develop and validate more detailed models that can fill this knowledge gap.

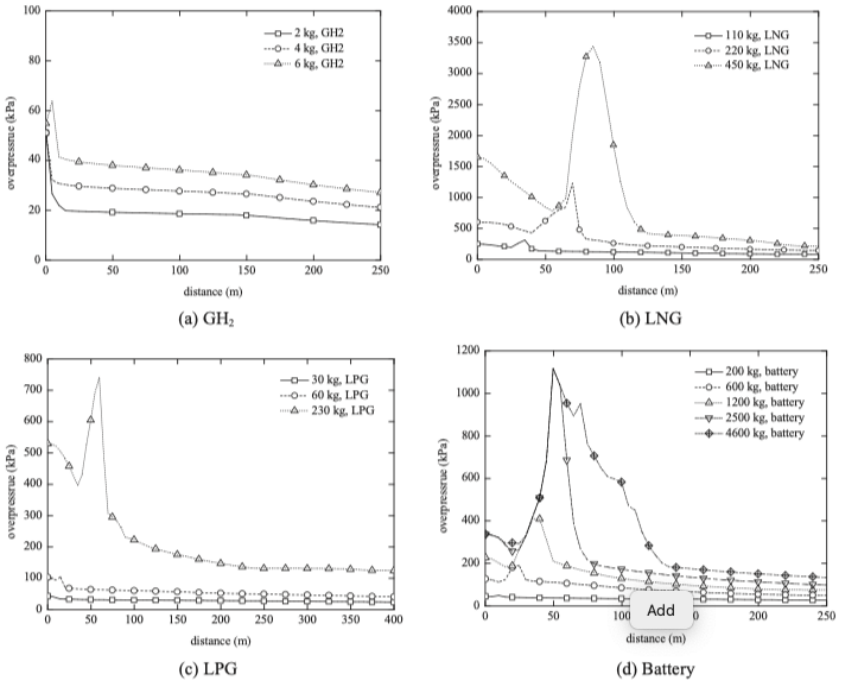

Figure 2 The peak overpressure vs. distance for cloud explosion of GH2, LNG, LPG and battery in the tunnel (reproduced from [1]).

Table 1 Summuary of the tests shown in Figure 3 (reproduced from [6])

Test No.	Tank	Pressure (bar)	Temperature (^{0}C)	Mechanical Energy, MJ	Gas
6	Type II	194	15	2.09	Hydrogen
4	Type IV	650	15	5.88	Helium
7	Type IV	520	15	7.39	Hydrogen

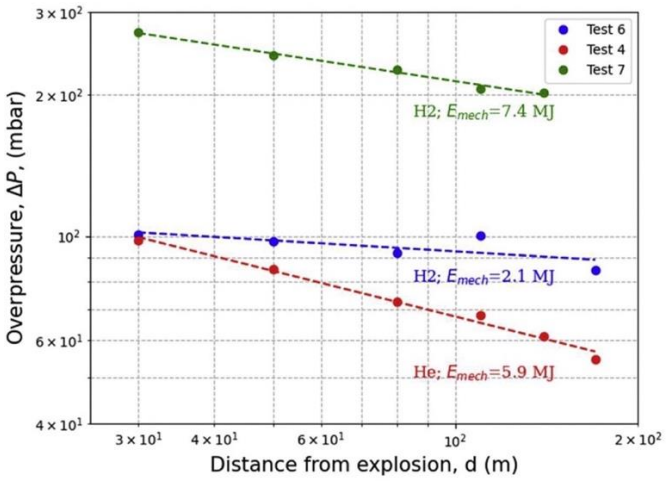

Figure 3 Results for maximum overpressure decay along the tunnel corresponding to the second group of tests. Type IV (reprocued from [6]).

Li et al. [8] conducted transient hydrogen release, dispersion, and combustion in a tunnel for FCVs using CFD code GASFLOW-MPI. The air velocity in the tunnel was not explicitly specified; but judging from the predicted jet fire in [8], the surrounding air was assumed to be quiescent. As expected, the results indicated that hydrogen accumulated beneath the ceiling, forming a thin hydrogen-air mixing layer with strong concentration gradients. The simulations of explosion due to delayed ignition revealed that the pressure wave propagated through the hydrogen cloud with the overpressure of around 8 bars. Beyond the flammable cloud, the blast wave decayed at a lower speed resulting in a lower overpressure to the surrounding cars. The predicted pressure wave exceeded the damage criterion on human being for causing lung damage, severe damage to man's ear drum, although is not lethal [8].

They also analysed flame acceleration (FA) and deflagration to detonation transition (DDT) for the hydrogen layer in the tunnel using the widely adopted σ (expansion ratio - the ratio of densities of reactants and products) and λ (detonation cell size) criterion [9] to calculate the hydrogen layer and compared the mass of hydrogen with the available hydrogen inventory. The anaylsis highlighted the risk for both FA and DDT. The thickness of the hydrogen layer δ calculated with average height along the cross-section of the tunnel was around 0.82 m. Figure 4 shows the λ criterion (above the threshold) at different locations, indicating a significant DDT cloud ($\delta/(14\lambda) > 1$) at the top of the tunnel in the absence of any mitigation. These results highlighted the likelihood of DDT potential associated with hydrogen explosion in tunnels.

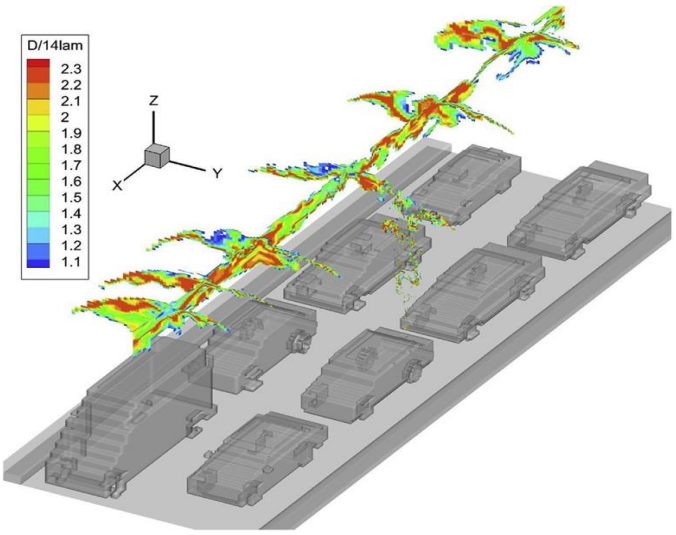

Figure 4 The DDT criterion with the maximum volume of DDT cloud (reproduced from [8]).

Skob et al. [10] numerically investigated the influence of the drift working space clutter by an electric locomotive on the distribution of the overpressure of the gaseous medium in a mine tunnel. Their predictions indicated that the closed nature of the working space and its blockage significantly altered the shape and size of the danger zone, indictaing the need for more detailed safety assessment.

Huang et al. [11] numerically investigated hydrogen dispersion and deflagration in an underground garage with regards to potential leaks from hydrogen fuel cell vehicles using CFD code FLACS. The environment condition of the underground parking garage was not explicitly specified in [11], most likely it was assumed to be quiescent in the simulations. The study was based on a geometric model of vehicles equipped with 70 MPa hydrogen tanks and considered various accidental scenarios by adjusting the orifice diameter and ignition time. Temperature and overpressure were monitored to evaluate the hazard distances. The results were used to help determing the affected areas and safety distances in hydrogen accidents, providing references for the design of parking intervals and the development of emergency plans.

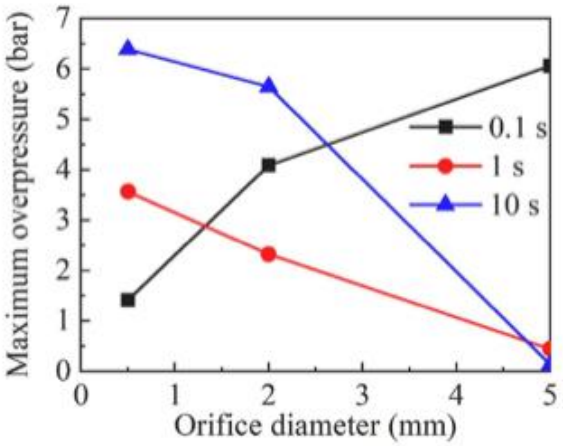

Figure 5 The predicted peak overpressure (d = 0.5/2/5 mm) as a function of orifice diamete (Reproducded from [11]).

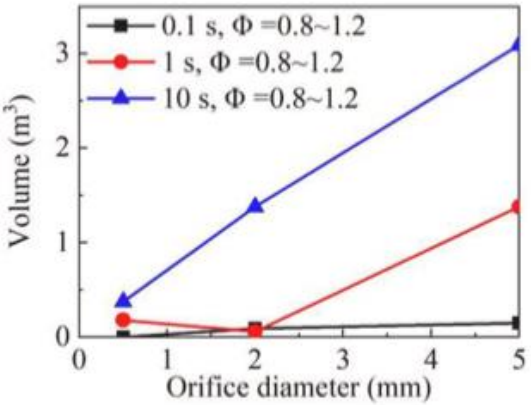

Figure 6 The predicted volume of the high overpressure region (Φ = 0.8–1.2) as a function of orifice diameter (Reproducded from [11]).

The author's group recently conducted 3-D CFD simulations of hydrogen explosion in a tunnel of 400 × 10 × 5 (m). The air velocity in the tunnel was assumed to be 0.5 m/s. Figure 7 is the predicted volume of flammable hydrogen cloud following a specified release condition scenario from a Thermal Pressure Relief Devices (TPRD) of 2.25 mm diameter. The cloud was ignited when the volume of the flammable cloud reached its maximum. The predicted explosion overpressure at four monitoing points are shown in Figure 8. The maximum explosion overpressure reached 57 kPa while the maximum pressure at the left and right ends of the vehicle in the tunnel reached 45 kPa. According to the recommended human harm criteria for overpressure [12], such level of overpressure can result in eardrum rupture, people standing up cab be thrown a distance and seriously injured by being projected against obstacles.

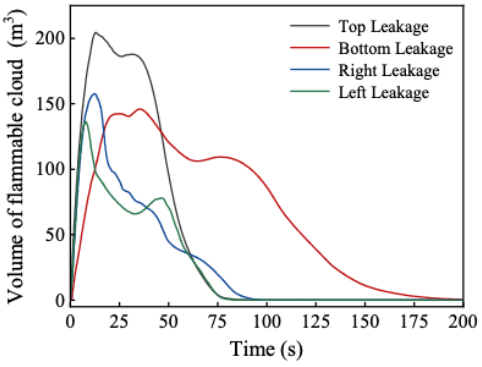

Figure 7 The predicted evolution of flammable cloud volume following TPRD opening in a tunnel.

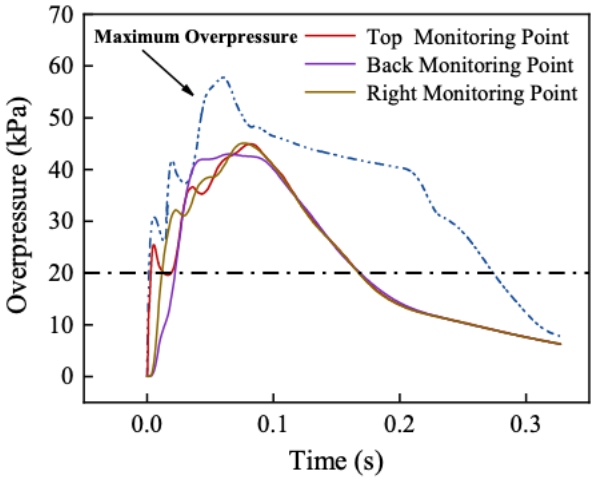

Figure 8 The predicted overpressure at 3 monitoring locations.

HYDROGREN NEV FIRES IN TUNNELS

Comparing compressed gas vehicles with traditional vehicles, the main differences are in the hazards of jet fires and fireball [1]. For compressed gas, generally the fire size is significantly larger than a traditional car or bus fire. The jet flame length can be much longer than that for liquefied fuels. A fireball is also a common phenomenon for a compressed gas tank rupture.

Comparing alternative liquid fuel vehicles with traditional vehicles, the main difference is in the pool fire hazards [1]. Li [1] analysed vehicles with four categories of alternative fuels including liquid fuels, liquefied fuels, compressed gases, and electricity, considering pool fires, jet fires and fireballs by comparing fire hazards of LPG, LNG and liquefied hydrogen (LH2). The results indicated that liquid fuels pose equivalent or even lower fire hazards compared to traditional gasolines. However, the hazards of liquefied fuels were found to be higher. For pressurized tanks, the fires were found to be generally much larger in size but shorter in duration showing highly transiuent characteristics [1]. Jet fires from hydrogen gas fueled vehicles were found to have longer flame lengths.

The 3-D CFD simulations of Li et al. [8] examined the effects of different ignition locations for HFCVs in a tunnel. They found that for ignition at the injection, the jet fire had the highest heat release rate (HRR). The predicted HRR decayed with the injection rate. The predictions also indicated that the region of the combustion cloud was limited to near the injection location and under the ceiling. Hence the activation of TPRD can mitigate the consequence of a tunnel accident for HFCVs.

EV FIRES IN TUNNELS

BEVs and PHEVs are already allowed in tunnels, including the Channel Tunnel without restrictions while some concerns remain due to the recurrent fire and explosion incidents involving these vehicles. When the LIBs are subjected to thermal, electrical and mechanical abuse conditions, the materials within the battery react with each other, generating heat accompanied by abnormal electrical behaviour, leading to the increase of the reaction rate due to temperature rise. As a result, thermal runaway (TR) will be induced and followed by fire or explosion. The TR of one single cell in a battery pack can trigger reactions in the adjacent cells, resulting in TR propagation. The propagation of TR from a single cell accompanied by the reactions chain can activate the TR of an entire LIB system and surroundings, resulting in catastrophic fire and explosion incidents [12].

Comparing electric battery vehicles with traditional vehicles, the main difference is in gas cloud explosion and toxic gas release [13]. Data concerning the HRR of electric vehicles are rather limited. Lecocq et al. [14] carried out four tests to compare the difference between internal combustion engine

cars and electric battery cars. The HRR results are replotted by Li and Ingason [15] for comparison with medium and fast fire curves, as shown in Figure 9. The fire was ignited inside the vehicle. The difference between traditional cars (car 1 and car 2) and the electric vehicles (EV 1 and EV 2) is not significant.

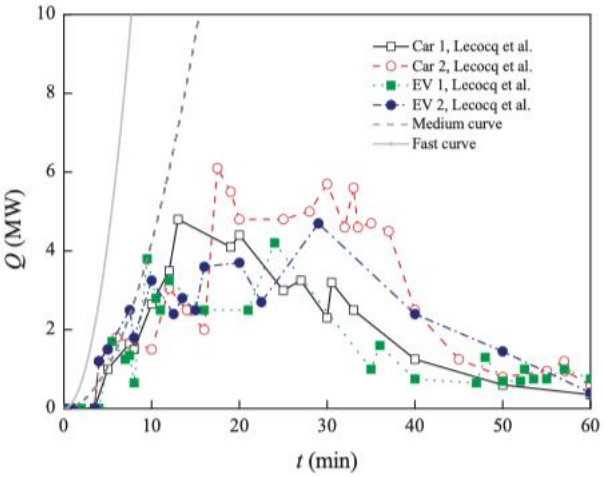

Figure 9 Summary of measured HRR for electric battery cars (Reproduced from [15]).

According to data collected by EV FireSafe [16], there were over 500 battery-related fires in light-duty EVs globally between 2010- mid 2024. With an estimated 40 million EVs operating globally as of early 2024, that's around a 1 in 100,000 rate of fire. Tesla estimated that one of its vehicles caught fire every 209 million km traveled [17]. Data from the U.S. National Transportation Safety Board [18] shows that there are approximately 25 fires for every 100,000 EVs sold. In comparison, there are approximately 1,530 fires for every 100,000 gas-powered vehicles sold. These statistics have led to the shift of concern for battery fires in BEVs and PHEVs to energy storage systems [19]. However, Hynynen et al. [20] recently commented that the available statistics shows that EV fires are not more likely than fires in ICEVs, rather the contrary by a factor of 8 - 10. However, as EVs are still relatively new and few, it might be that the number of EV fires will increase as the fleet becomes larger and as the fleet ages.

It should also be noted that, over 100 organic chemicals are generated during an electric vehicle fire, including some incredibly toxic gases such as hydrogen cyanide –which is fatal to humans. This would poses new chllenges of ventilation requirement in the cases of tunnels and should be duly addressed.

CONCLUDING REMARKS

Recent publications concerning fire and explosion safety issues of new energy vehicles in tunnels have been reviewed. For vehicles powered by conventional gasoline fuels as well as batteries, the dominant issues were fires. Statistics have shown that the fire risk of BEVs and PHEVs are no greater than vehicles powered by conventional fuels. However, the toxic gases emitted during fires of BEVs and PHEVs do pose some new challenges with regads to tunnel ventilation.

The reviewed studies have clearly indicated that when hydrogen is used as the fuel either in HFCVs or combustion engines, the explosion risks are of great concern. With regards to explosions, tunnels add another level of complextity. For a highly reactive fuel like hydrogen, this implies significant risk with serious consequences. While extensive experimental and numerical studies have been conducted for hydrogen FA and DDT in shock tubes at laboratory and industrial scales, few studies are conducted in real tunnels. As such, limited experimental data is available. Some of the reported numerical simulations have illustrated this risk. However, all these were limited to hydrogen cloud being of a limited size and releases of relatively short durations. The effects of air velocity in the tunnel were also insufficiently addressed in previous numerical simulations. Few of the simulations addressed the DDT potential. Furthermore, limited validations have been reported for tunnel configuration. For a more detailed review about hydrogen fire and explosions in general, covering both experiments and numerical simulations, the readers consult a recently published review paper [21].

It is of great importance to develop mitigation measures that can be effectively and practically deployed in tunnels for new energy vehicles, especially thosed powered by hydrogen. But so far, such efforts are limited and should be addressed by both researchers, designers and operators. It should also be noted the challenges to implement some of the conventional mitigation measures, such as venting, to limit explosion overpressure in long tunnels, especially those underneath the sea or large mountains. In the meantime, such mitigation measures should be considered for other enclosed underground spaces like car parks, etc. In such situation, consideration should also be given to the escape route of the vented flames in the content of the local environment.

As commented by Pasman [22], frequency risks can quickly turn up at large scale easily. Unless appropriate mitigation measures are ready to be deployed effectively, the safety issues concerning HFCVs or hydrogen engine powered vehicles entering long tunnels should be carefully assessed. There is an urgent need for relevant Regulations, Codes and Standards (RCS) to be developed and enforced.

REFERENCES

1. Y.Z. Li, Study of fire and explosion hazards of alternative fuel vehicles in tunnels, Fire Safety Journal, Volume 110, 2019, 102871.
2. https://h2tools.org
3. Wen, Jennifer X., Marono, Marta, Moretto, Pietro, Reinecke, Ernst-Arndt, Sathiah, Pratap, Studer, Etienne, Vyazmina, Elena and Melideo, Daniele; *Statistics, lessons learned and recommendations from analysis of HIAD 2.0 database.* Int J Hyd Energy 2022; 47 (38):17082-17096.
4. Melideo D, Moretto P, Wen JX. HIAD 2.0 - Hydrogen Incident and Accident Database, Proc. 8th Int Conf Hyd Safety, Yokohama, Adelaide, Australia, Sep.2019.
5. Y.Z. Li, Study of Fire and Explosion Hazards of Alternative Fuel Vehicles in Tunnels, RISE Research Institutes of Sweden, Borås, 2018 RISE Report 2018:20.
6. S. Kudriakov, E. Studer, G. Bernard-Michel, D. Bouix, L. Domergue, D. Forero, H. Gueguen, C. Ledier, P. Manicardi, M. Martin, F. Sauzedde, Full-scale tunnel experiments: Blast wave and fireball evolution following hydrogen tank rupture, International Journal of Hydrogen Energy, Volume 47, Issue 43, 2022, Pages 18911-18933.
7. Molkov V, Dery W. The blast wave decay correlation for hydrogen tank. Int J Hydrogen Energy 2020:31289-302.
8. Yabing Li, Jianjun Xiao, Han Zhang, Wolfgang Breitung, Jack Travis, Mike Kuznetsov, Thomas Jordan, Numerical analysis of hydrogen release, dispersion and combustion in a tunnel with fuel cell vehicles using all-speed CFD code GASFLOW-MPI, International Journal of Hydrogen Energy, Volume 46, Issue 23, 2021, Pages 12474-12486.
9. S.B. Dorofeev, M.S. Kuznetsov, V.I. Alekseev, A.A. Efimenko, W. Breitung, Evaluation of limits for effective flame acceleration in hydrogen mixtures, Journal of Loss Prevention in the Process Industries, Volume 14, Issue 6, 2001, Pages 583-589.
10. Y.A. Skob, M.L. Ugryumov, E.A. Granovskiy, Numerical assessment of hydrogen explosion consequences in a mine tunnel, International Journal of Hydrogen Energy, Volume 46, Issue 23, 2021, Pages 12361-12371.
11. Teng Huang, Fuyuan Yang, Xuefang Li, Tianze Wang, Minggao Ouyang, Modeling of hydrogen dispersion and explosion of a fuel cell vehicle in an underground parking garage, International Journal of Hydrogen Energy, Volume 51, Part D, 2024, Pages 1120-1129.
12. Gongquan Wang, Ping Ping, Depeng Kong, Rongqi Peng, Xu He, Yue Zhang, Xinyi Dai, Jennifer Wen, Advances and challenges in thermal runaway modeling of lithium-ion batteries, The Innovation, Volume 5, Issue 4, 2024, 100624.
13. LaChance, J, Tchouvelev, A and Engebo, A (2011). Development of uniform harm criteria for use in quantitative risk analysis of the hydrogen infrastructure. International Journal of Hydrogen Energy. Vol. 36 pp. 2381-2388.
14. A. Lecocq, M. Bertana, B. Truchot, G. Marlair, Comparison of the fire consequences of an electric vehicle and an internal combustion engine vehicle, 2nd International Conference on Fires in Vehicles - FIVE 2012, SP Technical Research Institute of Sweden, Chicago, 2012, pp. 183–194.

15. Y.Z. Li, H. Ingason, Overview of research on fire safety in underground road and railway tunnels, Tunnelling and Underground Space Technology, Volume 81, 2018, Pages 568-589.
16. https://theicct.org/clearing-the-air-evs-could-bring-lower-fire-risk-oct24
17. https://www.tesla.com/VehicleSafetyReport
18. https://www.ntsb.gov/Pages/home.aspx
19. Jens Conzen, Sunil Lakshmipathy, Anil Kapahi, Stefan Kraft, Matthew DiDomizio, Lithium ion battery energy storage systems (BESS) hazards, Journal of Loss Prevention in the Process Industries, Volume 81, 2023, 104932.
20. Hynynen, J., Quant, M., Pramanik, R., Olofsson, A., Li, Y. Z., Arvidson, M., & Andersson, P. (2023). Electric Vehicle Fire Safety in Enclosed Spaces. RISE Rapport 2023:42.
21. Jennifer X. Wen, Ethan S. Hecht, Remy Mevel, Recent advances in combustion science related to hydrogen safety, Progress in Energy and Combustion Science, Volume 107, 2025, 101202.
22. Hans Pasman, Edison Sripaul, Faisal Khan, Bruno Fabiano, Energy transition technology comes with new process safety challenges and risks, Process Safety and Environmental Protection, Volume 177, 2023, Pages 765-794.

Evacuation and human behaviours in tunnel fires

Håkan Frantzich[1]
[1]Lund University, Lund, Sweden

ABSTRACT

Tunnel evacuation is a challenge that requires a well-prepared strategy and relevant technical and organizational measures to be successful. The article focuses on the relation between knowledge about human behaviour during an evacuation process and how this knowledge is obtained through investigations after fires and through well-planned experiments. Furthermore, theories are introduced that explain and describe human behaviour in different situations, such as Canter's behavioural sequences, Sime's affiliation theory and the understanding of social influences within a group of individuals. A timeline model is presented that connects the behavioural description of how people in general act during fires with an engineering model that can be used for design. In addition, results from some experiments are presented where the effectiveness of different technical installations during an evacuation process has been investigated.

KEYWORDS: human behaviour, tunnel, fire, wayfinding, evacuation, affordance theory, affiliation theory, behaviour sequence, evacuation experiment

INTRODUCTION

In order to connect parts of a country efficiently and thus avoid long detours, it may be necessary to use road or rail tunnels. However, building tunnels for road and rail traffic can also pose major challenges, especially in the event of a fire. Evacuating a tunnel can be associated with great difficulties and this can apply even to relatively small fires. The conditions for evacuating tunnels, therefore, vary greatly depending on, among other things, geographical conditions, the fire development, the number of people involved and the technical installations of the tunnel. Many road tunnels, especially in urban environments, have a large traffic flow and are therefore often designed as double-tube tunnels with one-way traffic each and they are equipped with a number of technical installations and escape routes that make it easier in the event of a fire. This can be compared to single-tube tunnels with dual traffic direction in more rural areas where it may not be economically justifiable to provide the tunnel with escape routes to the same extent as an urban tunnel. The same may apply to many railway tunnels which often have fewer escape routes, but the reason may instead be that fire accidents are very uncommon in railway tunnels.

Experience shows that serious accidents can occur with fires in tunnels, even though most of them are relatively minor. Among the more serious ones we include the fire in the Mont Blanc tunnel in 1999, where 39 people died (Duffé och Marec, 1999). What is particularly serious about this fire from an evacuation perspective is that some of the motorists who died were found sitting in their cars. They had not even had time to start an evacuation. There were also people who had sought shelter in rescue chambers, but these were not safe enough and people died.

In Norway, there have been a number of fires in road tunnels and, fortunately, these have not resulted in fatalities. However, they still show the difficulty of evacuating tunnels where a fire has occurred. A couple of major accidents that have resulted in more extensive accident investigations have recently occurred in, among others, the Oslofjord Tunnel in 2011 (AIBN, 2013), and the Gudvanga Tunnel in 2013 (AIBN, 2015). In both cases, the fire occurred in a truck with extensive smoke spread and great

difficulty in evacuating the tunnels. Fortunately, the fires caused no deaths, but a large number of people suffered severe smoke injuries. Those who escaped through the smoke testified that the evacuation took place with great difficulty and in several cases it was done on foot in the tunnel and for several kilometres.

In the Oslofjord Tunnel, eight people were also forced to take refuge in a space between the tunnel wall and the rock face until they were helped by the rescue services to evacuate (AIBN, 2013). This space was not intended for evacuation, i.e. it was not a safe place, but the people fled there because conditions were better than in the smoke-filled tunnel.

In 2015, there was another fire in the Gudvanga Tunnel, but the consequences were milder. In that case, the fire was in a bus that stopped a couple of hundred meters into the tunnel. The rescue personnel had experience from the 2013 fire and were able to control the direction of the smoke in the tunnel, which reduced the number of people exposed and contributed to a smaller consequence (AIBN, 2016).

Typically, several Norwegian tunnels run under fjords, which means that the tunnel's slope can be considerable. This can be aggravating circumstances both because smoke spreads quickly along the sloped tunnel, but also because evacuation is made more difficult because evacuation may have to be done on a steep slope. A typical tunnel can be several kilometres long, with a steep slope down to the bottom of the tunnel and then a long, steep climb to ground level on the other side (Frantzich, Nilsson and Rød, 2016).

The design of a tunnel means that an evacuation will be problematic for those involved. When the tunnel has traffic in both directions in the same tunnel tube, it also means that in the event of a fire there will be motorists heading towards the fire from both directions. In this case, the smoke will spread in the tunnel in one or both directions and some motorists will inevitably encounter the smoke unless they turn around in time or are prevented from entering the tunnel. The direction of the smoke is controlled either by the prevailing wind direction or by mechanical fans. Motorists who are on their way out of the tunnel and have the fire behind them can usually drive out of the tunnel without any difficulties. These motorists do not pose any significant problems in the situation other than that they may be involved in secondary accidents if motorists heading into the tunnel, who have been informed of the fire ahead, turn their vehicles to drive out of the tunnel and cause further accidents (AIBN, 2018).

From these aspects, tunnel systems with double tunnel tubes where traffic only occurs in one direction in each tunnel tube are more favourable. Then there is also the possibility of using the second tunnel tube as a safe place and evacuation can take place from one tunnel tube to the other tube. Double tunnel tubes are usually only found in places where traffic flow is high, that is, in densely populated areas. But even in these cases, scenarios can arise that lead to motorists being exposed to smoke. One such case is accidents that occur during traffic jams and where it is not always possible to drive out of the tunnel due to vehicles in front. Evacuation on foot is therefore also necessary in these cases.

The evacuation conditions for railway tunnels are in general similar to those in a road tunnel, even though there are differences. The evacuation process can be more difficult by the fact that the tunnel's cross-section often is smaller, which means that even small fires can be problematic. The possibilities of moving around in a railway tunnel can also be somewhat more difficult as the ground surface is often uneven. However, several railway tunnels are equipped with walkways, which makes evacuation easier.

To facilitate an evacuation, a number of measures can be taken, which may be technical, organizational or related to the people staying in the tunnel.

Typical installations for handling a fire situation on the road may be:

- stations with emergency telephone and hand-held fire extinguisher
- radio intrusion into the radio network
- turning points for vehicles
- fire smoke ventilation along the tunnel tube
- mobile phone coverage
- stop signals and barriers outside the tunnel
- general lighting
- escape lighting
- fixed fire extinguishing systems
- fire and evacuation alarms
- escape routes to a safe place

Organizational measures or those that can be linked to the individual road user include the following:

- an active traffic control centre
- updated operation and maintenance plans for the tunnel
- prepared accident management plans
- a rescue service in the community with knowledge of the tunnel's conditions and facilities
- the ability to communicate with road users or train passengers
- road users' knowledge of what to do in the event of tunnel accidents
- personal ability to evacuate a tunnel

Which installations or measures are present in a specific tunnel depends on a number of factors such as the type of traffic, the traffic flow and the length of the tunnel, its design and geographical location. Often, there is a focus on technical installations as a solution to the assumed problems. But the aspect that is probably most important is that the measures taken can function in a context where technical systems must interact with the people in the tunnel who are forced to deal with an accident that has occurred. In order to be able to show that such interaction can take place, a tunnel's system for a fire-safe environment must be analysed and that this analysis is based on relevant and documented data and that knowledge of human behaviour is included. The person carrying out the analysis must therefore have knowledge of how people potentially can act in a fire situation and know how this behaviour is affected by how the development of the fire affects the environment in all the places where people are.

THEORY ON HUMAN BEHAVIOUR

People who are exposed to a fire must deal with the new situation that arises. Evacuation is a process that is unknown to most people and must be carried out under great uncertainty, which is especially evident early in the process. This means that a new situation must be assessed and new decisions must be made in relation to the new signals that arise, but also in an already existing context. People's behaviour in the event of a fire are influenced by what the person does before the fire starts. Actions are also not random, but they often follow a specific pattern or sequence. There are therefore a number of theories that describe why people act as they do in a fire.

The theory of behavioural sequences (Canter, Breaux and Sime, 1980) is based on the fact that evacuating people go through three stages in their decision-making and is often referred to as one of the fundamental theories in evacuation research. These stages, which can be repeated several times during an evacuation process, are:

- interpret the situation
- prepare
- act

During the evacuation phase, the person makes a number of decisions that all pass through these three stages, Figure 1. The illustration is a general description of different activities that people go through during an evacuation. The basis for the structure are investigations done in various occupancies mainly domestic premises. However, it is still likely, according to the authors, that the structure can be seen as

a general description that can be used for a range of evacuation situations. The links in the figure are the strongest relations found by the authors and they are not definitive. The decisions and activities that the person takes are determined, among other things, by where in the process the person is and the role that the person has. This means that different behavioural patterns arise between different activities and places. The actions included also depends on in what stage they occur. The Investigate action in the Interpret stage covers activities related to finding out what has happened. The Explore action in the Prepare stage could be seen as the same but the intentions are different. During the Prepare stage activities are related to finding different behavioural options once having interpreted the situation as related to fire. The general model presented by Canter et al. (1980) is later developed into the timeline model for describing human behaviour in fires and also for analysing a potential future evacuation during the design stage of for example a tunnel.

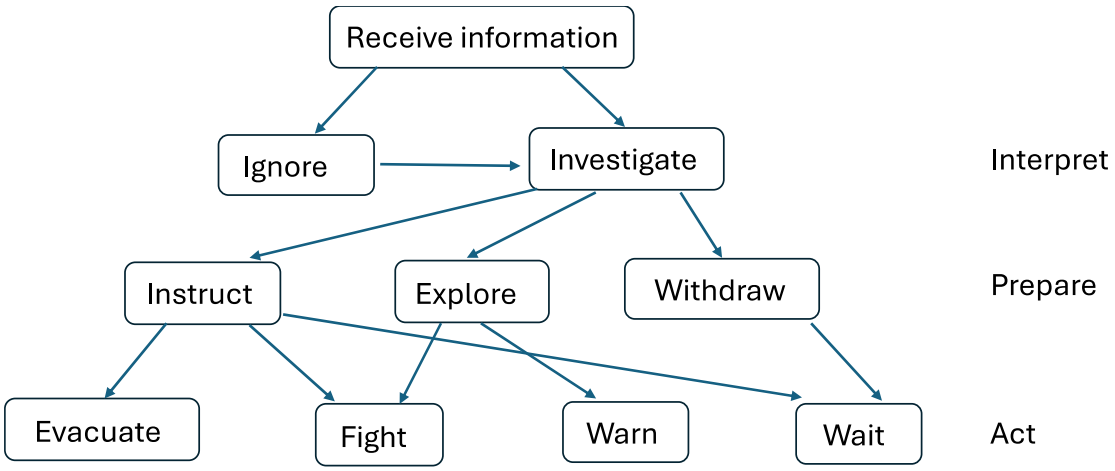

Figure 1. Behaviour sequence by Canter, Breaux and Sime (1980).

Studies show that the early stage of evacuation is often characterized by uncertainty, misunderstanding and inefficiency. Among the first actions that occur is that people try to inform themselves about what has happened. They then try to gradually translate this into practical actions such as fight the fire, help or warn others, save material things, call the emergency services and evacuate. Overall, it can be stated that people who evacuate are still relatively sensible and their behaviour is rational in its context. It can already be mentioned here that the occurrence of panic or other assumed irrational behaviour very rarely occurs in connection with fire and evacuation, despite the fact that the concept often appears as explanations for people's behaviour in the event of a fire (Sime, 1980 and Fahy et al., 2009).

What emerged from the fires that Canter et al. (1980) investigated was that people in similar situations exhibited similar behaviour, which is the basis for the behavioural sequences. The stages in the sequence are developed based on investigations of domestic, multiple occupancy and hospital fires. Still, the principles apply also to tunnel fires as the descriptions of actions are general but the specific actions may differ in likelihood from one occupancy to another, e.g. between residential buildings and tunnels.

It was also found by Canter et al. (1980) that the role different people have affects the expected behaviour, which was also later demonstrated, for example, in Sime and Kimura (1988). The trend is particularly evident in cases where there are hierarchies linked to some form of authority, for example, an authority person in relation to visitors or for staff in relation to customers (Canter, 1990). The connection between people's roles and their behaviour is explained by a theory called the role-rule model (Tong and Canter, 1985). According to the model, people's behaviour is governed by the rules that are linked to their role in the current situation.

Sime's affiliation theory (Sime, 1984) can be used to explain certain behaviours and is based on the fact that people prefer the familiar to the less familiar. This explains why people tend to evacuate in

groups, even with people they have not previously known, as it provides a sense of security. This can be seen in connection with tunnel accidents, when people who leave their cars evacuate in groups with people they have not previously known. Sime's theory also explains why people prefer to choose evacuation routes that are well-known, such as the tunnel entrance, instead of an emergency exit, even though the emergency exit may be closer.

Latané and Darley (1970) have investigated social interactions between people in various situations, resulting in the theory of social influence. People generally want to act in a way that is perceived as socially correct. Having multiple and clear cues that strengthen a person's perception of what is appropriate and correct behaviour makes it easier to take the first initiative. It can explain why there is a delay when people who do not know each other have to act together. Social influence can also be positive, so that if, for example, one person has made a decision to start evacuating, it is easier for others to follow with the same behaviour. It is therefore important that someone takes the first initiative, which should be a guide when technical systems are designed.

To investigate the function and benefit of technical systems and designs, the so-called "affordance" theory (Gibson, 1978 and Hartson, 2003) may be suitable. The affordance theory does not describe people's actions during an evacuation, but is a methodology for investigating how well, for example, technical installations can function and be interpreted by people exposed to the installation. The intention of an installation is that people should understand its message and act as expected. In an evacuation context, the theory can be useful in connection with the development and introduction of new installations and has been used by, among others, Ronchi, Nilsson, Modig and Lindgren Walter (2015) to suggest a design for variable message signs for road tunnels.

The different theories can be used to explain observed behaviours, but also serve as a basis for describing what is likely to happen in a future fire situation. This knowledge can therefore be used if new technologies are to be introduced in road tunnels to facilitate an evacuation. To connect theories of human behaviour with a practical design situation, the so-called timeline model can be useful.

To carry out such an analysis, a model is needed that describes how people act in the event of a fire and that can also be used to perform engineering analyses. The model should therefore be able to be used to analyse tunnel fires in a way that is consistent with how people are expected to act and can be used as a design tool or a way of thinking as a designer. A number of variants of a timeline model have been presented over the years (Proulx, 2008). A model is presented below, Figure 2, which forms the basis for the analysis that can be carried out to describe the fire safety of the tunnel.

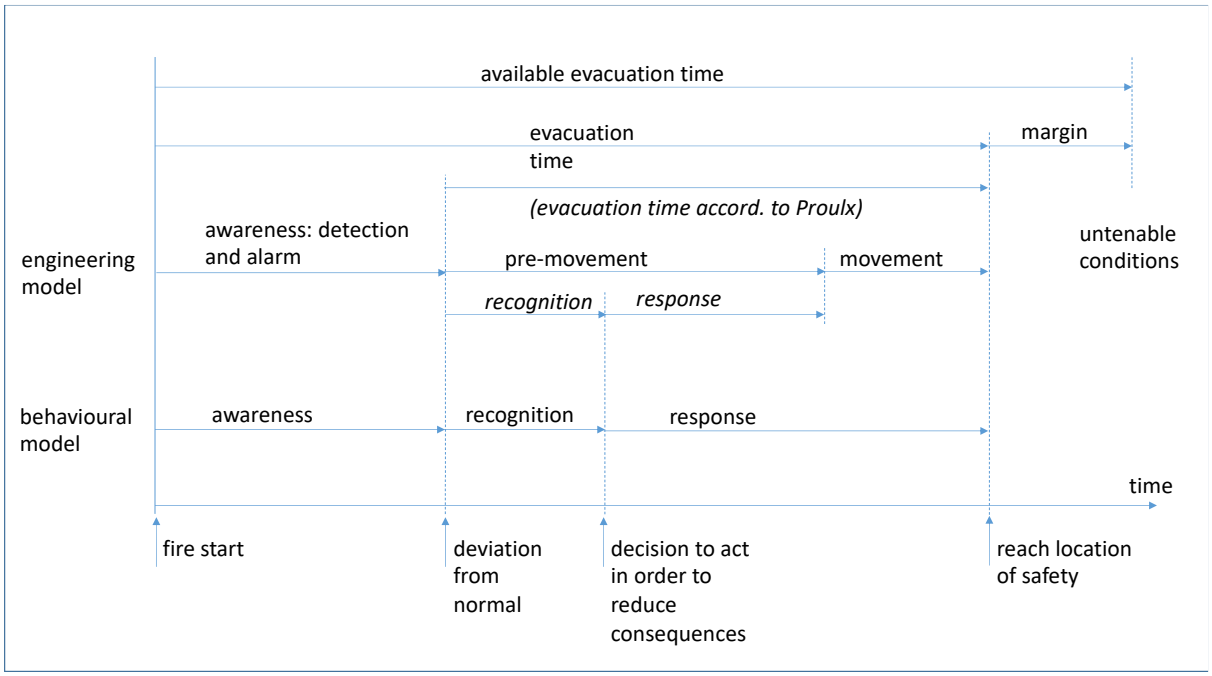

Figure 2. Evacuation time-line.

The timeline in the figure is structured so that it reflects the evacuation seen from a behavioural perspective (behavioural model) by explaining and describing how people act in the new situation but also as an engineering model of evacuation. The behavioural model is used as the basis for an engineering analysis of expected behaviour during emergencies and mainly to link behavioural research with engineering practice. In this way, the connection that must exist between an analysis and the expected behaviour during an evacuation is illustrated.

The behavioural model is based on the theory presented by Canter et al. (1980) but with some minor adjustments and can include the use of other models and theories such as Simes' attachment theory, the role-rule model and the effects of social influence.

The model is well known in the field of fire safety engineering and has been used in several cases to describe what happens during an evacuation linked to analyses of fires that have occurred, both in tunnels and in buildings, for example Fridolf (2010), Shields & Proulx (1999), Kobes, Oberijé, Post&Weges (2010), Kobes, Helsloot, de Vries & Post (2010), Zhao et al. (2009), Shields (2012) and Kuligowski (2013).

The timeline can be applied to individuals or to a group of individuals who are at approximately the same location in the tunnel. Each person will go through all phases of the behavioural sequence, interpretation and preparation (recognition) and action (response). How the process looks depends on the conditions for each individual, very much depending on where the person is in relation to the fire in the tunnel.

For an analysis of an evacuation process, it is essential to be able to define important events that distinguish the different phases. This is usually an aspect that is not well addressed when similar timelines are described.

Awareness

The timeline starts when the fire is initiated but people in the tunnel is still now aware of the eminent danger. The duration of the first phase depends on the location in the tunnel, people on different locations will receive the fire information at different time. Their behaviour is, therefore, still in a normal mode. The awareness phase continues until the people themselves notice that a deviation from

normal has occurred. In some cases, this event can also be initiated by a technical system, for example, the tunnel operator activating a fire warning system. This may be relevant for motorists who are far from the fire or outside the tunnel. A motorist who is closer to the fire can notice the deviation by the cars in front slowing down. For passengers on a train, the phase can end when a train suddenly stops in a tunnel. At that stage, it can be considered that the first phase has been completed and the person enters the next stage, i.e. recognition.

For the fire safety engineer this phase is important to determine and how it varies for different locations as it will influence when people are notified about the deviation from normal. Detection and alarm systems may effect when this notification time is reached.

Recognition
The second phase begins when the person has come to the realization that something is not as it should be, which means that the situation that has arisen should be interpreted so that the person understands what is happening. In most cases, the situation is something that has natural causes and then the process can return to a normal situation, but if a fire has occurred, the person will understand after a while that something is wrong.

In this phase, the person needs to get more information about what has happened in order to form an opinion about what needs to be done. The scope of the time period for interpretation can be long and it can also happen that a motorist stops the car and gets out to see what is happening, i.e. to seek more information. In the recognition phase, there is still not enough information to convince the person that a fire has occurred, but there is a gradual increase in information about the situation.

In the recognition phase, the motorist can decide to take certain actions, such as leaving their car, talking to other people or using the mobile phone. This means that this part of the evacuation process can also contain activities, i.e. people do things, which is otherwise connected to the next phase which is more associated with action to reduce the consequence, an evacuation action.

The link to the engineering part is to recognise the importance of information and support for decision making. The importance is to facilitate understanding the situation as initial cues are usually ambiguous. The presence of smoke will naturally make it easier to understand that a fire has occurred but remote from the fire, signals indicating an unnormal situation is most likely more diffuse. Information through radio channels or via signals in the tunnel may improve decision making.

The interpretation phase continues until the person is convinced that a fire has occurred and decides to act in a way that aims to reduce the consequence.

Response
When the person has realized that there has been a fire and has decided to take measures to reduce the consequences for themselves or another person, the response phase has begun. Examples of actions, which are called evacuation actions, include warning and helping other people, retrieving fire extinguishers and trying to fight the fire, gathering their luggage, trying to turn the car around and drive out, and evacuating on foot. For passengers on a train, this phase usually begins after a message from the train staff unless a spontaneous evacuation has already been initiated. A spontaneous evacuation from a train can be dangerous due to electrical wiring that may have been damaged in the accident.

In the engineering model, the response phase is often divided into a) preparatory action and b) movement. The main reason for this is that there is often a distinction between calculating the movement time and the time that has elapsed since the recognition phase began. For engineering purposes, installations that have an effect on the preparatory actions can be informative information signs telling people what to do. The purpose with these installations is to reduce time spent on activities that is not the most efficient and not desired according to the safety strategy.

The movement part of the response phase can, for the engineering side, be facilitated by having designated movement paths with handrails, escape lighting, short distances to the exits and so on. It is also possible to improve the hazardous exposure by for example limit the smoke concentration and reduce the fire hazard. The time spent on moving to a safer location is the driving force for finding improvements.

Evacuation process analysis

Now there is a model that can be used for analysis, the timeline model, and there is knowledge of some theories that can be applied to describe and explain human behaviour in the event of fires. The next step is to investigate the usefulness of the measures that are proposed for handling accidents, for example the usefulness of different forms of technical installations. The timeline model helps to describe when in the process an installation can be useful and how it will improve the evacuation efficiency.

The basis for an analysis is that there is access to reliable information that describes the current event and the system to be analysed. This often means that some form of test or experiment must be carried out. Nilsson (2009) presents a structure for how evacuation technology tests should be carried out, which is based on three levels: identify the problem, solve the problem and test the system, Figure 3.

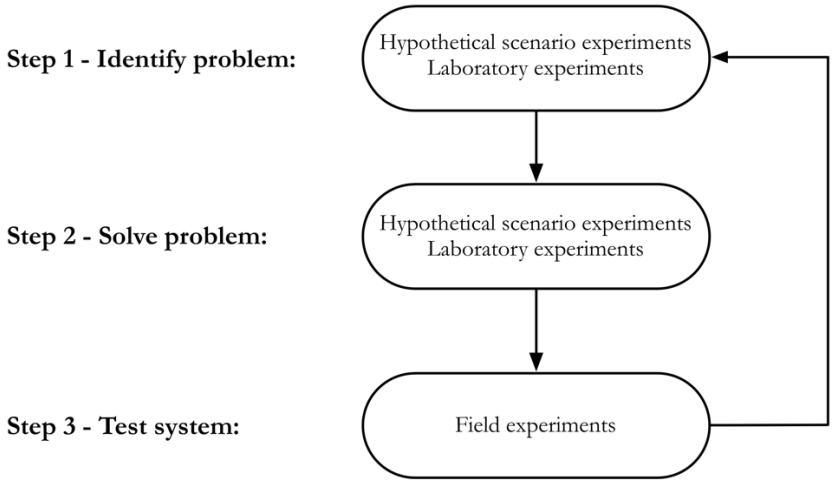

Figure 3. Method for investigating the usefulness of technical systems according to Nilsson (2009).

Ideally, a technical system or other measure should be tested at the different levels to identify what can work in a practical application. The final step is thus aimed at verifying that a particular installation actually works when it comes to a real tunnel environment. In many cases, however, there are no possibilities to utilize all three steps. But regardless of this, the purpose of the experiments carried out is to get people who are evacuating to make decisions that favour their evacuation to a safe place and therefore shorten the time they are exposed to the consequences of the fire.

The main problems identified in several fires that have occurred are that people:

(1) lack information about what has happened and what is expected of them.
(2) have difficulty interpreting the situation because the information may be unclear and not necessarily associated with fire.
(3) must quickly get to safety, either by moving directly to the open air or by moving to another safe place.

All of these types of problems mean that it takes time before an evacuation can begin and people have time to get to safety. Below are some examples of attempts that have been made to support one of the phases of the evacuation process.

HUMAN BEHAVIOUR DECISION MAKING DURING EVACUATION

This section presents results from some experiments conducted at Lund University over the years, where there are examples of systems that in practical application are found not to work at all, while others work beyond expectations.

The systems presented have their main benefit during the response phase, that is, when a person has made a decision to evacuate to a safe place to reduce the consequences for the person. Both presentations are examples of decisions made to select an escape route.

Using coloured lights at exits and directional lights

The first experiment (Frantzich&Nilsson, 2004) is a form of laboratory experiment that was carried out in a smoke-filled container tunnel. Subjects (a total of 45 subjects participated) walked one by one through the tunnel, which was about 35 m long and about 5 m wide with parked cars randomly placed, Figure 4.

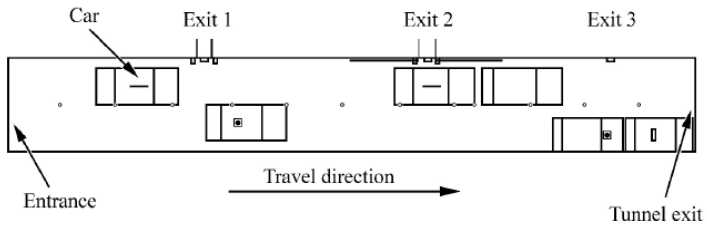

Figure 4. Illustration of the experimental tunnel.

Each subject was tasked with finding an escape route through the tunnel and getting out. The tunnel was filled with dark smoke that was very dense, with an average visibility of less than 1 m. In the tunnel there were two doors equipped with different technical systems (Exit 1 and 2) to be tested and an illustration of a door (Exit 3). In addition to the tested systems, there was a backlit escape sign above each door. The distance from the entrance to the farthest door was about 30 m, i.e. the distance the subject had to walk to find the door.

Three types of technical systems were tested one at a time; flashing orange lights, flashing green lights (at Exit 1 and 2) and a horizontal row of flashing lights on each side of the door (at Exit 2), Figure 5. The flashing lights were tested with one colour at a time (orange or green) and were placed at the top of the door, one light on each side. They flashed at about 1 Hz. The horizontal flashing points of light gave the illusion of light moving towards the door.

The motive for the various installations was that the flashing lights at the top of the door would be visible and attractive to people moving along the wall that did not have a door. Orange light is better visible through smoke compared to green light, which was also tested. The colours were chosen after initial laboratory tests in a neutral environment. The idea with the row of light points that appeared to move towards the door was that a person who saw them would follow the movement of the light and thus find the door.

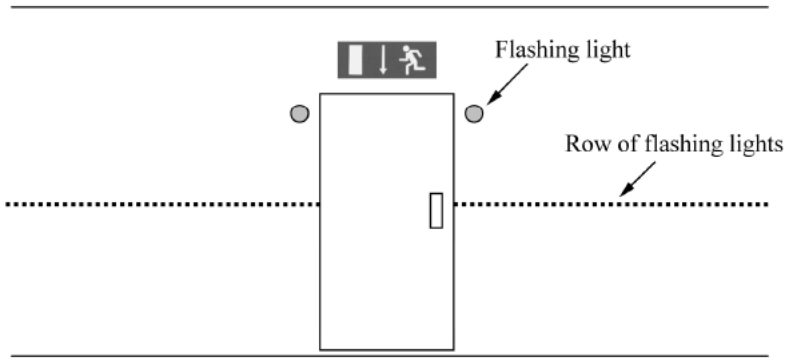

Figure 5. Evacuation door design (Exit 2) with added installations.

In general, the results were somewhat disappointing and the installations were not as effective as they had been assumed to be before the experiments were carried out. All the light installations were difficult to see due to the dense smoke. One reason why the installations were not perceived as useful was that the subjects had no previous knowledge of new types of escape installations. The orange lighting was also associated with fire and danger, which meant that the subjects instead moved away from the door when they saw a diffuse flashing orange light through the smoke, contrary to what was the desired purpose.

The movement that the horizontal rows of light points created was very clear when there was no smoke in the tunnel. However, when the tunnel was filled with smoke, the subjects could not perceive the movement pattern that the light points collectively illustrated; for them, it was only a few light points flashing as they only saw a small number of light points due to the smoke.

In summary, the experiments show that in a somewhat more realistic environment it may turn out that effects arise that could not be observed in initial tests. The parts that deal with decision-making to choose an escape route did not give any positive results but rather showed how a guiding system should not be implemented. There is therefore still value in testing installations on larger scales to really identify what works and what does not work.

Local fire alarm and simple information signs

The second experiment was performed in 2014 and was by far more successful (Fridolf, Ronchi, Frantzich, Nilsson, Lindgren Walter & Modig, 2016 and Fridolf & Frantzich, 2016). The experiment was carried out in a road tunnel in Stockholm and aimed to test various installations, including the design of the area around the door to an escape route from the tunnel. The tunnel is part of the so-called Northern Link in Stockholm, which is one of several major transport routes around the city. The tunnel system consists of double tunnel tubes, each with one-way traffic. Each tunnel tube has two lanes and a narrower space outside the right lane.

The experiments were part of a larger project *Project Bypass Stockholm, a study on safety in tunnels, co-financed by the EU Trans-European Transport Network (TEN-T)*. Figure 6 shows schematically the experimental area in the tunnel with the starting point for each subject on the right in the figure and a mock-up escape door marked EXIT on the left. The normal driving direction in this tunnel is from right to left in the figure. The experimental area was approximately 120 m long and 8.3 m wide. The mock-up door to be examined was equipped with several installations that were examined separately, Figure 7.

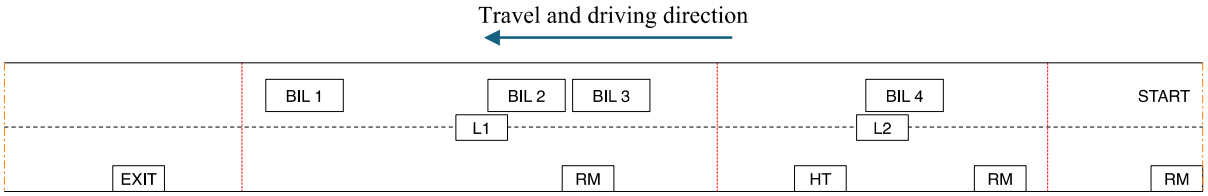

Figure 6. *Schematic diagram of the experimental area. BIL indicates the location of a car, RM are smoke generators, L1 and L2 indicate the location of smoke density meters and HT is a loudspeaker to create a background noise illustrating present jet fans.*

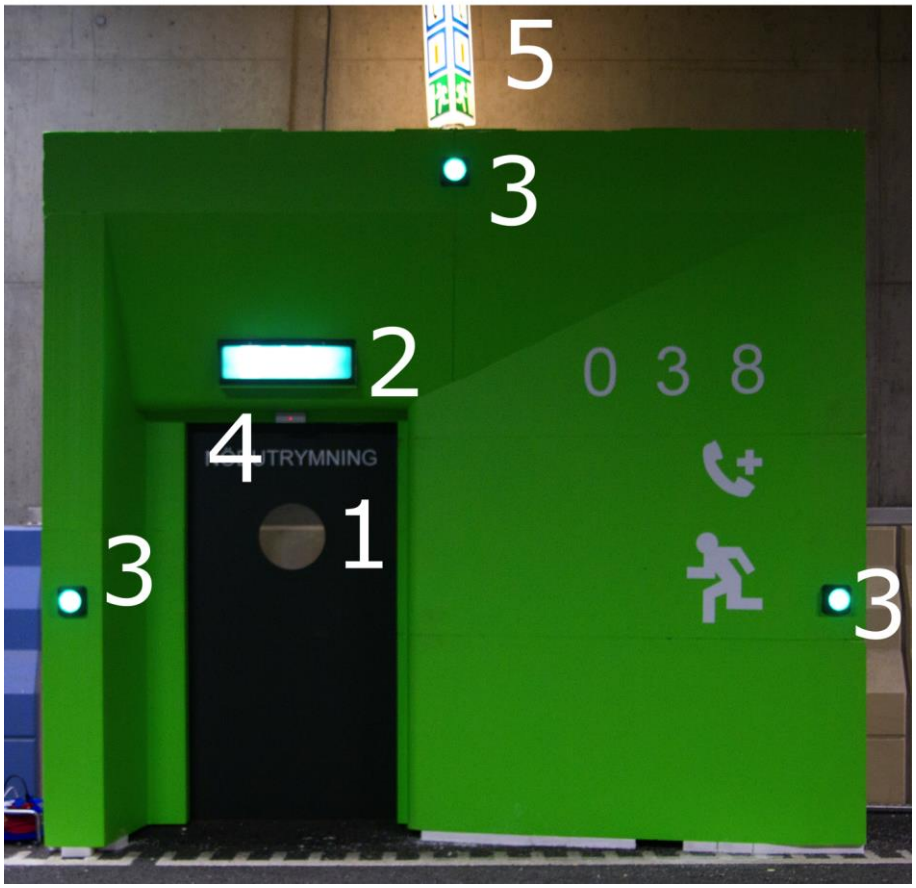

Figure 7. *Image of the mock-up escape door tested in the experiments. 1 = window in the door, 2 = escape sign above the door, 3 = three green LEDs flashing at approximately 1 Hz, 4 = local escape alarm and 5 = information sign about emergency equipment.*

A total of 66 people participated in the experiments and 64 of them completed the entire experiment they were exposed to. They participated individually with one person at a time. In all experiments, the tunnel was filled with dense white smoke, which limited visibility to less than 2 m on average. There was a total of five different scenarios in which the installations were combined in different ways. In two of the scenarios, the benefit of a local evacuation alarm was investigated, which was placed at the evacuation door, marked with "4" in the figure to inform that the door was an escape route. Installations 1, 2, 3 and 5 were active in all scenarios. The scenarios were combined with other installations in the tunnel that were not applied to the evacuation door.

For people who are close to the door, it is obvious that the door can be used for evacuation. This is relevant for a person who moves along the left side of the tunnel and who finally reaches the door. However, for people on the other side of the carriageways, while there is smoke in the tunnel, it is not

as easy to identify the door. The intention of the local evacuation alarm was to investigate whether people moving along the right side of the tunnel seen in the direction of travel (the upper part of Figure 6) could find the escape route even if they did not see the door due to the dense smoke.

In the scenarios where the local evacuation alarm was activated, it could be clearly heard from the opposite side of the tunnel. The alarm alternated with a spoken message and a varying tone signal. The spoken message was *"The sound comes from an exit. Follow the sound to get out"*. A total of 28 people were exposed to the local evacuation alarm. Of these, 27 people chose to use the escape door. Almost all of these, 25 people, stated that the sound was one of the reasons why they crossed from the right to the left side and chose the escape door. In the subsequent interviews, the suggestion that tunnels should be equipped with such an alarm was the most common suggestion for improving evacuation measures in tunnels. The people also stated that they had very great benefit from the installation during the evacuation.

One of the other installations that was investigated was to mount a simple sign on the wall on the right side of the tunnel opposite the place where the escape door was located. The sign was visible to those people who chose to move along the right side when they came close to the sign. The sign was present in all scenarios and had an appearance and message as shown in Figure 8. The sign was about 40 cm wide and 30 cm high and was only illuminated by the general lighting.

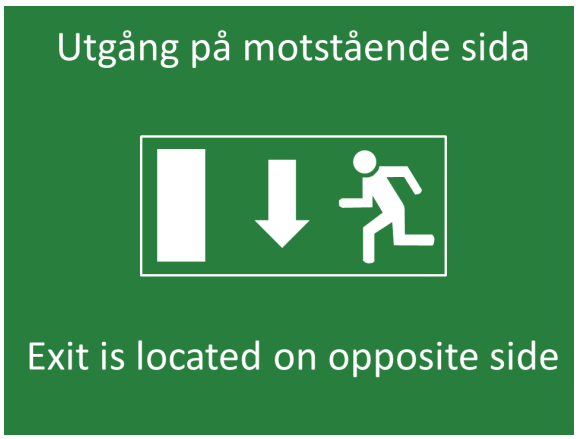

Figure 8. Sign located opposite the emergency door.

Since visibility during the experiments was very poor, the sign could only be detected when the person was close to it. In practice, all people walked very close to the tunnel wall and could then see objects on the wall as they passed. Of all the people who participated in the experiments, 34 people stated that they saw the sign. Of these, 23 stated that they chose the escape door on the other side of the tunnel because they had seen the sign. They may have chosen to walk towards the door for other reasons, such as hearing the local evacuation alarm in the scenarios where this was present. However, the fact that so many people still stated that the sign contributed to the decision to change sides in the tunnel indicates that it has a benefit. From a practical perspective, the results show that it is possible to influence people in an evacuation situation even with simple and inexpensive means, which may justify the installation of such a sign.

CONCLUSION

In general, people being exposed to an evacuation in a tunnel behave in a rational manner given the prevailing uncertainty. Typical actions related to human behaviour is to seek more information, contact other people in the tunnel, trying to extinguish the fire and try to get away from the danger, i.e. to evacuate. In road tunnels, motorists have also been seen to turn their vehicles and drive out of the tunnel. The main issue for people being trapped in a smoke filled tunnel is that evacuation takes time and measures must be taken to reduce the time taken for evacuation.

The prerequisites for an analysis of a tunnel system to facilitate an evacuation should be based on knowledge of how people are expected to act during an evacuation. The analysis should be based on relevant theories of how people act in the event of a fire.

The evacuation analysis should be based on the presented timeline model for an evacuation process that combines an engineering-based method with a description of how people behave during an evacuation process. Understanding the behavioural model and the engineering model is, therefore, important.

In addition two cases of evacuation research projects performed demonstrate how valid data can be achieved with a proper experimental design, even if the findings do not result in favour of the tested installations. Testing installations which indicate a poor performance for an efficient evacuation is also of importance.

But, the message is that experiments are of importance in demonstrating safety when installing novel technology so we do not need to rely only on judgements of assumed effects of the new installation being introduced.

REFERENCES

AIBN (2013). Rapport om brann i vogntog på RV23, Olsofjordtunnelen, 23 juni 2011, Rapport Vei 2013/05. Accindent Investigation Board Norway, Lillestrøm. (In Norwegian)

AIBN, (2015). Report on fire in a heavy goods vehicle in the Gudvanga tunnel on the E16 road in Aurland on 5 August 2013. Report Road 2015/02. Accindent Investigation Board Norway, Lillestrøm.

AIBN, (2016). Report on coach fire in the Gudvanga tunnel on the E16 road in Aurland on 11 August 2015. Report Road 2016/03. Accindent Investigation Board Norway, Lillestrøm.

AIBN, (2018). Report on fire in heavy goods vehicle in the Oslofjord tunnel on national road 23 on 5 May 2017. Report Road 2018/04. Accindent Investigation Board Norway, Lillestrøm.

Canter, D., Breaux, J., Sime, J. (1980). Domestic, Multiple Occupancy, and Hospital Fires. In Fires and Human Behaviour 1st ed., Ed. Canter, D. John Wiley & Sons.
Canter, D. (1990). An Overview of Human Behaviour in Fires. In D. Canter (Ed.), *Fires & Human Behaviour*, pp. 215-234. London: David Fulton Publishers Ltd.

Duffé, P., & Marec, M. (1999). Task Force for Technical Investigation of the 24 March 1999 Fire in the Mont Blanc Vehicular Tunnel. (No. Report of 30 June 1999): Minister of the Interior - Ministry of Equipment, Transportation and Housing.

Fahy R., Proulx G., Aiman L. (2009). 'Panic' and human behaviour in fire. Human behaviour in fire, Proceedings of the 4th International Symposium, Robinson College, Cambridge, pp387-398, 13-15 July.

Fridolf K., (2010). Fire evacuation in underground transportation systems: a review of accidents and empirical research. Report 3151. The Department of Fire Safety Engineering and Systems Safety, Lund University, Lund.

Fridolf, K., Frantzich, H. (2015) Test av vägledande system i en tunnel - slutrapport. Rapport 3189, Department of Fire Safety Engineering, Lund University, Lund.

Fridolf, K., Ronchi, E., Frantzich, H., Nilsson, D., Lindgren Walter, A. & Modig, H. (2016). 441 Full Scale Tunnel Evacuation Experiment to Determine Appropriate Emergency Exit Portal Designs in Road Tunnels. Int. Sym. on Tunnel Safety and Security, March 16-18, 2016, Montréal, Canada.

Frantzich, H., Nilsson, D. (2004) Evacuation experiments in a smoke filled tunnel. Proceedings of the 3rd International Symposium on Human Behaviour in Fire, Belfast UK, pp 229–238.

Frantzich, H., Nilsson, D. & Rød, K. (2016). Utrymning och tekniska installationer i vägtunnlar med dubbelriktad trafik. Report 3199, Fire safety En. Lund University, Lund. (In Swedish/Norwegian)

Gibson, J. J., (1978). The Ecological Approach to Visual Perception, Houghton Mifflin Company, Boston.

Hartson, H. R. (2003) Cognitive, Physical, Sensory and Functional Affordances in Interaction design, Behaviour & Information Technology 22(5): 315-338, doi:10.1080/01449290310001592587

Kobes, M., Oberijé, N., Post, J., Weges J. (2010). Fire response performance model for a systematic analysis of evacuation safety in buildings – a case study of a fire in a football stadium. Interflam 2010, Interscience Communications Ltd, London.

Kobes, M., Helsloot, I., de Vries, B., Post, J. (2010). Building safety and human behaviour in fire: A literature review Fire Safety Journal, Volume 45, Issue 1, January 2010, Pages 1-11

Kuligowski, E. (2013). Predicting Human Behavior During Fires. Fire Technol (2013) 49: 101. doi:10.1007/s10694-011-0245-6

Latané, B., & Darley, J. M. (1970). *The unresponsive bystander: Why doesn't he help?* Prentice Hall.

Nilsson, D. (2009). Exit choice in fire emergencies - influencing choice of exit with flashing lights. Report 1040, PhD thesis. Lund University, Lund.

Proulx, G. (2008). Evacuation Time. In The SFPE Handbook of Fire Protection Engineering 4th ed. Ed. DiNenno, P. J. pp 3-355 – 3-372, National Fire Protection Association, Quincy.

Ronchi, E., Nilsson, D., Modig, H., Lindgren Walter, A. (2016). Variable Message Signs for road tunnel emergency evacuations. Applied Ergonomics 52 (2016) 253-264. http://dx.doi.org/10.1016/j.apergo.2015.07.025

Shields, T. J. and Proulx, G. (1999). The Science of Human Behaviour: Past Research Endeavours, Current Developments and Fashioning a Research Agenda. Proc of 6th Int Conf. on Fire Safety Science, Poitiers, 5-9 July 1999.

Shields, T. J. (2012). Human behaviour during tunnel fires. In Handbook of tunnel Fire Safety 2nd ed. Ed. by Beard, A. and Carvel, R. ICE Publishing, London.

Sime J., (1980). The Concept of Panic. Fires and Human Behaviour Ed D Canter, J Wiley & Sons Chichester.

Sime, J. (1984). Escape behaviour in fires: 'Panic' or affiliation? PhD thesis, University of Surrey.

Sime J., Kimura M., (1988). The timing of escape: Exit choice behaviour in fires and building evacuation. Safety in the Built Environment, Ed J Sime, E & F.N Spon, London.

Tong, D., & Canter, D. (1985). The decision to evacuate: a study of the motivations which contribute to evacuation in the event of fire. *Fire Safety Journal*, *9*(3), 257-265.

Zhao, C. M., Lo, S. M., Zhang, S. P. et al. (2009) A Post-fire Survey on the Pre-evacuation Human Behavior. Fire Technol 45: 71. doi:10.1007/s10694-007-0040-6

Overview of confined fire plume behavior and smoke exhausting methods by natural and mechanical ways in tunnels

Jie Ji [1,*]
[1] State Key Laboratory of Fire Science, University of Science and Technology of China, JinZhai Road 96, Hefei, Anhui 230026, China

ABSTRACT
Due to the rapid increase in the number of tunnels and the occurrence of severe tunnel fires, attention to fire behavior and smoke control in tunnel has grown significantly in recent years. This paper presents an overview of research on confined fire plume behavior and smoke exhausting methods by natural and mechanical ways. Key topics related to the confined fire plume behavior include the ceiling jet distribution, the development of the fire plume under wall confinement, interactions of multiple fire plumes and characteristics of the smoke layer. Key topics concerning smoke exhaust methods include common mechanisms influencing smoke exhaust efficiency and the effectiveness of smoke exhaust.
KEYWORD: tunnel fire, fire plume, natural ventilation through shafts, mechanical smoke exhaust

INTRODUCTION

In recent decades, numerous severe and sometimes disastrous fires have unfortunately broken out in tunnels. Large fires in tunnels tend to spread quickly and the temperature of smoke and the concentration of toxic gas are high, leading to the difficulty of personnel evacuation and firefighting. The study of fire characteristics and smoke exhausting methods in tunnels is helpful for fire protection design, fire rescue, and personnel evacuation[1, 2].

The smoke spread process in long and narrow spaces can be classified into studies focusing on the near-fire area and the far-fire area in tunnel according to several stages of fire plume development. The near-fire area encompasses the rising plume stage and radial spreading stage. While the far-fire area corresponds to the one-dimensional spreading stage.

The active control of tunnel smoke management primarily consists of three methods, namely natural ventilation through shafts, mechanical smoke exhaust and longitudinal ventilation. Natural ventilation through shafts utilizes the stack effect created by the density difference between hot smoke inside the shaft and cold air outside the tunnel to exhaust smoke from the tunnel [3]. The objective of mechanical smoke exhaust is to confine and exhaust the smoke over a longitudinal distance as short as possible [4]. Longitudinal ventilation is used to push the whole fire-induced smoke downstream from the fire source location [5]. It is worth noting that both natural ventilation through shafts and mechanical smoke exhaust discharge smoke transversely (the focus of this study), while longitudinal ventilation blows away smoke longitudinally.

In this overview, for the near-fire area, the key research topics focus on the confined fire plume behavior, including the ceiling jet distribution, the development of the fire plume under wall confinement and the interaction of multiple fire plumes. For the far-fire area, key topics include the determination of the one-dimensional spreading stage, the characteristics of the smoke layer, and the effectiveness of natural ventilation through shafts and mechanical smoke exhaust.

1. TUNNEL FIRE DEVELOPMENT

1.1 Confined Fire Plume behavior in tunnel

Fire plume refers to the continuous upward flow of fluid driven by buoyancy generated during combustion [6]. The key characteristics of a fire plume include flame height, oscillation frequency,

combustion rate, and air entrainment intensity. In open spaces, the vertical plume behaves basically axisymmetric. However, for fires in confined long-narrow spaces such as natural ventilated tunnels, boundaries such as walls and ceilings restrict air entrainment, causing the smoke or fire plume to tilt toward the walls and impinging on the ceiling [1]. The impingement smoke or fire plume spreads horizontally beneath it and forms a ceiling jet [7]. For multiple fire plumes, negative pressure forms between adjacent fire plumes due to restricted air entrainment, leading to flame stretching and tilting towards each other. As the distance continues to decrease, the flames may eventually merge.

1.1.1 Fire at the tunnel centerline

Based on the interaction of fire plume with the ceiling, two types of plume behaviors are classified: weak plume impingement and strong plume impingement. For weak plumes, where the flame is lower than the ceiling, only the buoyancy plume impinges on the ceiling, the ceiling has little effect on flame height in tunnel. As the fire heat release rate (HRR) increases, the flame gradually impinges on the ceiling, forming a strong plume impinging flow [8]. The total flame extension can be defined as the combined vertical and horizontal extensions of flame. Ji et al. [9, 10] performed small-scale experiments with varying fire source heights to investigate strong plume-ceiling interactions in tunnel. Their research established a relationship for the longitudinal ceiling flame length, incorporating factors of HRR and effective ceiling height.

The aforementioned studies focused on fire plume characteristics in tunnel with flat ceiling and fixed cross section. To address practical tunnel design needs, researchers have also focused on the tunnel fires under different conditions. It includes the effects of cross-sectional shape [11], slope [12] and longitudinal airflow caused by natural or mechanical ventilation [11] on the confined flame behavior (the flame length, the temperature distributions and ceiling jet thickness) in tunnel and corresponding models have been developed to better understand and predict these phenomena [12].

1.1.2 Fire approaching the sidewall

In many tunnel fires, the vehicle that catches fire is often located near a sidewall. In such cases, the fire plume can entrain air only from the open side, resulting in a broader and more extensive flame spread. Gao et al. [13] observed that as the fire source moved from the centerline of the tunnel toward the sidewall, the flame transitioned from approximately symmetrical to wall-tilted, eventually resulting in spread along the wall. By adopting the concept of mirror model in tunnel [14], a dimensionless relationship was established between flame height and HRR, accounting for fires with different lateral positions in tunnel. Furthermore, Ji et al. [10, 15] studied the effects of pool aspect ratio of the wall fire in tunnel, finding that when the longer edge of a pool fire is adjacent to the wall, the flame attaches to the sidewall with relatively narrow ceiling jet flame forming. Conversely, when the shorter edge is adjacent to the wall, the flame is less attached and only part of it leans towards the sidewall, indicating weaker confinement of the fire source, as shown in Figure 1. On this basis, the influence of fire source height was also investigated further [9, 10]. When the fire source is adjacent to the tunnel sidewall, increasing the fire source height intensifies the restriction on air entrainment, leading to an extension of both longitudinal and transverse flame lengths.

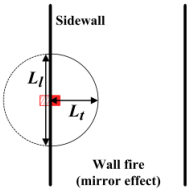

Figure 1 Mirror model for Fire behavior under sidewall constraints [15].

Building on the findings from previous studies on flame characteristics and sidewall confinement, the temperature distribution beneath the ceiling is inevitably affected. Ji et al. [16] experimentally found that applying the Alpert correlation [17] (without considering the limitations of the sidewall) to tunnel fire scenarios underestimated the maximum ceiling temperature compared to experimental results. This discrepancy arose because, after the fire plume impacted the ceiling and spread radially, the confinement of tunnel sidewalls caused smoke to flow back toward the fire source, resulting in an increase in the temperature beneath the ceiling. Subsequently, scholars conducted studies in tunnel with different ceiling types and proposed correlations to predict the maximum ceiling temperature [18]. Gao et al. [19] further investigated the relationship between the fire-sidewall distance and the maximum ceiling temperature, linking it to variations in flame height. Ji et al. [15] extended this work, finding that the

maximum ceiling temperature of a wall-adjacent fire was 1.59 times that of the centerline fire. These findings were also corroborated by Li et al. [20].

Moreover, under weak plume conditions, scholars have also studied the ceiling temperature distribution in various specific scenarios, such as inclined tunnels [21] and bifurcated tunnels [22]. As the fire HRR increases, intermittent and subsequent continuous flames impinge on the ceiling, forming strong plume impinging flow. By incorporating the distance between the fire source and the sidewall, Gao et al. [19] established a predictive formula for the temperature rise beneath the ceiling under various plume impingement conditions. Fang et al. [23] studied the temperature distribution caused by wall-adjacent fires at different fire source heights in tunnel. Their findings revealed that the ceiling temperature was strongly correlated with the fire HRR and its distance to the ceiling. Additionally, scholars have further considered the effects of longitudinal ventilation [24, 25], and established predictive formulas for both the maximum ceiling temperature and its corresponding position under ventilation conditions. Li et al. [24] also observed a particularly interesting finding that at critical conditions (when the backlayering just disappears), the maximum ceiling temperature always corresponds to the same position regardless of variations in heat release rate. In this scenario, the horizontal distance between it and the fire source is approximately 1.5 times the effective height of the tunnel.

1.1.3 Interaction of multiple fire plumes

When dual fire or multiple fires occur in a tunnel, it significantly increases fire risk in tunnel. Wan et al. [26] proposed a piecewise function to describe the flame height of dual fires in open space. And they developed a method to calculate the entrainment rate of dual fires using the Bernoulli theorem and mass conservation principles [26]. Subsequently, research on dual fires in tunnel was conducted by Ji et al. [27]. The interaction between dual fires in tunnel was categorized into four stages as the spacing decreased: non-interaction flames, tilted flames without merging, merging ceiling flames, and merging vertical flames [27]. And a correlation for predicting the effective ceiling flame length for dual fires in tunnel was proposed [27]. Based on this, Wan et al. [28] established models to predict ceiling temperature profiles induced by dual fire sources in tunnel, considering both weak and strong plumes impinging on the ceiling. They found that, due to the restriction imposed by tunnel sidewalls, more smoke accumulated under the ceiling, leading to higher ceiling temperatures compared to those predicted by Heskestad's [29] and Alpert's [17] correlations, which were derived under experimental conditions with unrestricted ceilings.

Additionally, other scholars have analyzed the flame merging criteria and ceiling temperature distribution [30] of dual fire sources in tunnels, considering various influencing factors such as tunnel lateral sidewall constraints [31], tunnel structure [32], longitudinal ventilation [33], low pressure [34, 35], and obstacles [36], etc.

1.2 Smoke spreading behavior

1.2.1 Smoke stratification and stability

After a tunnel fire goes through the radial spread and transition phases, it turns into the one-dimensional spread stage. In this stage, smoke continues to spread, entraining air and gradually forming a stable stratification. Ellison and Turner [37] studied the turbulent entrainment in stratified flows under an inclined roof, demonstrating that the entrainment coefficient depends on the Richardson number (*Ri*). Building on this, Newman [38] conducted experiments in a mine passage, quantifying the smoke stratification phenomenon at different distances from the fire source using the Froude number (*Fr*). And the smoke stratification was classified into three regions: 1) Stable buoyant flow stratification ($Fr < 0.9$); 2) Stratification with vortices at the interface ($0.9 < Fr < 10$); 3) No distinct stratification between buoyant flow and airflow ($Fr > 10$). Nyman and Ingason [39] compared data from various scaled experiments and found that the existing smoke stratification model based on the Froude number was not entirely accurate. They pointed out that the criterion results were affected by the experimental methodology, particularly whether the flame had developed to steady state.

Based on the previously discussed smoke stratification characteristics, the N-percentage rule [40] determines the smoke layer interface height using the vertical temperature distribution in a space. However, the N-percentage rule involves a certain degree of subjectivity and relies on the experiential selection of the N value. To address these limitations, He et al. [41] proposed the integral ratio method and the least squares method to determine the smoke layer interface. However, their experimental results

in real corridor fire scenarios revealed that the interface heights were overestimated compared to actual values. Gao et al. [42] introduced a new method based on buoyancy frequency to determine the smoke layer interface. The concept of buoyancy frequency was adopted to measure the rate of density change at different heights. Comparative scaled experiments demonstrated that the buoyancy frequency method achieves higher accuracy across all stages of fire development, as shown in Figure 2. At the same time, the buoyancy frequency method has a clear physical basis and does not rely on empirical parameters.

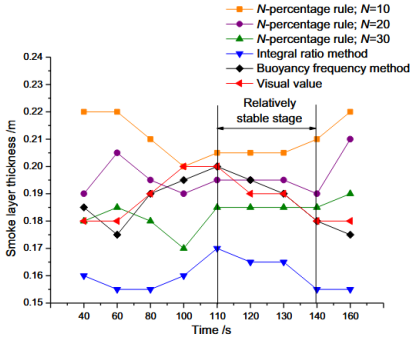

Figure 2 Comparison of smoke layer thickness of different approaches [42].

Oka et al. [43] experimentally investigated the distribution of smoke layer thickness along the tunnel axis and found that in the one-dimensional spread stage, the smoke layer thickness remains essentially constant. Guo et al. [44] developed a prediction model for smoke layer thickness in both the transitional stage and one-dimensional spread stage incorporating a non-Boussinesq approximation, through theoretical analysis and numerical simulations. Besides, Liu et al. [45] have numerically studied the impact of different altitudes on smoke layer.

1.2.2 Smoke spread velocity

Understanding the spread distance of smoke over time and estimating the time required for personnel to evacuate makes the velocity of smoke spread a critical factor in fire safety analysis.

Through an experimental study in an underground park facility, Hinkley [46] proposed a classic model for predicting the speed of the smoke front using the Froude number. Later, Kim et al. [47] conducted corridor experiments and pointed out that the smoke velocity calculated by Hinkley's model was 20% larger than the measured value. He [48] introduced a coefficient of 0.5 in the flame HRR term to correct Hinkley's model, achieving better consistency with Kim's experimental results. It is worth noting that the Hinkley model neglects the impact of sidewall heat loss. By taking smoke heat loss into consideration, Yang et al. [49] corrected Hinkley's model and achieved higher accuracy of smoke front velocity. Oka et al. [50] later pointed out that previous models did not consider the changes in Richardson number. Using this concept, they proposed a new smoke spread velocity model for the one-dimensional spread stage. Subsequently, Zhao et al. [51] studied the impact of dual fire sources and Liu et al. [52] explored the influence of altitude on smoke spread velocity in tunnel, respectively.

1.2.3 Smoke temperature attenuation

High-temperature smoke not only influences the dynamics of smoke movement but also poses a significant threat to tunnel structures[53].

Evers and Waterhouse [54] proposed a single exponential decay model of smoke temperature under the ceiling based on experimental data. Subsequently, further studies under various conditions have consistently validated the single exponential decay law of smoke temperature, such as different tunnel slopes [55], cross-sectional width [56], fuel mixing ratio [57], wall material [58], among others.

Ingason and Li [59] verified that a single exponential decay law was not suitable for temperature distribution under low longitudinal ventilation conditions. And they proposed an alternative correlation taking the form of the sum of two exponential functions, and verified its accuracy using both reduced-scale and full-scale experimental data. However, they noted that this correlation exhibits a prediction offset when the flame directly impinges on the ceiling. Additionally, the expression of the sum of two exponential functions has been further verified under the tunnel fire scenarios of various environmental pressures [60], and tunnel dimensions (tunnel slope, width) [61].

2. NATURAL VENTILATION THROUGH SHAFTS

Natural ventilation through shafts is an important smoke exhaust method in tunnel engineering. This method utilizes the stack effect created by the density difference between hot smoke inside the shaft and

cold air outside the tunnel as the driving force to exhaust the smoke out of the tunnel, as shown in Figure 3. Natural ventilation through shafts has been adopted in some underground tunnels in cities such as Tokyo in Japan and Nanjing in China (Figure 4).

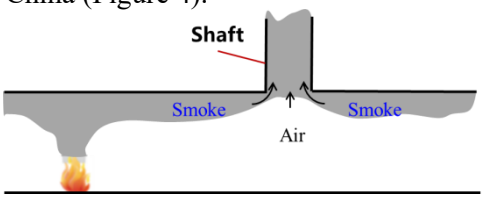

Figure 3 Natural ventilation through shafts

(a) Chiba section of Tokyo Outer Ring Road tunnel (b) Nanjing Xi 'an Gate Tunnel

Figure 4 The tunnels that adopt natural ventilation through shafts.

The difficulty in studying natural ventilation through shafts in tunnel lies in the numerous factors, such as the shaft size, shaft layout, fire location, etc. Prior to 2012, previous research [62-65] has primarily focused on the analysis of smoke exhausting effect by vertical shafts in one specific tunnel, i.e. case study, without addressing the common characteristics of smoke spread under the effect of shafts. The key to solving it lies in revealing the common influencing mechanisms and establishing universal mathematical models. Afterwards, Ji et al. [66] conducted a series of small-scale experiments on natural ventilation through shafts by varying HRR and shaft height. They firstly proposed two common mechanisms affecting the efficiency of smoke exhaust: the boundary layer separation and the plug-holing in Figure 5, which were widely used to describe the local smoke characteristics at the shaft in the studies related to natural ventilation through shafts under various conditions, subsequently [67-69].

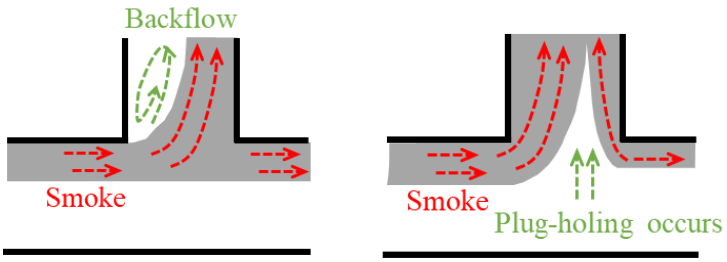

(a)The boundary layer separation (b)The plug-holing

Figure 5 Influencing mechanisms proposed by Ji et al. [66].

At relatively low shaft height, the boundary layer separation is significant and vortexes form on the upstream side of shaft, causing the backflow of a portion of discharged smoke and the effective exhausting section reduced. This is obviously detrimental to exhaust smoke effectively. If the shaft is too high, excessive vertical buoyancy force caused by the stack effect curbs the boundary layer separation and causes the occurrence of plug-holing. Ji et al. [70] employed numerical simulation methods to measure and calculate the mass flow rate of fresh cool air, smoke, and total gas exhausted through tunnel shafts. It was found that after the shaft height exceeded the critical plug-holing height, the mass flow rate of the total exhausted gas and fresh air gradually increased as the shaft height increased. However, the mass flow rate of exhausted smoke remained basically stable. This also leads to the smoke exhaust process inefficiency.

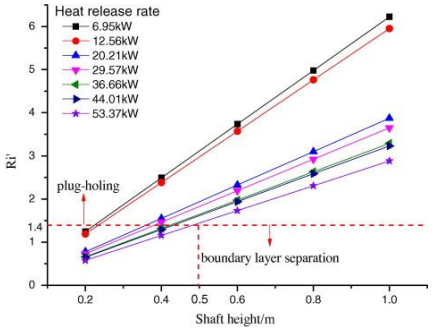

Figure 6 The criterion of Ri' proposed by Ji et al. [66].

Therefore, it is a clear choice to set the ventilation shaft at a critical value, at which the boundary layer separation is suppressed and plug-holing does not occur. Ji et al. [66] put forward a theoretically based criterion of *Ri'* by considering the vertical and horizontal inertial forces acting on the smoke, to determine the critical shaft height for different HRRs. The critical value of *Ri'* ($Ri'_{critical}$) is roughly determined as 1.4 on the basis of experimental results in Figure 6. This critical criterion has been subsequently adopted and verified in the studies conducted in the small-scale model tunnels with different scale ratios and aspect ratios [71] and the full-scale tunnels with different cross-sectional dimensions [72].

The main purpose of smoke control method is to ensure the safe evacuation of personnel and the access of firefighting and rescue personnel. Therefore, the smoke movement downstream of the shaft is highly focused on the study of natural ventilation through shafts. The two main evaluation indicators for assessing the smoke control effect are smoke spread distance and smoke layer thickness. Researches [63, 64, 68] in this aspect primarily focused on describing the variation of smoke spread distance and thickness downstream of shafts in specific scenarios and conditions, lacking theoretical analysis. Tanaka et al. [73] conducted a series of experiments using a 1:10 scale model tunnel with roof openings (shaft height of 0 m) of a 10% opening ratio. They proposed a simple model for predicting the smoke spread length in the tunnel based on flow and energy balance in smoke and fresh air. This work presented a good methodological approach for predicting the smoke spread distance under the effect of natural ventilation through shafts.

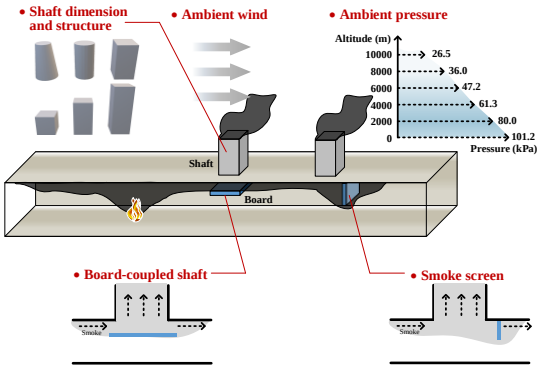

Figure 7 Factors affecting natural ventilation through shafts.

The impact of these factors (in Figure 7) such as shaft dimension [66, 74] and structure (bevel-angle connection shafts [75] and inclined shafts[76]), ambient wind [77]and pressure [78], board-coupled shafts [79-82]and smoke screens [83, 84] on natural ventilation through shafts has been further studied to assist in the design of shallow-buried urban tunnels.

3. MECHANICAL SMOKE EXHAUST METHOD

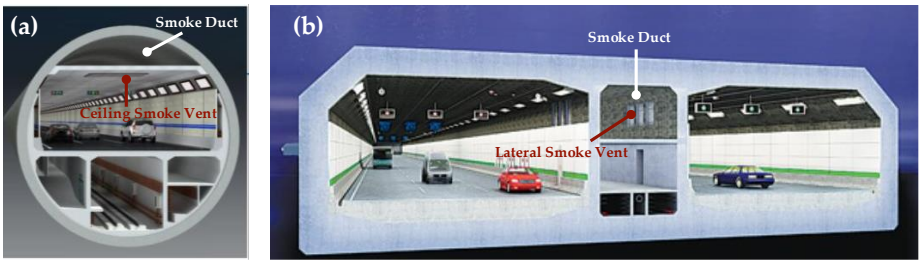

Figure 8 (a) Ceiling smoke exhaust; (b) Lateral smoke exhaust.

Mechanical smoke exhaust systems are commonly employed in long tunnels or single-hole two-way tunnels. According to the position of the smoke outlet, they can be further categorized into ceiling mechanical smoke exhaust and lateral mechanical smoke exhaust. The ceiling mechanical smoke exhaust is operated by positioning smoke vents at the tunnel roof, working with smoke extraction ducts, as shown in Figure 8(a). It is commonly used in urban traffic tunnels and extra-long highway tunnels. The lateral mechanical smoke exhaust is realized by setting smoke vents on the side wall of the tunnel. Since it is not restricted by the height of the tunnel, compared with ceiling smoke exhaust, it demonstrates remarkable flexibility and adaptability under certain complex tunnel conditions such as those in underwater tunnels (the Hong Kong-Zhuhai-Macao Bridge Tunnel (Figure 8(b)), the Shouxihu Tunnel and the Dalian Bay Undersea Tunnel).

3.1 Ceiling mechanical smoke exhaust

In earlier studies, Ji et al. [85] investigated smoke movement behaviors under various smoke extraction heights and rates through a series of ceiling mechanical smoke extraction experiments. Compared to natural ventilation, mechanical smoke extraction operates at a higher flow rate. On the one hand, this enhances the entrainment effect, disrupting the stratification of the smoke layer, and affects the thickness of the smoke layer. On the other hand, it may induce plug-holing phenomena, reducing the efficiency of smoke extraction (Figure 9).

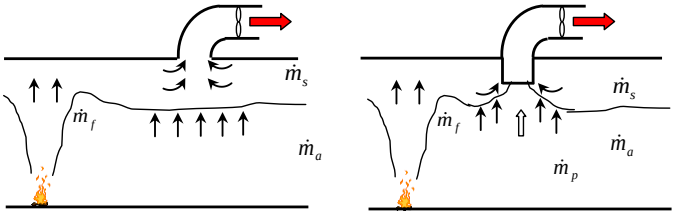

(a) No plug-holing; (b) Plug-holing

Figure 9 The flow field below the exhaust port in the ceiling exhaust [85].

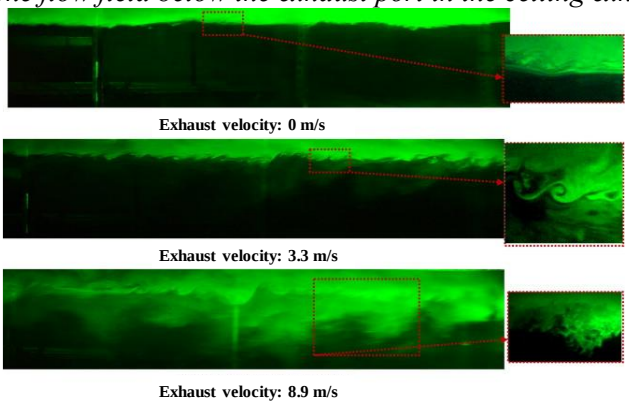

Figure 10 Typical configurations of smoke layer [86].

The effect of mechanical exhaust on the smoke structure in the tunnel is manifested by changing the stability of the smoke layer in Figure 10. With the increase of smoke exhaust velocity, the smoke layer gradually forms a vortex from stable stratification, and finally develops into an unstable structure which is strongly mixed with air [86]. The attribution of the above phenomenon is that the shear-induced counterflow generated by ceiling mechanical smoke extraction enhances thermal and mass exchange between the upper hot smoke layer and the lower air layer [86]. The smoke stratification states using the Froude number (Fr) and Richardson number (Ri) are classified: 1) stable buoyant flow stratification ($Ri > 0.9$ *or* $Fr < 1.2$); 2) the stable buoyant flow stratification with interfacial instability ($0.3 < Ri < 0.9$ *or* $1.2 < Fr < 2.4$); 3) unstable buoyant flow stratification ($Ri < 0.3$ *or* $Fr > 2.4$) [86].

The main concern of mechanical smoke extraction systems is to evaluate their smoke exhaust effect. The phenomenon of plug-holing occurs when the mechanical smoke extraction velocity is excessively high or the smoke layer beneath the extraction vent is too thin, thereby reducing smoke exhaust efficiency. The prediction of ceiling plug-holing using the Froude number was firstly proposed by Hinkley [46] in the context of natural ventilation systems. Lougheed [87] concluded that the Froude number can be used to determine the plug-holing in mechanical smoke exhaust in atria. Later Li et al.

[88] studied the suction problem of smoke in tunnel with a single ceiling exhaust port through numerical simulation, and found that the previous critical Froude number 1.5 [89] in building fires was not suitable to be used for tunnel fires, and re-determined the critical Froude number suitable for tunnel fires as 2.1 (Figure11). In addition, other researchers have explored various factors that affect the smoke plug-holing phenomenon of ceiling exhaust, including the size of vent [90], the number of vents [91] and so on.

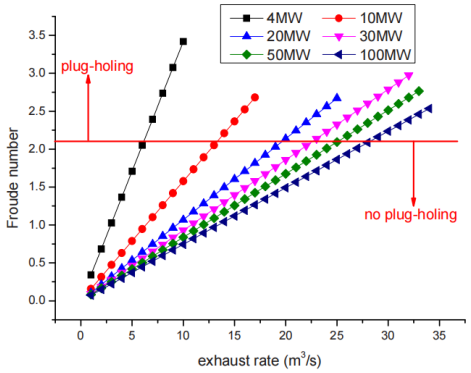

Figure 11 Critical Froude number of ceiling mechanical smoke exhaust in tunnel [88].

For the ceiling smoke exhaust effect of a single smoke vent, Ji et al. [92] determined that placing the smoke vent during the one-dimensional horizontal movement stage of smoke spread significantly increases turbulence and entrainment at the smoke layer interface, thereby reducing extraction efficiency. Subsequently, the heat extraction coefficient as a quantitative parameter is proposed to evaluate the efficiency of tunnel smoke extraction systems, defined as the ratio of the heat extraction rate to HRR [93]. It was found that the heat extraction coefficient gradually decreases with the increase of HRR and gradually increases with the increase of smoke exhaust velocity [93].

In actual tunnel fires, multiple smoke extraction outlets near the fire source are typically activated to expedite smoke removal which forms a multi-point extraction system. Researchers have studied the effectiveness of the multi-point smoke extraction system in controlling smoke through case study, aiming to identify strategies for optimizing smoke extraction performance[2, 4, 94-96].

3.2 Lateral mechanical smoke exhaust

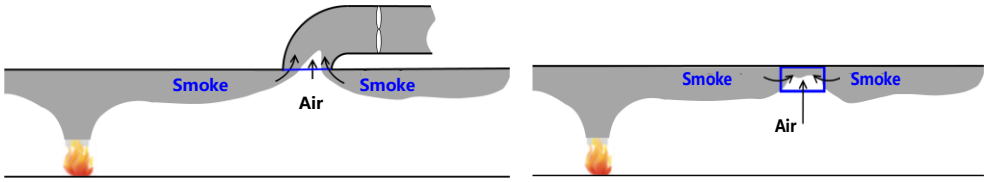

(a) Ceiling mechanical smoke exhaust; (b) Lateral mechanical smoke exhaust

Figure 12 Comparison of the two kinds of smoke exhaust modes.

Compared with the ceiling mechanical smoke exhaust, the lateral mechanical smoke exhaust vents are positioned closer to the smoke-air boundary layer. And the direction of the exhaust velocity also changes from vertical to horizontal, as shown in Figure 12.

Tang et al. [97] found that the critical standard of smoke stratification under the lateral smoke extraction was lower than that for ceiling exhaust. It can be explained that the suction force acts laterally under lateral extraction, intensifying mixing and disturbances during smoke transport. Further, Jin et al. [98] proposed a dimensionless number (F_{rs}) to classify the flow patterns of stratified smoke under lateral extraction in Fig.13: 1) stable buoyancy layer ($F_{rs} < 2.4$), 2) stable buoyancy stratification with unstable interfaces ($2.4 < F_{rs} < 4.8$), 3) unstable stratification ($F_{rs} > 4.8$).

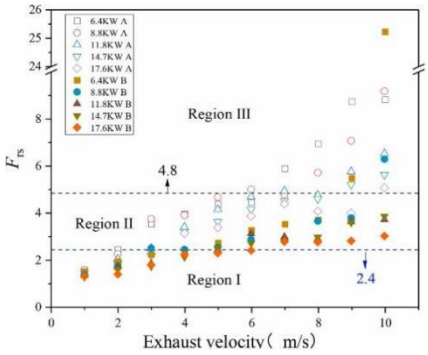

Figure 13 F_{rs} at different positions with different fire source power [98].

Due to the location of exhaust vents being closer to the air layer beneath the smoke, lateral smoke extraction systems are more prone to the phenomenon of plug-holing. Yang et al. [99] directly used the Froude number proposed by Hinkley [46] to predict the occurrence of plug-holing of lateral smoke exhaust, which is used for ceiling smoke exhaust in a stationary smoke reservoir [46]. It is debatable because the vertical inertial force of the smoke layer is mainly induced by the vertical exhaust velocity of the ceiling smoke exhaust. Zhong et al. [100] introduced a virtual exhaust vent that is perpendicular to the original lateral one for calculating the vertical inertial force, and proposed a modified Froude number to predict the occurrence of plug-holing of lateral smoke exhaust. By considering the vertical inertia force induced by the lateral exhaust vent and the horizontal inertial force generated by the fire source, Wang et al. [101] proposed a critical criterion ($Ri'_{critical}$) for predicting plug-holing in lateral mechanical smoke extraction systems. Its critical value is 0.6 in Fig.14. In subsequent studies, researchers explored conditions that mitigate the occurrence of-plug-holing by varying the dimensions of lateral smoke extraction vents [102, 103].

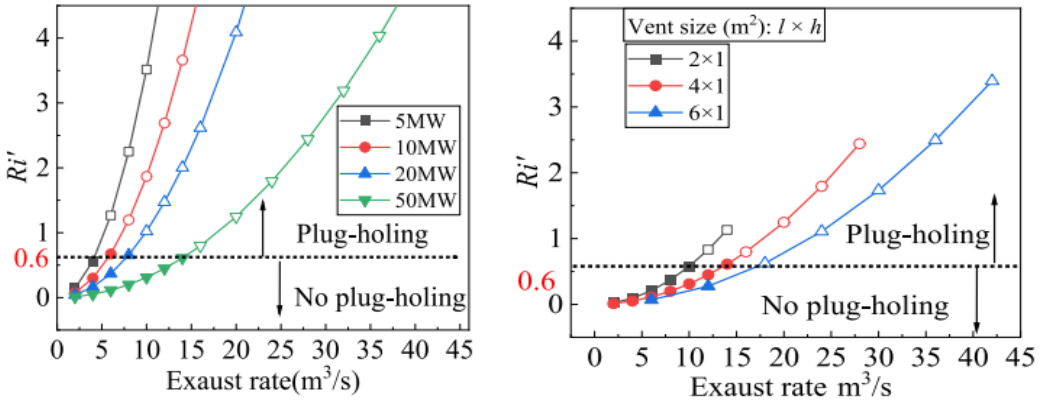

(a) Vent size: 4 m×1 m, different HRRs; (b) HRR: 50MW, different vent sizes.

Figure 14 $Ri'_{critical}$ of lateral mechanical smoke exhaust in tunnel [101].

In terms of smoke extraction efficiency, Xu et al. [104] found that it was directly proportional to the smoke exhaust rate and inversely proportional to HRR. Further, other studies also considered the influencing factors (the vent size, the distance between the exhaust vent and the ceiling, etc.[105]) of smoke exhaust efficiency and the methods to improve smoke exhaust efficiency [106], so as to better adapt to engineering practice.

3.3 Mechanical smoke exhaust combined with longitudinal ventilation

Due to the diverse and complex structural forms of tunnels, a single mechanical smoke extraction method has certain limitations in controlling smoke during tunnel fires. Therefore, engineers developed a hybrid smoke control strategy that leverages the synergy of longitudinal ventilation and concentrated extraction, as shown in Figure 15. By appropriately controlling the longitudinal ventilation velocity, smoke can be confined to a limited area near the fire source and efficiently discharged from the tunnel.

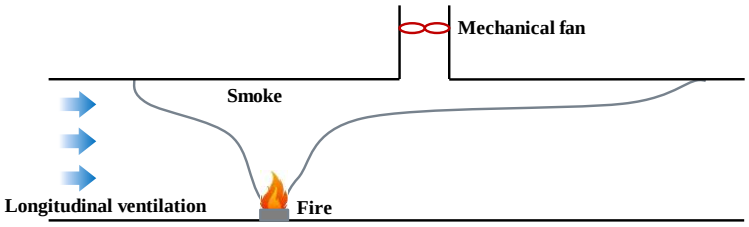

Figure 15 Longitudinal ventilation mixed with transverse exhaust smoke extraction mode.

Currently, many long tunnels primarily adopt a hybrid smoke exhaust mode that combines longitudinal ventilation with centralized smoke extraction, such as the Qianjiang Tunnel (Hangzhou, China), Yangtze River Tunnel (Shanghai, China), Central artery-190 and 193 (Boston, USA), Busan–Geoje tunnel (Busan, Korea) and so on. However, existing fire safety standards do not provide clear limits for key parameters in this hybrid smoke extraction mode. In response, numerous researchers have conducted experiments and simulations to study this mode, with a primary focus on addressing the challenge of controlling smoke back-layering in tunnels with exhaust ventilation. Vauquelin and Telle [107] simulated smoke and evaluated the induced longitudinal velocity under longitudinal ventilation through a small-scale tunnel model experiment. Ingason and Li [4] further gave the longitudinal ventilation speed required by single-point and two-point smoke exhaust systems. Recently, Tanaka et al. [108] verified the applicability of the longitudinal ventilation tunnel model in mixed smoke exhaust mode. The prediction models of smoke back-layering length and critical velocity were developed based on tunnel experiments with longitudinal ventilation with smoke extraction [109-113]. And other studies have also focused on the phenomenon of smoke stratification and ceiling temperature distribution [97, 114, 115].

4. FUTURE CHALLENGES

1) Current measurement methods in tunnel fire research mainly include point measurements and two-dimensional measurements, such as thermocouples, anemometers, planar light sources, etc. However, the development of tunnel fires is a three-dimensional process. Future research can develop three-dimensional measurement methods to gain a deeper understanding of the development of tunnel fire.
2) Alternative fuels, such as hydrogen, electricity, methanol, and biofuels, have been widely adopted in transportation. The combustion characteristics of these fuels differ markedly from those of traditional fuels, resulting in variations in fire growth rate, heat release rate (HRR), smoke composition, etc. Future research should focus on developing effective strategies to address fires involving new energy vehicles.
3) With the rapid development of artificial intelligence and the Internet of Things, the research direction of intelligent smoke extraction systems warrants attention. Smart control systems based on real-time data acquisition and dynamic analysis can significantly enhance the response efficiency and resource utilization of smoke extraction systems, providing more reliable support for smoke control and evacuation in complex fire scenarios.

REFERENCES

[1] Ingason, H., Li, Y.Z., Lönnermark, A., “Tunnel fire dynamics”, Springer, 2015.
[2] Li, Y.Z., Ingason, H., “Overview of research on fire safety in underground road and railway tunnels”, *Tunnelling and Underground Space Technology*, 81, 568-589, 2018.
[3] Fan, C., Ji, J., Wang, W., Sun, J., “Effects of vertical shaft arrangement on natural ventilation performance during tunnel fires”, *International journal of heat and mass transfer*, 3,158-169, 2014.
[4] Ingason, H., and Li, Y.Z., “Model scale tunnel fire tests with point extraction ventilation”, *Journal of Fire Protection Engineering*, 21, 5-36, 2011.
[5] Li, Y.Z., Lei, B., Ingason, H., “Study of critical velocity and backlayering length in longitudinally ventilated tunnel fires”, *Fire Safety Journal*, 45,361-370, 2010.
[6] Heskestad, G., “Dynamics of the fire plume”, *Philosophical Transactions of the Royal Society of London. Series A: Mathematical, Physical and Engineering Sciences*, 356, 2815-2833, 1998.
[7] Alpert, R.L., “Ceiling jet flows”, *SFPE handbook of fire protection engineering*, 429-454, 2016.
[8] Zhang, X., Teng, S., Cheng, Z., Li, L., Huang, Y., and Li, C., “Arc-top tunnel longitudinal ceiling temperature distribution under longitudinal ventilation with different fire-source–side-wall distances”, *International Journal of Thermal Sciences*, 205, 109258, 2024.
[9] Ji, J., Fu, Y. Y., Fan, C. G., Gao, Z. H., and Li, K. Y. “An experimental investigation on thermal

characteristics of sidewall fires in corridor-like structures with varying width", *International Journal of Heat and Mass Transfer*, 84, 562-570, 2015.
[10] Ji, J., Fu, Y., Li, K., Sun, J., Fan, C., and Shi, W., "Experimental study on behavior of sidewall fires at varying height in a corridor-like structure", *Proceedings of the Combustion Institute*, 35, 2639-2646, 2015.
[11]Fan, C.G., Yang, J., and Li, M.H., "A theoretical and experimental study of flame length under a tunnel ceiling", *Journal of Thermal Analysis and Calorimetry*, 128, 1143-1149, 2017.
[12] Xu, T., Deng, L., and Tang, F., "Flame extension scale and flow characteristics of inclined tunnel fires with various separation distances from sidewall", *Tunnelling and Underground Space Technology*, 154, 106090, 2024.
[13] Gao, Z.H., Ji, J., Fan, C.G., Sun, J.H., and Zhu, J.P., "Influence of sidewall restriction on the maximum ceiling gas temperature of buoyancy-driven thermal flow", *Energy and Buildings*, 84, 13-20, 2014.
[14] Hasemi, Y., and Tokunaga, T., "Some experimental aspects of turbulent diffusion flames and buoyant plumes from fire sources against a wall and in a corner of walls", *Combustion Science and Technology*, 40, 1-18, 1984.
[15] Ji, J., Fan, C.G., Li, Y.Z., Ingason, H., and Sun, J.H., "Experimental study of non-monotonous sidewall effect on flame characteristics and burning rate of n-heptane pool fires", *Fuel*, 145, 228-233, 2015.
[16] Ji, J., Fan, C.G., Zhong, W., Shen, X.B., and Sun, J. H., "Experimental investigation on influence of different transverse fire locations on maximum smoke temperature under the tunnel ceiling", *International Journal of Heat and Mass Transfer*, 55, 4817-4826, 2012.
[17] Alpert, R.L., "Calculation of response time of ceiling-mounted fire detectors", *Fire Technology*, 8, 181-195, 1972.
[18] Zhou, T., Zhou, Y., Fan, C., and Wang, J., "Experimental study on temperature distribution beneath an arced tunnel ceiling with various fire locations", *Tunnelling and Underground Space Technology*, 98, 103344, 2020.
[19] Gao, Z., Ji, J., Wan, H., Li, K., Sun, J., "An investigation of the detailed flame shape and flame length under the ceiling of a channel", *Proceedings of the Combustion Institute*, 35, 2657-2664, 2015.
[20] Li, Q., Kang, J., Xu, X., Feng, Y., and Wang, Y., "An experimental study on gas temperature characteristic in tunnel fires: The influences of sidewall restriction and sealing effect", *International Journal of Heat and Mass Transfer*, 214, 124385, 2023.
[21] Gao, Z., Li, L., Sun, C., Zhong, W., and Yan, C., "Effect of longitudinal slope on the smoke propagation and ceiling temperature characterization in sloping tunnel fires under natural ventilation", *Tunnelling and Underground Space Technology*, 123, 104396, 2022.
[22] Liu, C., Zhong, M., Tian, X., Zhang, P., Xiao, Y., Mei, Q., "Experimental and numerical study on fire-induced smoke temperature in connected area of metro tunnel under natural ventilation", *International Journal of Thermal Sciences*, 138, 84-97, 2019.
[23] Fang, X., Huang, Y., Ren, F., Zhang, H., and Li, C., "Experimental study of the temperature profile induced by the tunnel wall fire plume at various source-ceiling heights", *Case Studies in Thermal Engineering*, 60, 104761, 2024
[24] Li, Y.Z., Ingason, H., "Position of maximum ceiling temperature in a tunnel fire", *Fire Technology*", 50, 889-905, 2014.
[25] Chen, L., Li, X., Yang, Y., Li, Z., Li, T., Lan, Y., and Chen, Y., "Numerical investigation of the temperature characteristics beneath the ceiling driven by a strong plume in a longitudinal ventilated tunnel", *Fire and Materials*, 2024.
[26] Wan, H., Ji, J., Li, K., Huang, X., Sun, J., and Zhang, Y., "Effect of air entrainment on the height of buoyant turbulent diffusion flames for two fires in open space", *Proceedings of the Combustion Institute*, 36, 3003-3010, 2017.
[27] Ji, J., Wan, H.X., Gao, Z.H., Fu, Y.Y., Sun, J.H., Zhang, Y.M., Li, K.Y., and Hostikka, S., "Experimental study on flame merging behaviors from two pool fires along the longitudinal centerline of model tunnel with natural ventilation", *Combustion and Flame*, 173, 307-318, 2016.
[28] Wan, H., Gao, Z., Ji, J., Li, K., Sun, J., and Zhang, Y., "Experimental study on ceiling gas temperature and flame performances of two buoyancy-controlled propane burners located in a tunnel", *Applied Energy*, 185, 573-581, 2017.
[29] Heskestad, G., and Hamada, T., "Ceiling jets of strong fire plumes", *Fire Safety Journal*, 21, 69-82, 1993.
[30] Jia, Y., Fan, X., Deng, Y., Zhu, X., Yu, Q., and Zhao, W., "Study on the temperature characteristics

caused by two fires in a tunnel based on multi-layer zone model", *Tunnelling and Underground Space Technology*, 135, 105045, 2023.
[31] Zhao, S., Du, K., Yao, Y., Wang, F., Weng, M., Xu, L., and Lei, W., "Influence of sidewall restriction on flame characteristics of double fires in a channel", *Tunnelling and Underground Space Technology*, 140, 105297, 2023.
[32] Li, L., Nen, T., Wu, Z., Huang, H., Zhang, H., Sun, Y., and Gao, Z., "Experimental study on the flame merging and temperature profile produced by two pool fires beneath the curved ceiling", *Case Studies in Thermal Engineering*, 60,104600, 2024.
[33] Zhao, S., "Study on smoke movement under longitudinal ventilation in tunnel fires", A dissertation for doctor's degree, Chongqing University, Chongqing, China, 2019.
[34] Li, B., Zhu, X., Chen, Z., Duan, T., and Mao, S., "Research on characteristics of thermal smoke movements of twin fires in a tunnel under reduced pressure", *Case Studies in Thermal Engineering*, 54, 104066, 2024.
[35] Li, B., Wang, L., Mao, S., Lu, K., and Ni, X., "Study on the ceiling gas temperature distribution, fire merging, and flame length induced by twin tunnel fires under reduced pressures", *International Journal of Thermal Sciences*, 203, 109149, 2024.
[36] Heidarinejad, G., Mapar, M., and Pasdarshahri, H., "A comprehensive study of two fire sources in a road tunnel: Considering different arrangement of obstacles", *Tunnelling and Underground Space Technology*, 59, 91-99, 2016.
[37] Ellison, T.H., and Turner, J.S., "Turbulent entrainment in stratified flows", *Journal of Fluid Mechanics*, 6(3), 423-448, 1959.
[38] Newman, J.S., "Experimental evaluation of fire-induced stratification", *Combustion and Flame*, 57, 33-39, 1984.
[39] Nyman, H., and Ingason, H., "Temperature stratification in tunnels", *Fire Safety Journal*, 48, 30-37, 2012.
[40] Cooper, L.Y., Harkleroad, M., Quintiere, J., and Rinkinen, W., "An Experimental-study of Upper Hot Layer Stratification in Full-scale Multi-room Fire Scenarios", *ASME Journal of Heat and Mass Transfer*, 104, 741-749, 1982.
[41] He, Y.P., Fernando, A., and Luo, M.C., "Determination of interface height from measured parameter profile in enclosure fire experiment", *Fire Safety Journal*, 31, 19-38, 1998.
[42] Gao, Z.H., Ji, J., Fan, C.G., Li, L.J., and Sun, J.H., "Determination of smoke layer interface height of medium scale tunnel fire scenarios", *Tunnelling and Underground Space Technology*, 56, 118-24, 2016.
[43] Oka, Y., Oka, H., and Imazeki, O., "Ceiling-jet thickness and vertical distribution along flat-ceilinged horizontal tunnel with natural ventilation", *Tunnelling and Underground Space Technology*, 53, 68-77, 2016.
[44] Guo, Q., Li, Y.Z., Ingason, H., Yan, Z., and Zhu, H., "Theoretical studies on buoyancy-driven ceiling jets of tunnel fires with natural ventilation", *Fire Safety Journal*, 119, 103228, 2021.
[45] Liu, B., Mao, J., Xi, Y., and Hu, J., "Effect of altitude on vertical temperature distribution and longitudinal smoke layer thickness in long tunnel fires", *Fire and Materials*, 47, 16-27, 2023.
[46] Hinkley, P., "The flow of hot gases along an enclosed shopping mall a tentative theory", *Fire Safety Science*, 807, 1-1, 1970.
[47] Kim, M.B., Han, Y.S., and Yoon, M.O., "Laser-assisted visualization and measurement of corridor smoke spread", *Fire safety journal*, 31, 239-251, 1998.
[48] He, Y., "Smoke temperature and velocity decays along corridors", *Fire Safety Journal*, 33, 1999.
[49] Yang, D., Huo, R., Zhang, X.L., and Zhao, X.Y., "On the front velocity of buoyancy-driven transient ceiling jet in a horizontal corridor: Comparison of correlations with measurements", *Applied Thermal Engineering*, 31, 2992-2999, 2011.
[50] Oka, Y., and Oka, H., "Temperature and velocity distributions of a ceiling-jet along a flat-ceilinged tunnel with natural ventilation", *Fire Safety Journal*, 112, 102969, 2020.
[51] Zhao, W., Zong, R., Liu, J., Ye, J., and Zhu, K., "Study of the fire characteristics for multi-source fires in the confined corridor", *Journal of Wind Engineering and Industrial Aerodynamics*, 147, 239-250, 2015.
[52] Liu, B., Mao, J., Xi, Y., and Hu, J., "Effects of altitude on smoke movement velocity and longitudinal temperature distribution in tunnel fires", *Tunnelling and Underground Space Technology*, 112, 103850, 2021.
[53] Li, Y.Z., Lei, B., Ingason, H., "The maximum temperature of buoyancy-driven smoke flow beneath the ceiling in tunnel fires", *Fire Safety Journal*, 46, 204-210, 2011.

[54] Evers, E., and Waterhouse, A., "A computer model for analysing smoke movement in buildings", *Building Research Establishment*, 1-26, 1978.
[55] Jiao, W., Chen, C., Lin, Z., Bao, Y., and Shi, L., "Experimental study on the burning characteristics and smoke temperature distribution of continuous spill fires in sloped tunnels", *Tunnelling and Underground Space Technology*, 152, 105884, 2024.
[56] Ji, J., Bi, Y., Venkatasubbaiah, K., and Li, K., "Influence of aspect ratio of tunnel on smoke temperature distribution under ceiling in near field of fire source", *Applied Thermal Engineering*, 106, 1094-1102, 2016.
[57] Tian, X., Zhong, M., Shi, C., Zhang, P., and Liu, C., "Full-scale tunnel fire experimental study of fire-induced smoke temperature profiles with methanol-gasoline blends", *Applied Thermal Engineering*, 116, 233-243, 2017.
[58] Wang, K. H., Liu, Y. Q., Zhang, P. H., and Guo, Y. L., "Numerical study on the impact of wall thermal inertia on maximum smoke temperature and longitudinal attenuation in long channel fires", *International Journal of Thermal Sciences*, 184, 107940, 2023.
[59] Ingason, H., and Li, Y.Z., "Model scale tunnel fire tests with longitudinal ventilation", *Fire Safety Journal*, 45, 371-384, 2010.
[60] Ji, J., Guo, F., Gao, Z., Zhu, J., and Sun, J., "Numerical investigation on the effect of ambient pressure on smoke movement and temperature distribution in tunnel fires", *Applied Thermal Engineering*, 118, 663-669, 2017.
[61] Wang, Z., Ding, L., Wan, H., Ji, J., Gao, Z., and Yu, L., "Numerical investigation on the effect of tunnel width and slope on ceiling gas temperature in inclined tunnels", *International Journal of Thermal Sciences*, 152, 106272, 2020.
[62] Lin, C.J., Chuah, Y.K., and Liu, C.W., "A study on underground tunnel ventilation for piston effects influenced by draught relief shaft in subway system", *Applied Thermal Engineering*, 28, 372-379, 2008.
[63] Tong, Y., Shi, M.H., Gong, Y.F., and He, J.P., "Full-scale experimental study on smoke flow in natural ventilation road tunnel fires with shafts", *Tunnelling and Underground Space Technology*, 24, 627-633, 2009.
[64] Wang, Y., Jiang, J., and Zhu, D., "Full-scale experiment research and theoretical study for fires in tunnels with roof openings", *Fire Safety Journal*, 44, 339-348, 2009.
[65] Ko, J.S., Yoon, C.H., Yoon, S.W., and Kim, J., "Determination of the applicable exhaust airflow rate through a ventilation shaft in the case of road tunnel fires", *Safety Science*, 48, 722-728, 2010.
[66] Ji, J., Gao, Z.H., Fan, C.G., Zhong, W., and Sun, J.H., "A study of the effect of plug-holing and boundary layer separation on natural ventilation with vertical shaft in urban road tunnel fires", *International Journal of Heat and Mass Transfer*, 55, 6032-6041, 2012.
[67] Baek, D., Sung, K.H., and Ryou, H.S., "Experimental study on the effect of heat release rate and aspect ratio of tunnel on the plug-holing phenomena in shallow underground tunnels", *International Journal of Heat and Mass Transfer*, 113, 1135-1141, 2017.
[68] Yao, Y., Li, Y.Z., Ingason, H., and Cheng, X., "Numerical study on overall smoke control using naturally ventilated shafts during fires in a road tunnel", *International Journal of Thermal Sciences*, 140, 491-504, 2019.
[69] Guo, Q., Zhu, H., Zhang, Y., Shen, Y., Zhang, Y., and Yan, Z., "Smoke flow in full-scale urban road tunnel fires with large cross-sectional vertical shafts", *Tunnelling and Underground Space Technology*, 104, 103536, 2020
[70] Ji, J., Gao, Z.H., Fan, C.G., and Sun, J.H., "Large Eddy Simulation of stack effect on natural smoke exhausting effect in urban road tunnel fires", *International Journal of Heat and Mass Transfer*, 66, 531-542, 2013.
[71] Takeuchi, S., Tanaka, F., Yoshida, K., and Moinuddin, K.A., "Effects of scale ratio and aspect ratio in predicting the longitudinal smoke-temperature distribution during a fire in a road tunnel with vertical shafts", *Tunnelling and Underground Space Technology*, 80, 78-91, 2018.
[72] Zhang, G., Peng, T., Tong, Y., Gong, Y., Chen, Z., Huang, W., and Dai, B., "Full-scale experiments on the fire smoke extraction from naturally ventilated shafts for shallow-buried urban road tunnels in hot summer", *Tunnelling and Underground Space Technology*, 143, 105441, 2024.
[73] Tanaka, F., Yoshida, K., Ueda, K., and Ji, J., "A simple model for predicting the smoke spread length during a fire in a shallow urban road tunnel with roof openings under natural ventilation", *Fire Safety Journal*, 120, 103106, 2021.
[74] Ji, J., Han, J.Y., Fan, C.G., Gao, Z.H., and Sun, J.H., "Influence of cross-sectional area and aspect ratio of shaft on natural ventilation in urban road tunnel", *International Journal of Heat and Mass Transfer*, 67, 420-431, 2013.

[75] Ji, J., Fan, C.G., Gao, Z.H., and Sun, J.H., "Effects of Vertical Shaft Geometry on Natural Ventilation in Urban Road Tunnel Fires", *Journal of Civil Engineering and Management*, 20, 466-476, 2014.
[76] Yao, Y., Zhang, S., Shi, L., and Cheng, X., "Effects of shaft inclination angle on the capacity of smoke exhaust under tunnel fire", *Indoor and Built Environment*, 28, 77-87, 2019.
[77] Tanaka, F., Kawabata, N., and Ura, F., "Effects of a transverse external wind on natural ventilation during fires in shallow urban road tunnels with roof openings", *Fire Safety Journal*, 79, 20-36, 2016.
[78] Gao, Z., Cai, J., Jiang, L., Mensah, R.A., and Fan, C., "Investigation on the natural smoke exhaust performance by vertical shaft in tunnel fires under different ambient pressures", *Indoor and Built Environment*, 2024.
[79] Cong, H. Y., Wang, X. S., Zhu, P., Jiang, T. H., and Shi, X. J., "Improvement in smoke extraction efficiency by natural ventilation through a board-coupled shaft during tunnel fires", *Applied Thermal Engineering*, 118, 127-137, 2017.
[80] Cong, H.Y., Wang, X.S., Zhu, P., Jiang, T. H., and Shi, X. J., "Experimental study of the influences of board size and position on smoke extraction efficiency by natural ventilation through a board-coupled shaft during tunnel fires", *Applied Thermal Engineering*, 128, 614-624, 2018.
[81] Cong, H., Wang, X., Kong, X., and Xu, H., "Effects of fire source position on smoke extraction efficiency by natural ventilation through a board-coupled shaft during tunnel fires", *Proceedings of the Combustion Institute*, 37, 3975-3984, 2019.
[82] Cong, H., Bi, M., Bi, Y., Jiang, H., Li, Y., and Gao, W., "Experimental and theoretical studies on the smoke temperature distribution along the tunnel ceiling with natural ventilation by the board-coupled shafts", *International Journal of Thermal Sciences*, 159, 106639, 2021.
[83] Zhang, S., Huang, Y., Shi, L., Lin, B., Li, X., Wu, Y., and Wang, J., "A fly-wing smoke screen to improve the smoke exhaustion performance of a vertical shaft in road tunnel", *Tunnelling and Underground Space Technology*, 113, 103983, 2021.
[84] Zhang, S., Liao, S., Shi, L., Lin, B., Liu, J., and Wang, J., "Promotion effect of solid screen on the smoke extraction of vertical shaft in urban road tunnel fire", *Fire Technology*, 60, 1333-1355, 2024.
[85] Ji, J., Li, K., Zhong, W., and Huo, R., "Experimental investigation on influence of smoke venting velocity and vent height on mechanical smoke exhaust efficiency", *Journal of Hazardous Materials*, 177, 209-215, 2010.
[86] Yang, D., Hu, L., Huo, R., Jiang, Y., Liu, S., and Tang, F., "Experimental study on buoyant flow stratification induced by a fire in a horizontal channel", *Applied Thermal Engineering*, 30, 872-878, 2010.
[87] Lougheed, G.D., and Hadjisophocleous, G.V., "The smoke hazard from a fire in high spaces", *ASHRAE Transactions*, 107, 720-729, 2001.
[88] Li, L., Gao, Z., Ji, J., Han, J., and Sun, J., "Research on the phenomenon of plug-holing under mechanical smoke exhaust in tunnel fire", *Procedia Engineering*, 62, 1112-1120, 2013.
[89] Morgan, H., and Gardner, J.P., "Design principles for smoke ventilation in enclosed shopping centres", 1990.
[90] Zhao, P., Yuan, Z., Yu, N., and Liang, C., "Effect of heat release rate and exhaust vent settings on the occurrence of plug-holing during tunnel fires with two-point extraction ventilation", *Tunnelling and Underground Space Technology*, 106, 103617, 2020.
[91] Mei, F., Tang, F., Ling, X., and Yu, J., "Evolution characteristics of fire smoke layer thickness in a mechanical ventilation tunnel with multiple point extraction", *Applied Thermal Engineering*;111, 248-256, 2017.
[92] Ji, J., Huo, R., Hu, L., and Wang, H., "Influence of relative location of smoke exhaust opening to fire source on mechanical smoke exhaust efficiency in a long channel (in Chinese)", *Engineering Mechanics*, 26, 234, 2009.
[93] He, L., Xu, Z., Chen, H., Liu, Q., Wang, Y., and Zhou, Y., "Analysis of entrainment phenomenon near mechanical exhaust vent and a prediction model for smoke temperature in tunnel fire", *Tunnelling and Underground Space Technology*, 80, 143-150, 2018.
[94] Lin, C.J., and Chuah, Y.K., "A study on long tunnel smoke extraction strategies by numerical simulation", *Tunnelling and Underground Space Technology*, 23, 522-530, 2008.
[95] Yi, L., Wei, R., Peng, J., Ni, T., Xu, Z., and Wu, D., "Experimental study on heat exhaust coefficient of transversal smoke extraction system in tunnel under fire", *Tunnelling and Underground Space Technology*, 49, 268-278, 2015.
[96] Zhu, H., Shen, Y., Yan, Z., Guo, Q., and Guo, Q., "A numerical study on the feasibility and efficiency of point smoke extraction strategies in large cross-section shield tunnel fires using CFD

modeling", *Journal of Loss Prevention in the Process Industries*, 44, 158-170, 2016.
[97] Tang, F., Zhu, Y., and Chen, L., "Experimental study on the effect of lateral concentrated smoke extraction on smoke stratification in the longitudinal ventilated tunnel", *Fire and materials*, 44, 1004-1012, 2020.
[98] Jin, J., and Jiang, X., "A study of the characteristics of smoke stratification in lateral point smoke exhaust tunnel", *Fire safety journal*, 140, 103833, 2023.
[99] Yang, J., Pan, X., Wang, Z., Hua, M., and Jiang, J., "Numerical study on the smoke flow characterization and phenomenon of plug-holing under lateral smoke exhaust in tunnel fire", *Journal of Applied Fluid Mechanics*, 11, 115-26, 2018.
[100] Zhong, W., Sun, C., Bian, H., Gao, Z., and Zhao, J., "The plug-holing of lateral mechanical exhaust in subway station: phenomena, analysis, and numerical verification", *Tunnelling and Underground Space Technology*, 112, 103914, 2021.
[101] Wang, Z., Ji, J., Tan, T., Gao, Z., Zhou, Y., and Zhou, F., "Numerical study on the critical criterion for predicting the plug-holing under lateral mechanical exhaust in tunnel fires: Considering the effect of smoke flow in longitudinal direction", *Tunnelling and Underground Space Technology*, 128, 104666, 2022.
[102] Liu, Q., Xu, Z., Fan, C., Tao, H., Zhao, J., and He, L., "Experimental and numerical study of plug-holing with lateral smoke exhaust in tunnel fires", *Fire technology*, 60, 1357-1377, 2024.
[103] Zhu, Y., Tang, F., and Huang, Y., "Experimental study on the smoke plug-holing phenomenon and criteria in a tunnel under the lateral smoke extraction", *Tunnelling and Underground Space Technology*, 121, 104330, 2022.
[104] Xu, Z., Liu, Q., He, L., Tao, H., Zhao, J., Chen, H., Li, L., and Fan, C., "Study on the heat exhaust coefficient and smoke flow characteristics under lateral smoke exhaust in tunnel fires", *Fire and materials*, 43, 857-867, 2019.
[105] Liu, Q., Xu, Z., Zhu, J., Tagne, S.M.S., Mahmood, S., and Xie, B., "Study of the impact of the distance between the lateral exhaust vent and ceiling on heat exhaust coefficient and air entrainment in tunnel fires", *Tunnelling and Underground Space Technology*, 148, 105766, 2024.
[106] Xu, P., Xing, R., Jiang, S., and Li, L., "Theoretical prediction model and full-scale experimental study of central smoke extraction with a uniform smoke rate in a tunnel fire", *Tunnelling and Underground Space Technology*, 86, 63-74, 2019.
[107] Vauquelin, O., and Telle, D., "Definition and experimental evaluation of the smoke "confinement velocity" in tunnel fires", *Fire safety journal*, 40, 320-330, 2005.
[108] Tanaka, F., Majima, S., Kato, M., and Kawabata, N., "Performance validation of a hybrid ventilation strategy comprising longitudinal and point ventilation by a fire experiment using a model-scale tunnel", *Fire safety journal*, 71, 287-298, 2015.
[109] Chen, L. F., Hu, L. H., Tang, W., and Yi, L., "Studies on buoyancy driven two-directional smoke flow layering length with combination of point extraction and longitudinal ventilation in tunnel fires", *Fire safety journal*, 59, 94-101, 2013.
[110] Chen, L. F., Hu, L. H., Zhang, X. L., Zhang, X. Z., Zhang, X. C., and Yang, L. Z., "Thermal buoyant smoke back-layering flow length in a longitudinal ventilated tunnel with ceiling extraction at difference distance from heat source", *Applied Thermal Engineering*, 78, 129-135, 2015.
[111] Tang, F., Li, L. J., Mei, F. Z., and Dong, M. S., "Thermal smoke back-layering flow length with ceiling extraction at upstream side of fire source in a longitudinal ventilated tunnel", *Applied Thermal Engineering*, 106, 125-30, 2016.
[112] Tang, F., He, Q., Mei, F., Wang, Q., and Zhang, H., "Effect of ceiling centralized mechanical smoke exhaust on the critical velocity that inhibits the reverse flow of thermal plume in a longitudinal ventilated tunnel", *Tunnelling and Underground Space Technology*, 82, 191-198, 2018.
[113] Wang, J., Yuan, J., Fang, Z., Tang, Z., Qian, P., and Ye, J., "A model for predicting smoke back-layering length in tunnel fires with the combination of longitudinal ventilation and point extraction ventilation in the roof", *Tunnelling and Underground Space Technology*, 80, 16-25, 2018.
[114] Tang, F., Mei, F. Z., Wang, Q., He, Z., Fan, C. G., and Tao, C. F., "Maximum temperature beneath the ceiling in tunnel fires with combination of ceiling mechanical smoke extraction and longitudinal ventilation", *Tunnelling and Underground Space Technology*, 68, 231-237, 2017.
[115] Zhang, X., Xu, Z., Ni, T., Peng, J., Zeng, J., and Ran, Q., "Investigation on smoke temperature distribution in a double-deck tunnel fire with longitudinal ventilation and lateral smoke extraction", *Case Studies in Thermal Engineering*, 13, 100375, 2019.

Engineering Practice of Tunnel Fire Safety

Igor Maevski, PhD, PE
Jacobs, New York, USA, ASHRAE Fellow

ABSTRACT

The paper discusses previous practice, current practice, and trends for future engineering practice of tunnel Fire Safety systems design and operation. This includes historical information and development of engineering practice. Paper addresses fire prevention; fire detection; egress; tunnel ventilation; fixed firefighting and standpipe systems; and emergency response. New energy carriers, development of new tunnel construction technology; faster transportation needs; sustainability and energy saving pose additional challenges to tunnel fire safety practice. Paper discusses numerical modelling and importance of full-scale fire tests to verify models and technology and to address needs for engineering practice.

KEYWORD: emergency communication, point of safety, smoke management, standpipe, Saccardo ventilation system, critical velocity, water supply, water based fixed firefighting system.

PAST ENGINEERING PRACTICE OF TUNNEL FIRE SAFETY

Tunnel engineering and fire safety practice is over a century old. The oldest railway tunnel ventilation is found in the Summit tunnel in England built in 1841. The first known train fire in tunnel was in 1842 in a Menden tunnel, in France, which led to 150 fatalities. The first railway tunnel mechanical ventilation system was constructed in 1886 for Mersey railway tunnel of 1600 m (5250 ft) long. Longitudinal ventilation was provided with fresh air introduced at each of two stations designed on the basis of 18 kg (40lb) of coal burning per mile train travel and NO_2 emission of 1.8 m^3/kg (29 ft^3/lb) of coal. In 1898 Marco Saccardo patented an "Improved Method and Apparatus for Ventilating Tunnels" where he described the use of portal ring air jets to ventilate railway tunnel as shown in Figure 1. Saccardo ventilation was first applied in Italian tunnel in 1894 and then described for Gotthard Rail tunnel in 1899. Nowadays, more than a Century since then, Saccardo ventilation concept still remains the state-of-the art of engineering practice of tunnel ventilation for railway and road tunnels. Any nozzle airflow discharged into the tunnel at a small angle is used to call Saccardo ventilation, which differs from the method patented by Mr. Saccardo.

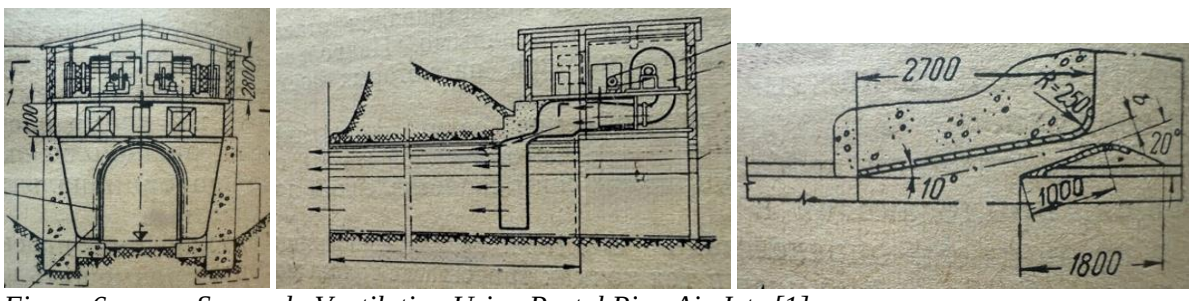

Figure 6 Saccardo Ventilation Using Portal Ring Air Jets [1].

The first passenger commuter railway tunnel ventilation system was installed in London tube in 1864 so-called ozonisers (air purifiers), which supplied fresh air to stations charging with ozone. This system was later abandoned and replaced with exhaust ducted tunnel ventilation system. To augment

this "piston-action" ventilation, fresh air was blown through shafts enclosed in staircase wells. In 1904 the first New York Subway from City Hall to 145th street was opened, which was built with no mechanical ventilation. However, during the summer of 1905 subway system developed hot air temperatures in tunnels, and fan chambers with central exhaust fans and flues were built between stations to remove heat. Fan capacity varied between 10 m^3/s (21,000 cfm) and 50 m^3/s (110,000 cfm). Piston effect of trains in tunnels was in-depth studied by G. Abramovich and published in 1939 [2]. Train piston-action ventilation augmented by mechanical longitudinal ventilation as needed remains in the engineering practice for metro tunnels and stations. The first known metro fire happened in 1903 in Couronnes metro in France, which led to eighty-four fatalities.

The first road tunnel ventilation fan plant was installed in 1922 for the Blackwall Tunnel under the Thames River in London capable of supplying 14 m^3/s (30,000 cfm) of air under the roadway to the middle of the tunnel. The single lane Elbe tunnel of 426.5 m (1,400 ft) long in Hamburg, Germany was opened in 1911 for vehicles and pedestrians; and had no mechanical ventilation but used elevators to transport vehicles between the tunnel roadway and the street surface.

In 1919 plans were under development by Clifford Holland to build a 2580 m (8,463 ft) long Holland tunnel in New York under the Hudson River, which was opened in 1927. No horse-drawn vehicles were allowed to pass through the tunnel. This tunnel was designed with tunnel ventilation system capable of exhausting gases from motor vehicles, such as carbon monoxide. It was determined that methods of tunnel ventilation used for railway tunnels, of blowing fresh air through the tunnel from one portal to the other could not be applied to road tunnel since air velocities would be excessive for the amount of ventilation air required, causing discomfort for traveling public, but also creating a hazard in case of fire in the tunnel. Investigations were carried out and based on measurements in a test tunnel, Ole Singstadt developed methodology and engineering equations for calculation of required fresh air and uniform air distribution along the ducts for full transverse tunnel ventilation system and published in 1929 [3]. Those equation were applied to design of Holland Tunnel and verified through testing between November 13, 1927, and March 12, 1929. For more than two decades tunnel ventilation systems were designed based on that data. As such, the full transverse ventilation system with 4 ventilation shafts (two on each side of the river) was introduced, eliminating the longitudinal airflow along the tunnel. This system was used later for most of the long US tunnels until the Memorial Tunnel Fire Tests were complete and proved eligibility to use jet fans and longitudinal system for road tunnels.

The first known major road tunnel fire happened in 1949 in Holland tunnel, which involved a truck carrying carbon bisulphate (in violation of regulations) [4]. A large fire developed which generated very long flames and ignited vehicle 100 m away. The fire department was unable to attack the fire due to dense smoke, strong heat and darkness and had to wait for the vehicles to burn out. No one was killed, although sixty-six people were injured and several people had to be rescued. Twenty-three vehicles were involved in the accident. The stream of fresh air from the supply air duct near the roadbed was a big help to the fleeing people and to firefighters, who put their heads to supply air flues to breath. Two thirds of the exhaust fans failed due to overheating. There was substantial damage to the tunnel ceiling and side wall lining due to fire.

In 1924, a twin tube (2 lanes in each direction) Liberty Tunnel in Pittsburgh, PA, which is 1775 m (5,823 ft) long was opened to traffic with longitudinal airflow in the direction of traffic. The mechanical vent plant was in the shaft in the middle of the tunnel. Fans exhaust air entering though the entrance portal in the middle of the tunnel, while another set of fans blow fresh air into the tunnel through nozzles pointing towards the exit portal. Lack of positive control and high air velocities were noted during the tests. The third street tunnel in Los Angeles, CA is 323 m (1,059 ft) long was completed in 1901 and was ventilated by two shafts equipped with exhaust fans providing approximately four air changes per hour was deemed insufficient under heavy traffic and two additional shafts were necessary to build later.

The Fixed Guideway Transit Systems Technical Committee was formed in 1975 and began work on

the development of NFPA 130 Standard [5]. One of the primary concerns of the committee in the preparation of this document centred on the potential for entrapment and injury of large numbers of people who routinely use these types of mass transportation facilities. During the preparation of the first edition of this document, several significant fires occurred in fixed guideway systems, but fortunately the loss of life was limited. In 1983 the first edition of NFPA 130 ”Standard for Fixed Guideway Transit Systems” was developed and adopted. Since then, NFPA 130 became the main standard which defines engineering practice for railway tunnels.

In 1965 Swiss Federal Bureau conducted fire simulation tests in the Ofenegg Tunnel (single track railroad tunnel). Using the data from the test intended to simulate the fire which could result from a collision of two passenger cars results concluded ventilation requirement of 0.15 m^3/s/lane/m (100 cfm / lane / foot) to remove smoke and soot from the tunnel. This requirement was published by ASHRAE [6] as a recommendation and was used for many years until it was revisited by NFPA 502 Standard [7]. Tests included application of sprinkler system in tunnels and documented challenges of their operation.

A tentative standard, NFPA 502T, Standard for Limited Access Highways, Tunnels, Bridges, and Elevated Structures, was prepared by the Technical Committee on Motor Vehicle Fire Protection and was adopted by the National Fire Protection Association on May 16, 1972. It was withdrawn in November 1975. In 1980, the committee rewrote the document as a recommended practice and included a chapter on air-right structures, which was adopted at the 1981.

Since 1961 several road tunnels have been fitted with a longitudinal ventilation system employing small jet blowers attached to the walls or the roof. In 1960-ies jet fans were installed in several relatively short road tunnels less than 1000 m (3280 ft) long in Europe and in Japan. Those include Munich Airport underpass on Munich-Salzburg autobahn, the Stuttgart airport runway underpass, Dutch Heinenoord Tunnel, a 735 m (2,411 ft) road tunnel in Caracas, Venezuela, and Okuda Tunnel in Japan. In 1937 a dissertation was published by Henschko in German language on “investigation on an improved Jet blower for tunnel ventilation” [8].

Initially tunnel ventilation was primarily designed for dilution of tunnel emissions. Physical modelling including wind tunnel modelling was widely used to study aerodynamics and ventilation of tunnels as shown in Figure 2.

Figure 2 Physical Modeling Experimental set-up.

However, the Holland Tunnel chemical fire served to sound a general alert on the need to implement proper control of foreseeable fire hazards by regulation of dangerous traffic. Vehicle fire and fuel explosion considerations were taken into consideration for the calculation of air requirements for St. Gotthard Road Tunnel project in 1972.

The fire risks in tunnels were examined in 1942 for the Alpine Road tunnel. Many countries use risk analysis as a tool to design tunnel fire life safety systems. It is important not to misinterpret results of the risk assessment models. For example, a probabilistic risk assessment was conducted for the

Channel Tunnel, which concluded: The total estimated rate of fatalities amongst passengers and staff in the Channel Tunnel is less than 6%. This may be seen alongside the fact that there have been several major fires since it opened in 1994.

The first fire control by automatic deluge water sprinkler system was installed in Seattle, WA in 1952 for 672 m (2200 ft) long Battery Street tunnel on SR99. George Massey Tunnel built in 1959 in Vancouver, British Columbia was also equipped with sprinkler system. Although the benefits of fire sprinkler systems in buildings have been widely recognized for over 100 years, they have not been used in many countries in tunnels for many years after Ofenegg tunnel tests. Sprinkler systems have been routinely used in Japanese tunnels since the 1963, and in Australian tunnels since early 1992 in the Sydney Harbor tunnel, however the use and effectiveness of fixed water-based fire-fighting systems in road tunnels were not universally accepted. In Japan, fixed water-based fire suppression systems are required in all tunnels longer than 10,000 m (32,808 ft) and in shorter tunnels longer than 3000 m (9843 ft) with heavy traffic. In 1989 the first deluge water based fixed firefighting system with 3% foam additives was installed in I-90 Mount Baker Ridge and First Hill Mercer Island tunnels in Seattle due to risk of flammable liquid tanker or hazardous materials vehicles fire since they are allowed for the unescorted passage. In 1999, the World Road Association (PIARC) stated that "sprinklers (FFFS) are generally not considered as cost effective and are not recommended in usual road tunnels"; however, severe fires in road tunnels in Europe have focused attention on the issue of fixed fire-fighting systems in road tunnels [9].

The first tunnel fire alarm system was installed in the Kanmon vehicular tunnel, which connects Honshu to Kyushu in Japan, and was opened to traffic in March 1958.

The first full scale series of experiments on automobile fire were performed in 1968 and 1969 in Japan for the purpose of understanding the state of tunnel fires by burning several cars and trucks in an actual road tunnel of384 m (1260ft) long) on the old Kuriko National Highway. Features of fires, temperature distribution in the tunnel, generation of hazardous gas, influence on the tunnel lining and so forth were studied in relation to the wind velocities in the tunnel.

Safety studied for road tunnels in 1967 concluded on the need of emergency exits in road tunnels and that the existed safety precautions were not sufficient to safeguard human life if fire breaks out. The Wallring tunnel in Hamburg, Maas Tunnel in Rotterdam and the Osterleden tunnel in Stockholm were first to include emergency exits such as a pedestrian tunnel which provides an escape route for drivers in case of fire. Studies examined type of ventilation system and possibilities of containing the fire by reversing the direction of air flow in crossflow ventilated tunnels.

For years the design of subway ventilation system was based on a rule of thumb. But in 1970's through the USDOT funding, the Subway Environment Simulation (SES) computer program was developed [10]. Since then, subway tunnel ventilation systems were designed using analytical means to enable more accurate assessment of the fire risk and ventilation response. This software was validated against full scale tests in many Metro tunnels. Analytical models were also developed in Europe by private companies. It was suggested that air velocity past the fire should be greater or equal to critical velocity in order to control the direction of spread of smoke and hot gases and push them downstream so that patrons could find a safe evacuation path upstream. If the air velocity is less than critical, backlayering will occur and smoke and hot gases will spread in the upstream direction endangering safety of the evacuating patrons and firefighters' access.

In 1958 Thomas proposed that the velocity head of fresh airflow should be comparable or greater than the buoyancy head of smoke flow in order to prevent backlayering and defined a critical Froude number [11]. In 1982 N. Danziger and W. Kennedy recommended using a critical Froude number of 4.5 for tunnels based on model scale experiments performed by Lee et al published in 1979. The total Heat Release Rate was replaced by the convective with the fractional convective heat reduction due to radiation. A correction for the tunnel slope was also introduced [11]. Equations were validated against the Memorial Tunnel Fire Tests results. Tests with fire sizes from 10 to 100MW were conducted from

September 1993 through March 1995. Since then, discussions on Critical Velocity and experimental results of Memorial Tunnel Fire Tests due to influences of blockages are on-going. There are many semi-empirical approaches based on dimensional or non-dimensional models. Several revisions to the methods of calculating critical velocity was made and likely will be made in the future.

In 1979 US DOT Federal Highway Administration issued TUNVEN and DUCT programs for calculations of tunnel ventilation systems in road tunnels along with reports Management of Air Quality in and Near Highway Tunnels [12]. The TUNVEN program solves the coupled one-dimensional steady-state tunnel aerodynamic equations to predict tunnel air velocities and concentration of different gasses for a wide range of tunnel designs, traffic loads and external ambient conditions. The DUCT program models the airflow through the ports for uniform air distribution through the ports and is limited to semi-transverse tunnel ventilation system.

In 1991 N. Rhodes, et al presented a paper [13] on Prediction of Smoke Movement Using CFD, where the acronym stands for Computational Fluid Dynamics. This was one of the first CFD applications for fire smoke management in tunnels. Since then, CFD became the software of choice for modelling tunnel fires and tunnel ventilation and suppression systems.

PRESENT ENGINEERING PRACTICE OF TUNNEL FIRE SAFETY

Present engineering practice is based on the engineering standards and guidelines. Standards accumulate best knowledge and practice of over a Century of fires in tunnels, or emergency responses, tunnel operations and maintenance. Each country has its own guidelines and standards [9]. In North America, NFPA standards such as NFPA 130 Standard for Fixed Guideway Transit and Passenger Rail Systems 2023 edition [5] and NFPA 502 Standard for Road Tunnels, Bridges, and Other Limited Access Highways 2023 edition [7] establish minimum fire protection and fire-life safety requirements, and are the most commonly used. Figure 3 shows an example of typical fire life safety systems for road and railway tunnels. Requirements for systems, equipment, construction, testing, commissioning, operation and maintenance can be found in ASHRAE Standard 217 [14] 2020 edition. NFPA standards are often referenced worldwide. While NFPA Standards committees make attempts to make those standards more performance based, many prescriptive requirements can be found in those documents, which could be considered strength or weakness of those documents.

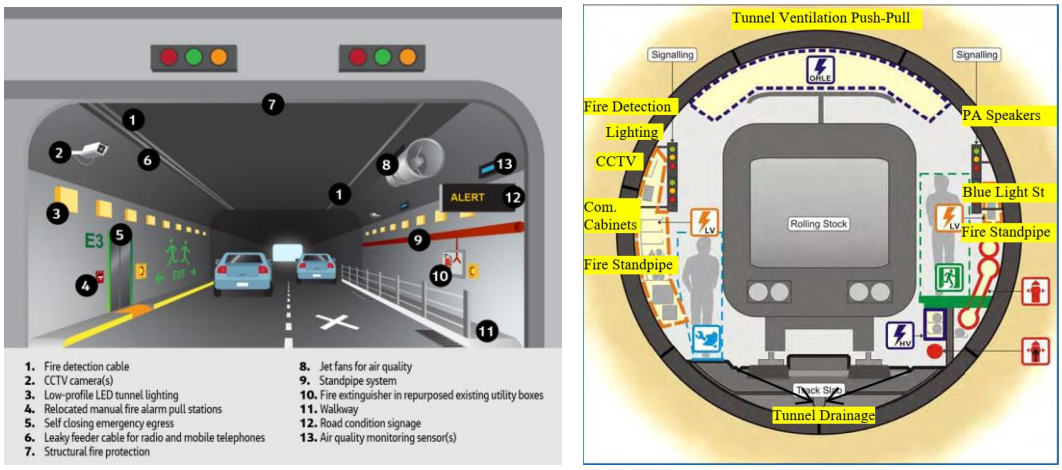

Figure 3 Example of Typical Fire and Life Safety Systems in Road and Rail Tunnels.

NFPA issues Fire Protection Handbook. The current 21 edition published in 2023 includes Chapter 10 Section 21 “Road Tunnels and Bridges” [9], which addresses engineering practice and unique fire protection and life safety considerations and challenges posed by road tunnels and bridges. Chapter 7

Section 21 “Fixed Guideway Transit and Light Rail Systems” [15] provides similar information on transit tunnels and underground stations. The handbook does not replace NFPA or other standards, but rather supplements providing best engineering practice discussion. Additional information can be found in ASHRAE Applications Handbook chapter on Enclosed Vehicular Facilities [6], in the Subway Environmental Design Handbook [10], in Tunnel Engineering Handbook, SFPE Handbook, and in the Transportation Research Board of the National Academies National Cooperative Highway Research Program Synthesis Studies (NCHRP) Reports, such as #415 Design Fires in Road Tunnels[16]; #836 “Guidelines for Emergency Ventilation Smoke Control in Road Tunnels [17]; #525 “Making Transportation Tunnels Safe and Secure” [18] and etc.

Publications of World Road Association (PIARC) are an excellent source of information on global current engineering practice of tunnel fire safety. EU Directive 2004/54/EC on minimum safety requirements for tunnels in the Trans- European Road network [19]; Australian Standard 4825 “Tunnel Fire Safety”, Japanese standard “Ventilation Technology Standard in Road Tunnels” and other national standards.

Many countries use qualitative and/or quantitative risk analysis based on fire hazard analysis to determine means of protection needed for tunnel fire safety [20]. This method allows for more economic approach and can lead to additional tunnel fire safety measures, or to measures which allow to reduce tunnel fire safety risk to as low as reasonably practical. Cost-benefit analysis is very effective for rehabilitation of existing tunnels.

Engineers over the globe share their practices of tunnel fire safety at International Conferences. The most known of them are International Symposium on Tunnel Safety and Security organized by RISE since 2004; International Symposium on Aerodynamics, Ventilation and Fires in Tunnels organized by BHR Group since 1973; International Conference “Tunnel Safety and Ventilation “organized by Graz University of Technology since 2002.

The following are the primary objectives of tunnel fire protection:

- Permit and encourage safe evacuation from the tunnel
- Facilitate the entrance of firefighting and first responders personnel into the tunnel to combat the fire
- Protect the tunnel structure and facilities from structural collapse.

An effective tunnel fire protection system program must contain the following elements:

- Prevention of a major fire event
- Fire identification, detection, and verification,
- Emergency communications
- Evacuation and rescue
- Smoke management
- Fire suppression
- Emergency response planning

Fire Prevention

Prevention of fire ignition and fire spread is of paramount importance. Fire prevention measures take place through reduction of risk of fires, restriction usage of combustible or flammable materials for tunnel construction and operations, fire hardening of vehicles and tunnel structures.

Railway vehicles are the primary fire hazard in railway tunnels. Construction and materials used in rolling stock are regulated by international standards such as NFPA 130 [5], EN 45545-1-7 and AS 7529.3. The objective is to minimize, control and isolate ignition sources, minimize combustible materials and reduce possible fire size through material selection and compartmentation. Fire barriers on rail vehicles include floors that resist spread of potential undercarriage fire to passenger compartment, partitions and equipment lockers. Some standards require traction and breaking train systems to be designed such that during a fire event, the train can proceed to a safe area.

Enclosed trainways and tunnels are required to be non-combustible construction and shall withstand high temperature requirements. Many single-track tunnels are separated from the adjacent bore through fire-resistance-rated walls or underground geological material, while connected via cross passages equipped with fire rated doors.

Many stations are equipped with full height platform screen doors, which could provide a physical separation between the station and the train guideway. Ancillary station spaces are also physically separated from public areas by fire resistance rating construction. Trash receptacles have been removed from platform areas in many stations to minimize the risk of ignition. Blast-resistant trash receptacles have been developed.

Road vehicles are getting safer as well, however it is difficult to regulate combustible loads traveling through road tunnels. Traffic control, which is part of prevention of a major fire event and traffic management is an effective road tunnel fire protection system program. Many tunnels do not allow traveling HAZMAT materials. Some do not allow flammable, combustible (fuel tankers), hydrogen vehicles and other dangerous goods to travel through. This reduces the potential fire size in road tunnels, which reduces consequences of such fires on traveling public and tunnel structural integrity.

However, taking all mitigation measures to prevent fires, we are unable to completely prevent fires in tunnels and stations. Once fire ignites, it is critical to detect it in a timely manner to initiate timely evacuation, timely activate fire life safety systems and get help from first responders to attack fire and rescue people.

Fire Detection

Fire protection system must be able to readily identify, detect and verify location of a fire anywhere within the tunnel. Determining the location of the fire in a timely manner is critical to safe evacuation, since the success of many companion fire and life safety systems such as smoke control (ventilation) and deluge fixed firefighting system activation depend on knowing where the fire is within the tunnel to permit the appropriate operational response.

Most transit tunnels are not equipped with automatic fire detection system, but rather rely on train operator communication with the control room and on blue light stations, which indicate emergency phone locations. With new development of more reliable means of fire detection, critical risky transit tunnels are equipped with linear heat detection for early temperature rise from fire heat detection, and with aspiration systems for smoke and products of combustion detection. Those fire detection systems do not necessarily automatically activate fire protection systems, but rather create an alarm to help control room operator to focus on relevant CCTV cameras and verify fire conditions.

Enclosed stations are protected by an addressable fire alarm system that is designed and installed in accordance with NFPA 72. Automatic fire detection is provided in all ancillary spaces. Public address system alerts and directs station occupants in the event of emergency. Occupants can report on fire emergency through the voice alarm communication devices located throughout the stations.

A reliable means to identify, detect and verify a fire incident location is required by NFPA 502 in all road tunnels over 90 m (300 ft). An automatic fire detection system in road tunnels, where provided, shall be able to provide detection in the early stages of a developing fire and detect a tunnel fire incident of 5 MW or less within 90 seconds or better in a testing environment of 3 m/sec (590 fpm) air velocity. Automatic fire detection shall be capable of identifying the location of fire within 15 m (50 ft). The key objective of the automatic tunnel fire detection and warning systems is to provide prompt, accurate, and reliable fire detection while preventing nuisance alarms.

Depending on the nature of the fire, any of the following can start developing first: smoke, flame, or heat. Consequently, multi-sensor alarm systems are better suited for automatic control. The most common tunnel fire detection principles are based on the fire products parameters and could be applied

individually or in combination:

- Smoke and combustion gases
- Heat
- Flames (radiation).

There are a range of methods available to detect fire and smoke within road tunnels including: linear (line-type) heat detection (LHD), CCTV video image smoke detection, flame detection, smoke and heat detectors, spot-type heat detectors, and smoke and gases detection and etc. The selection of the type of fire detection system(s) should be made depending on the fire safety goals/objectives and the overall fire safety strategy, which includes notifying occupants to allow for safe evacuation, modifying tunnel operations, initiating fire life safety systems operations, and notifying emergency responders. Application different types of fire detection systems in a tunnel significantly enhances the fire detection capabilities and tunnel fire safety. For example, installation of a linear heat detection system along with infra-red fire/smoke detection (IR) cameras equipped with CCTV ensures that air cooled fires or shielded fires will be detected in a timely manner and verified by the operator.

Recent live fire tests in road tunnels (see Figure 4) proved that fiber-optic type linear heat detection systems and infra-red fire/smoke detection cameras systems can reliably detect road tunnel fires under different tunnel conditions, while producing no or limited nuisance alarms depending on the devices sensitivity and set points. Linear heat detectors, infra-red flame detectors are the most applicable forms of automatic fire detection systems for road tunnels. Impact of natural ventilation has to be analysed when selecting the fire detection device.

Double looped redundant fiber-optic linear heat detection systems are the most commonly used devices for fire detection in tunnels. Fiber-optic Linear Heat Detectors consist of a control panel and quartz optical fibers. The control unit houses a laser that sends a beam through the fiber-optic cable. These systems provide detection using the Raman-Effect which senses temperature changes by evaluating the amount of light scattered. The rate of raise of temperature is adjustable and defines sensitivity. Fiber-optic cable suitable for harsh environments can be routed around obstructions with the single cable length up to 10 km (6.2 mi) and easy for installation. Some manufacturers of these systems claim a useful system life of 30 years.

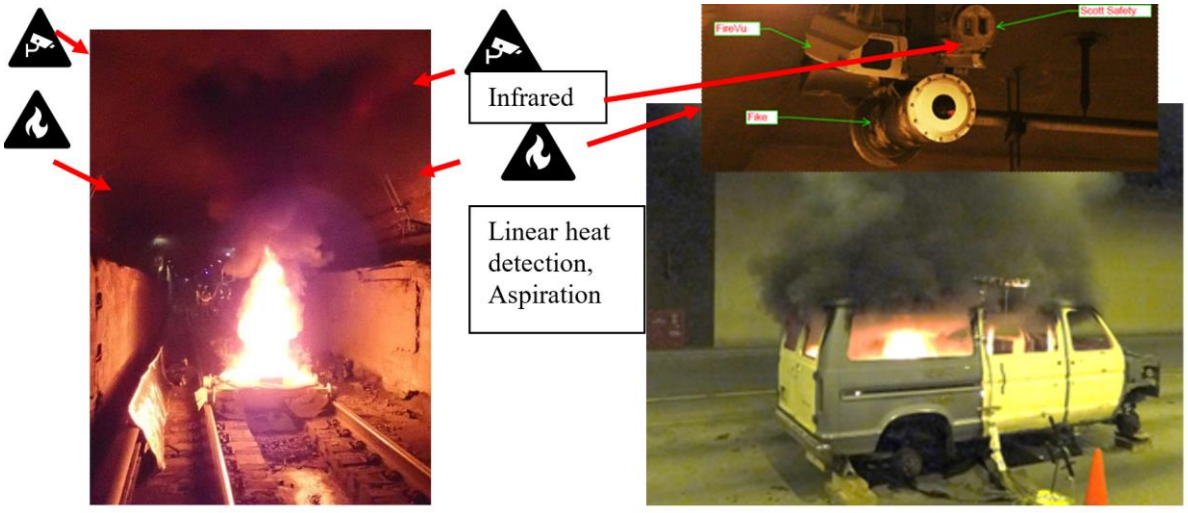

Figure 4. Recent full scale fire tests performed by Jacobs in railway tunnel (2019) and road tunnels (2012 -2014).

There are disadvantages to using linear heat detectors. Their performance can be impacted by tunnel airflow which cools down air temperature, moves heat along the tunnel, and reduces the rate of rise of the air temperature. Some models require replacement of the heat detection cable after a fire event. If the objective is to detect a fire from a moving vehicle, the design will need to assess whether the cable will be heated sufficiently as the vehicle moves to activate the alarm. In addition to airflow,

considerations should be given to shielded fires initiated inside or under vehicles or under vehicle's hood, which makes rapid heat detection at the tunnel ceiling level difficult.

Besides the automatic fire detection systems, fire can also be detected by the tunnel operator using Closed Circuit Television (CCTV) pan-tilt-zoom cameras installed in tunnels; by tunnel users notifying the operator using emergency phones installed at all cross-passages and other means of egress; or from tunnel users calling and notifying emergency services about the tunnel fire using cellular phone devices. Noise level within the tunnel roadway may pose difficulties for clear voice communications. CCTV and cellular phones notifications with capability for signal reception in tunnels, although not listed fire detection devices, has proven to be one of the most effective means for identifying and verifying a fire within a road tunnel. NFPA 502 considers CCTV monitoring an acceptable means to identify and locate fire if the tunnel is fully monitored by dedicated staff on a 24-hour basis.

There is an on-going debate if automatic fire detection system is needed for those tunnels or manual detection through CCTV cameras is sufficient. Human factor of tunnel operators needs to be taken into consideration. All tunnels equipped with automatic water based firefighting system and unmanned tunnels need automatic fire detection. Automatic fire detection does not necessarily mean automatic activation of the FLS systems, since verification to avoid nuisance alarms is still desirable.

Fire Emergency Response Procedures and Egress of Tunnel Users

An effective emergency response plan is most important from a safety viewpoint and includes the interaction of not only the operators of the tunnel but of all outside agencies that might become involved in an emergency response to a tunnel incident. Provisions should be made for tunnel access for outside aid services, and procedures for utilizing such access need to be included in the emergency response plan. Appropriate precautions should be taken at the points of entry to alert and control traffic to allow safe entrance by emergency equipment.

In the event of a train fire, the operators are often instructed to bring burning train to station, or outside the tunnel, or other relatively safe location, where evacuation is much easier. If train is disabled, passengers should leave the train and often rescue train should assist in evacuation. Tunnel evacuation by foot is typically the last resort. For this purpose, tunnels are typically equipped with means of egress to a point of safety. Such means of egress may include pressurized egress stairs, egress corridors or cross passages leading to a non-incident tunnel. Ventilation system shall provide smoke-free environment for evacuees, while directional signage and emergency lighting shall navigate to safe exits. In mass transit tunnels evacuation should be supervised and managed, which differs from road tunnels where self-evacuation takes place (except special or bus tunnels).

It is impossible to enforce to drive the burning vehicle out of the road tunnel. In addition, often road tunnel fires happen due to collisions or when vehicles are disabled. Emergency communications should permit the operator to communicate with the motorists within the tunnels and permit emergency responders to communicate with each other during an emergency in the tunnel. Emergency communication devices should have the following features:

- Conspicuous by means of indicating lights or other suitable markers
- Identified by a readily visible signs
- Posted with suitable instructions for use by motorists
- They shall be located in approved locations so that motorists can safely park vehicles.
- Shall be protected from physical damage from vehicle impact.
- Shall be connected to an approved constantly attended location.

Speech intelligibility during an emergency should be considered in the development of the facility and in the emergency response plan. A minimum level of speech intelligibility should be maintained along the emergency evacuation paths to allow for effective communication among first responders and between first responders and stranded or evacuating motorists. Speech intelligibility becomes difficult in background sound pressure levels exceeds 85 dBA. Other means of reliable communication such as

strobes or wayfinding signalling could be applied to support emergency communication and egress.

Loudspeakers are prevalent in many European road tunnels. These systems are used to alert the motorists of an emergency situation and to provide directions and guidance. The use of loudspeakers in road tunnels is not a universally accepted safety concept. There are several problems with their application to the tunnel environment, including the following:

- Hard surfaces within the tunnel roadway make it difficult to understand most announcements
- Motorists' vehicles and first responders moving
- Vehicle windows often closed (due to air conditioning)
- Potential language barriers

Radio communication systems, such as highway advisory radio (HAR) and AM/FM commercial station overrides can be an effective means to communicate an emergency to motorists and to provide them with direction.

Regardless of type, all communications and messaging systems used within road tunnels should be capable of real-time composition and selection by the emergency response authority. All areas planned for use of emergency refuge or assembly should be equipped with reliable two-way voice communication with the emergency response authority.

Means of egress in road tunnels are similar to mass transit tunnels, while due to self-rescue approach, communication and notification of tunnel occupants is getting more critical. A point of safety is defined as an exit enclosure that leads to a public way or safe location outside the structure, or an at-grade point beyond any enclosing structure, or another area that affords adequate protection for motorists [7]. Thus, in the case of a road tunnel, the potential points of safety are the outside, the properly protected longitudinal egress corridor and a safety refuge (if one is provided). The potential egress paths would include the roadway free from smoke, the pressurized cross passages, the emergency exits, the longitudinal egress corridor or parallel smoke-free egress tunnel and the safety refuge. The egress path must be provided with a tenable environment for a sufficient period of time to permit motorist evacuation from the incident bore.

Mobility impaired people would likely need assisted rescue, while relatively safe staging areas equipped with proper communication devices is often provided for those people throughout the means of egress.

Tunnel Ventilation

The primary purpose of tunnel ventilation systems in a tunnel fire emergency is to control and/or remove the heated gases and smoke from the egress path. However, it is well known that oxygen supports the combustion process and ventilation may further spread the fire. This generates the questions: To blow or not to blow? Can reliable evacuation system replace the need for tunnel ventilation, or can a strong reliable ventilation replace the need for the robust egress system?

Tunnels with natural ventilation only (no fans) primarily rely on both the ambient meteorological conditions and on the piston effect generated by the moving traffic to maintain a satisfactory environment within the tunnel during normal operations. However, to handle a fire-based emergency within the naturally ventilated tunnel, an emergency ventilation system may be needed. In essentially all emergency cases, protection of tunnel users is enhanced by prompt activation of emergency ventilation procedures as planned in advance.

Transit tunnels typically implement longitudinal ventilation system, where airflow is directed along the tunnel by introducing at one end and leaving in the other tunnel end. Such system directs smoke and hot gases along the tunnel in a predetermined direction, while allowing evacuees to move towards the fresh airflow to the nearest exit. It also supports firefighters access from the side of fresh airflow. Ventilation equipment is often installed at both ends of the station protecting station occupants from the oncoming tunnel smoke. Those fans are often used for station ventilation.

Type of station ventilation depends on station geometry and presence of platform screen doors. Often Over-Track Exhaust (OTE) system is found effective for station train fire as well as for train heat removal. In any case the objective of station ventilation is to maintain path of passengers' evacuation free from smoke and to extract smoke and hot gases from the fire origin.

NFPA 502 [7] requires the emergency ventilation for all road tunnels over 300 m (1000 ft) in length. For tunnels less than 300 m (1000 ft) in length engineering analysis are required to demonstrate that the level of safety provided by a mechanical ventilation system can be equalled or exceeded by enhancing the means of egress, the use of natural ventilation, or the use of smoke storage, and shall be permitted only where approved by the authority having jurisdiction. Engineering analysis for naturally ventilated short tunnels may need to demonstrate that tunnel occupants can safely leave the tunnel before ventilation could take smoke under control and smoke will be stratified leaving tunnel portals allowing first responders to access the fire site. Because of the number of different parameters that need to be considered in order to decide if mechanical ventilation is to be installed in a tunnel (length, location, traffic, type of vehicles using the tunnel, risks, and so forth), it is not possible to express universal recommendations about the limits of natural ventilation, particularly the allowable length without mechanical ventilation.

The systems used for mechanical, or fan-driven, road tunnel ventilation can be classified as longitudinal or transverse (fully transverse, semi-transverse, combination of, or modifications of the schemes). A longitudinal ventilation system achieves its objectives through the flow of air along the tunnel roadway, while a full or semi- transverse ventilation system achieves its objectives by means of continuous uniform distribution, collection, or simultaneous distribution and collection of air throughout the length of the tunnel roadway. There are also many combinations of different types of basic ventilation such as "single" point extraction, ventilation with intermediate shafts, etc.

Longitudinal ventilation is the most popular system for tunnels with free flowing uni-directional traffic in which air is introduced into or removed from the tunnel roadway at a limited number of points (such as at a portal or a shaft), thus creating a longitudinal flow of air along the length of the tunnel, from one portal to the other. Longitudinal ventilation can be achieved either by injection, central fans, jet fans mounted within the tunnel, nozzles (often installed at the portals and called a Saccardo system), or through a combination of injection and extraction at intermediate points. The system must generate sufficient longitudinal air velocity to control backlayering of smoke. Longitudinal ventilation systems can be further classified into those using central fans and those using local, or jet fans. Jet fan longitudinal ventilation employs a series of jet fans mounted at the ceiling level (or sometimes in a sidewall niches) of the tunnel roadway. These fans, through the effects of the high-velocity discharge thrust, induce a total longitudinal airflow through the length of the tunnel.

Other types of traffic flow, including bi-directional traffic and uni-directional congested traffic, are better supported by other ventilation schemes. Transverse Ventilation is a system that is applied for smoke control when the smoke stratification must be kept intact, leaving more or less clean and breathable air underneath the smoke layer to both sides of the fire while extracting smoke from the fire site. The stratified smoke is taken out of the tunnel through exhaust openings typically located at the tunnel ceiling or high sidewall areas. "Single" Point Extraction system is a modification of the semi-transverse exhaust system, where spreading of smoke over the tunnel length can be prevented by the large extraction of tunnel air directly above the fire incident with suitable extraction ports or large openings with remotely controlled dampers. When a fire is identified and located, the control system can open the damper or dampers nearest the fire and extract smoke and heated gases as close to the fire site as possible, thus removing most of the smoke. The capacity of the emergency ventilation system must be based on the design fire size selected for each specific tunnel. This system works best in conjunction with longitudinal jet fans, or Saccardo nozzles to localize smoke around openings and to prevent smoke driven by natural factors (such as wind and the tunnel grade) from spreading along the tunnel.

Fire Protection using standpipe and water based fixed firefighting systems

Standpipe system is typically required for installation in tunnels and stations for fire fighters' intervention. It provides reliable means for conveying water to locations accessible by firefighters to attack fire. Depending on the climate and tunnel length the standpipe systems could be either wet or dry provided that the system fill time is less than 10 minutes. Typical standpipe system supplies 16 L/sec (250 gpm) of water and at a minimum pressure of 6.9 bar (100 psi) at the most hydraulically remote hose valve. Tunnel standpipes typically utilize a minimum of 150 mm (6-inch) diameter pipe, and are required to be protected from damage, be inspectable and maintainable. Pipes are required to be designed to allow for thermal expansion and contraction and the piping support system needs to be anchored appropriately. Hydraulic analysis of the standpipe system is required. Pressure reducing hose valves are considered where the pressure exceeds 12 bar (175 psi). Hose valves need to be protected from physical damage by errant vehicles or vandals by placing them conspicuously and in a niche or providing a physical barrier that protects them from being struck by vehicles.

The water supply capacity of 1 hour for firefighting is typically required to include the demand for the fixed water based firefighting system and the standpipe system when both systems are provided. Fire pumps could be needed to provide the necessary flow capacity and pressure in tunnel standpipe systems. Pump components have to be inspected and tested annually or bi-annually.

Railway tunnels are typically not equipped with the fixed water based firefighting systems, with the few exceptions, where vehicles pose high risk to tunnel occupants or integrity of tunnel structures. Such examples may include mixed usage railway tunnels, where freight operation carrying dangerous goods is mixed with mass transit operation in long tunnels, or very steep tunnels (such as funicular tunnels), where tunnel ventilation system alone is unable to provide sufficient protection for evacuation of tunnel users, and water curtains, or means to control fire growth are essential.

Public areas of stations are typically not protected with automatic sprinkler system, except areas governed by building codes. There are few examples where railway undercarriage water mist system or platform sprinkler system is installed. Such installation was driven by presence of combustible materials in artwork or high risk of undercarriage train fires.

Lately, since 2002 Madrid Metro water mist system installation on new vehicles, there is a tendency to consider a water mist system on board the trains. Such system could provide early protection of passenger compartments (especially in case of arson fire) and prevent fire from rapid growth and development allowing passenger evacuation in less toxic and cooler environment.

In road tunnels, fixed fire-fighting systems are defined as consisting of fire-fighting equipment, permanently attached to the tunnel, consisting of a piping system with a fixed supply of water or extinguishing agent which, when operated, has the intended effect of reducing the heat release and fire growth rates by discharging the water or extinguishing agent directly on the fire and of cooling the surrounding area by water droplets absorbing convective and radiative heat from the fire. In cases where the deluge system was used, 90% of fires were extinguished within 30 minutes and tunnels were reopened to traffic in an average of 74 minutes. Examples of fixed fire-fighting systems include sprinkler, deluge and water mist systems. The primary difference between the two systems is the size of water droplet: water mist systems use a smaller droplet size and less amount of water than deluge systems. The high-water demand rate for deluge system needs to be available and requires that in-tunnel drainage piping, storage, and pumping systems all become much larger than for water mist system and need to be sized accordingly. Water mist systems are not suitable for use in windy environments and not effective in open or highly ventilated spaces. They are only suitable for a limited range of fire risks. Water mist systems are ideal for environments where water damage needs to be minimized. Deluge systems, on the other hand, are best suited for high-hazard areas where rapid and widespread fire suppression is required.

Typically, tunnels are divided by multiple deluge fire zones for effective delivery of large amount of water to the area. The fire zone length is typically defined as the length of two longest vehicles using

the tunnel, while activation of 2 – 3 zones is considered. Sprinkler heads are exposed to corrosive air environment, to heavy soot as well as flying debris from the roadway. When using mist system protection of the orifice, such as using a cap to prevent clogging from heavy soot is advisable.

For fighting liquid fuel fires, a deluge or water mist system is often considered with additives injected into the water stream. When additives are considered, the suppression system should have controls in places that allow for the release of either water or water with the additive and should have the ability to stop the additive at any time. New additive products have come to the market for application. When considering an additive, it's effectiveness, environmental impact, health impact and implementation should be investigated.

Portable fire extinguishers are also required for tunnels, stations, and are typically installed in fire wall cabinets at 90 m (300 ft) spacing. It is prudent to install a device to provide the operator with an alarm indication that a fire extinguisher has been removed from its station. This signal could be an indication either of a fire within the tunnel or of the theft of an extinguisher (a common security issue in tunnels).

Adequate tunnel drainage shall be able to carry all fire water not allowing to flood the tunnel. A tunnel drainage system of sufficient capacity must be provided in any railway and road tunnel over 90 m (300 ft) long to collect and discharge the water from seepage, rain, and fire-fighting activities, including the deployment of fixed fire-fighting systems. This system can be either gravity, pumped or a combination of gravity and pumped and should be designed, installed, and maintained in accordance with tunnel and plumbing codes [5, 7]. Drain inlets in road tunnels are required to be placed through the tunnel. Inlets have two major requirements – protect tunnel from flooding and prevent fire from propagation along the tunnel. 100% of the drainage should be captured by grate inlets prior to leaving the next downstream activated fire zone. Drainage inlets shall be placed in each fire zone defined by the fixed firefighting system. The inlet capacity often requires enhancement by adding a minimum of 3 m (10 feet) of back of curb inlet to each drainage box.

Engineering Design Practice

Rapid development of computers, computer memory and computational speed enhancements allowed to use numerical modelling as primary tools in engineering practice of tunnel fire safety. Such tools include:

- Aerodynamics, fire dynamics, fluid systems and environmental modelling for tunnel ventilation and water based fixed fire fighting systems simulations and design.
- Egress (people evacuation) modelling
- Other safety electrical and mechanical systems design analysis, such as
    - Tunnel lighting modelling;
    - Sound noise modelling;
    - Hydraulic analysis;
    - Energy modelling;
    - Electrical power and etc.

Linear, or one-dimensional (1D) modelling is used for preliminary evaluation of design alternatives for preliminary equipment selection and for required space allocation needs in tunnels and stations. Subway Environment Simulation (SES) program remains one of such tools, which has the ability to model the aerodynamic and thermodynamic effects of tunnel fire on ventilation system. IDA Tunnel software developed by Equa is an alternative to SES with similar capabilities, while has additional features to simulate road tunnels as well as railway tunnels. Results from simulations include air pressures and temperatures, flow rates, and pollution concentrations along the tunnel. Input data are tunnel geometry, including flow friction factors and loss coefficients, plus traffic and emission data and air pressures at boundaries. ThermoTun software was developed by Prof. Alan Vardy for high-speed rail tunnels and has fire modelling capabilities as well. 1D models are good for longitudinal ventilation to predict airflow movement along the tunnel and to compare against so-called "critical velocity" to prevent smoke backlayering. Critical velocity is still evolving parameter and as such it is advisable to use more detailed tree-dimensional (3D) modelling for verification and final system

evaluation.

Numerical 3D models solve Navier-Stokes equations along with other physical models represented in Computational Fluid Dynamics (CFD) techniques. CFD analysis allow for modelling all types of tunnel ventilation systems for observing smoke (products of combustion) stratification, smoke backlayering and smoke extraction. Most CFD software tools allow for water based fixed firefighting system modelling, however some limitations (such as foam additives modelling) still exist due to complicated physics. Stations and large volumes are best simulated using CFD software. Software allows for steady-state and for transient (time dependent) analysis, which allow to track smoke and hot gasses behaviour over time and over volume. There are different software tools on the market. The most popular for tunnel fire modelling are ANSYS Fluent, CFX and others. Many engineers and fire departments use Fire Dynamics Simulation (FDS) developed and maintained by the US National Institute of Standards and Technology (NIST) and are free, however there is an on-going industry discussion on validity of some of its results against the full-scale fire tests. We will see further development of those tools and their validation in the near future. As with any engineering software, verification and validation are critical for the users to be confident in the results.

Emergency egress modelling simulates people behaviour in case of fire emergency and allows to track people locations over time and over distance in 3 dimensions. Evacuation modelling software, such as SIMULEX, STEPS, FDS+EVAC or Pathfinder can be employed to simulate the escape movement of people to a point of safety during incidents within road tunnels. Egress modelling output allows to compare results with output from CFD models and can be coupled, which is the current engineering practice, and allows to evaluate effectiveness of ventilation system and egress elements and to optimize both systems. Location of evacuees at any time can be correlated to tenability, which could be represented as fractional effective dose (FED) of each individual at that location and at that time.

Sound noise calculations in tunnels could be very complicated and heavily depend on sources of noise, (such as fans, sprinkler system and etc.) tunnel wall construction and reverberation, along with other sources of noise. 3D SoundPlan modelling allows to evaluate noise while proper model calibration is advisable.

Rapid development of three-dimensional computer drafting and engineering tools result in design using 3D Building Information Modelling (BIM) tools which connect engineering disciplines, workflows, and data across the entire project. BIM, along with LIDAR Scanning allows for better design coordination which is especially important when rehabilitating existing tunnel fire safety systems.

FUTURE TRENDS FOR ENGINEERING PRACTICE OF TUNNEL FIRE SAFETY

Impact of new energy carriers on fire safety and engineering practice

New energy carrier vehicles are present on the roads and their quantity will increase. They may pose different risks to tunnels with adjustments needed to engineering practice of tunnel safety. It is reasonable to treat those vehicles consisting of two components – the vehicle body (which is largely remains the same) and the fuel on board. This could be battery electric vehicles (BEV); or compressed gas vehicles, such as hydrogen or other types of fuel, which could ignite more easily than hydrocarbon fuels. Each of this fuel poses different risks and should be evaluated separately. While for small vehicles, the difference between the new energy carriers fire risk and the existing vehicle fleet might be considered less significant, the large locomotives and trucks can make a difference. World's first hydrogen-powered trains began running in Germany 2018 and are in operation since 2022. Freight hydrogen trains locomotives are being tested. Fire spread and thus growth rate may also increase due to large ignition accelerant developing very high temperatures and long flames.

Some agencies prohibit hydrogen vehicles to pass through the tunnels, however the technology development will require to revisit those policies, to perform comprehensive hazards, risk assessment,

and develop mitigation means in order to allow new energy carriers to pass through.

Hydrogen or other gases often stored in high-pressure compressed gas form could be released at high pressure during accident, when safety systems (Pressure Relief Devices PRD and etc) malfunctioning, forming high-velocity jet flame reaching up to sonic velocity at very high temperature of up to 2130°C (3866°F). This rapid hot gas release poses additional risks to tunnel structural integrity, to tunnel users' ability to evacuate; to detect and timely activate fire life safety systems. It can be expected that more attention will be given to passive means of tunnel fire protection and pre-emptive measures, such as constant ventilation to prevent gas accumulation and explosion inside the tunnel. Rapid and more accurate gas analysis and rapid systems activation will be essential, while artificial intelligence technology and firefighting robots' application may help. It is also anticipated that vehicle safety design enhancements will reduce the risks of such accidents and vehicles will be designed according to international regulation.

Impact of new transportation technologies on engineering practice

We try to find faster and safer transportation means. They test hyperloop technology which uses electric propulsion and electromagnetic levitation under near-vacuum conditions at a speed of 1,200km/hr (745 mph) in pods in smaller diameter tunnels. The pod will quickly lift above the track using magnetic levitation and glide at airline speeds for long distances due to ultra-low aerodynamic drag. This near-vacuum tunnel conditions pose challenges for current engineering practice of tunnel fire safety and will force to apply elements of aircraft fire safety standards to this technology.

Autonomous and semi-autonomous vehicles capable of sensing the environment and navigate without human input are already present and more coming. They pose challenges to communicate on tunnel fire to other vehicles and to tunnel fire safety systems. Their sensors would need to recognize presence of smoke and hot gases and navigate in reduced visibility environment. Means of communication during tunnel fire events would need to be enhanced to accommodate autonomous vehicles.

Artificial Intelligence and future of tunnel fire safety engineering practice

Recent development of artificial intelligence (AI) and robot technique will soon start impacting engineering practice. AI have already been proposed to control tunnel ventilation system to optimize ventilation response, especially during normal operation; to extend the life of tunnel ventilation equipment using AI health monitor; to reduce and optimize energy usage of tunnel ventilation systems. However, this is just the beginning.

Fire-fighting robots (FFRs) have been playing an increasingly important role in fire source detection and firefighting. They have been tested in tunnel environment. Intelligence and autonomy are important trends in the development of intelligent fire-fighting robots. With the development of artificial intelligence, fire source identification and location have become critical for research. The objective is the prediction of the location and size of the tunnel fire by the trained robot. Such technology may reduce the need for standpipe and water based fixed firefighting systems; can be quickly employed and protecting lives of tunnel users, of first responders and owner's properties. They may operate in a near-vacuum environment and may provide some means of ventilation to dilute gas accumulation preventing explosions.

Virtual reality and 4D design tools will be developed for tunnel safety design applications. We are in need for new full scale fire tests to validate computer programs, new fire life safety systems, and we will continue debates on Critical Velocity.

CONCLUSIONS

Engineering practice on tunnel fire safety is a century old. We debate on accuracy of "critical velocity" and smoke backlayering based on interpretations of temperature results of Memorial tunnel fire tests performed over 30 years ago for different goals and objectives. We apply old proven technologies to

ventilate tunnels, such as Saccardo Ventilation, Jet Fans and still consider them new and innovative. We are still debating on old questions:

- Which means provide better safety for tunnel users - enhanced evacuation means or robust mechanical and fire protection systems?
- To blow or not to blow fresh air during tunnel fire emergency?
- To use fire suppression systems, or not? Can water mist protect from large tunnel fire?
- To detect fire automatically or to rely on operators to detect and activate fire life safety systems in a timely manner?
- Should firefighters attempt to fight catastrophic tunnel fires, or let it burn in tunnel environment?

We use new sophisticated computational tools which allow us to numerically model tunnel fire environment, however we are in need of new comprehensive full scale tunnel fire tests which would allow us to build confidence in verification of the numerical and physical models.

We are at the edge of new technologies which pose new challenges to engineering practice and there is a need for evolution of engineering practice meeting new objectives. The end goal remains the safe – public safety, while new technologies require us to achieve this goal much faster, and in more challenging environment.

REFERENCES

1. Poliakov, A. “Tunnel Ventilation Design”, Stroyizdat, Moscow 1971 (in Russian).
2. Abramovich G.N. “Train airflow resistance calculations in tunnels and in outside”, *CAGI Jukovsky,* #400**,** Moscow 1939 (in Russian).
3. Singstad O. “Ventilation of Vehicular Tunnels”, *New York State Bridge and Tunnel Commission,* Report, #339**,** pp 381 – 405, New York, USA 1929.
4. The Holland Tunnel Chemical Fire, National Board of Fire Underwriters (NBFU), New York, 1949.
5. NFPA 130. Standard for Fixed Guideway Transit and Passenger Rail Systems. 2023. National Fire Protection Association, Quincy, MA, USA.
6. Louie A., Maevski I., Smith R. Chapter 16 “Enclosed Vehicular Facilities”. In *ASHRAE Handbook. HVAC Applications,* ASHRAE, 16.1-16.44, Peachtree Corners, GA, 2023.
7. NFPA 502. Standard for Road Tunnels, Bridges, and Other Limited Access Highways. 2023. National Fire Protection Association, Quincy, MA, USA.
8. Henschko, “Investigation on an Improved Jet Blower for Tunnel Ventilation.”, *Thesis* 1937 (in German).
9. Maevski, I., “Road Tunnels and Bridges”. In *Fire Protection Handbook* 21st Edition, Volume 2, Section 21, Chapter 10. National Fire Protection Association, 21-167 – 21-212, Quincy, MA, USA, 2023.
10. US DOT, FTA. Subway Environmental Design Handbook. Subway Environment Simulation Computer Program. Office of Research, Demonstration, and Innovation**,** December 1997.
11. Ingason, H., Li, Y.Z., and Lönnermark, A., *Tunnel Fire Dynamics*. Springer, Cham, 2015
12. NTIS, User’s Guide for the TUNVEN and DUCT Programs, Publication PB80141575, National Technical Information Service, Springfield, VA., 1980.
13. Rhodes, N., Clark, I.W., Else, K., “Prediction of Smoke Movement Using CFD”, *IMechE EuroTech Conference,* Paper, C413/067**,** 1991.
14. ANSI/ASHRAE Standard 217. Non-Emergency Ventilation in Enclosed Road, Rail, and Mass Transit Facilities. 2020 ASHRAE Atlanta, GA, USA.
15. Alston, J., “Fixed Guideway Transit and Light Rail Systems”. In *Fire Protection Handbook* 21st Edition, Volume 2, Section 21, Chapter 7. National Fire Protection Association, 21-85 – 21-103, Quincy, MA, USA, 2023.
16. Maevski, I. “Design Fires in Road Tunnels”, National Cooperative Highway Research Program. Transportation Research Board of the National Academies, NCHRP Synthesis #415, Washington DC, USA, 2011.

17. Maevski, I. "Guidelines for Emergency Ventilation Smoke Control on Roadway Tunnels", National Cooperative Highway Research Program. Transportation Research Board of the National Academies of Science, Engineering, Medicine, NCHRP Research Report #836, Washington DC, USA, 2017.
18. Parsons Brinckerhoff Quade & Douglas, Inc., et al. "Making Transportation Tunnels Safe and Secure", National Cooperative Highway Research Program. Transportation Research Board of the National Academies, NCHRP Research Report 525, TCRP Report 86 Volume 12, 2006, Washington DC, USA, 2006.
19. European Union Directive 2004/54/EC of the European Parliament and of the Council on minimum safety requirements for tunnels in the trans-European road network, 29 April 2004
20. "Fire Dynamics in Tunnels". In *The Handbook of Tunnel Fire Safety* (R. O. Carvel and A. N. Beard, Eds.), Thomas Telford Publishing, 231-266, London, 2005

Review of the structural fire resistance in Tunnels

Daniel Joyeux[1]
[1]EFECTIS Group (FR)

Abstract

The standard fire ISO 834-1 (EN 1363-1 in Europe) developed at the end of 19th century drove the structural fire resistance of building and infrastructures. In particular, increased safety in construction. Prescriptive regulations were based on an ISO-Fire rating. European harmonisation allowed a Eurocode development for structural design and in particular structural fire design. However, large tunnel fires occurring at the end of the 20th century and the beginning of the 21st century have identified phenomenon which have not observed in ISO conventional fire conditions. New research was conducted notably for assessing the concrete spalling due to higher fire kinetics. RWS was initiated, and development of passive fire protection or a new design of concrete which may sustain direct exposed to fire. This phenomenon seems more or less contained, as we have observed less research on this topic which focuses on design details (equipment, structural supports, ..). However, when a risk can be monitored, new ones are appearing with a high fire kinetics and possibly combined with explosion effects. Structural fire research must continue. An ethos of continuous fire safety improvements should be implemented on existing high category tunnels. In addition, climate changes are limiting city expansions which increases the need to build over roads and rails creating new tunnels with a new specific structural fire safety objective of no collapse, even for small tunnels.

KEYWORD: Structural fire resistance, Fire protection, Fire Scenarios, Spalling of concrete

INTRODUCTION

Structural fire resistance aims to satisfy fire safety objectives, which may differ from country to country, from owner to owner, from the use and from the neighbourhood. Notably, for tunnels, the fire safety functional requirements were based on users' safety but have been improved to consider the continuity of operation. As noticed with the Mont-Blanc Tunnel fire in 1999, an operation's loss of such road tunnel produces large local, regional and national business, economic and environmental impacts [1]. This was also observed in the Channel tunnel, where initial fire scenarios for the structural fire design were underestimated. The 1996 and 2006 fires might have been fatal for Eurotunnel [2].

Internationally, legislation and guidance have been developed based on real fire experience and consequent research.

The paper aims to present an history of the structural fire resistance in tunnels. After a brief chapter dedicated to important real fires, and their impact on the research, a review of practices and development of legislations and guidance is done.

Performance-based design has often been the main practice in structural fire resistance design, but for many years, the fire kinetics and fire hazards in tunnels have been underestimated. At the initial design phase, solutions should be suitable for the required functional requirements. However, to reach the required fire safety level of existing tunnels, the solutions are often an effective cost / benefit optimization [3]. Global research about structural fire behaviour, as regularly observed during the "Structure In Fire" (SIF) conference, allowed the development of numerical methods for assessing the structural fire behaviour, but also for improving the fire part of Eurocode (EN 199x-1-2) for structural fire design. We can congratulate the CEN/TC250 for the new version that should be published soon, which includes large improvements in calculation methods.

However, an experimental approach to characterize concrete spalling and passive Fire protection efficiency remain unfortunately necessary, as used in 2023 for the Mont Blanc tunnel refurbishment [4]. However, as observed at the end of the 20th century, fire hazards in tunnels are continuously changing and unfortunately with an increase of the fire risk (in terms of frequency and in terms of consequence).

Refurbishment with fire safety improvements should be a continuous job, complimented with high-quality maintenance. In addition, due to urban covering of roads and rails, new tunnels are produced in cities with the objectives of erecting building above.

So, the paper will conclude with the new challenges for the structural fire resistance of tunnel as a part of fire protection measures to improve the overarching goal of tunnel safety.

FIRE ACCIDENT BASED INFORMATION

Fires in tunnels have always been investigated. However, the transportation of goods has increased since the 80's producing higher and higher risks in tunnels, in term of frequency (more traffic) and in term of consequence (severity of the fire with higher fire loads).

The Netherlands were the first to identify this fire risk in a tunnel, when a large fire occurred in Velsertunnel [5]. In 1978, following a traffic incident, a fire broke out in the Velsertunnel, the Netherlands, which cost the lives of 5 people, including 2 children. The incident drew the attention to the vulnerability of tunnels to vehicle fires. After this fire, the ministry of transportation requested TNO fire laboratory (now Efectis Nederland) to experimentally assess what may happen to the concrete structure of a tunnel [6] and defined a representative tunnel fire resistance test, which initiated the now famous RWS curve. The Table 1 shows the table 3 of the TNO report with a furnace temperature of 1350 °C as used in the current internationally renowned RWS curve.

The identification of this fire risk in tunnels has been propagated initially across Europe and then Internationally. The occurrence of the fires in the Mont Blanc Tunnel in 1999 and then in the Gothard tunnel has confirmed the increase of risk in tunnels and initiated a large review of legislation everywhere in the world. Haack [1] in the first International Symposium on Tunnel Safety and Security presented what we learnt from those large fires.

In 1999 a heavy goods vehicle caught fire in the Mont Blanc tunnel between France and Italy. Even though the fire was detected quite quickly by the tunnel operators, and the tunnel was closed to entry within minutes of the fire being detected, vehicles – including heavy goods vehicles – were already in the tunnel. Most of these vehicles could not pass the burning vehicle and became stuck behind it. The intervention conditions were not optimized, the ventilation was not efficient to allow fire fighters access. The fire kinetics of the initial truck were very high, and the propagation to other vehicles that occupants had left was also rather quick. It took 53 hours to extinguish the fire and hot spots had to be dealt with for 5 days after the fire. 39 people, including a fire fighter, died at the incident. Due, to the high kinetics and the long duration of the fire, the concrete structure was severely damaged by the fire, and it took nearly 3 years before the tunnel reopened for traffic. Consequently, there was a large impact on truck traffic between France and Italy with a deviation required through the Frejus tunnel, but these roads were not designed for such high traffic. This deviation also produced a large environmental impact. On the other hand, the stop of the traffic to Mont Blanc has impacted economically all that regions business.

This situation has not been limited to road tunnels, because in the same period, important rail tunnel fires have been recorded. The Fret in the channel tunnel opened in 1992, with a very large success for the railway transportation of trucks between France and UK. However, the fire risk of trucks in rail transportation was strongly underestimated. In 1996, a first large fire occurred, which due to the strong damage of the structure and equipment stopped the operation several years. This loss of operation might have led to the liquidation of the company. A second fire occurred in 2006 with again large damage, notably on the concrete lining. The structural surroundings of the natural land remain intact. The full

characteristics of the tunnel including their Heavy Vehicle Carriage, the equipment within the tunnel, and the concrete lining, have been revised for updating the fire safety level of the channel tunnel. Since 2006, no catastrophic fires have been observed.

Table 1 Table n°3 of the report [6]

Tijd	Temperatuur (°C)										
(min)	1	2	3	4	5	6	7	8	9	10	gem. 1t/m10
0	10	10	10	10	10	10	10	10	10	10	10
5	1000	1130	860	1140		1210	1290	1050	1180	1100	1140
10	1150	1210	810	1180		1250	1240	1080	1240	1240	1200
15	930	1230	1040	1250		1270	1250	1070	1260	1190	1180
20	1210	1310	980	1270		1320	1240	1060	1300	1270	1250
25	1050	1260	1160	1260	1270	1300	1270	1070	1240	1040	1190
30	1110	1310	1060	1300	1280	1310	1230	1080	1320	1190	1230
35	1190	1340	940	1210		1250	1290	1090	1290	1050	1210
40	1190	1290	900	1270	1290	1290	1280	1060	1350	1340	1260
45	900	1160	1050	1250	1300	1360	1240	1120	1270	1190	1190
50	920	1210	1030	1240		1340	1240	1070	1290	1050	1170
55	1000	1240	970	1260		1330	1180	1110	1320	1340	1220
60	980	1160	940	1240		1340	1250	1050	1290	1050	1140
65	870	1130	1020	1230	1270	1350	1210	1050	1250	1060	1140
70	910	1240	1000	1250		1340	1250	1070	1330	1250	1200
75	1000	1260	990	1270		1330	1280	1090	1320	1270	1230
80	1120	1160	1010	1240	1280	1350	1260	1020	1260	1180	1200
85	1150	1280	1000	1240	1260	1340	1260	1030	1350	1350	1250
90	930	1200	1070	1260		1270	1230	1010	1260	1130	1160
95	960	1230	1100	1250		1350	1220	1050	1320	1160	1190
100	920	1170	900	1050		1250	1000	700	1050	1040	1020
T	1030	1230	1000	1250	1280	1320	1250	1070	1230	1190	1200
σ	120	60	80	25	20	40	30	30	40	110	±60

FIRE SCENARIO DEPENDENT

The legislations require structural fire resistance that is mainly described in term of ISO fire rating. The ISO standard fire curve used worldwide has been derived from wood cribs tests in a room with enough ventilation [7]. The TNO development in 80ies has introduced a new standard fire curve called RWS, in the name of the ministry in charge of the transportation (Rijkswaterstaat) after the fire occurred in Velsertunnel. Shortly after, Rijkswaterstaat (RWS), the Dutch Ministry of Infrastructure, together with TNO Centre for Fire Safety (now called Efectis Nederland) started research to determine the fire load on the concrete structure of road tunnels for the worst-case scenarios. The research led to the well-known RWS fire curve and later to the development of a testing procedure for concrete tunnel lining. The curve introduced a very fast growth of temperature that may be representative of fires in heavy trucks with specific goods in tunnel, with a maximum temperature of 1350 °C.

More recently, CETU introduced a severe fire curve [8], similar to the RWS one: the majorated hydrocarbon curve, which is based on the formula of the Hydrocarbon curve defined in EN 1363-1 [9] based on a maximum temperature of 1100 °C, which is increased to 1300 °C. Those three standardized curves are presented in Figure 1. *Figure 1 Fire resistance standard fire curves*

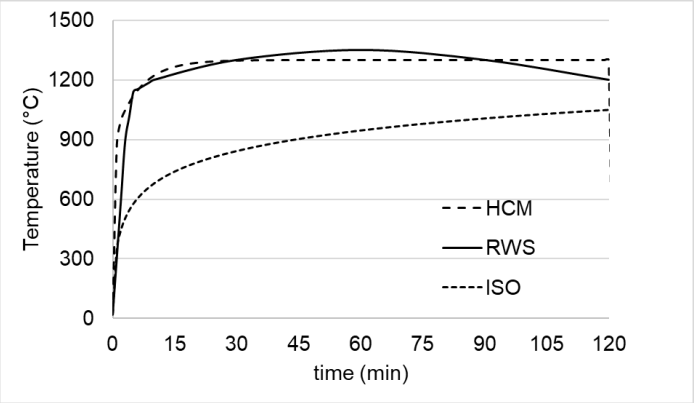

Figure 1 Fire resistance standard fire curves

These severe curves (HCM or RWS) have been confirmed as a representative standard curve for designing fire resistance in tunnels and is used internationally. In particular, the recommendations to use the RWS for designing the fire resistance of structure was introduced in NFPA 502 for Road Tunnels, Bridges, and Other Limited Access Highways in 2004 [10]. In 2022, the use of RWS for structural design was extended to the fire design of tunnel equipment and compartmentation [11].

To illustrate fire and life safety considerations, the article in Tunnel Business Magazine concerning the Elizabeth river tunnel and the Hugh L. Carey Tunnel [12] explores two projects involving tunnels, the construction of the Elizabeth River Tunnels in Virginia, and the rehabilitation of the Hugh L. Carey Tunnel in New York. Part of the fire and life safety scope for these tunnels was to protect the tunnel structure according to the NFPA 502, preventing explosive spalling and progressive collapse of the tunnel lining during a 2-hour RWS fire.

As an alternative, a fire curve tailored at the fire scenario may be determined based on a literature study, modelling or fire tests. To determine the fire load the following should be considered:

- Types of vehicles involved,
- Number of vehicles involved,
- Types of fuels that can be present (transport of hazardous materials, H_2 vehicles, etc.),
- Presence of a fixed firefighting system.

With specific traffic constraints, the refurbishment of the tunnel under La Defense [13] has been assessed by specific fire curve obtained from fire risk assessment and traffic analysis.

We may nevertheless wonder if those standard fire curves or tailored made fire curves remain representative of the evolution of the type of vehicles circulating in tunnels. Notably, new energy vehicles are generating new risks in terms of kinetics, of phenomenon (like additional overpressure), of effluents (like metal particles in fusion), of firefighting conditions.

A holistic approach is now necessary. As mentioned in NFPA 502, table A7.5.2 [14], but also required by several regulations, a fire engineering analysis should always be performed. However, they often require it at the safety design stage for new tunnels. But, as observed with the Mont-Blanc tunnel, the upgrade of fire safety measures (we may say fire and explosion safety measures to include the explosion effect when necessary) shall be regularly done to be adapted to the evolution of traffic and vehicle types.

The European Directive on critical entities [15] identifies on its article 2 transport as one of the categories. All member states shall have already transposed this directive in its regulation (foreseen before 17 October 2024), shall identify the entities before July 2026, and shall realize the risk assessment within 9 months. Thus in Europe, several road tunnels (rail tunnels as well) will be listed and risk assessment will be regularly completed. A review of scenarios according to the evolution of the use of the tunnel should be performed.

The fire risk assessment (Directive) or the fire engineering analysis (NFPA) utilises different tools. Globally, the assessment shall take into account all fire safety measures existing in the tunnel (ventilation, firefighting...) including their aging (for the passive fire protection as well), to characterize fire design scenarios. Probabilistic structural approaches may be used based on the basic background of Eurocodes. Safety coefficients and safety factors of Eurocodes have been calculated with a probabilistic approach [16].

STRUCTURAL FIRE SAFETY OBJECTIVES

Functional Requirements

According to the use of the tunnel, (traffic, bi-directional, number of lanes), to the characteristics of the tunnel (length, section, excavated...) and to its environment (urban with construction above, isolated in mountain, immersed...), the structural fire safety objectives will be different. They may be expressed in four main functional requirements:

- No collapse during a period of time: this functional requirement is allowing egress and firefighters intervention. It means that the tunnel is designed to satisfy egress of users and to allow easy and safe access to firefighters. The required time should be consistent with the time needed for firefighters to be operational, notably if the firefighters are not available on site (internal or external) or close by.
- No collapse during the full scenario: This functional requirement is imposed when the consequences of failure are very important. A collapse may lead to unacceptable consequences, like an immersed tunnel or tunnel with high construction above.
- Collapse is accepted without progressive collapse: This functional requirement is required when a structural collapse of the tunnel does not lead to large consequences, other than financial. But due to the size of the tunnel, progressive collapse is forbidden for securing firefighters' intervention and safe egress of the tunnel
- Collapse is accepted: This functional requirement is applied for small tunnels where the collapse provokes only financial reconstruction aspect.

Regulations and Standards

Those functional requirements are often indirectly defined in terms of conventional fire resistance duration taking into account the severity of the fire, notably using ISO fire rating or RWS fire rating (see fig 2), or a combination of both. Some regulations require a fire safety risk analysis to identify the corresponding fire structural behavior to satisfy the functional requirements expressed above. Fire safety in tunnels is governed by a complex framework of regulations and standards that take into account the nature of transported goods, vehicle types, and tunnel characteristics.

Key standards and regulations include:

- ISO 834-1 [7] / EN 1363-1 [9]: The initial standard used worldwide for fire resistance testing, based on a conventional time-temperature curve primarily designed for buildings and not fully representative of tunnel fire conditions. Over time, more severe curves like RWS and HCM have been integrated into the standards applicable to tunnels.
- NFPA 502 (Standard for Road Tunnels, Bridges, and Other Limited Access Highways) [10 - 14]: The NFPA 502 standard provides guidelines for fire protection and safety measures specific to tunnels, bridges, and other confined infrastructure. It mandates the use of severe fire scenarios like the RWS curve for the structural design of tunnels, particularly those handling hazardous materials or high traffic volumes.
- ADR (European Agreement Concerning the International Carriage of Dangerous Goods by Road) [17]: ADR regulates the transportation of hazardous goods through tunnels, specifying safety measures based on the nature of the cargo, such as explosive or flammable materials. The agreement defines tunnel restrictions based on risk levels and prescribes fire resistance standards

for tunnels frequently used by vehicles transporting dangerous goods.

- Directive 2004/54/EC of the European Parliament on Minimum Safety Requirements for Tunnels in the Trans-European Road Network [18]: This directive sets mandatory safety requirements for tunnels longer than 500 meters in the European network, including fire-resistant linings, emergency exits, and ventilation systems. The directive emphasizes the need for performance-based design to account for diverse fire scenarios. The directive is to be implemented into the national law of every member country of the EU.

National Standards and Local Regulations in different countries have additional requirements, often specifying particular fire curves (e.g., RWS, HCM, or Hydrocarbon Modified) depending on tunnel usage, location, and the nature of the transported goods. Without prejudice of additional measures, possibly provided at a national level, the Trans-European Road Network directive fixes with a certain ambivalence, some prescriptive regulatory safeguards, but also authorizes performance-based approaches through risk analyses included in the framework of a derogatory procedure provided for in §1.2.1 of its appendix and under its article 13.

In relation to fire resistance, the directive only sets the following objectives to achieve:

- Section 2.7: "The main structure of all tunnels where a local collapse of the structure could have catastrophic consequences, e.g. immersed tunnels or tunnels which can cause the collapse of important neighboring structures, shall ensure a sufficient level of fire resistance."
- Section 2.18: "The level of fire resistance of all tunnel equipment shall take into account the technological possibilities and aim at maintaining the necessary safety functions in the event of a fire".

It is then up to the designer to determine:

- In reference to section 2.7: Whether the tunnel structure studied or for instance equipment failure can have important consequences, and:
- In reference to section 2.18: What can be considered a sufficient level of fire resistance with respect to the safety functions to be satisfied.

The NFPA 502 requires a fire engineering analysis (§4.3.1) which shall verify the functional requirements according to the tunnel length (§7.2). In principle, this engineering analysis should be conducted to ensure that structural fire behavior will meet the functional requirements. In reality, unfortunately, these engineering analyses consist mainly in mentioning that the required fire rating (see table A7.2) is applied and is considering fulfilling the functional requirements.

As another example, the French requirements [8] is also expressed in term of functional requirements, scenarios are defined. HCM-Fire ratings and ISO Fire ratings are expressed. In many cases, structural fire risk analysis is not performed to confirm that those ratings are fulfilling the functional requirements. CETU (Centre Technique des Tunnels), with support of the official fire resistance fire laboratories, developed several guides allowing the application of procedures for analyzing the level of risk of structures, its improvement and ensuring that passive protection is properly considered [19]. This includes - but is not limited to:

- Guide N°4 of the road tunnel safety file guide detailing the fire source terms considered in most risk studies in road tunnels,
- The fire behavior guide for road tunnels, and its supplements, which specify different degrees of analysis (G1, G2 and G3) that can be used to check the fire resistance of structures depending on the complexity of the problems and the desired accuracy. However, this guidance is recommended implementation as soon as possible of a degree of analysis of G3 type (advanced calculations), and:
- Passive fire protection systems guide, performance justification for road tunnel structures.

Regarding the standardized levels of fire loads to be considered, the French prescriptive regulations limit for road tunnels to the use of the ISO 834 fire rating and the HCM fire rating, by defining levels of protection N0 to N3 according to the fire load considered:

Table 2 : Typical fire resistance level for French road tunnel

level	Reference fire curves*	Typical example
N0	Local failure	Structures without interfaces and without significant safety provisions (e.g. short tunnel in mountain)
N1	ISO 120	protection of direct means of egress, ventilation shaft important for firefighters
N2	HCM 120	Presence of a critical transport axe (e.g. railway, motorway), protection of egress means without direct outside communication
N3	ISO 240 & HCM120	Allowing to provide robustness for situations deemed to be the most critical likely to occur in tunnels
* for reduced gauge tunnels the different levels of requirements can be reduced to ISO 60		

Urban Development

The densification of urban environment is a current challenge for all cities in the world. The large high-rise buildings erected in the 60s – 70s were dismantled in 2000 to avoid ghettos and to build lower buildings (fewer floors). However, the increase of population, the need of green space to reduce temperature and trap CO_2 in cities changed the urban strategies of 2000, to come back urban strategies of the 60s by erecting higher buildings.

However, cities are looking for new areas to build. Thus, covering all road and rail tunnels is the main way of generating new urban construction. The tunnel covering may have a new structural design, with high consequences in case of uncontrolled fires. On the other hand, the erection of new buildings above those tunnels may lead to structural collapse of the building. What about the consequences on the tunnel.

Globally, there is a limited return of experience from fires developed in such tunnels coming from covering with buildings above, including also high rise. Very specific attention should be brought by municipalities which are mainly responsible for those new constructions. The application of prescriptive rules to existing tunnels is always a challenge. For existing tunnels, the use of functional requirements to verify the performance of the refurbishment should be via improved engineering. We can use the example of the Mont Blanc tunnel with its many steps and years of refurbishment, to demonstrate the improved safety levels.

STRUCTURAL FIRE BEHAVIOUR

Characteristics

The basic data concerning structure characteristics comes from the part regarding fire of Eurocodes notably concrete [20], steel [21] and composite [22]. The Eurocodes, developed by CEN/TC250, are regularly improved, including research input. The application of Eurocodes, out of the introduction of Fire Safety Engineering methodology, is limited to standardized fire curves from ISO to HC curves. For such conditions, the Eurocodes give all the details for designing the fire resistance of structure. The present paper focuses on the structural behavior that is not addressed by Eurocodes:

- Spalling of concrete
- Cracking of structures
- Passive fire protection
- Structural details
- Combination of actions and new risks

Spalling of Concrete (testing – new guidelines)

The phenomenon of spalling of concrete was clearly identified in 80s during the Velsertunnel fire in the Netherlands [5]. The fire in the channel tunnel in 1996 [2] confirmed the phenomenon and then it was re-confirmed by the next large fires in tunnels.

Concrete spalling is a critical issue in tunnel fires, where the rapid heating of concrete surfaces can lead to the explosive detachment of concrete layers. This phenomenon poses a significant risk to the structural integrity of tunnels, as it can expose reinforcement bars and weaken load-bearing elements. The spalling of concrete phenomenon is a complex mechanism combining the formulation of concrete, the aggregate characteristics, aging, moisture content, mechanical loading in particular the compressive stress [23], and the heating conditions notably the fire kinetics.

Different procedures of testing have been published. The historical one based on RWS development has been published by Efectis with the last version which includes equipment tests according to RWS [11]. Other, different procedures are already available in Sweden [24, 25], in the US [26], and in France [19]. The screening method for determining the spalling thickness after tests may also differ [27], using lasers, and radiography.

For tunnel segments most of the key parameters may lead to high spalling of concrete. The spalling of concrete will reduce the thickness of concrete, which may lead to a partial collapse of a structure, of ventilation ducts, of safety equipment losses, …. Avoiding, or limiting, the spalling of concrete is possible when working on the different main parameters as the following ones

Formulation of Concrete

The composition of concrete is a main factor of the spalling of concrete, which may reduce the phenomenon the spalling [28], but generally may not avoid it when a large increase of temperature is observed.

Incorporating lightweight aggregates such as expanded clay, pumice, or shale can reduce the spalling risk due to their lower thermal conductivity. These aggregates help manage thermal gradients within the concrete, reducing internal stresses during heating. However, they may require optimization with fiber reinforcement to maintain mechanical strength.

Supplementary Cementitious Materials (SCMs) like silica fume, fly ash, and slag improve concrete's thermal stability and reduce permeability, enhancing fire performance. However, the dense microstructure they create can impede steam escape, making polypropylene fibers crucial for managing spalling risks. As example, Anna-Lena Hammer [29] presented the impact of cement-free shotcrete in situations of thermal actions and mechanical conditions.

High-Performance and Ultra-High-Performance Concretes (HPC/UHPC): such concrete, characterized by their high strength and low permeability, are highly susceptible to spalling. The addition of polypropylene fibers at 0.2%, combined with adjustments to SCM content (e.g., reducing silica fume), can optimize the balance between strength and fire resistance.

The use of Carbon fiber reinforced Polymers (CFRP) composite to strengthen tunnel structure in case of fire has been analyzed by Yi Shen [30], as a local solution. However, currently, this formulation has only been a success on specific tunnel cases, where compress stress was limited or when heating conditions were also limited.

Polypropylene Fibers

Polypropylene fibers are a widely used solution to reduce the risk of concrete spalling in tunnel fires and have been the object of several research studies. These synthetic fibers help mitigate spalling by

melting at around 170 °C, forming micro-channels within the concrete that allow steam to escape. Since the initial ISTSS conference, many papers have been dedicated to the impact and design of PP fibers on the concrete spalling conditions, mainly with experimental approaches [31], while the numerical assessment remains very complex [32].

Optimal Proportion of Fibers: The recommended dosage of polypropylene fibers ranges from 0.1% to 0.3% by volume of the concrete mix, corresponding to 1 to 3 kg/m³. Research has shown that even at the lower end of this range, spalling resistance improves significantly, with reductions of up to 80% to 90% observed in full-scale fire tests under severe conditions like those of the RWS curve [33]. The effectiveness of polypropylene fibers depends on factors such as fiber length (typically 6 mm to 12 mm), type (monofilament vs. fibrillated), and uniformity within the mix. Shorter monofilament fibers are preferred for their consistent melting behavior and ability to create effective vapor release channels. Fiber proportions exceeding 0.3% do not substantially improve spalling resistance and can negatively impact the workability of the concrete. Some questions remain about regular small fires (cars) occurring during the life of the tunnel which may lead to large enough temperatures (over 170 °C) which may melt the PP fibers, and possibly impact the vulnerability of the concrete in case of large fires. The use of a probabilistic approach may be the answer, but it needs a high amount of information data. The analysis of tunnel fire statistics, and not only the large ones should be recorded for generating data for the probabilistic approach.

Cracking Phenomena

Concrete cracking is not critical in many configurations of road tunnels, notably bored tunnel. But in situations of immersed tunnel, cracking may initiate large damage or even worse. The phenomenon of concrete structure cracking is very complex, and is a multi-scale phenomenon, an opposite phenomenon to that like cement shrink and aggregate expansion. A limited number of studies have been performed in real tunnel conditions, like Stefan Smidgrowski [34] and Leander Noordijk [35].

Passive Fire Protection (including durability)

Road tunnel structures are almost always constructed from concrete and two types of passive fire protection are commonly used to protect concrete tunnel structures: systems based on spray-applied mortar and systems based on fire protection boards. Other spray-applied systems, such as intumescent coatings, are not available on the market for protecting concrete tunnel structures. However, for steel structures – such as used for covering urban roads – intumescent coatings may also be qualified.
The recent PfpNet guidance [36] can give more details about the nature of the type of products. The characterization of the passive fire protection performance is done experimentally while the final application may use a hybrid approach combining numerical evaluation and experimental assessment [32]. The oldest method for characterizing spalling and the passive fire protection performance was initiated by TNO [37] and regularly updated by Efectis [38]. The last version extends the qualification to products other than the structure. This method has been listed in NFPA 502, and recently ASTM has taken over the method in the ASTM E3134 standard [26] or in Norway with specific national application [39]. CETU, in cooperation with the French official fire resistance laboratories, has published specific guidelines for characterizing the performance of passive fire protection of concrete in road tunnel, which may be exposed of the standardized majorated Hydrocarbon fire curve [19]. Other guidelines for testing passive fire protection are published [40].

It has been demonstrated that in addition to the criteria of mechanical fire behavior of the structures, the limitation concrete spalling that is protected by passive fire protection shall be considered [41]. The criteria for avoiding the spalling of concrete protection by passive fire protection is generally defined by a temperature at the interface between the concrete and the passive fire protection. Several interface temperatures are defined as criteria (from 180 °C to 350 °C).

Initial performance assessment is required, but we can also refer to European Assessment Documents [42-43] to consider the durability of passive fire protection, which may be exposed to low temperatures,

even negative, and high humidity. However, it can be recommended to assess their performance with the existing European Assessment Documents published in September 2017, based on previous European Technical Assessment Guides. The durability performance of passive fire protection has been assessed when the product is put on the market, regular inspection of the quality of the existing product for verifying the aging and eventual local damages. Out of the EAD's application at qualification stage, studies and publications on the evaluation of the performance of aging passive fire protection are limited, even non-existent.

In order to assess the effectiveness of passive fire protection during the life of the tunnel (aging, damage) and estimating a cost-effective solution, notably in case of small fires, the use of passive fire protection after a fire has been assessed and can give a limit of use of passive fire protection compared to PP Fiber solution [44]. Kees Both gave a review of new challenges of passive fire protection in 2014 [45], but the present paper is updating the review with the new challenges as mentioned below.

Application on New or Existing Tunnels

Since the Mont Blanc tunnel fire, different passive fire protection has been characterized, and the fire behavior of concrete of any tunnels, located worldwide have been assessed: Port of Miami tunnel [46], Ohio River Bridge East End Crossing Tunnel [47], Waterwolftunnel in Netherlands [48]. Some guidelines have also been published [49]. Notable upgrades to the safety levels of tunnels have been made. The concept of applying a mobile fire resistance furnace to the existing lining has been used [50-51]. Generally, it allows exposing 1m² of concrete lining surface to RWS fire curve.

Figure 2 Application of mobifire® test in La défense, Paris (france)

Modelling approach

The thermal-Mechanical and Spalling Prediction Models are on two different bases:

- Finite Element Analysis (FEA): FEA models simulate the thermal and mechanical responses of tunnel linings, integrating temperature-dependent properties such as thermal conductivity, specific heat, and mechanical strength. These models help predict the onset of spalling and the structural impacts of severe fire exposure.
- Coupled Thermal-Hydraulic-Mechanical (THM) Models: THM models provide a detailed simulation of the interaction between heat transfer, water migration, and mechanical stress within the concrete. These models are particularly valuable in understanding the vapor pressure dynamics and water migration that led to spalling and optimizing the design of fire-resistant concretes. However, they need very accurate data at microscale of the structure.

Numerical modelling of the structural fire behaviour is strongly developed in conjunction with ISO fire curve. It means that the spalling phenomenon is generally neglected. In conditions of RWS fire curve,

or in case of specific fire scenarios, modelling shall consider the spalling effect. Thus, Hybrid method, combining experimental and modelling approaches is used.

On the one hand, the numerical approach allows designing the samples to be tested. The samples shall be the most critical samples representative of the global tunnel structure. In many cases, the tunnel is not a simple linear tube, but presents different geometrical aspects, different types and thickness of mining, the sections may also be distributed in different configurations. The numerical analysis can select the most critical samples. On the other hand, the test results, large scale or small scale, give input data to be applied in the risk analysis of the tunnel and the final structural fire assessment, like the maximum thickness of spalling to be considered.

The recent example of the refurbishment of the Mont Blanc tunnel [32] is a good example, presenting the method for evaluating the spalling sensitivity of concrete structures in laboratory conditions based on hybrid approach. In that case, the modelling is supporting the tests to be performed. The method consists of three phases:

- Phase 1: Designing the test set up for loading and/or constraining the structural element
- Phase 2: Structural modelling in the scope of reproducing the stress state
- Phase 3: Large-scale fire test of the representative test element

The second example [52] is a case where the tests support the modelling approach. It consists of assessing a precast concrete tunnel lining in case of major fire event within its final configuration, by using tests performed on medium scale. Those tests gave data about spalling and were used to validated method and tools. In this application, combination of CFD to assess the fire development and FEA to model the structural behaviour was used.

Characteristics of material are given from part fire of Eurocodes, notably from EN 1992-1-2 [20] for fire behaviour of reinforced concrete structures. Limitations are given as examples:

- Temperature is lower than 1200 °C, with large uncertainties above 1000°C
- Spalling is not included
- Strength is limited to 80 MPA when avoiding spalling effect

The modelling approach can assess local behaviour like simple friction isolator system used in urban tunnels to prevent vibration which may come from earthquake or other urban vibration like train and metro. Those connectors are made of polymers that may react at low temperature, (example of a loss of structural properties at 150 °C of EPDM, Ethylene Propylene Diene monomer, but other elastomer may lose thermal properties at lower temperature(between 80 °C to 120 °C) and produce structural damage. It is then essential to protect the structural connectors accordingly.

Figure 3 Friction isolar system - picture from [53]

New Risks and Combination of Actions

Climate change has introduced the need for new energy for vehicles: Electrical, based on batteries, and hydrogen. In only a few years, there has been an increased use of electric vehicles (EVs), hydrogen-powered vehicles, and other alternative fuel sources introduces new fire risks, including battery fires and jet flame risks. To reach its climate neutrality target by 2050, the EU is taking action to reduce

emissions from cars. Indeed, road transport accounts for a fifth of the EU's CO_2 emissions (54). The EU aims to reduce emissions from cars by 55 % and vans by 50 % by 2030, compared to 2021, to reach the zero-emission target for new cars and vans in 2035. Electrical vehicles are now common on the road, including buses, though the impetus of the European directive (For some countries as Norway, those percentage of EV is already very high).

On the one hand, these scenarios require updated fire curves and protective measures to address the unique challenges posed by these fuels. On the other hand, the combustion mode and the firefighting conditions concerning such fires are also modifying the global fire safety prevention and protection of the road tunnel, to avoid very long duration of fires which may become highly critical for structures, as seen in Mont Blanc (1999) or Channel tunnel (1996- 2006).

As hydrogen stations remain limited, it follows that the use of hydrogen vehicles is also limited for the time being. So, the fire engineering analysis shall verify the type of vehicles circulating the road tunnel and should be a multi-hazard analysis, notably that combine fire and explosion effects are essential for assessing the structural resilience of tunnels, especially those handling hazardous materials or situated in seismically active regions. These simulations assess the combined impacts of intense heat and shock waves, guiding the design of robust fire and explosion-resistant tunnels.

Structural behaviour assessment may also include explosion effect, with or without combination with fire impact. We can observe explosion producing a fire and a fire producing an explosion. Scenarios shall be established according to the identified hazard. Few studies are already performed to assess the impact of explosion in tunnels by calculations [55] or experimentally [56].

This evolution of risks should be combined with the aging of structural fire protection which may see their performance reduced with time. Update of risk analysis shall be performed to assess the improved risks in existing tunnel. Scenarios should be defined and should consider the global safety management of tunnels [57]. This will be also required by the European commission, with the application of the directive of critical entities [15] or due to climate change reasons [53], notably in combination with dangerous good circulation [58]. The same evaluation may be done in rail tunnel as well [59]. As mentioned above, covering urban roads to erect buildings is a further additional high risk to be assessed [60].

RESEARCH and STANDARDIZATION

Different large collective research projects performed more than 20 years ago are the current basis of regulations and engineering methods. Large fires were necessary to characteristics the fire risk in a tunnel. We can mention the 3 main projects:

- UpTun Project: A key European initiative that aimed to enhance fire safety in existing tunnels through innovative solutions such as advanced fire-resistant coatings, fibre-reinforced concrete formulations, and cost-effective retrofitting strategies. UpTun highlighted the critical need for continuous upgrades to meet evolving fire safety standards.
- FIT Project: Focused on understanding fire dynamics in rail tunnels, particularly with respect to the confined nature of rolling stock and the specific challenges posed by high-speed rail environments. The project's outcomes informed the development of targeted fire protection measures and advanced emergency response protocols.
- EUREKA FIRETUN Project: This project explored the interaction between fire suppression systems and tunnel linings, emphasizing the need for integrated fire safety solutions that account for the unique conditions of rail tunnels. The research supported the adoption of holistic fire protection strategies that combine active suppression with passive fire-resistant materials.

However, the evolution described in the present paper demonstrates the need of collective research for improving the rules, regulations, the engineering analysis and the design fire scenarios and design fires. This collective research is often the main basis of pre-standardization works.

CONCLUSION & REQUIREMENTS

A few years after the Mont Blanc Tunnel fire in 1999, a large amount of knowledge on fire scenarios and structural fire behaviour had been obtained. That knowledge has initiated standardization works internationally about structural behaviour (Efectis, NFPA, ASTM…) and has recently started at ISO TC92. However, new risks are highlighted, and their characterisation are limited. The risk is today managed because of a low frequency but not low consequences. The frequency will increase, but we should not face a new "Mont Blanc" type fire tunnel.

Mitigating concrete spalling in tunnel fires requires a comprehensive approach involving advanced concrete formulations, passive fire protection measures, and sophisticated modelling techniques. The integration of polypropylene fibres, optimized mixes, and state-of-the-art protective systems enhances tunnel resilience, safeguarding infrastructure and human life.

Future research should focus on refining fire resistance models, developing new materials to address emerging fire risks associated with new energy vehicles, and continuously updating fire safety strategies to adapt to evolving tunnel environments. Multi hazard engineering analysis becomes indispensable, with the complexity of the aging of passive fire protection.

The innovation on PP fibres introduced relationships between academic and all tunnel actors. New collective research may once again bring together all the players in applied research including academics. Notably, the integration of digital technologies, digital twins, sensor networks, and real-time monitoring systems into tunnel fire safety strategies can provide dynamic risk assessments, early warning systems, and data-driven decision-making to enhance fire protection and response measures.

REFERENCES

1. Haack, A. Catastrophic tunnel fires – What have we learnt? - Proceedings of the International Symposium on Catastrophic Tunnel Fires, 193-201, Borås, Sweden, 20-21 November, 2003
2. Franz Joel Ulm, Paul Acker and Michel lévy - Incendie dans le tunnel sous la manche, Analyse mécanique de l'écaillage du béton – Vol 2 Revue Française de génie Civil, 1998
3. Dr.ir. Kees Both, Technical Director Efectis Nederland BV, UPTUN: Cost effective sustainable and innovative Upgrading Methods for Fire Safety in existing Tunnel- Proceedings of the Third International Symposium on Tunnel Safety and Security , 353-362 Stockholm, Sweden, March 12-14, 2008
4. Dauti, D., PhD Thesis, A combined experimental and numerical approach to spalling of high-performance concrete due to fire. Mechanics of materials. Université Grenoble Alpes, 2018. English. (NNT : 2018GREAI062). (tel-01950731)
5. Haffmans L.J.M. - TNO test report – rapport betreffecde de beproeving van het gedrag van tweee isolatiematerialen ter bescherming van tunnels tegen brand – 00.65.3.2578 – B80-33 – 1980
6. Haffmans L.J.M and Dekkers J. report – beproeving van het gedrag bij verhitting van isolatiematerialen ter bescherming van tunnels bij brand, center voor brand veiligheid, B 79 391 - 1979
7. ISO 834-1, General principles, 1975
8. Interministerial circular no. 2006-20 of March 29, 2006
9. EN 1363-1, General principles, 2005
10. NFPA 502- 2004
11. J. Bienefelt, P. Kortekaas, A. Lemaire, M. van der Meulen, K. Parwani, T. Rakovec, M. Blom and B. Hendrix, "Fire testing procedure for concrete tunnel linings and other tunnel components," 2020
12. https://tunnelingonline.com/nfpa-502-fire-protection-case-histories-elizabeth-river-tunnel-and-the-hugh-l-carey-tunnel/
13. Pascal Van Hulle, Benoît Bertrand, Eric Cesmat, Bérénice Moreau et al Fire safety of underground structures of "La Défense" in Paris - Proceedings of the Sixth International

Symposium on Tunnel Safety and Security , 533-542, Marseille, France, March 12-14, 2014
14. NFPA 502 –2008
15. European directive 2022/2557 of the European Parliament and of the council of 14 december 2022 on resilience of critical entities and repealing Council Directive 2008/114/EC
16. National Annex to NEN-EN 1991-1-2+C3: Eurocode 1 - Actions on structures - Part 1-2: General actions - Actions on structures exposed to fire," 2019
17. ADR - Agreement concerning the International Carriage of Dangerous Goods by Road," 2023
18. Directive 2004/54/EC of the European Parliament and of the Council of 29 April 2004 on minimum safety requirements for tunnels in the Trans-European Road Network,"
19. CETU - Passive fire protection systems - Justification of performance for road tunnel structures," 2017.
20. EN 1992 Design of concrete structures - Part 1-2 : General rules - Structural fire design – 2004
21. EN 1993 Design of steel structures - Part 1-2 : General rules - Structural fire design – 2024
22. EN 1994 Design of composite structures - Part 1-2 : General rules - Structural fire design – 2006
23. Carré, H., Pimienta, P., La Borderie, C., Pereira, F., and Mindeguia, J.-C. ,"Effect of compressive loading on the risk of spalling". In: MATEC Web of Conferences 6, p. 01007. (2013).
24. Boström, L Spalling of tunnel structure linings – New Swedish result Proceedings of the International Symposium on Catastrophic Tunnel Fires, 193-201, Borås, Sweden, 20-21 November, 2003
25. Lars Boström, Robert Jansson, SP, Test Methods for Determining Fire Spalling of Concrete Proceedings of the Fifth International Symposium on Tunnel Safety and Security , 721-730, New York, USA, March 14-16, 2012
26. ASTM E 3134-20 "standard specification for transportation tunnel structural component and passive fire protection systems
27. Robert Mac Namee, Lars Boström, RISE, Experimental analysis of different screening test method for fire spalling of concrete - Proceedings of the Eighth International Symposium on Tunnel Safety and Security , 691-693, Borås, Sweden, March 14-16, 2018
28. Iravani, A. and Anders, S., "Effects of cement type, aggregate type and concrete age on the mass loss of concrete exposed to elevated temperature". In: : 5th International Workshop on Concrete Spalling due to Fire Exposure in Boras, Sweden, pp. 63–72 (2017)
29. Anna-Lena Hammer, Götz Vollmann Bochum University et al - Experimental investigation of a cement-free shotcrete in case of fire: Spalling tendency, thermal and mechanical properties, Proceedings of the Ninth International Symposium on Tunnel Safety and Security, 585-600, Munich, Germany, March 11-13, 2020
30. Yi Shen, Shi-qi Dou et al , 1State Key Laboratory of Disaster Reduction in Civil Engineering, bonding behaviour of CFRP composite strengthened tunnel structure under fire exposure - Proceedings of the tenth International Symposium on Tunnel Safety and Security, 602-617, Stavanger, Norway, April 26-28, 2023
31. Robert Jansson* & Lars Boström, Influence of polypropylene fibres on fire spalling and material properties of concrete, SP Technical Research Institute of Sweden, Borås, Sweden, Proceedings of the Third International Symposium on Tunnel Safety and Security, 249-260, , 87-94 Stockholm, Sweden, March 12-14, 2008
32. D. Dauti, J. Viale , J. Bienefelt, et al " structural modelling coupled with large scale fire tests for determining spalling of concrete structures : a real application case to the Mont Blanc Tunnel Vault" – 13th international conference on structures on fire, Coimbra, Portugal, June 19-21, 2024
33. Pimienta, P., McNamee, R., Robert, F. et al. Recommendation of RILEM TC 256-SPF on fire spalling assessment during standardised fire resistance tests: complementary guidance and requirements. Mater Struct 57, 3 (2024). https://doi.org/10.1617/s11527-023-02248-z
34. Stefan Zmigrodzki CIMA+ Consulting Engineers - Pre-stressing of structural tunnels as a method to control cracks resulting from the temperature loads - Proceedings of the Sixth International Symposium on Tunnel Safety and Security , 513-522, Marseille, France, March 12-14, 2014
35. Leander.M. Noordijk, P.G. Scholten, A.J. Breunese and C. Both, Efectis Nederland, Emerging

Problem for Immersed Tunnels: Fire Induced Concrete Cracking - Proceedings of the Fourth International Symposium on Tunnel Safety and Security, 211-220 Frankfurt am Main, Germany, March 17-19, 2010
36. PFPNet Guidance of structural passive fire protection in road tunnel
37. BI 86-69 Tunnel protection fire test procedure, TNO, 1986
38. Efectis R0695 Fire testing procedure for concrete linings, 2008
39. Claus K. Larsen "testing of fire proofing of concrete RWS fire curve - test method", TR 2494 – Norwegian Directorate of Public Roads, June 29, 2007
40. Maria Hjohlman, Lars Boström & Robert Jansson SP,Fire Testing of Concrete and Concrete Protection Systems for Tunnels in Sweden - An Overview - Proceedings of the Third International Symposium on Tunnel Safety and Security , 87-94 Stockholm, Sweden, March 12-14, 2008
41. Pierre Pimienta, CSTB, Octavian Anton, PRTC N.V et al - Fire Protection of Concrete Structures Exposed to Fast Fires - Proceedings of the Fourth International Symposium on Tunnel Safety and Security , 235-248 Frankfurt am Main, Germany, March 17-19, 2010
42. EAD 350140-00-1106- Fire Protective Products, Renderings and rendering kits intented for fire resisting applications – September 2017
43. EAD 350142-00-1106- Fire Protective Products, Fire Protective boards, slab and mat products and kits, September 2017
44. V. Venkov, D. Joyeux, T. Busson, X. Duponchel and C. Chinaya, "Operation of tunnels after a fire incident: the residual properties of concrete," 2017
45. Kees Both Promat International, New challenges in fire protection of tunnels - Proceedings of the Sixth International Symposium on Tunnel Safety and Security , 19-38, Marseille, France, March 12-14, 2014
46. Tim G. van der Waart van Gulik, , Larry DeGraff, Promat, Philippe Bourdon, Bouygues, Design, Assessment and Application of Passive Fire Protection in the Port of Miami Tunnel according to NFPA 502, Proceedings of the Seventh International Symposium on Tunnel Safety and Security , 147-158, Montreal, Canada, March 16-18, 2016
47. Wern-ping Nick Chen, Jacobs Engineering Concrete Explosive Spalling Test for the Ohio River Bridge East End Crossing Tunnel- Proceedings of the Seventh International Symposium on Tunnel Safety and Security , 159-170, Montreal, Canada, March 16-18, 2016
48. Leander Noordijk, Albert Kandelaar Arcadis Nederland BV , Assessment and upgrade of the fire resistance of the Waterwolftunnel, Proceedings of the Ninth International Symposium on Tunnel Safety and Security , 601-612, Munich, Germany, March 11-13, 2020
49. Leander Noordijk, Tim van der Waart & George Scholten, Efectis Nederland BV,
Coen van der Vliet, ARCADIS Nederland BV, Assessing the Fire Resistance in Existing Tunnels Proceedings of the Fifth International Symposium on Tunnel Safety and Security, 731-736, New York, USA, March 14-16, 2012
50. Martin Vermeer, Arnoud Breunese & Leander Noordijk, Efectis Nederland BV Mobile Furnace for Determining Spalling Sensitivity of Existing Concrete Tunnel Linings, Proceedings of the Fifth International Symposium on Tunnel Safety and Security , 703-712 New York, USA, March 14-16, 2012
51. Dominique Pardon, Pierre Pimienta, et al, CSTB- On site risk assessment of concrete spalling in tunnel by means of a mobile oil-fired furnace - Proceedings of the Sixth International Symposium on Tunnel Safety and Security , 523-532, Marseille, France, March 12-14, 2014
52. Amir Golpaygan, Jimmy Susetyo , Reza Shobayry, Nima Eslaminasab & Tomas Gregor Hatch, Mississauga, ON, Developing a Technique to Predict Concrete Spalling for Design of Tunnel Liner Exposed to a Major Fire Event in a Tunnel - Proceedings of the Seventh International Symposium on Tunnel Safety and Security , 171-180, Montreal, Canada, March 16-18, 2016
53. Naija Karimi, Roozbeh Sarem,Jawzjan University, Afghanistan, Seismic response of multistorey building using different vibration techniques, International Journal of Innovative Research and Scientific Studies
54. Regulation (EU) 2023/851 of the European parliament and of the council of 19 April 2023, amending regulations (EU) 2019/631 as regards strengthening the CO2 emission performance standards for new passage cars and new light commercial vehicles in line with the Union's

increased climate ambition

55. Wenqian Liu, Frank Markert et al, Technical University of Denmark , Nonlinear analysis of tunnel slab under hydrogen explosion - Proceedings of the tenth International Symposium on Tunnel Safety and Security, 240-253, Stavanger, Norway, April 26-28, 2023
56. Rickard Forsén and Anders Bryntse, FOI Swedish Defence Research Agency, An Analysis of the Consequences from an Explosion in a Road Tunnel with Concrete Walls and Roof - Proceedings of the Fourth International Symposium on Tunnel Safety and Security , 169-178 Frankfurt am Main, Germany, March 17-19, 2010
57. Didier Lacroix, Centre d'Etudes des Tunnels (CETU), Managing Road Tunnel Safety: Today's Challenge, Proceedings of the Third International Symposium on Tunnel Safety and Security, 7-20, Stockholm, Sweden, March 12-14, 2008
58. Directive 2008/68/EC of the European Parliament and of the Council of 24 September 2008 on the inland transport of dangerous goods
59. Jorrit Nieuwenhuis MSc, Art v/d Giessen MSc, Stefan Lezwijn MSc, ARCADIS Amersfoort - Safety Requirements & Transport of Dangerous Goods through the 53 Kilometer Railway Tunnel through the Alps between Lyon and Turin - Proceedings of the Third International Symposium on Tunnel Safety and Security , 119-128 Stockholm, Sweden, March 12-14, 2008
60. Erik Hall Midholm, Rosie Kvål & Johan Lundin , Brandskyddslaget AB, Risk evaluation in road and railroad overbuilding - Proceedings of the tenth International Symposium on Tunnel Safety and Security , 158-170, Stavanger, Norway, April 26-28, 2023

Numerical study of the influence of wind on the smoke spread between underpasses

Matteo Pachera[1]
[1]Sweco, Brussels, Belgium

ABSTRACT
Tunnels are complex and expensive infrastructure to build and to operate. In some cases, it is possible to optimize their geometry to limit their cost and complexity without compromising the safety level. This study investigates how a possible tunnel was downgraded to two underpasses separated by an open shaft. The two underpasses require less safety measures because of their limited length, however, they should remain independent in case of fire.
Computations fluid dynamics is used to investigate the smoke behaviour in case of fire and adverse wind conditions. A multiscale approach is proposed to simulate the wind at large scale and the fire at smaller scale. The second analysis uses the results of the first analysis as boundary conditions to take the wind field into account.
Given the short length of the open shaft different geometrical configurations are proposed to ensure that tenability conditions are maintained in the open zone and smoke spread between the underpasses is prevented. The results of the analyses show that the two underpasses are independent in case of fire and adverse wind conditions and how the different geometrical configurations can improve smoke management.

KEYWORD: wind, CFD, FDS, multiscale analysis, optimization

INTRODUCTION

Tunnels are infrastructures capable of crossing obstacles and improving traffic management. They can limit the effects of traffic above ground (noise, pollution, interaction with other means of transport) and improve the life quality of the surrounding area. Therefore, they became the preferred solution from an architectural perspective to reclaim urban areas [1, 2]. However, because of the tunnel's safety measures, the initial investment, exploitation costs and energy consumption are higher compared to open roads [3,4]. An optimal trade off should maintain high safety levels, limit the complexity, and guarantee an improvement in the landscape.

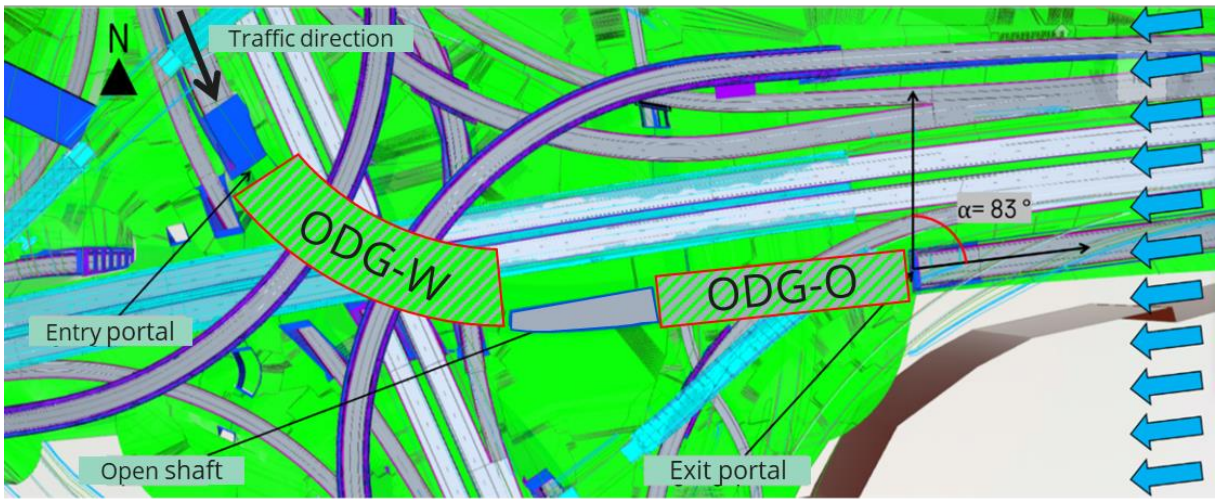

Figure 1: Infrastructure under analysis.

This study investigates the evolution of a possible tunnel (originally 365 m long) into two independent underpasses (ODG-W 155 m and ODG-O 135 m long) separated by an open shaft (75 m long) (see Figure 1). The underpasses, thanks to their short length, require less safety measures compared to a tunnel (separate evacuation route, ventilation, detection, monitoring) so the investment can be limited [4]. The underpasses are effectively independent, if in case of fire and adverse wind conditions, tenability conditions are negatively impacted only in the incident underpass, while they remain acceptable in the other underpass and part of the open shaft. Given the short length of the open shaft the possible smoke spread shall be investigated in detail [4,5]. Three different geometrical configurations are proposed for the open shaft to ensure that one or more solutions are available to limit smoke spread.

PROPOSED APPROACH

In the study computational fluid dynamics (CFD) is applied to study both the wind and fire induced flow fields. The software Fire Dynamics Simulator (FDS 6.8.1) is used to simulate both phenomena using a multiscale approach [6]. The wind driven flow is mainly affected by the morphology of the terrain and buildings in the proximity of the infrastructure. Therefore, wind is first modelled at large scale extending the computational domain beyond the infrastructure itself [7]. Given the large domain a lower spatial resolution is required to simulate the flow with the available computational resources. However, this resolution is insufficient to model accurately the fire induced flows which are strongly affected by the geometry of the infrastructure itself and the velocity close to the portals. Therefore, a second analysis is carried out with a smaller numerical domain, but with higher resolution, that considers both fire and wind. In the small scale analysis the wind velocity is imposed as boundary condition taking the results of the large scale analysis as input. The proposed strategy is a one way coupling strategy which assumes that the wind field on large scale is weakly affected by the fire itself [8].

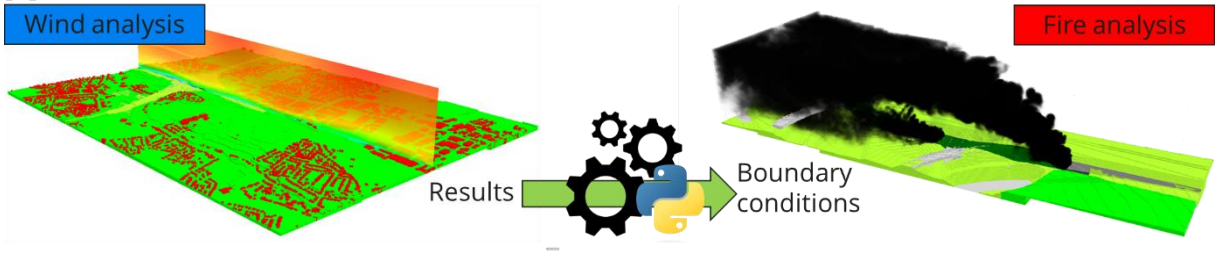

Figure 2: One-way multiscale approach for wind and fire analyses.

Large scale analysis

The large scale simulation is designed to predict the wind field near the infrastructure. Its numerical domain is mostly extended upstream the zone of interest to take into account the impact of the different obstacles on the wind field [7]. Figure 3 shows the morphology of the terrain (in green) and the existing buildings (in red) included in the model.

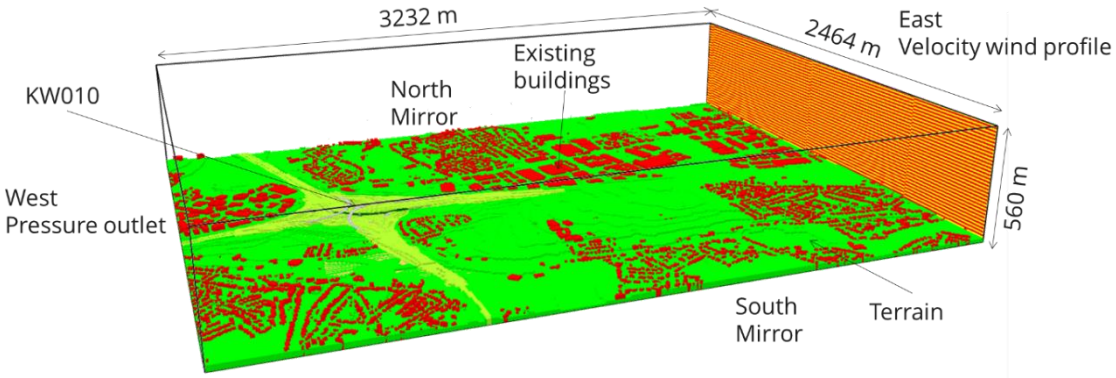

Figure 3: Numerical domain of the large scale wind analysis.

The domain is 3232 m long in the wind direction, 2464 m wide and 560 m high. The size of the domain is chosen based on the guidelines for wind simulations [7] and it is comparable to the domain used in similar types of studies [8,9]. The extension of the domain allows the flow to freely develop before impacting on the infrastructure [10]. The wind is imposed upstream in the domain using a power law wind velocity profile. The profile is calculated as function of the height using the reference wind speed of 3 m/s at 10 m and an α coefficient of 0.143. This wind profile is generally not applicable to urban area because it doesn't take into account the impact of obstacles that can affect the stability of the wind profiles, however, these are explicitly included in the model [10]. The boundary conditions are placed far upstream from the zone of interest therefore, the wind profile can freely develop before impacting on the infrastructure.

$$\frac{u}{u_r} = \left(\frac{z}{z_r}\right)^{\alpha} \tag{1}$$

The domain is discretized with different meshes that create layers around each other. The zone of interest is meshed with a uniform mesh of 1.0 m size, the zone with higher resolution is extended 100 m upstream the portals and 60 m above the open structure. The other zones further away are meshed with coarser meshes to reduce the computational load of the analysis.

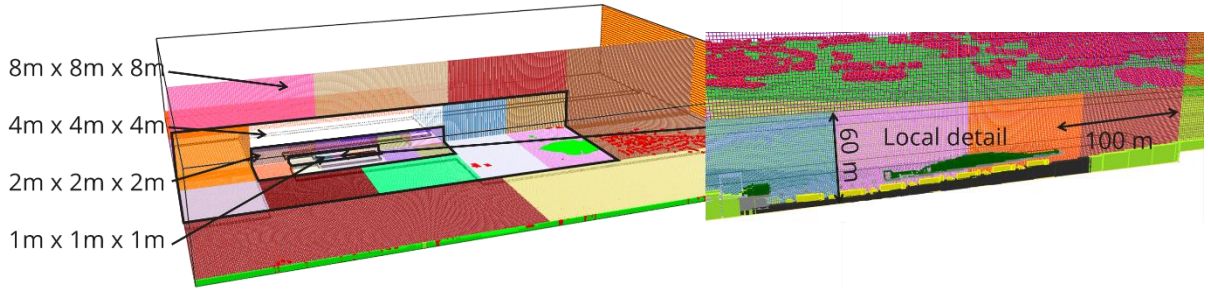

Figure 4: Grid resolution overview of the large scale analysis

Small scale analysis

The small scale analysis investigates the smoke propagation inside and between the underpasses with adverse wind conditions. The domain's size is reduced compared to the large scale analysis because of the higher spatial resolution. The domain is 496 m long in the wind direction, 218 m wide and 90 m high. The terrain and the different infrastructures are included as geometrical obstructions. On the lateral edges of the domain the velocity components are imposed as boundary conditions, based on the results of the large scale analysis. The top boundary condition is simulated as a local pressure boundary condition.

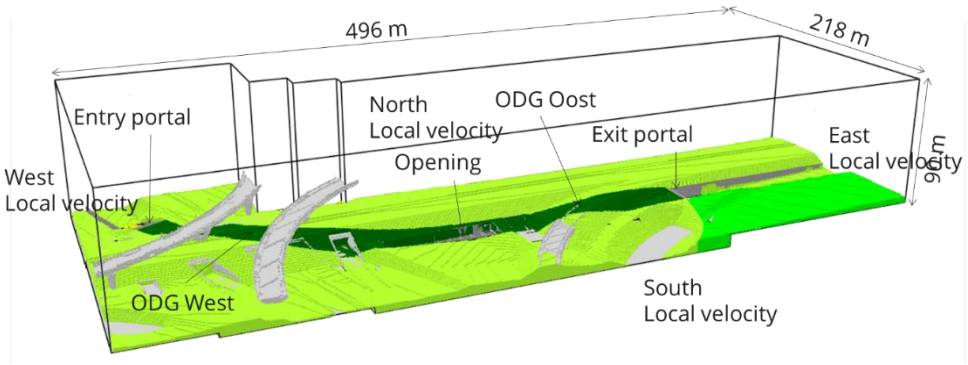

Figure 5: Domain overview of the small scale analysis

The domain's spatial resolution in the small scale analysis is much finer than in the large scale one. The tunnel is simulated with a mesh resolution of 0.25 m including a region near the portals and the opening between the underpasses [11,12]. The upper mesh layer has a mesh resolution of 0.5 m while the zone higher above has a mesh resolution of 1 m, *Figure 6*.

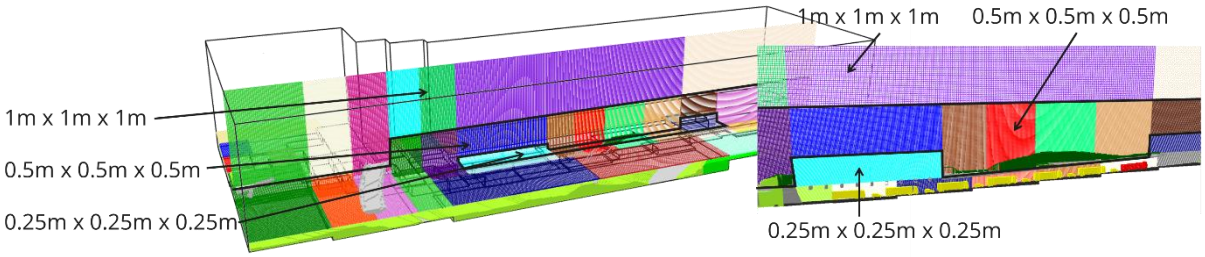

Figure 6: Grid resolution overview of the small scale analysis

PROPOSED SCENARIO

This paragraph describes the proposed fire scenario (location, magnitude, toxicity) and wind scenario (velocity, direction).

Fire scenario

The fire scenario is defined as a realistic worst case scenario for a large truck with a total HRR equal to 100 MW [4,13,14,15,16]. The soot yield of the fire is equal to 10%, the CO yield is equal to 10% and the HCN yield is equal to 1% [14,17]. The heat of combustion is equal to 25 MJ/kg, representing common plastic materials and the radiative fraction is equal to 35%. The model includes the burning vehicle and the other vehicles blocked upstream.

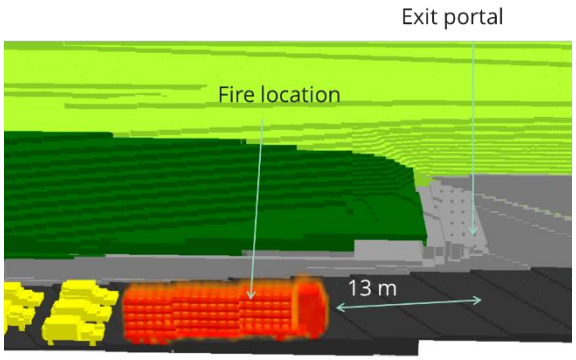

Figure 7: Side view of the burning truck

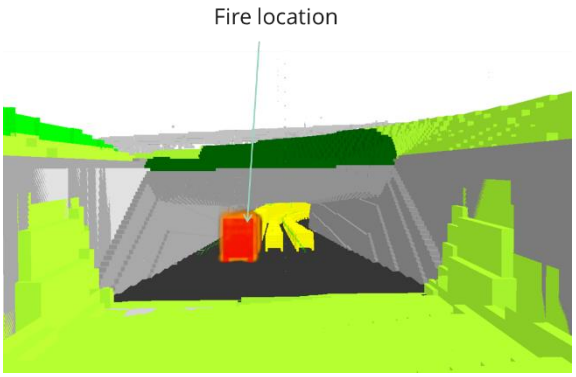

Figure 8: Front view of the burning truck

The fire's location is chosen to maximize the impact of smoke on road users [4]. The infrastructure under investigation is made of two unidirectional underpasses, therefore a fire in the first underpass ODG-W is not critical because the traffic downstream the fire in the opening and in the second

underpass can simply drive out. A fire in the second underpass ODG-O instead blocks the traffic upstream in both underpasses and in the opening possibly affecting more road users. The burning vehicle is located near the exit portal of the ODG-O in order to maximize the cooling effect of the smoke flowing back towards the shaft. The distance from the exit portal is about 13 m which represents 90% of the total length from the opening [4].

Wind scenario

The wind scenario should be a realistic worst case scenario that maximizes the smoke spread between underpasses, thus the number of exposed road users. The most conservative wind direction is the one blowing the smoke from the exit portal back towards the opening and the first underpass. This direction is equal to 83° N because of the orientation of the exit portal [4].
The magnitude of the wind is calculated starting from the measured wind distribution in all directions and computing the wind component along the direction of interest. In the region the wind mostly comes from south west, therefore the east component is relatively small as shown both in the wind rose, *Figure 9*, and in the histogram, *Figure 10*. The reference wind speed was calculated as the 95th percentile of the wind distribution in the worst case direction, *Figure 10*. This translates as only in 5% of the cases the wind speed in the direction of interest is higher than 3 m/s. This velocity is calculated at 10 m high and it is used to calculate the velocity profile shown in equation 1.

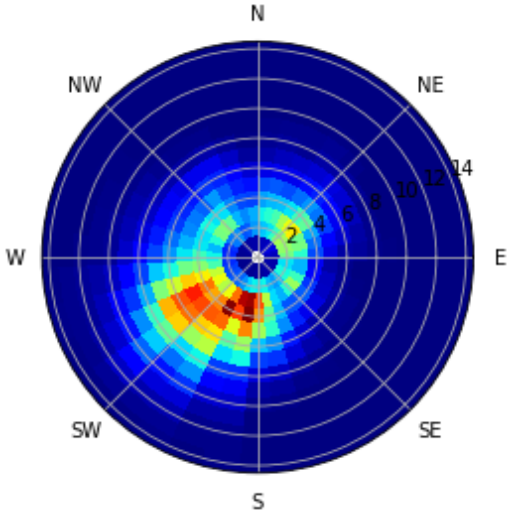

Figure 9: Wind rose used of the site under analysis.

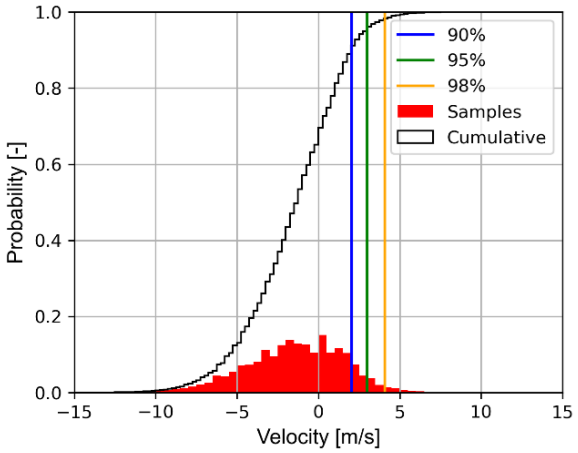

Figure 10: Distribution of the velocity component perpendicular to the exit portal

RESULTS

This paragraph discusses the results of the different analyses. The large scale wind analysis is presented first, its results are compared to a small scale analysis without wind to assess the correct implementation of the boundary conditions and the impact of the mesh resolution. The results of the different fire analysis are later presented showing the different tenability criteria along the two underpasses and in the open section, *Figure 11*. The acceptance criteria for the study are evaluated at 25 m from the exit portal of the ORG-W according to [4]. This location allows to create a safe space with good tenability conditions for the occupants of the ODG-O.

- Visibility > 10 m
- Temperature < 50 °C
- Radiative heat flux < 1 kW/m²
- CO concentration < 1000 ppm

All the criteria mentioned above are evaluated along the tunnel along two lines given the curvature of the infrastructure, *Figure 11*.

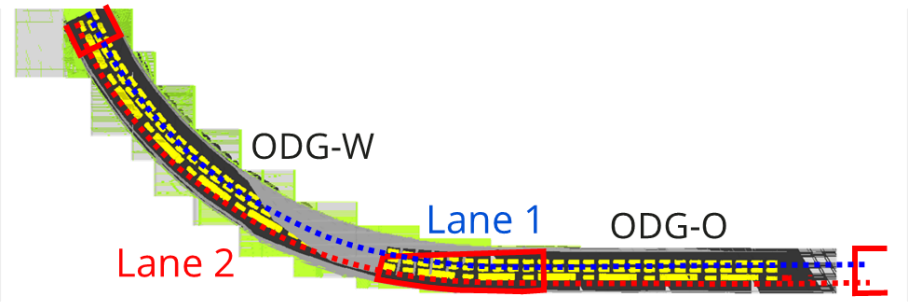

Figure 11:Locations where tenability conditions are evaluated.

In the figures below the exit portal of ODG-W is set at 0 m, the 25 m location is marked with a black line and the other portal are marked with dashed lines. The location of the portal slightly varies for Lane 1 and Lane 2 because of the curvature of the infrastructure.

Wind analysis

The main focus of the wind analysis is the velocity distribution near the infrastructure. The wind velocity is monitored at different locations and results are presented as function of the height in the figures below. Given the height variation of the terrain the z coordinate is referred to sea level. The first two profiles are monitored at 500m (Loc 4) and 1000m (Loc 5) upstream the exit portal, these are presented only for the large scale analysis.

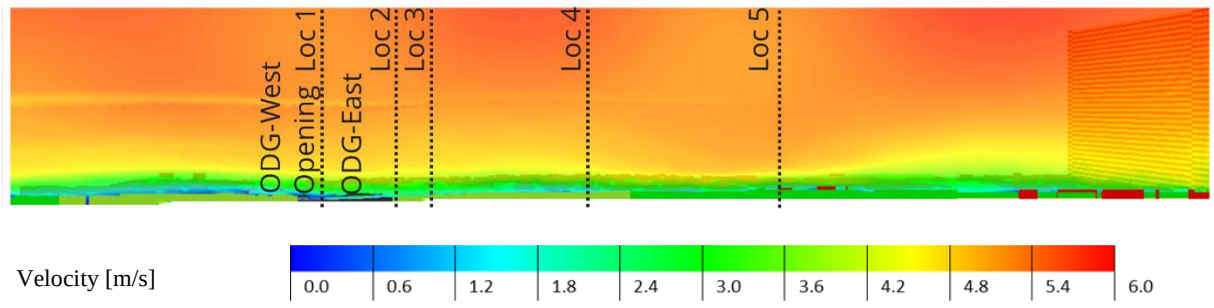

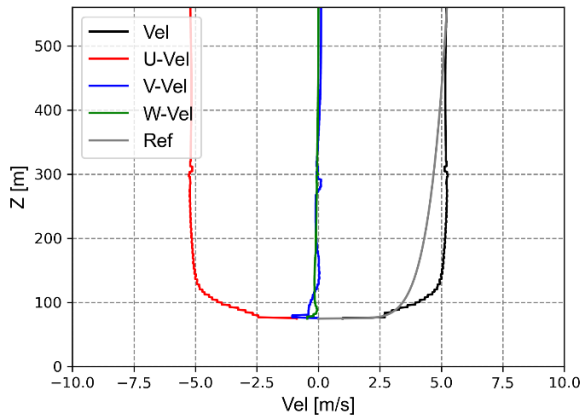

Figure 12: Velocity profile at Loc 5

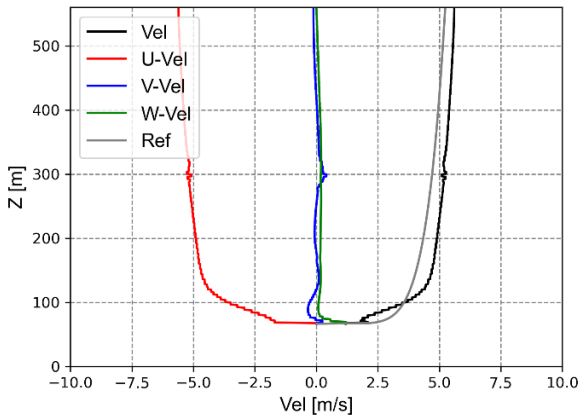

Figure 13: Velocity profile at Loc 4.

The velocity profiles closer to the infrastructure are monitored both in the large scale and in the small scale analyses. These are compared together in the figures below. The profile at Loc 1 is located in the open shaft, the profile at Loc 2 is located outside the exit portal of the ODG-O and the profile at Loc 3 is located 100 m outside the exit portal.

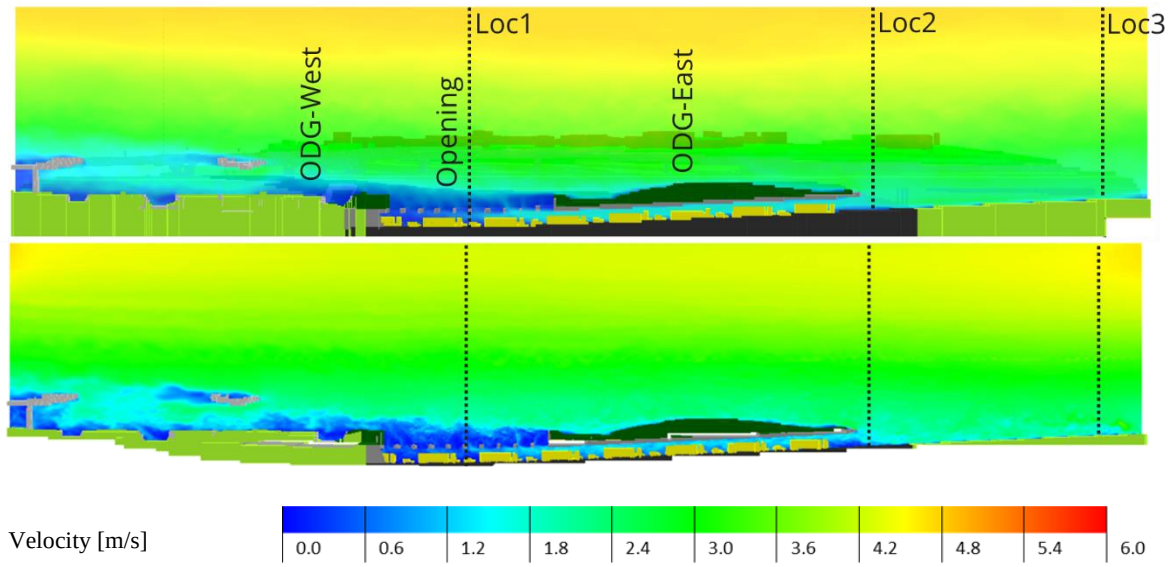

Figure 14: Velocity field near the underpasses obtained in the large scale analysis (top) and in the small scale analysis (bottom).

The results show that the velocity profiles in the small scale and in the large scale analysis are very close to each other. There are some differences near the top edge of the domain of the small scale analysis because a pressure boundary condition is imposed there, but this boundary condition doesn't allow to impose the tangential velocity. The velocity near the ground decreases close to the exit portal at Loc 2 and Loc 3 compared to the original profile and the possible explanation can be the lower height of the ground near the tunnel. The terrain's morphology is comparable to a divergent that locally reduces the velocity due to the flow expansion. The volume flow rates in the different portions of the underpasses and in the opening are also comparable given the large difference in mesh resolution (1.00 m for the large scale analysis, and 0.25 m for the small scale analysis) *Figure 18*.

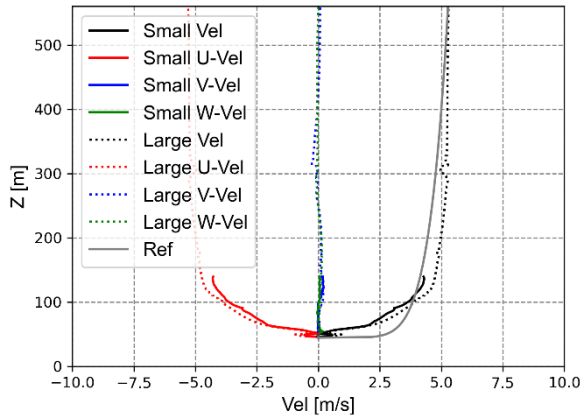

Figure 15: Velocity profile at Loc 1

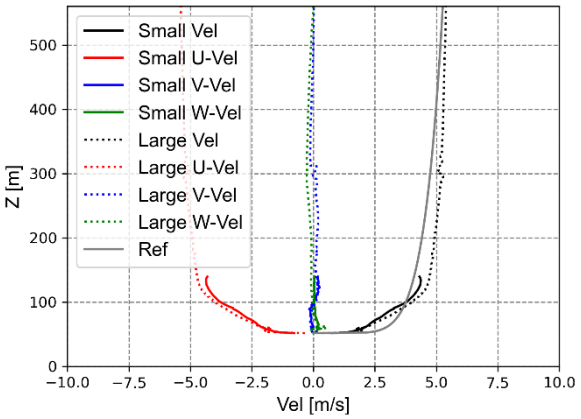

Figure 16: Velocity profile at Loc 2

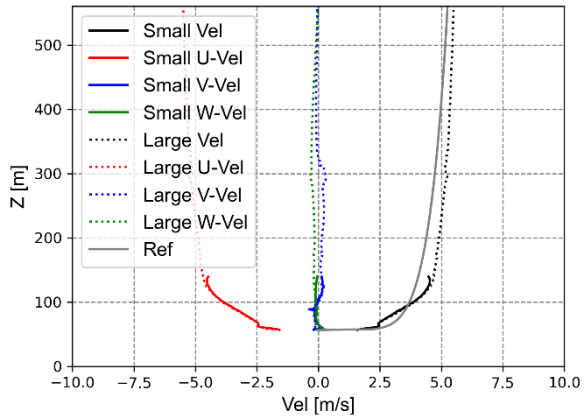

Figure 17: Velocity profile at Loc 3

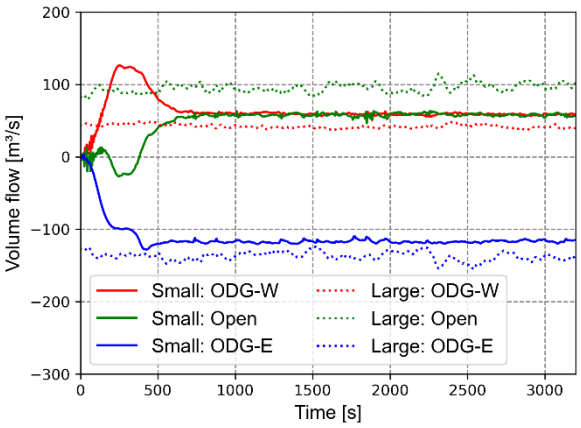

Figure 18:Volume flows in cold conditions

Fire analysis with geometry configuration 1

The first fire analysis is carried out considering the geometry of the open shaft without additional geometry optimization. The open shaft has transversal beams each 7 m to support the side walls, 6 m deep (see fig 19).

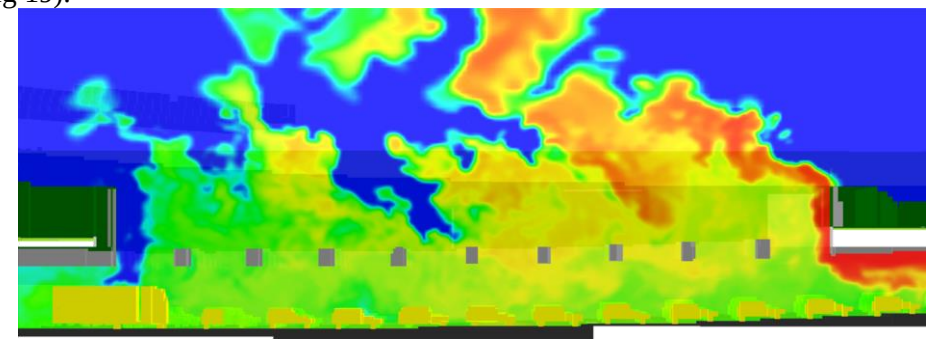

Figure 19: Detail of the open shaft for conf. 1

The results of the analysis are presented for the different tenability criteria described in the section above. The results are averaged in time over the last 200 s from 1000 s till 1200 s as the different flows in the underpasses become steady state, *Figure 20*, *Figure 21*.

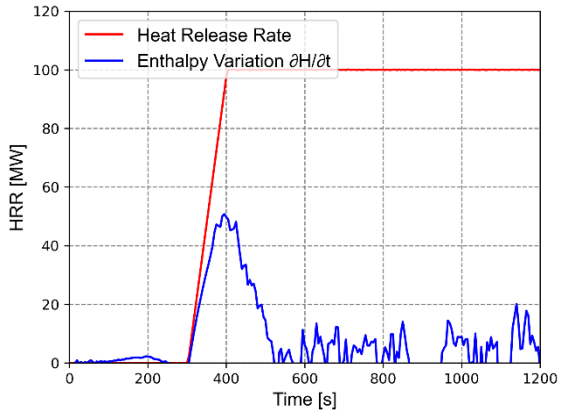

Figure 20: Energy balance for conf. 1

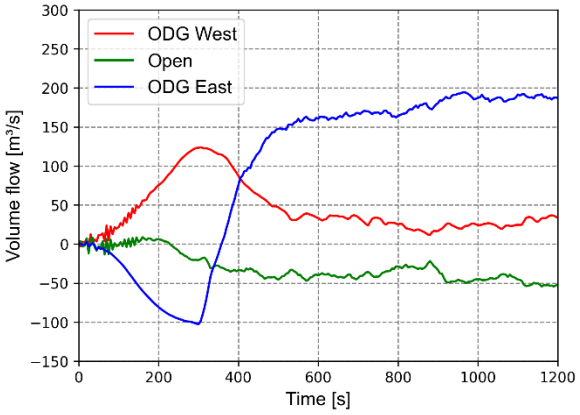

Figure 21:Volume flow rates for conf. 1

The visibility (fig 22), temperature (fig 23), radiative heat flux (fig 24) and CO concentration (fig 25) are monitored at 2 m high along the measurement lines inside the underpasses and in the open area. The results show that there is smoke spread between the two underpasses, however, the smoke is diluted by the wind and the visibility is just above 10 m at the reference point. The other tenability criteria are well within the acceptability limit.

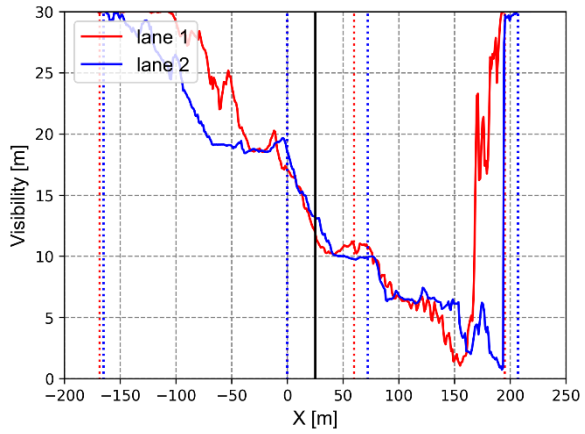

Figure 22: Visibility for conf. 1

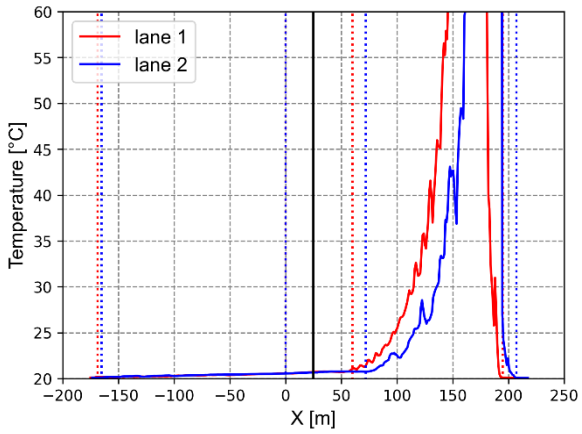

Figure 23: Temperature for conf. 1

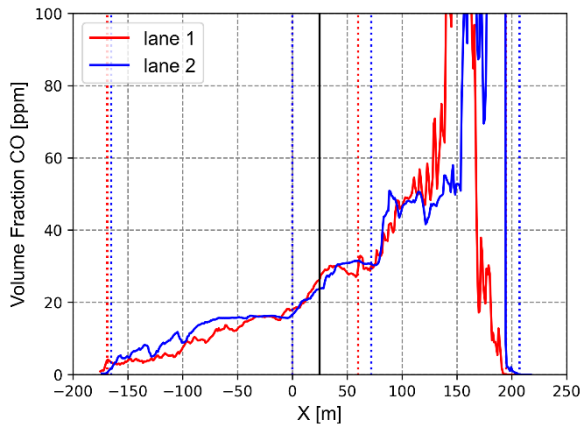

Figure 24: CO concentration for conf. 1

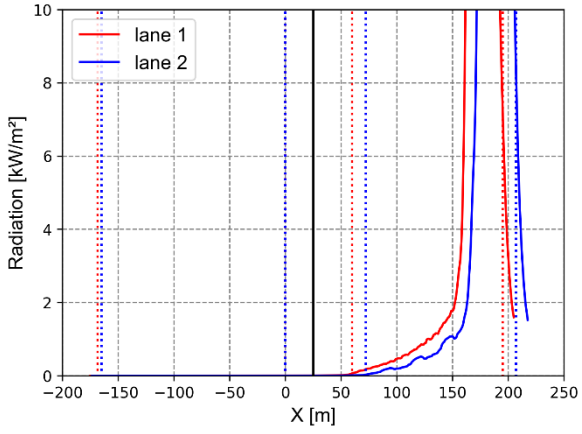

Figure 25: Radiative heat flux for conf. 1

The results are also presented in form of contour for the temperature (fig 27), visibility (fig 26), CO concentrations (fig 28) and velocity (fig 29). The mixing of smoke and fresh air causes loss of stratification and visibility, which is almost at the limit value at the reference point. The smoke is also partially pushed in the second underpass ODG-W however, the visibility remains higher than 10 m.

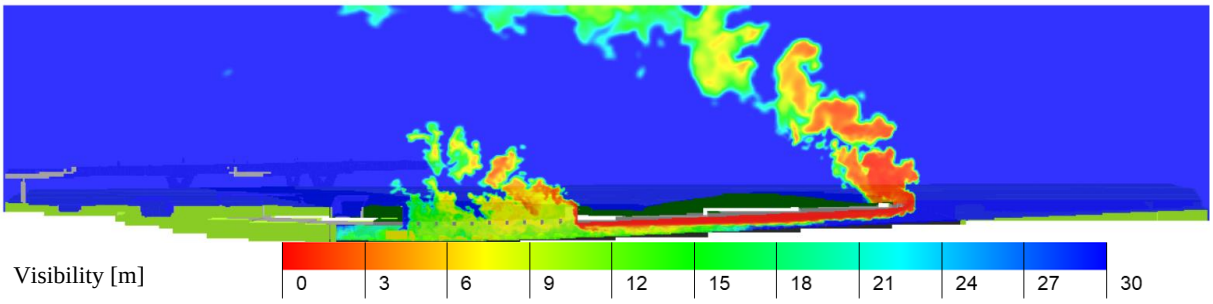

Figure 26: Side view of the visibility inside the ODG-O and the opening for conf.1

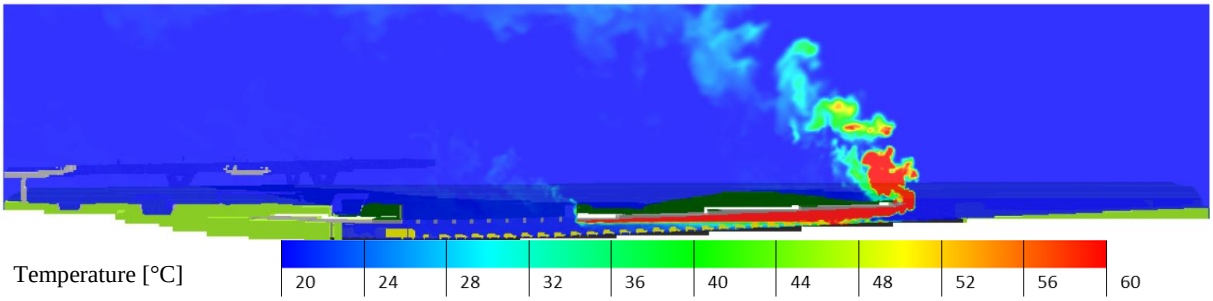

Figure 27: Side view of the temperature inside the ODG-O and the opening for conf. 1

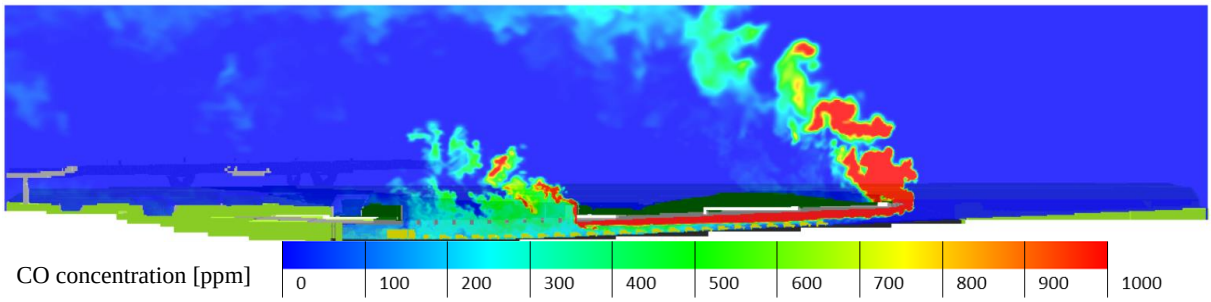

Figure 28: Side view of the CO concentration inside the ODG-O and the opening for conf.1

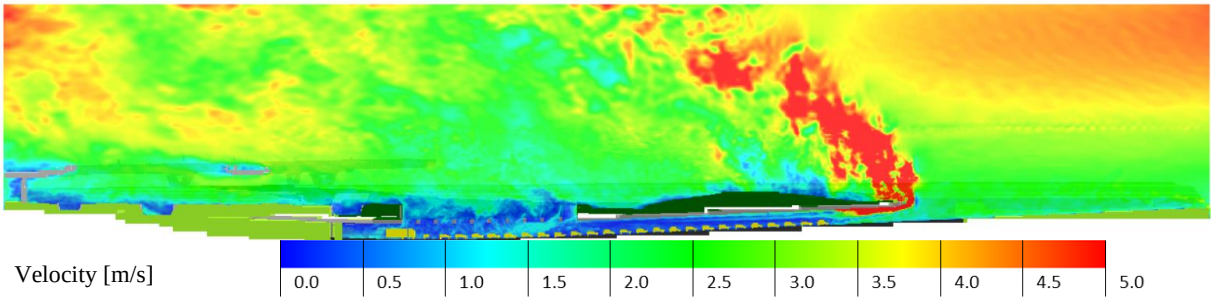

Figure 29: Side view of the velocity inside the ODG-O and the opening for conf.1

Fire analysis with geometry configuration 2

The first geometrical configuration provides acceptable results according to [4]. However, there is unwanted smoke spread between underpasses that should be limited, if possible. A first optimized configuration includes vertical elements above the beams to limit air and smoke recirculation. The vertical panels are 6 m high so they reach the top of the opening.

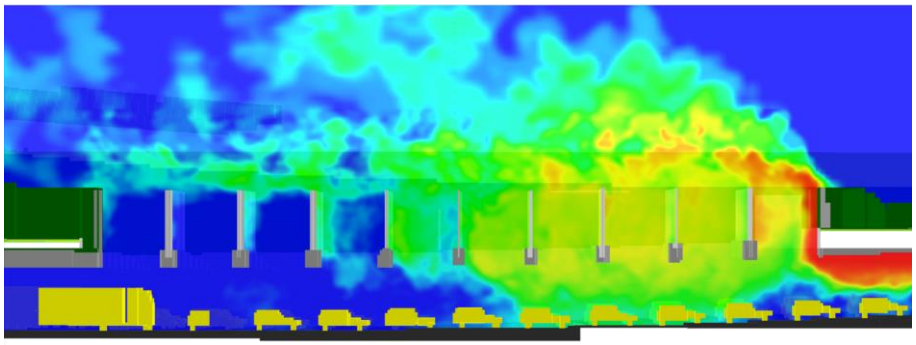

Figure 30: Detail of the open shaft for conf. 2

The results of the simulations are presented for the different tenability criteria described in the section above. The results are averaged in time over the last 200 s from 1000 s till 1200 s as the different flows in the underpasses become steady state (fig 31 and 32).

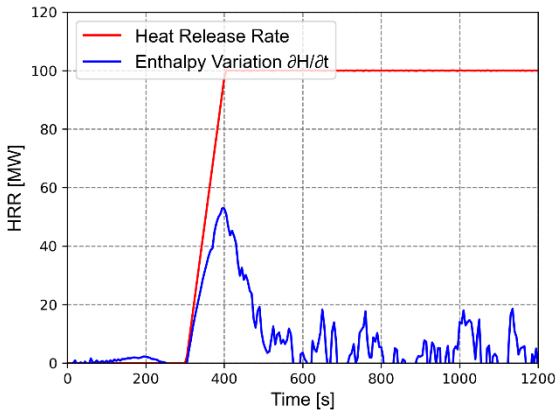

Figure 31: Energy balance for conf. 2

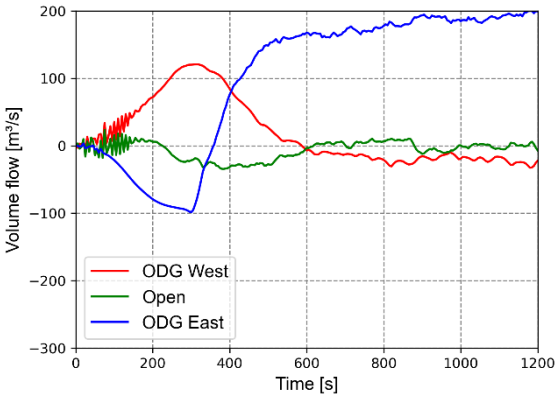

Figure 32:Volume flow rates for conf. 2

The visibility (fig 33), temperature(fig 34), radiative heat flux (fig 35) and CO concentration (fig 36) are presented along the measurement lines inside the underpasses. The different quantities are monitored at 2 m high above the road level. With this configuration the results, also for the visibility are well withing the acceptable limit.

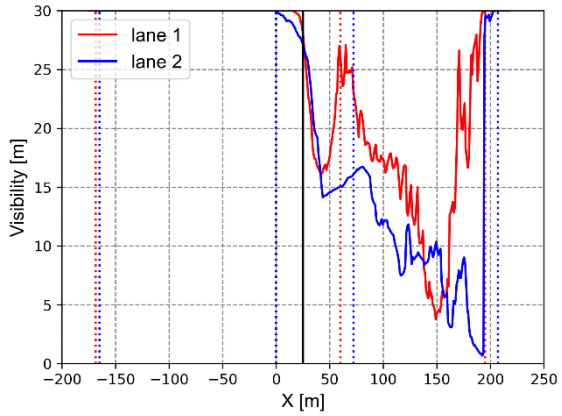

Figure 33: Visibility for conf. 2

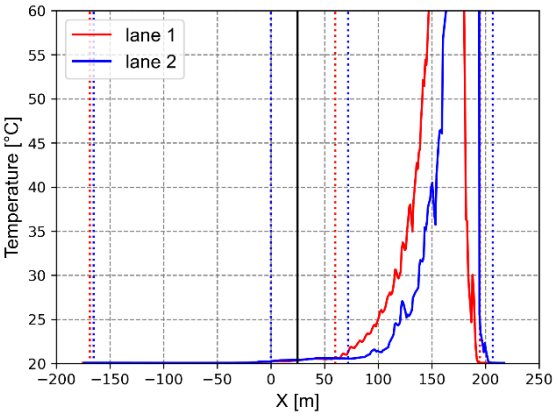

Figure 34: Temperature for conf. 2

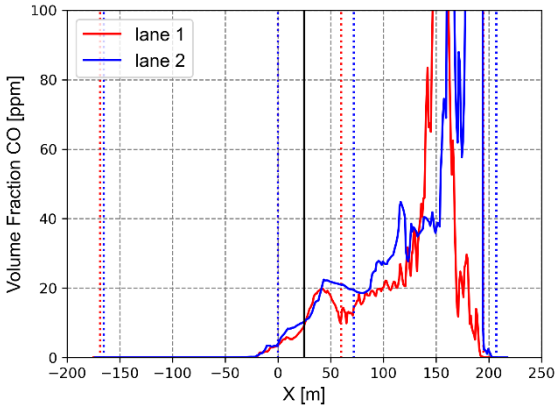

Figure 35: CO concentration for conf. 2

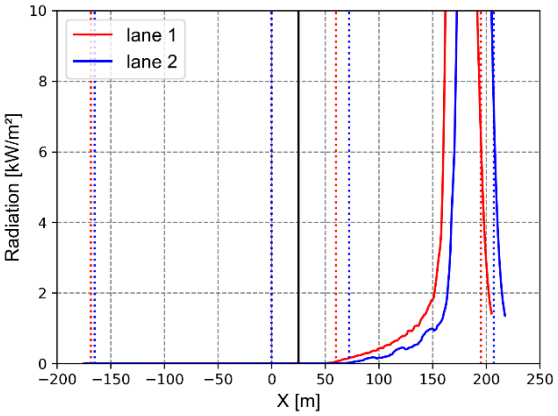

Figure 36: Radiative heat flux for conf. 2

The results are also presented in form of contour for the temperature, visibility (fig 37), CO concentrations (fig 38) and velocity (fig 39). In this second configuration the barriers block the formation of large eddies that mix the smoke and fresh air. As result, smoke doesn't spread to the second underpass ODG-W and it is only limited to a portion of the opening.

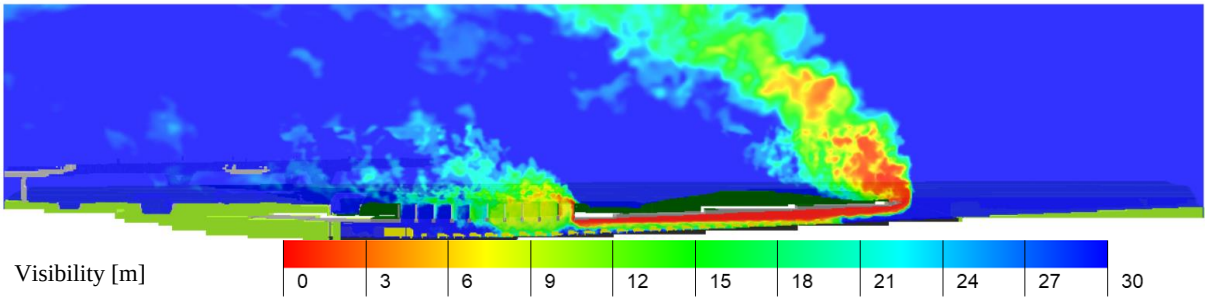

Figure 37: Side view of the visibility inside the ODG-O and the opening for conf.2

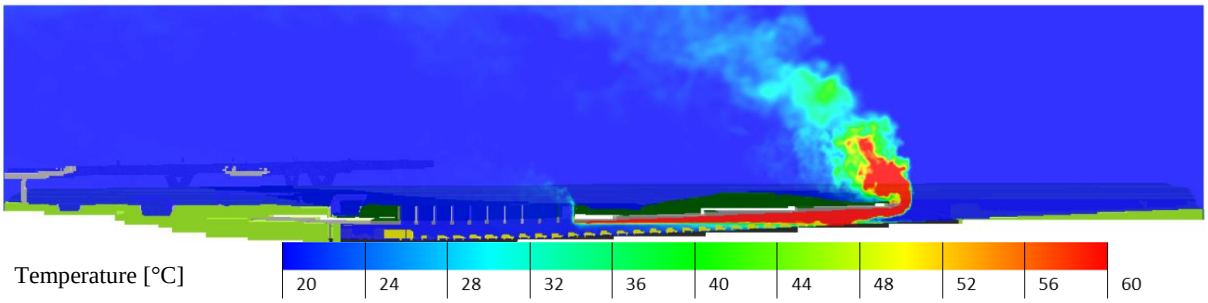

Figure 38: Side view of the temperature inside the ODG-O and the opening for conf.2

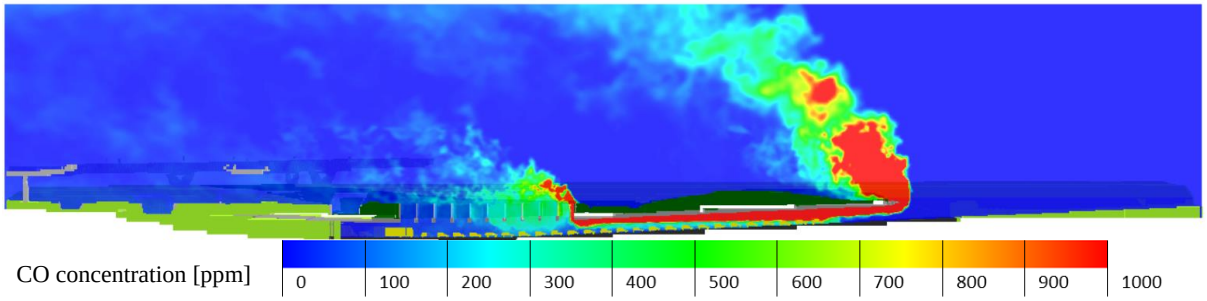

Figure 39: Side view of the CO concentration inside the ODG-O and the opening for conf.2

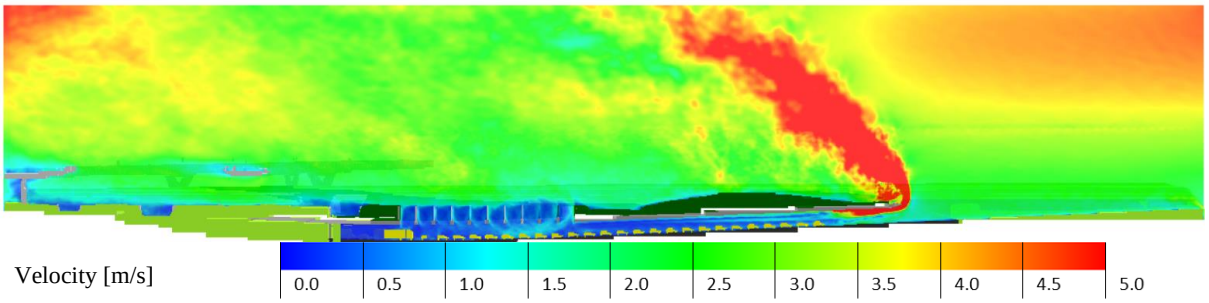

Figure 40: Side view of the velocity inside the ODG-O and the opening for conf.2

Fire simulation with geometry configuration 3

A second optimized configuration is proposed to further reduce mixing between smoke and fresh air. Diagonal vanes are installed at the top of the open shaft. Each vane is 2 m high and 2 m wide (inclined 45°) and they are spaced about 3.5 m from each other.

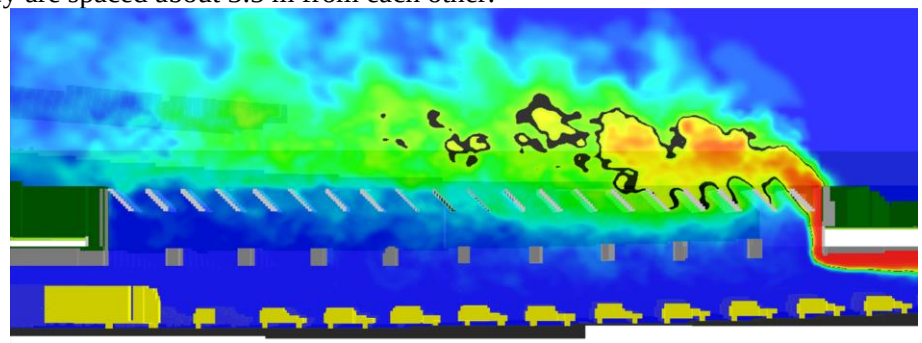

Figure 41: Detail of the open shaft for conf. 3

The results of the simulations are presented for the different tenability criteria described in the section above. The results are averaged in time over the last 200 s from 1000 s till 1200 s as the different flows in the underpasses become steady state (fig 42 and 43).

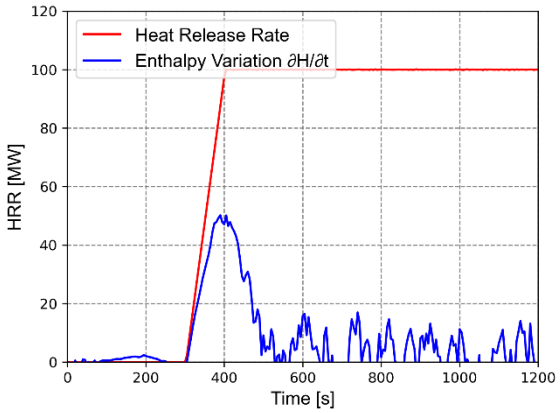

Figure 42: Energy balance for conf. 3

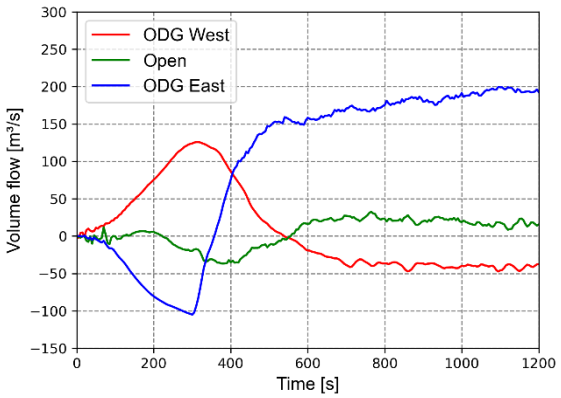

Figure 43:Volume flow rates for conf. 3

The visibility (fig 44), temperature (fig 45), radiative heat flux (fig 46) and CO concentration (fig 47) are presented along the measurement lines inside the underpasses. The different quantities are monitored at 2 m high above the road level.

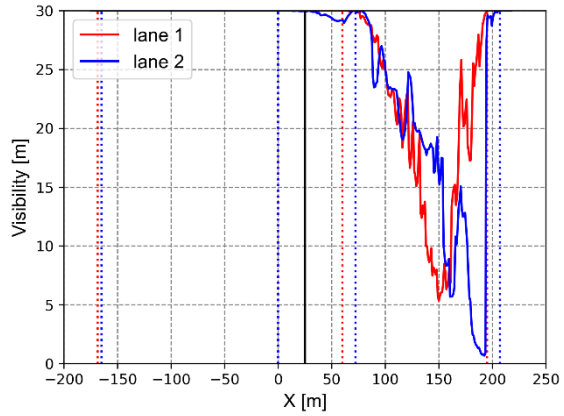

Figure 44: Visibility for conf. 3

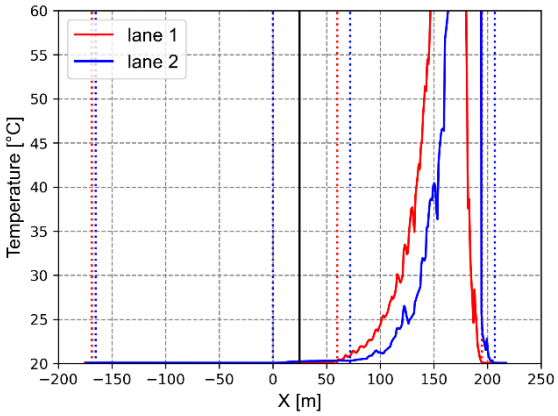

*Figure 45: Temperature for conf. 3**

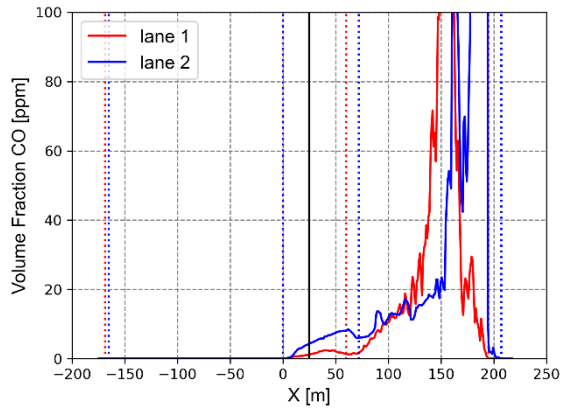

Figure 46: CO concentration for conf. 3

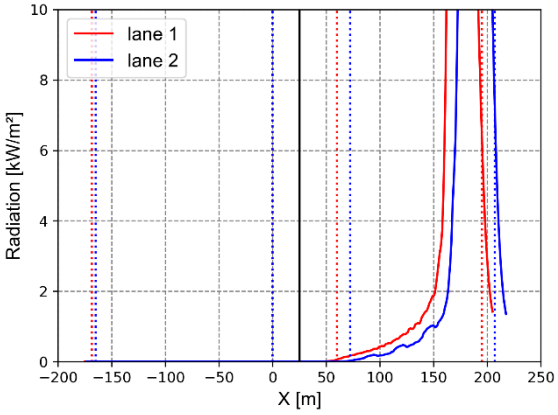

Figure 47: Radiative heat flux for conf. 3

The results are also presented in form of contour for the temperature, visibility ((fig 48), CO concentrations (fig 49) and velocity (fig 50). With this third configuration the diagonal vanes prevent the formation of large eddies that mix the smoke and fresh air. At the open shaft the smoke remains well stratified and flows out of the vanes, smoke and wind mostly interact outside the open shaft maintaining good tenability conditions in the zone of interest. This third configuration further improves the tenability conditions in the opening compared to the configuration 2.

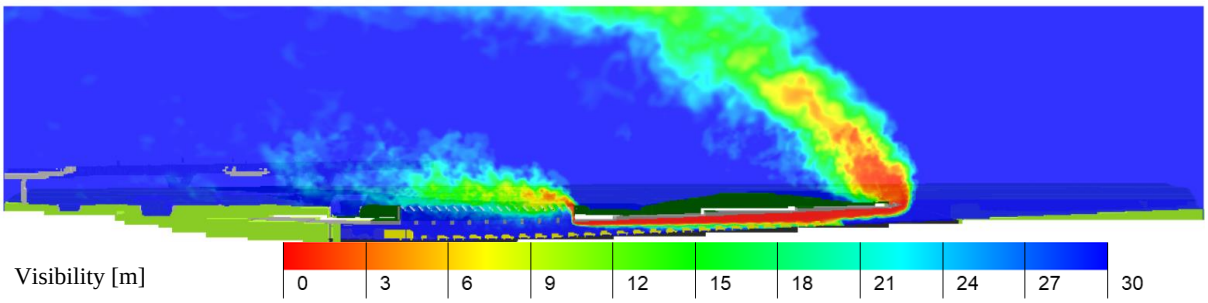

Figure 48: Side view of the visibility inside the ODG-O and the opening for scenario 3

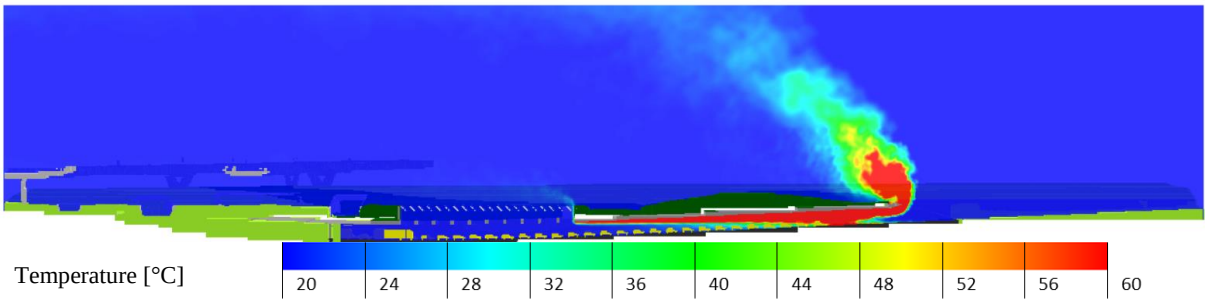

Figure 49: Side view of the temperature inside the ODG-O and the opening for scenario 3

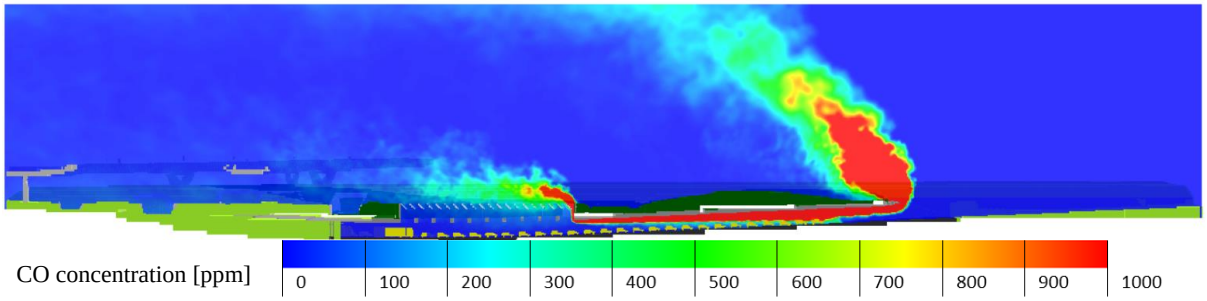

Figure 50: Side view of the CO concentration inside the ODG-O and the opening for scenario 3

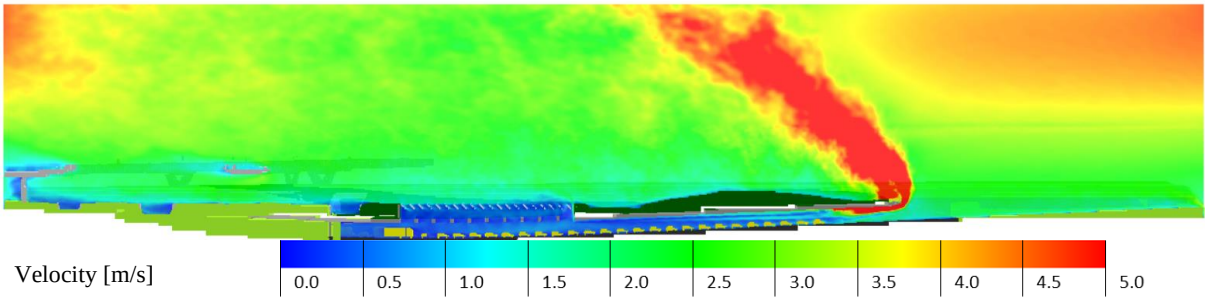

Figure 51: Side view of the velocity inside the ODG-O and the opening for scenario 3

CONCLUSIONS

This paper investigates the interaction between wind and smoke in a complex infrastructure made of two underpasses separated from an open shaft. The goal of the study was to assess whether the two underpasses can be considered independent from each other, limiting the required safety measures and simplifying the design process. The study shows how wind can be simulated first at large scale and then it can be implemented as boundary condition at smaller scale. The multiscale approach allows to include the terrain's morphology and the buildings on larger scale to provide a more realistic wind profile close to the zone of interest. The fire analyses show how the wind can negatively affect stratification in the underpasses and in the open shaft. The analysis of multiple configurations also shows how the smoke behaviour is impacted by the geometry of the shaft itself. The first configuration, without additional geometrical elements, shows smoke spread between the underpasses and loss of visibility at the target location. With the second configuration vertical plates are added to limit smoke and wind recirculation, this allows to improve visibility conditions in the open shaft and prevents smoke spread between underpasses. The use of diagonal vanes further limits the loss of stratification improving tenability conditions even more. The geometrical optimizations introduce additional complexity compared to the first configuration, but still very limited compared to a full tunnel. However it shall be verified that the use of diagonal vanes is not too scenario dependent especially for infrastructure with bidirectional traffic, and also give good results in case of other design scenario (wind direction and fire locations).

REFERENCES

1. De Oosterweelverbinding., https://www.oosterweelverbinding.be/het-project
2. De Werkvennootschap., https://dewerkvennootschap.vlaanderen/#projecten
3 Stammwitz, T., Rigert, S., Hoj, N., P., Bettelini, M., "On the aerodynamic characteristics of partly open galleries in case of fire" 8th International Conference 'Tunnel Safety and Ventilation', Graz, 2016
4 Mante, R., *Kader veiligheidsvoorzieningen verdiepte wegen, korte overkappingen en gedeeltelijk gesloten constructies*. RWS-GPO, afdeling Installaties en Bediening, Steunpunt Tunnelveiligheid, 2019. (in Dutch)
5 ASTRA 13001., "*7.2.6 Vermeidung von Strömungskurzschlüssen*" Richtlinie Lüftung der Strassentunnel, Systemwahl, Dimensionierung und Ausstattung, 2021 (in German)
6 McGrattan, M. B., Hostikka, S., Floyd, J., Vanella, M., & McDermott, R. J., *Fire Dynamics Simulator Users Guide, Sixth Edition*. Special Publication (NIST SP), 2022.
7 Franke, J., et al., "Recommendations on the use of CFD in wind engineering". Proceedings of the International Conference on Urban Wind Engineering and Building Aerodynamics, 2004.
8 Deevy, M., et al., "Innovative passive smoke control in Copthall Tunnel." HS2 Learning Legacy, 2020.
9 Yousaf, R., Gehrig, S., Buchmann, R.,"Evaluating Smoke Recirculation Potential at the Portal of a Swiss Road Tunnel in Case of a Fire" 7thInternational Conference 'Tunnel Safety and Ventilation', Graz, 2014,
10 Lee, B., Duckham, M., Van, J., Li, S., "A Method Of Smoke Dispersion Modelling Of Exhausted Tunnel Fire Smoke In Urban Areas", The 3rd Fire and Evacuation Modeling Technical Conference (FEMTC), Málaga, Spain. November 16-18, 2016.
11 Fixed Fire Fighting and Emergency Ventilation Systems for Highway Tunnels – Research Report
12 McGrattan, M. B., Hostikka, S., Floyd, J., Vanella, M., & McDermott, R. J., *Fire Dynamics Simulator Technical Reference Guide Volume 3: Validation*. Special Publication (NIST SP), 2022.
13 Ingason H, Li YZ, Lönnermark A. Tunnel fire dynamics. Springer New York; 2015
14 Gehandler, J., Ingason, H., Lönnermark, A., Frantzich, H., & Strömgren, M. (2014). Performance-based design of road tunnel fire safety: Proposal of new Swedish framework. Case Studies in Fire Safety, 18-28.
15 Huijben, J. W., P. Fournier, and B. P. Rigter. "Aanbevelingen ventilatie van verkeerstunnels." Utrecht: Ministerie van Verkeer en Waterstaat, Rijkswaterstaat, Bouwdienst 2006. (in Dutch)
16 Technical Committee 3.3 Road Tunnel Operation, "Design fire characteristics for road tunnels", PIARC, 2017
17 Purser, D. A. Combustion Toxicity. In M. J. Hurley, SFPE Handbook of Fire Protection Engineering (pp. 2207-2307). London: Springer. 2016

An improved model of smoke layer thickness in naturally ventilated tunnel fires considering the effects of aspect ratio

Liliang Yang[1], Mingjian Yin[2], Chuangang Fan[3], Jianda Xu[4], Ke Wu[1] & Tianhang Zhang[1]
[1]Research Center for Urban Fire Safety Engineering, Zhejiang University, Hangzhou 310058, China
[2]College of Energy, Environment and Safety Engineering, China Jiliang University, Hangzhou 310020, China
[3]School of Civil Engineering, Central South University, Changsha, China
[4]Zhejiang Communications Investment Expressway Operation Management Co.Ltd.

ABSTRACT

This study developed an improved model accounting for the effects of tunnel aspect ratio W/H on the smoke layer thickness h in naturally ventilated tunnel fires. The affecting mechanism of tunnel aspect was revealed by quantifying the contribution of air entrainment in each stage of smoke evolution using a FDS model. It was shown that the smoke flow rate generated in the radial spreading stage and the transitional stage from radial spread to one-dimensional flow increases significantly and finally takes the dominance with the increase of W/H. Accordingly, a novel model for predicting the smoke layer thickness was proposed by solving the correlation of m_s with tunnel aspect ratio and heat release rate. Finally, the reliability of this model was validated against both our newly conducted experiments and published experimental data, with an acceptable error range of 20% for all the conditions. Major findings of this work can provide reference for the design and optimization of fire rescue systems in tunnels with large aspect ratio.

KEYWORD: tunnel fire, aspect ratio, smoke layer thickness, smoke mass flow rate, predictive model

INTRODUCTION

Tunnels are typically semi-enclosed and extra-long structure. Once a fire occurs, high-temperature and toxic smoke will dramatically spread and accumulate in the tunnel, resulting in significant casualties, property damage, and adverse social impacts. For example, the fires in the Salang Tunnel (Parwan Province), the Yunzhongshan Tunnel (Shanxi Province), and the Housi Tunnel (Liaoning Province) resulted in 19, 7, and 9 deaths, respectively [1]. Therefore, the study on smoke flow characteristics and the associated prevention and control technologies in tunnel fires has garnered widespread attention [2-6].

The smoke layer thickness is one of the key parameters in tunnel fire studies. To be more specific, fire detectors and extinguishing systems must be immersed in the smoke layer to function effectively. Additionally, the safe height for evacuation and rescue should be below the smoke layer interface to prevent personnel from suffocation due to inhaling toxic smoke [7]. Therefore, quantifying the smoke layer thickness has become a research hotspot in recent years. Many scholars have established semi-empirical predictive models of smoke layer thickness by tunnel fire experiments, numerical simulations, and theoretical analysis [7-11].

The smoke spread process in naturally ventilated tunnel fires can be divided into four stages, including the plume-rising stage (Stage I), the radial spreading stage (Stage II), the transitional stage (Stage III) from radial spread to one-dimensional flow, and the one-dimensional spread stage (Stage IV) [12-14]. During each phase, the smoke flow rate increases through air entrainment, which further causes the

variation of the smoke layer thickness. In the early 1990s, Motevalli and Marks [8] conducted a series of experiments to investigate the variation characteristics of the ceiling-jet thickness near the fire source region by placing an unconstrained ceiling with a diameter of 2.13 meters above the burner with methane fuel. A calculation model to predict the smoke layer thickness in the near-fire field (i.e., 0.26 H to 2.0 H from the fire source) was proposed, as shown below:

$$\frac{h}{H} = 0.112\left[1-\exp\left(-2.24\frac{x_f}{H}\right)\right] \qquad 0.26 \le \frac{x_f}{H} \le 2.0 \tag{1}$$

Subsequently, Oka et al. [10] investigated the smoke thickness with methanol fuel in a model tunnel with dimensions of 10.0 m in length, 0.75 m in width, and 0.45 m in height. He found that the smoke layer thickness in the near-fire field and far-fire field is dominated by different physical phenomena, and a piecewise function is proposed to model the smoke thickness of the ceiling jet and the smoke stratification region, as given in Eq. (2).

$$\frac{h}{H} = \begin{cases} A\left(\frac{x_f}{H}-\frac{W}{2H}\right)+B\left(\frac{W}{2H}\right)^{-1/3}, & \text{Stage III} \\ C\left(\frac{W}{2H}\right)^{-1/3}, & \text{Stage IV} \end{cases} \tag{2}$$

where A, B and C are coefficients to be fitted by experimental data.

However, it should be pointed out that coefficients in the above-mentioned empirical formulas are highly related to the boundaries, e.g., tunnel dimensions, cross-sectional shape, which limits the generalization to tunnels with different sizes [15]. Based on the mass and energy balance principles of the smoke flow, Fan et al. [9] proposed a more general analysis framework for the prediction of the smoke thickness in the corridor-like long-narrow space, as shown below:

$$h = 0.56\left(\frac{m_s^{\,2}}{W^2\lambda_s(\lambda_a-\lambda_s)}\right)^{1/3} \tag{3}$$

Equation (3) indicates that the smoke layer height is positively correlated with smoke mass flow rate, while negatively correlated with the tunnel width. Xu et al. [11] further modified Eq. (3) by introducing the influence of the tunnel aspect ratio (*AR*) and derived the semi-empirical equation for smoke layer thickness in one dimensional region, as shown in Eq. (4).

$$h = 1.24(m_p/(W/H)^2)^{1/3} - 0.13 \tag{4}$$

Equations (3) and (4) indicate that the smoke mass flow rate plays a significant role in affecting the smoke layer thickness. Nevertheless, how to value the m_s remains a challenge in these studies. To be more specific, Eq. (3) adopts the empirical value and Eq. (4) uses the mass flow rate of the plume (m_p) to replace the m_s, which may cause systematic error in practice. To cover the knowledge gap, He et al. [7] fitted the distribution data of smoke mass flow rate for ARs in the range of 1.1 to 1.7 and developed a correlation for the smoke mass flow rate during the Stage IV, as shown in Eq. (5). Then the predictive model for the smoke layer thickness h could be obtained by solving the Bernoulli's Equation.

$$\begin{aligned} m_s &= Q^{*-0.13}W^{*0.43}(0.024Q_C^{\,1/3}(H-Z_0)^{5/3}+6.53\times10^{-4}Q_C) \quad H>l \\ m_s &= 0.002Q^{*-0.13}W^{*0.43}Q_C\frac{H}{l} \quad H<l \end{aligned} \tag{5}$$

$$h = \left(\frac{3m_s}{4C_d W \sqrt{2g\rho_s(\rho_a - \rho_s)}} \right)^{2/3} \quad (6)$$

In recent years, to alleviate traffic congestion and improve road capacity, many roads have significantly increased the number of lanes, leading to the emergence of tunnels with large AR [4, 5, 16]. For example, the Shenzhen–Zhongshan Link has an AR of 6.6 (Fig. 1a), and the confluence section of the Lishui Road Tunnel in Zhejiang has an AR that can even reach 10 (Fig. 1b). The increase in tunnel width results in a more complicated air entrainment and smoke formation process which have been hardly mentioned in previous literature. Therefore, existing equations fail to predict the smoke layer thickness accurately by nature.

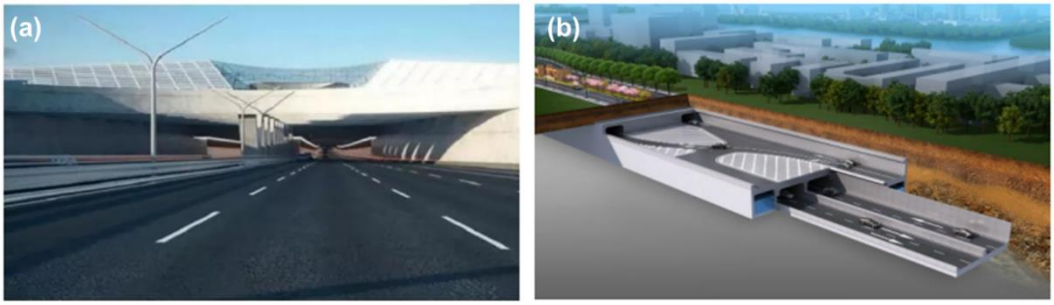

Figure 1 Large-section urban tunnel projects (a) Shenzhen – Zhongshan Link (AR≈6.6), and (b) Lishui Road Tunnel, Hangzhou (AR≈10)

To clarify the impact of increased tunnel width on smoke mass flow rate and smoke layer thickness, theoretical analysis and numerical simulation method are utilized in this study to investigate the distribution of smoke mass flow rate along the tunnel longitudinal direction under the influence of different ARs and HRRs. A correlation for the smoke mass flow rate at the one-dimensional region is proposed. Ultimately, a smoke layer thickness prediction model suitable for tunnel fires with various ARs is developed and experimentally validated.

NUMERICAL SIMULATION

Numerical model setup

Numerical model of a series of naturally ventilated tunnels were constructed using the Fire Dynamics Simulator (FDS), with their length L = 180 m and height H = 4.5 m. The tunnel width W in different conditions varied from 4.5 m to 45 m, covering an AR range of 1 to 10. The fire source was set on the centerline at 90 m downstream of the inlet portal, with a heat release rate between 5 - 20 MW, corresponding to the fire scenarios from small passenger vehicles to HGVs [17]. All the simulation conditions were summarized in Table 1. As shown in Fig. 2, the computational domain contained the whole tunnel, with two regions of open air (both with a length of 10 m, a height of 11.2 m and about 2 m wider than the tunnel) attached to the inlet and outlet portal of the tunnel. The tunnel walls together with the ground were set as “Concrete”, while all the other boundaries were set as “Open”.

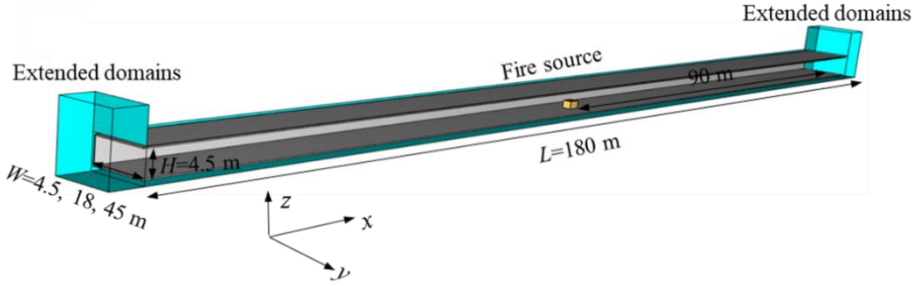

Figure 2 Diagram of the numerical model setup

Table 1 Simulation Conditions.

No.	W (m)	H (m)	AR	$\dot{Q}$ (MW)
1	4.5	4.5	1	
2	18	4.5	4	5
3	45	4.5	10	
4	4.5	4.5	1	
5	18	4.5	4	10
6	45	4.5	10	
7	4.5	4.5	1	
8	18	4.5	4	20
9	45	4.5	10	

Due to the symmetric feature of the smoke spreading process, measurement points were arranged only in the downstream half of the tunnel. Two series of thermocouples were set in parallel at an interval of 0.1 m to monitor the ceiling temperature difference between the centerline and the sidewall of the tunnel, and the detailed positions can be found in Fig. 3b & c. Meanwhile, monitoring surfaces were arranged at every 0.5 m along the longitudinal direction of the tunnel to measure the mass flow rate of the smoke layer and the air supple rate. A vertical section of temperature monitoring surface was set along the centerline to measure the temperature profile and thus obtained the smoke layer thickness using buoyancy frequency method [18].

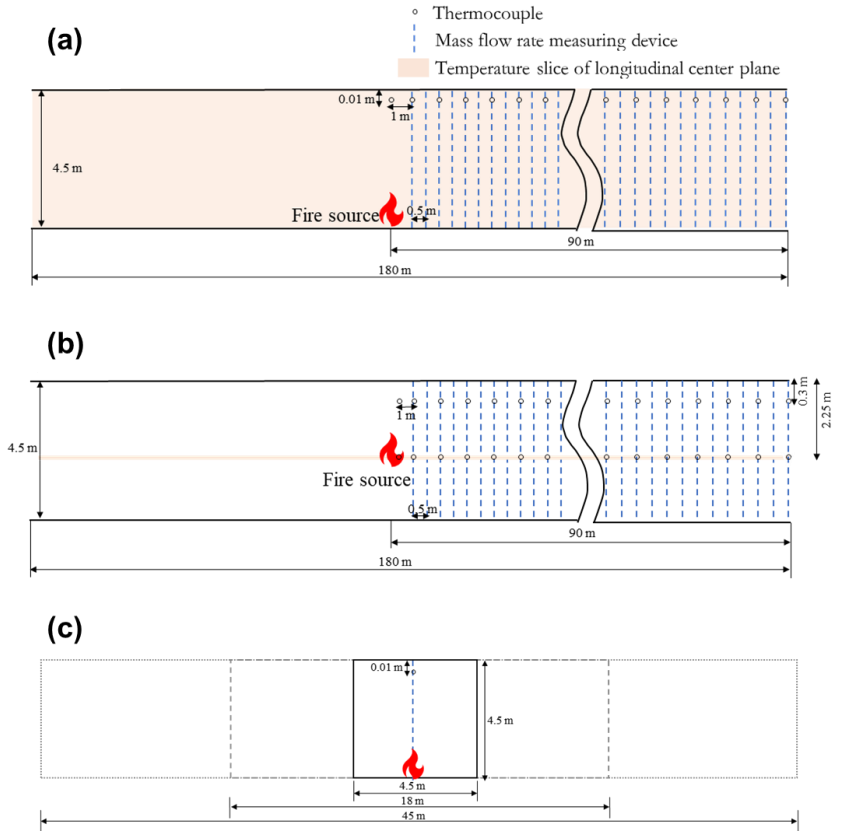

Figure 2 Numerical model setup (a) Full-scale numerical model (b) Measurement point layout (top view) (c) Measurement point layout (side view)

Grid independence analysis and numerical model validation

The grid resolution was determined following the FDS user guide, which recommends that the grid size δ_x should fall in the range of $D^*/\delta_x = 4 – 16$, with D^* calculated by Eq. (7).

$$D^* = \left(\frac{\dot{Q}}{\rho_a c_p T_a g^{1/2}} \right)^{2/5} \tag{7}$$

By referring to the grid resolutions adopted under similar fire scenarios in the literature [19, 20], δ_x was finally selected as 0.2 m in this work, which can satisfy the conditions requiring the finest grids (i.e. those with HRR = 5 MW).

To validate the numerical model of this study, simulation results of the maximum temperature rise ΔT_{max} together with the longitudinal temperature rise profile in the condition with HRR = 5 MW and W/H = 1 is compared against the predictive models by Li et al. [21] (Eq. (8)) and Ingason et al. [17] (Eq. (9)), which are derived experimentally and have been widely approved within their applicable range. Results show that the predicted and simulated ΔT_{max} are 820 ℃ and 941.8 ℃, respectively, with an acceptable error of 15%. Meanwhile, as shown in Fig. 3, the simulated results of the temperature rise profile closely matches the predictive curve, with a maximum error of 11%, which is acceptable.

$$\Delta T_{\max} = 17.5 \frac{\dot{Q}^{2/3}}{H_{ef}^{5/3}} \tag{8}$$

$$\frac{\Delta T(x)}{\Delta T_{\max}} = 0.55 \exp(-0.143 \frac{x - x_v}{H}) + 0.45 \exp(-0.024 \frac{x - x_v}{H}) \tag{9}$$

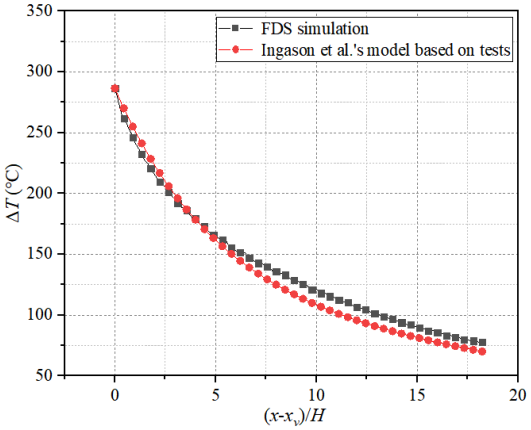

Figure 3 Comparison of predicted and simulated results of smoke temperature rise and decay along the longitudinal direction of the tunnel

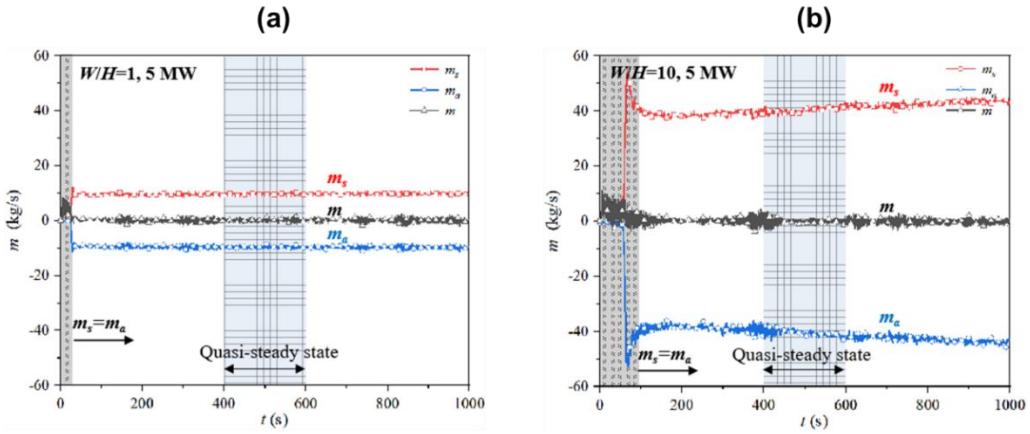

Figure 4 *Variation of mass flow rate with combustion time ($\dot{Q}$ = 5 MW) (a)AR=1, (b) AR=10*

Figure 4 compares the evolution of m_s and the flow rate of air supplementation m_a at a cross-section 50 m downstream of the fire source, with HRR = 5 MW. Results show that during this phase, m_s is almost in balance with m_a and the total mass flow rate m tends to 0, which indicates a quasi-steady state. Therefore, all the quantitative results subsequently are adopting the time-averaged value between 400 - 600 s.

RESULTS AND DISCUSSION

Effect of tunnel AR on mass flow rate and smoke layer thickness

To further clarify the contribution of each stage to m_s, boundaries between every two adjacent stages are defined by the following method. As shown in Fig. 5, based on the analysis of the smoke spread process in natural ventilation tunnel fire, Stage I ends as the plume hits the ceiling of the tunnel, and the range of Stage II is a circular region with a diameter equaling to the tunnel width W. Then after the transition of Stage III, the starting point of Stage IV, $x_{f\text{-}IV}$, can be located as the position where the temperature difference between the centerline and the sidewall drops below 5 ℃ [14, 22, 23].

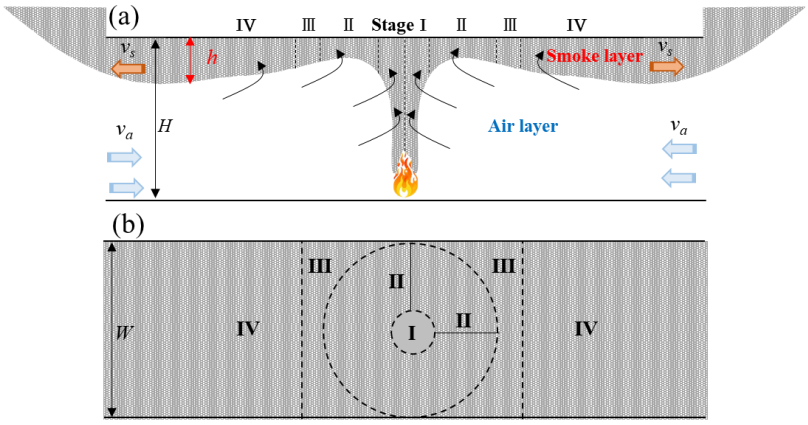

Figure 5 *Diagram of the smoke spread process in natural ventilation tunnel fire (a) view of the center cross-section, and (b) top view*

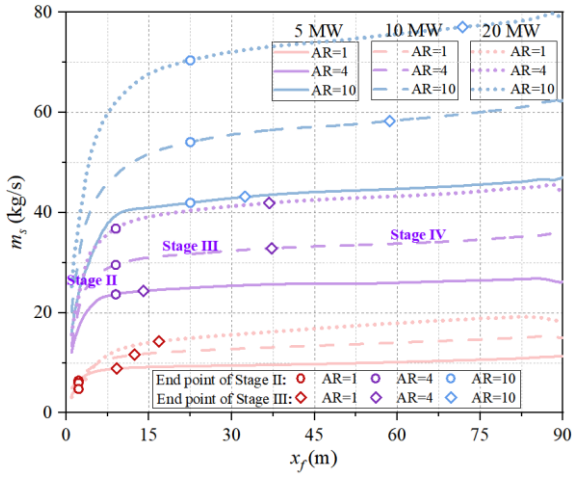

Figure 6 *Variation of the smoke mass flow rate along the longitudinal direction of the tunnel under different ARs and HRRs*

Based on the criteria to determine each stage, Fig. 6 presents the longitudinal distribution of m_s along the tunnel. It can be observed that for all the conditions, m_s increases sharply in the vicinity of the fire source and then turns to a slow growth towards the outlet of the tunnel, which agrees well with the four-stage developing pattern of smoke layer and indicates a minor air entrainment in the Stage IV. As AR increases from 1 to 10, m_s generally increases under all three HRRs, with its turning point moving downstream.

Figure 7 demonstrates the distribution of mass flow rate, smoke temperature below the ceiling, and smoke layer thickness at different stages with a HRR of 5 MW. As shown, the smoke mass flow rate increases significantly during the Stages II and III under all ARs, while it levels off during the Stage IV. Furthermore, as the tunnel AR increases, the increase in smoke mass flow rate during the Stages II and III becomes more pronounced. According to Eqs. (3 - 5), the smoke layer thickness increases with the increase in smoke mass flow rate. Therefore, the trend of smoke layer thickness variation is similar to that of the smoke mass flow rate, i.e., it increases sharply during the Stages II and III, while it shows little change during the Stage IV, with any changes being negligible.

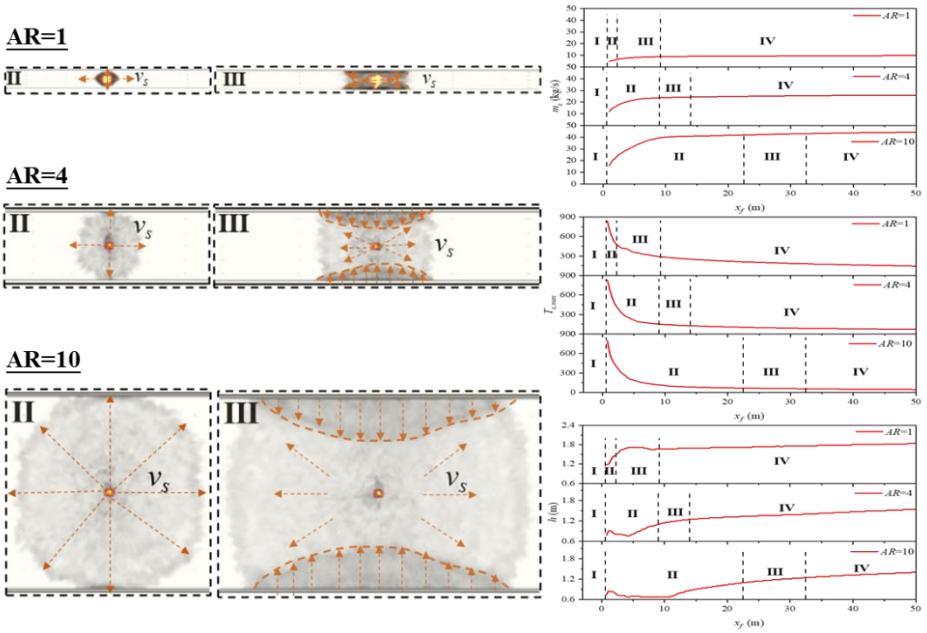

Figure 7 *Distribution patterns of mass flow rate, temperature below the ceiling, and smoke layer thickness, and smoke flow characteristics at different propagation stages*

Analysis of the flow behavior during the Stage II and Stage III under different ARs reveals that as the tunnel width increases, the extent of smoke spread in the Stage II and Stage III also increases, which leads to a larger range of air entrainment and promotes the increase in smoke mass flow rate. During these stages, after the smoke reaches the tunnel sidewalls, reverse buoyancy-induced wall jet occurs, continuously entraining air from below. Due to the high Froude number of the ceiling jet in this stage, the smoke velocity is high, and a large amount of air is entrained into the smoke layer, making the air entrainment effect in this stage significant. In contrast, during the Stage IV, the upward smoke flow and downward air flow move in opposite directions. Under the shear forces, the downward air is entrained into the smoke layer. However, studies have shown that the entrainment coefficient (the ratio of the entrainment velocity to the velocity difference between smoke and air) in the one-dimensional spread region is between 0.00015 and 0.0003, and the entrainment effect in this stage is generally negligible [24-26], which agrees well with the slowly increase trend of m_s during the Stage IV.

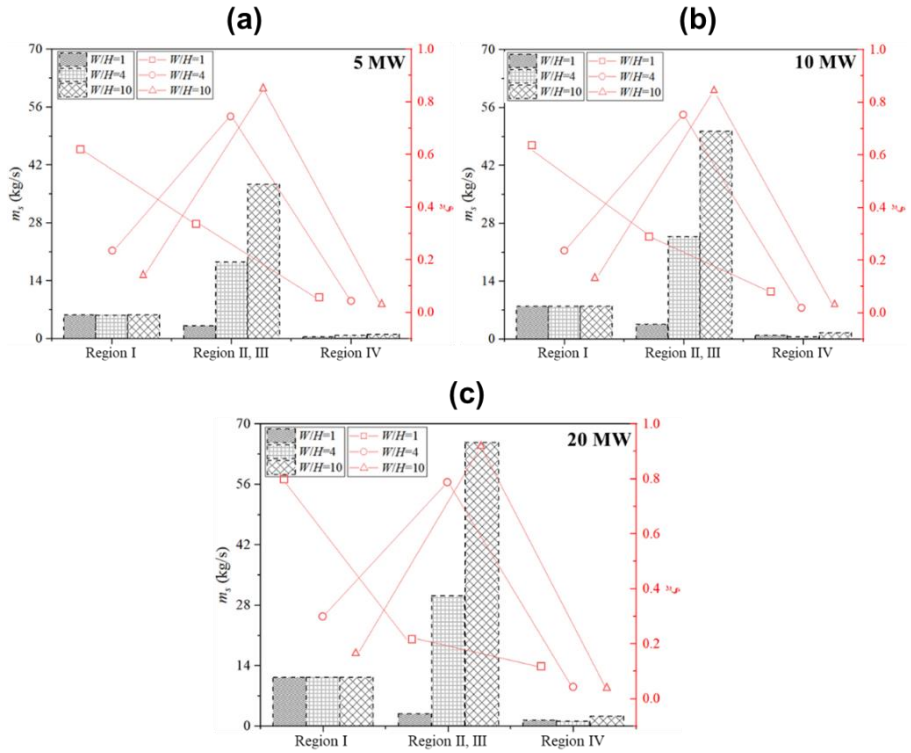

Figure 8 Variation of mass flow rate and its proportion at different smoke propagation stages (a) 5 MW (b) 10 MW and (c) 20MW

The smoke mass flow rate in each stage and the associated portion, ξ, are further quantitatively compared in Fig. 8. Since Stage I (the plume-rising stage) ends as the smoke hits the ceiling and hence is unlikely to be affected by the tunnel AR, smoke mass flow rate during this stage is evaluated following the classical model by Zukoski et al. [27]:

$$m_{\mathrm{p}} = 0.21\left(\frac{\rho_a^2 g}{c_p T_a}\right)^{1/3} \dot{Q}^{1/3} H^{5/3} \tag{10}$$

Considering the symmetric characteristic of the boundary so the contribution of Stage I on the right half of the tunnel, m_{sI}, is valued as 0.5 m_{p}. Besides, the smoke stratification mainly occurs in Stages II and III, smoke mass flow rate generated in these two stages are integrated here and denoted as $m_{\mathrm{sII\text{-}sIII}}$, representing the variation of smoke mass flow rate in the process forming a stable smoke layer. Afterwards, by measuring m_s at 75 m downstream of the fire source (i.e. Stage IV) and at $x_{f\text{-}IV}$ (i.e. the boundary of Stage III and IV) respectively, $m_{\mathrm{sII\text{-}sIII}}$ and m_{sIV} (the contribution of Stage IV) can be obtained.

It can be observed that for conditions with a conventional AR of W/H = 1, mass flow rate in Stage I takes the dominant position (especially under large *HRR* of 20MW, with the percentage of m_{sI} over 80%), which is the most common scenario of existing models for m_s and h. On the contrary, with the increase of AR, the percentage of $m_{sII\text{-}sIII}$ shows a rapid increase and has significantly overwhelmed m_{sI} when the AR reaches W/H = 4. This further highlights the contribution of radial entrainment in Stages II and III. Meanwhile, the percentage of m_{sIV} is below 10% for all the conditions, indicating that air entrainment is no longer the major factor to the smoke layer thickness in the Stage IV.

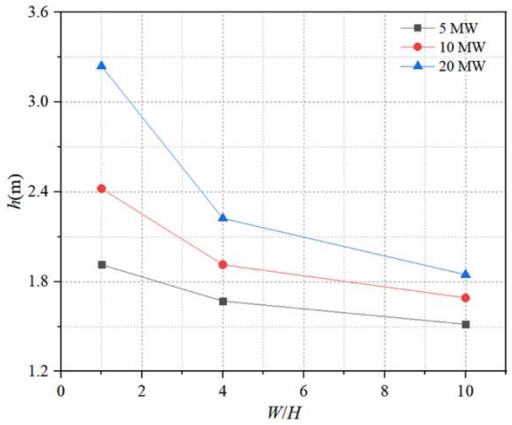

Figure 9 Variation of smoke layer thickness with AR under different HRRs (xf = 75 m)

Figure. 9 shows the variation of smoke layer thickness with the AR at a distance of 75 m from the fire source (i.e., the start point of the Stage IV) under different HRRs. According to previous studies, the smoke layer thickness is positively correlated with the smoke mass flow rate and negatively correlated with the tunnel width. From the figure, it can be observed that, under different HRRs, the smoke layer thickness decreases with the increase in the AR. This suggests that, although an increase in the AR leads to a rise in the smoke mass flow rate, which promotes an increase in the smoke layer thickness, the increase in tunnel width simultaneously suppresses the growth of the smoke layer thickness, leading to a reduction in its thickness. Overall, the increase in tunnel width has a dominant effect in thinning the smoke layer thickness.

Prediction model of smoke mass flow rate and smoke layer thickness

As illustrated previously, the intensified air entrainment during the radial spreading and stratification in Stage II and III is the major mechanism that reshapes the smoke evolution in tunnels with large AR. Therefore, this subsection develops an improved model for smoke layer thickness h by integrating the smoke mass flow rate in these two stages, $m_{sII\text{-}sIII}$, into the total m_s on the basis of Fan et al. [9] and thus accounting for the effects of tunnel AR. In the Stage IV, by assuming a nearly-uniform temperature profile in the smoke layer and neglecting the momentum provided by the fire plume, the buoyancy induced by the density difference can be considered as the only force driving the smoke flow [28], and thus the energy conservation equation of smoke flow at any height z can be written as:

$$\frac{1}{2}\rho_s v_s(z)^2 = (\rho_a - \rho_s) gz \tag{11}$$

with the local smoke velocity $v_s(z) = \sqrt{2(\rho_a - \rho_s) gz / \rho_s}$.

According to its definition, smoke mass flow rate m_s can be integrated from $v_s(z)$ as：

$$m_s = C_d \int_0^h \rho_s W v_s(z) dz = \frac{2}{3} C_d W h^{3/2} \sqrt{2(\rho_a - \rho_s)\rho_s g} \tag{12}$$

in which C_d the flow coefficient evaluated as 0.7 [29]. Taking $C_d\left[(\rho_a-\rho_s)\rho_s\right]^{1/3}$ as an empirical coefficient γ following Fan et al. and He et al. [7, 9], the relationship between h and m_s can be derived as:

$$h=\left(\frac{3m_s}{2C_dW\sqrt{2(\rho_a-\rho_s)\rho_s g}}\right)^{2/3}=\gamma\left(\frac{m_s}{W}\right)^{2/3} \tag{13}$$

Afterwards, a correlation of m_s is established as an intermediate step to the final predictive model of h. Essentially, m_s is consisted by the contribution of every stage. By reasonably neglecting the contribution of m_{sIV}, the percentage of which is generally below 10% (see Section 3.1), m_s can be expressed as:

$$m_s=m_{sI}+m_{sII\text{-}sIII}+m_{sIV}=\frac{m_p}{2}+m_{sII\text{-}sIII} \tag{14}$$

Factors of $m_{sII\text{-}sIII}$ can be written as follows:

$$m_{sII-sIII}=f(Q,\rho_a,c_p,T_a,g,H,W) \tag{15}$$

Using ρ_a, T_a, g and H as fundamental quantities, dimensionless expressions can be derived through dimensional analysis as:

$$m^*_{sII-sIII}=f(\dot{Q}^*,W^*) \tag{16}$$

with $m^*_{sII-sIII}=\frac{m_{sII-sIII}}{H^{\frac{5}{2}}\rho_a g^{\frac{1}{2}}}$, $\dot{Q}^*=\frac{\dot{Q}}{H^{5/2}\rho_a g^{1/2}c_pT_a}$, and $W^*=\frac{W}{H}$. Figure 10 shows the variation of $m^*_{sII-sIII}$, which indicates a tendency of power function with both Q^* and W^*. Accordingly, an empirical correlation of $m^*_{sII-sIII}$ is fitted from the data shown in Fig. 10, with R^2 = 0.98:

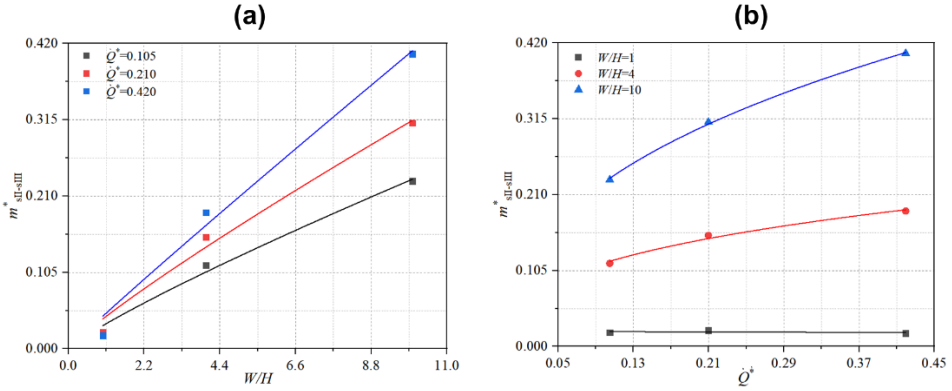

Figure 10 Variation of dimensionless smoke mass flow rate with AR and dimensionless HRR (a) Variation of dimensionless smoke mass flow rate with AR (b) Variation of dimensionless smoke mass flow rate with dimensionless HRR

$$m^*_{sII-sIII}=0.054(\dot{Q}^*)^{1/3}\frac{W}{H} \tag{17}$$

and thus m_s can be written as:

$$m_s = 0.054\frac{\dot{Q}^{1/3}}{c_p^{1/3}T_a^{1/3}}\frac{W}{H}H^{5/3}\rho_a^{2/3}g^{1/3} + 0.105(\frac{\rho_a^2 g}{c_p T_a})^{1/3}\dot{Q}^{1/3}H^{5/3} \quad (18)$$

Since it is helpful to find out the critical AR at which the air entrainment induced in the radial spreading stage and the transitional stage begins to take the dominance, a criterion is proposed here as $\varepsilon = \frac{m_{\text{sII-sIII}}}{m_{\text{sI}}}$. Once $\varepsilon \gg 1$, it can be considered that the air entrainment in Stages II and III have overwhelmed that in Stage I and become the major contributor to the smoke flow growth. For the convenience in applications, $m_{\text{s II-sIII}}$ can be directly evaluated using Eq. (17). Meanwhile, since the fuel mass flow rate is a minority in the plume rising stage[17, 27], $m_{\text{sI}} = \frac{m_p}{2}$ can be approximated as the air entrainment rate in Stage I. Following this method, $AR > 1.94$ can be considered as a criterion for tunnels with large aspect ratio.

For the final step, substituting Eq. (18) into Eq. (13) and fitting the empirical coefficient γ based on the simulation results, a predictive model of h can be obtained with a satisfactory correlation of R^2 = 0.98, as shown in Fig 11:

$$\frac{h}{H} = 1.09(\frac{m_s}{WH})^{2/3}H^{-1/3} \quad (20)$$

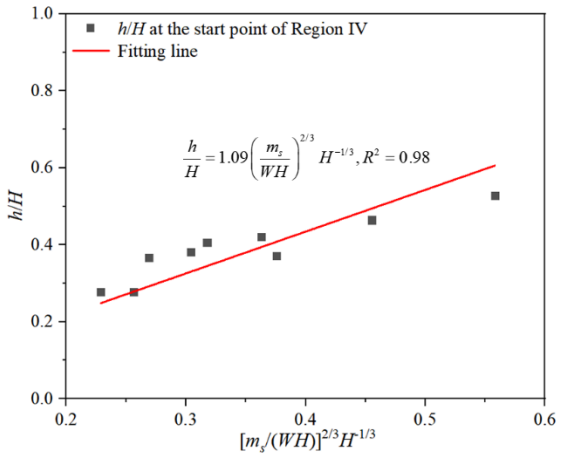

Figure 11 Variation of dimensionless smoke layer thickness with $\left[m_s/(WH)\right]^{2/3}H^{-1/3}$

Figure 12 presents a comparison between the predicted values from previous models and the simulation results. The model proposed in this study performs well in predicting the dimensionless smoke layer thickness during the Stage IV, applicable to different ARs and HRRs. The model by Fan et al [9]. also provides accurate predictions, but it requires monitoring of the mass flow rate. The model by Xu et al. [11] performs well only for small ARs. This is attributed to the fact that, as the AR increases, the mass flow rates in Stages II and III gradually become dominant, while the mass flow rate in Stage I increasingly underestimates that in Stage IV. Other models generally underestimate the numerical simulation values.

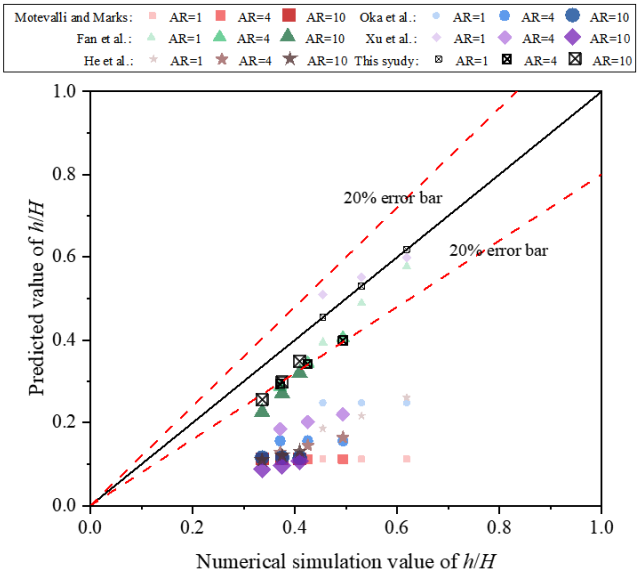

Figure 12 Comparison of predicted h/H obtained from previous models with numerical simulation values（x_f=75 m）

Comparative analysis of experimental results and prediction model results

Experimental design of 1/20 model tunnels

To further validate the reliability of the newly developed model for smoke layer thickness, a 1:20 scaled physical model was constructed following the Froude scaling law (Fig. 13). The model tunnel was made of 2 mm thick metal plates, with one tunnel having dimensions of 8 m in length, 0.6 m in width, and 0.25 m in height (AR=2.4), and the other having dimensions of 11 m in length, 1.5 m in width, and 0.25 m in height (AR=6). The n-heptane and 99% alcohol were used as fuels in square oil pans with side lengths of 4 cm, 6 cm, 8 cm, 14 cm and 20 cm, the HRR of which ranging from 1.6 kW to 15.7 kW according to the measured mass loss rate by an electronic balance.

Figure 13 1/20 tunnel model experimental setup

The test conditions in the present work, together with the experimental data in previous studies, are summarized in Table 2 [7, 11, 18, 30, 31]. It is worth noting that, except for the smoke layer thickness obtained by He et al. [7] using the integral ratio method, all other smoke layer thicknesses were calculated using the buoyancy frequency method [18].

Table 2. Experimental data on smoke layer thickness in natural ventilation tunnel fires

Reference	Experimental scales	Tunnel size (m)	AR	HRR (kW)	h (m)	h/H (EV)	h/H (PV)	x_f/H
Yang et al., 2010	Small scale experiment	7.5 (L)×1.5 (W)×0.6 (H)	2.5	11.8	0.126	0.211	0.260	2.58
					0.139	0.232	0.260	6.08
Gao et al., 2016	1/6	6 (L)×2 (W)×0.9 (H)	2.2	82	0.210	0.233	0.33	4.22
Tang et al., 2017	1/6	66 (L)×1.5 (W)×1.3 (H)	1.15	25	0.350	0.267	0.261	
				40	0.364	0.280	0.290	1.92
				55	0.350	0.269	0.311	
Xu et al., 2019	1/10	6.0 (L)×1.5 (W)×0.7 (H)	2.14	9.5	0.226	0.322	0.274	
				18.4	0.237	0.338	0.317	2.14
				30.1	0.256	0.366	0.354	
				63.5	0.289	0.412	0.419	
He et al., 2021	1/10	6.0 (L)×1.0 (W)×0.7 (H)	1.43	10.66	0.180	0.257	0.282	
				19.45	0.190	0.271	0.322	3.57
				33.30	0.200	0.286	0.363	
This study	1/20	8 (L)×0.6 (W)×0.25 (H)	2.4	1.6	0.057	0.230	0.275	3.2
				2.5	0.060	0.240	0.303	8.8
				8.2	0.090	0.358	0.395	8.8
		11 (L)×1.5 (W)×0.25 (H)	6	3.4	0.078	0.310	0.268	8
				5.2	0.082	0.326	0.295	8
				15.7	0.088	0.350	0.377	8

Figure 14 presents a comparison between the predicted and experimental results of the dimensionless smoke layer thickness. It can be seen that, overall, the prediction error is within a 20% margin, indicating that the experimental and predicted smoke layer thicknesses are in good agreement, thus validating the reliability of the prediction model. Furthermore, it can be observed that the prediction slightly overestimates the experimental results of Yang et al. [30], Gao et al. [18], and He et al. [7]. This is because, in the experiments by Yang et al. [30] and Gao et al. [18], the fire source was not located at the center of the tunnel, but rather near one end of the tunnel. The smoke layer thickness monitored in these experiments was at the opposite end, far from the fire source. Due to the influence of the fire source location, the smoke in the tunnel flows asymmetrically, with a large amount of smoke escaping from the tunnel entrance near the fire source, resulting in a thinner smoke layer at the other end.

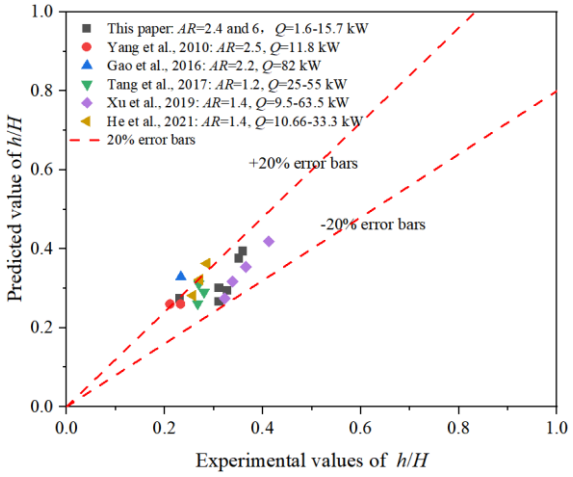

Figure 14 Comparison of predicted results with experimental results

Additionally, in the experiment by Yang et al. [30], a top smoke exhaust outlet was installed, further exacerbating the expulsion of smoke from the tunnel, which reduced the smoke layer thickness. Meanwhile,

previous studies have shown that the integral ratio method tends to yield a higher smoke layer interface, meaning that compared to the buoyancy frequency method, the smoke layer thickness obtained from this method is smaller, leading to an overestimation of the experimental results of He et al. [7].

It should be noted that the smoke layer thickness prediction model proposed in this paper for the Stage IV of smoke does not take into account factors such as the fire source location, smoke exhaust from the tunnel roof, and tunnel length. In long tunnels, after the smoke enters the Stage IV and travels a certain distance, the smoke temperature will decrease to the ambient temperature, resulting in insufficient buoyancy to maintain the stratification, causing the smoke to settle. The prediction model proposed in this paper is focused only on the smoke layer thickness during the one-dimensional steady stage. Future work will further consider the effects of the aforementioned factors on the distribution of the smoke layer thickness.

CONCLUSION

In this paper, the influence of tunnel aspect ratio (AR) and heat release rate (HRR) on smoke layer thickness in natural ventilation tunnel fires had been studied through numerical simulations. The present study revealed that the increase in the AR results in an expanded radial spreading range of smoke, so more air is entrained into the smoke flow during the stable smoke layer forming process. Therefore, the smoke mass flow rate increases significantly in tunnels with larger AR. On the other hand, the expansion of the tunnel width provides larger space to contain smoke, which finally causes the decrease of smoke layer with the increase of the tunnel aspect ratio.

Based on theoretical analysis, the relationship between smoke layer thickness, smoke mass flow rate, and AR had been derived. Finally, the predictive methods for smoke layer thickness, which is suitable for larger range AR had been proposed, by solving the correlation of smoke mass flow rate with the tunnel aspect ratio. Experimental validation showed that the prediction error is within 20%, indicating that the proposed prediction model has good reliability. This work deepens the understanding of the smoke evolution characteristics considering the effect of tunnel aspect ratio, thus providing a novel sight to classical tunnel fire dynamic theory.

REFERENCES

1. Deng, T., Norris, S., Wang, M., Yu, L., Yan, Z., Sharma, R. N., "Performance of water-based fixed fire fighting systems in road tunnels: A review". *Tunnelling and Underground Space Technology*, **157**, 2025.
2. Li, Y. Z., Lei, B., Ingason, H., "The maximum temperature of buoyancy-driven smoke flow beneath the ceiling in tunnel fires". *Fire Safety Journal*, **46,** 204-210, 2011.
3. Oka, Y., Oka, H., "Velocity and temperature attenuation of a ceiling-jet along a horizontal tunnel with a flat ceiling and natural ventilation". *Tunnelling and Underground Space Technology*, **56,** 79-89, 2016.
4. Zhang, T., Wang, G., Hu, H., Huang, Y., Zhu, K., Wu, K., "Study on temperature decay characteristics of fire smoke backflow layer in tunnels with wide-shallow cross-section". *Tunnelling and Underground Space Technology*, **112**, 2021.
5. Zhang, T., Wang, G., Li, J., Huang, Y., Zhu, K., Wu, K., "Experimental study of back-layering length and critical velocity in longitudinally ventilated tunnel fire with various rectangular cross-sections". *Fire Safety Journal*, **126**, 2021.
6. Wu, K., Li, J., Chen, X., Duan, X., Zhang, T., Wang, L., "Flame behavior and maximum ceiling temperature in traffic merging section tunnel fires: An experimental study and engineering modelling methodology". *Tunnelling and Underground Space Technology*, **156**, 2025.
7. He, L., Xu, Z., Markert, F., Zhao, J., Xie, E., Liu, Q., Tao, H., Tagne Sylvain Marcial, S., Wang, Z., Fan, C., "Study on the effect of tunnel dimensions on the smoke layer thickness in naturally ventilated short tunnel fires". *Tunnelling and Underground Space Technology*, **112,** 103941, 2021.
8. Motevalli, V., Marks, C. H., " Characterizing the unconfined ceiling jet under steadystate conditions: a reassessment". *Fire Safety Science*, **3,** 301–312., 1991.
9. Fan, W., Wang, Q., Jiang, F., *Concise Guide of Fire Science*, University of Science and Technology of China Press, 1995.
10. Oka, Y., Oka, H., Imazeki, O., "Ceiling-jet thickness and vertical distribution along flat-ceilinged horizontal tunnel with natural ventilation". *Tunnelling and Underground Space Technology*, **53,** 68-77, 2016.
11. Xu, Z., Zhao, J., Liu, Q., Chen, H., Liu, Y., Geng, Z., He, L., "Experimental investigation on smoke spread characteristics and smoke layer height in tunnels". *Fire and Materials*, **43,** 303-309, 2019.
12. Wang, H. B., Ji, J., Zhong, W., Huo, R., Hu, L. H. J. E. M., "Experimental study on air entrainment coefficient

during one-dimensional horizontal movement of fire-induced smoke in long channels". 2009.
13. Jiang, X., Liu, M., Wang, J., Li, K., "Study on air entrainment coefficient of one-dimensional horizontal movement stage of tunnel fire smoke in top central exhaust". *Tunnelling Underground Space Technology*, **60,** 1-9, 2016.
14. Gao, Z., Liu, M., Zhao, P., Yan, C., "Influence of tunnel slope on the one-dimensional spread of smoke transportation and temperature distribution in tunnel fires". *Tunnelling and Underground Space Technology*, **146**, 2024.
15. Hurley, M. J., Gottuk, D. T., Hall, J. R., Harada, K., Kuligowski, E. D., Puchovsky, M., Torero, J. L., Watts, J. M., Wieczorek, C. J., *SFPE handbook of fire protection engineering, fifth edition*, Springer New York, 2016.
16. Wu, K., Wang, G., Li, J., Huang, Y., Yan, X., Zhang, T., "Numerical study on plume bifurcation in longitudinally ventilated tunnel fires". *Tunnelling and Underground Space Technology*, **132**, 2023.
17. Ingason, H., Li, Y. Z., Lnnermark, A., *Tunnel Fire Dynamics*, Tunnel Fire Dynamics, 2015.
18. Gao, Z. H., Ji, J., Fan, C. G., Li, L. J., Sun, J. H., "Determination of smoke layer interface height of medium scale tunnel fire scenarios". *Tunnelling and Underground Space Technology*, **56,** 118-124, 2016.
19. Tilley, N., Deckers, X., Merci, B., "CFD study of relation between ventilation velocity and smoke backlayering distance in large closed car parks". *Fire Safety Journal*, **48,** 11-20, 2012.
20. Zhao, S., Yang, H., Li, Y. Z., Ingason, H., Liu, F., "Theoretical and numerical study on smoke descent during tunnel fires under natural ventilation condition". *Tunnelling and Underground Space Technology*, **142**, 2023.
21. Li, Y. Z., Ingason, H., "The maximum ceiling gas temperature in a large tunnel fire". *Fire Safety Journal*, **48,** 38-48, 2012.
22. Ji, J., Guo, F., Gao, Z., Zhu, J., Sun, J., "Numerical investigation on the effect of ambient pressure on smoke movement and temperature distribution in tunnel fires". *Applied Thermal Engineering*, **118,** 663-669, 2017.
23. Ji, J., Tan, T., Gao, Z., Wan, H., Zhu, J., Ding, L., "Numerical investigation on the influence of length–width ratio of fire source on the smoke movement and temperature distribution in tunnel fires". *Fire Technology*, **55,** 963-979, 2019.
24. Kunsch, J. P., "Critical velocity and range of a fire-gas plume in a ventilated tunnel". *Atmospheric Environment*, **33,** 13-24, 1999.
25. Hu, L. H., Huo, R., Chow, W. K., Wang, H. B., Yang, R. X., "Decay of buoyant smoke layer temperature along the longitudinal direction in tunnel fires". *Journal of Applied Fire Science*, **13,** 53-77, 2004.
26. Ji, J., Guo, F., Gao, Z., Zhu, J., "Effects of ambient pressure on transport characteristics of thermal-driven smoke flow in a tunnel". *International Journal of Thermal Sciences*, **125,** 210-217, 2018.
27. Zukoski, E., Kubota, T., Cetegen, B., "Entrainment in fire plumes". *Fire Safety Journal*, **3,** 107-121, 1981.
28. Delichatsios, M. A., "The flow of fire gases under a beamed ceiling". *Combustion Flame*, **43,** 1-10, 1981.
29. Takeuchi, S., Tanaka, F., Yoshida, K., Moinuddin, K. A. M., "Effects of scale ratio and aspect ratio in predicting the longitudinal smoke-temperature distribution during a fire in a road tunnel with vertical shafts". *Tunnelling Underground Space Technology*, **80,** 78-91, 2018.
30. Yang, D., Hu, L. H., Huo, R., Jiang, Y. Q., Liu, S., Tang, F., "Experimental study on buoyant flow stratification induced by a fire in a horizontal channel". *Applied Thermal Engineering*, **30,** 872-878, 2010.
31. Tang, F., He, Q., Shi, Q., "Experimental study on thermal smoke layer thickness with various upstream blockage–fire distances in a longitudinal ventilated tunnel". *Journal of Wind Engineering and Industrial Aerodynamics*, **170,** 141-148, 2017.

Nomenclature

Symbols		*Greeks*	
C_d	flow coefficient	ρ	density (kg/m^3)
c_p	specific heat (kJ/(kg · K))	λ	specific gravity of gas
D^*	characteristic diameter of fire source (m)	Superscripts	
g	acceleration of gravity (m/s^2)	*	dimensionless
h	smoke layer thickness (m)	Subscripts	
H	tunnel height (m)	a	ambient
l	flame height (m)	c	convection
L	tunnel length (m)	ef	effective
m	mass flow rate (kg/s)	max	maximum
$\dot{Q}$	heat release rate of fire (kW)	s	smoke

T	temperature (◦C)	p	rising plume
ΔT	excess temperature (◦C)	sI	Stage I
v	velocity (m/s)	sII	Stage II
W	tunnel width (m)	$sIII$	Stage III
x_f	distance from fire source (m)	sIV	Stage IV
x_v	distance from virtual origin (m)		
x	longitudinal length (m)		
y	horizontal width (m)		
z	vertical height (m)		
z_v	virtual origin (m)		

Study on the indoor-outdoor temperature difference-induced smoke re-stratification in naturally ventilated tunnel fires

Jiangdong Li[1,2], Ke Wu[1,2], Tianhang Zhang[1,2] & Lizhong Wang[1]
[1]Key Laboratory of Offshore Geotechnics and Material of Zhejiang Province, Zhejiang University, Hangzhou 310058, China
[2]Research Center for Urban Fire Safety Engineering, Zhejiang University, Hangzhou 310058, China

ABSTRACT

High-temperature, toxic smoke is a leading cause of casualties in tunnel fires, particularly caused by the descent of smoke due to the disruption of smoke stratification. In this work, the smoke stratification behaviour is investigated considering the effects of indoor-outdoor temperature difference and heat release rate in naturally ventilated tunnel fires using full-scale numerical simulations. Results show that thermodynamic equilibrium process between fire source and external high temperature causes smoke spreading stagnation and re-stratification, which means smoke lies beneath the air. The "double cycle" flow field generated by the hot smoke and external high temperature is the primary factor to trigger the smoke re-stratification behavior. Based on the smoke stagnation position and flow characteristics, the smoke propagation state can be divided into the one-dimensional spreading zone, the double circulation zone, and the smoke re-stratification zone. The length between the fire source and the smoke stagnation point increases with increasing the heat release rate and decreasing indoor-outdoor temperature difference at the quasi-steady state. By analyzing the dominant factors affecting longitudinal ceiling temperature rise in different regions, an empirical method for predicting the smoke stagnation point is proposed, based on the balance of the internal and external temperature rise. The predicted results show a good agreement with the existing data. This study provides valuable insights into the design of naturally ventilated tunnels and offers a theoretical basis for improving fire safety.

KEYWORD: tunnel fire, natural ventilation, indoor-outdoor temperature difference, smoke re-stratification

INTRODUCTION

The hot and toxic smoke is a main factor in casualties, resulting that the study about smoke movement becomes a hot spot [1]. Once a fire occurs, the hot smoke gathers at the tunnel ceiling and spreads along the tunnel, as shown in Fig. 1a. In near-fire areas, the smoke usually forms a stable stratification under the ceiling due to its thermal pressure or buoyancy force, which provides a clear height for the evacuation path (Fig. 1b). As the smoke spreads longitudinally, the smoke temperature gradually drops due to heat loss to the tunnel ceiling and cold air entrainment. Consequently, the buoyant force decreases over time (Fig. 1c), leading to the disruption of stratification and posing a threat to personnel safety. Therefore, it is of utmost importance to understand the characteristics of the smoke stratification and the smoke descent.

Buoyancy and inertial forces are the two primary factors influencing fire-induced thermal stratification [2]. The thermal buoyancy helps to maintain the stratification, while the inertial forces do the opposite. Based on this, *Fr* and *Ri* numbers are always used as dimensionless numbers to calibrate the stratified state. Newman [3] conducted experiments of duct fires and categorized the longitudinal layered structure into three distinct regions based on the *Fr* number. Ingason et.al [2] further refined the Froude number threshold to distinguish between different stratification regimes based on large-scale and reduced-scale tunnel fire tests.

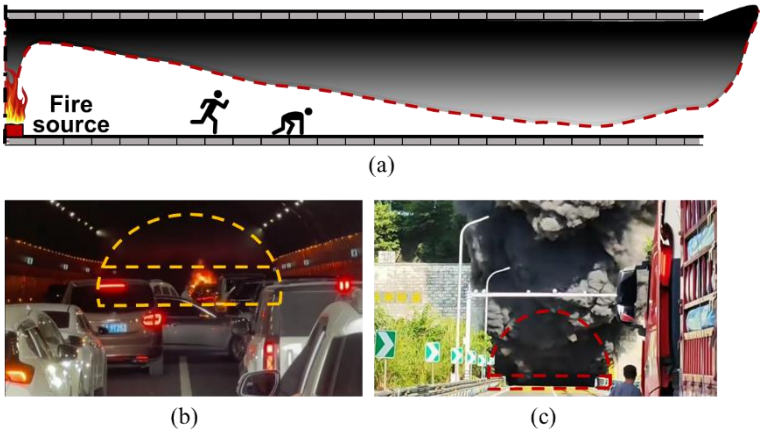

Figure 1 (a) Schematic diagram of fire smoke spread in a naturally ventilated tunnel, (b) Smoke stratification near the fire source, (c) Smoke stratification at the tunnel exit

Smoke descent is another critical phenomenon of the smoke layer behaviour, typically occurring when the buoyancy force cannot maintain the stratified flow. The smoke descent is an important factor determining tunnel fire safety caused by the increased smoke thickness. However, the smoke thickness is always assumed to be constant at the one-dimensional spread stage as the length of the tunnel structure is relatively short. As the length increases, the smoke thickness gradually increases, eventually leading to the smoke descent phenomenon [3]. Through full-scale numerical simulations, Zhao et al. [4] conducted a systematic study on smoke descent behaviour in naturally ventilated tunnels. They found that temperature decay along the tunnel and air entrainment at the smoke layer interface could be considered as reasons for smoke descent. Furthermore, smoke descent can hinder the supply of fresh air to the fire source, potentially even leading to fire self-extinction [5]. Smoke descent may be influenced by factors such as fire size [6,7], wall material [8], and tunnel cross-sectional area [4].

In addition to the internal factors mentioned, the external environment can also influence smoke movement and stratification. Factors like ambient pressure [9], crosswinds [10], and rainfall [11] at the tunnel entrance are increasingly drawing academic attention. Through FDS simulation, Zhang et al. [9] found that both ceiling temperature rise and induced velocity decrease with the decrease of ambient pressure, which has a complex coupling effect on smoke stratification. The intensification of both canyon cross winds and rainfall will lead to the increase of longitudinal airflow in the tunnel, which increases the smoke layer thickness downstream of the fire source [10,11]. Yang et al. [10] further proposed a *Fr* number to evaluate the stratification status of the smoke. However, the indoor-outdoor temperature difference, which has a potential impact on the flow field, has rarely been mentioned in existing studies.

During the diurnal cycle, the outdoor environment can rapidly attain a higher temperature due to solar radiation. In contrast, the temperature within the tunnel, influenced by the thermal inertia of the surrounding rock mass, may remain relatively low, exhibiting the indoor-outdoor temperature difference phenomenon. This kind of temperature difference is commonly-occurred during summer and winter in high-latitude regions whereas is often ignored in existing studies by setting the boundary temperature to be the same as the ambient temperature. Thus, the characteristics of the smoke movement will also change whereas the mechanism and critical condition remain unknown.

In this work, the smoke stratification and descent behaviour are investigated and analysed considering the effect of indoor-outdoor temperature difference and heat release rate in naturally ventilated tunnel fires using full-scale numerical simulations. By analysing the heat and mass transfer process during the smoke spread, a special smoke descent phenomenon, smoke re-stratification is proved and studied numerically. This study holds significant practical value for the design of naturally ventilated tunnels and provides a theoretical basis for fire science.

NUMERICAL SETUP

Full-scale or reduced-scale experiments can provide realistic fire scene information, such as flame shape, smoke movement characteristics, and temperature distribution. However, features of smoke stratification and descent require a long distance to be accurately represented, which can result in high costs and poor repeatability, especially in full-scale tunnel fire tests. Additionally, temperature differences between the inside and outside of tunnels are common, but reliable methods for accurately and stably controlling these temperatures are still lacking. Therefore, full-scale CFD simulations are conducted using Fire Dynamics Simulator (FDS 6.7.3) to analyze smoke spread and flow fields under the influence of indoor-outdoor temperature differences. Turbulence is modelled using Large Eddy Simulation (LES), while combustion and radiation transport are simulated using the Mixed Fraction Model and the Finite Volume Method, respectively.

Simulation setup

A series of numerical models with different indoor and outdoor temperatures are built up to study the smoke stratification behaviors. The layout of the numerical model is shown in Fig. 2. The cross-section of the full-size numerical model is 5.0 m (W) and 5.0 m (H) in height with a rectangular shape. The total length of the numerical tunnel is set to be 500 m (L). Heptane is selected as the fuel, with the fire source measuring 2.0 m in width and 2.5 m in length. The burner is positioned along the tunnel's centerline, near the left end. The soot yield and the CO yield are set to be 0.037 kg/kg, and 0.01 kg/kg, respectively [12]. The simple pyrolysis model is used, which ignores the mixing and reaction time between fuel and fresh air. In order to save computational resources, the left side of the numerical tunnel model is set to "MIRROR", which means that the heat release rate (HRR) and tunnel length in the numerical model are half of the actual values they represent. In other words, the fire scenario is a naturally ventilated tunnel fire with 1000 m in length, and the fire source positioned at the midpoint.

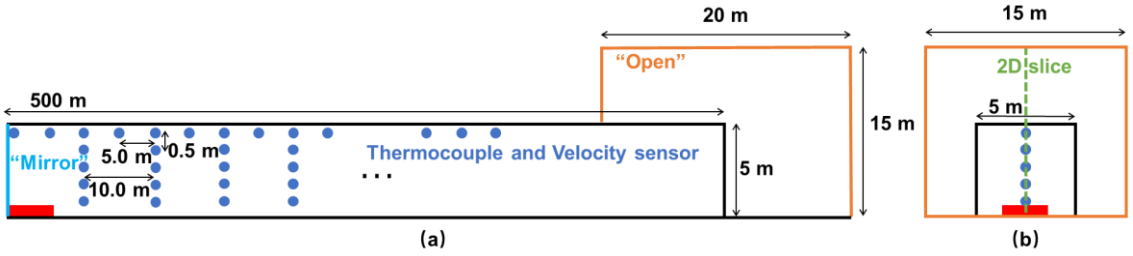

Figure 2 Numerical model of the tunnel (a) side view (b) cross-section view

An extended computational domain is set on the right side of the numerical model to simulate the external environment of the tunnel, with dimensions of 20 m (L) × 15 m (W) × 15 m (H). Except for the bottom surfaces, all other surfaces in the extended domain are set as 'OPEN,' allowing the 'Exterior Temperature' to be adjusted to reflect the ambient temperature outside the tunnel. To simulate the thermal hysteresis behavior of real tunnel temperatures, the solid boundaries of the tunnel are assigned the thermal and physical properties of concrete. The concrete has a density of 2280 kg/m^3, a thermal conductivity of 1.8 W/(m·K), and a specific heat capacity of 1.04 kJ/(kg·K), respectively.

In all simulations, the internal temperature (T_i), ambient pressure, and humidity are set to 10.0 ℃, 101.325 kPa, and 40%, respectively. Based on the vehicle fire load in the tunnel, the HRR in the numerical model is set to 1.25 MW, 2.5 MW, 5.0 MW, and 10.0 MW (presenting 2.5–20 MW in fact). According to the local daily average temperature difference and related work [13], the 'Exterior Temperature' values are selected as 10.0 ℃ (presenting no indoor-outdoor temperature difference), 15.0 ℃, 20.0 ℃, 30.0 ℃, 50.0 ℃ (i.e. external temperature of the tunnel, T_e). Therefore, the values of indoor-outdoor temperature difference (ΔT_{ie}) are 0 K, 5 K, 10 K, 20 K, and 40 K, respectively. Moreover, 4 cases with only external high temperature but no fire ignited (i.e. HRR = 0) are also simulated to investigate the flow and temperature field inside the tunnel caused by the external high-temperature environment. In total, 24 cases are conducted with various HRRs and external temperatures, as shown

in Table 1.

Fig. 2 also presents detailed information about the measuring points. Considering that the smoke stratification state and layer thickness are sensitive to buoyancy and inertial forces, the gas temperature and flow velocity at the tunnel ceiling are recorded with an interval of 5 m at 0-500 m from the fire source location. The temperature and velocity measurement trees are arranged at intervals of 10 m for recording the thickness of the smoke layer and the temperature stratification, with a vertical spacing of 0.5 m. Besides, several 2D slices are set for temperature, velocity, and visibility along the tunnel center line.

Table 1 Test conditions.

No.	Heat release rate (MW)	internal temperature (℃)	External temperature (℃)
1-20	2.5, 5.0, 10.0, 20.0	10	10, 15, 20, 30, 50
21-24	0	10	15, 20, 30, 50

Grid sensitivity

Grid size is a critical factor in determining computational accuracy and efficiency, making it essential to conduct a grid sensitivity analysis. Previous studies have shown that when the grid size of the computational domain ranges from 1/16 - 1/4 of the characteristic diameter D^* of the fire site, the simulation results align well with experimental data [14]. The D^* can be calculated using Eq. (1). It can be concluded that the smaller heat release rate needs the smaller the grid size to satisfy the sensitivity requirement. Therefore, in this study, the grid irrelevance analysis is carried out for a 2.5 MW fire and an ambient temperature of 10 ℃ inside and outside the tunnel.

$$D^* = \left(\frac{Q}{\rho_a c_p T_a \sqrt{g}} \right)^{2/5} \tag{1}$$

where Q is the total heat release rate of the fire (kW), ρ_a is ambient density (kg/m^3), c_p is specific heat capacity (kJ/(kg·K)), T_a is the ambient temperature (K), and g is the gravitational acceleration constant in (m/s^2).

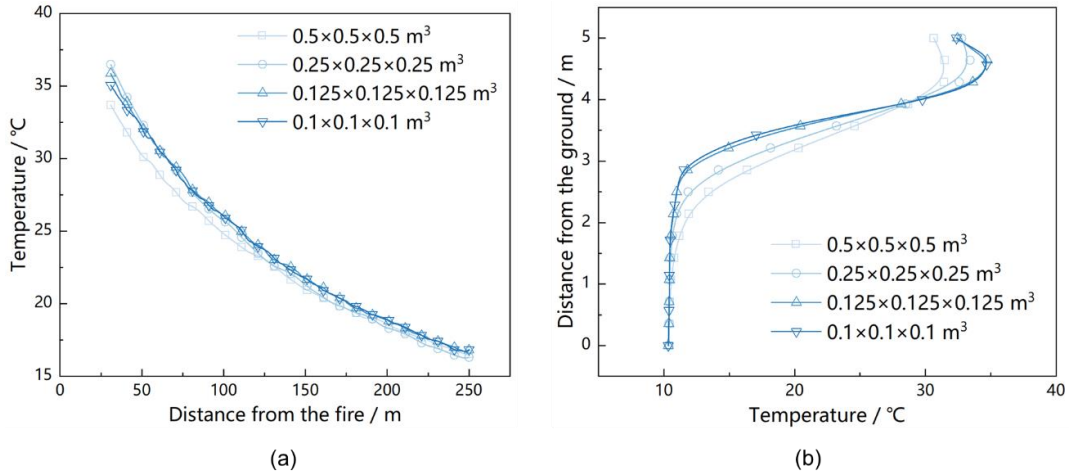

Figure 3 Temperature profile under different grid sizes (a) longitudinal ceiling temperature 30-250 m, and (b) vertical temperature 50 m from the fire (HRR = 2.5 MW, ΔT_{ie} = 0 K)

Based on the above analysis, for the 2.5 MW fire, four cubic grid sizes, including 0.1 m, 0.125 m, 0.25 m, and 0.5 m, are selected for the simulations, which are in the range of 0.07 – 0.36 D^*. Given that the primary focus of this study is to analyze smoke stratification through smoke temperature, the grid sensitivity analysis is performed using the longitudinal temperature at the ceiling 30-250 m from the fire

and the vertical temperature 50 m from the fire, as shown in Fig. 3, based on time-averaged values during 1200-1500 s. Qualitative analysis indicates that when the grid size is smaller than 0.125 m, the results converge closely. Therefore, a 0.125 m cubic grid will be used for subsequent simulations.

RESULT AND DISCUSSION

In order to understand the influence of temperature difference between inside and outside tunnel on the smoke movement, it is necessary to analyse the smoke spreading. According to previous studies, the smoke spreading in a naturally ventilated tunnel fire scenario can be divided into four regions, including the plume rising and impinging region beneath the ceiling, the radical spreading region, the transition region, and the one-dimensional spreading region. Since the smoke stratification phenomenon always occurs in the one-dimensional region, the present study will focus on this area.

The phenomenon of smoke re-stratification

Theoretically, when there is no temperature difference, the smoke will continue to spread toward to the tunnel exit forced by the buoyancy force [13]. Although hot smoke continuously exchanges heat with the boundary (i.e. ceiling and the side wall), the smoke temperature will never be lower than the ambient temperature under the "no indoor-outdoor temperature difference" assumption. Therefore, the smoke can keep a good stratified state at the front area and eventually be expelled outward and upward from the exit. On the contrary, if the internal boundary temperature is lower than that of the external space, the smoke temperature may drop below the ambient air temperature if the tunnel is sufficiently long. When this occurs, the smoke layer can descend to the lower space and spread along the ground, while the hot ambient air flows into the upper clear space and spreads near the ceiling, as shown in Fig. 4. Obviously, when there is a temperature difference, The smoke cannot spread directly to the tunnel exit but is instead halted at a certain distance. The place where the smoke stops moving forward is defined as *smoke stagnation point*. In the present case, the smoke stagnation point maintains a distance of 385 m from the fire source when t = 800 s.

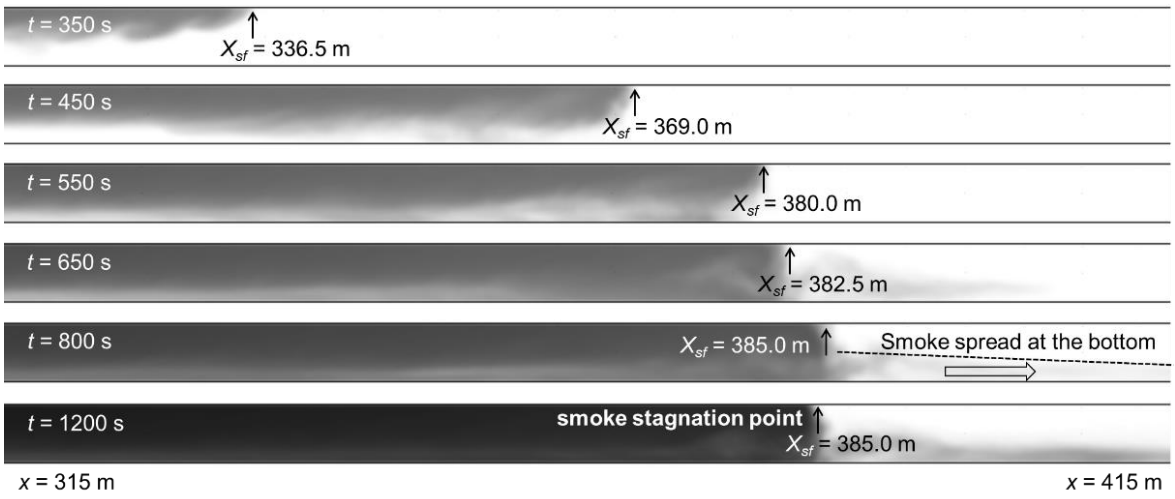

Figure 4 Typical smoke spreading process under the influence of high external ambient temperature (HRR = 5.0 MW and T_e = 30℃)

Besides, an increasing trend of the smoke layering thickness can be found especially during 450 s – 650 s after the ignition. The smoke gradually loses the stratified state which brings danger to the evacuation of people. After the smoke front stops spreading, most smoke goes back to the fire source direction, which means the smoke shows an internal circulation behavior. During the period of 800 s – 1200 s, the concentration of smoke increases significantly at the left side of smoke stagnation point. However, it needs to be pointed out that a small amount of the smoke separates and spreads from the bottom part of the tunnel towards to the tunnel exit, which is obviously different from the normal smoke spreading.

The special phenomenon of smoke at the tunnel bottom and air at the tunnel ceiling is first observed and named as *smoke re-stratification*.

When smoke re-stratification is induced by the indoor-outdoor temperature difference, the smoke spreading behavior can be divided into three zones: the *one-dimensional spreading zone*, the *double circulation zone*, and the *re-stratification zone*, based on the position of the smoke stagnation as plotted in Fig. 5.

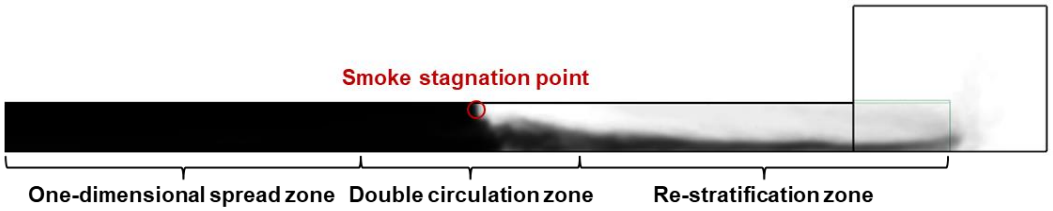

Figure 5 Schematic diagram of smoke re-stratification and different spreading zones

The mechanism of smoke re-stratification

The above-mentioned smoke spreading process shows that the internal and external temperature difference has a significant impact on the thermodynamic characteristics of the smoke, especially at the re-stratification zone. By analysing the temperature and velocity distribution near the smoke stagnation point, the mechanism of smoke re-stratification behaviour can be further revealed.

The vertical distributions of temperature rise and velocity in the longitudinal direction along the tunnel centerline are illustrated in Fig. 6 at quasi-steady conditions (1000 s to 1200 s after ignition). In this case, the heat release rate is 5 MW and indoor-outdoor temperature differences are 0 K (the dash curve) and 20 K (the solid curve). Key longitudinal positions are selected to evaluate the impact of external high temperatures, including the one-dimensional spreading zone (150 m, near-fire source region; 350 m, far-fire source region), the double circulation zone (385 m, the smoke stagnation point), and the re-stratification zone (450 m). For the vertical distribution of longitudinal velocity, positive values indicate flow in the positive x-direction, while negative values indicate flow in the opposite direction.

When there is no temperature difference between inside and outside (dashed line of hollow point in Fig. 6), the characteristics of the vertical temperature and velocity distributions remain in accordance with existing studies [13]. The closer to the tunnel ceiling, the higher the temperature rise, while the temperature rise near the floor is almost zero. The vertical distribution of wind velocity, on the other hand, shows typical stratified flow characteristics, with the upper fluid moving toward the tunnel exit and the lower fluid moving toward the fire source. In addition, the extremes and gradients of vertical temperature rise and wind velocity both decrease with distance from the fire source, which is related to factors such as the decrease of smoke temperature rise and the increase of smoke layer thickness.

When the indoor-outdoor temperature difference is 20 K, for the one-dimensional spreading region, the vertical temperature rise and velocity distributions have limited difference from that of no temperature difference, but show a tendency to increase with increasing distance from the fire source. As plotted in Fig .6 a & b, the temperature rise and velocity profiles for the two cases almost coincide when located at x = 150 m. However, the difference between the two cases increases slightly for the slice at x=350 m. Moreover, at the smoke stagnation point and the re-stratification zone, the temperature rise and velocity distributions for the two cases are obviously different (Fig. 6 c & d). Under the influence of high external temperature, the longitudinal velocity essentially disappears at the smoke stagnation point and the temperature distribution almost doesn't change. For the smoke re-stratification zone, the vertical temperature rise increases significantly compared to the case when there is no temperature difference. In addition, the trend of vertical velocity change is completely opposite, showing that the upper fluid moves toward the fire source, and the lower fluid moves toward the tunnel exit. This indicates that the external high temperature not only changes the temperature field inside the tunnel but also reshapes the

flow field structure near the tunnel portal.

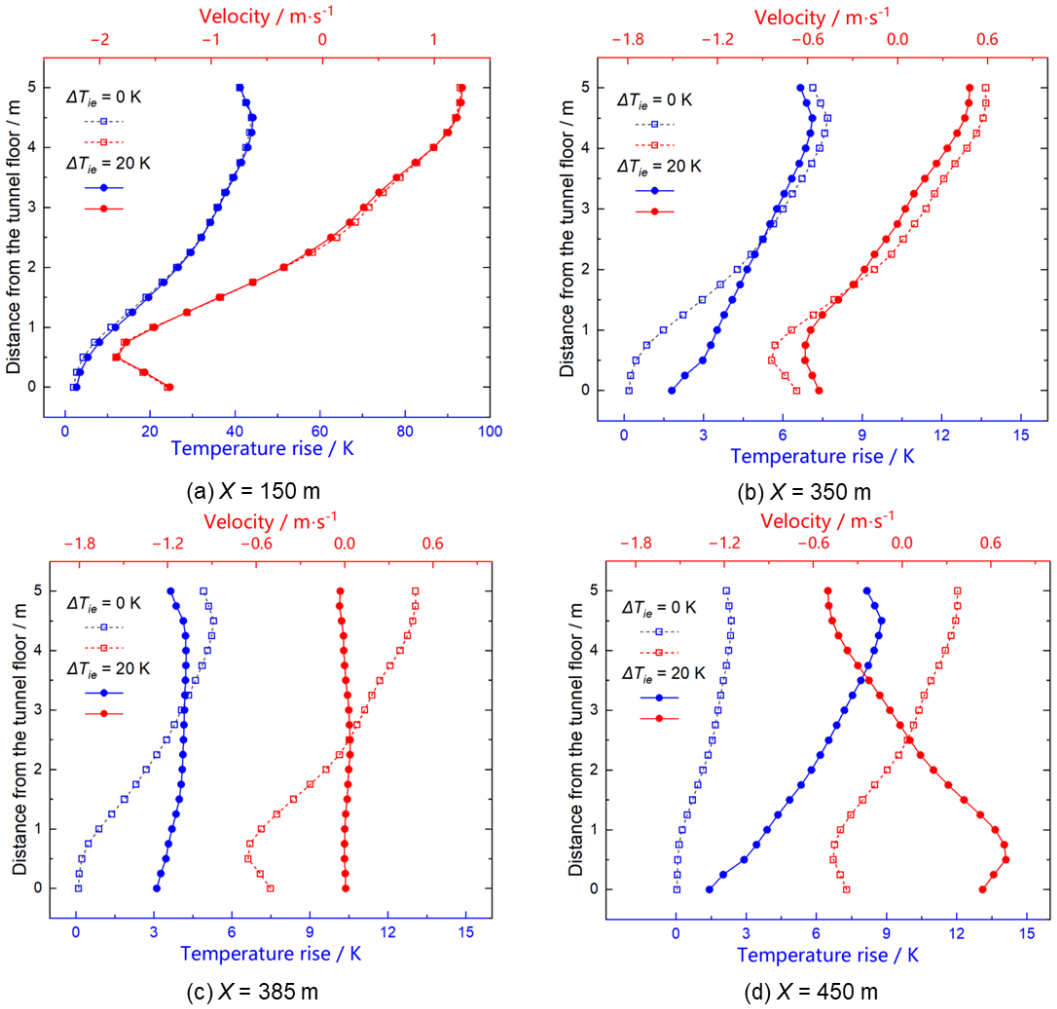

Figure 6 The influence of internal and external temperature difference on the vertical temperature rise and velocity distribution of the tunnel central axis (HRR = 5 MW, ΔT_{ie} = 0 K with the dash curve and 20 K with the solid curve)

Based on the above analysis, it can be seen that the external high temperature has a limited effect on the smoke one-dimensional spreading zone, but it can cause a significant increase in the temperature of the smoke re-stratification region as well as a reversal of the direction of the flow field. The special smoke movement behaviour described above (smoke stagnation and re-stratification) is associated with the unique vertical distributions of temperature and velocity in the re-stratification region. A deeper discussion for the thermodynamic at the stagnation point is presented for better demonstrate the mechanism of the smoke re-stratification. At the quasi-steady state, the smoke movement, temperature distribution, and longitudinal velocity distribution (as well as flow direction) near the smoke stagnation point under typical test conditions (5 MW and T_e = 30 °C) are shown in Fig. 7.

As shown in Fig. 7b, the smoke temperature decays while travelling along the ceiling with a gradient from the fire source to the tunnel portal. At the same time, the high-temperature external environment induces temperature rise near the portal but the temperature of the supplied air also drops due to the heat loss to the tunnel boundary. Eventually, on both sides of the stagnation point, the temperature fields of the hot smoke and the hot air reach the equilibrium state, causing the smoke stops its spread. From Fig. 7c, it can be observed that two incoming flows with opposite circular structures are generated by the temperature difference, including both clockwise (on the left) and counterclockwise (on the right), forming the “double cycle” flow field structure. As a result, the smoke spreading is blocked by opposing flow and the majority of smoke returns to the fire source with the clockwise flow structure. Besides, it

should be noticed that the rest smoke is drawn out of the tunnel along the tunnel floor with the counterclockwise flow field structure. Therefore, “double cycle” flow field structure near the stagnation point is the main factor contributing to the smoke re-stratification behavior.

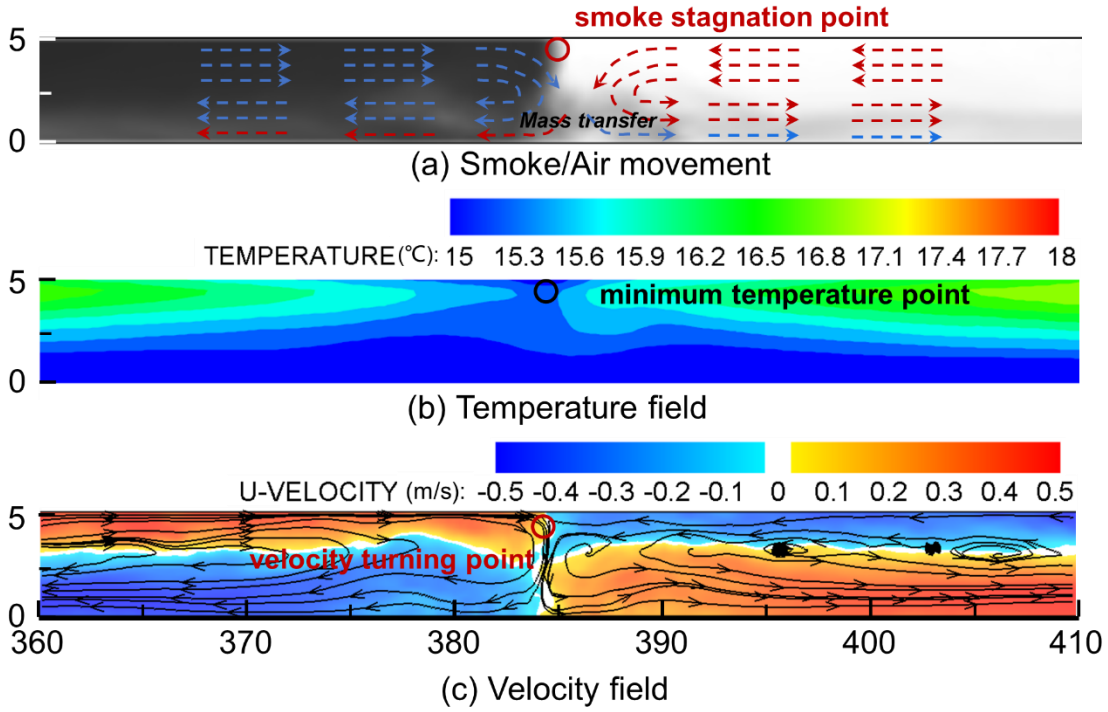

Figure 7 Contour of different physical quantities with 5 MW heat release rate and 30 ℃ external temperature: (a) Smoke movement contour, (b) Temperature distribution contour, and (c) Velocity distribution contour with flow field.

Based on the above analysis, the external high temperature of the tunnel can be treated as a virtual heat source, which generates a temperature field and velocity field distribution opposite to that of the actual fire source. The smoke stagnation behavior is mainly caused by the temperature field, while the smoke re-stratification is mainly produced by the “double cycle” flow field structure which is the consequence of the opposite velocity field.

Analysis of smoke spreading characteristics

As the smoke stagnation occurs, significant smoke settling is observed, leading to a notable reduction in evacuation safety. Therefore, it is essential to further analyse the characteristics of smoke spread, including its propagation speed and stagnation position, to provide valuable insights for evacuation.

Based on the longitudinal visibility slice at the center of the tunnel, the smoke front is considered to have spread to a specific region when the visibility at that location decreases. The time-history of the smoke front position under typical conditions is plotted in Fig. 8. It can be observed that in the early stages of the fire, the time-history curves of the smoke front position overlap regardless of the indoor-outdoor temperature difference. This indicates that the temperature difference has a limited impact on smoke propagation during the initial stage.

As shown in Fig. 8a, a higher heat release rate results in faster smoke propagation. For a 2.5 MW fire, it takes 1140 s for the smoke to travel 500 m, with an average velocity of 0.44 m/s. In contrast, a 20 MW fire reaches the tunnel exit in just 460 s, with an average velocity of 1.09 m/s, representing a 150 % increase. Additionally, under the same indoor-outdoor temperature difference, as the heat release rate increases, the smoke stagnation time (i.e., the time when the smoke front position becomes almost stable) decreases from 690 s to 420 s, and the smoke stagnation point moves farther from the fire source.

Conversely, as shown in Fig. 8b, under the same heat release rate, the increase in the indoor-outdoor temperature difference reduces the smoke stagnation time from 1010 s to 450 s, and the stagnation point shifts closer to the fire source. Although fully ideal, since the heat release rate varies with time in a real tunnel fire, this comparative analysis could still reveal the fact that the stagnation point where the triggers the smoke re-stratification is highly dependent on the heat the smoke spreading speed and the thermodynamic equilibrium process between hot smoke and hot air.

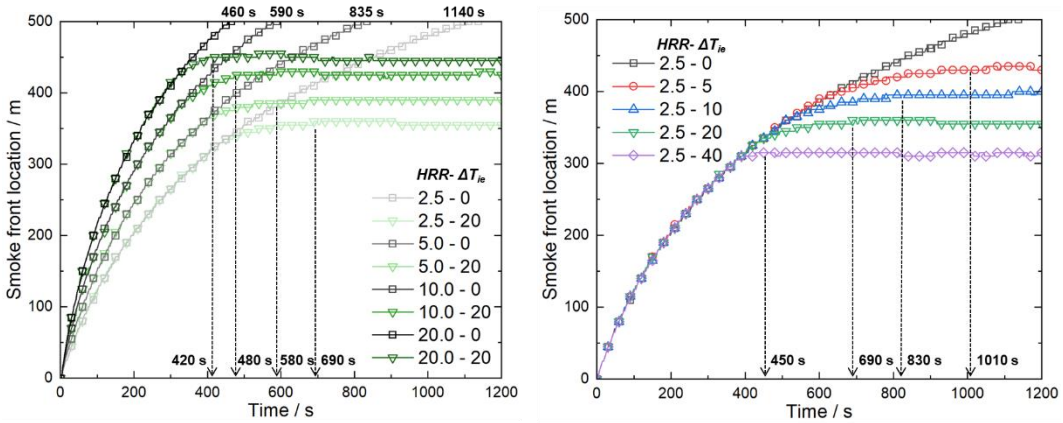

(a) influence of the heat release rate (b) influence of the ΔT_{ie}

Figure 8 the time-history curves of the smoke front position (x-y means heat release rate in MW and temperature difference in K), (a) influence of the heat release rate, and (b) influence of the indoor-outdoor temperature difference

The quantitative results based on smoke visibility are often challenging to apply in real fire scenarios, so it is necessary to develop a more practical method to identify the smoke stagnation point using measurable physical indicators. As shown in Fig. 7, the stagnation point identified from the smoke movement contour, the location of the minimum temperature, and the point where the flow field direction reverses are all approximately at 385 m, with their longitudinal positions nearly overlapping. Compared to wind speed sensors such as anemometers and weather stations, temperature sensors like thermocouples, distributed temperature sensing (DTS) fibers, and temperature gratings are more widely used in tunnels. Therefore, the location of the minimum temperature can be selected as the criterion for identifying the smoke stagnation point.

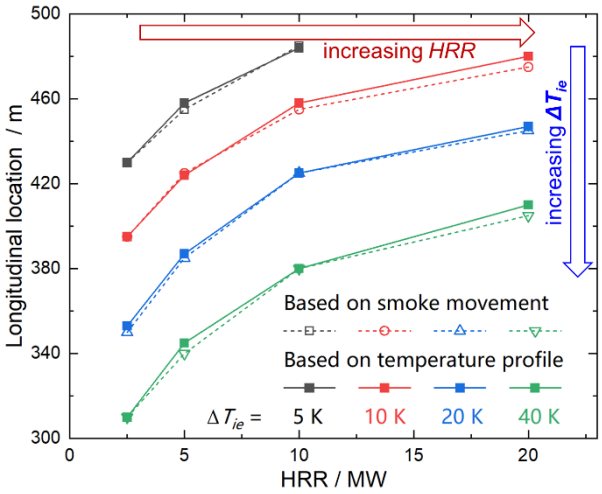

Figure 9 Quantitative and qualitative statistical results of the smoke stagnation point

The quantitative results (based on the location of the minimum temperature) and qualitative results (based on smoke movement contours) for the smoke stagnation points under various scenarios are shown in Fig. 9. The difference between the two methods is less than 5 m, indicating that the location of the

lowest temperature can be used as a reliable quantitative criterion for identifying smoke stagnation point. Furthermore, under different fire scenarios, the position of the smoke stagnation point consistently follows the same trend: it moves further from the fire source as the heat release rate increases and the indoor-outdoor temperature difference decreases.

Prediction of the smoke stagnation point

The above analysis indicates that the smoke stagnation position overlaps with the minimum ceiling temperature position, which may help to predict the smoke stagnation point. Therefore, Fig. 10 compares the longitudinal ceiling temperature rise under different scenarios during the quasi-steady state. The solid curve presents the temperature decay with no temperature difference and the coloured scatter represents cases with temperature difference.

When the indoor and outdoor temperatures are consistent, the ceiling temperature rise continuously decreases. However, it first decreases and then increases when the high temperature is outside the tunnel. It should be pointed out that the ceiling temperature rise has different features in different zones, with the location of the lowest temperature acting as the boundary. In the one-dimensional spreading zone, for the same heat release rate, the ceiling temperature rise overlaps under different external tunnel temperatures. Therefore, the ceiling temperature rise in this region is primarily controlled by the heat release rate, with limited influence from the external tunnel temperature. Similarly, in the smoke re-stratification zone, the ceiling temperature rise is mainly influenced by the external environmental temperature, while the heat release rate has little effect.

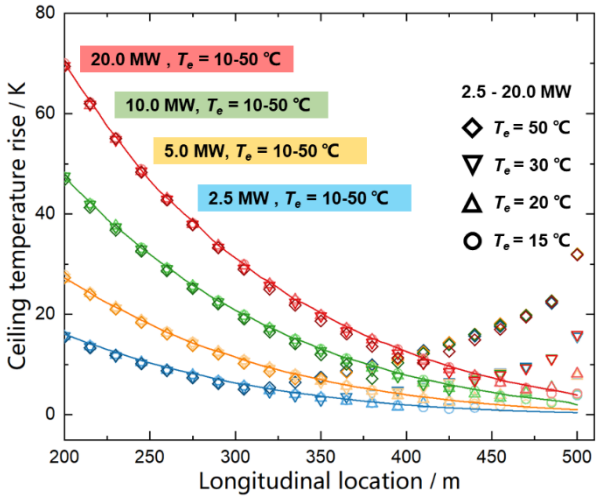

Figure 10 Longitudinal ceiling temperature rise under different heat release rates and indoor-outdoor temperature differences during the quasi-steady state

Based on the distinct ceiling temperature rise characteristics driven by different dominant factors in each zone, it can be reasonably inferred that the temperature rise curves produced by these dominant factors can be used to predict the smoke stagnation point. Specifically, the smoke stagnation point location can be predicted by comparing the ceiling temperature rise distribution under no fire source (induced by external high temperatures) with that during fire conditions with consistent indoor-outdoor temperatures. The intersection of these two curves in the longitudinal direction represents the predicted stagnation point.

The temperature rise distributions for different heat release rates and external high temperatures are shown in Fig. 11a, with the dashed lines in various colors representing the ceiling temperature rise for each scenario. The comparison between the predicted stagnation point (intersection of the curves) and the actual location of the lowest temperature (measured stagnation point) in the quasi-steady state is counted and presented in Fig. 11b. It can be seen that the proposed stagnation point prediction method

has an overall error of less than 5%, demonstrating good applicability.

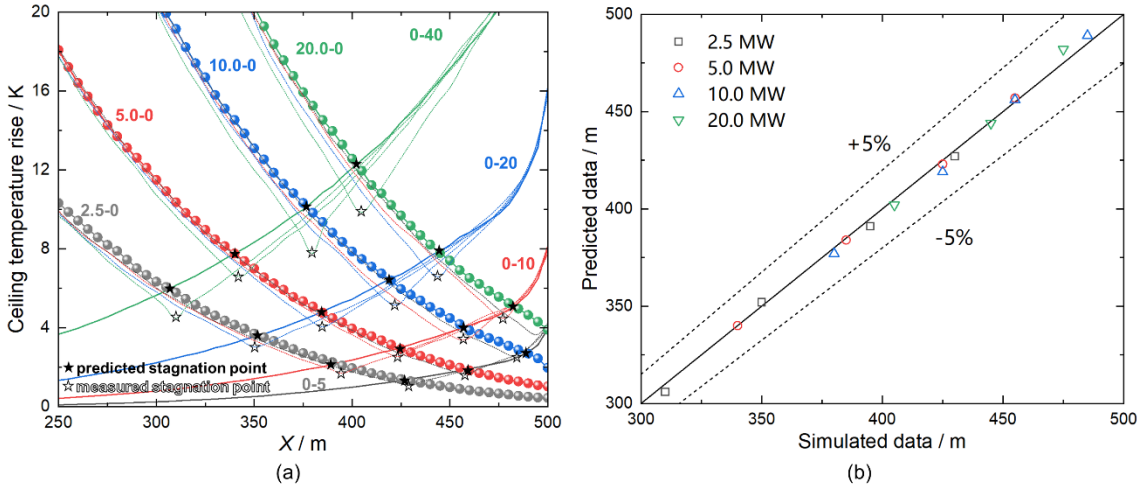

Figure 11 Prediction of the smoke stagnation point and validation: (a) Quasi-steady-state temperature rise distributions for various heat release rates and external high temperatures, and (b) validation of the smoke stagnation point prediction model (x-y indicates the heat release rate in MW and the temperature difference in K)

Since the tunnel length is 500 m in this work, the temperature and velocity of the smoke far from the fire source decrease to relatively low levels according to the above analysis. Under these conditions, a temperature difference of only 10 K can induce a significant smoke re-stratification phenomenon, even when the HRR reaches 20 MW. Correspondingly, as the tunnel length decreases or the HRR increases, the critical temperature difference required to induce significant smoke re-stratification also increases. This relationship will be further quantified in the future work.

Since it has already been proved that the smoke stagnation point could be predicted by combining the two kinds of virtual cases (namely, case without indoor-outdoor temperature difference, and case without fire source), it's feasible to calculate the stagnation point by solving the temperature decay functions of the smoke layer and external airflow layer. The temperature decay function could be adopted from existing studies [17-20] while the external airflow layer temperature decay model could be established based on the one-dimensional heat exchange model [21,22]. After solving the prediction of the smoke re-stratification position, the smoke travelling path (distance between the stagnation point and the fire source) could be compared with the tunnel length. Ideally, if the calculated smoke travelling path is shorter than the longest potential smoke travelling distance, the smoke re-stratification could happen, and vice versa.

The above-mentioned discussion also indicates that this smoke re-stratification phenomenon is more likely to occur in tunnels with smaller fire power and longer distance, which means lower initial heat and more heat loss. Since the smoke re-stratification will cause smoke descent and affect pedestrian evacuation, it is worthy to pay more attention to this kind of special danger caused by small fire in long tunnels in real firefighting applications.

CONCLUSION

In this work, a series of full-scale numerical simulations considering various heat release rates (2.5, 5.0, 10.0, and 20.0 MW) and indoor-outdoor temperature difference (0, 5, 10, 20, and 40 K) are conducted to investigate a special smoke stratification behavior, namely, the smoke re-stratification. The main conclusions are as follows:

(1) Thermodynamic equilibrium process between fire source and external high temperature results in smoke spreading stagnation and re-stratification, which means smoke lies beneath the air. The "double

cycle" flow field is the main factor contributing to the smoke re-stratification behavior. Based on the smoke stagnation point and flow field structure, the smoke propagation state can be divided into the one-dimensional spreading zone, double circulation zone, and the smoke re-stratification zone.

(2) The internal and external temperature difference has a limited impact on smoke propagation during the initial stage, but the length between the fire source and the smoke stagnation point increases with increasing the heat release rate and decreasing indoor-outdoor temperature difference at the quasi-steady state.

(3) The smoke stagnation point can be decided by the temperature profile as temperature rise in the one-dimensional spreading zone is mainly affected by the heat release rate, and that in the smoke re-stratification zone is mainly affected by the external temperature. A method for constructing the prediction model for the smoke stagnation point is proposed based on the balance of the ceiling temperature rise distributions with no fire and no indoor-outdoor temperature difference. The predicted results show good agreement with the existing data.

(4) Theoretically, based on the existing ceiling temperature decay and one-dimensional heat exchange model, the internal smoke and external air temperature distribution can be fitted. Thus, the smoke stagnation position can be calculated, and the occurrence of the smoke re-stratification can be predicted by solving the temperature decay functions above in future work.

Overall, this work discovers and defines the smoke re-stratification behaviour under the influence of indoor-outdoor temperature differences. The generation mechanism and the change law have been revealed, and a theoretical framework is proposed for predicting the re-stratification phenomenon. It provides a new vision to re-visit the danger in tunnel fire scenarios and highlight the potential risks induced by low-power fire.

REFERENCES

1. Wan, H., Jiang, Y., and Jiang, J., "A survey of fire accidents during the process of highway tunnel operation in China from 2010 to 2021: characteristics and countermeasures", *Tunnelling and Underground Space Technology*, **139**, 105237, 2023.
2. Ingason, H., Li, Y.Z., Lönnermark, A., *Tunnel Fire Dynamics*, Springer Nature, 2024.
3. Newman, J. S. (1984). "Experimental evaluation of fire-induced stratification", *Combustion and flame*,**57**(1), 33-39, 1984.
4. Zhao, S., Yang, H., Li, Y. Z., Ingason, H., and Liu, F., "Theoretical and numerical study on smoke descent during tunnel fires under natural ventilation condition", *Tunnelling and Underground Space Technology*, **142**, 105414, 2023.
5. Wang, K. H., Chen, J. M., Wang, Z. K., Gao, D. L., Wang, G. Y., and Lin, P., "An experimental study on self-extinction of tunnel fire under natural ventilation condition", *Tunnelling and underground space technology*, **84**, 177-188, 2019.
6. Guo, Q., Li, Y. Z., Ingason, H., Yan, Z., and Zhu, H., "Numerical study on thermally driven smoke flow characteristics in long tunnels under natural ventilation", *International journal of thermal sciences*, **192**, 108379, 2023.
7. Lin, P., Zuo, C., Xiong, Y. Y., Wang, K. H., Shi, J. K., Chen, Z. N., and Lu, X. X., "An experimental study of the self-extinction mechanism of fire in tunnels", *Tunnelling and Underground Space Technology*, 109, 103780, 2021.
8. Zhao, Z., Chen, X., Wu, X., Jia, J., Kang, N., Zhang, Y., ... and Lu, S., "Experimental study on the descent distance of fire smoke at the corridor corner", *Tunnelling and Underground Space Technology*, **144**, 105534, 2024.
9. Zhang, Y., Yao, Y., Ren, F., Zhu, H., Zhang, S., and Jiang, L., "Effects of ambient pressure on smoke propagation in inclined tunnel fires under natural ventilation", *Environmental Science and Pollution Research*, **30**(24), 65074-65085, 2023.
10. Yang, L., Fan, C., Luan, D., Ouyang, R., Tao, H., Xu, Z., and Wang, F., "Experimental study on thermal stratification characteristics in tunnel fires under the effect of canyon cross wind", *Journal*

of Wind Engineering and Industrial Aerodynamics, **218**, 104756, 2021.
11. Luan, D., Bu, R., Sheng, Z., Fan, C., & Huang, X., "Experimental study on the impact of asymmetric heavy rainfall on the smoke spread and stratification dynamics in tunnel fires", *Tunnelling and Underground Space Technology*, **134**, 104992, 2023.
12. Chen, X., Li, J., Ni, Y., Liang, Z., Ding, H., Liu, L., ... and Zhang, T., "Study on induced flow patterns and inlet velocity in inclined tunnel fire with natural ventilation", *Tunnelling and Underground Space Technology*, **155**, 106188, 2025.
13. Zhao, P., Chen, J., Luo, Y., Li, Y., Chen, L., Wang, C., & Hu, T., "Field measurement of air temperature in a cold region tunnel in northeast China", *Cold Regions Science and Technology*, **171**, 102957, 2020.
14. McGrattan, K., "Fire Dynamics Simulator User's Guide", *NIST special publication1019*, *6*, 2013.
15. Wu, K., Wang, G., Li, J., Huang, Y., Yan, X., and Zhang, T., "Numerical study on plume bifurcation in longitudinally ventilated tunnel fires", *Tunnelling and Underground Space Technology*, **132**, 104926, 2023.
16. Zhang, T., Wang, G., Li, J., Wu, K., and Wang, L., "Modelling the maximum ceiling temperature with bifurcated plume in tunnel fires", *Fire Safety Journal*, **150**, 104249, 2024.
17. Hu, L. H., Huo, R., and Chow, W. K., "Studies on buoyancy-driven back-layering flow in tunnel fires", *Experimental Thermal and Fluid Science*, *32*(8), 1468-1483, 2008.
18. Li, L., Cheng, X., Wang, X., and Zhang, H., "Temperature distribution of fire-induced flow along tunnels under natural ventilation", *Journal of fire sciences*, *30*(2), 122-137, 2012.
19. Ji, J., Bi, Y., Venkatasubbaiah, K., & Li, K., "Influence of aspect ratio of tunnel on smoke temperature distribution under ceiling in near field of fire source", *Applied Thermal Engineering*, *106*, 1094-1102, 2016.
20. Gong, L., Jiang, L., Li, S., Shen, N., Zhang, Y., and Sun, J., "Theoretical and experimental study on longitudinal smoke temperature distribution in tunnel fires", *International Journal of Thermal Sciences*, *102*, 319-328, 2016.
21. Hu, L. H., Huo, R., Chow, W. K., Wang, H. B., & Yang, R. X., "Decay of buoyant smoke layer temperature along the longitudinal direction in tunnel fires", *Journal of applied fire science*, *13*(1), 53-77, 2004.
22. Zhang, T., Wang, G., Hu, H., Huang, Y., Zhu, K., and Wu, K., "Study on temperature decay characteristics of fire smoke backflow layer in tunnels with wide-shallow cross-section", *Tunnelling and Underground Space Technology*, *112*, 103874, 2021.

Vehicles impact on smoke stratification

Benjamin TRUCHOT, Guillaume LEROY and Thierry DURUSSEL
Ineris
Parc ALATA 60550 Verneuil en Halatte, France
E-mail: benjamin.truchot@ineris.fr

ABSTRACT

This paper focuses on stratification characteristics for longitudinally ventilated tunnels in case of fire. In such tunnels, when traffic is congested, ventilation should be used to control the flow and maintain the stratification to enable people to evacuate. The objective of this paper is to evaluate the influence of different types of vehicles on the quality of the stratification for both upstream and downstream smoke layers. Based on a third-scale experimental tunnel with real fire, this paper proposes a cross-comparison between the stratification characteristics in an empty tunnel and for two configurations with vehicles: one upstream of the fire and one downstream of the fire. The primary learning of this experimental campaign is the confirmation of the well-known influence of the vehicle on the back-layering development and the associated relation with the critical velocity. This experimental test series, however, highlights that while the back-layering layer is significantly modified by vehicles in terms of length and, consequently, in terms of energy balance, the associated stratification criteria, commonly based on the vertical temperature distribution, remain similar, meaning that stratification is not influenced by vehicles. The same effect was observed in the downstream layers. This analysis should, however, be considered through visibility. While the temperature profile is slightly changed, visibility in the lower part of the tunnel decreases due to the increase in the mixture of fresh air and smoke. Such an influence is transparent for the commonly used stratification criteria but remains important for people's safety.

KEYWORDS: fire, smoke stratification, stratification disturbance

INTRODUCTION

Fire is the most critical event that can happen in a tunnel, and several past accidents have demonstrated that they could become dramatic when people are trapped in the tunnel when such a fire occurs. Following the major critical fires that occurred at the end of the 90s, the Mont Blanc and the Tauern fires, many research projects have been performed, leading to a real increase in the safety level in such underground infrastructure.

One of the most critical situations remains the congested tunnel, where many people can be located inside the tunnel when a vehicle catches fire. In such a case, the ventilation should be designed to maintain the stratification, enabling people to escape from the tunnel. One aspect behind this stratification is, first, critical velocity, the ventilation velocity that will prevent smoke from moving upstream from the fire, as listed by Li et al. (1). When the ventilation velocity exceeds this critical velocity, the smoke layer downstream the fire is commonly unstratified, meaning that, prior the end of people evacuation, ventilation velocity should be maintained lower than this critical value. In such a situation, a back-layering layer will progress upstream of the fire (2), and its stratification is crucial.
In most published studies, the smoke layer characterisation is achieved by considering an empty tunnel, while vehicles should strongly influence the smoke layer propagation and behaviour (1).

The present paper focuses on the smoke stratification characterisation for such a back-layering layer in the presence of vehicles. This paper does not deal with the influence of the blockage ratio on the

critical velocity but focuses on evaluating the relevance of a common approach that consists in designing safety systems in tunnel without vehicles, including for congested tunnels. Experimental tests were conducted with /without upstream obstacles to characterise the smoke flow stratification and the influence of obstacles on the smoke flow stratification.

EXPERIMENTAL CONDITIONS

Experimental tunnel description

This experimental campaign was achieved in the Ineris fire gallery, a 50 m long tunnel with 3 m width and 3.35 m height at the maximum. This section was modified for the present test series to represent a cut and cover introducing a horizontal roof 1.85 m above ground leading to a 5.4 m² section. The typical modified section is described hereafter in Figure 1. The initial shape of the experimental tunnel is an arched but the horizontal roof, marked in grey in this picture, leads to a cut and cover like geometry.

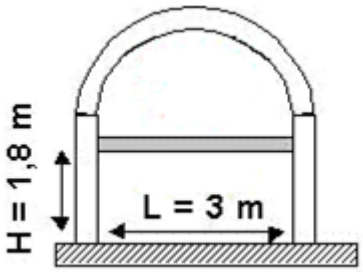

Figure 1: Typical section of the Ineris fire gallery.

Since one of the key aspects of stratification is the thermal interaction between the roof and smoke, specific attention was paid to the nature of the material used for this roof. For this test series, the roof was made of 0.112 m thick plywood with 0.038 m thick specific insulation mineral wool. The thermal characteristics of this wool were a density of 128 kg/m^3, 0,263 kJ/(kg.K) for the thermal capacity, and 0.05 W/(m.K) for the thermal conductivity.

During this campaign, vehicle mock-ups were introduced into the experimental tunnel to estimate their influence on the stratification. Those vehicle mock-ups were built respecting the global experiment scaling and distributed upstream of the fire (*Figure 2*). In this configuration, five cars were placed on the left lane, two cars and a truck were placed on the right lane, and the shape and size of the vehicle are also presented in this figure.

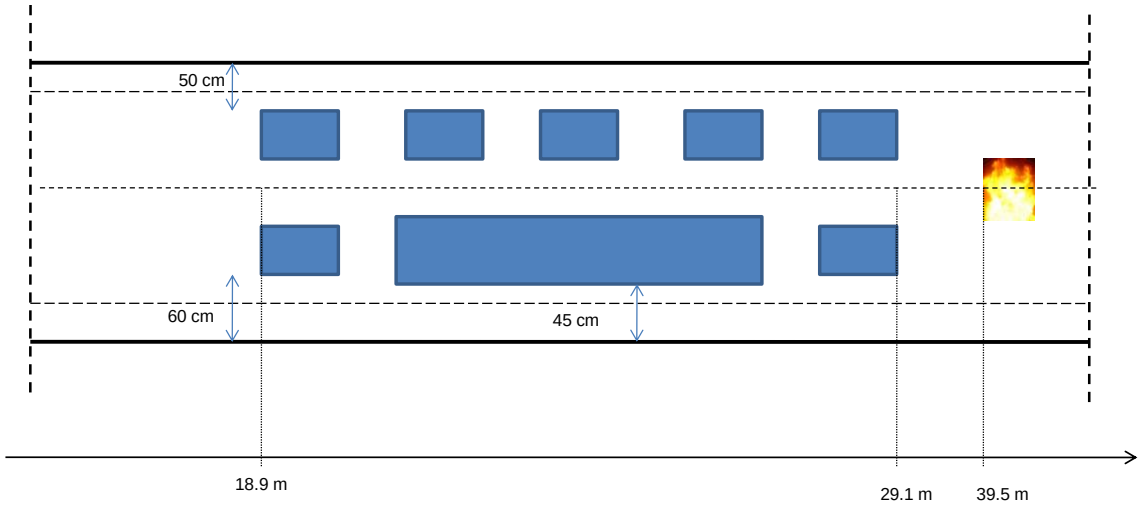

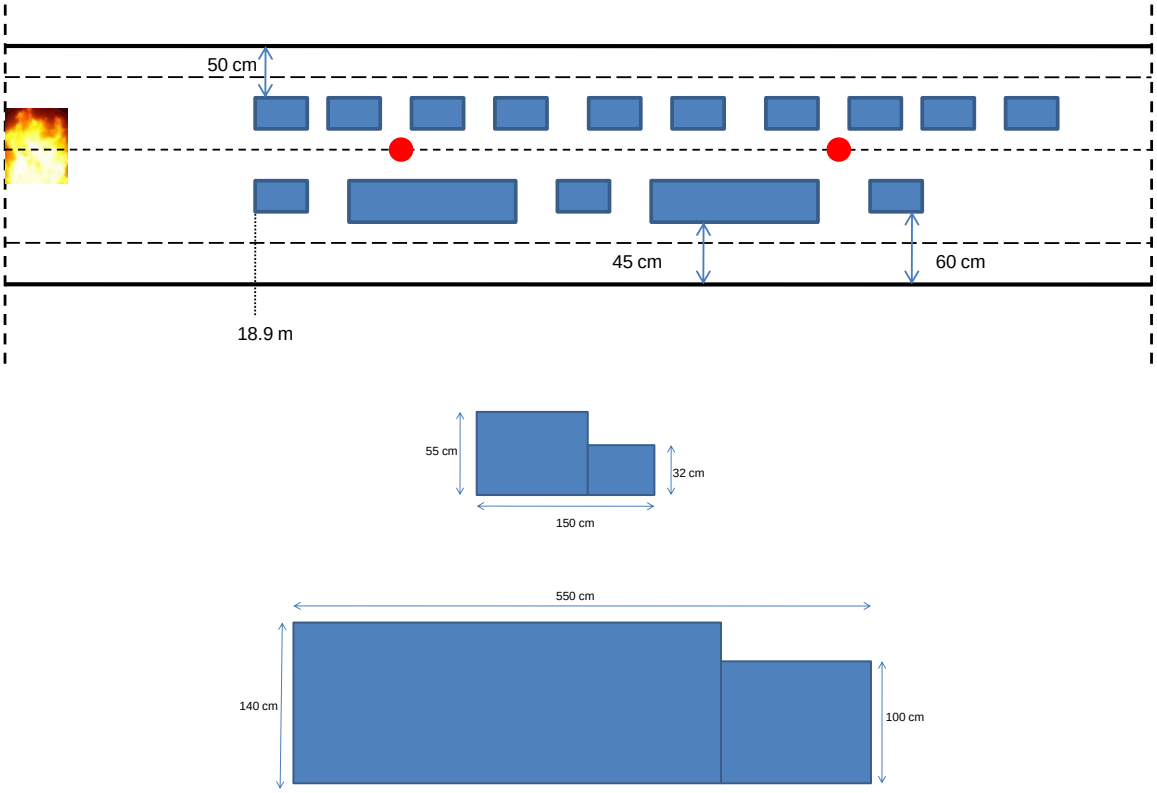

Figure 2: Vehicle distribution upstream of the fire in the experimental tunnel (top), vehicle distribution downstream of the fire in the experimental tunnel (middle) and vehicle size and shape (bottom).

Metrology

Key quantities to evaluate the vehicle impact on the back-layering behaviour and stratification are velocity, temperature, and, potentially, visibility. To get the maximum tunnel length for back-layering, the pool fire was placed, for this test series, 10 m before the end of the tunnel, i.e., the ventilation chimney, leaving 40 m for the smoke back-layering potential development.

Two sections were equipped with eight bidirectional velocity probes along the tunnel height for measurement. For temperature, a specific section was built, including 12 thermocouples distributed along the height of the section central line and four thermocouples on one section side*Figure 3*).

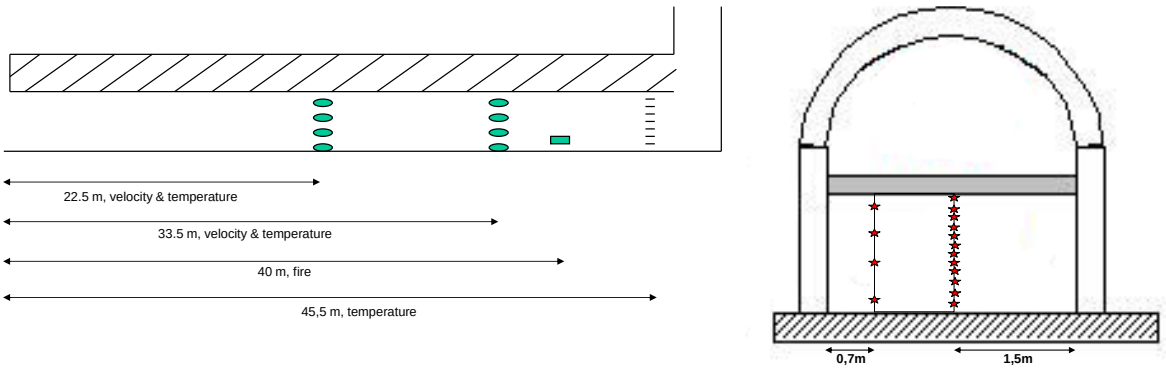

Figure 3: Position of the measurement sections (left) and thermocouple-specific section (right).

Several cameras were also distributed along the tunnel to estimate the local visibility in different situations.

Scaling rules

Scaling is key when dealing with experimentations since real-scale tests are highly expensive and do not enable repeatability. According to the experimental design characteristic dimension, the scaling factor, σ, ratio of the experimental characteristic length to the actual length, is about 1/3:

- 3 m width for the experiment leads to 9 m for the actual installation, i.e. a 2-lane tunnel;
- 1.8 m height induces a 5.4 m height, representing a standard cut and cover.

Scaling parameters in fluid mechanics means considering dimensionless numbers to create an experiment that respects those numbers. In that perspective, three main numbers should be considered: (1) the Froude number, Fr; the Reynolds number, Re; and the Prandtl number, Pr. The Froude number first represents the equilibrium between inertia and floatability and typically represents the stratification mechanism. The Reynolds number indicates the turbulence intensity through the ratio between inertia and viscosity effects. Last, the Prandtl number is the ratio between momentum and thermal diffusivity. Those numbers are respectively defined as follows:

$$Fr = \frac{U}{\sqrt{g.L}} \quad \text{Eq (1)}$$

$$Re = \frac{\rho.U.L}{\mu} \quad \text{Eq (2)}$$

$$Pr = \frac{\mu.C_p}{\lambda} \quad \text{Eq (3)}$$

These equations link the fluid velocity, U, the physical characteristic length, L, through fluid properties, viscosity, μ, thermal capacity, C_p, thermal conductivity, λ, density, ρ, and gravity, g. They let an intense difficulty when scaling a physical phenomenon appear, the impossibility of keeping all numbers constant since Fr and Re make the velocity and length vary differently. Respecting the Froude number induces a reciprocal variation of the Reynolds number.

According to the objective of the present experimental campaign, the Froude number was selected as a reference dimensionless number; this implies multiplying the Reynolds number by a coefficient $o\phi\ \sigma^{3/2}$. Not only should length be considered when scaling an experiment, but all other quantities should be connected to this scaling. Based on the Froude scaling, a coefficient σ on lengths implies a coefficient $\sigma^{1/2}$ for velocity. Using length and velocity, one can build the scaling factor for the volume flow rate, squared length, and section multiplied by a velocity, leading to $\sigma^{5/2}$ as a scale factor. Since the smoke emission rate depends on the fire heat release rate, this $\sigma^{5/2}$ scaling factor is also used for the fire intensity.

Design of a representative fire

Based on the above-mentioned scaling criteria, one should design the fire. Numerous publications in the literature provide typical heat release rate (HRR) curves for cars, from the Eureka test campaign at the beginning of the 2000s (3) to recent publications about electric vehicles (4)(5). According to the large variety of possible curves and peak HRR values, several standards and local regulations impose the representative HRR value, 5 to 10 MW for a car in the NFPA 502 (6), 2.5 to 5 MW for a vehicle in the AIPCR document (7) or 4 to 8 MW in the French CETu guide (8).

When scaling, a 5 MW fire with s=1/3 corresponds to a fire of about 350 kW. In the experiments, this fire was represented using a 0.25 m² heptane pool fire equipped with a cooling apparatus at the bottom of the pool to prevent any full boiling phenomena that induce an HRR peak at the end of the fire. The typical fire curve for the different tests is represented hereafter in *Figure 4*.

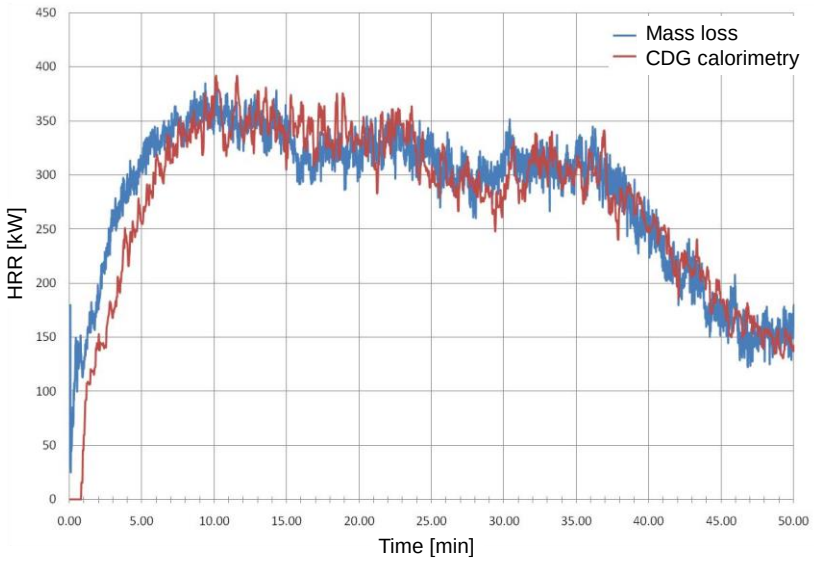

Figure 4: Typical fire curve obtained by mass loss and CDG calorimetry.

Fire repeatability is key since one of the present test series's objectives is comparing smoke layer behaviour in different situations. For the other tests made during this series, the peak HRR varies from 299 to 337 kW, with an average value of 317 kW and a standard deviation of 13 kW, representing about 4% of the average value. Analysing the temperature above the roof and the ventilation rate at the tunnel entrance also confirms the test repeatability.

Following Li et al (1), the critical velocity for this configuration, without restriction in the tunnel, can then be computed by:

$$u_c^* = \frac{u_c}{\sqrt{gh}} = \begin{cases} 0.81.\left(Q^*\varphi^{-\frac{1}{4}}\right)^{\frac{1}{3}} \text{ for } Q^*\varphi^{-\frac{1}{4}} \leq 0.15 \\ 0.43 \text{ if } Q^*\varphi^{-\frac{1}{4}} > 0.15 \end{cases} \qquad \text{Eq (4)}$$

In this relation, Q^* is the dimensionless heat release rate, based on the heat release rate, Q, and the fresh air density, ρ_0, and temperature, T_0, its thermal capacity, C_p, the gravity, g, and the tunnel height, h:

$$Q^* = \frac{Q}{\rho_0 C_p T_0 g^{1/2} h^{5/2}} \qquad \text{Eq (5)}$$

and ϕ is the tunnel aspect ratio, $\phi = w/h$, the ratio of the tunnel width, w, to its height, h.

The experimental configuration indicates a critical velocity of 1.3 m/s, corresponding to 3.9 m/s as critical velocity in actual conditions.

Since temperature is a key factor in stratification, the radiative fraction was also measured to provide a correct estimation of the influence of the fire and the hot gas layer. To meet this objective, assuming adiabatic walls and roof, the convective energy was measured by differentiating downstream, S_2, and upstream, S_1, energy by applying the thermodynamic first principle: $\Phi_{s1} + \Phi_{s2} + \Phi_\chi = 0$, where Φ is the energy flux in each section.

This method enables evaluating the radiative fraction to about 20% in the experimental conditions, *Figure 5*.

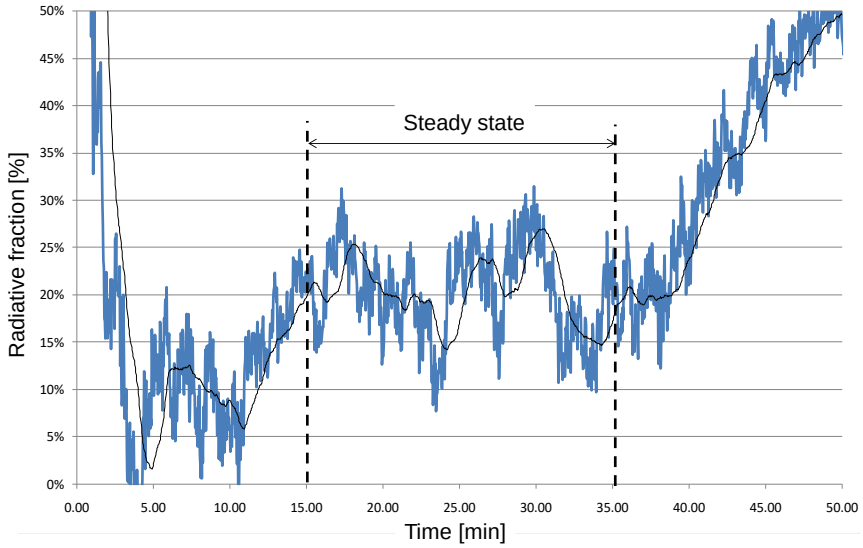

Figure 5: Radiative fraction measured during the experimental test series.

THEORETICAL DEFINITION OF STRATIFICATION PARAMETERS

Before going any further in presenting the experimental results, one should carefully define the stratification. Stratification should be connected to the potential consequences of fires on human beings; this includes temperature, toxic gas concentration, and visibility. Based on those three criteria, three stratification regimes can be considered. The velocity profile in the back-layering layer should also be used to evaluate the stratification. A theoretical representation of the different heights and values is given in *Figure 6*.

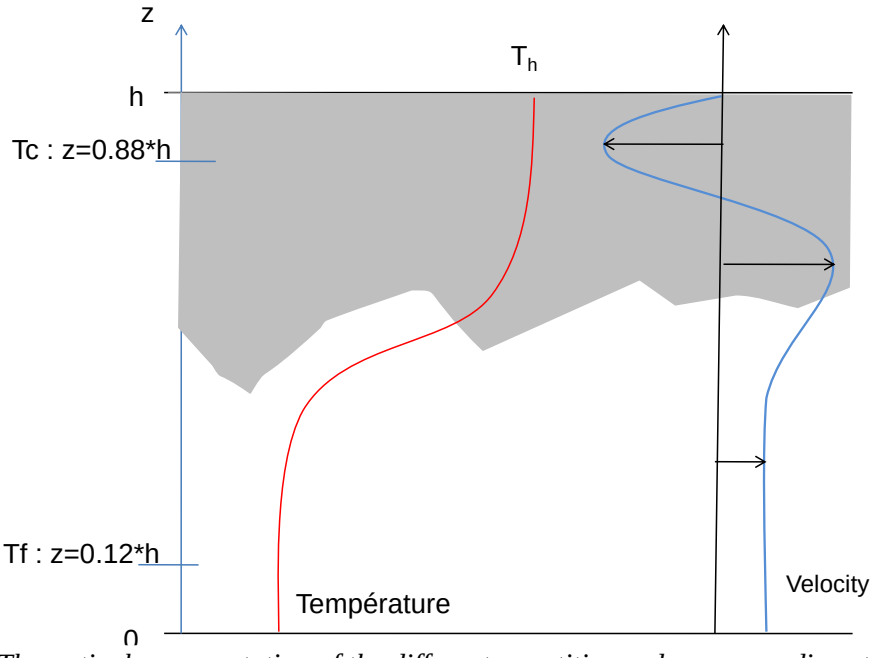

Figure 6: Theoretical representation of the different quantities and corresponding stratification.

Specific stratification criteria were previously published, for instance, by Newman (9)(10), who introduced two parameters to characterise the stratification:

$$\begin{cases} S_1 = \dfrac{T_c - T_f}{\Delta T_{avg}} \\ S_2 = \dfrac{T_c - T_f}{T_h - T_0} \end{cases} \quad \text{Eq (6)}$$

Those criteria are based on temperature distribution, using T_c, the temperature à 0.88H; T_f, the temperature at 0.12H; T_h, the temperature near the ceiling; and T0, the background temperature. ΔT_{avg} is the average temperature rise.

Newman shows that plotting those parameters in a graph leads to a specific pattern highlighting two regions (*Figure 7*). On this graph, region I corresponds to a stratified flow, and region II corresponds to an unstratified flow. Only thermal stratification is considered in this parameter.

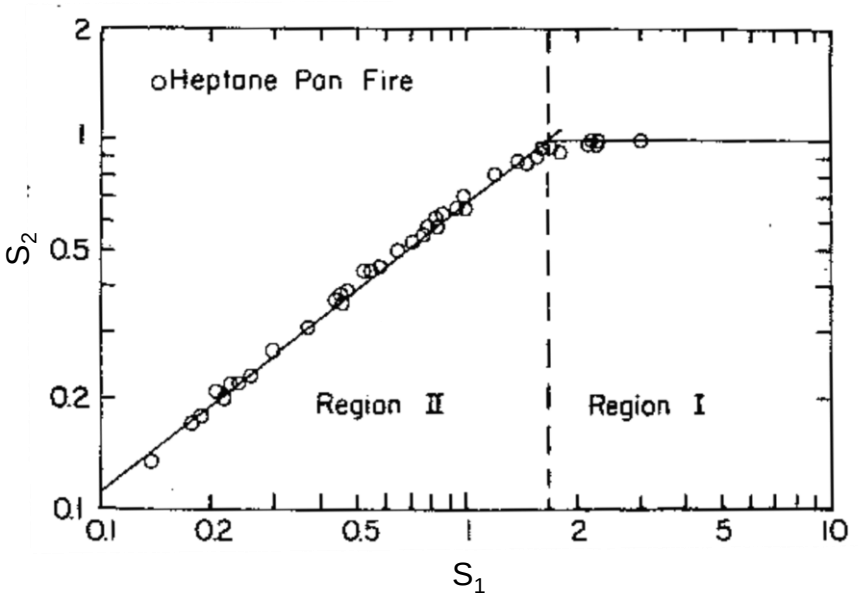

Figure 7: S_2 as a function of S_1 and corresponding regions, reproduced from (9).

The smoke thickness is another critical quantity when dealing with stratification and the definition of safe conditions for people under the stratified layer. Several methods were published to determine this thickness. According to the available data, the simple method published by Cooper et al. (11) proposes to define the interface height as the position where N% of the roof temperature increases the temperature; this means that the temperature at the interface height, h_{int}, is:

$$T_{h_{int}} = T_0 + N\% * T_{roof} \quad \text{Eq (7)}$$

Where T_{roof} is the smoke temperature near the roof, according to the literature, N should be between 10 and 20%.

EXPERIMENTAL RESULTS

Reference undisturbed back-layering layer

The two first tests were achieved without any obstacle along the back-layering layer development zone to obtain its reference behaviour. Once more, the objective of the two tests was to demonstrate the test's repeatability.

Ventilation conditions

A key parameter that influences the back-layering development is the ventilation velocity. For those two tests, the ventilation characteristic velocity, i.e., the velocity corresponding to the volumetric flow rate

with the tunnel section, was 1.06 and 1.05 m/s, respectively 1.84 and 1.85 m/s in actual dimensions. Those values remain lower than the critical velocity estimated for those conditions, meaning that a back-layering layer is expected in those conditions.

Temperature distribution

Since stratification is mainly defined according to the temperature distribution, temperature measurement in the back-layering is a key issue. Figure 8 presents velocity profiles at different distances upstream of the fire. According to these curves, the smoke layer seems stratified. This is confirmed by the evaluation of the Newmann parameters S_1, which is about 3.5 for this configuration.

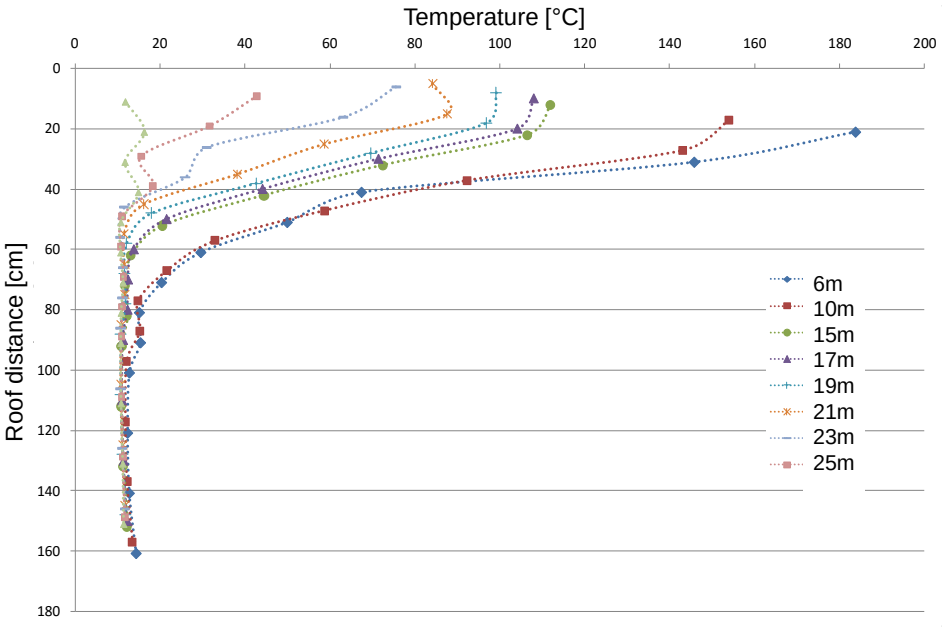

Figure 8: Temperature profile at different positions upstream of the fire.

Velocity distribution in the back-layering layer

Another key physical quantity in the back-layering layer is the velocity since the velocity direction, together with the velocity gradient, gives an interesting visualisation of the flow (*Figure 9*).

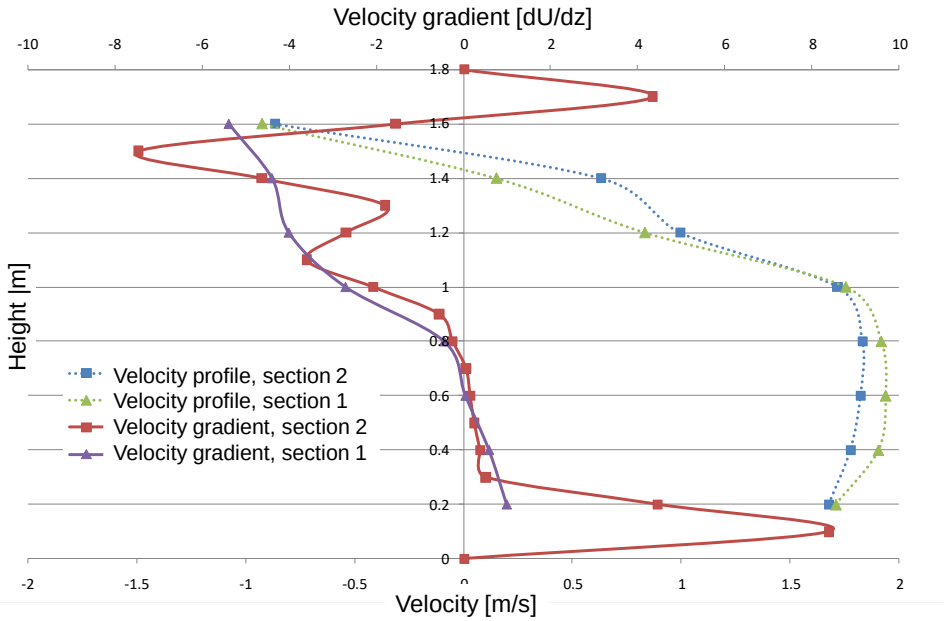

Figure 9: Velocity and velocity gradient profile on the two velocity measurement sections.

For measurement section 2, the closest to the fire, the profiles enable representing each flow zone in the section (*Figure 10*). For section 1, the tendencies are quite similar, but the distinction is less clear.

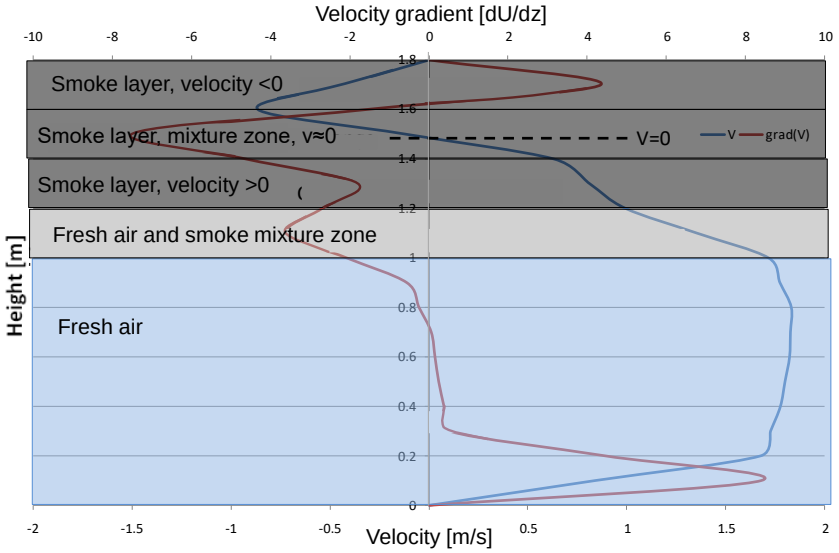

Figure 10: Flow zone in the back-layering layer for velocity measurement section 2.

Back-layering layer thickness

Based on the Cooper method presented previously, the back-layering layer thickness is estimated to be 0.65 cm at measurement section 2, 6.5 m upstream of the fire, and 0.55 m at measurement section 1, 17.5 m upstream of the fire.

Vehicle influence on the back-layering layer

Maintaining a stratified layer is an objective when vehicles are trapped in the tunnel in case of fire; the ventilation velocity is then fixed, in actual situation, to less than 2 m/s to make this stratification possible and allow the opportunity for people to escape. The previously described vehicle distribution was introduced into the tunnel to evaluate vehicle influence on the back-layering stratification quality.

Vehicle influence on the velocity profile

Since vehicles introduce a blockage ratio, they strongly influence the airflow, *Figure 11*.

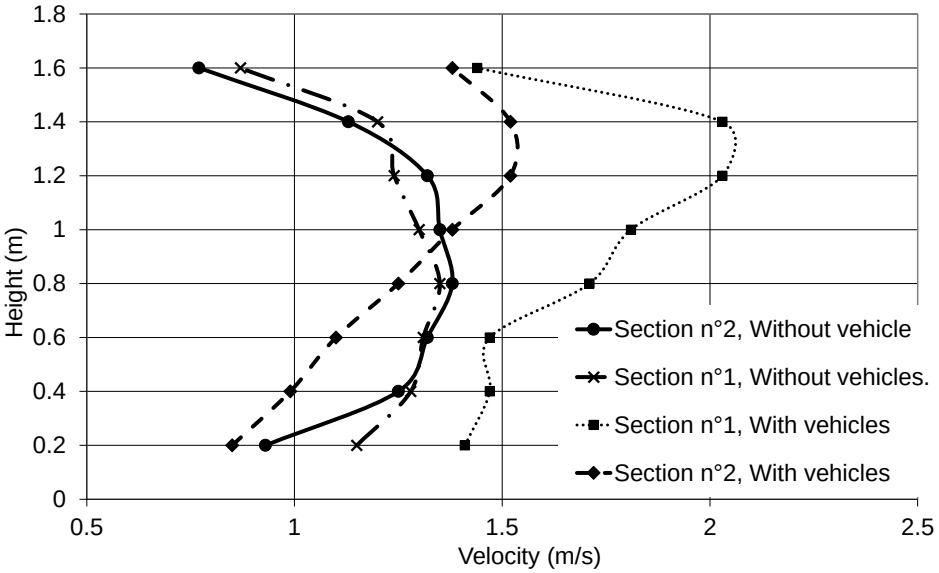

Figure 11: Velocity profiles with and without vehicles.

The typical blockage ratio, ϕ, is 53% in the section where both PL and VL are present, meaning that more than half of the tunnel section is occupied by a vehicle. This results in a strong velocity rise in such a section, as illustrated on this curve. Applying the formulae proposed by Li (1) for critical velocity in presence of blockage, $U_{c,blockage}$:

$$U_{c,blockage} = U_c(1 - 0.88.\phi) \qquad \text{Eq (8)}$$

For the present mock-up configuration, this leads to a $U_{c,blockage}$ of 0.7 m/s, a value in accordance with the observed phenomena since the layer is blocked, as expected, by vehicles.

A strong influence on the back-layering

Such a velocity increase directly reduces the back-layering length since the substantial velocity induced by the truck blockage counterbalances the back-layering energy. This result also illustrates trucks' strong influence on the development of the smoke layer.

Figure 12 plots the vertical temperature profiles 6 and 10 m upstream *Figure 12* of the fire. Before discussing stratification criteria, it should be noted that the temperature near the ground is increased for the configuration with vehicles, showing an increase in the fresh air and smoke mixture.

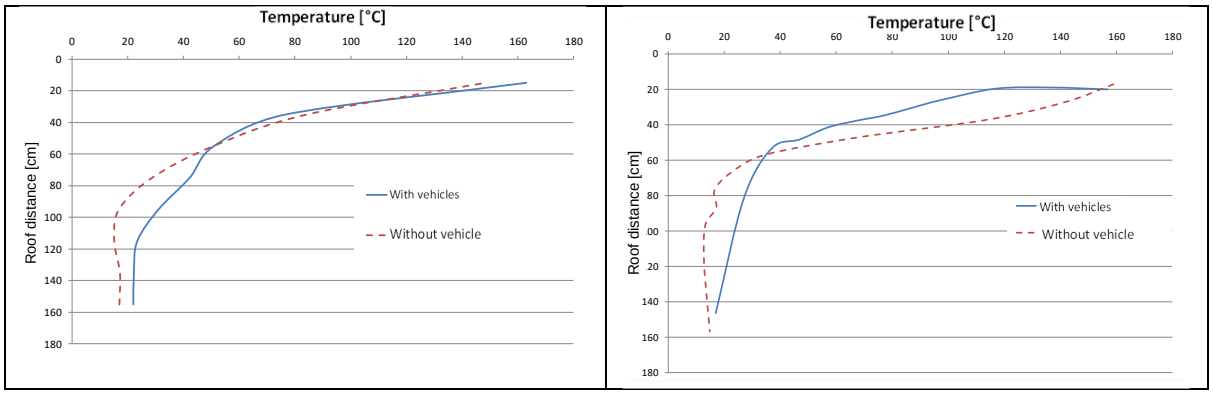

Figure 12: Temperature vertical profiles 6 m (left) and 10 m (right) from the fire.

When vehicles are introduced, the *S1* parameter becomes about 4, meaning a still stratified layer. Both situations, with and without obstacles, remain in the same region of the Newman graph representing stratification criteria, meaning the same stratification stability when dealing with temperature. Furthermore, while the interface between fresh air and smoke is more diffuse, based on the Cooper approach, the layer thickness is not significantly changed when vehicles are in the tunnel.

Those profiles show that, 6 m upstream of the fire, where there is no vehicle, the smoke layer's temperature distribution is quite similar. The temperature in the fresh air zone, where people potentially are, is slightly increased. 10 m upstream, the fire influence is more significant, the back-layering thickness seems reduced, and smoke temperatures are lower due to the strong influence of local velocities induced by the vehicle blockage. Furthermore, temperatures in the fresh air zone are also increased. At this same position, 10 m upstream of the fire, the velocity profile remains slightly modified (*Figure 13*).

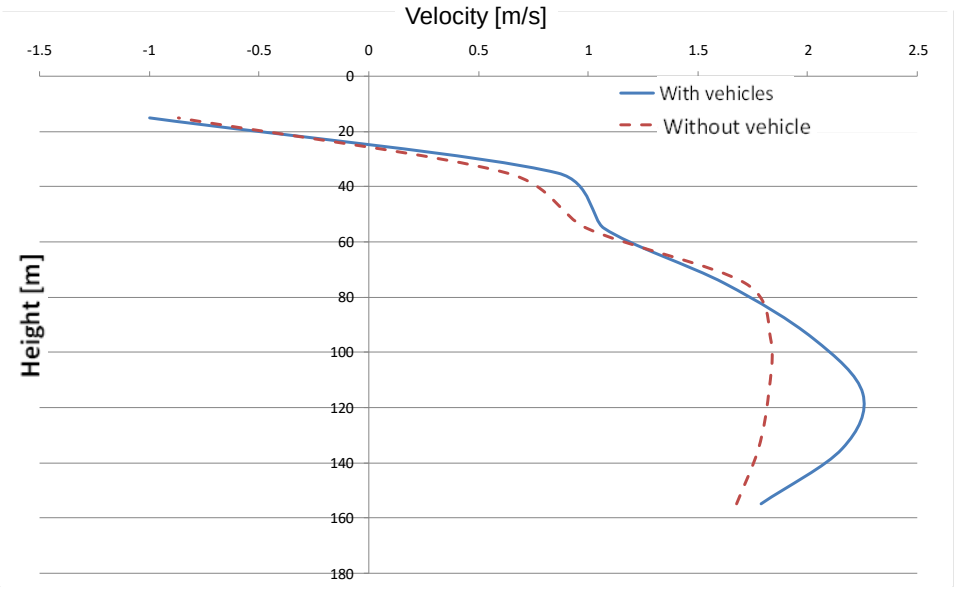

Figure 13: velocity profile 10 m upstream of the fire with and without vehicles.

While temperature-based stratification criteria do not strongly highlight a stratification loss, analysing the visibility conditions using cameras leads to a different conclusion. Those cameras show that visibility significantly decreases with the vehicle upstream of the fire. Since a low fraction of soot may lead to a substantial visibility decrease, one should consider building criteria based on a visibility-representative quantity.

Smoke layer downstream the fire

A similar analysis was performed focused on the layer downstream of the fire. For this situation, the measurement sections are located respectively at 12.5 m downstream of the fire for section 1 and 22.5 m for section 2, corresponding to actual distances of 37.5 m and 67.5 m applying the scaling factor. The analysis achieved for this configuration is identical to the one detailed for the upstream layer with a configuration without obstacles and a similar configuration but adding the vehicles distributed as detailed previously, keeping in mind that the fire is strongly repeatable, enabling comparison between the two situations.

As shown for the back-layering layer, vehicles strongly influence the velocity profile, with an identified recirculation for section 2 (Figure 14). Those velocity profiles show a velocity increase due to the section restriction and, potentially, a turbulence increase due to the modification of the flow's nature, typically with the recirculation.

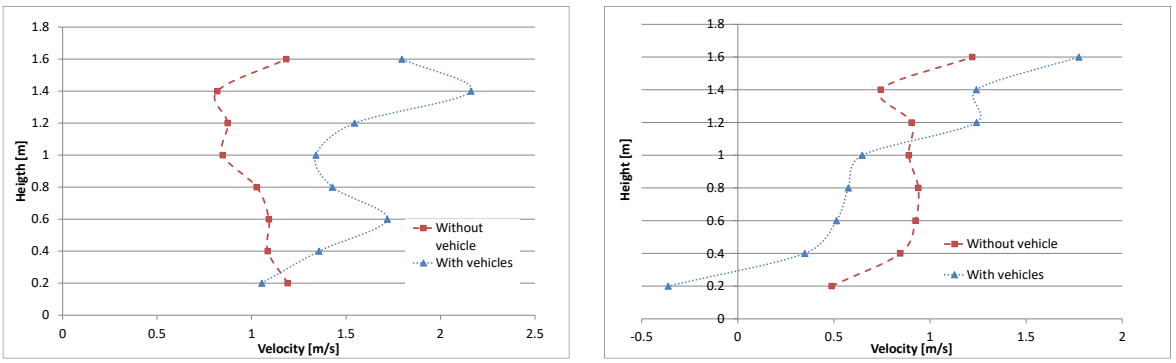

Figure 14: Velocity profile in the measurement sections, with and without vehicles.

However, the velocity observations are not confirmed when analysing temperature profiles, *Figure 15*.

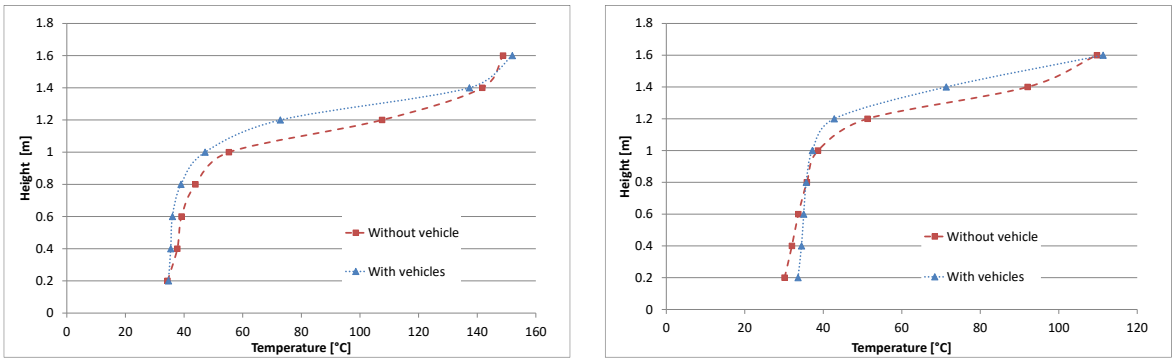

Figure 15: Temperature profile in the two measurement sections, section 1 on the left and section 2 on the right.

The stratification seems only disturbed downstream of the vehicles, 35.5 m after the fire (*Figure 16*). For this configuration, the temperature near the ground is also increased; this influence represents the increase of the mixture between fresh air and smoke.

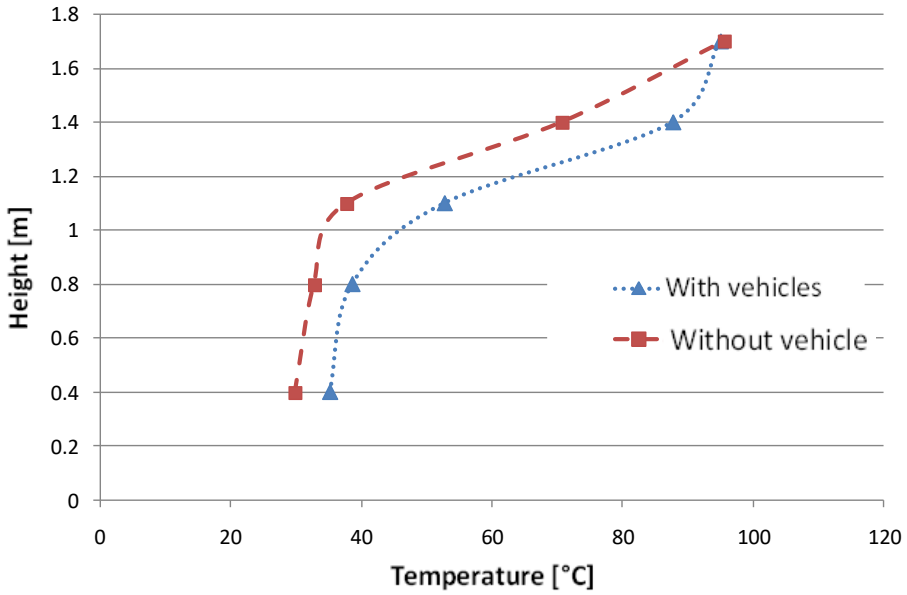

Figure 16: Temperature profile 35.5 m downstream of the fire.

This result shows that, close to the fire, the strong floatability effect due to the high temperature is not counterbalanced by the flow perturbation. The flow perturbation becomes significant on the stratification when roof temperature is reduced, limiting the floatability effect.

The Richardson number, representing the buoyancy effect on the flow shear, could be used to quantify this influence. The Richardson number, *Ri*, can be expressed, using the tunnel height, *h*, as the reference length, by:

$$Ri = g.\frac{(\rho_0 - \rho_{T_{roof}})}{\rho_{T_{roof}}}\frac{h}{V^2} \qquad \text{Eq (9)}$$

When Ri is more significant than 1, the flow is stratified; when it becomes lower than 1, it tends to be homogeneous. Considering the representative velocity is the ventilation characteristic velocity, which remains identical in each section, the evolution of the *Ri* could be analysed along the tunnel. It shows that it decreases from 10 close to the fire to about 5 in the last measurement section, translating a tendency to stratification loss. Using the maximum velocity as reference velocity for stratification evaluation through the *Ri* number leads to a value close to 1 in the last section, confirming this analysis.

CONCLUSIONS

This paper presents an experimental analysis of smoke layer characteristics in congested longitudinally ventilated tunnels. The main objective is to evaluate the influence of vehicles on the smoke stratification quality for both the upstream and downstream layers.

This experimental analysis is performed on a third-scale tunnel representative of a common cut and cover configuration, and all physical representative quantities are scaled using this factor. Comparisons with and without vehicles are performed using an identical configuration with the same scaled fire placed at the same position inside the tunnel after having demonstrated the fire reproducibility in terms of the heat release rate curve.

For both configurations, the upstream and downstream smoke layers, strong stratification of the smoke layer was observed through the temperature and velocity curves and thanks to specific criteria, such as the Newman parameter, which clearly shows a stratified regime.

When introducing vehicles, the first observation is the influence of the vehicle position on the back-layering development; local velocity increase stops the back-layering development. The characteristics of the residual shortened back-layering layer are slightly modified by vehicles; the temperature profiles remain similar, and the Newman stratification criteria are also conserved. Furthermore, the back-layering thermal thickness is also conserved, while the interface between fresh air and smoke is more diffusive. It was, however, observed that, while the thermal stratification seems unchanged, the visibility in the lower part of the tunnel is reduced downstream of the vehicle due to some mixture induced between smoke and fresh air in acceleration zones. This experimental result clearly shows that evaluating stratification only based on temperature values is not sufficient. Furthermore, in some situations, the temperature in the lower part of the tunnel is increased due to the rise of turbulent mixing, but this is not directly taken into account in some stratification criteria.

Conclusions are similar for the downstream smoke layer with few changes in the smoke layer characteristics, while the floatability effect remains important enough, i.e. close to the fire where the temperature above the roof is high. When the roof temperature decreases, leading to less floatability influence, the vehicle influence becomes significant. In actual configuration, stratification might be lost earlier with a vehicle than in an empty tunnel.

Those test series confirm the importance of considering vehicles when designing a stratification-based safety concept.

REFERENCES

1. Li, Y.Z. and Ingason, H., Influence of upstream blockage on smoke control in tunnel fires, Fire Safety Journal, vol 147 (2024).
2. Thomas, P., The movement of smoke in horizontal passages against an air flow, Fire Research Note (1968).
3. Ingason, H, Li, Y.Z. and Lönnermark, Tunnel fire Dynamics, Springer (2015).
4. Lecocq, A. et al., Comparisons of fire consequences of an electrical vehicle and an internal combustion engine vehicle, in: Second International Conference on Fire in Vehicles (2012).
5. Lam, C., MacNeil, D., Kroeker, R., Lougheed, G., and Lalime, G., Full-scale fire testing of electric and internal combustion engine vehicles, in: Fourth International Conference on Fire in Vehicles (2016).
6. NFPA 502 – Standard for road tunnels, Bridges and Other Limited Access highways, Edition 2008.
7. Fire and smoke control in road tunnels, Comité AIPCR des tunnels routiers (C5) (1999).
8. Guide to road tunnel safety documentation, booklet 4, Specific hazard investigations (2003).

9. Newman, J., Experimental evaluation of Fire-Induced stratification, Combustion and Flame 57:33 (1984).
10. Newman, J. and Tewarson, A., Flame propagation in Ducts; Combustion and Flame 51:347 (1983).
11. Cooper, L., Harkleroad, M., Quintiere, J. and Rinkinen, W., An experimental study of upper hot layer stratification in full-scale multiroom scenarios, Journal of Heat Transfer 104:741-749 (1982).

Laboratory Scale Tests Investigating Fixed Fire Fighting Systems and Emergency Ventilation Interaction for Highway Tunnels

Matt Bilson[1], Hasan Raza[1], Alexander Schmidt[2] & Max Lakkonen[2]
[1]WSP USA
One Penn Plaza, New York, NY, 10119, USA
E-mail: matt.bilson@wsp.com
[2]IFAB
Pankstraße 8A, 13127 Berlin, Germany

ABSTRACT

Laboratory scale testing was conducted as part of a United States Federal Highway Administration (FHWA) research program. The objective of the testing was to support the research project aiming to investigate the integration of highway tunnel emergency ventilation systems (EVS) with an installed fixed fire fighting system (FFFS). Laboratory scale tests were performed via the Institute for Applied Fire Safety Research (IFAB) in Germany. The tests used a custom made model tunnel (approximately 1:4 scale relative to similar full-size) with longitudinal ventilation. Measurements were recorded including velocity, temperature, pressure, humidity, and surface temperature. Video footage was taken as well. This paper summarizes the tests and some of the results from the published research report.

KEYWORD: Fixed water-based fire-fighting system, FFFS, deluge, water mist, tunnel, tunnel ventilation, CFD, FDS, testing, nozzle characterization

INTRODUCTION

The United States Federal Highway Administration (FHWA) has recently published a research project, conducted from 2018 to 2024, that looked into the use of fixed fire fighting systems (FFFS) in road tunnels. The objective of this research was to identify industry's current ability to consider the integration of highway tunnel emergency ventilation systems (EVS) with the installed fixed fire fighting system, and to then develop a set of suggested practices on the integration of FFFS and the EVS. The technical approach to this research project was divided into the following five distinct tasks: 1) Literature survey; 2) Industry workshop; 3) Computer modelling research; 4) Laboratory scale testing; and, 5) Research report with suggested practices. The research has been completed and reports have been published [1-5]. The present paper focuses on the laboratory scale testing.

The tests were performed to help better understand the interaction between a longitudinal EVS and the FFFS. Principal research hypotheses investigated included the following:

- That FFFS and EVS can be integrated and EVS capacity optimized because of the cooling effects of the FFFS water spray.
- That computational fluid dynamics (CFD) can be used to predict FFFS and EVS interaction for design integration.

As a result of these hypotheses, the tests were principally structured toward the goal of verifying critical/confinement velocity with an FFFS operating, and to provide data for computational fluid dynamics (CFD) model validation.

The following smoke management terminology was used in the research project:

- Backlayering is the movement of smoke and hot gasses counter to the direction of ventilation airflow.
- Critical velocity is the minimum steady-state velocity of the ventilation airflow moving toward the fire, within a tunnel or passageway, to prevent backlayering at the fire site.
- Confinement velocity is used to describe the steady-state velocity of the ventilation airflow moving toward the fire that is of a magnitude large enough to stop smoke movement upstream of the fire but not to prevent backlayering.

The tunnel was built to the laboratory scale, about 1:4 relative to full scale. For the laboratory tests the tunnel was 2.5 m wide and 1.25 m high. In the fire tests conducted the fire heat release rate (FHRR) was expected to be 0.63 MW or 1.3 MW based on the pool configuration, and the inlet velocity was varied to examine the effect of the FFFS on longitudinal smoke management. Eight distinct fire tests were recorded, and three nozzles were tested and characterised. The paper is structured to report on test description and procedures, test results, including water spray parameters, fire heat release rate, temperature, critical/confinement velocity observations, and pressure change due to the FFFS.

TEST DESCRIPTION AND PROCEDURES

The tests were conducted by the Institute for Applied Fire Safety Research (IFAB) in Germany. IFAB is an accredited fire test laboratory recognized by Deutsche Akkreditierungsstelle (DAkkS), Germany's national accreditation body, in accordance with DIN EN ISO/IEC 17025:2018-03. IFAB's accreditation covers the measurement of gas concentrations, temperatures, and pressures, which enables it to assess the effectiveness of water-based fire-fighting systems through fire tests for tunnel and transport infrastructure systems [4].

Test Tunnel

The test tunnel had dimensions of 2.5 m width, 1.25 m height, and 12.0 m length. The scale used was approximately 1 in 4, to give a full-scale equivalent of 10 m width and 5 m height, which is on the same order as a typical two-lane highway tunnel. Being limited somewhat by the test building site dimensions, the tunnel total length was 15.6 m. To limit outside wind influence on the air flow within the tunnel a porous plate was added at the breakthrough to the outer wall of the building. The tunnel was set up using a temporary construction comprised of dry wall with non-combustible and water resistant aquapanel boards, which were replaceable in case of fire damage during the tests. Figure 1, Figure 2, and Figure 3 show visual representations of the test tunnel.

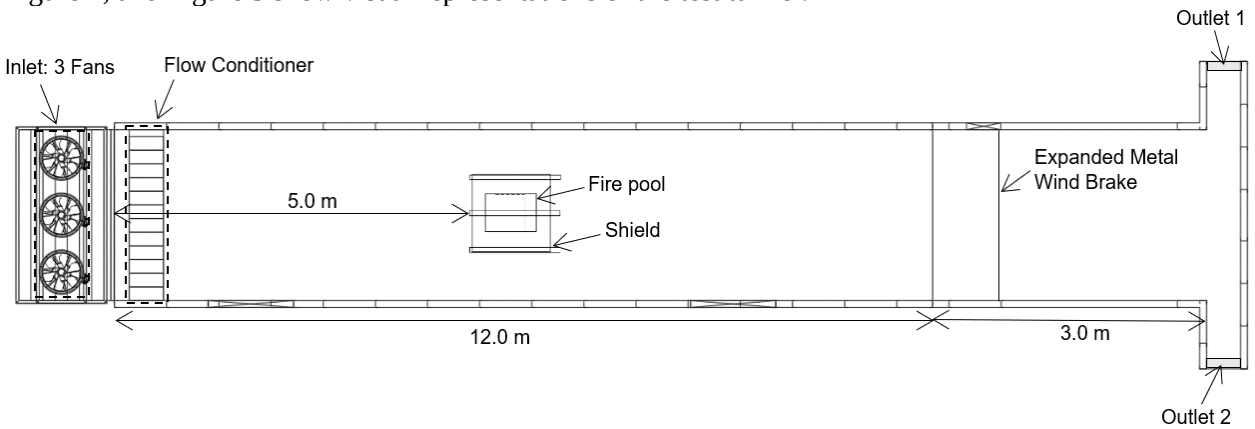

Figure 1 Test tunnel plan view.

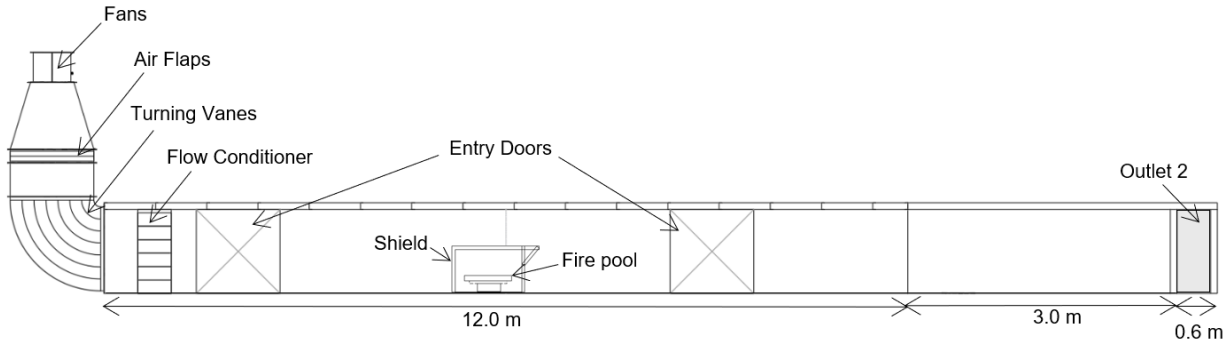

Figure 2 Test tunnel side view.

Figure 3 Constructed test tunnel.

Ventilation

The ventilation system was set up to supply an adjustable longitudinal air flow through the tunnel to investigate critical/confinement velocity and backlayering. Three fans were used to supply air (make and model type Ruck AL-560-D4-01) with a capacity of up to 34,000 m^3/h. The fans were operated on a variable frequency drive to enable adjustment of the velocity. Fresh air from outside was directed into the tunnel via a duct with a 90-degree bend with turning vanes followed by a flow conditioner. Figure 4 shows the sketch of the ventilation system.

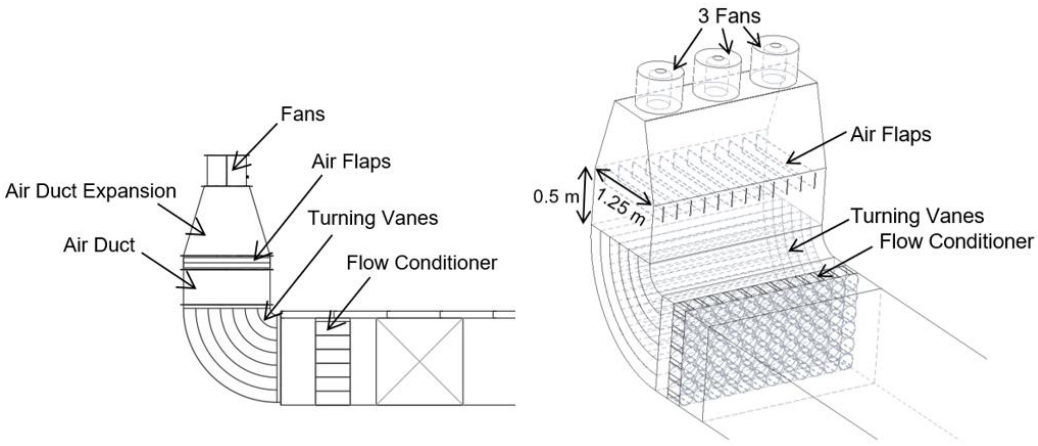

Figure 4 Sketch of the ventilation system.

Fire Loads

Fires were generated as class B fires using a pan of n-heptane or diesel. The fire loads were designed to generate an approximate fire heat release rate (FHRR) of 0.63 MW or 1.3 MW, depending on the size of the fire pan used. The fire load was shielded to prevent direct contact with water from the FFFS, with the goal of keeping the FHRR unaffected by the FFFS so that the impact of the FFFS on the critical/confinement velocity could be observed. Figure 5 shows the pool dimensions and setup from both the side and the top view, and Table 2 provides some quantitative information. The shield had a cross sectional dimension facing into the airflow of 1100 mm wide and 680 mm tall. To limit the direct impact of water spray on the fire, the shield was completely open at both sides, and closed at the front, top and rear.

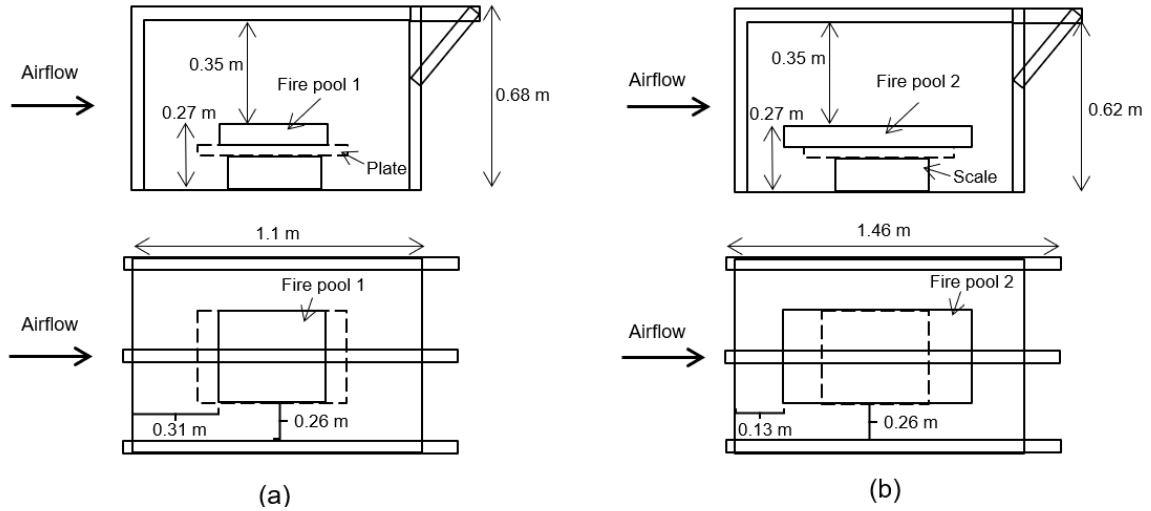

Figure 5 Fire pool dimensions and shields.

Table 2 Parameters of class B fire loads.

Parameter	Diesel	Heptane
Burning rate (kg/m^2/s)	0.045	0.101
Heat of combustion (MJ/kg)	44.4	44.6
Kβ (m^{-1})	2.1	1.1
D (m)	0.61	0.79
Flash point (^{o}C)	56	-7
Pool 1	0.49 m long, 0.59 m wide, and 0.10 m high, area of 0.29 m^2 for a nominal FHRR of 0.42 MW	As per diesel, but FHRR estimated to be 0.63 MW
Pool 2	0.84 m long, 0.59 m wide, and 0.10 m high, area of 0.50 m^2 for a nominal FHRR of 0.80 MW	As per diesel, but FHRR estimated to be 1.3 MW

Fixed Fire Fighting System and Water Spary Parameters

For the fire tests, nozzles were selected for characterization for laboratory testing based on the following factors:

- Application in U.S. tunnels, a nozzle that is approved and listed for the application per NFPA 13, where possible.
- Availability of sprinkler K-factor and spray pattern data.
- Availability of droplet size distribution or similarity of the nozzle to others where size distribution is available.
- Laboratory-scale suitability versus full-scale nozzle availability, noting that one key aspect of the testing was to compare laboratory-scale with full-scale nozzles (i.e. trying to balance a

nozzle that is well-suited for laboratory-scale tests versus a goal of the program to use nozzles that might be selected in a full-scale application).

Based on these factors, three different nozzles were used for the testing:

- Viking system (Nozzle A – large droplet size, typical nozzle listed for use in the United States).
- Lechler system (Nozzle B – smaller droplet size relative to Nozzle A, better suited to laboratory-scale).
- Fogtec system (Nozzle C – high pressure water mist).

The choice of nozzles was based on balancing the goals to use a nozzle listed for use in the United States and to use a nozzle that could work well at the laboratory scale. Nozzle A was used because it is a nozzle listed for use in the United States to NFPA 13 (i.e., a fire sprinkler), however, the flow rate from Nozzle A was large relative to the test scale, and the spray pattern was very wide. Therefore, Nozzle B was used because it had a smaller flow rate, spray pattern diameter and droplet size relative to Nozzle A, thus making it better suited to the laboratory scale test. Nozzle C was tested as it provided an interesting data point relative to the other two nozzles since it used a fine water droplet (mist). Figure 6, Figure 7 and Figure 8 show nozzle layouts, and Table 3 summarizes the nozzle parameters.

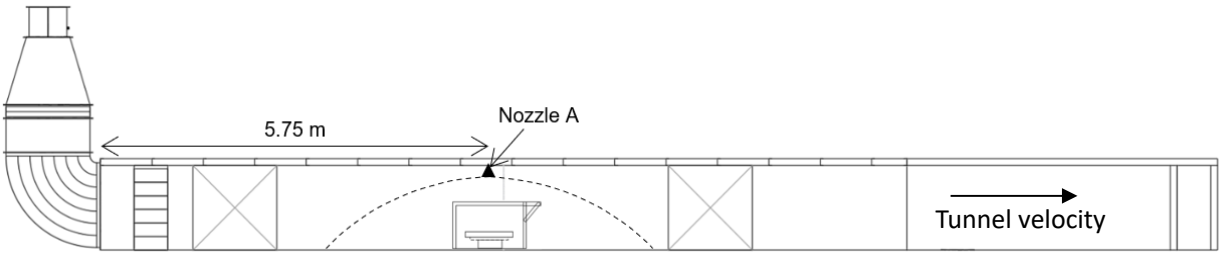

Figure 6 Nozzle A layout.

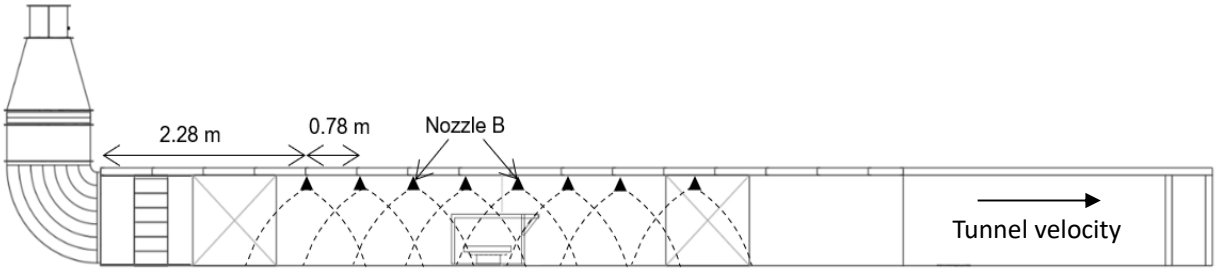

Figure 7 Nozzle B layout.

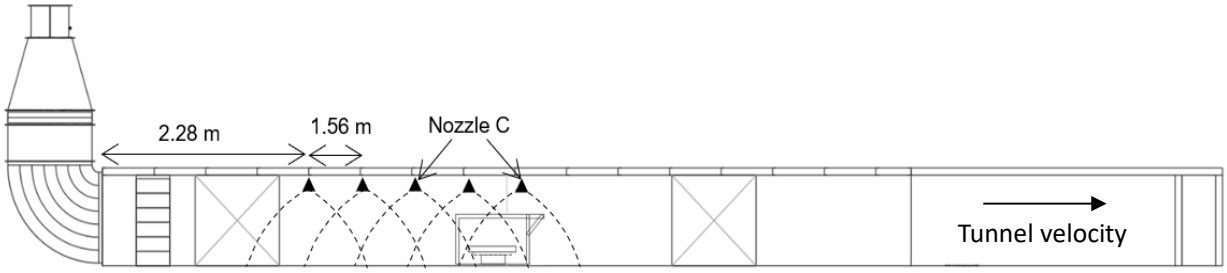

Figure 8 Nozzle C layout.

Measurements
The following parameters were measured and recorded during all tests:

- The gas temperature at the ceiling on the tunnel centerline (very near to the ceiling, typically within 50 mm) and at varying longitudinal locations and vertical heights.
- Air velocity at selected locations upstream and downstream of the fire.
- Adiabatic surface temperature (measured via a plate thermometer).
- Fire heat release rate via mass loss rate of the fire load (fuel), and from combustion product gas composition measurements (measurements of oxygen, carbon monoxide and carbon dioxide concentration at P115).
- Water pressure in the FFFS, which was used in conjunction with the manufacturer K factor to obtain the nozzle flow rate. The nozzle K factors were assumed to be reliable given they were per the nozzle specifications used for subsequent design development.
- Static pressure at selected locations along the tunnel. Pressure was recorded at one location (top corner of the tunnel) and as such, results need to be interpreted carefully as these measurements may not have been representative of an average over the cross section.
- Relative humidity upstream and downstream of the fire.
- Visual recording.

Table 3 FFFS parameters.

System parameter	Nozzle A	Nozzle B	Nozzle C
Nozzle type	Viking VK329, pendent	Lechler 490.648	Fogtec
Number of nozzle rows	1	2	1
Number of nozzles per row	1	4	5
Total number of nozzles	1	8	5
Nozzle pressure	1.5 bar	3.0 bar	90 bars
K-factor (L/min/bar$^{0.5}$)	40.83	2.83	0.48
Flow rate per nozzle	49.9 L/min	4.9 L/min	4.6 L/min
Total system flow rate	49.9 L/min	39.2 L/min	23 L/min
Water application rate (flow per area)	3.4 mm/min	2.0 mm/min	1.2 mm/min
Water application area (length is estimated from nozzle spray diameter) used to calculate water application rate	2.5 m (wide) by 5.8 m (long)	2.5 m (wide) by 7.68 m (long)	2.5 m (wide) by 7.74 m (long)
Spray radius at 1.25 m below nozzle (m) – approximate	2.9 m	1.5 m	1.5 m
Droplet diameter (Dv0.5)	1.12 mm	0.28 mm	0.13 mm
Nozzle spacing within rows	N/A (single nozzle)	1.56 m	1.56 m
Spacing between rows	N/A (single nozzle)	1.25 m	N/A (single row)
Distance to the nearest side wall	1.25 m	0.625 m	1.25 m
Orientation	Single nozzle above fire pool at the tunnel centerline	Four nozzles alternating per row above the fire pool	Five nozzles above the fire pool at the tunnel centerline

TEST SUMMARY

Results from testing included fire heat release rate (measured via fuel mass loss rate and oxygen consumption calorimetry), smoke spread extent (measured via temperature near the tunnel ceiling),

visualization of smoke spread, air velocity, and temperature. Other measurements taken included adiabatic surface temperature, static pressure, and humidity. Tests were performed under test series categories with mutliple tests sometimes performed. Each individual test was given its own numerical identification. Table 4 provides more details of the main tests. The categories of tests conducted were as follows:

- Test 1: Airflow only tests to attempt to establish pressure loss in the tunnel due to wall friction and FFFS pipework.
- Test 2: Not used.
- Test 3: Free burn tests with longitudinal ventilation; goal was to establish critical/confinement velocity with no FFFS operating.
- Test 4: As per Test 3 but with FFFS operating using Nozzle A; data point for critical/confinement velocity computation.
- Test 5: As per test 3, but with FFFS operating using Nozzle B; data point for critical/confinement velocity computation.
- Test 6: Laser Doppler analyses to determine nozzle spray pattern and droplet sizes (for Nozzles A, B and C).
- Test 7: As per test 3, but with FFFS operating using Nozzle C; data point for critical/confinement velocity computation.

Table 4 Fire test summary.

Series	Test number	Info	FHRR (MW) (expected and approximate observed in text in parentheses)	Inlet v (m/s)	Nozzle and water application rate (mm/min)
3A	IFAB22	Free burn, diesel pool fire	0.63 MW (0.9 MW)	1.2 m/s	None
3B	IFAB24	Free burn, diesel pool fire	1.3 MW (1.6 MW)	1.3 m/s	None
4A	IFAB11 IFAB10	Tests with FFFS, diesel pool fire	0.63 MW (0.5 MW)	1.1 m/s	A, 3.4 mm/min
4B	IFAB19	Tests with FFFS, diesel pool fire	1.3 MW (1.5 MW)	1.2 m/s	A, 3.4 mm/min
5A	IFAB13	Tests with FFFS, diesel pool fire	0.63 MW (0.4 MW)	1.0 m/s	B, 2.0 mm/min
5B	IFAB15	Tests with FFFS, diesel pool fire	1.3 MW (1.8 MW)	1.3 m/s	B, 2.0 mm/min
7A	IFAB21	High pressure water mist, diesel pool fire	0.63 MW (0.6 MW)	1.1 m/s	C, 1.4 mm/min
7B	IFAB20	High pressure water mist, diesel pool fire	1.3 MW (1.9 MW)	1.3 m/s	C, 1.4 mm/min

RESULTS

Water Spray Characteristics

The nozzle spray pattern was surveyed with a laser Doppler unit to measure drop size distribution and speed, and a bucket test was used at a location 1000 mm below the nozzle to measure the water flow distribution, see Figure 9. Results from the tests for drop sizes are summarised in Table 5. The results were used in a model of the sprinkler in Fire Dynamics Simulator (FDS), see Figure 10. For interest sake, the nozzle results with a velocity of 1.2 m/s are also displayed in Figure 10. The initial values for the unknown spray pattern parameters (spray angle, mean particle velocity, mean drop diameter) were estimated based on tests and available data sheets, and the FDS model water distribution was

compared with the measured distribution. The goodness of fit was based on the cumulative percentage of water within a certain radius. The spray pattern parameters were fine-tuned using a genetic algorithm that conducted multiple iterations to determine the best performing parameters which minimize the difference between the real and simulated spray pattern. The FDS model best fitting parameters gave results that followed the trend of tests, as shown in Figure 11. The water mist nozzle was not modelled due to that model needing a more complex spray pattern (six individual sprays rather than one conical spray).

Figure 9 Nozzle spray distribution test apparatus.

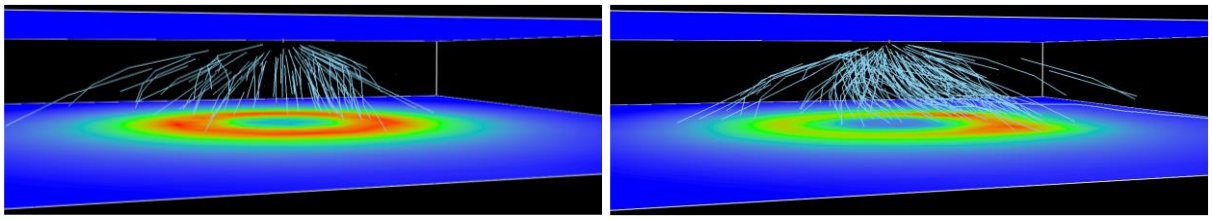

Figure 10 FDS visualization of the water spray for nozzle A, 0 m/s air velocity (left) and 1.2 m/s from left side of image (right).

Table 5 Nozzle parameters measured.

Parameter	**Nozzle A**	**Nozzle B**	**Nozzle C**
Pressure (bar)	1.5	3	90
Flow (L/min)	49.9	4.9	4.6
K factor (L/min/bar$^{0.5}$)	40.74	2.83	0.48
Drop count	2912	19370	282300
$Dv_{0.5}$ (µm)	1117	279.5	131.0
Vz (m/s) at 1 m	1.7	2.3	2.4
Vr (m/s) at 1 m	1.5	0.0	1.2
Best fit FDS particle velocity (m/s)	27.0	13.8	-
Best fit FDS spray angle (inner, degrees)	45	2.3	-
Best fit FDS spray angle (outer, degrees)	90	75	-
Best fit FDS particle diameter (µm)	1130	284.5	-

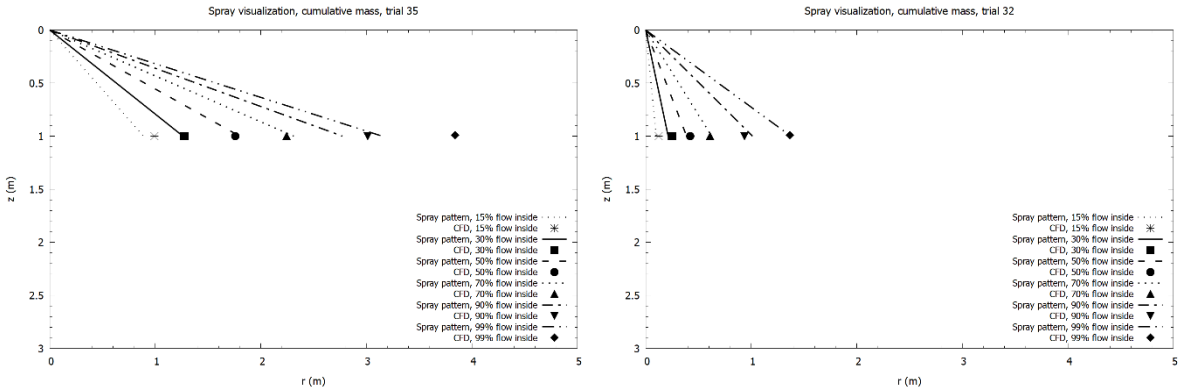

Figure 11 Spray pattern and FDS results for Nozzle A (left) and Nozzle B (right).

Fire Heat Release Rate (FHRR)

Two methods were used to calculate the FHRR, a weight loss based approach using a scale and the oxygen consumption method [6]. This procedure allows the comparision of both results and allows finding problems in the test setup or adjustment of results after finding the cause of errors by using video material and other measurement data.

The mass loss from the scale was used to calculate the combustion of fuel for every measured timestep. The values from the scale were adjusted by several processes to obtain corrected values for the FHRR (e.g., the evaporation of boiling water and the dripping of water into the pan). The fire pan configuration included water in the pan. This was done to guard against the pan deforming during the test, thus influencing the FHRR. In some of the tests water evaporated due to boiling (observed via real-time video footage) and sometimes there was water dripping into the pan from the shield (despite best efforts of design to avoid this, in some cases water found a pathway into the pan).

The water level in the pan as well as the level of water with fuel was measured at the beginning of the test. Additionally, the level of the remaining fluid, which can be water or a mixture of water and fuel, was measured at the end of the test. The change of the levels during the fire test was compared to the mass loss in the pan. The assumption is that the mass loss and change of levels is only generated by combustion of the fuel. If the mass loss does not match to the change of levels, there could be some amount of water responsible for the deviation. An adjustment to the mass loss rate was made accounting for water evaporation or dripping into the pan. The correction was based on integrated mass conservation and observation of video footage to quantify times when water was most likely entering or leaving the pan. Toward the end of some tests as the fuel had mostly burned off, water was observed to boil, and this caused a secondary peak in the FHRR due to the boiling disturbing the fuel surface and increasing the fuel surface area as a result (like the fire flare up phenomenon observed when water is thrown onto a burning oil fire).

The other method for the caclulcation of the FHRR was based on the oxygen consumption of the fire. For this, oxygen and other gas concentrations were measured downstream of the fire. Additionally, temperatures and differential pressures in the tunnel were measured with thermocouples and McCaffrey probes. The pressures and temperatures were used to calculate the velocities in different sections of the tunnel and to calculate sectionwise volume flows in segments of the tunnel. For every segment of the tunnel cross section, the FHRR was calculated. Summation of these components was then used to give the full FHRR in the tunnel.

Figure 12 provides some results comparing the FHRR determined from both methodologies. The results had similar trends but sometimes the variation between FHRR magnitudes with the two methods was more than within 20 percent. The oxygen consumption method tended toward a larger FHRR. After completion of the test series the scale was found to be damaged as part of some future unrelated work. FHRR data from the tests were revisited as a result. The damage was determined to have occurred most likely during test IFAB-13. This determination was based on the correction for

water level change failing to give reasonable results after this test, and also based on observations during the test. In test IFAB-13 a lot of n-heptane burned and water evaporated in a short amount of time, and the area next to the scale was surrounded by burning fuel. It was possible that a cable might have been damaged during this event, making the scale measurements after this time less reliable. For this reason, the rest of the results in this paper are shown from the oxygen consumption method FHRR.

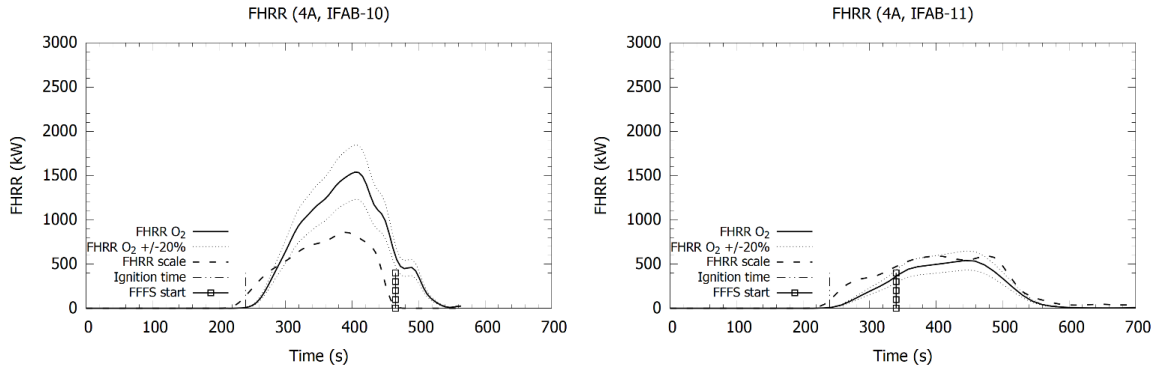

Figure 12 FHRR for test IFAB-10 (left) and IFAB-11 (right) per the two methods of computation.

The setup aimed to shield the fire so that the FHRR would not be directly impacted by the water spray. Results from the free burn tests (Test 3 series) are included in *Figure 13* for completeness (note in some cases the FFFS was operated toward the end of the test to protect the test rig). Prior to the FFFS operation, the free burn tests and FFFS tests are similar. Results are provided for Nozzle A, B and C in Figure 14, Figure 15, and Figure 16. The results suggest that the FHRR was not held constant as was desired, and it is suggested that future testing consider using a gas burner where FHRR is less likely to be affected. In these figures "FFFS start" indicates the approximate time at which the water pressure reached the target value, the actual pump start time was around 30 to 60 seconds before this. Ignition time indicates when the fuel was ignited.

Results with the FFFS show that Nozzle A FFFS with a large water droplet size (1.12 mm) had less impact on the FHRR than the Nozzle B FFFS with a small water droplet size (0.28 mm). Comparing results between Nozzle B and C FFFS (smaller drop sizes, 0.28 mm, and 0.13 mm respectively) shows that both test cases had FHRR profiles that were reduced after the FFFS was operated, which might have been due to droplet entrainment or heat feedback interuption. The smaller drops (relative to Nozzle A) have a greater cooling potential due to increased surface area and this reduced the heat feedback to the fire surface and hence the FHRR more than the larger drops. For tests with smaller fire potential (4a, 5a, 7a), this effect was not observed. It is noted that Nozzle B had a FHRR profile that decreased with time, while Nozzle C's FHRR profile remained approximately constant after an initial reduction when FFFS was operated. The reason for this was not able to be determined from the data. It might have been due to the Nozzle B droplets achieving an optimal balance between the total surface area (cooling potential, and heat feedback reduction, even with the shield in place) and droplet momentum, possibly allowing the Nozzle B drops to penetrate the fire plume (despite shielding) to result in an increased rate of fire suppression. The secondary peak of FHRR for Nozzle A was likely due to the water in the fire pan boiling and causing an increase in the FHRR.

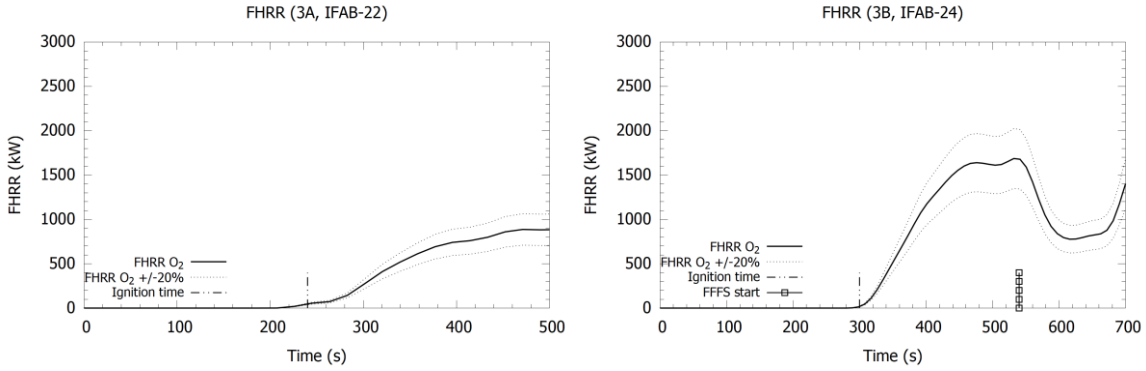

Figure 13 FHRR from test 3 series

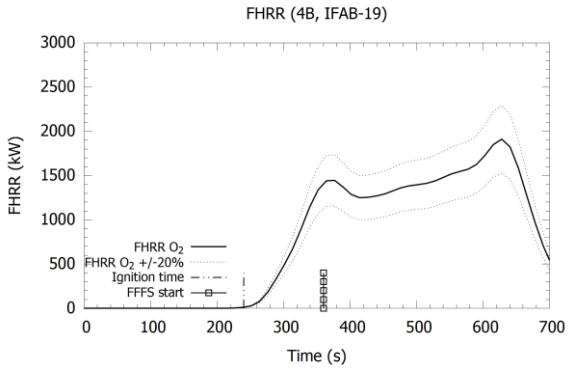

Figure 14 Test 4b, measured FHRR varying over time using Nozzle A.

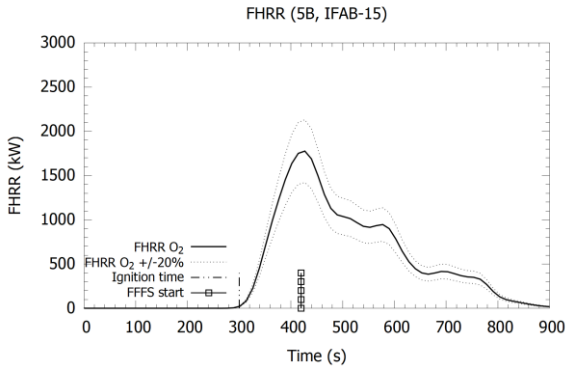

Figure 15 Test 5b, measured FHRR varying over time using Nozzle B.

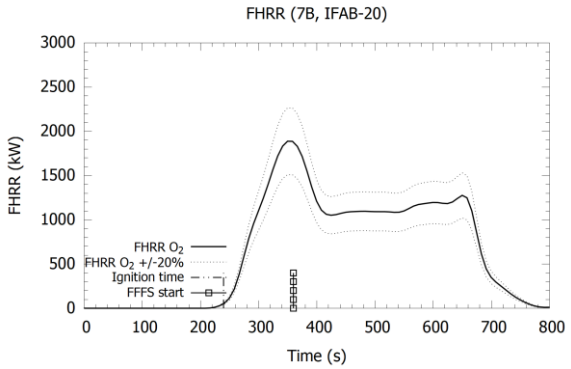

Figure 16 Test 7b, measured FHRR varying over time using Nozzle C.

FFFS and Temperature

Temperature measurements via thermocouples placed on the centreline just below the ceiling were used to assess the smoke control and thermal environment. Results for Nozzle A, Nozzle B and Nozzle C are provided in Figure 17, Figure 18, and Figure 19, respectively. Results are shown 10 seconds before the FFFS is operated and 60 seconds after the FFFS was operated. The fire location is at 0 m, indicated by the solid vertical line. The result in Figure 17 is suggestive of the FHRR not changing, or more likely increasing, since downstream of the fire the temperature is the same after FFFS was operated (i.e., cooling effect of the FFFS water is offset by the increasing FHRR, Figure 14). Figure 18 shows temperature with Nozzle B at 60 s after FFFS operation, with a downstream temperature of approximately 180 °C, FHRR approximately 1.1 MW per Figure 15. Figure 19 shows temperature with Nozzle C at 60 s after FFFS operation, with a downstream temperature of approximately 80 °C, FHRR approximately 1.1 MW per Figure 16). Overall, the temperature downstream was found to be lower for FFFS with smaller water droplets.

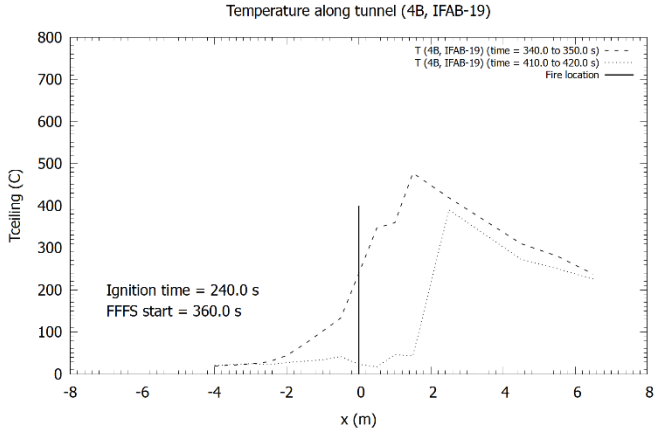

Figure 17 Test 4b, temperature at the ceiling with FFFS using Nozzle A (larger drop).

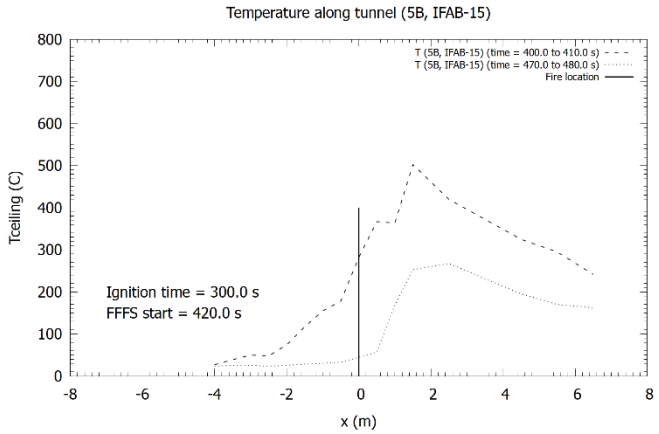

Figure 18 Test 5b, temperature at the ceiling with FFFS using Nozzle B (smaller drop).

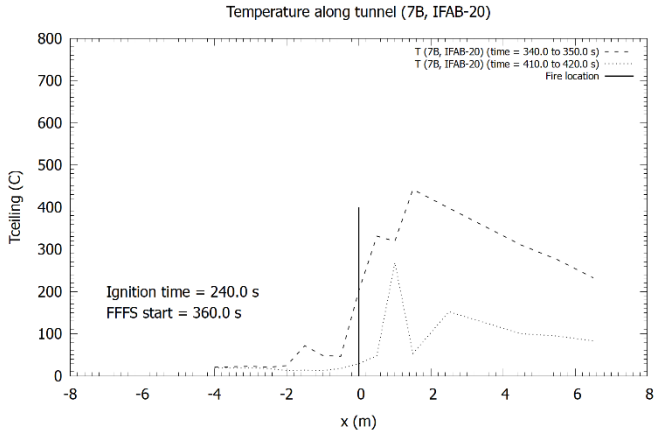

Figure 19 Test 7b, temperature at the ceiling with FFFS using Nozzle C (water mist).

Critical/Confinement Velocity

Smoke backlayering was judged based on monitoring the test videos as well as the FHRR, temperatures, and velocity data measured. The inlet velocity was controlled and remained fairly constant throughout the tests. However, as a result of fluctuating FHRR and uncertainty in both the velocity measurement and FHRR, it was not possible to finely tune the incoming velocity to precisely achieve critical velocity. The trend that could be reliably extracted from the data was the impact of the FFFS cooling as the upstream velocity was observed to remain approximately constant after FFFS operation (without changing the input speed on the fans). A visual result is provided in Figure 20.

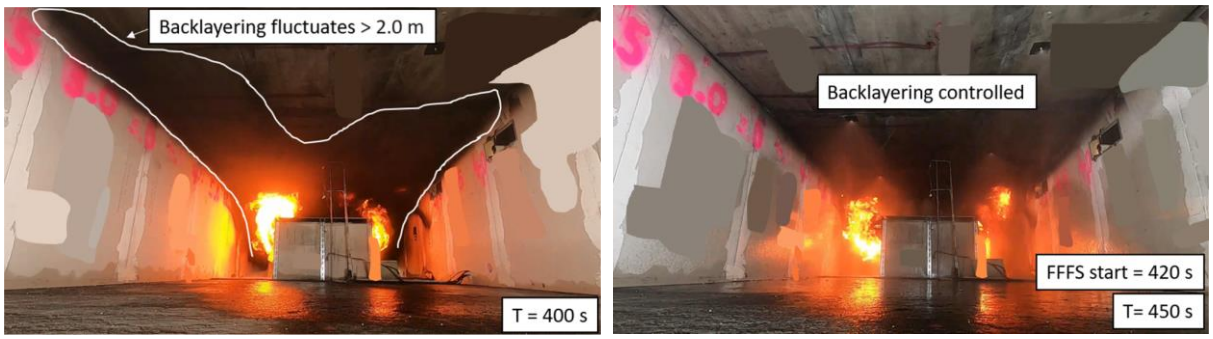

Figure 20 Visual test results, test 5b using Nozzle B.

Quantitative results from the tests are provided in Table 6. The results were determined at an instant in time (velocity and FHRR). The quantitative trend in the data supports visual observations with tests using the FFFS showing improved smoke control and similar upstream velocity and FHRR.

Table 6 Critical velocity test results.

Test and time reference (s)	FFFS on and nozzle	Upstream velocity (m/s)	FHRR (MW)	Backlayering
5B (IFAB15), 410 s	None	1.25	1.70	Yes
4B (IFAB19), 350 s	None	1.25	1.35	Yes
3A (IFAB22), 340 s	None	1.15	0.80	Yes
3B (IFAB24), 420 s	None	1.30	1.70	Yes
7B (IFAB20), 350 s	None	1.25	1.90	Yes
3A (IFAB22), 515 s	None	1.75	0.50	No
3B (IFAB24), 515 s	None	1.75	1.30	No
5B (IFAB15), 480 s	Yes, Nozzle B	1.10	1.10	No
4B (IFAB19), 420 s	Yes, Nozzle A	1.15	1.25	No
7B (IFAB20), 420 s	Yes, Nozzle C	1.15	1.10	No

Pressure Change Due to FFFS

In many tunnel projects it is discussed, whether the FFFS influences the flow field in the tunnel negatively, meaning the pressure of the ventilation system needs to be increased to overcome the additional mass of the droplets and friction effect in the tunnel. During the measurements in the test tunnel, it was found that the change in pressure difference due to the activation of the FFFS can be neglected as it was on the order of 0.5 Pa or less. Computation of pressure change due to FFFS via a momentum balance (to accelerate the droplets up to speed) was found to give similar order of magnitude pressure change for nozzles A and B.

Computational Fluid Dynamics Modelling

Computational fluid dynamics (CFD) models of the Tests 4B and 5B were conducted using Fire Dynamics Simulator (FDS) version 6.7.7 (nightly release), which is a free and open-source software provided by the National Institute of Standards and Technology (NIST) of the United States Department of Commerce. FDS was used as it is purpose-built for fire modeling and the software is developed to model turbulent flow, heat transfer, radiation, combustion, water droplets and cooling. Figure 21 shows the FDS models developed for Test 4b and Test 5b, with base grid resolution of 0.1 m along tunnel length, 0.1 m along tunnel width with refinement near the walls, and 0.125 m along the tunnel height with refinement near the walls [4].

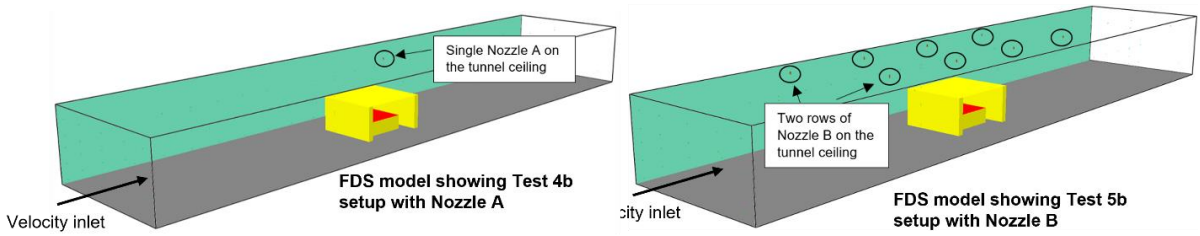

Figure 21 FDS models showing the different test setups.

A detailed comparison of the FDS results and the test data is presented in the full report [4]. Temperature and velocity results were compared between test data and FDS models. Note that the plots of results include a Pearson coefficient (r). The coefficient measures agreement between test and model based on a linear correlation. For purposes of using classifications in a consistent manner, the strength of association between test data and FDS is taken to be poor (r value between 0.0 and 0.25), fair (r value between 0.25 and 0.5), good (r value between 0.5 and 0.75), or very good (r value between 0.75 and 1.0). In the paper herein some general trends are discussed rather than focusing on the Pearson coefficient results.

Figure 22 shows the gas temperature results near the tunnel ceiling compared with the Test 4b data before and after the FFFS operation, using base grid resolution [4]. The fire location is marked at 0 m, shown with a vertical line. Some backlayering was seen in the tests prior to FFFS operation but this was not able to be replicated in the FDS models. Prior to operation of the FFFS the temperature downstream of the fire was similar between the test and FDS model. After FFFS operation the temperature profile downstream did not agree as well as it did prior to FFFS operation.

Comparison with Test 5B is provided before and after FFFS operation using the base grid resolution [4] in Figure 23. The results were like Test 4B; the FDS model did not predict the same extent of backlayering prior to FFFS operation. Following FFFS operation the temperature prediction downstream of the fire was improved for this model.

Grid resolution sensitivity (roughly halving the grid size) was performed for the FDS models for both Tests 4B and 5B, the results of which are presented in [4]. Grid sensitivity study showed that the temperature results and smoke backlayering were sensitive to the grid with the coarse grid predicting lower temperatures and less backlayering. The sensitivity to inlet bulk velocity was also investigated. The inlet velocity was varied based on a range derived from air velocity measurement during testing and uncertainty quantification of the measured data points, refer to [4] for more details. This factor

was not able to drastically improve the FDS model predictions. The sensitivity of results to the FHRR was tested. An increased FHRR did result in more backlayering, but temperatures downstream of the fire were much higher than the test data.

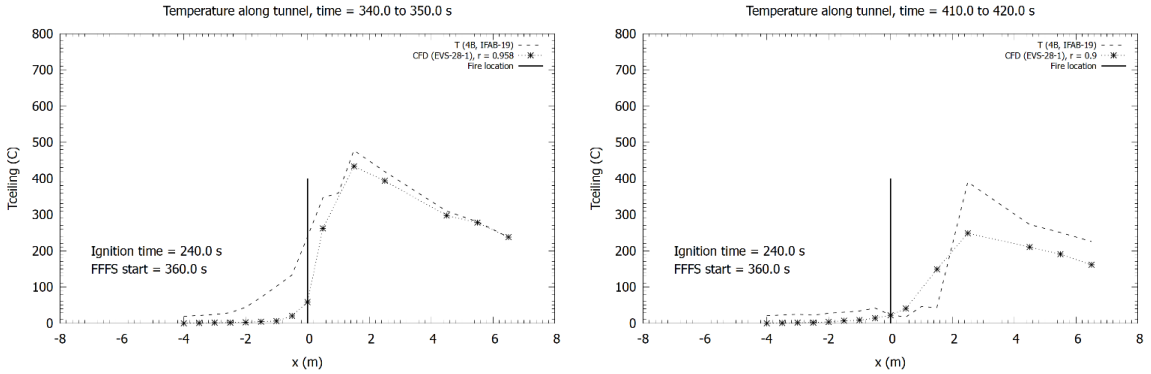

Figure 22 Test 4B, FDS results showing gas temperature near the ceiling before FFFS activation (left) and after (right).

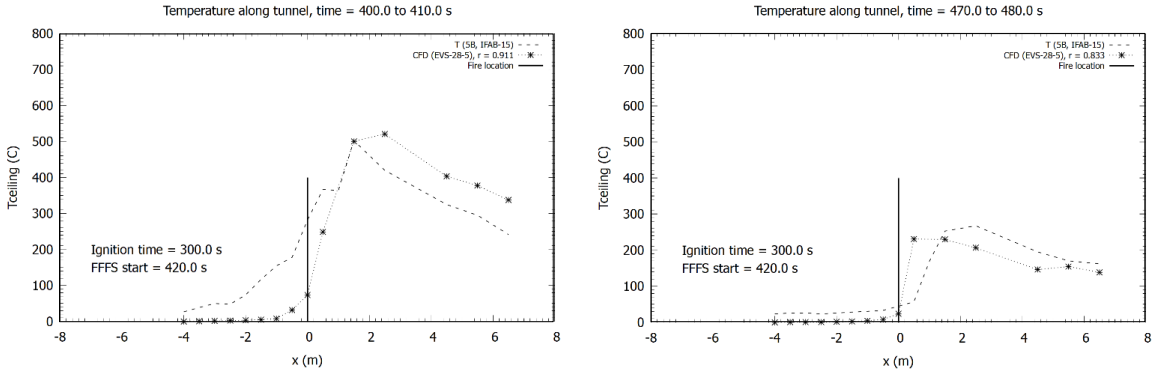

Figure 23 Test 5B, FDS results showing gas temperature near the ceiling before FFFS activation (left) and after (right).

The FDS results and test data (gas temperatures at the tunnel ceiling) showed qualitatively similar results downstream of the fire. The quantitative agreement was not as good, and the results were sensitive to the grid resolution. Backlayering proved difficult to predict with FDS, but in cases where the model did predict backlayering, a subsequent reduction in backlayering distance was seen when the FFFS was operated. Overall the FDS modeling did not produce good quantitative agreement with the tests, and a suggested area of further research was made with respect to improving FDS or considering other CFD software to perhaps improve the predictions.

DISCUSSION AND CONCLUDING REMARKS

Laboratory tests were performed to better understand the interaction between longitudinal EVS and FFFS. The tests were structured toward verifying the change in critical/confinement velocity with FFFS operating and providing data for CFD model validation. There were two main hypotheses considered:

- That FFFS and EVS can be integrated and EVS capacity optimized because of the cooling effects of the FFFS water spray.
- Computational fluid dynamics (CFD) can be used to predict FFFS and EVS interaction for design integration.

Results from the tests demonstrated qualitatively that the EVS capacity can be reduced, as the confinement velocity decreases due to the cooling of the FFFS water spray. The results also showed

that the backlayering is stopped (or backlayering distance reduced) once the FFFS is operated, even though the upstream velocity was observed to reduce slightly for two of the tests. This indicates a reduction in the longitudinal velocity needed to control the smoke spread upstream because of the cooling of combustion products. Smoke control, measured by the gas temperature at the ceiling, was found to be reduced when the FFFS was operated due to its cooling effect. Backlayering was controlled in all fire tests after FFFS was activated.

Optimization of the EVS because of cooling effects of the FFFS was not investigated in the tests. The focus was whether EVS capacity can be reduced due to FFFS integration, something that the results showed is feasible due to the improved smoke management with FFFS operating. Results from the tests were not able to be used to quantify the extent of critical/confinement velocity reduction when FFFS is operated. This was due to the transient FHRR and difficulty accurately controlling the upstream air speed at velocities encountered in the tests.

The magnitude of pressure changes measured was too small to allow for a quantification of resistance effects due to FFFS. The results reported for pressure did show small/negligible pressure changes due to the operation of FFFS. For design purposes, the FFFS resistance is suggested to be considered in the EVS design, although it is noted that the effect of this is likely to be negligible with respect to other aeroydnamic losses.

The test results reaffirmed that smaller water drop sizes provide increased cooling of the tunnel environment for less overall water application rate. In terms of suggested practices, it can be considered to utilise smaller water droplets if water supply is limited or optimal cooling efficiency is a key goal of the FFFS design.

The FDS results and test data (gas temperatures at the tunnel ceiling) showed qualitatively similar results downstream of the fire. The quantitative agreement was not as good, and the results were sensitive to the grid resolution. Backlayering proved difficult to predict with FDS, but in cases where the model did predict backlayering, a subsequent reduction in backlayering distance was seen when the FFFS was operated. Overall the FDS modeling did not produce good quantitative agreement with the tests, and a suggested area of further research was made with respect to improving FDS or considering other CFD software to perhaps improve the predictions.

REFERENCES

1. Fixed Fire Fighting and Emergency Ventilation Systems for Highway Tunnels – Literature Survey and Synthesis, Federal Highway Administration. FHWA-HIF-20-060, 2020 (https://rosap.ntl.bts.gov/view/dot/51767).
2. Fixed Fire Fighting and Emergency Ventilation Systems for Highway Tunnels – Workshop Report. FHWA-HIF-20-060, 2020 (https://rosap.ntl.bts.gov/view/dot/50664).
3. Fixed Fire Fighting and Emergency Ventilation Systems for Highway Tunnels – Computer Modeling Report. FHWA-HIF-22-021, 2022 (https://www.fhwa.dot.gov/bridge/tunnel/pubs/hif22021.pdf).
4. Fixed Fire Fighting and Emergency Ventilation Systems for Highway Tunnels – Laboratory Scale Testing. FHWA-HIF-23-022, 2024 (https://rosap.ntl.bts.gov/view/dot/75887).
5. Fixed Fire Fighting and Emergency Ventilation Systems for Highway Tunnels – Research Report. FHWA-HIF-24-005, 2024 (https://rosap.ntl.bts.gov/view/dot/75243).
6. M. L. Janssens, “Measuring Rate of Heat Release by Oxygen Consumption,” *Fire Technology*, vol. 27, no. 3, 234–249, 1991, doi: 10.1007/BF01038449.

Comparison of Fixed Water-Based Fire-fighting Systems for Road Tunnel Application

M.K Cheong, L.W Lim, C Tan, A Chong, H Wijaya, M Thong, K.W Leong
Land Transport Authority of Singapore
Singapore

ABSTRACT:

In a road tunnel, fires pose a significant threat to both assets and individuals, often resulting in catastrophic damages, injuries, and even loss of life. Specifically, fires involving heavy goods vehicles (HGV) carrying high fuel loads can rapidly propagate leading to severe and devastating consequences if not addressed in the early phase of fire development. An effective way to mitigate the potential impact of such fires is to install a fixed water-based fire-fighting system (FFFS) within the tunnel. Over the years, the Land Transport Authority of Singapore (LTA) have undertaken several large scale-fire test programs involving HGV and very heavy goods vehicle (VHGV) fires. The objectives of these large-scale fire tests were to investigate the effectiveness of FFFS such as deluge and low-pressure water mist systems for road tunnel projects in Singapore. Large-scale fire tests were conducted on simulated HGVs and VHGVs in test environments. The results demonstrate that both systems significantly reduce heat release rates in HGV and VHGV fires. In comparing the two systems, water mist proved more efficient, requiring less water than deluge systems to control VHGV fires.

KEY WORDS: fixed water-based fire-fighting systems, large-scale fire test

INTRODUCTION

Fire can be very dangerous as it poses significant threat to assets and individuals and can lead to catastrophic damages, injury, or even death. In road tunnels, fires involving high fuel load can propagate very quickly and lead to severe and catastrophic consequences. Notable examples of such major road tunnel fire incidents include: a) the Mont Blanc Tunnel fire in 1999 during which a transport truck caught fire in the tunnel connecting France and Italy, resulting in 39 facilities [1], and b) the St Gotthard tunnel fire incident in 2001, during which a collision between two heavy good vehicles transformed the tunnel into a smoking inferno resulting in the loss 20 lives and numerous injuries [2]. One way to mitigate the potential impact of the fire is to equip the tunnel with an appropriate fixed water-based fire-fighting system (FFFS) to control the fire. A FFFS, which is permanently installed in the tunnel, disperses a water-based extinguishing agent when a fire is detected [3]. Installation of a FFFS can provide benefits such as reducing the fire growth rate and fire spread, as demonstrated in the fire test programmes initiated by LTA in 2011 [4] and 2018 [5]. These benefits enhance the safety of motorists during the self-evacuation phase, aid fire-fighting operation and prevent prolonged road tunnel closures for repair work after a fire incident. This paper presents the findings from selected LTA fire tests and a comparison of the effectiveness of deluge and low-pressure water mist systems. This study aims to provide insights into the effectiveness of the FFFS in mitigating the impact of fires in road tunnels, offering valuable information for future tunnel safety measures.

BACKGROUND

If a fire in a tunnel is not promptly addressed in its early stages, it can lead to highly destructive and catastrophic consequences, especially if it involves a heavy goods vehicle (HGV) carrying goods with a high energy content. This can cause rapid production of heat, soot, and toxic combustibles, making it more challenging and dangerous for motorists to escape, and for rescue and firefighting operations.

Large-scale fire tests in Europe Road tunnel, have provided valuable insights into fire development, informing improved safety measures. The Runehamar fire tests revealed peak heat release rates (HRRs) of 66.4 MW to 201.9 MW for high energy content goods vehicles [6], while the EUREKA 499 recorded 128 MW for an HGV trailer carrying two tonnes of furniture [7]. These tests were conducted without intervention of fixed water-based firefighting systems (FFFS), and with 3 m/s to 6 m/s longitudinal air velocity in the tunnels. These findings highlighted the potential for catastrophic consequences from goods vehicle fires in road tunnels. Consequently, standards like NFPA 502 increased the recommended design fire for HGVs (e.g. 200 MW in the 2017 edition). However, the standards initially did not consider the mitigating effects of FFFS. Recent editions of NFPA 502 have recognised FFFS effectiveness, based on fire test programmes by Singapore's Land Transport Authority (LTA), Safety of Life in Tunnels (SOLIT) and Swedish Transport Administration (STA). In Singapore, long road tunnels are equipped with a tunnel ventilation system to create tenable conditions for safe evacuation of motorists during a tunnel fire. This is achieved by supplying fresh air in the opposite direction of escape, thereby creating a smoke-free path for motorists who are trapped upstream of the fire site to evacuate safely as shown in Figure 1.

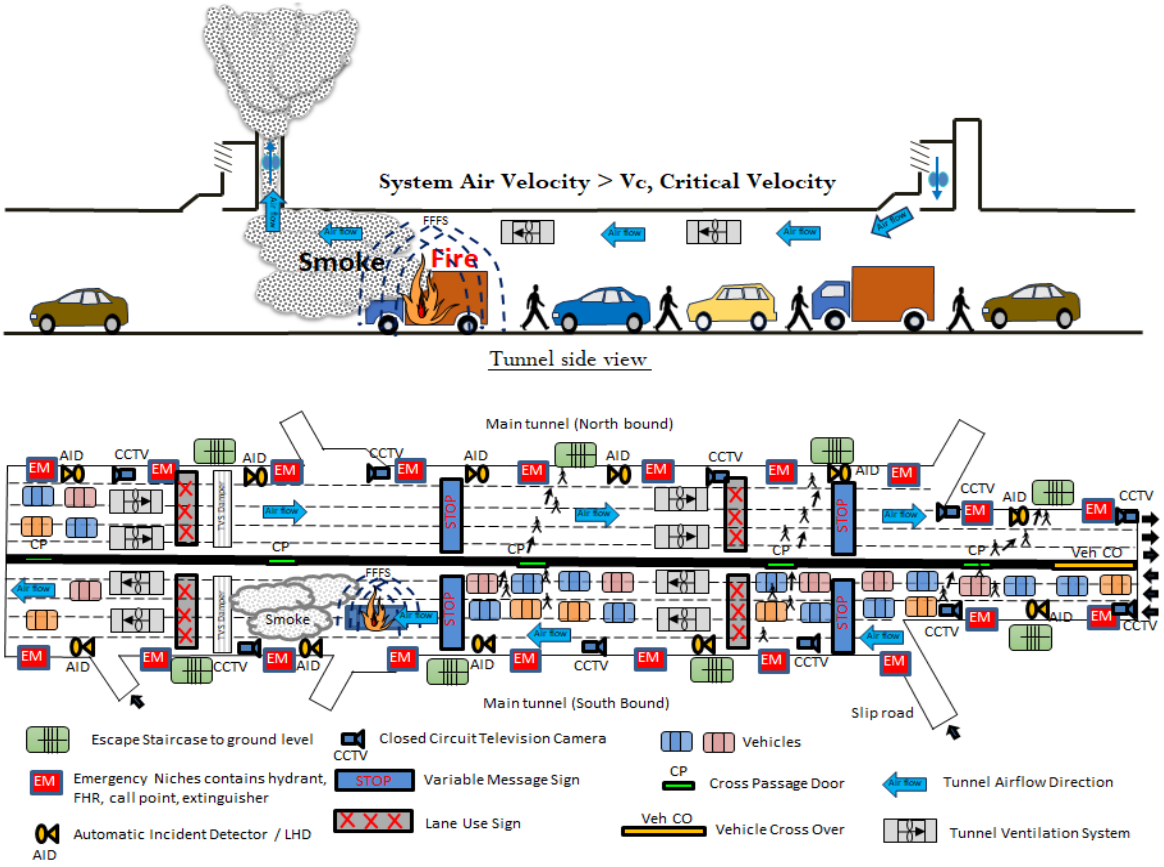

Figure 1: Smoke control and evacuation strategy in road tunnels in Singapore.

To achieve this, the air velocity generated at the fire incident site must be higher than the critical velocity to prevent backlayering of smoke (refer to Equations 1 and 2) [3]. The critical velocity is dependent on several factors, including the HRR of the fire, tunnel gradient, and tunnel geometry. Reducing the HRR of fire may allow the tunnel ventilation system capacity to be reduced. However, this is possible if, other design factors such as pollutant and temperature control during normal/congestion operation, do not necessitate an increase in the capacity of the tunnel ventilation system.

$$V_c = K_1 K_g \left[\frac{g H Q}{\rho C_p A T_f} \right]^{1/3} \qquad \text{Eq. (1)}$$

$$T_f = \left(\frac{Q}{\rho C_p A V_c} \right) + T_\infty \qquad \text{Eq. (2)}$$

Where:
V_c= Critical velocity [m/sec]
K_1= Froude number factor, $Fr^{-1/3}$ (e.g., K1= 0.87 for Q < 10MW)
K_g = Grade correction factor [Kg= 1 + 0.0374 (grade) $^{0.8}$]
g = Acceleration caused by gravity [m/sec^2]
H = Height of tunnel [m]
Q = Convective fire heat release rate [MW]
ρ = Average density of the approach air [kg/m^3]
C_p= Specific heat of air [kJ/kg K]
A = Area [m^2]
T_f= Average temperate of the fire site gases [K]
T_∞= Temperature of the approach air [K]

From a fire and life safety perspective, the main objectives of the FFFS are to limit the size of a fire by decreasing the HRR, pre-wetting the adjacent combustibles and controlling the gas temperatures to avoid damage to the structure. The reduction in HRR will enhance the ability for motorists to evacuate during the early phase of the fire development and facilitate the fire responders in fire-fighting activities during the later stage of the fire development. Most tunnel fires resulting from vehicle faults or collision will develop into flaming combustion, where the liquid fuel vaporises or solid fuel pyrolyzes to produce a flammable vapour. The combustion is an exothermic chemical reaction process that involves oxidation of the flammable vapour to produce flame, heat, and combustion products.

In NFPA 502 [3], FFFS are categorized according to the desired performance objective as follows: (1) fire suppression system - a system intended to sharply reduce the heat release rate of a fire and prevent its growth by means of direct and sufficient application of extinguishing agent to the burning surface, (2) fire control system – a system intended to limit the size of a fire by distribution of extinguishing agent to decrease the heat release rate and prewet adjacent combustible while controlling gas temperatures to avoid structure damage, (3) volume control system – a system intended to provide substantial cooling of products of combustion but is not intended to affect heat release rate directly and (4) surface cooling system – a system intended to provide direct cooling of critical structure or equipment without directly affecting heat release rate (as shown in Figure 2). It is important to establish the performance objective of the fire suppression system with the Authority Having Jurisdiction (AHJ) during the initial design phase of the project to avoid unnecessary redesign work or testing. Unlike the deluge system, most water mist systems utilise specially designed nozzles. As such, installation of listed water mist systems that have demonstrated their effectiveness in fire tests is a critical aspect of the approving process by the AHJ [8].

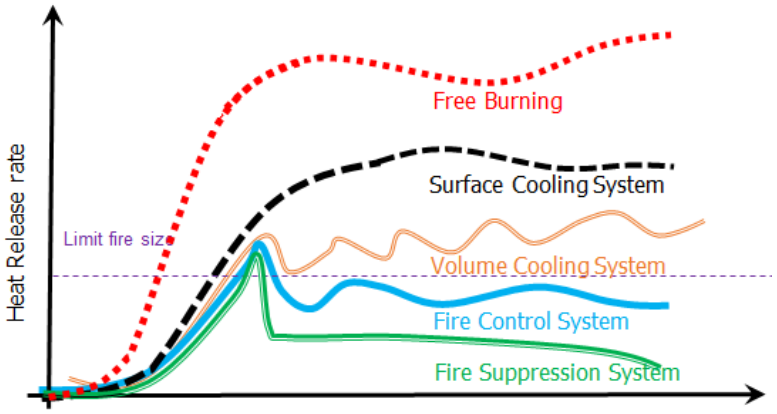

Figure 2: FFFS *categorization based on the performance objective.*

Various FFFS are available to enhance fire and life safety by limiting the heat release rate during a fire in a road tunnel. These systems include sprinkler systems, deluge water spray systems, foam water systems, and water mist systems. Among these, deluge water spray and water mist systems are the prevalent choices for application in Singapore's road tunnels.

Wet pipe sprinkler systems, commonly integrated into building designs, maintains water under pressure at all times and employ automatic sprinkler heads with a heat sensitive thermal element, typically a glass bulb or a solder link. When a fire generates sufficient heat, one or more sprinkler heads are activated, releasing water to suppress or control the fire. Deluge water spray systems utilise open sprinkler heads on dry pipework, with all heads discharge simultaneously in a designated zone when triggered by a detector system or by manual means. Deluge water spray systems are designed to deliver large volumes of water over a specific area within a short timeframe and are particularly effective for rapidly escalating fires and areas with substantial quantities of highly combustible materials [9]. In scenarios involving storage or handling of large amounts of flammable liquids, the performance of automatic sprinkler and deluge water spray systems can be enhanced by incorporating aqueous film-forming foam (AFFF). Water mist systems disperse fine droplets over combustible areas and the surrounding atmosphere to achieve rapid cooling with minimal water usage within a designated zone. These systems are particularly useful for tunnel projects motivated by the desire to minimize the impact on infrastructure, such as large drainage tanks and water storage tanks.

The primary fire suppression mechanisms of the water spray emitted from the FFFS on fire development consist of the following: (1) fuel surface wetting, (2) gas cooling, (3) oxygen displacement, (4) surface wetting and cooling (5) blocking of radiation heat, (6) influence on combustion kinetics and (7) de-stratification of the smoke layer [10]. Figure 3 illustrates the primary mechanisms involved in interaction of the water spray with the fire. More detailed descriptions of these mechanisms are also given below:

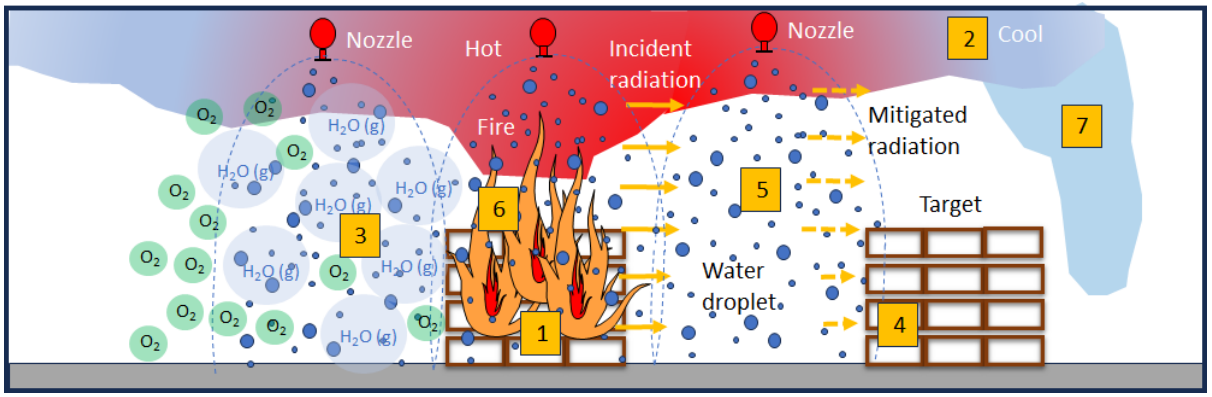

Figure 3: Primary mechanisms involved in the interaction of water sprays with a fire.

1. Fuel surface wetting: Spraying water directly onto the burning fuel surface slows down the burning process, affecting the fire's HRR and its impact on the structure and safety conditions.

2. Gas cooling: Droplets evaporate when falling through the hot smoke layer. This can influence the effects of the fire on structure and tenability.

3. Oxygen displacement: Rapid water evaporation in high temperatures displaces air, reducing oxygen concentration. Decreases oxygen availability for combustion results in less efficient fire and more controllable fire through cooling

4. Surface wetting and cooling: Water droplets reaching nearby objects can wet and cool their surfaces, preventing ignition and limiting temperature rise, thereby reducing risk of fire spread and decreased impact on the structure.

5. Blocking of radiation heat: Water droplets form a protective layer on surfaces, absorbing and reducing heat transmission from the fire to potential fuel sources.

6. Influence on combustion kinetics: Water droplets and vapor affect the fire's HRR. In some cases, water spray may temporarily intensify liquid pool fires by increasing fuel vaporization upon contact.

7. De-stratification of the smoke layer: Water droplets disrupt and cool the smoke layer, reducing ceiling stratification. This has mixed safety effects: decreased radiation from hot smoke, possible increase in air temperature and potential increase in smoke concentration at occupant level

FIRE TEST PERFORMANCE REQUIREMENTS

The main objectives of LTA's large-scale fire test programmes were twofold: Firstly, the tests aimed to investigate and validate the performance requirements as stipulated in NFPA 502, NFPA 750, Singapore Fire Code 2018 and by the AHJ. Secondly, the tests sought to provide evidence and data for the design of FFFS for road tunnels in Singapore.

The acceptance criteria used to evaluate the performance of the FFFS were:

a) The FFFS must be capable of controlling the total HRR. After activation, it must ensure that that the HRR does not exceed the design fire approved by the AHJ.

b) After activation of the FFFS, the heat radiation level measured shall not exceed 10 kW/m^2 when measured at a horizontal distance of 5 m downstream of the fire site and at the top of the target.

c) Ceiling surface temperature shall not exceed 380℃.

d) Temperature of steel reinforcement within the concrete shall not exceed 250℃.

e) Condition in the tunnel upstream of the fire site shall meet the tenable criteria stated in NFPA 502:
   - Heat radiation level shall not exceed 2.5 kW/m^2.
   - Air carbon monoxide content shall not to exceed 50 ppm.
   - Illuminated sign shall be discernible at 30 m.
   - Gas temperature shall not exceed 60℃.

FIRE TEST PROGRAMMES AND TEST SETUP

From 2011 to 2023, LTA commissioned three large-scale fire test programmes involving HGVs and VHGVs. These fire tests consisted of free burning scenarios and application of different FFFS, such as deluge water spray and low-pressure water mist systems with different discharge densities and nozzle arrangements. The tests in 2011 and 2018 were conducted in the "San Pedro de Anes" TST test tunnel facility in Spain. The more recent tests in 2023 took place at the TongJi AnTai Research & Development Center of Engineering Disaster Prevention (TJAT R&D Center) test tunnel facility in China.

The TST and TJAT test tunnels both have a rectangular cross-sectional area of 7.5 m (W) × 5.2 m (H) at the burning zone. The total length of the TST test tunnel is 660 m, while the TJAT is 330 m in length. Figure 4 provides an overview of the test tunnels and the locations of the fuel load, target, fans, pump house, water tank and measurement station. Due to the large amount of data recorded, only sensors relevant to this paper have been included (see Figure 5).

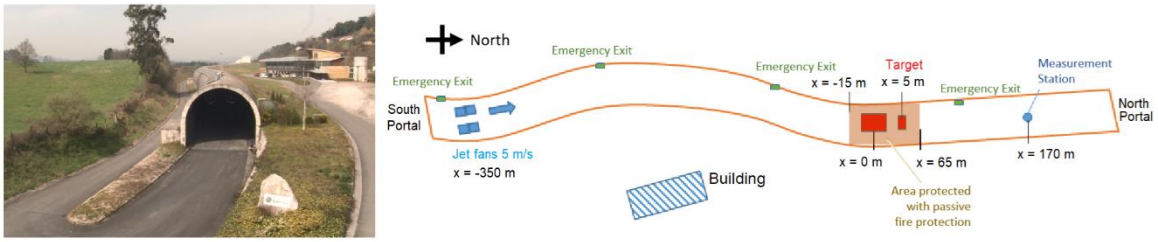

San Pedro de Anes test tunnel facility at TST tunnel (Spain)

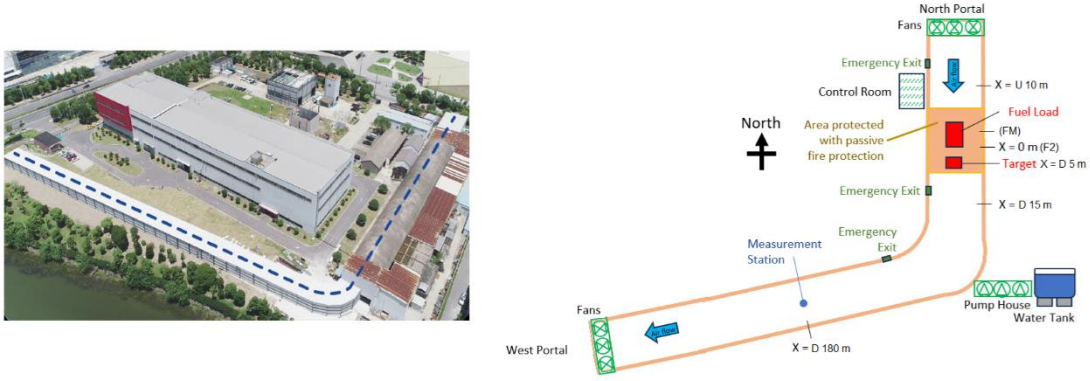

TongJi AnTai Research & Development Center of Engineering Disaster Prevention (TJAT) tunnel facility (China)

Figure 4: Plan view of test tunnel

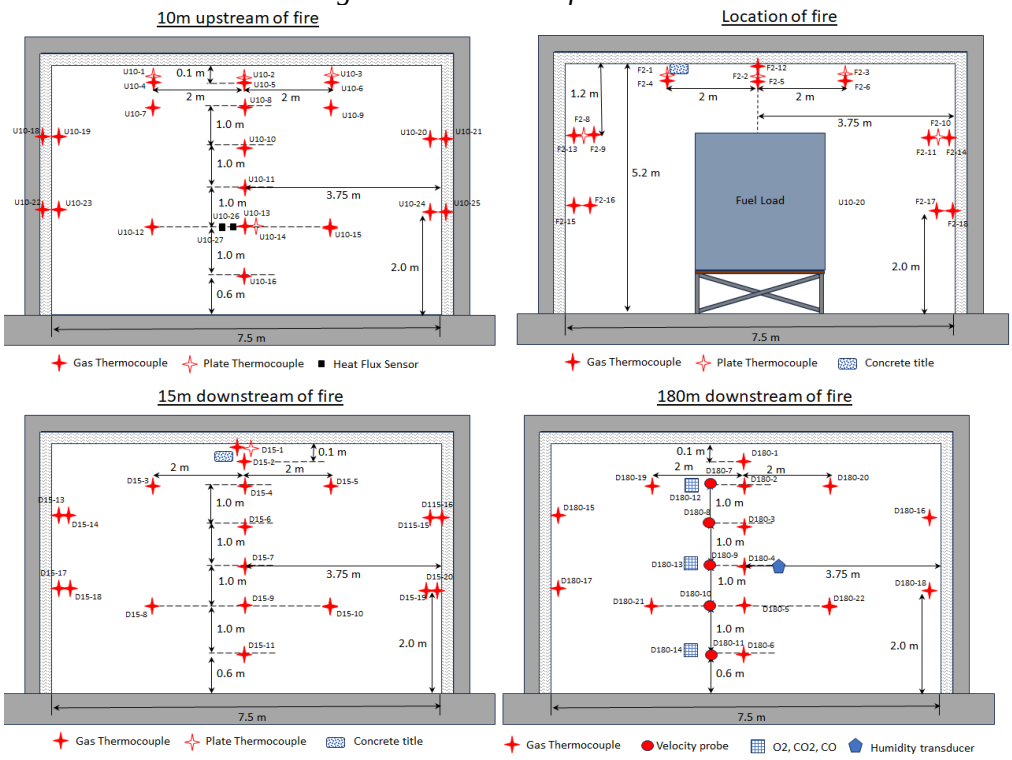

Figure 5: Cross-section of the test tunnel and instrumentation setup.

Fuel load quantity, arrangement, and ignition source

Singapore's regulations prohibit vehicles carrying hazardous material from entering road tunnels. The Singapore Civil Defence Force (SCDF) enforces this by using a Hazmat Transport Vehicle Tracking System (HTVTS). Hazmat vehicles, such as petrol tankers, are fitted with a tracking device allowing location monitoring and remote immobilisation if violation occurs. The system regulates the vehicle's throttle, restricting fuel injection which forces the driver to stop. Police are then dispatched to the site [11]. Singapore's Road Traffic Act also prohibits vehicles (including any load) exceeding 13 m and very heavy goods vehicle (VHGV), commonly known as trailers, from entering road tunnels. However, VHGV are not fitted with the tracking and immobilisation device. As such, a typical rigid very VHGV fully loaded with pallets was selected for the large-scale fire test programmes to assess the FFFS effectiveness in mitigating the VHGV fire risks in road tunnels.

Figure 6 shows the configurations of a typical VHGV and an HGV fully loaded with pallets, as well as the mock-up of the fuel load.

For the VHGV fire tests, the fuel load consisted of 494 EURO type pallets (1.20 m x 0.80 m x 0.15 m each): 104 plastic pallets (20%) and 390 wooden pallets (80%). The pallets were arranged in 26 stacks of 19 pallets shielded with 2 mm aluminium sheets on the top, front and back. A target pallet stack, consisting of two full pallet stacks, was positioned 5 m downstream from the end edge of the fire load.

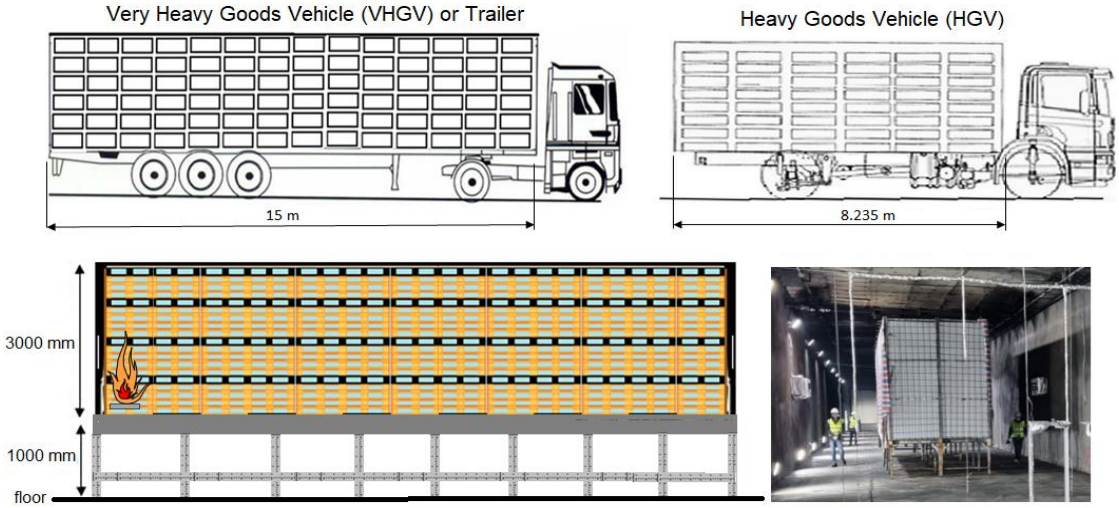

Figure 6: Diagram (Upper left – VHGV), (Upper right – HGV) and (Lower – Fuel load setup).

In the 2011 fire test programme, a scaled-down version of the fuel load was used to simulate an HGV. The fuel load comprised 228 EURO type pallets: 48 plastic pallets (20%) and 180 wooden pallets (80%). Like the VHGV test setup, the pallets were arranged in 12 stacks of 19 pallets each, on a 1 m elevation.

Fixed Firefighting System – Deluge Water Spray System

In the fire tests, the deluge water spray systems employed were low pressure systems with operating pressures of up to 5 bars, with each nozzle covering an area of at least 9 m^2. Two types of deluge nozzles were used: a pendent standard spray type and a directional 180° type. The deluge systems were designed to simultaneously activate two zones, each with a length of 25 m. A total of 46 nozzles were deployed across an area measuring 50 m in length and 7.2 m in width, with a water discharge density of 12 mm/min. Figure 7 shows part of the deluge system pipes at the ceiling for the tests.

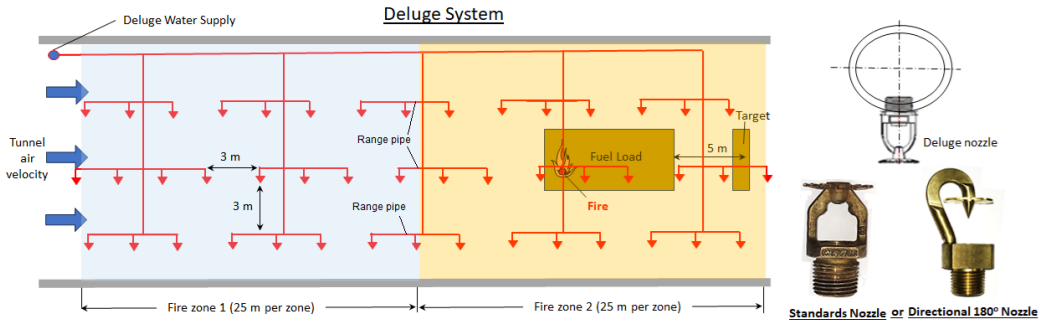

Figure 7: Deluge nozzle position, zone distance and fire location.

Two water mist systems utilising nozzles from two different vendors were tested: Water Mist System with Type A nozzles and Water Mist System with Type B nozzles.

Fixed Firefighting System – Water Mist System (with Type A Nozzles)

Like the deluge water spray system, the water mist system (with Type A nozzles) was designed to activate two zones simultaneously, each 25 m in length. The design operating pressure was set at 10 bars. Within the protection zones, two rows of pipes were installed with a 6.0 m spacing. The system utilized different types of nozzles and was arranged to discharge water mist in three directions. Fire tests were conducted with different water discharge densities. Figure 8 illustrates the layout of the water mist system.

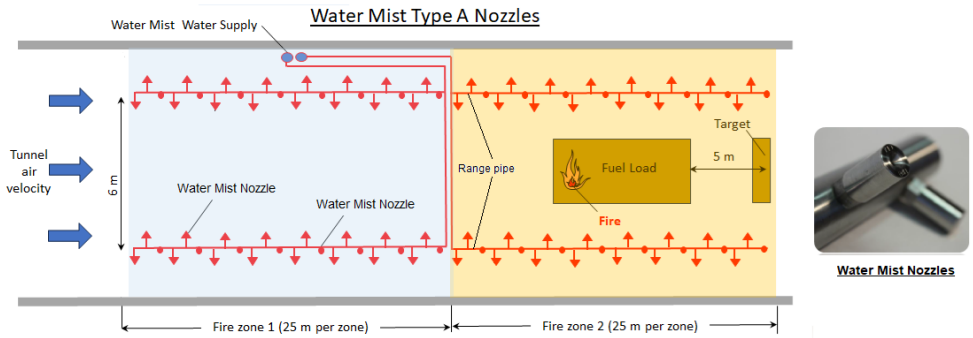

Figure 8: Water mist system with type A nozzle position, zone distance and the fire location.

Fixed Firefighting System – Water Mist System (Type B Nozzles)

The water mist system (with Type B nozzles) was also designed to simultaneously activate two zones, each with a length of 25 m. The design operating pressure was set at 10 bars. The two types of nozzle heads that were used, provided flow rates of 10 l/min to 17 l/min. The nozzle was spaced 0.52 m apart on each pipe and arranged to discharge water mist in three directions. A total of 192 nozzles were employed for the protection of the two zones, with a water discharge density of 7.5 mm/min. Figure 9 illustrates the water mist system layout.

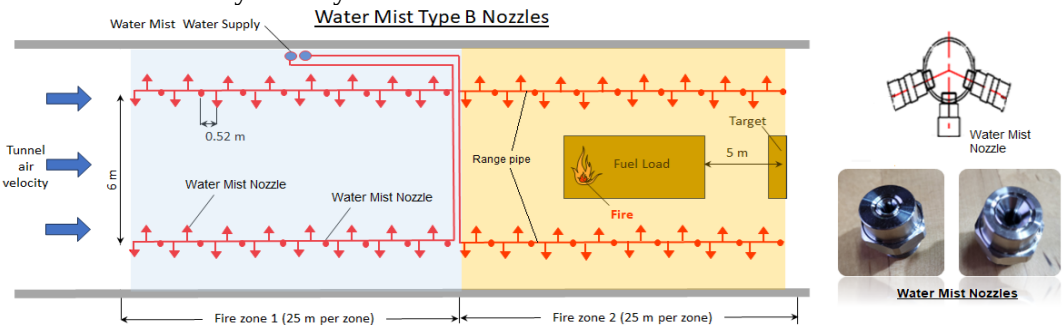

Figure 9: Water mist system with Type B nozzle position, zone distance and the fire location.

Large-Scale Fire Test Schedule

Table 1 provides a schedule of the LTA fire test programmes, including details such as the fuel load used, type of FFFS, types of nozzles, and discharge density of the FFFS.

Table 1 also includes information on the free burn tests of HGV and VHGV conducted in 2011 and 2018 at the TST facility in Spain. During these tests, the vehicles were ignited in the tunnel and allowed to burn without any FFFS intervention. The free burn tests aimed to determine the HRR and other fire characteristics under a non-suppression condition. The results were used to compare tunnel conditions with and without FFFS operation.

Table 1: Large Scale Fire Tests Schedule

Test	Fire Test Programme	Test description	Fuel Load	FFFS	Nozzle Type	Discharge density	Tunnel Facility
1	Fire Test 2011	Free Burn	HGV	N.A	N.A	N.A	TST
2	Fire Test 2018	Free Burn	VHGV	N.A	N.A	N.A	TST
3	Fire Test 2011	Suppression Test	HGV	Deluge	Directional 180°	8 mm/min	TST
4	Fire Test 2011	Suppression Test	HGV	Deluge	Directional 180°	12 mm/min	TST
5	Fire Test 2018	Suppression Test	VHGV	Deluge	Directional 180°	12 mm/min	TST
6	Fire Test 2018	Suppression Test	VHGV	Deluge	Standard	12 mm/min	TST
7	Fire Test 2018	Suppression Test	VHGV	Water Mist	Type A	4 mm/min	TST
8	Fire Test 2018	Suppression Test	VHGV	Water Mist	Type A	6 mm/min	TST
9	Fire Test 2018	Suppression Test	VHGV	Water Mist	Type A	8 mm/min	TST
10	Fire Test 2022	Suppression Test	VHGV	Water Mist	Type B	7.5mm/min	TJAT

Note: Tests 3 to 10 consist of two suppression zones each zone is 25 m
Fire Test with HGV - Longitudinal ventilation rate in the tunnel was in the range of 3 m/s
Fire Test with VHGV - Longitudinal ventilation rate in the tunnel was in the range of 5 m/s
Fire load was placed in the centre of the fire zone 2 and FFFS was activated 4 minutes after the detection time.

HEAT RELEASE RATE MEASUREMENT

Several methods can be used to measure the HRR, with the two most common ones being mass loss rate and oxygen depletion calorimetry.

The mass loss rate method determines the HRR by measuring the fuel source's rate of mass loss. This approach is based on the principle that the heat released by a fire is proportional to the amount of fuel consumed. Empirical correlations are used to calculate the HRR from the measured mass loss rate. However, in fire tests involving fire suppression systems, this method becomes impractical. The water discharge during system activation disturbs the measurement, affecting the accuracy of the HRR calculation.

The oxygen depletion calorimetry method, conversely, calculates the HRR based on the fire's oxygen consumption. It offers three measurement approaches: measuring oxygen only (method 1), measuring carbon dioxide (method 2), and measuring both carbon dioxide and carbon monoxide (method 3). The accuracy of HRR calculations increases as more gases are measured [12].

All the fire tests in Table 1 employed the oxygen depletion method to assess the HRR, measuring the fire's oxygen consumption. To enhance the precision of the HRR estimation, the study also monitored the carbon monoxide and carbon dioxide levels, alongside oxygen concentration.

The HRRs were calculated using equations 1 and 2 from Dlugogorski et al [12]. These equations account for water vapor content and are mathematically consistent with those developed by Janssen and Parker [13]. However, Dlugogorski's equations are simpler to use as they do not require calculating the molecular flow rate or incoming air humidity.

For easy reference, the equations are given below [12]:

$$\dot{q} = n^{e}_{total}(1 - X^{e}_{H2O})\left[0.5(E - E^{co})X^{e,d}_{co} + E(X^{i,d}_{o2}\frac{1 - X^{e,d}_{o2} - X^{e,d}_{co2} - X^{e,d}_{co}}{1 - X^{i,d}_{o2} - X^{i,d}_{co2}} - X^{e,d}_{o2})\right] \quad \text{Eq. (1)}$$

From Dlugogorski et al [10], the total molar flows rate for an ideal gas:

$$n^{e}_{total} = m^{e,d}_{air} / (M^{e}_{total} \times M^{i,d}_{air})^{0.5} \quad \text{Eq. (2)}$$

As the total molecular weight M^{e}_{total} differs from $M^{i,d}_{air}$ the relation in Eq. (2) is used to compute n^{e}_{total} with:

$$M^{e}_{total} = X^{e}_{H2O}M_{H2O} + (1 - X^{e}_{H2O})(X^{e,d}_{N2}M_{N2} + X^{e,d}_{O2}M_{O2} + X^{e,d}_{CO2}M_{CO2} + X^{e,d}_{CO}M_{CO}) \quad \text{Eq. (3)}$$

The required 'exhaust' mass flow rate of dry air and 'exhaust' molar fractions of H_2O vapour and dry O_2, CO_2 and CO gasses were determined from measurements taken 180 m downstream from the fire location. These measurements include air velocities, temperatures, and gas concentrations measured, accounting for the travel time of combustion products.

The required molar fraction of dry N_2 at exhaust is determined with the following equation:

$$X^{e,d}N_2 = 1 - X^{e,d}O_2 - X^{e,d}CO_2 - X^{e,d}CO \quad \text{Eq.(4)}$$

Given the measurement uncertainties and the observed profiles of air velocity, temperature, and gas concentration at the D180M downstream location, the calculated HRR was expected to have a relative error of approximately ±10%.

DISCUSSION OF FIRE TEST RESULTS

Figure 10 presents photographs of the tests while Figures 11 to 17 show estimated HRR curves for the tests. Table 2 summaries the peak HRR and integrated calorific energy for each test. Due to the substantial data collected, only the HRR information is presented here. The following paragraphs compare the tunnel conditions with and without FFFS operation.

Figure 10: Photographs of the fire tests.

Table 2: Peak HRR and calorific energy

Test	FFFS/ Nozzle	Fuel load	Discharge density (mm/min)	Approximate activation time (min)	Peak HRR (MW) [b]	Integrated calorific energy (GJ) [a]
1	N.A	HGV	N.A	N.A	150	99.2
2	N.A	VHGV	N.A	N.A	243	193.8
3	Deluge / Directional	HGV	8	4	44.1	52.7
4	Deluge / Directional	HGV	12	4	37.7	46.6
5	Deluge / Directional	VHGV	12	4	30.7	35
6	Deluge / Standard	VHGV	12	4	42.6	51
7	Water Mist / Type A	VHGV	4	4	32	40.7
8	Water Mist / Type A	VHGV	6	4	21	24.4
9	Water Mist / Type A	VHGV	8	4	8	13.2
10	Water Mist / Type B	VHGV	7.5	4	23.2	27.7

Note: [a] Calorific energy is based on 30 minutes burning duration
[b] Peak HRR after FFFD was activated.

Comparison of Free Burning and FFFS Tests (Deluge System)

Comparing HRRs between free burn and fire suppression tests is crucial for ensuring fire and life safety in road tunnels. This comparison provides vital insights into the design fire and capabilities of fire safety equipment, particularly the tunnel ventilation system, in managing fire events.

Figure 11 compares the HRR curves from free burn tests of HGV and VHGV fires with those where a deluge water spray system was activated. The deluge systems used directional nozzles with a water discharge density of 12 mm/min. Both free burn and deluge system suppression tests used the same fuel load types and quantities.

The HRR curves for the HGV and VHGV free burn tests showed faster growth rates than the T-square ultra-fast growth rate, reaching 150 MW and 249 MW respectively. The tests also recorded significant calorific energy: 99 GJ for the HGV and 194 GJ for the VHGV.

During deluge water spray system Test 4 (for HGV) and Test 5 (for VHGV), the systems were activated 4 minutes after fire detection by tunnel ceiling thermocouples. Upon activation, the peak HRRs for the HGV and VHGV fires were 37.7 MW and 30.7 MW, respectively. This represents a 75% reduction for HGV and an 87% reduction for VHGV compared to the free burn tests. The fires' growth rates were also reduced to that of a T-square fast fire, in contrast to the faster-than-ultra-fast growth rates observed in the free burn tests. Additionally, the calorific energies were significantly lower (HGV – 46.6 GJ and VHGV – 35 GJ), compared to the free burn tests.

These tests demonstrate that the deluge water spray system's positive impact on fire and life safety in tunnels by substantially reducing the fire size and HRR.

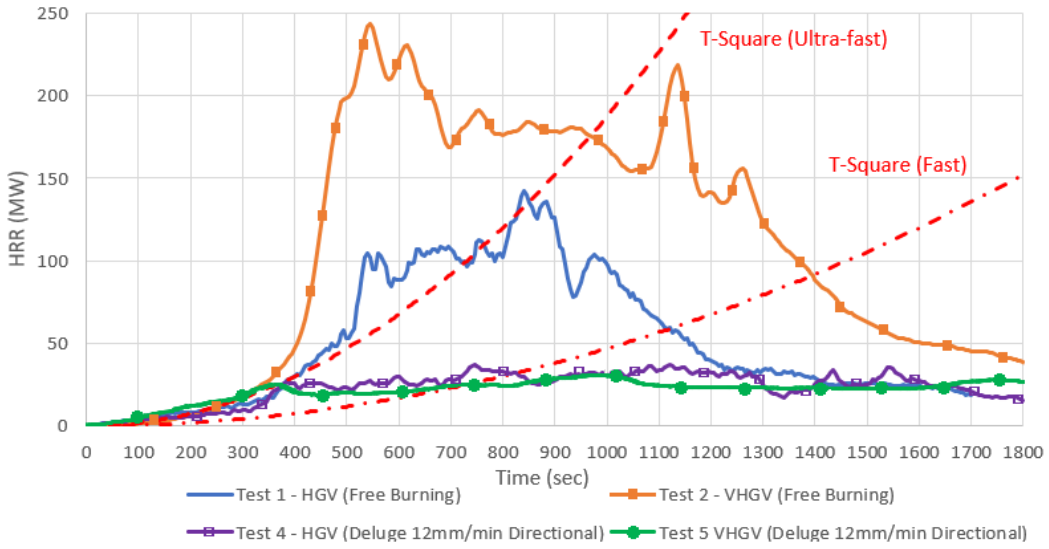

Figure 11: Free Burning and Suppression Tests for HGV Vs VHGV

Comparison of HGV Fire Tests with Different Discharge Density (Deluge System)

This section compares the fire test results conducted on an HGV with varying deluge system water discharge densities and assess their performance in controlling an HGV fire.

Two water discharge densities of 8 and 12 mm/min were tested using directional nozzles. In both tests, the fuel type and quantity were consistent. The deluge systems were activated 4 minutes after fire detection by thermocouples located at the tunnel ceiling.

At both discharge densities of 8 mm/min (Test 3) and 12 mm/min (Test 4), the fires exhibited a T-square fast growth rate, reaching peak HRRs of 44.1 MW and 37.7 MW, respectively, as shown in Figure 12. While the results did not show significant differences in fire suppression effectiveness, these tests suggested that increasing the amount of water would result in a reduced peak HRR and a lower amount of fuel load burned (i.e., 6.1 GJ or less). Further validation of this observation would be beneficial through a similar test with a deluge discharge density of 6 mm/min.

According to NFPA 502, the tested deluge water spray systems using directional nozzles and discharge densities can be classified as a 'fire control system' within the category of fixed water-based firefighting systems, when activated within 4 minutes of fire detection.

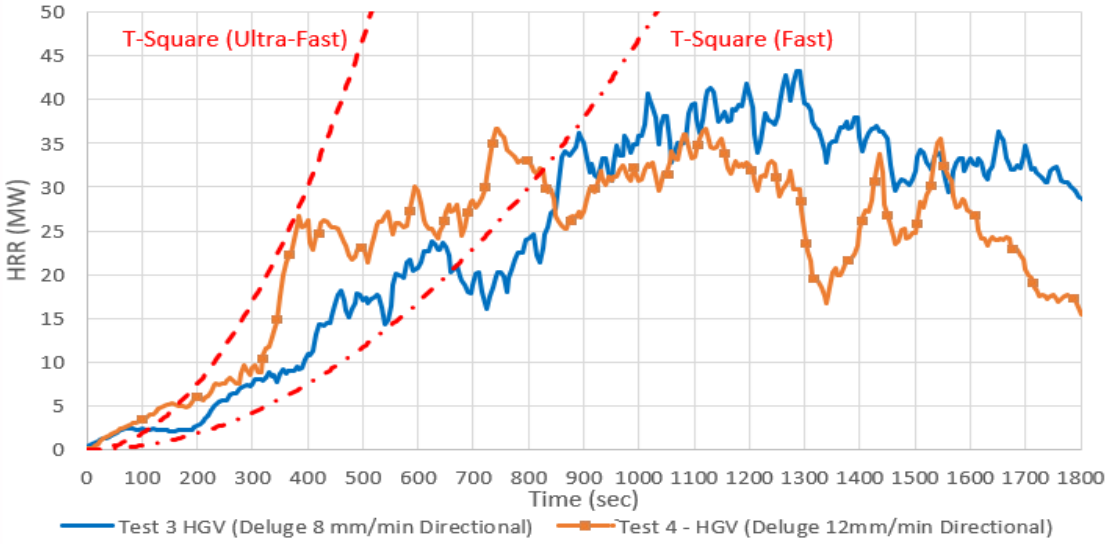

Figure 12: Different deluge discharge density tests on HGV fire

Comparison of VHGV Fire Tests Using Different Deluge Nozzles

This section compares the fire test results on a VHGV with deluge water spray systems using two types of nozzles: directional and standard. Both tests used a discharge density of 12 mm/min. In both tests, the fuel load type and quantity were consistent. The deluge systems were activated 4 minutes after fire detection by thermocouples at the tunnel ceiling.

Before the deluge system was activated, both tests exhibited a T-square ultra-fast fire growth rate, as shown in Figure 13. After activation, the HRR curves initially dropped and then rose to a 2nd peak of 30.7 MW for the directional nozzles (Test 5) and 3rd peak of 42.6 MW for the standard nozzles (Test 6). These later peaks may be attributed to the combustion of the subsequent pallets' stacks and the burnt pallets that had fallen during the tests. The fires' growth rates transitioned from a T-square ultra-fast fire to a T-square fast fire after deluge system activation. In addition to the lower peak HRR, the deluge system with directional nozzles demonstrated higher efficiency, with a lower integrated calorific energy of 35 GJ compared to the 51 GJ for the standard nozzles. The superior performance of directional nozzles could be attributed to their more efficient and narrower spray pattern, as shown in Figure 14, enhancing their suppression and gas cooling capabilities.

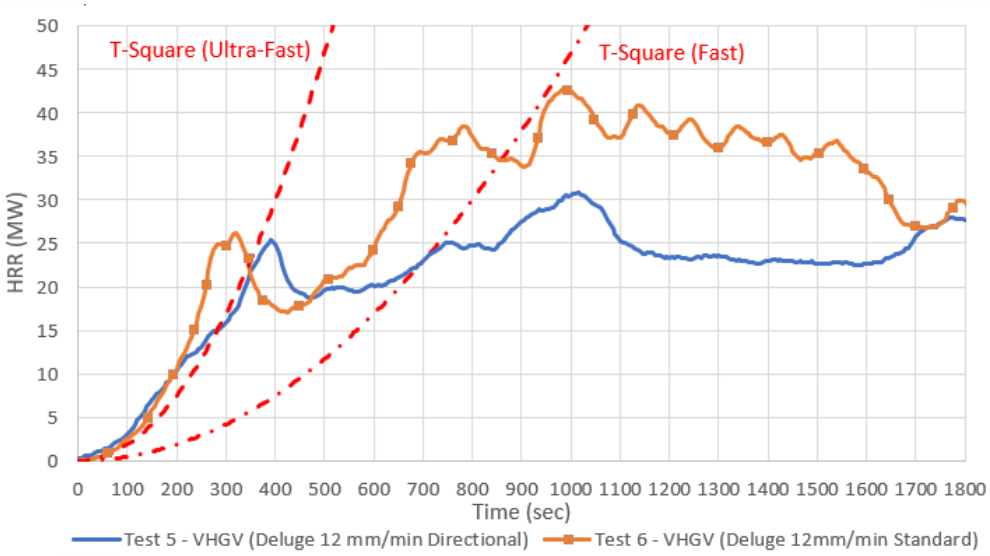

Figure 13: Different types of deluge nozzles tests on VHGV fire

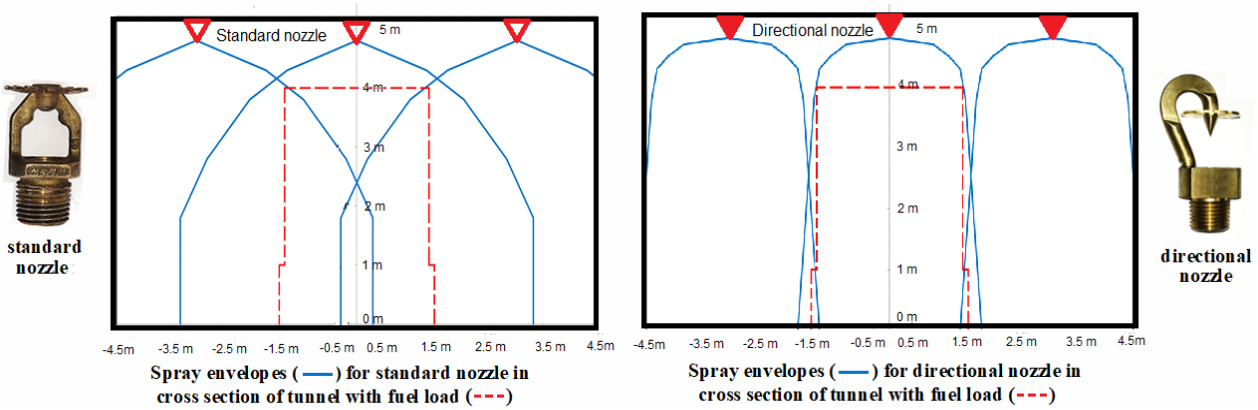

Figure 14: Spray envelopes of standards and directional nozzles [14].

Comparison of VHGV Fire Tests with Different Discharge Density (Water Mist System)

This section compares the fire test results on a VHGV with the varying the water mist system discharge densities and assesses their performance in suppressing a VHGV fire.

The fire tests used water mist systems discharging water at densities of 4, 6, and 8 mm/min, respectively. In all the tests, the fuel load type and quantity were consistent. The deluge systems were activated 4 minutes after fire detection by thermocouples at the tunnel ceiling.

Figure 15 (Test Nos. 7, 8 and 9) shows that as the discharge density increased, both the peak heat release rate (Test 7 - 32 MW, Test 8 - 21 MW, Test 9 - 8 MW) and calorific energy decreased (Test 7 - 40.7 GJ, Test 8 – 24.4 GJ, Test 9 – 13.2 GJ) due to more water being applied to the burning fuel load (Table 2). This trend is evident from the photographs below, which show fewer pallets were consumed by the fire when more water was applied.

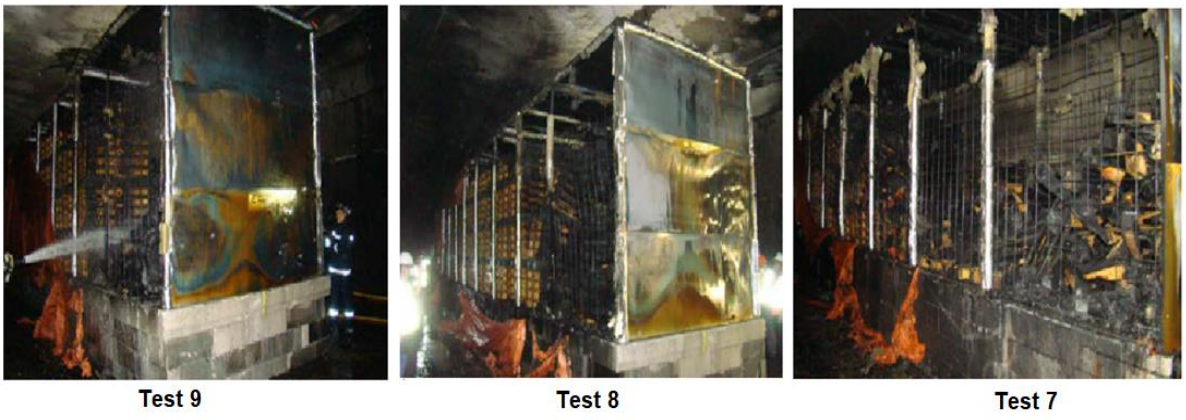

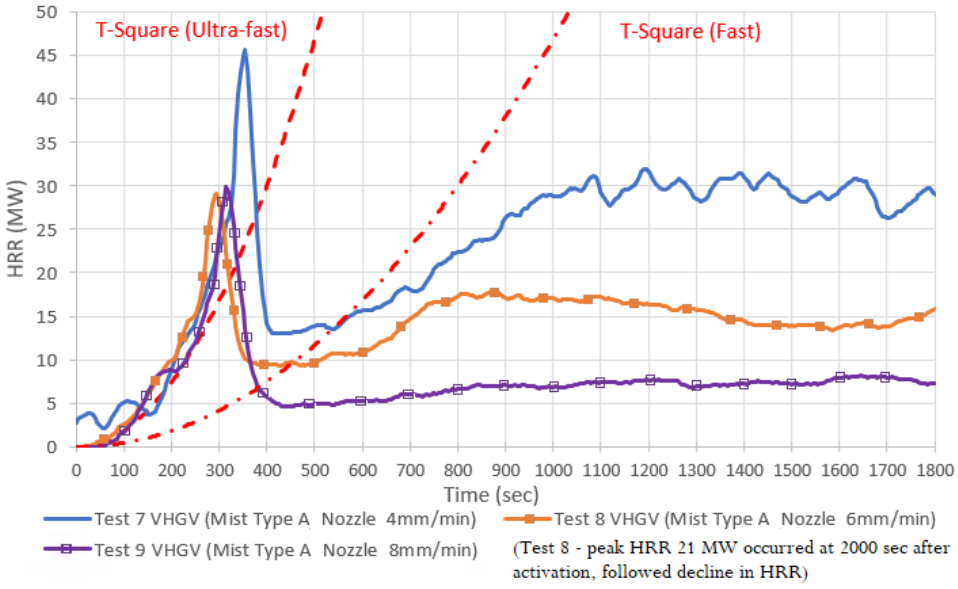

Figure 15: Water mist with different discharge densities tests on VHGV fire.

Comparison of VHGV Fire Tests Using Deluge Water Spray System vs Water Mist System

This section compares deluge water spray and water mist systems in controlling VHGV fires. Liu and Kim [15] note that water mist systems produce droplets smaller than 1000 microns, while conventional nozzles generate larger droplets of approximately 5000 micron. The smaller droplets create a larger surface area, enhancing evaporation and heat absorption. This characteristic allows the water mist system to effectively suppress a large area of the fire using lesser amount of water.

The comparison between deluge water spray and water mist systems utilized identical test conditions, including fuel type, quantity, and a 4-minute delay in system activation after fire detection. Results from two deluge water spray system tests (Test 5 with directional nozzles and Test 6 with standard nozzles, both at 12mm/min discharge density) demonstrated their effectiveness as 'fire control systems'. This effectiveness was evidenced by a slight initial increase in the HRR of the VHGV fire post-activation, followed by stabilization. Peak HRRs were recorded as 30.7 MW for directional and 42.6 MW for standard nozzles.

Water mist system tests using Type A nozzles (Test 8) and Type B nozzles (Test 10) employed lower discharge densities of 6 mm/min and 7.5 mm/min respectively, compared to the deluge water spray system tests (12 mm/min for Tests 6 and 7). Both water mist systems effectively controlled the HRR upon activation. The water mist systems demonstrated superior efficiency, achieving lower peak HRRs and integrated calorific energy: 21 MW and 24.4 GJ for Type A nozzles and 23.2 MW, and 27.7 GJ for Type B nozzles. In comparison, the deluge water spray systems recorded higher values: 30.7 MW and 35 GJ for directional nozzles, and 42.6 MW and 51 GJ for standard nozzles. The water mist systems with both nozzle types functioned as 'fire suppression systems' in these tests. Figure 17 illustrates that these systems effectively controlled the VHGV fires using less water than the deluge systems with either nozzle type.

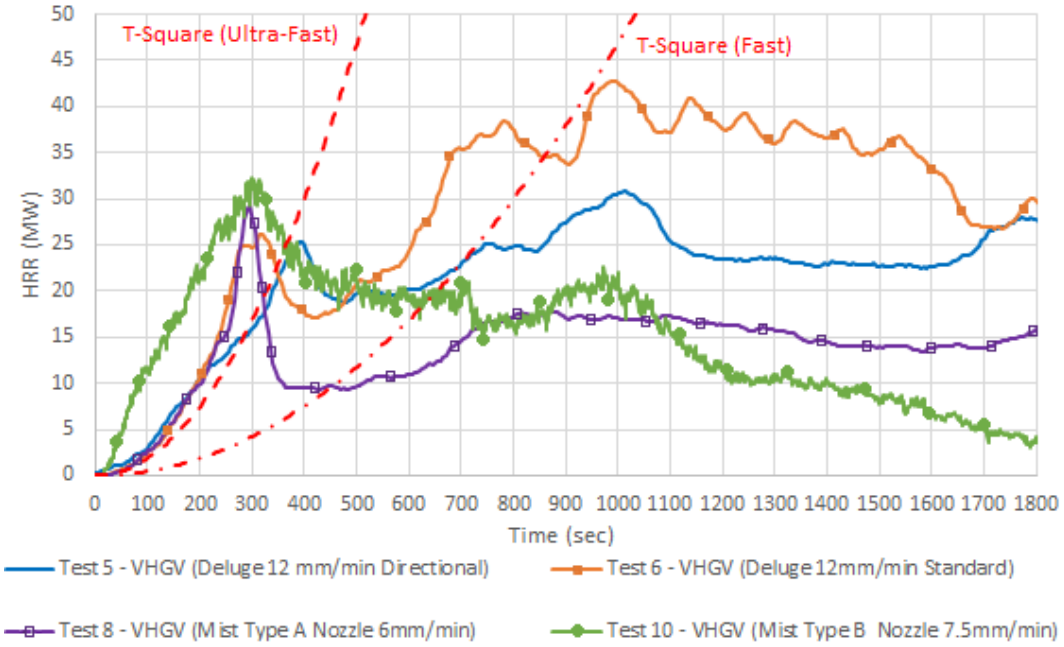

Figure 17: Deluge vs water mist tests on VHGV fire

From an installation perspective, the water mist systems detailed in this paper are easier to install than the deluge water spray systems, as illustrated in Figures 7, 8 and 9. The water mist system nozzles have a 6 m throw, requiring only two rows of range pipes, while the deluge system with a 3 m throw, needs three rows of range pipes for the road tunnel section. Reducing the number of range pipes is particularly advantageous during the upgrading of existing road tunnels, as it minimises tunnel downtime for the installation of the FFFS. The reduction in installation time is more significant with wider tunnels. For instance, an 18 m wide 3-lane road tunnel requires three range pipes for the water mist system, compared to the six range pipes for the deluge system.

Furthermore, the water mist system utilises smaller components, such as smaller control valves and smaller diameter pipes, further contributing to easier installation. It also requires a smaller water storage tank, leading to a reduced plant room footprint compared to the deluge water spray system. This is crucial for retrofitting and expanding existing road tunnel projects, where additional plant room space may not have been considered into the tunnel's original design. During upgrading of existing road tunnels, the tunnel drainage system may struggle to handle the significantly higher water discharge rate

of a deluge water spray system. Installation of a water mist system with lower discharge density could provide a solution. All the above highlights the importance of considering installation ease and infrastructure requirements when choosing a fire suppression system for road tunnels.

CONCLUSIONS

This paper compares the fire suppression and control performances of water mist systems and deluge water spray systems using results from large-scale fire tests conducted on mock-ups of HGVs and VHGVs in test tunnels. The tests found that both deluge water spray and water mist systems significantly reduced the heat release rates of HGV and VHGV fires, demonstrating their critical role in fire suppression. The tests also found that the varying the water discharge densities can impact the performance of both types of systems in controlling the fire. Increasing the water density resulted in lower heat release rates and reduced calorific energy.

Comparison of VGHV fire tests between deluge water spray and water mist systems showed that water mist systems required less water to control a VHGV fire compared to the deluge system. In summary, these tests provide valuable insights into the performance of deluge water spray and water mist suppression systems and their impact on fire control and safety in road tunnels.

REFERENCES

1. The Mont Blanc Tunnel Fire of 1999 - Online Safety Trainer, Access date: 2nd October 2023.
2. Up to 20 die in Swiss tunnel fire | World news | The Guardian, Access date: 2nd October 2023.
3. NFPA 502 [2023], Standards for Road Tunnels, Bridges and Other Limited Access Highways.
4. M. K. Cheong and et al, " Heat Release Rates of Heavy Goods Vehicle Fire in Tunnels with Fixed Water Based Fire-fighting System", Fire Technology, 50, 249–266, 2014.
5. M K Cheong and et al, "Heat Release Rates of Heavy Goods Vehicle Trailer in Tunnels with Fixed Water-based Fire Fighting System", 18th ISAVFT 2019, 25-27 September 2019.
6. Ingason H and Lonnermark A (2005), "Heat release rate from heavy goods vehicle trailer fires in tunnels" *Fire Safety Journal*, Vol 40, Issue 7, pp 646-668.
7. Dusseldorf, Eureka Project EU 499: FIRETUN, "Fire in Transport Tunnel", November 1995.
8. NFPA 750, Standard on Water Mist Fire Protection Systems, edition 2015.
9. Arthur. E. Cote and et al, Fire Protection Handbook, 19th edition Volume II, Chapter 11 Automatic Sprinkler Systems, NFPA.
10. Leander Noordijk and et al, "Time-Temperature Curve for Fires in Tunnels with Deluge System", SITCE Conference, October 2016.
11. M.K Cheong, M Thong, Soh L.T, Sng C.H, "Keeping Track", Fire prevention fire engineers journal, October 2007.
12. Dlugogorski B Z, Mawhinney J R and Duc V H, "The measurement of heat release rate by Oxygen consumption calorimetry in fires under suppression", Fire safety science – proceeding of the fourth international symposium pp 877 – 888, 1994.
13. Parker W.J, "Calculation of the Heat Release Rate by Oxygen Consumption for Various Applications", U.S. Department of Commerce, NBS, NBSIR 81-2427, 1-38, Feb, 1982.
14. F Tarada and et al, "The Effect of Nozzle Design on the Fire Heat Release Rates in Tunnel Deluge Systems" 18th ISAVFT 2019, 25-27 September 2019.
15. Liu, Z., & Kim, A. K. (2000). A Review of Water Mist Fire Suppression Systems—Fundamental Studies. Journal of Fire Protection Engineering, 10(3), 32-50.

Key findings from fire testing of water-based fixed fire fighting systems in a medium scale tunnel

Ying Zhen Li, Haukur Ingason, Joel Blom, Magnus Arvidson & Michael Försth
RISE Research Institutes of Sweden
Box 857, SE-501 15 Borås, Sweden
E-mail: yingzhen.li@ri.se

ABSTRACT

This paper summarises both small scale laboratory tests and medium scale tunnel fire tests. The main efforts are, by adopting the Froude scaling, seven series of tests conducted in a 49.2 m long container tunnel with a scale of 1 to 3. This paper presents results on the influence of low pressure, medium pressure and high pressure water-based fixed fire fighting systems (FFFSs) on fire development, fire spread to adjacent vehicles, structural protection, tenability, smoke control, spray deflection and spray resistances. The focus is to compare the performance of three default FFFSs and to evaluate the efficiency of each of the FFFS. The results show that the default low pressure FFFS performs well in term of suppressing the fire development, preventing the fire spread to nearby vehicles, providing tenable conditions for evacuation and rescue service, protecting tunnel structure and easing the problem with spray deflection due to tunnel ventilation. The default high pressure FFFS usually perform poorly while the default medium pressure FFFS usually lie in between.

KEYWORDS: Fire suppression, fire spread, critical velocity, tenability, spray deflection

INTRODUCTION

To meet the increasing needs of fast transportation, tunnels and underground structures are increasingly being built worldwide. Meanwhile, numerous catastrophic tunnel fires have occurred over the past decades, causing huge life and economic losses. For example, in the Mont Blanc tunnel in 1999, 34 vehicles caught fire, resulting in 39 casualties, a 900 m long severely damaged structure and 3 years closure [1]. These incidents have increased interest in the use of water-based fixed fire fighting systems (FFFSs) in tunnels. As an example, the Swedish Transport Administration has planned to use FFFS for the Stockholm Bypass and also for upgrading old road tunnels in Sweden [2]. It is recognized that FFFS can limit the fire growth rate and fire size, prevent the fire from spreading to adjacent vehicles, and protect the tunnel structure. Additionally, for vehicles with new energy carriers, FFFS has a great potential to minimize the risks of pressurized tank rupture and thermal runaway [3].

FFFS can be divided into low pressure and high pressure FFFS, depending on system operating pressure and water droplet size [1]. Besides, there exists also a low pressure water mist system, which we may call a “medium pressure system”. Low pressure FFFS in buildings and warehouses have been used for over 100 years while high pressure FFFS started to be used in the 1990s [4]. Japan introduced low pressure FFFS into its high-risk urban tunnels in 1963, and Australia has installed low pressure FFFS into road tunnels since 1992 [1]. Then some European countries also started to use FFFS in tunnels while most of them are high pressure FFFS. Despite many installations, there is a lack of knowledge on how to design and optimize FFFS in road tunnels. Most projects with FFFS requires full scale fire tests to validate its performance (see e.g.,. [1, 5-8]). The key mechanisms and technical issues related to FFFS in tunnels have not yet been well understood.
An evaluation of the conceptual difference between these systems in form of pressure and droplet size is of importance for tunnel fire safety. As the full scale testing is usually related to a narrowly focused testing of a given FFFS for a given tunnel project and not so much research oriented results aimed at comparison of systems, the use of 1:3 scale is a viable option at this stage. Many small scale studies

are available in the literature but raising it up to 1:3 scale is a necessary step forward. A comprehensive full scale study with a detailed parametric study as given here is difficult to accomplish, unless industry, research community and authorities decide to go for such research program. At this stage this study will work as knowledge gap finder related to the conceptual difference and the results should be a beacon for future full-scale studies.

The increased use of underground structures, together with several catastrophic fires occurred in such structures historically, calls for experimental and theoretical studies of fire mitigation mechanisms and performance of different FFFSs in tunnels, and the interaction mechanisms between ventilation system conditions and FFFS.

The objective of this study is to systematically investigate the mechanisms and performance of different water-based Fixed Fire Fighting Systems (FFFS) in tunnels by focusing on the conceptual difference between the systems rather than the exact design in a real tunnel project. More specifically, it is to study the influence of low pressure, medium pressure and high pressure FFFSs on fire development, fire spread to adjacent vehicles, structural protection and tenability, the interaction mechanisms between tunnel ventilation and FFFSs, and the use of computer tools to model FFFSs in tunnels. The aims are not only to improve the understanding of primary mechanisms and performance of these systems but also to provide technical solutions and guidance for the optimized design with the ultimate goal to improve the safety levels of tunnels and other underground structures.

FIRE TESTS

Material property tests

A number of tests were performed to characterize the pyrolysis model for wood and High-Density Polyethylene (HDPE) [9]. The pyrolysis kinetics parameters were tested based on Thermal Gravimetric Analysis (TGA) and Differential Scanning Calorimetry (DSC). TGA measures the mass of the sample exposed to a continually increasing temperature in either an inert environment (nitrogen) and under ambient conditions. An example of mass percentage, α, at different temperature rise rate, β (K/min), is given in Figure 1 for HDPE in nitrogen and in the air. Different oxygen concentrations were also tested to understand the oxidation behaviours of the wood char. In addition, thermal conductivity was measured using both Transient Plane Source (TPS) and Transient Line Source (TLS) for wood and HDPE. These tests provide thermal physical properties and the kinetic pyrolysis parameters for the fuels used in this project.

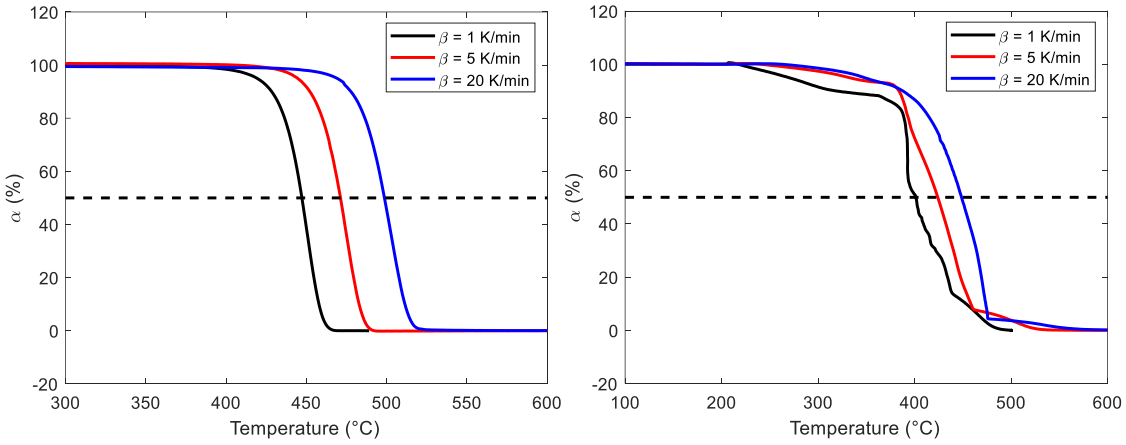

(a) Nitrogen (b) Air

Figure 1. Mass percentage vs. time for HDPE in various TGA test scenarios [9].

Cone calorimeter tests

Cone calorimeter tests were conducted for wood and HDPE using heat fluxes of 50 kW/m^2 and 75 kW/m^2, respectively to obtain necessary information for CFD modelling. In the tests, the burning of the HDPE sample resulted in too large fires and the tests had to be terminated after about 15 min when

using a heat flux of 50 kW/m^2, and after about 10 min when using 75 kW/m^2. As as an example, see *Figure 2*. The relevant results are summarized in reference [10].

Figure 2. The HDPE sample after the cone calorimeter test under 50 kW/m^2.

Spray tests with a water collection pan

The water densities below the nozzles were measured using a specially designed pan (see Figure 3). The pan was placed directly below the nozzle at a vertical distance between 10 – 16 cm. The distance is chosen such that almost all of the droplets were collected by the pan. The relevant results are summarized in reference [10].

Figure 3. Measurement of the water density below the medium pressure nozzle at 2.9 bar.

Water droplet characteristic tests

The distribution of water droplets and their velocities were tested using shadowgraph. The results are presented in reference [11]. The experimental set-up was configured to allow the characterization of water sprays produced by the injection of water into quiescent air at injection pressure ranging between 0.39 bar and 11.5 bar. The experimental set-up consisted of a pressurized liquid source, an electrically driven reciprocating pump, a pressure regulator, a flow meter, a nozzle, a high speed camera and optics. Measurements were done 500 mm downstream the nozzle exit and at three radial positions: 0 mm, 300 mm and 600 mm from the injection axis. A sketch of the measuring equipment in relation to the spray pattern is depicted in *Figure 4*.

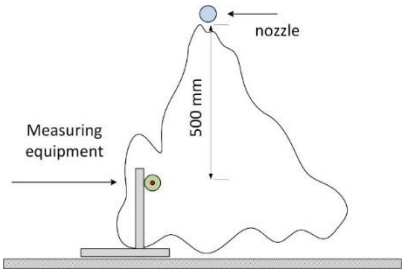

Figure 4. Sketch showing the placement of equipment in relation to spray pattern [11].

Tunnel tests

The Froude scaling was applied in the tunnel tests. The geometrical scale was 1:3. Previous research involving tunnel fires shows a good correlation between model and full scale on many focused issues [12, 13]. Scaling of FFFS has also been successfully applied, see for example [14] and [15]. The

scaling ratio of 1:3 was applied since a good correlation can be found by comparing the suppression results between this scale [15] and full scale [7]. In some tests with idle wood pallets as the fuel, the scaling method developed for wood pallet fires [16] was applied. Details about the Froude scaling can be found in the literature [1]. The length scaling ratio was 1:3 (1 length unit in model scale tunnel corresponds to 3 length units in full scale tunnel) which results in the following: time, velocity and water density are the square root of the length scale (1.73 times), water operating pressure is the length scale (3 times), and HRR is 5/2 power of the length scale (15.6 times). Gas temperatures and gas concentrations are approximately the same in both scales.

Seven series of tests were conducted for each FFFS system: Test series 1 – 4 (fire suppression tests), Test series 5 – Smoke control tests, Test series 6 – Spray deflection tests, Test series 7 – Spray resistance tests. In test series 6 and 7, no fire test source was used. In most of the fire tests, solid fuels were used as they are common fire loads in tunnels, but liquid fuels and gaseous fuels were also tested. Different FFFSs, water densities, ventilation conditions and activation times were tested.

The test tunnel was 49.2 m long, 2.39 m high and 2.35 m wide, as shown in *Figure 7* . It was constructed using regular freight containers. The tunnel ceiling and the upper parts of the tunnel walls (a height of 0.6 m) was protected with 10 mm thick Promatect H boards, within -2 m and +4 m from fire source center (x=0 m). Within -1.5 m and 1.5 m, the floor was also protected to avoid damage. Various longitudinal ventilation velocities were tested, ranging from 0.6 m/s to 5 m/s. However, in most of the tests, the velocity was within 1-2 m/s. Two electric fans were placed outside of the tunnel inlet to create longitudinal flows in the tunnel. In most of the tests, two perforated plates were used to control and uniform the air flow.

Different types of fire sources were tested, including idle wood pallets, wood/plastic cribs, pool fires and gas fires. Gas fires were mainly used for test series 5 where smoke control was evaluated.
The fire test sources were placed at around 26.5 m from the left tunnel portal, close to the middle point of the tunnel, see Figure 5. For the fires with idle wood pallets and wood/plastic cribs, the fire test sources were placed on a platform and near a wall, as shown in Figure 5. The platform consisted of a 0.55 m high steel frame and two layers of 10 mm thick Promatect H boards. In the tests with solid fuels, 2 mm thick steel covers were used to simulate heavy goods vehicles, as shown in Figure 5. Side curtain heavy goods vehicles (HGVs) with a roof are commonly used due to the convenience of loading. There are also many HGVs having tarpaulins on both sides and the tops. The front and back sides, however, are typically closed with plates. Therefore, in all tests, the front and the end covers were used. In most of the tests, a solid top cover was also applied. Note that a completely closed HGV, e.g. a steel container truck, is considered to provide a lower fire hazard, and thus not of key interest and therefore not tested in this study. Two small liquid pans were used as the ignition source, each having dimensions of 100 mm (L) × 250 mm (W) × 30 mm (H). In the wood pallet fires, each pan was filled with 150 mL heptane. In the wood crib tests and wood and plastic crib tests (see Figure 6), each pan was filled with 300 mL of commercial grade heptane as it was more difficult to ignite the wood crib. However, in one test 450 ml of heptane was used. In the gaseous fire and liquid pool fire tests, the fire test sources were placed along the longitudinal centerline of the tunnel. In liquid pool fire tests, a rectangular pool with dimensions of 0.8 m (W)×0.5 m (L) ×0.12 m (H) was used and heptane was used as the fuel. The fire size was estimated to be about 1.3 MW, corresponding to full scale fire of about 21 MW. In the tests with FFFS, 25 litres of fuel were used, while 35 litres were used in the free burn test. The pan was placed on the floor. For gaseous fires, a gas burner with dimensions of 0.45 m × 0.45 m × 0.30 m was placed on the floor. Propane was used as the fuel. The bottom of the burner was empty to allow around 100 mm high water filling. This was to avoid the influence of filled water on the fuel flow. Six wood samples were placed downstream of the main fire load at a height of around 1.6 m above floor in order to determine any fire spread. These samples had dimensions of around of 0.045 m (W) × 0.045 m (L) × 0.005m (H).

Three types of FFFS systems were tested. Each system had two longitudinal rows of nozzles covering a spray region of 9.4 m, corresponding to 28.2 m in full scale, as shown in see *Figure 7*. Each row consisted of eight nozzles. The spacing between the nozzles was 1.175 m, corresponding to 3.525 m in

full scale. A summary of the nozzles tested for various FFFSs is given in Table 1. The water pipes were made of stainless steel.

Three FFFSs were selected to represent a range of system types used in road tunnels, namely the default low pressure system, the default medium pressure system and the default high pressure system, having a water discharge density of 10 mm/min, 6.8 mm/min and 3.7 mm/min, respectively in full scale. Other water discharge densities were also tested to explore their effects, as well as the ventilation velocity and the activation criterion. Various fire test scenarios were considered, i.e., idle wood pallet fires simulating densely packed fuels, wood crib fires and wood and plastic crib fires simulating loosely packed fuels, and heptane pool fires, with or without a top cover of the solid fuel. The length of the deluge zone of the FFFS was 9.4 m, corresponding to 28.2 m in full scale.

Table 1. Summary of nozzles tested for various FFFSs.

FFFS System	Nozzle	Spray angle	K-factor	Diameter of narrowest hole	Operating pressure	Water density (model scale)	Water density (full scale)
			L/(min·bar$^{1/2}$)	mm	bar		mm/min
Low pressure	BETE MP156	120°	8.8	3.97	0.39	**4.0**	6.85
					0.82	**5.8**	10
					1.5	7.8	13.5
High pressure	Lechler 502.448	~130°	0.88	0.5	11.5	**2.2**	3.7
					20.5	**2.9**	5.0
Medium pressure	BETE WL1	120	2.35	2.08	2.9	**2.9**	5.0
					5.4	**4.0**	6.85
					11.5	5.8	10

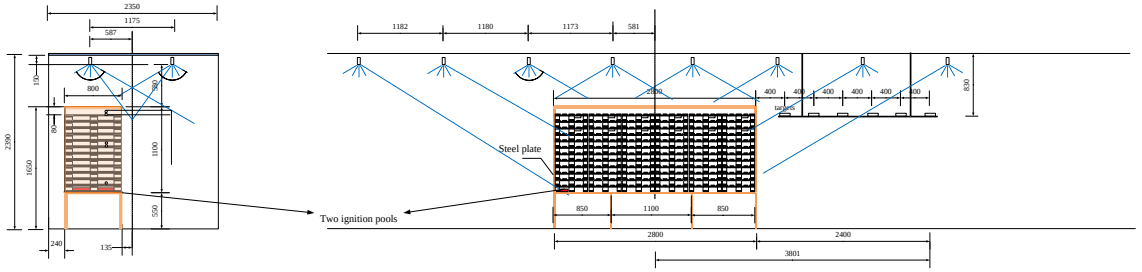

Figure 5. Fuel arrangement for the idle wood pallet test fires. Nozzles are also indicated.

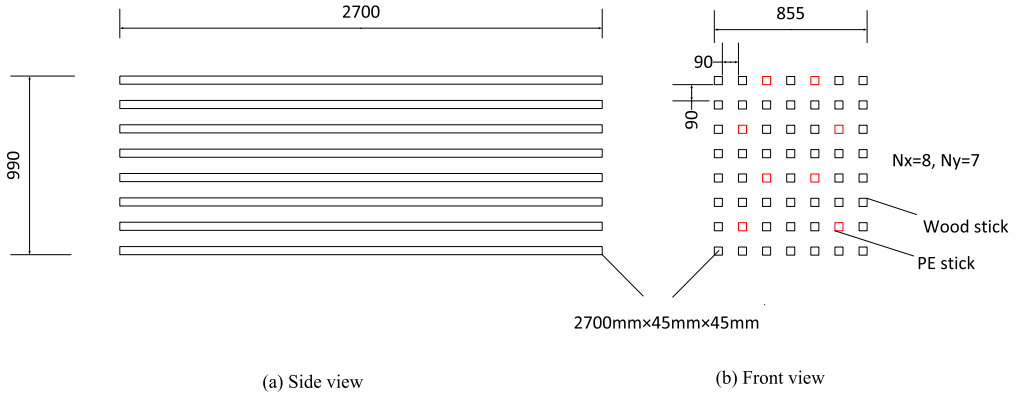

Figure 6. Detailed drawing of the wood/plastic crib.

In the tests, the gas temperature, gas concentrations, heat flux, light attenuation, and gas velocity were measured at various positions (including at the ceiling and at human height levels), and the heat release rate was measured using oxygen consumption calorimetry, also considering CO, by sampling close to the downstream tunnel portal (see *Figure 7*). Video cameras were placed both upstream and downstream to monitor the smoke movement and the fire development. For comparison, some free-burn tests were also conducted. All ceiling thermocouples were placed 150 mm below the ceiling,

except at thermocouple trees Pile A and Pile B. Thermocouple trees were placed at around 3.3 m upstream of the fire, and at 9.7 m and 16.7 m downstream of the fire. At Pile B, the gas analysis probes were placed at the centreline of the tunnel, and the bi-directional tubes and thermocouples were placed horizontally 50 mm from the gas analysis.

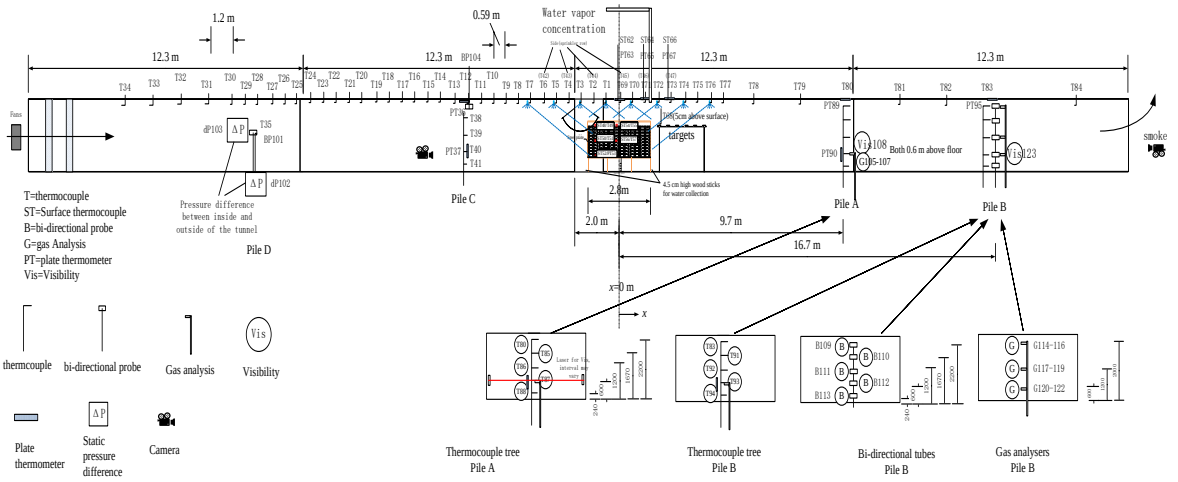

Figure 7. Instrumentation and measurements.

The FFFSs were activated when the maximum ceiling gas temperature reaches the detection temperature, mostly 141 °C, in accordance with the previous full scale tests [17, 18] and model scale tests [19, 20]. In some wood crib fire tests, a higher fire detection temperature of 300 °C was applied. In test series 4 with pool fires, the ceiling gas temperature at the early stage was not so high, and a fixed activation time of 3.5 min was used, corresponding to a gas temperature of around 100 °C.

RESULTS FROM TUNNEL TESTS

Key results and findings from these tunnel tests are presented below. More detailed results can be found in Ref. [21] and Ref. [22]. The relevant numerical simulations are presented in Ref. [10].

Free burn tests

The HRR curves from the free burn tests at a velocity of about 1.8 m/s are shown in Figure 8 and Figure 9 for wood pallet fires, Figure 10 for wood crib fires, Figure 11 for wood/HDPE crib fires and Figure 12 for heptane pool fires. In the wood pallet free burn fire test, the fire develops steadily up until 16.5 min (around 4 MW). At 17.5 min, the HRR reaches 5 MW, and 0.1 min later (17.6 min) the HRR suddenly rises to 6.3 MW (98 MW in full scale). This peak should be related to the collapse of the first wood pile on the upstream side, leading to a sudden increase in fuel surface area and an increase in HRR, as was noticed in previous tests [16, 23]. In general, the peak HRR correlates well with previous free burn test in 1:4 scale where the obtained peak HRR was 96 MW in full scale [20]. In the wood/HDPE crib free burn fire test, the maximum HRR is 7.5 MW, slightly lower than the previous estimate of 8.4 MW. This should be related to the use of upper limit for wood as stated above. If 165 kW/m^2 is used for heat release rate per unit area of wood, the heat release rate becomes 7.7 MW, much closer to the measured value of 7.5 MW in this test. The contribution from the HDPE to the HRR is rather significant, i.e., a volume portion of HDPE of only 14% contributes to about 50% to the total HRR. This fact has not been considered fully in full scale tests with FFFS systems. This has been a challenging scenario in testing and the use of pure wood pallets as a test commodity been accepted as can be seen in SOLIT guidelines [24] as well as NFPA502 [25]. In the heptane pool free burn fire test, the maximum HRR is around 0.9 MW before 13 min, but it rises to about 1.4 MW within a very short period. This phenomenon has also been observed in previous tests, e.g. [26] and could be attributed to enhanced heat transfer when the fuel layer becomes thin at the final stage of a pool fire [26].

Fire suppression performance

The performances of the three default FFFSs in the idle wood pallet fires without the top cover are compared in *Figure 8*. The HRR at activation is within 0.3 MW – 0.4 MW, as mentioned earlier. It is shown in *Figure 8* that the fire is effectively suppressed by the low pressure system. By contrast, when the high pressure system is activated, the fire continues to increase until it reaches a peak of 3.7 MW at 33 min. For the medium pressure system, a peak HRR of 1.4 MW is reached at 23 min. Clearly, in terms of reducing the HRR, the low pressure system performs the most efficient, the medium pressure system performs moderately well, and the high pressure system performs the less efficient.

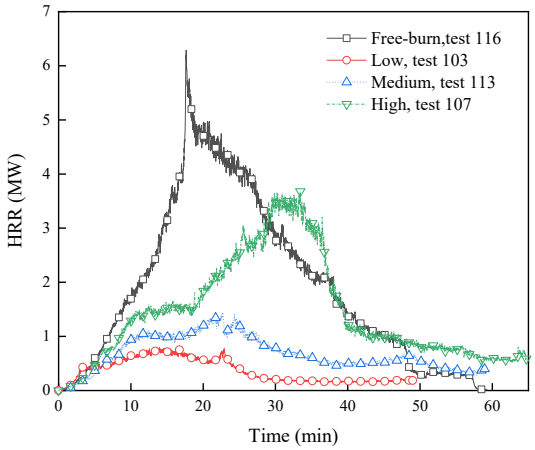

Figure 8. HRRs in wood pallet tests with various FFFSs and without top cover (u_o=1.8 m/s) [21].

The results for the three default FFFSs using the idle wood pallet fires with the top cover at 1.8 m/s are compared in *Figure 9*. The HRR at activation is within 0.3 – 0.4 MW, as mentioned above. The maximum HRRs for the default low, medium and high pressure systems are within 2.6 – 2.7 MW. They are rather close to each other, and only show an insignificant decrease of HRR with the increasing water density. The fire curves are also similar. The low pressure system performs better than the others at the early stage (before 12 min). However, between 12 min and 26 min, the medium pressure system performs better. After 26 min, the HRR curves for the low and medium pressure systems are close to each other. Between 12 min and 20 min, the HRRs for the low and high pressure systems are almost identical.

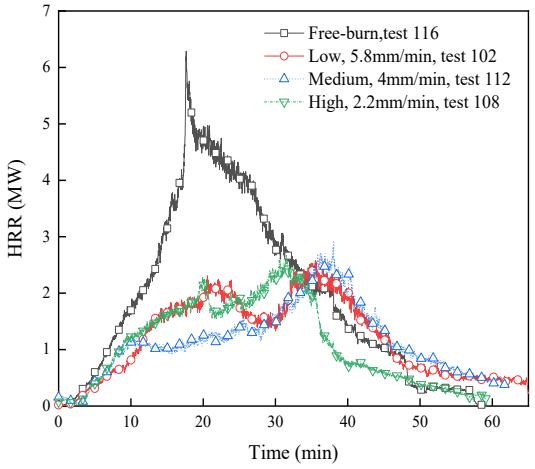

Figure 9. HRRs in the idle wood pallet tests with various FFFSs with top cover (u_o=1.8 m/s) [21].

For the wood crib fires, the HRR at activation is around 0.5 MW. In these tests, the maximum HRRs for the default low, medium, and high pressure systems are 0.9 MW, 1 MW and 2.8 MW, respectively. Overall, the default low pressure system performs satisfactory, and the fire is completely extinguished after around 7 min. The medium pressure system also performs relatively well. The fire with the medium pressure system is effectively suppressed but not extinguished after the system activation. For the high pressure system, the fire continues to burn intensely after the system activation, and reaches a

maximum HRR of 2.8 MW at 7.6 min.

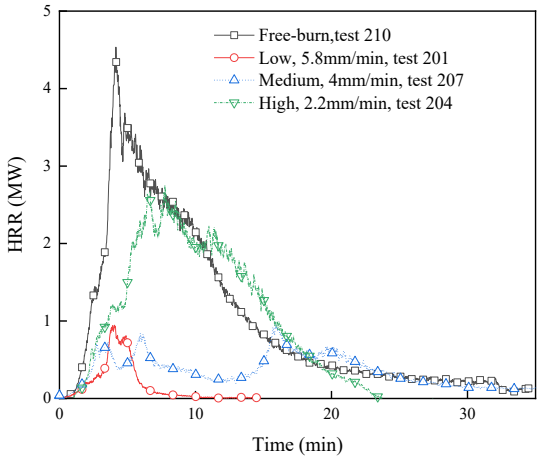

Figure 10. Comparison of HRRs for various FFFSs in the wood crib fires with top cover [21].

For the wood and HDPE crib fires, the results show that the default low pressure system performs better than the other two systems. By contrast, the HRR curve for the high pressure system is close to the free burn test. The performance of the medium pressure system is slightly better than the high pressure system. The results are consistent with those for the wood crib fires. Due to the presence of the plastics (HDPE), complete suppression of the fire becomes more difficult as for plastics a higher water density is required for effective suppression, compared to wood [27]. The water densities used for the default medium and high pressure systems seem to be insufficient to provide fire suppression.

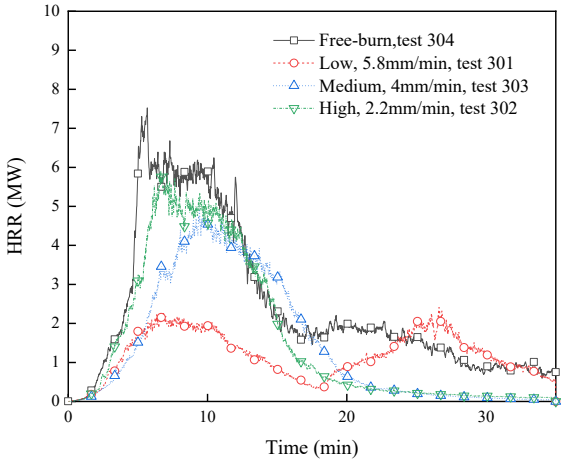

Figure 11. HRRs in wood and plastic crib tests with various FFFSs and the top cover. Data from the free-burn test is plotted for comparison.

In the heptane pool fire tests, for the low and medium pressure systems, the HRR decreases immediately to around 0.3 MW after the activation. The HRR for the high pressure system is close to the free burn test. For the low and medium system, the HRR is reduced by around 50% compared to the free burn HRR of 0.9 MW at the early stage, while the value is around 20% for the high pressure system.

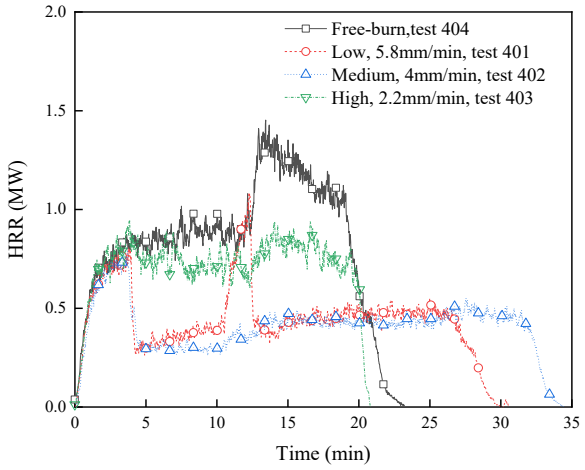

Figure 12. HRRs in heptane pool fire tests with various FFFSs. Data from the free-burn test is plotted for comparison.

Fire spread obervations

A summary of results related to the occurrence of fire spread based on visual observations of the wood samples (targets 1 to 6) after the fire tests is given in *Table 2* [21]. "No" indicates that the target was not affected by the fire. "Burnt" indicates that the target was completely burnt, however, if only part of the target was burnt, the approximate percentage of the burnt part based on visual observations is given. "Charred" indicates that the target was only charred but not burnt. Note that in the pool fire tests, the fire spread was not tested due to the different positions of the fire test source. It is clearly shown that in the free burn tests with solid fuels, all the targets were burnt.

Table 2. Summary of fire spread results in test series 1-4 on fire suppression [21].

Test no.	FFFS system	Fire spread to different targets (samples)					
		1 (nearby fire)	2	3	4	5	6 (furthest)
101	Low	*Charred*	No	No	No	No	No
102	Low	No	No	No	No	No	No
103	Low	No	No	No	No	No	No
104[a]	Low	No	No	No	No	No	No
105	Low	No	No	No	No	No	No
106	High	**Burnt~80%**	Charred	No	No	No	No
107	High	**Burnt~10%**	No	No	No	No	No
108	High	**Burnt~10%**	No	No	No	No	No
110	High	**Burnt~80%**	**Burnt~60%**	*Charred*	*Charred*	*Charred*	No
111	Medium	*Charred*	No	No	No	No	No
112	Medium	*Charred*	No	No	No	No	No
113	Medium	No	No	No	No	No	No
115	Medium	No	No	No	No	No	No
116	**Free burn**	**Burnt**	**Burnt**	**Burnt**	**Burnt**	**Burnt**	**Burnt**
200[a]	Low	No	No	No	No	No	No
201	Low	No	No	No	No	No	No
202	Low	No	No	No	No	No	No
203	Low	No	No	No	No	No	No
204	High	No	No	No	No	No	No
205	High	No	No	No	No	No	No
206[b]	High	*Charred*	No	No	No	No	No
207	Medium	No	No	No	No	No	No
208	Medium	No	No	No	No	No	No
210	**Free burn**	**Burnt**	**Burnt**	**Burnt**	**Burnt**	**Burnt**	**Burnt**
301	Low	No	No	No	No	No	No
302	High	**Burnt~70%**	**Burnt~40%**	**Burnt~30%**	*Charred*	*Charred*	*Charred*
303	Medium	No	No	No	No	No	No

304	Free burn	Burnt	Burnt	Burnt	Burnt	Burnt	Burnt
401	Low	NA					
402	High						
403	Medium						
404	**Free burn**						

[a] *Centered fire source.* [b] *Centered fire source and 1.5 times the amount of ignition fuel.*

In the presence of the FFFS, the targets were usually not burnt. In these tests, the low pressure system performed well in terms of preventing fire spread, and only in test 101 using the lower water density of 4 mm/min the first target was charred. The medium pressure system also performed relatively well in preventing fire spread, and only in two tests the first target was charred. By contrast, the high pressure system performed less effective in preventing the fire spread. In the majority of the tests with the high pressure system (5 out of 8 tests), one or more targets were partially burnt. In the following sections, more detailed comparisons of fire spread are made together with the HRR and the proportion of energy released.

Tenability

According to ISO 13571 [28], the time available for escape from a fire is the time after which occupants can no longer take effective action to accomplish their own escape, and it is the shortest of four distinct times estimated from consideration of asphyxiant fire gases, irritant fire gases, heat and visual obscuration due to smoke. The Fractional Effective Dose (FED) is commonly used to quantify the impacts of gases and heat on personnel. Besides the FED, the fractional effective concentration (FEC) is generally used for evaluating toxicity of irritant gas, which however was not measured in the tests. A FED threshold criterion of 0.3 refers to 11.4% of the population being susceptible and therefore statistically estimated to experience compromised tenability.

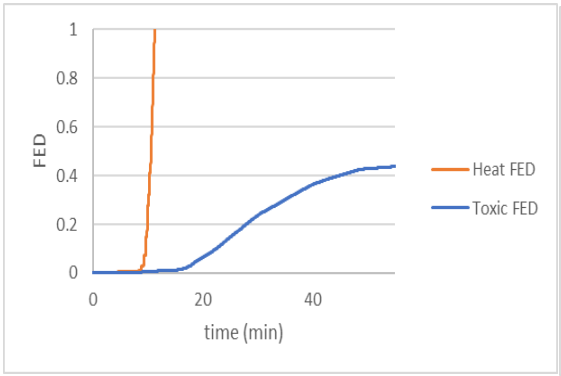

(a) free-burn

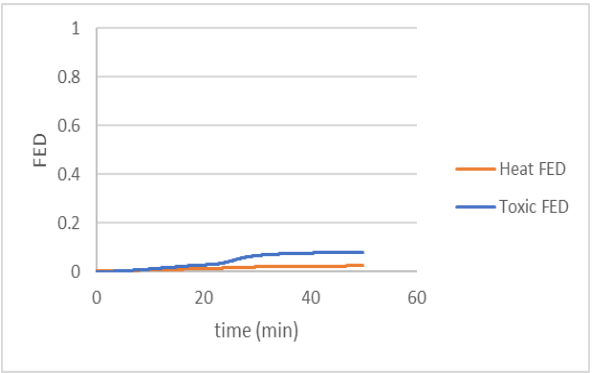

(b) default low pressure FFFS

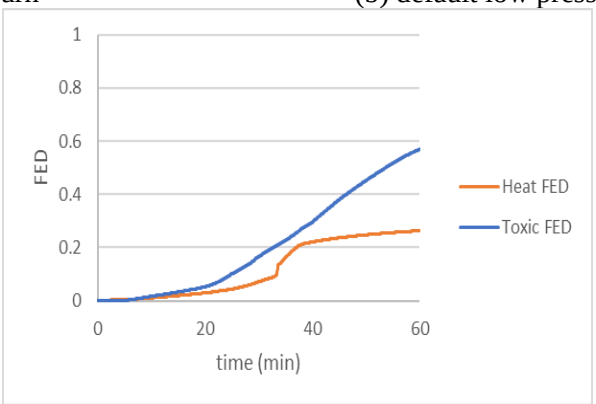

(c) default high pressure FFFS

Figure 13. FED at Pile B in Test 116, Free burn

The calculated FEDs at human height at Pile B (0.6 m above floor and 16.7 m from the fire source) for the free burn test, and the tests with default low and high pressure systems without the top cover are given in Figure 13. In the free burn test, the FED of heat exposure increases drastically at around 10 min when the HRR was around 2 MW. The FED related to gas concentration is much less. The FED is

the highest for the high pressure FFFS, and the lowest for the low pressure FFFS. This is in accordance with the measured heat release rates from these tests. It was also found that the high system FFFS results in much lower visibilities at Pile B than the other systems. Furthermore, it is found that in the free burn test, at Pile B, the heat exposure is more severe than the toxic gas, i.e., the FED due to heat exposure is the key criterion for evacuation. By contrast, the toxic gas tenability is the key criterion in all the tests with FFFS. The data from test series 2 on wood crib fires show similar results as presented above. The data from test series 3 on wood and HDPE fires show slightly different results. The results are similar for the low pressure system. However, for the medium and high pressure systems, the heat exposure criterion dominates, as the fires were not effectively suppressed. For the pool fires, the heat exposure and toxic gas criteria play similar roles. In all the free burn tests without FFFS, the heat exposure dominates at Pile B (around 50 m from the fire source) in terms of tenability. Note that at a location further away, the heat exposure will become less significant, and thus the toxic gas criterion becomes more and more important downstream the tunnel. This indicates that effective fire suppression is the key to reduce the toxic gas and increase evacuation time.

Structural protection

For structural protection, the incident heat fluxes received on the tunnel ceiling, the maximum ceiling gas temperatures and theceiling surface temperatures are of paramount importance. Three tests with the default FFFSs in the wood pallet fires with the top cover are compared with the free burn test. They are 34 kW/m^2, 34 kW/m^2 and 62 kW/m^2 for the low, medium and high pressure FFFS, respectively, compared to 106 kW/m^2 in the free burn test. This means that the low and medium pressure systems perform the best in reducing the ceiling heat fluxes. Note that the incident heat flux scales as ½ power of the length scale, i.e., it is higher in full scale. The maximum gas temperature for the high pressure FFFS is slightly higher than the other two systems. Further away from the fire, the gas temperatures are much lower in the tests with FFFS. All tests with FFFS produce quite similar temperatures further than 5 m downstream of the fire test source. The time to reach the maximum ceiling gas temperatures is significantly delayed in all the tests with FFFS. The maximum wall surface temperatures are 553 °C, 666 °C and 637 °C for the low, medium and high pressure FFFS, compared to 777 °C in the free burn test. Although the ceiling gas temperatures at Pile A and Pile B are within 160-270 °C, the floor temperatures at Pile A and Pile B are are all below 60 °C. The low pressure system refers to slightly higher ceiling gas temperatures, but the floor temperatures are similar to others and even lower than that for the high pressure FFFS at some locations. In all of the tests with FFFS, the maximum measured values for incident heat flux, ceiling gas temperature and surface temperature are lower compared to the corresponding free-burn tests. Note that they are highly correlated with the measured heat release rates. In the majority of the tests, the corresponding HRR for the low pressure system is the lowest among the three FFFSs, and these parameters (i.e., incident heat flux, etc.) are also at a low level. In terms of structural protection, the low pressure FFFS usually performs the most efficient, the high pressure system the least efficient, and the medium system in between. This is mainly due to the strong fire suppression performance of the low pressure FFFS, which overcomes the lower cooling effect due to its larger droplets.

Smoke control

Without FFFS

Figure 14 shows the critical velocities for smoke control based on extrapolation of the backlayering length curve from this test series and the TUSC fire tests conducted in the same tunnel [29]. Good agreement can be found between all the data and Li et al.'s equation [13, 30]. It shows clearly that the critical velocity becomes insensitive to the heat release rate for large fires.

$$u_c^* = \frac{u_c}{\sqrt{gH}} = \begin{cases} 0.81\varphi^{-1/12}Q^{*1/3} & Q^*\varphi^{-1/4} \le 0.15 \\ 0.43 & Q^*\varphi^{-1/4} > 0.15 \end{cases} \quad (5)$$

where the dimensionless heat release rate and tunnel aspect ratio are defined as:

$$Q^* = \frac{Q}{\rho_o c_p T_o g^{1/2} H^{5/2}},\ \varphi = \frac{W}{H}$$

In the above equation, u_c is critical velocity, Q is heat release rate (kW), ρ_o is air density, c_p is heat capacity (kJ/kg·K), T_o is ambient temperature (K), g is gravitational acceleration (m/s^2), H is tunnel height (m) and W is tunnel width (m). New experimental data for tunnels of various aspect ratios provide strong support to the above equation [31].

With FFFS

The critical velocities with FFFS are compared with those obtained in the free burn tests in *Figure 15*. Clearly, the critical air velocity in a test with FFFS is lower than that in the free burn test. The ratio of critical air velocity with FFFS tested in this study to that without it is in a range of 0.55 and 0.9. This indicates that after activation of FFFS, a smaller air velocity is required to prevent any smoke backlayering. An interesting question is whether various FFFSs influence the critical air velocity. From *Figure 15*, there are no clear differences or levels found for different FFFSs. When comparing the critical air velocities for the default low, medium and high pressure systems, it was found that the critical air velocities for these systems are very close to each other, and no significant difference was found. They are all around 70 % of the critical air velocity without FFFS, a reduction of about 30%. Considering the lower water density for the default high pressure system and the higher water density for the default low pressure system, this indicates that concerning critical air velocity, increasing the water pressure reduces the water density required to achieve the critical condition.

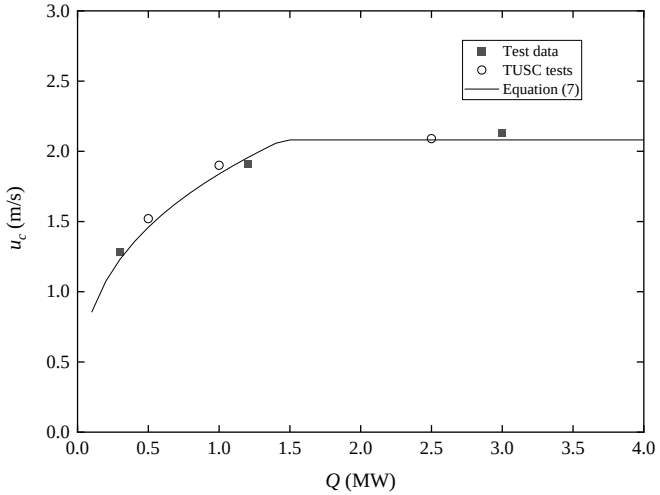

Figure 14. Comparison of measured and predicted critical velocity in free tunnel flow.

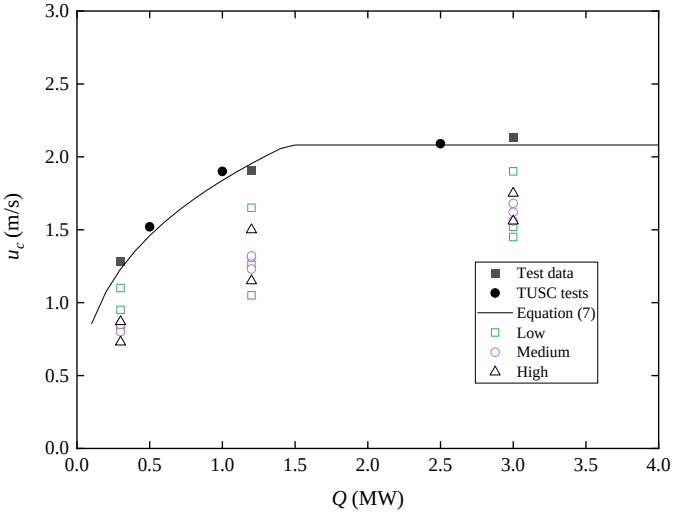

Figure 15. Comparison of critical longitudinal air velocity in tunnels with and without FFFS.

Spray deflection

The amounts of water collected in two rows of small containers (0.555 m (W)× 0.35m (L) ×0.08m (H)) placed on the tunnel floor for a period of 10 min are presented in *Figure 16* for the default low

pressure and medium pressure systems. The actual longitudinal ventilation velocity was around 2.2 m/s corresponding to 3.81 m/s in full scale. The water density distribution on floor approximately follows a normal distribution around the discharge point. Under no ventilation velocity (at 0 m/s), the centreline of the profile is about 0 m from the discharge point, i.e., there exists no influence of the ventilation on the water distribution. Below a longitudinal velocity of 2.2 m/s, the centreline of the distribution profile has been shifted to about 1.8 m for the default low pressure system and about 7 m - 8 m for the high pressure system. This clearly indicates that the deflection effect becomes more significant for smaller water droplets. These distances, however, are much shorter than what was found for single droplets. Similar trends can be found in the tests with all nozzles activated. Note that the nozzles lay within an 8.2 m long tunnel section. This means that at 2.2 m/s, if a fire occurs in the middle of the water spray zone as assumed in the tests, the majority of water droplets from the furthest upstream nozzle will be blown to the downstream end of the water spray zone when they arrive at the floor, rather than being discharged to the fire location to achieve fire suppression. It should, however, be noted that in case of a fire, the interaction between the fire plume and water droplets may probably exist during the travelling of water droplets. In any case, the deflection effect due to tunnel ventilation is significant, especially for the high pressure system, which may be a key reason for the deficiency of the system performance in fire suppression, and thus this effect should be well considered.

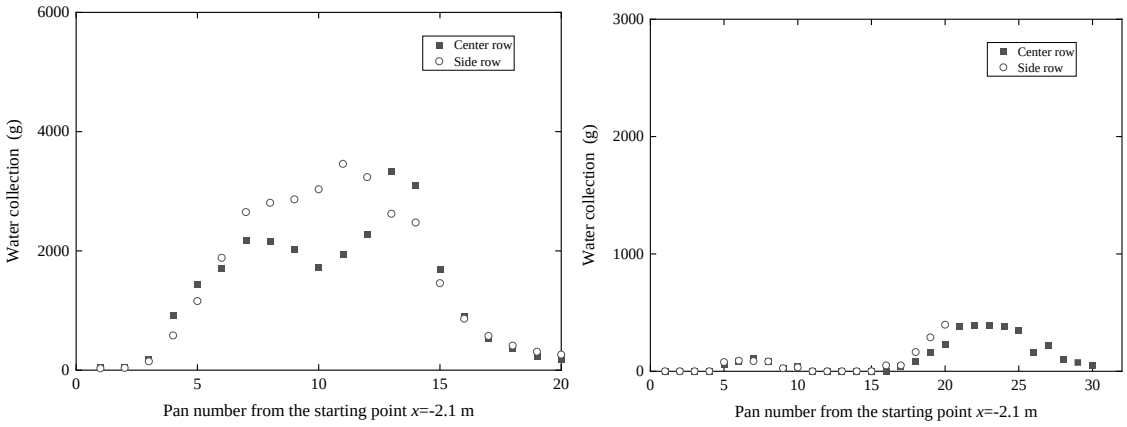

(a) Low pressure, 5.8 mm/min, 2.2 m/s (b) High pressure, 2.2 mm/min, 2.2 m/s.

Figure 16. Comparison of water collected from the tests. Each pan is 0.35 m long.

Spray resistance

The ventilation resistances caused by sprays were investigated in test series 7. The static pressure differences between -16.5 m and +16.7 m were measured in the tests. In each test, the fan was initially turned on without FFFS to measure a reference value for 3 min, and then the FFFS was activated to a lower level, and then raised step by step within an interval of 3 min. In all the spray resistance tests, the influence of FFFS on the tunnel air velocity is small and negligible. Furthermore, the influence of FFFS on the increases in the pressure difference above the reference value is also not significant, and this fraction of additional resistance related to FFFS becomes less as the velocity increases. The influence of FFFS on ventilation resistance due to FFFS can also be observed in test series 5 on smoke control. In those tests, the pressure differences usually decrease slightly after activation of FFFS, due to the fact that the FFFS reduces the gas temperatures and thus reduces the ventilation resistances. In a tunnel project, if a reduced design fire has been adopted due to the use of a FFFS, the ventilation resistances can be estimated using the new design fire without FFFS, to be on the safe side.

CONCLUSIONS

Both small scale laboratory tests and tunnel fire tests conducted in this project are summarized. The focus is on the results from the seven series of tests conducted in a 49.2 m long container tunnel with a scale of 1:3.

Three FFFSs were selected to represent a range of system types used in road tunnels, namely a low pressure system, a medium pressure system and a high pressure system, having a water discharge density of 10 mm/min, 6.8 mm/min and 3.7 mm/min, respectively, in full scale. Other water discharge densities were also tested to explore its effects, as well as the influence by ventilation velocity and the activation criterion. Various fire test scenarios were considered, i.e., idle wood pallet fires simulating densely packed fuels, wood crib fires and wood and plastic crib fires simulating loosely packed fuels, and heptane pool fires, with or without a top cover of the solid fuel. In the 1:3 scale tests the length of the deluge zone of the FFFS was 9.4 m, corresponding to 28.2 m in full scale.

Comparisons of the three default systems based on the HRR, the energy released and the possibility of fire spread to nearby targets show that the performance of the default low pressure system is usually the most effective in comparison to others in the densely packed fuel fires (without the top cover) and in all the loosely packed fuel fires (with or without the top cover). For the densely packed fuel fires with the top cover over the fuel, the three default system performs similarly but the low pressure system performs better at the early stage (before 12 min), and the medium pressure system performs better at the middle stage of the fire (between 12 min and 26 min). For the heptane pool fires, the low pressure and medium pressure systems perform similarly but significantly better than the high pressure system. For both systems, the maximum HRR is reduced by 50% of that in the free burn test, compared to 20% for the high pressure system. The high pressure system performs very differently in many aspects. Conclusively, in all the fire scenarios tested, the default low pressure system performs well and is usually the most effective, and the default high pressure system usually yields results less effective, when using the HRR, energy released and the potential for fire spread as the measures. The performance of the default medium pressure system usually lies in between them, but in the idle wood pallet fires with the top cover, the performance during a certain period is slightly better than the low pressure system.

In terms of preventing the fire spread to nearby targets, the low pressure system demonstrated good efficiency, and only in the test using the lowest water density of 4 mm/min the first target charred. The medium pressure system also performs relatively well in preventing fire spread, with the first target being charred in only two tests. By contrast, the high pressure system was not as efficient in preventing the fire spread. In the majority of the tests with the high pressure system, one or more targets were partially burnt.

Regarding smoke control, test data for critical ventilation velocity without FFFS correlate very well with Eq. (1). After activation of FFFS, the critical air velocity decreases. Comparing the default low, medium and high pressure system shows insignificant difference in the critical velocity to prevent any smoke backlayering, i.e., all around 70% of the critical velocity without FFFS.

Regarding tenability, in all the free burn tests, at 16.7 m from the fire source (at Pile B, around 50 m in full scale), the heat exposure is more severe than the toxic gas, i.e., the FED due to heat exposure is the key criterion for evacuation. By contrast, the toxic gas tenability is usually the key criterion in the tests with FFFS, except for the wood and HDPE fires where the fires were not effectively suppressed by the medium and high pressure systems. At a location further away, the toxic gas criterion becomes more important. Effective fire suppression is the key to reduce the toxic gas and increase evacuation time.

Regarding structural protection, in all of the tests with FFFS, the maximum measured values for incident heat flux towards the ceiling, walls and the floor level, ceiling gas temperature and surface temperature are much lower compared to the corresponding free-burn tests. They are highly correlated with the heat release rates. The low pressure FFFS usually performs the most efficient, the high pressure system less, and the medium system in between.

Regarding the influence of ventilation on the deflection of water sprays, it is apparent in the experiments that tunnel ventilation causes deflection of water sprays and this deflection effect is more significant for smaller droplets, i.e., for the high pressure system. The majority of water droplets from the furthest upstream nozzle will be blown to the downstream end of the water spray zone when they arrive at the floor, rather than being fully discharged to the fire site to achieve fire suppression. This effect has to be taken into account in the design of a high pressure system.

Regarding the ventilation resistance due to water sprays, it has been found that in all the spray resistance tests, the influence of FFFS on the tunnel velocity is small or negligible. In a tunnel project, if a reduced design fire has been adopted due to the use of a FFFS, the ventilation resistances can be estimated using the new design fire without FFFS, which should be on the safe side.

To sum up, the default low pressure FFFS performs well in term of suppressing the fire development, preventing the fire spread to nearby vehicles, providing tenable conditions for evacuation and rescue service, protecting tunnel structure and easing the problem with spray deflection due to tunnel ventilation. The default high pressure FFFS is usually on the opposite side while the default medium pressure FFFS usually lie in between.

ACKNOWLEDGEMENT

The work was financially supported by the Swedish Research Council Formas (2019-00521), which is gratefully acknowledged. The authors would also like to express their gratitude to Prof. Patrick van Hees at Lund University for his valuable input in the test planning process. Thanks also to our technicians at RISE for the great assistance in conducting the tests, and the Södra Älvsborg's Rescue Service for the support on site.

REFERENCES

1. Ingason, H., Y.Z. Li, and A. Lönnermark, *Tunnel Fire Dynamics*. 2nd ed. 2024, Cham: Springer.
2. Lundström, U. *Development of the Swedish road tunnel safety concept*. in *Proceedings from the Tenth International Symposium on Tunnel Safety and Security*. 2023. Stavanger, Norway, p. 45-55.
3. Li, Y.Z. *Study of fire and explosion hazards of alternative fuel vehicles in tunnels*. in *8th International Symposium on Tunnel Safety and Security*. 2018. Borås: RISE Research Institutes of Sweden.
4. Li, Y.Z. and H. Ingason, *Overview of research on fire safety in underground road and railway tunnels.* Tunnelling and Underground Space Technology, 2018. **81**: p. 568-589.
5. Lemaire, T. and Y. Kenyon, *Large Scale Fire Tests in the Second Benelux Tunnel.* Fire Technology, 2006. **42**: p. 329-350.
6. Cheong, M.K., W.O. Cheong, K.W. Leong, A.D. Lemaire, and L.M. Noordijk, *Heat Release Rates of Heavy Goods Vehicle Fire in Tunnels with Fire Suppression System.* Fire Technology, 2014. **50**: p. 249–266.
7. Ingason, H., Y.Z. Li, G. Appel, U. Lundström, and C. Becker, *Large Scale Tunnel Fire Tests with Large Droplet Water-Based Fixed Fire Fighting System.* Fire Technology, 2016. **52**(5): p. 1539-1558.
8. Mawhinney, J., *Fixed Fire Protection Systems in Tunnels: Issues and Directions.* Fire Technology, 2013. **49**: p. 477–508.
9. Sjöström, J., H. Sokoti, Y.Z. Li, and D. Brandon, *Pyrolysis and thermal properties of wood and high-density polyethylene*. 2024, RISE Research Institutes of Sweden, RISE Report 2024:24: Borås.
10. Li, Y.Z., R. Svensson, J. Wahlqvist, P. van Hees, and H. Ingason, *Numerical modelling of water sprays and fire suppression in tunnels*. 2024, RISE Research Institutes of Sweden, RISE Report 2024:23: Borås.

11. Otxoterena, P. and M. Försth, *Measurements of droplet size and velocity for three selected nozzles*. 2024, RISE Research Institutes of Sweden, RISE Report 2024:25: Borås.
12. Li, Y.Z., B. Lei, and H. Ingason, *The maximum temperature of buoyancy-driven smoke flow beneath the ceiling in tunnel fires.* Fire Safety Journal, 2011. **46**(4): p. 204-210.
13. Li, Y.Z., B. Lei, and H. Ingason, *Study of critical velocity and backlayering length in longitudinally ventilated tunnel fires.* Fire Safety Journal, 2010. **45**: p. 361-370.
14. Yu H.Z. *Physical scaling of water mist suppression of pool fires in enclosures*. in *10th International Symposium on Fire Safety Science*. 2011. Maryland, USA.
15. Li, Y.Z., G. Appel, H. Ingason, and H. Nyman, *Model scale tunnel fire tests with water-based fire suppression systems*. 2014, SP Report 2014:02, SP Technical Research Institute of Sweden: Borås, Sweden.
16. Li, Y.Z. and H. Ingason, *Scaling of wood pallet fires.* Fire Safety Journal, 2017. **88**: p. 96–103.
17. Ingason, H., Y.Z. Li, G. Appel, U. Lundström, and C. Becker, *Large scale tunnel fire tests with large droplet water-based fixed fire fighting system.* Fire Technology, 2016. **52**: p. 1539-1558.
18. Ingason, H. and Y.Z. Li, *Large scale tunnel fire tests with different types of large droplet fixed fire fighting systems.* Fire Safety Journal, 2019. **107**: p. 29-43.
19. Li, Y.Z. and H. Ingason, *Influence of fire suppression on combustion products in tunnel fires.* Fire Safety Journal, 2018. **97**: p. 96-110.
20. Li, Y.Z. and H. Ingason, *Parametric study of design fires for tunnels with water-based fire suppression systems.* Fire Safety Journal, 2021. **120**: p. 103107.
21. Li, Y.Z., H. Ingason, M. Arvidson, and M. Försth, *Performance of various water-based fire suppression systems in tunnels with longitudinal ventilation.* Fire Safety Journal, 2024: p. 104141.
22. Li, Y.Z., H. Ingason, J. Blom, M. Arvidson, and M. Försth, *Mechanisms and performance of different fixed fire fighting systems in tunnels – summary of laboratory and tunnel fire tests*. 2024, RISE Research Institutes of Sweden, RISE Report 2024:22: Borås.
23. Ingason, H., Y.Z. Li, M. Arvidson, and L. Jiang, *Fire tests with automatic sprinklers in an intermediate scale tunnel.* Fire Safety Journal, 2022. **129**: p. 103567.
24. SOLIT, *Engineering Guidance for a Comprehensive Evaluation of Tunnels with Fixed Fire Fighting Systems Scientific report of the SOLIT² research project*, in *Annex 3 - Engineering Guidance for Fixed Fire Fighting Systems in Tunnels*. 2012, The SOLIT² consor-tium.
25. *NFPA 502 - Standard for Road Tunnels, Bridges, and Other Limited Access Highways*. 2023 Edition, National Fire Protection Association.
26. Li, Y.Z., C.G. Fan, H. Ingason, A. Lönnermark, and J. Ji, *Effect of cross section and ventilation on heat release rates in tunnel fires.* Tunnelling and Underground Space Technology, 2016. **51**: p. 414-423.
27. Yu, H.-Z., J.L. Lee, and H.-C. Kung. *Suppression of Rack-Storage Fires by Water*. in *Fire Safety Science - Proceedings of the fourth International Symposium*. 1994.
28. ISO, *Life-threatening components of fire - Guidelines for estimation of time available for escape using fire data, ISO 13571:2012*. 2012.
29. Li, Y.Z. and H. Ingason. *Influence of blockage on smoke control in tunnels*. in *Proceedings from the Tenth International Symposium on Tunnel Safety and Security*. 2023. Stavanger: RISE Research Institutes of Sweden.
30. Li, Y.Z. and H. Ingason, *Effect of cross section on critical velocity in longitudinally ventilated tunnel fires.* Fire Safety Journal, 2017. **91**: p. 303–311.
31. Zhang, T., G. Wang, J. Li, Y. Huang, K. Zhu, and K. Wu, *Experimental study of back-layering length and critical velocity in longitudinally ventilated tunnel fire with various rectangular cross-sections.* Fire Safety Journal, 2021. **126**: p. 103483.

Preventing and managing NEC incidents in tunnels: Safety concepts

Christophe Willmann (1) &Pascal Blanc &Laurence Champin &Jean Marc Couvert &Yves Fleurial & David Giuliani &Daniel Lamarche &Christophe Lemierre &Olivier Peronne &Christophe Banos (1) &Antoine Mos (1)
(1) CETU - 25 avenue François Mitterrand 69674 Bron cedex
E-mail : Christophe.Willmann@developpement-durable.gouv.fr
& ATMB & DIR MC & SFTRF & Métropole Aix-Marseille Provence & GEIE-TMB & CD73 & DIRIF & SNCF (ex DGSCGC)

ABSTRACT

This paper focuses on the integration of new energy carrier (NEC) vehicles in the incident management procedures of tunnel operating bodies.
Firstly, the assessment of different identification means concludes that automated number plate recognition is the most reliable and a related safety concept is then presented. Secondly, the paper explains that in most cases, the fixed equipment investigated to detect initial signs of dangerous phenomena or even prevent them does not prove relevant. This is primarily due to the cost of such fixed systems and/or the very short time available to activate them for handling NEC phenomena.
Thirdly, the integration of NEC risks in the management of a collision or a fire is addressed. Indeed, specific NEC dangerous phenomena are always triggered by a collision or a fire or will trigger a fire. The paper first stresses that actions taken because of NEC risks should not reduce the effectiveness of collision or fire management procedures. Therefore, NEC-related identification will initially be limited to determining if a NEC vehicle is in the tunnel. No time will be spent on visual examination to know if a NEC vehicle is involved in the incident. Tunnel closure, user evacuation and ventilation are triggered in the event of fire and this should not change because of the NEC phenomena. In the event of a collision, likely to rapidly trigger a vapor cloud explosion on gas vehicles, closure, evacuation and ventilation are generally not carried out. The paper explains how and why choosing to adopt these three actions should be based on a cost-benefit analysis on a case-by-case basis.

KEYWORD: New energy carrier, NEC, collision, fire, explosion, prevention, safety management, procedure, identification, NEC specific incidents

INTRODUCTION

In recent years, work conducted within the scope of numerous research projects on vehicles using new energy carriers (NEC), has led to a better knowledge and understanding of specific dangerous phenomena in tunnels and the additional risks for user safety [1].
This knowledge now needs to be integrated into safety management systems as there is an urgent demand from national and local authorities in France to do so. As a first step, CETU has been working on how to integrate NEC vehicles into the main French risk analysis method [2]. As a second step, CETU has set up a work group of national operating bodies and emergency service representatives. The goal of this group is to study how an operating body could manage incidents involving NEC vehicles, so as to improve user safety.
The results of this collective work will be presented in the different sections of this article: the identification of NEC vehicles; the existing means to anticipate or prevent a NEC dangerous phenomenon and the management of a collision or a fire taking into account the NEC risk. Beforehand, some reminders about NEC vehicles will be given.

NEC VEHICLES: REMINDERS

The acronym "NEC" generally refers to 4 propulsion energies: electricity, hydrogen, compressed natural gas (CNG) and liquid natural gas (LNG). The case of vehicles powered by electricity will be discussed first, followed by that of vehicles powered by the three types of gas.

Accidents and fires that occur in tunnels are managed by tunnel stakeholders and can happen to both conventional and NEC vehicles. However, dangerous phenomena related to NEC are not explicitly taken into account in tunnel safety management. Whilst these phenomena can occur on NEC vehicles, their occurrence is highly unlikely, if not impossible, on conventional vehicles (except in the case of dangerous goods transport). The dangerous NEC-related phenomena will therefore be dealt with in more detail below.

The case of battery-powered vehicles

Technology
In an electric vehicle, one or more batteries power an electric motor.
The most common lithium-ion battery technologies are NMC or NCA cathode batteries, which have been the subject of numerous independent studies to assess their risks. Only these technologies have been investigated by CETU. In particular, current state of the art does not allow to assess how the risks specific to LMP (Lithium Metal Polymer) batteries have been reduced or even eliminated.
Batteries are stored in the lower part on light vehicles and HGVs, and in the upper part on buses.

The dangerous phenomena
With the most common battery technologies and a capacity of less than 80 kWh, accidents and fires involving electric vehicles do not present any additional risk compared with conventional vehicles [3].

For these most common technologies, the only dangerous phenomenon specific to batteries is thermal runaway. This can lead to a fire, which is difficult to extinguish. It can be caused by a short-circuit or a rise in temperature, the occurrence of which is limited by safety devices in the form of active and passive barriers. In the event of a temperature rise, thermal runaway will occur, on average, 10 minutes after a temperature of 150°C is reached [4].

Even if the risk of explosion cannot be totally ruled out, current state of the art does not allow us to assess the consequences, nor the rate of occurrence (which is a priori extremely low [3]).

Compressed gas vehicles

There are two types of compressed gas used to power vehicles: compressed natural gas (CNG) and hydrogen.

Technology
In a vehicle running on compressed natural gas, the internal combustion engine is fuelled by a gas stored in a tank pressurised to 200 bara.

A vehicle running on compressed hydrogen has a fuel cell that converts the hydrogen into electricity, which powers an electric motor and recharges a back-up battery (involved when there is a high demand for power). Tanks are generally pressurised to 350 bara for commercial vehicles, buses and HGVs, and 700 bara for light vehicles.

For both types of gas, the tanks are positioned at the bottom on light vehicles and HGVs, and at the top on buses.

The main safety device is the thermal pressure relief device (TPRD). The TPRD releases the gas

contained in the tank in order to lower its internal pressure and prevent degradation of the envelope and/or an increase in pressure from causing rupture. The TPRD opens at 110°C and there is at least one on each tank [3].

The dangerous phenomena

Accidents and fires involving gas-fuelled vehicles equipped with tanks containing 9 kg of CNG or 3.33 kg of hydrogen are not significantly more dangerous than with conventional vehicles, even in the event of TPRD activation [4]&[9].

Three specific dangerous phenomena exist for vehicles running on compressed gas:

- **jet fires,** which can occur following an impact or a fault during filling, if a source of sufficient temperature or energy is present in the immediate vicinity of the TPRD. Jet fires can of course also occur following a fire, but they do not significantly affect the fire, at least for the tank sizes mentioned above. A jet fire can occur within a few minutes of the collision or the fire that triggers it [3];
- **vapour cloud explosion**, which can occur following an impact or a fault during filling, if there is no source of temperature or sufficient energy in the immediate vicinity of the TPRD. Only a rupture of the TPRD could cause a significant explosion, given the various pressure regulator and supply cut-off systems in the rest of the gas circuit. The gas released by the TPRD then takes the form of a flammable cloud and could encounter such a source;
- **tank rupture**, which can occur following a failure of the TPRD in the event of a fire. The time taken for a gas tank to burst in the event of maximum thermal stress is 8 to 20 minutes, to which the (variable) time taken for the fire to spread to the tank must be added [3].

Heavy goods vehicles running on liquefied natural gas (LNG)

Technology

In a vehicle running on liquid natural gas, the internal combustion engine is supplied by a gas stored in a tank in a liquid state (10 bara and - 130°C or 1.1 bara and - 160°C).
Liquefied natural gas is used exclusively in HGVs, with the tanks positioned at the bottom.

The main safety device is the valve. The valve releases the gas contained in the tank in order to lower its internal pressure and prevent the envelope from deteriorating and/or the pressure from rising, causing the tank to rupture.
Each tank generally has two valves, set at 16 and 24 bara respectively.

The dangerous phenomena

Accidents and fires involving vehicles fuelled by tanks containing 150 kg of LNG are not significantly more dangerous than with conventional vehicles, even if the valves are activated [3].

The specific dangerous phenomena are the same as for CNG vehicles, the role of the TPRD being replaced by that of the valve. The time taken for LNG tanks to burst in the event of maximum thermal stress will be 15 to 20 minutes when stored at 10 bara and - 130°C. As with CNG, the (variable) time taken for the fire to spread to the tank must be added [3].

THE IDENTIFICATION OF A NEC VEHICLE INVOLVED IN A COLLISION OR A FIRE

As reminded in the previous section, specific NEC-related dangerous phenomena are always triggered by a collision or a fire (e.g., tank rupture by a fire) or will trigger a fire (e.g., thermal runaway). Therefore, when a collision or a fire occurs, it is of the utmost importance to know if a NEC vehicle is involved or not so that the first responders are aware of potential specific NEC-related risks.

However, trying to identify a vehicle after a collision or fire can pose two difficulties. Firstly, the vehicle may be so damaged that the means of identification is no longer effective. Secondly, depending on the means of identification considered, being able to identify a vehicle involved in a

collision or fire whatever its position may require a lot of identification equipment, which would be costly.

As a result, a second identification method was considered at CETU. This involves identifying NEC vehicles as they enter the tunnel, storing their characteristics in a database, then identifying them again as they leave the tunnel and deleting them from the database. This second method makes it possible to know whether a vehicle of a given energy type is in the tunnel when an accident or fire occurs. If the answer is negative, it is clear that there is no NEC vehicle involved in the collision or fire. If the answer is positive, a second step is to carry out a visual identification to determine whether or not the NEC vehicles identified at the entrance were involved.
The first method of trying to determine directly whether a NEC vehicle is involved will be referred to as "one-step identification". The second method of first determining whether NEC vehicles are present in the tunnel will be referred to as "second-step identification".

Numerous possible means to identify NEC vehicles have been investigated and analysed by the CETU, then assessed within the work group, taking into account the two possible identification methods. A first sub section below presents this assessment, then a second subsection presents the safety concept built around the most promising means.

Assessment of the identification means

Information provided by users

Following an accident or fire in a tunnel, it is generally advisable for one of the users involved to contact the control centre or the emergency services. When doing so, he or she should specify whether one of the vehicles involved runs on electricity or gas.

This means of information has the advantage of being free.

However, it has several disadvantages. First of all, it is only compatible with the one-step identification method. Secondly, it is possible that the user contacting the control centre or the emergency services has no information or the wrong information, particularly if he or she is not the driver. Thirdly, as feedback from French tunnels has shown, it is possible that no user will make contact, or that they will do so after a period longer than that in which the dangerous phenomena occur.

Symbols on the vehicles

This method simply consists in having symbols on NEC vehicles that indicates the alternative energy that could be seen by the operator through CCTV.

This means of information has the advantage of being free for the tunnel owner.

But it has several disadvantages. First of all, it is only compatible with the one-step identification method. Secondly, the identification may fail if the symbols are not readable (e.g., vehicle heavily damaged) or are masked (e.g., other vehicles or smoke) even if these symbols are big and colored. Thirsty, this method would place a new responsibility on the operator. Indeed, identifying the symbols on the vehicles would be in addition to identifying the incident and would be much more difficult, with a greater risk of error. Finally, it will need to have a specific regulation defining these symbols and requiring them on the NEC vehicles, which is beyond the tunnel context.

RFID chips

RFID chips fitted to the vehicles are already operational. They are of the ultra-high frequency (UHF) type.

In France you can find UHF readers with a range of 8 to 10 m at a cost around €300 excluding VAT, excluding installation and connection costs. In a two-lane tunnel 800m long, a sensor will be needed every 8 metres or so for one-step identification, which means 100 sensors at a total cost of €30,000 excluding VAT. This cost is reduced to €600 excluding VAT for two-step identification, since only two sensors would be needed: at the tunnel entrance and exit. Of course, it should be borne in mind that there will be maintenance costs, but overall, the cost can be considered reasonable.

Feedback from a French motorway operator highlighted an initial drawback to both identification methods: when two vehicles are travelling less than 4 metres apart at legal speed, the sensor could mistake one vehicle for the other.

A second disadvantage of this means of identification is that few vehicles are currently equipped with this type of chips, which greatly reduces its effectiveness. The obligation to equip vehicles with an RFID chip has only been compulsory in Europe since July 2024.

A third disadvantage is that, for the time being, the chips do not contain any information about the propulsion energy.

Ultimately, to meet the need for identification, whether in one or two steps, this method would first require very rapid technical adjustments to the sensors and to the information included in RFID chips. The modified chips would then have to be installed in all vehicles. Given the date of the regulatory obligation mentioned above and the average age of vehicles sold for destruction in France (19.6 years), this widespread use would take place in 2046 at best.

Communication between vehicles and/or with the infrastructure

Communication between vehicles and/or with the infrastructure is still evolving and maturing. The technologies are therefore not yet stabilised, nor is the regulatory framework for their use, specifying for example the information that will be exchanged.

Ecall system

In Europe, the ecall system enables the automatic transmission of data for information purposes and could be useful for the one-step identification method. The ecall system activates its SIM card and automatically calls the emergency centre (112) if the vehicle's sensors detect an accident. Among other things, it provides the VIN code, which contains information about the type of vehicles.

One advantage of this system is that it does not require any additional equipment in the tunnel, apart from the retransmission of GSM communications, which is generally already provided or possible.

A first disadvantage is that the VIN code does not always explicitly include the vehicle's propulsion energy. Post-processing, possibly automated, can generally be used to determine this. But, a priori, this requires the use of several different databases related to each vehicle brand.

A second disadvantage is that the call is transmitted to a general rescue centre which, in France, processes the information to ensure a rapid response. It is not the role of this type of centre to determine that the location corresponds to a position in the tunnel. This is a task that will have to be carried out by the local emergency services when they are contacted. Because of these delays in transmission and clarification, the operator runs the risk of being alerted too late on the involvement of an NEC vehicle. The responsiveness of the specific "NEC" measures will then be degraded.

A third disadvantage is that this system could be inoperative or operate late in certain situations. For example, in the event of breakdowns degenerating into fires, the sensors could react late or not at all, as they seem to be designed primarily for collisions.

Finally, this system came into force for new models in March 2018. Given the average age of vehicles sold for destruction in France (19.6 years), the scheme will not become widespread until around 2038.

Automated number plate recognition and identification with a national plate number data base

Automated number plate recognition operates thanks to a network of special cameras connected to a number recognition software. These cameras are separate from those used for automatic incident detection. This cameras system is used to read number plates. A national database links each number to the vehicle's characteristics, such as make, model, type, colour and propulsion energy. So, the camera system and an access to the data of the national database would theoretically make it possible to determine whether a vehicle runs on alternative propulsion energy.

Depending on the type of cameras, the reading range is 3 to 30 m and 3 to 45 m respectively. Only cameras capable of observing two lanes of traffic simultaneously were studied.

The advantage of this means of identification is that it works for all types of French vehicles. So, it could be used for purposes other than simply identifying NEC vehicles, such as counting vehicles by type.

What's more, the reliability of licence plate reading is now high, in the region of 90% to 95% on the French road network in normal traffic conditions [11]. These results mainly relate to the open-air network. In tunnels, if the cameras are directed towards the interior of the tunnel, these results could be even better. Indeed, reliability is degraded by unfavourable weather conditions such as rain, fog or snow that would generally not apply in tunnel. Specific tests are currently being carried out in tunnels by CEREMA's DTerSO/DM/MIM department and should provide further information.

One disadvantage is that, for the moment, it can only take French vehicles into account. Indeed, access to number plate data from other European countries is currently only possible via the Eucaris system in the event of an offence or theft. In bi-national tunnels and in tunnel in areas where foreign vehicle traffic may be significant, the relevance of this method will therefore be reduced.

In terms of cost, using the one-step identification method, coverage of a two-lane tunnel would require a camera every 15 to 20m at the usual ceiling heights. In an 800m structure, between 40 and 54 cameras would be needed, representing an investment of up to €380k, excluding installation and software acquisition costs. Each camera costs between €5k and €7k according to the feedback experience of two commands in France.
With the two-step identification method, only two cameras would be needed in the same structure, one at the entrance and the other at the exit. The cost would therefore be around €14k, excluding installation and software acquisition costs.
With regard to the cost of installing the cameras and acquiring the software, feedback from the implementation of such a camera system suggests a cost of around €55k for 4 cameras. This cost would of course decrease with the number of cameras installed.

Lastly, discussions with the French Home Office are well under way to ensure that tunnel operators have free access to the national database of the number plate for the identification of NEC vehicle. Indeed, this identification has as a safety purpose. If it were eventually not the case, the cost of receiving monthly updates for NEC vehicles alone would be a few thousand euros a year. For the same service for all types of energy, the cost would be several tens of thousands of Euros per year.

The one-step identification method raises a particular problem with this identification mean. Indeed, this method involves trying to determine directly whether or not a NEC vehicle is involved in an incident. However, a vehicle involved in a collision or a fire could have its number plate damaged or simply masked by another vehicle involved. The automated plate recognition would then be ineffective and the one-step identification method will fail.

The two-step identification method also raises a particular problem. Indeed, this method consists of identifying NEC vehicles on entering the tunnel, storing the characteristics in a database, then identifying them again on leaving in order to delete them from the database. As a result, when a collision or fire occurs, the operator will only know if there are NEC vehicles in the tunnel, not if they are involved. He/she will have to make an extra identification effort to find out. To do this, he/she will have to use the CCTV cameras to visually determine whether any of the vehicles involved have the characteristics linked to the number plates of the NEC vehicles present in the tunnel. If this identification action is undertaken immediately, it could waste precious time in carrying out other safety management tasks. It would also place a new responsibility on him/her, since identifying the vehicle would be in addition to identifying the incident and would be much more difficult, with a greater risk of error. However, this problem can be overcome. Firstly, the operator could immediately inform the emergency services of the presence or absence of a NEC vehicle in the tunnel in the event of a collision or fire. Then, he/she could apply the procedures conservatively, assuming that all the types of energy present are potentially involved. Possibly, in a second phase, once all the safety management tasks have been completed, he/she could try to visually identify the vehicle. If the identification is positive, the emergency services could be informed.

Summary and preferred means of identification

User information is an important means of identifying NEC vehicles involved in a collision or fire. However, because of its variable and uncertain reliability, this means of identification is not sufficient on its own. At the very most, it can be seen as an interesting complement.

Identification based on symbols on NEC vehicles visible through CCTV has the advantage to be free of charge for the owner. But it has several disadvantages including putting an unprecedent responsibility on operators ‘shoulders. At the very most, it can be seen as an interesting complement if a regulation is developed to require them.

Identification using RFID chips is not an immediate option, as all vehicles will not be equipped until around twenty years from now. In addition, the chips will have to contain information on the vehicle's propulsion energy, which is not currently the case.

Communication between vehicles and/or with the infrastructure is still evolving and maturing. The technologies are therefore not yet stabilised, nor is the regulatory framework for their use, specifying for example the information that will be exchanged.

Ecall cannot be adopted immediately, as it will only be fitted to all vehicles in around fifteen years' time. In addition, the data transmitted must clearly indicate the energy used to propel the vehicle. Currently, this information can’t not always be obtained without post-processing data bases of vehicle brands. The transmission of information to the local emergency services and even to the tunnel operator will also have to be much faster.

Identification using a system based on automatic number plate recognition is not without drawbacks. However, in the context of two-step identification, it could prove very useful, particularly for informing the emergency services. It could also be useful beyond the simple identification of NEC vehicles. So, it has been considered by the national group as the best mean of identification even if not perfect.

Safety concept based on number plate recognition and the related national data base

The envisaged framework for use would take the form of a four-step process:

1. Reading of vehicles plate numbers with cameras system at the tunnel’ entrance and recognition of number plate by using ad-hoc software;
2. Automatic search for plate numbers in data updated monthly from the Vehicle Registration System (BDD SIV); automatic identification of plate numbers corresponding to a NEC

vehicle; storage of these plate numbers and information describing the vehicles (e.g., make of vehicle, colours, model) in a dedicated database;

3. In the event of a collision or fire, the recorded information enables the operator to:
    1. indicate whether there are one or more NEC vehicles in the tunnel and give their characteristics, in particular their type of energy,
    2. try to determine by visual examination whether one of these NEC vehicles is one of the vehicles involved in the incident;
4. Reading of number plates when vehicles leave the tunnel to eliminate them from the dedicated database of number plates of vehicles that have left the tunnel.

The operation of the concept in a normal situation and in a collision or fire situation is illustrated by the following diagrams, respectively Figure 1 and Figure 2.

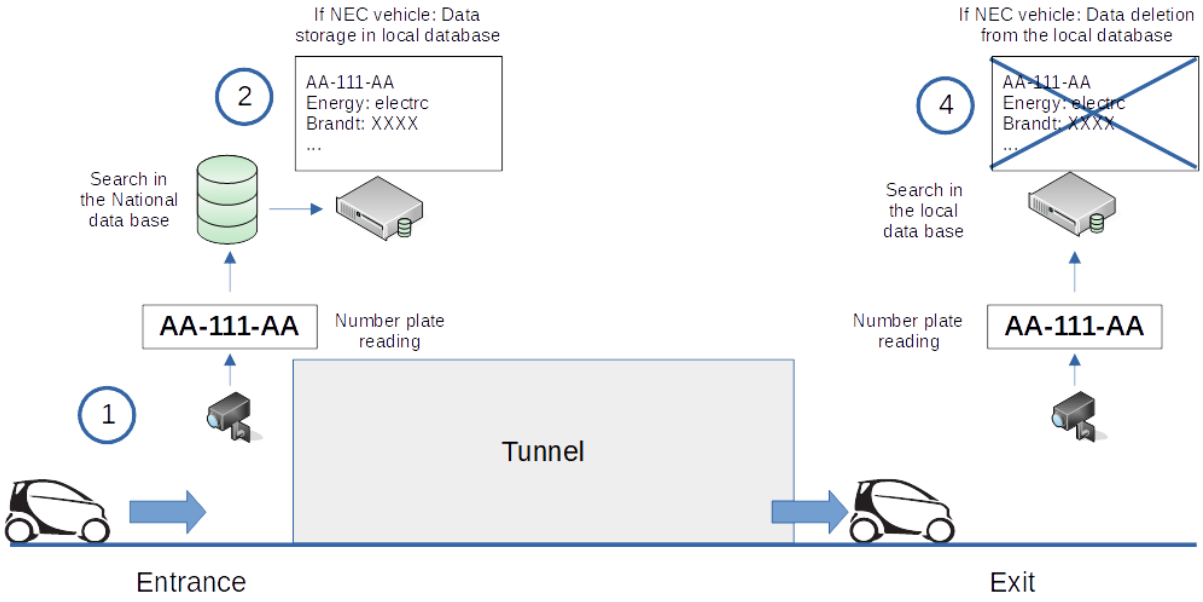

Figure 1 Scenario for current use (steps 1, 2 and 4)

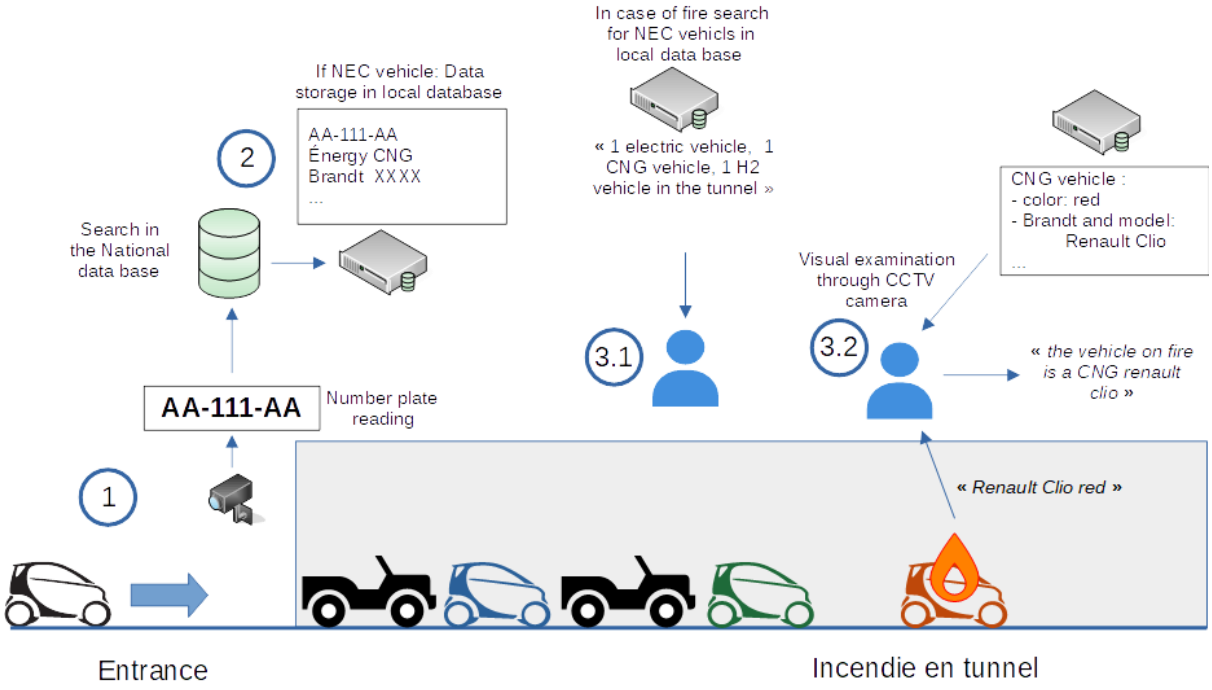

Figure 2 Usage scenario in the event of a collision or fire (steps 1, 2, 3.1 and 3.2)

MEANS TO DETECT THE FIRST SIGNS OF A DANGEROUS PHENOMENON OR EVEN PREVENT IT

Whether in normal traffic or following the occurrence of a collision or fire, it would be very useful to detect the beginnings of a specific NEC-related dangerous phenomenon or even to prevent it. In each of the paragraphs below, each means that could possibly contribute to these two objectives will be summarised, along with their possible use. The usefulness of each means will then be discussed. Developments will focus mainly on the case of vapor cloud explosions or tank ruptures that may occur following a collision or a fire. Indeed, with the most common battery technologies and a capacity of less than 80 kWh (vast majority of cases), an electric vehicle does not present a significant safety issue for users (see. section" nec vehicles: reminders). Finally, fire-fighting systems (FFS) were not included in the analysis. Many specific investigations remain to be carried out to determine their positive and negative impact. For example, it is necessary to determine the ability of a FFS to delay or even prevent a thermal runaway in an electric vehicle, given the position of the batteries in the vehicles and their cowling. We also need to know whether a FFS could inhibit the activation of the TPRDs when part of the tank is exposed to the flame, which could cause the tank to rupture.

Thermal camera

Thermal cameras installed in the tunnel may be of interest to detect a temperature increase before a fire occurs and impacts the battery or the tank. In case of an EV, it would also be interesting to detect a temperature increase in the battery before a thermal runaway happens.

Unfortunately, thermal imaging cameras cannot see through bodywork or glass. So, in the case of both electric and gas vehicles, it is unlikely that they will be able to detect a rise in temperature before the flame is visible.

On the other hand, portable cameras can be useful for first responders, for example, to identify the invisible part of the flame of a hydrogen jet fire. Depending on the quality of the equipment and the quantities ordered, each camera may cost between €1k and €2k excluding tax.

Gas sensors

Fixed systems

A system of gas detectors installed in the tunnel could detect an accidental release of gas from a TPRD. A so-called 4 gas sensor system is used in France. It generally consists of a control unit and a set of 4 sensors: 3 gas detectors (e.g., CO, NO, O2) and an explosimeter for detecting CH4. Of course, the sensors would have to be adapted for a specific 'NEC' use, for example, to enable hydrogen to be detected. Some of the devices available allow one or more sensors to be added as required.

However, the sensors only react when they are in contact with the gas. This raises the question of how much time remains after detection for any preventive or protective measures to be useful.

First of all, we need to determine the time range during which there is a risk of vapor cloud explosion. In most common cases, i.e., excluding special geometries, the flammable mass is controlled by the flow rate of the TPRD [4]. The flow rate decreases as the release progresses, due to the gradual drop in pressure inside the tank. The flammable mass therefore decreases over the duration of the release. In addition, the residual flammable mass will only remain in the tunnel for a very short time [1]. As a result, very soon after the end of the release, a vapor cloud explosion will be highly unlikely or its lethal effects will be very limited. For a tank containing 9 kg of CNG with a pressure of 200 bara, and TPRD diameter varying from 2mm to 4mm, the release time is between 20s and 80s [4]. It is between 7 and 40 seconds for a tank containing 3.33 kg of hydrogen with pressure of 350 bara or 700 bara and same TPRD diameter [9]. Almost all light vehicles and several types of HGV and bus have tanks with around these capacities. When these tanks are fitted to HGVs and buses, there are more of them (for

example 8 tanks on a CNG truck). It is therefore reasonable to assume that any measures to prevent or mitigate a vapor cloud explosion would have to be effective at the latest about 2 minutes after the release in order to be relevant.

The question is whether it is possible to meet this deadline. To answer this question, we need to assess the time required between the release of the gas and the effectiveness of a preventive or protective measure. To do this, we first need to determine the time needed for the gas to reach the sensor located near the vault (H2 and CH4 are lighter than air). In the most favourable case, where the release occurs under the sensor and is directed upwards, it will take at least a few seconds for the gas to reach the sensor. To this must be added the overall system reaction and transmission time, which would also be a few seconds with the most reactive sensors and optimum temperature and humidity conditions [5]&[6]. In the most favourable conditions, therefore, the time taken to detect a discharge and transmit the information would be around ten seconds. In France, in most cases, the operator's reaction time on detection of such an alarm would be at best 60 seconds, including the activation of predetermined ad-hoc measures. These measures to prevent or mitigate an explosion could include activating ventilation or triggering the evacuation of users. However, these measures will only have a tangible impact on the ground within 60 seconds at best. This is, for example, the time it takes for the ventilation system to ramp up. With regard to evacuating users, the time taken to take a decision after becoming aware of the danger is estimated in France at 90s [7]. Users would therefore only get out of their vehicles 150s after the release. To this time must be added the time needed for them to get out of range of the lethal effects that an explosion would cause. For the closest users, this would take 10s to 40s at a walking speed of 1m/s [7] given the lethal effect distances of a gas vapor cloud explosion (H2 or CH4) [4]&[9].

Consequently, the sensor system would enable certain preventive or protective actions to be effective within 130s at best after the discharge (150s to put users at a safety distance). This is longer than the time of about two minutes when these actions would be useful. It also corresponds to the most favourable situation in terms of the position of the discharge in relation to the sensors and the responsiveness of the latter.

For this favourable situation to be most likely, the sensor systems would have to be very close together (around ten metres), which would represent a very high investment cost. One supplier offers this type of 4-sensor system at around €15k each. Even if optimisations could be found, by equipping the system only with explosimeters for example, the cost would still be considerable.

The installation of fixed sensor systems in tunnels would therefore probably not provide any net added value, although it would be very costly in most cases. There may of course be special structures where the majority of gas-powered vehicles travel with tanks of much greater capacity than those taken into account in the previous reasoning. This could be the case for a dedicated bus tunnel in which mainly gas-powered buses are used. In this case, the time taken to empty the tanks and the persistence of the flammable mass could be significantly increased, making the sensors potentially relevant. The preceding reasoning would then have to be repeated and accompanied by a costing of the installation of sensor systems in the structure to assess their relevance.

Portable systems

Portable 4-gas sensor systems exist that can detect the same types of gas as fixed systems, but on a carrier scale. They are already used by some local fire services in France. They are very easy to use, and alert firefighter if he comes into contact with one of the 4 types of gas. He can then take cover if necessary (in the case of explosive gas, for example).

It could be of interest to the operating body staff who might have to intervene in the field, in the event of an accident for example.

In addition to their usefulness for alternative propulsion energies, they could also be of interest for

other uses: breakdowns or accidents during the transport of dangerous goods, the risk of a breakdown degenerating into a fire, etc.

The cost depends heavily on the quantity ordered and the supplier. Two commercial offers indicate a unit cost of between €850 and €1800 excluding VAT.

Ventilation

In the event of an accidental release of hydrogen from a TPRD, modelling has shown that the stronger the longitudinal airflow, the smaller the flammable mass [8]&[10]. The airflow helps to dilute the hydrogen and therefore to keep part of the gas below the lower flammable limit. This impact is significant for a longitudinal air flow of 2m/s. These results should remain valid for CNG. Indeed, in both cases, the size of the flammable mass is controlled by the diameter of the TPRDs and the range of diameters is the same for both gases. In addition, the lower explosive limits (LEL) of hydrogen and CNG are very close (4% and 5% respectively). Studies and tests are still needed, however, to test the robustness of this positive influence in different configurations (e.g., geometrical) and to specify it in these configurations.

In practice, however, the following factors need to be taken into account when deciding how best to use this positive influence.

Firstly, in a number of tunnels, there may already be a sufficient air flow during the periods and under the traffic conditions when a collision likely to cause a TPRD rupture is most likely. The natural air flow and/or the air flow created by the piston effect of the vehicles could dilute the gas sufficiently. This would be an initial point to include in any ventilation strategy.

Secondly, if the air flow is to be generated by a ventilation system, it must be effective within approximately 2 minutes after the collision in order to significantly reduce the risk of explosion (except in specific cases, see previous section). In order to achieve this objective, the ventilation system would have to be activated less than one minute after the collision. In some French road tunnels, this time has already been reduced to around 30 seconds. What's more, the system would have to be longitudinal to ensure the creation of such a current of air in around 1 minute. In fact, certain very specific procedures for activating transverse systems in road tunnels (push and pull) allow a longitudinal airflow to be created. However, it takes longer for this airflow to be effective (more than 2 minutes). With an activation time of 30s after the collision and a longitudinal ventilation, the longitudinal air flow may be effective in 1min30s.

Finally, if a ventilation system is activated when the flammable mass has reached a piece of ventilation equipment, such as an accelerator, the cloud could explode. Indeed, the energy supplied by the equipment could exceed the minimum ignition energy (MIE) of the gas, especially in the case of hydrogen where this MIE is only 17µJ. This risk would be eliminated if the accelerators in the explosive cloud were not activated. By far, the most likely scenario is for the explosion to occur when the gas is released or shortly afterwards, i.e., when the cloud is in the immediate vicinity of the vehicle (see previous section). So, the non-activation of certain accelerators above vehicles involved in an incident could be envisaged. This is already the case in certain ventilation procedures (e.g., collisions involving a transport of dangerous goods). As far as transverse systems are concerned, the risks associated with the suction of part of the flammable mass into the smoke extraction ducts are not yet fully understood. A priori, they depend on the system, in particular the location in the duct or at its ends of equipment likely to supply energy greater than the MIE.

THE MANAGEMENT OF A COLLISION OR A FIRE TAKING INTO ACCOUNT NEC RISK

As previously reminded, specific NEC-related dangerous phenomena are always triggered by a collision or a fire (e.g., tank rupture by a fire) or will trigger a fire (e.g., thermal runaway). The management of specific NEC phenomena must therefore be integrated with the management of the

fires or collisions to which they are linked. The previous sections presented the results of investigations on the means of identifying NEC vehicles, detecting the beginnings of specific phenomena and preventing them. On this basis, collision and fire management principles that take account of the NEC risk have been developed. They are presented below.

A golden rule: No action reducing the effectiveness of regular procedures

The risk of a specific NEC event occurring in the event of a collision or fire may lead the operator to modify the actions planned when only conventional vehicles are involved. This risk may also give rise to new actions designed to prevent or anticipate a specific NEC event. In either case, the handling of the collision or fire could be delayed. For example, the NEC vehicle identification process described above allows the operator to identify NEC vehicles involved in a collision or fire by visual inspection. However, if the operator carries out this examination immediately after the event in order to implement measures that take account of the NEC risk, this will delay the processing of the collision or fire.

Delaying the treatment of a collision or fire on the grounds of a possible NEC risk was deemed unacceptable by the working group. Indeed, it is not certain that a NEC vehicle is involved in the collision or fire, and even less certain that a specific NEC phenomenon will occur. The principles presented below have therefore been based on the assumption that nothing should delay or reduce the effectiveness of the treatment of the collision or fire possibly linked to the NEC phenomenon.

The detection of the collision or the fire

At this stage, the standard procedures apply unchanged.

Identifying a NEC risk

Identification of a NEC vehicle

If an operating body chooses to apply the identification concept presented above and to be equipped accordingly, the operator will not immediately know whether vehicles are involved in the collision or the fire. However, he/she will immediately know if NEC vehicles are present in the tunnel and what their propulsion energy is. It is therefore on the basis of this information alone that he/she will deal with the various aspects of incident management described below.

Detection of initial signs of NEC phenomena

In view of the results of the investigations carried out on the detection of the beginnings of a specific NEC phenomenon, no action to detect these beginnings is planned.

Tunnel closure

Fire (likely to be triggered by a specific NEC event or to trigger one)

In France, if a fire is suspected in a tube, the operator closes the entire tunnel. Therefore, the tunnel will be closed for any specific NEC phenomenon likely to be triggered by a fire or to trigger a fire without it being necessary to take this phenomenon into consideration. In particular, the operator will apply the procedure relating to fire and will close the tunnel without worrying about a tank rupture or a jet fire on a gas vehicle or a thermal runaway on an electric vehicle. There is therefore no need of specific procedure for closing the facility in the event of these phenomena.

Collision (likely to trigger a vapor cloud explosion on a gas-powered vehicle)

In the event of a collision, the tunnel is generally not closed systematically. The closure procedure may depend on the nature of the collision. For example, a tunnel will only be closed if the collision causes more than one lane of traffic to be obstructed, even partially. However, there may be systematic closure in the event of a collision in certain tunnels, for example in non-urban structures where the traffic is not significant and the number of collisions per year is low.

Choices in this area may be influenced by the risk of vapor cloud explosion. Three options can therefore be considered: closure procedure defined without taking into account the risk of vapor cloud explosion; procedure including closure if there is a gas vehicle in the tunnel; procedure reduced to systematic closure. These three options are described below, followed by a suggested approach for choosing between them.

Option 1- Closure procedure defined without taking account of the risk of a vapor cloud explosion
This option considers that the risk of a vapor cloud explosion is too low to influence the closure procedure in the event of a collision. Consequently, this procedure is defined without taking this risk into account. The advantage of this option is that it does not require gas vehicles to be identified, and the operating body may not need to equip the tunnel for this purpose, provided other actions do not require it. This option will not, however, make it possible to take account of the specific consequences of a vapor cloud explosion. The risk of explosion could nevertheless be covered without having been taken into account in cases where it is decided to close the structure in the event of a collision for other reasons.

Option 2: Closure procedure including closure if there is a gas vehicle in the tunnel
This option involves taking account of the risk of a vapor cloud explosion in the closure measures, provided that this risk is demonstrated by the presence of a gas-powered vehicle in the tunnel. As a reminder (cf. ***Identification of a NEC vehicle***), it is not possible for the operator to take the time to carry out a visual examination to determine whether a gas-powered vehicle was involved in the collision. Such a closure will have the advantage of limiting the number of vehicles in the tunnel. The phenomenon will occur so quickly that the closure should have no influence on the number of people exposed (cf. **Gas sensors**). Nevertheless, the reduction in the number of vehicles present will make it easier for emergency vehicles to intervene, particularly when their intervention strategy involves driving through the tube affected by the collision. This will enable them to provide more effective assistance to people injured by an explosion. The equipment and data needed to identify the NEC vehicles present in the tunnel will be necessary, but the cost remains reasonable (cf. "Automated number plate recognition…"). Nevertheless, even if the risk of identification error remains low in most cases (cf. previously), it will have to be taken into account and specified, particularly if foreign vehicles are travelling through the tunnel. In certain urban tunnels with very heavy traffic, the implementation of this option could cause major disruption to traffic over a significant area. However, these disruptions will be limited to cases of collision and the presence of a gas-fuelled vehicle in the tunnel.

Option 3: Procedure reduced to systematic closure
This option consists of closing the tunnel in the event of a collision without first identifying a gas-fuelled vehicle on the sole grounds that such a vehicle could be involved and cause a vapor cloud explosion. It offers the same advantages as option 2, without the need to bear the costs linked to the identification gas vehicles, or to deal with the risk of misidentification. However, in an urban tunnel with heavy traffic, major disruption to local traffic will occur in the event of a collision, i.e., even if there are no gas-powered vehicles in the tunnel. These disruptions should nevertheless be very limited in non-urban tunnels where the annual number of collisions is very low.

The choice between the three options
In order to choose between the three options, a risk -benefit analysis can be carried out, taking into account:

- the frequency of collisions,
- the frequency of vapor cloud explosions,
- the risk of misidentification of NEC vehicles, in particular by assessing the flow of foreign vehicles,
- the local consequences of a closure, which will make it possible to assess whether the risk, outside the tunnel is increased rather than reduced,
- the cost of equipment and access to data enabling NEC vehicles to be identified.

Users' evacuation

As with the closure of the tunnel, in the event of a suspected fire in a tube, the operator will evacuate users in all circumstances. There is therefore no specific procedure for a tank rupture, a jet fire in a gas vehicle or a thermal runaway in an electric vehicle.

In the event of a collision, except in rare cases (e.g., a collision involving the transport of dangerous goods), the evacuation of users is not triggered. This practice could be reviewed if gas-powered vehicles are used in the tunnel. If a collision involves a gas-powered vehicle, it is likely to cause a vapor cloud explosion. In this case, the explosion would occur very quickly after the collision. As previously indicated (cf. **Gas sensors**), triggering the evacuation of users would not allow them to distance themselves from the effects of such an explosion with the usual assumptions about reaction time. This observation has legitimately contributed to the decision not to recommend the installation of costly gas sensor systems. Nevertheless, it cannot be ruled out that some operators and users have more favourable reaction times and walking speeds. Besides, as previously indicated (cf. **Gas sensors**), in certain specific tunnels the time during which a significant vapor cloud explosion could occur may be greater. It is therefore conceivable that such a self-evacuation could be triggered in order to move users away from the release or even out of range of the lethal effects of a vapor cloud explosion. However, the working group felt that this provision should be made conditional on the presence of a gas vehicle in the tunnel. Self-evacuation can only be envisaged if it is accompanied by the closure of the tunnel. However, the experience of the working group members in incident management has shown that self-evacuation is particularly difficult to manage and leads to long delays in reopening the tunnel.

Consequently, apart from cases where evacuation is already planned in the event of a collision for reasons other than the risk of a vapor cloud explosion, two options could be considered:

- no evacuation,
- evacuation if there is a gas-powered vehicle in the tunnel.

The choice between these two options could be made using the same type of risk-benefit analysis as that presented for tunnel closure. In fact, the analysis of the two options could be carried out together, since self-evacuation without closure of the tunnel is out of the question.

Ventilation activation

Fire

As with the closure of the tunnel and the evacuation of users, in the event of a suspected fire in a tube, the operator triggers the ventilation system. There is therefore no specific procedure for a tank rupture, a jet fire on a gas-powered vehicle or a thermal runaway of an electric vehicle.

Collision

The treatment of the collision case is based on the previous sub-section "Ventilation".

First of all, as for tunnel closures and user evacuation, in rare cases the ventilation is already activated in case of collision, regardless of the risk of a vapor cloud explosion. Because of the "golden rule", this will not be called into question even with transverse ventilation, despite the risks linked to sucking in possible flammable gas. Concerning longitudinal ventilation, it will be necessary to study the possibility of not activating the accelerators above the vehicles involved.

With regard to taking into account the risk of a vapor cloud explosion when activating ventilation, the case of transverse ventilation will not be dealt with. Until there is better knowledge of the risk associated with sucking in a possible flammable gas, the existing procedure will not be put into question because of gas vehicles.

In the case of longitudinal ventilation, there are three possible options:

- ventilation procedure established independently of the risk of vapor cloud explosion,
- ventilation activated if a gas-powered vehicle is present in the tunnel
- systematic activation of ventilation regardless of the presence of a gas vehicle. This option

consists in activating ventilation in the event of a collision regardless of the presence of a gas vehicle, on the assumption that such a vehicle may be involved and could cause a vapor cloud explosion.

If longitudinal ventilation is activated, the accelerators located above the vehicles involved must not be activated. The three options proposed are the same as in the section entitled "Tunnel closure". The advantages and disadvantages presented in that section also apply here, and the question of power consumption must be added. Consumption will of course be a disadvantage for ventilation activation to an extent to be assessed. In order to choose between the three options, a cost-benefit analysis similar to that in the section " **Tunnel closure**" could be added, adding a criterion relating to electricity consumption.

Alerting emergency services

With regard to the alert, given the identification procedure adopted (see " ***Identification of a NEC vehicle***") and the "golden rule", the alert will take place in two stages:

1. Initially, the operator tells the emergency services whether there are one or more NEC vehicles in the tunnel and provides the information that he/she has, in particular the type of energy.
2. Secondly, the operator tries to determine by visual examination whether one of these NEC vehicles is involved in the collision or fire. If so, he informs the emergency services. For example, if a grey Citroën DS3 electric vehicle enters the tunnel, the operator will know this thanks to the identification system. If, after visual examination, he finds that a vehicle with the same apparent characteristics is involved, he will indicate that it is possible that one of the vehicles involved is an electric vehicle and transmit the vehicle's characteristics. In France, in most cases the information is likely to reach the emergency services before they arrive on the scene. This is because their journey time is generally around twenty minutes in urban areas, and up to forty minutes in non-urban areas.

CONCLUSION

A national group has been set up by the CETU in order to address the need to integrate NEC vehicles into tunnel operating body incident management processes. The paper presents the result of this work.

Concerning NEC vehicle identification, the most promising means appears to be automated number plate recognition combined with the use of a national plate number data base that contains vehicle characteristics. Although it is not without its drawbacks, it is operational and could prove very useful, particularly for informing emergency services. A safety concept based on this means has therefore been developed to identify NEC vehicles. It could also be useful beyond the simple identification of NEC vehicles. The information given by users or via symbols on vehicles could be useful but is not reliable enough to be the only means used. The other means investigated will need more time, generally dozens of years, before they are operational, as they require vehicle adaptations and/or technical adjustments to be reliable enough for the purpose.

Concerning the means to detect the first signs of dangerous phenomena or even prevent them, three means have been studied: thermal cameras, gas sensors, ventilation. It appears that the cost of fixed systems and/or the very short time available to activate them in the event of NEC phenomena for which they would be used, means that they are generally not a viable option. However, they could be more useful in specific situations where the time available is greater and/or the reaction time of tunnel operators or users is shorter. Portable gas sensors, already used by firefighters, could be useful for operating body staff who might have to intervene in the field.

As specific NEC dangerous phenomena are always triggered by a collision or a fire or may trigger a fire, the NEC-related risk has to be integrated into collision or fire management procedures. Any actions taken should not reduce the effectiveness of such procedures. Indeed, when such incidents

occur, a NEC vehicle will not necessarily be involved, and it is even less certain that a specific NEC phenomenon will occur. Therefore, in the initial stage of managing such incidents, NEC-related identification is limited to determining if a NEC vehicle is present in the tunnel or not. It is on this basis that the operator will apply procedures such as tunnel closure, user evacuation, ventilation activation and emergency service notification. Following this, the operator will need to use the CCTV cameras to determine if a NEC vehicle is involved in the collision or the fire. Tunnel closure, user evacuation and ventilation are triggered in the event of fire and any NEC phenomena linked to the fire (thermal runaway, jet fire and tank rupture) will not change these actions. In the event of a collision likely to rapidly trigger a vapor cloud explosion on gas-powered vehicles, the three previous actions are generally not carried out. Three main options could be considered for each action: no change in the existing procedure, action carried out if a gas vehicle is in the tunnel, action carried out systematically on the sole grounds that a gas vehicle could be involved and cause a vapor cloud explosion. The choice between these options may be based on a cost-benefit analysis taking into account the frequency of collisions, the frequency of vapor cloud explosions, the risk of misidentification of NEC vehicles (in particular due to foreign vehicles), consequences at a local level in the event of closure, the cost of equipment and energy consumption (especially for ventilation).

These proposals will strongly benefit from further research on four specific issues. Firstly, there is a need to more precisely determine the time, after a gas release, during which a significant vapor cloud explosion could occur. Secondly, the quantification of the airflow effect on the reduction of flammable mass needs to be more accurate. Thirdly, the reliability of automated plate number reading at legal speed has to be determined even if it is most probably greater than in the open air. Fourthly, the risk associated with the use of transverse ventilation in the event of a collision with gas release should be investigated. Finally, further investigations are needed concerning means that could detect and prevent NEC phenomena for example the self-venting tank studied within Hi-tunnel project.

REFERENCES

1. PIARC, TC 4.4, report, "impact of new propulsion technologies on road tunnel operations and safety - a PIARC technical report", 2024
2. Willmann C and Charles P, *"Integration of new energy carriers in French specific hazard investigations: overview of principal issues",* Tunnel Safety and Ventilation, Proceedings from the 12th International Conference, Graz, Austria, 274-282, 2024
3. CETU, Les documents d'information, "Les nouveaux modes de propulsion en tunnel routier - Risques et enjeux : état des lieux partagé", 2024
4. Christophe Willmann and Benjamin Truchot, *"New energy carriers and additional risks for user's safety in tunnels*", International symposium on tunnel safety and security, Proceedings from the Ninth International conference, 203-218, 2021
5. Hübert T and all, "*Response time measurement of hydrogen sensors",* h2knowledgecenter.com. 11p, 2017
6. J.J. Cepa, R.M. Pavón, P. Caramés, M.G. Alberti, "*A Review of Gas Measurement Practices and Sensors for Tunnels",* Sensors 23 (2023) 1090.
7. C.Willmann & A.Mos "Specific hazard study, help implementing the requirement of fascicle 4 of the guide to dafety files", CETU, 30p, 2023
8. Martin Aggarwal, Daniel Fruhwirt and all " Hydrogen powered vehicles in a tunnel incident - risks and consequences", Tunnel Safety and Ventilation, Proceedings from the 12th International Conference, Graz, Austria, 391-405, 2024
9. Christophe Willmann and Benjamin Truchot, *"User's safety in tunnels - additional risks of new energy carriers' vehicles"*, 18th International symposium on aerodynamics, ventilation&fire in tunnels, 878p, 2019
10. Maha Eleryan, "*Implementing Hydrogen-Fuelled Buses in the QRA-Tunnel Tool from the Dutch Authorities*", GEXCON report, Bergen, 2022
11. ANTAI "*Rapport d'activité 2019*", Report, 60 p, 2022

Deflagration consequences in a tunnel: Experimental evaluation of hydrogen leaks

Benjamin TRUCHOT[a] & Jerome DAUBECH[a,b]
[a]Ineris, Parc ALATA 60550 Verneuil en Halatte, France
[b]Sorbonne Universités, UTC-TIMR, 1 rue Dr Schweitzer, 60200 Compiègne, France
E-mail: benjamin.truchot@ineris.fr

ABSTRACT

Introducing new energy carriers in tunnels, mainly compressed gases, introduces explosion as a new phenomenon to be considered for safety design. An explosion in a tunnel strongly differs from an open explosion since the confinement directly interacts with the flame development and, then, with the resulting pressure wave propagation. This paper focuses on the specific deflagration of a flammable cloud in tunnel phenomenology and provides some engineering tools that can be used to estimate associated consequences. To meet this objective, a scaled experimental campaign was set up. The first main objective of the experimental test series consists of evaluating the scale factor by comparing very small-scale tests achieved in a small pipe and tests made in a several-diameter tunnel. This comparison shows that the pressure curve dynamic is similar, meaning the associated physical phenomena should be the same. This similarity also means that some models developed based on small-scale tests could remain valid. The test series also addresses the influence of some parameters, such as stratification, on flame development and its influence on the generated overpressure. This test series highlights a strong influence of stratification since it induces flame instabilities, and mainly for this specific case the hydrodynamic instabilities as the Rayleigh-Taylor one, that leads to flame acceleration and results in a stronger pressure wave.

KEYWORDS: hydrogen, flammable cloud deflagration, large-scale experiments

INTRODUCTION

Mitigating new risks in tunnels induced by the development of new energy carriers is a challenge for the coming years. Fire is the only dangerous phenomenon that can happen to vehicles, excluding hazardous goods. Following critical accidents that occurred at the end of the '90s and based on the results of several research projects such as EUREKA (12) or UPTUN (13), safety systems in the tunnels were strongly improved. Gas vehicles crossing tunnels let the potentiality of an explosion appear in the tunnel, a dangerous phenomenon generally not considered when designing tunnel safety. Explosion in tunnels is a specific topic that several authors addressed. Following the French EGSISTES project, a discussion of new risks in tunnels was published (14). More recently, the HyTunnel project (15) focussed on hydrogen safety in tunnels and proposed valuable results to deal with explosions in confined spaces.
When dealing with compressed gas, two different explosions may happen. The first type of explosion corresponds to the tank burst in case of surrounding fire, typically with safety depressurisation failure. Such an event leads to a blast wave induced by the gas expansion. The second type of explosion corresponds to a flammable gas dispersion with a delayed ignition leading, generally to deflagration and, in specific situation, transition to detonation. In both cases, a pressure wave will propagate through the tunnel with a strong influence of the confinement that modifies the pressure decrease along the tunnel, at least for the blast wave (16).

The present paper focuses on the flammable gas cloud deflagration. When dealing with such phenomena, it is well known that some key factors influence the flame propagation and the resulting pressure wave, such as the fundamental flame speed in the gas, the burnt gas expansion coefficient, the gas concentration or the turbulence in the cloud (17). These relations were quite well established in

atmospheric conditions, without confinement. Specific focuses were also published for confined explosions, for buildings or containers, for instance, where an additional secondary explosion may occur outside the confined space (18)(19). Understanding secondary explosion is a key issue for the explosion in the tunnels since the physical mechanisms that lead to this phenomenon are also, through some topics, responsible for vapour cloud deflagration in tunnels. During such an event, while the flame propagates into the cloud, the pressure increase in the room induces the opening of the weakest structure of the building. The gas is then pushed out of the room, generating an accelerated flammable cloud outside the building (Figure 1). While the initial cloud might be quiescent, the cloud induced outside the building is highly dynamic and turbulent, contributing to flame acceleration.

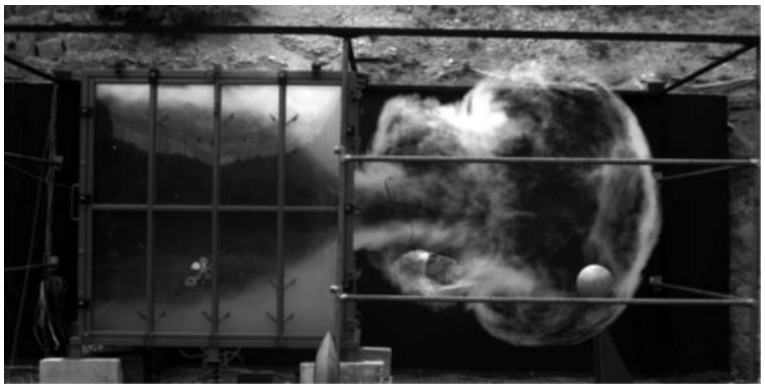

Figure 1: External explosion (uniform and quiescent mixture – 16.5% H2 – 0.49 m², (7))

In tunnel geometry, several additional factors will play a significant role in pressure wave characteristics. First, the flammable cloud is generated by a high-pressure release, which means a certain level of turbulence. The flame propagation in this cloud and the associated pressure rise and hot gas expansion will contribute to creating additional cloud acceleration with, potentially, additional turbulence, typically if vehicles are present inside the tunnel.

The present paper focusses on the fundamental mechanisms and their respective roles in flame propagation in the preliminary flammable cloud, with the influence of gas concentration, turbulence, and stratification. Deflagrations in tunnels can also be compared to deflagrations in pipes, which were strongly studied in the last two decades (20)(21).

THEORETICAL BACKGROUND

Assuming that an deflagration in a tunnel may be considered, for some situations, as deflagration in a pipe, it appears relevant to provide some principles based on existing models. When dealing with such a configuration, the first criterion for predicting deflagration behaviour is the pressure distribution in the volume. While pressure remains relatively homogeneous in the volume, which means low flame speed, lower than 30 m/s that typically corresponds to length L to diameter D ratio, lower than 5, some models enable flame behaviour and resulting pressure rise in the tunnel (22)(23). In contrast, some mechanisms, such as the role of flame instability, remain unclear (24)(25).

For a larger L/D ratio, typically in tunnels where length is more significant than five diameters, the flame propagation velocity becomes enormously more critical, pressure no longer remains uniform in the domain, and the maximum overpressure is directly proportional to the flame velocity. The associated physical mechanisms are numerous, including generated turbulence, combustion instabilities, flame and pressure wave interactions and local compression (26). Since all those mechanisms are well-known (27), how they interact and their relative influence on flame acceleration remain unclear (28).

Following Gilles (29), the pressure, $P(t)$ and flow velocity induced by the flame movement, $U(t)$, can

be linked using the density, ρ, and the sound velocity, c, by the following equation:

$$\Delta P(t) = \rho . c . U(t) \quad \text{(Eq 1)}$$

Introducing the expansion ratio of burnt gases, b, the flame trajectory, $f_p(t)$, can be evaluated by:

$$f_p(t) = \frac{\alpha}{\alpha - 1} \int_0^{\infty} U(t) dt \quad \text{(Eq 2)}$$

The theoretical expansion velocity, S_E, can be then written as the composition of the expansion ratio, α, and fundamental flame velocity, S_u:

$$S_E = \alpha . S_u$$

The fundamental flame speed and the expansion ratio depend on the nature of the gas, hydrogen in the present application, and the local concentration.

Based on previous test series, it has been shown that, when measuring the overpressure in a pipe resulting from such a deflagration, two pressure peaks are observed. A typical pressure measurement signal is represented hereafter in *Figure 2*. It corresponds to a methane-air explosion in a 100 mm in-diameter pipe. Such a signal clearly shows the two peaks, P1 and P2, with a relaxation phase in between.

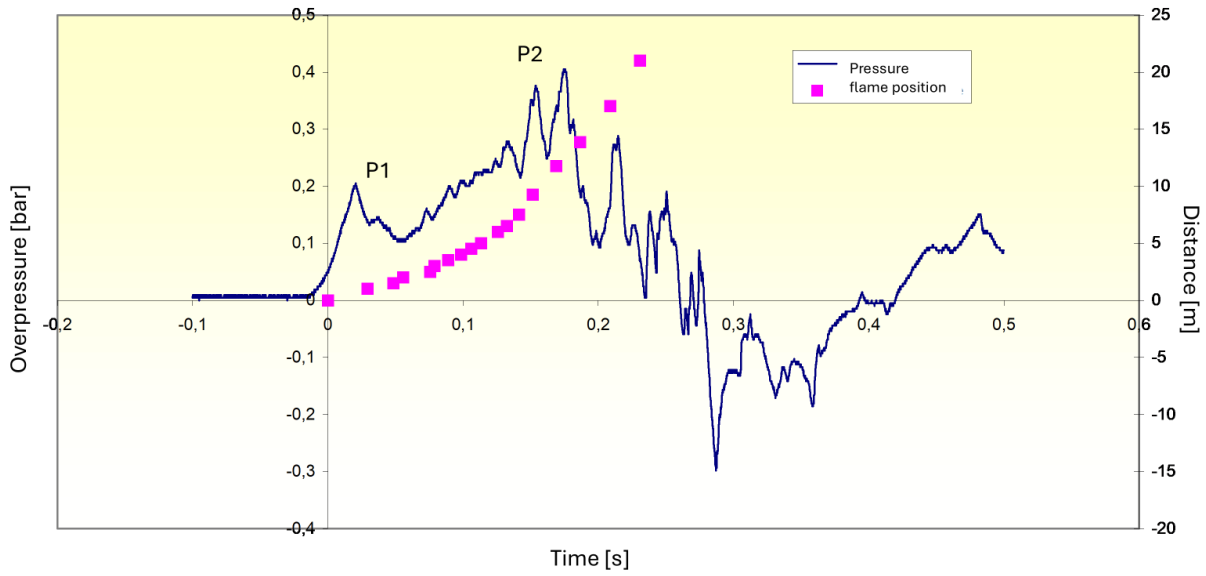

Figure 2: Typical pressure signal registered near the ignition source and flame position.

Proust et al. (10) interpret the two observed pressure peaks, attributing them to a two-stage propagation process. The first stage corresponds to the flame's initial development around the ignition point, forming an elongated parabolic shape. This elongation of the flame is accompanied by a significant increase in the flame surface area, reaching 10 to 15 times the cross-sectional area of the tube (19) (20). Once the sides of this parabola extinguish upon reaching the walls, the flame propagation slows down, as indicated by a decrease in the slope of the flame trajectory between 20 and 40 ms. Considering the time delay in the pressure measurement, the flame is estimated to be approximately 5 to 7 meters from the ignition point. Subsequently, a change in the slope of the flame trajectory is observed, marking the onset of a steady acceleration phase. Interactions with pressure waves periodically modulate this acceleration reflected from one extremity. At the end of this phase, the pressure reaches its second peak (P2), corresponding to the maximum overpressure.

One of the present test campaign's objectives is to evaluate whether such a methodology applies to larger geometry, such as tunnels. The following mechanisms are independent of the geometry diameter and correspond to a self-accelerated flame. The relation between expansion velocity and self-

acceleration is not as straightforward as in the first phase based on the existing test. The second objective of this campaign would be to evaluate this correlation in tunnel-representative geometries.

EXPERIMENTAL CONDITIONS

Experimental set-up geometry

The tests took place in gallery G1 at the Montlaville experimental site. Gallery G1 is a tunnel cut into the rock over a length of 144 m with a cross-section of ~ 3 x 3 m2. The natural cover is around 7 m high and consists partly of boulders. This tunnel is a blind gallery leading directly into the open air, with a vertical ventilation shaft fitted with an axial extractor at the closed end. This shaft can be closed using a hatch on the gallery roof, operated by a pneumatic jack. The walls are lined with concrete sprayed onto wire mesh. The roof has been reinforced with anchor bolts and, over 30 m from the tunnel end, steel hangers spaced 50 cm apart increase local resistance. Resistance to the effects of the explosion is estimated not to exceed 1.5 bar, *Figure 3*.

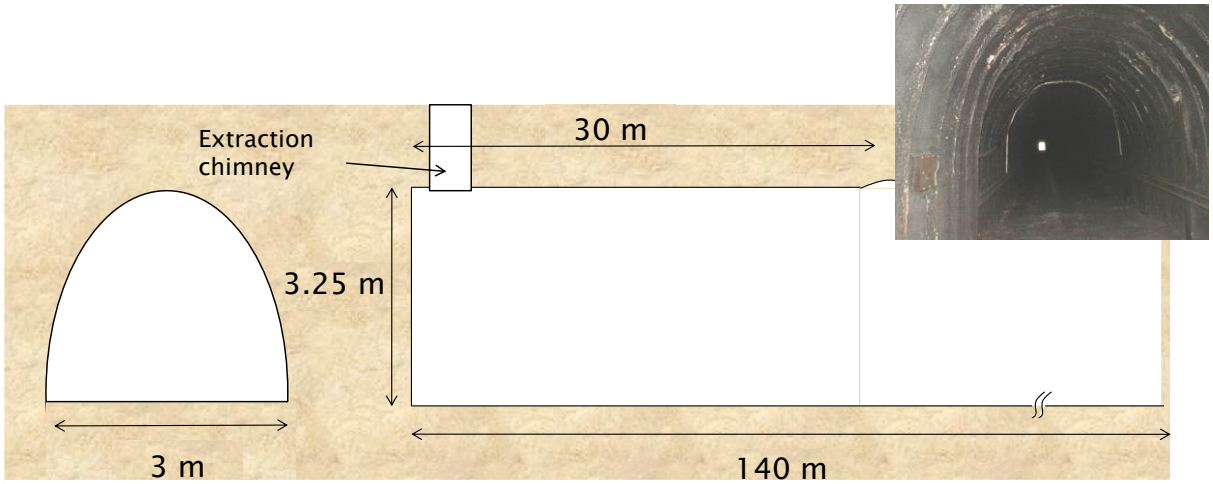

Figure 3: Schematic view of the explosion test gallery.

Measuring bases are installed every 15 m or so. The cables run in pipes inside or along the side walls. Three copper pipes link the 'cul-de-sac' area to the surface, near the ventilation shaft, and enable gas samples to be taken.

Gas and compressed air supply pipes run along the walls from the open end. The gas supply and control of the ventilation system (hatch and fan) are carried out from the 'firedamp station' along the cliff to the left of the gallery opening (10 m from the opening). The signals are acquired, and the shot is fired from the control room outside the pyrotechnic zone.

Generation of flammable clouds

The aim is to form homogeneous or stratified hydrogen clouds of different lengths, typically 7 and 15 m, at the bottom of gallery G1. These lengths were chosen because of the constraints at the bottom of gallery G1.

The gas plugs are formed between the blind section of the gallery and three sheets of transparent stretch plastic film magnetised to a metal structure (*Figure 4*) attached to the gallery walls by polyurethane foam. The polyurethane foam provides a hydrogen-tight seal between the metal profile and the walls.

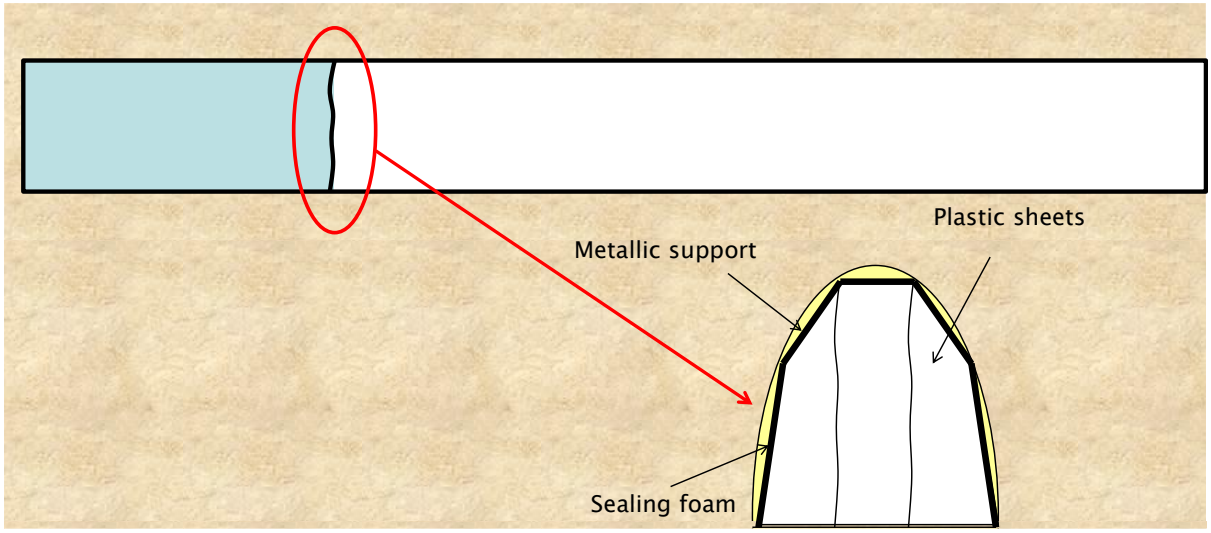

Figure 4: Schematic view of the generated flammable cloud.

The hydrogen is injected into the plug via the gas supply pipe along the walls from the open end and the firedamp station. The gas leaving the pipe is then distributed to the various injection nozzles (Figure 5). The diameter of the injection nozzles is 3 mm. Two and four nozzles were needed to form the 7 m long and 15 m plugs, respectively. The length of the flexible hose with an internal diameter of 8 mm between the outlet of the gas supply pipe and the injection nozzle is identical for each nozzle: 4 m for the 7 m plug and 10 m for the 15 m plug.

Hydrogen is supplied via a frame of interconnected cylinders. The maximum pressure in the frame is 197 bar. The internal volume is 903.6 litres. The nozzles are arranged on masts spaced 3 m apart. To form homogeneous mixes, they are located 50 cm from the ceiling, pointing towards the ground. To create stratified mixes, they are located 1.35 m from the ceiling, pointing upwards (*Figure 5*).

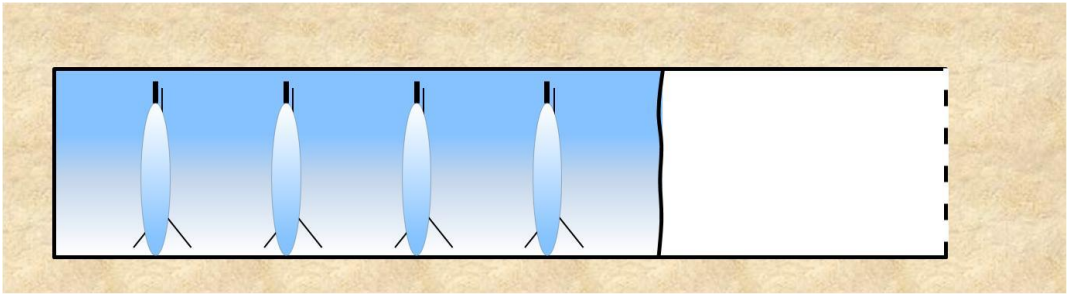

Figure 5: Typical injection procedure for the homogeneous 15m cloud.

Characterisation of the flammable cloud

During the injection, the hydrogen concentration is measured simultaneously and continuously at three points in the test chamber. Depending on the location of the measurement point, it varies between 0 and 20%v/v.

The measurement technique used is a paramagnetic measurement of the oxygen level (the hydrogen concentration being obtained by difference) for the following reasons (Figure 6):

- the concentration range 0 - 100% can be scanned with an uncertainty of less than 0.02 %v/v oxygen (0.1 %v/v H2),
- The measurement principle is very robust, easy to calibrate, interference-free and stable over time, making it possible to carry out continuous measurements over several hours,
- The equipment used operates by sampling, which means that the measurement points can be offset and, if necessary, the sampling points can be multiplied by automatic sampling

The gas samples are taken through three copper pipes linking the 'cul-de-sac' area to the surface. The measuring station is installed in the drill near the ventilation shaft. The sampling tubes are installed at three different heights in the gallery on one of the diagonals (*Figure 6*).

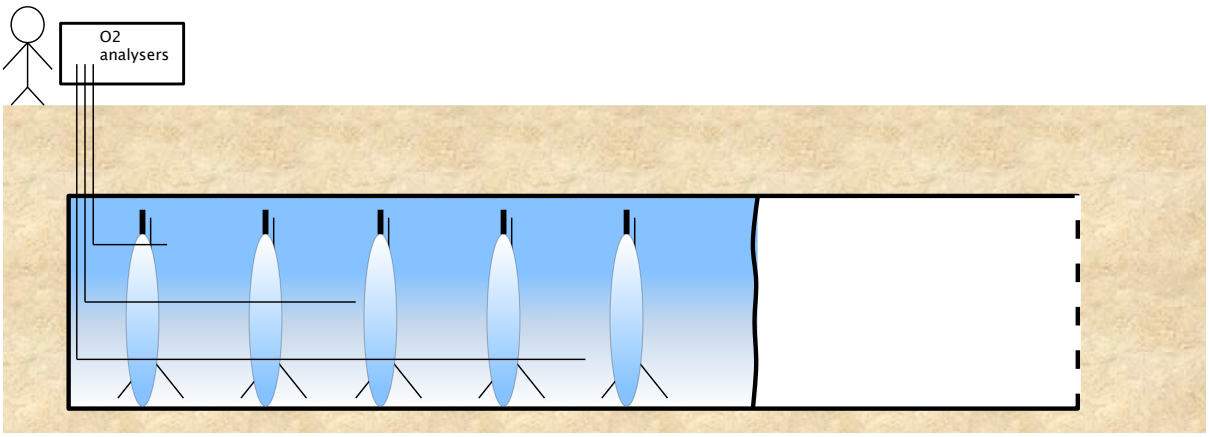

Figure 6: Sampling system installation and distribution.

Ignition procedure

The device used to ignite the gas mixture is a pyrotechnic bead with an energy output of 60 J. A sequencer ignites the bead by delivering a voltage of 220 V to its terminals.
The bead is placed halfway up the gallery, 10 cm from the wall.

Flame and pressure measurement

Figure 7 presents the pressure and flame detection system distribution during the test.

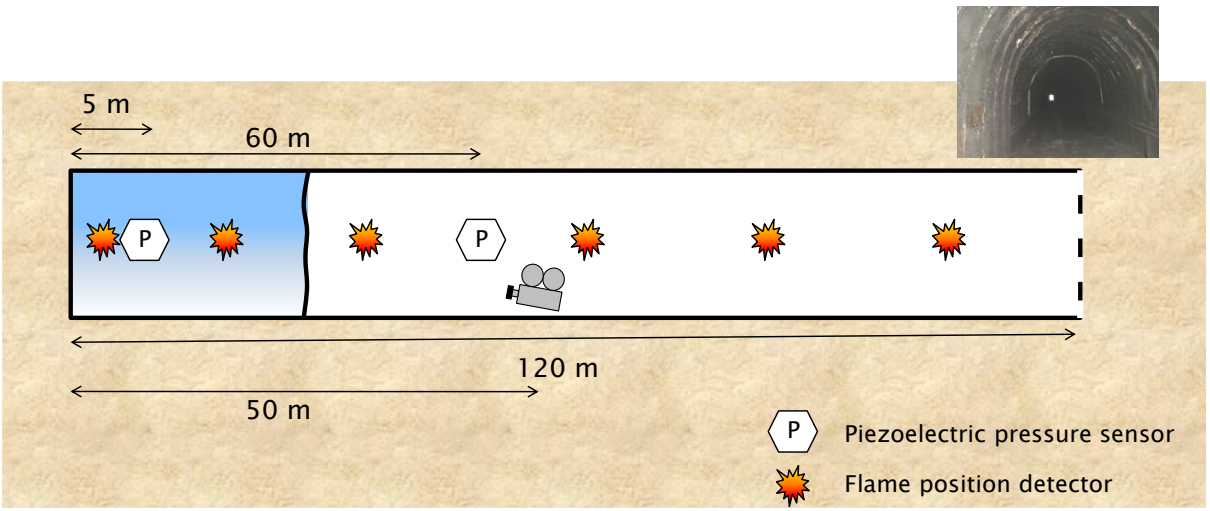

Figure 7: Location of in-gallery instrumentation

The pressure sensors used are absolute piezoresistive Kistler sensors. Two 0 - 10 bar sensors were installed flush with the gallery wall. One sensor is installed 5 m from the ignition source, the other 60 m from the ignition source.

A 0 - 2 bar sensor is installed at the gallery's exit to measure the explosion's external effects.
Flame sensors (Figure 7) are photovoltaic cells that deliver a voltage when light passes through them. This device reacts to the passage of a luminous flame and can, therefore, accurately detect the flame's arrival on the sensor.

These sensors are installed flush with the wall at distances of 5, 15, 35, 75, 105, 125 and 140 m from the ignition source.

Experimental test matrix

As mentioned in the introduction, the main objective of this campaign was to better understand the influence of the flammable cloud characteristics, size, concentration, turbulence, and stratification on flame propagation and associated pressure waves.

A series of 15 experiments were conducted to meet this objective, as shown in Table 1.

Table 1: characteristics of the conducted experiments

N°	Cloud length [m]	Homogeneous	Gas concentration [%v]	Turbulence
1	7	Yes	16.8	Medium
2	7	Yes	14.3	Medium
3	7	Yes	12.3	Medium
4	7	Yes	14.1	Medium
5	7	Yes	15.04	Medium
6	15	No	?	Medium
7	15	No	20.7-7.5-0	High
8	15	No	14.06-12-5.8	High
9	15	Yes	11.6	High
10	15	Yes	8.5	High
11	15	Yes	9.6	High
12	15	Yes	14.1	High
13	15	No	13.16-11.56-9.9	High
14	15	No	17.4-9.16-1.6	High

EXPERIMENTAL ANALYSIS

Flame behaviour and pressure wave propagation in a tunnel

Figure *8* presents the overpressure pressure signals measured at 5 m and 60 m for tests 11 and 12, representing a 15m long homogeneous mixture at 9.6 and 14.1 % H2 in air.

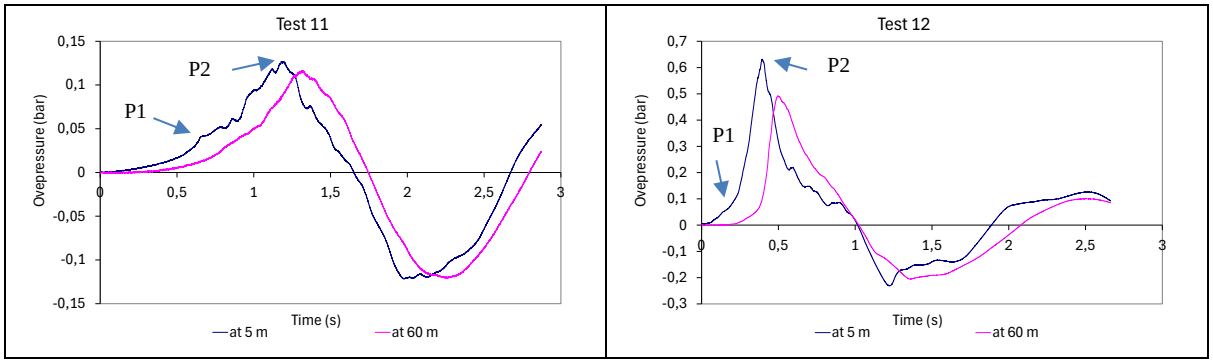

Figure *8:* overpressure pressure signals measured at 5 m and 60 m for tests 11 and 12

Figure 8 shows two distinct peaks, P1 and P2, can be observed. The first peak, P1, is more pronounced in test 11 than in test 12 due to the lower reactivity of the cloud in the latter. However, both tests exhibit a significant change in the slope of the overpressure evolution over time. This behaviour is reminiscent of flame propagation in a tube. The first peak, P1, is caused by the initial elongation of the flame as it expands until it reaches the tunnel walls. Subsequently, the flame undergoes a self-accelerating motion, ultimately reaching the edge of the cloud, where the second peak, P2, is observed. Unlike a fully gas-

filled tube, the gas cloud, in this case, has a limited length, preventing significant interaction between the tunnel's acoustics and the pressure wave. As a result, the overpressure signals are less oscillatory.

When analysing the pressure signals at 5 m and 60 m for both tests, it is evident that the signals have the same shape, similar pressure rise rates, and comparable magnitudes for the P1 and P2 peaks. This observation is consistent across all blast wave propagation tests conducted in this tunnel. Similarly, as reported in the Hytunnel project (21) for shock wave propagation in tunnels, a blast wave generated by a deflagration undergoes minimal attenuation as it travels through a tunnel.

Relevance of the theoretical correlation

Based on the measured overpressure and theoretical models, the experimental analysis identifies the worst-case situation. This analysis of cloud characteristics' influence is coupled with a theoretical analysis of flame propagation in a flammable cloud.

The first analysis in the present test campaign compares the measured flame propagation velocity with the theoretical value. Comparing the measured P1 pressure peak to the predicted value using the theoretical approach described previously shows an excellent agreement (*Figure 9*).

As observed on this graph, the magnitude of the overpressure is directly proportional to the material velocity of the flow, which is closely related to the flame velocity, as previously observed by Kerampran (19) and Daubech (20) for flame propagation in pipes. The maximum flame velocity is proportional to the burned gases' expansion velocity, represented by the parameter α.Su. The proportionality coefficient is simply the maximum flame elongation, expressed as A_f/A, also known as the "aspect ratio". The maximum flame elongation is approximately 10-15, a value consistent with measurements obtained from video analysis by Kerampran (19) and Daubech (20).

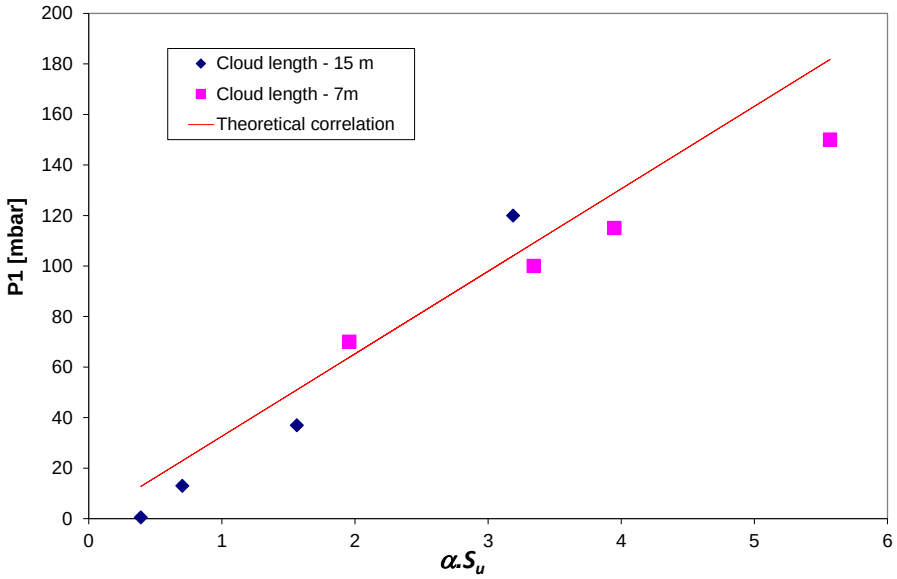

Figure 9: Predicted and measured P1 pressure peak for the different experimental conditions.

This analysis confirms that the simple method developed using small-scale tests, with hundreds of mm in-diameter pipes, seems to remain valid for large geometries such as tunnels to determine the value of the first peak P1.

After peak P1, peak P2 can be determined using an engineering model (22). This model allows the reconstruction of the pressure signal from peak P1 to peak P2 based on the self-accelerated motion of the flame. The self-accelerated motion can be estimated using the equation
$V_f = a_f \times t$, where V_f is the flame velocity, a_f is the flame acceleration, and t is the time. The resulting overpressure can then be calculated using Equation 1. The model assumes the peak is reached when the flame reaches the edge of the defined cloud.

The main challenge now lies in determining the flame acceleration coefficient. Proust's work (23), conducted under various configurations, has demonstrated that this acceleration factor depends on the product $\alpha.S_u$.

Applying this model to test 12, the expansion ratio of the combustion products α is 4.4, and the laminar burning velocity (Su) is 0.75 m/s, resulting in an acceleration factor of approximately 700 m/s². With an initial cloud length of 15 m, the combustion process concludes at approximately 30 meters.

Figure 10 compares the measured overpressure signal at 5 m and the calculated signal.

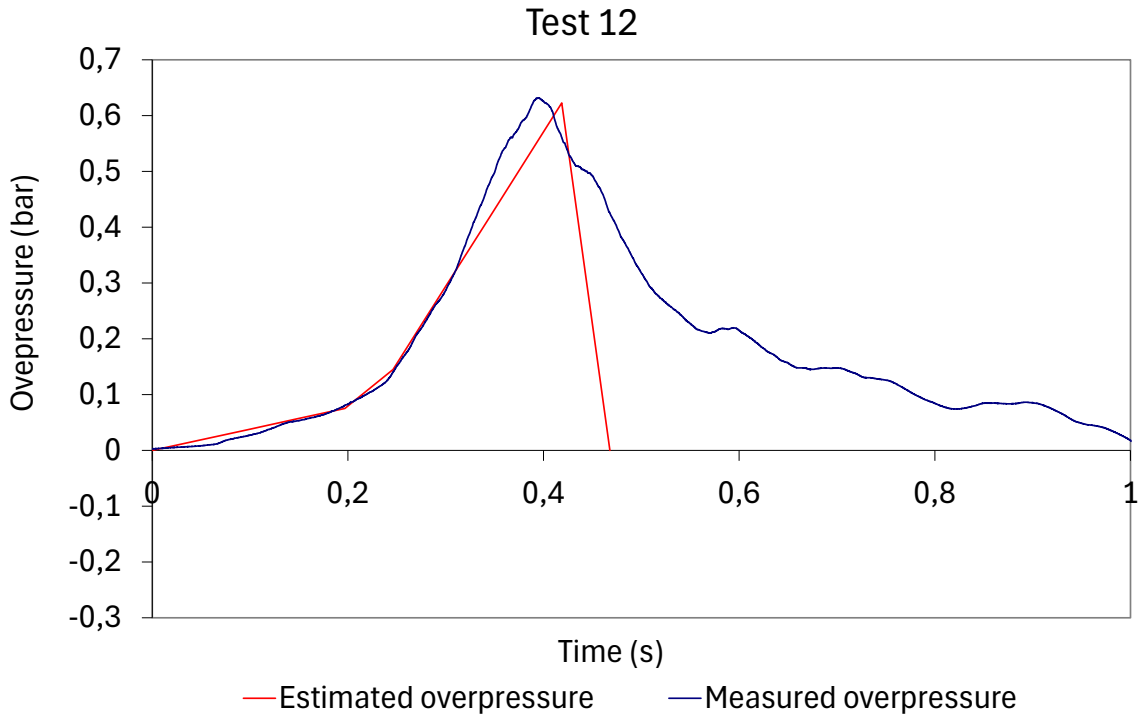

Figure 10: comparison between the measured overpressure signal at 5 m and the calculated signal

Gas concentration stratification influence

Another objective of this campaign was to evaluate the influence of the gas cloud characteristics on the resulting overpressure. Considering the impact of the concentration distribution, a comparison was performed between two 15 m long clouds containing the same quantity of hydrogen. The first is homogeneous, with a gas concentration of 11.5%. The second is a stratified one with a maximum concentration near the roof of 17.5% and a 1.5% concentration near the ground, with about 9.2% in the middle of the height. The flammable layer thickness is estimated to be 2 m. The resulting pressure signal 5 m to the end of the gallery is presented in *Figure 11*.

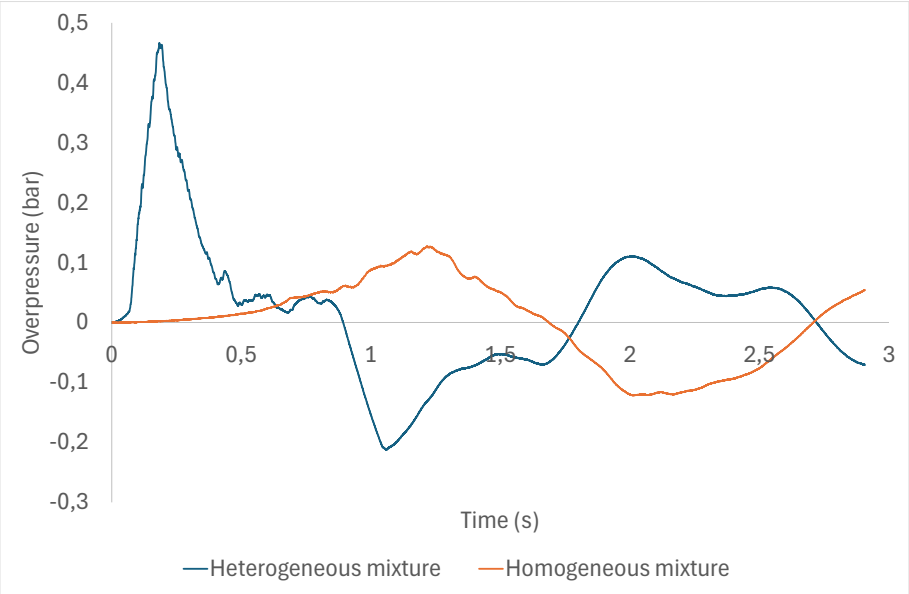

Figure 11: Pressure signal for two energetically equivalent clouds, homogeneous and stratified.

This curve clearly shows that introducing stratification strongly influences the maximum pressure reached in the geometry and the pressure variation over time. A more detailed analysis of this configuration, using video signals, highlights that the flame propagation is directly influenced by the most reactive layer of the cloud. This interaction increases the flame surface and a more significant flame acceleration. Since this mechanism directly influences the peak pressure (Eq 1), the observed peak pressure evolution is in good accordance with visual observation.

The flame velocity over time can then be plotted for those two situations (*Figure 12*).

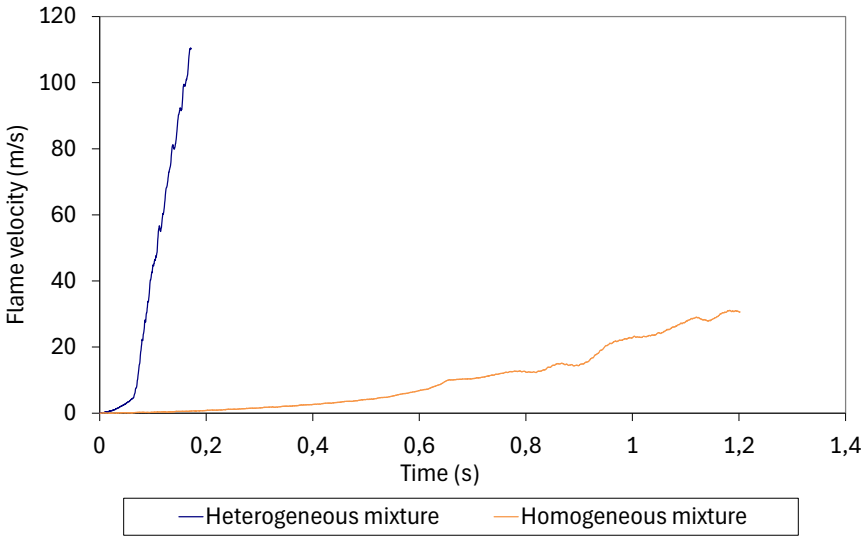

Figure 12: Flame velocity for homogeneous and stratified cloud deflagration.

This plot indicates that the flame velocity varies from about 30 m/s at the end of the propagation phase for a homogeneous cloud to about 115 m/s for a stratified one, i.e. a factor of 3.8 between the final propagation velocity.

One should consider some theoretical concepts based on flame-generated instabilities to propose a predictive approach for this acceleration mechanism. First, consider the theoretical flame expansion velocity, $S_E=\alpha.S_u$. This velocity equals about 6.1 m/s in the most reactive cloud layer and about 0.15 m/s in the lowest reactive cloud layer. Introducing the instability equations with:

- The Darrieus-Landau hydrodynamic mechanism (30)(31(32)(33):

$$S_{LD} = \left(1 + 4 \cdot \alpha \cdot \frac{(\alpha - 1)^2}{(\alpha^3 + \alpha^2 + 3 \cdot \alpha - 1)}\right) \cdot S_u$$

- the Rayleigh-Taylor instability (34)(35)(36):

$$S_{RT} = \left(0.51 \cdot \sqrt{\frac{\alpha - 1}{\alpha} \cdot \eta \cdot r}\right)$$

And considering their combination:

$$S_{Comp} = \sqrt{S_{RT}^2 + S_{LD}^2}$$

For a typical instability wavelength, the corresponding acceleration coefficient is about 3.2, which is quite good agreement with the experimental measurement.

CONCLUSIONS

This paper presents an experimental campaign to characterise the consequences of explosions in tunnels and the associated theoretical explanation.

First, this campaign shows that the physical mechanisms identified at tiny scale, hundreds of mm in diameter pipes, remain similar when dealing with several m in-diameter galleries, with two pressure peaks when analysing the pressure curve. The first peak, P1, is governed by the flame propagation in the cloud. Its intensity is directly correlated to the product of the fundamental flame speed and the gas expansion factor. The associated coefficient is the flame elongation factor. This approach enables predicting the P1 overpressure. When the flame reaches the tunnel wall, its influence decreases and, in some situations, the pressure also decreases by reducing the flame surface.

The flame self-acceleration makes the second pressure peak, P2, predictable. Predicting the acceleration coefficient remains a challenge, but some methods exist, and it can be shown that this coefficient does not depend on the fundamental flame velocity and gas expansion factor product.

Finally, a dedicated campaign was achieved to evaluate the influence of the gas concentration distribution in the tunnel and the effect of potential stratification. It has been shown that when stratification is in place, the resulting overpressure is strongly increased. This strong increase should be explained by the formation of instabilities resulting in flame disturbance by the concentration distribution.

REFERENCES

12. EUREKA 499, Fires in Transport Tunnels: Report on Full-Scale Test. EUREKA-Project EU499: FIRETUN Studiensgesellschaft Stahlanwendung e.V. D-40213 Dusseldorf 1995
13. Report for the UPTUN project - https://uptun.net/
14. Truchot, B., Oucherfi, M., Quezl-Ambrunaz, F., Duplantier, S., Fournier, L. and Waymel, F., Are the tunnel ventilation systems adapted for the different risk situations?, ISTSS conference (2010).
15. HyTunnel Deliverable D3.1, Detailed research program on hydrogen fires in confined structures (2019).
16. Molkov, V. and Dery, W., The blast wave decay correlation for hydrogen tank rupture in a tunnel fire, Int. J. Hydrogen Energy 45 (2020).
17. Van den Bosch C., Weterings, R., Methods for the calculation of physical effects: due to releases of hazardous materials (liquids and gases) ("Yellow Book"), TNO, Third edition

second revised print, 2005
18. Duclos, A., Développement de modèles phénoménologiques et de maitrise des risques d'explosion pour la filière émergente hydrogène-énergie. PhD thesis, Technical Univ. Of Compiègne, France (2019)
19. Daubech, J., Leprette, E., Proust., C., Influence of vent distribution on the violence of a gas explosion, 14. International symposium on hazards, prevention, and mitigation of industrial explosions (XIV ISHPMIE), July 2022, Braunschweig, Germany
20. Ciccarelli, G., Dorofeev, S., Flame acceleration and transition to detonation in ducts, Progress in Energy and Combustion Science, Volume 34, Issue 4, 2008
21. Proust, C., Gas flame acceleration in long ducts, Journal of Loss Prevention in the Process Industries, Volume 36, 2015, Pages 387-393
22. Rota R., Canu P., Carra S., Morbidelli M. (1991), " Vented gas deflagration modelling: a simplified approach ", Comb. and flame, vol. 85
23. Evans A.A., 1994, "Deflagrations in spherical vessels: comparison among four approximate burning velocity formulae", Comb. and Flame, vol 97.
24. Wu Y., Siddal R.G. (1996), " A mathematical model for vented explosions in a cylindrical chamber ", Trans IChemE, vol 74, part B
25. Dold J.W., Joulin G., 1995, " An evolution equation modelling inversion of tulip flames", Comb and Flame, vol 100, pp 112 - 126.
26. Proust C., 2004, "Habilitation à diriger des recherches : mémoires de travaux ", Institut National Polytechnique de Lorraine
27. Borghi R. (1988), " Turbulent combustion modelling ", Prog. Energy Comb. Sci., vol. 14
28. Evans A.A. (1994), " Deflagrations in spherical vessels: a comparison among four approximate burning velocity formulae ", Comb. and flame, vol. 97
29. Gilles S. (2000), "Propagation d'une explosion dans un réseau d'enceintes et de canalisations", mémoire de DEA de l'Université de Poitiers soutenue le 15 Octobre 2000 à Poitiers
30. Darrieus G., 1946, "Propagation d'une flamme. Essais des théories anormales de déflagration par développemen spontanée de la turbulence", 6th International Congress of Applied Mechanics
31. Landau L., 1944, "Theory of slow combustion", Acta Physicochim., vol 19, p 77.
32. Kerampran, S., Etude des mécanismes d'accélération des flammes se propageant depuis l'extrémité fermée vers l'extrémité ouverte de tubes horizontaux de longueur variable, PhD thesis, Univ. Of Poitiers, France (2000)
33. Daubech, J. Contribution à l'étude de l'impact d'une hétérogénéité de prémélange gazeux sur la propagation d'une flamme dans un tube, PhD thesis, Univ. Of Orléans, France (2008)
34. H.J. Kull, Theory of the Rayleigh-Taylor instability, Physics Reports, Volume 206, Issue 5, 1991, Pages 197-325
35. Kudriakov, S., Studer, E., Bernard-Michel, G., Bouix, D., Domergue, L., Forero, D., Gueguen, H., Ledier, C., Manicardi, P., Martin, M., Sauzedde, F., "Full-scale tunnel experiments: Blast wave and fireball evolution following hydrogen tank rupture", International Journal of Hydrogen Energy, 2022, 47(43), pp. 18911-18933
36. Daubech, J., Leprette, E., Proust, C. and Lecocq, G., Further insight into the gas flame acceleration mechanisms in pipes. Part I: Experimental work, Journal of Loss Prevention in the Process Industries, Volume 62, 2019, 103930S
37. Proust C., Propagation d`une explosion dans un reseau d`enceintes et de canalisatioNS, Ineris Report, 2002

In-Tunnel LIB Cargo Fire Emergency and Impacts on Tunnel Operational Capability

Adam Wood, Miguel Angel Fuentes & Sohail Alizadeh
Mott MacDonald
Renaissance House, 12 Dingwall Rd, Croydon, CR0 2NA, UK

ABSTRACT

With the recent trend of rapid development in battery technology, lithium-ion batteries (LIBs) are more frequently being transported by freight and in larger quantities. Thermal runaway of an LIB whilst in transit in a rail tunnel could lead to large fires with differing fire dynamics to regular cargo. This paper reports the Computational Fluid Dynamics (CFD) modelling of an LIB fire in a lorry being transported through a tunnel by rail. The study considers the scenario of a train on fire stopping in a tunnel with the activation of a tunnel ventilation system, while a second scenario considers the addition of a High Pressure Water Mist (HPWM) fire suppression system. CFD simulation results presented in the form of temperature contours and graphs of tunnel soffit temperatures show the peak temperature of the plume in the tunnel crown occurs when the train is stationary in the tunnel with low or no tunnel ventilation. The addition of tunnel ventilation dilutes the hot plume and reduces peak temperatures in the soffit to around 650 °C while the activation of the HPWM system further reduces temperatures to below 200 °C. The temperatures under the tunnel crown could lead to failure of tunnel systems and threaten the structural integrity of the tunnel walls.

KEYWORDS: CFD, train fire, cargo fire, battery fire, fire life safety, fire suppression, tunnel ventilation, operational impact.

INTRODUCTION

As battery technologies develop, high density energy storage devices such as lithium-ion batteries (LIBs) are more frequently being transported by rail. Owing to their high energy density, in the event of a fire these battery cargo loads combust with a much higher heat release rate than conventional loads. If a fire were to break out whilst a train passes through a tunnel, there is potential for damage to the tunnel structure, lineside equipment and rolling stock caused by a high intensity fire in an enclosed environment.

CFD modelling has the potential to assess the risks to tunnel structures, equipment and rolling stock during emergency incident scenarios of an LIB cargo fire in a tunnel. CFD can also assess the effectiveness of tunnel ventilation and fire suppression systems in limiting the maximum temperatures in the tunnel during an emergency fire scenario.

LIB fires develop in a more complex manner than conventional fires, owing to their propensity to undergo thermal runaway. Thermal runaway can be caused by faults in the battery construction, short-circuiting, overcharging or mechanical damage and abuse. Thermal runaway results in extremely high temperatures and is often self-sustaining due to oxygen producing exothermic reactions, making them difficult to extinguish and less effected by oxygen depletion compared to other types of combustion. Thermal runaway of an LIB on board a cargo train could trigger further thermal runaway in adjacent batteries, as well as combustion of other materials on board such as plastics and fuels.

In the present CFD study, a lorry transport train is considered travelling through a tunnel, with the incident lorry carrying a cargo of LIBs. Each individual combusting element of the incident lorry (e.g.

LIB cargo, lorry structure, fuel tank etc.) is given an individual composite fire curve with ignition times determined from a fire spread analysis calculation.

Tunnel ventilation systems are frequently used to minimise the danger to life during a fire emergency. Additionally, fire suppression systems such as sprinklers are more frequently being used in tunnel designs to reduce the potential impacts of fire damage. An example of their use can be seen in the Dartford road tunnel, which runs beneath the River Thames in England. Additionally, water mist fire suppression systems are installed on various trainsets across European rail operators [1], and may be considered during design stages of future rail and road tunnel projects. This study will consider the cases of a train on fire stopping in a tunnel with active tunnel ventilation, and stopping at a refuge where both ventilation and fire suppression is applied. Plume temperatures in the tunnel soffit and around key components are assessed and may inform future tunnel systems design and limitations on LIB cargo carrying capacity.

SCENARIO

Tunnel and Train Geometry

This CFD study was carried out on a mock-up tunnel geometry to simulate an emergency scenario of a lorry transport train carrying LIB cargo which ignites within the tunnel. The model includes the incident lorry aboard a carrier along with eight additional lorry carrier models, 4 ahead of the incident carrier and 4 behind, to provide a blockage to the flow in the tunnel mimicking the presence of the rest of the train, as shown in Figure 1. The tunnel has an hydraulic diameter of 8.6 m and extends 100 m to the front and rear of the modelled carriages giving an overall length of 388 m.

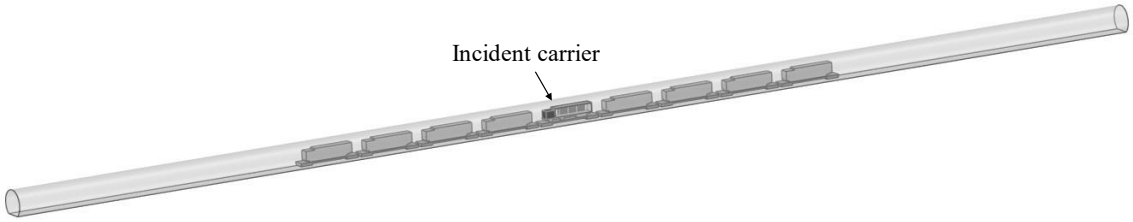

Figure 1 Tunnel geometry

A detailed view of the incident lorry and carrier is shown in Figure 1. The carrier is 20 m long and 4 m wide. The lorry is 16 m long, 2.8 m wide and 4 m tall and is made up of a trailer, cabin, solid chassis and a volume representing the combustible lorry components such as tyres and the diesel fuel tank. The trailer carries three containers of LIBs of length 3 m, width 1.6 m and height 2.1 m. No other internal features are included.

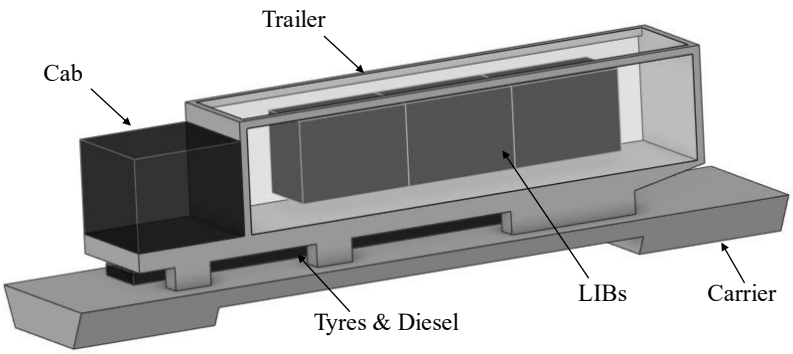

Figure 2 Incident lorry and carrier

Fire Definition

To produce an overall fire curve, the incident lorry was split into separate volumes to which individual fire curves are applied representing different combustible elements of the lorry. The method used to describe the time varying development of a lorry fire is based on the method described by Ingason H et al. [2]. The heat release rate (HRR) time history for each component is defined in terms of a t-squared fire growth phase, a constant (peak) HRR phase and an exponential decay phase. The area under each fire curve corresponds to the component's total fire load.

Assumptions of the fire definition of LIB fires have been made based on literature presenting information specifically from the fire testing of vehicle LIB packs [3] [4]. The fire curve for the three battery volumes are split into the LIBs themselves and the LIB casing. The total LIB fire size of each battery volume is assumed larger than the EVs in [3] and [4] with a maximum HRR of 10 MW, representing a cluster of LIBs stored together in a single casing. To maintain modelling simplicity, three battery volumes are included to represent fire spread within the trailer. The casings have an assumed HRR of 15 MW, based on a surface area of 30 m^2 and a heat release rate per unit area (HRRPUA) of 0.5 MW/m^2, representing a mixture of acrylic and metallic materials. As the state of charge (SOC) of batteries transported in the tunnel cannot be guaranteed, to be conservative, the SOC is assumed 100 %. The batteries are assumed to be new with a state of health (SOH) of 100 %. Both the batteries and the casings follow an ultra-fast t-squared fire growth parameter of 0.1876 kW/s^2 and a decay constant of 0.01. The cab volume, representing the combustion of materials in the lorry cab such as soft furnishings and plastics, is assumed to have a maximum HRR of 10 MW with a fast t-squared fire growth parameter of 0.01172 kW/s^2 and a decay constant of 0.0025. Finally, the volume on the underside of the lorry representing the tyres and diesel fuel is assumed to have a maximum HRR of 22.5 MW with a medium t-squared fire growth parameter of 0.0469 kW/s^2 and a decay constant of 0.01 [5].

Ignition time delays for each component are assessed based on an assumed fire spread pathway between the components. These delays are determined using engineering judgement based on material fire tests and the overall timescales for end-to-end fire spread observed in full scale lorry fire tests such as the Runehamar tunnel fire tests undertaken as part of the UPTUN project [6]. For this study it is assumed that the fire starts due to a fault in the front most LIB leading to thermal runaway which ignites the first battery casing. The fire spreads sequentially to the other two battery casings causing thermal runaway in their respective LIBs. The fire then spreads via radiation to the trailer's tyres and diesel tank before eventually spreading to the tractor unit (cab) which is constrained by being upstream of the burning trailer and its load.

The total and constituent fire curves for the LIBs, cab and tyres and diesel fuel are shown in *Figure 3*.

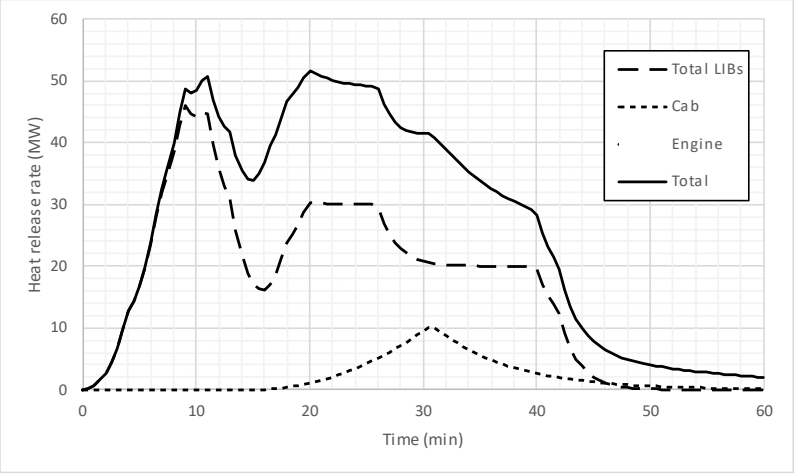

Figure 3 Component and total fire curves

Train Motion and Tunnel Ventilation

At the start of the simulation the train is assumed to be travelling through the tunnel at a constant speed of 100 km/h. The simulation follows a moving frame of reference methodology where the reference frame is fixed to the train. To model the train movement at the start of the simulation, a velocity inlet is prescribed at the upstream boundary to model the flow of air over the nose of the moving train and the tunnel walls and floor are given a moving wall boundary condition at the prescribed speed of the moving train. Due to piston effects inside the tunnel, the velocity of the air over the nose of the train is not equal to the train speed. The magnitude of the air velocity over the nose of the train has been determined using engineering judgement and experience from previous projects. A period of time after the fire starts, the train decelerates to a stop in the tunnel, controlled by varying the upstream velocity boundary condition and reducing the moving wall boundary condition speed to zero over the course of one minute. After a further minute the tunnel ventilation system is activated. For the purpose of this study the tunnel is assumed ventilated by a series of jet fan banks which are far from the incident carrier when the train comes to a stop. It is assumed the ventilation produces a uniform flow of 4 m/s with a ramp-up time of 2 minutes. The direction of ventilation is from the front of the train towards the rear.

Sprinkler System

In this study, a High-Pressure Water Mist (HPWM) system has been considered as part of the tunnel fire suppression system to limit the development and spread of a fire. It has been assumed that the HPWM system consists of two pipes located on either side of the track, split into sections slightly longer than a single train carriage. In this study, a total of 60 sprinkler heads are activated distributed along roughly 100 m of tunnel. Water coverage is achieved by the installation of sprinkler heads consisting of multiple injection ports per head, arranged for maximum water coverage within the tunnel.

When the train stops at the HPWM system, it is assumed that a heat detection system locates the fire and automatically tiggers the deployment of sprinklers over the hottest section and the two adjacent sections. It is assumed the HPWM system activates 2 minutes after the train comes to a stop. The train comes to a stop after 6 minutes, therefore the HPWM system is activated 8 minutes after the fire starts.

CFD METHODOLOGY

Software

The CFD study was performed using the ANSYS software suite with Fluent 2024 R1 as the CFD solver.

Computational Mesh

The computational domain was divided into 1,064,231 cells. The mesh resolution for the CFD model was tailored to resolve important flow features and where locally high spatial gradients of flow properties are anticipated i.e. in the vicinity of fires and in regions where flow area is restrained such as underneath the lorry. Mesh inflation layers were used at solid surfaces (tunnel walls, carrier bodies etc.) to appropriately represent the high gradients in flow field parameters. The general cell size was of the order of 0.2 m. In the region underneath the lorry the mesh size was more refined whereas in regions away from the fire the mesh was coarser to reduce computational time and maintain simulation efficiency. Mesh size expansion ratios were specified as 1.2 from higher to lower resolution regions. An example of the mesh structure and density is shown in *Figure 4*.

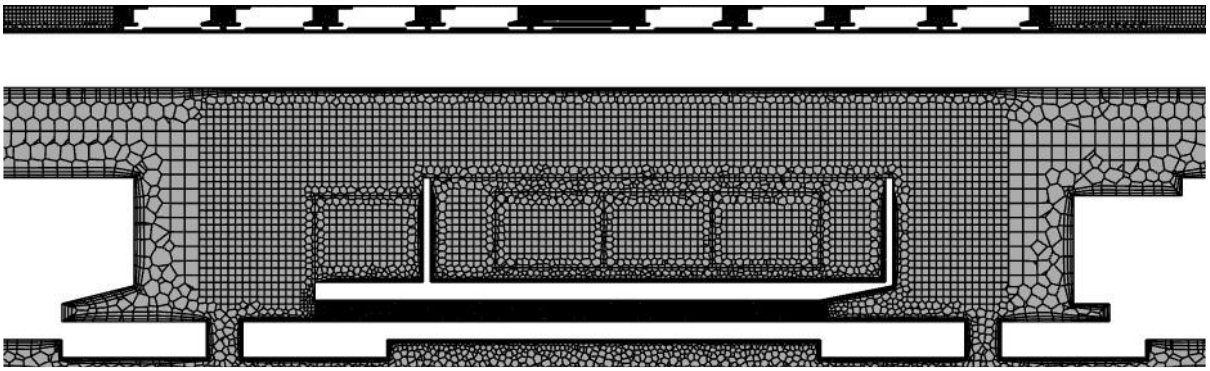

Figure 4 Section mesh of the tunnel and zoomed view of the incident carriage

Fire Representation

The definition of the fire curve within the CFD model is split into two methodologies. The HRR of the composite fire curve associated with the LIBs themselves is applied to the LIB fluid volumes as a volumetric heat source, controlled using a user specified profile. This models the LIBs' self-sustaining nature during thermal runaway as the LIBs produce heat without reliance on external oxygen. The HRR of the remaining components (i.e. the battery casings, lorry cabin, engine and tyres etc.) is modelled using a single step chemical reaction. The incomplete combustion of fuel with oxygen in the domain leads to the release of heat and combustion products. This models the more conventional type of fire associated with simple combustion where the fuel is reliant on the availability of oxygen to burn. Fuel is introduced to the domain via a volumetric source in the fluid zones, with the amount of fuel in each zone controlled using a user specified profile. The air fuel ratio (AFR) of the combustion reaction is specified to control the peak plume temperatures in the tunnel soffit to match experimental values [7] [8].

The summation of the total heat source plus the heat liberated via the single step combustion reaction gives the total heat release rate described in *Figure 3*. The convection fraction of the heat release rate is 0.65 [7]. The radiative portion is not modelled in the calculations as radiative effects are limited to the immediate vicinity of the fire. Radiative effects follow an inverse-square relationship with distance from the heat source. Therefore, smoke, and hot gases move primarily due to the convective component of the heat release from the fire.

Turbulence Model

The Reynolds Averaged Navier-Stokes (RANS) approach was adopted for the solution of the flow field conservation equations. The standard k-ε turbulence model was used in conjunction with Standard Wall Functions for near-wall boundary layer calculations. The buoyancy body force was incorporated into the fluid flow equations and in the turbulence model, based on localised differences in temperature and hence flow density.

Boundary Conditions

The no-slip boundary conditions is applied to the tunnel walls and floor which are given a moving wall boundary condition for the period where the train is modelled as moving through the tunnel and decelerating to a stop. The moving wall velocity profile is shown in *Figure 5*. The tunnel walls and floor are given an isothermal boundary condition with a far field temperature of 15 ºC and a wall thickness of 0.3 m. The walls are given the thermal properties of concrete i.e. density 2400 kg/m^3, specific heat 880 J/kgK and thermal conductivity 1.2 W/mK. The flow boundary conditions for the tunnel are specified at the upstream tunnel boundary ahead of the train as a velocity boundary condition. The velocity is prescribed as uniform across the surface and the velocity profile is show in *Figure 6*. The downstream tunnel boundary behind the train is prescribed as a pressure boundary.

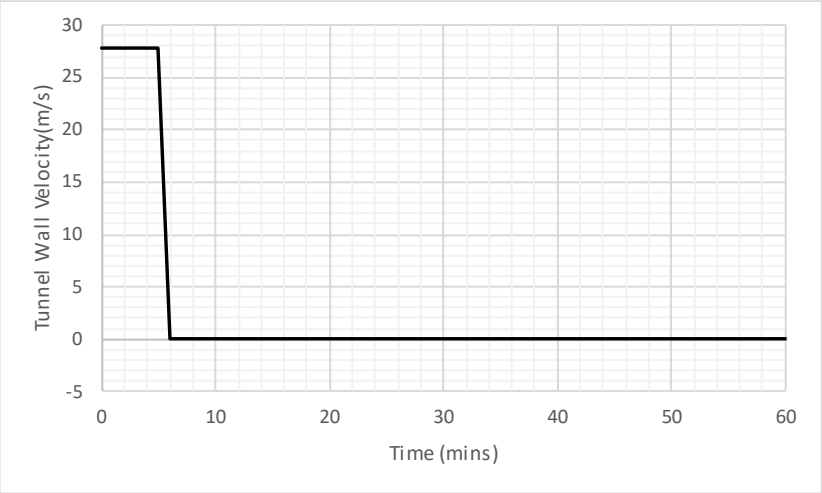

Figure 5 Tunnel walls and floor moving wall boundary profile

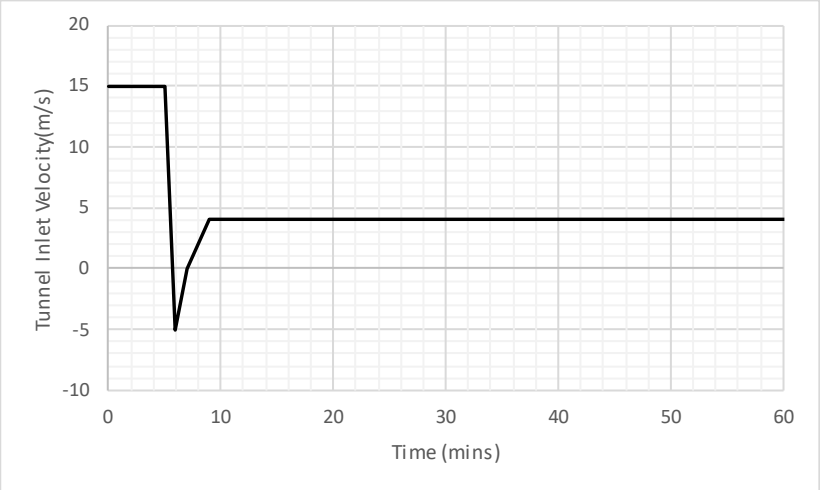

Figure 6 Upstream tunnel boundary velocity profile

The surface representing the tarpaulin of the lorry trailer is set to an internal boundary condition from the start of the fire on the assumption that the fire would quickly burn the tarpaulin away. The surface representing the lorry cab walls is specified as a wall boundary until the beginning of the cab fire at 15 minutes when the boundary is changed to internal to represent the cab materials being consumed by the fire. The remaining walls of the incident and non-incident carriers are given an adiabatic boundary condition.

Initial Conditions

The transient simulation begins upon ignition of the first LIB whilst the train is travelling through the tunnel at 100 km/h. As such, a steady state calculation was undertaken to determine the flow field around the train at this speed. This flow field was used to initialise the solution for the full transient calculation. It was assumed that the initial air temperature inside the tunnel is 25 ºC which is representative of a high ambient temperature for the tunnels and therefore more onerous.

Spray Modelling

The HPWM is represented via explicit representation of the individual sprinklers. The Discrete Phase Model (DPM) available in Ansys Fluent is used to model water droplet trajectories through the

domain. This solution uses a two-phase approach consisting of a fluid phase (air) and a discrete particle phase (sprinkler water droplets). Air as the fluid phase is treated as a continuum and is governed by the continuity and Navier-Stokes equations. Water droplets as the discrete phase consist of a definite number of particles that move through the continuous fluid flow, and which are tracked in a Lagrangian frame. A two-way interaction between droplets and the fluid is adopted. Further details about the methodology can be found in [9].

The spray pattern of each sprinkler is modelled by point-cone injectors which represent each of the five micro-nozzles per head. *Figure 7* illustrates the geometry of the nozzle. These injectors are modelled by specification of flow rate, cone angle, discharge velocity and droplet size distribution. The following parameters have been assumed about the HPWM system:

- The sprinklers have a flow rate of around 50 l/min at 50 bars.
- As the velocity distribution of droplets after atomization is unknown, a constant initial velocity of droplets is assumed. Initial velocity of droplet is set to 80 m/s based on Torricelli's law and an assumed orifice discharge coefficient of 0.8.
- A cone angle of 20° is estimated, which is the angle described in the near region of the micro-nozzles. The spray pattern of each micro-nozzle is assumed axisymmetric.
- It is assumed that the water jet is already atomised at the nozzle exit and the distribution of droplet sizes follows a Rosin-Rammler-Lognormal distribution and a $D_{v,0.5}$ of 150 µm (typical for ordinary high-pressure water mist systems).
- Initial temperature of water droplets is set to ambient, 25 °C.

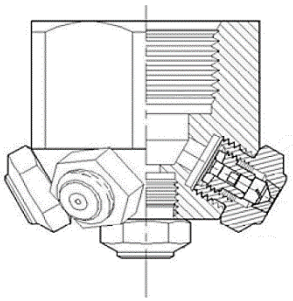

Figure 7 High-pressure fire suppression mist nozzle

The CFD modelling of the HPWM system presents the cooling of hot plumes resulting from sprinkler activation. The CFD model assumes that the HRR of the fire is reduced by 50 % after deployment of sprinklers. This assumption is in agreement with experimental tests carried out by researchers and suppliers of Fire Suppression Systems (FSS) found in public literature.

RESULTS

In the following section, all times are given in minutes with time t=0 referring to the time of the fire starting. Key events in the simulation timeline are outlined in Table 1.

Plots of tunnel soffit temperatures against time at three locations within tunnel are given for both scenarios with and without the sprinkler system active. The monitor points are set above the incident carrier along the tunnel centreline. The locations of these monitor points relative to the incident carrier are shown in *Figure 8*.

Table 1 Summary of key events in the simulation timeline

Time (mins)	Event
0	Simulation begins with the start of the fire
5	Train begins to decelerate from 100 km/h
6	Train comes to a full stop in the tunnel
7	Tunnel ventilation ramp up begins
8	HPWM system activates
9	Tunnel ventilation reaches a peak tunnel velocity of 4 m/s upstream of the fire
20	Fire reaches peak HRR
30	Simulation Ends

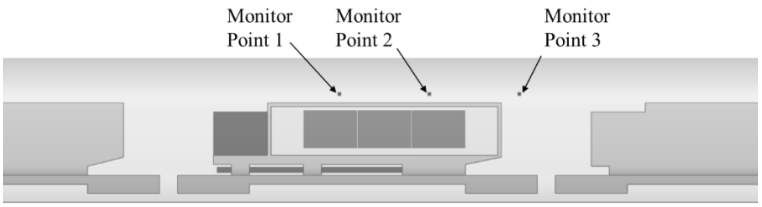

Figure 8 Locations of tunnel soffit temperature monitor points

Scenario 1 – Without Sprinklers

Figure 9 shows the temperature plots for the three monitor points in the tunnel soffit for the scenario without sprinkler activation.

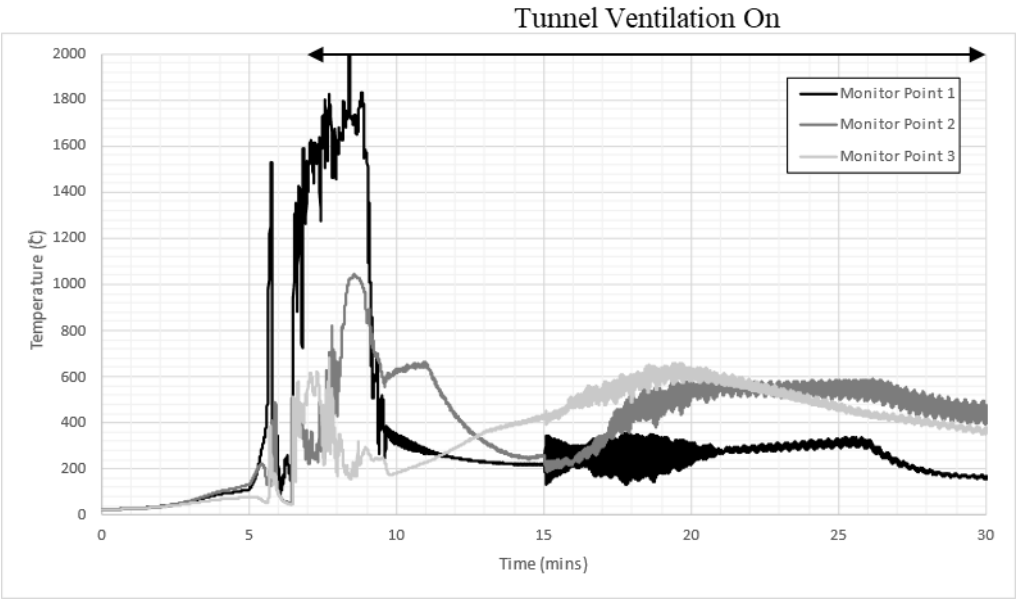

Figure 9 Temperature plots at monitor points in the tunnel soffit for the scenario without sprinkler activation

Figure 10 shows contour plots of static temperature on a vertical plane slicing through the centre of the tunnel for the scenario without sprinkler activation. *Figure 11* shows contour plots of static temperature on vertical planes slicing through the cross-section of the tunnel at the midpoint of the batteries, cab and behind the incident carrier.

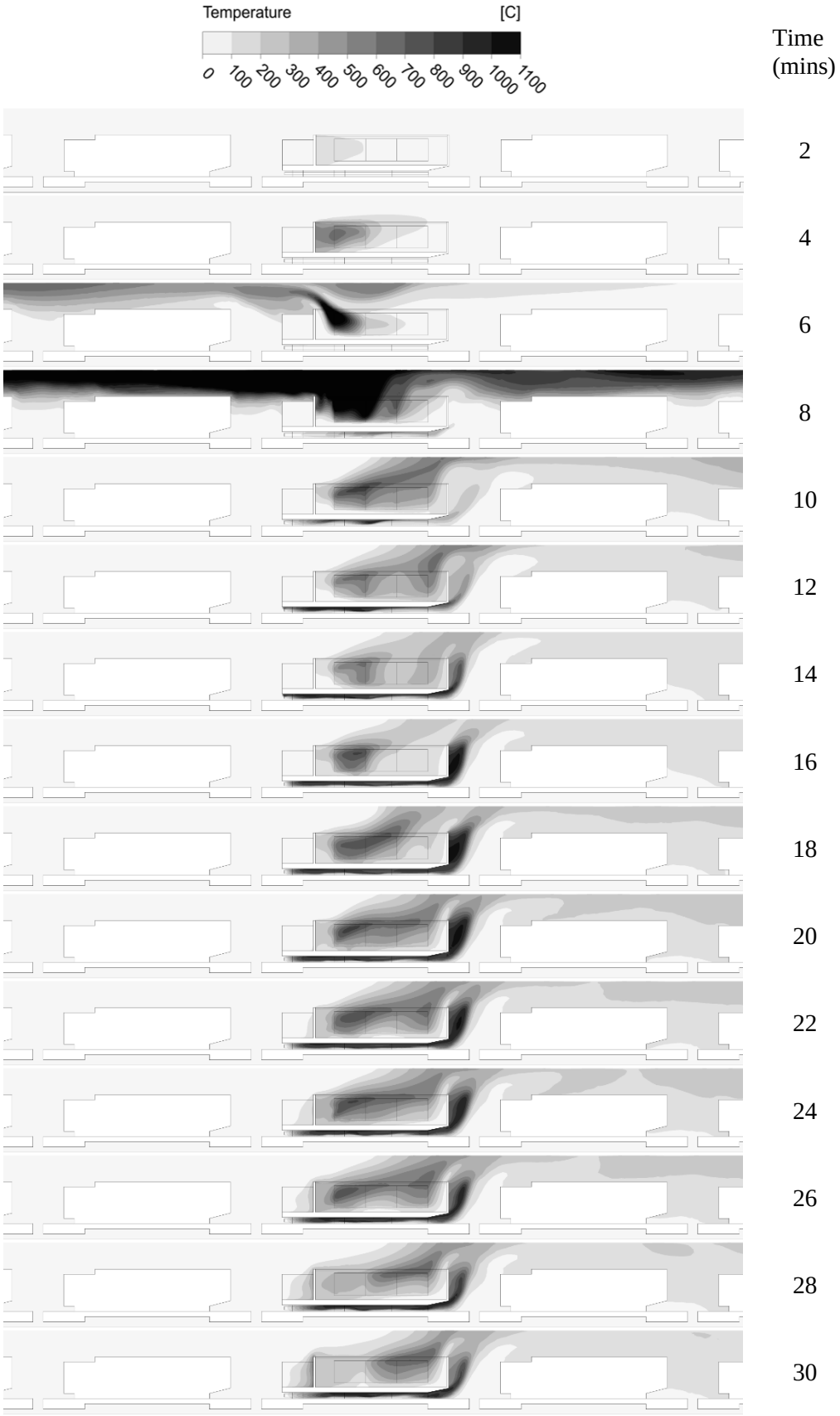

Figure 10 Air temperature on a vertical slice through the centre of the tunnel – without sprinkler activation

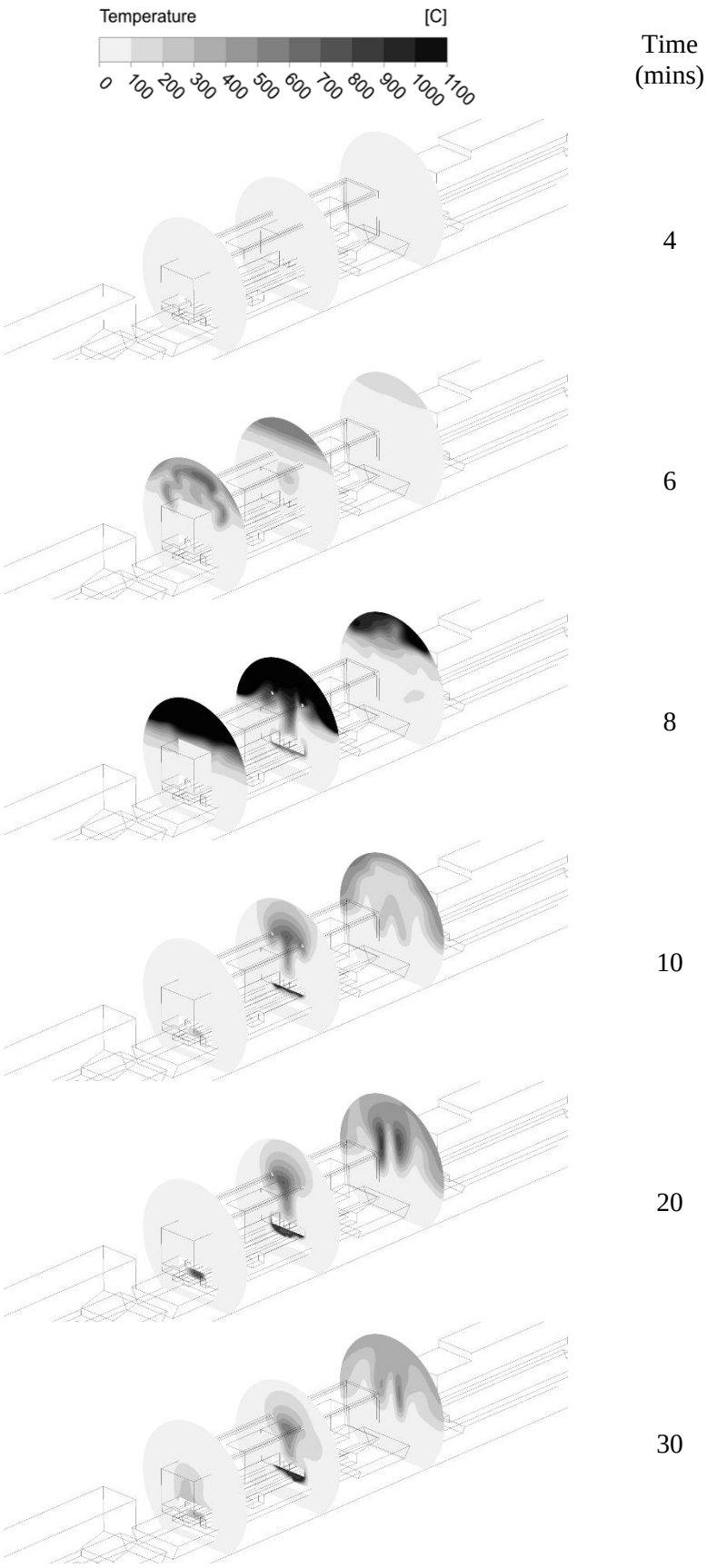

Figure 11 Air temperature on vertical slices through the centre of the batteries, cab and behind the incident carrier – without sprinkler activation

While the train is running in the tunnel at high speed, high temperatures remain within the trailer of the lorry and the plume is quickly mixed out in the high velocity airstream of the tunnel. When the train stops in the tunnel after around 6 minutes, a hot plume forms in the soffit of the tunnel above the carrier. Piston effects from the motion of trains within the tunnel network pushes this plume forwards of the lorry towards the front of the train. This piston effect then decays leaving a brief period of static flow in the tunnel at around 8 minutes at which time the hot plume starts to fill the tunnel from top down and spreads in both directions in the tunnel due to buoyancy effects. The peak temperature of the plume is significantly higher during this period as there is no dilution of the plume by the ventilation system. After around 10 minutes the active tunnel ventilation starts to push the hot plume back over the incident carrier towards the rear of the train, diluting the plume and lowering peak temperatures in the soffit. Temperature oscillations after 15 minutes are due to small scale unsteadiness in the hot flow field and coincide with the start of the lorry cab fire and the removal of the cab walls.

Temperatures in the tunnel soffit above the incident lorry peak at around 650 °C after activation of the tunnel ventilation from 9 minutes onwards. Temperatures underneath the lorry, but above the surface of the carrier, peak at around 1100 °C. Temperatures below the carriers remain cool (less than 100 °C) for the duration of the simulation. Overall peak plume temperatures agree largely with experimental data of tunnel fires [10].

Scenario 2 – With Sprinklers

Figure 12 shows the temperature plots for the three monitor points in the tunnel soffit for the scenario with sprinkler activation.

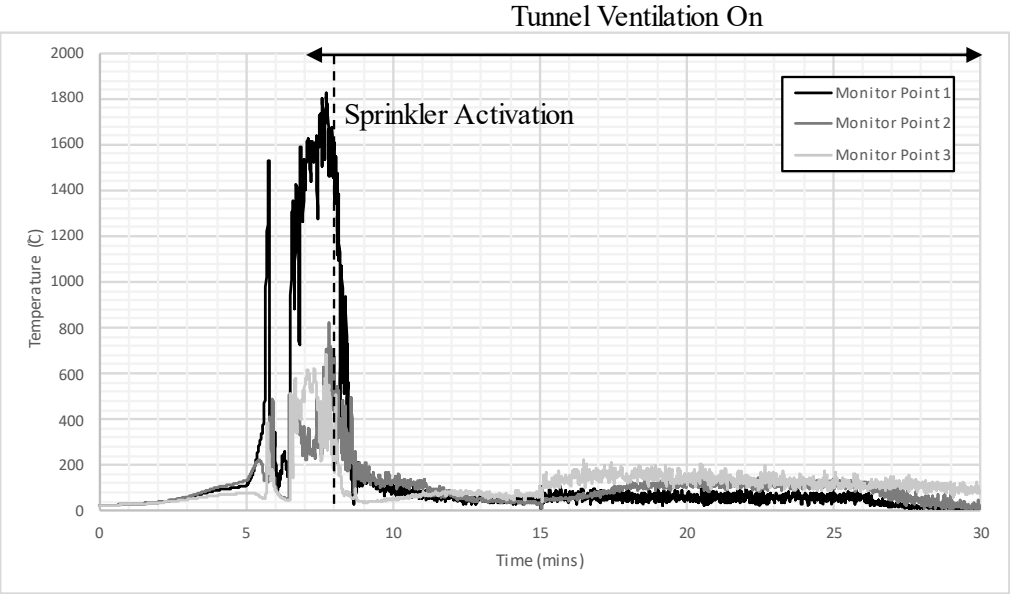

Figure 12 Temperature plots at monitor points in the tunnel soffit for the scenario with sprinkler activation

Figure 13 shows contour plots of static temperature on a vertical plane slicing through the centre of the tunnel for the scenario with sprinkler activation. *Figure 14* shows contour plots of static temperature on vertical planes slicing through the cross-section of the tunnel at the midpoint of the batteries, cab and behind the incident carrier.

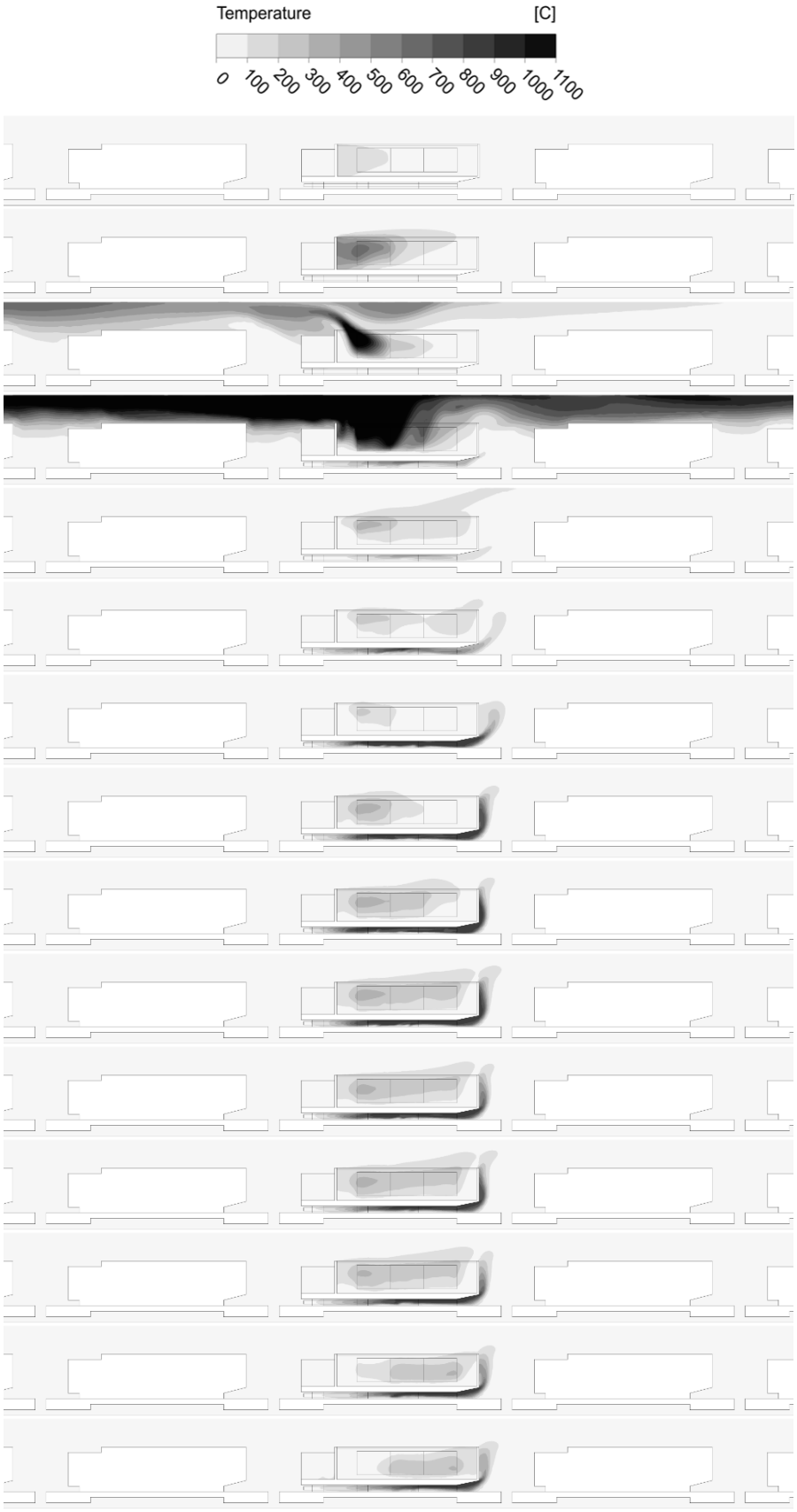

Figure 13 Air temperature on a vertical slice through the centre of the tunnel – with sprinkler activation

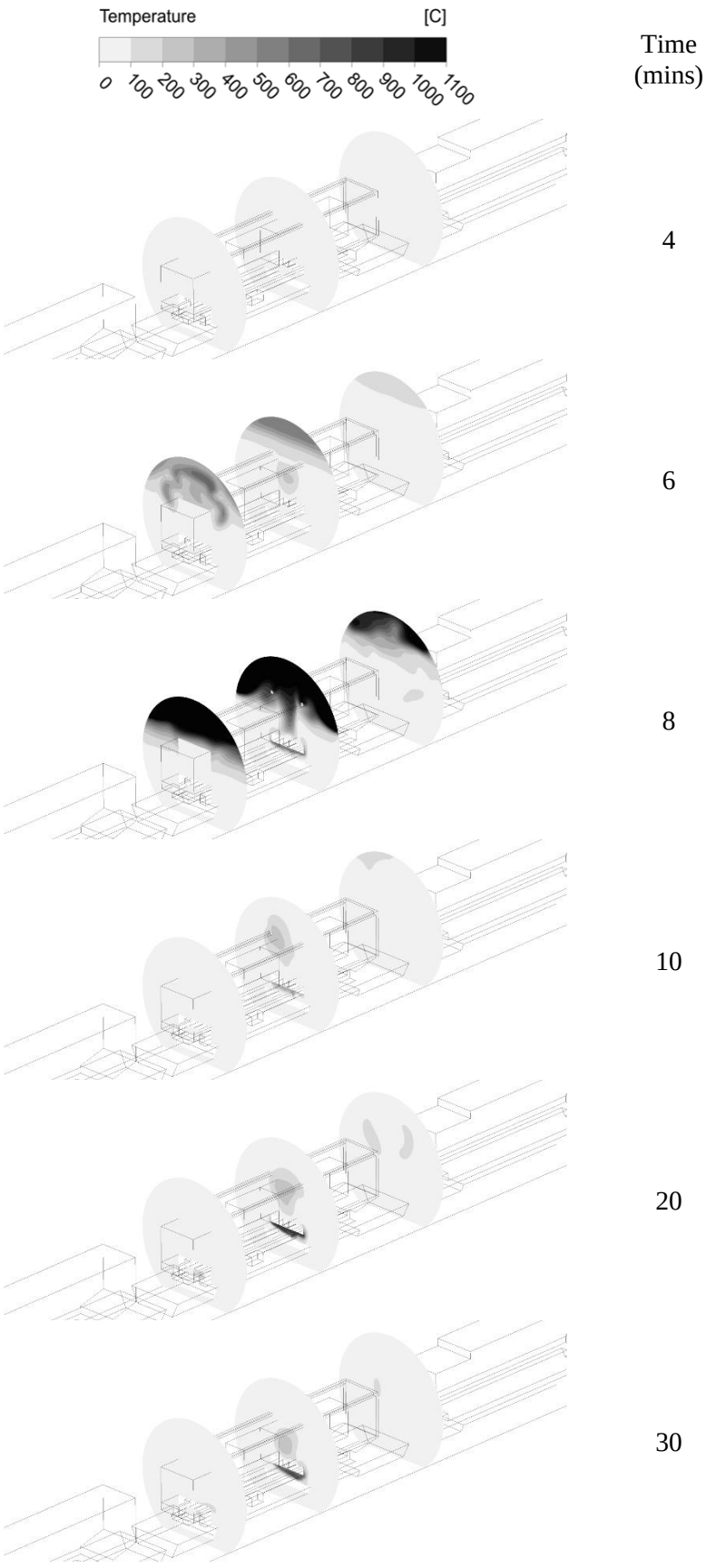

Figure 14 Air temperature on vertical slices through the centre of the batteries, cab and behind the incident carrier – with sprinkler activation

While the train is running in the tunnel at high speed, high temperatures remain within the trailer of the lorry and the plume is quickly mixed out in the high velocity airstream of the tunnel. When the train stops in the tunnel after around 6 minutes, a hot plume forms in the soffit of the tunnel above the carrier. Piston effects from the motion of trains within the tunnel network pushes this plume forwards of the lorry towards the front of the train. This piston effect then decays leaving a brief period of static flow in the tunnel at around 8 minutes at which time the hot plume starts to fill the tunnel from top down and spreads in both directions in the tunnel due to buoyancy effects. The peak temperature of the plume is significantly higher during this period as there is no dilution of the plume by the ventilation system. After 8 minutes the HPWM system is activated and from around 10 minutes the active tunnel ventilation starts to push the hot plume back over the incident carrier towards the rear of the train. Temperature oscillations after 15 minutes are due to small scale unsteadiness in the hot flow field and coincide with the start of the lorry cab fire and the removal of the cab walls.

Temperatures in the tunnel soffit above the incident lorry are reduced to below 200 °C after activation of the HPWM system and tunnel ventilation from 9 minutes onwards. Temperatures underneath the lorry, but above the surface of the carrier, still peak at around 1100 °C as this area is shielded from the HPWM system by the lorry chassis. Temperatures below the carriers remain cool (less than 100 °C) for the duration of the simulation. Overall peak plume temperatures agree largely with experimental data of tunnel fires [10].

DISCUSSION

Given the complexities of LIB fires, fire spread assessments, and fire suppression system interactions, together with the modelling and numerical uncertainties embedded in 3D detailed analyses, the solutions presented in this study are largely reliable from a qualitative perspective. Moreover, it can be envisaged that other train running and tunnel ventilation conditions can impact the detailed analyses solutions and outputs significantly.

In brief, some of the key uncertainties that impact the quantitative accuracy of the results and findings of this study include the following.

1. LIB fire physics and fire spread among battery packs and thermal runaway conditions.
2. General fire spread mechanism in lorry including cargo.
3. Ventilation conditions in the environment of the fire car for any given train speed and tunnel ventilation operation.
4. Combustion modelling physics, oxygen vitiation and applicability to given fire scenarios.
5. HPWM system interactions with fire plume and fire spread mechanisms.
6. Numerical uncertainties for turbulence, combustion, heat transfer, droplet modelling and interactions of these physical phenomena

The most vulnerable times for the tunnel structure, equipment and rolling stock, based on the scenarios modelled, are when the train slows down or is at a standstill with no or low levels of tunnel ventilation. It is observed that under such conditions, maximum temperatures are reached under the tunnel crown. Temperatures under the lorry peak much later in the simulation when the fire curve for the associated components (diesel tank and tyres) peaks.

Assessment of the temperatures in the tunnel soffit indicate that failure of tunnel systems under the tunnel crown is a significant risk, given the very high temperatures observed under the crown when the train is stationary. Furthermore, high temperatures in the tunnel crown could cause a risk to tunnel structures should the temperatures be excessive enough to cause explosive spalling of the concrete. Additionally, key plastic and rubber elements in rolling stock systems under the carrier have a failure temperature of very approximately 100 ºC. The CFD analyses show that the combination of the natural rise of the hot fire plumes in the scenarios investigated together with the carrier base acting as a shield, protect these components underneath the carrier. However, it’s observed that the margins are low. Furthermore, the fires above the carrier will significantly heat the carrier base and with conduction

through the material, the base will in turn radiate to these exposed components increasing their heat loading. This is most severe in the second half of the simulations when the fire representing the diesel tank and tyres reaches peak HRR.

For the scenario with HPWM sprinkler activation, large attenuation of peak temperatures are observed under the tunnel crown and within the lorry trailer after HPWM system activation, owing to both the reduction of the heat release from the fire together with the cooling of the plume as a results of the spray/mist and associated evaporation. However, the tunnel systems may still be impacted by the raised temperatures under the tunnel crown.

CONCLUSION

CFD analyses have been performed to assess the potential impact of transporting large quantities of LIBs through a rail tunnel. An assumed composite fire curve has been applied to a lorry model on a rail freight carrier using a mixture of a heat source model and a single step reaction model to represent the thermal runaway of the LIBs and material combustion respectively.

Temperature contours plotted on a vertical plane through the centreline of the tunnel show that while the train is running at high speed in the tunnel, the high temperature plume from the LIB fire is quickly mixed out in the high velocity air stream of the tunnel. However, when the train comes to a stop in the tunnel before the activation of any mechanical ventilation, a hot plume forms in the soffit of the tunnel above the carrier which starts to fill the tunnel from top down and spread in both directions in the tunnel due to buoyancy effects. The peak temperature of the fire plume is highest during this period of the simulation as there is no dilution of the plume by a ventilation system. Once the mechanical ventilation is activated in the tunnel, the tunnel ventilation starts to push the hot plume back over the incident carrier towards the rear of the train, diluting the plume and lowering peak temperatures in the soffit.

For the scenario with the activation of a HPWM system two minutes after the train comes to a stop in the tunnel, the HPWM reduces the measured temperature in the tunnel crown by around 400-500 °C. Temperatures underneath the lorry, but above the surface of the carrier, peak at around 1100 °C in both scenarios as this area is shielded from the HPWM system by the lorry chassis. Temperatures below the carriers remain cool (less than 100 °C) for the duration of both simulations.

The results of this study can be used to provide qualitative judgements on the likelihood of failure of the tunnel structure, lineside equipment and rolling stock. The most vulnerable times where tunnel operation is most at risk are when the train is at a standstill with no or low levels of tunnel ventilation. Maximum temperatures are reached under the tunnel crown which could lead to failure of tunnel systems and threaten the structural integrity of the tunnel walls through risk of explosive spalling. Additionally, key components of rolling stock are likely to be shielded from the rising hot plume by the carrier base, but may still be impacted due to their sensitivity to higher temperatures.

This study would benefit from further verification by means of testing. Some key uncertainties that may impact quantitative accuracy of the simulation results include the LIB fire physics and fire spread mechanisms within the incident lorry, and the operational sequence of the train including the time at which the train comes to a stop in the tunnel after fire start and the time at which ventilation and fire suppressions systems are activated. Additionally, the magnitude of the bulk flowrate in the tunnel due to mechanical ventilation could impact the calculated plume temperatures. Sensitivity studies around these areas of uncertainty could be the subjects of future studies.

REFERENCES

1. U.S Department of Transportation, “Water Mist Fire Suppression System Feasibility Study”, Federal Railroad Administration, Report Number DOT/FRA/ORD-23/08, 2022.
2. Ingason H., Li Y. Z., Lönnermark A., *Tunnel Fire Dynamics*, Springer, 2015.
3. Kang, S., Kwon, M., Yoon Choi, J., Choi, S., “Full-scale fire testing of battery electric vehicles”, Applied Energy, Vol 332, 2023.
4. Sun, P., Bisschop, R., Niu, H., Huang, X., “Review of Battery Fires in Electric Vehicles”, Fire Technology, Vol 56, 00. 1361-1410, 2020.
5. Wu, Guan-Yuan & Chen, Ruu-Chang. (2010). The Analysis of the Natural Smoke Filling Times in an Atrium. Journal of Combustion. 2010. 10.1155/2010/687039.
6. UPTUN, “Summary of Large Scale Fire Tests in the Runehamar Tunnel in Norway”, UPTUN publication, 2003
7. SFPE, *Handbook of Fire Protection Engineering*, Third Edition, ISBN: 087765-451-4, 2002.
8. Channel Tunnel Safety Authority, “Inquiry into the fire on Heavy Goods Vehicle shuttle 7539 on 18 November 1996”, 1997
9. Fuentes, M., Panos, I., Alizadeh, S., “Sprinkler System Design Using CFD Tools for Assessing Tenability Impact and Total Hydraulic Demand”. Tenth International Symposium on Tunnel Safety and Security, Stavanger, Norway, April 26-28, 2023.
10. Li, Y.Z., Ingason, H., “Maximum Ceiling Temperature in a Tunnel Fire”, SP Technical Research Institute of Sweden, Fire Technology, 2010.

Numerical investigation of the effects of ventilation on the tenability of egress paths in a metro tunnel fire

Ting-Hsuan Liao & Ricky Carvel
Edinburgh Fire Research Centre, School of Engineering, University of Edinburgh, UK

ABSTRACT

Smoke management in metro tunnels and stations is a concern when passengers exist on both sides of the fire. Longitudinal ventilation can only clear smoke for some, not all, of the passengers. Most smoke movement analyses for metro tunnels ignore the fact that ventilation influences fire dynamics, smoke production rate, and the toxicity of smoke. This study aims to include realistic variations of fire size and toxicity with applied ventilation in a metro carriage fire. FDS and Pathfinder are combined to predict the tenability of egress routes for escaping passengers in a metro tunnel. A novel method of incorporating a CO yield that varies with the global equivalence ratio was implemented into FDS. Egress paths along the track and a raised evacuation path were considered, and the tenability of these routes was evaluated using a fractional effective dose approach. The tenability of the egress routes is presented and discussed.

KEYWORDS: egress, tenability, fractional effective dose, ventilation, metro, tunnel

INTRODUCTION

Mass rapid transport systems (also known as metro systems) are a fast, efficient and generally safe means of moving people in modern urban areas. In many cities, these systems have extensive parts of their networks underground, which considerably increases the risk associated with incidents involving fire in these systems, due to issues of smoke movement in spaces used by passengers during travel and egress.

Commonly, ventilation systems are installed in underground facilities to provide a reasonably comfortable environment during normal operation, manage smoke movement in the event of a fire, and keep the environment as tenable as possible for the escaping passengers. However, the interactions of fire and smoke with ventilation and people are not simple, even in simple situations, let alone complex underground networks. Ventilation can sometimes clear smoke and reduce heat in the tunnel environment, but it can also enhance fire burning rates and generate greater volumes of smoke.

Previous research on fires on regular passenger trains in a tunnel with cross-passages has shown that applying a longitudinal airflow to clear smoke may, in some instances, result in less tenable conditions overall for escaping passengers than using no ventilation at all [1], [2]; the benefits of removing the smoke completely for some are more than negated by the negative effects of increased toxic exposures for others.

This study applies a similar, but more advanced methodology to investigate the effectiveness of available ventilation strategies on the tenability of egress routes from a metro train stopped in a tunnel in a typical modern underground metro system. Future work will extend the study into metro stations.

METHODOLOGY

A reasonably typical metro tunnel was modelled using the Fire Dynamics Simulator (FDS 6.9.1) and Pathfinder (2024.1.0813) models. The tunnel dimensions and ventilation flow patterns were based on a section of the Taipei metro system in Taiwan (specifically the westbound tunnel between Sun Yat-Sen Memorial Hall Station and Taipei City Hall Station). The tunnel is a single-directional and single-bore tunnel with a circular cross-section. It is 650 m long and has an internal diameter of 5.6 m. There is a walkway 0.6 m wide on the south side of the track in the tunnel. The train model was constructed by referring to the configuration of present trains operated by Metro Taipei. The train has 6 carriages; each 23 m long, 3.2 m wide and 3.6 m high, overall 141.6 m long. Every carriage has four doors 1.5 m wide and 1.8 m high on the side of the walkway (it was assumed that the doors on the opposite side did not open), there are also exit doors with emergency ramps at the front and rear of the train. See Figure 1 for details.

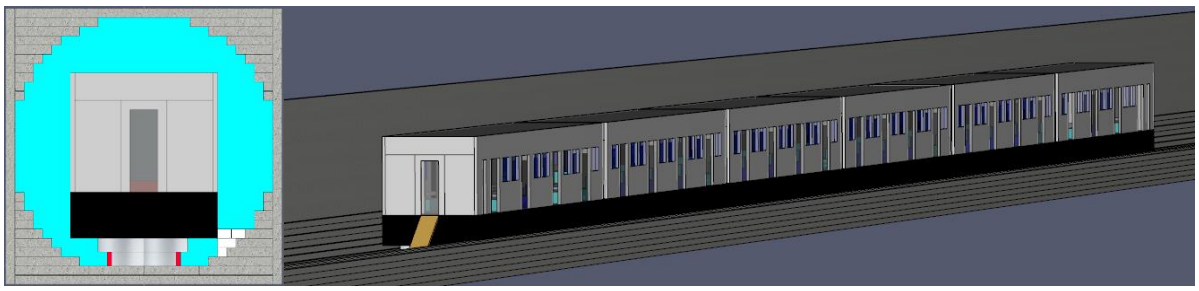

Figure 1 The cross-section and the schematic view of the fire model in FDS.

Fire Model

In the FDS model, an arson event was assumed to occur inside the train, at its midpoint. Simultaneously, the train lost power and stopped at the midpoint of the tunnel, this maximises the travel distance for escaping passengers on both sides of the fire. The fire was assumed to grow as a t^2 fire, with the growth parameter varying with longitudinal airflow, as described below. According to recent research (see Table), the peak heat release rate (HRR) of a modern metro vehicle fire can be in the range from 5 MW to 15 MW, or 1.5 MW to 2 MW for a luggage fire. In a recent experiment, the peak HRR of a metro carriage ($\dot{Q}_{max}$) was measured at 11.2 MW and was estimated to have been able to reach 12 MW if all the windows had broken [3]. Here it is assumed that the peak HRR was 12 MW and the fire growth rate (α) was 1.17×10^{-5} MW/s^2; a standard medium fire. Before the fire started to grow, the tunnel ventilation fans (TVFs) on the west side of the tunnel delivered forced longitudinal airflow with different airflow rates corresponding to one of four ventilation scenarios.

Table 1 Recent experimental and computational research for metro fires.

Type	Fuel	$\dot{Q}_{max}$ (MW)	α (kW/s^2)	Y_s (g/g)	Y_{CO} (g/g)	Ref
Experiment	1/3 mock-up carriage	3.5[a]	0.14[b]	-	-	[4]
Experiment	Real carriage	11.2	0.39	-	-	[3]
Simulation	Luggage	1.5	-	-	-	[5]
Simulation	Gasoline (arson)	0.5 - 2	0.1876	-	-	[6]
Simulation	Luggage	2	0.04689	0.113	0.024	[7]
Simulation	Luggage Train	2 5	0.04689	0.113	0.024	[8]
Simulation	Train	5 - 15	-	-	-	[9]
Simulation	Luggage	2 - 5	-	-	-	[10]
Simulation	Luggage	2 - 5	-	-	-	[11]

[a] Peak HRR can reach 17 MW if it is fully combusted.
[b] Calculated from the results.

Few literature sources provide specific values for the soot yield (Y_s) and carbon monoxide yield (Y_{CO})

for metro carriages. Here, the soot yield and CO yield for the fire were taken to be 0.113 and 0.024 respectively, assuming a luggage fire in a carriage [7], [8]. The longitudinal airflow rates (v) in the fire model varied from 0 m/s to 2 m/s based on the design of the Taipei metro system. The detailed information on parameters for the four general scenarios (V0, V1, V2, and V3) is shown in Table 2. The computational mesh used in this work was 0.2 m × 0.2 m × 0.2 m.

Table 2 Scenarios of this research

Scenario	v (m/s)	$\dot{Q}_{max}$ (MW)	α (MW/s^2)	Time to reach $\dot{Q}_{max}$ (s)	Y_s (g/g)	Y_{CO} (g/g)
V0	0	12	1.17×10^{-5}	1011.87	0.113	0.024
V1	0.66	12	1.17×10^{-5}	1011.87	0.113	0.024
V2	1.32	12	1.17×10^{-5}	1011.87	0.113	0.024
V3	2	12	1.17×10^{-5}	1011.87	0.113	0.024
M0	0	12	1.17×10^{-5}	1011.87	0.113	Varies
M1	0.66	12.8	1.59×10^{-5}	899.08	0.113	Varies
M2	1.32	13.7	2.00×10^{-5}	826.00	0.113	Varies
M3	2	14.5	2.43×10^{-5}	772.95	0.113	Varies

Usually, when different ventilation strategies are compared for a metro system, the behaviour of the fire is assumed not to change under different ventilation conditions; the airflow rate is changed to explore its impact on other factors such as toxicity and visibility, while the peak HRR, fire growth rate, soot yield, and CO yield are generally all kept fixed. This ignores real fire behaviour. The airflow brought by forced ventilation can change the burning behaviour, including modifying the growth rate, peak HRR, soot yield, and CO yield [12], [13].

Here, three additional modified scenarios (M1, M2, and M3) were designed with the specific parameters (peak HRR, fire growth rate, and CO yield) varying with airflow rates, to quantify the difference from the original scenarios (V0, V1, V2, and V3). To simplify the conditions in the present study, soot yield was fixed at a constant value, although this too can affect visibility in tunnel spaces, and impact evacuees' movement speed and decision-making. However, the effect of ventilation on soot yield will be considered and discussed in future research.

Forced longitudinal ventilation has been shown by Ingason & Li to enhance the mass loss rate per unit area (MLRPUA) and fire growth rate of wood cribs in a small-scale (1:23) tunnel [12]. Using their data, correlations between peak HRR and airflow rate, and between fire growth rate and airflow rate were devised, as shown in
Figure *2* (a) and (b). For full-scale, variables k_h and k_α were used, which are multipliers applied to the MLRPUA at 0 m/s velocity, and similarly for the fire growth rate, as shown in
Figure *2* (c) and (d). The correlations were devised assuming conventional Froude scaling laws [14].

Generally, peak HRR is reasonably proportional to maximal MLRPUA if the area of fuel doesn't change. Thus, the equation of the trendline in
Figure *2* (c) can be rewritten as follows:

$$\dot{Q}_{max} = k_h \times \dot{Q}_0 = (0.1054 \times v + 1) \times \dot{Q}_0 \quad (1)$$

where $\dot{Q}_{max}$ is the peak HRR under specific velocity (kW) and $\dot{Q}_0$ is the peak HRR in scenario V0 without forced ventilation (kW). Notice that the intercept of the equation was adjusted to 1 to assure $\dot{Q}_{max}$ is equal to $\dot{Q}_0$ with no forced ventilation. For the same reason, the correlation between fire growth rate and velocity in
Figure *2* (d) can be expressed as:

$$\alpha = k_\alpha \times \alpha_0 = (0.5375 \times v + 1) \times \alpha_0 \quad (2)$$

where α is the fire growth rate under specific velocity (kW/s^2) and α_0 is the fire growth rate without forced ventilation in scenario V0. Note that the unit of fire growth rate in Ingason & Li's research [12]

is kW/min while the units of α and α_0 in Eq. (2) are kW/sec^2. It is reasonable to assume a positive correlation between fire growth rate and velocity by Eq. (2) for this study. However, the exact correlation between these two variables still needs further exploration. Using Eq. (1) and Eq. (2), the $\dot{Q}_{max}$ for the modified scenarios (M1, M2, and M3) with different ventilation conditions were calculated and are shown in Table 2.

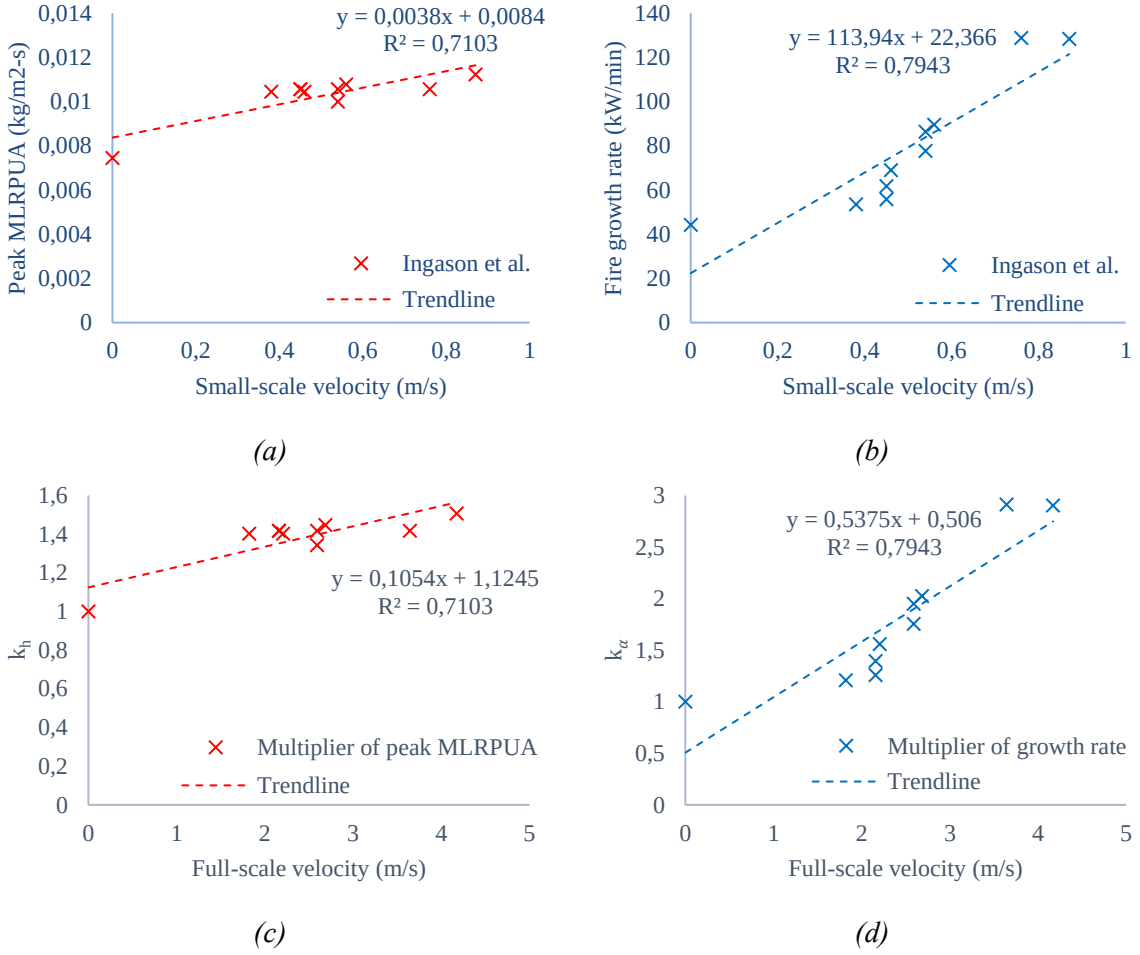

Figure 2 Correlations for (a) peak MLRPUA and small-scale velocity; (b) fire growth rate and small-scale velocity; (c) k_h and full-scale velocity and (d) k_α and full-scale velocity.

In addition to the influence of ventilation on HRR, CO yield also exhibits a ventilation dependency. Previous studies [13], [15], [16], [17] have shown that the CO yield of fire varies with the global equivalence ratio (GER) for compartment fires. Although these experiments were conducted in situations which have different geometry and spatial characteristics from tunnels, there is insufficient literature exploring the relationship between CO yield and GER in a tunnel. Thus, the metro carriage in the numerical model was considered as a compartment and the concept of GER was used to estimate the CO yield of the fire. The GER can be expressed as the following equation:

$$\mathrm{GER} = \frac{(\dot{m}_{fuel}/\dot{m}_{air})_{actual}}{(m_{fuel}/m_{air})_{stoich}} \tag{3}$$

where $\dot{m}_{fuel}$ is the actual mass loss rate of fuel (kg/s); $\dot{m}_{air}$ is the actual inlet mass flow rate of air (kg/s) to the fire area; m_{fuel} and m_{air} are the mass of fuel and air that is consumed while the burn reacts stoichiometrically (kg). When a fire is small, relative to the compartment, the GER will be small, when it is large relative to the compartment the GER will be large, that is, GER (and hence CO yield) is not a constant, but rather a function of time. The stoichiometric ratio of m_{fuel} and m_{air} can

be calculated assuming a single fuel chemistry. Here, the fuel used was "SFPE WOOD_OAK_fuel" from the FDS library (C1.0H1.7O0.72N0.001) and the ambient air was assumed to be 25°C and 1 atm. The stoichiometric ratio of fuel/air was 0.17.

To measure $\dot{m}_{air}$ of the fire area in the modified scenario, a pre-test fire model was used. In the pre-test fire model, two slices as devices were adopted to measure the inlet mass flow rate of air into the fire area (Figure 3). The simulation time was set as 1,200 seconds to obtain $\dot{m}_{air}$ for the whole duration. For stabilising the airflow in the tunnel, the TVFs at the west end of the tunnel were activated at the beginning of simulations and after 120 seconds the fire started using the specific values in Table 2. In the fire model, $\dot{m}_{fuel}$ is automatically recorded by FDS for each scenario. Thus, GER can be estimated for the region around the fire.

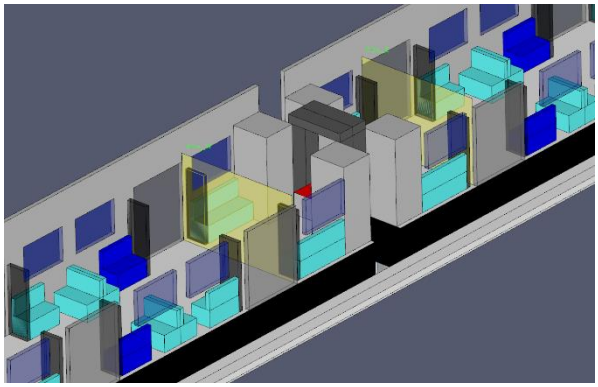

Figure 3 *The devices (two yellow slices) were adopted to measure the inlet mass flow rate of air in FDS.*

In enclosed space fires, CO generation is not limited to the fire source alone, as smoke layer temperature represents another significant factor affecting CO production [18]. When smoke layer temperatures are below 800 K, the fire plume primarily controls CO generation. However, at smoke layer temperatures exceeding 900 K under poor ventilation conditions, CO concentrations increase [19]. Here, the smoke layer temperature did not exceed 800 K, thus the following equation in the SFPE Handbook of Fire Protection Engineering [17] was adopted to calculate CO yield:

$$Y_{CO} = \left(\frac{0.19}{180}\right) tan^{-1}[10(GER - 0.8)] + 0.095 \quad (4)$$

where $\tan^{-1}[10(\mathrm{GER} - 0.8)]$ is in degrees. Equation 4 fits the empirical data of Beyler's experiment [20] for hexane combustion, while other studies show a similar pattern [13], [16], [21]. Therefore, it seems reasonable to use the curve of Eq. (4) to estimate the variation of CO yield in the modified scenarios. Using the same method for Eq. (1) and Eq. (2), the CO yield for a specific time can be written in multiplier form as follows:

$$Y_{CO} = k_{CO} \times Y_0 = \frac{Y_{CO}}{0.162} \times Y_0 \quad (5)$$

where k_{CO} is the multiplier for CO yield compared to the value of CO yield when GER is equal to 1 in Eq. (4), and Y_0 is the CO yield adopted for the general scenarios which is 0.024 g/g [8] as the assumption for scenarios V0 to V3. The CO yield calculated in this way varied with time in each scenario as shown in Figure 4.

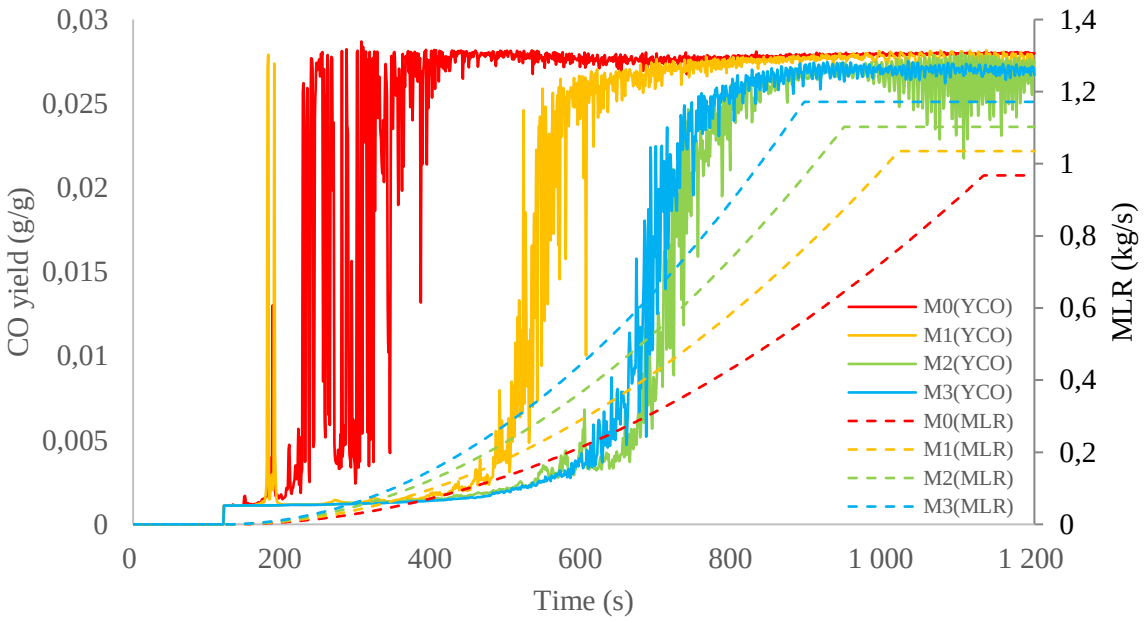

Figure 4 CO yield and mass loss rate against time in each scenario in FDS.

For general scenarios in FDS, CO can be generated by the fire with a fixed CO yield. However, for the modified scenarios, the CO yield changes along with time which FDS does not currently permit. To overcome this limitation, an alternative method was adopted which introduced the CO gas into the domain, separately from the fire source.

Figure 5 illustrates the fire source used in FDS, which consists of a burner on top of the red block with a surface area of 1 m², along with a CO source that features a single supply surface at the bottom of the cyan block, also with a surface area of 1 m², intended to generate CO during the fire. These supply surfaces were set to inject a specific amount of CO based on CO mass flux (kg/m^2-s) which was equal to CO yield times MLRPUA every second. The CO mass flux against time adopted for CO suppliers in the modified scenarios is shown in Figure 6.

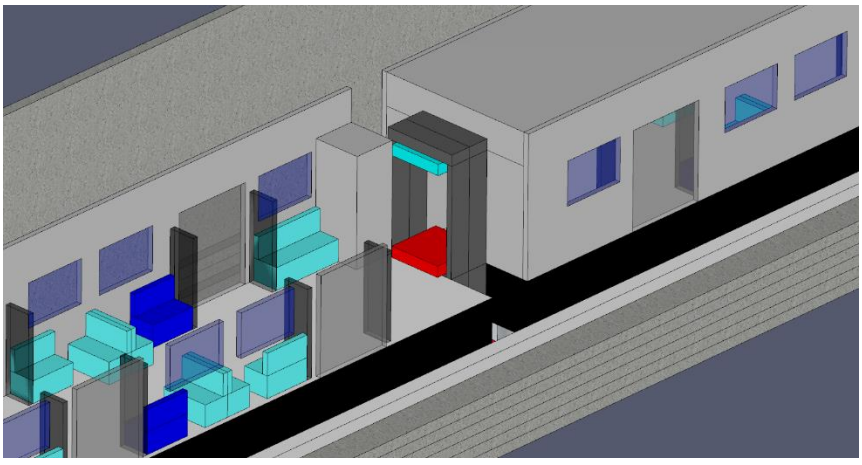

Figure 5 The source of fire and CO in FDS. The burner surface is on top of the red block, and the CO supply surface is at the bottom of the cyan block above the fire source.

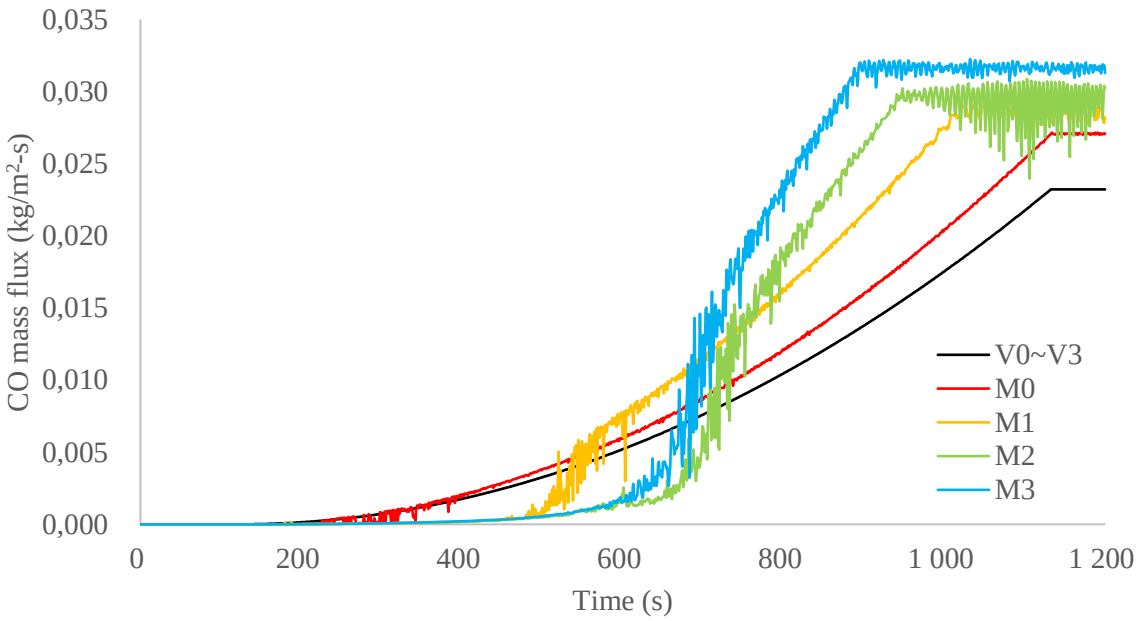

Figure 6 CO mass flux for modified scenarios.

Egress Model

According to the design capacity of carriages on the Taipei metro, each train can carry about 1,672 people (352 seats and 264 m^2 standing area with a density of 5 people/$m^{2)}$. However, due to the geometries of passengers (treated as cylinders in Pathfinder), they can occupy more projected area on the floor than people do in reality. Thus, in the egress model, all the seats in carriages were removed to deploy a total of 1,674 standing passengers inside. In each carriage, 279 passengers were initially distributed randomly and they started to evacuate when the fire was ignited at 120 s. As the evacuation time of passengers is not the primary focus of this research, pre-movement time was not considered in the simulation.

The passengers either used the emergency doors at the front and rear of the train to descend onto the track escape routes (254.2 m long and 1 m wide) or used the side doors to access the side egress paths (324.6 m long and 0.6 wide) (see Figure 7). Assuming that passengers could not pass the fire location, all passengers in carriages 1 to 3 escaped to the west side and the rest of the passengers travelled to the east side. It was assumed that passengers could not change routes between the track and the side egress path due to the 0.8 m vertical height between the two routes. Once all the passengers reached the exits at the end of the tunnel, the egress simulation was completed.

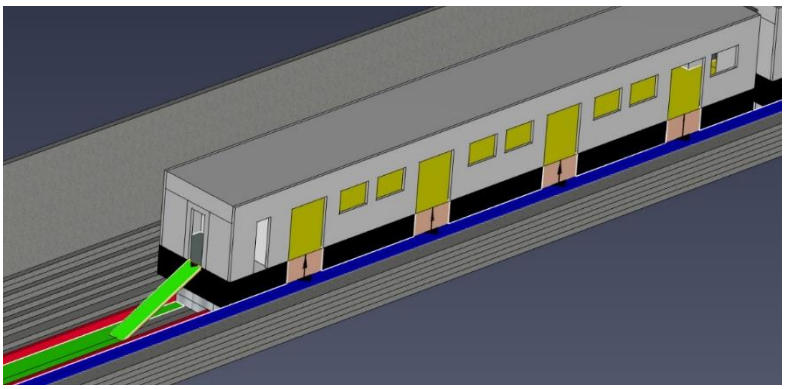

Figure 7 The two egress routes in the egress model: track (green) and side egress path (blue).

In egress studies, there are a lot of complex agent behaviours and characteristics that could be

modelled. Some studies [22], [23] consider passengers' movement speed and shoulder width as varying with age. Others adjust their behaviour according to, the slope of the ramp and visibility/smoke [24]. The height between the carriage floor and the side egress path can also influence the flow rate through the side doors during the egress process [25]. Here, the primary concern is the tenability of the egress path, and the intent is not to explore all aspects of egress in detail. Thus, to simplify the modelling assumptions, simple ramps were used to connect the end doors to the track, and the side doors were considered at the same height as the side egress path, which doesn't affect movement speeds or flow rates. All passengers were taken to have a shoulder width of 42.5 cm and an unimpeded walking speed of 1.19 m/s. Low visibility significantly impedes pedestrian walking speed, which delays the evacuation process for all passengers and potentially increases the Required Safe Egress Time (RSET). The relationship between visibility and walking speed has been clarified in relevant research [26], and these findings are extensively applied in evacuation simulation software. As this research is currently in an exploratory phase, and the relationship between soot yield and ventilation affecting visibility has rarely been examined in tunnel or metro fire scenarios, this study does not currently consider the impact of visibility on walking speed. However, these issues will be reconsidered and discussed in future studies.

Toxicity model and model coupling

To qualify the tenability of egress paths followed by escaping passengers, Purser's Fractional Effective Dose (FED) model is used [27]; this is implemented in both FDS and Pathfinder. The FED is the ratio of the dose received and the effective dose expected to cause incapacity or death, this gives a measure of the tenability of the environment which the agents pass through. When the FDS data is implemented into the Pathfinder models, the cumulative effect of the toxic gases experienced by the moving agents in the egress model can be quantified, and the tenability parameters of the possible egress routes can be compared. While numerical values of FED are calculated these should only be treated as indicative numbers, and the comparison between cases is more important here than the absolute numbers shown.

To estimate FED in FDS, devices were evenly located every 1 m along the x-axis of the tunnel from the location of the fire and were positioned 1.8 m above the level of the carriage floor, the track, or the side egress path. The total FED calculated by the simplified FED model implemented in FDS and Pathfinder can be expressed as follows:

$$FED_{total} = FED_{CO} \times HV_{CO_2} + FED_{O_2} \quad (5)$$

where FED_{CO} stand for the fraction of the incapacitating dose of CO; HV_{CO_2} is hyperventilation factor calculated by CO_2 concentration; and FED_{O_2} stands for the incapacitating dose of hypoxia. Generally, 0.3 is considered the minimum threshold for FED, deemed sufficient to cause serious effects on vulnerable populations (such as the elderly, children, or people with compromised immune systems). However, in this research, FED is used to measure the tenability of evacuation routes. Therefore, this study assumes that even if passengers' accumulated FED exceeds 0.3, they will continue to act according to the designed parameters without affecting the overall process. Nevertheless, it can be anticipated that in a real fire scenario, individuals with excessively high FED accumulation might lose consciousness, potentially obstructing escape routes or delaying evacuation times for specific groups.

It should be noted that Purser's model considers many asphyxiants and irritants, while only CO, CO2 and lack of oxygen were considered here. Equation 5 represents a simplified approach used in Pathfinder and FDS+Evac to evaluate evacuees' exposure to toxic or physical environmental effects. Irritants and asphyxiants such as heat, smoke, and hydrogen cyanide (HCN) can significantly impair evacuation efficiency during egress [27]. However, the current version of Pathfinder does not consider the effects of certain irritants and HCN on human behaviour. Currently, Pathfinder calculated FED for agents but does not modify their behaviour as a result of this calculation. Consequently, it can be expected that tenability will be optimistically overestimated when these negative factors are omitted from the assessment.

RESULTS & DISCUSSION

To assess egress path viability under varying ventilation conditions, FED devices were positioned at 1.8 m above the floor at 1 m intervals along the track and side egress path routes. (These devices show the tenability at fixed locations in the tunnel, and the FED values shown represent the cumulative exposure for an agent remaining at each fixed point for the entire duration of egress. In practice, no single agent would experience these levels of exposure, as agents will move.)

Figure 8 illustrates the FED variations at fixed points on the track route. The upstream measurements indicate that V0 exhibits higher FED values compared to standard scenarios (V1-V3), indicating (as expected) that longitudinal ventilation considerably improves upstream tenability. M0 and M1 demonstrate higher FED values than V0 and V1 separately, attributable to increased CO mass flux from the fire. Downstream measurements reveal that increased airflow rates generally correspond to reduced tenability of egress paths in standard scenarios. However, M0 and M1 display lower FED values at distances less than approximately 130 m, while M2 exhibits a higher peak than M3. A significant observation is the presence of two peaks in V0 and M0 scenarios, occurring approximately 220 m from the fire source. This phenomenon likely results from cooled smoke descending to head height at this distance.

Analysis of the side egress path route tenability, illustrated in Figure 9, reveals a distinct FED distribution pattern compared to the track route. An M-shaped distribution emerges due to the fire model geometry, with longitudinal airflow causing this pattern to shift downstream. The upstream peaks in V1 and M1 suggest that minimal airflow can result in higher FED values compared to scenarios without longitudinal ventilation, an effect attributed to train geometry and aerodynamic factors. On the downstream section, the interaction between train airflow and tunnel environment generates peaks approximately 70 m from the fire source. Beyond this point, ventilated scenarios demonstrate decreasing FED values, reaching a trough between 100 m and 230 m, followed by peaks before 325 m due to descending smoke. Similarly, V0 and M0 scenarios exhibit peaks at approximately 225 m from the fire source, reflecting the same descending smoke phenomenon.

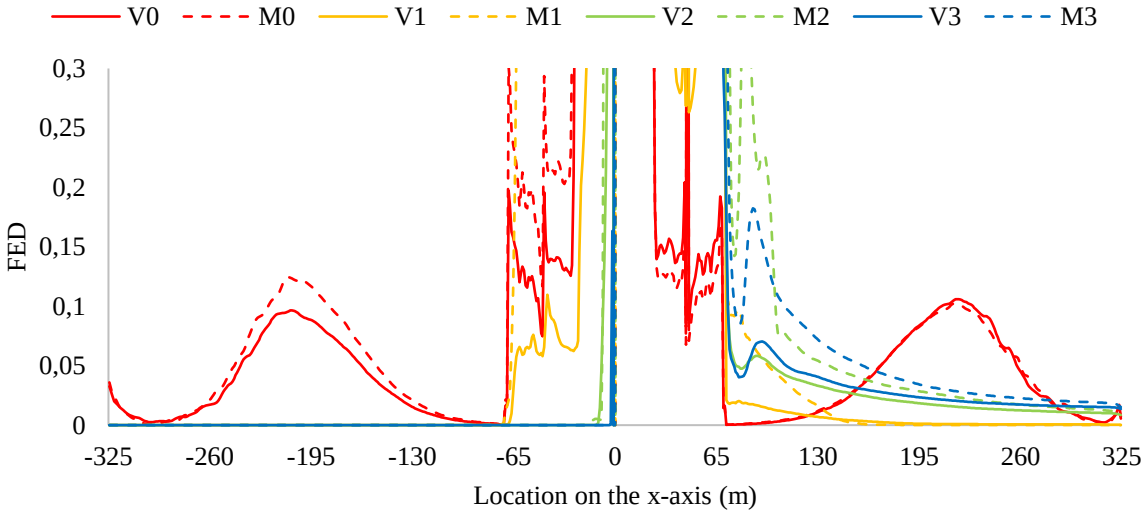

Figure 8 The tenability of the track egress path (train & track) against location on the x-axis.

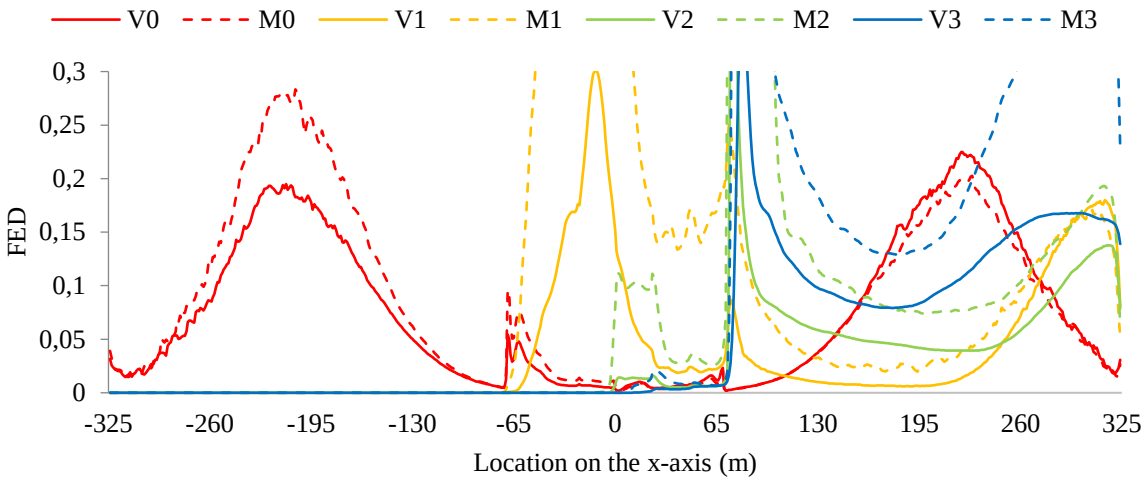

Figure 9 The tenability of the side egress path (train & path) against location on the x-axis.

The assessment of agent FED provides an essential measure for evaluating evacuation safety, complementing the analysis of egress path tenability. Based on previous findings regarding ventilation effects on egress paths, downstream passengers face greater exposure risks than those upstream. Therefore, the subsequent analysis focuses on downstream agents. Figure 10 and Figure 12 present FED values and inner time ratios (δ) for 167 agents, representing one-tenth of the total agent population across the different scenarios. The inner time ratio represents the proportion of time spent inside the train relative to the total evacuation duration, enabling analysis of the impact of train occupancy during evacuation.

Figure 10 reveals a distinct pattern for agents using the side egress path route. The left-side clusters indicate passengers who rapidly exited the train but encountered congestion on the side egress path. This congestion primarily occurred where agent flows merged at the final two side doors of the last carriage, as illustrated in Figure 11. The simulation showed that passengers on the path yielded to those newly emerging from the train, though this behaviour might not reflect actual emergency conditions. After congestion cleared, the queuing passengers resumed movement but encountered degraded environmental conditions due to fire growth during their wait period, as demonstrated in Figure 9. This explains the elevated FED values observed in scenarios V0, V1, M0, and M1 compared to other scenarios. The right side of Figure 10 depicts agents who experienced minimal or no congestion on the path. These results show FED values proportional to δ, reflecting toxic exposure during train queuing periods.

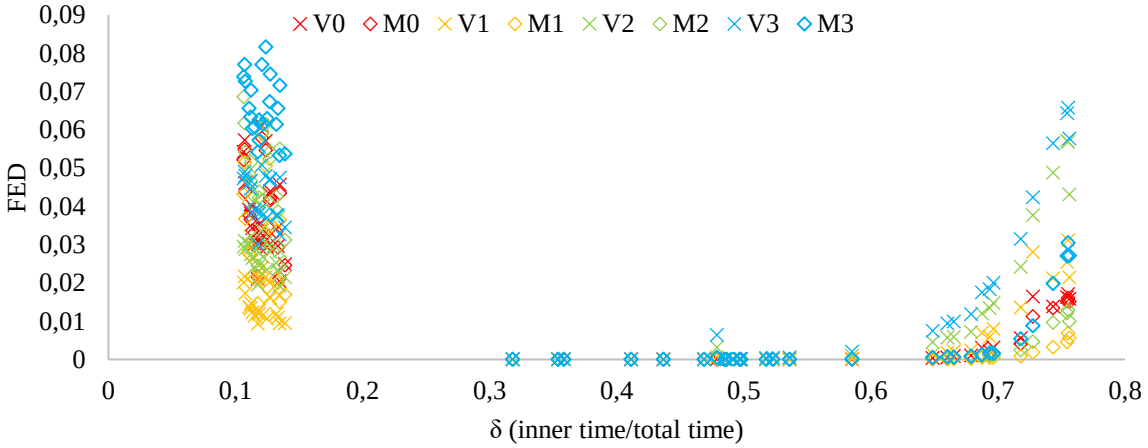

Figure 10 The FED of agents using the side egress path route against the δ.

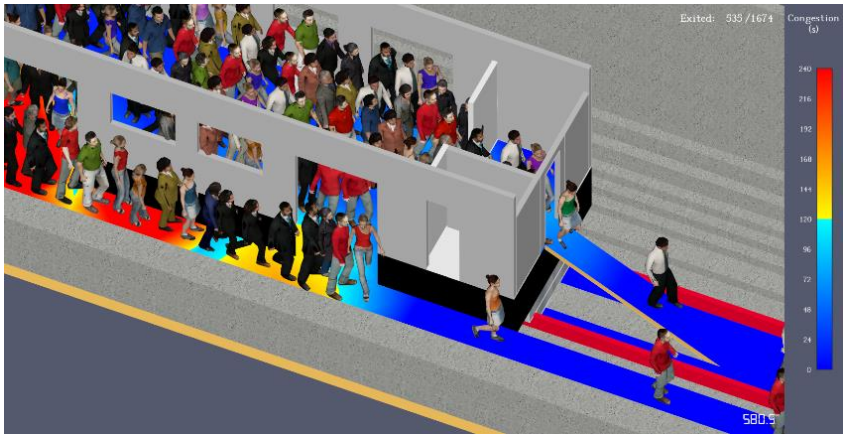

Figure 11 The congestion appeared at 580.5 seconds in scenario V3. The red area on the floor represents congestion while the blue area indicates the area without queuing.

For agents following the track route, FED demonstrates an exponential relationship with δ, indicating that extended train occupancy corresponds to higher final FED values. Ventilation airflow influences toxicity accumulation, as shown in Figure 12, with increased airflow rates corresponding to higher toxic gas exposure. Modified scenarios consistently demonstrate reduced values compared to their general scenario counterparts.

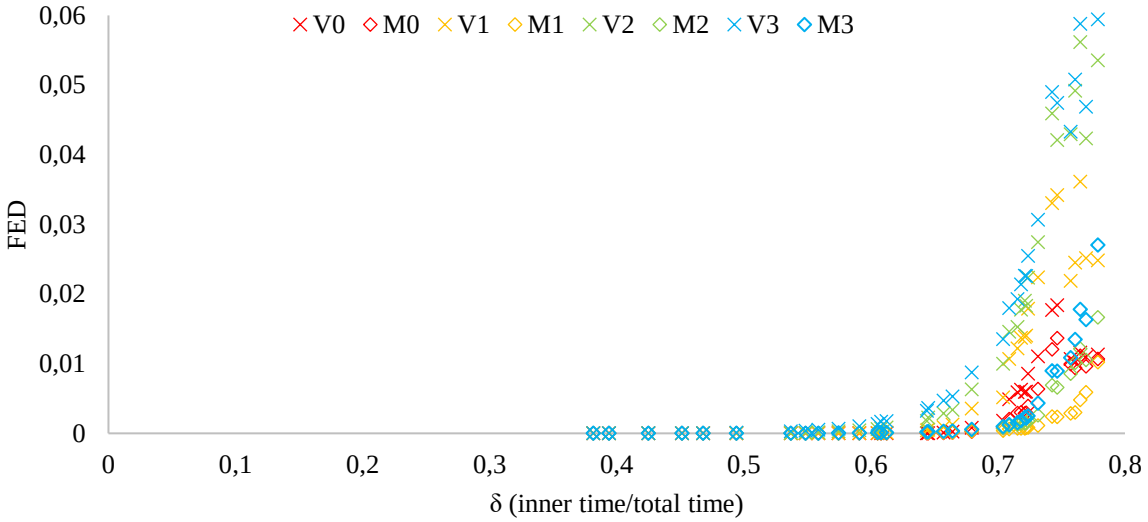

Figure 12 The FED of agents using the track route against the δ.

Investigation of agent trajectories and their corresponding FED values relative to x-axis positions provides additional insight into how changes in egress path tenability affect FED accumulation. Figure 13 shows that the upstream agent (C1_83) queued in the first carriage for the side door until congestion at the terminal door cleared, at which point the agent opted for the track route. The downstream agent (C6_156) exhibited comparable behaviour, waiting at the side door before ultimately using the track route. However, C6_156 accumulated higher FED than C1_83 due to ventilation airflow effects. As Figure 13 indicates, C6_156 remained stationary and accumulated toxic gases progressively due to high toxicity concentration in the carriage. Upon exiting the carriage, the agent encountered lower toxicity levels, resulting in reduced FED accumulation that aligns with the patterns shown in Figure 8. The data further demonstrates the influence of ventilation airflow on downstream tenability deterioration.

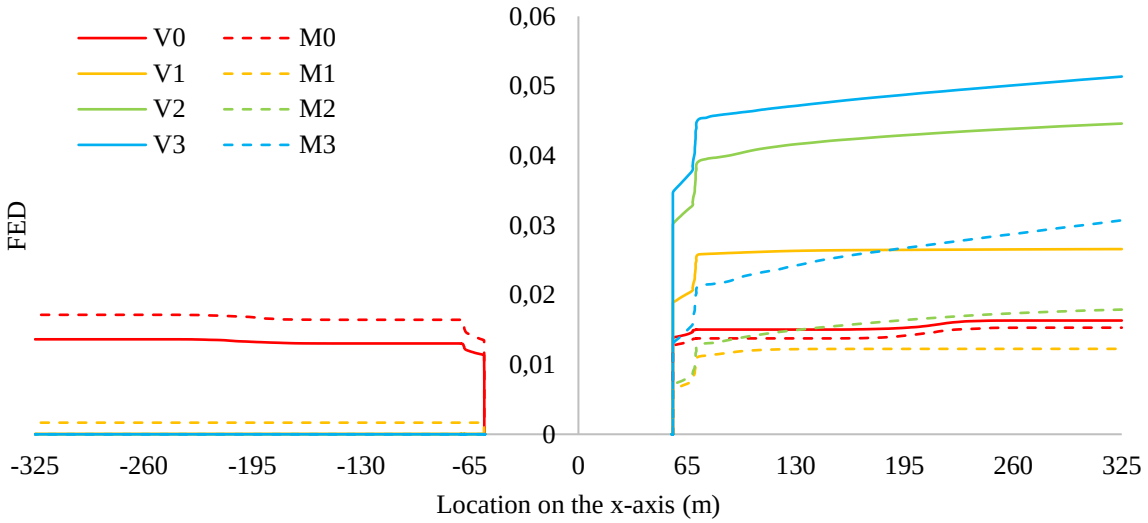

Figure 13 The track of the last agent arriving at the exit by the track route and its FED.

Figure 14 illustrates the FED values for the final agent reaching the exits via the side egress path, with corresponding positions plotted on the x-axis. For the upstream section of the side egress path, agent C3_4 experiences reduced FED levels when ventilation airflow is present in scenarios V2, V3, M2, and M3. In scenarios V1/M1, agent C3_4 encounters higher FED values before the -65 m mark from the fire source, while in scenarios V0/M0, higher FED values occur beyond -195 m, corresponding to the toxic gas distribution patterns shown in Figure 9. In the downstream section, agent C4_207 accumulates higher FED values with increased airflow strength. Similar to the upstream conditions, scenarios V0/M0 and V1/M1 demonstrate a reversal in FED accumulation at approximately 230 m. While the egress route patterns share similarities, the FED values along the side egress path route are approximately 10 times greater than those observed along the track route, attributed to the differences in toxic gas distribution and vertical positioning.

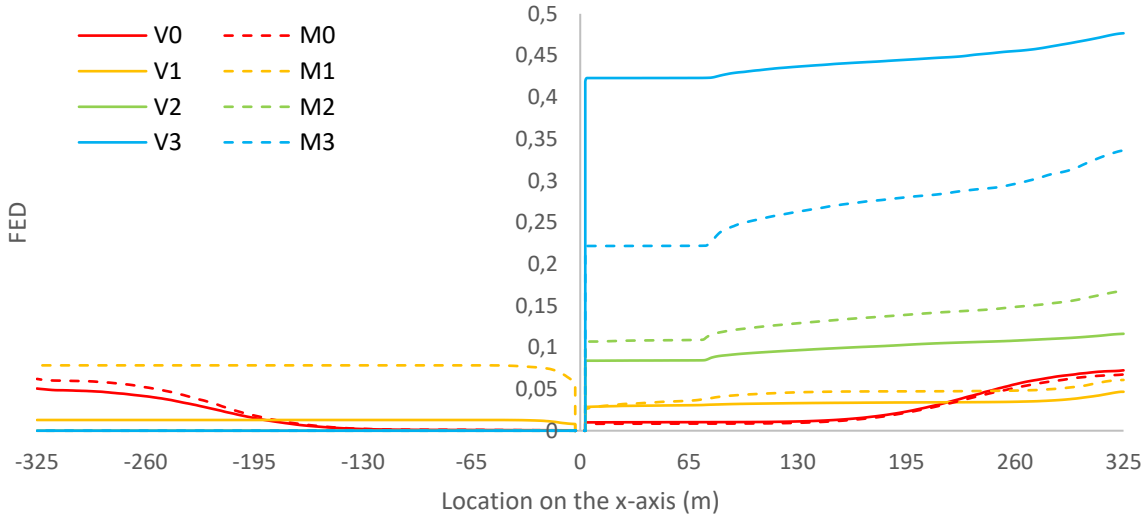

Figure 14 The track of the last agent arriving at the exit by the side egress path route and its FED.

LIMITATIONS OF THE METHODOLOGY

This preliminary study has investigated the use of a novel variable CO yield that changes with GER, and a variable HRR that depends on airflow velocity. Other factors that could vary have been considered fixed in this analysis, but need future consideration. It is intended to carry out future work addressing the following limitations of this study.

- This paper considers only CO as a measure of tenability. Tenability should also consider heat, visibility, and other factors.
- The location of the CO sources needs careful consideration. It is possible in the current configuration that FDS will have burned some of the injected CO at the fire source, reducing the modelled 'yield' lower than intended.
- Low visibility in smoke will impact movement and decision-making during evacuation, but the Pathfinder model does not currently adjust the behaviour according to the smoke present.
- Soot yield should also change according to the GER. This will have a considerable impact on human behaviour and visibility.
- The methodology is currently unvalidated.

CONCLUSIONS

This study examines the effects of ventilation airflow on evacuation route tenability, incorporating a novel variable carbon monoxide yield assumption.

The research methodology involved eight metro tunnel fire scenarios, analysed using FDS and Pathfinder software. Analysis indicates that for passengers upstream of the fire, the longitudinal airflow effectively reduces the FED accumulation and maintains tenable conditions. However, this same airflow compromises the survivability of downstream routes, creating hazardous conditions for occupants in these areas. Based on the assumptions of this study it would appear that higher ventilation rates result in considerably less tenable downstream conditions.

The findings also show that deterioration of environmental conditions occurs more rapidly on the elevated side egress path compared to the train then track route. Despite the need to transfer between levels, evidence suggests that evacuees should prioritise the track route to avoid exposure to more severe conditions in the side egress path.
Finally, the results of this study indicate that in the modified scenarios using new assumptions, regardless of upstream or downstream locations, there is a varying degree of reduction in spatial tenability compared to the original scenarios using basic assumptions. This suggests that if fire sources are assumed conventionally (i.e., maintaining the same peak HRR and growth rate regardless of ventilation conditions), the impact of toxic gases and environmental conditions on passengers may be underestimated. Furthermore, for passengers, some experienced a significant increase in FED accumulation under the modified scenarios, while others showed a relative decrease in FED under the same conditions. This phenomenon may be attributed to changes in the distribution of toxic gases within the geometric space due to altered fire behaviour assumptions. Therefore, the specific impact of these new assumptions on passengers requires further investigation and clarification in subsequent research.

REFERENCES

[1] M. Winkler and R. Carvel, 'The effect of longitudinal ventilation on tenability during egress from passenger trains in tunnels during fire emergencies', presented at the 16th International Symposium on Aerodynamics, Ventilation and Fire in Tunnels, Seattle, USA, Sep. 2016, pp. 211–226.
[2] M. Winkler and R. Carvel, 'Ventilation and egress strategies for passenger train fires in tunnels', presented at the 6th International Symposium on Tunnel Safety & Security, Montreal, Canada, Mar. 2016, pp. 454–464.
[3] C. Shi *et al.*, 'Metro train carriage combustion behaviors – Full-scale experiment study',

Tunnelling and Underground Space Technology, vol. 104, p. 103544, Oct. 2020, doi: 10.1016/j.tust.2020.103544.
[4] A. Lönnermark, H. Ingason, Y. Z. Li, and M. Kumm, 'Fire development in a 1/3 train carriage mock-up', *Fire Safety Journal*, vol. 91, pp. 432–440, Jul. 2017, doi: 10.1016/j.firesaf.2017.03.016.
[5] K. Wang, W. Cai, Y. Zhang, H. Hao, and Z. Wang, 'Numerical simulation of fire smoke control methods in subway stations and collaborative control system for emergency rescue', *Process Safety and Environmental Protection*, vol. 147, pp. 146–161, Mar. 2021, doi: 10.1016/j.psep.2020.09.033.
[6] Z. Zhang, X. Yao, Z. Xing, and X. Zhou, 'Understanding fire combustion characteristics and available safe egress time in underground metro trains: A simulation approach', *Chaos, Solitons & Fractals*, vol. 187, p. 115434, Oct. 2024, doi: 10.1016/j.chaos.2024.115434.
[7] D. Xu, Y. Li, J. Li, H. Zhong, J. Li, and Y. Huang, 'Climate-adaptive fire smoke ventilation strategies for atrium-type metro stations: A NSGA-II multi-objective optimisation study', *Energy*, vol. 306, p. 132390, Oct. 2024, doi: 10.1016/j.energy.2024.132390.
[8] D. Xu *et al.*, 'Investigating the influence of outdoor temperature variations on fire-induced smoke behavior in an atrium-type underground metro station using hybrid ventilation systems', *Energy*, vol. 287, 2024, doi: 10.1016/j.energy.2023.129570.
[9] Z. Wu *et al.*, 'Impact of ventilated tunnels on smoke peculiarities in train carriage fires with multiple lateral openings', *Case Studies in Thermal Engineering*, vol. 60, p. 104822, Aug. 2024, doi: 10.1016/j.csite.2024.104822.
[10] Z. Su *et al.*, 'Advancements in smoke control strategies for metro tunnel cross-passage: A theoretical and numerical study on critical velocity and driving force', *Tunnelling and Underground Space Technology*, vol. 147, p. 105734, May 2024, doi: 10.1016/j.tust.2024.105734.
[11] Z. Su *et al.*, 'A study of the critical velocity and the confinement velocity of fire accident in a longitudinally ventilated underground train with different door opening scenarios', *Tunnelling and Underground Space Technology*, vol. 131, p. 104776, Jan. 2023, doi: 10.1016/j.tust.2022.104776.
[12] H. Ingason and Y. Z. Li, 'Model scale tunnel fire tests with longitudinal ventilation', *Fire Safety Journal*, vol. 45, no. 6–8, pp. 371–384, Nov. 2010, doi: 10.1016/j.firesaf.2010.07.004.
[13] Y. M. M. Valoy, D. B. Mosiria, J.-C. Sautet, and A. Coppalle, 'Effect of ventilation on carbon monoxide and soot particles emissions in a confined and mechanically-ventilated fire', *Fire Safety Journal*, vol. 138, p. 103805, Jul. 2023, doi: 10.1016/j.firesaf.2023.103805.
[14] J. G. Quintiere, 'Scaling applications in fire research', *Fire Safety Journal*, vol. 15, no. 1, pp. 3–29, Jan. 1989, doi: 10.1016/0379-7112(89)90045-3.
[15] W. M. Pitts, 'The global equivalence ratio concept and the formation mechanisms of carbon monoxide in enclosure fires', *Progress in Energy and Combustion Science*, vol. 21, no. 3, pp. 197–237, Jan. 1995, doi: 10.1016/0360-1285(95)00004-2.
[16] R. J. Bray *et al.*, 'A comparison of carbon monoxide yields and particle formation at various global equivalence ratios in vitiated and under-ventilated conditions', *Fire Safety Journal*, vol. 141, p. 103915, Dec. 2023, doi: 10.1016/j.firesaf.2023.103915.
[17] M. J. Hurley *et al.*, Eds., *SFPE Handbook of Fire Protection Engineering*. New York, NY: Springer New York, 2016. doi: 10.1007/978-1-4939-2565-0.
[18] D. T. Gottuk, R. J. Roby, and C. L. Beyler, 'The role of temperature on carbon monoxide production in compartment fires', *Fire Safety Journal*, vol. 24, no. 4, pp. 315–331, Jan. 1995, doi: 10.1016/0379-7112(95)00027-5.
[19] E. E. Zukoski, J. H. Morehart, T. Kubota, and S. J. Toner, 'Species production and heat release rates in two-layered natural gas fires', *Combustion and Flame*, vol. 83, no. 3, pp. 325–332, Feb. 1991, doi: 10.1016/0010-2180(91)90079-Q.
[20] C. L. Beyler, 'Major species production by diffusion flames in a two-layer compartment fire environment', *Fire Safety Journal*, vol. 10, no. 1, pp. 47–56, Jan. 1986, doi: 10.1016/0379-7112(86)90031-7.
[21] D. T. Gottuk, R. J. Roby, M. J. Peatross, and C. L. Beyler, 'Carbon monoxide production in compartment fires', *Journal of Fire Protection Engineering*, vol. 4, no. 4, pp. 133–150, 1992.
[22] Z. Zhang, X. Yao, Z. Xing, and X. Zhou, 'Simulation on passenger evacuation of metro train fire in the tunnel', *Chaos, Solitons & Fractals*, vol. 187, p. 115429, Oct. 2024, doi: 10.1016/j.chaos.2024.115429.

[23] J. Tu, B. Peng, L. Bai, C. Li, and Y. Zhang, 'Study on Elevated Interval Evacuation of Metro Train considering the Influence of Fire, Railings, and Track Bed', *Modelling and Simulation in Engineering*, vol. 2024, no. 1, p. 6058039, 2024, doi: 10.1155/2024/6058039.
[24] T. Yamada and Y. Akizuki, 'Visibility and Human Behavior in Fire Smoke', in *SFPE Handbook of Fire Protection Engineering*, M. J. Hurley, D. Gottuk, J. R. Hall, K. Harada, E. Kuligowski, M. Puchovsky, J. Torero, J. M. Watts, and C. Wieczorek, Eds., New York, NY: Springer, 2016, pp. 2181–2206. doi: 10.1007/978-1-4939-2565-0_61.
[25] K. Fridolf, D. Nilsson, and H. Frantzich, 'The flow rate of people during train evacuation in rail tunnels: Effects of different train exit configurations', *Safety Science*, vol. 62, pp. 515–529, Feb. 2014, doi: 10.1016/j.ssci.2013.10.008.
[26] K. Fridolf, E. Ronchi, D. Nilsson, and H. Frantzich, 'The representation of evacuation movement in smoke-filled underground transportation systems', *Tunnelling and Underground Space Technology*, vol. 90, pp. 28–41, Aug. 2019, doi: 10.1016/j.tust.2019.04.016.
[27] D. A. Purser and J. L. McAllister, 'Assessment of Hazards to Occupants from Smoke, Toxic Gases, and Heat', in *SFPE Handbook of Fire Protection Engineering*, M. J. Hurley, D. Gottuk, J. R. Hall, K. Harada, E. Kuligowski, M. Puchovsky, J. Torero, J. M. Watts, and C. Wieczorek, Eds., New York, NY: Springer, 2016, pp. 2308–2428. doi: 10.1007/978-1-4939-2565-0_63.

Ventilation and Fire Life Safety upgrades to an existing rail tunnel facility considering modern requirements

Jeffrey Bott, Jackie Chen, Kevin Ficarra, Igor Maevski, & Andrew Page
Jacobs
One Penn Plaza, 24th Floor, Suite 2400 | New York, NY, USA 10119

ABSTRACT
Increased ridership, aging infrastructure, and more stringent code requirements create new challenges when considering replacement of existing equipment within an existing rail tunnel. Additionally, the presence and quantity of open cross passages within the subject facility provides unique challenges and opportunities for innovative analysis and design. This existing rail tunnel, originally built in the early 1900's and totalling nearly 1,500 meters in length, runs beneath the city center of one of the United States most populous cities. The ventilation system is being considered for replacement and upgrade, with numerous concepts being proposed in this study. A key factor in recommending an alternative ventilation concept is the existing, open cross passages spaced evenly throughout the twin tunnel. Closure of these cross passages, via doors or permanent means, increases the ventilation system performance but limits maintenance escape capabilities while adding additional owner maintenance costs. This study demonstrates, through engineering analysis, that there are viable ventilation fire safety solutions that may avoid the need for closure of the existing cross passages.

KEYWORDS: rail tunnel, tunnel ventilation, fire life safety, emergency egress, cross passageways, fire protection

INTRODUCTION

The existing tunnel currently serves a variety of railway vehicles including diesel locomotives, catenary powered commuter rails, and freight trains with various cargos. The existing tunnel ventilation system consists of two centrifugal ventilation fans that appear to be of original construction. The intended distribution system for these fans, through original Saccardo Nozzles, has been previously modified due to changes in vehicle fleet and the vehicle dynamic envelope that further diminish the already limited system capacity. Further challenging the existing system is the twin tunnel's forty open cross passages, spaced every 30.5 meters along its 1,230 meter length. The tunnel owner prefers to keep these cross passages open since they are used as an escape haven for maintenance workers during regular maintenance operations and also have concerns regarding cross passage door maintenance costs.

Fire protection and egress capabilities were not considered in the original facility's design and as such, the systems are not compliant with modern code requirements. This study is focused on the tunnel ventilation system upgrades, cross passage considerations, and supporting improvements necessary to achieve compliance with NFPA 130 and ASHRAE 217, as practicable under the existing site constraints with minimal impacts to the facility operation.

NFPA 130, Section 6.3.1.6 states that cross passageways shall not be farther than 244 meters apart and where cross passageways are utilized in lieu of exits, cross passageways shall be separated from the trainway with self-closing fire door assemblies having a fire protection rating of 1½ hours [1]. This paper demonstrates that, in some cases, tunnel safety can be better achieved via viable ventilation fire safety solutions that may avoid the need to comply with this requirement. The ongoing design considers that spacing between cross passages exceeds NFPA 130 requirements, while completely open, and how to implement possible solutions in a space restricted, fully operational, and highly secure facility.

EXISTING CONDITIONS

This facility, as shown in Figure , totals 1,500 meters in length and is comprised of a 1,230 meter twin tunnel that is directly connected to an overbuild subway area consisting of a 110 meter track switch area and 160 meter multi-track area with track on ballast throughout.

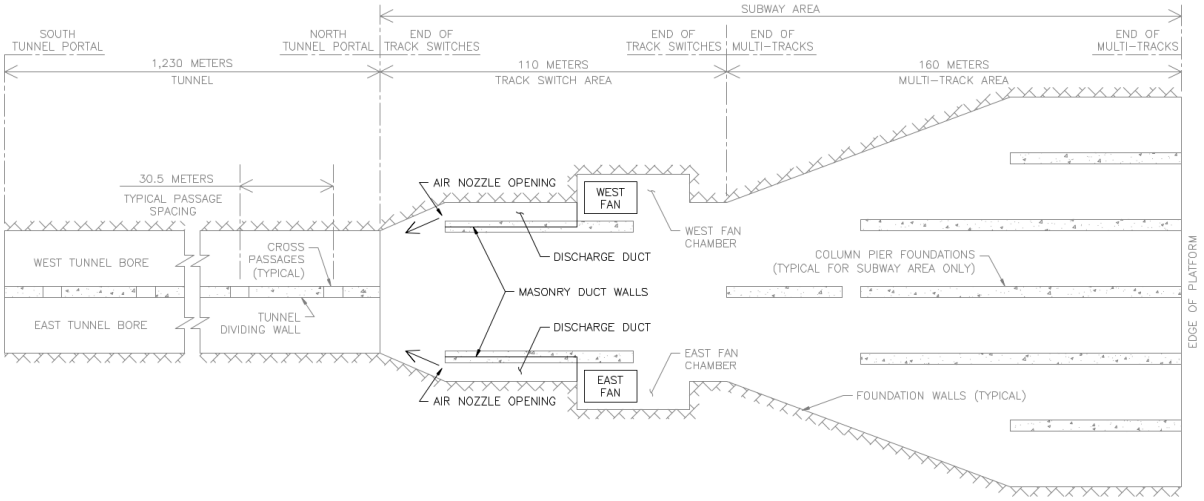

Figure 1: Schematic diagram of existing tunnel layout.

The tunnel structure consists of a 1.2-meter-thick inner stone masonry wall, concrete outer walls, and brick crown arch. Each bore is approximately 4.9 meters in width and 5.8 meters in height at the top of the arch. The bores of the tunnel are connected through their inner wall by forty open cross passageways approximately 1.2 meters wide and 2.3 meters in height spaced at regular intervals of 30.5 meters through the entire twin tunnel length. The subway area has similar height to the tunnel although it varies in width. A column pier foundation approximately 2.4 meters in height provide footings for columns which support the overbuild structures above. An existing catenary system extends from the adjacent platforms through the subway area to the twin tunnel but does not extend throughout the twin tunnels.

Tunnel Ventilation

The primary means of ventilation to the tunnel is provided by two, double inlet centrifugal fans. Originally, these fans were designed for use with steam locomotives. The current intended use of these fans is to influence air movement through the tunnel to prevent diesel smoke stagnation and control temperature, especially when diesel engine locomotives are idling in the tunnel or subway area. One fan is operated as primary and runs continuously and the second fan is maintained as a standby unit and is typically operated in the event the primary fan is taken out of service. The existing ventilation fans appear to be beyond their useful life and any improvements to the tunnel ventilation will require replacement of the existing centrifugal fans.

Each fan is installed in a dedicated fan chamber located adjacent to the railway of the track switch area as shown in Figure 1. Air is drawn from the track switch area and discharged toward the tunnel portal through a Saccardo Nozzle duct cavity formed by the foundation walls, the column pier foundations, masonry walls, and a framed ceiling. Near the tunnel portal, a cross duct connects both fan airflows below the track level and discharges into a vertical duct between the tracks. The original intent of the vertical duct was to distribute air to the inner portion of the existing Saccardo Nozzle system, but currently the duct is open to the switch area and discharges air upwards to the deck above. If the existing duct system is to be reused for ventilation improvements, the duct ceilings and masonry walls will require repair or replacement.

The original ventilation system utilized a steel framed Saccardo Nozzle system at the tunnel portal which was used to direct discharge air into the tunnels and induce unidirectional airflow from the subway area. The nozzle framing has been previously removed to provide additional envelope clearance for larger carriages. The performance of the Nozzle is ineffective as it currently exists. If improvements to the

ventilation system are to utilize the remaining of the existing Saccardo Nozzle system, modifications will be required to ensure discharge air is delivered to the point of discharge at design flow velocities and at desired angles of discharge.

Cross Passages & Egress

Cross passages are open to both the east and west tunnels via their respective inner walls, as shown in *Figure 2*, and are in compliance with the owner's protocol for rail workers' safety. This allows open communication between the twin tunnel environments resulting in difficult to control airflows during a fire emergency. In the event of a fire emergency, fresh air supplied to an incident tunnel will escape through the open cross passages, not reaching the fire site, and the non-incident tunnel could be compromised with smoke if critical velocities in the tunnels are not maintained. The proposed ventilation strategy improvements will heavily depend on the cross passage approach. Considerations could include the installation of cross passage doors in compliance with NFPA 130, or avoiding cross passages modification entirely and therefore relying on a powerful tunnel ventilation system in conjunction with short spacing between exits to the non-incident tunnel allowing quick escape for the tunnel users.

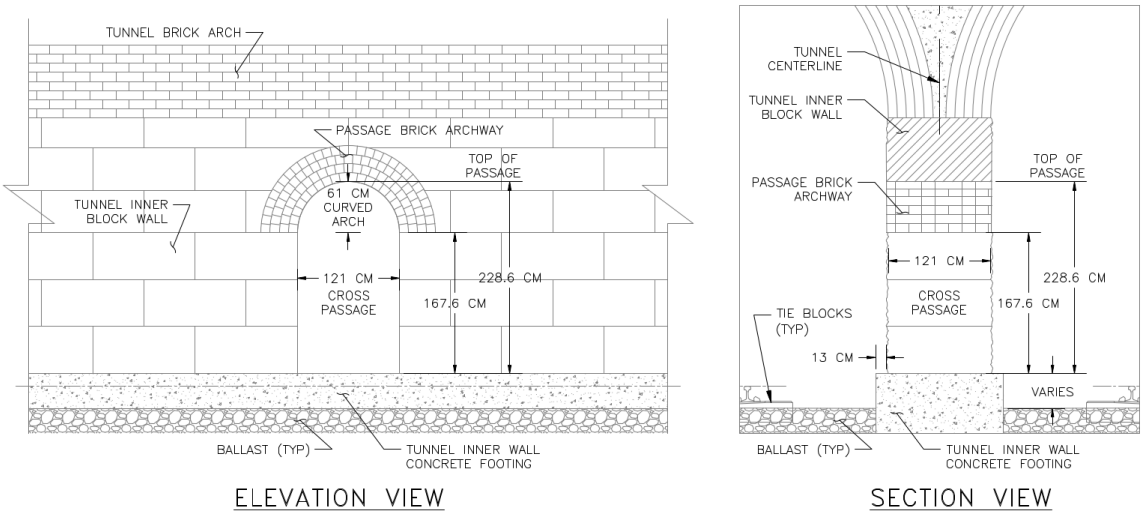

Figure 2: Existing cross passages

Fire Protection

Fire protection for the tunnel, rail switch area, and station track area is provided by a single, dedicated dry manual standpipe in the east tunnel. Within the tunnel, fire hose valves are spaced at 91.5 meter intervals to correspond with location of cross passageways. The general layout of the existing standpipe system is shown in *Figure 3*.

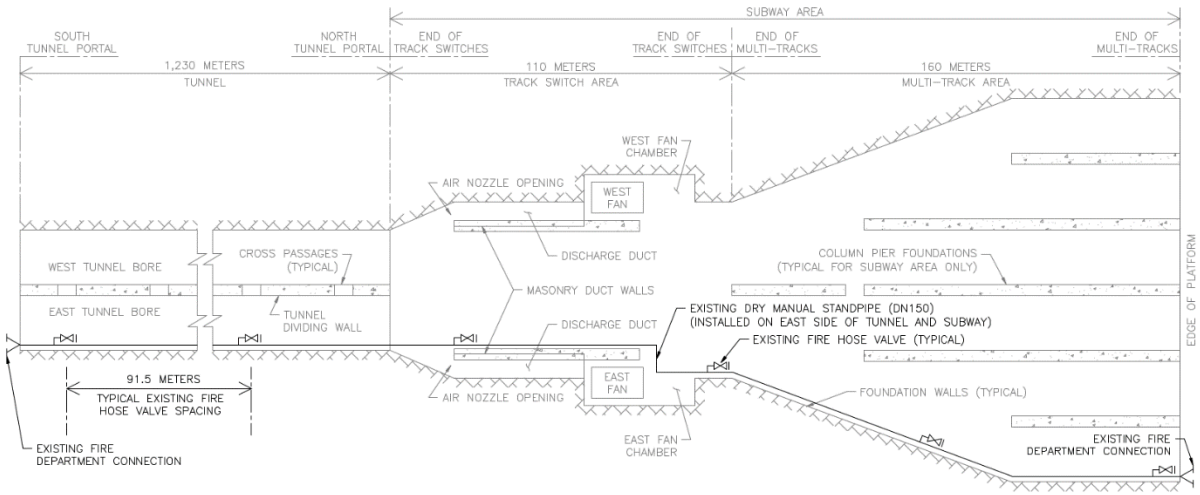

Figure 3:Schematic diagram of existing standpipe system.

Currently, to serve the west tunnel and west side of the subway area, fire hoses are required to foul the east track and be routed through the cross passageways. This can currently be easily achieved with the open cross passages but will face additional challenges if the cross passages are to be equipped with self-closing doors.

Summary

As described, the existing tunnel ventilation system is in a state of disrepair and the tunnel ventilation fans are beyond their useful service life. The current ventilation system does not provide sufficient airflow to manage smoke during fire emergency. Additionally, the numerous twin tunnel cross passages are open which provides additional challenges for the existing ventilation system and considerations for any proposed ventilation approach.

SYSTEM IMPROVEMENT APPROACH OVERVIEW

Considering the existing conditions, a conceptual design feasibility study has been performed. The focus of this study is to identify feasible alternatives to upgrade the ventilation system and fire life safety system components for compliance with current codes and standards, as practicable under the existing site constraints with minimal impacts to the facility operation [2].

A key consideration for the ventilation alternatives is the existing cross passageways and their interaction with the tunnel ventilation system. Initial owner feedback has stated that operation and maintenance concerns, specifically within the twin tunnel structure where the cross passages reside, will be a major evaluation criterion for selection of the preferred ventilation alternative. As such, each ventilation option has been evaluated considering open and closed cross passageways despite NFPA 130 requirements on fire rated separation. However, prior to in depth analysis of the ventilation options, it is important to understand the impact of the cross passageways and their possible closure.

SMOKE CONTROL EVALUATION CRITERIA

Improvements to the ventilation system were evaluated for various levels of performance, including allowable backlayering of smoke, with considerations to the cross passage approach. The following criteria were evaluated for each proposed ventilation strategy:

Smoke Control in the Tunnel with Open Cross Passages

Maintain critical velocity in both tunnel tubes, including in the incident tunnel at the location of the fire to prevent backlayering of smoke and allow for immediate safe egress of occupants to the non-incident tunnel. Egress can be achieved using regularly spaced open cross passages which are roughly spaced at a distance of a train car throughout the tunnel. Occupants downstream of the fire location may see smoke while in the incident tunnel and will need to immediately egress through a cross passage to the non-incident tunnel in the direction towards upstream of the fire. For this ventilation strategy, no closure or doors to the cross passages is considered. Air velocities in the non-incident tunnel will exceed air velocities in the incident tunnel, with the ability to control smoke in both tunnels.

Smoke Control in Tunnel with Open Cross Passages, Permitting Backlayering

NFPA 130 Annex B acknowledges that the area immediately proximate to the fire will unavoidably create untenable conditions, and that this area may extend as much as 30 meters from the fire location [1], which is equal to the spacing between cross passages in the design tunnel. As cross passages in the tunnel are spaced at 30.5 meter intervals, conditions at the cross passage immediately upstream of the fire location may be considered compromised. Therefore, ventilation performance was studied to ensure critical velocity is maintained upstream of this cross passage. Occupants upstream of this cross passage (i.e., any occupants more than 30 meters upstream of the fire location) will have safe egress either in the incident or non-incident tunnel, whereas occupants downstream may see smoke while in the incident tunnel and will need to immediately egress through a nearby cross passage to the non-incident tunnel in the direction towards upstream of the fire (in the direction of fresh airflow) [3]. For this ventilation strategy, no closure or doors to the cross passages is considered.

Smoke Control in Tunnel with Closed Cross Passages

Open cross passages allow for significant flow from the incident tunnel to the non-incident tunnel due to blockages from the incident train and throttling due to thermal effects from the fire. To mitigate this, closure of the cross passages prevents air leakage from the incident to non-incident tunnel, reducing ventilation requirements to maintain critical velocity in the incident tunnel and reduces the requirements for ventilation of the non-incident tunnel. To support emergency egress during a fire event, closure of passages may be achieved through the installation of doors. Occupants upstream of the fire location may safely egress either in the incident or non-incident tunnel. Occupants downstream of the fire location may see smoke while in the incident tunnel and will need to egress through a cross passage door to the non-incident tunnel in the direction of the closest exit.

CROSS PASSAGES IMPROVEMENT STRATEGY

Although the closure of the cross passages provides additional flexibility and saving related to the ventilation design, there are additional negative considerations which are not favorable to the owner. Currently these open passageways are utilized by maintenance personnel for clear-out procedures during track foul time, which will not allow the design to consider their permanent closure. An alternative is to consider cross passage doors at each location; however, there are significant capital costs and maintenance concerns with the additional door equipment. Such options are described in depth below, however weighted priority will be given to ventilation options that do not require cross passage doors.

Conclusions can be drawn by comparing the two scenarios, one fully NFPA 130 compliant with closed cross passages at 244 meter intervals and the other with open cross passages at 30.5 meter intervals,. Considering a fire in the middle of an 8-car train, it appears that half of the train passengers downstream of fire will be exposed to untenable smoke conditions while walking in the incident tunnel towards the nearest cross passage. In the case of open cross passages, spaced at 30.5 meter intervals (every train car), those passengers will spend minimum time in the incident tunnel while walking into the non-incident tunnel. Within the non-incident tunnel passengers might be exposed to some smoke leaking from the incident tunnel, especially when ventilation fans are started and reaching full operating speed, but the concentration is much less. Note, that air velocities in the non-incident tunnel will exceed velocities in the incident tunnel. Airflow pressure in the incident tunnel downstream of the fire is expected to be less than in the non-incident tunnel which minimizes smoke leakages through the open cross passages. As such it could be concluded that open cross passages at 30.5 meter intervals provide safer conditions for occupants compared to an NFPA 130 compliant solution with closed cross passages, provided that ventilation in both cases is sufficient to prevent smoke backlayering.

It is anticipated that the proposed longitudinal ventilation systems will de-stratify the smoke layers downstream away from fire during emergency smoke control, and mixed smoke-and-air will descend to the level of the cross passageway openings further away and potentially migrate to the non-incident tunnel at some distance from the incident car and the evacuation shall be managed in the direction of fresh airflow only.

Cross Passage Doors

Although cross passage doors are not preferred, they provide ventilation equipment cost savings and multiple alternatives have been considered to support ventilation options requiring their closure. All concepts considered are required to be operable or movable while sustaining repetitive pressure pulses and air movement influenced by trains. Door type alternatives that can be considered include single leaf sliding, single leaf swinging, double leaf swinging, pivot sliding double leaf, and roll-up. Criteria used to vet the door concepts focused on not modifying the existing passage, clearances to train and egress envelopes, complexity of the assembly, resilience to train pressure, power requirements, maintenance, and relevant listings. Dependent on selection, the considered doors may not necessarily meet the fire protection rating of 1½ hours, but would provide significant resistance for airflow and smoke leakages. Note that occupants will not consider using a cross passage door which is exposed to high heat temperatures.

A standard gravity closing, single leaf, sliding door assembly, as shown in *Figure 4*, is regularly

produced and installed in the tunnel environment. Fire resistance and other listings are available for this type of assemblies which can be applied as required to meet the project needs.

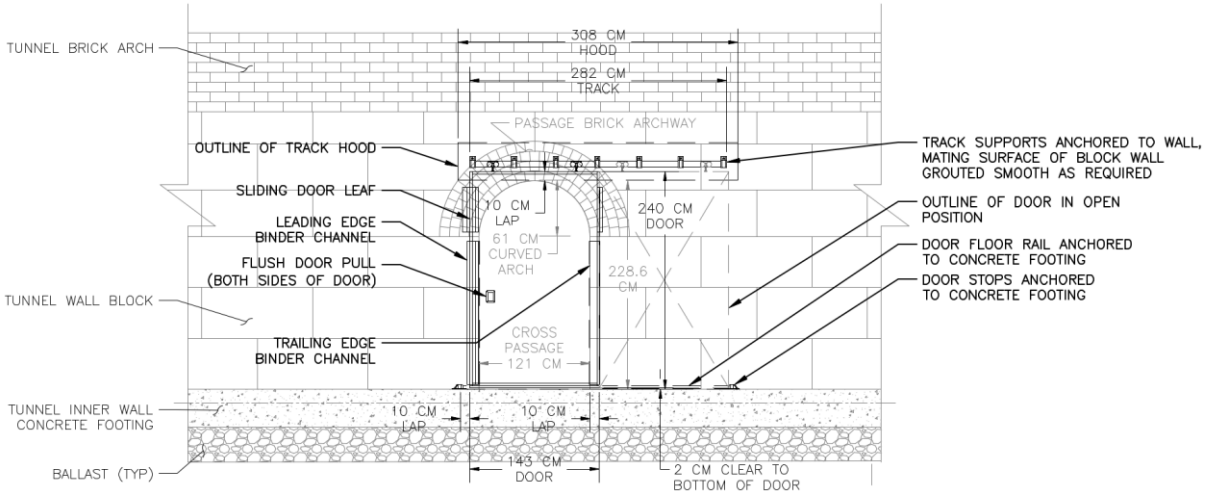

Figure 4:Elevation of proposed cross passage door assemblies.

To allow for the owner's clear-out procedures, and to limit the quantity of door assemblies, each cross passage could be provided with one door. The installed location of the doors will alternate their positions in the east and west tunnels such that the cavity of every other passage may still be used to clear-out without the need to open a door. A single installed door on cross passages is depicted in *Figure 5* below.

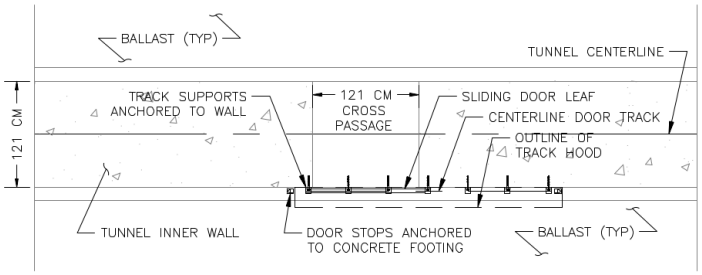

Figure 5:Plan view of proposed cross passage door assemblies.

FIRE PROTECTION IMPROVEMENT STRATEGY

The closure of the cross passageways also has additional fire protection considerations. The tunnel, switch area, and station track area are currently served by a dry manual standpipe provided with air release valves to assist in filling procedures. The standpipe is installed on the east outer wall of the east tunnel. The standpipe is fitted with three fire department connections and eighteen single connection fire hose valves. The fire hose valves are spaced in 91.5 meter intervals and are positioned such that they land at, or near an adjacent cross passage for coverage of both east and west tunnel bores. In the switch and station area, fire hose valves are located along the east wall directly connected to the standpipe main. Several tracks would need to be fouled by first responders and hoses in order to respond to an event on the west side of the tracks.

Currently the system does not fully meet the current requirements of NFPA 130 and NFPA 14 standards, and the closure of any cross passages will further diminish the level of compliance [4]. Inherently, the closure of the passageways separates the tunnel into individual environments and introduces obstruction to the existing standpipe hose valves.

Parallel Standpipe

Although cross passage doors are not preferred, modifications required to the standpipe system have been considered to support this approach. Closure of the passages would require provisions of a parallel standpipe through the length the facility to provide proper coverage. The new, parallel standpipe would

be routed on the outer wall of the west tunnel and subway area. To limit alterations to the existing standpipe, the layout of the new standpipe is proposed to mimic the existing conditions such that the fire hose valves would be positioned at staggered intervals of 91.5 meters and located near cross passages in the tunnel as shown in *Figure 6*. Additional considerations such as fire department connections and air release valves will also be required.

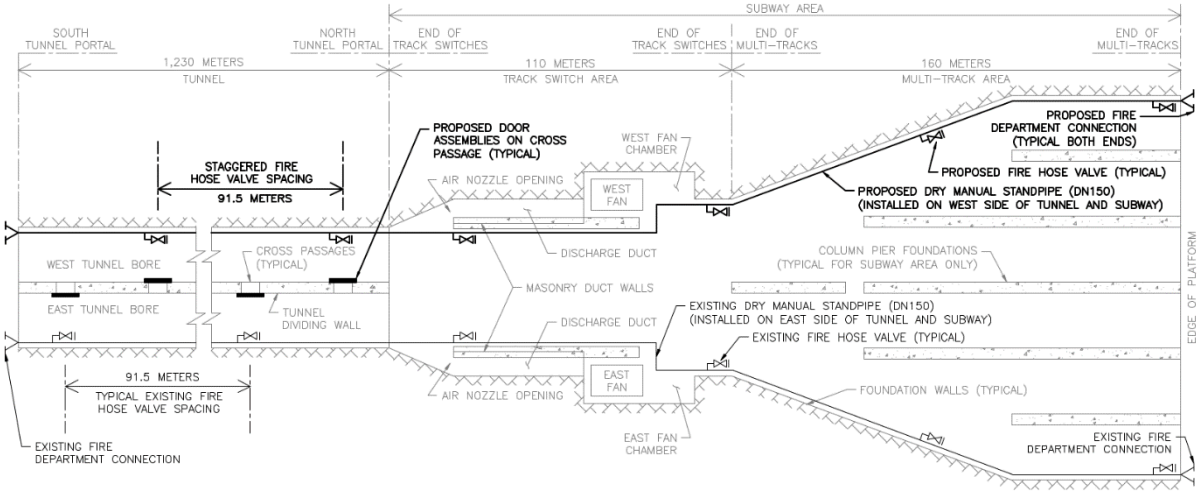

Figure 6:Schematic diagram of proposed parallel standpipe system.

This strategy poses additional upfront costs and subsequently increases assets requiring testing and maintenance. At this time, similar to the cross passage door concerns, a parallel new standpipe system is undesirable for the owners.

VENTILATION APPROACH AND METHODOLOGY

An in-depth ventilation analysis has been performed to quantify the ventilation requirements and compliance with current industry codes and standards. Considering existing conditions, including cross passages, multiple fan configurations and styles were considered to achieve carrying degrees of compliance. Considerations included replacement of the existing fans, unidirectional and bi-directional jet fans, push/pull ventilation via a supply/exhaust configuration, and other supporting improvements. Performance of each of the ventilation system concepts was evaluated using Subway Environment Simulation (SES) for multiple train fire scenarios located in the tunnel and subway area, with and without cross passage doors installed. The assumption was made for one fire in a tunnel at a time and for a single train in the incident tunnel. Evaluation was performed to determine the efficacy of each ventilation concept to provide ventilation and smoke control during an emergency fire event in the twin tunnel or underground subway area.

Saccardo Nozzle

As described above the Saccardo Nozzle is currently only partially remaining; however, replacement of fans and repair of the existing ductwork could restore functionality of the system. Unlike a typical modern Saccardo Nozzle ventilation system, where fresh air is drawn in from ambient and injected into the tunnel at high speed through the nozzle, the system serving the tunnel draws air from the crossover switch area and re-injects it at a high-speed jet approximately 50 meters downstream of the fans, inducing flow into the tunnel.

The existing configuration of the remaining nozzle considers air injected along the outer walls as well as along the middle wall separating the northbound and southbound tunnels as shown in *Figure 7*.

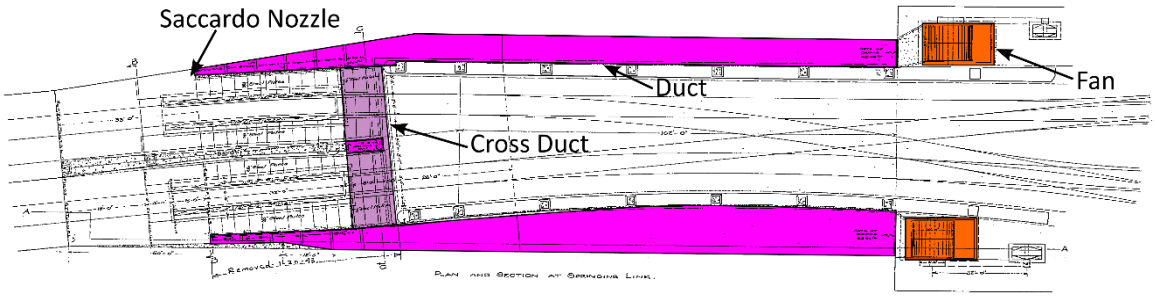

Figure 7:Saccardo Nozzle Geometry

Rolling Stock

Rolling stock information for the tunnel was provided by the operator and users. The longest train consist travelling through the tunnel for current and future operating plans includes two locomotives and eleven coaches. The largest locomotive cross section provided in the documentation is 13.66 m^2.

Design Fire

The design fire in the tunnel is based on an owner specified peak heat release rate (HRR) of 31 MW. It is noted that a fire growth curve is also defined; however, steady state analysis, including SES analysis presented, uses a constant peak HRR of 31 MW.

Jet Fan Configurations

Several of the presented options propose supplemental small diameter jet fans be installed in the subway area between existing structural columns. Due to structural space constraints these fans are located closer than typical installation and are proposed to be equipped with deflector vanes. The vanes, and their subsequent deflection at individually engineered angles, allow for full development of each flow while mitigating the interactions between fans. Computational Fluid Dynamics (CFD) modelling has been performed to show the developed flow paths. Figure 8, shown below, shows the CFD results for the most equipment intensive case. Adjustments to the jet fan efficiency was also made due to the anticipated losses due to the deflection and proximity, resulting in 70%.

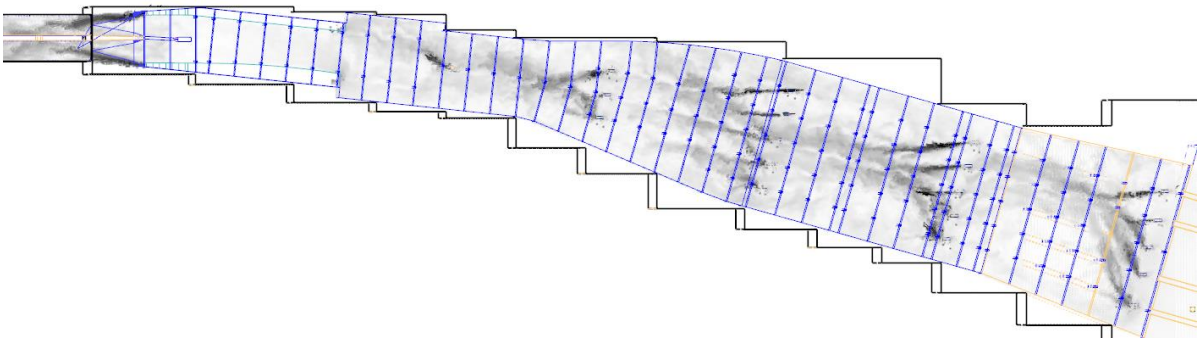

Figure 8: Jet Fan Flow Development and Deflection

Additional analysis was performed to confirm the flow through the jet fans does not exceed the flow in the upstream section. Table 1, shown below, compares the total airflow compared to the flow through the jet fans in the subway area for Options D, E, and F, all of which are below the minimum total flow in the tunnel (similar for tunnel and fan velocity). A detailed explanation for each option is provided in the following section.

Table 1: Comparison of Total Airflow to Flow through Subway Area Jet Fans

Option	Total Airflow	Jet Fan Airflow per Bank	Ratio of Jet Fan to Total Airflow
D	272.3 m^3/s	67.5 m^3/s	25%
E	271.4 m^3/s	67.5 m^3/s	25%
F	320.5 m^3/s	135.0 m^3/s	42%

TUNNEL VENTILATION ANALYSIS AND ALTERNATIVES

Through engineering analysis, discussions with fan manufacturers, and conceptual design, the feasible ventilation solutions have been narrowed down to six options. Presented below, these options vary from; with or without smoke backlayering (partially or fully protecting users), with or without needs to close cross passages, with or without abilities to reverse tunnel airflow, and with different numbers of mechanical and electrical equipment needed. Each ventilation option is considered against the smoke control evaluation criteria to determine performance considering backlayering, cross passages, and the remainder of the facility.

Ventilation Option A – Centrifugal Fans (No Backlayering, Closed Cross Passages)

The most straightforward ventilation option involves replacing the existing centrifugal fans with two new centrifugal fans, each driving 127.4 m^3/s of air through the Saccardo Nozzles with no additional fans in the subway area. A plan view of the overall installation is presented *Figure 9*.

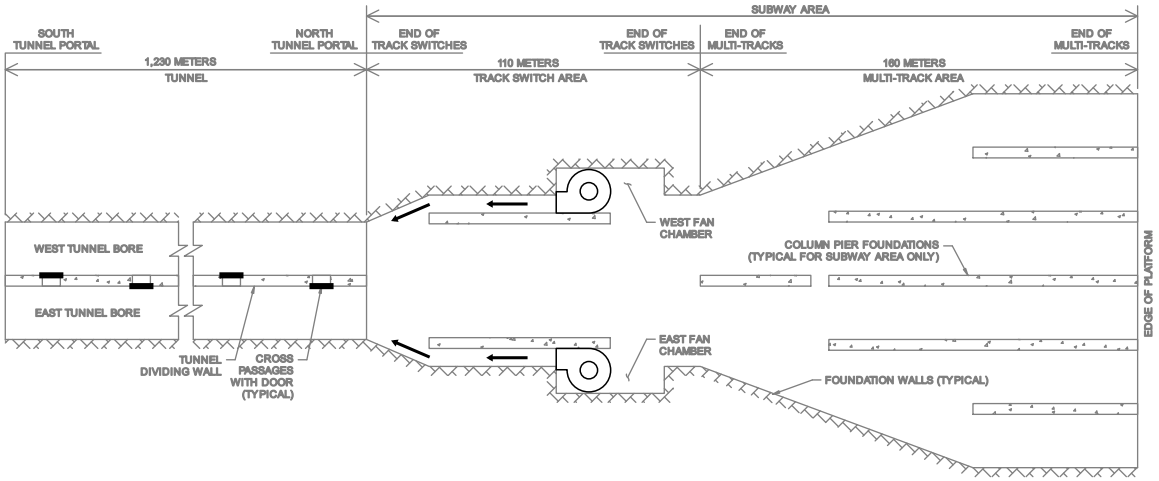

Figure 9:Ventilation Option A

Two centrifugal fans are to be installed to supply air to the reconstructed Saccardo Nozzles, one in the east fan chamber and one in the west fan chamber. The nozzle discharge velocity of this option must increase to 28.1 m/s to achieve minimum ventilation performance. Increased velocities will have negative impacts egress conditions due to high air velocities, and noise local to the Saccardo Nozzles. Discharge velocities are achieved by modifying the existing nozzle structure by cutting back the nozzle such that the discharge area is increased to 3.34 m^2.

It was found that critical velocity could only be achieved in the incident tunnel if cross passages were closed (e.g., with cross passage doors). With cross passages open critical velocity is not maintained in the incident tunnel; however, airflows in the non-incident tunnel were found to be high enough to ensure that any smoke that leaks into the non-incident tunnel will be directed downstream. This raises an additional question on the need to achieve critical velocity in the incident tunnel if cross passages to the non-incident tunnel are located at each train car. Airflows in the subway area were found to be below critical velocity though 3D CFD analysis would be necessary to verify the extent of smoke propagation during a fire in the subway area. A summary of ventilation performance is presented in *Table 2*.

Table 2: Ventilation Performance of Option A

Number of Fans	Fan Airflow [m^3/s]	Passages Open (Crit 34.5 m^3/s)	Passages Open 30m backlayering (Crit 34.5 m^3/s)	Subway Area (Crit 262.9 m^3/s)	Passages Closed (Crit 34.5 m^3/s)
2	127.4 m^3/s	✗ (21.2 m^3/s)	✗ (27.4 m^3/s)	✗ (217.1 m^3/s)	✓ (35.9 m^3/s)

Benefits of this alternative includes simplicity, by replacing the existing centrifugal fans with similar centrifugal fans. However, the required centrifugal fans (at required dimensions, flow, and pressure) are

not easily available on the market and need to be assembled in place.

Ventilation Option B – Axial Flow Fans (No Backlayering, Closed Cross Passages)
This straightforward ventilation option involves installation of two axial fans to each drive 127.4 m^3/s of air through the Saccardo Nozzles with no additional jet fans in the subway area. A plan view of the overall installation is presented in Figure 10.

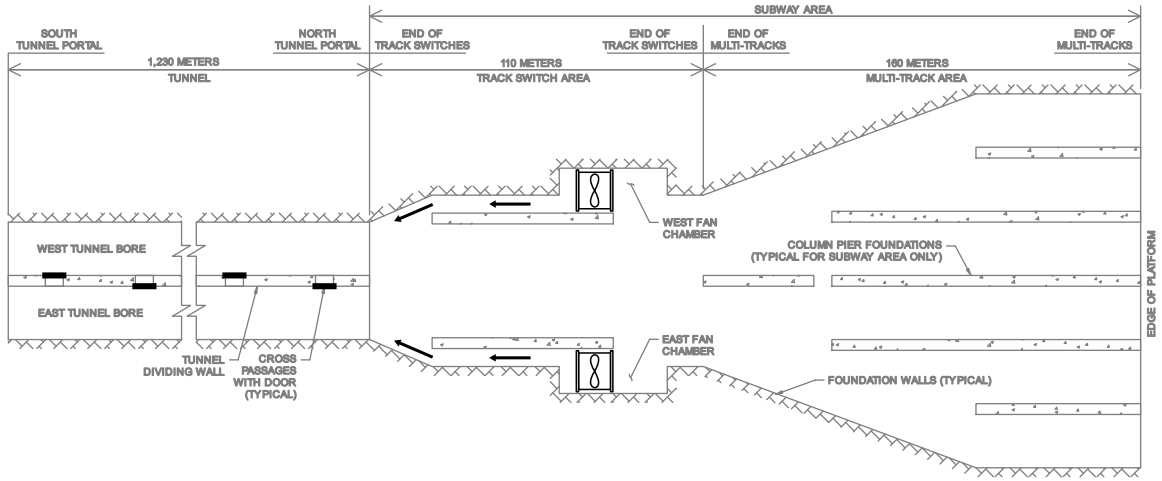

Figure 10: Ventilation Option B

The two axial fans are to be installed to supply air to the Saccardo Nozzles. Similar to the previous option, one in the east fan chamber and one in the west fan chamber replacing the existing centrifugal fans. The nozzle discharge velocity of this option must increase to 38.1 m/s to achieve minimum ventilation performance. Increased velocities will have negative impacts on egress conditions due to high air velocities, and noise at the Saccardo Nozzles. Discharge velocities are achieved by modifying the existing nozzle structure by cutting back the nozzle such that the discharge area is increased to 3.34 m^2.

It was found that critical velocity could only be maintained in the incident tunnel if cross passages were closed (e.g., with cross passage doors). With cross passages open critical velocity is not maintained in the incident tunnel; however, airflows in the non-incident tunnel were found to be high enough to ensure that any smoke that leaks into the non-incident tunnel will be directed downstream. Airflows in the switch and Subway area were found to be below critical velocity though 3D CFD analysis would be necessary to verify the extent of smoke propagation during a fire in the subway area. A summary of ventilation performance using SES is presented in *Table 3*.

Table 3: Ventilation Performance of Option B

Number of Fans	Fan Airflow [m^3/s]	Passages Open (Crit 34.5 m^3/s)	Passages Open 30m backlayering (Crit 34.5 m^3/s)	Subway Area (Crit 262.9 m^3/s)	Passages Closed (Crit 34.5 m^3/s)
2	127.4 m^3/s	✗ (21.2 m^3/s)	✗ (27.4 m^3/s)	✗ (217.1 m^3/s)	✓ (35.9 m^3/s)

Benefits of this alternative includes simplicity, by replacing the existing centrifugal fans with adequate axial flow fans more widely available on the market from many manufacturers.

Ventilation Option C – Jet Fans (No Backlayering, Closed Cross Passages)
An additional option which increases the quantity of ventilation equipment is to demolish the Saccardo Nozzle and ductwork and replace with eight large jet fans in the newly open space, each providing 2,200 N of thrust with no jet fans in the subway area. A plan view of the overall installation is presented in *Figure 11*.

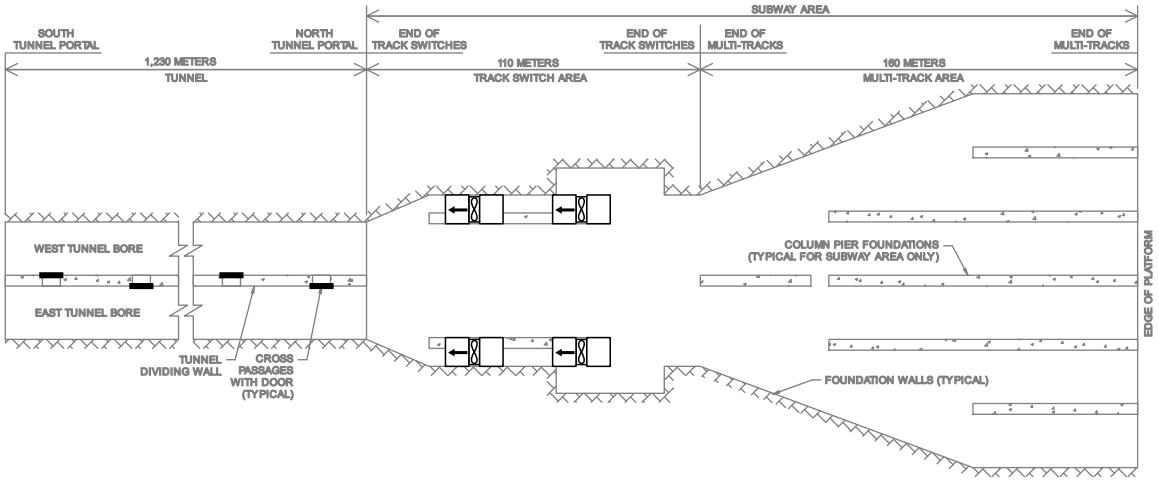

Figure 11:Ventilation Option C

The eight large jet fans are proposed to be installed along the east and west walls of the crossover area to provide thrust to generate flow through the tunnels. To execute this fan arrangement, the existing non-load bearing duct walls, ceiling, and nozzle walls are required to be removed in order to provide the needed space. These larger, reversible jet fans are proposed to be elevated above the top of column foundation piers to limit obstruction to air flow. This constrains the available height for installation of elevated fans to a maximum inner diameter of 1,120 mm with one or two-diameter silencers, each providing a thrust of 2,200 N.

It was found that critical velocity could only be maintained in the incident tunnel if cross passages were closed (e.g., with cross passage doors). With cross passages open critical velocity is not maintained in the incident tunnel; however, airflows in the non-incident tunnel were found to be high enough to ensure that any smoke that leaks into the non-incident tunnel will be directed downstream. Airflows in the subway area were found to be below critical velocity, though 3D CFD analysis would be necessary to verify the extent of smoke propagation during a fire in the subway area. A summary of ventilation performance is presented in Table 4.

Table 4: Ventilation Performance of Option C

Number of Fans	Fan Thrust [N]	Passages Open (Crit 34.5 m^3/s)	Passages Open 30m backlayering (Crit 34.5 m^3/s)	Subway Area (Crit 262.9 m^3/s)	Passages Closed (Crit 34.5 m^3/s)
8	2,200 N	✗ (23.6 m^3/s)	✗ (29.7 m^3/s)	✗ (231.3 m^3/s)	✓ (38.2 m^3/s)

Benefits of this alternative include the ability to reverse tunnel airflow, elimination of the ductwork and nozzle, and allowing for additional space in the switch area for egressing.

Ventilation Option D – Jet Fans (Compliant Backlayering, Open Cross Passages)
Keeping the cross passages open, while allowing for reversal of tunnel airflow, requires supplemental small jet fans in addition to the large jet fans described in Option C. Option D considers to demolish the Saccardo Nozzle and ductwork and to provide eight large jet fans in the newly open space, each providing 2,200 N of thrust in addition to nineteen small jet fans installed in the switch and subway area, each providing 700 N of thrust to help drive flow through the tunnel. A plan view of the overall installation is presented in Figure 12.

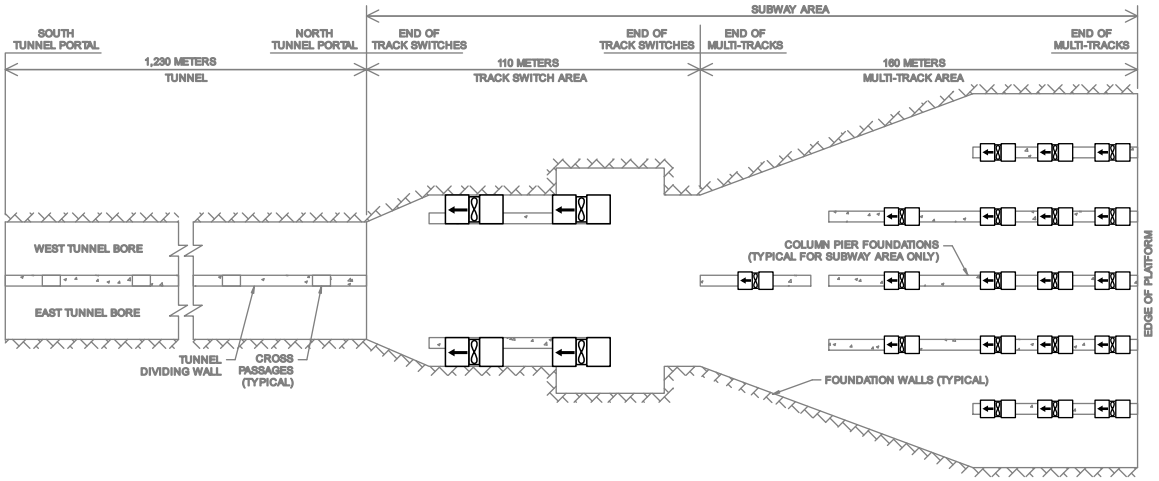

Figure 12: Ventilation Option D

The eight large jet fans are proposed to be installed along the east and west walls of the crossover area to provide thrust to generate flow through the tunnels. To execute this fan arrangement, the existing non-load bearing duct walls, ceiling, and nozzle walls are required to be removed. These larger jet fans are proposed to be elevated above the top of column foundation piers to limit obstruction to air flow. This constrains the available height for installation of elevated fans to a maximum inner diameter of 1,120 mm with one or two-diameter silencers, each providing a thrust of 2,200 N.

Nineteen small jet fans are to be installed in the switch and subway areas on top of column footings dividing the tracks in these areas. One jet fan is installed at each location, near the top of the column footing, to remain clear of the overhead catenary system while maintaining clearances from vehicle dynamic envelopes. Jet fans are proposed to be centered between the existing structural columns. Due to the limited space available, the jet fan size is limited to 630 mm inner diameter fans with one diameter silencers and deflector vanes.

It was found that while critical velocity was not met at the tunnel fire location with all cross passages open, smoke was controlled with backlayering not exceeding 30 meters and in the subway area. A summary of ventilation performance is presented in Table 5.

Table 5: Ventilation Performance of Option D

Number of Fans	Fan Thrust [N]	Passages Open (Crit 34.5 m^3/s)	Passages Open 30m backlayering (Crit 34.5 m^3/s)	Subway Area (Crit 262.9 m^3/s)	Non-Incident Tunnel (Crit 34.5 m^3/s)
8 **19**	2,200 N 700 N	✗ (29.3 m^3/s)	✓ (36.3 m^3/s)	✓ (272.3 m^3/s)	✓ (193.9 m^3/s)

Benefits of this alternative include no need for cross passage doors and reversible airflow in the tunnel. Note that NFPA 130 allows for some tenability compromise within 30 meters of the fire location.

Ventilation Option E – Axial Flow and Jet Fan (Compliant Backlayering, Open Cross Passages)
A slightly improved level of compliance with further increased quantities of equipment includes installation of two axial fans to each drive 165.2 m^3/s of air through the Saccardo Nozzles and nineteen jet fans installed in the switch and subway area, each providing 700 N of thrust to help drive flow through the tunnel. A plan view of the overall installation is presented in Figure 13.

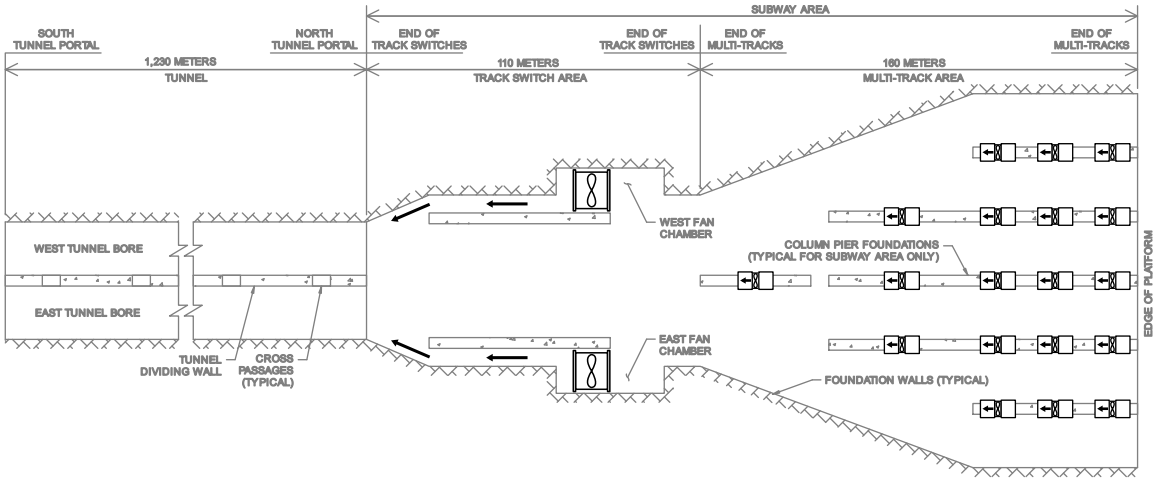

Figure 13: Ventilation Option E

The two axial fans are to be installed to supply air to the Saccardo Nozzles, one in the east fan chamber and one in the west fan chamber. Each fan supplies 165.2 m^3/s of air to the Saccardo Nozzle through the existing discharge ducts. The nozzle discharge velocity is limited to 33.0 m/s due to excessive velocities that could have negative impacts with regard to egress and noise. To achieve this discharge air velocity, modification to the existing nozzle structure is required which includes cutting back the nozzle such that the discharge area is increased to 5.02 m^2.

Nineteen jet fans are to be installed in the switch and subway areas on top of column foundation piers dividing the tracks in these areas. One jet fan is installed at each location, near the top of the column footing, to remain clear of the overhead catenary system while maintaining clearances from vehicle dynamic envelopes. Jet fans are proposed to be centered between the existing structural columns. Due to the limited available width on top of the column foundation piers, the jet fan size is limited to 630 mm inner diameter fans with one diameter silencers and deflector vanes.

It was found that while critical velocity was not met at the tunnel fire location with all cross passages open smoke was controlled with backlayering not exceeding 30 meters, as well as with closed cross passages or a fire in the subway area. A summary of ventilation performance is presented in Table 6.

Table 6: Ventilation Performance of Option E

Number of Fans	Fan Airflow/Thrust [m^3/s, N]	Passages Open (Crit 34.5 m^3/s)	Passages Open 30m backlayering (Crit 34.5 m^3/s)	Subway Area (Crit 262.9 m^3/s)	Non-Incident Tunnel (Crit 34.5 m^3/s)
2 **19**	165.2 m^3/s 700 N	✗ (28.8 m^3/s)	✓ (35.9 m^3/s)	✓ (271.4 m^3/s)	✓ (179.7 m^3/s)

Benefits of this alternative includes less large mechanical equipment needed in comparison to Option F without the need for fans to be stacked, which simplifies maintenance and reduces construction costs. Note that NFPA 130 allows for some tenability compromise within 30 meters of the fire location.

Ventilation Option F – Axial Flow and Jet Fan (No Backlayering, Open Cross Passages)
The ventilation option with the greatest level of compliance and no smoke backlayering with open cross passages includes installation of four axial fans, each providing 94.4 m^3/s of air through the Saccardo Nozzles (188.8 m^3/s per nozzle), and thirty-eight jet fans installed in the switch and subway area, each providing 700 N of thrust to help drive flow through the tunnel. A plan view of the overall installation is presented in Figure 14.

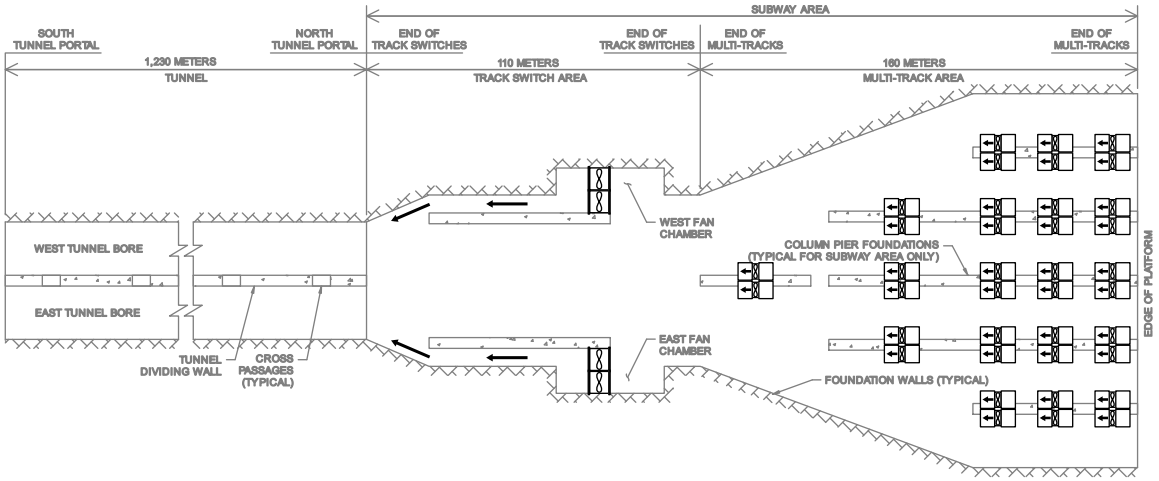

Figure 14: Ventilation Option F

The four axial fans are to be installed in pairs to supply to each Saccardo Nozzle, two in the east fan chamber and two in the west fan chamber. Each fan supplies 94.4 m^3/s of air to the Saccardo Nozzle (188.8 m^3/s per nozzle) through the existing repaired discharge ducts. Each pair of axial fans is proposed to be stacked in the existing fan chamber. The nozzle discharge velocity is limited to 33.0 m/s due to excessive velocities that could have negative impacts regarding egress and noise. To achieve this discharge air velocity, modification to the existing nozzle structure is required, which includes cutting back the wall such that the discharge area is increased to 5.76 m^2.

Thirty-eight jet fans are to be installed in the switch and subway areas on top of column foundation piers dividing the tracks in these areas. At each installation location, two jet fans are positioned vertically one above the other while maintaining clearances from vehicle dynamic envelope and below the overhead catenary system above the tracks. Jet fans are proposed to be centered between the existing structural columns. Due to the limited available width on top of the column foundation piers, the jet fan size is limited to 630 mm inner diameter fans with one diameter silencers and deflector vanes.

It was found that critical velocity could be maintained for all levels of ventilation compliance, including the most onerous condition for full smoke control of a fire in the tunnel with cross passages open. A summary of ventilation performance is presented in Table 7.

Table 7: Ventilation Performance of Option F

Number of Fans	Fan Airflow/Thrust [m^3/s, N]	Passages Open (Crit 34.5 m^3/s)	Passages Open 30m backlayering (Crit 34.5 m^3/s)	Subway Area (Crit 262.9 m^3/s)	Non-Incident Tunnel (Crit 34.5 m^3/s)
4 **38**	94.4 m^3/s (188.8 m^3/s / tunnel) 700 N	✓ (35.4 m^3/s)	✓ (43.4 m^3/s)	✓ (320.5 m^3/s)	✓ (210.3 m^3/s)

CONCLUSIONS

Multiple ventilation solutions have been proposed with varying levels of performance and compliance. A driving factor when selecting a viable alternative is the forty existing, open cross passageways within the twin tunnel structure. Initial owner input suggests that closing of the cross passageways with doors is not preferred due to safety considerations and increased maintenance requirements. However, these open airways play a large role in the ventilation performance, including backlayering and the control of smoke spread within the tunnels.

To meet the ventilation requirements, while considering the owner's preference of open cross passages, investigation of various ventilation and fire-life safety refurbishments and upgrades have been analyzed resulting in six ventilation concepts with varying levels of equipment requirements and performance for smoke control of a fire in the tunnel. The compliance of the various ventilation concepts to control smoke spread for various configurations has been evaluated, ranging from full control of smoke spread

in the incident tunnel with cross passages open, limited control of smoke spread (i.e., permitting up to 30 meters of backlayering) in the incident tunnel with cross passages open, control of smoke spread in the incident tunnel with cross passages closed, and control of smoke spread in the station track area. A summary of the performance of various ventilation concepts is presented in Table 8.

Table 8: Summary of Ventilation Performance

Arrangement	Option	Number of Fans	Fan Airflow/Thrust [m^3/s, N]	Passages Open (Crit 34.5 m^3/s)	Passages Open 30m backlayering (Crit 34.5 m^3/s)	Subway Area (Crit 262.9 m^3/s)	Passages Closed (Crit 34.5 m^3/s)
Centrifugal Fans	A	2	127.4 m^3/s	✗ (21.2 m^3/s)	✗ (27.4 m^3/s)	✗ (217.1 m^3/s)	✓ (35.9 m^3/s)
Axial Fans	B	2	127.4 m^3/s	✗ (21.2 m^3/s)	✗ (27.4 m^3/s)	✗ (217.1 m^3/s)	✓ (35.9 m^3/s)
Jet Fans	C	8	2,200 N	✗ (23.6 m^3/s)	✗ (29.7 m^3/s)	✗ (231.3 m^3/s)	✓ (38.2 m^3/s)
Arrangement	**Option**	**Number of Fans**	**Fan Airflow/Thrust [m3/s, N]**	**Passages Open (Crit 34.5 m3/s)**	**Passages Open 30m backlayering (Crit 34.5 m3/s)**	**Subway Area (Crit 262.9 m3/s)**	**Non-Incident Tunnel (Crit 34.5 m3/s)**
Jet Fans	D	8 19	2,200 N 700 N	✗ (29.3 m^3/s)	✓ (36.3 m^3/s)	✓ (272.3 m^3/s)	✓ (193.9 m^3/s)
Axial & Jet Fans	E	2 19	165.2 m^3/s 700 N	✗ (28.8 m^3/s)	✓ (35.9 m^3/s)	✓ (271.4 m^3/s)	✓ (179.7 m^3/s)
Axial & Jet Fans	F	4 38	94.4 m^3/s (188.8 m^3/s / tunnel) 700 N	✓ (35.4 m^3/s)	✓ (43.4 m^3/s)	✓ (320.5 m^3/s)	✓ (210.3 m^3/s)

Supporting alternatives for fire and life safety have been identified and evaluated, including cross passage doors and fire standpipe, each of which has increased costs and maintenance considerations within the twin tunnel.

It was concluded that while closing cross passages would reduce the required ventilation equipment for fire emergencies, and might be a cost savings alternative, open cross passages could provide increased safety for tunnel occupants when spaced at 30.5 meters intervals. This approach exceeds the NFPA 130 requirements for fire protected closed cross passages, when considering that critical velocity is achieved in the incident tunnel for both scenarios.

ACKNOWLEDGEMENTS

Authors would like to thank all of the Jacobs team members who have contributed to the ongoing project work and execution. Authors would also like to acknowledge Dr. Sai Doddi for his efforts with computational fluid dynamics modeling.

REFERENCES

1. National Fire Protection Association, NFPA 130. Standard for Fixed Guideway Transit and Passenger Rail Systems. 2023 edition. ISBN: 978-145592346-5. NFPA, 1 Batterymarch Park, P.O. Box 9101, Quincy, MA 02269-9101
2. American Society of Heating, Refrigerating, and Air-Conditioning Engineers, 2020 ASHRAE Standard 217: Non-Emergency Ventilation in Enclosed Roda, Rial, and Mass Transit Facilities, Atlanta, GA: ASHRAE, 2021.
3. H. Biteau, J. Donovan, A. Went, A. Berry, A. Smith, N. Birmingham. Review of Emergency Egress and Rescue Challenges in Rail Tunnels. 2024 Fire Protection Research Foundation. 1 Batterymarch Park, Quincy MA 02169. January 2024
4. National Fire Protection Association, NFPA 14. Standard for the Installation of Standpipe and Hose Systems. 2024 edition. ISBN: 978-1455920327. NFPA, 1 Batterymarch Park, P.O. Box 9101, Quincy, MA 02269-9101

Disposal of Emergency Telephones in Swedish Railway Tunnels: Practical application of the CSM RA-regulation

Karl Fridolf[a] & Johan Lundin[b]
[a]The Swedish Transport Administration
Box 366, SE-201 23 Malmö, Sweden,
E-mail: karl.fridolf@trafikverket.se
[b]Brandskyddslaget AB, Stockholm, Sweden

ABSTRACT
In this paper, the safety implications of removing emergency telephones from railway tunnels owned by the Swedish Transport Administration is assessed. Employing the European common safety method for risk evaluation and assessment (CSM RA), it involves risk and expert analysis of various tunnel designs and communication equipment. The study finds that emergency telephones mainly serve as a redundant system, with other wireless options like GSM-R providing similar functions. The conclusion is that telephones can be safely removed, provided that for tunnels longer than 1 km, adequate radio communication and fixed connections are established in safe areas. This approach offers a balanced solution for maintaining safety while managing costs and infrastructure efficiency.

KEYWORDS: emergency telephones, common safety methods, CSM RA, removal, disposing, tunnel safety

INTRODUCTION

In order to prevent and/or mitigate railway tunnel-incident scenarios, such as collisions, derailments, and fires, technical and administrative measures are typically introduced as part of a tunnel safety concept. Providing means for emergency communication in general, and emergency telephones in particular, is an example of a technical measure, which historically has been used to allow people in a tunnel to communicate with the control center of a tunnel infrastructure manager. Consequently, emergency telephones are today installed in approximately 70 of the Swedish Transport Administration's (Trafikverket's) railway tunnels. Facing large costs related to maintenance and reinvestments as part of the life cycle management of these emergency telephones, the question was raised whether or not they could be removed. As such action is a change to the railway system in Sweden, regulation (EU) no 402/2013 shall be applied. The regulation establishes a common safety method (CSM) for risk evaluation and assessment (RA), and in this paper, the practical application of the so called CSM RA-regulation to assess the impact of the proposed change on safety levels is presented. This paper gives a brief overview of the work conducted that is presented in a project report (TRV 2022/102615).

Purpose and objectives

The primary purpose of the work presented in this paper was to conduct a comprehensive analysis of the safety implications associated with the decommissioning of emergency telephone systems within railway tunnels owned by Trafikverket. The objective was to evaluate the impact of removing these systems on overall safety measures and communication protocols within these tunnels. Through meticulous examination and risk assessment, this research aimed to identify potential challenges, risks, and alternative communication measures post the removal of emergency telephone systems. By understanding the consequences of this action, the study sought to propose viable strategies and guidelines to ensure the maintenance or enhancement of safety standards within railway tunnels, aligning with EU directives while accommodating the evolving technological landscape and safety protocols.

Scope

The proposed change was expected to primarily impact on-board staff and passenger safety. This is because emergency telephones in tunnels are unlikely to be utilized by rescue personnel during an emergency response. Additionally, operations and maintenance staff are not expected to use emergency telephones as they rely on other communication systems both during regular operation and in emergency situations, primarily GSM-R. However, the safety of maintenance staff needs assessment based on the facility's status and the nature of their work.

The risk identification was mainly focused on how on-board staff and passengers are affected, while the consequences of removing emergency telephones for operation and maintenance personnel's communication with Trafikverket's traffic control center (TTCC) was not thoroughly examined. It is essential to note that although the focus was limited to the implications for on-board staff and passengers, the risk analysis encompassed the entire sequence of events from cause to effect, including alarm chains and the TTCC's actions.

An emergency telephone itself is not expected to increase the risk of an initial accident. Its primary purpose is to mitigate damages and consequences after an accident has occurred. Therefore, the activities to identify risk sources, especially during the below-mentioned risk workshop, focused on describing how various accident scenarios in tunnels unfold and how on-board staff and passengers are expected to act during these events.

Special attention was given to the use of different communication systems (regardless of type) and the anticipated severity of damage based on various actors' actions during an accident. The method resembles a combination of 'what-if' scenarios and sensitivity analysis, where accident scenarios were developed, focusing on one communication system at a time.

A collision between trains in a single-track tunnel without derailment was assessed as highly unlikely and not specific to tunnels. Such an event could occur anywhere in the railway system with severe consequences, but several safety systems are already in place to minimize the risk, such as signaling systems and traffic control. Therefore, this event was not further explored in the subsequent work.

DEFINING THE SYSTEM UNDER ASSESSMENT

As a first step, the system under assessment was defined and described in a so called system definition. The system was defined to include Trafikverket's railway tunnels (belonging to subsystem infrastructure) and all measures that has been taken to enable emergency communication with TTCC. A distinction was made between the following types of tunnels equipped with emergency telephones:

A. Single-track tunnels with safe areas[1] (such as service tunnels and service shafts)
B. Single-track tunnels without safe areas
C. Double-track tunnels with safe areas
D. Double-track tunnel without safe areas
E. One of two (or more) fire-separated single-track tunnels with cross-passages
F. One of two (or more) single-track tunnels that are not fire-separated

The tunnels were categorized based on length and system design, impacting the requisite communication infrastructure. Tunnels shorter than 1 km exhibited relatively simpler communication needs compared to longer counterparts.

DECIDING THE SIGNIFICANCE OF THE PROPOSED CHANGE

It was early established that the proposed change had an impact on safety. Hence, the significance of

[1] a safe area is defined as a temporary survivable space for passengers and staff to find refuge after they have evacuated from a train.

the change had to be assessed by expert judgement. A group of experts representing individuals with knowledge and experience within of tunnel safety, CSM RA, radio and telecommunications systems, facility monitoring and work as a train driver assessed the significance based on the following criteria: failure consequence; novelty used in implementing the change; complexity of the change; monitoring; reversibility; additionality. It was unanimously decided to consider the proposed change as significant. Consequently, the risk management process described in the CSM RA-regulation had to be applied (TRV 2022/102615).

IDENTIFICATION OF RISK SOURCES AND SCENARIO REPRESENTATION

The risk analysis work included examining and analyzing how the risk in existing tunnels where emergency telephones are part of the safety concept is affected if they are disposed, and assessing whether the remaining risk is acceptable. Prior to the risk assessment, the system design for the facility inventory was categorized and specified. This constituted an important starting point for structuring the risk analysis. The risk assessment, in broad terms, involved the following activities:

1. Identifying sources of risk and risk scenarios, including a pre-study, during a risk workshop and in subsequent meetings with individuals with knowledge about experience from train driving.
2. Estimating relevant sources of risk and risk scenarios using a semi-quantitative risk estimation method.
3. Evaluating risks and applying code of practices as a principle for risk acceptance.

Since all risk sources are controlled through code of practice, the risk management process was limited to the following:

a) Identification of risk sources

b) Recording the use of code of practice in the hazard record

c) Documentation of the application of the risk management process

d) Independent assessment

The risk analysis method initially involved the identification and analysis of accident scenarios using a functional communication system to determine the importance of contacting TTCC in various types of accidents, facilitated by the emergency telephone. The following step in the assessment was to consider the emergency telephone in comparison to other communication methods.

The risk assessment commenced with a workshop involving the same participants as the significance assessment. Efforts were made to contact the chairperson of the Railway Companies' Safety Focus Group, but despite an initial response, there was no further reply regarding invitations to coordination meetings. Therefore, the initial risk workshop was followed up with a meeting involving the Swedish Traffic Administration employees previously working as train drivers to ensure the accurate documentation of identified risks, accident scenarios, and actions.

Types of Accidents

The process of identifying sources of risk was based on studying the types of accidents that can occur in a tunnel and that are specific to tunnel environments according to regulation (EU) no. 1303/2014 concerning the technical specification of interoperability relating to safety in railway tunnels (TSI SRT). These include:

- Fire (combination of heat, flames, and smoke)
    - Fire occurring on board trains
    - Fire occurring in traffic or ancillary spaces (such as the tunnel or a utility space in a service tunnel)
    - Explosion followed by fire

- Release of toxic smoke or gas
- Collision
- Derailment
- Spontaneous evacuation

During the risk workshop and the subsequent meeting conducted with former train drivers, participants were given the opportunity to supplement this list. However, no such addition was deemed necessary at that time.

Identification of Relevant Risk Sources and Scenarios

In the risk assessment, the railway tunnel was viewed as a complex facility with numerous interdependencies among its various components and systems, especially during emergencies and different types of accidents and their consequences. An accident might result from multiple interacting hazards, leading to several similar consequences. Due to the lack of a practical method to identify relevant risk sources in this complexity, a customized risk identification method was devised. The objective was to pinpoint which accident scenarios needed closer examination to assess the risk associated with the proposed change, particularly where an emergency telephone reduces risk. A traditional risk model (Figure 1) was adapted and adjusted (Figure 2) to analyze the effect of emergency telephones during tunnel-specific accidents.

According to the CSM RA-regulation, the identification of risk sources only needs to be detailed enough to determine when safety measures can control the risks. In addition, selecting the risk acceptance principle is challenging before an initial risk identification has been made, making the work iterative. The assessment was that a structured accident development according to the adapted model meets the requirements. Code of practice was deemed applicable as the risk assessment principle for all identified risks within the scope of this work.

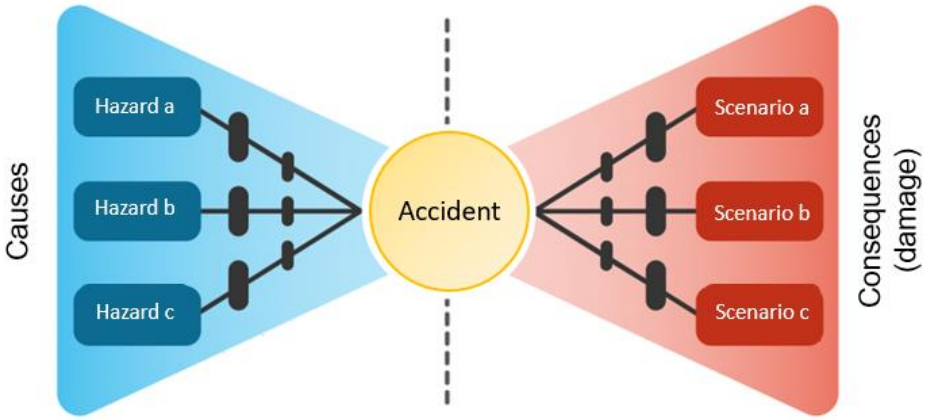

Figure 1. Traditional model for dividing and describing risk.

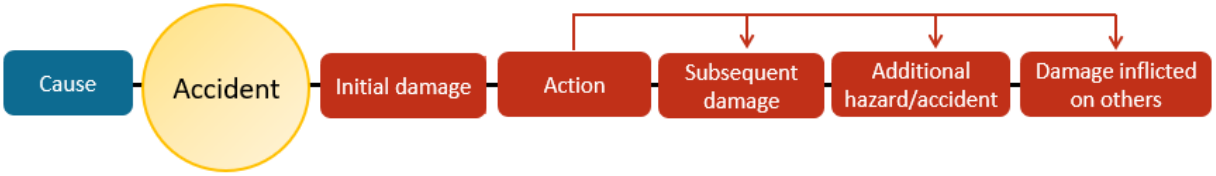

Figure 2. Adapted model for risk in the current application.

Below is a concise description of the different components in the adapted model:

- Cause: The causes of accidents in a tunnel can be diverse.
- Accident: Represented by tunnel-specific accidents.

- Initial damage: Harm to passengers and on-board staff during the initial phase of the accident.
- Actions: Expected actions of on-board staff and passengers during the accident.
- Subsequent damage: Harm occurring later during the accident sequence due to the initial incident, for instance, the spread of smoke in the tunnel as a fire develops.
- Additional hazard/accident: Beyond the initial incident, various additional accidents can affect individuals on the train or during evacuation, such as fallen power lines, traffic in the tunnel on other tracks, etc.
- Damage inflicted on others: Initially affecting individuals on-board the affected train, the consequences can extend to other individuals, including people on other trains or maintenance staff.

Scenarios specific to tunnel events are described using an adapted model (see *Figure 2*). Participants in the risk workshop and train driver representatives contributed to describing various actors' actions after the initial damage.

Based on the accident sequence in *Figure 2*, each communication system was analyzed separately (GSM-R, public mobile phones, and emergency telephones), in an assessment of how on-board staff and passengers can be expected to react depending on the available communication systems in a given accident scenario. During the risk workshop, the model followed a repetition of the following points:

1. What could be the cause this tunnel-specific accident?
2. What can be expected to be the initial damage?
3. How would on-board staff and passengers act if they only had access to this communication system (GSM-R, public mobile phones, or emergency telephones)?
4. What consequences and additional dangers/accidents can be identified and how does this impact other individuals?

The following uncertainties in the accident sequence have been identified and considered in the risk analysis:

- Actors' actions and regulatory compliance
- Functionality of communication systems
- Factors influencing the scale of the accident, such as fire and smoke spread
- Location of the accident in the tunnel
- Tunnel design

These uncertainties were important input values in the construction and structuring of the risk analysis, from risk identification, division of the accident sequences into different parts, to the presentation of results. During the risk workshop, it was observed that behaviour can be expected to be influenced by several factors, which is expected to be similar under different conditions. This information constitutes input values for the risk estimation.

Causes
Causes of accidents, i.e. hazards, encompass both the reasons for the original incident and additional hazards and accidents that can threaten individuals in a tunnel. These causes were mapped during the risk workshop.

Type of Damage in Different Stages of the Accident Sequence
A hazard record for various tunnel accidents and their impact due to delayed alarm to TTCC was documented and constituted input to risk index calculations. In summary:

1. Additional accidents may occur after the evacuation starts, except in track incidents in a double-track tunnel when a passing train collides with a still standing. This assumes a lack of alarm to TTCC.
2. Alarms to TTCC reduce the dangers for evacuating individuals, especially in the case of electrical accidents involving fallen power lines or train collisions with individuals.
3. Individuals within the tunnel can evade the effects of the accident through alerts from GSM-R or TTCC via public GSM.
4. Alarms to TTCC can reduce subsequent injuries for passengers and facilitate faster emergency services response. The effect is considered to be small because the time it takes for the emergency services to reach the accident site is expected to be long in relation to the progression of the accident. The tunnel safety concept relies on the self-evacuation principle, meaning individuals in the tunnel should be able to rescue themselves without assistance from emergency services, which has been the standard even before the introduction of the TSI SRT.

Actions of Train Drivers, On-board Staff, and Passengers
An overview of how on-board staff and passengers can be expected to act given their access to (only) a specific communication system (GSM-R, public mobile phones, or emergency telephones) is presented briefly in Table 1. The presentation also outlines actions in the absence of communication systems.

Significance of System Design
The tunnel design outlined in the introduction of the paper impacts the development of an accident, extent of damage, and the effectiveness of emergency communication. Below is an overview of the differences in types and sizes of damage at different stages:

1. The cause of the accident influences the extent of the initial damage. A fire onboard a train can spread at different rates, influenced by where in the train it starts.
2. Initial damage is usually similar, except in double tracks involving multiple train sets. In such cases, more individuals may be affected, potentially increasing the damage's size.
3. Subsequent damages vary depending on the tunnel's design. Some designs allow protection against fire or toxic gas through evacuation spaces, while double tracks may involve more trains and larger damage.
4. Tunnel design impacts the risk of injuries during evacuation, such as falls or electric shocks, especially during train evacuation.
5. In single-track tunnels, the extent of damage partly depends on the distance to eemergency exits, varying based on the accident's location within the tunnel.
6. In double-track tunnels, damages are similar to single-track tunnels but pose risks of additional injuries such as train collisions or being struck by trains.
7. In facilities with multiple tunnel tubes, there's still a risk of being struck by trains or sustaining injuries during evacuation due to traffic, fire, or abrupt braking during evacuation.

Table 1. Description of Expected Actions Following an Accident by Train drivers/On-board staff and Passengers Based on Analysis in the Risk Workshop and Subsequent Meeting with Former Train drivers.

Communication system	**Subsequent activities train driver/on-board staff**	**Subsequent activities passengers**
Only GSM-R (MobiSIR)	Train driver: "Ordinary alarm chain in case of apparent threat": Emergency call to TTCC and all trains in nearby area. Supplementary alarm call to TTCC. The alarm receiver forwards the alarm to, among others, the emergency services according to an alarm receiver checklist. Communication with other on-board staff occurs via the train's internal communication system. Extensive additional activities are outlined in the National Railway Traffic Regulations, e.g., emergency signs should be displayed. On-board staff: If they have GSM-R, they receive emergency calls. Railway companies have safety regulations. The staff is expected to inform that leaving the train is dangerous. Typically, the onboard supervisor does not have their own GSM-R, but has been trained to send emergency calls via a GSM-R device. Initiates possible evacuation. The decision on this is made by the driver in consultation with the train dispatcher and electrical engineer at TTCC. A GSM-R phone is typically available in both driver cabs of the train. Whether the unit is fixed or mobile varies between train types.	Instruction: Move from danger to the next carriage. Presumed spontaneous evacuation (quite common). Lower risk during spontaneous evacuation as long as there is no apparent danger. Good information from the driver reduces the risk of this.
Only public GSM	Train driver: Alarm number is available in the route book. The GSM-R phone can be used via the public network through roaming, with normal functionality. Some time delay due to delayed alarm and more to handle. The alarm receiver at TTCC has more tasks because the emergency call has not been made. Otherwise, the same conditions. Possible initiation of evacuation. The train driver decides this in consultation with the train controller and the electrical engineer at TTCC.	The risk of spontaneous evacuation increases as the time elapses. Several are expected to call relatives, friends, or emergency services. Risk of overload on the GSM network used by train drivers in case of non-functioning GSM-R. It is not possible to rule out overload on the GSM system. 112 may have reserved channels, but whether operators have implemented this is uncertain.
Only emergency telephone	Train Driver: Contacts TTCC via the nearest emergency telephone, but there is no guarantee for this. Should be signposted and emergency lit. Dependent on the person. On-board staff: Unclear if they sound the alarm. Probably stay on board. May initiate evacuation. The train driver decides on this in consultation with the train dispatcher and the electrical operation engineer at TTCC. The route book indicates the presence of an emergency telephone, but not its exact location.	Depends on the circumstances. May vary in different parts of the train. Emergency telephone might be used.
No communication system	Evacuation. Possibly faster in the absence of dialogue with TTCC. Uncertain. Organized evacuation and/or spontaneous evacuation. Lack of possibility for consultation with the train controller and electrical engineer.	Evacuation. Organized evacuation and/or spontaneous evacuation.

The Importance of Notifying TTCC for the Size of the Damage
During the risk workshop, the importance of notifying TTCC to assess the extent of the damage was emphasized. Below are the summarized conclusions from the workshop:

1. Communication systems for alerts have the greatest impact on damages in additional accidents outside the affected train, such as electrical accidents involving downed overhead lines and collisions with evacuating trains or trains on adjacent tracks or in adjacent tunnel tubes.
2. Emergency telephones are part of the alert process, but their impact varies. The study focuses on stages where the alarm is relevant.
3. The difference in alert times between different systems is estimated to be a few minutes, but the system initiating the alert is less important compared to the alert reaching TTCC on time.
4. The presence of emergency telephones in a railway tunnel affects the ability to sound an alarm and possibly (under certain circumstances) the timeline until an alarm is raised, which can impact the risk. GSM-R is assumed to be quicker. The primary function of the emergency telephone is to serve as a redundant system.
5. The effect of alerts to TTCC is similar regardless of system. It has the least impact in single-track tunnels with functional ancillary spaces (technical rooms) since the risk of train-person collisions is minimal.
6. Simultaneous alerting through multiple systems is not advantageous and can overload the public mobile network. Preventing staff alerts is considered as a negative safety impact.
7. Traffic Administration staff at the traffic control take actions using the control and monitoring system, not solely based on emergency alerts. The safety concept relies on their continuous monitoring and intervention.

The Importance of Choosing Communication Systems for Notifying TTCC for the Size of the Damage
During the risk workshop, the behavior and sequence of events during accidents were examined, along with how the alerting process was affected by different communication systems. It was clarified that the impact of the alerting process was confined to damages from additional accidents and injuries to other individuals. The assessment concluded that the alerting process had minimal impact on the initial damage and subsequent injuries. GSM-R is presumed to provide faster alerts than emergency telephones, with the primary effect of the emergency telephone being an additional communication system.

RISK ESTIMATION

During the risk workshop, a thorough analysis was conducted on how different communication systems and risk identification affect the consequences of accidents in tunnel environments. Several crucial conclusions emerged, forming the basis for understanding how emergency communication impacts safety during accidents.

A key finding was that if risk sources are managed according to code of practices, the associated risks can be deemed acceptable. This implies that further analyses are not required for these specific risk sources, and the use of such practices is recorded as safety requirements for the relevant risks. Despite this conclusion, the authors of this paper chose to conduct a rough risk estimation to enhance understanding of how emergency communication affects the complex sequence of accidents in tunnel environments. Through discussions in the risk workshop and meetings with train driver representatives, combined with experiences and literature reviews, an assessment was made of the magnitude of damage in various scenarios.

The method of risk estimation involved a semi-quantitative approach, assessing the likelihood of different types of accidents and system designs, represented by indices from 1 to 3. This index aimed to reflect the relative likelihood of each type of accident, considering that tunnel accidents occur with very low frequency.

The consequence for each type of accident and system design was also assessed with an index ranging from 1 to 3 for different stages of the sequence of events. Furthermore, a risk index for each type of accident and system design was calculated by multiplying the probability and consequence indices. Subsequently, the significance of having at least one functioning communication system during an accident was evaluated by assessing the difference in risk indices between the scenario with and without a functioning communication system.

This approach provided a deeper understanding of the expected effect of emergency communication at various stages of an accident. The reporting of results primarily aimed to enhance understanding of the effects of proposed measures from a risk and safety perspective.

The Impact of Alarming on the Risk Profile

Detailed results of the risk indices for the types of accidents are presented in the project report and are summarized in Table 2. In the table, the difference in risk indices between functioning and non-functioning alarms to TTCC is presented for various tunnel configurations, with a particular focus on scenarios with the most impact on the risk index. The difference in RI values is calculated by subtracting the RI for scenarios with functioning alarms from those without functioning alarms, reflecting the added safety value of operational alarm systems. As an example, a train fire in a double-track tunnel without functioning alarms to the TTCC can escalate risks due to delayed responses. Key hazards include potential collisions with oncoming trains or electric shocks during evacuation if power is not promptly cut. With an operational alarm system, these risks are significantly reduced by enabling quick actions such as halting train operations and alerting evacuation personnel. In the project report detailed risk index comparisons under these scenarios are provided. The summary table aided the identification of situations where functional communication systems have the greatest influence. The data serves as the basis for subsequent risk assessment and review of safety requirements to mitigate these risks in new constructions and renovations.

Findings

The risk analysis indicates that emergency communication with TTCC is significant for the risk profile, particularly in later stages of an accident, especially in double-track tunnels and tunnels with parallel tubes. In the absence of this communication, the risk of damage in additional accidents increases, especially through electrical accidents involving downed overhead lines and collisions with evacuating trains or trains in adjacent tunnel tubes. Deficiencies in communication also affect warnings to maintenance personnel and increase the risk of another train entering the affected tunnel tube. However, the significance of this is less in single-track tunnel with side space featuring emergency functions compared to other tunnel designs.

RISK ASSESSMENT AND RISK ACCEPTANCE

The risk analysis evaluates the acceptance of one or multiple risk sources within the assessed system according to the CSM RA-regulation. Principles for risk acceptance include the use of code of practices, comparison with similar systems, and an explicit risk estimation. This assessment, subject to review by an independent assessment body (AsBo), is crucial for documenting safety requirements and maintaining an acceptable level of risk.

Code of practices, applied as a principle for risk acceptance for all risks, involve a set of written rules used to control one or multiple risk sources. These rules are widely accepted within the railway sector and include TSIs, national regulations, and EN standards. To be considered code of practice, these rules must be recognized within the railway domain, relevant for managing the risk sources within the assessed system, and available for review by assessing bodies.

If the risk sources are controlled according to such code of practices, the associated risks are considered acceptable, and thus do not require further analysis. Registering the use of code of practices serves as safety requirements for relevant risk sources in the hazard record. The use of code of practices in this context were justified by the existing emergency communication practices during tunnel accidents, the relevance of this practice in controlling the identified risk sources, the absence of

other applicable national or international standards, and the lack of additional requirements from the Swedish Transport Agency regarding communication in railway tunnels.

Table 2. Difference in risk index between functioning and non-functioning alarms to TTCC for various tunnel configurations.

Tunnel specific accidents	**Initial damage**	**Subsequent damage**	**Damage du to additional hazard/accident**						**Damage inflicted on others**					
			Single-track tunnel - safe areas		Double-track tunnel - safe areas		Parallell tubes - fire separated		Single-track tunnel - safe areas		Double-track tunnel - safe areas		Parallell tubes - fire separated	
System design			YES	NO	YES	NO	YES	NO	YES	NO	YES	NO	YES	NO
			A	*B*	*C*	*D*	*E*	*F*	*A*	*B*	*C*	*D*	*E*	*F*
Fire in a train stopping in the tunnel	0	0	0	0	4	4	4	4	2	2	2	2	2	2
Fire in a train on the adjacent track causing trains to stop in the tunnel	0	0	N.A.	N.A.	4	4	N.A.	N.A.	N.A.	N.A.	2	2	N.A.	N.A.
Fire in infrastructure or side space causes trains to stop in the tunnel	0	0	0	0	4	4	4	4	2	2	2	2	2	2
Explosion followed by fire affecting a train stopped in the tunnel or causing a passenger train to stop in the tunnel	0	0	1	1	2	2	2	2	1	1	1	1	1	1
Gas leak affecting a train stopped in the tunnel or causing a passenger train to stop in the tunnel	0	0	1	1	2	2	2	2	1	1	2	2	2	2
Collision	0	0	0	0	4	4	4	4	0	0	0	0	0	0
Collision leading to derailment	0	0	0	0	4	4	4	4	0	0	0	0	0	0
Collision with subsequent fire	0	0	0	0	4	4	4	4	2	2	2	2	2	2
Derailment	0	0	0	0	4	4	4	4	0	0	0	0	0	0
Derailment causing a fire	0	0	0	0	4	4	4	4	2	2	2	2	2	2
Derailment leading to collision	0	0	0	0	4	4	4	4	0	0	0	0	0	0
Spontaneous evacuation	0	0	3	3	6	6	6	6	0	0	0	0	0	0

Medium or high impact of functioning alarm

1-3 low

4-6 medium

7-9 high

Note: The values in each column represent the difference in Risk Index (RI) calculated as RI_non-functioning_alarm – RI_functioning_alarm for each tunnel configuration and stage in the accident sequence. Absolute RI values for functioning and non-functioning alarm systems are presented in the project report.

Code of practices
Tunnels in the rail system of the European Union are critical facilitites that demand hig safety standards. To ensure this safety, the TSI SRT prescribe specifications guiding the design, construction, and assessment of new or modified tunnels. This encompasses a range of measures aimed at minimizing specific risks to on-board staff and passengers within tunnels.

Technical specifications for interoperability are considered as codes of practice within the framework of the Railway Safety Directive (2016/798/EC) and are guiding in assessments according to the CSM RA-regulation. Therefore, these principles were applied and assessed as relevant and compliant with the requirements of the CSM RA-regulation for the current system.

Within the TSI SRT, there are detailed requirements and clarifications regarding emergency communication in tunnels. Specific sections apply to tunnels longer than one kilometer, while shorter tunnels do not explicitly demand emergency communication. Clarifications also encompass the definition of a 'mobile phone' and emphasize the necessity of communication between on-board staff and the TTCC in emergency situations.

It's crucial to note that the overall safety of the tunnel is not solely reliant on passengers' or on-board staff members' ability to make emergency calls. There is, for example, no direct link between requirements for safe areas and those for emergency communication, even concerning general radio coverage.

Furthermore, the requirements for radio coverage for emergency services during crises are not linked to or reliant upon communication between traffic and side areas. The principle that mobile communication via GSM-R reduces the need for fixed connections, such as emergency telephones or radio coverage for general mobile communication, has been consistent since the initial versions of the TSI SRT.

There's a history where emergency telephones have been used in Swedish railway tunnels due to the absence of other communication solutions. When GSM-R was implemented, signal telephones along the track vanished but were retained in the Swedish Transport Administration's tunnels, renamed emergency telephones following guidelines like BVS 545.22200 and later TDOK 2015:0287. This example highlights the evolutionary development of communication systems in these environments.

Findings
According to code of practices, communication via GSM-R constitutes a necessary safety requirement to achieve an acceptable level of safety for the identified risks. A prerequisite is the ability to communicate from a mobile phone or fixed connection both from the tunnel's traffic area and from a safe area. As per code of practices, GSM-R provides sufficient reliability for alarm signaling without additional redundancy. This implies that the residual risk due to the absence of alarm signaling with GSM-R or malfunctioning GSM-R is acceptable.

SAFETY REQUIREMENTS
The risk assessment suggests that the existing emergency telephones in the Swedish Transport Administration’s tunnels can be phased out, but before this occurs, safety measures must be verified to achieve an acceptable risk level in accordance with code of practices. The technical requirements vary depending on the tunnel's system design and length. For tunnels longer than 1 km, specific communication capabilities are required as per practice, with different requirements for different system designs.

System designs A, C, and E must enable radio communication between trains and the TTCC, either via GSM-R, public GSM, or fixed connections in the side spaces. Systems B and D do not require more than GSM-R between trains and the traffic center, as they lack safe areas for emergency communication.

Emergency communication requirements vary for tunnels over 1 km depending on the system, and some options are more complicated to implement than others. Relying solely on public GSM in emergencies may lead to overload, preventing contact with the TTCC in severe events. The recommendation is to use fixed connections in safe areas together with GSM-R in the tunnel to ensure robust communication and adequate safety. However, this alternative requires train companies to provide GSM-R terminals, while relying solely on GSM requires prediction of the expected number of users to avoid overload.

ACTIONS REQUIRED IN DISPOSAL PROJECTS

To ensure emergency communication between traffic and side spaces in the Swedish Transport Administration's railway tunnels, each disposal project should adhere to the following requirements:

1. In tunnels ≤1 km, no additional safety requirements need to be fulfilled after disposal

2. In tunnels >1 km with safe areas, radio communication between the train and TTCC shall be provided in the tunnel, as well as one of the the following in the safe area(s):
    a. communication by GSM-R, or
    b. communication by GSM, or
    c. communication by fixed connection.

In tunnels >1 km (systems A, C, and E), alt. c) is the recommended option, thus providing fixed connections in safe areas. Additionally, the following must be done regardless of the tunnel's length:

- The basis for the Route book (section L) should be updated according to TDOK 2013:0240 and TDOK 2014:0553.

- Train companies on the route must be informed about the change and its consequences.

- Trafikverket's facility registry in BIS should be updated in accordance with TDOK 2016:0407, TMALL 0594, and TMALL 0588.

Technical documentation, such as fire protection information and safety concepts, should be revised or removed for decommissioned facilities according to tunnel personnel safety.

These steps are part of Trafikverket's process for implementing measures on roads and railways and are managed by the responsible project manager. According to TDOK 2018:0193, the project manager leads the project and ensures compliance with the requirements by following the Swedish Transport Administration's documents. This mainly involves managing facility requirements and handing over new or modified infrastructure according to various regulatory documents (such as TDOK 2018:0099 and TDOK 2012:139).

The person responsible for IT and telecommunication infrastructure, especially the emergency telephone system, must include safety requirements in the planning and implementation of each change project. This is part of their responsibility for the technical management, operation, and maintenance of these facility components.

DISCUSSION

Balancing Safety and Technological Advancements

The disposal of emergency telephone systems from railway tunnels marks a significant shift toward modernizing communication infrastructure. However, this transition necessitates a delicate equilibrium between safety imperatives and technological upgrades. The evaluation revealed the critical importance of maintaining robust communication links within tunnels, especially during emergencies, to ensure passenger safety and expedite response times.

Challenges in Implementing Alternative Systems
While advocating for the integration of GSM-R-based systems supplemented by public GSM networks or fixed communication lines, challenges surface in ensuring seamless implementation. Foremost among these challenges is guaranteeing consistent coverage across tunnels, avoiding overloads on public mobile networks, and estimating the potential number of simultaneous users during emergencies.

Transition Strategy for Optimal Safety
The study's recommendations propose a phased compliance roadmap, advocating for a strategic transition plan. This approach aims to minimize potential disruptions while ensuring uninterrupted communication capabilities during emergencies. Implementing such a transition necessitates collaboration among various stakeholders, including railway authorities, technology providers, and regulatory bodies, to ensure a harmonized and systematic adoption process.

Challenges during the practical application of the CSM RA-regulation
The CSM RA-regulation specifies a method for capturing, assessing, controlling and accepting risks arising from changes that can affect adversely the safety on the European Railways, tunnels included. Thus, it has a broad scope and is formulated to be applicable with regard to changes of technical, operational and organisational nature. As such, a large responsibility is put on the risk assessment leader to adapt and adopt the method to fit the scope of the proposed change. In the study presented in this paper these are some of the observations were made by the authors of this paper:

1. The decision or rather interpretation of whether a proposed change has an impact on safety varies between individuals. Although presented with the same information about the proposed change, different experts initially judged the impact on safety differently. Discussion during the work shop eventually led to consensus.

2. Deciding the significance of the change, particularly in the current study, was difficult as one of the six criteria to be judged was failure consequence: credible worst-case scenario in the event of failure of the system under assessment. Given the proposed change, failure of the system under assessment was irrelevant to judge (the system would no longer be there to eventually fail). This was solved by instead judging not the possible failure of the system, but rather the consequence of actually removing the system, taking into account the existence of other safety barriers (communication systems).

3. Initially, there seemed to be a reluctancy among some experts to classify the proposed change to be significant. Discussion during the workshop eventually led to consensus, after having described that such a decision would facilitate both communication with internal and external bodies, and also – to some degree – facilitate, for example, the selection of principle for risk acceptance.

4. The eventual involvement of the AsBo was not friction free. The AsBo was contracted based on an individual call-off from a pre-defined business framework agreement in which they were to be given priority. The initial offer to review and assess the risk assessment was roughly 500 % higher than what they eventually were compensated for, despite pre-meetings and explanations of the scope of the study. In addition, it by far exceeded the actual effort to execute the actual risk evaluation and assessment. From a practitioner point of view, it is difficult not to view a large part of the work to be related to unnecessary documentation.

CONCLUSIONS

The investigation into the removal of emergency telephone systems within railway tunnels has revealed multifaceted insights into the intricate balance between safety, communication infrastructure, and risk management. This comprehensive study aimed to address the implications of decommissioning these systems while proposing viable alternatives in accordance with European Union safety directives.

The risk assessment framework employed in this study was designed to holistically evaluate the safety implications associated with the removal of emergency telephones, emphasizing the diverse parameters inherent in railway tunnel configurations. It became evident through meticulous analysis that the safety requirements vary significantly based on tunnel length, tunnel system design, and communication infrastructure compatibility.

The identified risk factors encompassed potential disruptions in communication between trains and traffic control centers, particularly in tunnels longer than 1 kilometer, highlighting the critical need for reliable communication systems. The scenario-based analysis vividly portrayed the vulnerability of passengers and railway staff during emergency situations, accentuating the significance of effective and resilient communication protocols.

In conclusion, the removal of emergency telephone systems in railway tunnels demands a careful approach considering the multifaceted challenges posed by varying tunnel configurations and safety requirements. The findings highlight the criticality of robust communication infrastructure to mitigate risks, safeguard passenger safety, and enable efficient emergency response protocols. By adhering to the proposed recommendations and compliance roadmap, stakeholders can effectively navigate this transition, ensuring enhanced safety standards and seamless communication within railway tunnel environments.

REFERENCES

Banverket, 2006. Telesystem: Telefoni längs spår (BVS 545.22200).

Commission Regulation (EU) No 402/2013 of 30 April 2013 on the common safety method for risk evaluation and assessment

Commission Regulation (EU) No 1303/2014 of 18 November 2014 concerning the technical specification for interoperability relating to safety in railway tunnels of the rail system of the European Union

Commission Implementing Regulation (EU) No 2015/1136 of 13 July 2015 amending Implementing Regulation (EU) No 402/2013 on the common safety method for risk evaluation and assessment

Commission Implementing Regulation (EU) 2019/773 of 16 May 2019 on the technical specification for interoperability relating to the operation and traffic management subsystem of the rail system within the European Union

Decommissioning of emergency telephone systems in the Swedish Transport Administration's railway tunnels: System definition and assessment of safety impact (TRV 2022/102615)

Directive (EU) 2016/798 of the European Parliament and of the Council of 11 May 2016 on railway safety

Trafikverket, 2015. Telesystem. Telefoni längs spår (TDOK 2015:0287).

Trafikverket, 2020. Metod för riskhantering vid ändringar gällande trafiksäkerhet järnväg (CSM RA; TDOK 2020:0236).

Trafikverket, 2022. Riskbedömning: Skrotning av nödtelefonisystem i Trafikverkets järnvägstunnlar (TRV 2022/102615).

Trafikverket, 2022. Väsentlighetsbedömning – Skrotning av nödtelefon i befintliga tunnlar (TRV 2022/102615).

Trafikverket, 2022. Upprättande av underlag till linjeboken (TDOK 2013:0240).

Trafikverket, 2023. Data och dokumentation till förvaltande system – Järnväg (TDOK 2016:0407).

Trafikverket, 2023. Hantering av anläggningsspecifika krav (TDOK 2018:0099).

Trafikverket, 2023. Linjeboken – underlag till linjeboken, uppdatering och publicering (TDOK 2014:0553).

Trafikverket, 2023. Projektledare Genomföra åtgärder (TDOK 2018:0193).

Trafikverket, 2023. Överlämnande av ny eller förändrad infrastruktur (TDOK 2012:0139).

Safety Enhancement by Introduction of Evacuation Assisting Light for Long Distance Road Tunnel Fires

Yuika Sakamoto[1], Shoichi Kume[1], Yudai Matsunaga[2] & Tomoki Kikumoto[3]
[1]Hanshin Expressway Company Limited, Osaka, Japan
[2]Hanshin Expressway R&D Company Limited, Osaka, Japan
[3]Techno Hanshin Company Limited, Osaka, Japan

ABSTRACT

Hanshin Expressway Co., Ltd. aims to enhance evacuation safety in tunnel fires by introducing new devices and improving the operation of existing equipment. The paper has verified the influence of visibility and walking speed in fire smoke by introduction of evacuation assisting light that considered effective for people to continue evacuation activities even in severer condition. The verification was conducted at an abandoned tunnel filled with pseudo smoke by measuring walking speed of about 40 people and taking feedback on questionnaires. The 3D CFD simulations were also conducted to optimize the airflow velocity for smoke control in a way that mitigates the negative effect of smoke and to make evacuation assisting light more visible. These studies have led to the conclusion that the evacuation assisting light is effective for the people in smoke to continue evacuation activities and the average walking speeds are 1.5 m/s at Cs = 0.5 m^{-1}, 1.2 m/s at Cs = 1.0 m^{-1}, and 1.0 m/s at Cs = 1.5 m^{-1}. Introducing evacuation assisting lights and optimizing existing equipment operations can improve tunnel fire safety, especially where civil construction measures are challenging to implement.

KEYWORD: Tunnel safety, fire evacuation, footlight, assisting light, 3D fire numerical simulation, tunnel renovation

INTRODUCTION

Hanshin Expressway Co., Ltd. (“HEX”) is currently working on improving the existing safety measures for the Shin-kobe Tunnel, one of her long distance tunnels, which reaches the time for refurbishment. As the Shin-Kobe Tunnel was designed to meet the old safety standards, the refurbishment plan is to be built to comply with the present safety guidelines such as the interval of emergency exits and fire emergency ventilation. However the refurbishment which requires civil construction is difficult to implement considering the space limitation and social impact of tunnel traffic closure. It was decided to approach the safety improvement with the study of introduction of new equipment and revision of operation procedures. The study focuses on the *evacuation assisting light* (simply *“assisting light”)* in tunnel fires where ensuring visibility becomes particularly important. Experiments were carried out on the feasibility of the assisting light to verify the effectiveness and decide the installation condition which becomes basic data for design of the assisting light. The installation guidelines for the similar equipment are published [1], but validation for effectiveness is not completed. Examples verifying walking speed in the smoke are published [2, 3]. None of them, however, have dealt with the assisting light. The experiment was conducted at an abandoned tunnel filled with pseudo smoke to measure the variation of walking speed of subjects against the smoke concentration, and collect their feedback on questionnaires. The results of the experiment were taken into consideration in 3D simulation studies on the south-bound tube of the Shin-Kobe Tunnel, and the interval of the assiting light was decided.

OUTLINE OF SHIN-KOBE TUNNEL AND ISSUE OF FIRE SAFETY

The Shin-kobe Tunnel consists of two unidirectional traffic tubes, the north-bound line of which was open to public in 1976 (operated in two-directional tunnel upon opening) and the south-bound line of which was open in 1988. In 2006 the tunnel was extended to the south, becoming the present configuration as shown in Figure 1. The tunnel was originally owned and operated by the Kobe City Road Public Corporation and the tunnel equipment except the tunnel structure were modified to become compliant with the HEX's standards when the ownership was transferred to HEX in 2014. The south-bound line which this paper is concerned with is made of the NATM and the cut-and-cover method. The tunnel connects two rampway tubes, making a complex structure. The total length is about 8 km.

The tunnel adopts a longitudinal ventilation which combines a centralized exhaust and jet-fans. The entire polluted air is to be exhausted outiside the tunnel at the ventilation station to prevent degradation of air quality arround tunnel exit portal. The cross-passage and emergency exits are located in 10 positions in the south-bound tube, where the intervals are 330 m in the shortest and 1,146 m in the longest. The HEX's standard interval of emergency exits in tunnel is 300 m in the condition that locates in urban area with rampway tube. Therefore additional evacuation tubes and emergency exits were needed to meet the stanard. However civil construction of these was almost impossible to implement when considering the difficulty of construction, space limitation and social impact of tunnel closure. Measures must be adopted to secure the safety for tunnel fires with the present tunnel configuration. Minimizing the effect of fire smoke in a way that allows people to walk to the emergency exits under an improved visibility is considered a feasible solution.

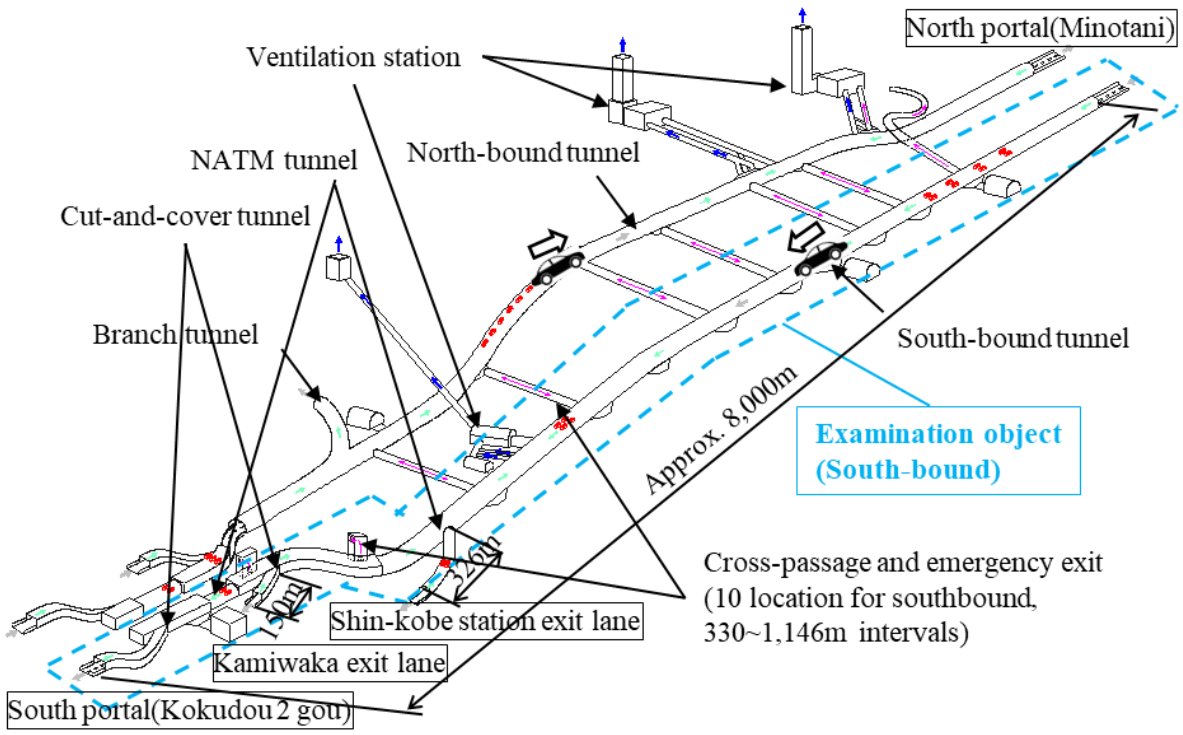

Figure 1 Schmatic views of Shin-kobe tunnel.

NUMERICAL SIMULATION OF SMOKE CONCENTRATION IN CASE OF TUNNEL FIRE

As the first step, 3D fire simulation was studied to predict smoke behavior to confirm the safety level of the present south-bound tube of the Shin-kobe Tunnel. Simulations were studied with the simulation software "Fireles" [4] which has been used widely as a standard tool in Japan.

Analysis condition

An outline of the longitudinal slope of the south-bound line of the Shin-kobe Tunnel is illustrated in Figure 2. It shows the NATM section which makes up of the most of the main tube (Case1), and two

ramp tunnels with smaller cross section area (Case2 & Case3). Simulations were conducted for Case1, Case2 and Case3. Table 1 lists the cross sectional parameters used in the simulatons. The model fire size was set in 30 MW as in many of the fire evacuation simulations in Japan. This paper adopted the Heat Release Rate ("HRR") curve as shown in Figure 3, taking from that of the EUREKA bus fire reported as 30 MW fire[5]. As the longitudinal airflow velocity affects a lot to the smoke behavior, 1D airflow velocity simulation for the entire tunnel was conducted and the results were used as the boundary conditions of the 3D fire simulations to reproduce the dynamic airflow in the tunnel. The parameters of the grid partitioning conditions and thermophysical property in the 3D fire simulation study are given in Table 2.

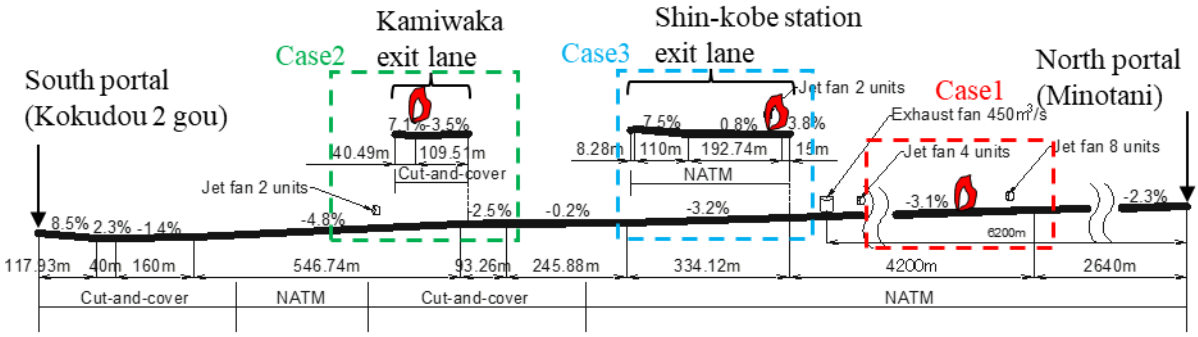

Figure 2 Longitudinal slope of Shin-kobe tunnel(South-bound).

Table 1 Cross-section of each simulation case.

Typical cross-section of NATM	Cross-section of Kamiwaka exit lane	Cross-section of Shin-kobe exit lane (General section)	Cross-section of Shin-kobe exit lane (Raising section)
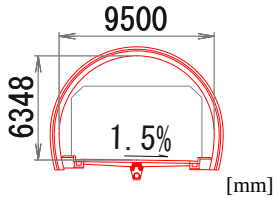 50.1m²(2 lane)	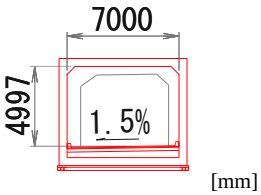 34.7m²(1 lane)	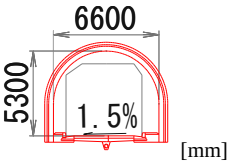 30.0m²(1 lane)	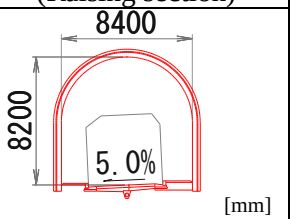 60.7m²(1 lane)
Case1	Case2	Case3	

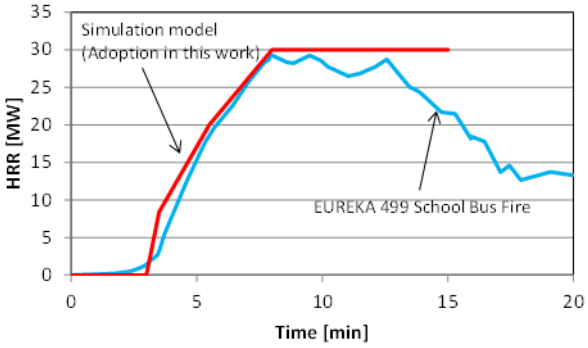

Figure 3 Heat Release Rate curve.

Table 2 Grid partitioning condition and thermophysical property on CFD.

Grid partitioning condition		Thermophysical property of wall(Concrete)	
x direction	0.4 m	Heat transfer rate	1.1(W/mK)
y direction	Approx. 0.3 m	Specific heat	879(J/kgK)
z direction	Approx. 0.27 m	Density	2100(kg/m^3)

Safety index of tunnel fire in HEX

HEX has a policy to achieve safety of the tunnel users by making their evacuation possible to a safety facility such as emergency exits. Thus securing visibility becomes important so that users can continue to evacuate in the main tube. The tunnel safety is evaluated primarily by the smoke concentration. Optical smoke concentration Cs (or extinction coefficient) was used for evaluation in this study. For example, there are some literatures [6, 7] which judge the people unable to continue evacuation when they face the smoke concentration of Cs = 0.4 m^{-1}. The height of the smoke is usually set at 1.5 m high, which is evacuee eye-level height from the road surface. The walking speed of 1.0 m/s is widely used after considering aged people and children. In addition to these, it is assumed that it takes about four (4) minutes from recognizing fire and beginning evacuation (decision to evacuate by hearing loud speaker announcement: about 2 minutes to leave vehicles, about 2 minutes to leave a large bus). Having considered the above, HEX adopted their evaluation index of self evacuation stage as ahown in Table 3.

Table 3 Evaluation index of evacuation.

Smoke concentration (Extinction coefficient)	Cs=0.4m^{-1}: Limit smoke density at which evacuation actions can be taken.
Evaluation height	Within 1.5m height from road surface
Walking speed	1.0m/s: Consideration of lower walking speed than average like a eldery and children.
Start time and location of evacuation action	4 min after ignition, start from near the fire source.

Simulation result of main tube(Case1)

The south-bound tube of the Shin-kobe Tunnel experiences chronic traffic congestion inside the tunnel because there is a traffic light near the exit portal. This leads to a situation where users exist in both sides of the fire location, although it is unidirectional traffic. If ventilation works to exhaust smoke in the traffic direction, evacuees leaving fire will face a weak visibility due to smoke expansion. Therefore, low-speed airflow velocity control is adopted not to disturb the smoke stratification. The basic in this control is to keep the velocity at 0 m/s.

Figure 4 illustrates the airflow velocity change and Figure 5 shows a distribution of smoke density over the longitudinal direction at 240 s and 360 s after the fire occurrence. The airflow velocity is controlled to 0 m/s at 231 sec after the ignition. However, the smoke does not propagate symmetrically to each direction. Most of the smoke moves toward in the direction of the high gradient due to the buoyancy and smoke falling down near the road surface is observed. In this situation, evacuees will be exposed to the smoke concentration of Cs = 0.4 m^{-1} before they reach the emergency exit and the sufficient visibility required for safe evacuation is not secured.

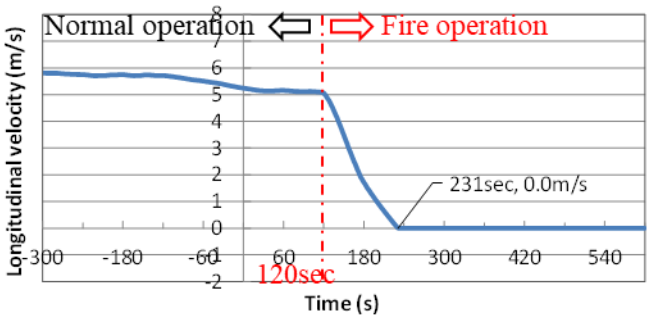

Figure 4 Velocity change in case of fire(Case1: Target velocity 0.0m/s).

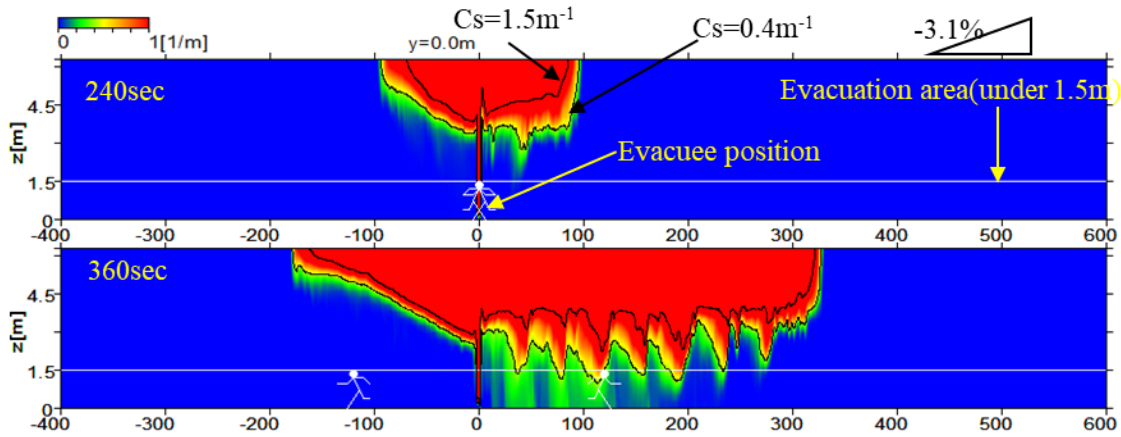

Figure 5 *Smoke distribution in NATM section(Case1: Target velocity 0.0m/s).*

The primary reason for the high concentration smoke falling down in Figure 5 is considered due to the unbalanced smoke propagation, namely most in the direction of upper side of the fire point. To mitigate the unbalanced smoke propagation, the target airflow velocity is changed to 0.6 m/s. Figure 6 shows 1D airflow velocity simulation and Figure 7 illustrates 3D fire simulation. The airflow velocity in the tunnel is controlled to the target 0.6 m/s at 212 s. In this simulations, the smoke propagation toward the upper side direction is reduced and the negative effect of smoke on evacuees can be mitigated. With that results, the target airflow velocity in the NATM section of the main tube (Case1) was decided to change to 0.6 m/s. However there are still remaining areas of the smoke concentration exceeding 0.4 m^{-1}. And accurate ventilation control will be required in actual operations if the same effect of smoke suppression will obtain. Therefore, additional measures are required to ensure a sufficient visibility for evacuation.

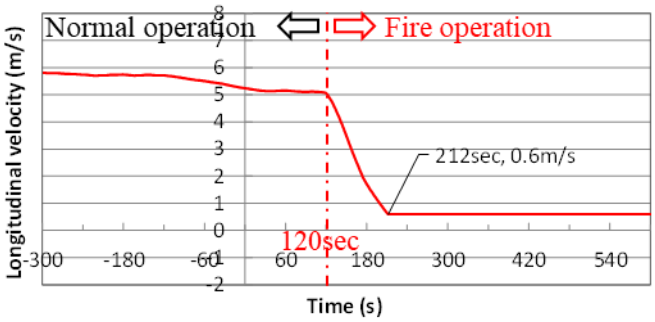

Figure 6 *Velocity change in case of fire(Case1: Target velocity 0.6m/s).*

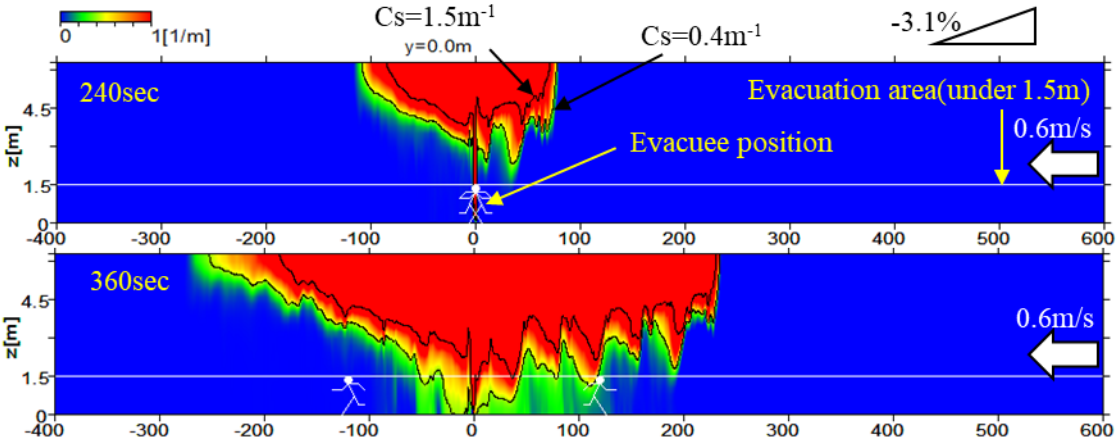

Figure 7 *Smoke distribution in NATM section(Case1: Target velocity 0.6m/s).*

Simulation result of rampway tunnel(Case2 & Case3)

The rampway tunnels have one lane for traffic with the small cross secton. As they have steeper slope than main tube, securing visibility is considered difficult when people evacuate. With these in mind, two target airflow velocities were simulated: 0 m/s and 0.5 m/s for the Kamiwaka Rampway (Case2), and 0 m/s and -0.6m/s for the Shin-kobe Station Rampway (Case3). Figure 8 and Figure 10 show 1D airflow simulation results, while Figure 9 and Figure 11 illustrate 3D fire simulation results. In ramp fires, smoke tends to diffuse in the direction of cross section due to the low ceiling and smoke movement distracted by the stationary large vehicles. In the Kamiwaka Rampway fire, the target airflow velocity of 0.5 m/s delayed smoke propagation more than that of 0 m/s, mitigating the smoke filling in the direction of cross section. Similar effect of the target airflow velocity control at -0.6 m/s shows a better effect in ensuring the better visibility than that of 0 m/s in the Shin-kobe Station Rampway. Adjustment of the target airflow velocity improved the visibility to some extent but it still left areas where Cs exceeded 0.4 m^{-1}. Adjustment of target airflow velocity alone was not enough to secure the visibility required for safe evacuation.

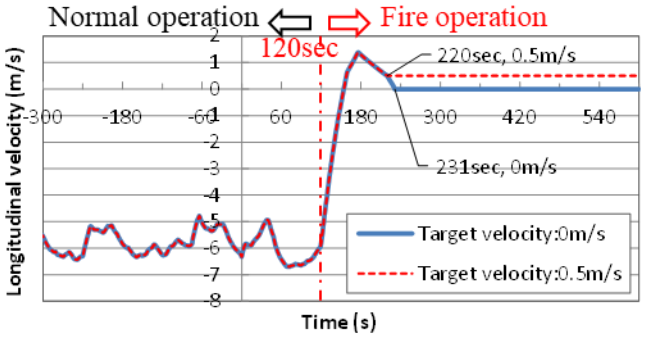

Figure 8 *Velocity change in case of fire(Case2: Target velocity 0.0m/s & 0.5m/s).*

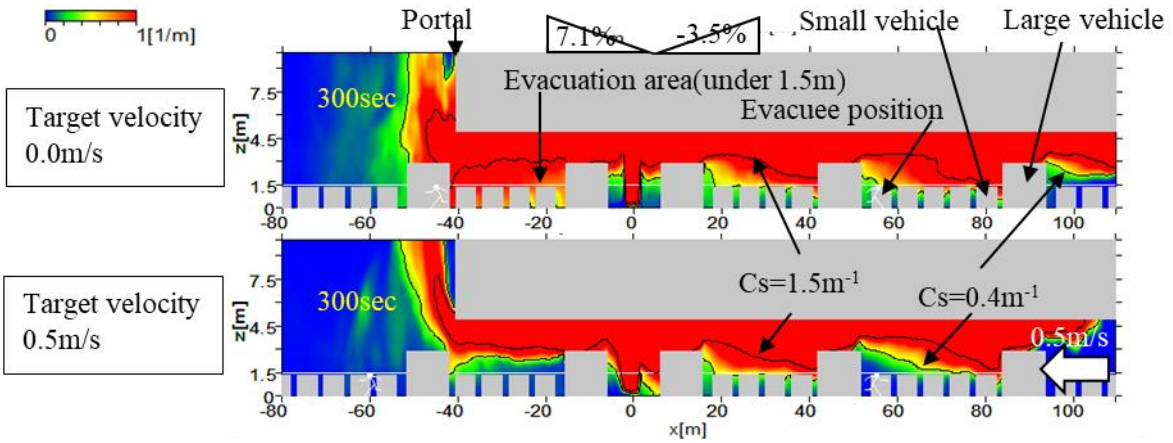

Figure 9 *Smoke distribution in ramp tunnel(Case2: Target velocity 0.0m/s & 0.5m/s).*

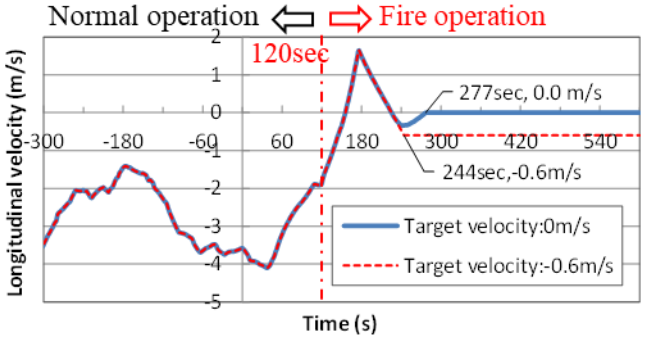

Figure 10 *Velocity change in case of fire(Case3: Target velocity 0.0m/s & -0.6m/s).*

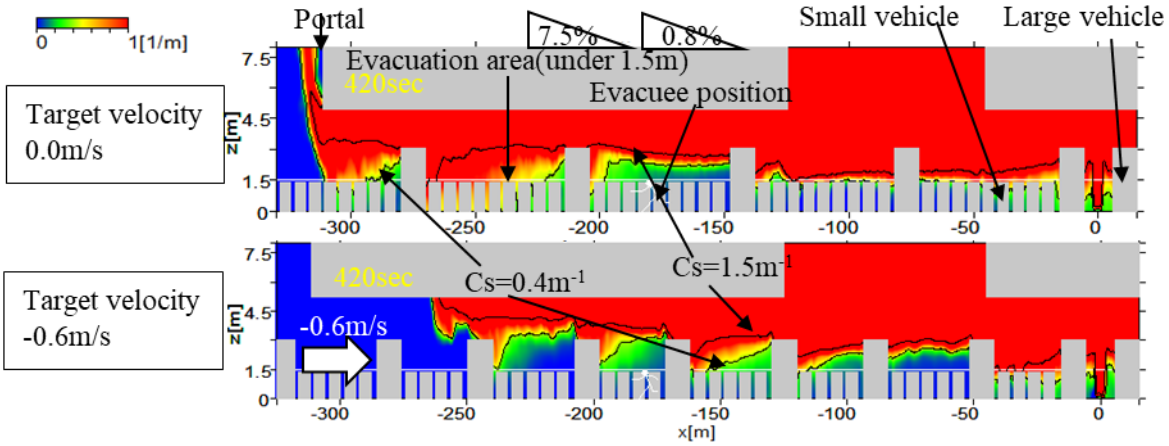

Figure 11 *Smoke distribution in ramp tunnel(Case3: Target velocity 0.0m/s & -0.6m/s).*

FIELD TEST ON EVACUATION ASSISTING LIGHT

The simulaton studies in the previous chapter clarified that the adjustment of ventilation operations alone was insufficient in ensuring the visibility required for the safe evacuation at the time of tunnel fires. Then installation of light source in the tunnel area of evacuation was verified to see if it was effective for users to continue evacuation. The system with such light source is called “evacuation assisting light” (“assisting light” in short) in this paper.

Examination of effectiveness

The walking experiment by subjects were conducted for the purpose of investigation on the effectiveness of the assisting light in regard to the visibility and continuation of evacuation actions in the abandoned tunnel filled with pseudo smoke. Tests were carried out to clarify the influence of lighting pattern, color of the light source and light interval on the walking speed and confidence of evacuation activities in the smoke. As the assisting light is demanded for the effectiveness of continued evacuation activities under Cs >0.4 m^{-1}, the experiments were performed with a focus on the smoke concentration of Cs > 0.4 m^{-1}. Figure 12 shows the outline of the abandoned tunnel where the experiments were carried out. The tunnel was 488 m in length and the experiments were conducted within the area covering 150 m around the center of the tunnel. Both portals were closed by the sheet completely to prevent outside air from entering. The tunnel light is usually installed at the crown part of the tunnel cross section, but the experiments went on with the tunnel light shut down to emulate the situation that the tunnel lights did not help for visibility because they were shaded by smoke layers in actual tunel fires.

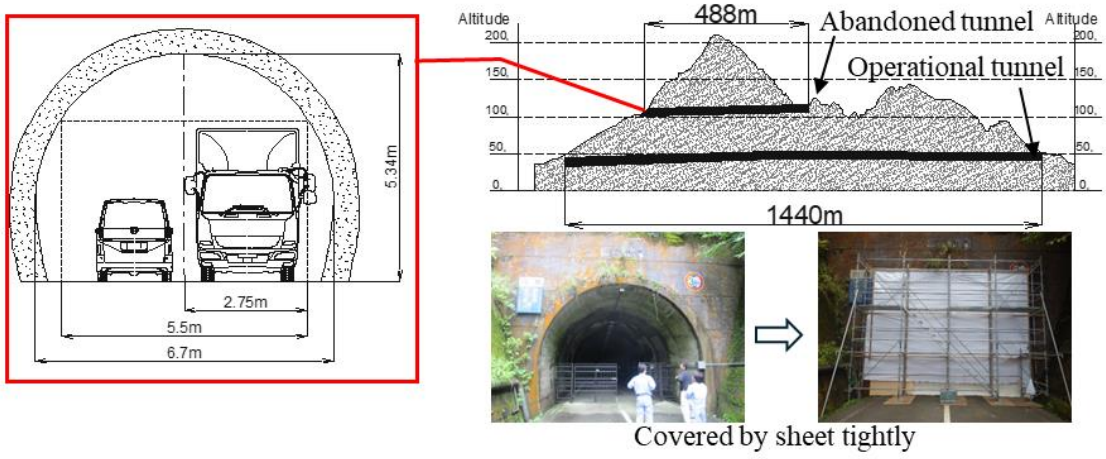

Figure 12 *Outline of test site(Abandoned tunnel).*

The areas of experiment and the location of the assisting light are provided in Figure 13. The assisting light was installed on the wall of one side, and obstructions mimicking the passenger vehicles were placed as shown in Figure 13. The area of experiment was divided into four Area1, Area2, Area3 and Area4 by considering the relative position of the assisting light and obstructions. Figure 14 gives a system configuration of the assisting light used for verification. LED light source in white and green are installed at 0.8 m high from the road surface and with an interval of 1.5 m in staggered arrangement. The specifications of LED light source are given in Table 4.

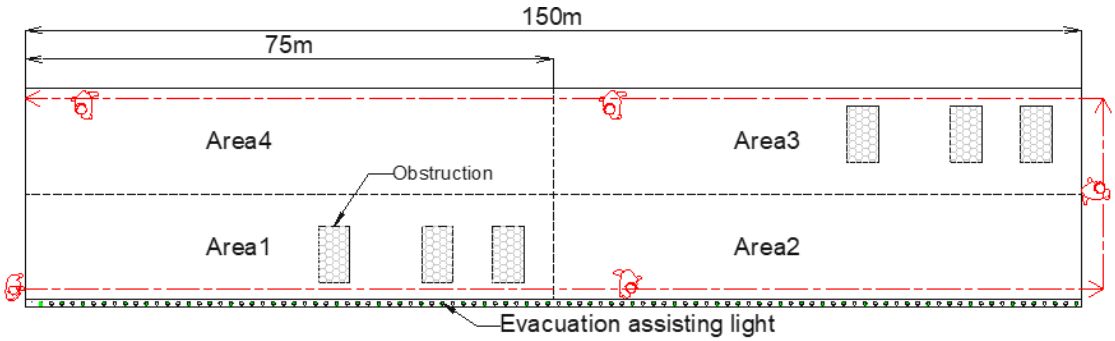

Figure 13 Overview of walking area and location of evacuation assisting light.

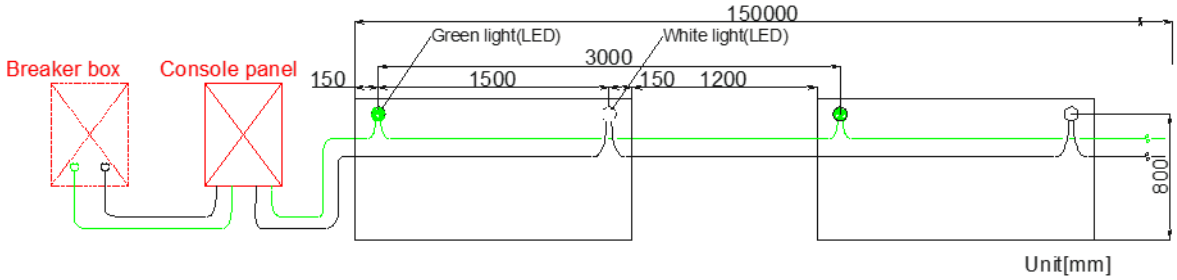

Figure 14 System configulation of evacuation assiisting light.

Table 4 Specifications of light source.

Specification	Optical property	
	Correlated color temperature	5,000K（4,800K～5,400K）
	Total luminous flux	Typ：590lm Min：425lm
	Average color renderringindex （Ra）	85
	Central luminosity	Over 165cd
	Beam angle（2θ1/2）	110°
Dimensioal drawing	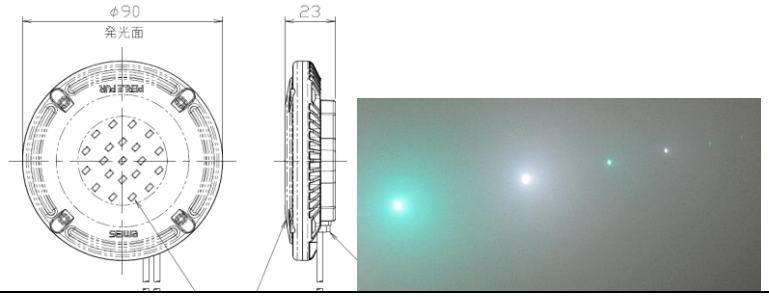	

Three smoke concentrations were studied: Cs = 0.5 m^{-1}, 1.0 m^{-1} and 1.5 m^{-1}. The uniform smoke density was maintained by operating six (6) units of pseudo smoke generators (white) and stirring fans arranged in equal distance, and monitoring the measurement of the optical densitometer.
Table 5 lists the subjects in the experiment. Most of the subjects were male and covered wide range of age from 20's to 60's.

Table 5 Breakdown list of participant.

Smoke concentration	Cs＝0.5m^{-1}		Cs＝1.0m^{-1}		Cs＝1.5m^{-1}	
	Man	Woman	Man	Woman	Man	Woman
20s	11	0	16	0	12	1
30s	3	0	3	0	9	0
40s	14	1	12	1	8	0
50s	4	1	5	1	5	0
60s	4	0	4	0	7	0
Unknown	0	0	1	0	0	0
All	36	2	41	2	41	1
	38		43		42	

Lighting pattern of the assisting light is shown in Table 6. The white light source was Constant lighting and the green light was varied in three (3) patterns: Off, Blinking, and Consant lighting.

Table 6 Lighting pattern.

Pattern name	Lighting image	Lighting pattern
P1	White: On Green: Off	P1=White: Constant lighting Green: Off
P2	White: On Green: Blinking	P2=White: Constant lighting Green: Blinking
P3	White: On Green: On	P3=White: Constant lighting Green: Constant lighting

Walking speed of each age group to the lighting pattern is shown in Figure 15 for three (3) concentrations of Cs . Slowing down of the walking speed to thicker smoke is observed, and the average speed of all ages and lighting patterns under Cs = 0.5 m^{-1} was about 1.5 m/s and it became 1.1 m/s under Cs = 1.5 m^{-1}. Large difference in walking speed of each age group was not observed to different lighting patterns, and this led to an observation that the lighting pattern did not influence so much on the walking speed within this experiment condition. Figure 16 illustrates the walking speed in each Area to different smoke concentrations. When Cs equals to 0.5 m^{-1}, any large difference in walking speed was not observed. The reason for this is considered that subjects could recognize the obstruction and the assisting light sufficiently from the opposite side of wall while they were walking. Under Cs = 1.0 m^{-1} and Cs = 1.5 m^{-1}, slowing down of the walking speed in Area3 and Area4 could be observed compared with Area1 and Area2, but the walking speed of faster than 1.0 m/s was achieved. It is considered that the assisting light helped subjects to keep walking and achieved the original effect. Furthermore the walking speed difference between Area1 and Area2 or Area3 and Area4 was marginally small. The effect of sight obstruction by passenger vehicles was limited and it was confirmed that the assisting light could be seen from the opposite side of wall.

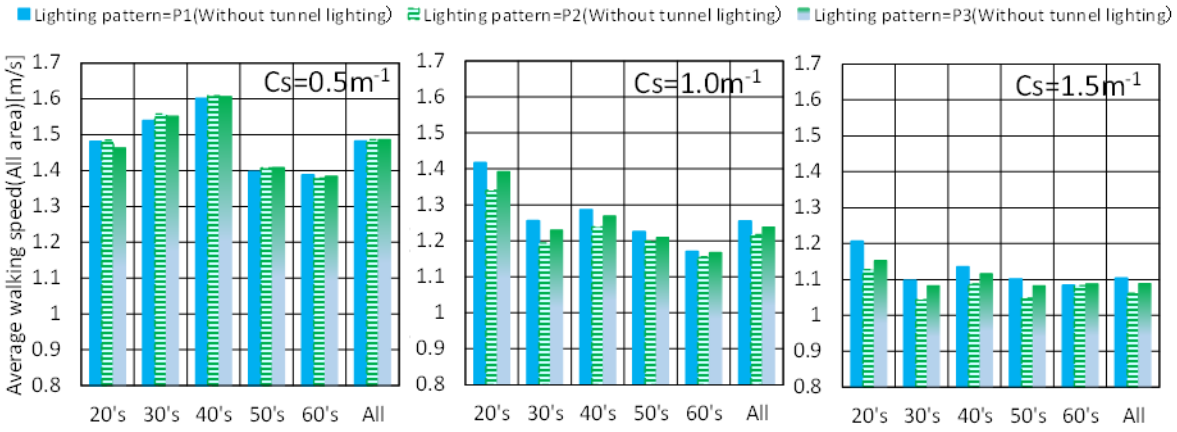

Figure 15 Walking speed in smoke with evacuation assiisting light(Influence of lighting pattern).

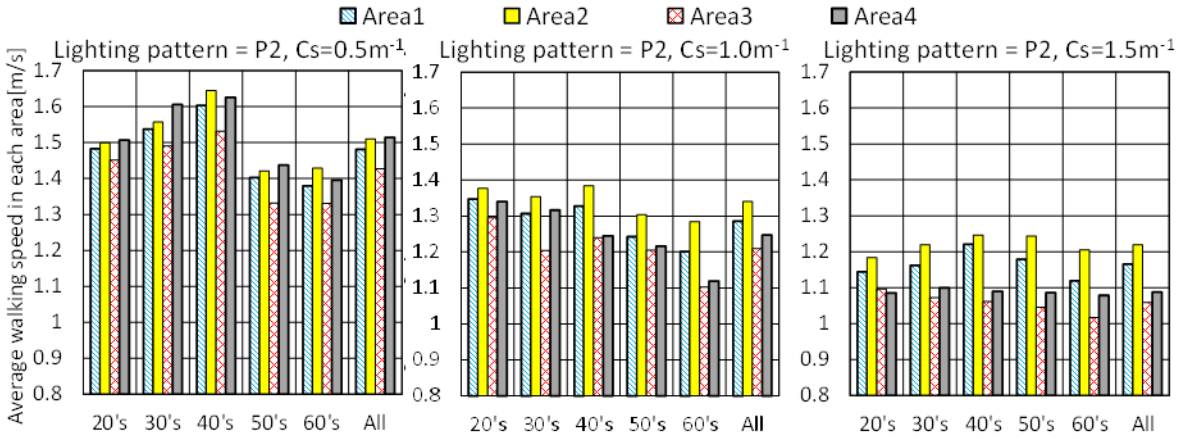

Figure 16 Walking speed in smoke with evacuation assiisting light(Influence of walking area).

The subjects' feedback to the questionnaires on the height of the light are summarized in Figure 17. The feedback that lower position is better was answered by more subjects in Area1 and Area2 who walked same side of the wall with the asisiting light than those in Area3 and Area4 who walked on the other side of the wall without the light. This is considered as the lights were installed horizontally on the wall and thus the light did not reach the road surface nearby. This led to an insight that the visibility near the foot is important to evacuation in the smoke, and the assisting light requires lighting effects.

The subjects' feedback to the questionnaires on the interval of the light are summarized in Figure 18. Lighting pattern P2 and P3 with the intervals of 1.5 m received a positive response from the majority of subjects even in Area3 and Area4 under Cs = 1.5 m^{-1}. Lighting pattern P1 with the interval of 3.0 m received a positive response from the majority until Cs = 1.0 m^{-1}, but the majority responded to P1 as shorter interval was better under Cs = 1.5 m^{-1}. However the walking speed was faster than 1.0 m/s and subjects could continue evacuation although they felt some difficulty to walk.

Those test results led to a finding that the assisting light has a positive impact on continuing evacuation activities under the smoke of Cs > 0.4 m^{-1}. Moreover, subjects feedback to the questionnaires on effectiveness of the assisting light and lighting pattern shown in Figure 19 indicated ninety (90) percent of the subjects responded as the light was effective or rather effective. With that result, the assiting light has proven effective to evacuation in the smoke. Majority responded that the lighting pattern P2 is better than the others. It has been verified that the combination of constant lighting and blinking was effective to evacuation activities.

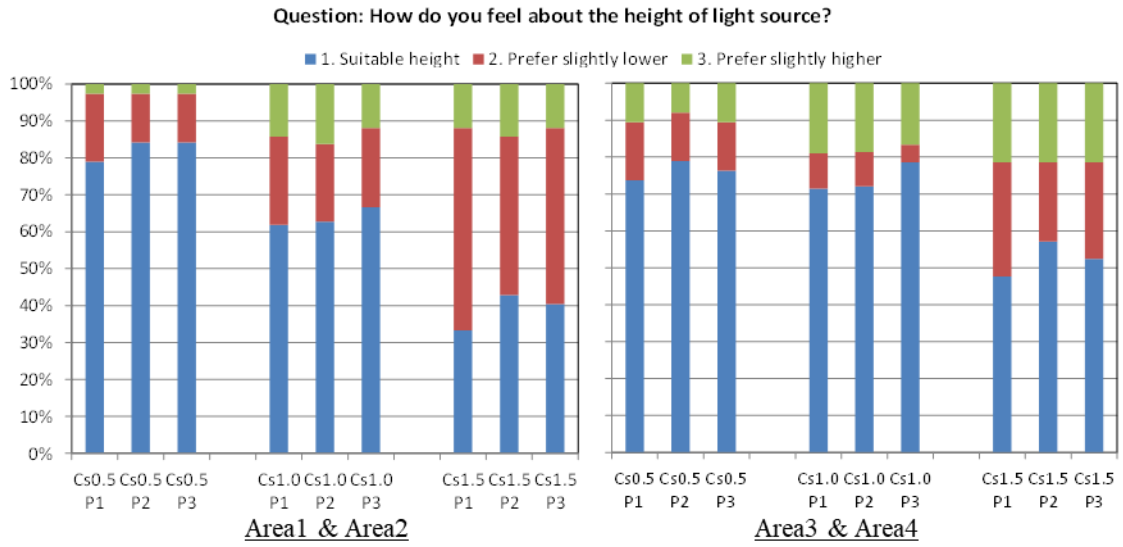

Figure 17 Questionnaire on the height of light source.

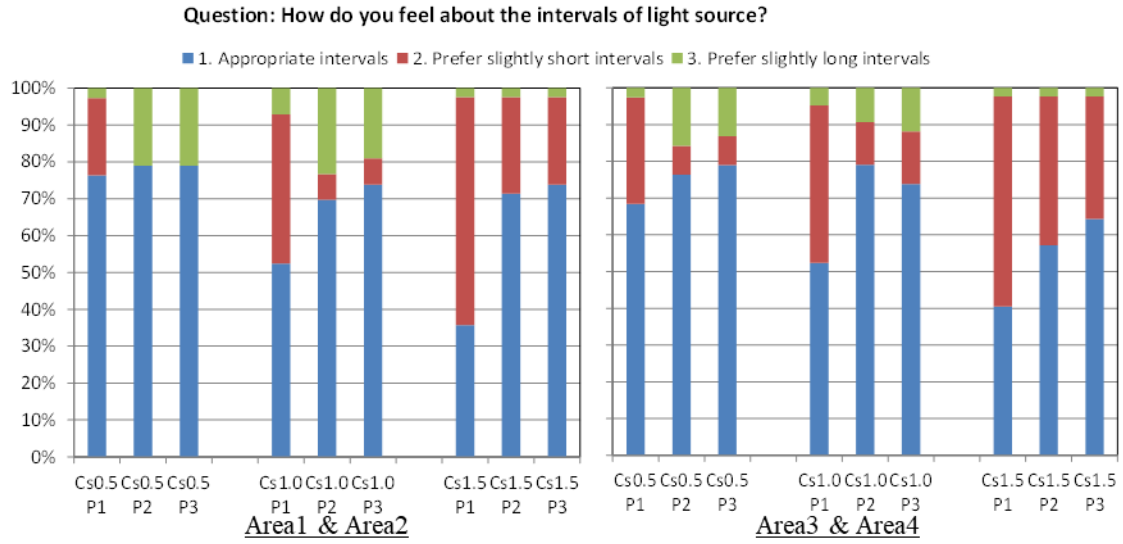

Figure 18 Questionnaire on the intervals of light source.

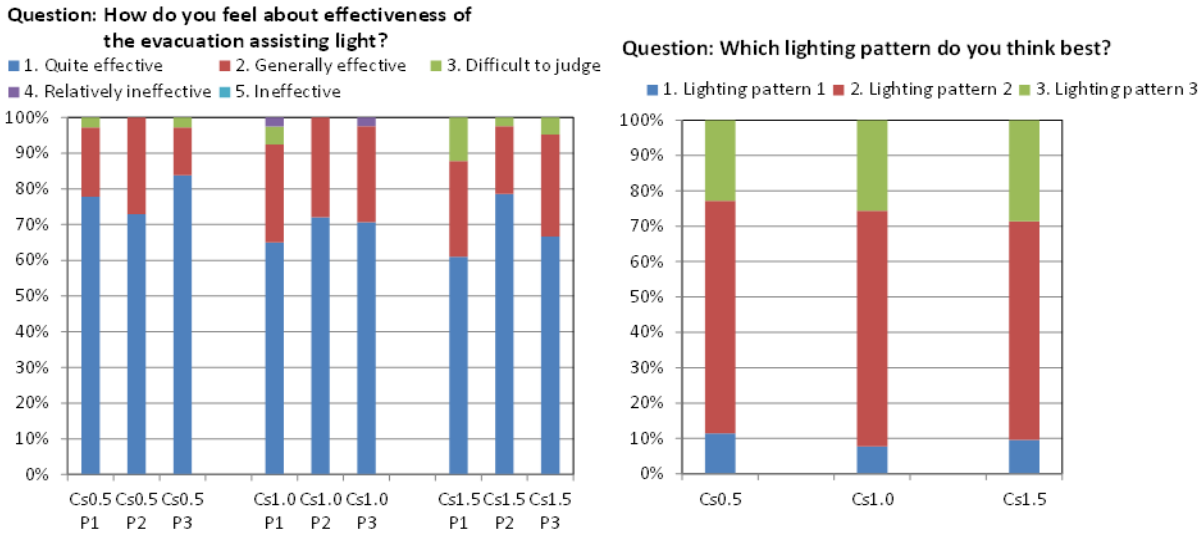

Figure 19 Questionnaire on the effectiveness and lighting pattern.

Decision of specification on evacuation assisting light

The field test proved the effectiveness and visibility of the assisting light, but did not verify the viewable distance of the light source. The white pseudo smoke was used in the tests from the safety consideration. However, the black smoke in the real tunnel fires needs to be verified. The viewale distance test was conducted at a large experimental facility where black smoke was generated from gasoline pool fire. The verification test was carried out by the limited members. The viewable distance was confirmed by observation as 11 m under Cs = 0.8 m^{-1} and 4 m under Cs = 2.4 m^{-1}.

Figure 20 Visibility of evacuation assisting light in black smoke.

Numerical fire simulation indicates that the assisting light is presumed to use in the smoke range of Cs = 1.5 m^{-1}. If the interval of light fixture is 4 m, the assisting light is considered viewable enough. Having taken into account the field test result that prefers the lighting effects near the foot, and the combination of constant lighting and blinking, it was decided that the light fixture of the assisting light was installed in minimum 4 m interval with the white and green light source directed toward the road surface as shown in Figure 21. The height of the center of green light is 1.5m above the road surface.

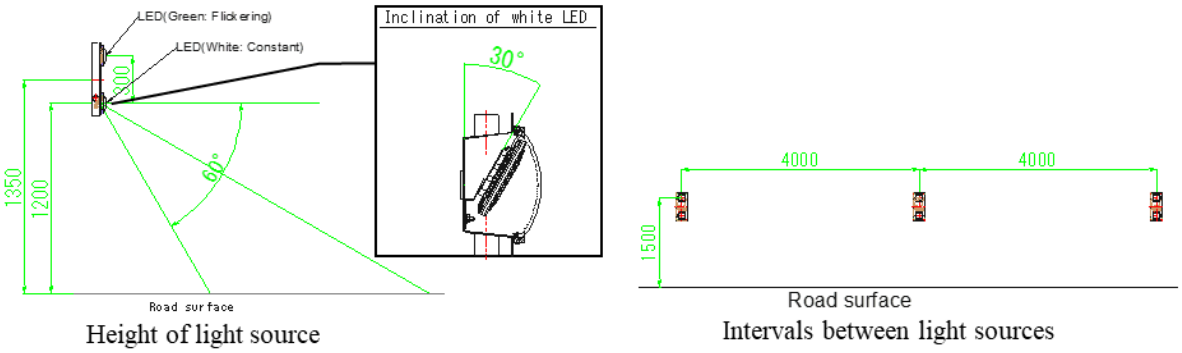

Figure 21 Specification of evacuation assisting light.

Additional tests

Additional walking test took place using the assisting light installed as specified in the previous chapter. An exhaust duct of the tunnel under construction was used for evacuation path. Figure 22 illustrates the outline of the test area. The assisting light was installed 100 m long and walking speed was measured. The walking path includes a crank-shaped jump, which makes the light partially invisible. The walking speed was measured for ten (10) subjects under the smoke concentration of Cs = 0.5, 1.0, 1.5 and 2.0 m^{-1} modelled by white pseudo smoke, and the light interval of 4 m and 8 m. To avoid an experience, each subject participated only one case. In these tests, 22% were women, and the age range was from their 20s to 50s. No significant difference in walking speed was observed based on gender within this experimental condition.

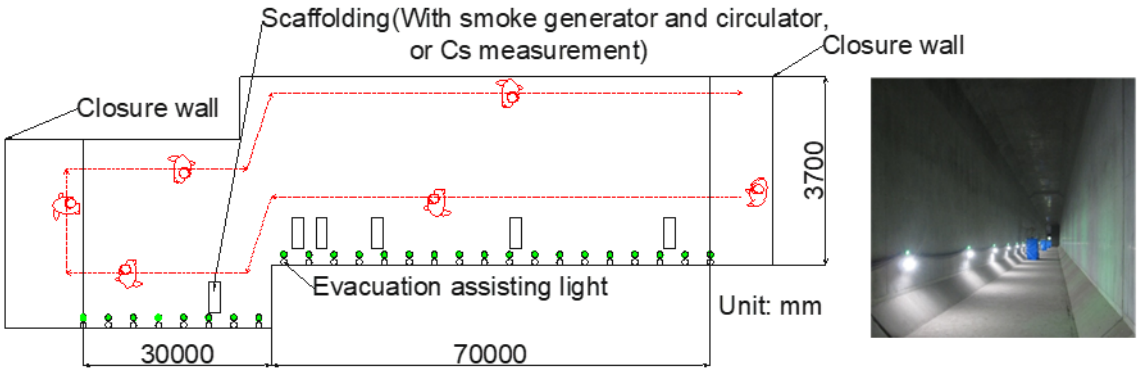

Figure 22 Overview of walking area in exhaust duct.

The results of the walking speed of each subject was summarized to the smoke density as shown in Figure 23. The walking speed in Cs=0.5m^{-1} had no distinctive difference between the two intervals of the light. The interval of 8 m worked effectively to continue evacuation because of the average walking speed of 1.2m/s. The interval of 8 m slowed down the walking speed to 1.0 m/s for Cs = 1.0 m^{-1}, 0.8 m/s for Cs = 1.5 m^{-1} and 0.6 m/s for Cs = 2.0 m^{-1}. Based on the evaluation index for walking speed of 1.0m/s shown in table 3, the interval of 8 m is considered applicable for Cs = 1.0 m^{-1} and lower. The interval of 4 m achieved the average walking speed of 1.2 m/s up to Cs = 1.0 m^{-1}. It also slowed down but very slightly the speed to 0.9 m/s for Cs =1.5 m^{-1}, and 1.0 m/s for Cs = 2.0 m^{-1}, confirming the assisting light effective enough to continue evacuation.

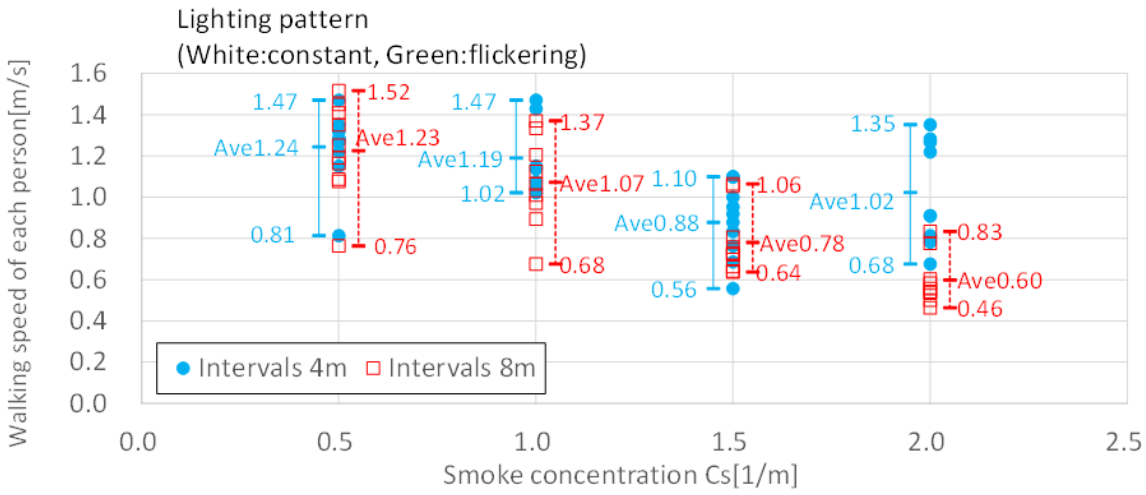

Figure 23 Walking speed of each person on additional tests.

INSTALLATION TO CURRENTLY OPERATIONAL TUNNEL

Evaluation on introduction of evacuation assisting light

The conventional safety evaluation at the tunnel fires made a judgment that continuing evacuation is impsossible when people are exposed to the smoke concentration of Cs = 0.4 m^{-1}. The experiment above has clarified that introduction of the assisting light allows people to continue evacuation in the smoke beyond Cs = 0.4 m^{-1}. The possibillity of continuing evacuation was evaluated by using the 3D CFD simulations shown in the previous chapter when the assisting light is introduced into the Shin-kobe tunnel. The walking speed under the assisting light was defined as Table 7 taking the minimum speed given in Figure 23 for each smoke concentratin range. Moreover the experiment inidctaed that continuing evacuation was possible even in Cs > 1.5 m^{-1}, but the assisting light was treated as an effective equipment only for the smoke concentration range Cs < 1.5 m^{-1} to avoid over judgment at the planning stage.

Table 7 Evaluation index of walking speed in smoke.

Smoke concentration	Walking speed	Requirement of installation intervals
Cs ≦ 0.4m^{-1}	1.0m/s(Conventional index)	Unnecessuary
0.4m^{-1} < Cs ≦ 1.0m^{-1}	0.8m/s	8m
1.0m^{-1} < Cs ≦ 1.5m^{-1}	0.6m/s	4m
1.5m^{-1} < Cs	Impossible to evacuate	-

The evaluation results for the NATM section of the main tube are shown in Figure 24. All parameters except the walking speed were same in Table 3. The longest evacuation distance was about 120 m as Cs = 0.4 m^{-1} bounds evacuation when evacuation assisting light was not installed. In case the assisting light was installed, people could escape the smoke after 9 minutes, and could escape always in front of the tip of smoke to arrive in the safety zone by the suitable fire ventilation velocity restricts the expansion of the smoke layer. The maximum smoke concentration to which people were exposed was Cs < 0.9 m^{-1}, and the interval of 8 m will be sufficient for the NATM section of the main tube.
The evaluatin results for Kamiwaka Rampway and Shin-kobe Rampway are showin in Figure 25 and Figure 26 respectively. As the rampway tube has smaller cross section area, smoke tends to concentrate thicker than the main tube. The Kamiwaka Rampway experienced a region which exceeds Cs = 1.5 m^{-1} for an instant, but showed Cs < 1.5 m^{-1} all the time, while the Shin-kobe Station Rampway did it too. Therefore the interval of 4 m for the assisting light will make possible continuing evacuation.
The studies above have come to a conclusion about the refurbishment policy as shown in Table 8 to improve the fire safety in the south-bound tube of the Shin-kobe Tunnel. The cut-and-cover section of the main tube was not studied for numerical simulation. As it has smaller cross section area than the NATM section, the interval of assisting light was set to 4 m. As shown in the photo of Table 8, the assisting light is already installed in this section. The installation in other sections is underway now.

Table 8 Evaluation index of walking speed in smoke.

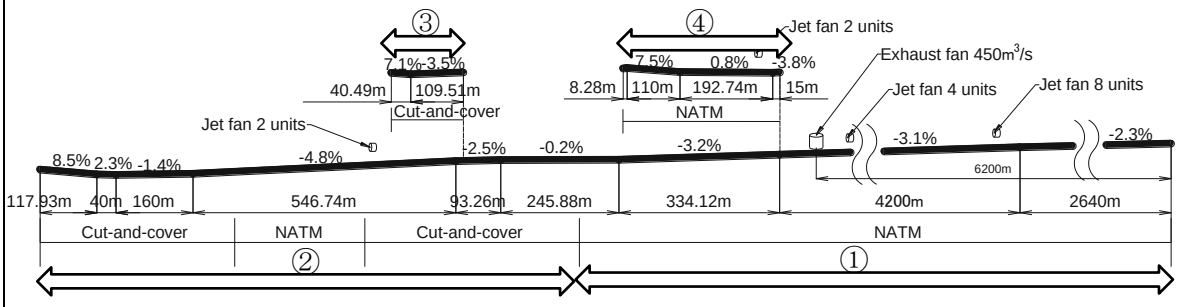

	①Main tunnel (NATM)	②Main tunnel (Cut-and-cover)	③Ramp tunnel (Kamiwaka exit)	④Ramp tunnel (Shin-kobe station exit)
Installation intervals evacuation assisting light	8m	4m	4m	4m

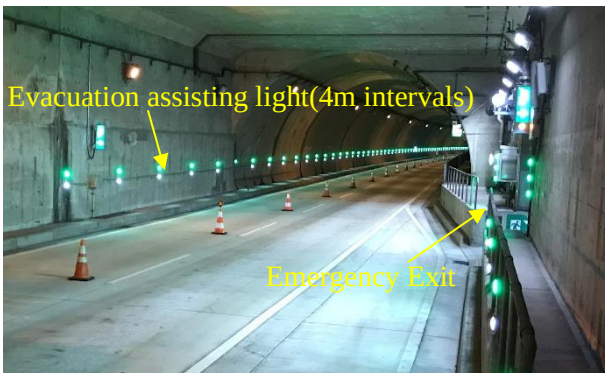

Installation case of cut-and cover area in main tunnel

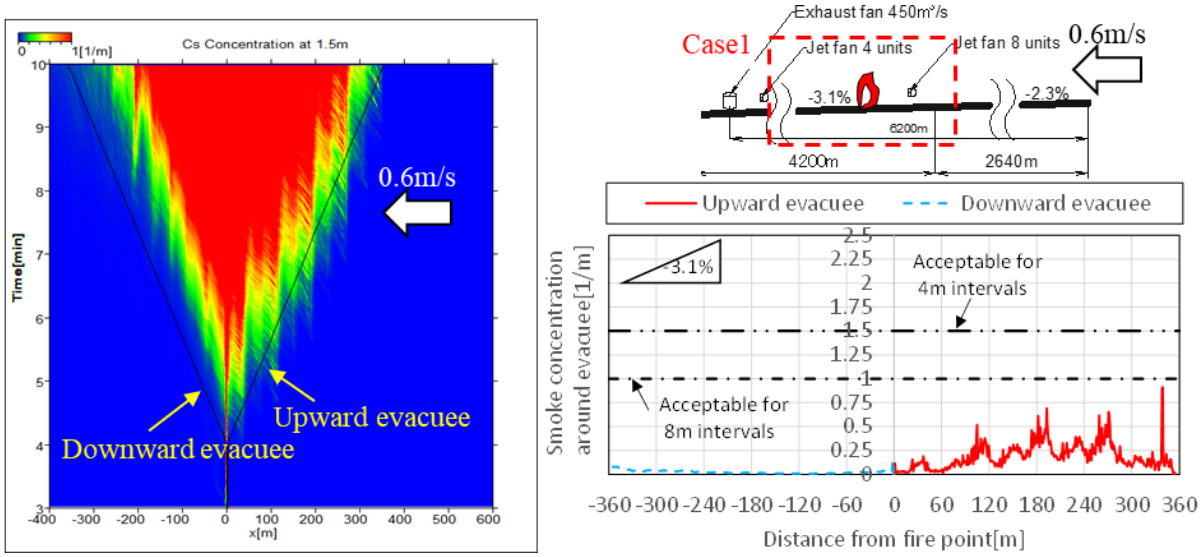

Figure 24 Evaluation of evacuation activity in NATM section.

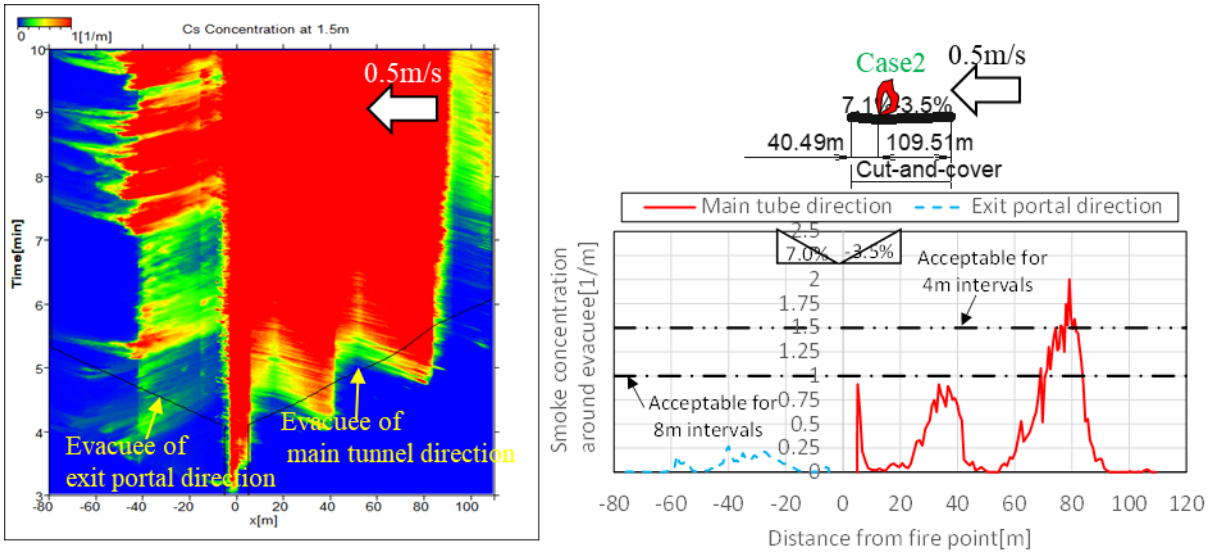

Figure 25 Evaluation of evacuation activity in ramp tunnel section(Kamiwaka exit lane).

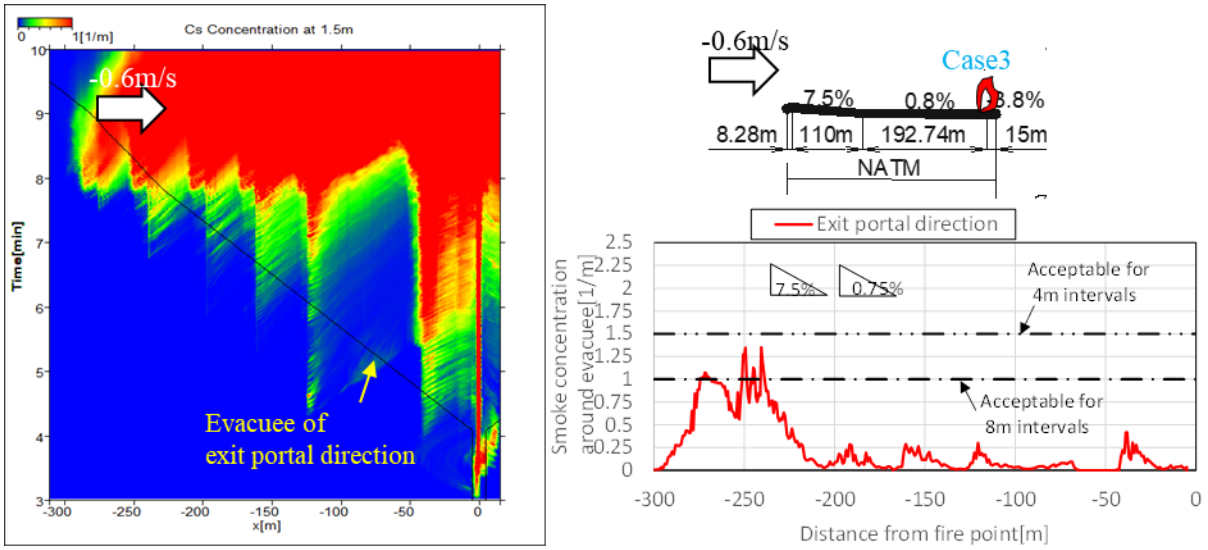

Figure 26 Evaluation of evacuation activity in ramp tunnel section(Shin-Kobe station exit lane).

CONCLUSIONS

Revision of the current operation procedures for existing equipment and introduction of the evacuation assisting light have been evaluated on the effectiveness for helping people to continue evacuation by securing visibility in the fire smoke when civil construction is difficult to implement in enhancing the equipment of existing tunnels for safey improvement at the time of tunnel fire. Following are the summary.

(1) Target airflow velocities in ventilation control were clarified to the type of cross section and longitudinal slope of the Shin-kobe Tunnel for effectively restricting smoke propagation.
(2) With respect to the evacuation assisting light which allows to continue evacuation under the smoke, applicable smoke concentration, light installation interval, and walking speed were specified from the field tests. It was verified that the new system of assisting light worked effectively for people to continue evacuation under the smoke concentration of Cs = 1.5 m^{-1}.
(3) The safey of the Shin-kobe Tunnel was evaluated by simulating the evacuation under the smoke concentration profile forecasted by 3D CFD simulatiom when the evacuation assisting light was introduced, and the assisting light interval was determined for each area of the Tunnel.

There are several topics which are not addressed in the experimental design for the evacuation assisting light. White vs. black smoke effects and psychological factors of evacuees are some of them and they are suggested as further studies. It is the basic policy of HEX to generate a refurbishment plan which meets the current technology standards when existing tunnel is updated.
At present the refurbishing construction has been underway in the Shin-kobe Tunnel with the insight obtained from the tests and experiments described in this paper. HEX will continue to investigate measures for further improvement of their road tunnels.

ACKNOWLEDGEMENT

The experiments were conducted at the facility provided by the Tan-nan Civil Engineering Office of Fukui Prefecture. Special gratitudes are due to the Emeritus Professor Nobuyoshi Kawabata of Kanazawa University for his kind and polite technical advice to the experiments. The authors also would like to express their thanks to subjects for participation in the experiments, Dr. Toshiaki Sakaguchi of Sohatsu Systems Laboratory Inc., and the colleagues of Hanshin Expressway Co., Ltd., for their help with writing the paper.

REFERENCES

1. PIARC., “ROAD TUNNELS MANUAL”, Available from: https://tunnelsmanual.piarc.org/en

2. Jin T., “Studies on Human Behavior and Tenability in Fire Smoke”, *Fire Safety Science – Proceedings of The fifth International Symposium*, pp.3-21, 1997.

3. Fridolf K. et al, “Walking Speed in Smoke: Representation in Life Safety Verifications”, *The 12th International Conference on Performance Based Codes and Fire Safety Design Methods*, Oahu, Hawaii ,April 2018.

4. Q. Wang, Kawabata N. et al, “Evaluation of Critical Velocity Employed to Prevent the Backlayering of Thermal Fume during Tunnel Fires”, *Proceedings of International Conference on Applied Computational Fluid Dynamics*, pp.404-411, 2000.

5. Ingason H., Gustavsson S. and Dahlberg M., “Heat Release Rate Measurements in Tunnel Fires”, *SP Report 1994:08*, Swedish National Testing and Research Institute.

6. Horikoshi K., “An Examination on Smoke Control by means of Numerical Simulation in a Long Urban Tunnel(The Yamatogawa Tunnel)”, *13th REAAA Conference*, Incheon city, Korea, 2009.

7. Hirose T., “Measures against Fire Disaster for Long Urban Tunnel of the Hanshin-Expressway Yamatogawa line”, *13th REAAA Conference*, Incheon city, Korea, 2009.

Tunnel safety, requirements for self-rescue and evacuation - the (mis)use of traffic volume to define the level of safety

Pål Andreas Dahl
COWI AS
E-mail: pada@cowi.com

ABSTRACT
The study reported in this paper examines tunnel evacuation as a design parameter for tunnel safety. Average Annual Daily Traffic (AADT) through tunnels is according to regulations important in defining the level of safety. Compared to evacuation in other parts of society, tunnel users are less prepared for events that require immediate evacuation. Evacuations from buildings and air traffic are designed with clearly defined maximum expected person loads, unlike in tunnels where these values are often unknown.

The number of vehicles that must be expected inside a tunnel during a fire incident and the number of vehicles trapped in fire is of major concern. The expected time it takes for evacuees to exit the tunnel on foot has been assessed in this paper, provided that the tunnel user has recognized the urgent need to evacuate. The traffic work or traffic flow (often expressed by AADT) and tunnel length contribute to the number of vehicles inside a tunnel with a fire incident. Other factors, especially the time to close the tunnel after ignition influences the amount of vehicles inside a tunnel and hence, the evacuation times. The comparison of hypothetical tunnels in this paper demonstrates significant variations in the expected evacuation times.

The EU Directive (TSR) sets demanding requirements for individual self-rescue. With current regulations and exceptions in Norwegian regulations (emergency exits should only be established with AADT of 8.000 in long tunnels), the requirements for self-rescue are rarely met. We conclude that Average Annual Daily Traffic should be integrated in an analysis of traffic flow and traffic conditions combined with analysis of actual scenarios rather than relying solely on threshold values to define requirements. Given that AADT represents an average rather than capturing short-term fluctuations or peak conditions, it is insufficient as a direct measure of risk. Instead, risk assessments should prioritize metrics that more accurately reflect real-time exposure, such as Peak ADT, which better represents the maximum number of individuals affected during critical incidents like fires.

Currently, the road users in Norwegian tunnels are left with unrealistic self-rescue demands, which undermines the self-rescue principle, the cooperation principle and the universal design principle.

KEYWORD: Tunnel Safety, Emergency Exit, Average Annual Daily Traffic (AADT)

INTRODUCTION

The EU directive [3] was enacted to establish minimum safety requirements for tunnels within the trans-European road network (TERN). This directive has served as the foundation for the Norwegian Tunnel Safety Regulations (TSR) [1]. This paper examines the prerequisites for the requirements concerning the self-rescue assumption, the establishment of escape routes from tunnels in accordance with the directive, as well as the adaptations made in the Norwegian regulations. The introductory considerations of the EU directive, point 11, state: “Safety measures should enable individuals involved in incidents to rescue themselves, allow road users to take immediate action to prevent more serious consequences, ensure that emergency services can operate effectively, and protect the environment while limiting material damage.”

The Tunnel Safety Regulations require the inclusion of emergency exits for tunnels with an Average Annual Daily Traffic (AADT) exceeding 4.000 vehicles. Additionally, if other risk factors are critical, establishment of emergency exits may be needed. This could be particularly relevant in cases where the tunnel slope exceeds 3%. According to § 8 of the Tunnel Safety Regulations, the Norwegian Public Roads Directorate (NPRD) is given the authority to make exceptions to the emergency exit requirement for tunnels shorter than 10 km and with an AADT less than 8.000 vehicles. This exception is contingent upon a risk analysis demonstrating that equivalent safety or safer system can be achieved through alternative measures.

This paper has analyzed the following research questions:

- *How do Norwegian tunnel owners ensure that the self-rescue requirements stated in the introductory considerations of the EU directive, pt. 11, are fulfilled through the Tunnel Safety Regulations?*
- *How does the use of AADT justify self-rescue requirements as the governing parameter for the establishment of emergency exits?*

Emergency exits from inside tunnels are rarely established in Norway. Primarily, this is undertaken when tunnels with two tubes are constructed, wherein escape is facilitated by cross-connections to the opposite tunnel tube. The motivation behind this study is to explore the reasons behind the limited establishment of escape tunnels in Norway and to analyze the implications of traffic volume being the sole parameter utilized as the basis for this requirement.

EVACUATION FROM TUNNELS IN THE EVENT OF FIRE

Current Methods for Ensuring Safe Evacuation

Experts agree that the evacuation of tunnels during a fire can be complex. There is often an unknown number of individuals within the tunnel, each possessing varying levels of knowledge regarding evacuation procedures. The outcome of an incident will depend on numerous factors, which may vary between different tunnels and events. Such factors include: the length of the tunnel, the tunnel profile, fuel composition, dynamics of the fire, ventilation systems, detection and monitoring, tunnel traffic management, communication with road users, closing barriers at the tunnel entrances, niches to turn around vehicles, the competence of individuals regarding evacuation, occupancy levels, etc.

One of the most critical factors to clarify is: "How many individuals are present in the tunnel during an event that necessitates evacuation?" This can be referred to as occupancy levels, and it should guide the selection of most safety measures within the tunnel. To ensure that the implemented evacuation measures correspond with the risks posed by the expected occupancy, it is currently facilitated by utilizing the tunnel's Average Annual Daily Traffic (AADT).

What is AADT and How Does It Affect Tunnel Safety Levels?

According to the Norwegian Public Roads Administration (NPRA), AADT is defined as follows: "The total number of vehicles, in both directions, that pass a given point on a road over the course of one year, divided by 365." It is a measure based on past observations, an average which does not say anything about the distribution, the variation over the year, seasons, weeks and days. In other words, AADT alone cannot indicate how many individuals are present in a specific tunnel during an incident. Number of vehicles and tunnel-users must be predicted, with inherent uncertainties as well as identifying the assumption of time horizon as basis for the prediction. AADT becomes the presented mean of a distribution rarely described by the risk analysts. To account for increases in traffic, hazardous traffic conditions, and seasonal variations, AADT must be analyzed more closely in each project. Examples of this include the following:

- AADT forecasts for 10 to 30 years into the future are used for capacity planning.
- If proportion of heavier vehicles in the AADT exceeds 15%, AADT must be risk-adjusted/increased.
- If summer daily traffic (SDT) during June, July, and August is significantly higher than the annual average, the AADT must be risk-adjusted/increased.

Thus, AADT is not a static value, and there are numerous uncertainties associated with AADT predictions. It is essential to understand the underlying historical data, the precision of measurement tools, and what premises that are laid down for the prediction of future traffic work. Furthermore, the connection between number of vehicles/traffic users and the performance of the self-rescue system also contains huge uncertainties.

What Does AADT Mean for the Selection of Safety Measures?
Both the EU directive (Tunnel Safety Regulations) and the NPRA's Handbook N500 [5] base safety requirements on AADT. Both documents have the status as a formal regulation. These regulations stipulate safety measures and tunnel designs based on the tunnel's length and AADT. However, the traditional approach regarding tunnel fire rescue and evacuation seem to prevail, it is in general sufficient with evacuation through tunnel entrances.

The uncertainties associated with the use of AADT result in variability regarding how many individuals may be considered present in a tunnel during a fire incident and whether the safety measures have been designed for the specific event. It would be prudent for the risk analysis, as stipulated in §10 of the TSR, to be used as an active tool for analyzing how AADT impacts risk. Additionally, the provisions in Appendix I, pts. 1.1.1 and 1.1.2 of the regulations must be considered, ensuring that the established safety measures are based on a systematic evaluation of all aspects of the system.

Several parameters in 1.1.2 are affected to varying degrees by the segment or tunnel's AADT. By analyzing AADT in a more nuanced manner for each individual tunnel, it becomes possible to identify risks associated with AADT beyond merely constructing facilities based on the frequency of expected incidents. For instance, ferry traffic on each side of a tunnel may lead to significant fluctuations in traffic volumes during certain times of the day, which is not necessarily reflected in the statistics for maximum hourly traffic. If there is a ferry arriving once an hour, most of the traffic may occur within a 15-minute window rather than being evenly distributed over a full hour. The Byfjord tunnel is close to a ferry connection. Consequently, the number of vehicles in the tunnel during an incident could far exceed what the AADT suggests as an average. This exemplifies why AADT may not accurately represent the risk within the tunnel. The scenario highlighted could also be typical for an undersea tunnel, where the observed number of fire occurrences is much higher than tunnels onshore, mostly due to the combination of long tunnels and steep slopes.

There exists an established practice in Norway of not building escape routes before AADT exceeds 8.000, even though this should be evaluated on a case-by-case basis according to the regulations.

Self-Rescue with and without Escape Routes
Self-rescue means that each road user must ensure their own safety, either by using their vehicle, evacuating on foot, or receiving assistance from other motorists. Most tunnels in Norway have longitudinal ventilation, which creates a smoke-free side and a smoke-affected side during a fire. Consequently, the conditions for self-rescue can vary significantly depending on which side of the fire a person is located.

If evacuation on foot is necessary, there is a substantial difference between evacuating a tunnel with escape routes and one without. The TSR mandate a maximum distance of 500 meters between escape routes, while in Manual N500 its a maximum of 250 meters (between cross-connections in dual tube tunnels). In the case of a long single tube tunnel (up to 10 km) without emergency exits, the distance to evacuate may extend several kilometers. Experiences from tunnel fires in Norway, such as those in the Gudvangatunnel [11, 12, 14] and the Oslofjord Tunnel [10, 13], demonstrate that self-rescue was complicated and that individuals were trapped in smoke. In other societal sectors this is approached differently:

Buildings. Evacuation requirements are defined according to the Regulations on Technical Requirements for Construction Works, TEK 17 [2], along with the accompanying guidelines, VTEK 17 [15]. A standard assumption is made of 1 cm exit width per person, with the dimensioning scenario based on the incident with the highest number of occupants present simultaneously. The maximum number of individuals anticipated to be present is thus known in advance. Based on this, evacuation plans and instructions are developed to ensure that individuals within the building are informed about evacuation procedures. In all public and occupational buildings, there are designated individuals tasked with ensuring that the evacuation can occur safely and efficiently. Evacuation plans are typically posted at escape routes and within hotel rooms, among other locations.

Passenger Aircraft. For the evacuation of an aircraft, specific requirements regarding the number and size of emergency exits are established based on the aircraft's passenger capacity. Design requirements are rigorously regulated by national and international standards. The worst-case scenario, with the maximum number of occupants known in advance, guides the requirements for ensuring safe evacuation. Additionally, crew members on all flights are responsible for giving passengers information, as well as managing situations that necessitate evacuation. Information about safety and evacuation procedures is available at each seat.

Summary. Evacuation systems from other constructions than tunnels are based on the scenario in which the maximum allowable number of individuals is present. Also, more information about safety and evacuation is provided to users of buildings and aircrafts than to users of tunnels. Lack of acceptance criteria and dimensioning assumptions for tunnels results in uncertainty regarding the expected number of individuals who may need to evacuate during a given incident. The self-rescue principle requires individuals to take proactive measures to secure their own safety, but the tunnel users are not provided with information and practical advice. There exist many Norwegian tunnels that will engulf tunnel users in smoke in case of fire inside.

METHOD

The following documents has been analyzed:

- Tunnel Safety Directive [3]
- The Norwegian Tunnel Safety Regulations [1]
- Handbook N500-2024 Road Tunnels, including previous versions [5]
- Guidelines for Risk Analyses of Road Tunnels, TS 2007:11 [7]
- Guideline V721 Risk Assessment of Road Traffic Systems [4]
- SINTEF Risk Analysis, AADT 4.000/8.000 [6]

The document analysis shows that there is limited justification for the central role of AADT in the safety management of tunnels and how the threshold values are established.

Analysis of safety in existing tunnels and three hypothetical tunnels

Two existing tunnels were chosen for examination, both without longitudinal escape routes. Traffic data from several years is available for both tunnels, the Byfjord Tunnel in the outskirt of Stavanger and the Oslofjord Tunnel south of Oslo. Both tunnels are subsea with steep slopes. The focus of the analysis has been on examining AADTs and its development in relation to the requirements or needs for emergency exits. The study includes 3 hypothetical tunnels to study variations in safety levels using the current regulation.

Variations in safety levels in tunnels utilizing current regulations

The purpose of the TSR is described in §1; to ensure the lowest permissible safety level for tunnel-users by mandating the prevention of critical incidents that could endanger human lives, the environment and tunnel infrastructure, and to provide protection in the event of accidents. So, what variations are considered acceptable when using the current criteria for safety management in tunnels? The outcome of an incident may be determined by several parameters, including:

- Length of the tunnel
- Availability of emergency exits or rescue rooms

- Gradient/vertical curvature of the tunnel
- Ventilation solutions
- Alarm systems and monitoring
- Barriers to close tunnel
- The number of individuals present in the tunnel at the time of the incident
- Possibilities for turning vehicles around in the tunnel
- Manual firefighting capabilities
- Emergency response times

To narrow and ease the analysis, the tunnel's gradient and profile were not taken into consideration, allowing the assumption that the probability of a fire per vehicle per km remains constant. It is assumed that the tunnels are equipped with longitudinal ventilation. Requirements for emergency exits are based on scenarios with an AADT exceeding 8.000. Requirements for Automatic Incident Detection/Incident Traffic Vision (AID/ITV) are based on the specifications in N500. The analysis will focus on the following parameters:

- Length of the tunnel
- Traffic volume (AADT), with further assessments of occupancy levels
- Availability of emergency exits
- Alarm systems and monitoring
- Barriers to close off tunnel entrances

The analysis examines variations in measures and expected outcomes resulting from these factors. It focuses on the number of vehicles expected to be in the tunnels during an incident, which will have implications for how far the users will need to travel or walk to reach the exit.

RESULTS

Analysis of safety based on AADT in existing tunnels

This chapter provides an analysis of the safety measures established in the Byfjord Tunnel and the Oslofjord Tunnel in relation to the development of AADT over time.

Description of the Byfjord Tunnel

The Byfjord Tunnel is part of the E39 Rennfast connection, which opened in 1992. The bi-directional tunnel is 5.875 meters long and has a maximum gradient of 8%. The tunnel profile is T11.5. It contains three lanes and has a speed limit of 80 km/h. There are speed cameras in both directions (average speed in the northern lane and point camera in southern lane). Safety measures include:

- Emergency niches and niches to turn around vehicles
- Emergency stations: 57 in total (approximately every 100 meters)
- Barriers for tunnel closure in the event of an incident
- Video surveillance (ITV) and Automatic Incident Detection (AID)
- Emergency lighting

The tunnel has longitudinal ventilation, which is typical for tunnels in the Norwegian road network. On www.trafikkdata.no, the NPRA website, there is a vehicle counting point located at Sokn, north of the tunnel. This counting point has only been operational since 2006. Detailed data from 1992 to 2006 is not readily available. However, an article published in Stavanger Aftenblad (newspaper) on June 18, 2012 [19], indicated that the AADT in 1992 was approximately 4.000. There has been a steady increase in AADT from 2006 to 2023. In 2023 it was 11.313, following a constant upward trend since the initial opening. The tunnel experiences steady traffic throughout the year, with little seasonal variation. However, the highest daily traffic recorded was 16.275 vehicles on June 23, 2023. To further investigate peak loads during worst-case scenarios, data on maximum hourly traffic in 2023 was also reviewed, with a peak of 1.676 vehicles recorded in one hour. The tunnel is connected with a ferry terminal in the north (approx. 12 km from the north entrance of the tunnel), resulting in fluctuations in the traffic pattern.

Description of the Oslofjord Tunnel

The Oslofjord Tunnel opened in 2000. It is 7.306 meters long and has a maximum gradient of 7%. The tunnel profile is T11. The bi-directional tunnel has three lanes and a speed limit of 70 km/h. Notable safety measures include:

- Emergency niches and niches to turn around vehicles
- Emergency stations: approximately every 250 meters, with fire cabinets located between emergency stations
- Evacuation rooms/rescue rooms: distances between rooms range from 150 to 475 meters. One location has a distance of 475 m, and another has 350 m; the rest are 250 m or shorter.
- Emergency exit: Approximately 2 km from the Drammen portal, leading directly to safety
- Barriers for tunnel closure in the event of an incident
- AID in traffic rooms and evacuation rooms, along with ITV in the escape tunnel
- Emergency lighting

On www.trafikkdata.no, there is a vehicle counting point inside the tunnel; however, data is missing for the years 2014 to 2016, and it was closed in 2017. Another counting point is located just outside the tunnel on the eastern side and has been operational since 2000. There has been a steady increase in AADT from 2000 to 2023, rising from 3.419 to 10.860. The tunnel maintains a consistent traffic flow throughout the year, with slight seasonal variations. The variations are larger than those observed for the Byfjord Tunnel but not substantial enough to warrant emphasis in further analyses. The highest recorded daily traffic was 15.748 vehicles on May 26, 2023. To examine peak loads during worst-case scenarios, data regarding maximum hourly traffic in 2023 has also been collected, with a maximum of 1.529 vehicles recorded in one hour.

Analysis of AADT and safety level - assumptions

It is assumed that the requirements outlined in the TSR apply to both tunnels, and reference is made to §2 and §14 of the regulations, which state that tunnels not meeting the criteria should be upgraded and approved by the NPRD. TSR further states that "for existing tunnels longer than 1.000 meters with a traffic volume exceeding 2.000 vehicles per lane, it must be assessed whether it is feasible and effective to create new emergency exits." In Norway, it is understood through §8 and prevailing practices that this threshold is at 4.000 vehicles per lane, corresponding to an AADT of 8.000.

The regulations direct that emergency exits should be established when AADT exceeds 8.000. At the same time, it must be evaluated whether such measures are feasible and effective. While the feasibility will not be challenged in this study, it is evident that establishing emergency exits would be beneficial in the event of a fire, bearing in mind the obvious threat of individuals being trapped by fire and smoke within the tunnel.

Analysis of AADT and safety level – Byfjord Tunnel

The TSR came into force in 2007, and according to www.trafikkdata.no, the AADT exceeded the 8.000 threshold since 2010. According to §14, renovations for tunnels were required to be completed by April 30, 2014, with an option to extend the deadline by five years. Since the tunnel has not established escape routes, it must be concluded that it has not been considered feasible and effective. This is despite the traffic volume being 2.83 times higher than the AADT threshold in the EU directive and 1.4 times higher than the AADT threshold in §8 of the regulations.

It is anticipated that traffic through the Rennfast connection, and subsequently through the Byfjord Tunnel, will decrease significantly when the Rogfast project opens in 2033, as E39 will no longer pass through Rennfast. The extent of the reduction in traffic through the Byfjord Tunnel is currently unknown, but a substantial decrease is expected. The AADT for the Byfjord Tunnel heading toward 2033 is not known, but applying an increase similar to the previous decade (2013-2023) from 9.270 to 11.313 (approximately 22%) would result in an expected AADT of 13.802. According to the E39 Rogfast Risk and Vulnerability Analysis from 2012 [17], AADT is predicted to be 13.000 20 years after opening.

Analysis of AADT and safety level – Oslofjord Tunnel

According to www.trafikkdata.no, the AADT surpassed the 8.000 threshold in 2016. There is access to an escape tunnel located approximately 2 km from the Drammen portal. However, this escape route has only one exit from the tunnel, resulting in long distances compared to longitudinal escape tunnels as required by the TSR, which stipulate a maximum of 500 meters between emergency exits. The escape tunnel contributes to the performance of the evacuation system and provides the fire services with an alternative access route, but it does not meet the regulatory requirements. Following the fire in in 2011 [10], rescue rooms were constructed in 2012, providing escape options to temporary safe locations. These rescue rooms conflict with the EU directive and TSR requirements. This analysis does not assess the safety of the rescue rooms, but it can be concluded that these measures were established to enhance safety.

In 2023, the AADT was recorded at 10.860, which is 2.72 times higher than the AADT limit established in the EU directive and 1.36 times higher than the AADT limit in §8 of the Tunnel Safety Regulations. There are plans to establish an additional tunnel section through the E134 Oslofjord Connection – Construction Phase 2. The completion date is not known but can be assumed to be around 2032. The AADT for the Oslofjord Tunnel heading toward 2032 is also unknown, but a similar increase to the previous nine-year period (2014-2023) from 7.459 to 10.860 (approximately 46%) would yield an expected AADT of 15.856.

Byfjord and Oslofjord Tunnels – AADT as a basis for safety management

The two tunnels exhibit a somewhat similar trend in traffic volume and, aside from their lengths, are constructed with comparable specifications in terms of gradient and number of lanes. Furthermore, both tunnels must comply with the same requirements for emergency exits as per the TSR. The AADT for both tunnels indicates that, unless it can be demonstrated that establishing emergency exits is not feasible and effective, such exits should have been established for both tunnels. For the Byfjord Tunnel, the AADT exceeded 8.000 in 2010, and for the Oslofjord Tunnel, this threshold was exceeded in 2016. With the anticipated opening of Rogfast in 2033, leading to a subsequent expected reduction in AADT, the Byfjord Tunnel has had 23 years with an AADT greater than 8.000 without any emergency exits being established. For the Oslofjord Tunnel, the establishment of emergency exits is expected to occur with the addition of a new tunnel section, assumed to be completed by 2032. Thus, the Oslofjord Tunnel would have had 16 years with an AADT exceeding 8.000.

Both tunnels have undergone extensive upgrades. Assuming that the rescue rooms sufficiently protect individuals from fire and smoke in the event of a fire, there is a significant difference in the self-rescue abilities between the two tunnels. Additionally, the escape tunnel in the Oslofjord Tunnel provides a positive contribution to evacuation options, along with facilitating the fire service's access capabilities. Nevertheless, questions need to be raised why it has been accepted not to establish emergency exits, especially for the Byfjord Tunnel, and why there are substantial differences in the implemented measures in the two tunnels. Furthermore, it should be noted that the Byfjord Tunnel may experience larger accumulations of traffic due to the ferry connection between Arsvågen and Mortavika. Whether this effect is captured in the maximum hourly traffic is uncertain and has not been further studied in this paper. According to TØI Report 1948/2023 [8], 112 out of 226 fires and fire incidents in tunnels occurred in tunnels with steep gradients, with 23 of the fires in the Byfjord Tunnel and 40 in the Oslofjord Tunnel.

Variations in safety levels in tunnels under current regulations

This chapter presents an analysis of the variations in safety levels that can be expected under current regulations, taking three hypothetical tunnels into considerations. The highest hourly traffic is determined to be 14.8%, which aligns with the proportion observed in the Byfjord Tunnel in 2023. The speed limit for all tunnels is set at 80 km/h, except for the Oslofjord Tunnel, which has a speed limit of 70 km/h. For each tunnel, safety equipment is defined on actual conditions for the existing tunnels or in accordance with N500 for the hypothetical tunnels. Based on this, the analysis contain:

- Differences in self-rescue capabilities (with or without emergency exits).
- Expected number of vehicles during an incident.

- Anticipated number of vehicles that would be caught downstream and upstream of the fire, and which would need to evacuate either by vehicle or on foot in smoke.
- Estimated time required for evacuation on foot (based on the stopping point in the middle of the tunnel or worst-case scenarios between escape alternatives).

The analysis assesses how variations in AADT influence safety levels and how this, in turn, affects the drivers' ability to perform self-rescue. The expected number of vehicles in the tunnel during an incident will be statistically calculated based on maximum hourly traffic and speed/travel time. Additionally, the time to close the tunnel is crucial for the outcome of the incident response. For comparison, in tunnels equipped with ITV/AID and barriers, the closing time will be set to 60 seconds. In tunnels without ITV/AID, but with barriers or traffic lights for tunnel closure, this time will vary significantly and depend on how long it takes for road users to notify the Traffic Control Center to initiate closure. This will also depend on how many people are present in the tunnel, how individuals assess the situation, the speed of fire progression, etc. For the purpose of comparison, the time to close the tunnel will be set to 5 minutes (300 seconds). This is just an assumption since no data has been collected for this and its likely to be large variations between events.

It is assumed that the same number of vehicles travel in each direction in the tunnel during a fire incident. It is also assumed that the ventilation system has a fixed direction which activates in the event of a fire. The analysis does not calculate the impact of ventilation on the evacuation process other than noting that it will create an upstream (smoke-free) and a downstream (smoke-filled) zone, which will subsequently affect drivers' opportunities for self-rescue.

The size of the fire is not explicitly defined in the analysis, but it is assumed to involve a fire/accident that blocks both lanes of traffic. It is further assumed that vehicles that have passed the fire, regardless of whether they are upstream or downstream, will drive out of the tunnel. The figure below (Figure 1) illustrates an expected normal distribution scenario for defining how many individuals would be blocked by the fire/accident. In the analysis this is based on maximum hourly traffic, length of the tunnel and travel speed. Consequently, these individuals would need to either turn their vehicles around or evacuate on foot, leading to different outcomes depending on whether they are positioned upstream or downstream of the fire. Safety measures such as emergency niches are not illustrated, as they vary among the different tunnels.

Walking speed is set to 1.4 m/s [16] for comparison between the tunnels, but it will vary and does not consider evacuation in smoke or the evacuation of wheelchair users, elderly persons, etc. Regarding evacuation time on foot, a simplification has been made by assuming that evacuation starts without accounting for reaction and decision-making time. This results in an unrealistically short evacuation time; in reality, the total time required for evacuation will be longer. Evacuation time on foot is only used for comparison between the various tunnels, and the method is therefore considered relevant. Calculating reaction and decision-making time will represent large uncertainties and will be complex to calculate.

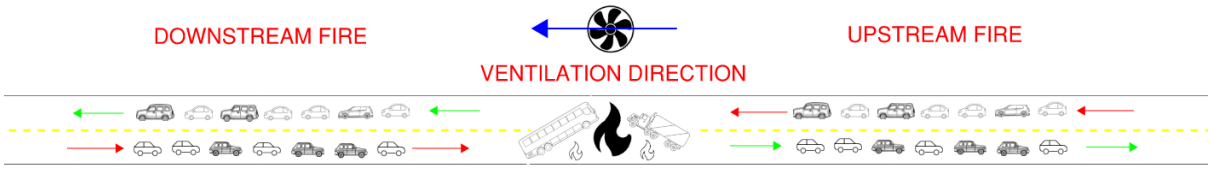

Figure 1 *Vehicles blocked in the tunnel by fire/accident. Vehicles traveling in the direction of the green arrow are assumed not to be involved in the accident, while vehicles traveling in the direction of the red arrow are blocked by the accident/fire and tunnel users must either turn around or evacuate on foot.*

Tunnel Analysis – Byfjord Tunnel

Table 1 *Byfjord tunnel*

AADT	11.313	Vehicles/sec	0,47
Length (m)	5.875	Time from fire start to closure	60
Tunnel Class (according to current regulations)	D	Total vehicles at fire start	123
Emergency exits	No	Total vehicles between fire start and closure	28
AID og ITV	Yes	Total vehicles in tunnel at fire	151
Barriers to close tunnel	Yes	Total vehicles downstream fire – blocked by fire	45
Maximum hourly traffic (vehicles/hour)	1.676	Total vehicles downstream fire – passed the fire	31
Speed (m/s)	22,2	Total vehicles upstream fire – blocked by fire	45
Travel time	265	Total vehicles upstream fire – passed the fire	31

The analysis is based on the current situation. It shows that at the start of the fire, there will be 123 vehicles in the tunnel, and after 60 seconds before closure, an additional 28 will have entered the tunnel. The latter are all expected to become trapped in the tunnel due to the fire/accident. This implies that there will be 45 vehicles on either side of the fire that must either turn around and exit, get assistance from other motorists, or evacuate on foot. The expected evacuation time on foot, assuming one is located at the center of the tunnel and moving at a walking speed of 1.4 m/s, will be approximately 35 minutes. The walking speed will be dramatically reduced if evacuating in smoke.

Tunnel Analysis – Oslofjord Tunnel

Table 2 *Oslofjord tunnel*

AADT	10.860	Vehicles/sec	0,42
Length (m)	7.306	Time from fire start to closure	60
Tunnel Class (according to current regulations)	D	Total vehicles at fire start	160
Emergency exits	1 + rescue rooms	Total vehicles between fire start and closure	25
AID og ITV	Yes	Total vehicles in tunnel at fire	185
Barriers to close tunnel	Yes	Total vehicles downstream fire – blocked by fire	53
Maximum hourly traffic (vehicles/hour)	1.529	Total vehicles downstream fire – passed the fire	40
Speed (m/s)	19,4	Total vehicles upstream fire – blocked by fire	53
Travel time	377	Total vehicles upstream fire – passed the fire	40

The Oslofjord Tunnel is equipped with an escape route and rescue rooms, with distances ranging from 150 to 475 meters. This analysis is based on the current situation. It shows that at the start of the fire, there will be 160 vehicles in the tunnel, and after 60 seconds before closure, an additional 25 vehicles will have entered the tunnel. The latter are all expected to become trapped in the tunnel due to the fire/accident.

This implies that there will be 53 vehicles on either side of the fire that must either turn around and exit, get assistance from other motorists, or evacuate on foot. The walking time to the nearest rescue room and to the emergency exit is calculated. The maximum distance between two rescue rooms is considered to be 475 meters. Given that the emergency exit is approximately 2 km from the Drammen portal, the distance between the escape route and the Drøbak portal is established (7.306 m – 2.000 m = 5.306 m / 2 = 2.653 m). The expected evacuation time on foot to the nearest rescue room, based on a walking speed of 1.4 m/s, will be approximately 3 minutes, and the expected evacuation time to the emergency exit will be around 31.5 minutes. The expected time to fully exit the tunnel will be approximately 43.5 minutes. The walking speed will be dramatically reduced if evacuating in smoke.

Tunnel Analysis 1 – Tunnel Class B, Length 4.990 meters / AADT 3.990

This hypothetical tunnel will have a length of 4.990 meters and an AADT of 3.990. This gives the requirements Tunnel Class C, thus exempting it from AID and ITV requirements. It would be reasonable to install these measures, as the tunnel is marginally shorter than the requirements, but this example is used to illustrate how this can affect the number of vehicles that may be trapped by a fire in the tunnel due to delayed detection and closure.

Table 3 *Tunnel Class B, length 4.990 meter / AADT 3.990*

AADT	3.990	Vehicles/sec	0,16
Length (m)	4.990	Time from fire start to closure	300
Tunnel Class (according to current regulations)	B	Total vehicles at fire start	37
Emergency exits	No	Total vehicles between fire start and closure	49
AID og ITV	No	Total vehicles in tunnel at fire	86
Barriers to close tunnel	Only light signal	Total vehicles downstream fire – blocked by fire	34
Maximum hourly traffic (vehicles/hour)	591	Total vehicles downstream fire – passed the fire	9
Speed (m/s)	22,2	Total vehicles upstream fire – blocked by fire	34
Travel time	225	Total vehicles upstream fire – passed the fire	9

The analysis shows that at the start of the fire, there will be 37 vehicles in the tunnel, and after 300 seconds before closure, an additional 49 vehicles will have entered the tunnel. The latter are all expected to become trapped in the tunnel due to the fire/accident. This implies that there will be 34 vehicles on either side of the fire that must either turn around and exit, get assistance from other motorists, or evacuate on foot. The expected evacuation time on foot, assuming one is located at the center of the tunnel and walking at a speed of 1.4 m/s, will be approximately 29.5 minutes. The walking speed will be dramatically reduced if evacuating in smoke.

Tunnel Analysis 2 – Tunnel Class C, Length 9.990 meters / AADT 7.000

This hypothetical tunnel will have a length of 9.990 meters and an AADT of 7.000. This places it just under the 10 km threshold permitted by N500. Furthermore, the AADT is 1.000 vehicles below the requirement for establishing emergency exits.

Table 4 *Tunnel Class C, length 9.990 meter / AADT 7.000*

AADT	7.000	Vehicles/sec	0,29
Length (m)	9.990	Time from fire start to closure	60
Tunnel Class (according to current regulations)	C	Total vehicles at fire start	130
Emergency exits	No	Total vehicles between fire start and closure	17
AID og ITV	Yes	Total vehicles in tunnel at fire	147
Barriers to close tunnel	Yes	Total vehicles downstream fire – blocked by fire	41
Maximum hourly traffic (vehicles/hour)	1.036	Total vehicles downstream fire – passed the fire	32
Speed (m/s)	22,2	Total vehicles upstream fire – blocked by fire	41
Travel time	450	Total vehicles upstream fire – passed the fire	32

The analysis shows that at the start of the fire, there will be 130 vehicles in the tunnel, and after 60 seconds before closure, an additional 17 vehicles will have entered the tunnel. The latter are all expected to become trapped in the tunnel due to the fire/accident. This means that there will be 41 vehicles on either side of the fire that must either turn around and exit, get assistance from other motorists, or evacuate on foot. The expected evacuation time on foot, assuming one is located at the center of the tunnel and walking at a speed of 1.4 m/s, will be approximately 59.5 minutes. The walking speed will be dramatically reduced if evacuating in smoke.

Tunnel Analysis 3 – Tunnel Class D, Length 5.000 meters / AADT 8.000

This hypothetical tunnel will have a length of 5.000 meters and an AADT of 8.000. This places it exactly at the threshold for establishing emergency exits, as previously described.

Table 5 *Tunnel Class D, length 5.000 meter / AADT 8.000*

AADT	8.000	Vehicles/sec	0,33
Length (m)	5.000	Time from fire start to closure	60
Tunnel Class (according to current regulations)	D	Total vehicles at fire start	74
Emergency exits	Yes	Total vehicles between fire start and closure	20
AID og ITV	Yes	Total vehicles in tunnel at fire	94
Barriers to close tunnel	Yes	Total vehicles downstream fire – blocked by fire	28
Maximum hourly traffic (vehicles/hour)	1.184	Total vehicles downstream fire – passed the fire	19

Speed (m/s)	22,2	Total vehicles upstream fire – blocked by fire	28
Travel time	225	Total vehicles upstream fire – passed the fire	19

This tunnel is equipped with emergency exits. The distance between emergency exits should, according to TSR, be maximum 500 meters. The analysis shows that at the start of the fire, there will be 74 vehicles in the tunnel, and after 60 seconds of closure, an additional 20 vehicles will have entered the tunnel. The latter are all expected to become trapped in the tunnel due to the fire/accident. This means that there will be 28 vehicles on either side of the fire that must either turn around and exit, get assistance from other motorists, or evacuate on foot. When evacuating on foot, the assumption is made that individuals will head towards the nearest escape route. With a maximum distance of 500 meters between escape routes, a distance of 250 meters is assumed if one is located midway between two exits. The expected evacuation time on foot will be approximately 3 minutes.

Comparing the safety of tunnels

It is essential to distinguish between the results of the two existing tunnels and the three hypothetical tunnels due to their different conditions, particularly regarding their construction dates. However, it is interesting to observe the differences in safety levels since all tunnels must meet the requirements outlined in the TSR. To compare the risks in the various tunnels, the table below shows the number of vehicles blocked by fire/accident downstream and upstream of the fire, as well as the expected time for evacuation on foot in cases where individuals are unable to reach a safe or temporary safe location using their own or others' vehicles.

Table 6 *Comparison of analyzed objects*

	AADT	*Length*	*Vehicles in tunnel fire*	*Vehicles blocked upstream fire*	*Vehicles blocked downstream fire*	*Evacuation time on foot**
Byfjord tunnel	11.313	5.875 meters	151	45	45	35 minutes
Oslofjord tunnel	10.860	7.306 meters	185	53	53	3 minutes
Tunnel 1	3.990	4.990 meters	86	34	34	29,5 minutes
Tunnel 2	7.000	9.990 meters	147	41	41	59,5 minutes
Tunnel 3	8.000	5.000 meters	94	28	28	3 minutes

* Evacuation time calculated from the center of the tunnel where individuals evacuate fully and from the midpoint between emergency exits where applicable. For the Oslofjord Tunnel, the distance is considered midway between two rescue rooms involving the longest distance.

The analysis indicates that AADT plays a significant role in defining how many vehicles may become trapped in the tunnel during a fire. The length of the tunnel is also a decisive factor; however, how quickly the tunnel is closed are crucial for reducing the number of vehicles present during a fire.

There are significant differences in walking evacuation times, which is critical when smoke is travelling the same direction. Tunnel 3, which is 5.000 meters long, will be evacuated within approximately 3 minutes, whereas Tunnel 1, at 4.990 meters needs 29.5 minutes. If this tunnel were 10 meters longer, it would be classified as Tunnel Class C, requiring AID and ITS, resulting in a faster closure of the tunnel and a reduction from 68 vehicles to 28 vehicles trapped by the accident. However, this does not impact the requirements for emergency exits with this AADT, nor does it affect evacuation times on foot.

Furthermore, individuals evacuating on foot in the Oslofjord Tunnel would be able to reach a safe location in just 3 minutes, whereas individuals in the Byfjord Tunnel would take approximately 35 minutes. The difference in safety levels regarding self-rescue during a fire for two otherwise similar tunnels is considered substantial. It should be noted that the use of rescue rooms contradicts the requirements of the EU directive. Assuming these rescue rooms are constructed with adequate safety levels, they represent a significant enhancement in self-rescue safety. The quality and effectiveness of the rescue rooms have not been further evaluated in this paper.

There is also substantial discrepancy in the safety levels between Tunnel 2 and Tunnel 3. This illustrates how an increase in AADT from 7.000 to 8.000 require better conditions for self-rescue, even though the tunnel without emergency exits is nearly twice as long and has an estimated evacuation time of close to one hour.

DISCUSSION

The study claims that the use of AADT, as it is currently approached, places greater emphasis on the likelihood of an adverse event occurring rather than on the consequences of such an event.

Safety Levels in Existing Tunnels

The safety levels of the Byfjord Tunnel and the Oslofjord Tunnel have been evaluated based on the information gathered. Comprehensive analyses of the tunnels' safety levels, in accordance with the requirements of §10 of the TSR, have not been carried out in this paper. The intention has been to study the development of AADT in the tunnels and how this has affected safety level requirements, particularly concerning the establishment of emergency exits. The findings show that traffic has largely exceeded the values that require emergency exits as per Appendix I, section 2.3.6 of the TSR (and §8 of the regulations), if it is deemed both feasible and effective to establish them. With the expected completion of the Rogfast project in 2033, the Byfjord Tunnel will have been in operation for 23 years with an AADT greater than 8.000 without any escape routes being established. In comparison, the Oslofjord Tunnel will have been in service for 16 years with an AADT exceeding 8.000, awaiting the completion of a new tunnel section in 2032. The tunnel has one perpendicular emergency tunnel, and rescue rooms. They must be seen as compensatory measures for the establishment of emergency exits, providing protection against the effects of fire and smoke. The two tunnels appear quite similar in terms of safety level when considering length, gradient, and AADT.

Whether past incidents have prompted these differences, or if other underlying factors exist, has not been further studied. Given the number of fires and near-fires between 2008 and 2021 [8] - 23 incidents in the Byfjord Tunnel compared to 40 in the Oslofjord Tunnel, it would seem reasonable that similar measures had been considered for both tunnels. From the outset of the regulatory plans for single-tube tunnels, it is essential to stipulate the conditions under which emergency exits should be established. This could provide greater predictability in safety management and necessitate the allocation of investments for upgrades in a long-term perspective.

Variations in safety levels under current regulations

The results from the analysis of three hypothetical tunnels based on length and AADT indicate significant discrepancies regarding the safety measures required in relation to the expected incident considered. AADT has some influence on the number of vehicles anticipated to be trapped by a fire accident. Moreover, the differences between vehicles being trapped in the three hypothetical tunnels are minor, ranging from 56 vehicles in Tunnel 3, 68 vehicles in Tunnel 1, and 82 vehicles in Tunnel 2. Since emergency exits are established in Tunnel 3, the evacuation time on foot is projected to be only 3 minutes, while the time will be nearly 30 minutes for Tunnel 1 and almost 60 minutes for Tunnel 2. These differences in safety levels are considered to be unreasonable.

Tunnel 1 may be seen as somewhat inappropriately dimensioned since it is at the threshold of requiring the establishment of AID and to be classified as Tunnel Class C. To test variations, the length could be set to 5.000 meters while the AADT is simultaneously decreased to 2.000. In this case, the time to close the tunnel could similarly be set to 60 seconds, as for the others. This,

combined with a halving of the traffic volume, would lead to a reduction in the number of vehicles trapped by fire from 68 to 14. This is a significant reduction; however, evacuating those positioned downstream of the fire would still be complex, both by vehicle and on foot, potentially taking around 30 minutes.

Considerations regarding consequences of fire incidents in current regulations

One may question whether the use of AADT focuses too heavily on reducing the probability of an incident occurring. The examples provided indicate that safety management of buildings and air traffic, maximum anticipated occupancy is used, while for tunnels, the expected value (AADT) is employed. So, how are the consequences incorporated into the risk management for tunnels? Does a lower assumed AADT justify low likelihood of fire and subsequently low risk? Analyses indicate that tunnels without emergency exits and without rescue rooms may experience a variation of between 68 and 90 vehicles trapped by a fire accident.

If vehicles located upstream of a fire can evacuate safely to an exit, the various tunnels, including Tunnel 1 with the reduced AADT, would have between 7 and 45 vehicles blocked downstream of the fire. With just 7 vehicles, for example one tourist bus carrying 50 people involved, implying that in the worst-case scenario there could be an incident involving 60-70 people downstream. An incident involving 45 vehicles downstream could lead to far more individuals trapped in the tunnel, presenting the potential for a major disaster under the Major Accident Regulations [18].

It is essential to differentiate between risks associated with traffic safety, which encompass numerous incidents throughout the year, and the rare, critical incidents such as a fire in a tunnel. It is challenging to contend that safety management utilizing AADT is particularly suited to address these situations.

Discussion of research questions

The first research question in the study is described as follows: *How do Norwegian tunnel owners ensure that the self-rescue requirements stated in the introductory considerations of the EU directive, pt. 11, are fulfilled through the Tunnel Safety Regulations?*

It is difficult to assert that the current tunnels, and those constructed under current regulations, will adequately address the self-rescue requirements. This concern arises from the uncertain number of vehicles that may be involved in fires where self-rescue must be considered complicated, especially for those located downstream of a fire. Additionally, the knowledge regarding self-rescue among road users varies significantly. Experiences from incidents, such as the fire in the Gudvanga tunnel, demonstrate that self-rescue can be complex even with a small number of vehicles involved.

If the self-rescue requirement in pt 11 of the EU directive is to be fulfilled, there must be a greater commitment to a practice where the overall safety of tunnels is assessed according to the intention of Appendix I, section 1.1.1 of the TSR, which states: *"Safety measures implemented in a tunnel shall be based on a systematic assessment of all aspects of the system, comprising infrastructure, usage, road users, and vehicles."* Section 1.1.2 further specifies the parameters to be considered. This approach would better tailor the safety levels to the specific risks of each tunnel.

The second research question in the study is described as follows: *How does the use of AADT justify self-rescue requirements as the governing parameter for the establishment of emergency exits?*

As described in the analysis, AADT is a predicted mean value. The associated figures will introduce significant uncertainties regarding future developments and, importantly, how to define a dimensioning scenario based on an annual average. If AADT is to be used appropriately, seasonal adjustments, risk adjustments, and assessments of maximum values for daily and hourly traffic must be performed. This would provide a more solid foundation for evaluating actual scenarios instead of relying solely on average figures to define requirements derived from the AADT thresholds stipulated in the regulations. As shown, the use of AADT can lead to substantial fluctuations in safety measures and overall safety levels.

Recommendations for further work

Self-rescue is complicated in tunnels, and adherence to current regulatory requirements results in highly variable safety level across Norwegian tunnels. Is it acceptable to continue constructing single-tube tunnels without emergency exits, reserving such measures primarily for tunnels with two tubes?

It is recommended to consider alternative approaches for defining when the establishment of escape tunnels is warranted in Norway. A greater emphasis on the provisions outlined in Appendix I, sections 1.1.1 and 1.1.2 of the TSR would facilitate this. In addition, methods for analyzing these parameters within a holistic tunnel safety framework should be explored. This could lead to a change in practice that moves away from strictly defined thresholds and requirements. A careful application of AADT should be integrated into this process, as it remains prerequisite under section 1.1.2 of the TSR. However, it's role should not be weighted too heavily in defining minimum safety levels.

Historically, AADT was likely chosen for its simplicity, availability, ease of standardization across tunnels, and alignment with the regulatory framework. While it provides a convenient, generalized measure, it's reliance on historical data, often infrequently updated, limits its accuracy in reflecting current traffic conditions.

Given that AADT represents an average rather than capturing short-term fluctuations or peak conditions, it is insufficient as a direct measure of risk. Instead, risk assessments should prioritize metrics that more accurately reflect real-time exposure, such as Peak ADT, which better represents the maximum number of individuals affected during critical incidents like fires. This shift would enhance the reliability of safety analyses and ensure that emergency measures, including evacuation planning and emergency exits, are based on actual peak usage rather than historical administrative conventions.

In relation to methods for analyzing tunnel safety, it is also advisable to establish a practice for defining design scenarios for critical incidents and clear acceptance criteria that can be verified through risk analyses.

Typically, emergency exits are only established in single-tube tunnels when the tunnel is extended with another full-size tube. One reason for this could be that the cost of establishing a parallel escape tunnel, given today's requirements (tunnel profile T5.5 according to N500) is too high. It is therefore recommended to investigate whether it is possible to establish emergency exits within the same profile while allowing a narrower escape route. If simpler methods for constructing emergency exits that meet sufficient safety levels can be identified, this may also promote greater utilization of emergency exits through lower costs.

CONCLUSION

It is challenging to justify that self-rescue is adequately addressed in existing and new tunnels in Norway. The difficulty arises from numerous uncertainties concerning the varying assumptions about how many and which individuals are present in the tunnels, where self-rescue in many instances can be complicated. Often, these situations also involve very long distances to evacuate.

Managing safety in tunnels based on AADT, particularly for the purpose of establishing emergency exits, introduces substantial uncertainties and necessitates more detailed analyses than merely utilizing expected values. Furthermore, AADT conveys little about the consequences of incidents requiring self-rescue. It is crucial to distinguish between risks associated with traffic safety, where incidents occur frequently throughout the year, and the rare and critical incidents such as fires in tunnels. AADT is not adequately suited for assessing the risks associated with these critical events. The use of Peak ADT would better represent the maximum individuals affected during a critical event.

Experience demonstrates that both in existing tunnels and in the planning of new tunnels, substantial variations in safety levels for self-rescue during tunnel fires are anticipated. The results indicate significant differences in evacuation distances and evacuation times on foot. The notable disparities in

measures between the Oslofjord Tunnel and the Byfjord Tunnel are striking, given that both tunnels are expected to meet the same regulatory requirements and appear to have similar conditions and risk profiles. However, there have been more critical incidents in the Oslofjord Tunnel compared to the Byfjord Tunnel, which may suggest that incident frequency shapes the safety management practices. This approach could result in high-risk tunnels, where the consequences of accidents could be severe, not receiving the necessary safety upgrades due to the absence of critical incidents. The analysis of the hypothetical tunnels also reveals significant differences in safety levels, which is expected since measures are typically triggered at threshold values associated with increased lengths and AADT. Developing methodologies for conducting more comprehensive analyses of tunnel safety concepts may facilitate a more uniform safety level among various tunnels, thereby placing greater emphasis on the requirements outlined in Appendix I, sections 1.1.1 and 1.1.2 of the TSR.

In comparison to evacuation in other areas of society, it is assessed that road users are poorly prepared for potential incidents that may occur. Evacuation from buildings and air traffic are more clearly defined, with maximum expected occupancy, in contrast to road tunnels where such values are often unknown.

REFERENCES

1. Tunnel Safety Regulations (TSR). (2020). Ministry of Transport
2. Regulations on Technical Requirements for Construction Works (TEK 17). 2017 Ministry of Local Government and Regional Development
3. Directive 2004/51/EC of the European Parliament and og the Council og 29 April 2004 on minimum safety requirements for tunnels in the Trans-European Road Network (2004). The European Parliament and the Council og the European Union.
4. Handbook V721 Risk assessment of road traffic. (2014). Norwegian Public Roads Directorate
5. Handbook N500:2024 Road Tunnels. (2024). Norwegian Public Roads Directorate
6. Risk Analysis AADT 4000/8000. (2018). Sintef
7. TS 2007:11 – Guidlines for Risk Analyses of Road Tunnels. (2007). Norwegian Public Roads Directorate
8. TØI Report 1948/2023, Vehicle fires in Norwegian road tunnels 2008-2021. (2023). Institute of Transport Economics
9. Handbook N500:2020. Norwegian Public Roads Directorate, 2020
10. Report 2013/05 – Lorry truck fire on the Rv 23, Oslofjord Tunnel, 23. June 2011. (2013). Norwegian Safety Investigation Authority
11. Report 2015/02 - Lorry truck fire on the E16 in the Gudvanga Tunnel in Aurland 5. August 2013. (2015). Norwegian Safety Investigation Authority
12. Report 2016/03 – Coach fire in the Gudvanga Tunnel on the E16 in Aurland 11. August 2015. (2016). Norwegian Safety Investigation Authority
13. Report 2018/04 – Fire in heavy goods vehicle in the Oslofjord Tunnel 5. May 2017. (2018). Norwegian Safety Investigation Authority
14. Vei rapport 2020/04 - Lorry truck fire on the E16 in the Gudvanga Tunnel in Aurland 30. March 2019. (2020). Norwegian Safety Investigation Authority
15. Guidance for Regulations on Technical Requirements for Construction Works, VTEK 17. (2017). Norwegian Building Authority

16. Building Research Design Guide 520.385, Required evacuation time in case of fire. (2016). SINTEF Building Research
17. A22149 / RAP_201 Åpen - E-39 Rogfast, Risk and vulnerability analysis tunnel. (2012). Sintef.
18. Major Accident Regulations. (2016, last updated 2024). Ministry og Justice and Public Security
19. News article rescue rooms Rennfast connection, 18 June 2012, Stavanger Aftenblad

A modified approach to walking speed within smoke-filled rail tunnels

Emil Persson, Niclas Åhnberg & Santiago Nordlund Gendra
Brandskyddslaget AB
Långholmsgatan 27, 117 33 Stockholm, Sweden

ABSTRACT

Lighting and walkway configuration have a clear impact on movement in a smoke-filled rail tunnel. During design, analysis and evacuation modelling, occupants' walking speed should be adjusted according to the visibility and the configuration of the tunnel. The walking speeds proposed in standards and default values in evacuation modelling tools are often based on an environment which does not fully correspond to environments as seen in today's newer rail tunnels.

Newer rail tunnels are often equipped with adequate lighting, walkways free from obstructions and handrails providing guidance and support. If the walking speed used during design and analysis can be increased to reflect a more beneficial environment in new tunnels, it could lead to distances between exits being extended leading to fewer escape routes being needed. Hence, refined analysis can provide large cost-savings.

This paper presents a case study where walking speed reduction due to visibility is varied within egress simulations. This given varied lighting configurations. The constant K, used for calculating visibility, is varied to illustrate impact of sufficient lighting. The paper also studies the impact of an increased minimum walking speed given a more preferable egress environment. For this part, the usage of wayfinding aids, e.g. handrails, is focus. Based on these aspects, the effect in terms of toxic exposure on the evacuees in case of fire will be studied.

Using CFD for fire modelling coupled with evacuation modelling, this study aims to highlight the shortcomings in current knowledge and provide a greater understanding for important input parameters when conducting egress analysis. Results show that an enhanced lighting configuration and tunnel environment can lead to significantly lower smoke exposure during egress. However, it is clear that a refined analysis approach equals greater challenges for the engineer conducting the analysis.

KEYWORDS: Walking speed reduction, rail tunnels, tunnel environment, evacuation, light configuration

PURPOSE

This case study investigates the impact of lighting configuration on walking speed, focusing on the constant K used for visibility calculations. The paper also studies the impact of an increased minimum walking speed given more preferable egress environments, e.g. use of continuous handrail. Using Computational Fluid Dynamics (CFD) and evacuation simulations, the toxic impact of smoke under varied conditions is analyzed. Findings aim to refine egress modeling, ensuring safety while optimizing design and cost efficiency.

DESIGN STANDARDS

The driving factor for conducting fire and egress analysis within rail tunnels is often optimizing distance between emergency exits.

The governing standard for subway systems in Sweden (Swedish Transport Agency) states that:

"If the distance between two escape routes is greater than 300 meters in one tunnel, the developer must determine threshold values for critical impact for evacuation. These limit values must not be exceeded during the required time for the evacuation."

The standard outlines threshold values which should not be exceeded during evacuation. Criterias include smoke and heat exposure and are listed below. These limits can be considered acceptable conditions to determine whether self-evacuation is possible or not. Within this study, the focus is on exposure to toxic gases. Based on experience, the threshold values for toxic gases are often exceeded earlier than the threshold values for heat and temperature exposure.

Toxic gases	The last group to evacuate can reach a point of safety before the toxic gases cause unconsciousness. A fractional incapacitation dosis (FID) of maximum 0.3 (excluding effects of Hydrogen Cyanide, HCN) is used as a criteria. *Note: A fractional incapacitation dose (FID) of 0.3 corresponds to approximately the most vulnerable 11% of the population being susceptible to compromised tenability, and an FID of 1.0 corresponds to 50% of the occupants experiencing compromised tenability.* Toxic gases 2.0 meters above walkways should contain at least 15% oxygen by volume, no more than 5% carbon dioxide by volume and no more than 0.2% carbon monoxide by volume.
Heat exposure	Prolonged exposure < 2,5 kW/m^2
Temperature	Air temperature should be below 80 degrees celsius.

Similar type of design standards, highlighting a need for fire and evacuation analysis, exists in other parts of the world.

ISO/TS 21602:2022

Walking speed reduction due to a decreased visibility can be found in some design standards.

ISO/TS 21602:2022 (ISO/TS 21602:2022, 2022) provides correlation between movement speed and smoke characteristics. However, the document does not consider the effects of smoke on way-finding behaviour.

The standard provides correlations for walking speed reduction to be used for deterministic analyses. For Method II within the standard, the first step is to define three different movement speeds in smoke

free environments (unimpeded walking speed). The movement speeds should reflect the population evacuating. During the second step, correlations describing the reduction of movement speed as a function of visibility distance shall be selected. *Figure* 1 below shows the correlation of three groups and how walking speed is reduced based on visibility.

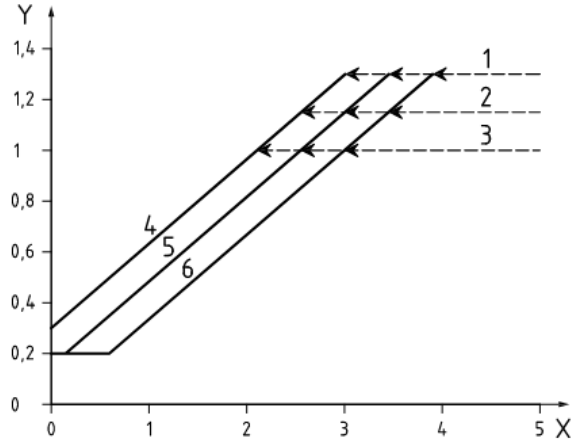

Key

X	visibility distance, *V* (m)	4	medium reduction
Y	movement speed, *v* (m/s)	5	early reduction
1	medium	6	very early reduction
2	slow		
3	very slow		

Figure 1 Example of correlation between movement speed and visibility according to Method II

The movement speed starts to reduce once low visibility prohibits free movement, i.e. when people are no longer able to move at their unimpeded speed without risking injury due to a collision or fall. The lower visibility distance typically corresponds to smoke-filled conditions, which create a situation similar to moving in complete darkness. Below the lower visibility distance, people move at a constant low movement speed at which collisions or falls lead to limited injuries.

The standard highlights that handrails along a wall can lead to a higher minimum movement speed in smoke. It also highlights that a continuous visual way-guidance system (e.g. light strip) can lead to a higher minimum movement speed. Uneven or coarse floor surfaces along with geometry requiring decision making leads to lower unimpeded movement speed and a more rapid reduction of movement speed in smoke. The impact of these factors are however not quantified and are therefore not explicitly included within the standard.

The standard also highlights the need of taking irritans species into consideration during analysis.

PREVIOUS STUDIES AND EXPERIMENTS

Research focusing on walking speed within smoke-filled rail tunnels is scarce. In Sweden, a minimum walking speed of 0,3 m/s have historically been used in analysis when evacuating through heavy smoke. The basis for this goes back to experiments conducted during the 1980s. In the upcoming sections some more recent research deemed suitable for the study herein is summarised.

Fridolf et al. (2016)
The report investigates how reduced visibility in smoke-filled environments affects walking speeds, based on data from several full-scale experiments conducted in different settings. The studies mentioned in the literature review include experiments where participants navigated through smoke with varying visibility distances.

One of the key findings is that the current state of research shows that there are major uncertainties

linked to the movement of people in smoke. A recommendation to represent occupants' walking speed in smoke is however presented, handling some of the these uncertainties. Three different methods are presented within the recommendation. Independent of method, the recommendation is that peoples' walking speed in smoke should be dependent on the unimpeded walking speed in a smoke-free environment. Hence, an individual assumed to move faster than another individual in a smoke-free environment will always be assumed to do so in a smoke-filled environment as well.

Method 2 in the report splits the population into the different categories; medium, slow and very slow. The figure below shows the walking speed for the different categories. It is up to the designer to choose the distribution of occupants for each category.

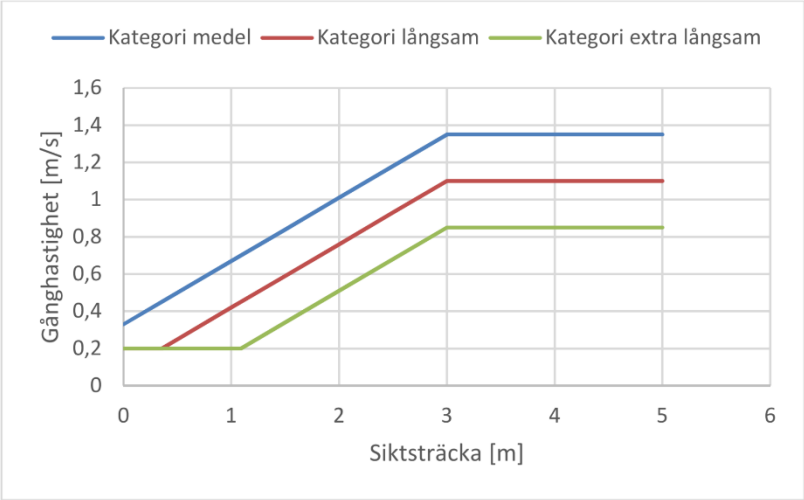

Figure 2 Diagram showing the applied relationship between walking speed (y-axis) and visibility (x-axis) for the three categories.

The minimum walking speed is 0,2 m/s, corresponding to situations where visibility is extremely limited. Note that walking speeds below 0,4 m/s have only been observed in environments containing obstacles in the form of cars in a road tunnel.

The literature review also contains an experiment in a complex environment representing a ferry or a hotel including stairs. In this experiment walking speeds below 0,4 m/s, including pauses for wayfinding decisions, were observed in low visibility. These experiments included different smoke environments and wayfinding aids with or without a handrail. It could be observed that a combination of wayfinding aids in form of handrail and reflective strips on the floor, or a reflective strip on the handrail (scenario 10,11 and 13), was significantly more effective than having only visual wayfinding aids (scenario 2-8) or only handrail (scenario 9 and 12).

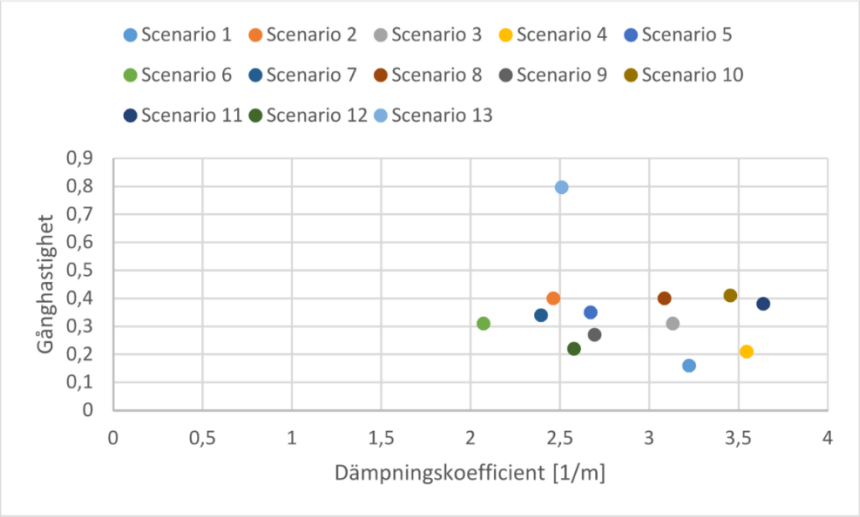

Figure 3 Correlation between walking speed (y-axis) and extinction coefficient (x-axis)

The report emphasizes the need for further research. Explicitly movement within environments with a visibility <3 metres is deemed important to study further. In addtion, the study recommends that future research aim to quantify the effect of other parameters and variables than visibility itself, both in relation to the behavior of people as well as their walking speed. Within this context, the use of handrails and light installation are mentioned.

Fridolf et al. (2013)
The report examines how smoke density affects evacuation speed, based on full-scale experiments. In total, 146 participants navigated smoke-filled tunnels, with extinction coefficients ranging from 1.2 to 7.5 m^{-1}. The tests included both a road tunnel setup and a rail tunnel setup.

At lower smoke levels, the average walking speed was 1.02 m/s, but it dropped to 0.42 m/s at higher densities. Factors like age, gender, and tunnel slope had no significant effect, but it was clear that most participants used the walls for guidance.

Ronchi et al. (2012)
The report focuses on how smoke density affects walking speeds in evacuation simulations and examines the role of different experimental data sets and model interpretations. The study compares two primary data sets being Jin's experiments and Frantzich and Nilsson's tunnel trials. It analyzes six evacuation models, including STEPS, to assess how embedded assumptions and default settings influence simulation outcomes.

The study underscores the importance of understanding how evacuation models interpret smoke-related data to avoid misinterpretations and emphasizes the need for the designer to re-evaluate the appropriateness of the default values for a certain evacuation model.

Fridolf et al. (2019)
The article provides an in-depth analysis regarding how walking speed is affected by smoke in tunnels and suggests methods for incorporating this data into fire safety design. Many of the findings presented inherit from (Fridolf, Nilsson, Frantzich, Ronchi, & Arias, 2016).

The document highlights the importance of visibility rather than extinction coefficient to represent walking speed, as people adjust their speed based on what they can see in the environment rather than theoretical smoke metrics.

The report emphasizes the importance of tactile or visual guidance, noting that people tend to follow walls in smoke to maintain direction and stability. This aligns with our interest in investigating

whether e.g. illuminated handrails can help evacuees maintain higher walking speeds in smoke-filled tunnels.

Additionally, the report reference to real-life incidents, such as the Gudvanga Tunnel, in which a fire occurred in a truck in Norway 2013. During this incident, a family of two adults and a 10 year old child managed to evacuate a distance corresponding to approximately 8 km in 90 minutes. The relatively high walking speeds observed in the Gudvanga tunnel fire could be linked to the limited irritating effects of the smoke due to the large air volme within the tunnel. However, the fire crew reported visibility as low as 0-2 m within the tunnel (Accident Investigation Board Norway, 2015). Hence, the incident indicates that a high minimum walking speed is possible even in smoke-filled environments. It also highlights how environmental conditions, such as ventilation and smoke irritancy, can affect walking speeds.

Yamada T. & AkiZuki Y. (Yamada T., 2016)
The correlation between soot density and visibility is described in the SFPE Handbook. The human eye can distinguish a sign from the background in smoke only when the difference between the luminance of the sign and the background luminance is larger than some threshold value of luminance contrast. Visibility therefore depends on the intensity of luminous flux from the background, the luminous flux from the sign and the properties of smoke.

In the range of visibility of 5–15 m, the constant K, of the visibility, V, at the obscuration threshold and the smoke density, Cs, is almost constant as expressed in equation below.

$$V = k\frac{I}{C_s}$$

Where:

V	Visibility of signs at the obscuration threshold [m]
k	Constant K
I	The intensity of light through smoke [cd]
C_s	Smoke density expressed by the extinction coefficient [1/m]

For reflecting signs, the product of the visibility and smoke density is almost constant as well. The product depends mainly on the reflectance of the sign and the brightness of illuminating light. The constant K varies between 2 and 4 for reflective signs and between 5 and 10 for light emitting signs. The visibility of other objects such as walls, floors ,doors, stairways, and so forth in an underground shopping mall or a long corridor varies depending on the interior and its contrast condition; however, the minimum value for reflecting signs may be applicable.

Note that the presented relation between the visibility of self-illuminated signs at the obscurity threshold and smoke density (extinction coefficient) from the experiments performed in Japan indicates that the constant K does not decrease at lower visibilities. The equation is used in FDS User's guide for all visibilities with a recommendation for constant K of 3 at light reflecting signs and 8 for light emitting sign. The equation is also used in ISO ISO/TS 21602:2022 for all ranges of visibility and a recommended range of constant K between 2 and 10.

METHODOLOGY

This paper presents a case study. It couples fire simulations with egress simulations to understand the impact on egress given the following two parameters:

- Lighting configuration along the walkway. This is conducted by varying the constant K, used for calculating visibility distance.
- Built environment along the walkway, e.g. continuous handrails. This is conducted by varying the minimum walking speed in smoke.

A quantitative approach is used studying the fractional incapacitation dose (FID) of toxic gases (excluding effects of Hydrogen Cyanide, HCN) experienced during evacuation. The calculation of FID is based on equations given in the SFPE Handbook (SFPE Handbook of Fire Protection Engineering, 5th edition, Society of Fire Protection Engineers , 2016). The FID values experienced are compared against the threshold previously explained (mainly a toxic FID < 0.3).

MODEL CONFIGURATION

Fire and smoke simulations were initially conducted using CFD. The results from the CFD simulation were thereafter input for egress simulations using the software STEPS. Further explanation regarding the modelling setup in given in the upcoming sections.

Fire simulations

A geometry representative of a generic single bore tunnel was used as a basis. The model consisted of a tunnel with a width of 5,6 m and a height of 4,8 m. A train with two cars was modelled within the tunnel. Each car was approximately 30 m. A walkway on one side of the trains was modelled within the tunnel. The walkway was modelled without elevation. Hence, the difference in elevation between the floor of the train cars and the walkway was 0,8 m.

The totalt length of the tunnel within the study was 800 m. The fire was located inside the train car closest to the North tunnel portal. The incident car was placed 200 m from the North Portal. A wind was applied from north as a pressure boundary. During cold condition, the airflow within the tunnel was around 1,2 m/s. See below for configuration.

Figure 4 Fire simulation configuration

The incident car was equipped with three doors leading to the walkway. Each door was 1.4 x 2.2 meters (width x height). Doors facing the walkway were all modeled as open throughout the simulation enabling smoke to reach the walkway early on. Doors on the other side of the train were modeled as closed throughout the simulation.

Windows in the incident car were modelled to break at different times depending on proximity to the fire sources. The windows have been estimated to brake at around 450 °C. The times for when windows fail are shown in Table 1. Note that these times are estimates and have been taken slightly earlier than when the temperature reaches 450 °C at window level, in order to avoid the risk of the fire becoming ventilation-controlled.

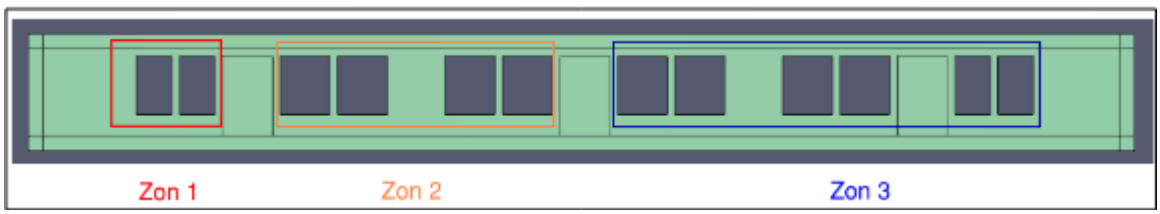

Figure 5 Window zones in the incident train car

A single fire size was simulated within this study. This includes a 20 MW fire with a medium growth

rate. The fire was deemed suitable based on experience and similar fire sizes are often used in Sweden to study egress. Three different burners were used as indicated in *Figure 4*.

Fire parameters were based on general recommendation within Swedish guidelines (Boverket, 2013) and the SFPE handbook (SFPE Handbook of Fire Protection Engineering, 5th edition, Society of Fire Protection Engineers , 2016).

Slice files were placed in the fire model to study results. The most eminent slice file being soot density at a height of 2 meters above the walkway. This was later to be used as an input in egress calculations.

Table 1 presents the parameters used for the fire simulation.

Table 1 Parameters for the fire simulation

Parameter	Value	Comment
Area of tunnel	27 m^2	Height 4,8 m Width 5,6 m
Length of tunnel	800 m	Deemed satisfactory for the current study.
Heat release rate	20 MW	Note that this fire size and growth rate is often not used strictly as a design fire. However, it is a common fire size used to study egress.
Fire growth rate	0,012 kW/s^2	
Window breakage (after fire start)	Zon 1 – 600 s Zon 2 – 900 s Zon 3 – 1200 s	See Figure 5 for applicable zones.
Simulation time	3600 s	This extent of time was modelled after the start of the fire. An extensive simulation time was modelled to ensure sufficient inputs for egress studies.
Slope	-	The tunnel was modelled without slope.
Surface roughness	250 mm	Based on experience and deemed suitable for the study.
Software	FDS 6.7.9.	
Fire parameters		
Yields	Soot – 0,09 g/g CO – 0,10 g/g CO_2 – 2,5 g/g	Deemed suitable based on Swedish guidelines (Boverket, 2013) and SFPE handbook (SFPE Handbook of Fire Protection Engineering, 5th edition, Society of Fire Protection Engineers , 2016).
Heat of combustion	20 000 MJ/kg	Based on Swedish guidelines (Boverket, 2013).
Constant K	8	Constant K, used for calculating visibility distance (slice files). This was later varied within STEPS as part of the purpose of the study.

The output from the fire simulation where used as input parameters for the evacuation simulations.

Evacuations simulations

It was assumed that the first egress point was 150 m into the tunnel (from the North portal), hence 50 m upstream from the incident train car. The second egress point was placed 600 m into the tunnel (from the North portal). Hence, there is a significant distance between the two egress points, see *Figure 6*. Note that the figure below does not show the entire length of the tunnel used in the fire simulation and shown in *Figure 4*.

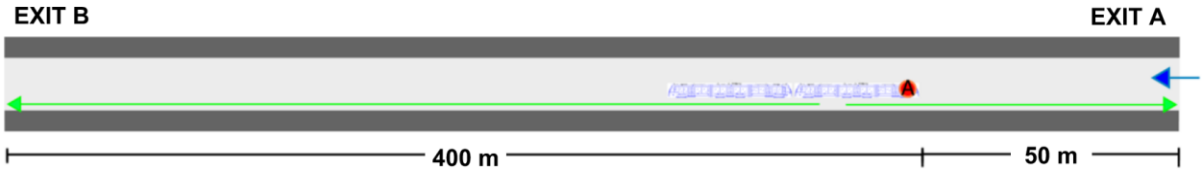

Figure 6 Distance from the fire-affected train car to the evacuation routes

The main principle is that passengers move away from the fire during evacuation. Hence, occupants within the non-incident train car were modelled to evacuated downstream, towards Exit B.

The train in the egress simulations had 1,35 m wide doors, with three doors per train car leading to the walkway.

The flow rate from the train cars to the walkway has been set at 0,52 p/s per door. The flow rate is based on experiments and recommendations (Niclas Åhnberg, 2017) regarding the flow capacity of the Swedish railway system for different door widths and height differences between the door and the walkway.

The walkway was 1,2 m wide in the evacuation simulations. For the walkway, a flow rate of 1,2 p/sm was assumed, corresponding to Swedish guidelines (Boverket, 2013), allowing two people to walk side by side.

The tenability criterias allow for movement in a smoke-filled environment, and walking speeds must therefore be adapted depending on the specific visibility. The unimpeded walking speeds and the walking speed reduction along the walkway used in the simulations can be linked to the research presented by Fridolf et al. (Fridolf, Nilsson, Frantzich, Ronchi, & Arias, 2016). The walking speed reduction due to a decreased visility is more significant for the slowest individuals than the reductions specified in ISO/TS 21602:2022 (ISO/TS 21602:2022, 2022). However, ISO/TS 21602:2022 includes correlations which do not cover individuals without full mobility, such as children (covering only the 80th percentile), whereas the proposal from Fridolf et al. (Fridolf, Nilsson, Frantzich, Ronchi, & Arias, 2016) includes the 97th percentile. *Figure 7* presents the applied walking speeds relative to the visibility distance in this case study. Note that the minimum walking speed presented in the figure is 0,4 m/s and that for some of the simulations the minimum walking speed was set to 0,2 m/s.

Individuals in the simulations are assigned one of the three representations of unimpeded walking speeds according to the distribution in *Table 2*.

Table 2 Distribution of representations of walking speeds in the evacuation scenarios.

Representation of walking speed	Distribution
Average	80 %
Slow	15 %
Extra slow	5 %

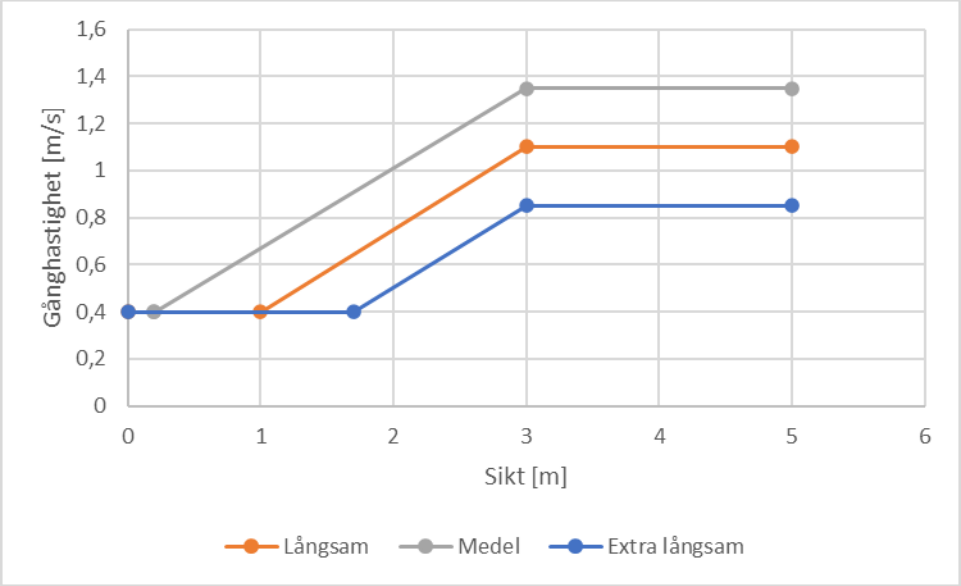

Figure 7 Diagram showing the applied relationship between walking speed (y-axis) and visibility (x-axis) for three groups.

Visibility distance which affects the walking speed of evacuees, is calculated using the soot density from the fire simulations according to the following equation:

$$V_s(t,x) = \frac{K}{\sigma * \rho_{sm}}$$

Where:

$V_s(t,x)$ Visibility as a function of time and distance from the fire [m]

ρ_{sm} Soot density from the fire simulations [kg/m^3]

K Constant K

σ Mass extinction coefficient, 8700 [m^2/kg] (Mulholland)

The soot density, used to calculate visibility, is taken at the height of 2 m above the walkway, in line with the perspective of a standing adult. The visibility is generally better at lower heights, even if the smoke layer is not clearly defined.

Within the simulations, visibility affects the movement of individuals, while doses of various gases are recorded for the evacuees. This is possible because output data from the fire simulations is imported into the evacuation simulation model.

Table 3 Parameters for the evacuation simulations

Parameter	Value	Comment
Constant K	Base value = 3 Alternative value = 8	For the scenarios with a value of 8, continuous light emitting LED handrails (1 m above ground) with sufficient light intensity are assumed.
Minimum walking speed	Base value = 0,2 m/s Alternative value = 0,4 m/s	For scenarios with a minimum walking speed of 0,4 m/s, a flat walkway, level with its surrounding is assumed, with handrails to follow a path without any obstacles along the way.
Occupant load	145 occupants per train car	The simulations were conducted with 2 train

		cars. Hence, a total of 290 occupants were simulated.
Time to initiation of evacuation	Fire-affected train car: 2 min Second train car: 4 min	Based on time to untenable conditions in the car and travelling time between safe areas.
Distance between evacuation routes	450 m	

Toxic exposure

The evacuation simulations generates output in the form of accumulated doses per individual. To calculate toxic exposure during evacuation, a so called fractional dose model is used. This model describes the combined effects of the toxic gases carbon monoxide (CO) and carbon dioxide (CO_2), as well as the impact of reduced oxygen concentration (O_2). The model indicates the sum of contributions to the dose an individual can tolerate for each gas at a given concentration and exposure time. The total fractional dose is calculated in time steps and then accumulated. When the sum of the doses exceeds a certain value, self evacuation can no longer be assumed for all individuals. In this case a FID value of 0,3 is used the threshold value. ISO-13571:2012 have been used for calculation the number of fatalities depending on the FID value. (SS-ISO 13571:2012 Livshotande parametrar i händelse av brand - Vägledning för bedömning av tiden till kritiska förhållanden vid brand,, 2012)

Simulation descriptions

A totalt of four different egress simulations were conducted as described below in *Table 4*. Except for the parameters outlined in *Table 4*, the inputs followed parameters shown in *Table 3*.

Table 4 Evacuation simulation descriptions

Evacuation simulation	Constant K	Minimum walking speed
Sim_A_1 (Base scenario)	3	0,2 m/s
Sim_A_2	8	0,2 m/s
Sim_A_3	3	0,4 m/s
Sim_A_4	8	0,4 m/s

RESULTS

The results from the fire simulations show that smoke spread is extensive downstream throughout the simulation. Once the fire grows in intensity, the backlayering increases. However, smoke does not reach the North portal.

Exposure to toxic gases

The maximum toxic gases FID, average egress time, number of individuals with FID over 0,3 and number of fatalities for each of the four egress cases are shown in *Table 5*.

Table 5 Analysis results

Scenario	Description	Avg. egress time [min][1]	Max toxic exposure FID	Number of personens FID > 0,3	Max time with visibility < 3m [min]	Consequence (Fatalities)
Sim_A_1	Constant K: 3 Minimum walking speed: 0,2 m/s	26	1,64	8	18	5
Sim_A_2	Constant K: 8 Minimum walking speed: 0,2 m/s	13	0,06	0	5,5	0
Sim_A_3	Constant K: 3 Minimum walking speed: 0,4 m/s	18	0,28	0	11	0
Sim_A_4	Constant K: 8 Minimum walking	13	0,07	0	5,5	0

	speed: 0,4 m/s					
[1] Average egress time according to the evacuation simulations						

Radiation and temperature exposure
For prolonged exposure, which can be equated to queuing for more that a few minutes, a threshold value of 2,5 kW/m^2 is applied as previously described. This corresponds to the radiation from fire gases at approximately 200 °C.

Results from fire simulations indicate that ceiling temperatures approaching these levels only occus after approximately 15 minutes into the fire development and above the fire affected train car. At this point, high radiation levels from the fire are localized, and the evacuees have already left the area near the fire.

Results also indicate that a temperature of 80 °C at a height of 2 m above the walkway is only evident beyond the proximity of the incident car after approximately 20 minutes. At this time, occupants have left this area and are therefore not exposed to temperatures above 80 °C.

DISCUSSION

The results from the egress simulations shows the significant impact the constant K can have. This highlights the importance that lighting configuration can have on evacuation. By changing the constant K , used for calculating visibility, to 8 instead of 3, the FID values are significantly lower (see Sim_A_1 vs. Sim_A_2, and Sim_A_3 vs. Sim_A_4). This emphasizes the importance of the engineer understanding the prerequisites for lighting and other visual way-finding aids within each tunnel project.

The results also indicate that an increased minimum walking speed can have a great impact on evacuation. When increasing the minimum walking speed from 0,2 m/s to 0,4 m/s, for simulations with a constant K of 3, the maximum toxic FID is significantly lower (Sim_A_1 vs. Sim_A_3). This highlights the importance of having an environment where navigation is possible with a limited risk for collisions or falls that lead to injuries.

The impact of the increased minimum walking speed is however not evident when comparing simulations with a constant K of 8. This since the visibility that evacuaees experience remains above 2 metres due to the relatively short evacuation times. If a greater occupant load was modelled, leading to an extended evacuation time, the impact of increasing the minimum walking speed is expected to be greater.

Based on the results, it is clear that the designer is faced by several challenges when analyzing egress. These challenges are both connected to inputs to use for evacuation simulations but also regarding which requirements to be set for the tunnel environment. Some of these challenges are deeper discussed below.

- **How should the constant K (used for calculating visibility) be assessed?**
  A constant K is chosen based on the lighting within the tunnel. A constant K of 3 is typically used for light-reflecting surfaces and a constant K of 8 is used for light-emitting surfaces. In many existing rail tunnels, the lighting configuration consists of light-emitting items placed approximately 25 m apart. Hence, within a heavy smoke-filled environment, e.g. visibility <3 m, these items will not be seen. Therefore, a constant K of 3 has historically been used when conducting egress analysis. Based on newer rail tunnels often being equipped with more sufficient lighting, e.g. continuous light strip, it is important that the designer takes this into account when selecting constant K. It can also be mentioned that contrasts have an impact on how a human eye distinguish a sign. Hence, a handrail, or walkway, being in clear contrast to a tunnel wall impose usage of a greater constant K. Also a greater illumination flux directed at the walkway, handrail or directly at the evacuee is of importance.

- **How should the walking speed be assessed based on the occupants' trust for the tunnel environment?**
  The answer to this question is not fully given in current research. The main aspect affecting this is the configuration of the walkway and a tactile guidance. Occupants are expected to walk faster if being comfortable with the layout of the walkway without fear for serious injury from fall or collision. Factors expected to lead to a greater walking speed includes;

  - walkway being straight throughout the tunnel,
  - no height differences between the walkway and the surroundings being present,
  - the walkway being even,
  - no obstacles narrowing the walkway being present, e.g. signaling systems,
  - and a continuous handrail being provided.

  The tunnel in the case study herein is assumed to be provided with the above. Therefore a minimum walking greater than 0,2 m/s, as suggested in ISO/TS 21602:2022 (ISO/TS 21602:2022, 2022) and Fridolf et al. (Fridolf, Nilsson, Frantzich, Ronchi, & Arias, 2016), was used for some of the cases. A minimum walking speed of 0,4 m/s was deemed reasonable, as the factors above were assumed, and the walking speeds below 0,4 m/s have only been observed in experiments containing obstacles in the form of cars in a road tunnel or stairs. However, a scientific basis for a precise effect of the parameters above or the explicit use of walking speeds greater than 0,4 m/s does not exist. If comparing to the Gudvanga accident, where a family evacuated with a walking speed of approximately 1,5 m/s (8 km in 90 minutes), a walking speed of 0,4 m/s is still deemed conservative.

- **How should walkways and lighting be designed?**
  The answer to this question depends on who is deemed suitable for selecting walkway and lighting design. In the end, the AHJ (Authority Having Jurisdiction) will decide the minimum requirements. However, an engineer responsible for evacuation assessment, should have an idea of how improvements can be cost-effective.

It should be noted that no explicit impact of irritant smoke is studied within this paper. Limited data exists regarding experiments in irritant smoke due to ethical restrains. Therefore, the impact on occupants evacuating is uncertain.

CONCLUSION

During design of rail tunnels, focus is often around design fires. Design fires play a major role in the design of fire-life safety systems for a rail system and can be the principal factor responsible for the sizing of the ventilation system or distance between exit routes. However, factors affecting walking speed during evacuation is another important parameter with uncertainties in need of focused research and guidance on selecting design values.

It is clear from the literature review provided that data from evacuation tests performed within a rail tunnel environment are few. Therefore, many of the input parameters being used within evacuation calculations are based on test and research inheriting from buildings and road tunnels.

The study has shown that enhanced design and refined analysishave the potential of providing more preferable results in terms of smoke exposure. Meaning that the distance between egress points can be longer, leading to great cost-savings. However, it is also evident that a refined analysis gives the engineer greater challenges connected to selecting both inputs and requirements.

The study focuses on impact of toxic exposure, due to a varied constant K and increased minimum walking speed given more preferable egress environments. Many simplifications have been made within the analysis and the extent of the study is rather narrow, e.g. only one fire sizes has been

studied. Hence, there is a clear need for sensitivity analysis and further research. Some parameters deemed suitable for sensitivity analysis include a varying walkway width and different fire parameters, e.g. heat release rate. Further research is needed regarding the impact on walking speeds in reduced visibility due to exposure of irritants, varying age of evacuees, functionality impairment and walkway surface.

REFERENCES

1. Swedish Transport Agency, ”Transportstyrelsens föreskrifter och allmänna råd om personsäkerhet i tunnlar och plattformsrum för tunnelbana och spårväg, TSFS 2017:119”.
2. ISO/TS 21602:2022, Fire safety engineering - Estimating the reduction in movement speed based on visibility and irritant species concentration, ISO, 2022.
3. K. Fridolf, D. Nilsson, H. Frantzich, E. Ronchi och S. Arias, ”Människors gånghastighet i rök: Förslag till representation vid brandteknisk projektering,” SP Sveriges Tekniska Forskningsinstitut, Borås, 2016.
4. K. Fridolf, K. Andrée, D. Nilsson och H. Frantzich, ”The impact of smoke on walking speed,” John Wiley & Sons, Ltd, Lund, Sweden, 2013.
5. E. Ronchi, P. Colonna, S. M. V. Gwynne och D. A. Purser, ”Representation of the Impact of Smoke on Agent Walking Speeds in Evacuation Models,” Springer Science + Business Media, LLC, The United States, 2012.
6. K. Fridolf, E. Ronchi, D. Nilsson och H. Frantzich, ”The representation of evacuation movement in smoke-filled underground transportation systems,” Elsevier Ltd, Lund, Sweden, 2019.
7. Accident Investigation Board Norway, ”Report on Fire in a Heavy Goods Vehicle in the Gudvanga Tunnel on the E16 road in Aurland on August 2013,” Lilleström, 2015.
8. A. Y. Yamada T., ”Visibility and Human Behaviour in Fire Smoke,” i *Handbook of Fire Protection Engineering, Fifth ed*, New York, Springer, 2016.
9. SFPE Handbook of Fire Protection Engineering, 5th edition, Society of Fire Protection Engineers, 2016.
10. Boverket, ”Boverkets ändring av verkets allmänna råd (2011:27) om analytisk dimensionering av byggnaders brandskydd; BFS 2013:12 - BBRAD 3,” Boverket, 2013.
11. K. H. &. A. E. Niclas Åhnberg, ”Report 2017:243 Utrymningsdimensionering vid upphöjda gångbanor,” Swedish Transport Administration, Borlänge, 2017.
12. G. Mulholland, ”SFPE Handbook of Fire Protection Engineering, chapter Enclosure Smoke Filling and Fire-Generated Environmental Conditions, 5th edition,” New York, Springer, 2016..
13. ”SS-ISO 13571:2012 Livshotande parametrar i händelse av brand - Vägledning för bedömning av tiden till kritiska förhållanden vid brand,,” Swedish Standards Institute, Stockholm, 2012.

Cross River Rail – Innovations in Metro Tunnel Ventilation and Fire Life Safety

Dr Nick Agnew, Michael Meissner, Dr Michael Beyer, & Ben Tuckwell
Stacey Agnew Pty Ltd, Brisbane, Australia

ABSTRACT

Cross River Rail (CRR) is a new metro rail line in Brisbane, Australia. Currently under construction, and nearing completion, the project includes 5.9 kilometres of twin tunnels and four new underground stations.

Tunnel ventilation is one of the key systems that will keep users of this city-shaping infrastructure comfortable and safe. The design of the CRR tunnel ventilation system incorporates numerous industry innovations in form and function. The CRR tunnel ventilation system (TVS) is discussed with respect to design philosophy and challenges, particular 1-D and 3-D numerical simulations undertaken, and the practical implementation of hardware and controls. A discussion is presented of interesting ventilation features, and importantly, how they interact with other life safety controls in the tunnels, on the rollingstock, and in the stations. To help minimise excavated station volumes, fan plant is centralised, tunnel ventilation ducts are integrated into station structural elements, draught relief paths are rationalised, and over-platform exhaust ducts are designed to also service air-conditioning supply. To minimise the number of fans, tunnel ventilation fans are used for both tunnel and station exhaust functions. Design challenges included working with structural constraints for trackway exhaust points and alignment of train operations and a new signalling design.

Underground fire life safety (FLS) is largely about smoke management. To provide a robust emergency response in tunnels, CRR utilises Saccardo nozzles at all station ends. For station trackway fires, CRR employs tunnel ventilation exhaust fans to bias smoke extraction over the platform, instead of over the train, and makes use of fire-hardened platform screen elements to reduce risk. To facilitate station evacuation, escalators automatically stop and reverse in certain fire emergencies, and front-of-house (FoH) lifts remain operational during a fire. These approaches are not common for modern metro systems.

This paper presents CRR as a case study in modern FLS and TVS thinking. Rather than dwell on design features, modelling, and design approaches considered to be “business-as-usual” for a modern greenfield metro system, the discussion focuses on a number of innovations and novel aspects of the CRR design which help to reduce asset and life safety risks, particularly during fire emergencies.

KEYWORDS: Rail, Metro, Fire Life Safety, Tunnel Ventilation, Cross River Rail

INTRODUCTION

With a total length, including surface lines, of 10.2 km, CRR connects the Brisbane suburbs of Dutton Park and Bowen Hills, and interfaces with the existing surface network. The project includes 5.9 km twin tunnels that pass under the Brisbane River and Brisbane central business district (CBD). CRR also includes construction of four new high-capacity underground stations at Boggo Road, Woolloongabba, Albert Street, and Roma Street. Figure 1 illustrates the underground portion of the layout, highlighting the location of the new stations. More general project information is available at

https://crossriverrail.qld.gov.au/. CRR will provide a second river crossing at the centre of the Brisbane suburban rail network, with future-proofed capacity to run up to 24 trains per hour in each direction. CRR is being delivered in partnership with the private sector through three major infrastructure packages of work: the Tunnel, Stations and Development (TSD) public-private partnership, the Rail, Integration and Systems (RIS) alliance, and the European Train Control System (ETCS) contract. The prime contractor, CBGU JV, is a joint venture of CPB Contractors Pty Ltd, BAM International Australia Pty Ltd, Ghella Pty Ltd, and United Group Limited. Stacey Agnew Pty Ltd was engaged by CBGU JV as the Fire Engineer of record for the tunnels and stations, and TVS scheme designer for the project.

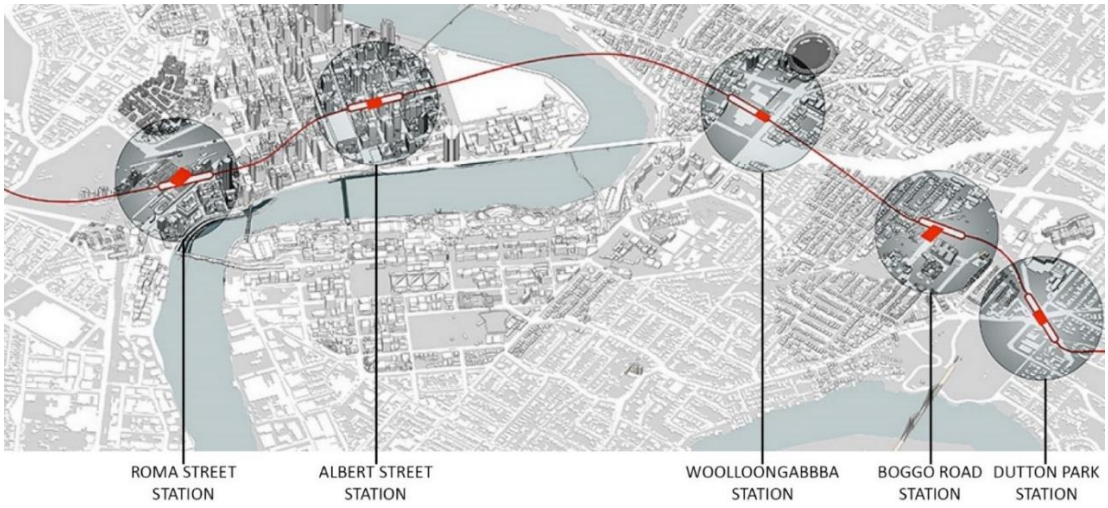

Figure 1 Project layout.

As the vertical alignment in Figure 2 shows, the tunnels were constructed mainly with tunnel boring machines (typically 6.2 m ID). The northern and southern ends incorporate cut-and-cover dive structures, and road headers were used to mine the tunnel between Boggo Road and Woolloongabba stations.

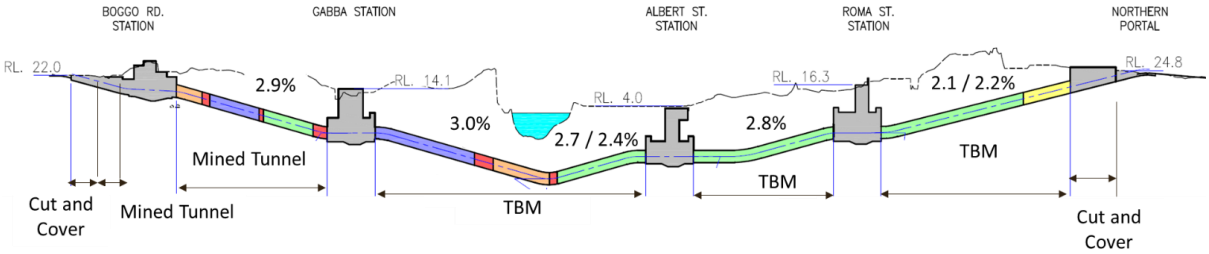

Figure 2 Vertical alignment.

The four new underground stations have a similar form, and range in rail depth between approximately 20 m and 30 m (refer Figure 3). Station functional elements include 220 m-long centre platforms to accommodate future 9-car New Generation rolling stock (NGR), a paid concourse level, and a shaft containing lifts and escalators to a surface entry structure (Albert Street Station has two access shafts connected to the station cavern via adits, refer Figure 4). Plant and other operational spaces are either located on levels below ground, or in separate service buildings. A common constraint for all stations was the limited surface access at each end of the main cavern. End egress routes and TVS duct paths to the surface or plant inevitably had to be reticulated back towards the centre of the station or substantially offset to the side of the main cavern.

Roma Street Station is somewhat more complex than the other stations as it is sited beneath existing surface rail and busway stations which it interfaces with, and which have been kept operational throughout construction of the new station.

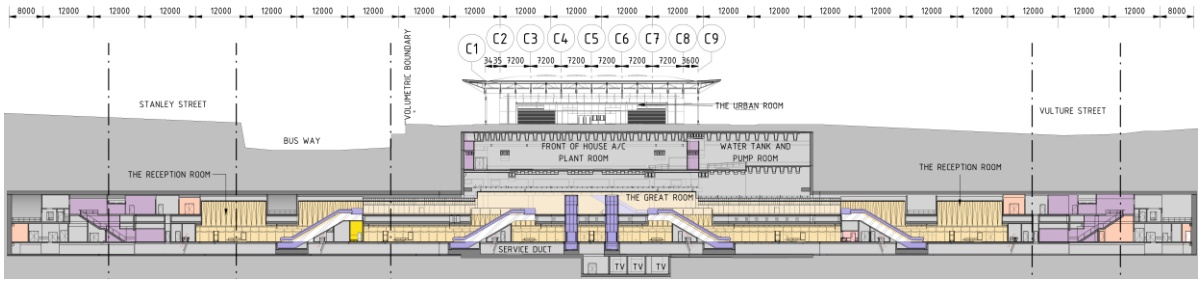

Figure 3 Section through Woolloongabba Station cavern showing public escalators, lifts, and end egress stairs.

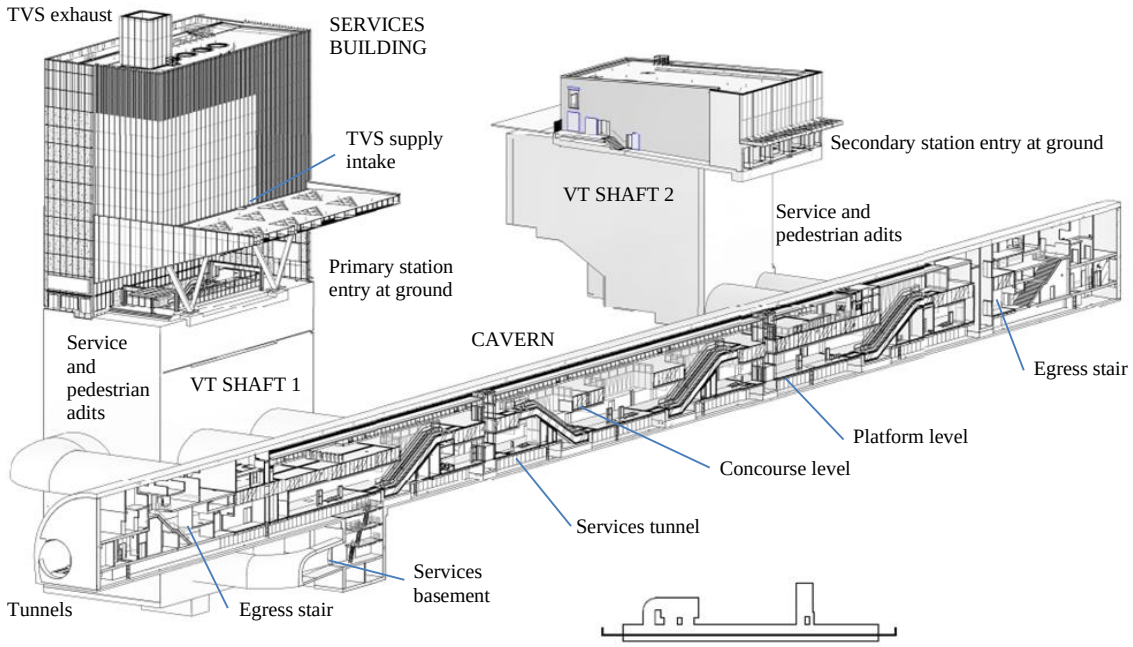

Figure 4 Isometric of Albert Street Station cavern centre showing buildings, shafts, and cavern.

Business-As-Usual Design Features

Underground rail networks are complex machines that transport people and keep people safe through various interacting physical and human-based systems. Compliance with the Rail Safety National Law in Australia requires that safety risks have been reduced so far as is reasonably practicable (SFAIRP). To demonstrate that objective with respect to FLS involves several sub-systems working in concert. At a high level, we consider the three broad elements of rolling stock, operations, and infrastructure in developing the overarching FLS strategy and subordinate FLS systems. Each system has been designed so that the network provides a level of safety that is intended to meet the owner's and operator's societal obligations. This introduces interfaces that do not exist for regular surface buildings. As a result, the FLS design required a "back-to-fundamentals" approach to engineering.

To provide context for the detailed topics below, there are features of CRR that experienced FLS and TVS practitioners would reasonably be expected to adopt, if not, at least consider, after applying applicable and required standards, accepted best industry custom and practice, and ultimately, due diligence. Additionally, the CRR Project Scope and Technical Requirements (PSTR) nominated certain approaches, standards, and explicit requirements, which were contractual obligations.

For the tunnels:

- 850 mm wide elevated tunnel walkway to facilitate detraining with fine expanded steel mesh surface and handrail (Figure 5), and integrated ladders to trackway. The chosen elevated

walkway width of 850 mm is consistent with that applied for all recent metro projects in the region, including Melbourne Metro, Forrestfield Airport Link in Perth, Sydney Metro, and City Rail Link in Auckland. 850 mm meets the minimum requirement of 800 mm set by the European Technical Specification for Interoperability (TSI) dealing with safety in railway tunnels, and is more than the 610 mm width required by NFPA 130

- Cross passages between tunnels spaced at approximately 244 m with sliding 1 m-wide doors, and clear passage width of 1.5 m (exits are more closely spaced at 60 m in the northern cut and cover portal section)
- Reversible longitudinal tunnel ventilation to control smoke, pressurise the non-incident tunnel, and prevent recirculation at portals
- Emergency lighting, directional wayfinding signage, CCTV
- Help phones in cross passages, and mobile and radio coverage
- Stringent control on fire performance of all materials
- Fire resistance to RABT-ZTV (train) and 4-hour ISO curve for structures adjacent to train
- Double hydrants spaced at 60 m to suit local fire department requirements with boosted ring main water supply for 30 L/s capacity
- Rail management centre supervision.

Figure 5 CRR TBM tunnel showing the elevated walkway and expanded steel mesh with 23 mm x 9 mm perforations (minimised in size to the extent that sufficient galvanizing thickness could be still applied).

For the stations:

- Station smoke management systems (mechanical and natural ventilation) with typically tens of metres of separation between discharge points and station entries and TVS intakes
- Smoke baffles/downstands around platform voids and other smoke reservoir interfaces
- Platform screen doors (PSDs)
- Reliance on normal station access routes for evacuation supplemented with pressurised fire-separated platform end stairs and corridors to the surface with an equivalent total clear width of 8 m
- Automatic stopping of downward escalators
- Evacuation populations calculated assuming various train populations, network perturbations and, for Roma Street and Woolloongabba stations, event loading
- Refuges, and back-of-house (BoH) lifts or stair lifts to assist people with reduced mobility (PRM) evacuate to the surface
- Fire detection (combination of aspirating, point smoke, multi criteria, heat and optical beam for public areas) and alarm systems in the stations, and fire control room
- Emergency lights and signage, strobe lights, repurposing of passenger and advertising signs for wayfinding for emergencies

- Combined public address and emergency warning system with a minimum speech intelligibility performance level of 0.6 STIPA
- Fixed fire suppression systems in station BoH areas (water or IG-541 gas in critical rooms), but not in any open public space
- Hydrants throughout with boosted supply and 30 m spacing on platforms, extinguishers, and hose reels in BoH areas
- Stringent control on fire performance of all materials
- Fire resistance to RABT-ZTV (train) and 4-hour ISO curve for structures adjacent to train
- Fire separation between BoH and FoH areas
- Minimum construction to the National Construction Code (NCC) of Australia for public assembly buildings
- Full staffing during operating hours and management centre supervision.

The NGR will be the only passenger rolling stock to use the CRR infrastructure and therefore will be the main fire hazard relative to the travelling public. While efforts to facilitate egress and control smoke vary widely (for example, there is very little possibility in some old London, New York, and Sydney tunnels), it is the low probability of an adverse event that allows the operational risk to be acceptable. That is, all underground railways inherently rely on taking a view of the risk, and not on a deterministic 'proof' of safe egress. A major part of that approach is to recognise the contribution to risk reduction of controlling rolling stock fire performance.

The NGR were specified with several features which act together to reduce FLS risk. It is important to understand these also for context, and to acknowledge the significant contribution to the network FLS safety case.

- 30-minute intercar fire doors that automatically close only on smoke detection
- Maximum fire power of 15 MW per carriage calculated using Duggan's method
- Minimum running capability of 10 minutes (with a fire on board)
- Materials and fire barriers compliant to BS6853 (Code of practice for fire precautions in the design and construction of passenger carrying trains) category 1b.

Demonstration of proper risk minimisation starts with being transparent about the risks. For CRR, a return period of the order of 500 years was estimated for a major fire occurring underground. Because of the exceptional fire performance of the NGR materials, the fire separation employed, and containment of services, a return period of 5000 years was estimated for a large saloon fire that causes a train to be disabled in a tunnel. This value was used to support aspects of the Safety Case.

TVS SCHEME

The CRR tunnels are longitudinally ventilated for smoke management, normal operations, congestion, and maintenance operations. For the purposes of this paper, only emergency functions will be discussed in detail. For design, the TVS was analysed using IDA Tunnel (Equa) for the primary 1D network simulations, and Fluent (ANSYS) and Fire Dynamics Simulator (NIST) for the 3D computational fluid dynamics (CFD). At the time of writing this paper, preliminary commissioning activities were underway to validate aspects of the design modelling. One modelling input, friction factor for the TBM tunnels, has been measured to be approximately 0.025, which is less than the value of 0.032 assumed for design. It is also consistent with a recent measurement undertaken for the new Melbourne Metro project in Australia.
At the Northern Portal, there is a significant step change in tunnel cross-section (28.8 m^2 to 96 m^2). Due to the significantly larger area, the target smoke control velocity cannot be practically achieved there. This required a different ventilation response for fires in the northern cut and cover section compared to the TBM tunnel sections. More closely spaced exits at a spacing of 60 m were constructed compared to the TBM tunnels to expedite evacuation. Similarly, at the Southern Portal there are step changes in the cross-sectional area where the target smoke control velocity cannot be achieved. CFD was used to demonstrate that the fire life safety requirements are met in the northern

and southern cut and cover tunnel sections during an emergency.

Plant is only located at the stations, and includes provisions for tunnel exhaust, over trackway exhaust (OTE), Saccardo nozzles for supply flow and thrust, tunnel-to-surface draught relief, and tunnel-to-tunnel draught relief (Figure6). With rolling stock that substantially regenerates braking effort, and roof-mounted air conditioning units, under-platform exhaust was considered unnecessary. For CRR, the TVS also services station smoke management requirements, and so the other exhaust elements connected to the TVS fans include the over platform exhaust (OPE), over mezzanine exhaust (OME), and over concourse exhaust (OCE). The OME exhausts smoke from the paid concourse area directly above the platform space. The OME duct is also used for station cooling supply during normal operations. The OCE typically exhausts from the upper escalator landing in the main access shaft.

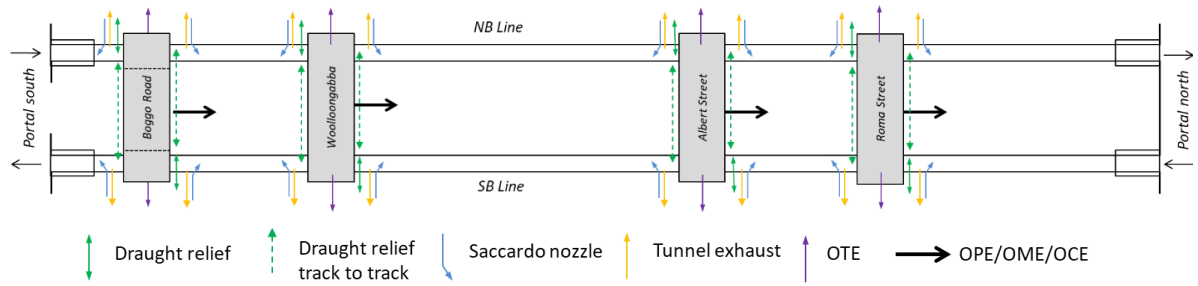

Figure 6 CRR TVS scheme.

The TVS design incorporates Saccardo nozzles at every station end of every tunnel. Saccardo nozzles generate thrust using a high-speed jet of supply air. TVS schemes that use nozzles are less sensitive to open PSDs than traditional push-pull systems that supply without injecting directional momentum into the flow. Nozzles provide greater flexibility and robustness than traditional push-pull TVS schemes. Safety during tunnel evacuation is increased.

Analysis confirmed that PSD state (open or closed) at the downstream station in the incident line will have a major influence on ventilation requirements. With downstream PSDs closed, the non-incident nozzle at the downstream station is not required to achieve minimum cross passage flows (non-incident tunnel to incident tunnel) and the upstream nozzle flow is reduced in most cases (subject to the system meeting minimum non-incident tunnel requirements). In practice, non-incident tunnel nozzle operation at the downstream station will not be required for most tunnel fire scenarios along the network as it is expected that downstream trains will depart, and so PSDs will be closed.

A dedicated system wide Tunnel Ventilation Control System (TVCS) will control the ventilation elements. The TVCS interfaces with the:

- Signalling system (either traffic management system or signal interlock system), to provide a stopped train (with location and train direction) signal to allow initiation of pre-programmed ventilation responses
- Fire system, which is networked and will action responses at stations
- Train management system, which will provide an indication of a fire alarm on the train (saloon smoke detector or linear heat detector around transformer).

The network is broken up into fire zones, each with a specific TVS response or “mode”. Other modes have also been defined to address fires occurring externally to the system as well as interface scenarios, where the incident train stops partly in a station and partly in the adjacent tunnel. Sub-modes are also included to account for open downstream PSDs, which reduce the effectiveness of the downstream tunnel exhaust.

For managing smoke in a tunnel, the Saccardo nozzles typically have a design capacity of up to 65 m^3/s (38 m/s throat velocity and 15° inclination), and the downstream exhaust, typically a capacity of up to 200 m^3/s (split between OTE and tunnel exhaust) (Figure 7). Ultimate system sizing assumed

open PSDs downstream. Although the automatic default response will be to drive smoke in the direction of train travel, the TVS has been designed to be reversible. Because tunnel air does not instantaneously stop and reverse direction because of the inertia of the air column, reversing the established flow in a tunnel will often involve risks associated with drawing smoke back over occupants. There is also significant uncertainty in determining the exact fire location on a train.

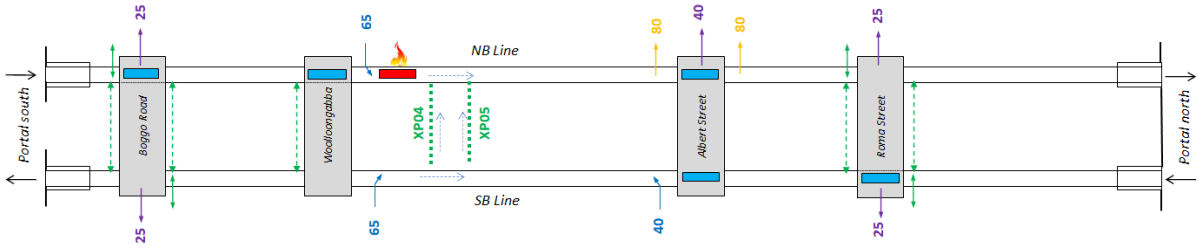

Figure 7 Example tunnel smoke management response (eg fire between Woolloongabba and Albert Street, with PSDs open downstream. Two open cross passages and smoke driven from Woolloongabba to Albert Street. Values indicate the supply or exhaust rate in m^3/s).

It is usual for metro stations to incorporate a common plenum at each station end, typically with reversible fans and a duct to the surface that can be used for exhaust, supply, or draught relief. A key feature of the CRR scheme was the capability for simultaneous exhaust on one trackway and supply on the other, at every station end. To achieve that, a manifold system was required, as described in the TVS plant configuration section below. That improves flexibility in response and ensures a robust outcome for tunnel fire incidents by providing positive flow from the non-incident tunnel to the incident tunnel at all open cross passages upstream and downstream of the incident.

The CRR TVS design has reduced performance risks associated with downstream trains not being able to move or downstream PSDs not being closed, so far as is reasonably practicable.

NGR Fire Size

Accepting that there is a continuum of possible fire scenarios, underground rail infrastructure for electric rolling stock is typically designed for a peak heat release rate (PHRR) of approximately 10 MW to 20 MW, with some down to 5 MW. With the NGR, the inter-car fire barriers will help contain the fire and limit its PHRR for some period of time to that of a single car. Design PHRR is not the same as ‘fire power’, which is often used to characterise rolling stock in a comparative way. A 15 MW to 20 MW fire power can be readily achieved with modest materials and moderate fire hardening. A fire power below approximately 10 MW to 12 MW is achievable but is more difficult and expensive. The CRR TVS and station smoke management design is based on a PHRR of 15 MW, as a high challenge scenario of a fully-involved carriage, a value consistent with the mandatory rollingstock interface requirements for the project. From the NGR design documentation, a maximum “PHRR” per carriage of approximately 11.5 MW was claimed based on a Duggan’s method calculation supported by benchtop test data. To highlight the conservative nature of the Duggan’s calculation, the NGR supplier data were processed in an alternative way with an assumed realistic longitudinal spread rate, which delayed the contribution of fuels along the carriage. For a fire spreading in two directions away from the fire seat in the saloon, the design analysis indicated that a more realistic PHRR for the vehicle is of the order of 8 MW (including the 1.5 MW ignition value incorporated into the calculations). On that basis, the TVS and station smoke management designs therefore include a safety margin.

Smoke Control Velocity

Early in design in 2020, calculations were performed to determine a suitable longitudinal velocity for smoke management. The PSTR required compliance with NFPA 502, excluding the NFPA critical velocity calculation in its Annexure D. For a maximum 3% gradient and PHRR of 15 MW, annular critical velocity estimates ranged from 2.2 m/s (NFPA 502:2014), to 3.2 m/s (NFPA 502:2017), to 3.5 m/s (NFPA 502:2020). In order to determine a reasonable tunnel air speed applicable to metro

tunnels for controlling backlayering to meet fire safety objectives, a CFD analysis was eventually undertaken using FDS, with later comparison to ANSYS Fluent used to verify robustness (using a volumetric heat source method).

Based on the FDS results, confirmed by Fluent results using volumetric heat source, an annular critical velocity of 2.6 m/s was recommended for the steepest tunnel sections along the alignment. Later analysis with Fluent using an updated methodology with a combustion model as a heat source and validated against the Memorial Tunnel (road tunnel) full-scale testing [1][2], indicated that, with no design margin, the critical annular velocity for CRR should be of the order of 2.15 m/s (refer Figure 8). Using the proposed semi-empirical formulae in [1] also results in a similar low velocity (~1.8 m/s for a nearly unobstructed tunnel based on a pool fire). The transition from no backlayering to uncontrolled backlayering of the train fire occurs quickly across a very narrow velocity range, highlighting the unstable nature of this physical phenomenon (ie practically, there is no "confinement velocity" that controls backlayering to a certain distance). The CFD methodology used was validated for a road tunnel scenario [1][2] with a blockage ratio much lower than typical metro rail tunnels, however, highlighting the need for future research on how the local 3D blockage effects impact critical velocity for metro tunnels. At the 2.6 m/s value adopted for design, backlayering is clearly prevented, ensuring a very robust response. Regardless, in many instances, ventilation capacity was driven by thermal management requirements and not smoke management.

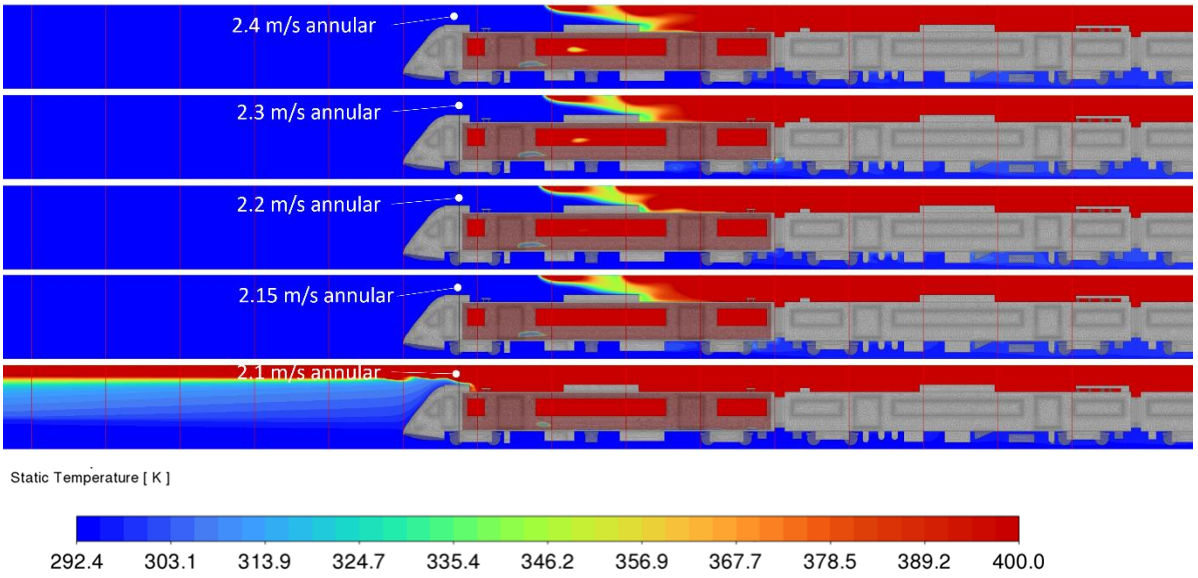

Figure 8 Modelling of critical velocity using ANSYS Fluent, and methodology calibrated against the Memorial Tunnel tests.

Two Trains

Allowing multiple trains in a ventilation section is normally avoided (eg as discussed in Australian Standard AS 4825) because FLS risk is increased when longitudinal ventilation is employed to manage smoke. Two stopped trains in a tunnel could result in smoke being driven over the non-incident train. Should an incident occur, the TVS provides longitudinal flow along the tunnel to prevent smoke spread upstream of the fire. In the case where a second train is present in the same ventilation section, smoke could be driven over the downstream train, and potentially many more people could be exposed to the hazard.

The probability of more than one train being present in a tunnel is a function of alignment and headway. If the system headway dictates multiple trains, intermediate ventilation shafts are sometimes required to divide long tunnels into smaller ventilated sections. With the nominal two-minute travel time between Woolloongabba and Albert Street Stations, constraining the system to a single train in that tunnel in all circumstances is not possible, especially for 9-car NGR operations, and considering the possibility of system perturbations following recovery after an operational event.

This “two-trains” issue is not unique to CRR, as other recent local projects have faced the same problem (eg Melbourne Metro and Sydney Metro). There are numerous systems around the world where the residual risk associated with having multiple trains in a ventilation section has been accepted by the operator. CRR uses ETCS to minimise the chance of more than one train being in a ventilation section at a time through block placement and minimum separation distances, supported with virtual home signals placed in the tunnel prior to platforms. Virtual home signals are placed at defined distances (typically 100 m to 300 m) ahead of station platforms. Trains will not be given a movement authority to leave a platform until the train ahead has passed the next home signal on route into the next station platform. Rail operations modelling was used to optimise home signal placement such that system headway and capacity would not be impacted.

During normal operations, under a two-minute recovery headway, it may still be possible for part of one train to enter the tunnels between Woolloongabba and Albert Street Stations at the same time as part of a second train that is close to entering the next station. With the imposed signalling constraint, it will not be possible for two trains to be present in any of the other tunnels because the travel time is much less than two minutes.

For two trains to be forced to stop in a ventilation section, a critical fault would need to occur on the leading train, or an unrecoverable operational condition would need to rapidly develop at the next station. For example, a train could break down just as it pulls out from Woolloongabba Station heading north. At that time, the following train in the tunnel is given authority to proceed beyond the home signal, and into the Woolloongabba platform. That scenario could result in parts of two trains being stopped in the Woolloongabba Station northbound trackway/ventilation section or in the tunnel between Albert Street Station and Woolloongabba Station.

ETCS will have other train management constraints to ensure that the platform ahead of any train on fire will be clear or at least will be able to be cleared without significant delay. As an example of such a constraint, no more than two trains in total will be allowed to occupy the first three ventilation sections immediately inside an entrance portal. Also, no more than two trains in total will be allowed to occupy the combination of Albert Street station platform and the tunnel between Woolloongabba Station and Albert Street Station.

These controls highlight the safety benefits of enabling the Fire Engineer, TVS designer, rail operations, and signalling designers to work together to reduce risk. In any case, if two trains were to stop in any tunnel, and one of those trains was on fire, the TVS has been designed to have capacity to generate sufficient velocity over both trains in either direction.

Smoke Dispersion

The CRR stations are located amongst other existing buildings. Albert Street Station is located in the middle of the Brisbane CBD, and Boggo Road Station is located in a medical research precinct and close to a hospital. Smoke dispersion modelling was undertaken with ANSYS Fluent for each station for a range of wind speeds and directions for the location (Figure 9). The discharge components assessed included soot, CO, CO_2, HCL, HCN, and SO_2 and were represented by a smoke fraction. Knowing the fraction of the individual components in the smoke allowed appropriate post processing of the overall smoke fraction. The assessments focused on potential for smoke ingress into station entries and supply points, adverse effects on fire department intervention points, and impacts on adjacent buildings in the vicinity of the station. The dispersion modelling was used to establish a minimum exhaust efflux velocity (typically 10 m/s), and for optimising the location and height of exhaust stacks and supply points which are several storeys above ground level. Guidance from HVAC standards with respect to separation of exhausts from other receptors is typically not applicable to modern metro TVS systems.

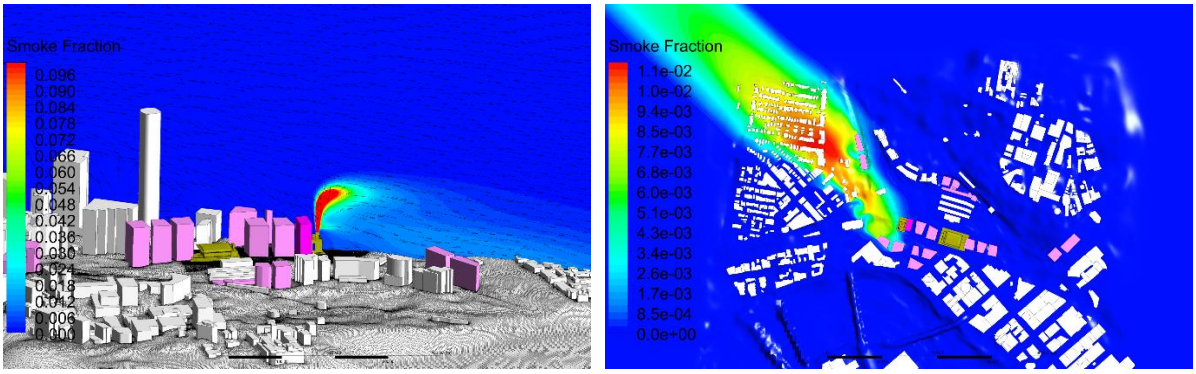

Figure 9 Example of smoke dispersion modelling undertaken, Roma Street Station, scalar smoke fraction shown, isometric (left), ground level concentrations (right).

TVS PLANT CONFIGURATION

Due to the CRR rail alignment, direct vertical access to the surface for TVS shafts at the ends of each station was not possible. A TVS plant arrangement was designed for all four stations with end plenum ducting connected back to a single central or offset plant space.

The following high-level objectives guided the development of the CRR TVS plant layout:

- Minimise the ventilation plant footprint and duct areas and hence the excavated volumes to reduce construction risk and costs
- Centralise TVS plant for ease of maintenance
- Minimise the number of fans to reduce capital and ongoing maintenance costs while ensuring adequate redundancy
- Use uni-directional fans; to maximise reliability and efficiency
- Maximise separation of station stacks from intakes and station entries to prevent re-circulation of smoke ejected to atmosphere in the event of a fire emergency with sizing of stacks and flow rates to meet minimum efflux velocity.

The CRR TVS plant layout (refer Figure 10 and 11) connects four corner plenums (located at each end of a station above each tunnel interface) to under-platform ducts, which in turn connect to supply and exhaust manifolds. One set of unidirectional axial fans service the exhaust manifold, and one set of unidirectional axial fans service the supply manifold. The supply manifold includes a single draught relief bypass. The system includes one single supply/draught relief shaft from the surface, and one exhaust shaft (with an area of approximately 20 m^2). Using dampers, each end corner plenum can be tasked with providing a draught relief path to the surface, supplying a Saccardo nozzle, or exhausting from the tunnel, OTE, OPE, OME, or, at several locations, the OCE. The TVS layout includes tunnel-to-tunnel cross over dampers at each station end for draught relief for normal operations, and plenum cross over dampers for enabling end plenums to share flows for certain modes. For metro stations, it is common practice to construct a draught relief shaft (normally 20 m^2 in free area) at each end of a station. CRR effectively utilises one 8 m^2 draught relief path to the surface at each end during normal operations. Modelling has shown that the tunnel-to-tunnel cross over paths provide higher draught relief flows than the tunnel-to-surface draught relief paths, however TVS thermal and air exchange criteria are still met for normal operations. Oversized draught relief paths to surface can limit air exchange effectiveness, as a larger proportion of the expelled vitiated air can be pulled back into the tunnel with train movements.

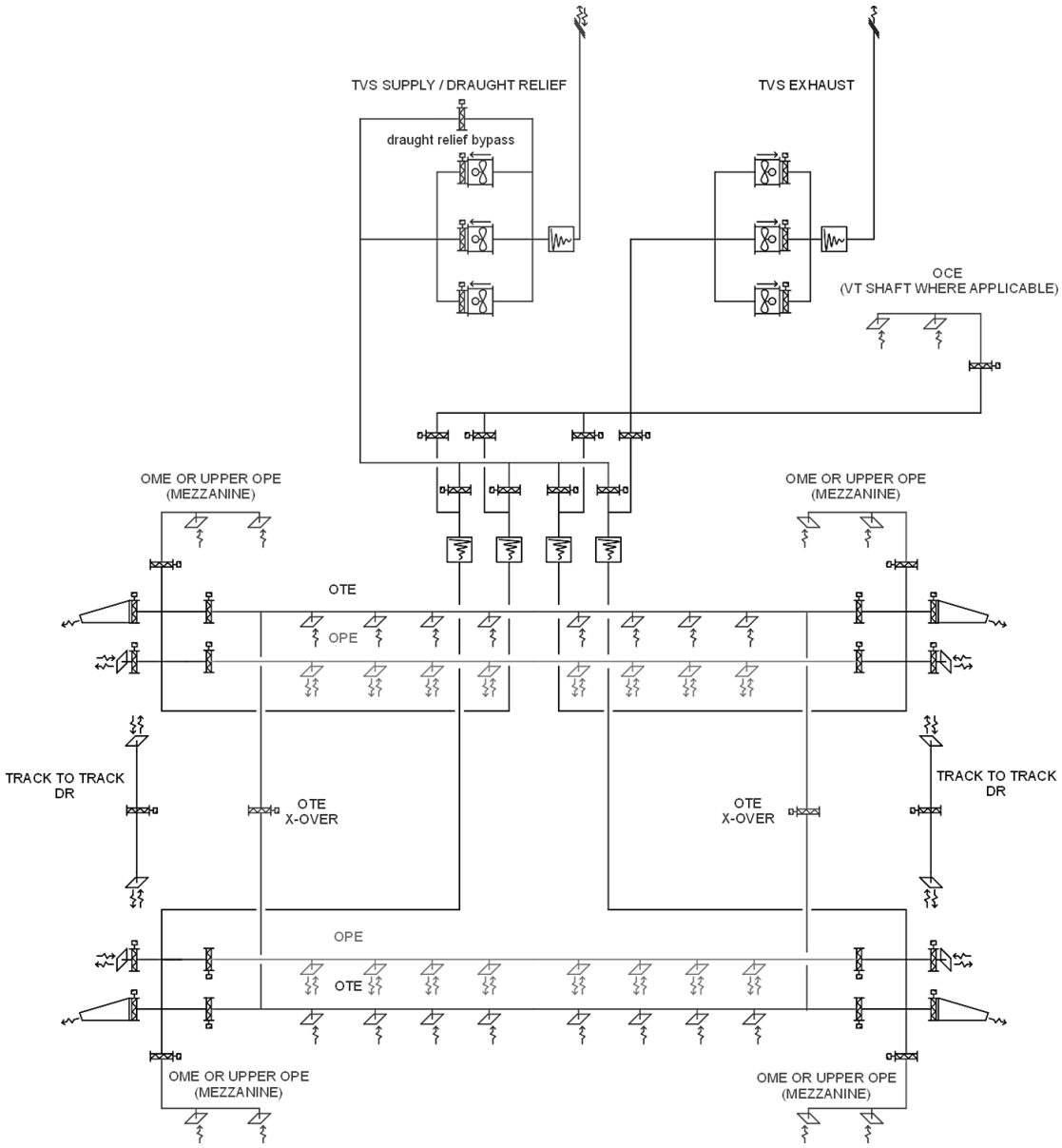

Figure 10 Generic CRR TVS plant layout schematic (details vary between stations).

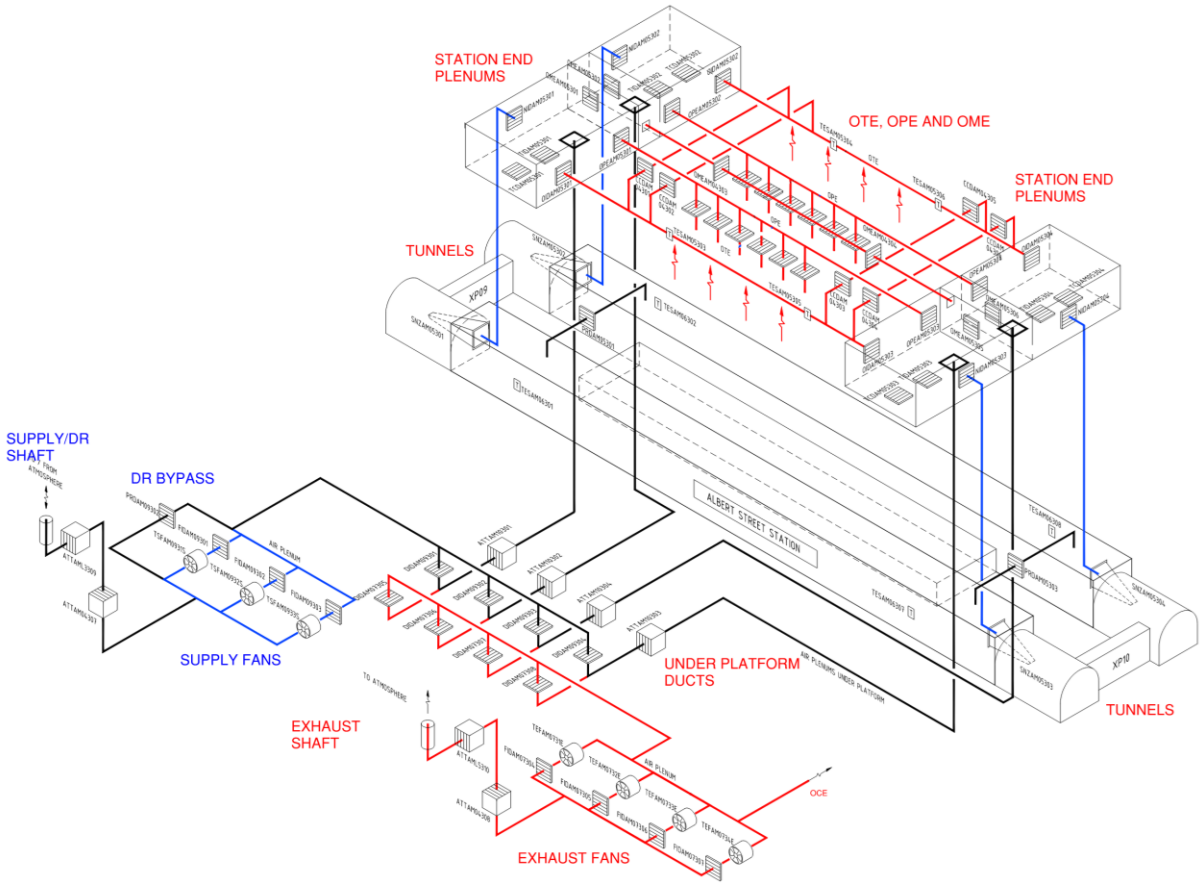

Figure 11 Generic CRR TVS plant layout isometric example – Albert Street Station.

PLATFORM SMOKE MANAGEMENT

For a train on fire at a station platform, it is common practice to manage smoke by exhausting over the train itself, or by using the tunnel exhaust points at each end of the platform. Some projects include supplementary mechanical exhaust over the platform space itself, but often at a much lower rate than from the trackway.

For a train fire at a platform, most smoke is ejected sideways into the station space. The CRR stations therefore bias the extraction over the platform, relative to the trackway in a 4 to 1 ratio. For a train fire scenario, the CRR OPE capacities range from 170 m^3/s to 200 m^3/s, while the OTE capacity is 40 m^3/s to 50 m^3/s. Such a high distributed exhaust rate along the platform is shown to greatly reduce the extent of spread along the platform, and to other levels of the station due to the high air velocities attained at voids. For the CRR stations, the aerodynamic connection (void areas) between the platform and concourse spaces has been minimised SFAIRP, with the Fire Engineer working closely with the project architects very early in the design. Smoke spread from the platform to higher levels in the station is minimised (refer Figure 12), due to the higher air velocities generated at voids. This important safety feature conflicts with typical political and architectural aspirations of openness and natural light.

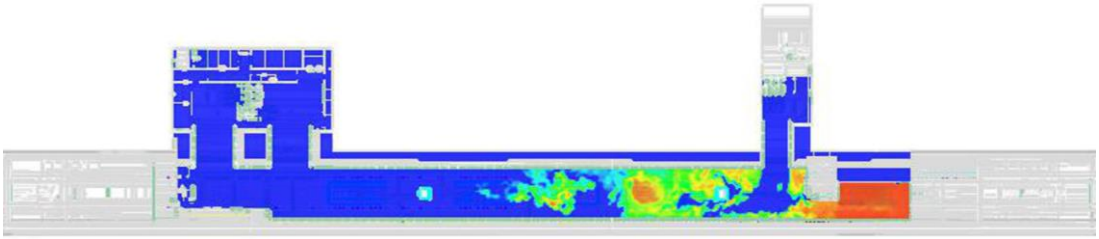

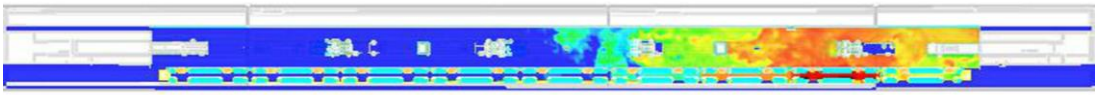

Figure 12 Example of modelled smoke from a train fire (15 MW PHRR) being controlled. Albert St Station, concourse level (top), platform level (bottom), visibility cropped to 0 (blue)-10 m (red), 900 seconds from ignition. The majority of platform and concourse kept clear of smoke. Adits and shafts to surface also kept clear of smoke.

As a good example of collaborative design optimisation, the OTE / OPE ducts were integrated into precast Vierendeel trusses spanning the station caverns (Figure 13), supported on corbels and with internal transverse and longitudinal ligaments. The OPE ducts also serve a secondary function as a cooling supply duct during normal operations, which is isolated when the duct is used in smoke exhaust mode, and non-return smoke dampers above the platform open. These features contributed significantly to minimising cavern excavation.

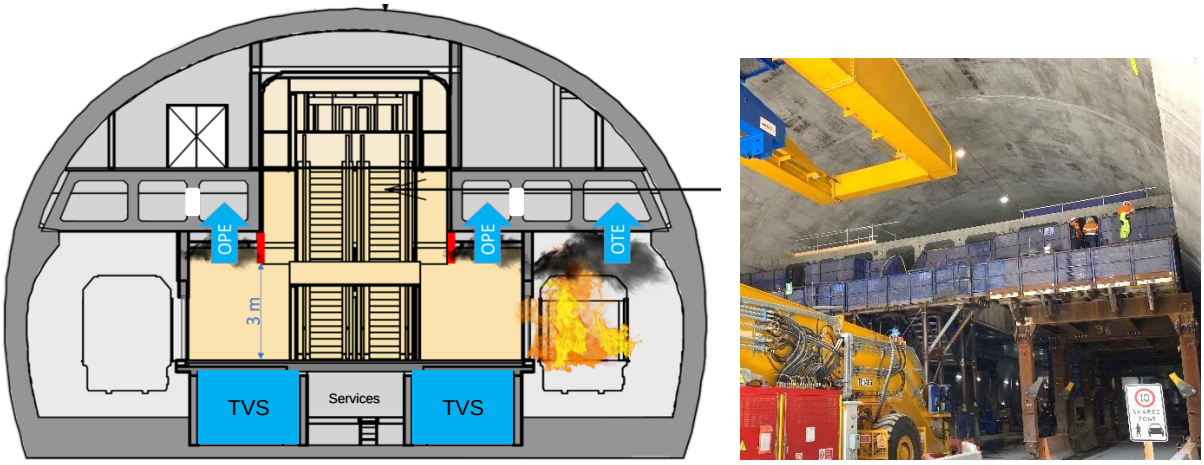

Figure 13 Platform OTE/OPE scheme (left) showing OTE/OPE response for a train fire at a platform, installation of a cavern Vierendeel truss showing voids used for TVS ducting (right).

Each CRR station is fitted with full height PSDs to enable bulk air-conditioning of the station FoH areas, to improve rail safety, and minimise smoke and dust infiltration from the tunnels. Fixed glazed panels and double-leaf hinged emergency egress doors (EEDs) are located between the automatic sliding doors (ASDs) at certain locations. Single leaf driver and guard doors are also provided. The number and setout of the EEDs was optimised following a risk assessment by the supplier, with input from the Fire Engineer. Similar to the ASDs, the EEDs and driver/guard doors are also equipped with manual release devices which allow them to be manually operated from the trackside in an emergency. During a train fire at a station platform, the ASDs are expected to remain open to enable passenger evacuation. If the fire continues to spread to involve a substantial portion for the carriage, the adjacent PSD line structure, EEDs and fixed glazing will fail after a short period of time following break out from the carriage. That failure process greatly promotes smoke spread into the station, stimulates a greater volumetric generation rate, and reduces the effectiveness of the OTE.

Platform Screen Door Design

It is not industry practice to intentionally design PSD assemblies for any fire resistance. To support the objective of reducing FLS risk SFAIRP, CBGU JV and the Fire Engineer worked closely with the PSD supplier to partially modify their existing product to have better fire performance, particularly for

the fixed PSD panels and EEDs. E30 glazing was incorporated into the safety glass laminate (11.52 mm for the EED and 13.52 mm for the fixed panels), aluminum cover plates and other structures were replaced with stainless steel, stress concentrators were removed around EED hardware, and retaining clips were included to support the glass when the main gaskets/seals failed. The PSD bulkhead, which forms the smoke reservoir over the train which is expected to see high temperatures, and hangers and beams supporting the PSD line were encapsulated to provide a minimum 60-minute fire resistance.

Additionally, the lower guide on the sliding PSDs was modified to include a roller bearing to ensure the doors are less sensitive to differential pressures driven by trains or TVS. This has been an issue on two other recent metro projects in Australia. In both cases the lower guides were a simple tongue-in-groove arrangement.

The EEDs and fixed panels were fire tested (Figure 14). The fixed assembly did not fail for the duration of the 30-minute test. This outcome was considered acceptable, and consistent with reducing risk SFAIRP. For the EED, failure of the assembly commenced approximately 7.5 minutes into the test. 7.5 minutes is longer than the time required for evacuation of the station platforms. Failure appeared to be due to the frame of the hinged EED flexing while being constrained by the corner locking pins. There was no apparent solution to improve this response without a complete redesign of the platform screen system. On that basis, the EED test outcome was considered acceptable, and also consistent with reducing risk SFAIRP.

Figure 14 Fixed panel fire test after 30 minutes (left), EED assembly fire test after 7.5 minutes (right).

VERTICAL TRANSPORT

The CRR FLS strategy includes using vertical transport elements such as FoH escalators and lifts to facilitate evacuation. Other emergency egress paths are also provided (eg pressurised fire-isolated end stairs with an adjacent BoH lift or stair lift for PRM); however, people are likely to preference access paths they are familiar with.

Automatic Escalator Reversal

On an initial fire alarm, escalators operating in the downward direction will be automatically stopped by the fire system, following thirty seconds (NFPA 130 requires a minimum of 15 seconds) of an audible signal or warning, and flashing visual warning (including flashing under-handrail lighting). On a second or verified FoH fire, the escalators will also automatically reverse after being stopped. Reversing any downward escalator instead of just stopping it, doubles its available egress capacity (from approximately 56 ppm to 121 ppm). It is noted that the egress calculations also considered escalators out of service and unavailable for evacuation.

As the tread rise of escalators is higher than for normal stairs, many people may find it difficult to ascend a stopped escalator for any significant distance. Given the depth of the CRR stations, an egress

path to the surface would require ascending three or four escalators. It is expected that such a path using stopped escalators alone would be arduous for many people, resulting in an extended evacuation time. Falling forward on a stopped escalator is also a credible safety concern. Risk would be increased in life-threatening circumstances.

Station staff are provided with the ability to arrest the reversal process if the fire is small, or conditions are clearly tenable. For fires or evacuation circumstances that exceed design assumptions, reversal is still considered to be a safer option, as the risks of trips and falls due to the reversal process are considered to be very low. By automatically reversing the escalators, station staff will be kept free to provide evacuation assistance to station occupants such as PRM. This approach has been adopted only for station FoH fires and not BoH or tunnel fire scenarios. One risk associated with automatic escalator reversal is the potential for slips, trips, and falls due to the acceleration in the reverse upward direction while people are facing downwards. This risk was considered and balanced against the benefits of automatic reversal. The escalators are designed with controlled automatic deceleration and acceleration rates of less than 0.052 m/s^2. The ASME Handbook on Safety Code for Elevators and Escalators (2016), nominates a maximum acceleration/deceleration rate of 0.3 m/s^2 to ensure passenger safety when speeding up or slowing down escalators and moving walkways. The specified value for CRR is clearly well below this value. Literature also suggests 1 m/s^2 as the recommended value to be used as a design and acceptance value for escalator braking system performance in order to prevent passenger falls [3]. In accordance with EN115-1, escalators or moving walks which start or accelerate automatically by the entering of a passenger shall move with at least 0.2 times the nominal speed and then accelerate at a rate of less than 0.5 m/s^2. The CRR escalators have also been designed such that any passenger who steps onto an escalator at mezzanine level at the time of a fire alarm, will likely make it to the platform level at the bottom as the escalator stops, and well before the escalator reverses.

FoH Lifts

Normally lifts in buildings are either stopped or forced to home to a designated level on fire alarm in accordance with local standards or building code. The FoH lifts in the CRR stations, which are typically contained in glazed shafts, are kept operating on fire alarm to aid the evacuation process. They will only stop/home if smoke is locally detected at the base or within the shaft. If the FoH lifts become unavailable, other fire-isolated and pressurised egress paths are available at all FoH levels. FoH lifts are not provided with smoke lobbies or pressurisation systems.

NO SPRINKLERS IN OPEN FOH AREAS

Sprinklers are normally intended to reduce fire growth and prevent spread (if there is fuel to burn), protect people in other (adjacent) building areas, and protect structure and assets. Sprinklers are not intended to facilitate egress or protect people in the space where the fire is located. Sprinklers or gas suppression is installed in BoH areas where there is sufficient fuel load. In the FoH areas, sprinkler coverage will be limited to locations with elevated hazard such as amenities, vending machine alcoves, and offices. Sprinklers are not being installed in the fire-sterile open FoH areas such as platform, mezzanine, or concourse circulation areas used by the public. The station smoke management systems and station structures have been designed to account for foreseeable fires in those areas, as an alternative means for managing risk. In such areas, sprinklers would increase FLS risk with all things considered and so are inconsistent with the life safety intent of both the Australian National Construction Code (the Building Code) and NFPA codes.

By not installing automatic sprinklers in the public areas:

- The volumetric rate of smoke generation will be minimised (sprinkler activation generates a higher volume of smoke). This is due to the additional entrainment
- The effectiveness of the smoke management system will be maximised to remove smoke and improve egress opportunity. Less smoke volume and hotter smoke will both act to improve extraction effectiveness

- Visibility will be maintained to facilitate safe evacuation. The action of sprinklers introduces a downward momentum source which causes smoke to be mixed downwards. Such mixing spreads smoke and lowers the smoke layer which will affect visibility locally where sprinklers have discharged, and remotely
- Visibility will be maintained to assist intervention, and therefore fire fighter effectiveness and safety will be improved
- Risks associated with steam generation and flaring are mitigated
- Risks associated with installation and maintenance are mitigated. Sprinklers require occasional maintenance and inspection at high level which would not be required if there were no sprinklers
- Risks associated with slips, trips and falls are mitigated. In the author's opinion this has a negative safety implication, albeit a minor one. Water on any walking surface clearly elevates slip, trip and fall risk to an extent, albeit to a minor extent
- Risks associated with extended duration of sprinkler flows causing anxiety and potentially crowd panic are mitigated. This is a logical conclusion and is supported by the opinion of the Project's human factors specialist. It is considered that such risk is minor.

Fusible sprinkler heads remote from the fire site can be inadvertently activated with no potential for suppression of the fuel sustaining the fire. The dynamic air flows along the platform will cause smoke to spread, potentially via the trackway through multiple open PSDs also.

For major train fires (which need to involve materials in the saloon), platform sprinklers will do little to get water onto the fire seat and fuel within the incident carriage. This is logical, given that the fire is shielded, and the sprinklers are to the side of the PSD line.

For minor under-train fires (expected to be more common than saloon fires), platform sprinklers will do little to get water onto the fire seat and fuel. This is also logical given that the fire is shielded, and the sprinklers are to the side of the PSD line.

All materials used in the stations (and tunnels) are strictly controlled to ensure low flammability, low smoke emission, low toxicity and zero halogen, so far as is reasonably practicable. In some cases, where a risk assessment has been required, material fire performance has been tested in a semi-qualitatively way by the Fire Engineer. All combustible materials in the stations and tunnels have been (or will be) assessed, with the approvals and supporting information being captured in a database with proforma site inputs, and any relevant evidence of test certification.

With the factors above considered holistically, it was determined that sprinklers in any of the public FoH circulation areas would increase FLS risk. This direction was accepted by the reviewers and local fire department and is at the extreme of the various approaches taken on other metro projects in Australia. The new Melbourne Metro employs sprinklers throughout all FoH areas. The new Sydney Metro employs sprinklers throughout FoH concourse spaces, but not platforms.

CONCLUSIONS

Cross River Rail in Brisbane, Australia, incorporates several TVS and FLS design features discussed above that demonstrate fresh design thinking and novel implementation, resulting in safer infrastructure and reduced construction costs. Key to the successful delivery of the project and the realisation of these design features were:

- Removal of an often-problematic design interface between FLS strategy and TVS/station smoke management schemes by having the same responsible person fulfilling both functions
- Willingness by the contractor to explore design improvements and industry innovation
- Early collaborative coordination between the Fire Engineer/TVS designer, the constructor, other design disciplines, such as architecture, structural engineering, geotechnical

engineering, tunnel and building Mechanical and electrical services, and PSD designer/supplier
- Early and proactive engagement with the state client, railway operator, local fire brigade, and various project reviewers
- Efficient professional and collegial design peer review and safety case assessment processes.

REFERENCES

1. Beyer, M., Stacey, C. & Brenn, G. A Mixed Convection Model for Estimating the Critical Velocity to Prevent Smoke Backlayering in Tunnels. Fire Technol 61, 295–342 (2025). https://doi.org/10.1007/s10694-024-01607-8.
2. Beyer, M and Stacey, C., "CFD Validation for Tunnel Smoke Control Design," in 11th International Conference Tunnel Safety and Ventilation, Graz, 9th and 10th May 2022, https://openlib.tugraz.at/download.php?id=6315edb636dbb&location=browse.
3. Al-Sharif, L., "Modelling of Passenger Falls on Escalators and the Control of Braking Systems to prevent them: Putting it all together", Elevcon 2012, Florida, USA, Volume: 19.

Smoke Management, Differential Pressures on Egress Doors and Controls during Fire Evacuation in Metros

Evangelos Krokos[1] & Marios Kalyvas[1]
[1]Mott MacDonald, Sydney, Australia

ABSTRACT

Metros require the design, engineering and assurance of a plethora of rail and station systems. Among these systems, the tunnel ventilation and smoke management systems typically give rise to a lot of controversy. One of the reasons is the lack of prescriptive standards on smoke management along the trackway and at the station levels. Another is the absence of a holistic view in their design that could allow the set out of design objectives accounting for the functions provided by other systems and the pragmatic risk assessment of the simultaneous occurrence of multiple events and faults. As a result, the Tunnel Ventilation Fans (TVF) are predominantly sized to manage the temperature along a tunnel section in which trains are congested, resulting in airflows typically above 100 m^3/s and high negative differential pressures along the trackway that can obstruct the evacuation of passengers through the Trackway Exit Doors (TEDs) to the platform. In this study, we argue that such oversized airflows are not required since the Grade-of-Automation-4 (GoA4) enabled Communications-Based Train Control (CBTC) rail signalling system and the Command-and-Control Centre can minimize (if not eliminate) the potential risk on trains being congested in the tunnel. We, thus, recommend the sizing of the tunnel ventilation fans to be performed only considering the tunnel critical velocity. To justify our argument and recommendation we have calculated with 1D and 3D Computational Fluid Dynamics (CFD) the differential static pressure between trackway and platform as well as the smoke propagation in two distinct fire-in-train events, respectively. In the first one (FE-1) the train stops at the platform, whilst in the second one (FE-2) the train stops in the tunnel between two adjacent stations. The results demonstrate that by extracting smoke using the platform smoke exhaust fans in FE-1 and by sizing the TVFs considering only the critical velocity in FE-2, not only smoke is managed effectively, but also the high negative differential pressure between trackway and platform is eliminated, enabling unobstructed evacuation through the TEDs. Finally, we propose the incorporation of a novel control system architecture that will allow the seamless integration of the involved systems, simplify the testing and commissioning processes and enable the on-time delivery of the entire system without functional gaps and flaws.

KEYWORD: Smoke Management, Tunnel Ventilation, Fire Engineering, Fire Life Safety, Industrial Control Systems, Systems Engineering, Systems Assurance, Systems Integration, Metro, Rail.

INTRODUCTION

Efficient design, engineering and assurance of Metro systems is a challenging task that requires careful consideration of many aspects of the systems life cycle. When systems provide critical functions in fire evacuation operating conditions, which are required to assist passengers to reach safely a pre-determined point-of-safety, their functional integration is of the utmost importance. Unfortunately, more often than not, the latter is overlooked, and systems are designed as if operating in isolation rather than integrated with other rail and station systems. Tunnel and station smoke management systems are not an exception, hence, they are usually overdesigned and complex in terms of their operation under different circumstances. Regarding the tunnel ventilation system, it has been observed in some Metros that high differential static pressures are developed between the trackway and the platform, separated by the ceiling-to-platform wall of the platform screen doors, when the

tunnel ventilation system operates in smoke management. As a result, opening of the evacuation exit door from the trackway to the platform could potentially be obstructed. This may not be a problem when an incident train stops at the platform and passengers evacuate through the platform screen doors, but it is undesirable in the occasion that the platform screen doors cannot open, or the train stops in the tunnel between adjacent stations. Motivated by these observations we modelled different system configurations and investigated with 1D and 3D CFD potential solutions to overcome this issue. In addition, we considered the functionality of CBTC signalling and SCADA-based systems which are able to automatically, semi-automatically, or manually adjust the configuration of the entire rail system. In so doing, we investigated potential synergies and their impact in the identified issue of high differential static pressure build up along the trackway. To the best of our knowledge, a fully integrated approach for ensuring unimpeded opening of trackway egress doors under operation of smoke management systems at underground metro stations has not been investigated in the relevant literature [1]. Instead, analyses [2] and testing [3] are focused on examining mechanical ventilation induced forces on cross-passage doors and prevention of smoke ingress through them. In the following sections, we present the system configurations we used; the various parameters involved in the modelling of the infrastructure, the systems and the fire event; the results of the CFD calculations; and we discuss two topics which we consider important for the design and implementation of smoke management or other Metro systems, i.e. the architecture and attributes of a centralized control system, and the risk analyses and assessment of multiple-events (faults).

SYSTEM CONFIGURATIONS & PARAMETERS

The modelled system comprises of a railway Tunnel Section (TS); Station Platform (PL); Platform Screen Doors (PSDs); Trackway Egress Doors (TEDs); Tunnel Ventilation Fans (TVFs); Smoke Extraction Fans (SEFs); and Motorized Dampers (MDs). It is assumed that the mechanical equipment is utilized by means of timely sequences of control signals generated by an Industrial Control Signal (ICS) designed to provide Fire and Life Safety (FLS) functions. The control signals are engineered to implement pre-determined system configurations for two specific fire-in-a-train events, i.e. activation of specific TVFs, SMEs, and MDs.

In the first fire event (FE-1), the train on fire is stopped at the station platform and the passengers evacuate through the platform screen doors to the station platform. In the second fire event (FE-2), the train on fire is stopped between two adjacent Metro stations (upstream and downstream with respect to the train movement direction) and the passengers evacuate through the trackway exit doors to the platforms of the stations adjacent to the tunnel section where the train is stopped. The TEDs can be accessed by the walkway along the incident tunnel or the non-incident tunnel through the cross-passages. In FE-1, the purpose of the activated mechanical equipment is to manage smoke propagation at the station platform in such a way that along the egress routes smoke is adequately stratified to enable self-rescue. In FE-2, the purpose of the activated mechanical equipment is to provide an egress path by controlling the smoke spread in the upstream direction in respect to the train movement. It is noted that smoke can be pushed and extracted either downstream or upstream. We chose the former being mindful that passengers may attempt evacuation in this direction. To the best of our knowledge, the only way to enable safe evacuation in both directions is by means of vertical smoke extraction (transverse type) along the tunnel. This alternative requires careful consideration of many parameters, including the tunnel geometry, and is currently under investigation. The results of this investigation may be presented in the future. Figure 1 and Figure 2 depict the modelled system in case of FE-1 and FE-2, respectively. Table 1 summarizes the parameters used for modelling of the station, the tunnel, and the train.

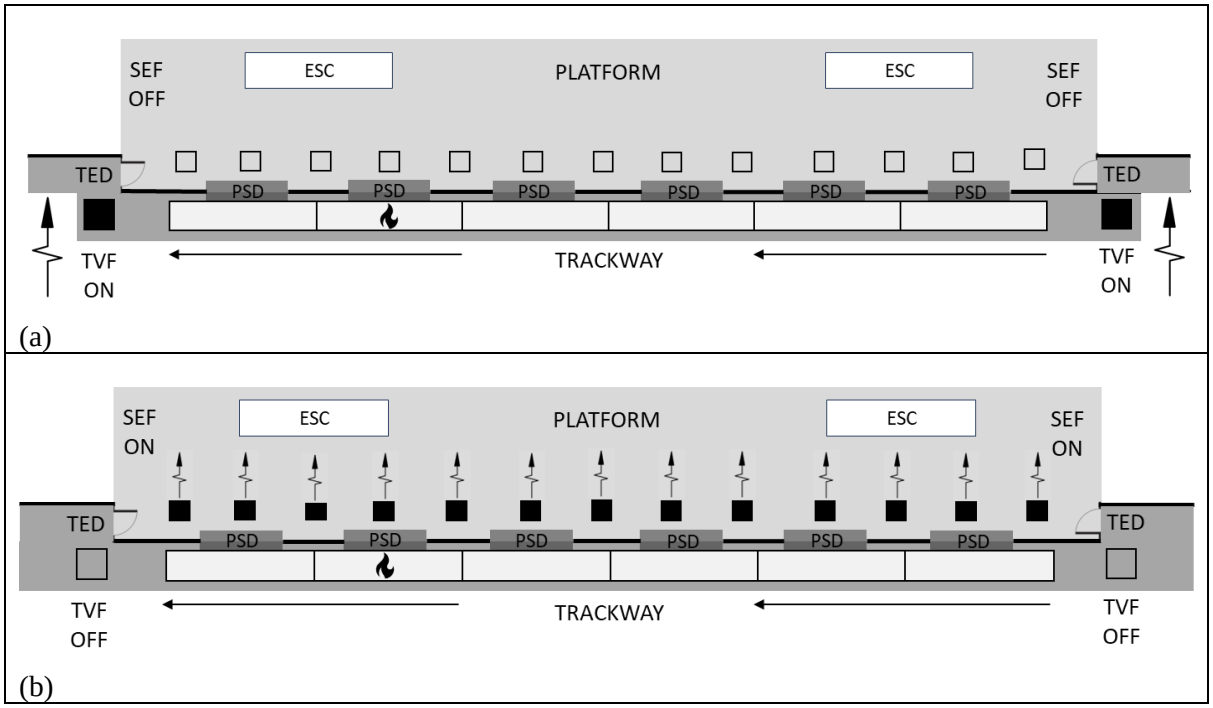

Figure 1 Representation of the modelled system in case of FE-1 (a) typical system configuration utilizing TVFs in smoke exhaust mode and (b) proposed system configuration utilizing platform SEFs. The vertical arrows depict smoke extraction, whilst the horizontal the train movement direction. (ESC: Escalator / Staircase opening.)

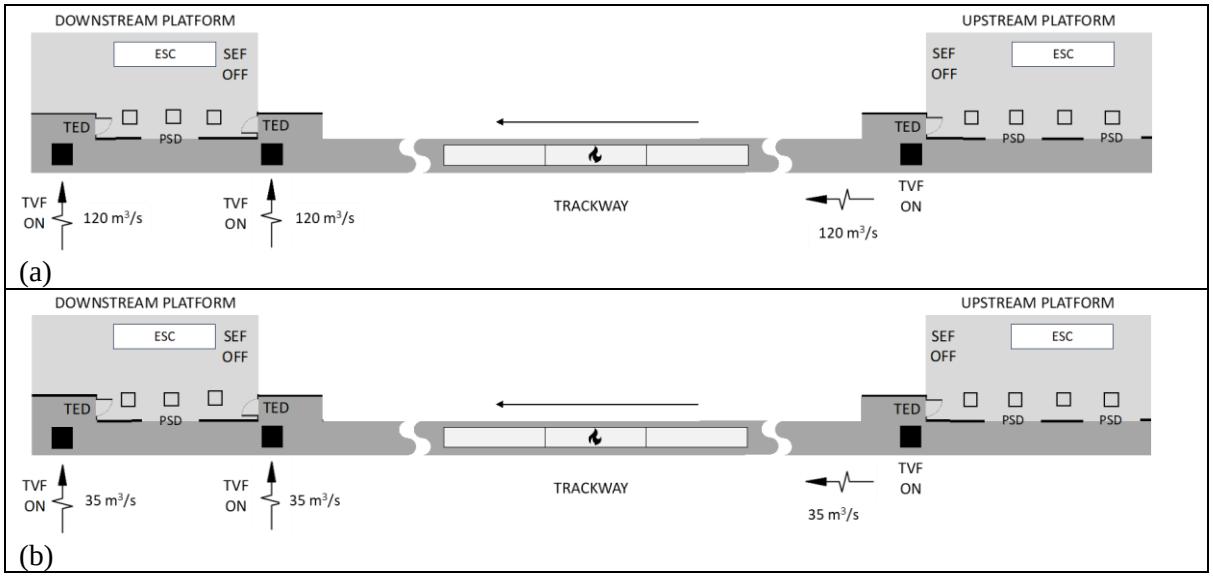

Figure 2 Representation of the modelled system in case of FE-2 (a) typical push-pull system configuration consisting of TVFs sized for train congestion in the tunnel and (b) proposed push-pull system configuration consisting of TVFs sized only for fire (tunnel critical velocity). The vertical arrows depict smoke extraction, whilst the horizontal the train movement direction. Only the first three cars of the train are depicted but the model consists of a six-car train. (ESC: Escalator / Staircase opening.)

Table 1 Infrastructure and Train modeling parameters.

Station Geometry		
Platform length	150	m
Platform width	12	m
PSD height	2.1	m
PSD width	2.0	m
TED height	2.1	m
TED width	1.1	m
Tunnel Geometry		
Tunnel area	25	m^2
Tunnel hydraulic height	5.2	m
Tunnel length	500	m
Train Configuration		
Train cross sectional area	11	m^2
Train length	120	m
Train cars	6	-
Train side doors	18	-
Cars on fire	1 (2^{nd})	-

In the case of FE-1, the typical system configuration is depicted in Figure 1(a), whilst the proposed system configuration in Figure 1(b). The former requires smoke to be extracted from the smoke exhaust openings at the roof of the tunnel (TVFs are ON and SEFs are OFF), whilst the latter extracts the smoke through the platform smoke exhaust openings (TVFs are OFF and SEFs are ON). The airflow of each tunnel ventilation fan (TVF) is calculated accounting for the case of train congestion in the tunnel (to maintain the temperature of the A/C condenser units on top of the train < 46°C) and is equal to 120 m^3/s. The combined airflow of the smoke extraction fans (SEFs) is calculated equal to 120 m^3/s considering the smoke production rate at steady state conditions (>30 m^3/s) and the distributed arrangement of the platform smoke exhaust openings which are assumed to be always open.

In the case of FE-2, the typical system configuration is the one depicted in Figure 2(a), whilst the proposed system configuration in Figure 2(b). In both system configurations smoke is pushed (by the upstream TVF) along the tunnel section at the direction of the train movement and pulled (by the downstream TVFs). Thus, smoke is extracted from the trackway of the downstream station (Downstream TVFs are ON, Downstream SEFs are OFF, Upstream TVFs are ON and Upstream SEFs are OFF). In the typical configuration, each tunnel ventilation fan (TVF) airflow is equal to 120 m^3/s (train congestion condition). In the proposed configuration, each tunnel ventilation fan (TVF) airflow is calculated considering only the critical velocity requirement in case of a fire in the tunnel [4] and is equal to 35 m^3/s. The smoke extraction fans (SEFs) at the downstream station may be activated automatically if smoke will penetrate at the platform. In this case, smoke at the platform will be extracted by the SEFs as in the FE-1(b) system configuration.

The ability of each system configuration to manage the smoke and satisfy the baseline tenability criteria is assessed by 3D CFD. The results are a function of the designed fire, and particularly the Heat Release Rate (HRR) of the fire and the production rate of pollutants and heat that need to be removed from the tunnel [5]. Currently the HRR is not standardized, while the values used in international projects vary from 5 MW to 32 MW [6]. For the purposes of this analysis, we used a HRR value equal to 10 MW and a t^2-fast growth rate equal to 0.047 kW/s^2 [7]. We believe this is a pragmatic selection for the HRR value considering available data for fire-in-a-train experiments [8]. The location of the fire in all simulations is set in the second car behind the leading one in respect to the train movement direction. *Table 2* summarizes the fire modelling parameters used in this study.

Table 2 Fire modelling parameters.

Parameter	Value	Unit	Reference
Fire Heat Release Rate	10	MW	
Fire Growth rate	0.047	kW/s^2	[7]
Reaction	Polyurethane	Not Applicable	[5]
Soot yield	0.198	kg/kg	[5]
CO yield	0.042	kg/kg	[5]
Radiative/convective	0.3/0.7	Not Applicable	[5]
Heat of combustion	19855	kJ/kg	[5]

The critical velocity calculation results for a 10 MW fire with a -3% gradient are presented in *Table 3*. A 10% safety factor has been added to the calculated value. The critical velocity (v_c) represents the velocity in the train annulus, and it is used to calculate the minimum supply airflow needed for preventing backlayering in FE-2(b).

Table 3 Critical velocity results.

Fire HRR (MW)	Gradient (%)	Annulus Tunnel Area (m^2)	v_c (m/s)	Annulus Airflow (m^3/s)
10	-3	12	2.9	35

The forced airflows at each system configuration result in a differential pressure between trackway and platform areas with the physical interface being determined by the platform screen doors and trackway exit doors. To determine the maximum allowable differential static pressure (*DPmax*) that will not obstruct the opening of the egress doors from the train side we used Eq. 1 shown below. When static pressures are equalized, the maximum allowable force (*Fmax*) to set the egress door leaf in motion is 133 N [9]. Therefore, the maximum differential pressure between trackway and platform cannot exceed 105 Pa. The values we used for the other equation parameters are: 1.1 m trackway exit door width (*W*); 2.31 m trackway exit door area (*A*); and 0.1 m distance between the point where the opening force is applied and the trackway exit door edge (*D*).

$$DP_{max} = 2F_{\max}\frac{W-D}{WA} \quad (1)$$

RESULTS

The 3D CFD calculations were performed using ANSYS Fluent 24r2 utilizing the SIMPLE solution algorithm with turbulence closure via the realizable k-epsilon model. Buoyancy forces were accounted for using the incompressible ideal gas model and species transport (transport and mixing of combustion products) was modelled using a single-phase convection-diffusion model. At the trackway boundaries, and area adjusted k-factor of 20 was applied corresponding to the airflow resistance of neighbouring stations draught relief shafts and associated tunnel. A k-factor of 2.5 was applied on the escalator boundaries mirroring the airflow resistance of station geometry. The quality of the simulation results was assured by setting the convergence criteria sufficiently low to ensure that residuals converge at each timestep.

The 1D CFD calculations of the static pressure at the trackway were performed by modelling a metro line comprising of seven underground stations over a length of 20 km [10]. The calculated static differential pressures are shown in Table 4 and Table 5 for FE-1 and FE-2, respectively. These results are calculated at the fourth station (S4) located approximately at the middle of the line as depicted in Figure 3, with the platform screen doors closed. Fire simulations or train movements were not included. The shafts at all stations were modelled with an area adjusted k-factor of 18.

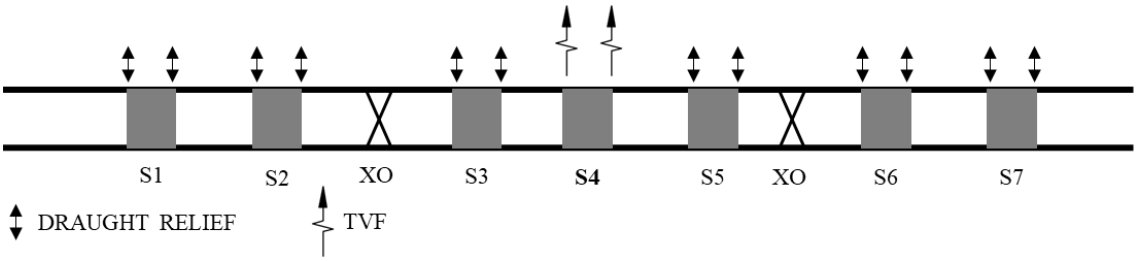

Figure 3 1D CFD model for estimation of differential static pressure at trackway.

It is noted that the application of mechanically assisted doors cannot resolve the issue in the case of the typical system configuration (FE-1(a) and FE-2(a)). This is a consequence of the air velocity through the opened trackway exit doors, which is calculated to 14-16 m/s and, thus, above the maximum allowable value of 11 m/s [9]. On the other hand, in the proposed configuration (FE-2(b)) it is 5 m/s and, thus, below the maximum allowable value of 11 m/s.

Table 4 Summary of calculated static differential pressures in FE-1.

	SEF (m^3/s)	TVF (m^3/s)	DP (Pa)
FE-1(a)	OFF	2 x 120	- 160
FE-1(b)	120	OFF	+10

Table 5 Summary of calculated static differential pressures in FE-2.

	Upstream SEF (m^3/s)	Upstream TVF (m^3/s)	Downstream SEF (m^3/s)	Downstream TVF (m^3/s)	DP (Pa)
FE-2(a)	OFF	1 x 120	OFF	2 x 120	- 230
FE-2(b)	OFF	1 x 35	OFF	2 x 35	- 20

In case of FE-1 the CFD computations for both the typical and the proposed system configuration are shown in *Figure 4* (a) and (b), respectively. The plan views depict smoke propagation at 2 m above the platform level and the sections are at the middle of the platform. In both cases the egress path to the point of safety remains smoke free (or smoke is sufficiently stratified) during the maximum evacuation time of 180 sec [9]. Therefore, from a smoke management perspective, both solutions comply with the baseline tenability criteria. The traditional system configuration, however, will result in – 160 Pa (>> – 105 Pa) high negative differential pressure at the trackway area when the platform screen doors remain closed. In this case, potential passenger evacuation through the trackway exit doors will be obstructed since manual operation of the trackway exit doors demand the application of forces >> 133 N. In contrast, using the proposed system configuration the differential static pressure is + 10 Pa when the platform screen doors remain closed. Therefore, passenger evacuation from the train side to the platform through the trackway exit doors is not obstructed. In addition, most the platform area remains smoke free even at the steady state, allowing easier intervention of the emergency intervention team and the fire-fighters.

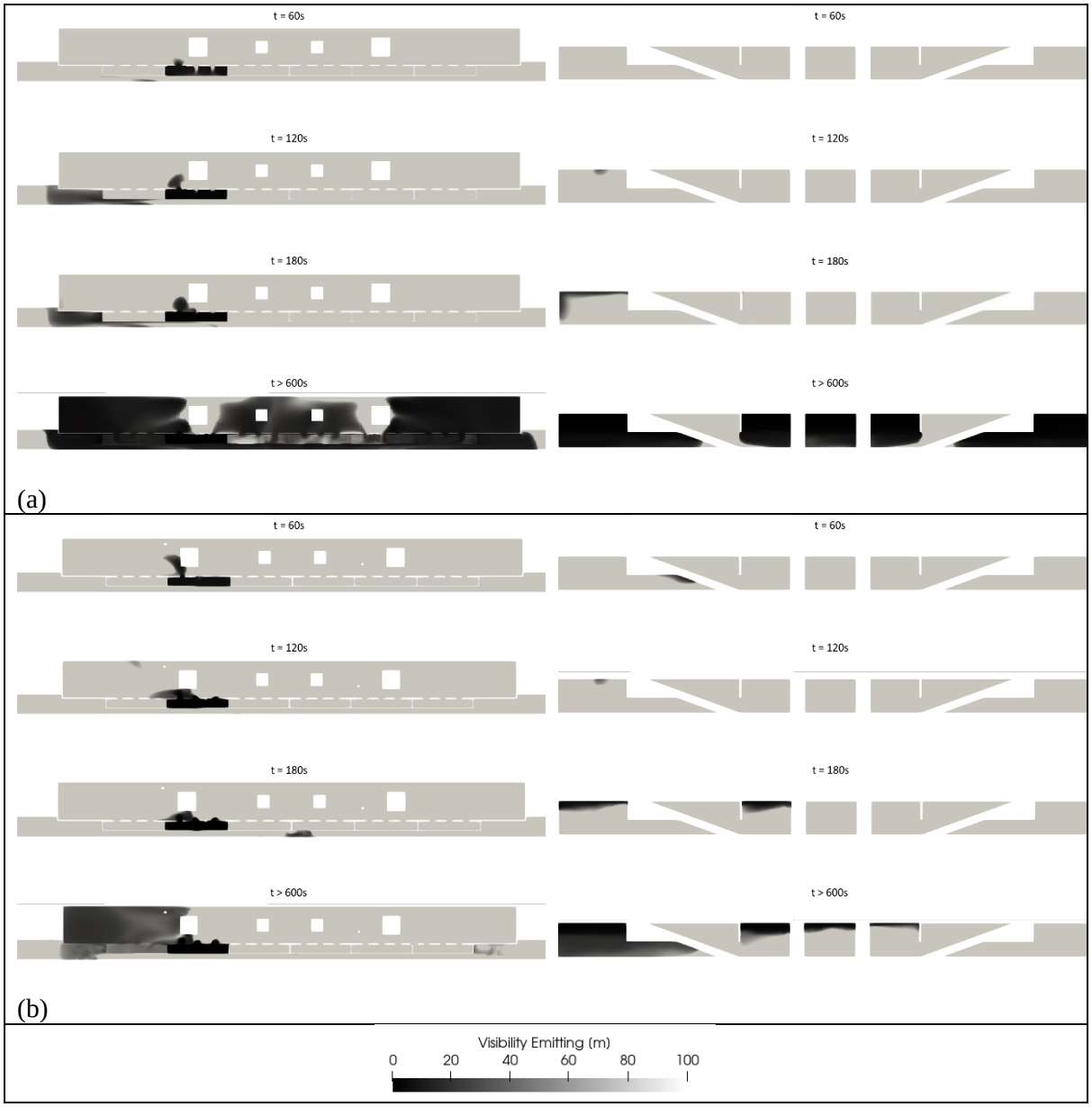

Figure 4 3D CFD results in case of FE-1 (a) typical system configuration utilizing TVFs in smoke exhaust mode and (b) proposed system configuration utilizing platform SEFs.The plan view is at 2m above the platform level and the section at the middle of the platform.

In case of FE-2 the 3D CFD computations for both the typical and the proposed system configuration are shown in *Figure 5* (a) and (b), respectively. In both cases smoke is extracted efficiently (no backlayering) at the downstream station. The traditional system configuration, however, will result in a negative differential static pressure at the trackway area of – 230 Pa (>> – 105 Pa). In this case, the passengers that will cross the cross-passages will evacuate safely through the trackway exit doors at the non-incident tunnel, but those passengers that will attempt to reach the platform through the trackway exit doors at the incident tunnel will be obstructed since manual operation of the trackway exit doors demand the application of forces >> 133 N. On the other hand, using the proposed system configuration the negative differential pressure at the trackway is maintained at – 20 Pa (<< – 105 Pa) and, as a result, the evacuation through the trackway exit doors at the incident tube will be unobstructed.

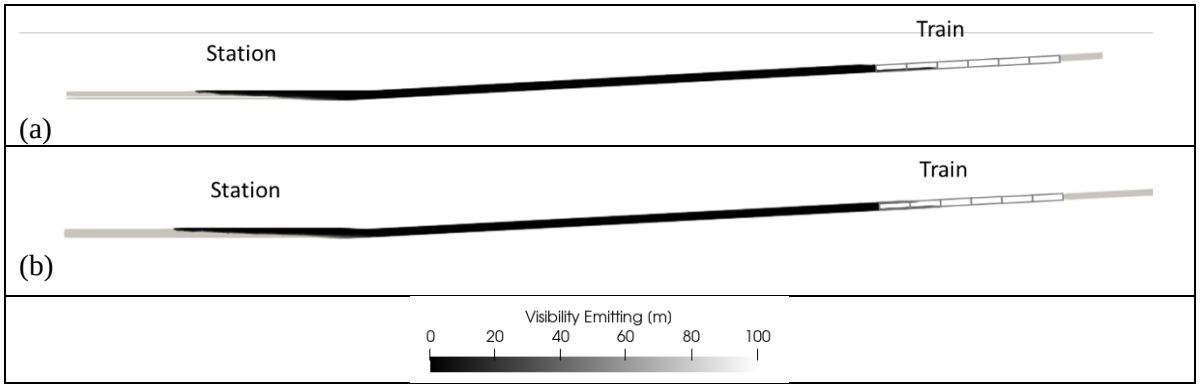

Figure 5 3D CFD results in case of FE-2 (a) typical system configuration consisting of TVFs sized for train congestion in the tunnel and (b) proposed system configuration consisting of TVFs sized only for fire (tunnel critical velocity). Vertical section views through the tunnel middle.

CONCLUSION & DISCUSSION

In conclusion, the presented analysis suggests that by extracting smoke using the platform SEFs in FE-1 and by sizing the TVFs considering only the critical velocity in FE-2, not only smoke is managed effectively, but also the negative high negative differential pressure between trackway and platform is eliminated. The later cannot be achieved with the typical smoke management system configurations which utilize large TVF airflows accounting for the possibility of train congestion in the tunnel (above 100 m^3/s when less than 40 m^3/s is required). As a result, the force that is required to manually operate the trackway exit doors is very high (>> 133 N) and practically impossible to be applied by the passengers that will not be able to evacuate safely from the train side to the platform and the point of safety.

The solution to this undesirable side effects is to design the tunnel ventilation system by sizing the TVFs considering only the critical velocity of the tunnel. The potential risk of trains being congested in the tunnel will be effectively mitigated through the CBTC (GoA4) control and signalling functions, and the Operating Command Centre (OCC) standard operating procedures. Even though a detail analysis of such measures is outside the scope of this study, the main functions involved are the following:

1. Isolation of the zone affected by the fire event.
2. Adjustment of train headways and frequencies.
3. Re-routing of trains to alternative paths.
4. Disembark passengers in adjacent stations.
5. Move empty trains to designated holding areas.

These functions can be implemented automatically by the GoA4 enabled CBTC signalling system through pre-programmed control sequences based on a carefully designed zoning scheme. Alternatively, they can be manually commanded by the OCC (human intervention) by applying pre-planned emergency operating procedures. A combination of both approaches is also feasible. The complexity of the network and the level of the available operating capabilities will eventually determine the configuration that is more suitable. Despite the differences of each implementation, when properly designed, tested, and maintained, these functions can minimize (if not eliminate) the risk of congestion in a zone that has been affected by fire or other event.

Notwithstanding the above, the successful response on an emergency depends on many parameters which need to be viewed with a holistic system engineering and assurance approach. In both FE-1 and FE-2 cases, several systems need to be in synch and react in real-time in order the fire event is effectively resolved (i.e. passengers evacuate safely). Initiated by the onboard fire alarm signal, the normal operating mode must switch to the pre-configured (for the affected zone) emergency operating

mode. To this end, a series of electronic systems and subsystems need to exchange information, process incoming data, command field devices, monitor feedback signals and adjust outputs accordingly. The plethora of these systems and subsystems as well as the complexity of the required functionality at the level of input and output signals, challenges the usually simplistic testing and commissioning processes. As a result, many physical and logical interfaces remain unresolved, and revenue operation is temporarily achieved by putting in place costly operating procedures with questionable effectiveness in case of an emergency. Indicatively, some of the involved electronic systems and subsystems are: CBTC Signalling; Centralized Control System (CCS); Tunnel Ventilation Control System (TVCS); Building Management and Control System (BMCS); Fire Detection and Alarm System (FDAS); Public Address System (PAS); Public Information System (PIS); Closed-Circuit TV (CCTV); Central Battery Control System (CBCS); Lighting Control System (LCS); Vertical Transportation Control System (VTCS) and Ventilation and Air-Conditioning (VAC) Controllers.

One way to overcome this issue is to reduce the number of stand-alone control systems (TVCS, BMCS, CCTV, PAS, PIS, CBCS, LCS, VTCS, VAC Controllers) and rather introduce a centralized Industrial Control System (ICS) with an architecture that is able to provide high signalling capacity, real-time response and seamless integration with the CBTC, CCS and FDAS systems. The successful design and implementation of such ICS has been documented in [11] and [12]. For the purposes of this study suffice to summarize that it is engineered with one central controller, one cluster of servers, one switched optical ring and multiple sensing and actuating devices on copper rings, amalgamating automation technologies and data networking techniques over one common communication platform. This centralized architecture allows for seamless systems integration and enables fast systems testing and commissioning both off-site and on-site. Furthermore, due to the ICS inbuild fault recovery technologies for its hardware and software components, it is capable to provide functions with safety integrity level (SIL) 2 or more, being thus suitable to integrate and coordinate fire-life-safety and mission critical systems.

Finally, the outcomes of this analysis put forward for consideration an important matter in the design of Metro systems and subsystems. This is the number and type of events that may occur simultaneously and for which the rail and station systems must provide safety functions. In our study, FE-1 represents the situation of a single-event scenario. There is a fire in the train (one event) while all systems operate without faults (zero additional events). On the other hand, FE-2 represents a multiple-event scenario. There is fire in the train (one event) and at the same time the train stops in the tunnel between two stations (another event due to one or more faults in the systems involved in the train movement). It could be argued that the probability of such multiple-event scenarios is practically, and theoretically, very low taking into consideration the high operating availabilities of the involved systems. We argue that by carefully assessing the risk of multiple events, using operating and maintenance data from live Metros, pragmatic design objectives can be set, resulting in simple yet effective smoke management or other systems in large-scale industrial or infrastructure projects.

REFERENCES

1. Huijben, J.W., Huijben, M.E., Thesing, E., “Egress Way Ventilation for Escape Routes in Tunnels – The Design of Overpressure Systems”, 8th International Conference ‘Tunnel Safety and Ventilation’, Graz, Austria, 2016.
2. De los Rios, N., Harvey, N., Li, K., Hall, R., “Safe Passage-Evacuation Provisions for Road Tunnel Users”, 18th International Symposium on Aerodynamics, Ventilation & Fire in Tunnels, Athens, Greece, 2019.
3. Thaller, T., Sturm, P., Rodler, J., “Keeping Cross Passages Smoke-Free Results From Full Scale Tests In Rail Tunnels”, 9th International Conference ‘Tunnel Safety and Ventilation’, Graz, Austria, 2018.
4. Subway Environmental Design handbook, Volume II, Subway Environmental Simulation Computer Program SES Version 4.1, Part I, User’s Manual.
5. Khan, M., Tewarson, A., Chaos, M., The SFPE Handbook of Fire Protection Engineering

(Hurley M. et al Eds.), SFPE Publication, Fifth Edition, 2016.
6. Darmody, M., Weaver, S., "Design Fires for Passenger Trains – How Do We Know We Have Them Right?", Conference on Railway Excellence, Adelaide, Australia, 2014
7. NFPA 92, Standard for Smoke Control Systems, 2023.
8. Shi, C., Zhong, M., Chen, C., Jiao, W., Li, J., Zhang, Y., Zhang, L, Li, Y., He, L., "Metro train carriage combustion behaviors – Full-scale experiment study, Tunnelling and Underground Space Technology", Volume 104, October 2020.
9. NFPA 130, Standard for Fixed Guideway Transit and Passenger Rail Systems, 2023.
10. Henson, A., Lowndes, F., "Practical applications of a method of assessing the ventilation and draught relief requirements for underground railways", Paper C2, Proceedings of the 2nd International Symposium on the Aerodynamics and Ventilation of Vehicle Tunnels, BHRA 1976.
11. Kalyvas, M., "An innovative industrial control system architecture for real-time response, fault-tolerant operation and seamless plant integration", IET The Journal of Engineering, 1–13, 2021.
12. Kalyvas, M., and McCracken, A., "Doha Metro Novel Building Automation and Control System (BACS)", Journal of Industrial Integration and Management - Innovation and Entrepreneurship, 1–26, 2023.

Tunnel Ventilation in India: State-of-the-Art and Evolution

Ravi Shankar[1] & Marco Bettelini[2]
[1]Amberg Engineering AG, Gurugram, India
[2]Amberg Engineering AG, Regensdorf-Watt, Switzerland

ABSTRACT

India's infrastructure development has witnessed remarkable growth in the past decade, with tunnels forming a critical part of both road and rail networks. Tunnel Ventilation Systems (TVS) play a crucial role in ensuring safety, operational efficiency, and environmental compliance. This paper examines TVS practices in major road and rail tunnel projects, including Banihal-Qazigund, Chenani-Nashri, Z-Morh, Thane-Borivali (road tunnels), USBRL (T-13, T1-T47), Sivok-Rangpo, and T7-Teesta (rail tunnels). It highlights the evolution from fully transverse systems to optimized semi-transverse and longitudinal systems. This study explores future trends in tunnel ventilation and discusses strategies to optimize costs, improve safety, and enhance efficiency in Indian tunnel projects.

KEYWORDS: tunnel ventilation, semi-transverse, longitudinal, road tunnels, rail tunnels, India

INTRODUCTION AND OBJECTIVES

India's diverse geography presents significant challenges for transportation infrastructure, with its rugged mountains, dense urban centres, and vast plains necessitating the construction of tunnels. Tunnels have transformed connectivity across India, enabling faster transit, reducing fuel consumption, and ensuring year-round access to remote regions. The design and operation of tunnels, however, bring unique challenges, particularly in ensuring proper ventilation. Tunnel Ventilation Systems (TVS) must maintain air quality, control smoke during emergencies, and optimize construction, operational and maintenance costs, especially for long tunnels in high-altitude or urban settings. The lack of robust infrastructure represents a primary constraint for national development. India is increasingly looking to the private sector for forging partnerships via effective models for co-working between public and private sectors. The National Infrastructure Pipeline (NIP) [1] is a step in this direction. Road and rail represent a key component and over 280 km of tunnels are planned within the framework of NIP. The National Highway network increased by 60% from 91,287 km in 2014 to 1,46,145 km in year 2024 [2]. A recent review of TVS for road tunnels in India is provided by Sharma et al. [3].

India's rapid infrastructure development has led to the construction of several significant tunnels, each incorporating advanced ventilation systems to ensure safety and operational efficiency. For instance, the 9.29 km long Chenani-Nashri Tunnel, inaugurated in 2017, is among India's longest bi-directional highway tunnels and the first in India to feature a fully transverse ventilation system. This system provides a continuous air exchange to passengers throughout the tunnel, enhancing safety and comfort. Similarly, the 9 km long single-tube Atal Tunnel, opened in 2020, employs a semi-transverse ventilation system with large fans circulating air, ensuring optimal air quality and safety for travellers. A specific challenge for this tunnel was the high altitude, over 3100 m over sea level. These examples underscore the critical role of advanced tunnel ventilation systems in India's infrastructure projects, ensuring safety, efficiency, and cost-effectiveness.

This paper analyses the evolution of TVS in India, from the predominance of fully transverse systems to the adoption of semi-transverse and longitudinal systems. Both road and rail tunnels are considered, with detailed case studies to highlight advancements, challenges, and best practices. It provides insights into optimizing ventilation design, addressing project-specific challenges, and aligning with international safety standards. The objectives of the present paper are:

1. To analyse the evolution of TVS practices across major road and rail tunnels in India.
2. To assess the transition from fully transverse to semi-transverse and longitudinal systems.
3. To identify the challenges and opportunities in adopting innovative TVS strategies.
4. To provide recommendations for improving TVS design and implementation under the NIP framework.

METHODOLOGICAL APPROACH

The analysis incorporates technical reports for Banihal-Qazigund, Chenani-Nashri, Z-Morh, Thane-Borivali, USBRL (T13, T1-T47), and Sivok-Rangpo rail tunnel projects, designed by the authors of this paper. Government documents and industry publications were also reviewed.

The evaluation of Tunnel Ventilation Systems (TVS) in this study was based on comprehensive technical, operational, and economic criteria to ensure safety, efficiency, and sustainability in the context of Indian infrastructure. These criteria include:

1. Smoke and Heat Control

Smoke and heat control are critical during emergencies such as fires within tunnels and for ensuring tunnel safety. The evaluation focused on:

- **Smoke extraction efficiency**: The ability of the ventilation system to remove smoke from the tunnel to create safe self-rescue paths. Fully and semi-transverse systems, for instance, excel in smoke control for long and congested tunnels, as seen in Chenani-Nashri.
- **Longitudinal smoke management**: This issue is particularly relevant in road tunnels with frequent congestion or bidirectional traffic, as well as in rail tunnels.
- **Readiness for emergency**: Systems such as the sector-based reversible fans in Teesta station, India's first underground railway station, were assessed for their capacity to isolate and extract smoke from specific zones, minimizing risks to tunnel users and rescue personnel.

2. Pollutant Management and Thermal Control Efficiency

Modern tunnels handle significant traffic volumes, leading to high emissions of carbon monoxide (CO), nitrogen oxides (NOx), and particulate matter (PM). This represents a key issue for all road tunnels but is a real challenge also for long rail tunnels operated with diesel trains. Key considerations include:

- **Air quality standards**: Compliance with air-quality regulations, particularly in urban tunnels like Thane-Borivali in Mumbai, where pollutant levels must be managed to ensure driver safety. Specific issues result in tunnels located at high altitude, such as Z-Morh in the lower Himalayas, due to increased motor-vehicle emissions.
- **Fresh-air supply**: The capacity of jet fans or axial fans to ensure uniform fresh-air circulation, preventing the accumulation of harmful gases within the tunnel.
- **Tunnel geometry and traffic profile**: Adjustments to ventilation flow based on tunnel dimensions and traffic load, such as the twin-tube unidirectional design of Banihal-Qazigund.
- **Thermal management**: Effective dispersion of heat generated by vehicle engines, particularly large diesel locomotives, and environmental conditions to prevent overheating of tunnel structures.
- **Environmental impact**: Mitigation of environmental impact is a specific issue particularly in urban areas, such as Thane-Borivali in Mumbai.

3. Energy Efficiency

Energy consumption represents a significant operational cost for ventilation systems. Evaluation metrics included:

- **Fan power requirements and operating times**: Comparing the energy consumption of fully transverse systems versus semi-transverse and longitudinal systems. For example, the semi-transverse system in Z-Morh resulted in reduced energy demands compared to fully transverse configurations.
- **Optimization strategies**: Incorporation of energy-efficient systems such as semi-transverse systems instead of fully transverse systems.
- **Dynamic operation**: Systems that adapt fan speed and airflow based on real-time traffic conditions, operating at part load to conserve energy without compromising safety.

4. System Maintenance and Durability

The maintenance requirements of TVS were evaluated to ensure long-term availability and reliability, particularly in remote or challenging environments:

- **Component lifespan**: Assessing the durability of jet fans, axial fans, and ductwork under continuous use and extreme climatic conditions.
- **Ease of access**: Maintenance access was analysed for projects like USBRL, where the mountainous terrain complicates servicing and repairs.
- **Spare parts and cost**: Availability of replacement components and associated costs were factored into the evaluation, highlighting the importance of cost-effective designs for projects like Z-Morh.

5. Availability in Case of Emergency

The capacity of the TVS to respond swiftly to emergencies is a critical parameter:

- **Evacuation readiness**: Evaluating cross passages, emergency adits, and escape tunnels for facilitating safe evacuation, as implemented in USBRL T13.
- **Zone-based control**: Systems such as Teesta's sector-based reversible fans were assessed for their ability to isolate hazardous zones during emergencies.
- **Smoke modelling simulations**: Comprehensive 1-dimensional and 3-dimensional Computational Fluid Dynamics (CFD) simulations were utilized to validate smoke flow patterns and emergency preparedness for various tunnel designs.

6. Adaptability to Environmental Conditions

Tunnels in India must address diverse environmental challenges, including:

- **Extreme weather conditions**: Ventilation systems must perform efficiently in high-altitude, cold climates (Banihal-Qazigund) and humid, tropical conditions (Sivok-Rangpo).
- **Barometric pressure differences**: Particularly in mountainous regions such as the high Himalayas, where pressure gradients can significantly impact airflow dynamics.

CASE STUDIES

Banihal-Qazigund Road Tunnel

The Banihal-Qazigund Tunnel, also known as the Jawahar Tunnel Replacement Project, is an 8.5 km twin-tube unidirectional road tunnel located in the challenging terrain of Jammu and Kashmir. This state-of-the-art infrastructure replaces the older Jawahar Tunnel, providing year-round connectivity between the Kashmir Valley and the rest of India under the 2,832 m high Banihal Pass. The tunnel was built between 2016 and 2021 and was commissioned in August 2021. The traffic volumes are low, but the high tunnel elevation represents a particular challenge.

Table 1 Key parameters of Banihal-Qazigund tunnel.

Parameter	*Details*
Tunnel length	8.45 km
Number of tunnel tubes	2
Cross passages	Every 500 m
Longitudinal slope	1.2%
Traffic volume (AADT)	7,000 vehicles/day
Design speed	70 km/h
Altitude	1,790 m above sea level
Meteorological conditions	Cold climate with snowfall and high humidity during winter
Ventilation system	Fully transverse ventilation and jet fans
Tunnel commissioning	August 2021

AADT = Annual Average Daily Traffic

The tunnel is equipped with a fully transverse ventilation system operated as follows:

- Normal operation: Distributed fresh air injection and exhaust extraction.
- Fire emergency: Concentrated smoke-extraction through motorized dampers.

Remarks:

- The tunnel is equipped with 126 jet fans for mastering longitudinal airflow, installed in side niches on both sides of the carriageway.
- The ventilation stations are installed at the portals and there are no intermediate shafts.

This system is well-suited for managing emissions and ensuring optimal air quality in normal operating conditions in case of high traffic volumes.

Chenani-Nashri Road Tunnel

The Chenani-Nashri Tunnel, officially known as the Dr. Syama Prasad Mookerjee Tunnel, is India's longest road tunnel, spanning over 9 km. Situated in the Jammu region, it is a twin-tube road tunnel designed to provide an all-weather route to the Kashmir Valley. The challenging terrain and high vehicular emissions necessitated a state-of-the-art TVS.

Table 1 Key parameters of Chenani-Nashri Tunnel.

Parameter	*Details*
Tunnel length	9.3 km
Number of tunnel tubes	1 + safety tunnel
Cross passages	Every 300 m
Longitudinal slope	0.5%
Traffic volume (AADT)	15 000 vehicles/day
Design speed	50 km/h
Altitude	1,200 m above sea level
Meteorological conditions	Moderate temperature with significant seasonal variations
Ventilation system	Fully transverse ventilation, no jet fans
Tunnel commissioning	April 2017

The tunnel is equipped with a fully transverse ventilation. The ventilation stations are installed only at the portals and the required ventilation cross section is very large (*Figure* 1). There are no jet fans for

controlling longitudinal air velocity. The fresh-air injection ports are installed every 8 m, the smoke-extraction dampers every 100 m and the fire ventilation is designed for a fire rate of 30 MW.

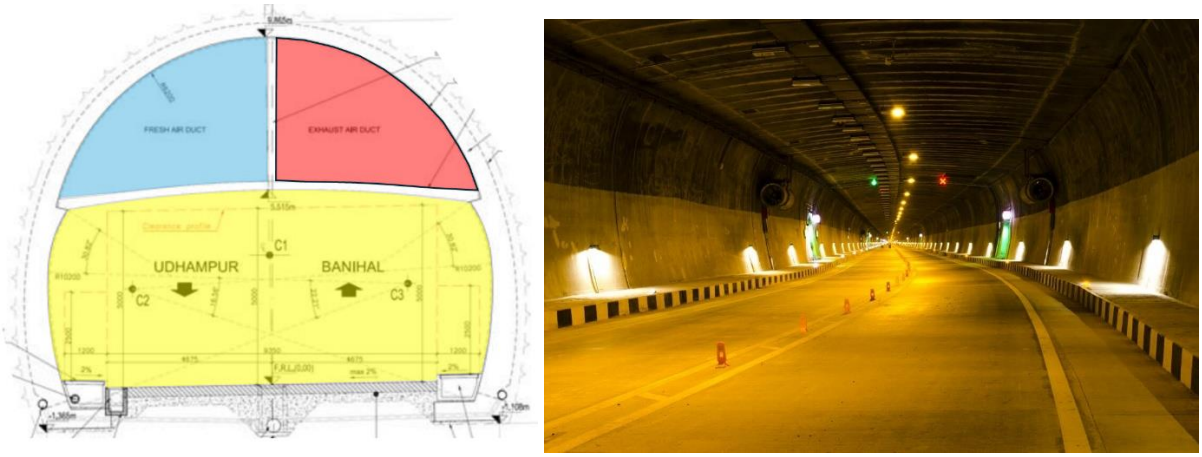

Figure 1 Cross section with ventilation ducts (left [4]) and interior view (right, Wikipedia) of the Chenani-Nashri Tunnel.

Z-Morh Road Tunnel

The Z-Morh Road Tunnel, spanning 6.5 km, is a vital infrastructure project in Jammu and Kashmir, designed to ensure year-round connectivity along the Srinagar-Leh highway. The tunnel is located at a very high altitude, which poses extreme requirements in terms of operation and maintenance. The tunnel, commissioned in January 2025, incorporates state-of-the-art ventilation systems to manage air quality, ensure fire safety, and adapt to the region's challenging environmental and operational conditions.

Table 2 Key parameters of Z-Morh Tunnel.

Parameter	*Details*
Tunnel length	6.5 km
Number of tunnel tubes	1 + safety gallery
Cross passages	Every 250 m
Longitudinal lope	2.27%
Traffic volume (AADT)	~12,000 vehicles/day with 25% HGVs
Design speed	80 km/h
Altitude	~2,600 m above sea level
Meteorological conditions	Heavy snowfall and temperatures dropping below -15°C
Ventilation system	Semi-transverse ventilation with concentrated smoke extraction and jet fans
Tunnel commissioning	January 2025

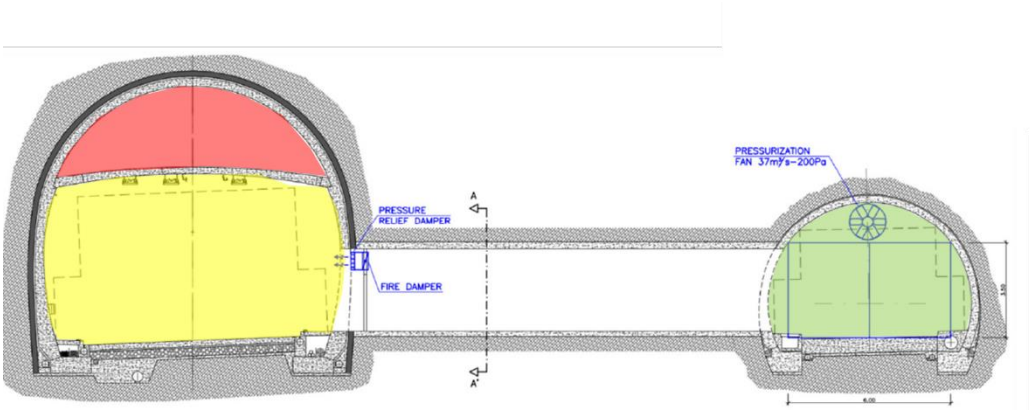

Figure 2 Typical cross section of the Z-Morh tunnel with bidirectional tunnel with exhaust duct, safety gallery and cross connection.

A fully transverse ventilation system was proposed originally at DPR (Detailed Project Report) stage, with four ventilation sectors and three ventilation stations at the portal and at the centre of the tunnel (*Figure 3*). Each ventilation sector was equipped with a fresh-air and an exhaust fan, with a total of 8 axial fans. Butterfly flaps between the different segments of the ventilation ducts allowed for the simultaneous use of two smoke-extraction fans in the fire sector. Jet-fan installation required the construction of expensive side niches. Maintenance was very challenging, because of the remote location and very high altitude of the tunnel.

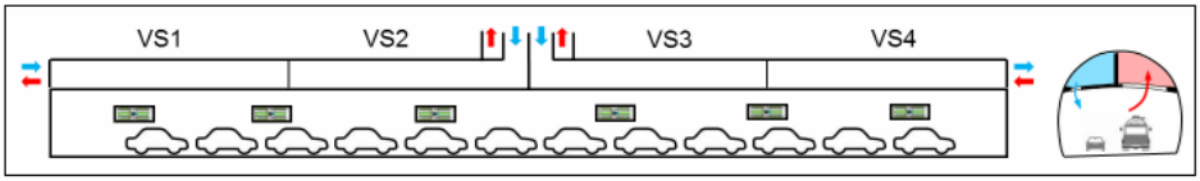

Figure 3 Original ventilation system for Z-Morh Tunnel (DPR stage), fully transverse ventilation.

After careful evaluation of all operational requirements in normal and emergency conditions as well as preventive and curative maintenance, a semi-transverse ventilation system was implemented for Z-Morh Tunnel due to its ability to balance cost-effectiveness, energy efficiency, and safety requirements. This decision marks a departure from fully transverse systems used in earlier Indian tunnels, focusing instead on operational simplicity and reliability. Detailed measurements of the barometric pressure difference were carried out for over a year during tunnel construction. These resulted in surprising high pressure differences up to 300 Pa, due to the extreme weather conditions characterizing this area in the southern part of the Himalayas.

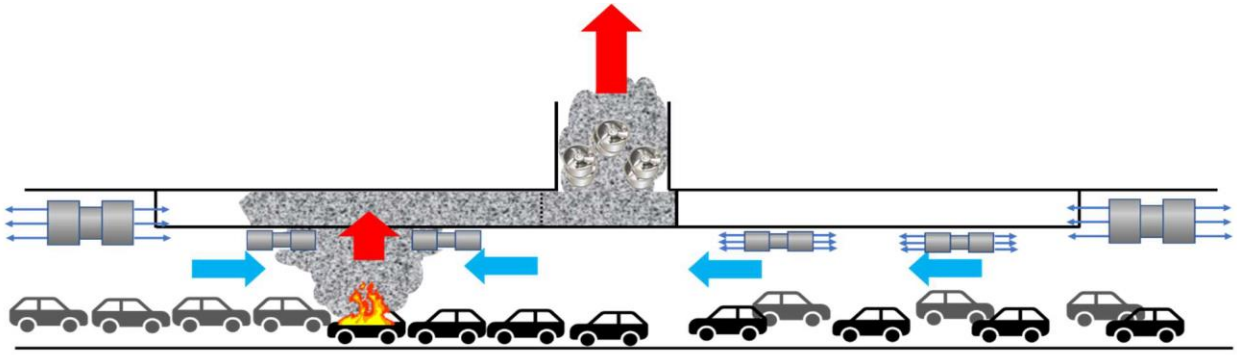

Figure 4 Semi-transverse ventilation scheme for the Z-Morh tunnel.

The transition from fully to semi-transverse ventilation allows to use the whole cross section of the ventilation duct for smoke extraction and the two ventilation stations at the portals can be removed,

with great benefits in term of investment cost and maintenance. Additionally, the ventilation ducts can now be eliminated in the vicinity of the portals, providing space for installing large jet fans. Because of the very high barometric pressure difference, smaller jet fans are installed in the lay-bys inside the tunnel.

In normal operating conditions with large traffic asymmetry and/or barometric pressure differences, the tunnel is ventilated naturally or operated as purely longitudinal ventilation with jet fans supporting the natural airflow. In case of aerodynamically symmetric conditions, polluted air can be extracted through 5 dampers on the centre of the tunnel and fresh air enters both portals. In case of fire, a high-capacity smoke extraction system (253 m^3/s, based on the design HRR of 50 MW) is activated and smoke is extracted through the dampers located in the immediate vicinity of the fire zone. Jet fans manage airflow to ensure smoke-free evacuation zones and optimum smoke extraction.

The Z-Morh Tunnel showcases the adaptability of semi-transverse ventilation systems in addressing the specific needs of Indian infrastructure projects. The new concept allowed to enhance the tunnel safety level while significantly reducing its investment, operation and maintenance cost. Key achievements include:

- Cost-effective normal operation using jet fans, which fully take into advantage natural airflow generated by traffic and meteorological effects.
- Enhanced longitudinal airflow management in normal and emergency conditions through a powerful longitudinal ventilation system.
- Enhanced fire safety through powerful localized smoke extraction, owing to the significantly increased cross section of the exhaust duct achieved by eliminating the fresh-air duct.
- Drastic reduction of the number of ventilation stations and axial fans, with great benefits in terms of investment and maintenance requirements.
- Systematic use of variable-frequency drives for optimizing effectiveness at part load and managing power peaks at startup.
- Energy-efficient designs tailored to high-altitude conditions, which require particularly long and expensive power supply lines.

Thane-Borivali Road Tunnel

The Thane-Borivali Tunnel, a 10.3 km twin-tube tunnel in the north of Mumbai's metropolitan area, represents a significant step in improving urban connectivity and reducing congestion on existing road networks. Designed to connect Thane and Borivali, the tunnel underpasses the Sanjay Gandhi National Park and no ventilation shafts are allowed.

Table 3 Key parameters of Thane-Borivali Tunnel.

Parameter	*Details*
Tunnel length	10.3 km
Number of tunnel tubes	2
Cross passages	Every 300 m (33 cross passages)
Longitudinal slope	<2%
Traffic volume (AADT)	~40,000 vehicles/day with about 8% HGVs
Design speed	80 km/h
Altitude	30 m to 480m above sea level
Meteorological conditions	Coastal, high humidity
Ventilation system	Semi-transverse ventilation with concentrated smoke extraction
Tunnel commissioning	(under construction)

The Thane-Borivali is a typical long urban tunnel with heavy traffic volumes and high congestion frequency. The portals are located in densely urbanized areas and the realization of intermediate ventilation shafts is not allowable for environmental reasons. A purely longitudinal ventilation system with reversible Saccardo nozzles was proposed at DPR stage. However, after detailed risk assessments and technical evaluations, this system was rejected for the following reasons:

1. Inadequate smoke management capabilities: The longitudinal system lacked the capability to manage smoke effectively during emergencies in a tunnel of this length, especially in high-congestion scenarios. The safety level was therefore deemed insufficient.
2. Lack of flexibility: Saccardo-type ventilations are predominantly used in retrofits, where there is no space for installing jet fans. Longitudinal ventilations with jet fans are significantly more flexible both in terms of operation and maintenance.
3. Traffic growth: With projected traffic growth of ~6% annually and increasing risk of traffic congestion, the system could not ensure the required air quality and safety standards.
4. Regulatory concerns: The proposed design did not align with international best practices for urban tunnels exceeding 10 km in length, as referenced in NFPA 502, PIARC, and EU Directive 2004/54/EC.

To address these challenges, a semi-transverse ventilation system with air extraction was proposed. The key characteristics and advantages of this ventilation system are:

- Normal operation: Airflow is managed using jet fans supporting the natural airflow induced by the moving vehicles for pollutant removal, while the extraction system remains inactive.
- Emergency operation: Smoke is extracted through strategically located dampers, with a high smoke-extraction capability of 250–300 m³/s. Jet fans manage the longitudinal airflow for best smoke-extraction effectiveness. The system is designed for a high fire heat-release rate of 100 MW.
- Flexible jet-fan placement: Three groups of jet fans (each group with three fans) installed in the vicinity of each portal allow for longitudinal airflow management. Short distances to the portal stations reduce cabling costs and electric losses.

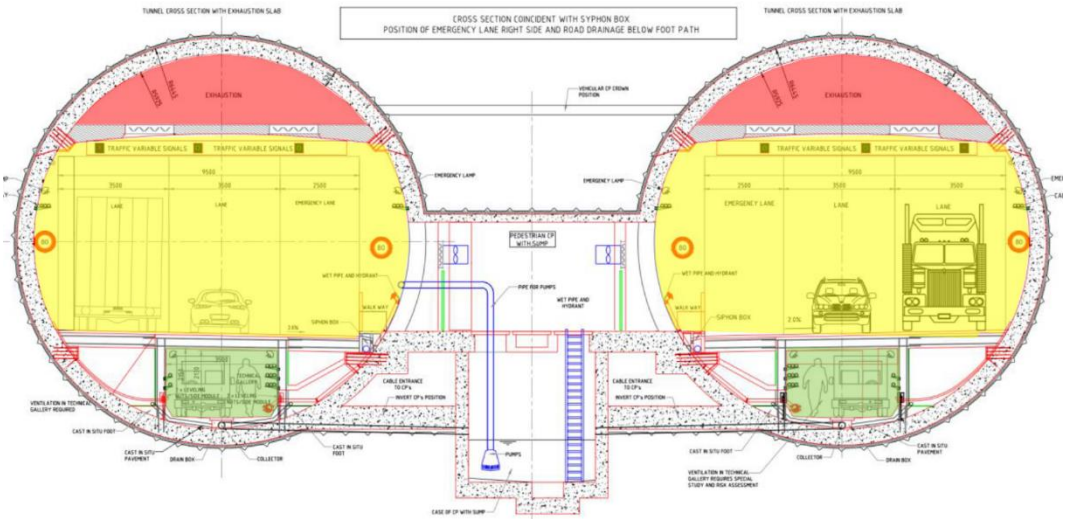

Figure 5 Normal profile of the tunnel Thane-Borivali showing the two traffic tubes with exhaust duct on top and technical gallery under the carriageway, a cross connection and the water sump at the lowest point.

USBRL Rail Tunnels (T13, T1-T47)

The Udhampur-Srinagar-Baramulla Rail Link (USBRL) project encompasses several critical rail tunnels designed to connect Jammu to Srinagar, including T13, the longest tunnel in the project at 9.3

km. Other tunnels have significant lengths, e.g. T1 (3,159 m), T3 (3,009 m), T5 (5,959 m), T6 (3,493m), T12 (2,146 m), T42/43 (2,595 m) and T47 (2,230 m). Ventilation systems for these tunnels were designed to meet stringent safety, operational, and environmental requirements, reflecting advancements in longitudinal ventilation strategies.

Table 4 Key parameters of Tunnel T13 on Udhampur-Srinagar-Baramulla Rail Link.

Parameter	*Details*
Tunnel length	9.3 km
Number of tunnel tubes	1 + safety gallery
Cross passages	Every 375 m
Longitudinal slope	Average 1.05% (0.25 to 1.25%)
Traffic volume	10-14 trains per day (mixed traffic with freight and passenger trains)
Design speed	100 km/h for passenger trains, 60 km/h for freight trains
Altitude	938 to 1,036 m above sea level
Meteorological conditions	Temperate
Ventilation system	Longitudinal
Tunnel commissioning	2025

All USBRL tunnels over 2.0 km are equipped with longitudinal ventilation systems. The jet fans are distributed along the tunnel length and clustered in the vicinity of the electrical substations. The ventilation is designed for achieving the critical velocity with a 40 MW fire. Significant barometric pressure differences were accounted for.

Significant requirements on tunnel ventilation result also from diesel operation with heavy freight trains. Under such conditions, natural ventilation is not sufficient. The ventilation system is automatically activated during the transit of freight trains, based on measurements of CO, NOx and opacity in the tunnel. Depending on train intervals and on the effect of meteorological conditions on natural airflow in the tunnel after trains transit, the ventilation stays in operation well after trains transit, since the pollutants released by the locomotives need to be convected out of the tunnel. This energy-consuming process will need a careful fine-tuning during the initial months of operation.

Tunnel T13 has a safety gallery with 24 cross connections. These fundamental safety features require an appropriate ventilation system. The safety gallery is pressurized with jet fans, which allow for optimum adaptation to the very high portal pressure differences and allow for maximum accessibility. The cross connections have doors on both ends and are equipped with a dedicated ventilation system with small axial fans and dampers. They are operated according to the measured pressure difference between the interior of the cross connections and the rail tunnel.

Tunnel T-7 with Underground Teesta Station on Sivok Rangpo Rail Project

The Sivok–Rangpo Rail Tunnel Project, spanning approximately 45 km, includes 14 tunnels and one underground railway station, Teesta Bazaar, located within Tunnel T-7. The project represents a vital step in connecting Sikkim to the Indian rail network. This ambitious design required advanced Tunnel Ventilation Systems (TVS) to ensure safety, air quality, and operational reliability under mixed traffic conditions (freight and passenger).

Table 5 Key parameters of Tunnel T-7 on Sivok Rangpo Rail Project.

Parameter	*Details*
Tunnel Length	3,083 m
Number of tunnel tubes	1
Cross passages	6 adits inside Teesta station (typical distance 120 m)
Longitudinal slope	0.215%
Traffic volume	~5 trains per day (1-2 freight + 2-3 passenger trains)
Design speed	80 km/h
Altitude	246 m above sea level
Meteorological conditions	high annual rainfall, elevated humidity (>80%), moderate temperature variations (5°C–30°C)
Ventilation system	Longitudinal for tunnel, transverse for Teesta Bazaar Station
Tunnel commissioning	2027

Testa Bazaar station is a 650 m long underground station located about 1,810 m from the south portal and 1,273 m from the north portal of tunnel T-7, as shown in *Figure 6*. This is the very first totally underground rail station in India. The station ventilation system was designed to:

- Ensure effective air circulation during normal operations.
- Facilitate smoke extraction during emergencies.
- Maintain ambient conditions suitable for passengers in all operating conditions.

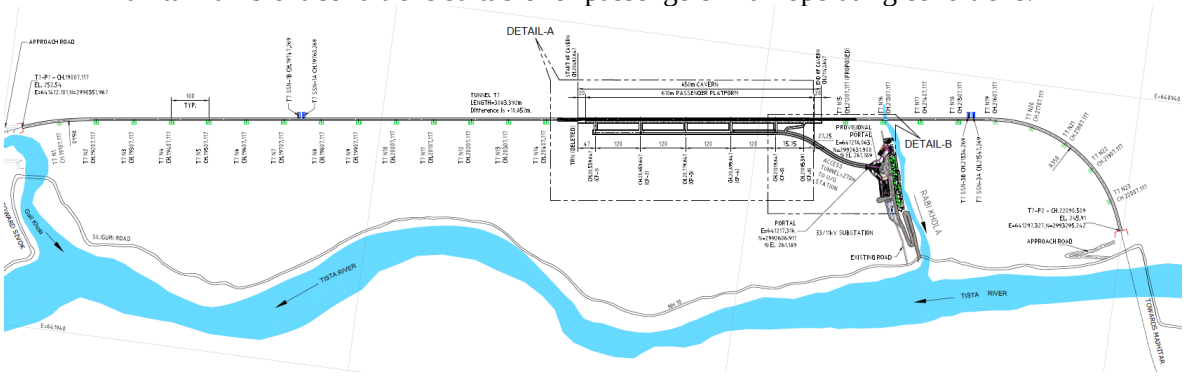

Figure 6 Tunnel T-7 with Teesta Bazaar station.

The tunnel is equipped with a longitudinal ventilation with jet fans and Teesta Bazaar station with a reversible system with fresh-air supply and smoke extraction in case of emergency (*Figure 7* to *Figure 9*). Tunnel and station are designed for a 40 MW fire. The ventilation system is operated as follows:

1. Normal operating conditions
    - Fresh air is supplied to the platform and access tunnels via axial fans installed at strategic locations.
    - Pollutants are extracted through ducts running along the station.

2. Emergency operations with fire inside the station (*Figure 8*):
    - Concentrated smoke extraction (up to 200 m^3/s) is achieved through dedicated ducts with motorized dampers located at sector boundaries.
    - Ventilation zones are isolated to prevent smoke propagation to unaffected areas.
    - The airflow in the tunnel is controlled using jet fans for enhancing smoke extraction.

3. Emergency operations with fire outside the station:

- All jet fans are activated for ejecting smoke from the nearest portal and protecting the station.
- Fresh-air injection through the station is activated at full power for protection the interior of the station from smoke penetration.

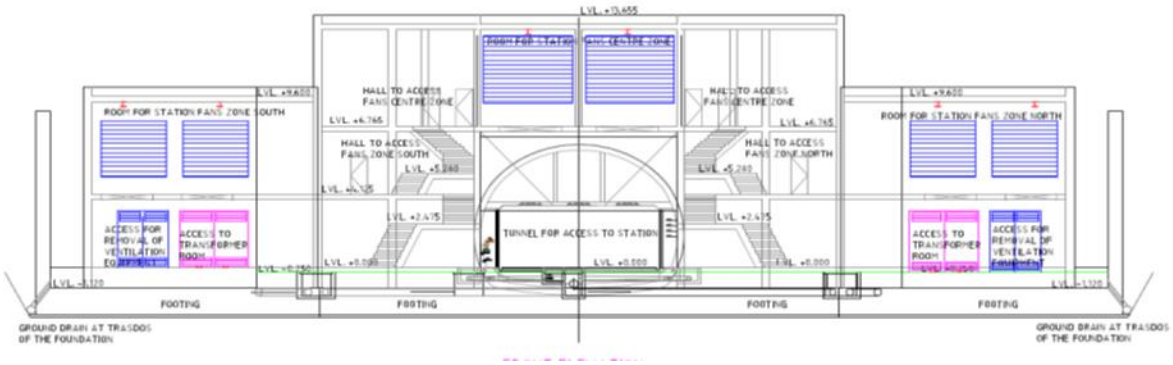

Figure 7 Front view of Teesta station with air intakes for the south (left), north (right) and center sectors of the station.

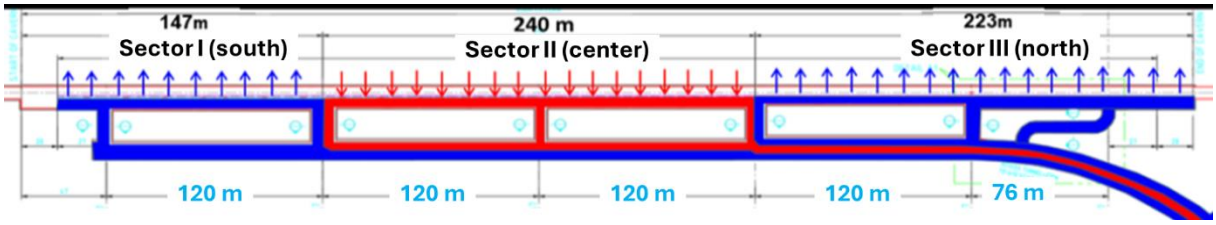

Figure 8 Schematic view of ventilation operation in case of fire in Sector II (center), with full smoke extraction in sector II and fresh-air injection in Sectors I and III.

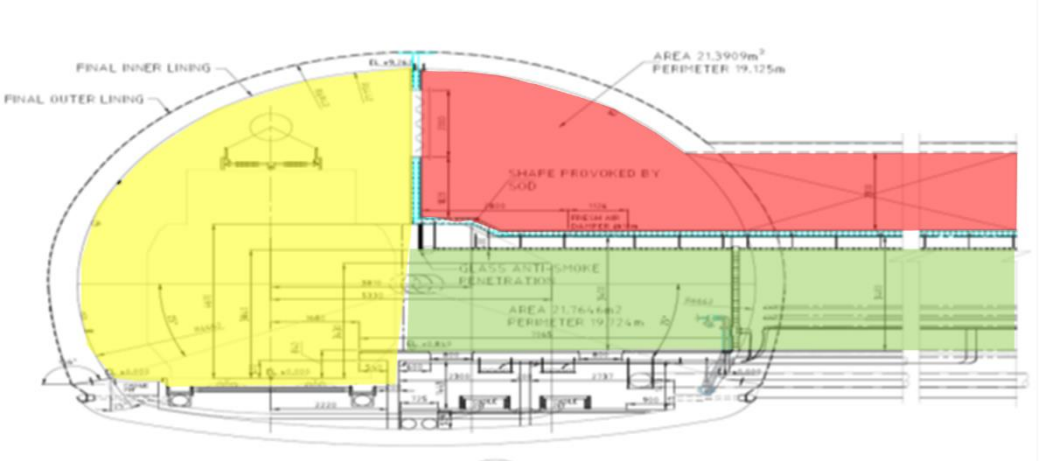

Figure 9 Cross section through Teesta station, showing the rail tunnel, the passenger platform, a cross connection to the interior of the station and the ventilation ducts.

FINDINGS AND DISCUSSION

Insights from Indian Projects

India does not yet have a national regulation for safety and ventilation of tunnels. Design was so far influenced by several different national tunnelling cultures and traditions and was not always properly adapted to the specific conditions and requirements characterizing India's diverse geography and conditions. The case studies presented in the previous chapter illustrate a wide spectrum of technical solutions and a general lack of technical consistency. This concerns primarily the choice of ventilation systems, their proper integration in civil design and specific ventilation-design issues, such as design

fires, management of longitudinal airflow and smoke-extraction capacity. On the other side, there is a clear trend towards safe but cost- and energy-optimized solutions for both road and rail tunnels.

As tunnel construction in India expands, ventilation systems must adapt to increasingly complex requirements. These challenges include:

1. Longer tunnels:
    - The average length of Indian tunnels has increased, with several tunnels exceeding 10 km. This results in increasing requirements for both normal operation and fire safety.
    - Long, steep single-track rail tunnels operated with diesel-powered trains, such as USBRL's T-13, pose unusual challenges in terms of air-quality in normal operating conditions.
2. Widely different traffic volumes:
    - Urban tunnels like the Thane-Borivali Tunnel are designed for over 40,000 vehicles per day, requiring robust ventilation systems to handle heavy congestion and emergency scenarios.
    - On the other side, many new tunnels in peripheric areas are frequently characterized by low but seasonally variable traffic volumes.
    - Traffic forecast is frequently very uncertain.
3. Environmental factors:
    - Mountain tunnels, such as the ones in the Himalaya range, face extreme meteorological conditions, such as very cold winters and extreme winds and barometric pressure differences.
    - The extreme elevation of some tunnels, such as Z-Morh, pose severe challenges e.g. for the analysis of fresh-air requirements for normal operation [5][6].
    - Tunnels located in remote areas impose several severe constraints, ranging from ventilation design to maintenance constraints.
4. New types of infrastructure:
    - New types of infrastructure, such as the T-7's Teesta underground station, pose entirely new challenges.
    - The lack of national experience and regulations, coupled with unusual requirements, represents a challenge for both designer and owner.
5. Cost of construction and maintenance:
    - The pressure on investment cost is very high, particularly for peripheric tunnels with low traffic volumes, such as the Z-Morh Tunnel.
    - Power efficiency is an increasing factor, because of operational costs and sustainability issues, but also for limitations of available power supply in remote areas.
    - Maintenance can be extremely challenging, particularly in remote mountain areas in the lower Himalayas.

Road Tunnels

In the past, purely longitudinal ventilation systems were proposed even for very long urban tunnels such as Thane-Borivali in the northern Mumbai metropolitan area. Such concepts, largely based on purely economic constraint, should be rejected for safety reasons, based on the international state-of the art. A national guideline would be a great support for preventing such very expensive mistakes.

On the opposite end of the complexity spectrum, there is a clear trend from fully transverse ventilation to semi-transverse ventilation with localized smoke extraction and full control of longitudinal air velocity. This results from the general evolution towards cleaner vehicle concepts [5][6] and from significant pressure on construction and operational costs. Semi-transverse systems, as seen in Z-Morh and Thane-Borivali, strike a balance between cost-effectiveness and operational reliability. The distinct advantages are:

- Operational efficiency and simplicity resulting from purely longitudinal ventilation in normal operating conditions. Jet fans support natural ventilation whenever the air-quality sensors indicate a deterioration of air quality. The operational costs are significantly lower than in the case of fully transverse ventilation, which does not fully take advantage of natural ventilation and intrinsically involves higher energy consumptions, particularly in case of narrow ventilation ducts.
- High safety levels in case of fire, owing to powerful smoke-management and extraction systems. Semi-transverse ventilation does not require fresh-air ducts and allow for significantly larger smoke-extraction capabilities for a given overall tunnel cross section.
- Reduced net excavation cross section and possibility of increasing smoke-extraction rates through elimination of fresh-air ducts.
- Easier integration and cost-optimized installation of jet fans in the portal areas without false ceiling.
- Great simplification of the ventilation layout, with less fans, smaller ventilation stations and reduced maintenance requirements.

Because of extreme cost pressure, particularly for peripheric tunnels, in the past fully transverse ventilation systems were designed with insufficient cross sections for the ventilation ducts. This can result in severe operational problems and should be avoided:

- Very high installed power and energy consumption for fresh-air supply and exhaust in normal operating conditions. This intrinsic limitation is even more relevant because transverse ventilation cannot fully take advantage of natural ventilation and transverse ventilations generally require frequent activation during the day hours.
- Insufficient smoke-extraction capabilities in case of fire. This leads to insufficient smoke confinement and reduced safety levels.
- Leakages in the exhaust system increase significantly in case of high pressure differences in exhaust ducts, as shown in *Figure 10* [7]. Full details are provided in [8] and [9].

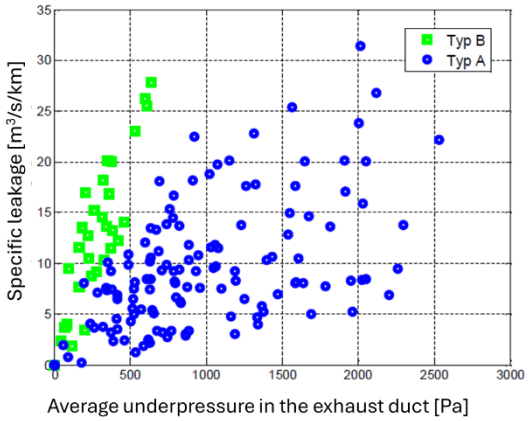

Figure 10 *Specific leakages vs. underpressure in the exhaust duct for new ("Typ A") and aging ("Typ B") tunnels (measurements in Swiss tunnels [7]).*

As an illustration of the potential weaknesses of fully transverse ventilation, air quality in the 9.2 km Chenani-Nashri tunnel on the Jammu-Srinagar highway originated many complaints. A regular user was quoted as follows: "The ventilation system inside the tunnel probably doesn't work effectively. As soon as we enter the tunnel during peak hours, the visibility starts plummeting." [10][11]

In the past, some ventilation systems were designed without jet fans or other devices for controlling longitudinal airflow. This can result in significant issues in normal operating conditions and poor smoke management capabilities in case of fire, particularly in the case of the extreme winds and

barometric portal pressure differences met in the Himalayas (e.g. up to 300 Pa for the comparatively short Z-Morh Tunnel).

Reversible semi-transverse ventilation systems, with distributed fresh-air supply in normal operating conditions and distributed or concentrated smoke extraction in case of fire, were built in the past but are now less popular. The main disadvantages of these cost-efficient systems are pollution at the portals, the risk of smoke destratification in the first minutes after fire onset and the significant time required for reversal and activation of smoke extraction. Reversible systems are seldom used for new road-tunnel projects.

Rail Tunnels

Rail tunnels are currently built and operated under widely different conditions, ranging from the extreme mountain conditions characterizing USBRL's tunnels to modern high-speed lines, such as the Broad-Gauge Double Railway Line Project between Pune – Nashik, operated at 250 km/h with modern trains. While the latter can be broadly developed based on overseas standards, the peripheric tunnels are significantly more challenging for the ventilation engineer. As an example, the USBRL project between Jammu to Srinagar includes a large number of single-tube, single-track tunnels up to 9 km long, operated in alternate direction with diesel passenger and freight trains.

Efforts for unifying requirements and design of rail-tunnel ventilation were not successful so far. Mechanical ventilation of rail tunnels in India is generally required for tunnels longer than 2.0 km. Longitudinal systems dominate rail tunnel designs due to their adaptability and cost-efficiency. Design is generally based on achieving the critical velocity for fires of typically 40 MW. This value is larger than typical design fires used in Europe for state-of-the-art passenger trains and accounts for the use of older rolling stock with lower standards in case of fire. Mechanical ventilation is generally used only in case of fire emergency. Specific issues arise in case of operation with diesel locomotives, particularly in case of heavy freight trains through tunnels with significant slopes, as for example in Kashmir:

- Locomotives pollutant emissions and heat release can be high and require careful analysis.
- Emissions from freight trains can be extremely high, requiring a powerful ventilation for pollution management and thermal control.
- Emissions from a single train can be so high, that longitudinal ventilation needs to be operated between two train transits for achieving full air exchange before the following train can access the tunnel. A particular challenge is presented by single-track tunnels with alternate mixed traffic, where natural ventilation is not sufficient for ensuring proper air quality and temperature.

Specific challenges to be met at design stage include:

- Space requirements for jet fans is not always available in existing tunnels, requiring ad-hoc solutions such as the use of a large number of small jet fans, installation within enlarged sections at the portals or realization of cost-intensive jet-fan niches. Such situations should obviously be prevented at designs stage.
- Development of advanced, automatic fire-ventilation control strategies taking properly into account fire location, other trains in the tunnel, underground stations etc.
- Specific CFD studies are mostly required for illustrating smoke-management capabilities and verifying the possibility of self-rescue and intervention.

The main and frequently neglected task for the ventilation of such tunnels is ventilation control. Clear rules, or at least specific guidance and training of the operators are required for preventing fatal operator mistakes in case of fire. Tunnels like T-7 with Teesta underground station are particularly challenging, with several different ventilation strategies to be activated in case of fire at different

locations in the station or in the tunnel. For increased safety, passengers are not allowed to wait inside Teesta station but access the platform just before boarding.

COLCLUSIONS AND OUTLOOK

India's infrastructure development is undergoing a transformative phase with the government investing heavily in tunnel construction under the National Infrastructure Pipeline (NIP). Over 280 km of new tunnels are planned for roads, railways, and urban transit systems by 2030, addressing critical connectivity challenges in the country. Projects such as the Thane-Borivali Road Tunnel, Sivok-Rangpo Rail Tunnel, and Chardham Highway Tunnels exemplify the scale of these developments. The relevant trends can be summarized as follows:

1. Investment Projections:
    - The NIP allocates nearly ₹1 lakh crore (₹1,000,000,000,000 corresponding to roughly 11.4 billion US$) exclusively for tunnel construction in the next decade, signifying a massive boost in funding compared to earlier years.
    - Major financing comes from public-private partnerships (PPPs), international lenders, and national funding bodies such as the Ministry of Road Transport and Highways (MoRTH) and the Ministry of Railways.
2. Strategic Importance:
    - Mountainous Regions: Tunnels like the Atal Tunnel and Banihal-Qazigund Tunnel ensure year-round connectivity for regions previously inaccessible due to snowfall and landslides.
    - Urban Areas: Projects like the Chennai Metro and Mumbai's Coastal Road Tunnel demonstrate how urban tunnels can mitigate traffic congestion and reduce pollution.
3. Freight and Passenger Benefits:
    - Rail tunnels in projects like USBRL improve freight logistics, reducing transit times and boosting trade.
    - Road tunnels shorten travel distances, cut fuel costs, and enhance regional tourism.

To address the growing demand for efficient tunnel ventilation systems, several policy initiatives can guide future projects:

1. Standardized TVS guidelines:
    - India should establish national standards for TVS design tailored to regional and project-specific needs.
2. Incentives for innovation:
    - Public-private partnerships should prioritize funding for innovative ventilation designs, such as hybrid systems combining natural and mechanical ventilation.
3. Skill development:
    - Training programs for engineers and technicians on advanced TVS technologies will ensure proper implementation and maintenance.
4. Enhanced regulatory frameworks:
    - Collaboration between agencies such as MoRTH, Ministry of Railways, and environmental bodies will ensure integrated planning for safety and sustainability.

The future of tunnel ventilation in India is promising, with a focus on:

- **Efficiency:** Adopting designs that minimize energy consumption while maintaining performance.
- **Safety:** Implementing advanced smoke control systems to enable high safety levels.
- **Sustainability:** Aligning tunnel ventilation practices with global environmental standards.

India's tunnel infrastructure demonstrates a remarkable trajectory of innovation and adaptation. The county's rapidly growing growing network of road and rail tunnels represents an opportunity to set

new benchmarks in ventilation design, ensuring proper leadership in safety, efficiency, and innovation.

REFERENCES

1. The Government of India, "National Infrastructure Pipeline (NIP)", https://indiainvestmentgrid.gov.in/national-infrastructure-pipeline.
2. Government of India, Ministry of Road Transport and Highways, New Delhi "Annual Report 2023-2024", 2024.
3. Sharma, A.K., Pady, T.P, and Ahirwar, Y., "Tunnel Ventilation in Road Tunnels", IARJSET, International Advanced Research Journal in Science, Engineering and Technology, Vol. 11, Issue 2, February 2024.
4. Palomba, M., Russo, G., Carrieri, G. and Jain, A.R., "Chenani-Nashri Tunnel, the longest road tunnel in India: a challenging case for design-optimization during construction", WTC 2013, Geneva, Switzerland.
5. AIPCR/PIARC, "Road Tunnels - Vehicles Emissions and Air Demand for Ventilation", Report 2012R05EN, 2012.
6. AIPCR/PIARC, "Road Tunnels - Vehicles Emissions and Air Demand for Ventilation", Report 2019R02EN, 2019.
7. Buchmann, R. and Gehrig, S., "Quantifizierung von Leckagen in Abluftkanälen bei Strassentunneln mit konzentrierter Rauchabsaugung", Forschungsauftrag ASTRA 2007/004 auf Antrag des Bundesamtes für Strassen (ASTRA), Bericht 1346, Dezember 2011 (in German).
8. Bettelini, M., "Measuring Flow Rates and Leakages in Long Tunnels", ITA-AITES World Tunnel Congress, Sept. 19-25, 2008, Agra, India.
9. Bettelini, M., "Measuring leakages in road tunnels", 4th International Conference "Tunnel Safety and Ventilation" 2008, 21-22 April 2008, Graz.
10. The New Indian Express, "New Kashmir tunnel: Commuters complain of high pollution, poor visibility", 16.04.2017, New Kashmir tunnel: Commuters complain of high pollution, poor visibility.
11. Gulf News, "Pollution chokes Chenani-Nashri tunnel", https://gulfnews.com/world/asia/india/pollution-chokes-chenani-nashri-tunnel-1.2012252, 1.11.2018.

Experimental study on smoke temperature and carbon monoxide diffusion of channel fires under the synergistic action of air curtain and lateral centralized smoke exhaust

Xinyang Fan, Fei Tang*, Xinyu Peng, Nannan Zhu, Xiaolei Zhang, Longhua Hu
State Key Laboratory of Fire Science, University of Science and Technology of China, China

ABSTRACT

The objective of this study is to experimentally investigate the characteristics of smoke temperature and carbon monoxide diffusion in channel fires under the synergistic effect of air curtain and lateral centralised smoke exhaust. There are 270 fire experiments designed to simulate fire scenarios with different fire heat release rates, different air curtain velocities and lateral smoke exhaust velocities. The experimental results show that the introduction of air curtain effectively blocks the spread of smoke in the evacuation direction, while the lateral centralised smoke exhaust system plays an active role in reducing the overall temperature and smoke concentration in the tunnel. The synergistic effect of both systems significantly improved the temperature and smoke control effect in tunnel fires. As the lateral exhaust velocity increases, lower air curtain velocities are required to reduce the temperature to a certain value. After the effect of lateral smoke exhaust, the airflow of the air curtain is deflected and effectively reduces the diffusion of toxic gases in the direction of evacuation due to the impact of the air curtain on the channel floor. As a result, smoke sealing efficiency tends to be close to 100% when the the air curtain speed is 1 m/s to 2 m/s under the synergy of air curtains and lateral smoke evacuation, and the required air curtain jet velocity is about 4 m/s when the air curtain is acting alone. Considering the fire heat release rate, the lateral centralised smoke exhaust velocity and the air curtain velocity, a prediction model for smoke control efficiency is established based on dimensionless analysis. This study provides experimental basis and theoretical support for the optimal design of the fire smoke control system.

KEYWORD: Channel fires, air curtain, lateral smoke exhaust, smoke temperature, carbon monoxide

INTRODUCTION

With the process of urbanization, many narrow and long spaces have emerged in urban infrastructure, such as urban tunnels, narrow channels and narrow passages [1, 2]. The fire safety design is one of the important factors, which can effectively avoid more casualties and property losses. In this kind of long channel fire, the diffusion of smoke and the propagation of toxic and harmful gases are the important parameters of fire research , and how to effectively control the smoke is an important research content[3].

Longitudinal ventilation and concentrated smoke extraction has been widely used in tunnel or channel fires and has been extensively studied by previous researchers[4-12]. These traditional methods can discharge smoke to reduce the smoke hazard but are unable to effectively stop the smoke from spreading and creating an effective and safe escape route. Air curtains have attracted a lot of attention as a new means of smoke protection[13-21]. For example, Hu et al. [13]investigated the effect of air curtains in channel fires through experiments and numerical simulations, showing that air curtains are an effective means of limiting smoke migration. The efficiency of the air curtain system in terms of its structural parameters, installation location, etc. in blocking harmful gases was studied experimentally by Zhang et al [14].

Based on the findings of the aforementioned studies, air curtains create a high-velocity air barrier that effectively prevents smoke and heat from travelling through a designated area, while smoke evacuation

systems remove smoke from the fire-affected area through strategically placed ducts. Combining air curtains with smoke evacuation systems appears to be a promising smoke evacuation solution. However, there has been limited research on how the synergy of air curtains and smoke exhaust systems affects fire behaviour. Li et al. [6] investigated the effects of the synergistic effect of longitudinal ventilation and air curtain on the ceiling temperature rise distribution by conducting experiments in a 1:10 scaled-down bifurcated tunnel and proposed a prediction model for the corresponding maximum temperature rise. Lu et al. [19] explored the feasibility of using smoke curtains in bifurcated tunnels through experiments and numerical simulations and proposed a prediction model for determining the optimal air curtain jet velocity in bifurcated tunnels by means of quantitative analysis. Chen et al. [20] investigated the plug-holing phenomenon under the effect of ceiling centralized smoke exhaust system with air curtains and proposed a new modified critical Fr value for prediction the plug-holing phenomenon.

The selection of smoke exhaust systems depends on the specific design requirements and structural characteristics of the building. Lateral centralised smoke exhaust is more commonly used in long passages, and there is a lack of research on fires under the action of lateral centralised smoke exhaust and air curtain systems, particularly in terms of smoke temperature distribution and the diffusion of carbon monoxide. diffusion of carbon monoxide. The aim of this study is to provide a comprehensive experimental investigation of the combined effects of air curtains and transverse centralised smoke extraction systems on smoke temperature and carbon monoxide dispersion in an access fire scenario, taking into account the effects of different fire heat release rates and ventilation speeds. This study is essential for optimising fire safety strategies in enclosed and complex environments.

EXPERIMENTAL SETUP

The experiments were carried out on a 1:8 reduced scaled channel experimental platform[5, 22, 23], as shown in Figure 1. The dimensions of the channel are 22 m long, 1.20 m wide and 0.80 m high. The ceiling, floor and one side wall of the channel are steel plates covered by fireproofing panels, and the other side wall is made of fire-resistant glass that can be opened. The square burner (Side length: 0.12 m, Height: 0.30 m) was placed in the centre of the channel at a distance of 1.0m from the lateral centralized smoke vent.The lateral smoke vent (Width: 0.30 m, Height: 0.36 m) is positioned in the upper part of the channel sidewalls, the distance between the upper edge of the vent and the channel ceiling is 0.05 m. Air curtain (Length: 1.20 m Width: 0.20 m) and lateral centralized smoke vent are located downstream of the fire source, and the air curtain spaced 2.50 m apart from the fire source.

The experimental instrumentations are also shown in Figure.1. Two cameras ware placed on the exterior of the glass side of the channel to photograph the flame patterns and smoke flow. K-type thermocouples are arranged at 0.02 m beneath the channel ceiling to measure the ceiling temperature distribution. The thermocouples were spaced at intervals of 0.10 m-0.15 m. The CO concentration was measured with two gas analyzer (TESTO 330) based on built-in sensors. Two probes of the gas analyzers at 0.50 m centres on either side of the air curtain (S1 and S2)were used to measure the CO concentration at 0.02 m below the channel ceiling. In addition, smoke cakes were used in the experiment to generate artificial smoke, which was combined with a laser light source placed in the centreline of the channel to observe the smoke flow.

Ethylene was used as the fuel and the flow rate was controlled by a mass flow meter. During the tests, nine different fire heat release rates ranging from 26.5 kW to 90.3 kW, five lateral smoke exhaust velocities ranging from 0 m/s to 2 m/s (Corresponding full-size velocities of 0 m/s -5.7m/s), and six air curtain velocities ranging from 0 m/s to 4 m/s (Corresponding full-size velocities of 0 m/s -11.3m/s) were considered. A total of 270 sets of experimental test conditions, as shown in Table 1. The ambient temperature was about 26±2 °C. Each condition was repeated three times and averaged for further analysis.

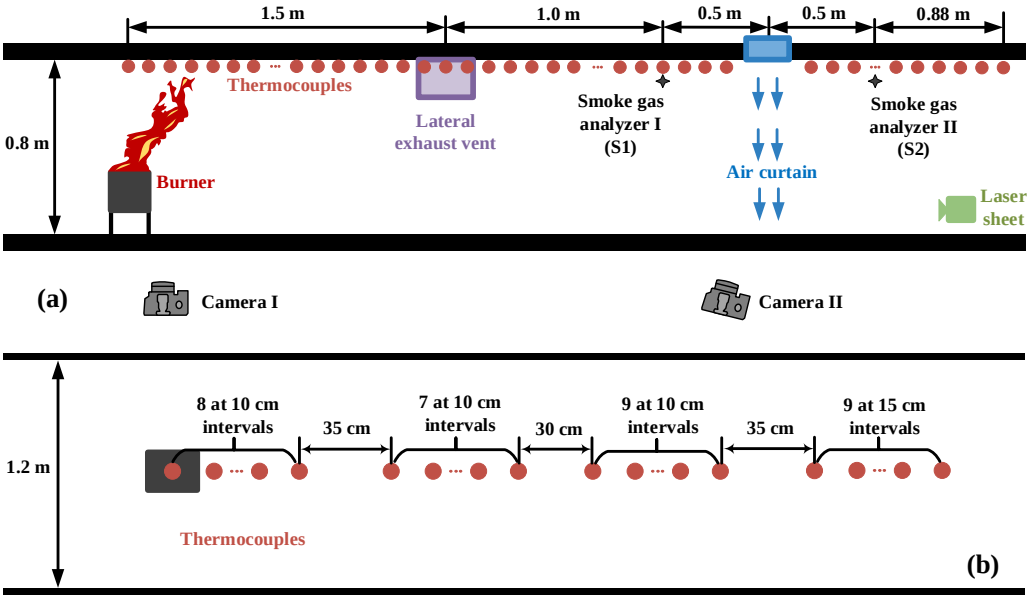

Figure 1 Experimental setup.

Table 1 Experimental conditions.

Test number	Burner size (cm)	Heat release rate /HRR (kW)	Lateral exhaust vent velocity (m/s)	Air curtain velocity (m/s)
1-270	12 cm; Ethylene	26.5, 31.9, 37.2, 42.5, 47.8, 58.4, 69.0, 79.6, 90.3	0, 0.5, 1.0, 1.5, 2.0	0, 0.5, 1.0, 2.0, 3.0, 4.0

RESULT AND DISCUSSION

Individual effect of air curtain or lateral centralized smoke exhaust

The temperature distribution of the tunnel ceiling and the local ceiling temperature distribution in the vicinity of the air curtain under the individual action of the air curtain and lateral smoke extraction as shown in Figure 2 and Figure 3. The air curtain can block the diffusion of high temperature smoke [13], so it has greater influence on the ceiling temperature of air curtain downstream. When the air curtain is not switched on, the overall ceiling temperature shows power exponential decay law. After the air curtain is turned on, the downstream ceiling temperature rapidly decreases and converges to the ambient temperature with the increase of the exit velocity of the air curtain. However, the upstream ceiling temperature gradually decreases only when the velocity of the air curtain is large enough ($v_A \geqslant 3$m/s). The lateral smoke vent can facilitate smoke evacuation under certain conditions so that part of the heat and smoke is discharged out of the tunnel [5]. Therefore, the ceiling temperature of the channel will gradually decrease with the increase of the lateral exhaust velocity.

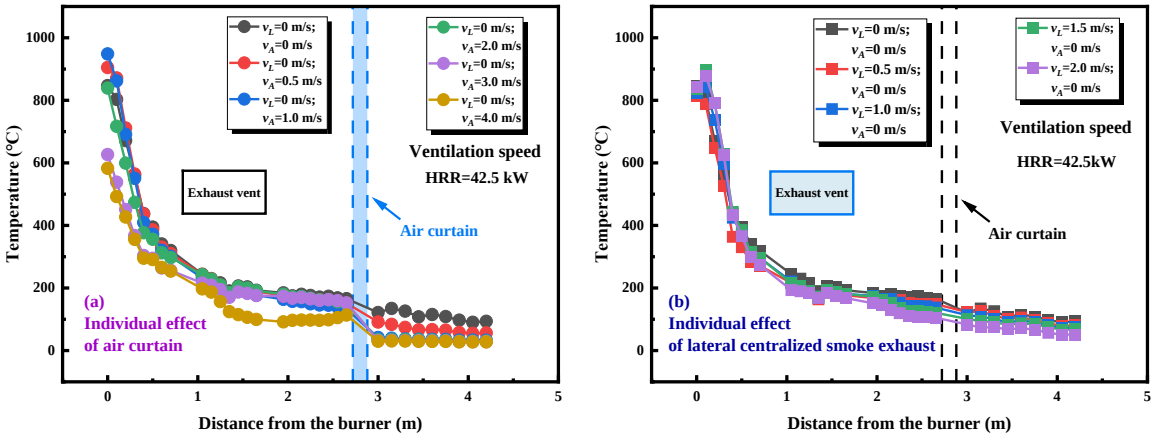

Figure 2 Ceiling temperature distribution.

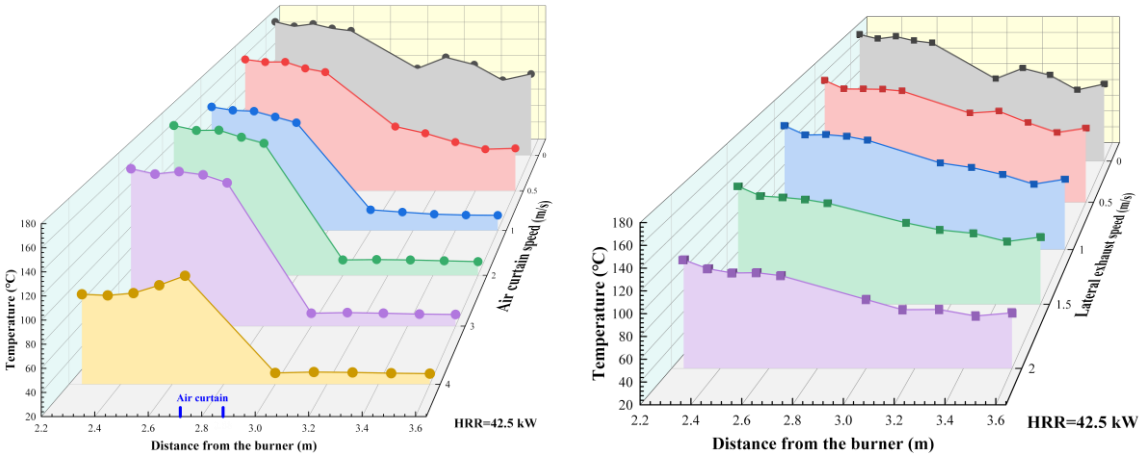

Figure 3 Local ceiling temperature distribution in the vicinity of the air curtain.

In order to visualise the effect of the air curtain and lateral smoke evacuation, the smoke flow field of the channel was further photographed in combination with a sheet light source[5, 19]. As can be seen from Figure 4, when the fire occurs in the passageway and there is no ventilation to control the smoke, the heat smoke forms a distinct stratification spreading along the channel ceiling. When the air curtain acts individually, the air curtain deflects significantly at smaller ventilation velocities and the smoke flows downstream from the bottom of the channel. The deflection angle of the air curtain becomes smaller and the air curtain carries little smoke to the downstream after impacting the bottom plate as the air curtain velocity increase. The unilateral pumping force of the lateral smoke vent creates longitudinal air velocity in the channel. Therefore, when the lateral smoke vent is acting individually, part of the smoke below the channel ceiling flows from both sides towards the lateral smoke vent but the smoke flow near the channel ceiling tends to stagnate under the competition of pumping force and buoyancy drive.

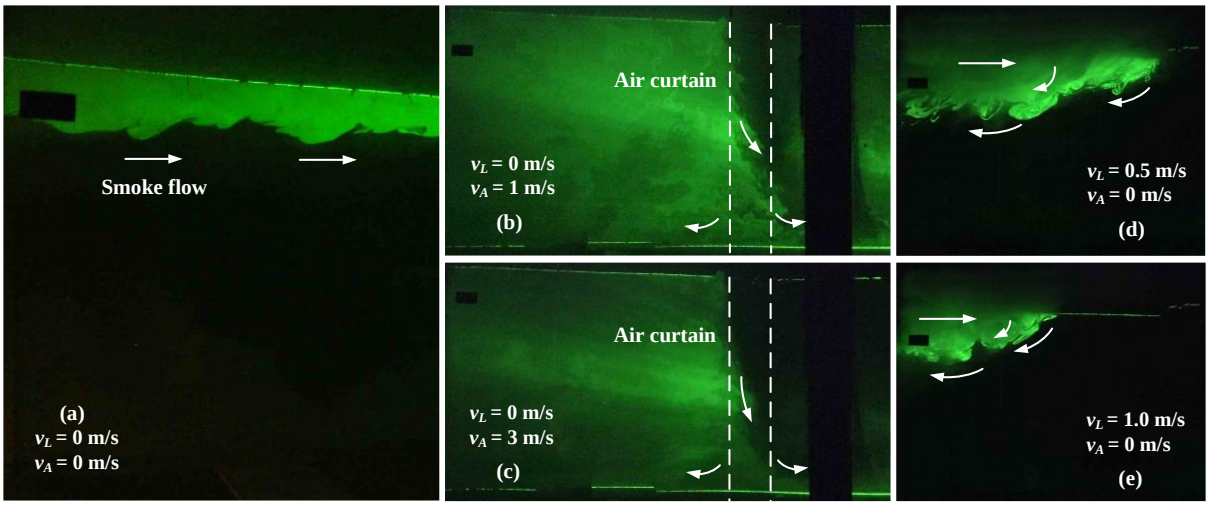

Figure 4 Smoke flow pattern of individual effect.

Synergistic action of air curtain and lateral centralized smoke exhaust

The occurrence of fire in a channel can generate high temperature smoke and release toxic gases, seriously threatening the safety of personnel. The combination of air curtain and lateral smoke exhaust system, both of which work together through different mechanisms of action (air curtain barrier and smoke exhaust flow), can effectively control the flow of smoke and improve the safety of personnel evacuation.

Then the effect of the synergistic action of the air curtain and lateral smoke exhaust is further explored and the ceiling temperature distribution in this case is shown in Figure 5. It can be seen that the temperature upstream and downstream of the air curtain are affected and decreased. When the lateral exhaust air velocity is constant, the ceiling temperature upstream of the air curtain decreases significantly with the increase of the air curtain velocity. The ceiling temperature downstream of the air curtain decreases rapidly when the air curtain velocity is small, but does not change greatly with the further increase of the air curtain velocity.

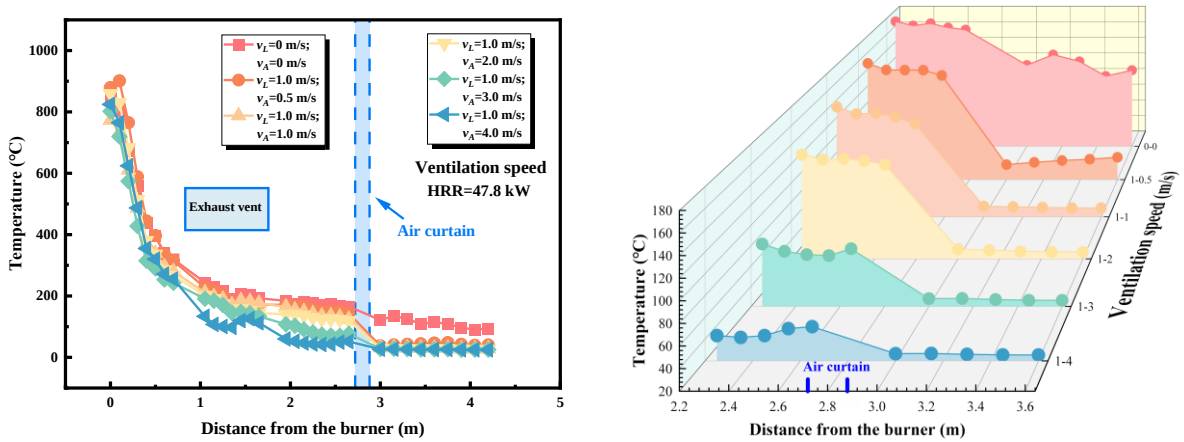

Figure 5 Ceiling temperature distribution under synergistic action of air curtain and lateral centralized smoke exhaust.

The evolution of the maximum channel ceiling temperature after the air curtain is shown in Figure 6. Figure 6a shows the variation of the maximum ceiling temperature with the air curtain velocity for different heat release rate at certain lateral smoke exhaust velocity. It can be seen that the maximum ceiling temperature decreases rapidly with the increase of the air curtain velocity under a certain fire heat release rate when the air curtain velocity is small ($v_A \leqslant 1.0$ m/s) and increases with the increase of the fire heat release rate for a certain ventilation velocity. When the air curtain is further increased (v_A

> 1.0 m/s), the maximum ceiling temperature does not change significantly, and the fire heat release rate has less influence on the maximum ceiling temperature. Figure 6b shows the effect of different lateral ventilation velocities on the ceiling temperature control for the maximum fire heat release rate in the experiment. It illustrates that the maximum temperature corresponding to a given air curtain velocity is lower as the lateral exhaust velocity increases, while the critical speed at which the air curtain velocity has little effect on the maximum temperature decreases.

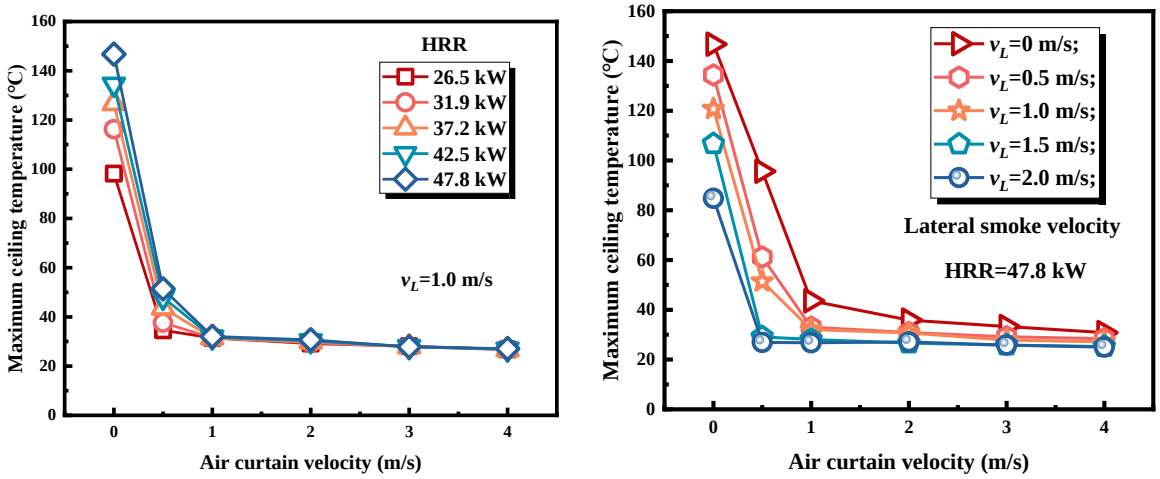

Figure 6 Maximum ceiling temperature after air curtain

Toxic and hazardous gases, in addition to temperature, are also a contributing factor in fires. Figure 7 demonstrates the concentration of carbon monoxide beneath the ceiling at different HRRs. In this case, the carbon monoxide concentration at the two measurement points on the left and right side of the air curtain under the same ventilation rate is shown in Fig. 7a. It can be seen that the CO concentration at both S1 and S2 increases with the increase of fire heat release rate, while the difference of CO concentration between the two sides of the air curtain also increases gradually with the increase of fire heat release rate under the effect of ventilation and smoke extraction. At the same position on the right side of the wind screen, the CO concentrations without ventilation and with ventilation are shown in Fig. 7b. It is found that the fire heat release rate is still one of the main influencing factors of CO concentration under a certain ventilation speed, and the difference of CO concentration before and after ventilation increases with the increase of fire heat release rate.

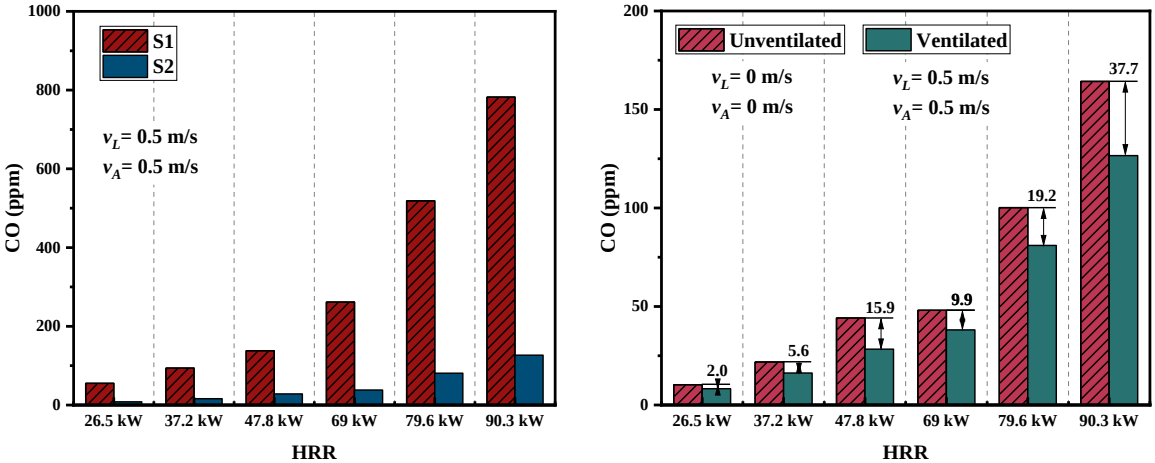

Figure 7 Carbon monoxide concentration beneath the ceiling at different HRRs.

Figure 8 illustrates the CO concentration underneath the ceiling at HRR = 47.8 kW. For the measured values of probe S1, the CO concentration increases and then decreases with the increase of the air curtain velocity at a certain lateral exhaust velocity. This is because the low-velocity air curtain has blocking effect on the smoke that makes the smoke accumulate upstream of the air curtain and the

lateral smoke exhaust cannot discharge the accumulated smoke effectively, thus the CO concentration shows an increasing trend with the increase of the air curtain velocity first. With the further increase of the air curtain velocity, the flow field upstream of the air curtain changes and makes the nearby smoke blow away (as shown in Figure 9), so the CO concentration gradually decreases with the increase of the air curtain speed. For the same air curtain speed, CO concentration shows a decreasing trend with the increase of lateral exhaust speed, which is mainly because the increase of lateral exhaust wind speed makes its exhaust capacity gradually increase to exhaust more smoke.

For measurements at probe S2which shown in Figure 8, the carbon monoxide concentration decreases with increasing the air curtain velocity and lateral exhaust velocity, except for the v_A = 0 m/s. For the case of v_A = 0 m/s, the CO concentration downstream of the air curtain did not decrease with increasing lateral exhaust velocity, which is mainly due to stagnant flow in the flue gas layer (analysed in Figure 4). Under other conditions, both the air curtain and the lateral exhaust have positive effect on the CO concentration downstream of the air curtain, and the CO concentration decreases rapidly with the increase of both velocities.

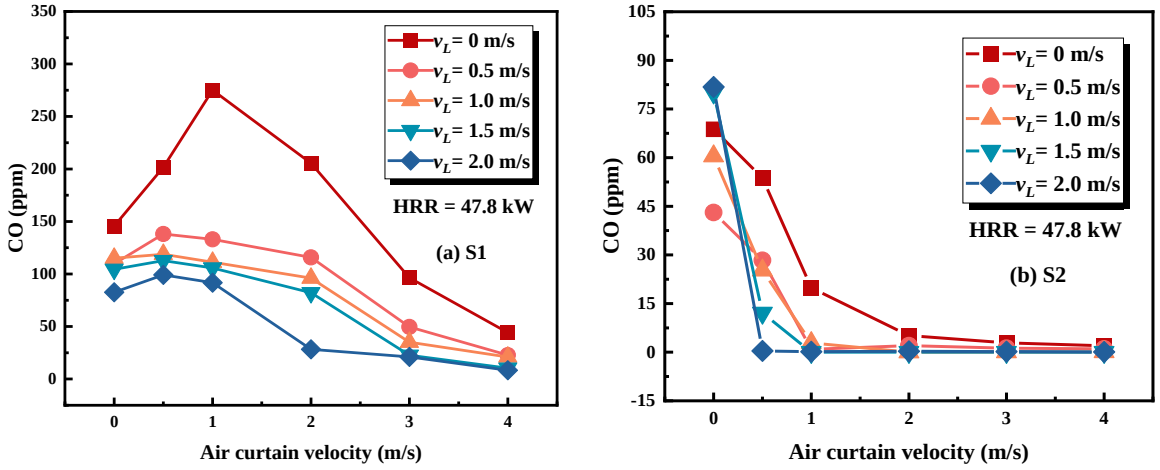

Figure 8 Carbon monoxide concentration beneath the ceiling under different ventilation speed at HRR=47.8 kW.

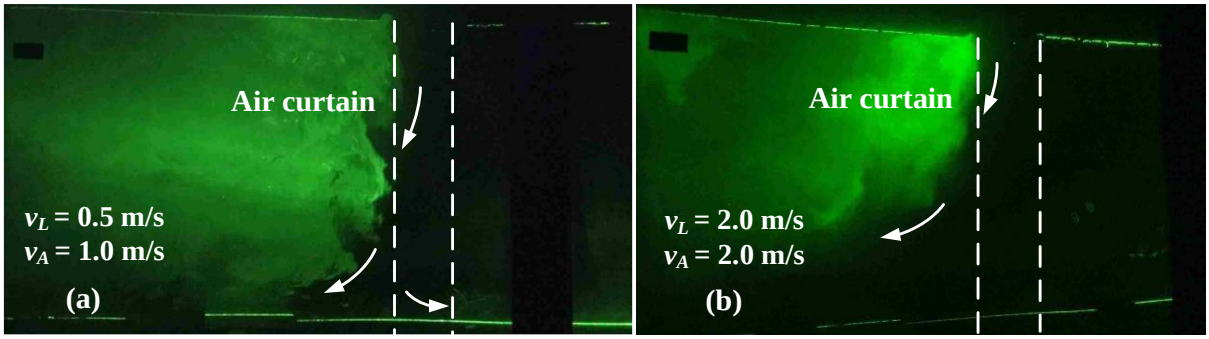

Figure 9 Smoke flow pattern of synergistic action.

The main function of air curtain and lateral smoke evacuation is to reduce the spread of high temperature smoke and toxic gases in the direction of evacuation. The effectiveness of air curtains in controlling smoke can be measured using the smoke sealing efficiency[14]:

$$\eta = \frac{C_0 - C_v}{C_0} \tag{1}$$

where C_0 is the CO concentration at S2 in the no-wind condition, C_v is the CO concentration at S2 under the synergistic effect of the air curtain and lateral smoke extraction.

The change in CO concentration at S2 downstream of the air curtain was used to calculate the smoke sealing efficiency in the work and the reault shows in Figure 10. Both air curtain and lateral smoke evacuation individually cannot achieve effective smoke control rapidly, and the synergistic effect of the two methods demonstrates excellent advantages.It can be seen that the greater the lateral smoke exhaust velocity, the smaller the air curtain velocity required for the smoke sealing efficiency to converge to 1. At the same time, after the smoke sealing efficiency exceeds approximately 90%, increasing the air curtain or lateral exhaust velocity has little effect on the efficiency. And at the corresponding air curtain and lateral exhaust velocity, the tunnel ceiling temperature is close to the ambient temperature, and the CO concentration after the air curtain is close to zero. It is worth noting that lateral smoke exhaust is used to remove smoke, and its exhaust efficiency is not suitable to be expressed in terms of the smoke sealing efficiency. Therefore, the subsequent analysis of the smoke sealing efficiency does not consider the case where the air curtain velocity is 0.

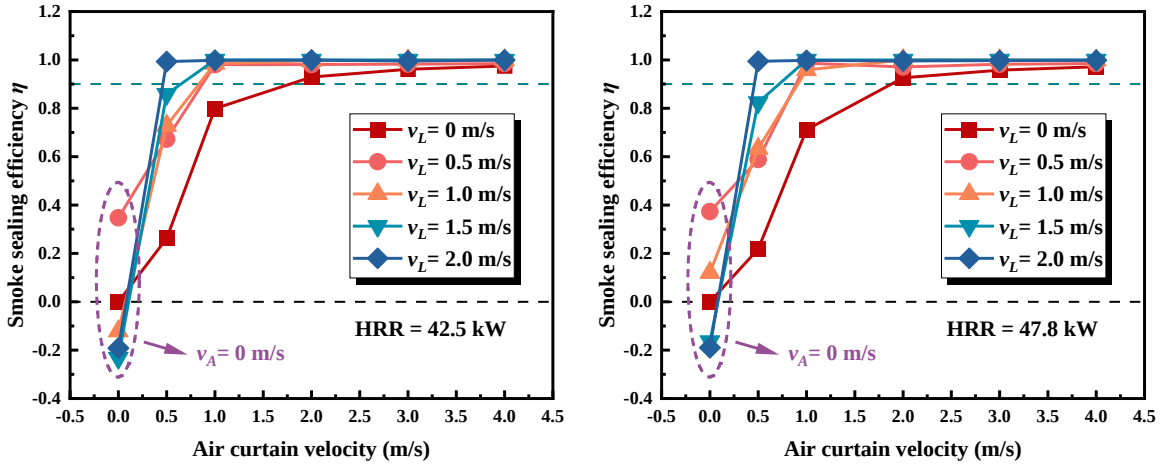

Figure 10 Smoke sealing efficiency of different ventilation velocities

Investigating and predicting the efficiency of smoke control with the synergistic effect of air curtains and lateral smoke extraction is essential to improve fire safety and optimise smoke control in buildings. In this paper, the smoke sealing efficiency under the synergistic action of air curtain and lateral centralized smoke exhaust will be studied using dimensional analysis method. According to the previous analysis, it can be concluded that the efficiency of smoke sealing efficiency is related to the fire heat release rate, lateral smoke exhaust velocity and air curtain velocity:

$$\eta = f\left(\frac{\dot{Q}}{\rho_a c_p T_a g^{1/2} H^{5/2}}, \frac{v_A}{\sqrt{gH}}, \frac{v_L}{\sqrt{gH}}\right) \tag{2}$$

Previous studies have shown that after the smoke sealing efficiency is greater than or equal to a certain threshold, the effect of increasing ventilation speed on the tunnel temperature, visibility, and smoke sealing efficiency is very small and the corresponding smoke sealing efficiency can be satisfied with the evacuation requirements [19]. According to the experimental results of this study, the smoke sealing efficiency threshold is about 90%, so the following smoke sealing efficiency prediction model is applicable to the efficiency less than or equal to 90%. Smoke sealing efficiency responds differently to air curtain velocity with and without lateral smoke exhaust. Thus the smoke sealing efficiency predictive model when the air curtain acts individually ($v_L = 0$ m/s)was obtained by fitting the dimensionless fire heat release rate and air curtain velocity. And the prediction equation for smoke sealing efficiency under the synergistic effect of air curtain and lateral smoke exhaust ($v_L \neq 0$ m/s) was developed by optimally fitting the three dimensionless parameters. The results in Figure 11 show that the prediction of smoke sealing efficiency is relatively good when the lateral exhaust is 0. But when the air curtain and lateral exhaust work in tandem, the smoke sealing efficiency is not predicted well for some fire heat release rates due to the complex tunnel airflow.

$$\eta = \begin{cases} 0.58\left(\dfrac{\dot{Q}}{\rho_a c_p T_a g^{1/2} H^{5/2}}\right)^{-0.35}\left(\dfrac{v_A}{\sqrt{gH}}\right)^{0.7}, v_L = 0 \\ 0.36\left(\dfrac{\dot{Q}}{\rho_a c_p T_a g^{1/2} H^{5/2}}\right)^{-0.60}\left(\dfrac{v_A}{\sqrt{gH}}\right)^{0.06}\left(\dfrac{v_L}{\sqrt{gH}}\right)^{0.26}, v_L \neq 0 \end{cases} \quad (3)$$

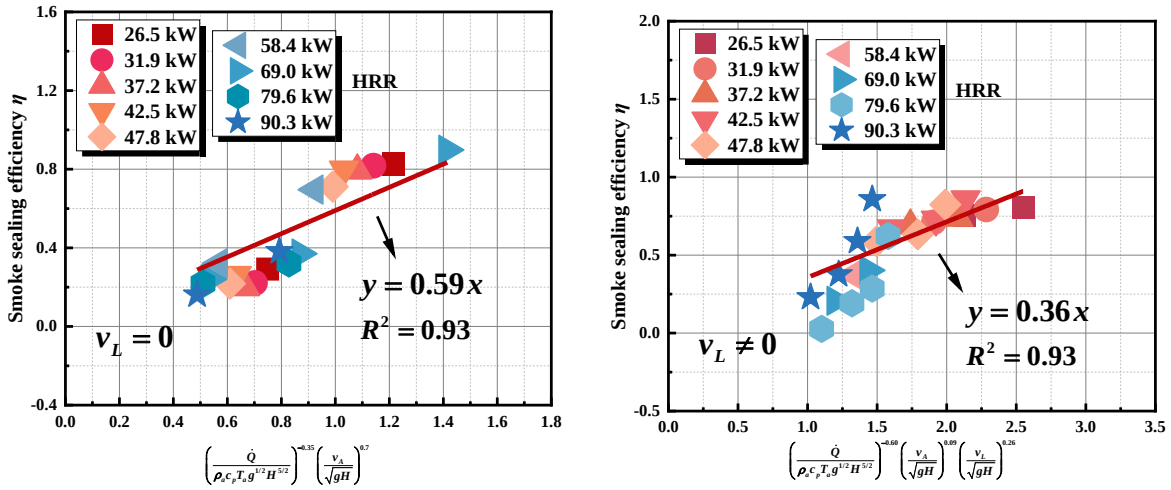

Figure 11 Smoke sealing efficiency model

CONCLUSION

In this work, the characteristics of smoke temperature and carbon monoxide diffusion in channel fires under the synergistic effect of an air curtain and a lateral centralised smoke extraction system were experimentally investigated. Key findings were drawn:

(1) Air curtains are effective in blocking the spread of smoke, but will roll smoke in the direction of evacuation upon impact with the channel floor. And the lateral centralised smoke exhaust system accelerates the discharge of smoke, and can reduce the overall temperature of the channel.

(2) With the synergistic effect of lateral smoke extraction and air curtains, the ceiling temperature and CO concentration on both sides of the air curtains are significantly reduced.

(3) The air curtain airflow is deflected by the synergistic action of the lateral smoke evacuation and the air curtain, effectively reducing the spread of toxic gases in the direction of the smoke evacuation. In the tunnel with a downscale of 1:8 and a height of 0.8 m, air curtain velocities of only 1 m/s to 2 m/s are required when the smoke sealing efficiency is approximately 100%.

(4) A predictive model for smoke sealing efficiency based on dimensionless analysis was developed by integrating the effects of fire heat release rate, lateral centralised smoke exhaust velocity and air curtain speed.

REFERENCES

1. Zhao, S., K. Du, Y. Yao, F. Wang, M. Weng, L. Xu, and W. Lei, *Influence of sidewall restriction on flame characteristics of double fires in a channel.* Tunnelling and Underground Space Technology, 2023. **140**: p. 105297.
2. Han, J., Y. Chen, W. Tan, W. Ma, C. Fan, Z. An, and H. Gao, *Field investigation of fire and smoke spreading characteristics in the high-altitude tunnel with strongly longitudinal ventilation.* Tunnelling and Underground Space Technology, 2025. **155**: p. 106235.
3. Li, Y.Z. and H. Ingason, *Influence of upstream blockage on smoke control in tunnel fires.* Fire Safety Journal, 2024. **147**: p. 104197.
4. Wang, Q., F. Guo, Y. Yao, and X. Zhang, *Numerical study on plug-holing of double fires in tunnel with centralized smoke exhaust.* Tunnelling and Underground Space Technology, 2023. **142**: p. 105419.

5. Zhu, Y., F. Tang, and Y. Huang, *Experimental study on the smoke plug-holing phenomenon and criteria in a tunnel under the lateral smoke extraction.* Tunnelling and Underground Space Technology, 2022. **121**: p. 104330.
6. Liu, Y., J. Chen, and D. Yang, *Experimental study on the effects of exhaust vent layout on plug-holing for ceiling central smoke extraction in road tunnel fires.* Tunnelling and Underground Space Technology, 2022. **126**: p. 104550.
7. Li, Y.Z. and H. Ingason, *Effect of cross section on critical velocity in longitudinally ventilated tunnel fires.* Fire Safety Journal, 2017. **91**: p. 303-311.
8. Zhu, Z., Q. Guo, S.E. Quiel, and C.J. Naito, *Rapid prediction of fire-induced heat flux on the liners of horseshoe and circular tunnels with longitudinal ventilation at critical velocity.* Fire Safety Journal, 2022. **130**: p. 103590.
9. Tang, F., L. Deng, N. Meng, M. McNamee, P. Van Hees, and L. Hu, *Critical longitudinal ventilation velocity for smoke control in a tunnel induced by two nearby fires of various distances: Experiments and a revisited model.* Tunnelling and Underground Space Technology, 2020. **105**: p. 103559.
10. Chen, X., J. Li, Y. Ni, Z. Liang, H. Ding, L. Liu, X. Zhang, K. Wu, and T. Zhang, *Study on induced flow patterns and inlet velocity in inclined tunnel fire with natural ventilation.* Tunnelling and Underground Space Technology, 2025. **155**: p. 106188.
11. Liu, Y., D. Yang, and X. Guo, *Theoretical model for predicting smoke back-layering length downstream of centralised ceiling exhaust vent in tunnel fires.* Tunnelling and Underground Space Technology, 2023. **137**: p. 105134.
12. Tang, F., Q. He, F. Mei, Q. Wang, and H. Zhang, *Effect of ceiling centralized mechanical smoke exhaust on the critical velocity that inhibits the reverse flow of thermal plume in a longitudinal ventilated tunnel.* Tunnelling and Underground Space Technology, 2018. **82**: p. 191-198.
13. Hu, L.H., J.W. Zhou, R. Huo, W. Peng, and H.B. Wang, *Confinement of fire-induced smoke and carbon monoxide transportation by air curtain in channels.* Journal of Hazardous Materials, 2008. **156**(1): p. 327-334.
14. Zhang, Z., Y. Yuan, K. Wang, X. Gao, and X. Cao, *Experimental investigation on Influencing Factors of air curtain systems barrier efficiency for mine refuge chamber.* Process Safety and Environmental Protection, 2016. **102**: p. 534-546.
15. Chen, Z., Z. Liu, X. Li, H. Linqi, and G. Niu, *Numerical study of the effect of air curtains on smoke blocking and leakage heat flux in tunnel fires.* Case Studies in Thermal Engineering, 2022. **35**: p. 102164.
16. Felis, F., M. Pavageau, J.C. Elicer-Cortés, and T. Dassonville, *Simultaneous measurements of temperature and velocity fluctuations in a double stream-twin jet air curtain for heat confinement in case of tunnel fire.* International Communications in Heat and Mass Transfer, 2010. **37**(9): p. 1191-1196.
17. Gupta, S., M. Pavageau, and J.-C. Elicer-Cortés, *Cellular confinement of tunnel sections between two air curtains.* Building and Environment, 2007. **42**(9): p. 3352-3365.
18. Li, T., Y. Yang, X. Li, C. Mi, C. Wang, Z. Chen, L. Chen, and Y. Zhang, *Experimental study of air curtain thermal insulation efficiency and maximum temperature rise beneath the ceiling under longitudinal ventilation in bifurcated tunnels.* Tunnelling and Underground Space Technology, 2023. **137**: p. 105112.
19. Lu, X., M. Weng, F. Liu, and J. Yu, *Study on smoke sealing effectiveness of the air curtain in exit bifurcated tunnel fires.* Case Studies in Thermal Engineering, 2024. **63**: p. 105380.
20. Chen, Z., Z. Liu, L. Huang, G. Niu, J. Yan, and J. Wang, *Research on the effect of ceiling centralized smoke exhaust system with air curtains on heat confinement and plug-holing phenomenon in tunnel fires.* Process Safety and Environmental Protection, 2023. **169**: p. 646-659.
21. Jung, U.-H., S. Kim, S.-H. Yang, J.-H. Kim, and Y.-S. Choi, *Numerical study of air curtain systems for blocking smoke in tunnel fires.* Journal of Mechanical Science and Technology, 2016. **30**(11): p. 4961-4969.
22. Hu, P., X. Peng, and F. Tang, *Prediction of maximum ceiling temperature of rectangular fire against wall in longitudinally ventilation tunnels: Experimental analysis and machine*

learning modeling. Tunnelling and Underground Space Technology, 2023. **140**: p. 105275.
23. He, Q., F. Tang, Y. Zhao, P. Hu, and M. Gu, *An experimental study on the intermittent flame ejecting behavior and critical excess heat release rate of carriage fires in tunnels with longitudinal ventilation.* International Journal of Thermal Sciences, 2022. **176**: p. 107483.

A paramedic study of fire conditions in naturally ventilated road tunnels

Imad Obadi, George Hadjisophocleous
Department of Civil and Environmental Engineering, Carleton University, Ottawa, Canada

abstract

The Ofenegg Tunnel Fire Test was conducted in a full-scale experimental study aimed at gaining a better understanding of fire behavior in road tunnels. Documented and validated experiments of this nature are limited in existing literature, highlighting the unique contribution of this research. For validation, two fire scenarios representing minimum and maximum heat release rates of 17 and 43 MW under natural ventilation conditions were selected. The Fire Dynamics Simulator (FDS) was used to compare the predicted temperature distribution, oxygen levels, carbon monoxide concentrations, and gas flow rates with experimental data. The findings demonstrated good agreement between FDS predictions and experimental values. Following validation, a parametric study was conducted to investigate the effects of varying fire sizes (1.5, 75, and 150 MW) and slopes (0.5%, 3%, and 6%) on time-temperature profiles reaching 60°C, assessed at 2 m to represent human height. The study tracked the temperature progression 10 meters upstream and downstream from the fire origin and along the entire 450-meter tunnel length, underlining the effect of these factors on temperature magnitudes. Results showed that the small fire (1.5 MW) is considered safe regardless of the slope, while larger fires (75 and 150 MW), combined with steeper slopes (3% and 6%) in the downstream direction, represent a worst-case scenario, as they lead to accelerated temperature increases and reduced Available Safe Egress Time (ASET). However, for large fires with a slope of 0.5%, the time required to reach 60°C was similar in both directions but resulted in a higher ASET compared to steeper slopes. Additionally, the temperature distribution at the downstream gradually became more uniform, resembling the conditions observed in longitudinally ventilated tunnels.

KEYWORD: road tunnel, naturally ventilation, validation, FDS, time-temperature.

INTRODUCTION

Tunnel fires have been rising globally, ranking among the most severe traffic accidents occurring in these confined spaces (1–4). Such incidents often result in numerous casualties and cause wide damage to tunnel structures. Furthermore, they frequently lead to regional traffic paralysis and disrupt communication systems, causing significant indirect losses (5,6). Given these serious consequences, tunnel fires have garnered considerable attention in recent years. The unique structural characteristics of tunnels contribute to rapid temperature increases and the quick spread of smoke, complicating emergency rescue efforts.

During the early stages of a fire, the lower part of a tunnel often serves as an evacuation pathway (7). However, temperatures exceeding 60°C can be life-threatening, as the human body cannot tolerate such heat for extended durations (8–10). Therefore, understanding smoke stratification and its downward movement is essential for ensuring the safe evacuation of personnel. To effectively evaluate associated risks, it is essential to understand the dynamics of smoke movement and the temperature distribution. In this context, managing smoke temperature becomes a key aspect of fire safety, with ventilation systems playing an integral role in controlling smoke flow and maintaining safe temperature levels. Tunnel ventilation is typically either natural or mechanical (11). Mechanical systems are suited for

longer tunnels, require substantial power and cost, and they may disrupt smoke stratification, potentially hindering safe evacuation in early fire stages (12). Natural ventilation in shorter tunnels often relies on buoyancy-driven airflow to remove smoke through openings with minimal disruption to smoke layers (7,13–15). Its simplicity and cost-effectiveness have made natural ventilation increasingly prevalent and a focus of recent research (16). During a fire, the temperature distribution of smoke varies between upstream and downstream directions due to fire sizes, as larger fires with higher HRRs produce stronger buoyant forces, driving smoke flow and temperature more significantly downstream while also affecting upstream movement. These affects are further influenced by the tunnel slope (17–19), which complicates evacuation and emergency rescue efforts, making it essential to understand this interaction for accurately characterizing fire severity in road tunnels.

In recent years, many scholars have conducted numerous studies on the rise of maximum temperature in naturally ventilated tunnels. For example, Huang et al. (20) examined how the position of a fire within a tunnel influences the ceiling temperature, using HRR values of 1, 2, and 3 MW. Their results indicate that fires located closer to the tunnel entrance tend to produce lower maximum temperatures compared to those located deeper within the tunnel. Kong et al. (21) investigated the effect of the hot gas movement and smoke distribution in a slopping tunnel fire varies from 0 to 10%, with HRR of 15 MW and located at the centerline in the middle of the 500 m tunnel geometry. The results indicate that the smoke temperature at the downstream exit first increased and then decreased with a higher slope. Cong et al. (22) conducted a series of numerical simulations to study the rise in maximum temperature in tunnels with varying widths and slopes under natural ventilation. Their findings indicate that the stack effect becomes more pronounced with an increase in tunnel slope or a decrease in tunnel width. In another study, Merci (23) has concluded that the stack effect becomes stronger as the slope of tunnel increases. Therefore, the smoke movement in an inclined tunnel is different from the one in a horizontal tunnel. Ji et al. (24) investigated the effects of tunnel slope and on the upstream maximum temperature along the centerline of modelling tunnel. The results indicate that the upstream maximum temperature drops progressively as the distance from fire source increases.

The combination of inclined tunnel fires coupled with varying fire sizes under natural ventilation adds further complexity concerning occupants' safety. However, limited research focused on time-temperature profiles at human body height in both upstream and downstream directions, particularly for large- scale fires, such as tanker fires, in naturally ventilated road tunnels. To address this gap, the present study conducts a detailed numerical analysis of these scenarios, as presented in the parametric study section.

Large-scale tunnel fire testing is essential for the development of tunnel safety standards and also contributes to the development of theoretical models and deepening understanding of fire dynamics in tunnels (25). This approach allows researchers and engineers to investigate the impact of key parameters such as tunnel geometry and ventilation systems that sometimes cannot be accurately replicated through smaller-scale testing. Also, large-scale testing is invaluable for the validation of models dealing with fire-related hazards in road tunnels (26). However, conducting large-scale tunnel tests for every configuration is not possible due to their high cost, logistical complexities, and time-intensive nature, which results in a limited number of such experiments (27).

In this study, the Ofenegg Tunnel Fire Tests, conducted in 1965 in Switzerland and recognized as the "first large-scale fire test series" (28). These tests aimed to provide a fundamental understanding of the fire behaviour, including temperature distribution, visibility and smoke concentrations caused by gasoline tank fires, thereby providing key data on potentially hazardous conditions for tunnel users. For the validation, two of these fire tests that used natural ventilation were selected. One having the lowest (17 MW) and the other the highest (43 MW) Heat Release Rate.

THE OFENEGG TUNNEL FIRE TESTS

The schematic diagram in Figure 1 shows the Ofenegg Tunnel fire test. The tunnel featured a portal on its western side, while the eastern portal served as a dead end. The tunnel spanned a total length of 189.25 m with a cross-section in the shape of a horseshoe and offered a clear area of approximately 24 m^2. The maximum clear height was 6.0 m and the width at the base 4.0 m. Typically, the dimensions of this cross-sectional are intended to provide a single traffic lane for a unidirectional road tunnel (29). The tunnel vault consists of a combination of rock and concrete materials. The fuel pan dimensions were 3.80 m in width and 0.40 m in height, and with two different lengths of 1.75 and 12.50 m, representing areas of 6.60 and 47.50 m^2, respectively. The smallest pool represented the volume of two vehicles' fuel tanks, while the largest was approximately equivalent to a significant spill from a petrol tanker (27). The distance from the portal to the fire origin was 131.50 m. Gasoline with a heat of combustion of 43.7 MJ/kg was used, and the fuel density was assumed to be 740 kg/m^3. The maximum fuel burning rates for 100 and 500 Liter (L) were set at 0.074 and 0.026 $kg/m^2.s$, respectively. The maximum HRR for each pool fire was then calculated using Equation (1), assuming a combustion efficiency of 0.8 within the tunnel (30)

$$HRR = \eta\, \dot{m}_f^{''}.A_f.\Delta H_c \quad (1)$$

where, η represents combustion efficiency, $\dot{m}_f^{''}$ denotes the burning rate per square meter, A_f denotes the fuel area, ΔH_c represents the heat of combustion.

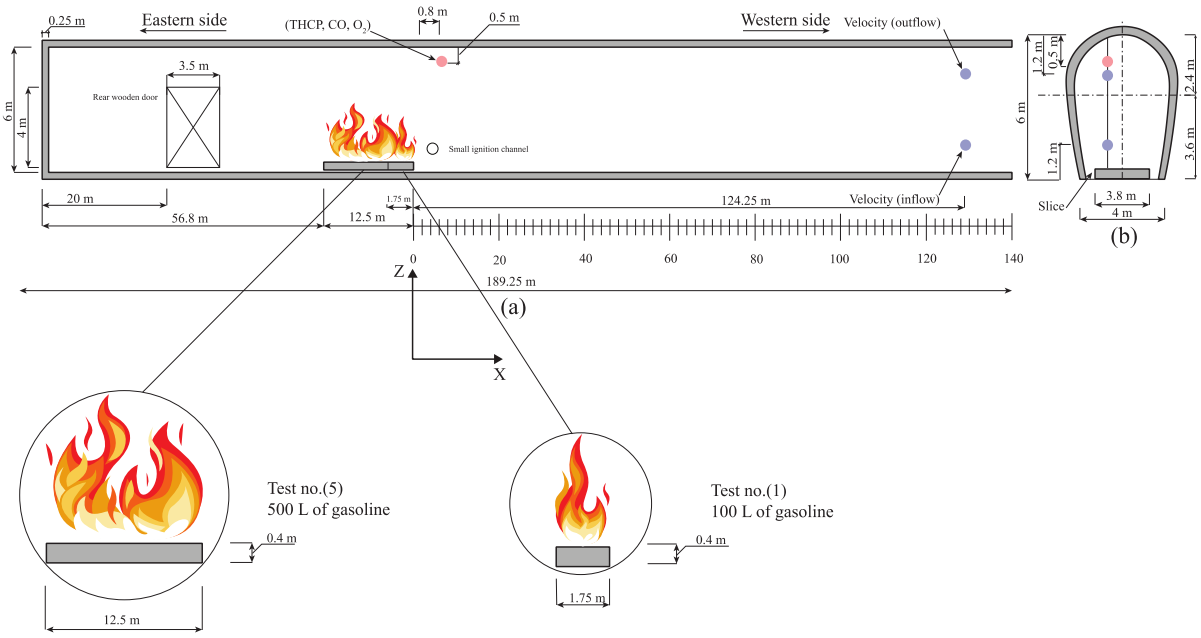

Figure 1 Schematic diagram of the Ofenegg Tunnel fire test and the FDS model setup (a) Side view, (b) Cross-section view (not to scale).

Experimental setup

From the experimental setup described in (28,31), the fuel used consisted of pure gasoline, with volumes of 100 and 500 L, contained within a concrete pan. During the experiment, ventilation was achieved solely using a natural system. The test tunnel had two openings: first, a window positioned near the concrete tub was sealed off with bricks, except for a small resistant cable serving as the ignition channel. Second, a rear wooden door remained open throughout the test. This setup helps fresh air to be drawn in through the rear door, aided by the injector effect. The ambient wind velocity outside the tunnel portal was measured before the test began, and the readings were taken between 20 and 30 m away from the tunnel portal at an elevation of 3 to 5 meters above ground. Furthermore, two flow measurement devices

were positioned 124.25 m from the western edge of the tub, at depths of 1.2 m below the ceiling and 1.2 m above the tunnel floor. Temperature sensing was conducted using Chromel–Alumel thermocouples connected to multiple recorders via cables made of the same material. A mono gas analyzer was used, with copper pipes running from each intake port to the central sampling point, which had an outside and inside diameter of 8 and 6 mm, respectively.

Test No. 1 (100 L of gasoline used)

In the initial stage of Test No. 1 (31), the temperature was 16 °C, humidity was 92%, and barometric pressure was 713.9 mm HG. Wind velocity ranged from 0 to 1.6 m/s at a fixed point (i.e., 20 meters in front of the tunnel portal and 4 meters above its base), where wind conditions were noted as gusty and westerly. The experimental setup included a burning area measuring 1.75 m x 3.80 m, totalling 6.65 m2, with 100 L of pure petrol. The fire lasted approximately 2.5 to 3 minutes, indicating sufficient oxygen for combustion, similar to how such a fire would occur outside (31). Under open conditions, HRRs per unit area can reach up to 2.40 MW/m², with a mass loss rate per unit area of 0.055 kg/m².s and a heat of combustion of 43.70 MJ/kg (30). The smoke plume traveled from the fire origin toward the tunnel entrance at an average speed of approximately 2.5 – 3 m/s. However, at the fire location, the speed was around 4 m/s and was gradually reduced towards the entrance. Table 1 summarizes the observations from the experiment report (31), showing the progression of fire at each test stage, and providing a comprehensive overview of its development throughout the testing period.

Table 1 Summary of fire behavior observations from experiment report - Test No. 1 (100 L of gasoline used).

Time after ignition		Remarks from the experimental test
Minute(s)	Second(s)	
0	10	Flames extended across the entire width of the tub, and airflow at the portal was observed to be escaping at a rate of 1.5 to 1.7 m/s.
0	20	The layer of smoke in the tub is well-defined and measures 2.5 m in thickness.
0	30	Smoke becomes thicker.
0	45	The smoke exits the tunnel at different speeds: 2.4 m/s at the upper part of the portal and 1.2 m/s at the lower part.
1	00	Heavy smoke emissions were seen from the entrance, leading to a 2.7-m-thick smoke layer.
2	00	The tunnel portal is filled with smoke, experiencing strong turbulence and heat generation from the fire source at its peak intensity.
2	30	The fire intensity decreases.
3	00	The fire is likely extinguished, but smoke emission continues.
6	00	The smoke at the entrance disappears gradually.
10	00	Smoke remains within the tunnel, with extremely low levels observed at the portal.
32	00	The tunnel is cleared for repair work.

Test No. 5 (500 L of gasoline used)

During the initial stage of Test No. 5 (31), the temperature was 10.30 °C, humidity 85%, and barometric pressure 711.5 mm HG. Wind velocity ranged from 2.3 to 3.3 m/s at a fixed point (i.e., 20 meters in front of the tunnel portal and 4 meters above its base), where gusty westerly winds were observed. The experimental setup consisted of a burning area measuring 12.50 x 3.80 m, totaling 47.50 m^2, and with 500 L of pure gasoline. The entire experiment, from ignition to the appearance of smoke at the tunnel portal, progressed rapidly. The fire lasted 6 minutes, but insufficient oxygen was available to sustain normal combustion, with most burning concentrated at the tub's two-end cross-sections. The smoke plume traveled from the fire source to the portal with an average speed of between 5 and 5.5 m/s. Maximum temperatures for all profiles between the fire source and the tunnel portal were recorded 2 minutes after ignition, with the peak reaching at the highest point after 1 minute. Two minutes after ignition, the peak temperature had advanced 11.60 meters away from the fire location, probably due to

flame redirection on the vault and possible vapor ignition in that area (32). Table 2 summarizes observations from the experiment report (31), showing the progression of fire behavior at each stage and providing a comprehensive overview of its development throughout the testing period.

Table 2 Summary of fire behavior observations from experiment report - Test No. 5 (500 L of gasoline used).

Time after ignition		Remarks from the experimental test
Minute(s)	Second(s)	
0	6	A visible sign at a distance of 11 m had become covered in flames on its upper section. The intensity of the fire was higher on the closed side of the tunnel compared to the open side.
0	12	The fire was no longer visible, concealed by dense smoke. The flow velocity at the portal measured 4 m/sec at the top and 5.8 m/sec at the bottom.
0	25	Smoke is observed at the portal, indicating that countercurrent flow is occurring in the tunnel's lower half. Current flows at a rate of 4 m/sec at the top and 2.1 m/sec at the bottom.
0	30	The anemometer positioned at the top has failed, with the cables melted.
1	00	Intense smoke is accumulating near the entrance, while the lower part remains smoke-free.
2	00	A short circuit in the tunnel caused the failure of the lighting system for the visible markers. At the tunnel portal, the flow rate at the top varies between 2 and 5 m/sec, while the flow rate below is 2.3 m/sec.
3	00	At the portal, the smoke emissions are thicker.
5	00	The fire is getting close to its final stage; however, the release of smoke remains.
6	00	The fire in the tub is most likely extinguished.
7	00	Smoke emissions at the entrance are somewhat decreasing. The flow out of the tunnel portal varies between 1.8 and 2.3 m/sec at the top and 1.1 to 1.6 m/sec at the bottom.
10	00	A visible flame remains in the tunnel, likely originating from burning vehicles.
12	00	The disturbances at the portal are diminishing, but there are still notable fluctuations: the outflow at the upper section is 2.3 m/sec with a maximum deviation of more than 5 m/sec, while the inflow at the lower section fluctuates between 0.9 and 1.1 m/sec.
15	00	The amount of smoke produced is small, yet there is still a faint glow of fire in the tunnel.
20	00	Smoke production has almost stopped.
72	00	The test is completed, and the tunnel is now cleared for repair work.

Numerical model

The FDS (33), developed by the National Institute of Standards and Technology, is an open-source code commonly used for fire simulations. It uses the numerical solution of a modified version of the Navier-Stokes equations customized for low-speed, thermally driven flows, with a special emphasis on the movement of smoke and heat produced by combustion. This is performed using a second-order accurate finite difference approach and more information can be found in Ref. (34). FDS incorporates both direct numerical simulation (DNS) and large eddy simulation (LES). In this paper, LES approach is combined with the constant coefficient Smagorinsky model to simulate turbulent flow, with the turbulence viscosity represented by Equation (2 and 3) (35). Furthermore, thermal conductivity and material diffusivity are correlated with turbulent viscosity by means of Equation (3). Simulations are done using version 6.8.0.

$$\mu_{LES} = \rho(C_s\Delta)^2[2\overline{S}ij:\overline{S}ij - \frac{2}{3}(\nabla \cdot \overline{u})^2]^{0.5} \quad (2)$$

$$k_{LES} = \frac{\mu_{LES}\, c_p}{Pr}, \qquad (\rho D)_{LES} = \frac{\mu_{LES}}{Sc} \quad (3)$$

Initial and boundary condition

The initial parameters in the FDS model (Figure 1), are configured according to those of the experimental setup within the tunnel as explained in the previous section for each test, these parameters include ambient temperature, barometric pressure, and relative humidity. A fire fueled by 100 L generated an HRR of approximately 17 MW, while a fire fueled by 500 L produced an HRR of around 43 MW. In the FDS model, we used a simple pyrolysis model to replicate these fires using "BURNER," and N-Octane (C_8H_{18}) as the fuel. The carbon monoxide (CO) yield and soot production during fuel combustion were set to be 0.01 and 0.034 mol/mol, respectively (36). However, due to a lack of information on the thermal properties of hard gneiss rock, the thermal properties of "CONCRETE" were used as a reference benchmark. The tunnel ceiling, floor, and side walls were each assumed to have a thickness of 0.25 m. "OPEN" boundary conditions were applied for all directions to simulate the open space condition. The simulations were executed for a duration of up to 250 s for fires with HRR of 17 MW, and 400 s for fires with HRR of 43 MW. The simulation used thermal conductivity, density, and specific heat values for concrete set at 1.2 W/m/K, 2200 kg/m^3, and 0.88 kJ/kg/K, respectively (37). To account for the gusty wind reported during the experiment, extended domains were added in the x direction extending 20 meters from the portal. Accordingly, Test 1 was assigned to a wind velocity of 1 m/s, while Test 5 was assigned to a wind velocity of 2.5 m/s. The wind velocity was modelled using vents placed at the boundaries of the domain to simulate the gusty conditions. Horizontal thermocouples and gas-phase instruments were installed to measure temperature distribution, oxygen concentration, and CO levels inside the tunnel. These devices were positioned 0.8 m from the fire pan's endpoint, 0.5 m below the ceiling, and spaced at 5 m intervals to capture longitudinal temperature distribution. Additionally, a single set of gas-phase instruments for smoke velocity measurements was placed 124.25 m from the fire pan. These instruments were installed at two heights: 1.2 m above the ground to measure inflow velocity and 1.2 m below the ceiling to measure outflow velocity.

Meshes

In FDS simulations, the grid size is an important element that contributes to the accuracy of the numerical simulations. For example, when opting for a coarse mesh, the resolution of the fire becomes inadequately resolved and therefore inaccuracy in fuel transport and combustion processes becomes increased due to numerical diffusion effects (38). Therefore, the selection of an appropriate mesh size is essential to ensure consistent outcomes and meet two key criteria: good accuracy results and low calculation time (39). The non-dimensional expression Z^*/δ_x gives the appropriate mesh size for the domain, where δ_x is the nominal mesh size and Z^* is the characteristic fire length, and calculated using the following formula (33):

$$Z^* = \left(\frac{\dot{Q}}{\rho_\infty c_p T_\infty \mathrm{g}^{0.5}}\right)^{\frac{2}{5}} \quad (4)$$

where $\dot{Q}$ is the heat release rate (MW); ρ_∞ is the air density (kg/m^3); C_p is the air heat capacity (J/(kg.K)); T_∞ is the ambient temperature (°C); and g is the acceleration of gravity (kg/m^3).

McGrattan (33) recommended that the value of Z^*/δ_x should be in the range of 4 –16 for simulations to provide favorable outcomes while consuming a minimal amount of processing time. The accuracy of the simulation output improves with higher values of Z^*/δ_x. The following equation can thus be used to determine the appropriate range of mesh sizes. Further clarifications are provided in (34)

$$\frac{Z^*}{16} \leq \delta_x \leq \frac{Z^*}{4} \quad (5)$$

Table 3 shows the cell size range obtained through Equation (5) and the simulated HRR for both scenarios, a grid size of 0.25 m was consistently used all over the domain.

Table 3 Cell size range with HRRs.

HRRs (MW)	Z^*	Cell size range (m)
17	3.06	0.20 – 0.75
43	4.44	0.25 – 1.0

Comparison of experimental and numerical data (Validation)

To verify the accuracy of FDS to model tunnel fires with natural ventilation, the numerical results are compared with the data from the full-scale experiments. The results of these comparisons are presented below.

Longitudinal temperature distribution

Figure 2(a) and (b) illustrate the maximum temperature distributions, comparing numerical results with experimental data range for two fire sizes (17 and 43 MW), respectively. The experimental results are presented as a range, as documented in the experimental report (28,31). Measurements were taken longitudinally from a distance of X = 0.8 m from the fire pan's endpoint toward the exit portal, at a height of Z = 5.5 m and width of Y = 2.8 m. For the numerical results, the maximum temperature reached was 670 °C with an HRR of 17 MW, and 1055 °C for a fire with an HRR of 43 MW. Temperatures decreased downstream as the distance from the fire source increased. The simulated curve was in very close agreement with the experimental data for a fire for 17 MW. However, for the 43 MW fire, the temperatures calculated by FDS were slightly lower than those measured experimentally. This discrepancy may be attributed to some materials used in the experimental tests that could have ignited within the tunnel, contributing to higher recorded temperatures compared to the actual values. These materials include non-engine-fueled vehicles, meat carcasses hung both inside and outside the vehicles, wood, fabric, and textiles. They were included solely to assess the degree of skin burn at the driver's head height, and the samples were later tested in the laboratories of the Scientific Service of the Zurich City Police. Generally, in both scenarios, the numerical results show good agreement with the experimental data, with only slight deviations observed in the temperature curve for the larger HRR.

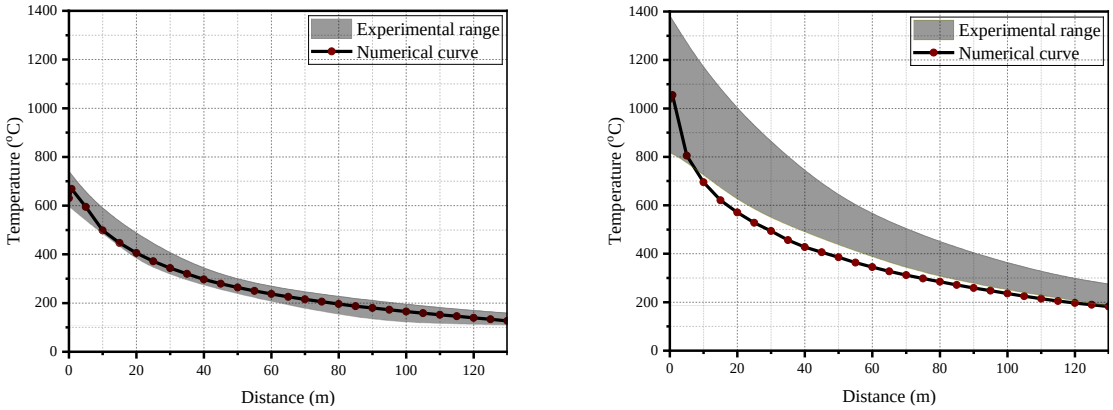

(a) *(b)*

Figure 2 Experimental temperature-distance range versus numerical maximum temperature-distance curve for entire the tunnel length started at 0.8m from Fire Endpoint's Pan. (a) HRR= 17 MW, (b) HRR= 43 MW.

Time–temperature distribution

Figures 3(a) and (b) show temperature curves over time, measured at a distance of 0.8 m from the fire pan's endpoint and 0.5 m below the ceiling. In Figure 3(a), a rapid temperature rise is observed after ignition, with the peak reaching approximately 670°C within two minutes, indicating that the fire quickly reaches maximum intensity. After 2 minutes, the temperature drops sharply, falling below

200°C, indicating that the fire has been extinguished (40). In contrast, Figure 3(b), shows a much faster temperature rise after ignition, reaching a maximum temperature of about 1055°C in one minute. This sharp rise implies that the greater the volume of fuel (500 L of gasoline), the more quickly heat reaches the ceiling due to upward gas flow (41). The subsequent temperature decrease is slower than in Figure 3(a), with the temperatures falling below 500°C six minutes after ignition. This is due to the fact that the fire continues to burn until 6 min after ignition. Both figures show good agreement between the numerical results and the experiments.

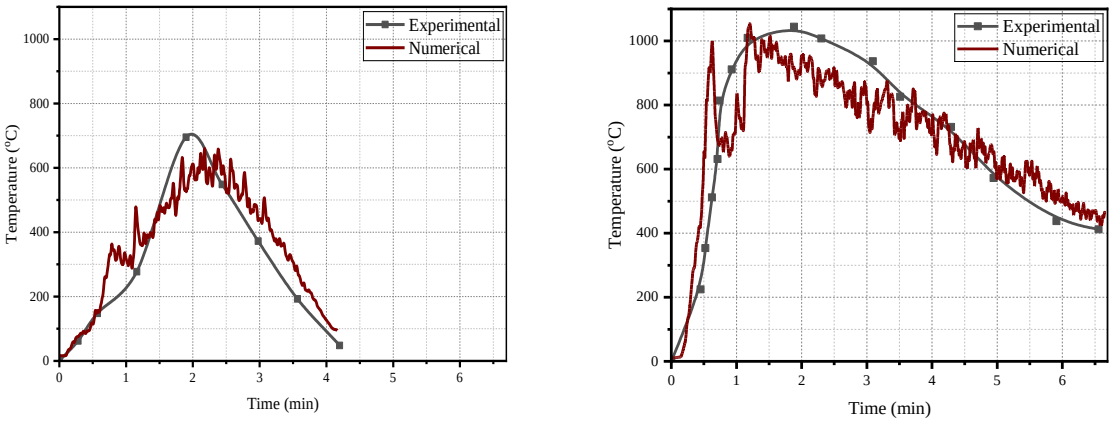

Figure 3 Temperature curves versus time at 0.8m from Fire Endpoint's Pan and 0.5m below Ceiling. (a) HRR=17 MW, (b) HRR=43 MW.

Oxygen concentration

Figures 4(a) and (b) show the oxygen concentration (%) over time (min) for two cases with different HRRs at a distance of 0.8 m from the fire endpoint and 0.5 m below the ceiling. The corresponding oxygen consumption rate for a fire with HRR of 17 MW is approximately 5–6 $l/(m^2.min)$ and for a fire of 43 MW is around 1.7-1.9 $l/(m^2.min)$ (31). These rates can be estimated using equation (6) (37,42):

$$\alpha_t = \frac{Q}{B_t \times A} \tag{6}$$

where, α_t is the fuel burning rate in ($l/(m^2.min)$), Q is the fuel quantity (l), B_t is the burn duration (min), and A is the surface area of the fuel pool (m²).

For the small fire (HRR = 17 MW), substituting $Q = 100\,l$, $B_t = 3\,min$, and $A = 1.75\,m \times 3.8\,m$ ($6.6\,m^2$), the oxygen consumption rate (α_t) is approximately 5.05 $l/(m^2.min)$. This value is consistent with typical outdoor burning fires, which generally exhibit oxygen consumption rates around 5 $l/(m^2.min)$ (31,43). For the larger fire (HRR=43 MW), substituting $Q = 500\,l$, $B_t = 3\,min$, and $A = 12.5\,m \times 3.8\,m$ ($47.5\,m^2$), the α_t is approximately 1.75 $l/(m^2.min)$. This value indicates an insufficient oxygen supply within the tunnel, limiting the fire's combustion efficiency. The slower oxygen consumption rate (1.7–1.9 $l/(m^2.min)$) reflects oxygen-limited combustion, as observed in both the experimental report and the FDS modeling results. The comparison between the numerical results and experimental outcomes shows a reasonable agreement. The average oxygen concentrations in experimental fires with HRRs of 17 and 43 MW were 16.55% and 10.40%, respectively. In the FDS models, the average oxygen concentrations were estimated to be 16.00% for the fire with an HRR of 17 MW and 12.60% for the fire with an HRR of 43 MW. Furthermore, the minimum oxygen concentration for the 17 MW fire in the experiment was 10.3%, while the FDS model predicted 9.6%. For the 43 MW fire, the minimum oxygen concentration observed in the experiment was 3.3%, compared to 4.5% in the FDS model. This discrepancy is due to the FDS assumption of 21% ambient oxygen, whereas the actual tunnel oxygen level was lower because of restricted fresh air exchange in the dead-end tunnel. Additionally, since the experimental report lacked detailed fuel composition data, the FDS model used the default gasoline composition, which may have further contributed to the variation in results.

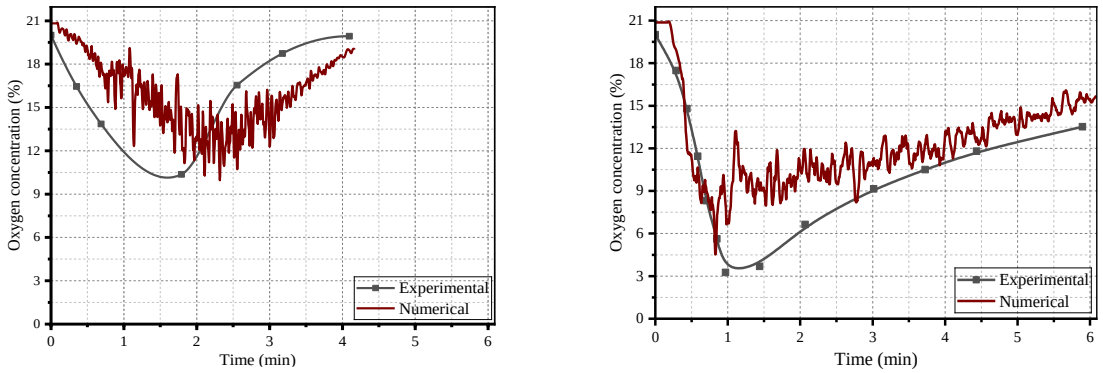

Figure 4 Oxygen Levels versus time at 0.8m from Fire Endpoint's Pan and 0.5m below Ceiling (a) HRR= 17 MW, (b) HRR=43 MW.

CO concentration

Figures 5(a) and (b) illustrate a comparison of CO concentrations over time at a location 0.8 m from the fire endpoint and 0.5 m below the ceiling. In both cases, CO levels rise immediately after ignition to a peak, and then gradually decline. However, the behavior of the two curves differs, influenced by fire intensity, ventilation conditions, and fuel consumption. In Figure 5(a), for a fire with an HRR of 17 MW, the CO peak is less intense and decays more rapidly due to fuel consumption and the effects of ventilation on gas dispersion. By comparison, in Figure 5(b), with a higher HRR, the fire is more intense, leading to higher peak CO levels and decay more slowly. However, it can be noted that the intensity of fire has a significant impact on the production and emission of CO. The discrepancy between the FDS and experimental CO concentration curves may be attributed the variation in available oxygen levels shown in Figure 4, which influences incomplete combustion, leading to differences in CO production between the numerical and experimental.

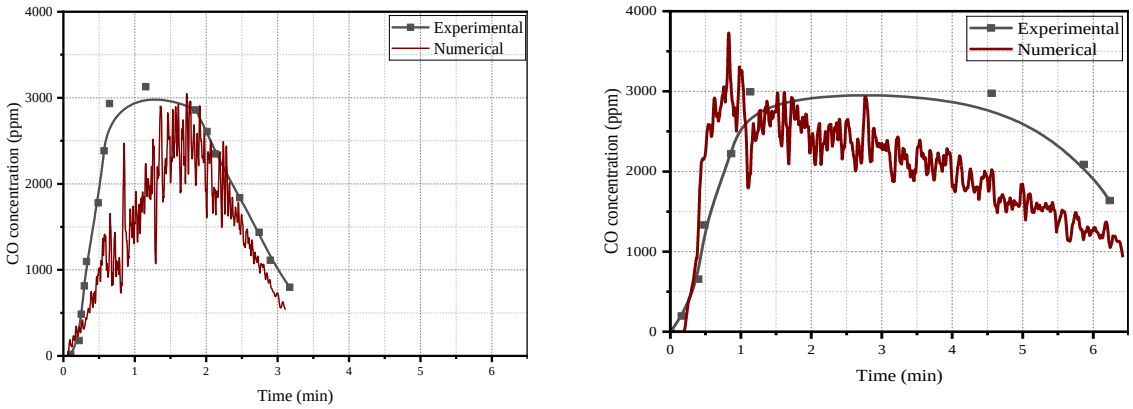

Figure 5 CO concentrations versus time at 0.8m from Fire Endpoint's Pan and 0.5m below Ceiling (a) HRR= 17 MW, (b) HRR=43 MW.

Gas velocity

Figures 6(a) and (b) depict measured gas velocities at 124.25 m from the end of fire pan at two levels: 1.2 m above the floor (inflow) and 1.2 m below the ceiling (outflow), recorded 2 minutes after ignition for fires with HRRs of 17 MW and 43 MW, respectively. In Figure 6(a), the smoke plume moves toward the tunnel entrance at an average speed of 2.5 – 3 m/s, and gradually slowing as it nears the entrance. As the smoke passes, the outflow in the upper section increases to 2.5 m/s, while the lower region draws air inward at a rate of approximately 1.4 m/s. In Figure 6(b), the smoke plume advances toward the portal at a faster rate. Following the passage of smoke, a counterflow develops, with the outflow in the upper section fluctuating up to 4 m/s and the inflow in the lower section reduced to around 2.3 m/s. These observations highlight the influence of fire intensity on ventilation dynamics within the tunnel.

Furthermore, the measured velocities closely align with FDS simulation predictions, reinforcing the validity of the model in replicating observed fire-driven ventilation dynamic.

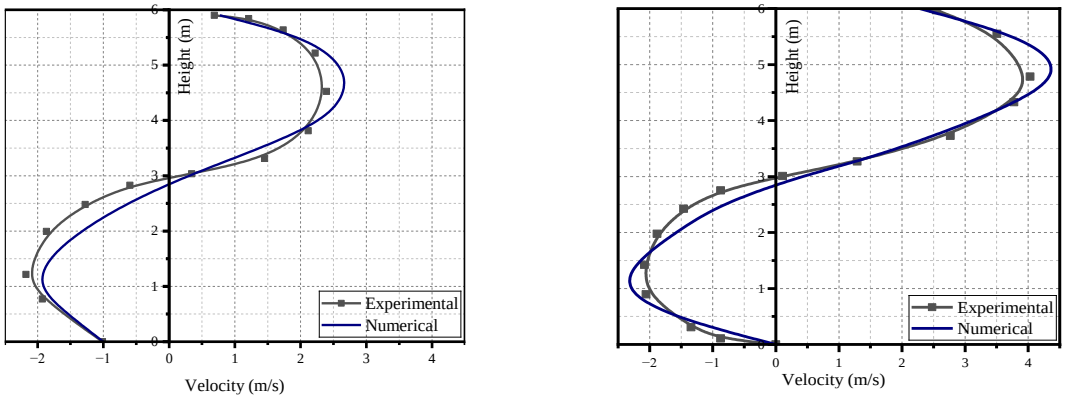

Figure 6 Velocity versus height at time (2 minutes) (a) HRR= 17 MW, (b) HRR=43 MW.

Summary of validation

Table 4 summarizes the comparison between experimental and numerical data, highlighting key parameters and their levels of agreement to demonstrate the reliability of the FDS model. Maximum values were used for temperature and velocity, while average values were considered for oxygen and CO concentrations. The percentage deviation between the FDS predictions and experimental results is calculated using the formula:

$$\text{Percentage deviation} = \frac{\text{FDS Output} - \text{Experimental Finding}}{\text{Experimental Finding}} \times 100\% \quad (7)$$

In summary, the FDS model's predictions show reasonable agreement with the experimental results, with deviations generally falling within an acceptable range of 15–25% (27).

Table 4 Summary of the relevant data obtained during the naturally ventilated experiments conducted in the Ofenegg Tunnel, along with the corresponding output from FDS.

Test No.	Gasoline (L)	*Max. HRR (MW)*	Max. Temp. (°C)		Avg.O_2 level (%)		Avg. CO conc. (ppm)		Max. gas velocity (outflow/inflow) (m/s)	
			at X= 0.8 m and Z= 5.5 m							
			Exp.	FDS	Exp.	FDS	Exp.	FDS	Exp.	FDS
1	100	17	665	670	16.55	16.00	1545	1555	2.3/1.9	2.7/2.2
5	500	43	1100	1055	10.40	12.60	1565	1925	4.0/2.0	4.5/2.4

Parametric study

Following the validation exercise, FDS was used to simulate fires in a 450-meter-long arbitrary tunnel model. As shown in Figure 7, three fire scenarios of varying sizes were simulated under different slopes. The tunnel cross-section represents a unidirectional tunnel (single lane) with an area of 25 m². The fire source was positioned at the middle of the tunnel length, with HRRs of 1.5, 75, and 150 MW, corresponding to fuel loads for a small vehicle, heavy goods vehicle (HGV), and a petrol tanker, respectively (40). The simulation covers the transition from ultra-fast fire growth to quasi-steady-state conditions. Three different tunnel slopes were modeled with gradients of 0.5%, 3%, and 6%. The slope was modified by adjusting the direction of gravity from the downward (negative z-direction) to an inclined angle relative to the vertical, calculated by the arc tangent of α (representing the slope) (44).
The height from the tunnel floor to the burner surface, along with its thermal and combustion properties, matched the conditions described in the experiments used for the validation exercise. Open boundary conditions were applied at both tunnel ends, with no initial air velocity introduced, allowing only for

natural ventilation. The cell sizes were determined using Equation (5), and the model was discretized into cubic cells. For the small fire, a cell size of 0.0625 cm was used, while for the large fire, the cell size was 0.25 cm. This resulted in a total of 2.9312 and 1.44256 million cubic cells, respectively. All simulations were performed using supercomputers supported by the Digital Research Alliance of Canada. The ambient temperature was set to 20°C. Thermocouples were positioned centrally within the cross-section along the tunnel length, 2 meters above the ground level, with intervals of 1 meter. A total of nine cases were simulated, as summarized in Table 5.

Table 5. List of FDS simulation cases.

Case No.	Tunnel length (m)	Fire size (MW)	Slope (%)
1, 2, 3	450	1.5	0.5, 3, 6
4, 5, 6		75	
7, 8, 9		150	

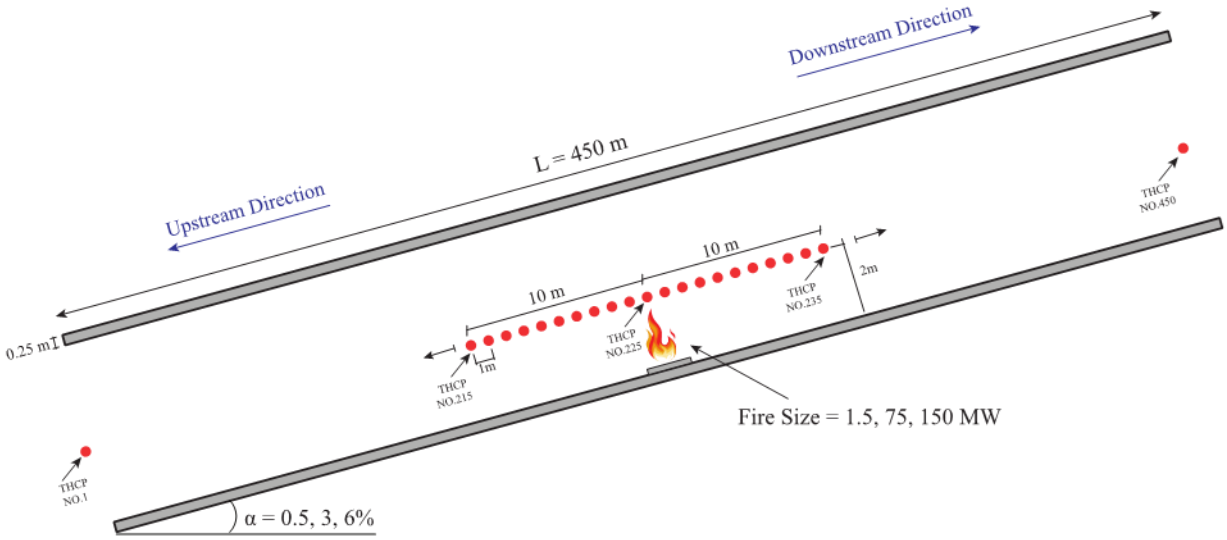

Figure 7 Side view of 450 m long tunnel model (not in scale).

Results and discussion of parametric study

It is widely known that smoke temperature distribution patterns vary significantly in sloped and horizontal tunnels. In horizontal tunnels, smoke and heat propagate symmetrically, producing similar magnitudes on both sides. In contrast, sloped tunnels exhibit asymmetrical distribution due to buoyancy and the chimney effect caused by elevation differences along the tunnel. This phenomenon results in smoke and heat traveling faster and reaching higher temperatures on the uphill (downstream) side, while moving more slowly with lower temperatures on the downhill (upstream) side (45–47). In a sloping tunnel, the elevation difference between the tunnel portals induces an upstream longitudinal airflow. Under these conditions, the stack effect becomes the primary driving force for smoke movement. As the tunnel slope increases, the upstream outflow of smoke is suppressed due to the higher air supply rate. Additionally, the downstream temperature distribution gradually becomes more uniform, resembling the conditions observed in longitudinally ventilated tunnels (48).

Figures 8–10 present the time-temperature curves (in seconds) from the start of the fire until a steady state is reached, measured at a height of 2 meters above the ground, 10 meters from the center of the fire in both upstream and downstream directions with varying fire sizes and slopes. The gray empty regions in the center of the graphs represent the fire sources, corresponding to vehicle lengths of 2 meters (small vehicle), 7.5 meters (HGV), and 12.5 meters (tanker), for fire sizes of 1.5 MW, 75 MW, and 150 MW, respectively. These fire source areas are omitted for better visualization of the interactions between fire size, slope, and their effect on temperature distribution over time.

As expected, larger fires (75 and 150 MW) reach their peak more rapidly and sustain higher temperatures over a longer duration and distance. In contrast, smaller fires (1.5 MW) exhibit a more gradual temperature rise and require more time to stabilize. Additionally, increasing the tunnel slope introduces a compensatory effect in the temperature distribution: larger temperature rises occur downstream, while smaller rises are observed upstream. This behavior emphasizes the impact of fire size and tunnel slope on temperature dynamics, with larger fires and steeper slopes increasing risks to safety and structural integrity. These findings align with previous studies on the effects of tunnel inclination on fire behavior (18,19,44,49–56), underscoring the crucial role of slope and fire size in determining temperature distribution in tunnel fires.

Figures 11 and 12 illustrate the time required for the temperature to reach 60°C under various scenarios with slopes of 0.5%, 3%, and 6%, and fire sizes of (a) 1.5 MW, (b) 75 MW, and (c) 150 MW, with Figure 11 showing the data at a distance of 10 meters from the fire source center and Figure 12 presenting the data along the tunnel length, both in upstream and downstream directions.

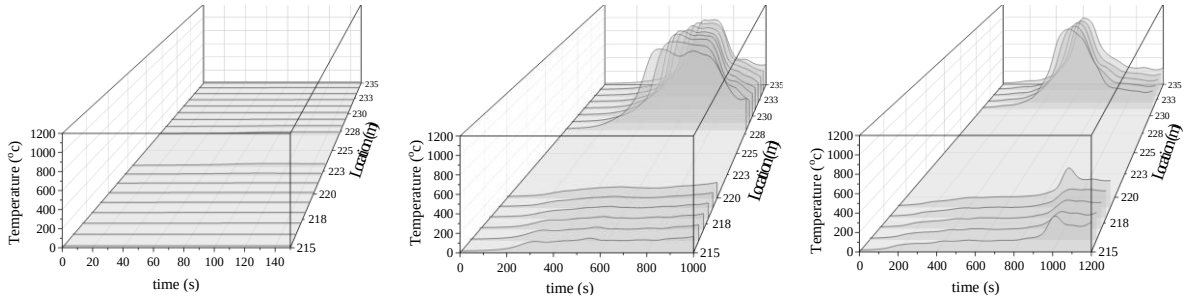

(a) *(b)* *(c)*

Figure 8 Time-temperature curves at 10 m from the center of the fire in both upstream and downstream directions with a 0.5% slope, for fire sizes of: (a) 1.5 MW, (b) 75 MW, and (c) 150 MW.

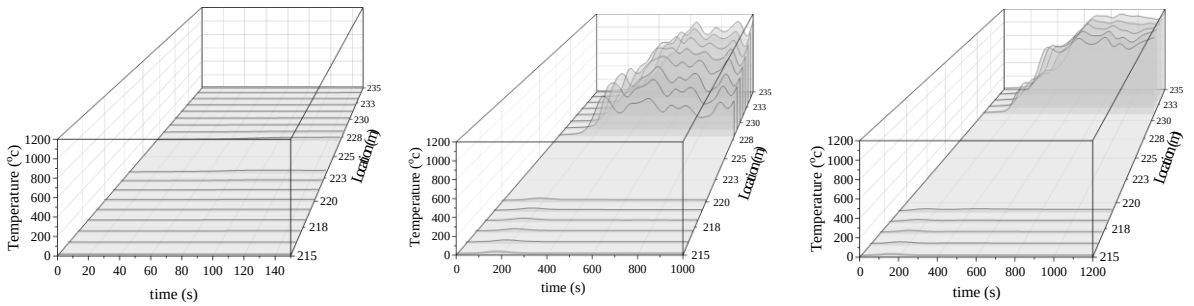

(a) *(b)* *(c)*

Figure 9 Time-temperature curves at 10 m from the center of the fire in both upstream and downstream directions with a 3% slope, for fire sizes of: (a) 1.5 MW, (b) 75 MW, and (c) 150 MW.

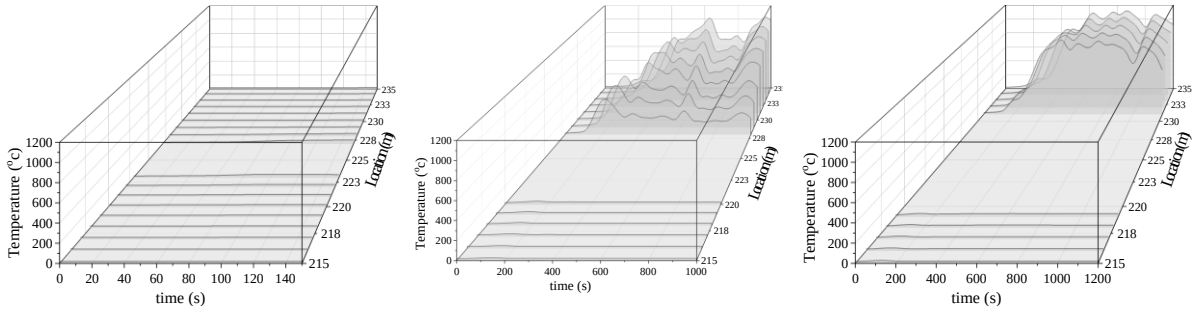

(a) *(b)* *(c)*

Figure 10 Time-temperature curves at 10 m from the center of the fire in both upstream and downstream directions with a 6% slope, for fire sizes of: (a) 1.5 MW, (b) 75 MW, and (c) 150 MW.

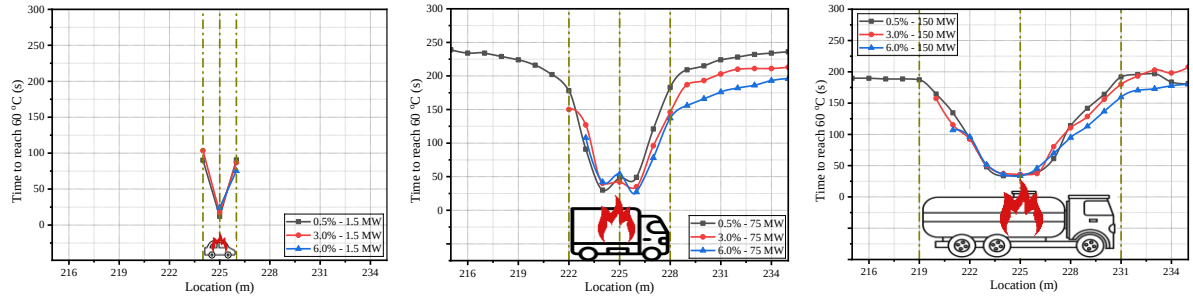

(a) (b) (c)

Figure 11 Time to reach 60°C at 10 m from the center of the fire in both upstream and downstream directions for slopes of 0.5%, 3%, and 6%, with fire sizes of: (a) 1.5 MW, (b) 75 MW, and (c) 150 MW.

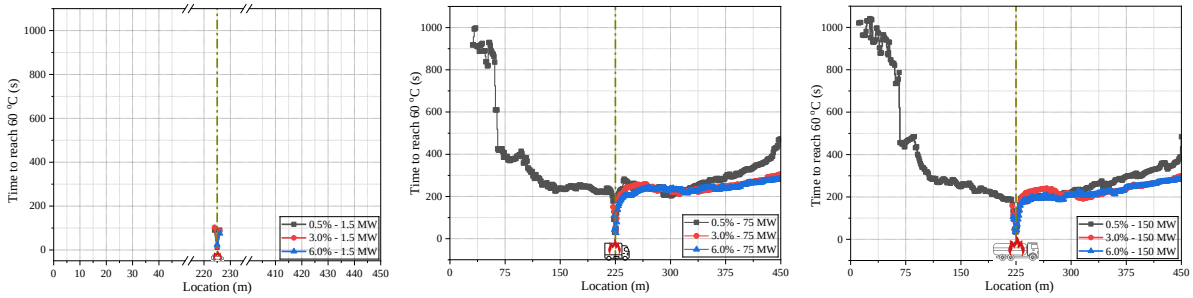

(a) (b) (c)

Figure 12 Time to reach 60°C along the tunnel length from the center of the fire in both upstream and downstream directions for slopes of 0.5%, 3%, and 6%, with fire sizes of: (a) 1.5 MW, (b) 75 MW, and (c) 150 MW.

As an estimate of the Available Safe Egress Time (ASET) for occupants in the tunnel is assumed to be the time when the air temperature at a height of 2 m. In Figure 11(a), the small fire (1.5 MW) is considered safe regardless of the slope. This behavior is attributed to the limited heat generation of smaller fires, resulting in weaker buoyancy forces and rapid heat dissipation as the distance from the fire source increases (57). In contrast, for larger fires (75 and 150 MW), the temperature varies depending on the slope and direction. For example, in Figure 11(b) and 11(c), at a slope of 0.5%, the temperature exceeds 60°C in both directions. In the upstream direction, the ASET is 202 and 190 seconds, while in the downstream direction, the ASET is 210 and 195 seconds for a 75 and 150 MW, respectively. For the same larger fires, with a steeper slope (i.e., 3% and 6%), the temperature remains below 60°C in the upstream direction, while the downstream ASET decreases as the slope increases. For instance, for 75 MW, the ASET is 187 seconds at slope of 3%, and 156 seconds at slope of 6%. Similarly, for 150 MW, the downstream ASET is 193 seconds at slope of 3%, and 170 seconds at slope of 6%, The larger fire pans lead to a slightly faster time to reach the 60°C threshold compared to 75 MW. Therefore, the downstream direction with a steeper slope (3% and 6%) and larger fire (75 and 150 MW) represents the worst-case scenarios.

Figure 12 shows similar results as Figure 11, but for the whole tunnel length. In Figure 12(a), for the small fire, conditions are safe along the entire length in both directions due to the very small fire. However, in Figures 12(b) and 12(c), the time required for the temperature to reach 60°C along the tunnel length in the downstream direction becomes nearly identical and relatively consistent as both fire size and slope increase. In addition, for larger fires, i.e., greater than 75 MW, the ASET is independent of the slope. For the large fires with a slope of 0.5%, the time required for the temperature to reach 60°C is quite similar in both directions, as shown in Figures 12(b) and 12(c), with a higher ASET compared

to steeper slopes. This trend becomes more evident as the distance from the fire increases, particularly after 150 meters in the downstream direction and after 200 meters in the upstream direction.

ConclusionS

This study comprises two main components:

(i) Validation of the fire dynamics simulator (FDS) with data from the large-scale naturally ventilated Ofenegg Tunnel Fire Tests; validation was done using different experimental results, including temperature distribution, oxygen levels, CO concentration, and gas flow rates; and

(ii) A parametric analysis investigating the impact of different fire sizes (1.5, 75, and 150 MW) and tunnel slopes (0.5%, 3%, and 6%) on the time required for the temperature to reach 60°C at human height (2 m).

For the FDS validation two tests were simulated: a 100 and 500-L gasoline fire generating 17, and 43 MW of heat. For both cases, the FDS results compared well with the experimental data, illustrating the ability of FDS to model fires in naturally ventilated tunnels under well- and under-ventilated fires.

The parametric analysis investigated how various fire sizes (1.5, 75, and 150 MW) and slopes (0.5%, 3%, and 6%) influence time-temperature profiles, focusing on occupant safety at human height. Temperature changes were measured 10 meters upstream and downstream of the fire origin, as well as along the 450-meter tunnel length. It was shown that the downstream temperature distribution gradually becomes more uniform, resembling the conditions observed in longitudinally ventilated tunnels. For the small fire, conditions are safe along the entire length in both directions, while for larger fires, i.e., greater than 75 MW, the ASET is independent of the slope. Nevertheless, for the large fires with a slope of 0.5%, the time required for the temperature to reach 60°C is quite similar in both directions with a higher ASET compared to the steeper slope cases.

REFERENCES

1. Haack A. Current safety issues in traffic tunnels. Tunnelling and underground space technology. 2002;17(2):117–27.
2. Caliendo C, De Guglielmo ML. Accident rates in road tunnels and social cost evaluation. Procedia-Social and Behavioral Sciences. 2012;53:166–77.
3. Bassan S. Overview of traffic safety aspects and design in road tunnels. IATSS research. 2016;40(1):35–46.
4. Lin CL, Chien CF. Lessons learned from critical accidental fires in tunnels. Tunnelling and Underground Space Technology. 2021;113:103944.
5. Gehandler J. Road tunnel fire safety and risk: a review. Fire Sci Rev. 2015;4:1–27.
6. Balog JN. Public transportation security. Vol. 12. Transportation Research Board; 2002.
7. Zhao S, Yang H, Li YZ, Ingason H, Liu F. Theoretical and numerical study on smoke descent during tunnel fires under natural ventilation condition. Tunnelling and Underground Space Technology. 2023;142:105414.
8. Gehandler J, Eymann L, Regeffe M. Limit-based fire hazard model for evaluating tunnel life safety. Fire Technol. 2015;51:585–614.
9. Ingason H. Workpackage 2 fire development and mitigation measures D221—target criteria. Upgrading of existing Tunnels for fire safety (UPTUN). 2008;
10. Standardization IO for, Technical Committee ISO/TC 92 Fire threat to people and environment F safety. SSC 3. Life-threatening Components of Fire: Guidelines for the Estimation of Time to Compromised Tenability in Fires. ISO; 2012.
11. Maevski I. Guidelines for emergency ventilation smoke control in roadway tunnels. NCHRP research report. 2017;(836):1–81.

12. Fan C, Zhang L, Jiao S, Yang Z, Li M, Liu X. Smoke spread characteristics inside a tunnel with natural ventilation under a strong environmental wind. Tunnelling and underground space technology. 2018;82:99–110.
13. Harish R, Venkatasubbaiah K. Effects of buoyancy induced roof ventilation systems for smoke removal in tunnel fires. Tunnelling and Underground Space Technology. 2014;42:195–205.
14. Jin S, Jin J, Gong Y. Natural ventilation of urban shallowly-buried road tunnels with roof openings. Tunnelling and Underground Space Technology. 2017;63:217–27.
15. Wang YF, Li YL, Yan PN, Zhang B, Jiang JC, Zhang L. Maximum temperature of smoke beneath ceiling in tunnel fire with vertical shafts. Tunnelling and Underground Space Technology. 2015;50:189–98.
16. Liang C, Yuan Z, Qu H, Yu N. The Effect of Slope on Smoke Characteristics of Natural Ventilation Tunnel with Shafts. Buildings. 2024;14(7):1963.
17. Hu LH, Huo R, Wang HB, Yang RX. Experimental and numerical studies on longitudinal smoke temperature distribution upstream and downstream from the fire in a road tunnel. J Fire Sci. 2007;25(1):23–43.
18. Yang Y, Long Z, Cheng H, Chen J, Liu C, Zhong M. Experimental and numerical study of smoke temperature distribution characteristics in a sloped tunnel. Sustain Cities Soc. 2021;73:103091.
19. Sun C, Weng M, Liu F, Yang H, Zhu X. Study on the maximum ceiling temperature and downstream temperature distribution in inclined tunnel fire. Tunnelling and Underground Space Technology. 2024;153:106057.
20. Huang P, Ye S, Xie J, Chen M, Liu C, Yu L. Study on the maximum and longitudinal distribution of ceiling gas temperature in a naturally ventilated tunnel: The effect of longitudinal fire location. International Journal of Thermal Sciences. 2023;185:108037.
21. Kong J, You W, Xu Z, Liu H, Li H. A numerical study on smoke behaviors in inclined tunnel fires under natural ventilation. Journal of safety science and resilience. 2022;3(2):169–78.
22. Cong W, Nie S, He K, Liu X, Peng W. Numerical Study on the Maximum Ceiling Gas Temperature Rise in Inclined Tunnel Fires Under Natural Ventilation. Available at SSRN 4682945.
23. Merci B. One-dimensional analysis of the global chimney effect in the case of fire in an inclined tunnel. Fire Saf J. 2008;43(5):376–89.
24. Ji J, Wan H, Li K, Han J, Sun J. A numerical study on upstream maximum temperature in inclined urban road tunnel fires. Int J Heat Mass Transf. 2015;88:516–26.
25. Ingason H, Li YZ, Lönnermark A. Tunnel Fire Dynamics. Vol. 2nd ed., Tunnel Fire Dynamics. Springer International Publishing; 2024. XVII–580.
26. Carvel R. A history of experimental tunnel fires. The Handbook of Tunnel Fire Safety, Thomas Telford, London. 2005;201–30.
27. Ingason H. Fire testing in road and railway tunnels. In: Flammability testing of materials used in construction, transport and mining. Elsevier; 2022. p. 237–80.
28. Haerter A. Fire tests in the Ofenegg-Tunnel in 1965. In: International Conference on Fires in Tunnels, SP Report Vol 54. 1994. p. 195–214.
29. AASHTO L. Road Tunnel Design and Construction Guide Specifications. AASHTO; 2017.
30. Burning rates. SFPE handbook of fire protection engineering. 1995;
31. KFSS. Kommission für Sicherheitsmassnahmen in Strassentunneln Schlussbericht der Versuche im Ofenegg Tunnel von 17.5–31.5. 1965;
32. Carvel R, Beard A. The influence of tunnel ventilation on fire behaviour. The handbook of tunnel fire safety. 2005;184–98.
33. McGrattan K, Hostikka S, McDermott R, Floyd J, Vanella M. Fire Dynamics Simulator User's Guide, NIST special publication. 2019;1019.
34. McGrattan K, Hostikka S, Floyd J, Baum H, Rehm R. Fire Dynamics Simulator (Sixth Edition), Technical Reference Guide. NIST Special Publication. 2013;
35. McGrattan K, Hostikka S, Floyd J, McDermott R, Prasad K. Fire Dynamics Simulator, Technical Reference Guide Volume 3: Validation. NIST Special Publication. 2013;
36. SFPE handbook of fire protection engineering. Springer; 2015.
37. Drysdale D. An introduction to fire dynamics. John wiley & sons; 2011.
38. McDermott RJ. Quality assessment in the Fire Dynamics Simulator: A bridge to reliable simulations. In: Proceedings of the Fire and Evacuation Modeling Technical Conference. 2011.

39. Vermesi I, Rein G, Colella F, Valkvist M, Jomaas G. Reducing the computational requirements for simulating tunnel fires by combining multiscale modelling and multiple processor calculation. Tunnelling and Underground Space Technology. 2017;64:146–53.
40. Lönnermark A, Ingason H. Recent achievements regarding heat release and temperatures during fires in tunnels. In: Safety in Infrastructure-Svédületes, Budapest 20th-21st October. 2004.
41. Li YZ, Ingason H. Maximum ceiling temperature in a tunnel fire. SP report. 2010;51.
42. Quintiere JG. Fundamentals of fire phenomena. 2006;
43. Jiang C, Li Y, Huang H, Zhao J, Wang Z, Zhang J. Experimental study of burning rate in large-scale rectangular pool fire. J Fire Sci. 2016;34(4):323–34.
44. Gao Z, Li L, Sun C, Zhong W, Yan C. Effect of longitudinal slope on the smoke propagation and ceiling temperature characterization in sloping tunnel fires under natural ventilation. Tunnelling and Underground Space Technology. 2022;123:104396.
45. Cong W, Nie S, Li X, Peng W. Numerical study on smoke temperature distribution in naturally ventilated inclined tunnels: Effects of tunnel width and tunnel slope. Case Studies in Thermal Engineering. 2024;62:105202.
46. Zhao S, Li YZ, Kumm M, Ingason H, Liu F. Re-direction of smoke flow in inclined tunnel fires. Tunnelling and Underground Space Technology. 2019;86:113–27.
47. Yu L, Wan H, Ji J. Asymmetric flow effect in a horizontal natural ventilated tunnel with different aspect ratios under the influence of longitudinal fire locations. In: Building Simulation. Springer; 2021. p. 1311–23.
48. Gao Z, Li L, Sun C, Zhong W, Yan C. Effect of longitudinal slope on the smoke propagation and ceiling temperature characterization in sloping tunnel fires under natural ventilation. Tunnelling and Underground Space Technology. 2022;123:104396.
49. Wang P, She C, Chen J, Xu Z, Chen Y. Study of slope effect on smoke back-layering length and ceiling temperature in tunnel fires under natural ventilation. International Journal of Thermal Sciences. 2023;185:108046.
50. Han J, Liu F, Wang F, Weng M, Wang J. Study on the smoke movement and downstream temperature distribution in a sloping tunnel with one closed portal. International Journal of Thermal Sciences [Internet]. 2020;149(July 2019):106165. Available from: https://doi.org/10.1016/j.ijthermalsci.2019.106165
51. Wang Z, Ding L, Wan H, Ji J, Gao Z, Yu L. Numerical investigation on the effect of tunnel width and slope on ceiling gas temperature in inclined tunnels. International journal of thermal sciences. 2020;152:106272.
52. Gao Z, Liu M, Zhao P, Yan C. Influence of tunnel slope on the one-dimensional spread of smoke transportation and temperature distribution in tunnel fires. Tunnelling and Underground Space Technology. 2024;146:105650.
53. Zhang X, Lin Y, Shi C, Zhang J. Numerical simulation on the maximum temperature and smoke back-layering length in a tilted tunnel under natural ventilation. Tunnelling and Underground Space Technology. 2021;107(June 2020):103661.
54. Li YZ, Ingason H, Jiang L. Influence of tunnel slope on smoke control. 2018.
55. Chen Y, Jia J, Tang J, Liu X, Meng F, Sun Y. Study on the influence of branch slope on smoke movement mechanism in bifurcated tunnel fire under natural ventilation. Case Studies in Thermal Engineering. 2024;59:104545.
56. Chen C, Zhang Y, Lei P, Jiao W. A study for predicting the maximum gas temperature beneath ceiling in sealing tactics against tunnel fire. Tunnelling and Underground Space Technology. 2020;98:103275.
57. Lönnermark A. On the characteristics of fires in tunnels. 2005;

Impact of external wind with upward and downward angles on smoke layer development in tunnel fires

Tzu-Yan Tseng[1], Kuang-Chung Tsai[1*]
[1] Dept. of Safety, Health and Environmental Engineering,
National Kaohsiung University of Science and Technology, Yanchao, Kaohsiung, Taiwan
[*]Corresponding author : tsaikc@nkust.edu.tw

ABSTRACT

Longitudinal ventilation is the most commonly used system in modern tunnels, with which smoke back-layering can be prevented while tunnel's ventilation velocity reaches a critical value, i.e. critical ventilation velocity, u_{cr}. The value of u_{cr} has been investigated for decades, however, in an environment without external winds. However, tunnels are often constructed in rural areas, where they are frequently subjected to external wind influences. Previous studies have exhibited that horizontal external winds with various angles affect the smoke flows within the tunnels, and the u_{cr} of the axial fan must increase. Clearly, the external wind does not only blow horizontally; it can also blow at upward or downward angles. Accordingly, this study investigated the impact of external winds blowing at downward and upward angles on the smoke flow and u_{cr} within tunnels. This study conducted two series of experiments using a 1:20 scale model of a real tunnel, measuring 6 m in length, 0.6 m in width, and 0.6 m in height. The first series of experiment investigated the flow field without a fire under the influence of external wind, while the other explored the effect of external wind on the fire and smoke behaviours. The study designed two wind directions, with downward and upward angles, although the upward-angle scenario may not be realistic. Three external wind angles (0˚, 15˚, and 30˚), and four different external wind velocities (0 m/s, 0.4 m/s, 0.6 m/s, and 0.8 m/s) were applied to explore the smoke layer behaviour inside the tunnel. The experimental results revealed that the airflow inside the tunnel could be divided into turbulent and unidirectional flow zones when the external winds entered the tunnel. Additionally, the flame began to tilt due to the influence of the wind, affecting the mass loss rate. When the fire source was located in the unidirectional flow zone, the mass loss rate decreased as the wind increased. Conversely, the mass loss rate increased with the wind velocity when the fire source was in the turbulent flow zone. Furthermore, a higher u_{cr} to prevent smoke back-layering was needed for both the wind velocity and angle increased.

KEYWORDS: Tunnel fire, longitudinal ventilation, external wind, critical ventilation velocity

INTRODUCTION

In the event of a fire inside a tunnel, the unique structural characteristics of tunnels cause the smoke to spread horizontally toward both sides of the fire source. When the smoke spreads in the same direction as the evacuation of people, it can lead to severe casualties. Thus, in order to prevent the hazards of smoke, the smoke control in tunnel fires is an important issue [1], which typically use ventilation systems to control the spread of smoke. The main ventilation systems used in modern tunnels include longitudinal ventilation, transverse ventilation, and point extraction ventilation, with longitudinal ventilation being the most common. Longitudinal ventilation exhausts smoke in a horizontal direction, ensuring all the smoke spread toward the downstream direction of the tunnel and back-layering of smoke can be prevented. A safe environment can consequently be formed. The back-layering corresponds to the smoke flow to the upstream of the fire source. The length of smoke back-layering is determined by the tunnel size, heat release rate (HRR), and longitudinal ventilation velocity [2-3]. When

the horizontal inertial force caused by the buoyancy of hot smoke equals to the inertial force of the longitudinal ventilation air, i.e. the critical ventilation velocity, u_{cr}, is reached, the stagnation of hot smoke would be performed [4]. Thomas [3] proposed an equation to define the critical Froude number, which could be used to predict the u_{cr}. Moreover, the predicted model shows the u_{cr} affected by the aspect ratio of the tunnel [5] and HRR. Since the HRR would influence the Froude number, the higher HRR resulted in the higher u_{cr}. However, the dimensionless u_{cr} is proportional to one-third power of the dimensionless HRR in the case of small and medium-scale HRRs, and is independent of HRR in the case of large HRR [6-8]. Furthermore, some special scenarios such as the vehicular blockage [9] and multiple fire sources in the tunnel [10] on the u_{cr} were investigated.

Tunnels are often constructed in rural areas, and the wind speed may be high. For example, the wind speed reaches 7 m/s near the surrounding area of the Su-Hua tunnel groups in Taiwan. In order to evaluate the external wind effect on tunnel fires, the flow field characteristics in tunnel under external wind have been investigated [11-14]. Shen *et al.* [14] and Zhao *et al*. [11] proposed that when canyon winds flow through a tunnel, it creates three regions in the internal airflow field: a negative pressure zone, a transition zone, and a unidirectional flow zone. The negative pressure zone occurs at the tunnel portals, where the canyon wind passing through the tunnel entrance leads to two conditions: one is that external airflow enters the tunnel, and the other is that external airflow creates a suction effect at the tunnel portal, resulting in negative pressure and turbulence. However, the suction effect only occurs at the tunnel portals. As the external wind moves deeper into the tunnel, external airflow may become influencial. Additionally, as the tunnel length increases, the airflow tends to stabilize, forming a unidirectional flow zone. Furthermore, a transition zone forms between the unidirectional flow zone and the negative pressure zone, where the turbulent state caused by the front-end negative pressure zone leads to an increase in airflow velocity.

Ouyang *et al.* [13] studied the effect of horizontal canyon cross wind on the burning rate and the flame characteristics. Their results showed that the burning rate and the flame height both decreased under canyon cross wind before the application of longitudinal ventilation, but they increased after the longitudinal ventilation was applied. Due to the canyon cross wind, the flame inside the tunnel was tilted to the upstream of fire source which resulted in the poor heat feedback and also decreased the flame height. After applying the longitudinal ventilation, the airflows from two sides were interacted at the fire source and resulted in the vertical flame structure. Therefore, the burning rate and the flame height increased with the vertical flame. Additionally, Zhao *et al.* [11] and Jiao *et al.* [12] furthermore had experimentally explored the u_{cr} under different canyon cross winds and wind angles, focusing primarily on the effects of winds from the same level and various horizontal angles. The experimental results show that the airflow direction in the tunnel is mainly toward the upstream side of the tunnel when there is a canyon cross wind. After a certain longitudinal ventilation velocity is applied, the overall airflow velocity in the tunnel slows down due to the competition of the two airflows, so the burning rate of the fire also decreases. As the longitudinal ventilation velocity continues to increase, the airflow in the tunnel is dominated by the longitudinal ventilation, and the airflow velocity increases accordingly.

Horizontal winds with various angles can affect the smoke flow within the tunnel, and the u_{cr} of the axial fan must also increase. However, the external wind does not only blow horizontally; it can also blow directly in the tunnel at upward or downward angles. Therefore, this study investigates the impact of external winds blowing at downward and upward angles on the smoke flow and u_{cr} within tunnels.

EXPERIMENTAL DESIGN

The aim of this study was to investigate the impact of external winds with varying vertical angles on the smoke behaviour within tunnels. Two series of experiments were conducted herein. The first series of experiment investigated the flow field inside the tunnel with external winds without fires, and the other one explored the effect of external winds on fire and smoke behaviours. The external wind effect on the u_{cr} was also evaluated in the latter series.

Figure 1 showed the experimental rig, which included a tunnel, fans, and honeycombs. This study conducted experiments using a 1:20 scale model of a real tunnel, measuring 6 m in length, 0.6 m in width, and 0.6 m in height. The tunnel ceiling, floor, and one sidewall were made of 10 mm thick marinate (with a thermal conductivity of 0.49 W/m•K, density of 1000 kg/m^3 and specific heat of 1.354 kJ/kg•K), and the other sidewall was made of 6 mm thick transparent glass. This transparent glass wall, which was designed to facilitate visual observations, can withstand high temperatures.

Figure 1 additionally shows the experimental set-up of the latter series of experiment. The fire source was set using 95-octane unleaded gasoline in a square fuel pan with a side length of 0.06 m at the middle of the tunnel, generating a HRR of 2.7 kW [10]. The size of the fire source was chosen to simulate fires with a HRR of 5 MW in a typical tunnel. A load cell with a capability of 10 kg and accuracy of 1 g was used to measure the mass loss rate of fuel. There were two axial fans placed at both portals of the tunnel, respectively. One simulated the external wind, while the other one was used to simulate the longitudinal ventilation throughout the full tunnel cross section. The distance from the longitudinal ventilation fan to the upstream portal was 5 cm. Additionally, the shortest distance from the external wind fan to the downstream portal was 10 cm.Tthe shortest distance existed for the experiments with external winds with upward and downward angles, and it was present at the top or bottom of the downstream portal when the experiments with downward or upward angles were conducted, respectively. The existence of the gaps allowed smoke to exit. Both fans could adjust the velocity from 0 to 10 m/s. A 1 m long mesh screen was made of plastic pipes (10 mm in diameter), i.e. honeycomb, to keep flows uniform throughout the tunnel cross section. The study designed two wind directions (with downward and upward angles), three different external wind angles, θ, (0˚, 15˚, and 30˚), and four different external wind velocities (0 m/s, 0.4 m/s, 0.6 m/s, and 0.8 m/s) to explore the effect of external wind angles on the smoke layer inside the tunnel. The external wind velocities in the 1/20 tunnel: 0.4 m/s, 0.6 m/s and 0.8 m/s were equivalent to 1.8 m/s, 2.7 m/s and 3.6 m/s in a real tunnel. (The average wind in the rural area is 2.8 m/s.) Note that the upward wind may not be realistic and was for analysis. In order to observe the smoke back-layering, the thermocouples were set 0.1 m below the ceiling and along with the tunnel. For upstream of the fire source, each thermocouple was set 0.1 m apart in 1 m of the fire source, 0.3 m apart between 1 and 2 m, and 0.5 m apart after 2 m. For downstream of the fire source, each thermocouple was set 0.3 m apart in 2 m of the fire source and 0.5 m apart after 2 m. A digital camera was set to observe the flame shape and the smoke behaviour. The flow field and air velocity inside the tunnel were measured by the anemometer with accuracy of 0.1 m/s.

Figure 2 illustrated the measuring points of anemometer for the first series of experiment, investigating the flow field inside the tunnel with external winds. It is worth to note that the flow field experiment was under no fire condition. The cross sectional area of tunnel was divided into three parts and the measured points of air velocity were set at the centre of each parts. Moreover, the horizontal distance of each measuring points was 0.5 m and total of 30 points were measured. Each test was conducted three times for the repeatability. The limitation of this study might be the length of the tunnel, since the tunnel was not long enough to present the external wind effect on the smoke spreading length and also the smoke back-layering behaviour completely. However, it still showed the difference between the smoke behaviour with or without different angled external wind.

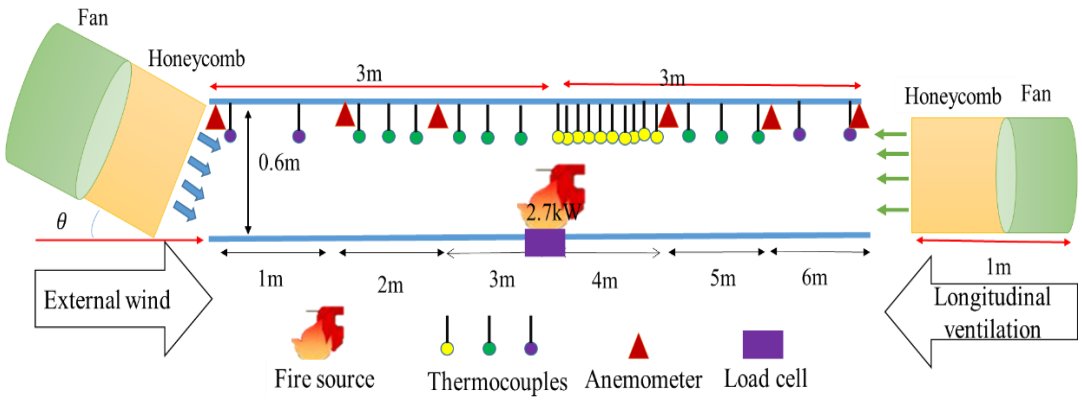

Figure 1 Experimental set-up (draw not to scale).

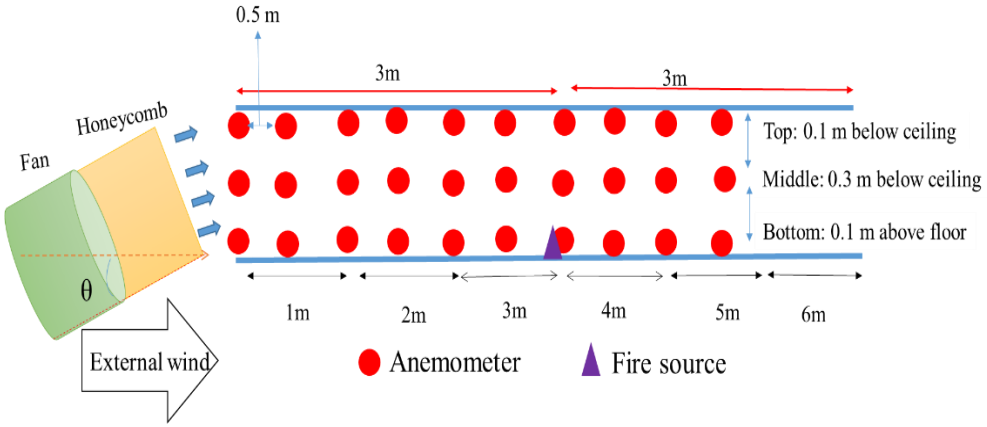

Figure 2 The set-up of air velocity measurement (draw not to scale).

RESULTS AND DISCUSSION

Flow field analysis inside the tunnel

The distribution of airflow within the tunnel is a crucial phenomenon to analyze, as it can cause changes in the behavior of dense smoke and variations in the ventilation and smoke extraction system. Thus, exploring the impact of external airflow on the airflow distribution within the tunnel even with the absence of a fire is important.

Flow field with different downward angles

This study divided the tunnel into three sections: top, middle, and bottom, and measured the wind velocity in each region to observe the changes in the airflow field after vertical external wind flowed into the tunnel. Figure 3 presented airflow field analysis for different downward angles of the external wind velocity of 0.4 m/s: (a) 0˚, (b) 15˚, and (c) 30˚. The diagrams showed that when the external wind angle was 0˚ (Figure 3(a)) and with a downward angle of 15˚ (Figure 3(b)), the airflow entering the tunnel was relatively uniform and stable due to the installation of a honeycomb in front of the fan. The flow within the tunnel was unidirectional, with airflow moving towards the tunnel's upstream. The wind velocity within the tunnel decreased with distance, demonstrating the effect of friction. Additionally, at a distance of 3 m from the tunnel entrance, the airflow began to stratify under the 15˚ external wind, causing the wind velocity at the bottom of the tunnel to gradually increase compared to the top. However, the effect was minimal due to the small angle. When the external wind angle was 30˚ (Figure 3(c)), significant changes in the flow field could be observed around the positions of 0.5 m inside the tunnel. The wind velocity in the middle and bottom sections of the tunnel reached 0.6 m/s, which was higher than the external wind velocity, while the wind velocity in the top section was less than 0.2 m/s.

The wind velocity in the middle and bottom parts stabilized and remained higher than the initial external wind velocity, showing no decrease with increasing distance. Meanwhile, the wind velocity in the top section gradually increased to match the original external wind velocity. The higher external wind angle caused the wind to first hit the ground and then rebound to the ceiling, creating a situation where the wind velocity in the top part of the tunnel first dropped and then rose, forming a turbulent airflow field. This turbulence extended further into the tunnel due to the continuous external wind, resulting in a chaotic airflow field throughout the tunnel.

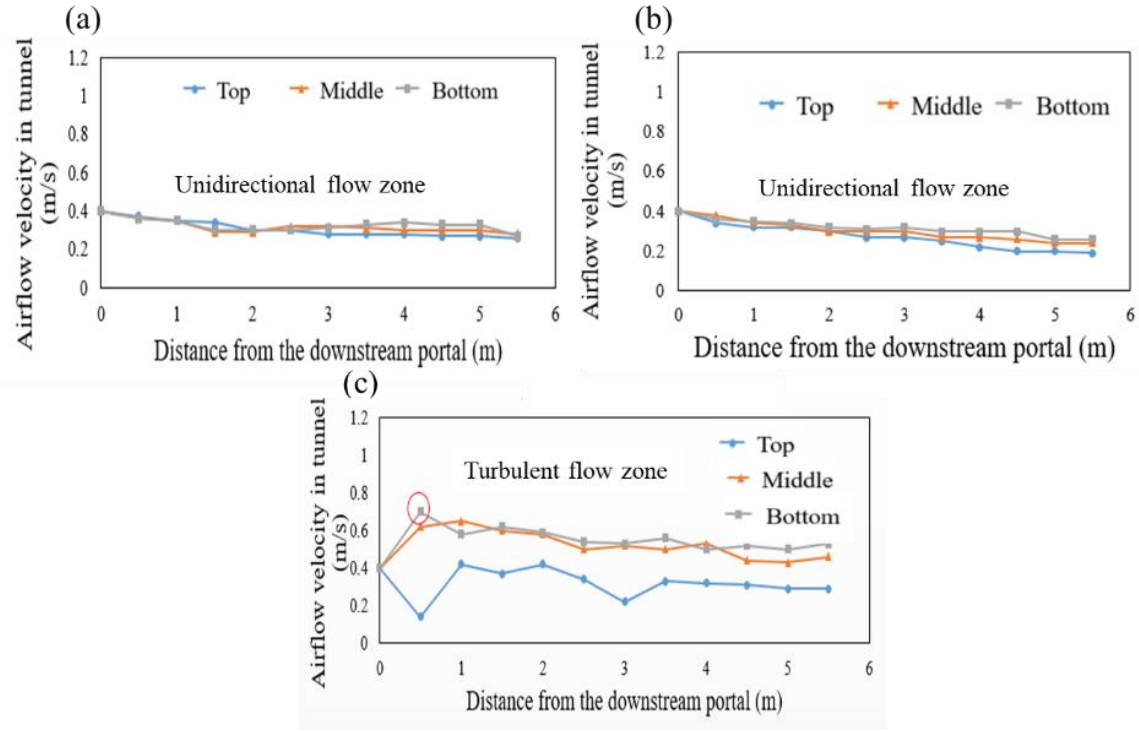

Figure 3 The flow field of downward angles (a)0 ˚;(b)15 ˚;(c)30 ˚ with external wind velocity of 0.4 m/s.

Figure 4 and Figure 5 show airflow field analysis for different downward angles of external wind at a velocity of 0.6 m/s and 0.8 m/s: (a) 0˚, (b) 15˚, and (c) 30˚. Similar trends were followed to those of the airflow field at 0.4 m/s, but with a higher wind velocity. Figure 4 shows airflow field analysis for different downward angles of external wind at a velocity of 0.6 m/s. The wind velocity at a 0˚ external wind angle decreased more rapidly with distance compared to the 0.4 m/s wind velocity. On the other hand, for the 15˚ downward angle, the wind velocity at 5.5 m in the tunnel was higher than at the 0˚ external wind angle. This suggests that the change in the external wind angle caused the airflow to form small-scale vortices after hitting the ground, reducing the distance-based decay and maintaining a more consistent wind velocity. The airflow with a 15˚ external wind angle also showed stratification at 3 m in the tunnel, and as the external wind velocity increased, the bottom part of the airflow after stratification became significantly faster than the top part. With a higher wind velocity, the stratification of airflow at a 30˚ external wind angle was more pronounced, lasting until 4.5 m inside the tunnel, with the middle and bottom wind velocities eventually becoming similar. Furthermore, Figure 5 presented airflow field analysis for different downward angles of external wind at a velocity of 0.8 m/s. The airflow with a 15˚ external wind angle also showed stratification at 3 m in the tunnel, with the bottom part of the airflow becoming significantly faster than the top part as the external wind velocity increased. The higher external wind angle of 30˚ caused the wind entering the tunnel with greater intensity, and the rebound velocity was also higher, leading to even more chaotic airflow patterns in the first 3 m of the tunnel and causing uneven wind velocities across the tunnel section.

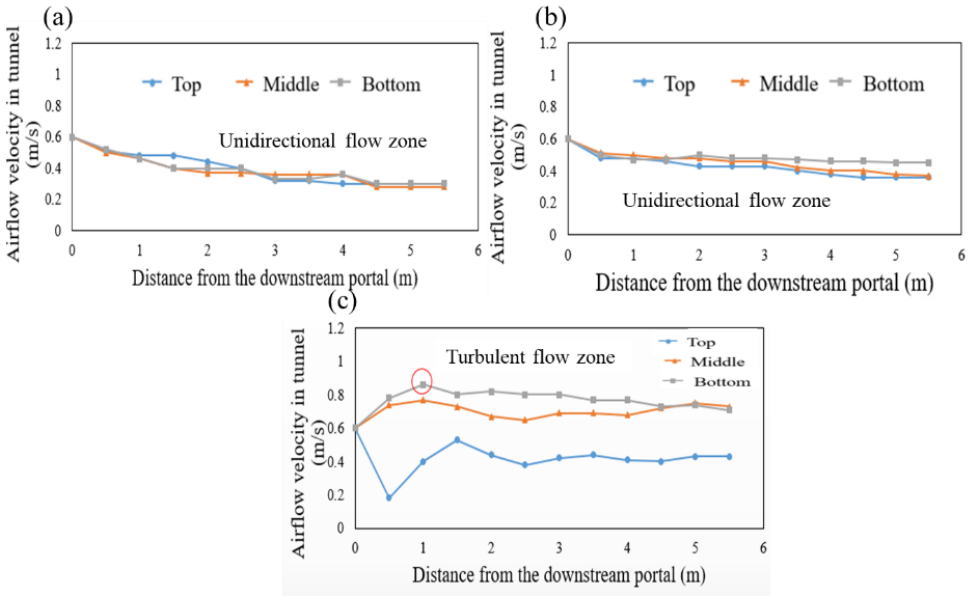

Figure 4 *The flow field of downward angles (a)0 ˚;(b)15 ˚;(c)30 ˚ with external wind velocity of 0.6 m/s.*

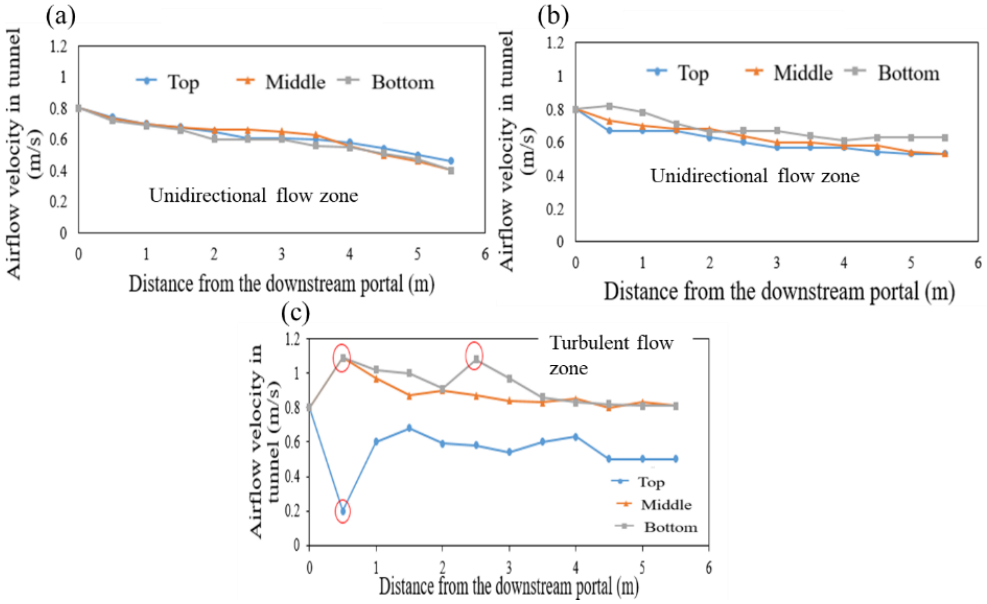

Figure 5 *The flow field of downward angles (a)0 ˚;(b)15 ˚;(c)30 ˚ with external wind velocity of 0.8 m/s.*

Flow field with different upward angles

Figure 6 presented airflow field analysis for different upward angles of external wind at a velocity of 0.4 m/s: (a) 0˚, (b) 15˚, and (c) 30˚. Since the tunnel opening did not extend with a ceiling, the upward-angle airflow cannot effectively enter the tunnel, causing the airflow velocity to decrease at the tunnel entrance. As the angle increased, the airflow decayed more, and due to the reduced amount of airflow entering the tunnel, the length of the turbulent zone also shortened with increasing angle. Additionally, the effect of stratification of airflow within the tunnel did not significantly strengthen with the increase in the external wind angle. On the contrary, because of the reduced wind velocity, unidirectional airflow was more likely to occur.

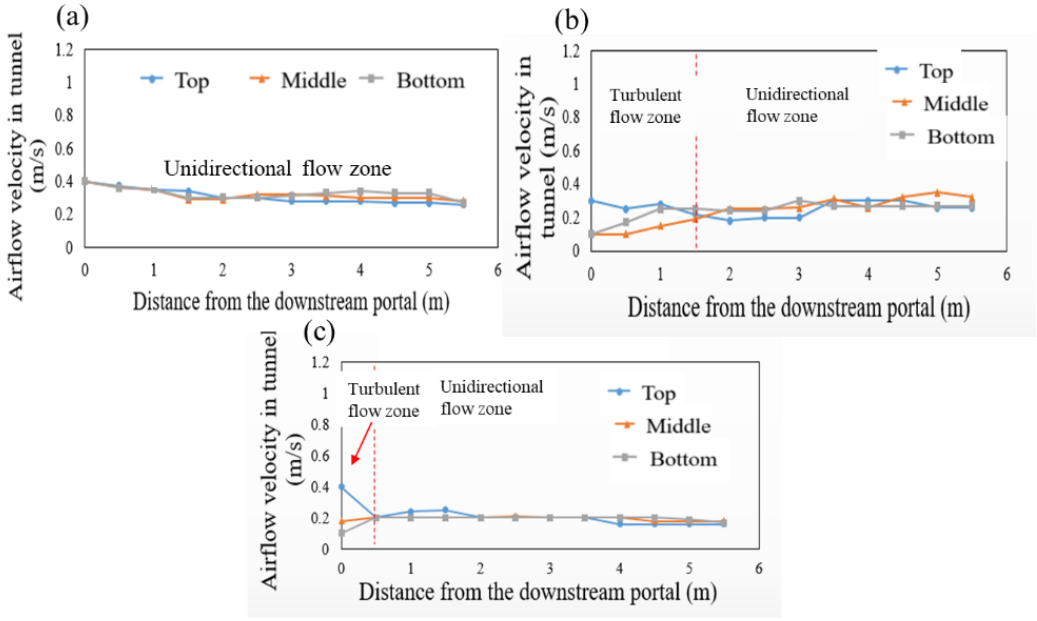

Figure 6 The flow field of upward angles (a)0 ˚;(b)15 ˚;(c)30 ˚with external wind velocity of 0.4 m/s.

Figure 7 and Figure 8 present airflow field analysis for different upward angles of external wind at a velocity of 0.6 m/s and 0.8 m/s. The basic results followed a similar trend to those of the airflow field at 0.4 m/s, but with a higher wind velocity. As the external wind velocity increased, the length of the turbulent zone also increased. When the external wind angle was 15˚, stratification occurred in the airflow field beyond 4 m in the tunnel. In contrast, the group with an external wind angle of 30˚ did not exhibit this phenomenon, possibly because the airflow tended to become unidirectional earlier, causing the subsequent airflow field to resemble that of the 0˚ external wind group. Furthermore, Figure 8 presented airflow field analysis for different upward angles of external wind at a velocity of 0.8 m/s. The airflow velocity at the tunnel opening decreased more as the external wind velocity and angle increased. Due to the inertia of the airflow, excessive airflow escaped above the tunnel opening and fails to enter the tunnel, resulting in a reduction in the overall wind velocity and a decrease in turbulent effects within the tunnel.

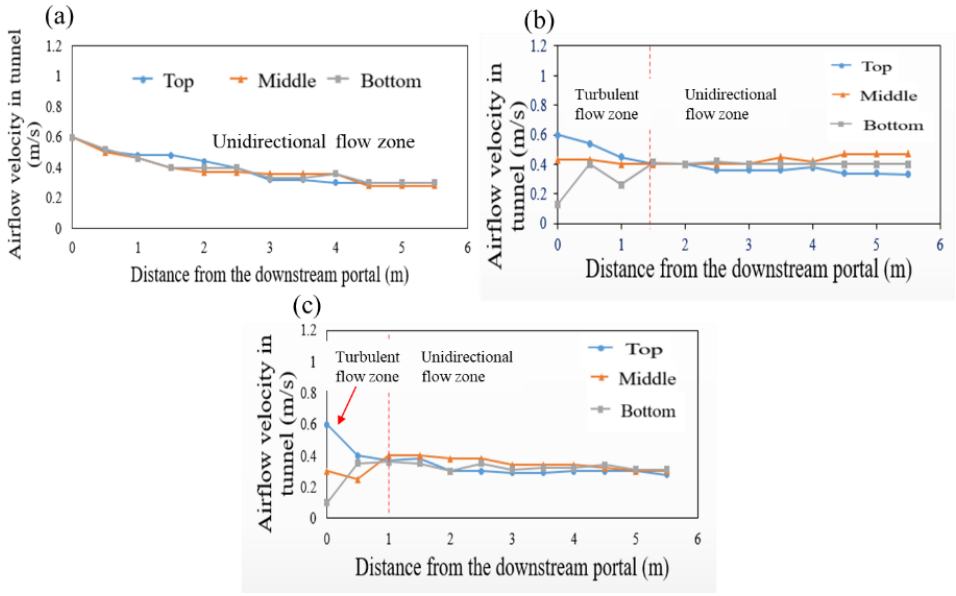

Figure 7 The flow field of upward angles (a)0 ˚;(b)15 ˚;(c)30 ˚with external wind velocity of 0.6 m/s.

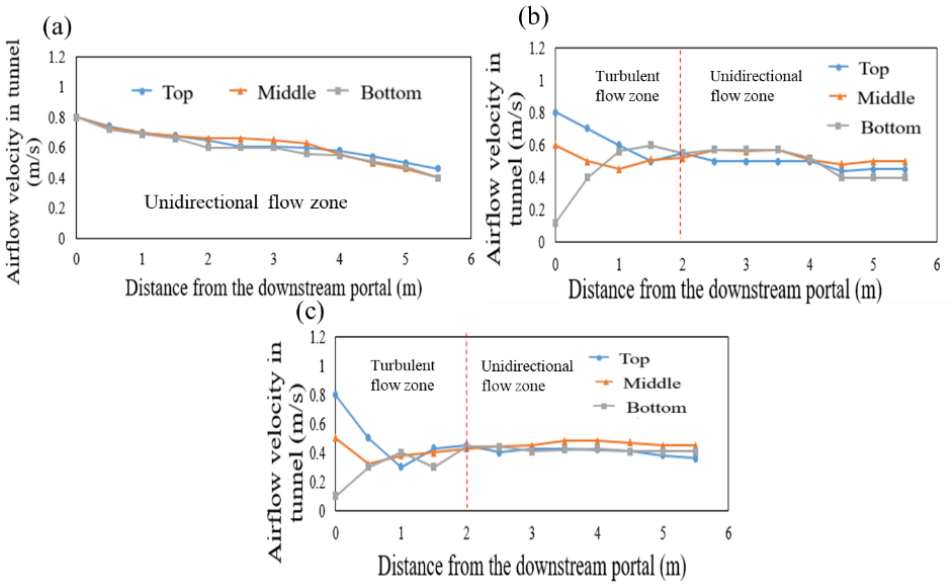

Figure 8 The flow field of upward angles (a)0 ˚;(b)15 ˚;(c)30 ˚with external wind velocity of 0.8 m/s.

Mass loss rate under different external wind velocity with varying angles

Mass loss rate without longitudinal ventilation

Figure 9 and Figure 10 show the effect of external winds on mass loss rate. Figure 9 compares the mass loss rate under different downward external wind angles and wind velocities in the absence of axial ventilation. For the groups with external wind angles of 0° and 15°, the mass loss rate decreased as the external wind velocity increased. The burning rate of pool fires was influenced by heat transfer [15]. Therefore, when the external wind velocity increased, the flame shape became tilted (as shown in Figure 11), which reduced the heat feedback from the flame to the fuel. Under cross-flow conditions, the interaction between the flame and the fuel was strongly affected [16], leading to a decrease in the mass loss rate. Conversely, when the downward external wind angle was 30°, the airflow field in the tunnel became more turbulent, resulting in higher airflow velocities inside the tunnel. The flame tilted more (as shown in Figure 11), and according to Rafael *et al*. [17], when the airflow intensity inside the tunnel increased, heat feedback shifted from heat radiation to heat convection. As the external wind velocity increased, the heat convection feedback was enhanced, which increased the mass loss rate. Therefore, it can be observed that the downward external wind angle and wind velocity affected the airflow distribution inside the tunnel, causing the flame to tilt and enhancing the heat convection effect. These two effects interact, influencing the mass loss rate inside the tunnel by both increasing the heat convection effect and lowering the tunnel temperature. However, the results of this experiment showed that the heat convection effect still dominated in tunnel fires, while the cooling effect played a secondary role. Thus, despite the decrease in tunnel temperature, the mass loss rate increased, indicating that the heat convection effect had a more significant impact.

Figure 10 showed the comparison of mass loss rates under different upward external wind angles and wind velocities in the absence of axial ventilation. The mass loss rate decreased as the upward external wind velocity increased, but it slightly increased as the upward external wind angle increased. According to the airflow field analysis, under the same upward external wind velocity, increasing the upward external wind angle caused the airflow velocity inside the tunnel to decrease. As the airflow velocity increased, the mass loss rate decreased.

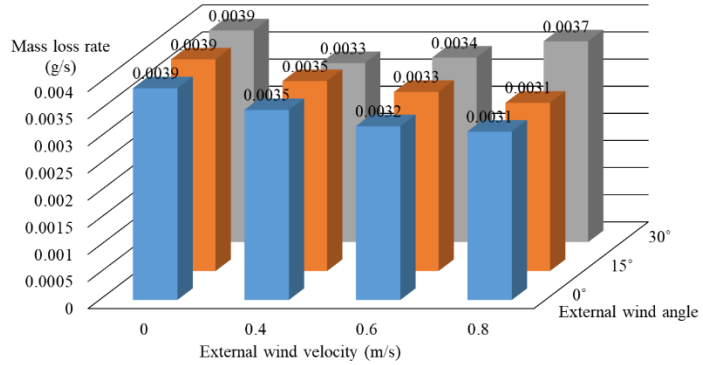

Figure 9 *The mass loss rate of different downward angles external wind and wind velocity without longitudinal ventilation.*

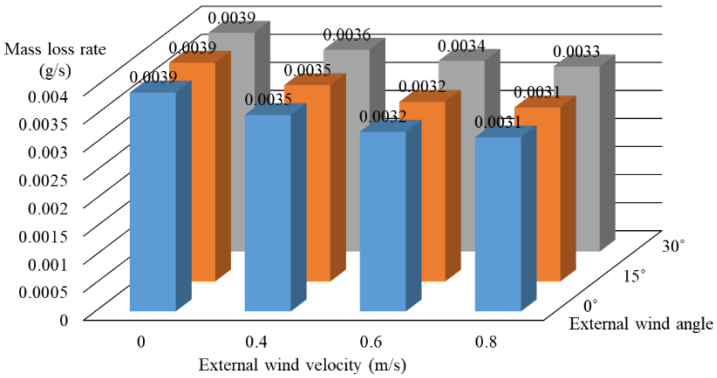

Figure 10 *The mass loss rate of different upward angles external wind and wind velocity without longitudinal ventilation.*

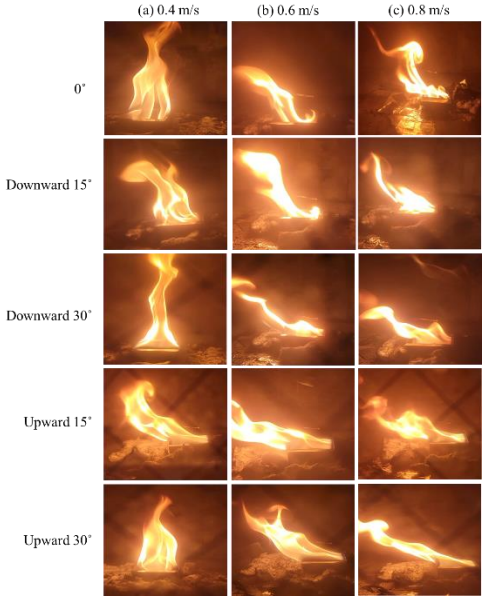

Figure 11 *The flame shapes of different downward angles external wind and wind velocity without longitudinal ventilation.*

Mass loss rate with longitudinal ventilation

Figure 12 compared the mass loss rates under different downward external wind angles and wind velocities in the presence of axial ventilation. The axial ventilation velocity was 0.38 m/s which was calculated according to the equation of Wu and Bakar [7] with a heat release rate of 2.7 kW. For the

group with a 0˚ external wind angle, as the external wind velocity increased, the mass loss rate first increased and then decreased. When the external wind velocity was 0.4 m/s, the airflow field was in a unidirectional flow zone, and with the interaction with the axial flow fan, the flame did not tilt, keeping the heat feedback unchanged. This enhanced the air entrainment effect, increasing the mass loss rate. However, as the downward external wind velocity increased, the airflow inside the tunnel strengthened, causing the heat feedback to decrease, resulting in a reduction in the mass loss rate. Conversely, when the downward external wind angle increased, the airflow field inside the tunnel became more turbulent, with higher airflow velocities, causing a larger flame tilt (as shown in Figure 11). According to Rafael *et al*. [17], when the airflow intensity inside the tunnel increased, heat feedback shifted from heat radiation to heat convection, and as the external wind velocity increased, heat convection feedback strengthened, increasing the mass loss rate. However, when the external wind velocity was large, the axial flow fan became less effective at reducing the external wind influence, making the flame tilt more due to the external wind. As a result, the mass loss rate decreased.

Figure 13 compared the mass loss rates under different upward external wind angles and wind velocities in the presence of axial ventilation. The axial ventilation velocity was 0.38 m/s. When the external wind angle was 30° upward, the airflow inside the tunnel became more stable. Additionally, when interacting with the axial flow fan, the flame tilt decreased, allowing the heat to be more effectively transferred back to the fuel, increasing the mass loss rate. However, as the wind velocity increased, it caused an imbalance in the airflow on both sides, leading to a tilted flame, which reduced the heat feedback. Therefore, the mass loss rate was higher in the case of both external wind and axial flow ventilation than with external wind alone. This was because, when there was only external wind in the tunnel, the generated airflow tilted the fire source, causing poor heat feedback. In contrast, when both fans were operating, the axial flow fan counteracted the effect of the external wind, reducing the external wind's influence on the fire source. As a result, heat feedback became more stable, and the increased airflow can provide more oxygen to support combustion.

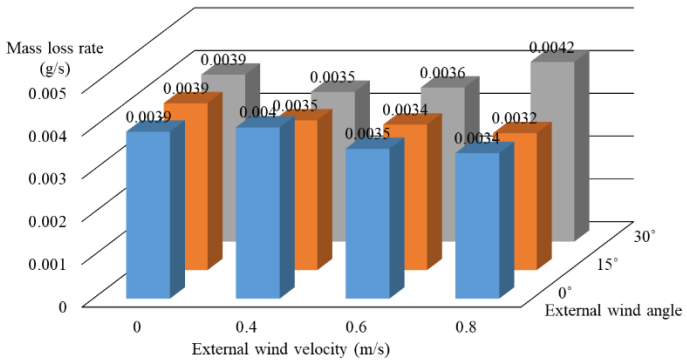

Figure 12 The mass loss rate of different downward angles external wind and wind velocity with longitudinal ventilation.

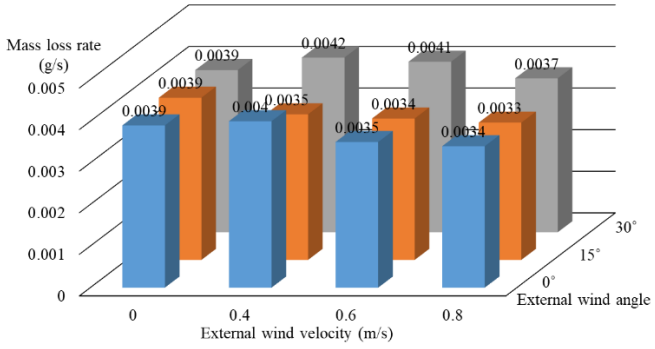

Figure 13 The mass loss rate of different upward angles external wind and wind velocity with longitudinal ventilation.

Smoke behaviours and critical ventilation velocity analysis

Smoke spreading length

Figure 14 illustrated the smoke spreading length with (a) 0˚; (b) Downward 15˚; (c) Upward 15˚. By observing the position of the dense smoke and comparing the temperature data, it can be determined that if the measured temperature was higher than the ambient temperature by 6°C (indicated by the black dashed line), it indicated that the dense smoke had reached that position, which is similar to the 5°C temperature difference proposed by Zhao *et al*. [11]. The blue line in the figure represented the group with no external wind influence and with axial ventilation at 0.38 m/s (the critical ventilation velocity calculated based on a heat release rate of 2.7 kW). It can be observed that, due to the effect of axial ventilation, the highest temperature in the tunnel was located 0.5 m downstream from the fire source, and the downstream smoke layer spread to the tunnel exit. For the external wind angle of 0 ˚ (Figure 14 (a)), regardless of wind velocity, the smoke layer spread to the downstream exit of the tunnel, only affecting the position of the highest temperature and reducing the temperature. As the external wind velocity increased, the position of the highest temperature moved further upstream toward the fire source, and the cooling effect inside the tunnel became stronger. In the group with a 15˚ downward external wind angle (Figure 14 (b)), when the external wind velocity was 0.8 m/s, the smoke layer spread over a length of 2.3 m. Since the wind velocity entering the tunnel was higher, the kinetic energy of the smoke layer was hindered, causing it to stagnate. According to the airflow field analysis, the larger the downward external wind angle, the stronger the airflow inside the tunnel, which resulted in a decrease in the smoke layer's spreading length as the downward external wind angle increased. Figure 14 (c) compared the smoke layer spreading length at different external wind velocities when the external wind angle was 15 ˚ upward. When the external wind velocity was 0.8 m/s, the smoke layer spread over a length of 0.9 m. Because of the upward external wind forms a unidirectional flow earlier in the front section of the tunnel, with uniform wind velocity across the section, which strongly hindered the spread of the smoke layer. According to the airflow field analysis, as the upward external wind angle increased, the internal airflow velocity decreased, allowing the dense smoke to spread toward the downstream exit. When the external wind angle was 30 ˚ upward, the smoke layer spread over a length of 1.8 mm.

Smoke back-layering

Figure 15 showed the smoke back-layering with (a) 0˚; (b) Downward 15˚and (c) Upward 15˚. The blue line in the figure represents the group with no external wind influence and axial ventilation at 0.38 m/s (the critical ventilation velocity calculated based on a heat release rate of 2.7 kW). It can be observed that, due to the effect of axial ventilation, the smoke layer was pushed downstream of the fire source. Therefore, the highest temperature was located 0.5 m downstream of the fire source, and the temperature difference upstream of the fire source did not exceed 6°C, indicating no smoke back-layering. Thus, the critical ventilation velocity of 0.38 m/s matched the theoretical calculation. However, once external wind was introduced, regardless of its angle or velocity, the smoke layer backflows to the upstream exit of the tunnel. As the external wind velocity increased, the position of the highest temperature moved further upstream toward the fire source, and the cooling effect inside the tunnel became stronger, reducing the highest temperature in the tunnel. Therefore, it was evident that no matter how large the external wind was, the kinetic energy generated will obstruct the ventilation system inside the tunnel, preventing the original ventilation from sufficiently restricting the smoke flow, which in turn increased the difficulty for personnel to evacuate safely.

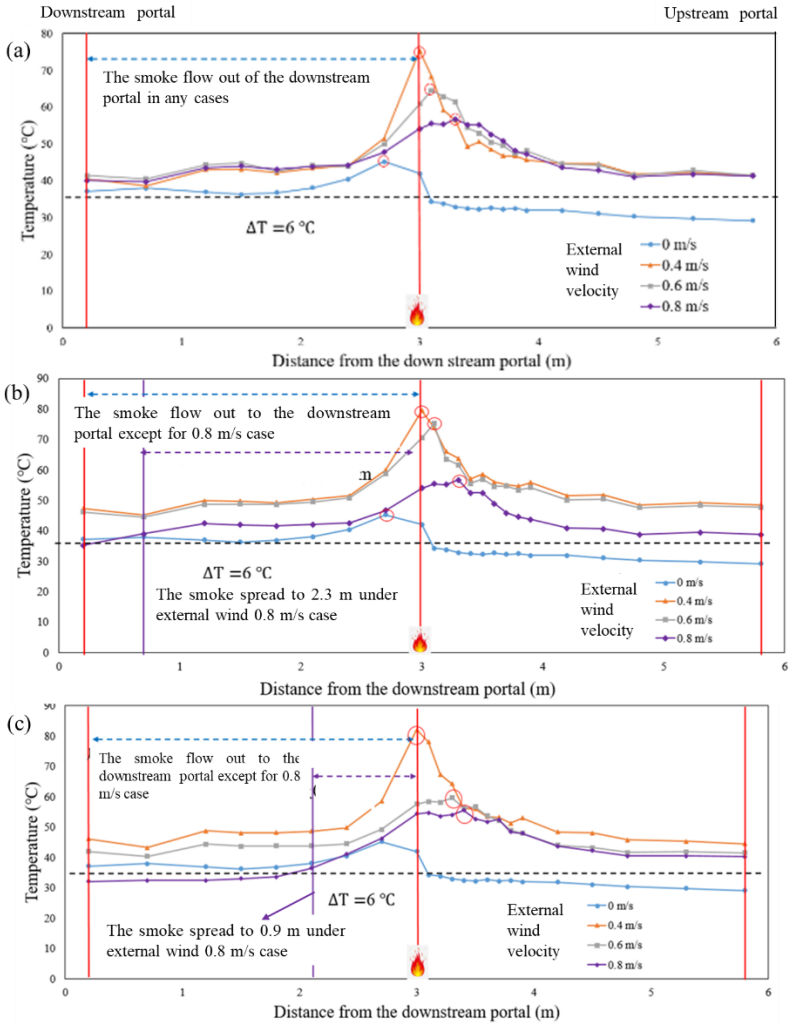

Figure 14 The smoke spreading length with (a) 0°; (b) Downward 15°; (c) Upward 15°.

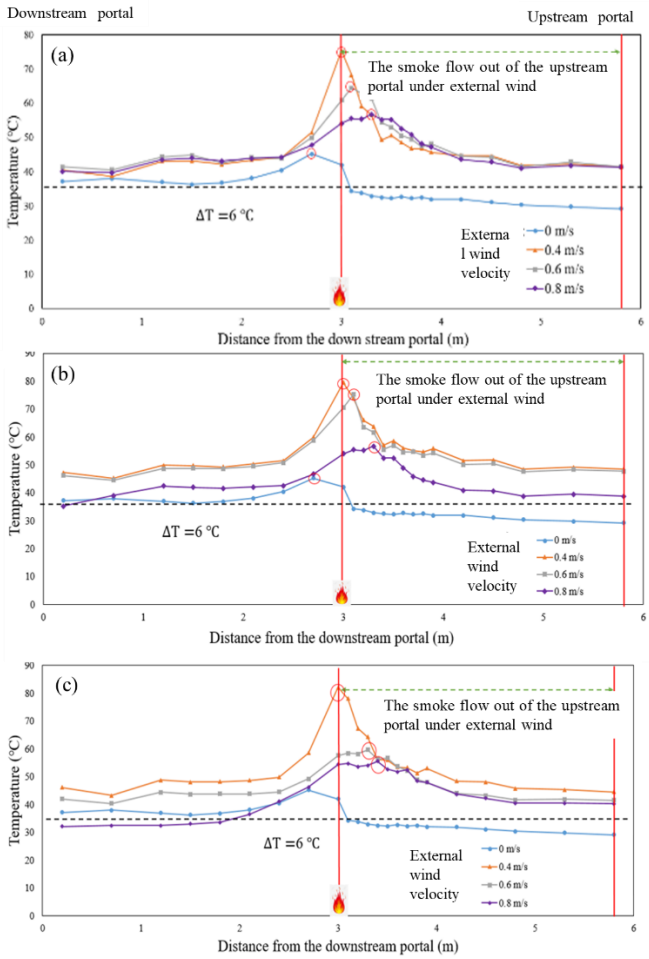

Figure 15 The smoke back-layering with (a) 0°; (b) Downward 15°; (c) Upward 15°.

Critical ventilation velocity

When external wind enters the tunnel, it affects the smoke layer inside the tunnel by altering the airflow and increasing the required critical ventilation velocity to prevent smoke back-layering. In this study, when external wind at an angle of 0° blew into the tunnel at a velocity of 0.8 m/s, the new critical ventilation velocity was tested by trial and error methods, which was 1.2 m/s. The new critical velocity was determined by adjusting the longitudinal ventilation velocity to prevent the smoke flow back to the upstream of fire source. The method to characterize the critical velocity condition was consistent with the one used for the cases with only one-dimensional longitudinal ventilation. When the external wind was at a downward angle of 15° at 0.8 m/s, the critical ventilation velocity was 1.25 m/s. For a downward angle of 30° at the same wind velocity, the critical ventilation velocity increased to 1.35 m/s. Conversely, when the external wind was at an upward angle of 15°, the critical ventilation velocity was 1.25 m/s; at an upward angle of 30°, it was 1.3 m/s. As the external wind velocity increased, the kinetic energy generated by the wind also increased, causing the smoke layer to be more affected, which resulted in a greater spreading distance. Furthermore, as the angle of the external wind increased, a higher critical wind velocity was required since external wind entering the tunnel influenced the inclination angle of the heat source, thereby affecting the movement of the smoke layer. At an angle of 0°, the inclination angle of the heat source was smaller, so the smoke layer was less affected. However, as both the wind velocity and the angle increase, the inclination angle of the heat source in the tunnel became larger, leading to a greater distance covered by the smoke layer.

CONCLUSION

This study examined the effects of different external wind angles and wind velocities on the flow field inside a tunnel, mass loss rate, smoke back-layering, smoke spread, and new critical wind velocity, based on the results of a 1:20 scaled-down experiment. The conclusions of this study are as follows:

1. The turbulent zone and unidirectional zone were formed under the external wind effect inside the tunnel. The flow field would be more turbulent and the wind velocity increase as the increased angle of the downward angled external wind. However, upward external winds are affected by the tunnel opening, resulting in a decrease in the airflow entering the tunnel as the angle and wind speed increase. Additionally, the unstable airflow field also shortens accordingly.
2. External wind had two different effects on the mass loss rate. One effect occurred when the airflow inside the tunnel was high and unstable, causing an increase in the flame's tilt angle, which reduced the flame's heat feedback to the fuel and lowered the mass loss rate. Conversely, if the airflow inside the tunnel was lower and more stable, it increased the intake volume and enhanced the heat convection effect, which boosted the flame's heat feedback to the fuel and increased the mass loss rate.
3. The external wind imparted kinetic energy to the smoke flow inside the tunnel, limiting the diffusion of the smoke layer. The original critical ventilation velocity will be affected by the external wind entering the tunnel, causing an increase in the kinetic energy of the smoke layer, which prevented it from effectively stopping the backflow of the smoke layer.
4. The external wind and its angle entering the tunnel will caused changes in the flow field inside the tunnel. As more airflow entered the tunnel, the smoke flow became more susceptible to the kinetic energy of the external wind, which made the original critical ventilation velocity unable to prevent the backflow of the smoke layer. Therefore, when the external wind angle and wind velocity increased, the new critical wind velocity must also be increased to prevent the smoke layer from backflowing to the upstream section of the tunnel.

ACKNOWLEDGEMENT

The authors would like to thanks Mr. Meng-Hsun Wu for conducting the experiment.

REFERENCES

1. Zhang, X., Wu, X., Park, Y., Zhang, T., Huang, X., Xiao, F., Usmani, A., “Perspectives of big experimental database and artificial intelligence in tunnel fire research”, *Tunn. Undergr. Space Technol.* 108, 103691, 2021, https://doi.org/10.1016/j.tust.2020.103691.
2. Thomas, P.H., The movement of buoyant fluid against a stream and venting of underground fire. Fire Research Note No, p. 351, 1958.
3. Thomas, P.H., The movement of smoke in horizontal passages against an air flow. Fire Research Note No, p. 723, 1968.
4. Hu, L.H., Huo, R., Chow, W.K., “Studies on buoyancy-driven back-layering flow in tunnel fires” *Exp. Therm. Fluid Sci.* 32, 1468–1483, 2008.
5. Li, Y.Z., Ingason, H., “Discussions on ucr and critical Froude number for smoke control in tunnels with longitudinal ventilation”, *Fire Saf. J.* 99, 22–26, 2018.
6. Oka, Y., Atkinson, G.T., “Control of smoke flow in tunnel fires”, *Fire Saf. J.* 25, 305–322, 1995.
7. Wu, Y., Bakar, M.Z.A., “Control of smoke flow in tunnel fires using longitudinal ventilation systems - a study of the ucr”, *Fire Saf. J.* 35, 363–390, 2000.
8. Li, Y.Z., Lei, B., Ingason, H., “Study of ucr and backlayering length in longitudinally ventilated tunnel fires.” *Fire Saf. J.* 45, 361–370, 2010.
9. Lee, Y.P., Tsai, K.C., “Effect of vehicular blockage on critical ventilation velocity and tunnel fire behaviour in longitudinally ventilated tunnels”. *Fire Saf. J.* 53, 35–42, 2012.
10. Tsai, K.C., Chen, H.H., Lee, S.K., “Critical ventilation velocity for multi-source tunnel fires.” *J. Wind Eng. Ind. Aerod.* 98, 650–660, 2010.
11. Zhao, W., Ouyang, R., Ran, Q., Chen, T., Xu, Z., Zou, M., Fan, C., “An experimental study on smoke back-layering and ucr in tunnel fires with canyon cross wind”, *J. Wind Eng. Ind. Aerod.* 209, 104477, 2021.

12. Jiao, A., Shen, Y., Wang, Z., Chen, T., Tao, H., Xu, Z., Fan, C., "Experimental study on the effect of canyon cross wind yaw angle on airflow and flame characteristics in a tunnel", *J. Wind Eng. Ind. Aerod.* 213, 104616, 2021.
13. Ouyang, R., Zhao, W., Yang, L., Jiao, A., Xu, Z., Fan, C., "An experimental investigation of burning rate and flame geometric param of tunnel fires under canyon cross wind and longitudinal ventilation", *Fire Saf. J*. 126, 103474, 2021.
14. Shen, Y., Jiao, A., Chen, T., Li, Y., Gao, Y., Xu, Z., Jiang, B., Fan, C., "Experimental study on smoke movement characteristics in tunnel fires with different canyon cross wind yaw angles." *Tunnelling and Underground Space Technology*, 117, 104129, 2021.
15. Blinov, V.I., and Khudyakov, G. N., "Diffusion burning of liquids." US Army Engineer Research and Development Laboratories, 1961.
16. Hu, L., Hu, J., Liu, S., Tang, W., Zhang, X., "Evolution of heat feedback in medium pool fires with cross air flow and scaling of mass burning flux by a stagnant layer theory solution." Proceedings of the Combustion Institute, 35.3, 2511-2518, 2015.
17. Salvagni, R.G., Centeno, F.R., Indrusiak, M.L.S., "Burning rate, flame geometry and temperature of convection-controlled circular diesel oil pool fire under air crossflow conditions." *Journal of hazardous materials*, 368, 560-568, 2019.

When is a Tunnel a Tunnel?

Salvatore Marsico, Luis Robles & Alexa Laszlo
WSP USA, New York, USA

ABSTRACT

The National Fire Protection Association (NFPA) 502 defines a "Road Tunnel" as "An enclosed roadway for motor vehicle traffic with vehicle access that is limited to portals" however when a roadway is not "fully" enclosed, the decision to consider it a road tunnel shall be made by the authority having jurisdiction (AHJ). The onus is on the engineer to make a recommendation supported by engineering analysis as to whether to classify and thus design the facility as a tunnel or otherwise.

NFPA 502 is a United States national standard that establishes the minimum fire life safety provisions for road tunnels, bridges, limited access highways and roadways beneath air-right structures. Some structures will not cleanly fall into one category or the other and so requires an assessment by the engineer to determine how to approach the fire life safety design of the facility. Chapter 7 of NFPA 502 [1] Section 7.2.1 states that "Where a roadway or portion of a roadway is not fully enclosed on both sides, is not fully enclosed on top, or any combination thereof, the decision by the authority having jurisdiction (AHJ) to consider the roadway as a road tunnel shall be made after an engineering analysis is performed in accordance with 4.3.1." Section 4.3.1 provides 21 factors that are, at a minimum, required to be considered as part of the engineering analysis to support the classification recommendation. The framework of the engineering analysis required by NFPA 502 is not defined and requires the engineer to develop the analytical approach.

This paper will examine a case study for a unique road structure consisting of several stacked roadways in a semi-enclosed configuration and establish an engineering analysis framework for evaluating what fire protection measures should be included in the design to meet fire and life safety requirements.

KEYWORD: Fire, NFPA 502, classification, roadway, tunnel

INTRODUCTION

A project in the design phase, in North America includes a ramp structure in a multi-level ramp configuration. The purpose of the ramp structure was to facilitate the movement of buses between a multilevel bus terminal and ground level for incoming and outgoing buses. Because of the roadways being positioned on top of one another as well as the partial closure of the exterior of the roadways per National Fire Protection Association (NFPA) 502 Standard for Road Tunnels, Bridges and Other Limited Access Highways (National Fire Protection Association, 2020) an engineering analysis had to be conducted to assess the classification of the facility. This paper will examine this case study and establish an engineering analysis framework for evaluating what fire protection measures should be included in the design to meet fire and life safety requirements.

Facility description

The facility consists of a ramp structure above grade that connects to each level of a bus terminal. The ramps will function to facilitate the movement of buses between the multilevel terminal and ground level for incoming and outgoing buses. Figure shows a sketch of a typical section of the ramp. The ramps are multilevel. The outer façade of the facility will be cladded with a partially open

architectural screen structurally supported via connections to the adjacent ramps, while the inner side of the ramps will not contain a façade, i.e. it will be 100% open, with the exception of structural elements required to support the roadways, which affords minimal blockage to airflow. Other key variables that will impact analytical results include: roadway width, roadway grade, and vertical and horizontal offset between roadway levels the details of which will not be provided given the sensitive nature of the facility

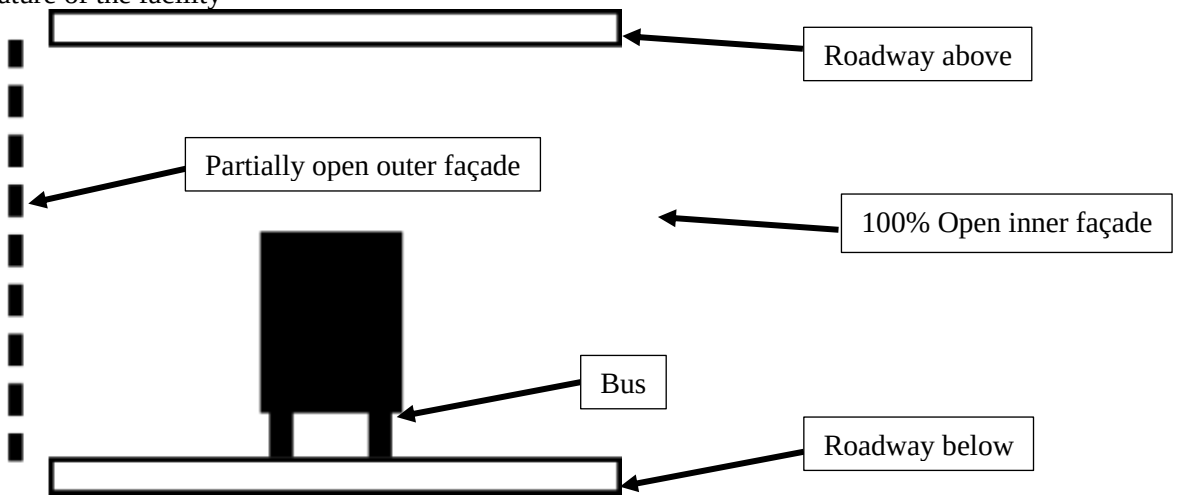

Figure 1 Sketch Typical Ramp Level.

NFPA 502 – GOVERNING STANDARD

The facility, which is used to allow only the travel of buses into and out of the bus terminal, falls under the scope of NFPA 502 2020 edition per section 1.1.4.1. The 2020 version of NFPA 502 is used instead of the newer version of the standard as it is the most up to date version referenced by the latest local building code and we were thus contractually obligated to use it.

The ramps are partially enclosed which triggers an engineering analysis per section 7.2.1 and section 4.3.1 only goes so far as to indicate that an engineering analysis is required regardless of the facility type and length to determine the fire protection and life safety provisions required. Section 4.3.1 does not indicate the type of engineering analysis that should be conducted (e.g. qualitative or quantitative, CFD, etc), but only goes on to list 21 minimum considerations. Therefore, the framework of the engineering analysis to be conducted is based on the judgement of the engineer.

FACILITY CLASSIFICATION

Qualitative Engineering Analysis

A qualitative analysis is the most appropriate approach for this facility. The ramp facility most closely resembles a bridge, therefore, each consideration from NFPA 502 Section 4.3.1 was evaluated to determine if the facility's characteristics were more similar to that of a bridge, or a tunnel, or neutral, meaning it applies equally to both.

Table provides a summary of the considerations, associated qualitative analysis, and engineering assessment. The engineering assessments for each consideration resulted in either a "Neutral" or "Bridge" classification, therefore, the classification for the facility was determined to be that of a Bridge. For this ramp facility, the classification was straightforward, however, had the ramp structure been more enclosed, access been more restricted etc, it may have resulted in more considerations qualitatively assessed to be more like a tunnel. NFPA 502 requires that regardless of classification, the engineer must develop a design that protects against loss of life and property.

Table 1 NFPA 502 Section 4.3.1 Engineering Analysis for Facility Classification of the Ramps.

#	NFPA 502 Section 4.3.1 Consideration	Engineering Analysis	Engineering Assessment (Bridge/Neutral/Tunnel)
1	New facility or alteration of a facility	New facility.	Neutral-
2	Transportation modes using the facility	Buses only. Unidirectional traffic on separated ramps.	Neutral-
3	Anticipated traffic mix and volume	Buses only.	Neutral-
4	Restricted vehicle access and egress	Yes – restricted to buses. Egress has protected egress stairs.	Neutral-
5	Fire emergencies ranging from minor incidents to major catastrophes	A worst-case single battery electric bus fire was evaluated.	Bridge – Smoke and hot gases are released more like a bridge than a tunnel through the partially and 100% open sides of the roadway.
6	Potential fire emergencies including but not limited to the following: (a) At one or more locations inside or on the facility (b) In close proximity to the facility (c) At facilities a long distance from emergency response facilities	(a) multiple fire locations were evaluated. (b) not the worst case from tenability perspective (c) closest fire department is 2 blocks away.	Bridge- Smoke and hot gases are released more like a bridge than a tunnel. Access for the fire department is more like a bridge than a tunnel due to easier access. Ladder trucks can access elevated roadways.
7	Exposure of emergency systems and structures to elevated temperatures	CFD analysis was performed to determine exposure requirements.	Bridge- Fires are readily visible from the outside ambient much like a bridge, which can reduce response time from the Fire Department and minimize temperatures. Due to the release of smoke and hot gases like a bridge, exposure to high temperatures is less stringent.
8	Traffic congestion and control requirements during emergencies	Traffic control will be provided to stop additional traffic from entering the ramps. Traffic ahead of the fire is assumed to move away from the fire incident.	Neutral-
9	Fire protection features, including but not limited to the following:	Fire protection provisions are determined based on NFPA 502 for bridges, engineering analysis and relevant project precedent. See item 10.	Bridge- Fire protection features like a bridge due to the 100% open on one side and partially open on the other side of the

	(a) Fire alarm and detection systems (b) Standpipe systems (c) Water-based fire-fighting systems (d) Ventilation systems (e) Emergency communications systems (f) Protection of structural elements (g) electrical cable		ramps, the release of smoke and hot gases and access for fire department.
10	Facility components, including emergency systems	1) One side of ramp partially open façade, other side of ramp 100% open except for structural elements 2) 3 egress stairs of 54" wide (based on engineering analysis and local building code for accessible means of egress) 3) Directional and exit signage (engineering analysis) 4) Emergency lighting 5) Traffic control (engineering analysis) 6) Standpipe 7) CCTV 8) Naturally ventilated 9) No fixed fire suppression needed for tenability (based on engineering analysis)	Bridge- Emergency systems provisions like a bridge due to 100% open on one side and partially open on the other side of the ramps, the release of smoke and hot gases and access for fire department. Neutral- All other components/ systems listed under “Engineering Analysis” column fall under Neutral
11	Evacuation and rescue requirements	Size of egress provisions will be based on providing a tenable environment for evacuation during a design fire incident. Areas for rescue assistance will also be provided in the egress stairs. Fire department will be able to use inbound ramps for their vehicles. Fire fighter ingress can also be accomplished through stairs.	Bridge- Evacuation and rescue like a bridge due to 100% open on one side and partially open on the other side of the ramps, the release of smoke and hot gases, egress and access for fire department.
12	Emergency response time	Expected faster emergency response than a tunnel. Trained and familiar bus operators. Closest fire department is 2 blocks away.	Bridge- Open design of the ramps is expected to produce a faster response time for the Fire Department, due to restricted access to only trained and familiar bus operators, multiple access locations, better visibility, open exterior when compared to a tunnel.

13	Emergency vehicle access points	If there is a fire on the outbound ramp, the inbound ramps are available for access, vice versa.	Neutral-
14	Emergency communications to appropriate agencies	Two way communication provided via an enhanced radio infrastructure using radiating cable.	Bridge- Aboveground ramps provide better emergency communications to appropriate agencies than a tunnel.
15	Facility location such as urban or rural (risk level and response capacity)	Urban. Response capacity is expected to be significant, response time to site expected to be faster.	Bridge- The risk level, response capacity and time are that of a bridge.
16	Physical dimensions, number of traffic lanes, and roadway geometry	Dimensions, number of traffic lanes and roadway geometry are accounted for in the smoke/egress CFD analysis.	Bridge- A significant amount of smoke propagates out of the ramps like a bridge. Tenable egress path more like a bridge than a tunnel.
17	Natural factors, including prevailing wind and pressure conditions	Natural factors are included in the smoke/egress CFD analysis.	Bridge- Openness and wind help with toxicity and heat concerns more like a bridge. Lessens concerns with gas and heat confinement than a tunnel.
18	Anticipated cargo	Buses.	Neutral-
19	Impact to buildings or landmarks near the facility	Assessing grandfather status of adjacent infrastructure	Neutral-
20	Impacts to facility from external conditions and/or incidents	External conditions and/or incidents are included in the smoke/egress CFD analysis.	Bridge- Openness and wind help with toxicity and heat concerns more like a bridge. Having more points of access mitigates risk of external incident impact.
21	Traffic operating mode (unidirectional, bidirectional, switchable, or reversible)	Buses only. Unidirectional traffic on separated ramps.	Neutral

Authority Having Jurisdiction

The Authority Having Jurisdiction (AHJ) per NFPA 502 Chapter 3 is "…an organization, office, or individual responsible for enforcing the requirements of a code or standard, or for approving equipment, materials, an installation, or a procedure." The responsibility of the engineer of record is to perform the analysis and provide a recommendation to the AHJ. The AHJ, in this case, was the owner/operator of the facility. The AHJ reviewed the analysis and recommendation for the Bridge classification, and provided no objection.

Key Requirement Differences Between a Bridge and Tunnel Classification under NFPA 502

The requirements for a bridge classification are prescriptively less stringent than that of a tunnel classification. Table 2 provides a comparison between the requirements as it relates to key fire life safety provisions under the bridge or tunnel classification. The table shows that for the two key provisions listed, a bridge classification would result in a Conditionally Mandatory

Requirement (CMR) for both, whereas a tunnel classification would result in a Mandatory Requirement (MR) for both. A CMR requires the engineer to perform engineering analysis to determine if it is required as opposed to a MR where the provision would be prescriptively required.

Table 2 Comparison of Key Fire Life Safety Provisions for Bridge and Tunnel Classification under NFPA 502.

Fire Life Safety Provision	Bridge Classification	Tunnel Classification[1]
Mechanical Ventilation	CMR[2]	MR – NFPA 502 11.1.1
Exits spaced at a maximum of 1000 ft	CMR[2]	MR – NFPA 502 7.16.6.2

CMR = Conditionally Mandatory Requirement
MR = Mandatory Requirement
[1] = Tunnel Category D
[2] = No mention in relevant chapter, thus determined by engineering analysis (i.e. CMR) per NFPA 502 Section 4.3.1

STRUCTURAL FIRE TEMPERATURE ANALYSIS

As part of a holistic multidisciplinary analysis as required by NFPA 502, the structural integrity of the facility as it relates to design fire exposure must be assessed to determine if the design meets NFPA 502. That analysis was conducted under a separate group and will not be discussed in detail in this paper. The impact of the design fire on the structural design has been analytically assessed and meets the requirements of NFPA 502.

EMERGENCY VENTILATION AND EGRESS ANALYSIS

Pass/Fail Criteria

The overarching criteria for engineering analysis to assess the appropriate ventilation and egress provisions is to provide a tenable environment for evacuation for the time required for egress. A tenable environment is defined in NFPA 502 Section 3 as "An environment that permits evacuation or rescue, or both, of occupants for a specific period of time." The pass/fail criteria were developed based on the information found in "Annex B Tenable Environment" of NFPA 502. The criteria are presented in Table 3.

Table 3 CFD/Egress Analysis Pass/Fail Criteria (no objection by the AHJ).

Parameters	Value	Units	Source and notes
Air temperature	60 140	deg C deg F	Annex B of NFPA 502 lists guidelines for a tenable environment. 60°C gives a maximum exposure time without incapacitation of 10.1 min 10 m of visibility where wayfinding is critical. CO limit is for 30 minutes.
Visibility of a light reflecting surface	10	m	
Carbon monoxide	225	ppm	
Radiation	2.5	kW/m^2	
Height clear of smoke	2.5	m	
Air speed	11	m/s	

Modelling

A Computational Fluid Dynamics (CFD) analysis using Fire Dynamics Simulation (FDS) (Fire Dynamics Simulator (FDS) Version 6.8.0, (CFD Software), 2023) was performed to assess the tenability on the ramp facility for design fire scenarios. FDS was used for this case because it captured the most relevant physics for this problem i.e. combustion, smoke movement, heat transfer and turbulence. The geometry of the structures investigated was more like a building/atrium rather than a tunnel and thus many of the usual issues that arise in tunnels did not arise (i.e. instability due to the

pressure solver). Precautions were taken by putting domain boundaries away from regions of interest. The modelling domain encompassed the entire ramping system and was resolved to a cell size of 0.3m x 0.3m x 0.3m established from other project work. In cases with no wind the external boundary conditions, excluding those at grade, were modelled as "Open," while the cases with wind included a velocity boundary via the built-in "&WIND" function of FDS.

Design Fire

NFPA 502 section 4.3.1 requires the engineer to establish a design fire size. The facility limits traffic to that of buses only and Annex A of NFPA 502 provides some guidance on representative fire heat release rates for a bus class, however, the bus types that are expected to use the facility include battery electric buses (BEB). Fire heat release rate data on BEB fires could not be found at the time of the analysis so a BEB fire curve was developed based on existing fire testing data. For example, the Eureka Tests (Eureka Project, 1995) included test B11, which was that of a conventional diesel bus. The composition of these buses; diesel vs BEB, are assumed to be effectively identical as it relates to combustibles except for the propulsion/fuel system i.e. internal combustion engine (ICE) and diesel fuel vs electric motor and batteries. A peak fire heat release rate for a BEB, which included its battery packs, was established to be 53 MW (Raza, 2019) using a conventional ultrafast heat release (α = 0.1876 kW/s^2) rate based on a t^2 curve.

Ventilation Design

The bridge classification requires an engineering analysis to determine the ventilation provisions. Although the facility roadways are stacked on top of one another, they are 100% open on one side and partially open on the other side. The openness of the facility and CFD Analysis demonstrated that natural ventilation was sufficient to meet the criteria found under section "Pass/Fail Criteria" above. It was found that the worst-case scenario included no wind, where smoke and heat propagated to the levels above the fire bus level resulting in untenable conditions on those levels. Buses could be found on these levels above as the design case included a design fire on the departure ramp, which would result in non-incident buses stopped and trapped behind the fire bus. CFD analysis captured this smoke and heat propagation behaviour. The driving criteria was that of visibility, which was quantified based on the calculated soot present in the air. The visibility results were coupled with egress modelling to assess if the natural ventilation provisions incorporated in the design were sufficient to meet criteria. This behaviour of smoke and heat propagating to levels above the fire bus level is inconsistent with typical fully enclosed tunnels as the smoke and heat would be trapped on the fire bus level in this case. The fire bus level for this design was not observed to be a critical level when it came to meeting tenability criteria.

Egress Design

The bridge classification requires an engineering analysis to determine the required egress provisions. The approach here was twofold: 1) Establish obvious exits that would be required based on potential fire locations and 2) use CFD and egress modelling to adjust the established exit locations and add any additional exits that may not have been obvious due to the behaviour of smoke propagation and the impact to tenability. Figure 2 shows an elevation sketch of the ramps with "Egress Stair 1" shown. The location for "Egress stair 1" was established based on inspection, without CFD. Smoke from a fire on the lower level of the ramps could result in a smoky condition on the levels above, and block access for people on the ramps trying to egress towards the bus terminal resulted in the need for Egress Stair 1. The need for additional egress stairs was determined based on CFD analysis. Due to the sensitive nature of the project, we are not able to share any more information regarding egress stair locations. In choosing design fire locations under design development, it is the intent to choose those that are most critical that can reveal weaknesses in the fire life safety design so that the design can be adjusted and improved. Due to the natural propagation of the smoke from different fire locations, it was found that an additional egress stair location was necessary as the smoke from the additional fire location managed to block access to Egress Stair 1 and the roadway connection to the bus terminal.

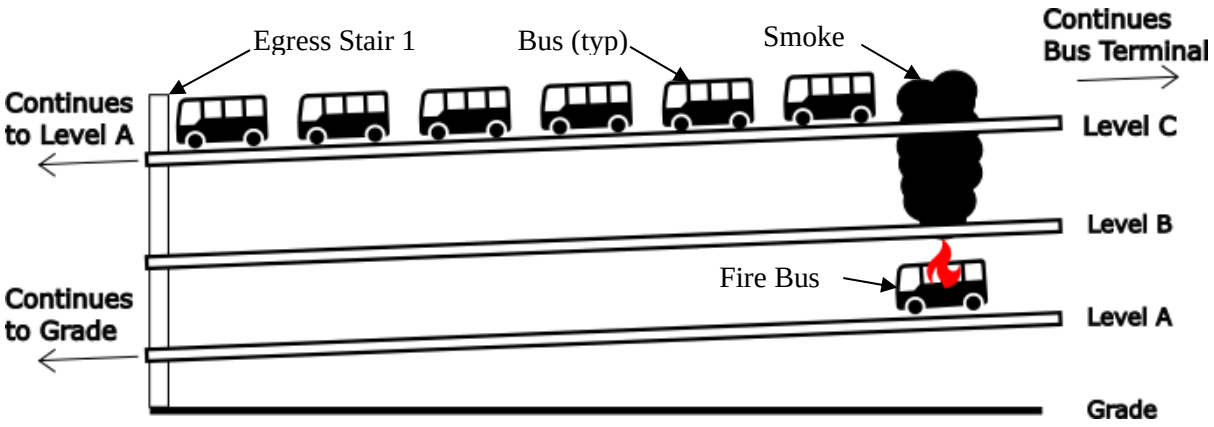

Figure 2 Sketch of Egress Stair Location - Elevation View.

CFD and Egress simulation results

CFD and egress analysis were conducted for a few fire locations throughout the ramping system. A key smoke behaviour that was observed deviating from tunnel behaviour was the contamination of the ramp levels above the fire location, while the fire bus level itself remained clear at the criteria height of 2.5m above the roadway. The analysis included natural ventilation, and with the grade of the ramping system, encouraged the hot smoke in the uphill direction. Due to the sensitive nature of the project detailed results cannot be shared, but a tenable environment was provided for evacuating passengers without the use of a mechanical ventilation system, therefore, a mechanical ventilation system was not needed.

DISCUSSION

The focus of this paper is to provide a framework for determining the fire life safety provisions for a facility that does not quite fall into the classification of a tunnel, but includes characteristics that resemble a tunnel e.g. a ceiling. As shown, the first step to determine the minimum required fire life safety provisions is establishing the classification of the facility. This project used a qualitative analytical approach incorporating the 21 considerations required by NFPA 502 under Section 4.3.1. The classification establishes the required “baseline” provisions, but required the engineering to perform analysis to determine the minimum requirements beyond the “baseline.” This paper focuses on two key fire life safety elements: emergency ventilation and egress provisions. Through quantitative analysis using CFD and egress simulation software it was determined that mechanical ventilation is not required, consistent with the baseline requirements of a bridge classification, while emergency exits were required, which is beyond the baseline requirement of the bridge classification.

CONCLUSION

The facility discussed was classified as a bridge under NFPA 502 establishing the baseline provisions, however, analysis showed that the baseline provisions were not sufficient to provide a tenable environment for evacuation and thus additional provisions beyond the baseline were required to protect life, however, the analysis also showed that the tunnel classification would have resulted in an overdesign as mechanical ventilation was not required, where under a tunnel classification, it would have been part of the baseline requirements. The structural fire temperature analysis was conducted by a different group and the design has met the requirements of NFPA 502.

REFERENCES

1. National Fire Protection Association. NFPA 502: Standard for Road Tunnels, Bridges and Other Limited Access Highways. Quincy, Massachusetts : National Fire Protection Association, 2020.
2. Fire Dynamics Simulator (FDS) Version 6.8.0, (CFD Software). NIST. Maryland : Building and

Research Laboratory, National Institute of Standards and Technology (NIST), 2023.
3. Eureka Project. Fire in Transport Tunnels, Report on Full-Scale Tests. 1995.
4. The impact of battery electric bus fire on road tunnel. Raza, H., Li, S. Athens, Greece : BHR Group, 2019, 18th International Syposium on Aerodynamics, Ventilation & Fire in Tunnels.

Reykjavik's Sæbraut Road Tunnel: Balancing Development and Safety

Böðvar Tómasson[1], Johan Lundin[2], Erik Hall Midholm[2] & Birgir Þór Guðbrandsson[1]
[1]ÖRUGG verkfræðistofa, Reykjavík, Iceland
[2]Brandskyddslaget AB, Stockholm, Sweden

ABSTRACT

The Sæbraut Road Tunnel project in Reykjavik enhances connectivity in the Vogar neighbourhood, tackling a unique opportunity for urban development and the transport of dangerous goods. This project adds to existing knowledge due to the project's complex infrastructure, diverse risk profile, and multiple competing objectives from various stakeholders. It aims to achieve sustainable urban development while addressing the challenges of transporting dangerous goods, with few or no alternatives available for reaching key destinations not accessible by sea. Additionally, the lack of detailed regulations both nationally and internationally for such an infrastructure necessitates innovative solutions, as the traditional Icelandic approach of adopting infrastructure design regulations from other Nordic countries is no longer viable. This paper presents and discusses the comprehensive risk analysis conducted to address some of these challenges and ensure a safe and sustainable built environment in the area, focusing on the evaluated challenges, opportunities, and solutions. The paper will present how these issues were tackled in an Icelandic context, with key measures like QRA, sprinklers, buffer zones, and transport restrictions reducing risks, aligning with the ALARP principle. The project illustrates effective risk management for resilient urban development.

KEYWORDS: tunnel, decking, capping, overbuilding, fire, safety, risk analysis, life safety, dangerous goods, sprinkler.

INTRODUCTION

Background

The initiative to construct city tunnels in Reykjavík presents several challenges that need careful consideration. While Iceland has existing tunnels, the city has not previously implemented this type of infrastructure. One major challenge is Reykjavík's low population and population density, which can complicate the need for such extensive projects. The city’s harsh weather conditions also demand designs that prioritize safety and durability to withstand extreme elements. Geotechnical challenges also play a crucial role, as the local geology may impact construction techniques and overall feasibility. Moreover, the current infrastructure has limited capacity for emergency response, making it essential that new tunnels are designed to enhance access for emergency services.

There is a growing determination within Reykjavík to shift away from a long-standing tradition of prioritizing car usage towards developing more environmentally sustainable transportation options. This project is part of a broader vision to establish a bus metro system to reduce reliance on cars and promote public transport. Lastly, by integrating city tunnels into the urban landscape, Reykjavík aims to increase population density while simultaneously creating more green spaces, thereby enhancing the quality of life for residents and improving the overall urban environment. These challenges and opportunities must be navigated strategically to ensure the success of the city tunnel project.

Transitioning from open roads in developed neighbourhoods to tunnels, along with the potential for sustainable urban development above, can significantly enhance traffic flow, create more green spaces, increase population density, and support greater sustainability in public transportation operations. This project established a foundation for city-tunnel design, essential for guiding future development and decision-making. Supporting future development on the road to better urban development.

Sæbraut Road Tunnel

The Sæbraut Road Tunnel project in Reykjavik is a significant urban development initiative by the Icelandic Road and Coastal Administration (Vegagerðin) and the Reykjavík city (Reykjavíkurborg). It aims to enhance connectivity between the older and newer sections of the Vogar neighbourhood (see Figure 1). This undertaking is characterized by its complex infrastructure and diverse risk profile, addressing multiple competing objectives from various stakeholders. A significant aim is to achieve sustainable urban development while managing the unique challenges posed by the transportation of dangerous goods, given the limited alternatives for accessing key destinations. ÖRUGG Consulting Engineers was responsible for fire safety design, which included a risk analysis for the superstructure carried out with Brandskyddslaget AB. The main design contractor is Verkís Engineering.

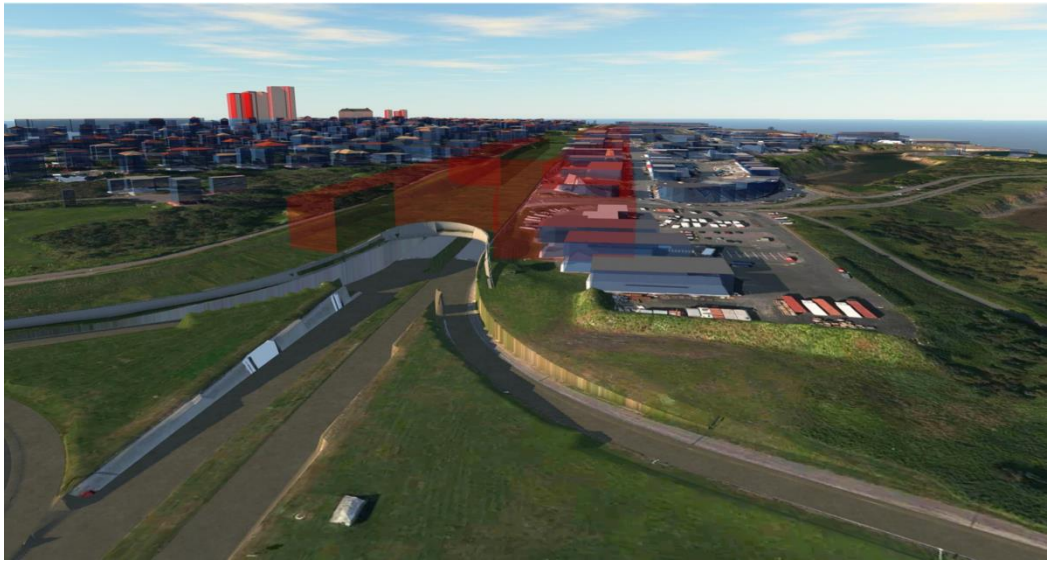

Figure 1 Tunnel entrance, seen from south with proposed overbuild example/Verkís.

Regulations and risk

There are no city tunnels nor covering and decking in Iceland, making this project unique in nature. This also poses a challenge for both designers, clients, authorities and other stakeholders. At the same time, it can create an opportunity for improved traffic flow, lowering accidents regarding pedestrians, increasing green spaces, and reducing pollution related to sound and vehicle exhaust, ultimately enhancing the overall quality of life for residents and dwellers.

Typically, Iceland has relied on infrastructure design regulations from other Nordic countries, but the lack of detailed national and international regulations for this type of infrastructure has necessitated innovative approaches. The project involves integrating housing, offices, retail, and public transport around and above the tunnel, fostering a vibrant urban community and improving accessibility within Reykjavik. This development is a collaboration between Vegagerðin (the Icelandic Road Administration) and the City of Reykjavik.

Transport systems are essential in industrial societies and urban, economic, and social development. Utilizing underground space for transport has been a continuing trend across the globe during past decades [1]. Underground transport systems, such as city tunnels, have been chosen by cities as

potential solutions for solving urbanization problems, such as noise and air pollution and traffic congestion, allowing cities with land shortages to expand [1], [2]. This suggests that underground infrastructure, such as city tunnels contributes to sustainable urban development [3]. However, city tunnels are not without risks. Palm et al. [4] mention that underground structures represent a complex environment with other risks than everyday enclosure fires. As J. Gehandler mentions in his thesis, tunnel fire safety is largely a low probability-high consequence risk issue [5].

Projects involving the covering, decking, or overbuilding of transportation routes are becoming increasingly common, often involving underpasses beneath populated areas where the transportation of hazardous materials takes place. Recent studies show that there is a lack of research in this area, hence significant uncertainty remains regarding how to manage the risks associated with such projects effectively [6].

Guidelines exist internationally for assessing and evaluating risk in spatial planning around tunnels or overbuild (see, e.g. Swedish Road Administration, Trafikverket). However, there are no established regulations or guidelines specifically for land use directly on top of or close to an overbuild. The key distinction lies in population density and potential catastrophic consequences. The impact outside a road or rail tunnel is generally limited due to lower population density, whereas overbuilds are typically located in areas with higher population density. Consequently, the potential damage outside and below the overbuild significantly contributes to the overall risk.

The risk acceptance guidelines for decking, developed by the City of Stockholm [7], require an advanced analysis of potential barriers. This involves identifying and evaluating measures that can reduce either the likelihood or the consequences of catastrophic events. A common approach involves extending the criteria from Det Norske Veritas (DNV) and applying the same valuation principles for scenarios involving fewer than 1,000 fatalities. However, this approach does not align with the original intent behind the criteria [8]. The absence of established guidelines and practices for conducting risk assessments within the ALARP framework, as well as for addressing catastrophic scenarios, complicates the challenges associated with overbuild projects. The capacity of the emergency servises in the Reykjavik capital area is very limited which affects the „catastrophic“ level. Due to this lack of specific guidance or accepted standards, project-specific adaptations are currently required.

Safety for road tunnel users

A considerable amount of literature has been published about city tunnels. Previous studies show that the accident rate in road tunnels (excluding portals) is lower than on open roads, but the consequences tend to be more severe [9], [10]. By allowing traffic to flow through tunnels instead of an open road, the negative effect on drivers of sudden weather changes is lowered, distances between pedestrians and vehicles are lengthened, and surveillance cameras can be more efficient due to more constant sight without the effect of rain, sun, snow, and etcetera. A study from Israel shows that redirecting traffic from open roads to tunnels saves travel time, reduces air pollution, and decreases traffic noise in the environment and its surroundings [11], commonly appreciated by city dwellers.

Purpose and objective

The purpose of the project was to assess the risk of overbuild and compare it to the international context. The objective is to propose risk measures that meet these requirements and identify potential barriers that need to be included in further design. The lack of acceptable Icelandic risk measures requires an extensive summarization of the proposed project.

Delimitations

In this paper, the project-specific tunnels are “dug and covered twin tube tunnels” and, therefore, possibly not representable for tunnels buried deeper in the ground or with two-way traffic in the same tube regarding consequences from larger explosions. The transport of dangerous goods ratio related to daily traffic is not known, but it is likely to be higher than the average ratio due to the close proximity to the harbour and the largest fossil fuel storage/depot in Iceland.

METHOD

The risk analysis utilized a Quantitative Risk Analysis (QRA) approach to evaluate various scenarios and their potential impacts. The QRA involved calculating the societal and individual risk levels, considering factors such as traffic volumes, types of dangerous goods transported, and the tunnel's structural integrity, along with other safety measures which can impact the risk for people on top of, and alongside the tunnel. The analysis only covers sudden and unexpected accidents with acute consequences for the life and health of people staying within the studied area. In the analysis, the long-term effects of substances hazardous to health, noise, or environmentally hazardous emissions have not been taken into account. Nor are risks for operational disruptions studied. Natural disasters (for example, flooding), suicide or antagonistic threats have not been considered. The analysis does not cover the safety of road users within the tunnel, which is covered by the analysis "Sæbraut Road Tunnel – Risk Analysis" [12]. The analysis only includes consequences in the form of the number of fatalities. The analysis is focused solely on studying fatalities, as there are no evaluation criteria available for assessing injuries. The risk analysis is limited to the operational stage of the tunnel and urban development, i.e. the risk impact when the facility is completed.

RISK ASSESSMENT

General Overview

The risk analysis serves as a foundation for the municipality's development plan, evaluating urban development's suitability concerning human health and safety. It provides recommendations for managing identified risks in line with current legislation based on the proposed land use in the master plan. Building placement and design is guided by initial concepts from Vegagerðin and Veitur [13].

Risk Identification

Risk identification begins with an inventory of potential hazards within the studied area, focusing specifically on sources that could lead to sudden and significant accidents with extensive consequences.

Dangerous goods are categorized under the European Agreement concerning the International Carriage of Dangerous Goods by Road (ADR) into nine classes, each representing different chemical properties and associated risks. Key challenges include managing high population density and the risks posed by transporting hazardous materials such as ADR Class 1 (explosives, which may cause mass explosions, fragmentation, or intense fires) and ADR Class 5 (oxidizing substances and organic peroxides, which can intensify or sustain fires). These materials increase the potential for severe accidents involving explosions, toxic gas releases, or uncontrolled fires within the tunnel.

Infrastructure limitations and unique tunnel geometry further complicate traditional safety concepts, requiring tailored evacuation and emergency response adaptations. Addressing these challenges involves comprehensive risk management strategies to ensure a resilient and safe built environment.

Initial Qualitative Risk Analysis

Following the risk inventory, a qualitative assessment determines the consequences and likelihood of identified risks affecting individuals in the area. Risks associated with fatal injuries are prioritized for further analysis, while those with low consequences and probabilities are typically excluded from deeper assessment.

Quantitative Risk Analysis (QRA)

For risks deemed impactful, a quantitative risk analysis (QRA) is conducted. This involves calculating societal and individual risk levels, incorporating factors such as traffic volumes, tunnel design, and proximity to hazardous goods transports. Societal risk measures the risk a source poses to the surrounding environment, reflecting the expected number of fatalities per year based on frequency and consequences. The assessment considers planned building structures and their implications on regional safety.

Individual risk evaluates the likelihood of fatal injury for a specific person in proximity to a risk source, presented as location-specific profiles. This analysis accounts for the height of structures above the tunnel, differing from traditional distance-dependent risk calculations.

Risk criteria ALARP (As Low As Reasonably Practicable)

To evaluate the acceptability of risk levels, they must be compared against established acceptance criteria, which are not clearly defined by legislation. It is recommended to use the ALARP criterion, which establishes lower and upper limits for acceptable risks. Risks falling below the lower limit are deemed acceptable, while those above the upper limit are classified as unacceptable and require mitigation measures. Risks between these limits require cost-efficiency assessments of additional safety measures to be considered tolerable.

No specific criteria for acceptable risks related to the transport of dangerous goods exist in Iceland, although various countries have proposed such measures, resulting in considerable disparities. Specific acceptance criteria examples shown in Figure 2 are from DNV report (Sweden) [14], the Netherlands [15], and the United Kingdom [16] and highlight this variability.

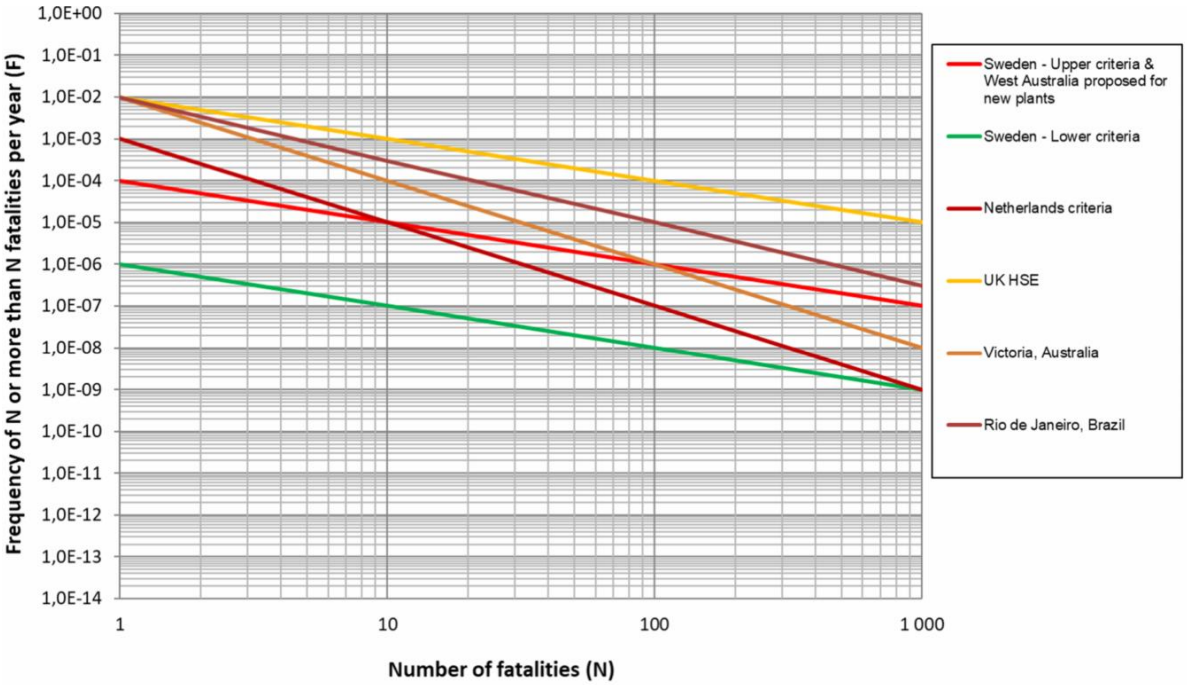

Figure 2 Acceptance criteria in different countries for societal risk regarding third party (the criteria is based on a 1 km road/railway section.

In this project, societal risk assessments will adopt the recommended acceptance criteria from Sweden for conservative evaluations of limited consequences (lesssp than 10 deaths). In contrast, larger consequences necessitate using the ALARP framework for enhanced risk evaluation without exceeding higher risk levels observed in other countries. Furthermore, there are currently no universally accepted criteria for disaster scenarios exceeding 1,000 fatalities. While society typically views such catastrophic risks as unacceptable, the methodologies for assessing these risks remain underdeveloped. Given the potential for large fatality numbers, especially in densely populated areas like around the Sæbraut Road Tunnel, special consideration is needed for scenarios involving dangerous goods.

Existing societal risk criteria often apply an upper limit of 1,000 casualties, beyond which it remains unclear if risk acceptance can be appropriately extrapolated [8]. Therefore, decision-making should prioritize risk-informed strategies over rigid risk-based approaches. Lacking national guidelines and international consensus, there is a critical need to establish project-specific acceptance criteria. Initial

suggestions for assessing catastrophic risk scenarios may be proposed, yet any evidence of potential large-scale incidents necessitates specialized analysis to ascertain risk tolerance.

Sensitivity analysis

In risk assessments, various input data such as design specifications, traffic flows, accident statistics, anticipated population levels, and the behavior of different constructions are essential. Given the infrequent occurrence of the studied accident types, many assumptions are necessary, often leading to limited knowledge of the event sequences and environmental impacts. Conservative estimates are employed to address uncertainties related to these assumptions, providing a safety margin in frequency and consequence calculations.

The calculated risk levels presented should not be interpreted as absolute but serve as guideline values that indicate the approximate risk in the area. To emphasize these uncertainties, a sensitivity analysis was conducted on the most critical input parameters affecting the societal risk level. The analysis aims to demonstrate the robustness of the methods used, revealing how variations in uncertain parameters influence risk levels. The sensitivity analysis encompasses multiple parameters. By adjusting these parameters, both upward and downward, the analysis assesses their impact on the societal risk level, which can inform risk assessments and decisions regarding mitigation measures.

RISK EXPOSURE TO SURROUNDINGS

Societal risk level

Figure 3 plots the societal risk level for third parties and for the planned development on top of, alongside, the tunnel and for surroundings. The societal risk level is plotted in total, both planned development and its surroundings and serves as a baseline for evaluating risk-reducing measures. The Figure shows the societal risk for the planned development in the year 2045 and acceptance with upper and lower criteria according to Sweden.

Figures 4 and 5 plot the societal risk for third parties as well as for planned development on top of and alongside the tunnel and for surroundings. Figure 4 evaluates the impact of a sprinkler system, reduced footprint of the built population, and 20m minimum distance to development. This combination reduces the risk significantly. Figure 5 adds restrictions for the transport of dangerous goods during rush hours, which in particular greatly affects the risk with catastrophic consequences.

The Figures illustrate how different types of buildings, land use and consequence-reducing barriers affect the total societal risk, which can be used in the continued discussion around potential safety-enhancing measures.

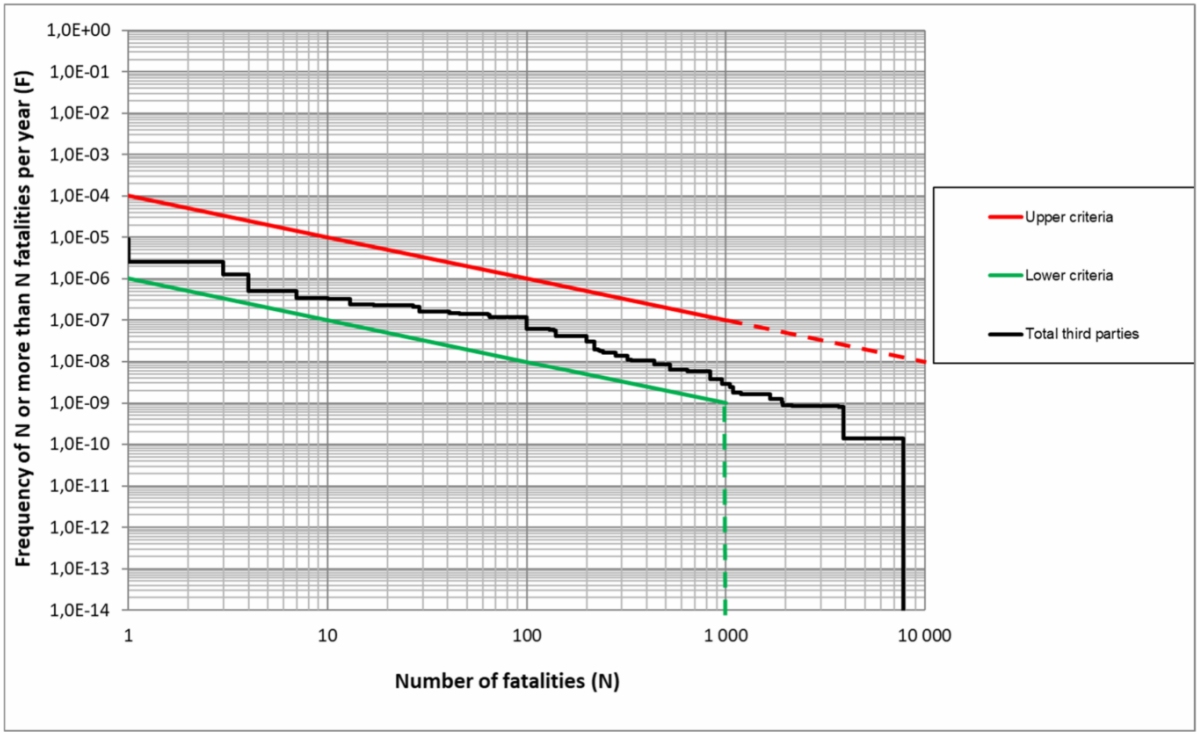

Figure 3 *F/N curve that reports the societal risk level for third parties: total for third parties and for planned development on top of, alongside, the tunnel and for surroundings.*

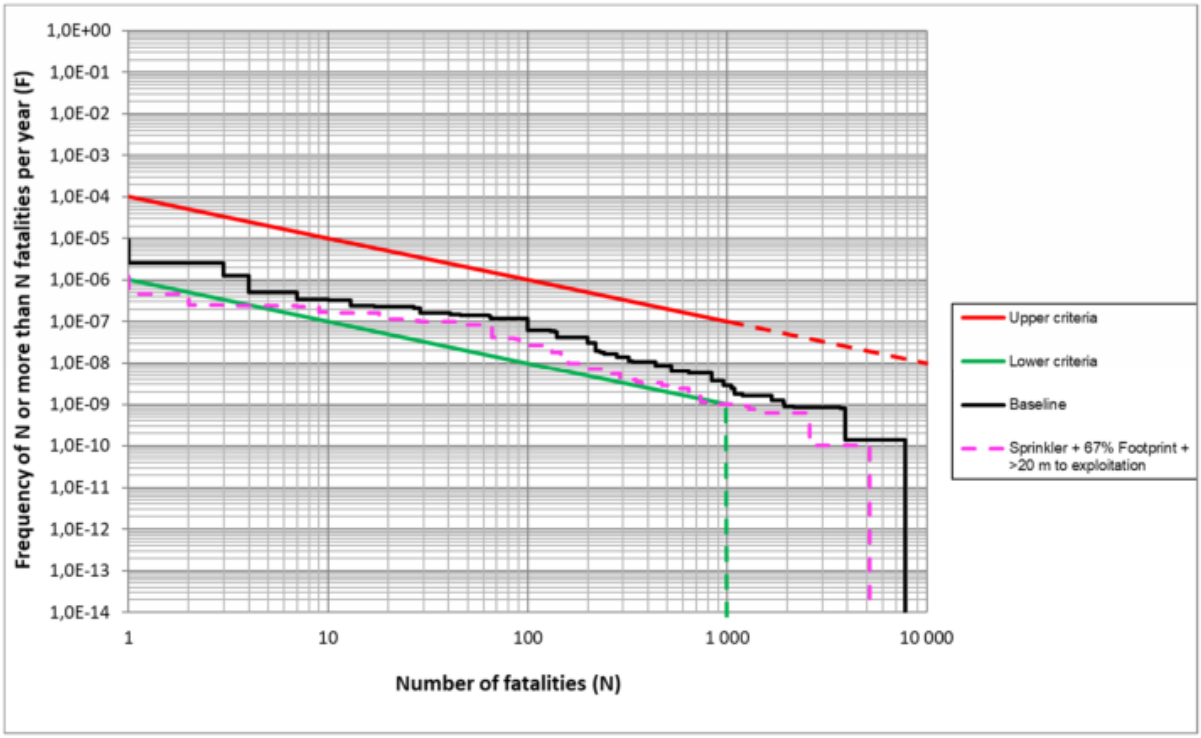

Figure 4 *F/N curve that reports the societal risk level for third parties (planned development and surroundings) + Sprinklers, limited planned development 2/3 of the footprint and 20m safety distance within southern tunnel portal.*

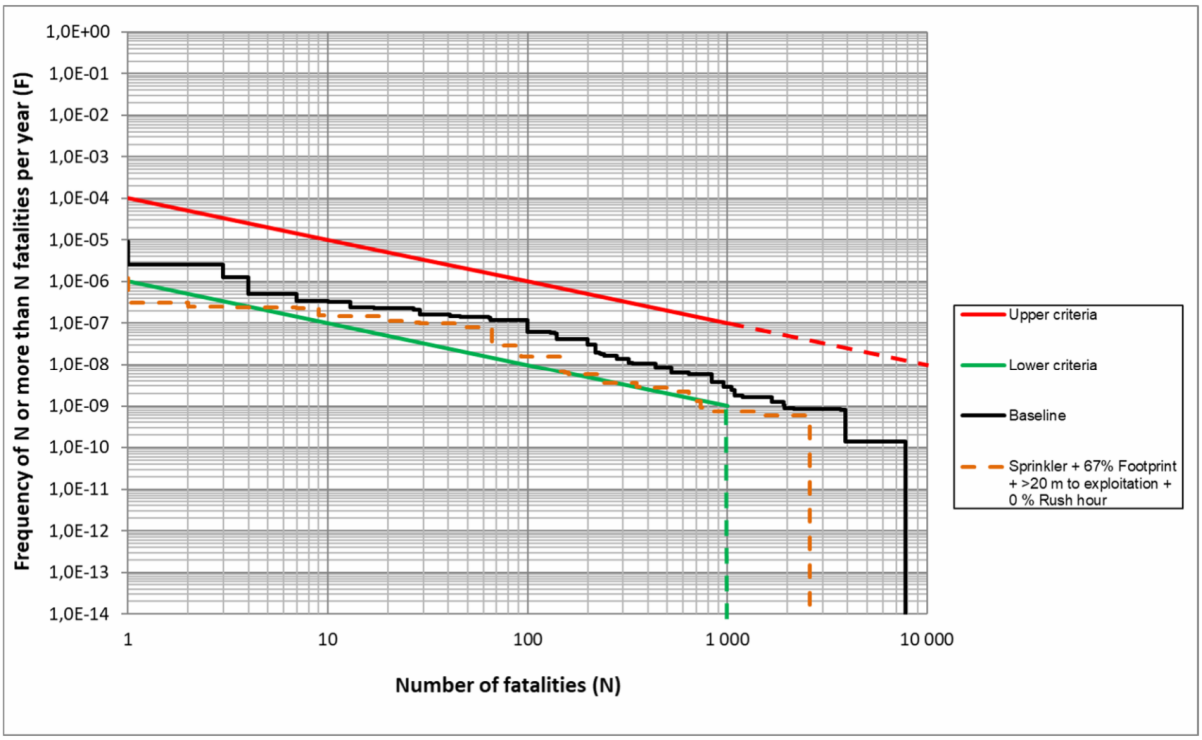

Figure 5 *F/N curve that reports the societal risk level for third parties (planned development and surroundings) + Sprinklers, limit the planned development 2/3 of the footprint, 20m distance within southern tunnel portal and restriction regulation on dangerous goods during rush hour.*

Individual risk

Figure 6 shows the individual risk level as a function of the distance from the roadside. The diagram shows the individual risk for traffic data in the year 2045. The diagram also plots acceptance criteria.

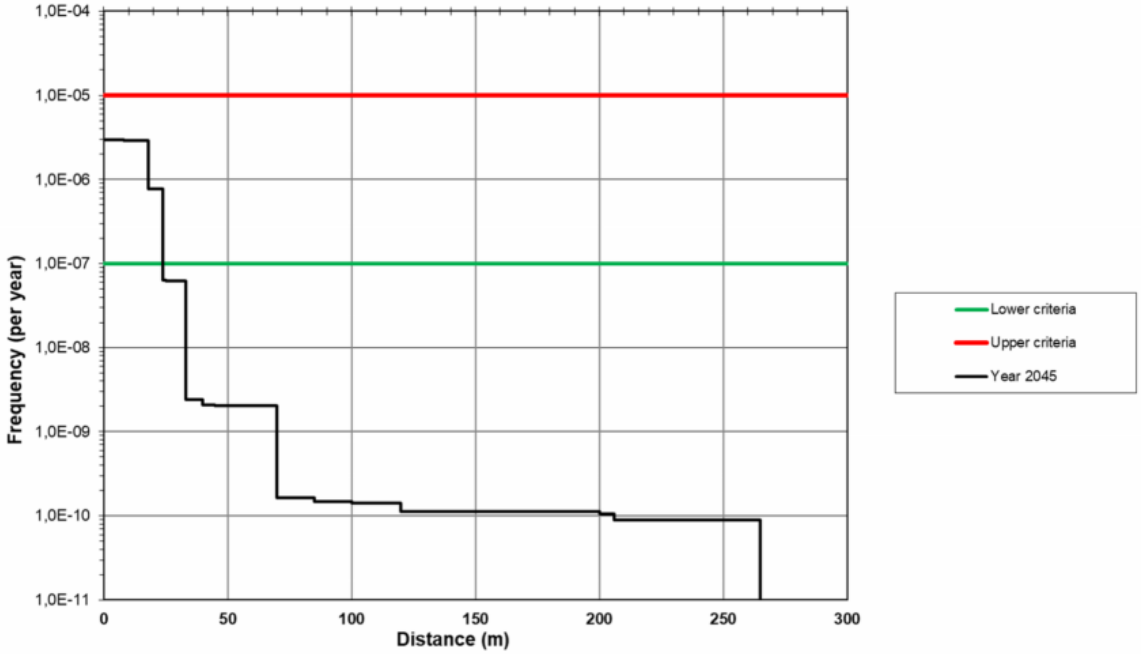

Figure 6 *Individual risk profile as a function of distance to the roadside. Open road accident.*

For areas on top of and alongside the Sæbraut Road Tunnel, the calculation of the individual risk will

differ slightly. This is because the tunnel means that the individual risk level is dependent on the level in relation to the risk source rather than distance-dependent, as described above. For people on top of the tunnel, the individual risk is calculated by summing up the frequency of all scenarios that are expected to lead to fatalities on top of the tunnel.

By summing up the frequency of all the scenarios within the tunnel which are expected to have an impact on the societal risk on top of the tunnel, the total frequency can be calculated as 3.50 x 10-7 per year. This frequency is roughly assumed to contribute to the individual risk level within the planned development. You can call it a baseline of the individual risk on top of the tunnel. In addition, there are scenarios that also contribute to the individual risk on top of the tunnel when they occur in the open, mainly in connection with the tunnel portals. The contribution to the individual risk level on top of the tunnel from surface road scenarios is assumed based on the individual risk profile in Figure 6.

Figure 7 shows the individual risk level on top of the tunnel as a function of the distance from each tunnel portal. The diagram shows the individual risk for traffic data in the year 2045.

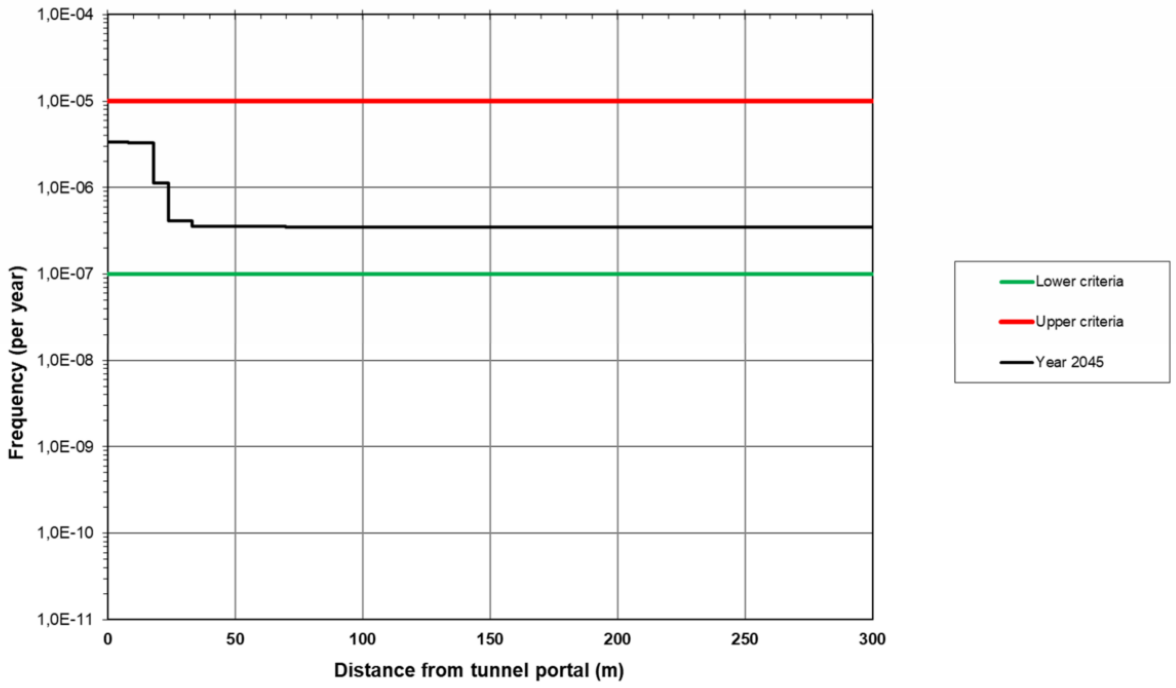

Figure 7 Individual risk profile as a function of distance to tunnel portal. Underground accident + open road accident.

Risk evaluation

The societal risk for planned development and its surroundings has been calculated. Based on the examples of acceptance criteria presented in Figure 2, accidents with dangerous goods are assessed to have a critical effect on the societal risk level within the area. Compared to acceptance criteria in Sweden the societal risk level is within ALARP, which means that cost-efficient safety measures need to be introduced. Within the consequence interval >1.000 deaths, the societal risk is at a level which means, according to the initial suggestion of the chosen acceptance criteria from Sweden, given in Figure 2, that a special analysis of scenarios and measures must be carried out to determine whether the level of risk can be tolerated or not.

The individual risk level for areas on top of the tunnel exceeds 10-7 per year but is less than 10-6 per year, except within approx. 25 meters from the tunnel portals where the individual risk level can exceed 10-6 per year. However, the individual risk level never exceeds 10-5. Along surface road

sections, the individual risk level for areas alongside the tunnel is less than 10-7 per year beyond approx. 30 meters from the roadside. Beyond approx. 25 meters from the roadside, the individual risk level is less than 10-6 per year. The individual risk level never exceeds 10-5.

Based on the individual risk, the risk level is generally within ALARP of the chosen criteria, which means that cost-efficient safety measures or restrictions need to be introduced on top of the tunnel. The same applies to areas closer to 30 meters alongside the surface road, such as the ramps to/from nearby intersection.

Results of Sensitivity Analysis

The sensitivity analysis indicates that only a few parameters significantly affect the risk levels. Major contributors to the societal risk include scenarios involving explosions categorized as ADR Class 1 and ADR Class 5, while ADR Class 2 (For example. LPG, acetylene, chlorine, ammonia, nitrogen etc.) and ADR Class 3 (For example. Gasoline, diesel and fuel oils, solvents and industrial chemicals) scenarios have minimal impact. Notably, the calculations related to ADR Class 1 and ADR Class 5 entail the most assumptions and uncertainties due to the limited statistical data available for these incidents. Additionally, a critical factor not included in the quantitative sensitivity analyses is the planned development above and alongside the tunnel, which may include high-density housing, commercial facilities and transport systems. This development substantially influences societal risk. The consequence calculations rely on conservative assumptions regarding the footprint of this planned development. Therefore, incorporating more detailed information about the planned development will yield a more accurate assessment of the risk level, and this parameter should be considered in the analysis of safety measures.

MITIGATING RISK BARRIERS

The tunnel design is supposed to fulfil Icelandic requirements for new tunnel constructions and the Norwegian requirements for tunnels, N500:2022 [17]. In those requirements, only a few guidelines are provided about rescue services and how to ensure that they can fulfil their task in case of an emergency. The European Union regulations for tunnel structures, state, that safety measures should ensure that emergency services can act effectively [18], but without further guidelines.

Given the complex combinations of scenarios possible in road tunnel accidents, mitigating procedures can be very important. Explosions can have a devasting effect on the tunnel structure causing collapse or serious damage to the tunnel lining and technical equipment. Release of chemical substances might not only cause health hazards and fatilities within the tunnel, but also have a far reach effect on nearby businesses and residences. Large scale consequences can also cause a lack of faith in authorities and limit further development. One crucial aspect of minimizing the consequences of incidents in tunnels is enhancing the efficiency of emergency rescue operations. Early implementation of key measures during the design and planning phases of new tunnels can significantly influence this efficiency. For the fire brigade the key considerations include:

- Training for firefighters and tunnel control center operators to support fluent communications and detailed scene rapport, short responce time, accurate location of emergency and etc.
- The availability and strategic location of access and emergency egress points are critical for minimizing response time and improving firefighters safety. Proper placement can reduce required fire hose length and egress travel distances, while also decreasing the risk of access points being obstructed by a single hazard.
- Design of the smoke ventilation system to increase visability during firefighters egress as well as minimizing the affect of heat ratiation, conduction and convection from smoke layer.
- Availability of fixed firefighting systems/fire sprinklers witch to control and or suppress (reduce) fires.
- Design of the drainage system and holding tanks for combustible liquid to prevent downstream contamination, ignition in drainage, minimizing possible spillage and therefor possible poolfire.

By incorporating these measures, response times can improve, and the effectiveness of emergency services in managing tunnel incidents can be increased, ultimately reducing their impact [19]. Therefore, findings from a risk analysis can serve as valuable input for determining which measures will have the most significant impact on both the probability and consequences of incidents within tunnels. This analysis not only aids in assessing the likelihood of requiring emergency services but may also enhance the chances of executing a safer and more effective rescue operation.

The holistic approach in the mitigating phase involves the interwoven responses of tunnel operators and responders, including the information to and response of the tunnel users, proximate dwellers and buisnesses. At the design stage, it is paramount to include these factors as they may include both the technical design of tunnels and more general road and traffic management. However, from the risk assessment perspective, these barriers involve complex behavioural and technical factors that are difficult to assess quantitatively but involve an uncertainty that must be taken into consideration.

VULNERABILITY IN A SOCIETAL CONTEXT

When faced with a decision on whether or not to implement a protection measure to limit the risk of catastrophic failures, it is important to assess the vulnerability of the road system network in a larger context. By adding vulnerability, the traditional risk assessment framework is broadened in two key ways. First, it expands the focus to include areas with high consequences and low or uncertain (but non-zero) probabilities of occurrence. This shift acknowledges that accurately measuring the likelihood and impact (both human and economic) of many incidents is challenging. Furthermore, society often deems inevitable potential consequences unacceptable and worth mitigating, even when their probabilities are uncertain. Second, vulnerability analysis offers a structured approach to prioritizing and refining risk assessments.

The unavailability of key roads is poised to lead to unacceptable congestion for the road network [20]. The lack of measures and acceptable levels of service for the road system could lead to significant disruptions to traffic flow, increased travel times, and economic losses, highlighting the urgent need for strategic planning and investment in infrastructure resilience and alternative routes. Any accident affecting large and complex infrastructure, such as a tunnel, will have a long-term effect on the entire network since it might take several months or years until the network is put back in working conditions. Hence, it is of large importance to reduce the risks at these links or to increase the redundancy since the consequences of a failure of these links might be regarded as unacceptable.

CONCLUSION AND KEY FINDINGS

This risk analysis initially includes an inventory of possible risks. The inventory shows that only accidents with the transport of dangerous goods impact the risk level for planned development on top of and alongside the tunnel.

Key conclusions include:

- Buffer zones around tunnel portals are crucial in mitigating the impact of accidents on surrounding buildings and inhabitants.
- Limiting the footprint of the development and regulating land use can effectively manage population density and reduce potential casualties in the event of an accident.
- The installation of sprinklers and other fire suppression systems in the tunnel can significantly reduce the risk of vehicle fires escalating to dangerous goods incidents, enhancing the efficiency and safety of the fire brigade when approaching.
- The fire brigade access and response possibilities are important but are difficult to evaluate in quantitative assessment.
- Prohibiting the transport of dangerous goods can lower the probability of high-impact accidents, especially during rush hours.

The findings highlight the importance of a multi-faceted approach to urban development, incorporating safety measures and risk management strategies to create a resilient and sustainable built environment. The project demonstrates how quantitative risk analysis can guide decision-making and ensure that complex urban development initiatives prioritize public safety and well-being.

The initial risk analysis includes an inventory of potential risks, revealing that only accidents involving the transport of dangerous goods significantly impact the risk levels for the planned development atop and alongside the tunnel. Other substantial risk sources were not identified. The tunnel's construction reduces the risk impact on surrounding areas for most potential accidents compared to current open-air road conditions.

The quantitative risk analysis (QRA) indicates that the overall risk level aligns with the ALARP principle, suggesting that additional safety measures should be implemented if they are practical and economically feasible. However, the societal risk demonstrates a catastrophic potential, and even result in accidents with fatalities exceeding 1,000, while unlikely. The absence of national guidelines for third-party risk assessment and international consensus on acceptance criteria underscores the need for establishing project-specific criteria during the design process. This can start with developing a project-specific risk valuation proposal for stakeholder consultation.

The QRA identifies that extensive explosions involving ADR Class 1 and ADR Class 5 significantly elevate societal risk, primarily due to increased population density and the potential for large-scale impacts. While accidents with ADR Class 2 (gases) and ADR Class 3 (flammable liquids) may have devestating effect within the tunnel, the effect outside of the tunnel will be smaller, due to the distances between planned development and the southern tunnel portal. However, they still pose risks that warrant attention in further design.

Based on the QRA's findings regarding their risk-reducing effects, an initial inventory of possible risk mitigation measures and barriers has been made. It is important to note that these measures are preliminary and ultimately depend on project decision-making. Additionally, some conservative assumptions in the risk analysis can be refined through further customization, potentially resulting in a lower calculated risk.

ACKNOWLEDGEMENTS
The authors would like to thank the Icelandic Road Administration for initiating the risk assessment for the overbuild and the cooperation with Verkís Consulting Engineers.

REFERENCES

[1] J. Cui and J. D. Nelson, "Underground transport: An overview," vol. 87, pp. 122–126, 2019, doi: 10.1016/j.tust.2019.01.003.

[2] F. van der Hoeven, "A review of the impact of the RingRing study for multifunctional motorway tunnels in the Netherlands and beyond," *Tunnelling and Underground Space Technology*, vol. 26, no. 2, pp. 292–309, Mar. 2011, doi: 10.1016/j.tust.2010.11.001.

[3] S. Raymond and P. Nelson, "City resiliency and underground space use," *Advances in Underground Space Development*, vol. 7, pp. 43–55, 2013.

[4] A. Palm, M. Kumm, and H. Ingason, "Full Scale Firefighting Tests in the Tistbrottet Mine," *Fire Technology*, vol. 52, pp. 1519–1537, 2016.

[5] J. Gehandler, "Fire safety design of road tunnels," thesis/doccomp, Lund University, 2020. Accessed: Mar. 17, 2023. [Online]. Available: http://lup.lub.lu.se/record/7abf687e-c873-4d0d-ae44-cd45809284c5

[6] H. Tehler and J. Lundin, "Risk Assessment of Deckings of Dangerous Goods Routes -A knowledge inventory," presented at the Tenth International Symposium on Tunnel Safety and Security (ISTSS 2023), Stavanger, Norway, Apr. 2023, pp. 171–186.

[7] "PM Bedömningsgrund för olycksrisk – ovan överdäckning, detaljplan för Centralstationsområdet," Stadsbyggnadskontoret Stockholms stad, Sweden, 2021.

[8] J. Lundin, "Risk Evaluation and Risk Control in Road Overbuilding of Transport Routes for Dangerous Goods," *Journal of Civil Engineering and Architecture*, vol. 12, pp. 428–446, Jun. 2018, doi: 10.17265/1934-7359/2018.06.004.

[9] F. H. Amundsen and G. Ranes, "Studies on traffic accidents in Norwegian road tunnels," *Tunnelling and Underground Space Technology*, vol. 15, no. 1, pp. 3–11, Jan. 2000, doi: 10.1016/S0886-7798(00)00024-9.

[10] C. Nussbaumer, "Comparative analysis of safety in tunnels," Austrian Road Safety Board, Wien, Young Researchers Seminar, 2007. Accessed: Apr. 11, 2023. [Online]. Available: https://www.scribd.com/document/635574419/Nussbaumer-COMPARATIVE-ANALYSIS-OF-SAFETY-IN-TUNNELS

[11] O. Ayalon, L. Shmueli, S. F. Koren, and M. Z. Zerbib, "Evaluating Market Benefits of Transportation Tunnels—The Carmel Tunnels as a Case Study," *JEP*, vol. 07, no. 10, pp. 1259–1272, 2016, doi: 10.4236/jep.2016.710111.

[12] N. P. Høj, "Sæbraut Road Tunnel," Switzerland, Risk Analysis H-IS-009, Apr. 2023.

[13] Vegagerðin and Veitur, "Forsendur Vegagerðarinnar á forhönnunarstigi varðandi byggingar í kringum/ofan á stokk." Sep. 2020.

[14] G. Davidsson, M. Lindgren, and L. Mett, "Värdering av Risk," Statens Räddningsverk, Karlstad, 1997.

[15] "Guidance on the Duty of Accountability for Societal Risk, VROM," Ministry of Housing, Spatial Panning and the Environment, Aug. 2004.

[16] "Reducing Risks: Protecting People - HSE's decision making process," HSE (Health and Safety Executive), UK, 2001.

[17] *N500:2022*. 2022. Accessed: Mar. 25, 2023. [Online]. Available: https://viewers.vegnorm.vegvesen.no/product/859938/nb

[18] *2004/54/EC*. 2004. Accessed: Mar. 24, 2023. [Online]. Available: https://eur-lex.europa.eu/legal-content/EN/TXT/?uri=CELEX%3A02004L0054-20090807

[19] B. Þ. Guðbrandsson, "Firefighting safety and efficiency in twin-tube city road tunnels," Lund University, Lund, LUTVDG/TVBB--5701--SE, 2023. [Online]. Available: http://lup.lub.lu.se/student-papers/record/9135358

[20] B. Tómasson and J. Bengtson, "Vulnerability and risk analysis of road infrastructre in Reykjavík," Línuhönnun hf, Prelm. report VR07RA, Mar. 2008.

The Ferney Cut-and-cover: a project with several specific challenges

Raphaël Defert[1], Justine Vivien[1] & Christophe Zing[1]
[1]WSP Ingénieurs Conseils SA, Lausanne, Switzerland

ABSTRACT

In a few years' time, the Ferney Cut-and-cover, which is operated by the Canton of Geneva, owned by the Geneva Airport and located on the French-Swiss border, will be used for both road and tramway traffic. This particularity induced the necessity to build a safety concept able to reach both road and rail safety requirements, in order to ensure users safety in case of fire. Besides, since the Ferney Cut-and-cover is located underneath the airport's runways, business continuity issues are also critical (i.e., the tunnel's fire resistance). As a result, one of the requirements for this project involved reviewing the structure's safety concept – particularly regarding fire hazards.

To meet these requirements, different safety studies have been carried out, including:

- Definition of a safety program based both and road and rail standards
- Hazard analysis to ensure measures from this safety concept are proportionate and sufficient
- Transport of Dangerous Goods (TGD) analysis ensure that the Ferney Cut-and-cover could still be authorised for TDG traffic

These studies made it possible to validate and implement a complete and appropriate work program, including in particular a water mix sprinkler system, a first in Switzerland.

As far as operational issues and the safety plan are concerned, working group sessions were held, bringing together all the players involved (road and tramway operators, public and private emergency services, customs, etc.). This made it possible to define, in advance of the working and operating phases, the main principles of intervention and tunnel safety, in particular the interactions to be formalised or even automated between the various players.

KEYWORD: fire hazards in tunnel, mixed-traffic operation, safety concept, fire modelling, water mist system, emergency plan, coordination between emergency services

PROJECT PRESENTATION

Historic and administrative aspects

Situated under Geneva Airport (GVA) runways, close to the French-Swiss border, the Ferney Cut-and-cover (CCT) is 430 m long. It was built in the late 1950s to provide a link between Geneva and Ferney-Voltaire, a commune across the border in France, while allowing the airport to expand (Figure 1). This was originally a cantonal project, but its ownership has since been transferred to GVA. Its operation remains cantonal. Two emergency services work together in the event of an incident: the cantonal fire department and GVA response teams (ARFF).

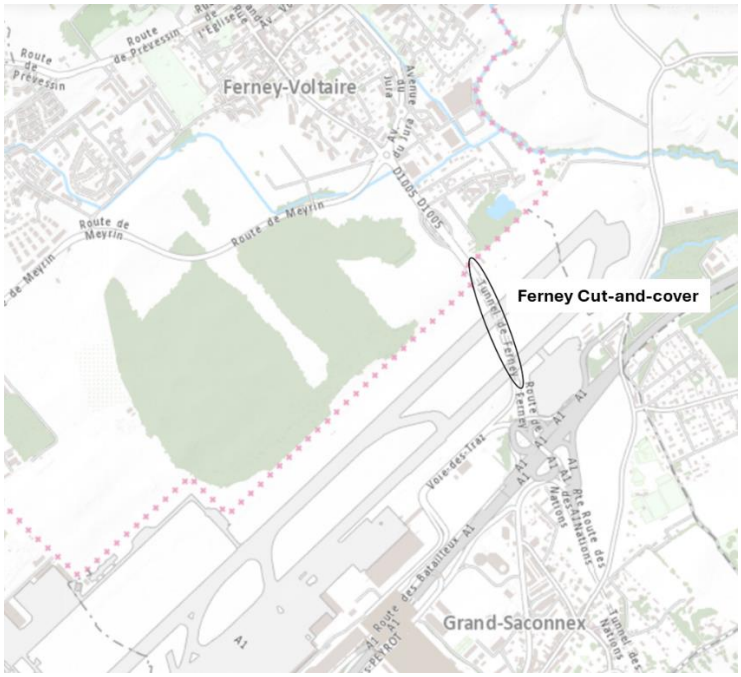

Figure 1 Ferney Cut-and-cover's location

At present, the Ferney CCT structure consists of two tubes with bidirectional traffic (Figure 2):

- The Ferney tube: Two lanes in each direction, including one reserved for buses and cabs, customs transit and the N1 motorway
- The customs tube: One lane in each direction, serving the French GVA zone from Ferney-Voltaire, without crossing customs. This tube also has a dedicated area for alternative mobility modes (a bicycle path and pedestrian walkway), which is separated from the road by a customs fence

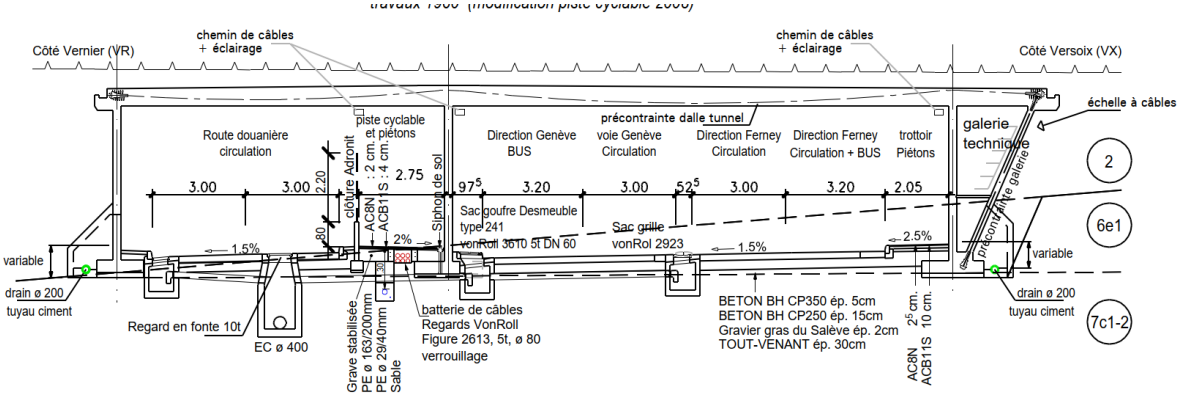

Figure 2 Ferney Cut-and-cover's section – Current situation

Currently, there are two emergency exits between the two tubes so that, in case of fire, the other tube can be used as a fire escape area. This complies with the current Swiss Standard [3], which states that the maximum distance between emergency exits in CCTs must not exceed 300 meters (for the record the Ferney CCT is 430 m long, therefore only one emergency exit would be sufficient). For tunnels built underground, the maximum distance between emergency exits is:

- 300 meters for twin-bores tunnels
- Between 300 and 500 meters for bidirectional tunnels (depends on their longitudinal gradient)

Traffic and challenges

In 2019, traffic levels amounted to 22,800 vehicles per day, of which 2% were heavy goods vehicles (HGVs). Even though it is not extremely long, the Ferney CCT represents a major economic challenge – with its substantial cross-border traffic. Closing the CCT would cause severe congestion on secondary roads, which are already saturated with commuter traffic.

The Ferney CCT is authorized for transporting dangerous goods (TDG), but the number of TDG vehicles is extremely low according to a survey conducted in 2021 (less than one vehicle per day on average.)

Construction methods and airport interfaces

The structure is made of reinforced and pre-stressed concrete, originally built to support the weight of the land cover, the taxiway slabs and the airport runway above.

Over the years, the CCT's load-bearing slab has been doubled (1986) and then reinforced (2007) to guarantee the passage of 600-tonne aircrafts. The structure's fire resistance, as well as the continued operation of the CCT and the GVA, are therefore major issues to work with.

Future use

As part of the Nations-Grand-Saconnex tramway project, the Ferney CCT is set to accommodate a mix of road, tramway and bus traffic. Two of the four existing traffic lanes will be dedicated to public transport in Geneva (PTG) (Figure 3). This concept is part of the incentive to create different types of environmentally friendly transport infrastructure.

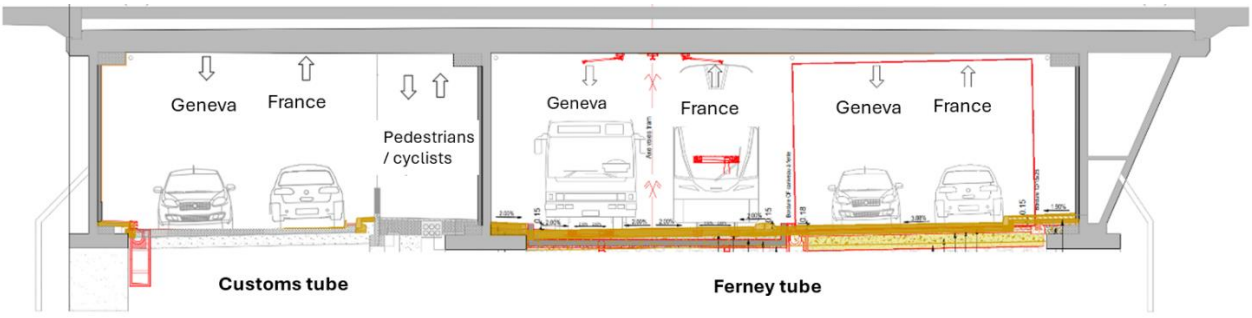

Figure 3 Ferney Cut-and-cover's section – Future situation including tramway traffic

This substantial change in operations raises questions about safety, particularly regarding fire risks and evacuation issues – especially given the potential increase in the number of people in the CCT in certain circumstances.

DESIGNING A SAFETY IMPROVEMENT PROGRAMME BASED ON A GLOBAL SAFETY ANALYSIS APPROACH

The tramway development project has resulted in an opportunity to assess the overall safety of the Ferney CCT in order to define a comprehensive and consistent renovation programme. The goal is to develop a coherent, cross-functional vision that incorporates both modes of transport and their specific operating characteristics.

A safety analysis approach has been applied to people (to identify the best safety measures for reducing the occurrence and severity of potential incidents) and operating issues (incidents analysed in terms of their social and economic impact).

These two approaches complement each other and have resulted in a coherent, rational programme that will ensure the highest possible level of safety for the planned structure – even during its construction phase (site operations).

As part of the federal planning approval procedure for the tramway, it was therefore agreed to carry out the following:

- A safety concept for the two tubes as part of renovation work
- A Hazard Analysis, including modelling and fire scenarios simulation (smoke propagation and emergency evacuation), to validate the safety concept and make additional recommendations
- A dangerous goods risk assessment to quantify the level of risk corresponding to the CCT's current and future condition. The thereof goal is to confirm the transit of dangerous goods in this infrastructure

These elements will be presented in the following chapters.

Safety concept

First, a regulatory comparison was carried out with the relevant technical standards to identify discrepancies and, therefore, possible safety provisions to be incorporated in the project.

SIA Standards 197 (tunnels) [1], 197-1 (railway tunnels) [2] and 197-2 (road tunnels) [3] provide the basis for underground construction projects in terms of the construction itself, environment and safety. Although they concern planned tunnels and not tunnels in operation, these standards can be used as technical benchmarks for tunnels in operation, hence their relevance for the Ferney CCT. The FEDRO (Federal Roads Office) [4] - [9] and FOT (Federal Office of Transport) [10] Standards were also used as a basis for defining the safety provisions to be included.

In concrete terms, all possible provisions relating to civil engineering and equipment provided for by these road and rail standards will be incorporated into the CCT in its final state – with mixed traffic operation. This includes the detection, warning, traffic management (cars and tramway), users' evacuation, smoke management, intervention by emergency services… In addition, certain safety provisions will even go beyond the requirements of these technical standards (for example, the number of emergency exits, dynamic exit signage, etc.).

As a result of the CCT'S profile change and the new type of traffic planned, the new challenges coming to light mainly concern the following points:

- Adapting current equipment to ensure the CCT remains 100% operational and suited to future traffic (e.g., lighting, signalling, video surveillance)
- The potential risk of a tram stopping at an emergency exit in the event of an incident, which could restrict and/or lengthen the emergency route for road users, or even prevent them from seeing certain exits. Wherever possible, PTG tram or bus exits will be included in PTG operating instructions in the event of an incident. Enhanced signage for exits (illuminated arrows on both sides) will help improve visibility
- The risk of dual traffic operation in the CCT. It is vital that, in the event of an incident, traffic is stopped at the gates for all vehicles in order to limit the number of people in the CCT as much as possible and to facilitate emergency evacuation
- The risk of recurring road congestion within the structure (an aggravating factor in the event of fire), potentially linked to the reduction in the number of road lanes for traffic levels similar to current levels (currently, taxis and motorised two-wheelers use the lanes reserved for buses, which will no longer exist in the future)

These analyses have also made it possible to examine issues that are not specific to the future mixed-traffic operation concept, such as the structure's fire resistance, which is not linked to introducing the tramway. Regarding the structure's fire resistance, analyses were performed based on temperature curves (RWS) which correspond to the maximum power of a TDG pool fire (maximum calorific potential).

The safety concept drawn up for the two tubes has made it possible to prepare a construction programme that addresses the various issues inherent in the CCT, whether or not they relate to the future mixed-traffic operation concept. The main construction projects are as follows:

- Adapting the principle of collecting effluent from roadways and the tramway/bus platform (potentially hydrocarbons or toxic materials) and installing a slotted gutter with siphonic manholes to limit the size of a hydrocarbon slick in the event of accidental spillage
- Lowering the current height of the CCT shoulder (wheelchair accessibility)
- Adding three emergency exits, limiting the distance between exits to 75 m and ensuring that existing exit doors comply with fire regulations, even though an emergency exit is necessary every 300 meters in Cut-and-covers according to Swiss standards [3]
- Reinforcing signage at these exits
- Installing closing barriers at the entrances to the two tubes
- Adding smoke detectors (fire detection)
- Installing ventilation in the technical gallery (in the CTT, the ventilation is natural)
- Resetting the AID (Automatic Incident Detection) system and adapting the monitoring system
- Adding a leaky feeder cable for radio communications (operators, emergency services and inlaying radio messages for CCT users)
- Fire protection for the building structure (installing protective plates under the slabs)
- Setting up a water mist sprinkler system

Hazard Analysis

The Hazard Analysis (HA) [11] aims to:

- Describe incidents likely to occur during the operating phase and assess the nature and significance of their potential consequences
- Identify measures to reduce the probability of these accidents and their consequences from occurring

This is a cross-functional, scenario-based approach. Using this systemic approach, the HA ensures:

- The consistency and validity of the safety concept is verified
- There are no safety deficiencies
- The provision of additional recommendations on operating instructions and procedures in consultation with the fire brigade during incidents (fire, serious accidents)

The scenarios considered in the HA are presented in a Frequency x Severity Matrix (Figure 4).

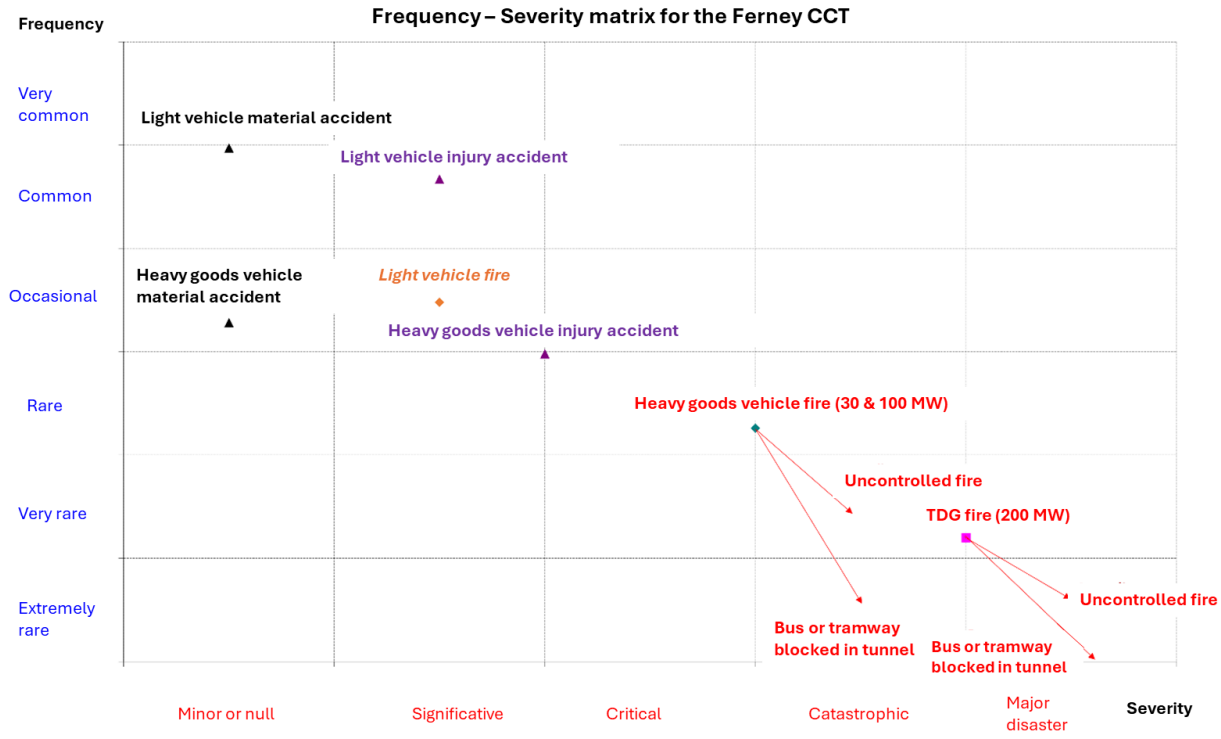

Figure 4 Hazard analysis scenarios for the Ferney Cut-and-cover represented in a Frequency x Severity matrix

The HGV fire scenarios (Table 1) were modelled using dedicated 3D software to analyse smoke propagation within the structure at any given moment and over time, as well as changes in survival conditions within the CCT (temperature, toxicity, visibility, etc.) (Figure 5).

Table 1 Parameters used to model the HGV fire scenarios

Scenario	Heat release rate (MW)	Position of potential fire in relation to north gate - customs side (m)	Air pressure difference between the 2 portals - from France to Switzerland (Pa)	Traffic from Switzerland to France (vehicles per hour)	Traffic from France to Switzerland (vehicles per hour)	Blocked tramway
1	30	215 (center)	5	1240	600	No
1 again	30	215	5	1240	600	Yes
2	30	215	20	1240	600	No
3	100	215	5	1240	600	No
4	200	215	5	1240	600	No
5	200	215	0	1240	600	No

In this table, the basis used for fire heat release rates is described in the CETU (Centre for Tunnel Studies) Guide to Road Tunnel Safety Documentation, in particular Booklet 4 Specific Hazard

Investigations [11].

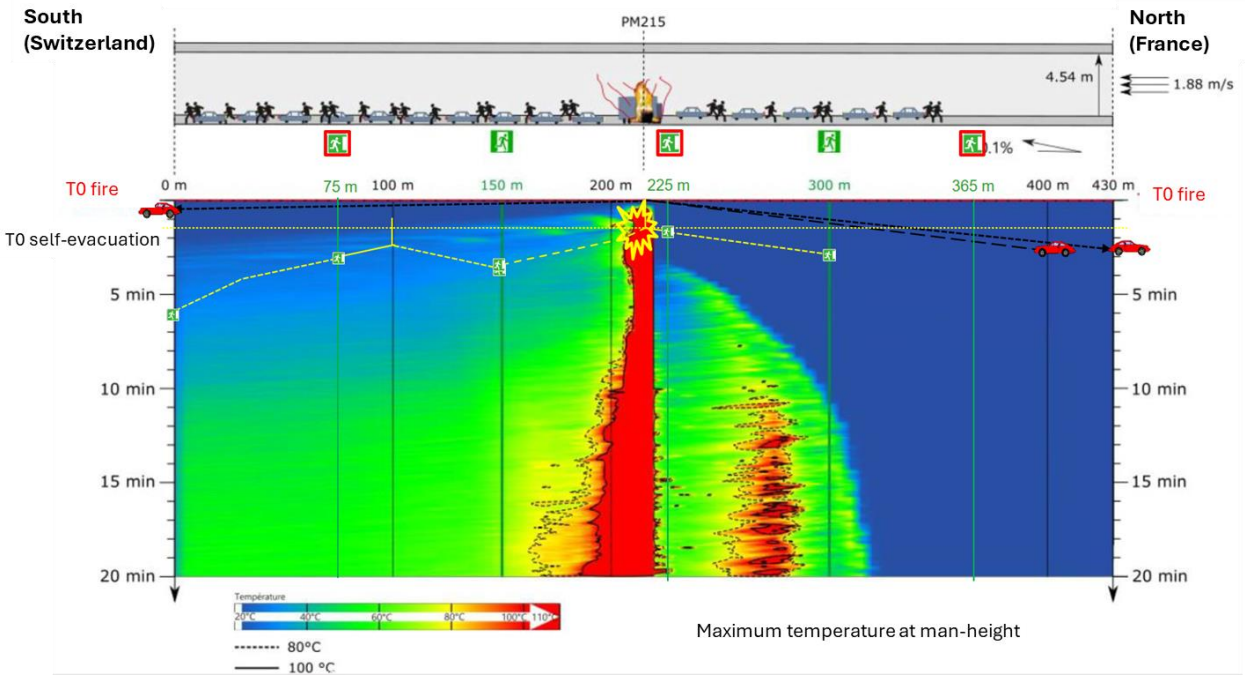

Figure 5 Space-time graph transposing the user path into the temperature diagram

For remark, the acceptable temperature criteria used in Figure 5 is 80°C [11].

The HA concluded that the work proposed in the Ferney CCT safety concept will lead to a satisfactory safety situation in its future operation (the scenarios studied correspond to major overall situations). The two tubes and their interactions (one serving as an escape route for the other in the event of a fire) were studied.

Although the safety level is satisfactory without a water mist sprinkler system (which is designed to protect the structure from fire), this system also represents significant added value in terms of tunnel user safety by significantly reducing the strength of a fire and, therefore, the temperature and toxicity of smoke (*Figure 6*). This system is triggered by different fire detection systems in the Ferney CCT, especially the thermal cable thanks to its precision.

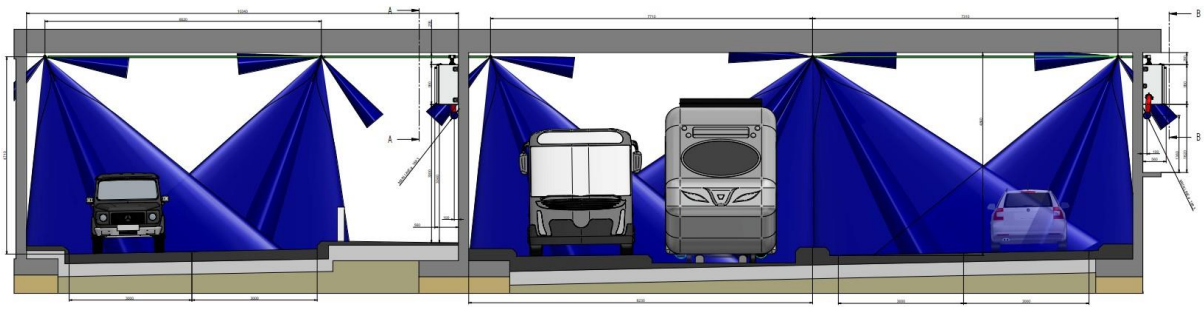

Figure 6 Water mist sprinkler system to be implemented in the Ferney Cut-and-cover

TDG risk analysis

The consequences of a TDG accident in a tunnel are very different from those of an accident in the open air. It is therefore necessary to carry out a tunnel risk assessment using a specific model.

The "OECD/PIARC Swiss Model" [12] was developed on behalf of FEDRO (WSP development) in order to be able to quantitatively assess these risks, compare them with acceptability criteria, and ultimately decide on the authorisation regime for dangerous goods in accordance with international ADR regulations (Agreement concerning the International Carriage of Dangerous Goods by Road) [13]. To achieve these objectives, five TDG restriction categories are possible to implement (Table 2).

Tunnel category	Restrictions
A	No restrictions apply transporting dangerous goods
B	Restrictions on dangerous goods that could cause a very large explosion
C	Restrictions on dangerous goods that could cause a very large explosion, a large explosion or a large discharge of toxic substances
D	Restrictions on dangerous goods that could cause a very large explosion, a large explosion, a large toxic leak or a large fire.
E	Restrictions on all dangerous goods except UN numbers 2919, 3291, 3331, 3359 and 3373

Table 2 TDG restriction categories [13]

Like each other signatory country, Switzerland can choose its own criteria and methodology for defining the category of its tunnels [14] and [15]. The method used by FEDRO [12] is shown in Figure 7.

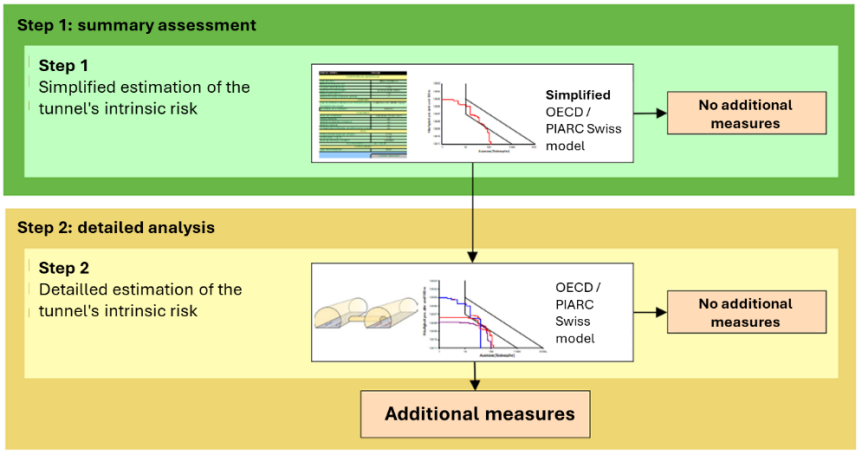

Figure 7 Methodology used by FEDRO (Switzerland) to define its tunnels TDG restriction category (traduction from French)

This method was applied to the Ferney CCT to ensure that it could be authorised for TDG traffic even in its current state – which was confirmed.

In its future state, the calculations carried out have led to the conclusion that TDG risk in the structure is also acceptable (particularly in view of the safety provisions and the low level of TDG traffic in the CCT). For remark, the previous method does not take into account ventilation in tunnels, as it is in the Ferney CCT.

Therefore, the TDG restriction category for both the existing and future Ferney CCT is category A.

INTERVENTION AND SAFETY PLAN

Challenges and implementation methods

Drawing up the intervention and safety plan for the Ferney CCT involves several operational and intervention issues for such a complex infrastructure, which is in addition characterized by the interaction of many different parties:

- The Canton of Geneva and the PTG, which operate the structure, and the GVA, which owns it
- Airport and cantonal fire brigades, which need to work together to combat potential incidents
- Border control within the structure (interface with customs)
- Proper use of the sprinkler system

Workshops bringing together all these parties have made it possible to draw up the Ferney CCT ISP (including the customs road) according to three timeframes, or reference statuses:

- Current status
- Status during construction
- Future status

The ultimate goal is to define and coordinate emergency resources and to specify the principles of managing incidents. An ISP must be drawn up for each phase of existence (current state/construction/future operation) to ensure that the document is operational in all circumstances and in accordance with the specific operating conditions.

Operational documents

In particular, the following schemes have been drawn up in a collegiate manner:

- Warning system: guarantees the transmission of information between all parties involved and rapid access for public emergency services
- Synoptic Tables of Action (STA): summarise and plan coordination and actions to be taken by each party, depending on the nature of the incident.
- A flow chart and timetable to trigger the sprinkler system to ensure that it is not implemented incorrectly or triggered too late.
- Minimum Operating Conditions (MOCs): defining, for each piece of technical equipment, acceptable or unacceptable malfunction thresholds for the safe operation of the structure, as well as compensatory measures and emergency maintenance levels (Figure 8).

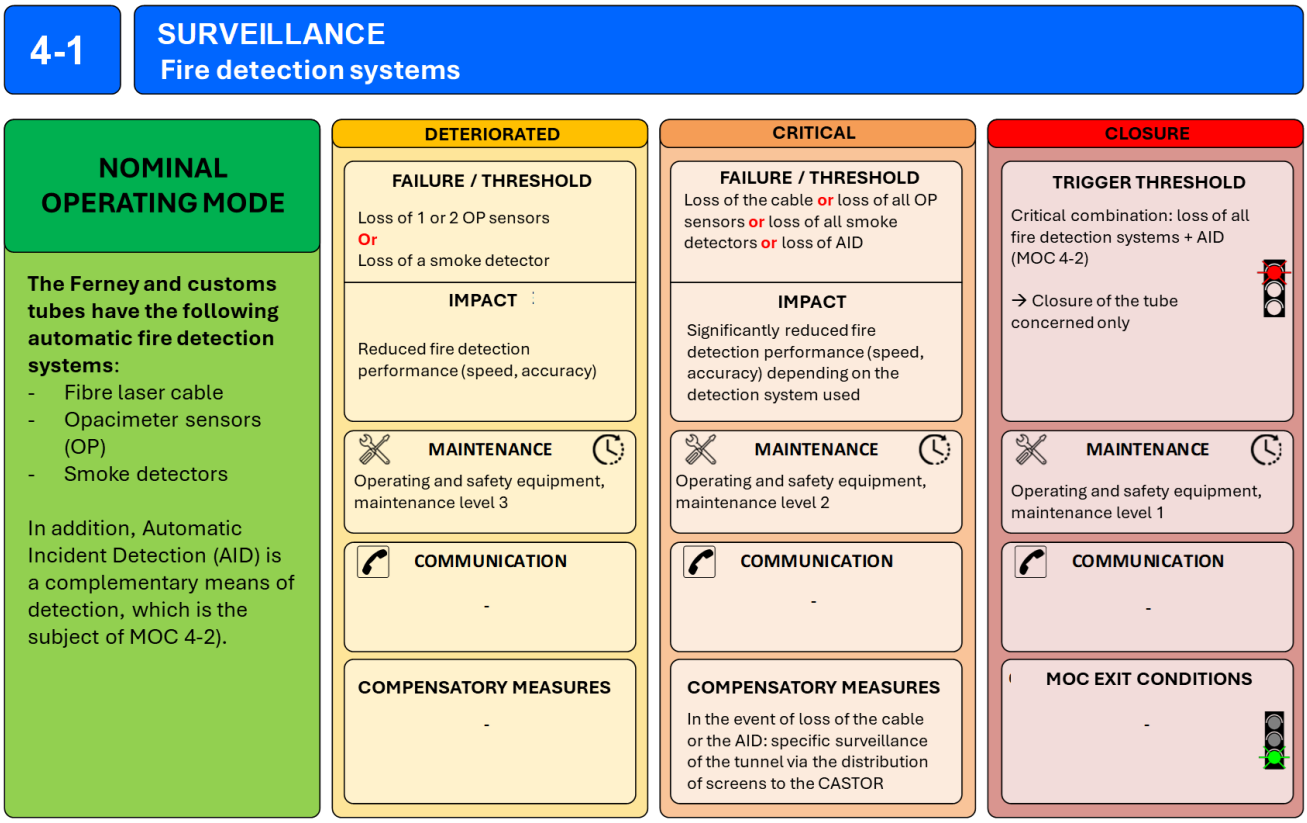

Figure 8 Example of Ferney' Minimum Operating Conditions (fire detection systems)

Conducting one or more of these exercises will allow us to test the implementation of the emergency response plan and coordination between the various parties involved so that the plan can be adapted if necessary.

CONCLUSION

To conclude, all the studies carried out have enabled to establish a safety concept and operational plans which completely face issues encountered in this special infrastructure:

- Mixed operation: road and rail safety requirements to be met
- Geneva Airport business continuity issues
- Both public and private emergency services to coordinate
- Customs to take into account, etc.

Besides the safety concept, WSP is in charge of all the project phases (design, call for tenders, works supervision, tests…), as far as operating and safety equipment are concerned. This enables to have a complete vision of all issues linked to this innovative project in Switzerland (for instance the water mist sprinkler system), and to guarantee the following of the safety concept until the commissioning.

While works on road lanes have begun this year, works for the tramway lane are scheduled for 2026.

REFERENCES

1. SIA Standard 197:2004, Tunnel projects, general principles
2. SIA Standard 197/1:2019, Tunnel projects, railway tunnels
3. SIA Standard 197/2:2004, Tunnel projects, road tunnels
4. FEDRO Directive 13001 “Ventilation of road tunnels, System selection, dimensioning and equipment”, 2008 Edition, V2.03
5. FEDRO Directive 13004 “Fire detection in road tunnels”, 2007 Edition, V2.10
6. FEDRO Directive 13010 “Safety signage in road tunnels”, Edition 2011, V2.07
7. FEDRO Directive 13015 “Lighting installations”, Edition 2017, V1.12
8. FEDRO Directive 15003 “Traffic management on national roads (Framework Directive VM-NS)”, 2016 Edition, V2.01
9. FEDRO Technical Manual 23001 “Operating and safety equipment”, Edition from January 2021
10. FOT Directive “Safety requirements for existing railway tunnels”, 10 Aug. 2009
11. CETU (Centre for Tunnel Studies) Guide to Road Tunnel Safety Documentation
12. FEDRO Documentation 84002 “Transporting dangerous goods in road tunnels – Analysis and evaluation of risks to people”, Edition 2023, V2.01
13. European Agreement concerning the International transport of dangerous goods by road, version in force on 1 January 2021
14. Ordinance on transporting dangerous goods by road dated 29 November 2002 (SDR) – 741.621, status as of 1 January 2021
15. Ordinance on protection against major accidents dated 27 February 1991 (OPAM), 814.012

Managing Disaster Risks in Underground Transportation Infrastructure - A Comprehensive Analysis of Safety Targets and Practices

Johan Lundin
Brandskyddslaget AB
Box 9196, SE-102 73 Stockholm
E-mail: johan.lundin@bsl.se
www.brandskyddslaget.se

ABSTRACT

This study examines the management of disaster risks in underground transportation infrastructure, focusing on the safety challenges posed by large-scale accidents. By reviewing international guidelines and evaluating Swedish projects, the research identifies risk criteria, such as FN- curves and the ALARP principle, used to assess societal risks across sectors like nuclear power and dam safety. The findings reveal gaps in Swedish regulations regarding disaster risk management, especially for complex environments such as the space surrounding platform area in underground stations. Recommendations are provided to strengthen Swedish regulations and standards by incorporating international best practices and enhancing risk-informed decision-making. This work aims to contribute to safer, more resilient transportation systems and supports sustainable urban development by addressing the specific challenges of large-scale accident prevention in underground infrastructure.

KEYWORDS: Disaster, catastrophic risk, underground transportation infrastructure, safety criteria, FN-curves, ALARP principle, societal risk assessment, risk-informed decision-making, sustainable urban development.

Introduction

Context and relevance

This paper forms part of the research project Safety Objectives for Underground Stations [1], initiated by the Swedish Transport Agency and the Swedish Transport Administration. The project aimed at developing a unified model for defining and verifying minimum acceptable safety levels for platform enclosures, based on risk and socio-economic analysis. This paper presents a segment of this work, an analysis of disaster risk, contributing to the project's overarching goal of improving safety and efficiency in regulatory development.

In the event of a major accident in a location where large groups of people are present, there is potential for mass casualties under catastrophic circumstances. Society generally views accidents with multiple fatalities as unacceptable, yet this perspective often emerges only after an incident has occurred. The development of safety regulations is often accident driven. Beforehand, it is challenging to assess whether a risk is acceptable, particularly in preventive work for both minor and major accidents. Explicit guidelines are frequently lacking to support such assessments across sectors. Fortunately, no such accidents resulting in a very high number of casualties have yet occurred in modern underground infrastructure. However, this does not mean that it is appropriate to refrain from regulating this type of risk, thereby effectively leaving it to chance. While incidents involving multiple individuals have taken place, they have so far been of a smaller magnitude than the catastrophic scenarios considered in this context. Such an approach is not consistent with sustainable development and sound disaster risk management [2].

For certain environments, such as underground platform enclosure in mass transport systems, the risk of severe consequences exists, especially in complex evacuation scenarios involving large numbers of people and/or concurrent transport of hazardous materials. This raises questions about the need for special regulatory requirements to address such risks, potentially influencing infrastructure design and operation to mitigate unacceptable risks. Eliminating these risks entirely could restrict current or future transportation system capacity, necessitating a careful balance in decision-making and a thoughtful assessment of which stakeholders are best suited to make these determinations. Should decisions on such risks be made within individual projects, or should national guidance be established to standardize decision-making?

Although the primary focus of this study is Swedish risk regulation, its findings have broader relevance for countries facing similar challenges in managing disaster risks in underground transport infrastructure. Several international safety standards, such as those in nuclear and dam safety, demonstrate how systematic approaches to disaster risk management can enhance regulatory frameworks. Lessons learned from Sweden's approach may therefore be applicable to other nations developing safety targets for transportation infrastructure. Existing EU directives, such as those for tunnel safety [3], further highlight the role of national regulatory refinement, complementing the broader international perspective discussed above.

Purpose and objectives

The purpose of this paper is to enhance understanding of requirements for managing — through analysis, assessment, and control — accidents with significant consequences. The goal is to outline how the risk of severe accidents is addressed in various regulations. In addition to reviewing the scientific literature and regulations, the study examines two Swedish infrastructure projects, Sundbyberg Station and Centralstaden in Stockholm, to illustrate how risk assessment and disaster risk management are applied in practice. Based on these analyses, the study also provides recommendations for improving risk governance in the Swedish transport sector, particularly in underground infrastructure projects.

This study adopts an empirical approach by systematically analyzing how disaster risks are regulated across multiple sectors and jurisdictions. The research seeks to identify patterns, gaps, and regulatory principles that influence risk acceptance criteria. By examining documented safety regulations, risk criteria, and decision-making processes, the study contributes to the broader field of applied risk research. The methodology aligns with comparative policy studies, where regulatory frameworks are empirically assessed to provide insights into risk governance. This approach is commonly applied in disciplines such as disaster risk management, regulatory science, and safety engineering. While the work does not fit strictly within experimental research paradigms, it provides an empirical foundation for understanding how safety targets evolve and function in practice.

Background

Safety regulations have evolved from strictly risk-based comparisons to risk-informed frameworks that integrate quantitative criteria (e.g., FN-curves) with qualitative assessments. This shift, seen in nuclear power and dam safety, ensures a broader evaluation of risk beyond numerical thresholds. In some situations, additional factors must be considered to determine whether safety requirements are met. This is particularly relevant when evaluating if a safety goal has been achieved. Consequently, for certain assessments, criteria comparisons may need to be supplemented with other considerations, thus broadening the basis for evaluation. At the same time, risk level estimation remains an important component, requiring support to determine what constitutes high or low risk. Therefore, the question of how criteria are appropriately formulated cannot be disregarded. This approach has been primarily driven by the energy production sector, notably nuclear power and hydroelectric dams, where decision-making support in risk analysis has increasingly included information on uncertainty, cost-benefit analyses, risk reduction, and the impacts of different risk-reducing measures. Additionally, restrictions and limitations for facilities and infrastructure systems should also be part of such analyses.

An earlier project report summarizing the first part of the Safety Targets for Platform enclosure project [2] noted that risk acceptance criteria (RAC) are commonly used across several industries to

aid decision-making. Many industries establish clear boundaries for acceptance criteria as the number of people exposed to risk increases, and separate evaluations are often needed for accidents with very large-scale consequences. While catastrophic incidents involving over 1,000 fatalities are a common benchmark for additional scrutiny, smaller-scale incidents can also have severe societal impacts. This paper focuses on risks with "catastrophic potential" or "disaster risk," for which standardized definitions and thresholds are often lacking. Nonetheless, many sectors employ quantitative criteria to guide decisions when managing risks of significant societal impact.

Systematic risk analyses, such as those utilizing FN-curves, are critical for assessing societal risks, but they inherently involve epistemic and aleatory uncertainties, which influence the reliability of probability and consequence estimates. This study highlights that risk assessment is not simply a mechanical comparison of probabilities and consequences; it also requires qualitative judgments about knowledge strength and the ability to predict rare, high-impact events. Addressing uncertainties, such as evaluating data quality and assumptions, plays a crucial role in risk-informed decision-making. While such uncertainties cannot be eliminated, they should not serve as a justification to neglect studying or managing these risks. Instead, systematic approaches provide a robust framework for navigating incomplete knowledge and ensuring decisions are informed by both quantitative data and qualitative insight.

Method

To understand and analyze how disaster risks are managed across various sectors and countries, a three-step approach was undertaken. The aim of this method was both to identify international applications of risk management and to examine how Swedish infrastructure projects address these risks in practice. A summary of the approach is provided below.

- Literature Review: A review of international and sector-specific guidelines and criteria was conducted to explore how quantitative risk criteria are applied across various sectors relevant to disaster risks. The study initially took a broad approach, aiming to identify diverse methods and principles used for managing large-scale risks. As the review progressed, it became evident that FN-curves and the ALARP principle are among the most commonly employed measures in sectors such as nuclear power, dam safety, and transport infrastructure where explicit risk governance was conducted. These tools were therefore given particular attention in the analysis due to their prominence and applicability in disaster risk management.
- Case Studies of Swedish Infrastructure Projects: Two Swedish infrastructure projects, Sundbyberg Station and Centralstaden in Stockholm, were analyzed to highlight how risk assessment and disaster risk management are applied in practice. These projects were selected based on their complexity and potential impact on large groups of people in underground environments.
- Analysis and Comparison: Identified criteria and methods from the literature review and case studies were compared to highlight similarities and differences between international and Swedish approaches to managing major accidents. The findings are used to suggest improvements to Swedish regulations and guidelines in the transport sector.

1. REGULATION OF DISASTER RISKS

Regulations addressing disaster risks are often reactive and based on past events. This approach poses challenges, given the limited empirical data on very large-scale accidents, primarily due to their low probability. Therefore, while empirical experience remains valuable, it must be supplemented with proactive strategies. Without such approaches, new risks could emerge without adequate mitigation, potentially for extended periods. In urban development, this could lead to long-term limitations in addressing these risks, embedding vulnerabilities that later become difficult to rectify.

In several industries, the need to explicitly account for disaster risks and to adopt protective measures that reduce both the likelihood and consequences of such events has grown significantly over the last

30 years. While some sectors have had these requirements for a long time, the 2011 Fukushima nuclear disaster highlighted the importance of this issue, accelerating both research and implementation of protective measures in areas where accidents with extensive consequences are possible.

In international agreements, such as the Sendai Framework [2], countries have committed to avoiding activities that introduce disaster risks into society as part of sustainable development goals. In Sweden, the responsibility for implementing this framework rests with MSB (the Swedish Civil Contingencies Agency); however, so far, implementation has not resulted in pronounced requirements that clearly influence how disaster risks are managed across different sectors or in planning and design. Notably, the Sendai Framework emphasizes the importance of proactive measures to reduce vulnerabilities and prevent new risks. Yet, despite these commitments, reports indicate that there has been limited progress in translating these principles into actionable, sector-specific guidelines or robust risk governance strategies [5].

Across sectors, there has been a growing emphasis on the need for specific requirements addressing disaster risk management. This is a recent trend, and various terms in international literature, such as Design Extension Condition, Beyond Design Accidents, and Severe Accident Management, are used to highlight this need. These terms refer to accidents with the potential for extensive injuries and fatalities, events that present significantly greater consequences than traditionally managed risks. This paper refers to such accidents as "disaster risks," a term that, while potentially subject to future refinement, aligns with international terminology.

The regulation of disaster risks typically includes requirements across multiple aspects of an organization's safety management system, from technical standards to training and emergency response, as well as facility location, management, and governance. Hence, it is not limited to be covered by only expressing a quantitative criteria on an acceptable risk level due to such accidents. Across all studied sectors, requirements related to "disaster" are integrated within the broader safety management framework rather than as isolated additions to traditional accident regulations. However, distinct requirements can be identified that specifically address large-scale accidents and disaster potential as one important component in such a safety management system.

Within organizations, requirements for disaster risk management are divided into various categories (comparable to high-level safety goals), including requirements for risk analysis, specific safety measures, and emergency management. For instance, in the nuclear industry, specific "design requirements" are established:

"A set of design extension conditions shall be derived on the basis of engineering judgement, deterministic assessments, and probabilistic assessments for the purpose of further improving the safety of the nuclear power plant by enhancing the plant's capabilities to withstand, without unacceptable radiological consequences, accidents that are either more severe than design basis accidents or that involve additional failures. These design extension conditions shall be used to identify the additional accident scenarios to be addressed in the design and to plan practicable provisions for the prevention of such accidents or mitigation of their consequences" [4].

The requirement above clarifies, at a relatively high level within regulatory hierarchies, that very large accidents, those exceeding the design basis of the facility, need to be considered during facility design. Additionally, such analyses should influence both the preventive and mitigative safety measures. This requirement sits high within the requirements and objectives hierarchy and is subsequently broken down into more detailed requirements and quantitative criteria. In parallel, an emergency management requirement is set at the same hierarchical level, emphasizing the need for handling (analysis, assessment, decision-making, and implementation of measures) very large accidents within this domain.

Examples of Quantitative Criteria from Different Countries and Sectors

A literature review was conducted to identify countries and sectors where quantitative criteria are incorporated into managing large-scale accident risks. The figures below present several such criteria. It is evident that in countries and sectors where specific requirements exist for assessing the acceptability of disaster risks—particularly for incidents that could result in over 1,000 fatalities

(intense scrutiny)—this determination is generally part of a formal approval process carried out by an external regulatory authority rather than by the developer alone. Thus, it is not solely the responsibility of the developer to decide, after conducting an assessment, whether the disaster risk has been sufficiently managed, even though the developer is ultimately accountable for the facility's safety during operation, including potential accident scenarios.

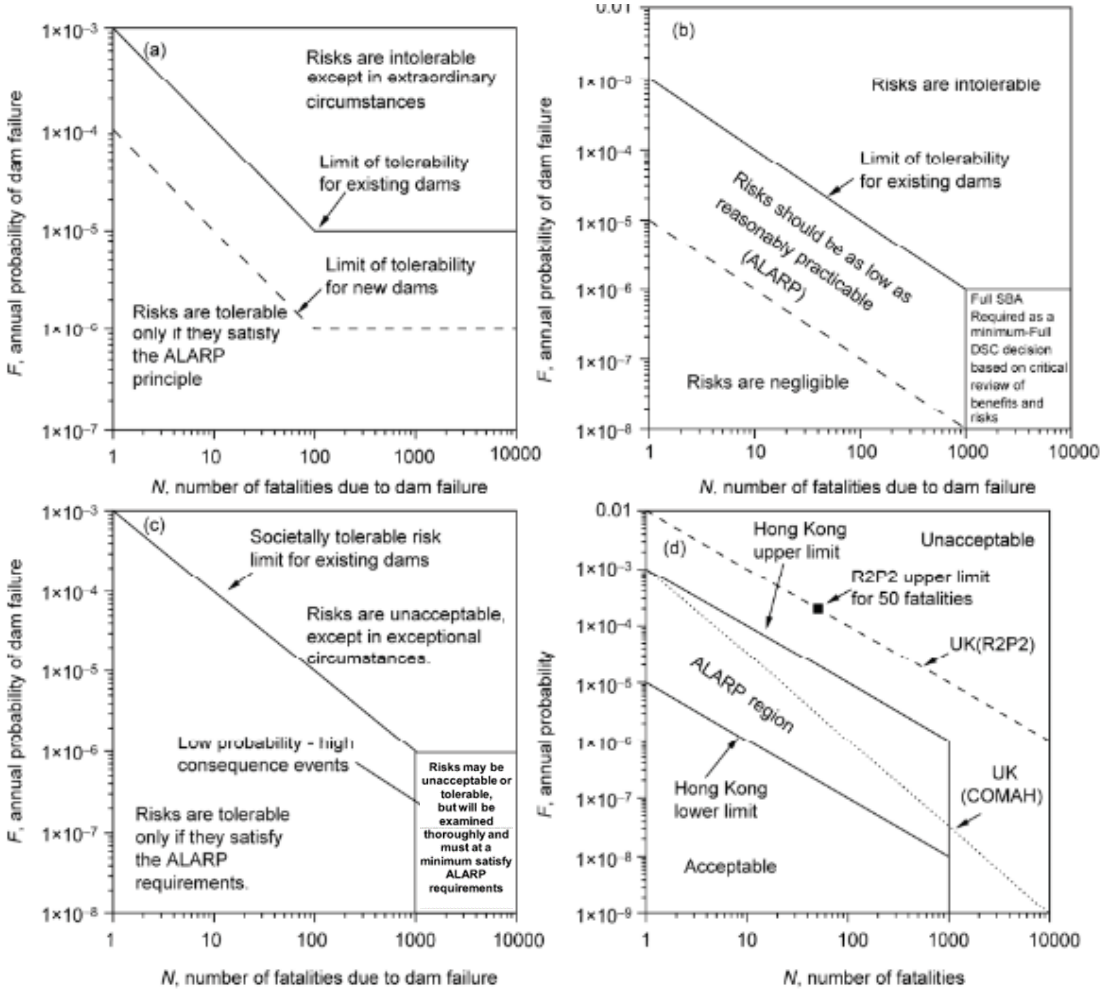

Figure 9. Examples of International Risk Criteria in the Power Plant and Dam Safety Sectors (a) ANCOLD [7], b NSW [8], (c) USACE [9] och (d) UK and Hong Kong [10] [11].

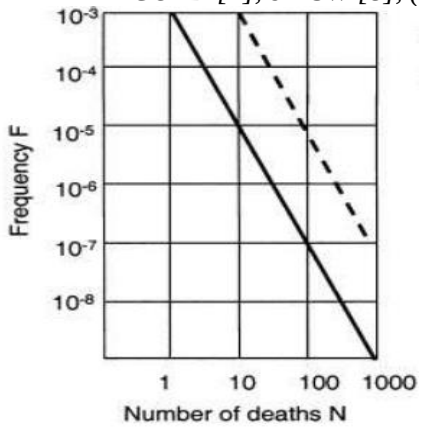

Figure 10. Country: Netherlands, Sector: Industrial Activities (solid line) and Transport (dashed line) [12].

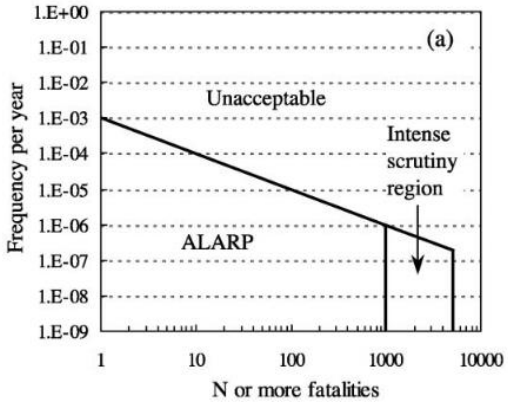

Figure 11. Country: Hong Kong, Sector: Landslides [13].

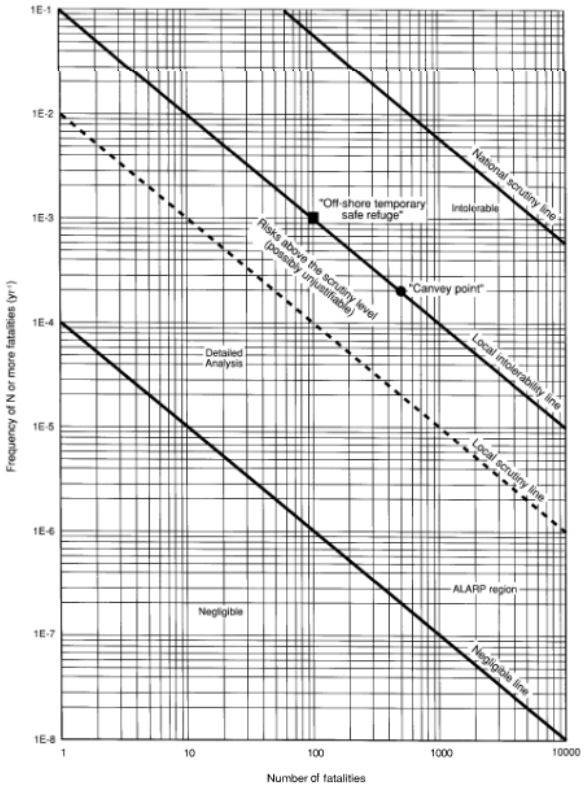

In Sweden, the so-called DNV criteria [12] have long served as standard practice in land-use planning, such as for developments adjacent to hazardous facilities or dangerous goods transport routes. No upper threshold for fatalities is included in the societal risk criteria. Instead, it is recommended that such issues be addressed qualitatively. Consequently, extrapolation to the right in Figure 13 is not advised, even if the dotted lines in the figure suggest it. The DNV report does not further elaborate on the practical application of qualitative assessments for such accidents.

Limited information has been identified within the road and rail sectors. Some European countries have established risk criteria that consider consequence magnitude in terms of societal risk (F/N curves, see Figure 6 and Figure 7), but it remains unclear how these apply to very large consequences (disaster risks). This issue appears to be unexplored in the transport sector and has a low level of maturity.

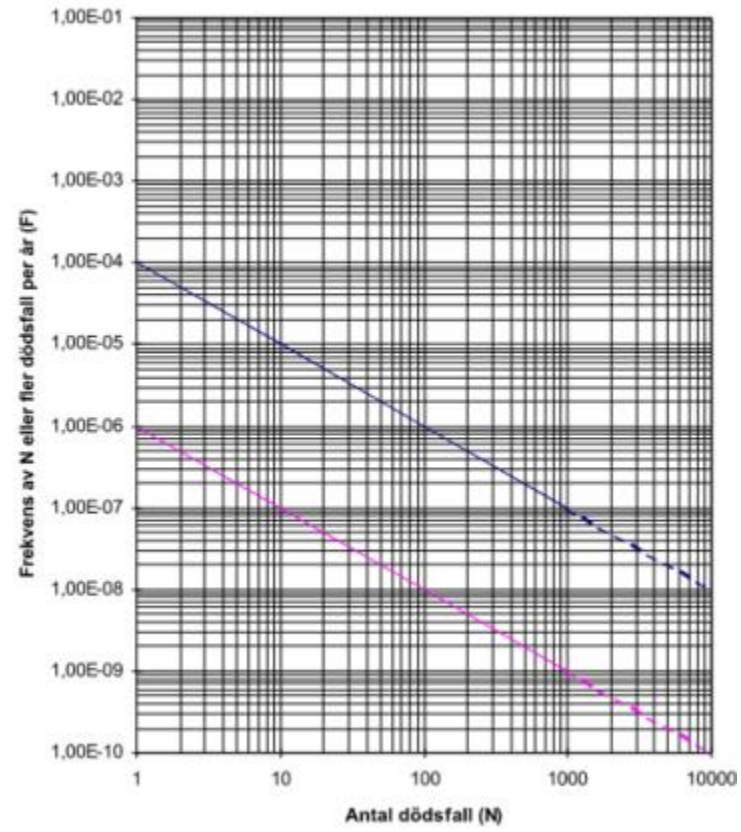

Figure 13. Country: Sweden, Sector: Physical Planning and Hazardous Activities. [8].

In the Swedish Transport Administration's Tunnel Construction Requirements (TRVINFRA-00233) [12], societal risk criteria are specified according to Figure 16. These assessment criteria apply to accident frequencies per train kilometre with consequences of up to N ≤ 1,000 fatalities. The Tunnel Construction Requirements also state that if the maximum potential consequence is estimated to exceed 1,000 fatalities, a project-specific safety target should be determined through a special investigation. However, no additional guidance is provided on how this special investigation should be conducted.

In the Swedish Transport Agency's Road Tunnel Safety Regulations TSFS 2022:13 [15], the acceptance level is presented in the form of FN-curves, as shown in Figure 9. These regulations include criteria for incidents with up to 10,000 fatalities.

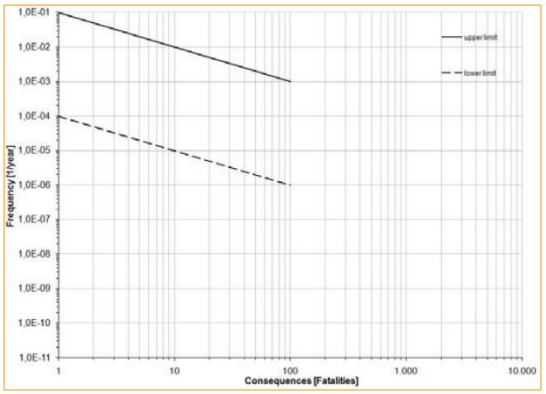

Figure 14. Country: Italy, Sector: Road Tunnels. [18]

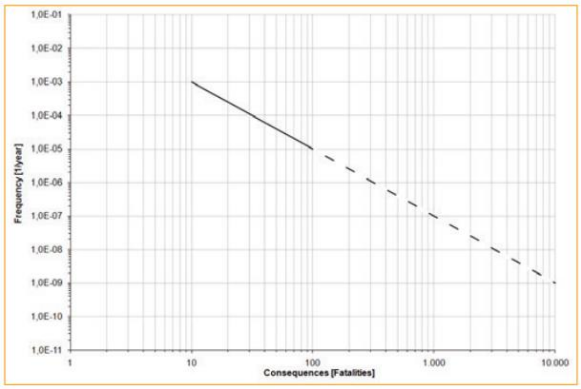

Figure 15. Country: Austria, Sector: Road Tunnels. [18]

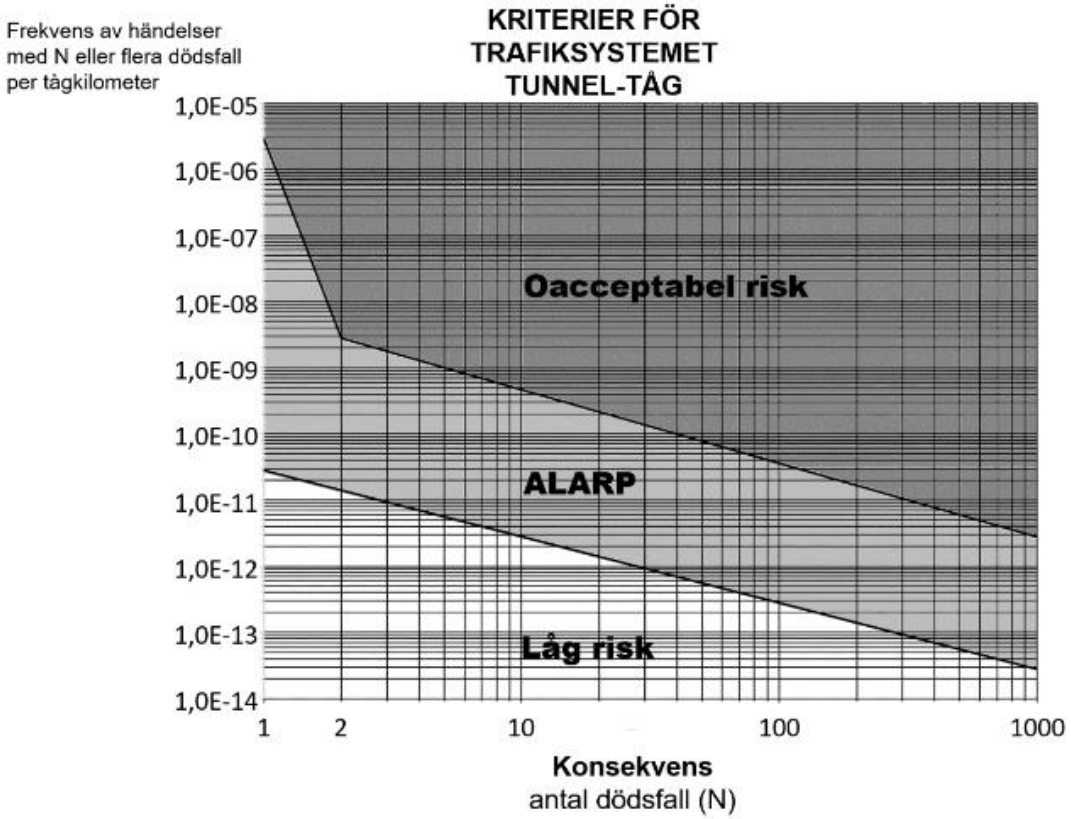

Figure 16. Societal risk criterion for individuals traveling by train in railway tunnels, from Trafikverket's Tunnel Construction Requirements regulations. [16]

The results of the presented examples show that risk criteria are exclusively reported as FN-curves, which were the most common measure found in the literature review. However, there are also risk criteria for certain industries expressed differently than FN-curves, such as in the nuclear sector, where criteria are defined as radiation levels in relation to distance from the facility. These types of criteria are considered challenging to apply within the transport sector and are therefore not presented in the graphs.

The concept of risk acceptability varies significantly between sectors and jurisdictions. While some industries, such as nuclear power, adopt rigid quantitative thresholds, other sectors rely more on qualitative assessments. Risk acceptance criteria are not absolute scientific truths but are shaped by societal values, political decisions, and historical experiences.

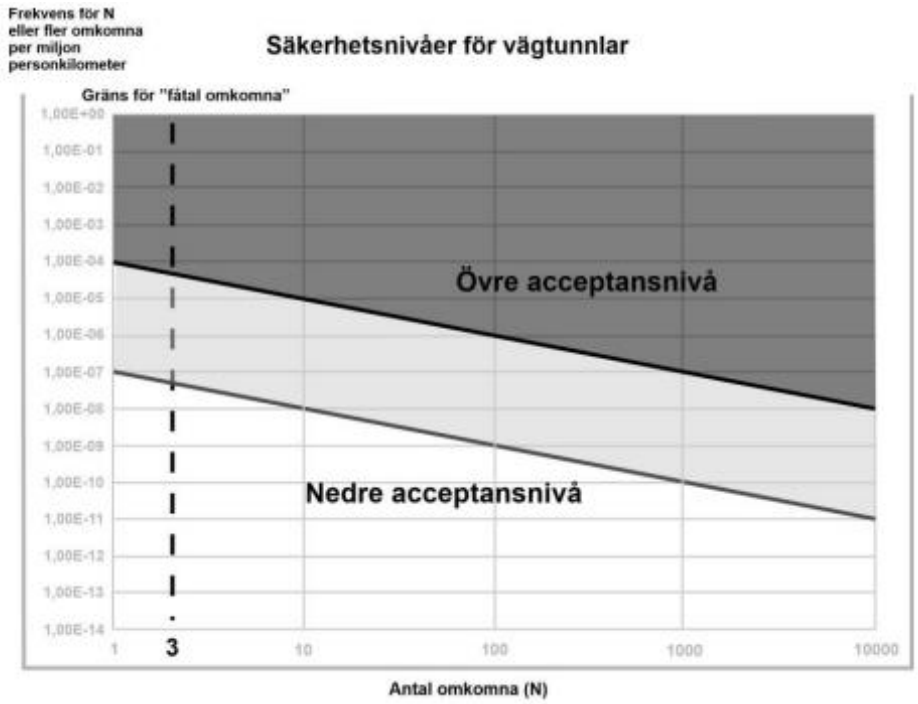

Figure 17. F/N diagram showing the upper and lower acceptance levels for road tunnels in the Swedish Transport Agency's regulations TSFS 2022:13. [17]

This study does not argue for a universal standard but rather examines how different regulatory approaches manage disaster risks. A balance must be struck between comparability across sectors and respecting national decision-making autonomy. The EU's directive on tunnel safety, for instance, encourages nations to develop their own provisions rather than enforcing a uniform threshold.

The findings reveal that quantitative risk acceptance criteria concerning consequence magnitude vary by industry/facility type and by country. There is no unified set of criteria applied consistently across sectors, whether in terms of curve slopes (risk aversion, curve position) or maximum allowable consequences. Based on these insights, the following section outlines key recommendations for enhancing disaster risk management in the transport sector. Additionally, variations exist regarding lower thresholds, i.e., areas where additional risk-reduction measures are not mandated even if they are cost-effective. It is important to note that the literature review does not provide a comprehensive overview of all risk acceptance criteria but does indicate the current level of knowledge.

There are examples where quantitative criteria impose no limits on the severity of allowable accidents, and conversely, where the presence of disaster risks renders the activity unacceptable. Some criteria specify that the potential for large consequences requires stricter application of ALARP (As Low As Reasonably Practicable) and intense scrutiny, often permitting such risks only under exceptional circumstances. For instance, exceptional circumstances may apply if the risk exists only temporarily, such as while permanent risk-reduction measures are being implemented. When no other options are feasible, operational limitations such as restrictions may need to be thoroughly examined [19].

In some dam safety charts, risks are only acceptable under exceptional circumstances, such as war-time, where the government may determine acceptability if societal benefits are deemed significant. The rationale for establishing a threshold on the maximum acceptable damage in risk acceptance criteria relates both to clarifying when additional assessment is required and to signalling an unwillingness to introduce new, more extensive catastrophic scenarios into society. Such a threshold is not dictated by natural law but is instead a practice established in some fields, while unused in others. Management tends to be binary; that is, either a distinction is made for very large accidents, or it is not. In all situations where the need for special treatment is identified in the acceptance criteria, >1,000 fatalities represent the scale at which such requirements are applied.

Thus, a clear recommendation regarding the limitation or allowance of disaster risks based on regulations and guidance from other countries and industries cannot be made. No single established methodology exists for constructing such curves, with approaches varying across sectors and countries. However, it appears appropriate that specific investigation and assessment should be undertaken in these cases, and that general guidelines for conducting such assessments and structuring decision support (in terms of both content and quality) should be developed. It is also reasonable to consider whether such risks should be accepted before there are established rules to limit them, and under what conditions, and to determine who should assess their acceptability. This is especially challenging within infrastructure compared to geographically isolated facilities, as measures like limiting freight transport capacity can have impacts on the whole transport system that extend beyond the scope of a specific project. In practice, this can mean that such decisions cannot be made within a specific project, even if the measure itself may be reasonable from a broader perspective.

Conclusions from the Literature Review

The literature review led to several key conclusions:

- Explicit requirements are set for managing "disaster risks" through risk analysis, regardless of consequence size.
- Decisions on risk-reducing measures are made using risk-informed decision-making, where risk analysis and "quantitative criteria" are part of the decision-making basis.
- Requirements for disaster risk management are not solely based on "quantitative criteria" or technical standards for facilities.
- Prescriptive requirements include a subset of necessary requirements for addressing "disaster risks."
- ALARP is present in some form across all studied examples.
- Collaboration with emergency services, including emergency planning, is a critical component of the requirements for risk reduction.
- In several areas, allowing activities with large potential consequences is not self-evident, which is also reflected in quantitative criteria.
- Requirements for risk reduction include both preventive and damage-limiting measures.
- Safety requirements, especially for preventing catastrophic incidents, have a strong reactive element.
- The transport sector's requirements in this area are relatively underdeveloped compared to high-hazard industries.
- Incidents with extensive casualties are (fortunately) rare, so strategies for managing disaster risks cannot rely mainly on empirical data or past event experience.

There are also examples of different regulations for existing facilities versus new developments, where higher risks are tolerated for existing activities, but new disaster risks must not be introduced in new developments.

EXPERIENCE WITH DEFINING DISASTER RISK CRITERIA FOR UNDERGROUND FACILITIES

In Sweden, there is limited experience with explicitly defining criteria for disaster risks involving high-consequence scenarios in underground facilities. Currently, two projects in the railway sector have examined this issue in greater depth, with proposed criteria developed by the infrastructure manager. One project involves a partially covered platform area along the Huvudsta–Duvbo section of the Mälarbanan line near Sundbyberg, while the other is at Stockholm Central Station, where plans include covering part of the rail area with an overbuilding. These projects are at different planning stages and have not yet been finalized or approved for operation by the Swedish Transport Agency.

There are existing facilities with similar platform conditions in operation, but at the time of their development, general knowledge and requirements for managing risks associated with hazardous goods transportation were different, and disaster risks were not explicitly addressed in the planning processes. Consequently, these examples will not be highlighted or discussed here.

Mälarbanan - Sundbyberg Station
In the risk assessment for Sundbyberg Station, it was determined that there is a very low but not negligible probability of an accident with a potentially large number of fatalities (over 1,000 fatalities). Individuals at Sundbyberg Station were classified as passengers and included in the safety assessment calculations for the Sundbyberg Tunnel. In the event of a major accident with dangerous goods at the station or tunnel exit, people at the station could also be affected and potentially fatally injured. These individuals were therefore considered in the risk assessment for the tunnel.

It was also noted that there is no widely accepted criterion or procedure for evaluating incidents with over 1,000 fatalities within either the Swedish Transport Administration's own regulations or those of other authorities. This lack of clear criteria created uncertainty in managing the situation, as the proposed facility design allowed limited flexibility for risk reduction without exceeding the project's scope. Consequently, a project-specific risk evaluation was conducted based on the following elements:

- Examination of assumptions, causes, and frequencies for high-consequence scenarios.
- Comparison of PLL (Potential Loss of Life) values with other rail tunnels in Sweden.
- Review of possible measures to reduce the risk of major accidents.
- Management of uncertainties.
- Consideration of the facility's societal benefits, including sustainability, capacity enhancement, urban development, and third-party risk reduction.

The overall assessment concluded that the risk could be accepted based on the extremely low frequency of severe accidents, the project's net reduction in societal risk for third parties, and acceptable individual risk levels for passengers and third parties. Furthermore, the Mälarbanan expansion is expected to provide significant societal benefits by increasing transport capacity and supporting urban development in Solna and Sundbyberg. The railway plan for this section has been approved by the Stockholm County Administrative Board and submitted for planning review by the Swedish Transport Administration.

Stockholm Central Station / Centralstaden
Another project recognizing the risk of a single accident affecting a large number of people is the planned covering of Stockholm Central Station. This project, known as Centralstaden, includes development with high rise buildings on top of the covered platform area. Currently in the detailed planning stage, the proposed design is set to undergo public consultation in 2025. As the facility will include both an underground station and overhead development, separate acceptance criteria have been established for risks above and below the covering. This study focuses on the risk acceptance criteria for the spaces under the covering, i.e. the platform area, which have been developed in a project memo by the Swedish Transport Administration [20].

The criteria state: "The safety level in the platform area under the covering structure should be comparable to that of other modern platform enclosure. Comparable platform enclosure include those designed or built in Västlänken, Citybanan, and suitable stations where freight trains pass. Trafikverket recommends using the future Sundbyberg Station as a reference."

Given that dangerous goods do not pass through Västlänken or Citybanan, Sundbyberg is the primary reference point for comparing disaster risk aspects. As this underground station represents the first example in this paper, no alternative methods for disaster risk assessment are added.

A separate risk assessment approach has also been prepared for safety above the covering, led by the Stockholm City Building Office. The basis for assessing risks around and above the covering includes the following components:

- Risk Profile
    - As catastrophic potential is inherent, a deeper analysis should focus on this to improve knowledge and reduce uncertainties.
    - Other unique risk profile characteristics impacting the needs of barriers should be identified.
    - The risk profile will guide the depth and scope of further analysis.
- Barriers
    - Both technical/physical and organizational barriers are considered essential for safety throughout the system.
    - Different types of barriers are evaluated, including those within the rail facility, other parts of the planning area, readiness of on-site actors, and societal crisis preparedness.
    - Barriers should be possible to regulate and verify over time.

In this risk assessment, the unacceptable risk threshold is extrapolated with an unchanged slope into the area exceeding 1,000 fatalities. However, there is no designated zone for more than 1,000 fatalities where risk is considered directly acceptable. Therefore, in cases where potential catastrophic scenarios are identified, as is the case for the Centralstaden area, a detailed analysis of scenarios and barriers is always required to determine if the risk level is tolerable. These analyses are proposed in three sequential steps: (1) barrier identification, (2) barrier analysis, and (3) safety assessment.
For incidents with catastrophic potential, no definition exists for a directly acceptable risk level, meaning the assessment basis does not specify the exact barriers required to achieve an acceptable risk. Instead, decision-makers are expected to evaluate this by reviewing different barrier combinations and their risk-reducing effects, including the responsibility distribution among involved actors. Additionally, the assessment basis specifies that barrier selection should consider factors such as risk reduction, safety level, and the acceptability of associated uncertainties. In summary, the assessment framework demands a more robust decision basis than is typical for physical planning risk evaluations, but it still leaves decision-makers in a challenging situation with limited guidance on what is considered reasonable.

These case studies illustrate the practical challenges of implementing disaster risk criteria in infrastructure projects. They highlight the need for clearer regulatory guidance and structured decision-making processes to ensure consistent risk management practices.

2. DISCUSSION

Lack of Consensus in the Literature

The knowledge base for regulating disaster risk in the transport sector is limited. This work suggests initial steps towards such regulation, but further research and development are necessary to establish effective standards. Evaluating disaster risks and deciding on suitable risk-reduction measures is a knowledge area that currently lacks sufficient answers to identified challenges. This gap increases the risk that the analysis and implementation of effective preventive measures may be overlooked in projects, potentially embedding vulnerabilities that could have been mitigated through proactive action.

There is no consensus among countries or sectors on what constitutes acceptable, tolerable, or permissible risk exposure. This also applies to low-probability events with the potential for mass casualties, i.e., events with disaster risk potential. Moreover, scientific literature provides little support for ignoring disaster risk simply due to low probability. Across industries, no such risks are deliberately left unaddressed.

While guidelines and regulations for disaster risk management exist in other sectors, few examples have been identified within the transport sector. One reason may be that unrestricted dangerous goods transportations through underground platform enclosure is rare or prohibited. Although certain European countries have criteria for road tunnels involving major accidents, the transport sector's standards are relatively underdeveloped compared to other sectors. Specific criteria for platform enclosure have not been identified.

The Existence of Disaster risks

Whether a facility poses a disaster risk depends on factors not fully regulated by the Planning and Building Act. The Swedish Transport Agency should determine if, and under what conditions, it is permissible to design facilities with disaster risk potential as described in this study. Not allowing such designs could impact transportation efficiency, while allowing them may introduce disaster risks.

Project Experiences

In Sweden, some projects have acknowledged the potential for high-casualty incidents in platform enclosure and attempted to assess disaster risks. However, risk assessment remains vague, leaving project-level decision-makers to determine acceptability. Despite this, identified disaster risks have not halted project planning.

Establishing clear safety targets helps prevent Black Swan events—low-probability, high-impact incidents often overlooked in traditional risk models. By integrating disaster risk scenarios into infrastructure planning, extreme but plausible events are addressed early, opening for reducing unforeseen disasters explicitly.

Rather than dismissing these risks due to low probability or political sensitivity, a structured framework offers two rational approaches: (1) designing resilient systems that mitigate their impact or (2) prohibiting intolerable risks outright. Defining and regulating disaster risks does not impose unnecessary constraints but enables informed decision-making, ensuring that extreme events are neither ignored nor implicitly accepted through regulatory gaps. Neglecting this increases the likelihood of true Black Swan events, not because they are unpredictable, but because they were avoidably overlooked.

Decision-Making Responsibility

Certain sectors, like dam safety, permit disaster risks but elevate decision-making to higher political levels, emphasizing that such decisions are exceptional and require careful investigation and scrutiny. The appropriate division of responsibility for the transport sector in Sweden is not discussed further here, but ought to be revisited by authorities having jurisdiction.

Need to Supplement Basic Standards

The basic standard (prescriptive requirements) for accidents with multiple fatalities provides a baseline safety level, but it is unclear if this is sufficient. Additional analysis of the need for risk-reduction measures for accidents covered by proposed safety targets, such as FN-curves, is necessary for complex platform enclosure. Basic standards are primarily derived from empirical data, so supplementary requirements for disaster risk management are needed, especially for rare and high-consequence events. This includes understanding potential scenarios and exploring risk-reduction options, complemented by requirements for facility design—such as redundancy, approach to untested solutions, and safety system maintenance.

Control over Risk-Reduction Measures

Reducing disaster risks, for instance in dangerous goods transport, can be challenging, as some risk-reduction measures lie outside project-specific infrastructure design, e.g., tunnels and platform enclosure. Restriction on transportation of certain substances is one such example. Determining if measures outside facility design are necessary to ensure acceptable risk levels within the Planning and Building Act is complex.

Clarity on facility requirements, including any external measures, would help avoid sub-optimization and uncertainty in operational safety.

Balancing Interests

Decisions to reduce disaster risk inherently require balancing multiple interests. Who makes these trade-offs and how significantly impacts the outcomes. This should be factored into regulations for disaster risk management.

The suitability of constructing infrastructure, including tunnels and/or platform enclosure with disaster risk potential, requires deeper investigation and is not solely a matter of engineering or scientific judgment. Until clearer guidance exists, strict investigation requirements should be in place if such facilities are permitted at all.

Disaster risk Threshold
Platform enclosure may, under certain circumstances, pose a risk of high-casualty incidents. If such designs are to be allowed, specific requirements for managing these risks should be developed. Existing design methods, aimed at other types of accidents, may not provide adequate protection. The 1,000-fatality threshold serves as a rough indicator for incidents requiring additional risk management. Other countries and sectors use similar thresholds, reflecting a limit above which incidents are either prohibited or require additional scrutiny.

Low-Probability Dismissal
In some cases, arguments suggest that disaster risks can be accepted if the probability of occurrence is sufficiently low. However, scientific literature provides very limited support for this rationale. Even with a low probability, the risk contribution of a scenario cannot be fully understood without examining the potential magnitude of its consequences [19]. If an activity could lead to a catastrophic scenario, it may not necessarily align with sustainable urban development and might require alternative design approaches or may not be permissible at all. However, certain aspects of societal development mean that some level of risk to human life cannot be entirely avoided, including within infrastructure systems or in large facilities like stadiums or hospitals.

The Need for a Holistic Approach
Disaster risk management, like safety management, requires standards across multiple system components, which interact in design and operation. However, regulations often target specific parts of the safety management system or facility, missing the overall system functionality. To address this, it is essential to clarify how different system components interconnect and how requirements relate across domains.

Decisions on disaster risk acceptance may depend on both facility design and infrastructure management systems. The interface between these two is challenging to address in standards and regulations.

Role of Emergency Services
The role of emergency services presents challenges in setting facility requirements. Emergency personnel must be able to safely operate in complex environments like underground platform enclosure, but their operational capacity can sometimes vary between different regions and municipalities. Consistent requirements for factors like distances, water supply, and evacuation sites are needed to create safe operational conditions. Simultaneously, emergency services need to practice in such facilities to ensure readiness, though mandating this in regulations is challenging.

Need for Guidance
Due to the lack of guidance on evaluating disaster risks, significant project-level differences are likely conducting these assessments. It is worth investigating whether disaster risks align with long-term, sustainable infrastructure planning, and, if so, how to determine adequate risk management. Consideration should also be given to which authority decides acceptability and the principles governing such decisions.

Evaluating Disaster risks
If incidents with extensive casualties are to be managed effectively, certain aspects require further study and clear standards for evaluation and decision-making. Leaving these complex assessments to individual projects may not reach optimal results. Furthermore, "creeping vulnerability" may be introduced as infrastructure, once built, is difficult to modify. A low-probability scenario may be viewed as plausible over the system’s lifespan, particularly as system configurations and risk

perceptions evolve. An unnoticed increase in vulnerability may only become apparent upon catastrophe, threatening society's functionality and safety.

ALARP and cost-benefit analyses often guide these decisions, but this approach has challenges. Highly improbable events with large impacts may be undervalued compared to certain, immediate benefits. Rational decisions may be difficult when costs, risks, and benefits are distributed among multiple actors, and uncertainty is high.

The challenges of safety through quantitative risk assessment and cost-benefit decisions are recognized. These tools, while part of a broader decision basis, are insufficient alone. Therefore, additional considerations must be included in regulations.

Introducing risk-informed decision-making requirements in current standards could help clarify the need for additional factors in risk assessments. For example, refining "comprehensive assessment" criteria and integrating risk-informed decision-making could enhance clarity and effectiveness.

Need for Improved Decision Support

Disaster risks in underground platform enclosure require more than technical standards; requirements for training, preparedness, and safety management systems are also essential. Quantitative criteria alone are insufficient; risk-informed decision-making considers additional aspects, including safety margins, barrier properties, uncertainty, cost-effectiveness, and decision quality. Control over disaster risks requires regulatory focus on these elements.

In addition to technical standards for disaster risks, operational requirements are needed to ensure effective disaster response. Design-stage decisions impact operational safety, necessitating alignment between design and operation.

RECOMMENDATIONS FOR THE TRANSPORT SECTOR

The following recommendations are derived from the study's findings and aim to provide policymakers with practical measures for strengthening disaster risk governance in the transport sector. These recommendations do not propose a universal methodology but highlight key areas where regulatory improvements can enhance safety outcomes. Based on the findings presented in this study, the following recommendations outline key steps to improve disaster risk governance in the Swedish transport sector.

1. Develop sector-specific risk acceptance criteria:
    - Introduce explicit risk criteria for catastrophic events in underground transportation infrastructure, drawing on methodologies from other sectors (e.g., nuclear and dam safety).
    - Establish guidelines for when FN-curves should be used and how they should be interpreted in transport context.
2. Strengthen risk assessment methodologies:
    - Require transport infrastructure projects to integrate both probabilistic risk models and qualitative assessments to account for uncertainties and decision-making under incomplete information.
    - Introduce scenario-based stress tests for underground stations and tunnels to evaluate worst-case scenarios and response capacities.
3. Clarify the division of responsibilities between regulators and project developers:
    - Define clear regulatory requirements for when special investigations must be conducted for projects involving potential disaster risks.

   - Ensure that decision-making responsibility for high-impact risks is elevated to an appropriate policy level, rather than being determined solely within individual projects.

4. Introduce regulatory refinements based on international best practices:
   - Explore the application of ALARP (As Low As Reasonably Practicable) or de minimis thresholds in transport safety regulations.
   - Consider implementing adaptive regulatory approaches that allow flexibility in risk acceptance depending on specific project conditions.
5. Operational requirements and periodic evaluations:
   - Regular risk assessments should be conducted at least every five years, and emergency response exercises should involve relevant stakeholders, including the fire and rescue services.
   - Ensure that risk assessments are well-documented, include uncertainty analysis, and provide clear justifications for accepted risks and trade-offs.

By implementing these recommendations, the Swedish transport sector can adopt a more structured and consistent approach to disaster risk management. These proposals are grounded in the study's findings and provide a framework for improving regulatory consistency and safety outcomes. The following section summarizes the key insights from this research, reinforcing the basis for these recommendations.

CONCLUSIONS AND SUGGESTED DIRECTION

This section provides a synthesis of the study's key insights, summarizing the empirical findings and their implications for transport risk governance. This study has examined the governance of disaster risks in underground transportation infrastructure by analyzing regulatory frameworks across multiple sectors and jurisdictions. The findings highlight several key insights:

- Sectoral differences in risk governance: Industries such as nuclear power and dam safety have well-defined risk acceptance criteria for catastrophic events, whereas the transport sector has yet to develop an equally systematic approach.
- Fragmented regulatory landscape: Existing Swedish regulations lack a unified framework for addressing disaster risks in underground transportation, leaving risk assessment methodologies inconsistent across different projects.
- Need for risk-informed decision-making: Effective disaster risk management requires a combination of quantitative approaches (e.g., FN-curves) and qualitative considerations, including epistemic uncertainty and societal values.
- No universal methodology for disaster risk assessment: Regulatory approaches vary significantly across industries and countries, suggesting that solutions must be sector-specific and context-sensitive rather than relying on rigidly applied global standards.
- Regulatory responsibility: A key question remains whether the Swedish Transport Agency should regulate disaster risks at the national level or leave such decisions to project-specific assessments.

These insights provide a foundation for further regulatory improvements and future research on disaster risk governance.

REFERENCES

[1] B. Wahlström, O. Jansson, E. Hall Midholm och J. Lundin, ”Säkerhetsmål i plattformsrum,” Transportstyrelsen, 2022.

[2] United Nations, Sendai Framework for Disaster Risk Reduction 2015-2030, 2015.

[3] Council, European Parliament and of the, Directive 2004/54/EC on minimum safety requirements for tunnels in the trans-European road network, 2004.

[4] Jansson, O. Wahlström, B., Lundin, J, & Midholm, E., ”Säkerhetsmål för plattformsrum (del 1),” Brandskyddslaget/Risktec, 2021.

[5] MSB, Sendairamverket för katastrofriskreducering 2015–2030, 2017.

[6] IAEA, Safety of Nuclear Power Plants: Design, Specific Safety Requirements No SSR-2/1 (Rev 1), 2016.

[7] Australian National Committee on Large Dams (ANCOLD), Guidelines on Dam Safety Management, 2003.

[8] New South Wales Dam Safety Committee, Risk Guidelines, 2006.

[9] US Army Corps of Engineers (USCE), Safety of dams - policy and procedures, 2014.

[10] Hong Kong Planning Department, Hong Kong Planning Standards and Guidelines, 2006.

[11] Health and Safety Excecutive (HSE), Reducing Risks, Protecting People, 2001.

[12] G. Davidsson, M. Lindgren och M. Liane, ”Värdering av risk,” Statens Räddningsverk, Karlstad, 1997.

[13] Geotechnical Engineering Office, Landslides and Boulder Falls from Natural Terrain: Interim Risk Guidelines. GEO Re-port No. 75., Hong Kong, 1998.

[14] Health and Safety Executive (HSE), The Tolerability of Risk from Nuclear Power Stations, 1992.

[15] Statens Räddningsverk , Värdering av risk (DNV), 1997.

[16] Trafikverket, *TRVINFRA-00233, Krav Tunnelbyggande version 1.0,* 2021.

[17] *Transportstyrelsens ändringar i föreskrifter och allmänna råd (TSFS 2019:93) om säkerhet i vägtunnlar, TSFS 2022:13,* Transportstyrelsen.

[18] PIARC, Current Practice for Risk Evaluation for Road Tunnels, 2012.

[19] D. Bowles, What is ALARP and how can it improve dam safety decisions?, ASDSO 2013 Conference on Dams , 2013.

[20] Trafikverket, ”PM – Bedömningsgrund för olycksrisk - under överdäckning. Detaljplan Centralstationsområdet. TRV 2020/135500.,” 2022.

Using Deep Learning to Predict Traffic Dynamics in Road Tunnels

Naeem Khademi, Vinothini Aravindan, Parvathy Anil Kumar & Erlend Tøssebro
University of Stavanger, Stavanger, Norway

ABSTRACT

This paper investigates the applicability of deep learning models for predicting traffic dynamics in road tunnels. While the ability to predict traffic dynamics is important for both real-time and long-term safety and risk management, it has rarely been investigated in the context of road tunnels, specially more so using advanced deep learning models. Our paper aims to address this shortcoming by taking an experimental methodology. Using real-life measurement data from carefully selected road tunnels in Norway – a country with the highest number of tunnels per capita – spanning across various tunnel classes, profiles and average daily traffic volumes within urban, suburban and countryside areas, this paper explores the performance of baseline — e.g., RNN — and advanced deep learning models — e.g., GRU and (Bi)LSTM in comparison with selected machine learning models such as Linear Regression and Random Forest. Our evaluation results reveal that advanced deep learning models perform significantly better than baseline deep learning or machine learning models and can effectively be utilized for predicting rush hours, average speed, and traffic volume by considering various features such as time of day, weekday and season, thus capturing both temporal and spatial aspects. Prediction of traffic dynamics using such models can be leveraged by various systems such as for real-time use in safety-based decision support systems for road tunnels, automated incident detection, and for design and planning of tunnel systems.

KEYWORDS: Deep learning, traffic forecasting, neutral networks, LSTM, RNN, GRU, tunnel

INTRODUCTION

Road tunnels are critical infrastructures within the road network and efficient traffic flow within them is significantly important for the public notion of safety, in addition to socio-economic reasons. In countries with complex geographical terrains — e.g., Norway or Switzerland — they can potentially become major bottlenecks in the country's road system if the traffic flow is hindered. Hence, better understanding of the dynamics of traffic flow in tunnels is vital to forecast the future traffic flow and take necessary measures to manage it effectively. The importance of traffic forecasting for road safety is well-established [1] [2]. For instance, traffic forecasting can be leveraged for accident risk mitigation and emergency preparedness through proactive traffic management, as well as data-driven policy decisions. It is also a requirement for real-time decision support systems such as those intended for road tunnel safety, an example of which is our proposed RiskTUN Decision Support System (DSS) framework [3].

Owing to the rapid proliferation of applied Artificial Intelligence (AI) in recent years, data-driven models leveraging Machine Learning (ML), and neural networks have been utilized for traffic and congestion prediction within the road system [4][5][6]. Common approaches of traffic prediction have included parameter-based approaches (e.g., time-series models [7]), non-parametric approaches (e.g., Artificial Neural Networks (ANN) [8]) or simulation-based approaches, mostly focusing on the generic road networks. In addition, benefits and challenges of using Deep Learning (DL) models for short-term road traffic forecasting in comparison to traditional ML models are critically explored by Manibardo et al. [9] as they are assumed to be well-suited to model complex phenomena and can potentially better capture the dynamic nature of traffic in both spatial and temporal aspects.

Specifically, there has been limited research on traffic forecasting within the road tunnels so far. In particular, the use of DL models for traffic prediction in road tunnels is yet to be fully explored. An exception to this is the work of Yu & Liu [10] which proposes a hybrid prediction approach for road tunnel traffic based on temporospatial data fusion using Shanghai Dalian Road Tunnel as its main use-case scenario. Although a promising preliminary work, this work's scope and applicability is limited to a single tunnel while a thorough investigation of deep learning-based prediction models for various tunnel classes – e.g., with various lengths and traffic volumes – is needed. Among other things, this paper aims to address this shortcoming.

In this paper we explore how various deep learning models can be leveraged for forecasting the traffic in road tunnels. We perform our investigations relying on real-life measurements from road-side sensor data provided by the Norwegian Public Roads Administration (NPRA), for various tunnel types across Norway. These include data from several tunnels with various profiles and classes as well as geographical location – e.g., urban, sub-urban and countryside.

Paper's Scope

In this work we focus on Norway, a country with more than one thousand road tunnels and with the highest number of road tunnels per capita in the world. Due to its complex geographical terrain, tunnels in Norway are very diverse in characteristics, varying across different length, traffic volume, seasonal traffic patterns, tunnel profiles and slopes, all of which affect how traffic flows within them. Although there are other countries like Norway – e.g., Switzerland or Italy, in this paper we choose to solely focus on Norway because: (1) Norway is a sufficiently good representative candidate with diverse set of tunnels; and (2) we have access to the sensor data from roadside measurement points in this country. In addition, we take the relationship between tunnel safety and traffic forecasting for granted based on scientific literature [1][2][3] and will therefore for the remainder of this paper mainly focus on the performance of ML/DL traffic forecasting methods for road tunnels. However, in Section 6 we will provide some insights on the potential use of DL-based tunnel traffic forecasting models for tunnel safety.

Paper Contributions

The contributions of this paper are as following:

a) We analyse the traffic patterns within road tunnels through data integration and pattern analysis techniques to identify the key factors influencing congestion in the road tunnels including during the rush hours. In doing so, we also study the impact of tunnel profile and class as well as location (i.e., urban, sub-urban, countryside) on the traffic pattern.
b) We implement and evaluate a range of ML models including traditional models such as Random Forest and Linear Regression as well as DL-based models such as simple RNN, Long Short-Term Memory (LSTM), Gated Recurrent Units (GRU), and Bi-directional LSTM (BiLSTM) to predict the traffic pattern and congestion in the road tunnels. We identify which approach produces the most accurate and reliable prediction in tunnel environments.
c) We optimize the beforementioned models through hyperparameter tuning to enhance the performance of traffic modelling while preventing the overfitting of such models.

Paper Structure

The remainder of this paper is structured as follows: Section 2 lays out the related works on traffic forecasting using ML/DL with emphasis on road tunnels; Section 3 provides some insights from measured tunnel data; Section 4 presents our research methodology and ML/DL model setup and implementation; Section 5 presents the evaluation results using the ML/DL models for three use-cases of rush-hour, influence of day, and traffic volume and average speed predictions; Section 6 discusses the obtained results and puts them in context; and finally Section 7 concludes the paper and discusses the future work.

RELATED WORKS

Traffic forecasting plays a crucial role in the management and planning of transportation systems. Its importance has become even more profound with the emergence of Intelligent Transport Systems (ITS) where traffic forecasting tools can become a vital component in the system to manage traffic congestion [6]. ML techniques have been widely adopted in traffic congestion prediction due to their ability to learn from historical data and make predictions about future traffic conditions. Traditional ML methods, including Support Vector Machines (SVM), Decision Trees (DT), and Random Forests (RF), have shown effectiveness in predicting short-term traffic flow and congestion levels by considering various features such as traffic volume, speed, and time of day. For instance, Vlahogianni et al. [11] demonstrated the effectiveness of SVM in short-term traffic forecasting, emphasizing its capacity to handle nonlinear relationships in traffic data. Similarly, Zhong et al. [4] utilized Random Forests to predict traffic flow, noting the model's robustness in managing large datasets with multiple features. However, these *traditional* methods often require extensive feature engineering and may struggle with the temporal and spatial complexities inherent in traffic data, especially in dynamic environments like tunnels [5].

DL, a subset of ML, has significantly advanced traffic forecasting by automatically extracting features from raw data. It utilizes multi-layer or deep architectures to extract intrinsic features of data from the lowest to the highest levels. Given the inherently complex nature of traffic flow, DL algorithms can represent traffic characteristics without necessarily requiring prior knowledge, potentially providing strong performance in traffic flow prediction [6]. Deep learning models, especially Recurrent Neural Networks (RNN) and their variants like Long Short-Term Memory (LSTM) networks and Gated Recurrent Units (GRUs), are well-suited for time series forecasting, making the ability to better capture temporal dependencies. For instance, Zhao et al. [12] applied LSTM networks for short-term traffic forecasting, finding that LSTMs outperformed traditional ML models in capturing long-term dependencies in traffic data. Similarly, Ma et al. [13] employed GRUs for traffic speed prediction, demonstrating their efficiency in learning temporal patterns and improving accuracy in traffic forecasting.

Moreover, Convolutional Neural Networks (CNNs) have been adapted for traffic forecasting by treating traffic data as spatial-temporal grids. Yu et al. [14] combined CNNs with LSTMs in a hybrid model, achieving high accuracy in predicting traffic flow by leveraging the strengths of both spatial and temporal feature extraction. In another approach by Rusul et al. [15], Bidirectional LSTM (BiLSTM) models were used that outperformed other models in traffic flow prediction by capturing complicated time-related connections. This approach employs bidirectional data flow to improve the precision of traffic predictions, particularly in circumstances where traffic patterns are influenced by both past and future conditions. BiLSTM units are particularly excellent at grasping sequences completely because they combine insights from both temporal directions – i.e., using a *forward* and *backward* LSTM process.

It is worth noting that combining CNN and RNN may potentially provide superior accuracy in traffic forecasting by capturing complex spatial-temporal dependencies. However, these models require large datasets and significant computational resources. In contrast, traditional ML models still rely heavily on feature engineering, which can be labor-intensive and may not capture all relevant traffic dynamics. Automated feature extraction in DL models offers a solution but at the cost of interpretability. The ability to adapt to real-time data is crucial for traffic forecasting models. Integrating data from diverse sources may improve model's performance, but it can also introduce challenges related to data fusion and real-time processing. Models should generalize well across different traffic environments, including in tunnels. The scalability of DL models to new, unseen data and different geographic locations remains a significant challenge. The black-box nature of DL models poses a challenge for interpretability and trust in predictions. Efforts to improve *explainability* of these models are ongoing, formalized in a broader sense in recent EU AI act [16].

So far, the application of ML/DL models in traffic forecasting has mainly been investigated in the

context of generic road networks, while specific research on traffic in road tunnels remains scarce. An exception is the work of Yu & Liu [10] which focuses on a single tunnel in China using a hybrid approach for spatial-temporal data fusion. Two predictors – i.e., *local* and *global* – are used where local tunnel data and data from peripheral road segments are incorporated respectively. While it offers valuable insights, this work is limited in its scope due to: (1) absence of diversity in tunnel profiles/classes in the investigation; (2) baseline comparisons not including advanced DL models such as GRU and LSTM. Our work, among other things, tries to address these shortcomings by conducting a performance evaluation study of various ML/DL models for a diverse set of tunnels. We view this as a foundational step in direction of understanding the dynamics of traffic forecasting in road tunnels, and as a result our paper differs in scope from Yu & Liu's [10] as it does not include the study of peripheral road segments since we consider this as the next step forward.

INSIGHTS FROM TUNNEL DATA

Before implementing our ML/DL study, we aim to analyse the traffic patterns within road tunnels through data integration and pattern analysis techniques to identify the key factors influencing congestion in the road tunnels. For this goal, we select several representative tunnels in Norway from various classes/profiles as shown in Table 1. Classes and their associated profiles are defined in [17]. Since classes C and D share the same tunnel profile, we exclude the use of a class D tunnel in this investigation. In addition, since class A tunnels are designed for very low Average Daily Traffic (ADT) volumes of fewer than 300 vehicles, they are excluded from our study. For data acquisition and preprocessing methods, see Section 4. Figure 1 shows the average hourly traffic flow per weekday for the tunnels in Table 1 based on measurement data. Several features can be manually extracted. For instance, Fannefjordtunnelen, a C-class suburban tunnel near the city of Molde shows a distinct traffic peak in early hours of the workdays. The same workday pattern can be observed for E-class suburban Ryfylketunnelen near the city of Stavanger, although to a lesser extent. These patterns demonstrate the morning commute from the suburban areas to the city centers. In addition, a distinct peak in Sunday afternoon traffic can be observed for Ryfylketunnelen, unlike other tunnels. This is perhaps due to tourists and residents returning to the city from recreational locations by the end of the weekend. In general, a peak in traffic level can be observed for all tunnels in the afternoon. However, this pattern can be observed at a slightly earlier time (i.e., around noon) for B-class county-side Gudvangatunnelen. This is potentially due to the remote nature of the tunnel as most traffic from cities (e.g., Bergen or Oslo) departing in the morning reach the tunnel in mid-day. Although following the general trend, the traffic pattern in F-class urban Ekebergtunnelen is smoother compared to other tunnels due to the urban and high-volume nature of the traffic in capital Oslo.

The next step is to explore the relationship between vehicle speed and traffic levels. Figure 2 provides a comparison of hourly average speed versus average traffic volume for two tunnels. From Table 1, we select two significantly different tunnels, the urban Ekebergtunnelen and the countryside Gudvangatunnelen for brevity. It can be observed that in both tunnels, an inverse relationship between traffic volume and average speed can be observed. Interestingly, the average speed in early morning hours is slightly higher than late evenings with similar traffic volumes. Among other things, this can hypothetically be due to drivers' behavior factor during different times of the day.

Table 1 Tunnels in Norway selected for traffic trend analysis.

Tunnel Name	County	Class	Profile	Lane	ADT (vehicles)
Gudvangatunnelen	Vestland	B	T9.5	Single	2260
Fannefjordtunnelen	Møre og Romsdals	C	T10.5	Single	4368
Ryfylketunnelen mot Stavanger	Rogaland	E	2xT9.5	Dual	2360
Ekebergtunnelen	Oslo	F	2xT9.5	Three	37800

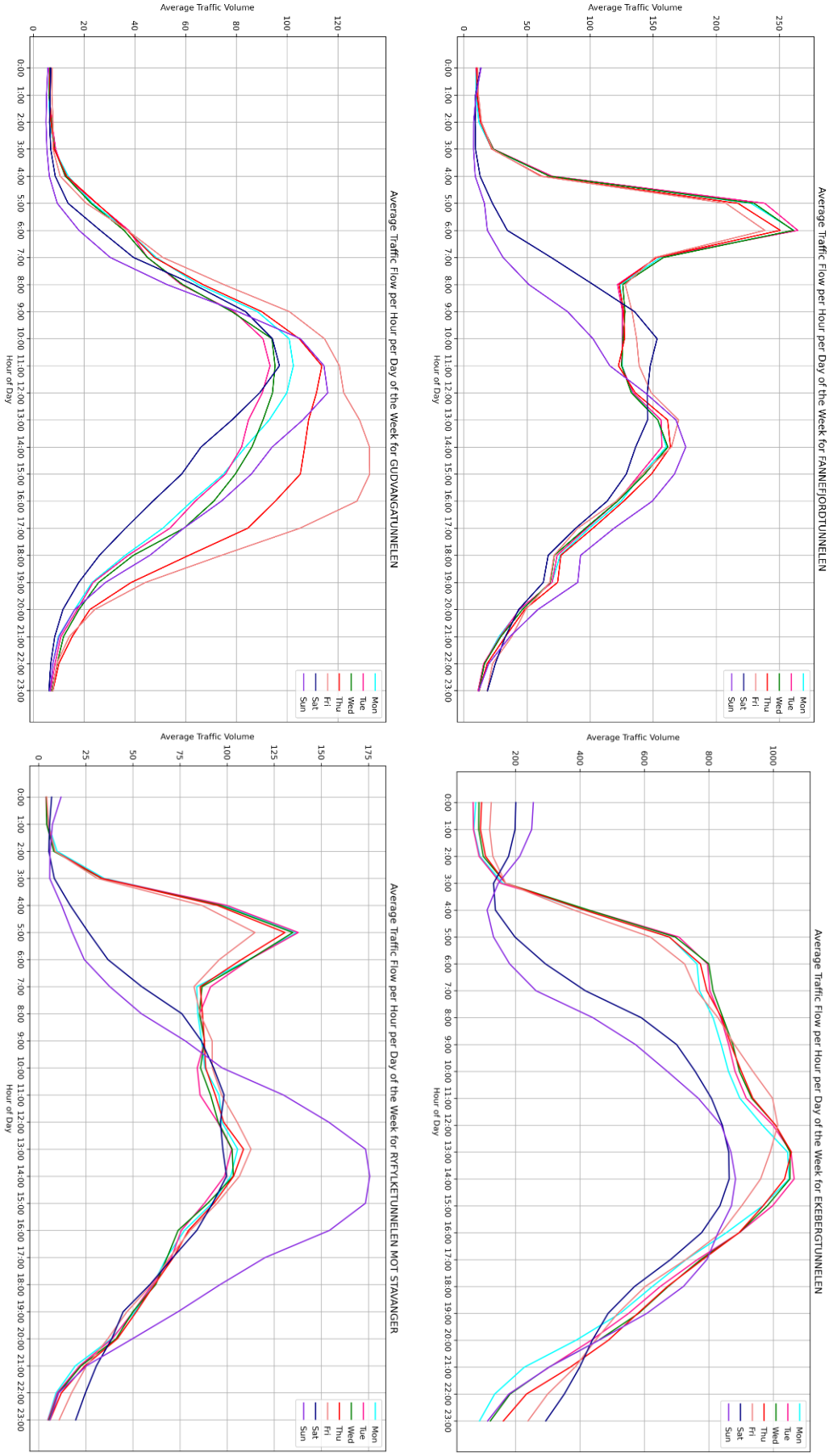

Figure 1 Average hourly traffic flow per day of the week.

Another important feature to investigate is the seasonal variations in traffic volume in road tunnels. Figure 3 shows the seasonal changes in traffic for Ekebergtunnelen and Gudvangatunnelen. While the seasonal variation is minimal in an urban tunnel such as Ekebergtunnelen, it is significant in a countryside tunnel such as Gudvangatunnelen – e.g., due to seasonal nature of tourism in the area.

Now that we have been able to extract certain features from tunnel-related measurement data, we aim to investigate to what extent DL models can help automatically predict these features – e.g., rush hours, influence of day and season, traffic volume and average speed.

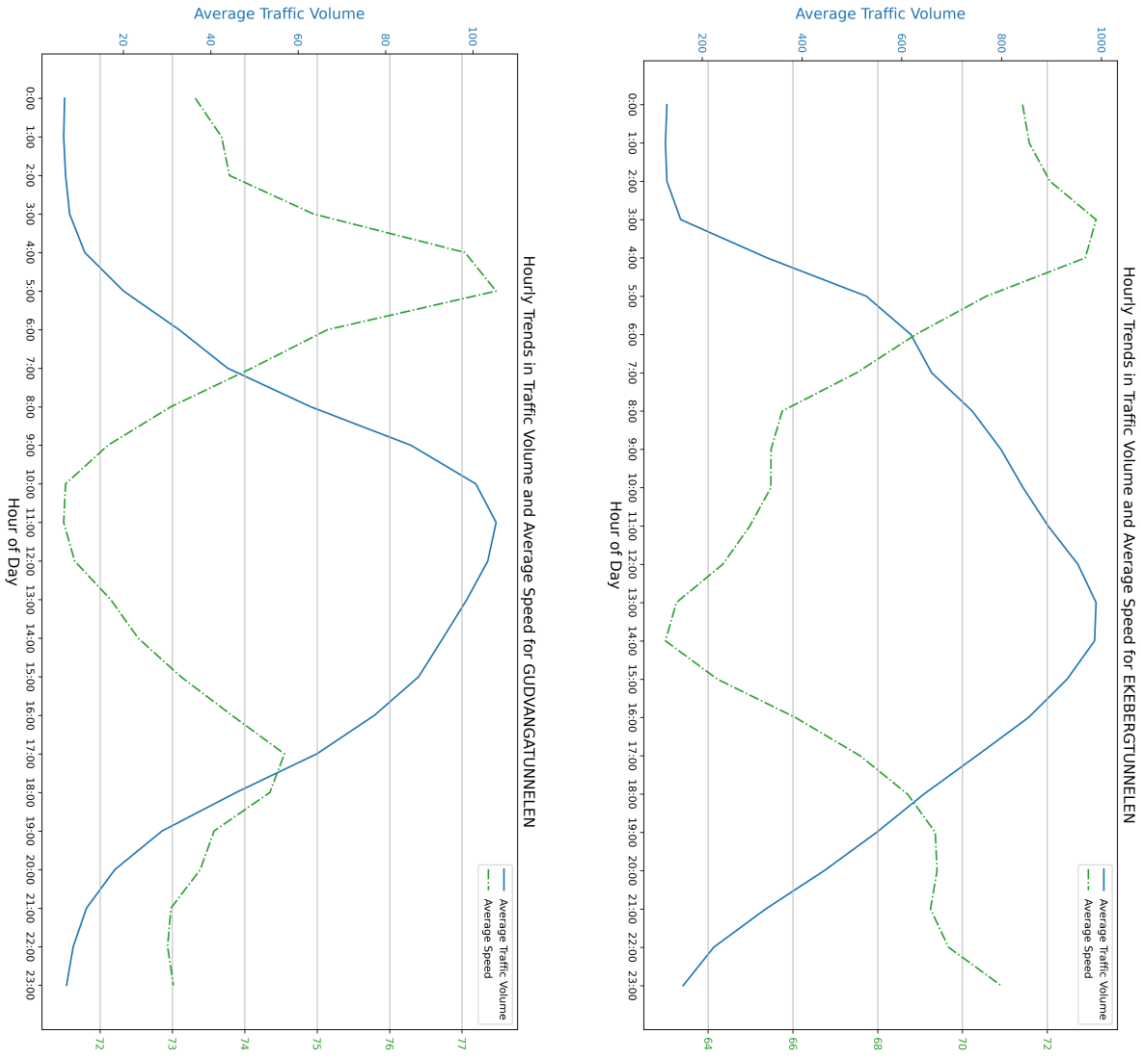

Figure 2 Comparison of hourly average speed versus average traffic volume for urban Ekebergtunnelen and countryside Gudvangatunnelen.

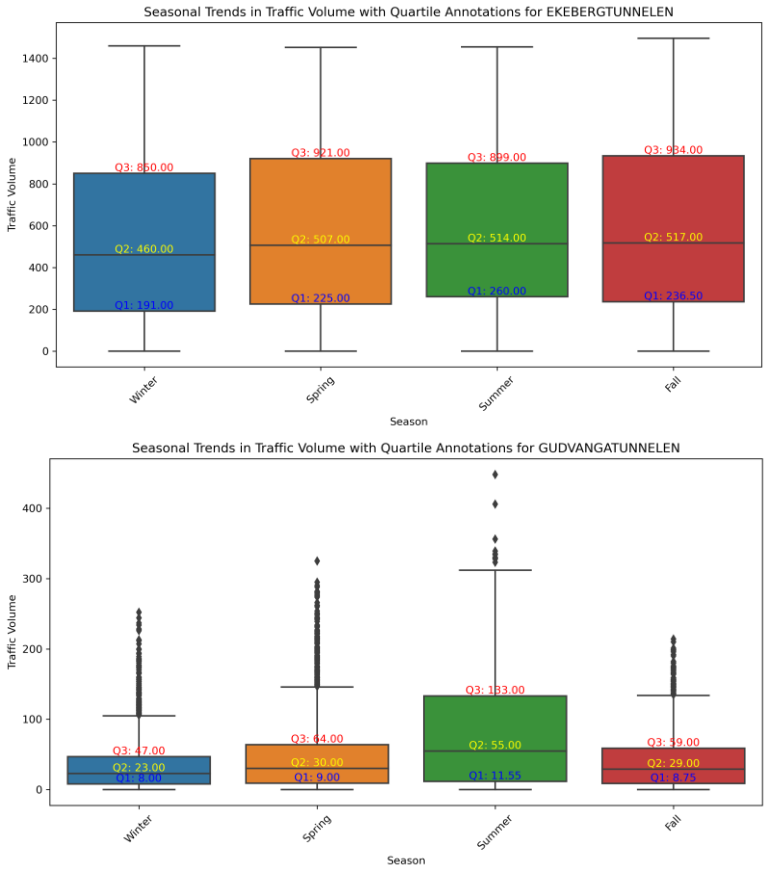

Figure 3 Seasonal traffic volume analysis for urban Ekebergtunnelen and countryside Gudvangatunnelen.Q1, Q2, Q3 show 25th, 50th and 75th percentiles respectively.

RESEARCH METHODOLOGY AND ML/DL MODEL SETUP

This section presents the methodology and ML/DL model setup used in this paper. Data acquisition and preprocessing methods, as well as model implementation are explained in detail.

Data Acquisition

Vehicle count and speed are collected at the roadside measuring points on the national and municipal roads by the NPRA and are available through *trafikkdata* DATEX system [18]. DATEX is a European standard for seamless exchange of traffic data [19]. The data is gathered using inductive loops embedded in the roadway. For any given tunnel, the nearest traffic measurement points were selected via the spatial join using the data provided by national road databank through RESTful NVDB API version 3 [20]. Spatial join operation was performed using QGIS tool [21]. Other tunnel-related data is also available using the NVDB API. To classify a tunnel – i.e., as urban, suburban, or countryside – we have developed Python scripts for QGIS that make use of population data from SSB [22].

Data Preprocessing

Data cleaning was performed on the dataset obtained from *trafikkdata* handling the nil or missing values. For average speed, median imputation was performed – i.e., the missing values were filled with the median value of the column. This was chosen to ensure that the extreme values which are common in speed data, do not skew the imputed data [23]. For traffic volume, we use linear interpolation for a smooth and continuous distribution. Further, we conduct feature engineering by extracting spatial and temporal properties in the data – e.g., time of day, day of week, geographic location, weekend identifier – to allow for the ML/DL model to differentiate traffic behaviours based on spatial-temporal data. For trend analysis, see Section 3.

Model Implementation

This subsection explains how ML/DL models were implemented in a step-by-step fashion. These steps include data scaling, encoding and sequence creation, and ML/DL model implementation. ML/DL model implementation include training and validation, feature selection, DL input layer configuration, hyperparameter selection and parameter optimization.

Data Scaling. Due to significant variation in traffic levels among the tunnels, data scaling was used to normalize the data. We use *RobustScalar* method [24] which is less sensitive to the outliers in the data – e.g., in comparison to *StandardScaler* method [25]. This normalization allows for processing of data from multiple tunnels simultaneously.

Data Encoding. Further, data encoding methods were used to tailor the data for use by ML/DL algorithms. Among other things, these include conversion of text-based timestamps into numerical date-time timeseries, as well as conversion of data labels (e.g., feature categories) into distinct integer values. The encoder objects were stored in a dictionary keyed by their corresponding feature names for potential inverse transformations when needed. The dataset was organized into 24 hours long sequences of consecutive values. Each segment of the data was transformed into a matrix with dimensions determined by the number of features multiplied by the sequence length. This matrix serves as input for ML/DL models, where each row represents a sequence of features, and the corresponding target values are stored separately. The amount of data that the model receives at once to modify the weights based on the Mean Squared Error (MSE), the actual and the predicted value is known as *batch size*.

ML/DL Model Training and Validation. In the ML workflow of this paper, the dataset was divided into two parts, 20% of which was allocated to the test set, with the remaining 80% used for training, by consistently using a predetermined random seed for data splitting to maintain reproducibility. Models are trained based on splitted data, and parameters are adjusted accordingly to minimize the prediction error on unseen data. The prediction accuracy is characterized using several Key Performance Indicators (KPIs) such as Mean Absolute Error (MAE), Mean Squared Error (MSE), Root Mean Squared Error (RMSE), and the coefficient of determination R^2. In addition to ML models of Random Forest and Linear Regression, various DL models are also evaluated. These include Simple RNN, LSTM, GRU and BiLSTM. During the training process, a portion of data is reserved for validation set, separate from training set. Validation set is used to monitor the performance to detect overfitting and tune the model effectively. The *EarlyStopping* callback is incorporated in the LSTM model's training to halt the training process if the model's performance on the validation set doesn't improve after a certain number of epochs. This helps save computational resources and avoid over-fitting by restoring the weights of the best iteration once training is halted.

Feature Selection. For ML models each feature was specifically chosen to improve the model's capacity to recognize patterns and generate accurate predictions. Certain features, such as *IsRushHour*, *encoded_month*, *encoded_day*, and *encoded_season*, were used in models that analyze traffic during rush hours. The hourly data is used to generate the *IsRushHour* feature, which determines peak traffic hours that are important for forecasting traffic volume. Evaluating traffic changes according to these temporal variables offer valuable insights into the dynamics that shape traffic patterns. In addition to Linear Regression, a Random Forest model is used in this paper to investigate *MultiOutputRegressor* [26], expanding the analysis to predict traffic volume and average speed concurrently. A better understanding of the relationship between traffic volume and speed which are closely related – but may behave differently depending on the situation – is made possible by this dual prediction technique. To detect long-term trends and seasonal fluctuations, extended feature tests employing *encoded_day* and *encoded_season* evaluate the impact of particular days and seasonal shifts on traffic. For DL models, *lane*, *traffic_volume*, *DayOfWeek*, *IsWeekend*, *Hour*, *DayOfMonth*, *encoded_month*, *encoded_day*, and *encoded_season* were among the numerical features used. These were selected since they can reveal time cycle patterns, including weekly, monthly, and seasonal fluctuations, which are essential for forecasting the *average_speed* variable.

Configuration of the DL Input Layer. The Input layer is essential for the DL model implementations by holding the data sequences. The input to the DL model is created in such a way that it can be trained on a single tunnel or multiple tunnels, having the same amount of data points. This means that the model can handle a dynamic shape of input data, where the dimensions can be changed by the sequence length and the number of features used. Because of this structure, the model can process the incoming data sequentially and capture the temporal relationships among the chosen features.

Hyperparameter Selection. The models incorporate various optimized hyperparameters to enhance the performance. The RNN utilizes a SimpleRNN layer with the Rectified Linear Unit (ReLU) activation to address the vanishing gradient problem. It is set up using the Adam optimizer [27] with the learning rate of 0.001. While the GRU model – similar to SimpleRNN – uses ReLU activation, the LSTM model employs hyperbolic tangent (tanh) activation. SimpleRNN, LSTM and GRU models are all using 50 units (i.e., neurons). Both LSTM and GRU models incorporate an *EarlyStopping* callback during training. This callback tracks the validation loss and halts training if no improvements are observed after 10 epochs, at which point it reverts to the best weights. This feature is vital to prevent overfitting and to ensure that the model performs well on unseen data. Table 2 presents the hyperparameters used in this work.

Table 2 List of hyperparameters used for DL models in this work.

Model Name	Hyperparameter	Value
Baseline RNN	Layers	2
	Activation function	ReLU
	Optimizer	Adam
	Learning rate	0.001
	Batch size	32
	Validation split	0.2
Advanced LSTM	Units	128,256
	Activation function	tanh
	Optimizer	Adam
	Learning rate	0.0005
	Batch size	32
	kernel_regularizer	l2(0.001)
	Dropout	0.5
	Validation split	0.3
Advanced GRU	Units	128,256
	Activation function	ReLU
	Learning rate	0.0005
	Batch size	32
	Optimizer	Adam
	kernel_regularizer	l2(0.001)
	Validation split	0.3
BiLSTM	Units	64,128,256
	Activation function	tanh
	Learning rate	0.0005
	Batch size	32
	Optimizer	Adam
	batchnormalization	–
	kernel_regularizer	l2(0.001)

Parameter optimization. Overfitting is a significant issue in training ML models, including in complex DL models. To address this, we use a 20% *validation* split during training. This method monitors the model's performance on data that is not used for training, offering insights into how well

the model is generalizing, while allowing for potential early stopping when needed. We chose the learning rate of 0.0005 with the batch size of 32, because smaller learning rates allow for better convergence and reduction of overfitting. In addition, we also utilize L2 regularisation [28] and dropout algorithms [29] to prevent further overfitting.

EVALUATION RESULTS

This section presents the performance evaluation results based on the methodology outlined in Section 4. Our evaluations are conducted on five representative tunnels, each representative of a certain class except for class A which has very limited daily traffic. These tunnels are those listed in Table 1 in addition to Ilsvika tunnel which is an urban class D tunnel near the city of Trondheim.

Rush Hours Traffic Prediction

Table 3 shows the KPI values for ML models in predicting rush hours. It shows that Random Forest yields better prediction results in comparison with Linear Regression except for Ryfylke tunnel (class E) with 0.2 increase in RMSE. Better results correspond to lower prediction errors – e.g., lower RMSE. In addition, rush hour prediction has been explored by applying DL models as shown in Table 4. It shows that RNN model, as the baseline DL model, performs better in predicting rush hours within tunnels than ML-based Random Forest. Amongst the DL models, BiLSTM yields the best results although GRU follows trend quite closely.

Table 3 KPI of ML models for predicting rush hours per tunnel class.

Tunnel Class	Linear Regression			Random Forest		
KPI	MAE	MSE	RMSE	MAE	MSE	RMSE
B	38.7	27774.9	52.6	**34.7**	**2219.7**	**47.1**
C	50.1	4528.1	67.3	**49.8**	**4300.4**	**65.6**
D	60.5	5926.6	76.9	**60.4**	**5616.3**	**74.9**
E	**65.3**	**6550.9**	**80.9**	65.9	6581.7	81.1
F	311.8	137016.7	370.1	**306.4**	**132080.9**	**363.4**

Table 4 KPI of DL models for predicting rush hours per tunnel class.

Tunnel Class	RNN			LSTM			GRU			BiLSTM		
KPI	MAE	MSE	RMSE	MAE	MSE	RMSE	MAE	MSE	RMSE	MAE	MSE	RMSE
B	32.7	1786.5	42.2	31.4	1412.5	37.5	19.6	746.8	27.3	**14.4**	**752.5**	**27.4**
C	49.6	4762.8	69.0	18.6	1141.8	33.7	19.7	1187.2	34.4	**16.5**	**1046.0**	**32.3**
D	29.1	1734.4	41.6	22.7	1144.4	33.8	23.1	1173.4	34.2	**22.3**	**1148.5**	**33.8**
E	67.9	6780.2	82.3	27.6	2110.7	45.9	27.0	2081.0	45.6	**25.7**	**1936.3**	**44.0**
F	256.9	94845.5	307.9	91.7	22416.7	149.7	**85.1**	20791.3	144.1	87.2	**20596.8**	**143.5**

Table 5 KPI of ML models for predicting traffic volume based on the weekday and season.

Tunnel Class	Linear Regression			Random Forest		
KPI	MAE	MSE	RMSE	MAE	MSE	RMSE
B	40.0	2885.0	53.7	**37.1**	**2456.2**	**49.5**
C	57.2	5271.376	72.6	**55.5**	**5061.0**	**71.1**
D	68.5	7166.5	84.6	**66.8**	**6865.2**	**82.8**
E	**68.4**	**6748.6**	**82.1**	68.6	6704.4	81.9
F	340.9	161189.7	401.4	**338.9**	**158855.1**	**398.5**

Table 6 KPI of DL models for predicting traffic volume based on the weekday and season.

Tunnel Class	RNN			LSTM			GRU			BiLSTM		
KPI	MAE	MSE	RMSE	MAE	MSE	RMSE	MAE	MSE	RMSE	MAE	MSE	RMSE
B	30.3	1507.3	38.8	30.2	1503.6	38.7	**16.9**	**770.5**	**27.5**	17.3	800.1	28.2
C	58.8	5787.6	76.0	54.4	5376.4	73.3	**21.2**	**1446.1**	**38.0**	21.4	1461.2	38.2
D	63.6	6156.6	78.4	63.7	6162.8	78.5	**25.7**	**1468.8**	**38.3**	27.2	1627.5	40.3
E	67.8	6780.2	82.3	67.7	6780.3	82.3	58.5	5466.7	73.9	**57.8**	**5460.0**	**73.8**
F	347.3	164728.6	405.8	347.3	164731.9	405.8	206.7	79744.7	282.3	**190.3**	**74673.1**	**273.2**

Influence of Day and Season

In the next step of our evaluations, we use the weekday and the season as features to predict the traffic volume. Tables 5 and 6 show the performance of ML and DL models respectively. With regards to ML models, similar to rush hour traffic prediction, Random Forest performs slightly better than Linear Regression. With regards to DL models, baseline RNN and LSTM perform similar to ML models in overall and no particular pattern in either directions can be observed. However, GRU and BiLSTM show significant improvements over baseline RNN, LSTM and ML models. In overall, performance of GRU and BiLSTM are relatively similar.

Traffic Volume and Average Speed

In the last part of this section, we explore the prediction performance for traffic volume and average speed. Initially, as a baseline ML model a *MultiOutput Regressor* is used with a Random Forest as the base estimator. Multiple target variables used are traffic volume and average speed with seasonal features. Table 7 shows the KPI results corresponding to these evaluations.

In addition, DL-based models such as baseline RNN, LSTM and GRU are evaluated for predicting average speed and traffic volume as presented in Tables 8 and 9. The average speed prediction performance is these models are varied depending on the tunnel class – i.e., GRU and RNN perform best for classes B and C respectively while LSTM is the best performed for classes D-F. In overall, LSTM shows the best performance. In comparison with a selected ML model, the best DL performer (shown as bold in Table 8) performs better than Random Forest *MultiOutput Regressor* (Table 7) except for class D tunnel. For predicting traffic volume, LSTM performs the best amongst all DL models as shown in Table 9. LSTM also performs significantly better in predicting traffic volume than the ML-based Random Forest *MultiOutput Regressor*.

Table 7 KPI of MultiOutput Regressor for predicting traffic volume and average speed.

Tunnel Class	Traffic Volume			Average Speed		
KPI	MAE	MSE	RMSE	MAE	MSE	RMSE
B	37.1	2456.2	49.5	3.7	39.4	6.2
C	55.5	5061.0	71.1	3.4	27.2	5.22
D	66.8	6800	82.8	1.1	2.7	1.6
E	68.6	6704.4	81.9	4.6	43.4	6.6
F	338.9	150000	398.5	3.4	26	5.1

Table 8 KPI of DL models for predicting average speed.

Tunnel Class	RNN			LSTM			GRU		
KPI	MAE	MSE	RMSE	MAE	MSE	RMSE	MAE	MSE	RMSE
B	3.30	33.20	5.70	3.60	38.50	6.20	**3.20**	**32.0**	**5.6**
C	**2.90**	**26.10**	**5.10**	3.30	29.60	5.40	2.90	26.50	5.20
D	2.50	9.90	3.10	**1.20**	**2.80**	**1.70**	1.80	6.70	2.60
E	3.70	26.90	5.20	**2.60**	**17.40**	**4.20**	3.0	22.10	4.70
F	2.0	14.60	3.80	**1.80**	**12.60**	**3.50**	2.10	16.70	4.0

Table 9 KPI of DL models for predicting traffic volume.

Tunnel Class	RNN			LSTM			GRU		
KPI	MAE	MSE	RMSE	MAE	MSE	RMSE	MAE	MSE	RMSE
B	32.60	2158.7	46.40	**25.50**	**1120.90**	**33.40**	26.90	1478.9	38.40
C	21.20	1602.10	40.0	**18.0**	**988.0**	**31.40**	23.60	1506.3	38.8
D	37.70	2659.6	51.50	**27.10**	**1680.8**	**40.90**	30.3	1935.8	43.90
E	16.8	781.6	27.9	**13.6**	**547.7**	**23.40**	15.90	687.5	26.20
F	90.8	16859.9	129.8	**62.20**	**8457.7**	**91.9**	88.6	17894.3	133.7

From these evaluations it is evident that, in overall LSTM is the best performer amongst all considered ML- and DL-based models in this paper. We therefore would like to explore if LSTM's performance can further be improved using the BiLSTM extension in a similar fashion to previous subsections. Due to bidirectional nature of BiLSTM – by capturing patterns in both past (backward) and future (forward) directions, it is expected that it provides a better understanding of the entire data sequence, leading to better prediction results. Figures 4 and 5 compare the performance of LSTM and BiLSTM in terms of average speed and traffic volume predictions respectively. With regards to average speed prediction, comparing LSTM and BiLSTM's performance do not reveal a particular trend in favour of either of the models as each perform better than the other under a particular tunnel scenario. However, it can be observed BiLSTM performs significantly better than LSTM for the selected tunnel class E – i.e., Ryfylketunnelen (Figure 4). On the other hand, with regards to traffic volume prediction, BiLSTM clearly performs better than LSTM in most scenarios (Figure 5).

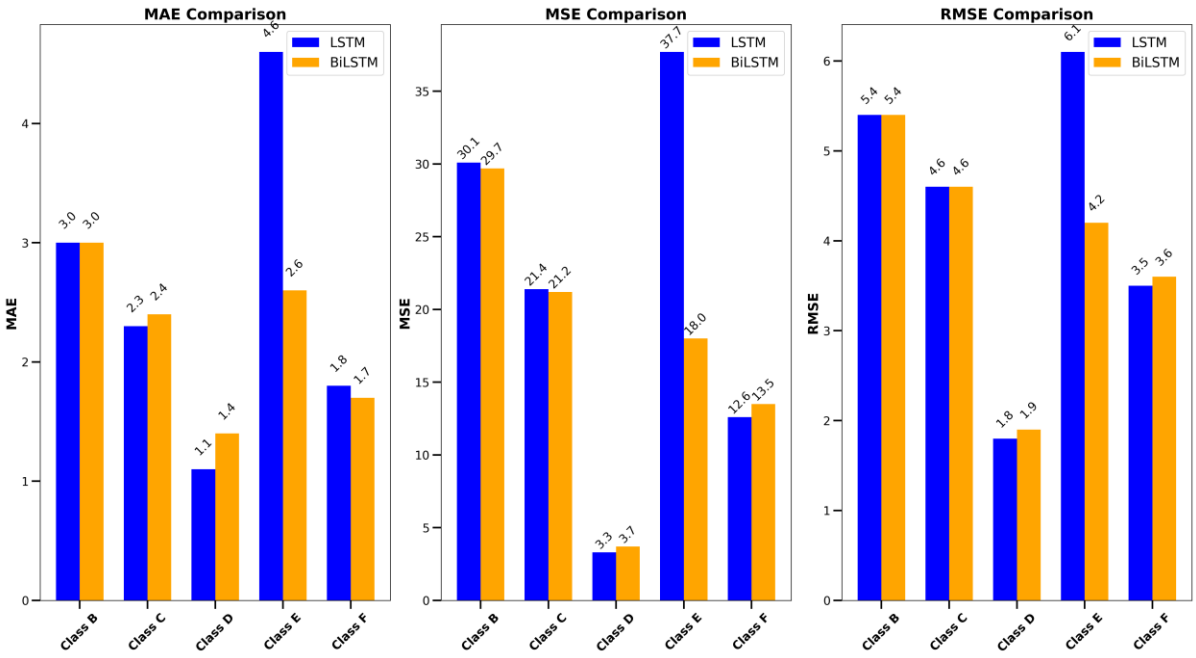

Figure 4 Average speed prediction KPI comparison of LSTM and BiLSTM.

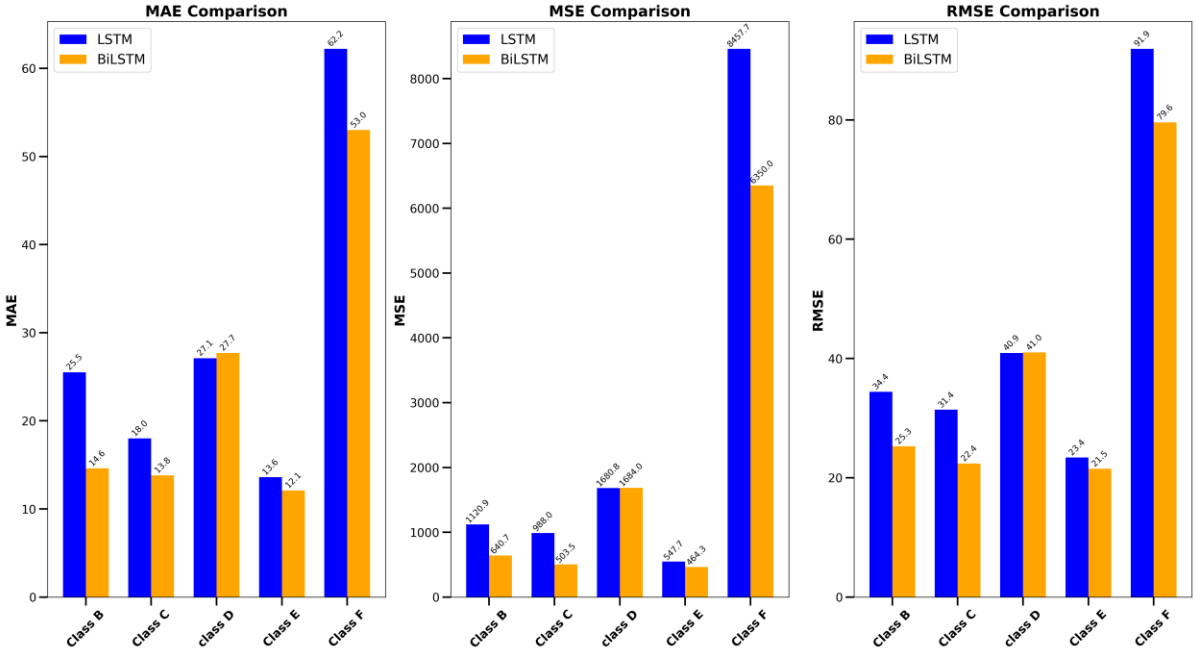

Figure 5 Traffic volume prediction KPI comparison of LSTM and BiLSTM

DISCUSSION

This section presents the outcomes of our investigations into applicability of DL for predicting tunnel traffic, lays out the challenges and limitations of our work, and discusses the potentials of using our models in safety-based DSS, traffic management and policy making.

Deep Learning as a Potential Way Forward

In this paper, we have demonstrated – through utilizing real-life measurement data – that deep learning models can be applied for forecasting traffic in road tunnels. Through exploring various scenarios, we have observed that application of advanced DL models such as GRU, LSTM and its variants (e.g., BiLSTM) can yield better prediction accuracy in most scenarios. These include predicting features such as traffic volume, average speed, and rush hour by, among other things, considering the impact of time of day and season. Our investigations reveal that using advanced DL models such as GRU and BiLSTM can yield better results than traditional ML models such as Linear Regression and Random Forest while performance of baseline DL models (e.g., RNN) can be comparative with ML models. This improved performance of advanced DL models comes with higher computational complexity which may be justified depending on the use-case. It can also be observed that, advantage of BiLSTM versus LSTM is more profoundly visible in traffic volume prediction in contrast to average speed prediction. Our findings in this paper are generally in line with those of Manibardo et al. [9] which critically explores the use of DL for short-term road traffic forecasting, albeit in a road tunnel specific context.

Challenges and Limitations

One of the major challenges of any research like ours is the access to fine-granular traffic data from a large number of measurement points for training ML/DL models. Our work relies on aggregated traffic volume and average speed statistics from nearest roadside measurement points to tunnel portals, averaged on an hourly basis. Access to raw instantaneous in-tunnel traffic data would have likely been beneficial but remains a practical challenge thus far. This is both due to the lack of an access method to raw tunnel traffic data, and the absence of necessary measurement equipment in large number of existing tunnels. In our work, we have addressed this by selecting one representative from each tunnel class to address the latter issue partially. Having an appropriate access method to fine-granular data, in contrast to hourly data, requires further development by road authorities in

collaboration with research organizations and industry. Despite these practical limitations in data access, our work successfully sheds light on the practicality of applying ML/DL for forecasting traffic and its features in road tunnels. Finally, the black-box nature of DL remains a challenge in integration of DL models with other safety-critical systems. However, this is something that is expected to be addressed gradually through *explainable AI* initiatives in the future and by application of EU's AI act [16].

Use of Tunnel Traffic Forecasting for Safety-based Decision Support, Traffic Management and Policy Making

Traffic forecasting is an essential element in design and planning of transportation systems including for road tunnels [1]. This includes congestion and traffic management in both design and operational phases of tunnels' lifespan. Efficient flow of traffic within road tunnels has a more profound implication on safety in comparison with general roads due to special characteristics of road tunnels, as safety-related incidents can lead to tunnel closures and high-risk situations – e.g., involving fire and hazardous smoke in closed environments – creating challenging situations for emergency response. In this sense, the ability to understand and predict the dynamics of traffic within the road tunnels, both in real-time and over long-term, will have significant implications on safety management. Combined with other sources of real-time and historical data, these insights can be therefore used as an important input into safety-based DSS for road tunnels such as our proposed RiskTUN framework [3]. Knowledge and prediction of traffic dynamics within road tunnels can be leveraged in *reasoning* mechanisms within the DSS such as RiskTUN – e.g., to recommend preventive measures. In addition, such traffic forecasting – e.g., average speed or traffic volume predictions – can also be used in combination with Automated Incident Detection (AID) mechanisms – e.g., for real-time detection of traffic queues, or other anomalies that deviate from the expected traffic behaviour – leading to improved safety levels in real-time. Further, knowledge of traffic dynamics and the ability to predict future behaviour can be leveraged in long-term transportation planning including in design and development of future road tunnels enhancing the tunnel safety in long-term.

CONCLUSIVE REMARKS & FUTURE WORK

In this paper we have explored the use of ML/DL for predicting traffic dynamics within road tunnels. To the best of our knowledge, this is the first comprehensive work on this subject considering a variety of tunnel types with various classes, profiles and daily traffic levels spanning over urban, suburban and countryside areas. In doing so, we have explored the ML/DL's ability to predict rush hours, traffic volume and average speed by considering various features including the impact of time of day, weekday and season capturing tunnel traffic dynamics in both spatial and temporal dimensions. Taking selected Norwegian road tunnels as our main use-cases, in this work we use real-life data from measurement points near the tunnel portals, enhancing the validity of our results. Our evaluation results reveal that while advanced DL models such as GRU and (Bi)LSTM perform significantly better, performance of baseline DL models such as RNN is similar to ML models such as Linear Regression and Random Forest. We have demonstrated that BiLSTM can appropriately capture the dynamics of traffic data in timeseries in both forward and backward directions yielding the best results among the studied models. As discussed in previous section, our work in this paper can be considered as a necessary building block within safety-based DSS frameworks for road tunnels. As applied AI sees proliferation in a vast number of areas, it is anticipated that such safety-based DSS will make use of DL to predict the expected traffic behaviour and take necessary preventive measures to mitigate risks and increase overall safety both in real-time and in long-term scopes. Integration of DL-based traffic forecasting in RiskTUN remains a future work.

REFERENCES

1. Button K., "Transport Safety and Traffic Forecasting: An economist's Perspective", *IATSS Research*, **38**, Issue 1, 27-31, 2014. https://doi.org/10.1016/j.iatssr.2014.05.002.
2. Alajali, W., Zhou, W. and Wen, S., "Traffic Flow Prediction for Road Intersection Safety," IEEE SmartWorld, Ubiquitous Intelligence & Computing, Advanced & Trusted Computing, Scalable Computing & Communications, Cloud & Big Data Computing, Internet of People and Smart City Innovation, Guangzhou, China, 2018.
3. Khademi, N., Bjelland, H., Nilsson, E.G., and Boletsis, K., "RiskTUN: An ICT-based Concept for a Riskaware Decision Support System for Tunnel Safety," ISTSS Conference, Stavanger, Norway, April 2023.
4. Zhong, M., Sharma, S., and Lingras, P., "Traffic Flow Prediction using Time Series Analysis", *Transportation Engineering*, **140(6)**, 2014.
5. Lim, J.M., Parthiban, R., Soon, K.L., Chan, R.K.C, "Short-term Traffic Forecasting Model: Prevailing Trends and Guidelines", *Transportation Safety and Environment*, **5**, Issue 3, 2023.
6. Huang, M., and Zheng, J., "Traffic Flow Forecast through Time Series Analysis Based on Deep Learning", *IEEE Access*, **8**, 2020.
7. Chen, Y., Shu, L., and Wang, L., "Poster Abstract: Traffic Flow Prediction with Big Data: A Deep Learning based Time Series Model", IEEE Conference on Computer Communications Workshops (INFOCOM WKSHPS), Atlanta, GA, USA, 2017.
8. Kumar, K., Parida, M., Katiyar, V.K., "Short Term Traffic Flow Prediction for a Non Urban Highway Using Artificial Neural Network", *Procedia - Social and Behavioral Sciences*, **104**, 755-764, 2013. https://doi.org/10.1016/j.sbspro.2013.11.170.
9. Manibardo, E. L., Laña, I., and Ser, J. D., "Deep Learning for Road Traffic Forecasting: Does it Make a Difference?", *IEEE Transactions on Intelligent Transportation Systems*, **23**, 7, 6164-6188, July 2022.
10. Yu, G., and Liu, J., "A Hybrid Prediction Approach for Road Tunnel Traffic based on Spatial-Temporary Data Fusion", *Applied Intelligence*, **49**, 4, 1421–1436, April 2019. https://doi.org/10.1007/s10489-018-1339-3
11. Vlahogianni, E. I., Karlaftis, M. G., Golias, J. C., "Short-term Traffic Forecasting: Where We are and Where We're Going", *Transportation Research Part C: Emerging Technologies*, **43**, 1, 3-19, 2014. https://doi.org/10.1016/j.trc.2014.01.005.
12. Zhao, Z., Chen, W., Wu, X., Chen, P.C.Y. and Liu, J., "LSTM Network: a Deep Learning Approach for Short-term Traffic Forecast", *IET Intelligent Transport Systems*, **11**, 68-75, 2017. https://doi.org/10.1049/iet-its.2016.0208
13. Ma, X., Tao, Z., Wang, Y., Yu, H., and Wang, Y., "Long Short-term Memory Neural Network for Traffic Speed Prediction using Remote Microwave Sensor Data", *Transportation Research Part C: Emerging Technologies*, **54**, 187–197, 2015. https://doi.org/10.1016/j.trc.2015.03.014.
14. Yu, B., Yin, H., and Zhu, Z., "Spatio-temporal Graph Convolutional Networks: A Deep Learning Framework for Traffic Forecasting", 27th International Joint Conference on Artificial Intelligence (IJCAI), 3634–3640, 2017.
15. Abduljabbar, R. L., Dia, H., Tsai, P., "Unidirectional and Bidirectional LSTM Models for Short-Term Traffic Prediction", *Advanced Transportation*, **5589075**, 2021. https://doi.org/10.1155/2021/5589075
16. Regulation (EU) 2024/1689 of the European Parliament and of the Council of 13 June 2024 laying down harmonised rules on artificial intelligence and amending Regulations (EC) No 300/2008, (EU) No 167/2013, (EU) No 168/2013, (EU) 2018/858, (EU) 2018/1139 and (EU) 2019/2144 and Directives 2014/90/EU, (EU) 2016/797 and (EU) 2020/1828 (Artificial Intelligence Act). http://data.europa.eu/eli/reg/2024/1689/oj
17. Vegtunneler håndbok N500, Vegdirektoratet, 2014. http://hdl.handle.net/11250/2419303
18. Trafikkdata, Statens Vegvesen. https://trafikkdata.atlas.vegvesen.no/#/om-trafikkdata
19. DATEX II, CEN/TS 16157. https://datex2.eu/
20. NVDB API v3 Documentation, Statens Vegvesen. https://nvdbapiles-v3.atlas.vegvesen.no/dokumentasjon/openapi/swagger-ui/index.html

21. QGIS Geographic Information System Software. https://qgis.org/
22. Statistics Norway (SSB), https://www.ssb.no/en
23. Wilcox, R.R., Keselman, H. J., "Modern Robust Data Analysis Methods: Measures of Central Tendency", *Psychol Methods*., **8(3)**, 254-74, September 2003. PMID: 14596490.
24. RobustScaler, scikit-learn, API documentation. https://scikit-learn.org/stable/modules/generated/sklearn.preprocessing.RobustScaler.html
25. StandardScaler, scikit-learn, API documentation. https://scikit-learn.org/1.5/modules/generated/sklearn.preprocessing.StandardScaler.html
26. MultiOutputRegressor, scikit-learn, API documentation. https://scikit-learn.org/1.5/modules/generated/sklearn.multioutput.MultiOutputRegressor.html
27. Kingma, D. P., Ba, J., "Adam: A Method for Stochastic Optimization", **v9**, January 2017. https://arxiv.org/abs/1412.6980
28. Cortes, C., Mohri, M., and Rostamizadeh, A. "L2 Regularization for Learning Kernels", 25th Conference on Uncertainty in Artificial Intelligence (UAI '09). AUAI Press, Arlington, Virginia, USA, 109–116, 2009. https://dl.acm.org/doi/10.5555/1795114.1795128
29. Srivastava, N., Hinton, G. E., Krizhevsky, A., Sutskever, I., and Salakhutdinov, R., "Dropout: A Simple Way to Prevent Neural Networks from Overfitting", *Machine Learning Research*, 2014.

Use of a Risk Model to Evaluate Tunnel Safety Features

Sigurjon Ingolfsson[1], Peter Woodburn[2], Frederik Møller Paulsen[3], Rory Turnbull[1]
COWI Arup Joint Venture
Copenhagen, Denmark
[2]now Jacobs
[3] now University College London

ABSTRACT

Sustainability goals are driving designers to re-think business as usual and propose new solutions. For fire safety, these solutions need to be documented as equally safe or safer than the original solution. For Copenhagen Metro M5 line evacuation shafts have been identified as a significant contributor to the project's carbon footprint and impact on the city and as such alternative solution was proposed of evacuation using cross passages to the non-incident tunnel tube. A quantitative risk model was developed to demonstrate that the alternative evacuation strategy of using cross passages at extended spacing is as safe as the previous approach based on shafts.

KEYWORDS: Quantitative risk, Case study, Risk informed design

INTRODUCTION

The Copenhagen Metro M5 line project is a planned automated (driverless) metro system, that aims to link new city development areas in the east of Copenhagen with the existing city. The project will include considerable lengths of bored tunnel alignment and underground stations. One of the project's goals is to reduce carbon emissions by 50% of the construction of the line compared to previous Copenhagen Metro lines.

The fire strategy and design of both the rolling stock and the tunnel is to support the ability of a train experiencing a fire incident to continue to the nearest station (or portal) and safely evacuate the passengers via the station. However, there is a possibility that a train with a fire onboard is not able to continue and could stop within the tunnel. This scenario would increase the risk to the passengers and present additional challenges for the fire and rescue service.

The M5 scheme is being developed using the methodologies set out in the Common Safety Method (CSM)[1]. In accordance with Clause 2.1.4. of CSM, the design team have principally sought to demonstrate compliance by application of recognised codes of practice, such as BOStrab [2] and NFPA 130 [3]. BOStrab recommends the provision of intervention shafts at regular intervals, limiting the distance between exits to not greater than 600 m. However, informed by the projects carbon reduction goal, the M5 scheme proposes an alternative approach, whereby cross-passages are provided between each station with distances between exits in excess of 600 m (the cross passages have been placed at approximately 6-800 m intervals depending on station) and firefighting trolleys provided to enable firefighters to access any incidents within the tunnels. This alternative approach has been evaluated on the basis of the quantitative risk model discussed in this paper.

More specifically, the quantitative risk model is used to assess whether the risk posed to M5 passengers is comparable to the risk for an older Copenhagen Metro line, the M3 (also known as Cityringen, built in 2009) which is considered to have a proven track record of safety. Additionally, the quantitative risk model provides an absolute comparison with a risk matrix developed for all metro lines in Copenhagen.

The use of a quantitative risk model as described above is considered an acceptable route to demonstrate compliance with the CSM, based on the similarities of the two schemes, the M3 and M5 (with the exception of the use of cross passages). By utilising cross passages in lieu of exit shafts, it is estimated that approximately 1.4 million kg carbon dioxide equivalent (CO_2e) are reduced per shaft, on the expectation that each shaft is duly replaced with a cross passage.

MODEL BACKGROUND

The quantitative risk model, employed to evaluate the risk to passengers for the tunnel sections of the M5 line, has been developed to answer the following questions:

1) Do the egress arrangements proposed within the tunnel sections comply with the risk matrix utilised by the metro operator for other lines? The matrix is based on the frequency of incidents and associated fatalities.
2) Can the proposed system have comparable or lower risk to that of the reference system (Copenhagen's M3 line)?

MODEL FUNCTIONALITY AND SETUP

The quantitative risk model is set up as a Monte-Carlo simulation of scenarios with parameters varied in accordance with probabilistic distributions (Figure). The model set-up enabled the design team and other stakeholders to interrogate:

1. Elements of the system that contribute the most to the overall risk of the system.
2. Benefits of individual specific fire safety measures.
3. Model assumptions: which ones are firmly founded in literature and which ones are based on engineering judgement.
4. Resolution of uncertainties.

MODEL ASSUMPTIONS

The model and assumptions have been set up to account for the M5 fire strategy and specific layout of the M5 scheme:

1. The passengers are in a safe area as soon as they reach the nearest cross passage behind the train on fire.
2. The operational procedure for M3 is to avoid trains ramping up in case of a failure somewhere in the ring. All trains are stopped immediately and will then be maneuvered to achieve as many trains as possible within, or close to, stations. The same operational procedure is assumed in this analysis.
3. It is assumed that the 3-car rolling stock, fire suppression and the train control systems will be as safe and reliable as those for the existing lines. Further improvements are anticipated but no account has been taken in the present risk model.
4. The passenger space in the rolling stuck will be equipped with a suppression system. The contribution of this life safety system is not considered within the risk model.
5. It is assumed that the tunnel is always ventilated in the direction of travel and evacuation is directed against the direction of travel i.e. towards the previous station. This leads to the tunnel section from the train towards the destination station being the downstream section of tunnel (smoke is expected in this zone) and the tunnel section from the incident train towards the previous station being the upstream tunnel section (clear air is expected in this zone).

Delay in the activation of fire life safety systems and evacuation – the model assumes that that the fire has brought the train to a halt within a tunnel segment, compromising train control systems that are programmed to continue to the next station. A significant fire would be required to achieve this and as such it is likely that the fire will have been detected, causing activation of the tunnel ventilation

system and the evacuation procedures prior or shortly after the train has been brought to a halt. Any delay between train halt and activation of the afore mentioned system is likely to be negligible and therefore has not been explicitly included.

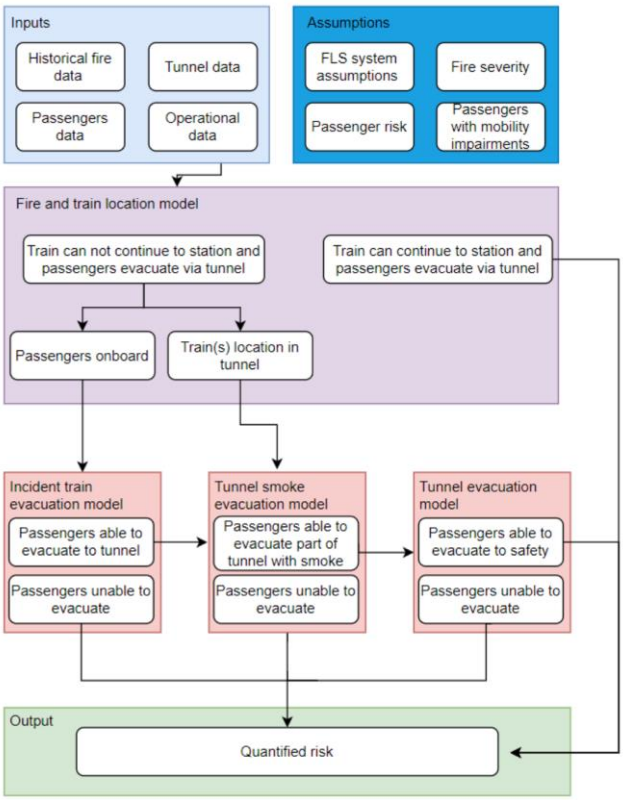

Figure 1 Functionality of the quantitative risk model.

Additionally, there are two major differences between the M3 design and M5 which require evaluation within the model:

1. The increase in expected occupancy of trains and the increase in tunnel lengths. The increase in expected occupancy (maximum occupancy changed from 300 to 350) leads to a change in the model such that each occupant is considered separately rather than as a group of occupants.
2. Due to the longer distances between stations there is an increased likelihood of multiple trains between tunnel ventilation points. It is assumed that the train spacing is such that there is a cross passage in between trains at all times which reflects the operational reality.

MODEL SET-UP

Tunnel Evacuation Model

Evacuation conditions are determined by the effectiveness of the mitigation measures, location of the fire, and the smoke conditions. The primary mitigation measure is for the rolling stock to have sufficient resilience for the train to continue to the next station and evacuate passengers via the station.

However, if this mitigation measure fails and the train comes to a stop in the tunnel, there are four possible fire scenarios based on the tunnel being ventilated/unventilated (smoke conditions) and the fire location being internal/external. The resultant evacuation conditions are indicated in Figure 2.

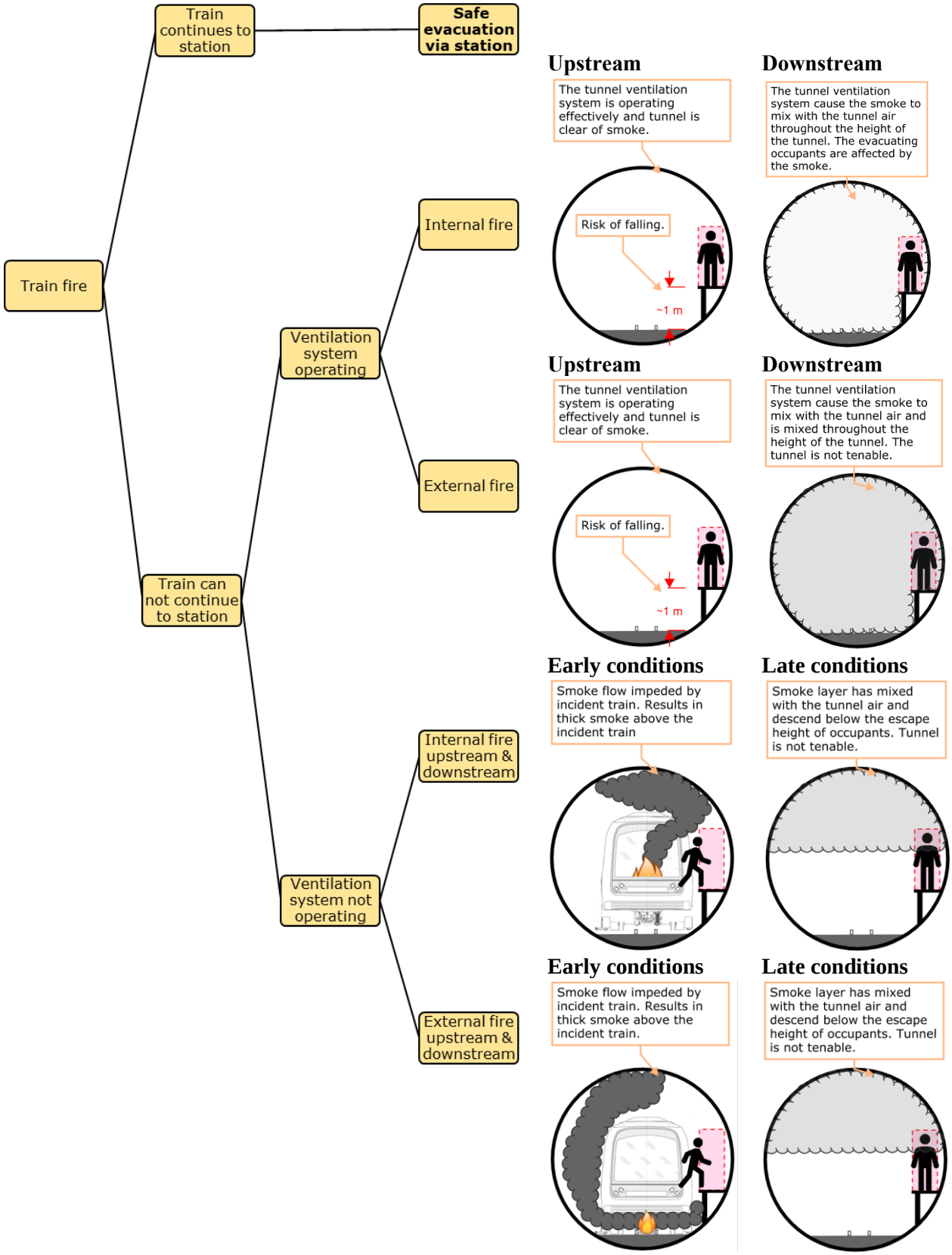

Figure 2 Smoke conditions in tunnel included in the quantitative risk model.

Persons with reduced mobility and other impairments (PRMs)

The definition of PRMs can be broad. For the purpose of the model, Person with Reduced Mobility (PRM) refers to individuals who may have difficulty evacuating due to physical, sensory, and/or

cognitive impairments. This includes people with physical disabilities, elderly people, pregnant women, individuals under the effects of alcohol, and those with temporary impairments (e.g., broken bones). PRMs can be at higher risk, if a fire was to occur and cause the train to a stop within the tunnel. This is due to potentially slower evacuation, as well as wheelchairs, walking aids, able-bodied assistants or similar, being unlikely to fit on the walkway. For this paper, PRMs are categorised into two groups: those that can evacuate independently and those that cannot and may require assistance.

Those that can evacuate independently are included in the non-PRM passenger number. Their reduced walking speed has been accounted for using a triangular distribution of walking speeds, applied to the entire population.

For those that cannot evacuate independently, there is not a specific proportion of the population recommended as PRMs. The population of PRMs is applied as a uniform discrete distribution (a distribution where every one of the outcome values has equal probability) of 0-5 persons on the M5 model. This reflects Danish guidance within DS/ISO 21542, DS handbook 186:2018.

Under the established procedures for Copenhagen Metro, these passengers can move to the upstream area of the train, but may require rescue by firefighters for further evacuation.

Rolling stock safety measures

The M5 line is expected to operate on similar driverless EMU rolling stock as those provided for the M3 line). These trains will meet contemporary fire safety design standards for rolling stock specifically, EN 45545 Hazard Level 2 and OC2. These measures may be active, such as tunnel ventilation, or passive, such as compartmentation. The aspects related to provision of safe evacuation conditions are summarised below (*Table*).

Table 1: Fire protection measures within rolling stock

Fire Protection Measure		**Response Tier**	**Reactive / Active / Passive measure**
Resistance to immobilisation	Fire separation of onboard systems	Primary	Passive
	Redundancy of onboard systems	Primary	Passive
	Fire separation of undercarriage and passenger compartment	Primary	Passive
	Construction of materials of favourable fire performance	Primary	Passive
	Watermist	Primary	Active
Automatic and Visual Detection		Primary	Active
Tunnel Ventilation		Secondary	Active
Communication Systems		Secondary	Reactive

These measures are considered when establishing the assumptions for evacuating the incident train.

Probability the train is within the tunnel

In line with Cityringen (M3), a probability of the train being within a tunnel upon fire ignition as opposed to the station is an input to the model. The probability is calculated based on the travel and dwell times for the scheme. The probability that the train is in the tunnel estimated for M5 is 79.5 % which is considered reasonable given the current dwell and run times estimated for the line.

Location of train within the tunnel

There is a risk that trains are unable to continue onto the next station and become stranded in the tunnel. This is accounted for within the model by describing their location in the tunnel section using a uniform distribution in the model.

If the train is blocked by a non-incident train or the station is blocked, a minimum distance of 50 m between incident and non-incident trains is set in the model in the model as a conservative assumption. This is conservative as the exit ahead is close but occupants are guided to evacuate backwards in the upstream ventilation direction.

Probability a non-incident train is stuck
In line with Cityringen (M3), it is assumed that there is a 0.001% probability that a non-incident train is stuck prior to the station. It is acknowledged that there is a limited dataset to substantiate this number. However, the actual train failure rate per kilometre evidenced on other lines in Copenhagen has been reported to be lower than this, and it therefore presents an onerous probability of a stuck non-incident train.

Probability station ahead is blocked
In line with Cityringen (M3) data, it is assumed that the probability a station ahead is blocked is 1% at 90 seconds headway, with the value being inversely proportional to the headway.

Probability an external fire strands the train
It is assumed that the probability an external fire strands the train is 1/150. Since this scenario has not occurred to date on M3, data for other systems has been used for benchmarking. This rate is supported by data from London Underground having recorded 79 ignitions outside the compartment between 1999 and 2007 [4] whilst recording zero (0) incidents which brought the train to a stop within the tunnel.

Probability an internal fire strands the train
In line with Cityringen (M3), it is assumed that the probability that an internal fire strands the train is 1/1000. The internal compartment is separated from the train control system and motors with fire-rated construction, and motors and critical control systems have redundancy. This probability set recognises that a number of failures of safety systems must occur to lead to a train being stranded in a tunnel.

Ratio of internal to external fires
In line with Cityringen (M3) and data from the operation of Copenhagen Metro trains the ratio of internal to external fires was assumed to be 67% internal and 33% external fires.

Fatality rate for occupants unable to leave train
The quantitative risk model assumes that every occupant unable to leave the incident train within the tenable time limit is a fatality. This conservative assumption has been implemented, as it cannot be demonstrated that occupants inside the train after the tenable time is reached will be rescued or otherwise evacuated. A conservative estimate of 100 % fatality is therefore assumed.

Pre-movement time
The premovement time has been selected to account for the behaviour which is usually observed in fire events. Studies show that occupants generally start evacuation simultaneously and with little delay if the fire or smoke is visible [5]. The fire scenario considered in this risk model is a fire capable of bringing the train to a stop. In addition to this, the rolling stock is supplied with water mist (aimed at internal fires), detection in the external systems for external fires, and voice alarm system providing directions for evacuation. A triangular distribution of 1,2 and 3 minutes (low, peak, high) is implimented in the M5 model for pre-movement time

Tenability time
The time for the train coming to a stand and for the conditions becoming hazardous to life inside the train depend upon the quantity and type of the material ignited and if the fire spread to other materials. Untenable conditions are caused by temperature or smoke. The probability distribution for the time of tenability taken from the risk model for Cityringen is adopted for the M5 model and replicated in *Figure 3*.

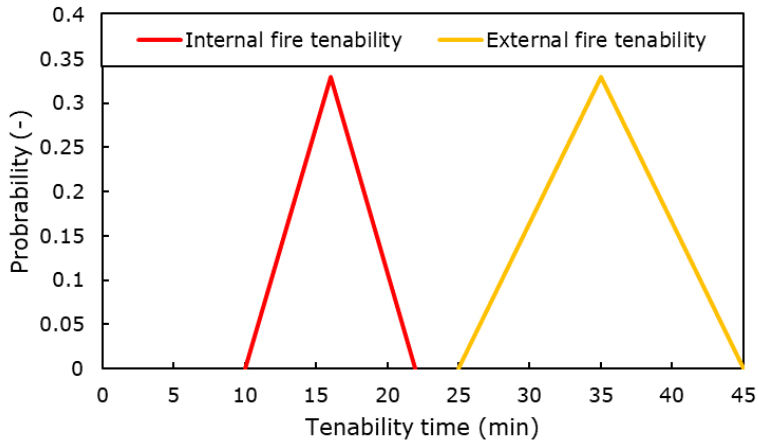

Figure 3: Probability distribution assumed for the fime of tenability for internal and external train fires.

Table 2: Tenable time for an internal and external fire.

	Internal fire	External fire
Minimum tenability (minutes)	10	25
Mean tenability (minutes)	16	35
Maximum tenability (minutes)	22	45

Downstream fatalities

In line with the fire strategy, when the passengers have evacuated from the incident train, they will be directed upstream. The principles for a fire incident with a non-incident train behind is shown in Figure 4.

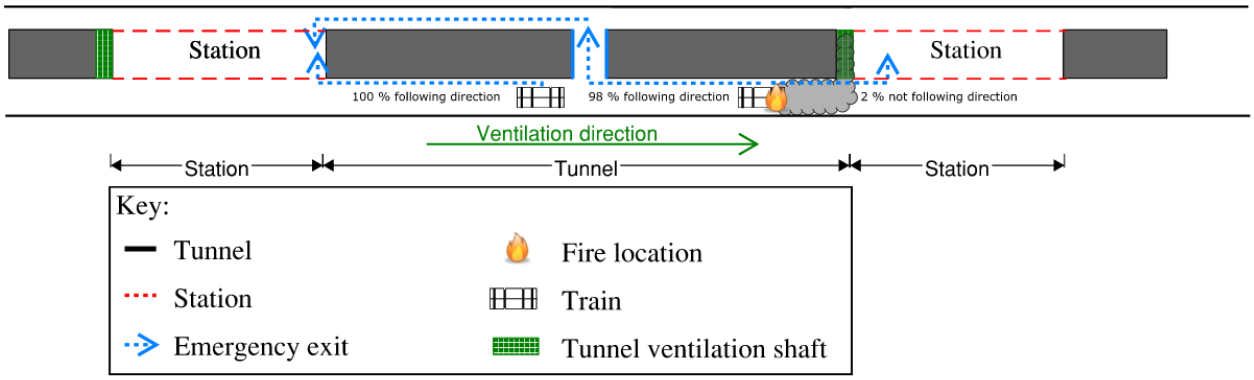

Figure 4: Assumption of evacuation behaviour for a fire incident in the tunnel.

There is a risk that occupants leaving the train onto the walkway may become confused or blocked by the fire, leading to occupants escaping in the wrong direction downstream of the fire via a smoke-logged route.

The authors have not to date found data in the literature on the number of passengers that may become confused and evacuate downstream in the event of fire. For the purpose of the model, a conservative engineering judgement has been made for both schemes:

- **Cityringen** – Cityringen is not provided with Adaptive Dynamic Signage Systems (ADSS) although it is equipped with static directional signage. Therefore, it is assumed that up to

10% of occupants act irrationally and evacuate downstream of a fire, representing a "panic scenario". 20% of this group are assumed to be fatalities. This is implemented as a uniform distribution between 0 and 2%.

- **M5 scheme** – M5 is proposed to be provided with ADSS, which enhances wayfinding, it is assumed that up to 8% occupants may evacuate irrationally, reflecting a 20 % improvement over Cityringen. Of this 8%, it is assumed that 0 to1.6% of these are fatalities as a uniform distribution.

Inclusion of this scenario is considered to be conservative, on the basis that it is unlikely to occur, based on the following points:

- **Trains are unlikely to come to stop within a tunnel in the event of fire:**
  - The fire strategy requires the rolling stock meets the requirements of EC L64/1 2008, which stipulates that the trains must have a running capability of 15 minutes with a fire onboard.
  - The distance between each station takes less than 15 minute travel time. The maximum travel time is expected to be approximately 5 minutes.
- **Occupants are likely to act in a rational manner:**
  - Research suggests that assumptions about human behaviour has shifted from viewing evacuee's behaviour as instinctive, irrational, and even self-destructive, to recognising them as adaptive cooperative decision makers [6],[7],[8]
  - Fire evacuations are usually done in an orderly manner and that people make rational choices based on the instructions received and the cues provided by the fire [9].
  - Research indicates that panic scenarios are more likely to occur where there are physical constraints (e.g. rapidly closing exits) and a lack of adequate communication [10]. These are valid risks that will be addressed in the fire strategy through the provision of a PA system, automatic opening exit doors from the train, ADSS, mist suppression inside the train, and a tunnel ventilation system.
- **There is likely to be strong visual cues of the fire:**
  - Should a fire bring the train to a halt, in light of the rolling stock requirements, it is likely that this would be a significant fire to bring the train to a halt. In such an event there would likely be strong visual cues of the fire and a clear, smoke-free route upstream due to the tunnel ventilation system being activated.
  - Therefore, it is unlikely that occupants would choose to evacuate downstream via the smoke-logged route.

If the system works as intended and in line with evacuation research, all passengers would be expected to either:

- Make a rational choice to evacuate to the direction where there is no smoke due to the tunnel ventilation system.
- Follow the cues of the rest of the crowd which has made the correct choice.

In both these cases, all passengers would be considered to escape safely. Therefore, the assumption that a fraction of occupants choose to evacuate downstream in spite of the cues and instructions available to them is considered to be conservative.

EVACUATION CONDITIONS

Evacuation in upstream conditions

To account for the risk present evacuating via a walkway without a railing, an incident rate is assigned per meter walked in the tunnel in fresh air. In line with Cityringen, an incident rate of 1 per 30,000 metres walked is adopted, with the most likely incident being a trip or a fall. The walkway on M5 is approximately 1 m above the tracks as indicated in Figure 5.

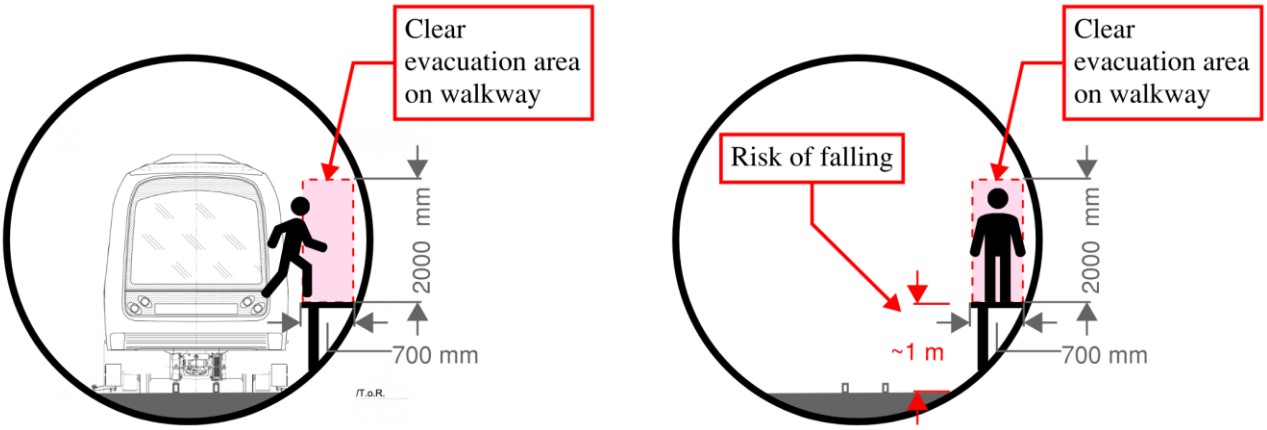

Figure 5: Evacuation via walkway in fresh air and associated risk.

Retrospective research [11] has shown that 2.1 % of falls from heights in the range 0 - 1 m results in a fatality. The fatality rate is rounded up to 2.5 % as a conservative estimate. The remaining 97.5 % of incidents would either result in the occupant continuing towards the exit or being rescued by the fire and rescue services when they arrive.

Evacuation in smoke with operational ventilation system

The tunnel ventilation system is assumed to be effective 99 % of the time. This is based on each set of fans operating effectively i.e. providing sufficient airflow to prevent backlayering allowing intervention and escape. Each of the two fans in each tunnel ventilation shaft are assumed to be 90% reliable as evidenced by historical datasets supplied by the manufacturers.

For the group of occupants evacuating downstream of an incident train discussed in the prior section there is a high likelihood that they will be affected by the smoke. The forced ventilation will cause the smoke layer to mix over the entire cross section of the tunnel. The concentration of this mixture is dependent on the fire size. This gives rise to two separate evacuation scenarios:

- Internal fire – for the internal fire it is assumed that the suppression system fails to control the fire and that a large fire develops. A significant volume of smoke will be produced and the mixture downstream of the incident may not be tenable.

- External fire – for the external fire bringing the train to a stop, it is assumed to be systems fire which has a limited fuel load by design. The initial growth rate will therefore be slowed

- by the fire-resistant floor until the fire breaks into the train causing baggage and the train interior to become involved in a fire.

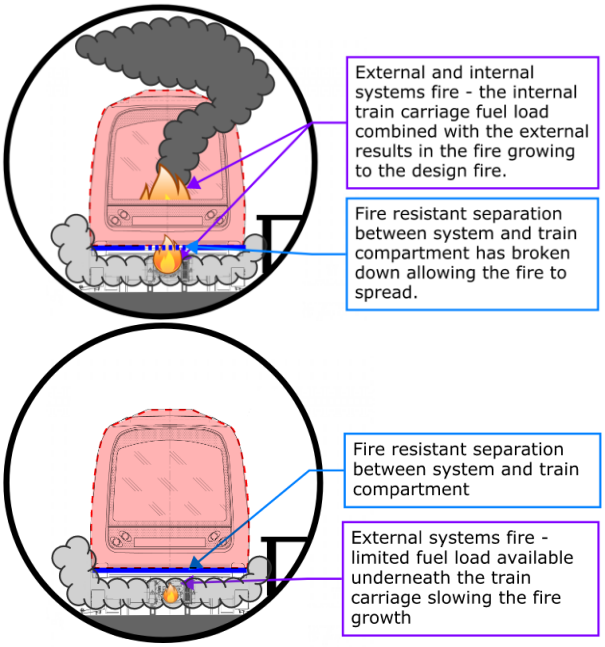

Figure 6: External systems fire breaking into the train compartment with a delay due to the fire resistant floor construction.

Evacuation in smoke without an operational ventilation system

For the unlikely scenario in which the tunnel ventilation system fails to operate and provide critical velocity, smoke is assumed in the model to spread uniformly backwards and forwards. Initially, the air movement within the tunnel is expected to depend on the airflow induced by the trains. As the trains come to a stop the effects of the train, such as the 'piston effect' will decrease and the airflow will be governed by the buoyancy of the smoke. The smoke layer is assumed to stratify initially, but later to become fully mixed over the tunnel cross section within a few minutes and over a short distance in the range of 200-300 meters [12]. The concept is shown in Figure 7.

This leads to the following assumptions for the smoke model:

- Acceleration model – the smoke front acceleration is assumed to be a triangular distribution of 1.5-4.5-9.0 m/min/min (low, peak, high acceleration). This produces a smoke velocity in the expected range of 1 m/s in 7 to 40 minutes for the upper and lower ranges of acceleration respectively.
- Velocity cap – the smoke front velocity is capped at 1 m/s.
- Fatality rate – the fatality rate is assumed to be 100 % if a passenger does not evacuate beyond the smoke layer before it descends or if the passenger is caught by the smoke front before reaching an exit. This is a conservative assumption as smoke exposure is not inherently fatal.

The authors acknowledge that this is a simplistic representation of the complex interactions of smoke and residual airflows within the tunnel system which cannot be fully captured in this type of model. In the results from the model, the assumption of smoke from a large fire which mixes down after a few minutes results in a high number of fatalities (all passengers not initially in front of the smoke) which is considered to be conservative. The same behaviour was assumed for both Cityringen and M5, so allowing comparison.

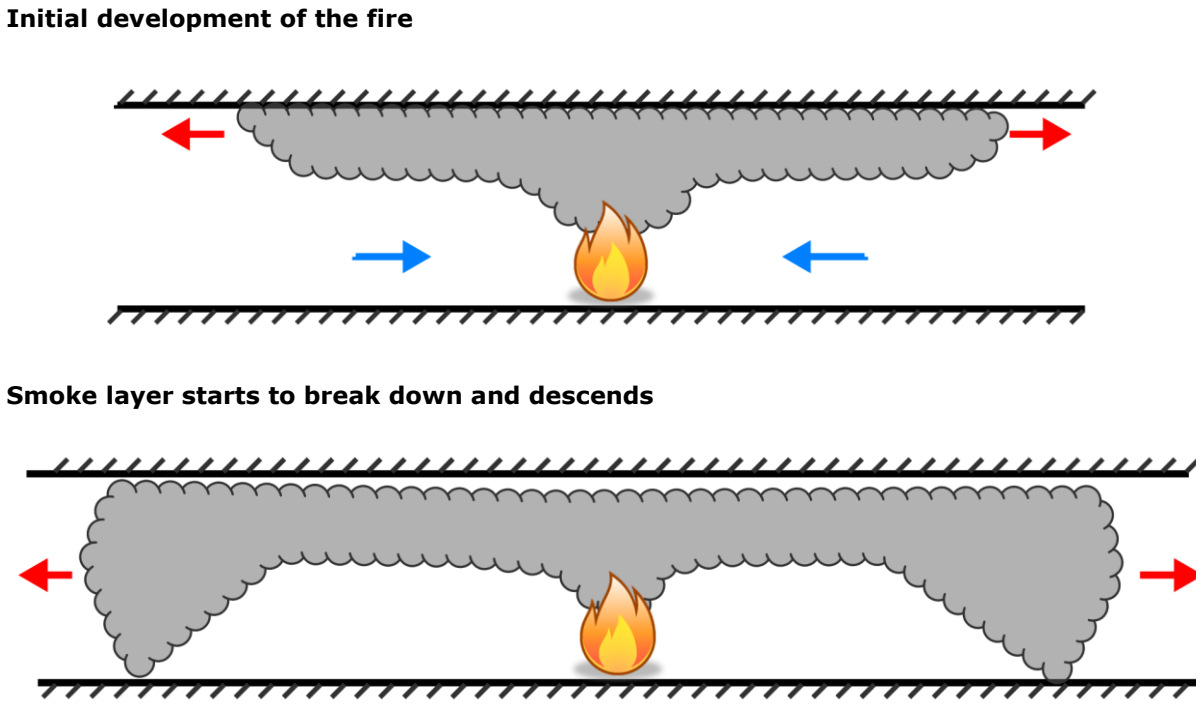

Figure 7: Assumed smoke front development for a naturally ventilated fire.

Train fire and location model
The train and fire location model established the occupancy in the incident and non-incident train, the train's location in the tunnel and the frequency of which a train comes to a stop with a fire.

The evacuation from the incident train model is structured in accordance with Figure 8.

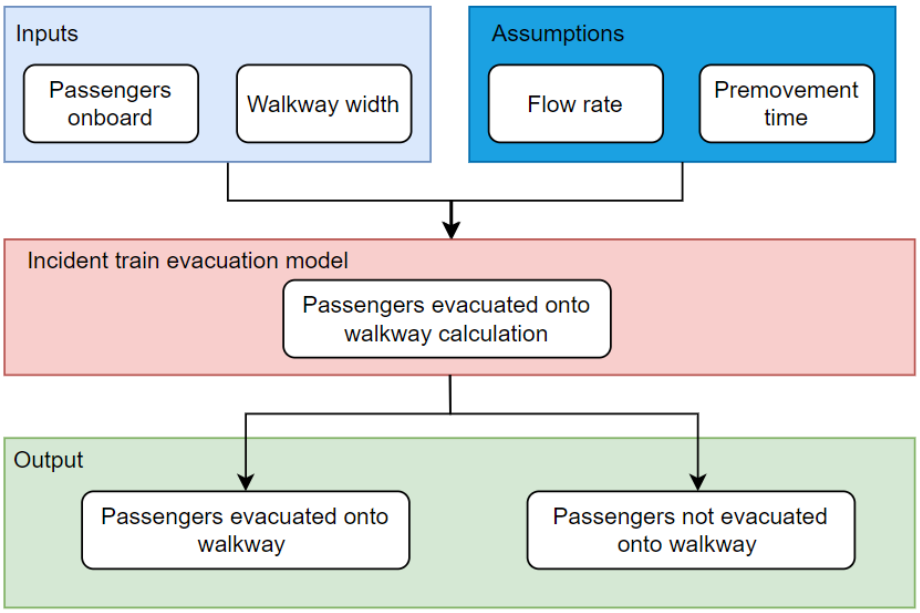

Figure 8: Incident train evacuation model.

Evacuation via the walkway in smoke

Occupant evacuation via the walkway to the cross passage, intervention shaft or station is at risk to smoke from the fire. It is assumed that evacuation with smoke exposure can be grouped into the following:

- Occupants evacuating downstream with a functioning ventilation system
- Evacuation without a functioning ventilation system

Evacuating without a functioning ventilation system would result in the smoke behaviour of a natural ventilated tunnel as outlined in the previous section. This leads to the smoke conditions in the tunnel as indicated in Figure 9.

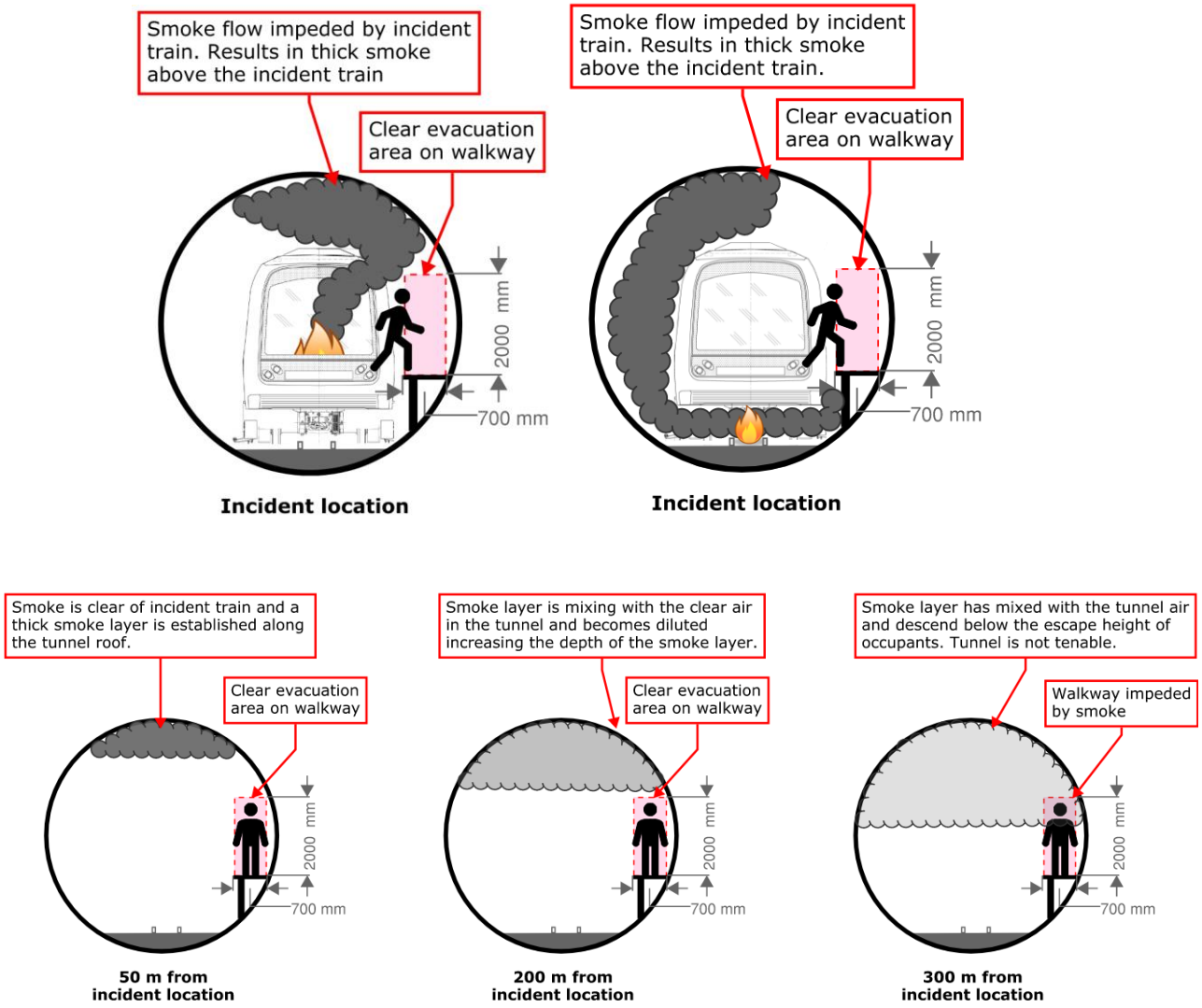

Figure 9: Assumed smoke condition in the tunnel as the smoke front arrives a given distance from the incident location.

For occupants evacuating downstream with a functioning ventilation system the fatality rates outlined in the prior section are applied. This means that the model for evacuation via the walkway in smoke is structured in accordance with Figure 10.

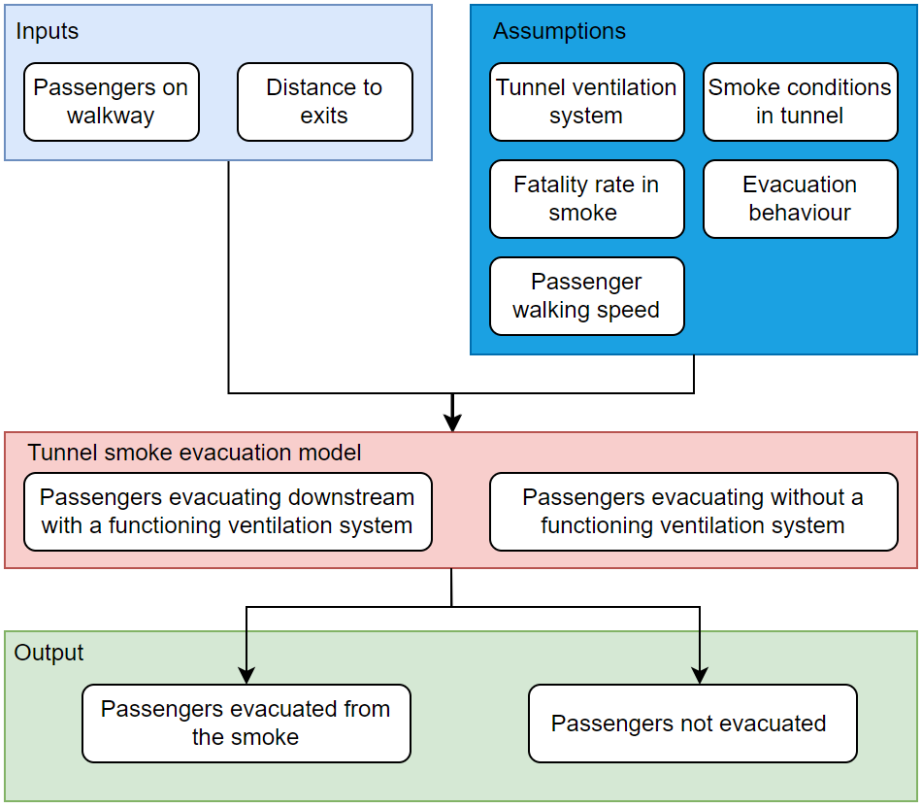

Figure 10: Tunnel smoke evacuation model.

HAZARD MATRIX

As part of the quantitative risk model, a hazard matrix was introduced in line with the frequency and consequence classes outlined in Table 3. The consequence table includes two categories (S0 and S1) for incidents without fatalities. For the current assessment, all S0 and S1 injuries have conservatively been assessed as S1, and recorded as incidents in which no fatalities occurred.

Table 3: Frequency(left) and consequence (right) table.

Class	Description	Frequency range [per year]
F0	Frequent	> 3 x 10^{-1}
F1	Probable	3 x 10^{-2} – 3 x 10^{-1}
F2	Occasional	3 x 10^{-3} – 3 x 10^{-2}
F3	Remote	3 x 10^{-4} – 3 x 10^{-3}
F4	Improbable	3 x 10^{-5} – 3 x 10^{-4}
F5	Very unlikely	3 x 10^{-6} – 3 x 10^{-5}
F6	Barely credible	< 3 x 10^{-6}

Class	Description	No. of fatalities [people]
S0	Minor injury	-
S1	Major injury	-
S2	Serious	1-3
S3	Severe	3-30
S4	Catastrophic	30-300
S5	Disastrous	>300

The corresponding risk matrix is as follows:

Table 4: Risk matrix

		Hazard Consequence class					
		S0	**S1**	**S2**	**S3**	**S4**	**S5**
Hazard Frequency Class	**F0**	Undesirable	Undesirable	Intolerable	Intolerable	Intolerable	Intolerable
	F1	Tolerable	Undesirable	Intolerable	Intolerable	Intolerable	Intolerable
	F2	Acceptable	Tolerable	Undesirable	Intolerable	Intolerable	Intolerable
	F3	Acceptable	Acceptable	Undesirable	Undesirable	Intolerable	Intolerable
	F4	Acceptable	Acceptable	Tolerable	Undesirable	Undesirable	Intolerable
	F5	Acceptable	Acceptable	Acceptable	Tolerable	Undesirable	Intolerable
	F6	Acceptable	Acceptable	Acceptable	Acceptable	Tolerable	Undesirable

And risk classes are to be as defined as follows:

Table 5: Risk class definitions

Risk Class	Action required
Intolerable	Shall be eliminated.
Undesirable	Shall only be accepted when risk reduction is impracticable and with the agreement of the Safety Regulatory Authority.
Tolerable	Acceptable with adequate control and agreement of the Safety Regulatory Authority. Risks shall be further mitigated where practicable.
Acceptable	Acceptable (without needing to consult the Safety Regulatory Authority).

RESULTS

Using the quantitative risk model set-up and assumptions described above, risks have been calculated for the M5 scheme. The hazard matrix results for the M5 scheme, and its variations and reference Cityringen (M3) are shown below in Table 6 (S0 injuries included in S1 for both).

Table 6: Hazard matrix for M5 base scheme (3-carriage trains), 4-carriage train and 70s peak headway variant, and Cityringen (M3). The relevant outcome for each consequence class is bolded in the tables.

M5 scheme (cross passages, including 3 train-carriage, 4 train-carriage and 70 s headway case)

		Hazard Consequence class					
		S0	**S1**	**S2**	**S3**	**S4**	**S5**
Hazard Frequency Class	**F0**	Undesirable	Undesirable	Intolerable	Intolerable	Intolerable	Intolerable
	F1	Tolerable	Undesirable	Intolerable	Intolerable	Intolerable	Intolerable
	F2	Acceptable	Tolerable	Undesirable	Intolerable	Intolerable	Intolerable
	F3	Acceptable	Acceptable	Undesirable	Undesirable	Intolerable	Intolerable
	F4	Acceptable	**Acceptable**	**Tolerable**	Undesirable	Undesirable	Intolerable
	F5	Acceptable	Acceptable	Acceptable	**Tolerable**	Undesirable	Intolerable
	F6	Acceptable	Acceptable	Acceptable	Acceptable	**Tolerable**	**Undesirable**

Cityringen (M3) evacuation shafts

		Hazard Consequence class					
		S0	**S1**	**S2**	**S3**	**S4**	**S5**
Hazard Frequency Class	**F0**	Undesirable	Undesirable	Intolerable	Intolerable	Intolerable	Intolerable
	F1	Tolerable	Undesirable	Intolerable	Intolerable	Intolerable	Intolerable
	F2	Acceptable	Tolerable	Undesirable	Intolerable	Intolerable	Intolerable
	F3	Acceptable	Acceptable	Undesirable	Undesirable	Intolerable	Intolerable
	F4	Acceptable	**Acceptable**	**Tolerable**	Undesirable	Undesirable	Intolerable
	F5	Acceptable	Acceptable	Acceptable	**Tolerable**	Undesirable	Intolerable
	F6	Acceptable	Acceptable	Acceptable	Acceptable	**Tolerable**	**Undesirable**

As shown in Table 6, the M5 scheme and its variants are generally within the acceptable and tolerable consequence classes with the exception of the S5 consequence class where the lowest risk class is 'Undesirable'. However, it is noted that Cityringen also achieves "Undesirable" against the S5 consequence class. It is noted that these were primarily driven by extremely low probability events (in the region of 10^{-9}) which are not affected by the choice between cross passages and shaft. It was demonstrated to the Safety Regulatory Authority that further mitigation of these remaining S5 risks is not considered reasonably practicable.

DISCUSSION

General notes

The following observations can be made from the experience of applying and refining the model:

1. Utilising a model such as the one described in this paper provides a level of insight into the aspects of the design and impact of proposed safety measures which is not available to a designer when designing in line with codified norms.
2. The comparison to a similar (but not identical) system enables the impact of specific design choices (such as distance between intervention shafts) to be clearly identified.
3. Due to its complexity and sensitivity to inputs, using the model as an explicit estimator of risk needs to be done with caution (though this is possible with enough refinement). It provides an indication as to the origin of risk and the benefits of individual mitigation measures.
4. Due to the lack of reliable, verifiable and generally applicable data sets, a degree of engineering assumptions have to be made. These were supported by sensitivity studies to ensure the conclusions are not unexpectedly impacted by the assumptions made. This was undertaken for each parameter where robust data was not available.
5. Similarly, adding complexity (e.g. a highly refined fire brigade intervention model), needs to be done with caution as additional complexity may require additional assumptions and increase uncertainty which may not ultimately benefit the analysis.
6. Inputs which heavily influence the outcome of the model as constructed include:
    a. Decision making for occupants has a large influence on the risk level. This particularly applies to occupants who choose to evacuate downstream into smoke. Therefore, improving the information given to occupants is highlighted as a significant risk reduction measure.
    b. Similarly, the reliability of the tunnel ventilation system has a significant contribution to the risk outcome.
    c. The importance of enabling an incident train to reach the nearest safe area is highlighted by the model.
    d. The rate of ignition and potential for rolling stock to stop in a tunnel environment; as envisaged by modern approaches to safety: the fire survivability of rolling stock yields greater safety benefits than adding measures to the tunnels.

Specific observations

Operational strategy with shafts or cross passages

Evacuation

In terms of evacuation, as evidenced by the model, there is no material risk difference between the provision of a shaft or cross passage for the system under examination. Occupants will either need to use a vertical stair in an intervention shaft or walk horizontally to the next station after utilising the cross passage but either way they would be considered to be in a place of relative safety.

Firefighter intervention

No estimation of fire service arrival time or the explicit benefit of their intervention has been made as no benefit of fire service intervention has been taken into account in the model. The model assumes that the fire develops freely, without suppression from the mist suppression system or the fire service.

This is considered to be a conservative assumption for occupant fatality rates within the model, as this results in a more onerous conditions to evaluate tenability and increases the fatality rate along the walkway. Accounting for intervention would result in a less onerous outcome (lower fatalities and injuries).

However, it should not be taken to mean that no facilities or access to tunnels for firefighting should be provided. This is more a reflection that the model as constructed is not well suited to evaluate the risk posed to firefighters. As such, firefighting provision has been undertaken on a more qualitative basis and in collaboration with first responders, but it can be summarized as follows:

Upon arrival at the station, fire fighters will access the tunnels through stairs and escalators at the stations.
A walkway will be provided for horizontal movement through the tunnel, firefighting trolleys will also be located at the stations.
In the event of a single cross passage between stations, where the fire location is at or before the cross passage, there is no difference in fire fighter operation procedures, as the tunnel vent system would operate to clear smoke downstream in the incident tunnel and the fire fighters would access the tunnel at the nearest station upstream, traversing down the incident bore using the firefighting trolleys.

Reversing non-incident trains
The model does not consider the potential for non-incident trains behind the incident trains to be reversed. This can have a significant benefit for firefighting operations and reduce the overall risk posed to occupants.

Model purpose
It important to note that the intent of the risk model is to assess whether the provision of additional cross-passages and/or intervention shafts is adequate, through comparison with Cityringen as a "similar system". As such, factors which are different between the two systems are of importance but factors which remain the same do not impact the comparative assessment.

CONCLUSIONS

As part of a sustainability-led design, a quantitative risk model was developed which enabled the identification of the principal sources of risk within the tunnel system and the benefits of individual mitigation measures.
These insights have been used to develop a significantly more sustainable design through the reduction of the number of evacuation shafts while maintaining the risk to passengers to levels which are comparable with or lower than those of the existing rail lines. Measures which have clear safety benefits were highlighted by the model; these have been identified for further development as the M5 design progresses.

REFERENCES

1. European Union Agency for Railways, *Common Safety Method (CSMs),* 2016
2. German Federal Ministry of Transport, *Verordnung über den Bau und Betrieb der Strassenbahnen.* 2010.
3. National Fire Protection Association, NFPA 130, *Standard for Guideway Transit and Passenger Rail Systems*. 2023
4. London Underground data
5. E. Kuligowski, "Human Behaviour in Fire," in *SFPE handbook*, 2016, pp. 2070-2110.
6. E. Kuligowski, "Terror Defeated: Occupant Sense-making, Decision-making and Protective Action in the 2001 World Trade Center Disaster," University of Colorado, 2011, p. Ph.D. Thesis.
7. S. Gwynne, E.D. Kuligowski, M.Kinsey, "Human Behaviour in Fire - Model Development and Application," in *Human Behaviour in Fire Conference*, Cambridge, UK, 2015.

8. E. D, Kuligowski, S.M.V. Gwynne, M.J.Kinsey, L.Hulse, "Guidance for the Model User on Representing Human Behaviour in Egress Models," *Fire Technology,* no. doi: 10.1007/s10694-016-0586-2, 2017.
9. E. Kuligowski and S. Gwynne, "The Need for Behavioral Theory in Evacuation," in Pedestrian and Evacuation Dynamics 2008, Berlin, 2010.
10. CTIF, "Panic and Human Behaviour in Fire and Emergency Situations," 10 Jul 2018. [Online]. Available: https://www.ctif.org/news/panic-and-human-behavior-fire-emergency-situations. [Accessed 16 08 2024].
11. Kasim Turgut et al, "Falls from height: A retrospective analysis," *World Journal of Emergency Medicine ,* vol. 9, no. 1, 2018.
12. R. C. Hall, "Ventilation during road tunnel emergencies," Mott MacDonald, 2006.

Dutch road tunnel firefighting in the future: outlook from a Dutch fire fighter's perspective

Nils Rosmuller & Arjen van Barreveld
NIPV, Netherlands Institute for Public Safety
Box 7010, 6801 HA Arnhem, The Netherlands
E-mail: nils.rosmuller@nipv.nl

ABSTRACT

The tunnel safety landscape is changing. New energy carriers and bigger vehicles cause bigger and more complex fires. Meanwhile, fire suppression techniques evolve as well, and the firefighters become more defensive in their tactics. We studied fire characteristics of green vehicles (Battery electric, liquid bio-fuels, liquid gasses (LPG and LNG) and compressed gasses (CNG and hydrogen) and compared them with the traditional fuels such as petrol and diesel. In addition, we studied tunnel and fire suppression developments. As a result, we think that the current (Dutch) SoP for tunnel fire-fighting should be re-evaluated by the tunnel providers and fire fighters together, taking into account the three above described developments. Despite the fact that we studied tunnel fire suppression from the Dutch perspective (Dutch road tunnels, Dutch SoP's and the car population), the arguments that we formulated for seriously (re) considering daily practise in tunnel fire suppression could be of great value for other countries and their tunnel providers and firefighters as well.

KEYWORDS: road tunnel, firefighting, future scan, new energy carriers

1. INTRODUCTION

Dutch road tunnels exceeding 250 meters are recognized for their high safety standards. Tunnel safety regulations are established in the Tunnel Safety law (2006) [1], and includes amongst others one way driving per tunnel tube, tunnel ventilation, emergency and traffic control rooms, emergency response cabinets and emergency procedures. However, since 2006, things are changing. Road vehicles' fire characteristics deteriorate (heavier and bigger vehicles containing more rubbers and plastics) and change (battery electric vehicles, LNG, CNG, hydrogen fuel systems) [2]. In addition, fire suppression technologies such as sprinklers, autonomous systems,,..) evolve. And finally, the fire suppression tactics change from an almost irrefutable offensive tactic (fire crew in the tunnel suppressing the fire) to a more defensive tactic (no fire crew in the tunnel or at a relatively large distance from the fire safeguarding the infrastructure and other vehicles) [3]. These three developments may affect road tunnel fire suppression. Therefore, an exploration of the future Dutch tunnel fire suppression tactics is necessary. Together with the Dutch fire association, we performed a project that explores the developments.

The aim of this article is to describe the trends in road traffic, fire suppression technology and the consequences for Dutch future fire suppression tactics [4]. We first present the common Dutch standard operating procedure for tunnel fires (section 2). Then, our focus will be on the future (2030-2035). Our research approach for the future scan was threefold. We studied literature to get a grip on the future vehicle trends that affect tunnel safety (section 3). We studied developments in fire suppression technologies (section 4). Finally, we deduced topics for (re)consideration of the current Dutch tunnel fire suppression standard operating procedure (SoP) (section 5).

2. DUTCH STANDARD OPERATING PROCEDURE FOR TUNNEL FIRE FIGHTING

The road tunnel safety requirements in The Netherlands is pretty complex. It is based on four laws, including the Building code, the Road tunnel safety law, The Dutch Security Regions Act (a set of regulations and tasks for fire brigades) and the Labor law. In the end, it results in a national standard for tunnels (with two separated tunnels tubes (one for each traffic direction), mostly connected via either a middle tunnel service corridor or cross connections, and prescribed technical features such as tunnel ventilation, escape routes, emergency cabinets), and a standard method to quantify the road user risk (and a risk threshold). Like the safety measures, there is a kind of 'standardized' fire suppression procedure in Dutch road tunnels [5]. Of course fire tactics may change as a result of the specific tunnel design, the fire scenario and the capabilities of the fire crew and improved fire suppression methods.

As for the tunnel fire scenarios, there are several numbers of heat release rates (MW) for different vehicle fires. Based on those numbers and sources, some ranges of heat release rates and the time taken to reach peak heat release rates (minutes) are presented below. These numbers are intended only as a guide for the officer-in-charge. Fires having a capacity of more than 50 MW are labelled 'big' (M2/M3 vehicles/buses). This comes down to the category of 'big' vehicles (weight, size, more than 4 wheels). The category M1 vehicles concerns passenger cars.

Table 1 Summary of key HRR-figures from the literature [6], [7] and [8, based on] (NFPA 502, Oosterveld (2013), (Rosmuller (2017), based on [9]

Vehicle	Heat release rate (HRR) in MW	Time to peak heat release rate (PHRR) in minutes
'Small' fires: <50MW		
1. Passenger car	5-10	10
2. Multiple passenger cars	10-20	20
3. Van	15-30*	10
'Large' fires: >50MW		
4. Bus	45-60	15
5. Truck including load	50-150	15
6. Tank lorry with flammable liquid	200**	??

* Based on [10].
** There have been incidents where significantly higher heat release rates have been reported: Caldecott USA, 1982 and Skatestraum Norway, 2015.

The main responsibility of firefighters in the Netherlands, as outlined in the Dutch Security Regions Act, is suppression and the rescue of individuals. Damage control and the tunnel's operational reliability may be considered but are not part of the fire department's primary duties. Tunnel firefighting in the Netherlands in the first minutes after a (fire) report is quite standardized and written down in a uniform way [11]. Consequently, we can speak of a standard operating procedure (SoP) in (road) tunnel firefighting that applies to the standard tunnel situation described above. Exceptions are when the 1) doors are located further apart (e.g. 250 m) and 2) when there is a traffic jam downwind. In addition, it is always the decision of the officer-in-charge on site which incident response strategy is followed. The phases in case of fire are basically as follows:

> The traffic controller/tunnel operator at the traffic center is alerted to an incident or emergency by

standstill detection and/or fire alarm. The situation on site - like the fire location and spread to other vehicles - can be assessed using CCTV camera images.

> The traffic controller/tunnel operator activates 'emergency operation' if necessary. The illumination system, tunnel (longitudinal) ventilation in the traffic tube (>500 m) and ventilation in the middle tunnel channel are activated to create overpressure. The lanes are closed by traffic lights and barriers and the fire extinguishing facilities are pressurized. If evacuation of the incident tube proves necessary, 'evacuation mode' will also be activated. Evacuation instructions via sound beacons and radio will be broadcast. In addition, contour lighting around the escape doors will be activated.

> Alarms are sent to the joint emergency services control room (dispatch center). The information transfer that takes place is prescribed by law in appendix 3 of the regulation for additional road tunnel safety rules (Rarvw) [12]. Information such as the exact location and nature of the incident, desired deployment and best approach route will be communicated, after which a fire engine will be dispatched to the tunnel fire.

The approach procedure in emergencies for the fire brigade is in principle as follows:

> From the nearest fire station, at least one fire engine with priority drives to the entrance of the supporting tunnel tube. The priority vehicle approaches the tunnel entrance in accordance with the regular traffic direction. Normally, one fire engine will be dispatched for a vehicle fire. However local policy deviations , such as having two trucks approach the scene from different directions, are common. Furthermore the incident commander can escalate the fire department's response if deemed necessary.

> Arriving at the tunnel tube, the fire engine can contact the traffic control center via the emergency services panel located outside the tunnel and view camera images to form a picture of the nature and extent of the incident.

> The fire engine, at the indication of the traffic control center, enters the parallel and save tunnel tube as far as the first door beyond the incident.

> Through the escape doors and the cut-through, the incident tube is reached and the incident is approached 'upwind'. An initial reconnaissance is carried out answering the following questions:

Is it a small or large fire? ?
Is the tunnel ventilation working?
Is there a change of incident escalation?
Are there additional hazards?(?

> Via the cross connection, firemen crosses over form the parallel tube to the incident tube, where the low pressure hoses are connected to the Storz couplings present in the emergency cabinet.

> Final extinguishment takes place in compliance with the *Basic Principles of Tunnel Fire Fighting* [5].

By systematically addressing the key questions above, a well-informed and evidence-based decision can be made regarding the appropriate firefighting strategy to be implemented. The term 'small' does not mean small fire, but is intended to indicate fires with one or more somewhat smaller vehicles in terms of weight, size and heat release rate (passenger car and van: see table 1) and to distinguish them from fires with large vehicles such as buses and trucks. Combined, the size of the fire and the operation of tunnel ventilation give four quadrants [5]. The preferred action is labelled in each of the quadrants.

Table 2 Quadrant model for tunnel firefighting [5]

		Tunnel ventilation	
		Does work	**Does not work**
Fire	**'Small' (<50MW)**	Offensive inside: deployment in the incident tube, from the supporting tube and aimed at rescuing victims/extinguishing the fire[1)]	Defensive inside: deployment from the supporting tube, aimed at creating safe escape/approach[2)]
	'Large' (>50MW)	Offensive outside: outside deployment from the tunnel mouth of the incident tube, and aimed at rescuing victims/extinguishing the fire	Defensive outside: deployment from outside the tunnel, preventing spread to surrounding area

1) In this case, the low pressure hoses or O-bundles are taken from the support tube to the incident tube and there attached to a special coupling in the auxiliary box.

2) In that case, the officer-in-charge may consider laying the hoses from the fire truck through the cross section to the incident pipe rather than connecting them (only) to the aid station. In a fire of this size, the emergency stations may not have enough water to fight the fire. These are situations where the available capacity of 120m^3 /h from the aid station proves insufficient. The fire truck with 1.5m^3 water on board can itself be used as the first water supply. Soon that quantity of water will be exhausted, and so it will have to be relayed to another (continuous) water supply. To this end, large scale water supplies will presumably be deployed. If the hoses are routed through a culvert or the middle tunnel duct, doors to the middle tunnel duct remain open and there is a risk of smoke spreading. In that case, however, structural safety, or maintaining the tunnel structure, prevails over keeping the middle tunnel channel smoke-free. In our opinion, this is also justified in such cases because (if all goes well) no one will be in the middle tunnel channel anyway by the time the fire has escalated to > 50 MW and the fire brigade is on site by then.

The traffic controller/tunnel operator will provide valuable information and have an advisory role. However it is always the fire commander, in coordination with the Duty Officer, who determines the deployment tactics based on his own professionalism, experience and familiarity with the location, and on the basis of the equipment, the incident scenario progression et cetera.

3. NEW ENERGY CARRIERS IN TRAFFIC

The vehicle population in the Netherlands is changing rapidly. For decades, passenger vehicles have been growing in size and weight.

Use of plastics in passenger cars
Government-imposed or otherwise, in terms of fuel efficiency, durability and safety, metal parts have mostly been replaced by durable plastics in recent decades. These tend to make a vehicle safer, lighter, more rust-resistant and cheaper. However, the downside is that a fire can develop faster and the potential heat release rates are higher. This leads to fires increasing in size faster, which has implications for described firefighting [14].

In recent years, new types of zero-emission/new energy carriers vehicles enter the passenger car markets, such as battery electric cars or hydrogen-powered cars. A similar sustainability trend is also visible in public transport and freight transport. New energy carriers will potentially lead to different fire scenarios compared to the traditional fossil fueled vehicles. Below, we present the upcoming and already ongoing larger changes in new energy carriers, including their impact on fire development. Battery electric; liquid biofuels; liquefied gases and compressed gases We conclude this part of the paper considering any additional risks arising from the new energy carriers entering the vehicle

population.

Battery electric vehicles

The total heat release rate of an electric vehicle is comparable to that of a similar vehicle running on fossil fuels. The bulk of the fire load is in the chassis and body of the car; the battery contributes only a limited amount to the total heat release rate.

There is, however, a substantial difference between the fire progression of electric vehicles and fossil fuel engine vehicles. Although the lead time is similar, varying between 10 and 20 minutes until peak heat release rate is reached, electric vehicle fires are characterized by multiple peaks.

In addition, a fire in a Li-Ion pack proves difficult to extinguish because it is difficult to penetrate the battery pack with the extinguishing agent, mostly water. In addition, a 'thermal runaway' can occur within the battery pack. This is a process in which there can be re-ignition of the battery pack for an extended period of time. This means that a fire can keep reigniting, especially with much lager truck batteries, up to days after it has started.

Liquid bio fuels: bioethanol and biodiesel

Liquid biofuels generally have a lower energy density than fossil fuels. Whereas petrol and diesel have an energy density of around 43 MJ/kg, this is significantly lower for liquid biofuels: 27 MJ/kg and 37MJ/kg for bioethanol and biodiesel, respectively [15]. Although exact data are lacking, it is therefore plausible that the heat release rate for liquid biofuels *is lower* than for fossil fuels. However, there is no reason to believe that the burn rate is significantly, in terms of risk, different from that of conventional liquid fuels. This applies to all types of vehicles, from passenger cars to trucks.

Liquid gases: LNG and LPG

Vehicles can also run on gases formed into liquids in two different ways. First, we know gases cooled to liquid. LNG is an example of this. In an incident, part of the gas may evaporate immediately, while another part forms a puddle and then evaporates. LNG is used in trucks, and also has a renewable variant with Bio-LNG. Secondly, we know gases compressed to liquid, such as LPG. Again, part of the gas may evaporate in an incident, and the other part forms a puddle which then evaporates and form an explosive risk.

Vehicles with liquefied compressed or refrigerated gases do not significantly outperform conventional vehicles in terms of total heat release rate. However, the fire behavior may be different, especially with liquefied compacted gases. When the storage tank becomes pressurized due to heating, the overpressure protection (pressured relief device (PRD) will be activated causing it to blow off, until the excess pressure is levelled out. This creates a risk of short-term recurring flares. For a truck running on LNG, some impact distances have been depicted based on modelling. Tank rupture, or similar damage, can result in a flare fire up to 96 meters; an irradiation-induced hot BLEVE can result in a fireball up to 31 meters from the source [16].

Compressed gasses: CNG and Hydrogen

The data for hydrogen and CNG are similar. The heat release rate of a hydrogen car is similar to that of a conventional car, although the heat release rate when a flare occurs can be temporarily significantly higher: 5-10 MW without flare, up to as much as 25-30 MW with flare. CNG and hydrogen cars contain thermally pressured relief devices (TPRD). Contrary to the PRD's in LPG and LNG tanks, the *thermally* pressure relief device remains open only until excessive pressure is blown off. This means that in case of fire, the overpressure protection device is activated again and again in case of temperature rises above 110degrees Celsius. The pressure relief prevents for the tank to explode, and is therefore a relevant safety measure [17]. The heat release rate of a CNG truck (around 80 MW) is also similar to that of a regular truck [18]. The flare is created the moment a tank is ignited, and the 'thermal pressure relief device' (TPRD) is activated. Since a hydrogen vehicle may have multiple tanks, the peak heat release rate may occur at multiple times. When multiple tanks are irradiated at the same time, multiple TPRDs may also be activated at the same time, even though this is not obvious. The size of the flare depends on the diameter of the TPRD combined with the pressure of the tank, and usually of short duration. In case the CNH of hydrogen tank rolls onto side, the TPRD

may be below the liquid level in the tank and the heated tank might force liquid out of the TPRD, causing a spray of flammable liquid.

Assessment of the new energy carrier fire characteristics
Table 3 shows our comparison of heat release rates and fire behavior of new energy carriers and conventional fuels in a qualitative way.

Table 3 Heat release rate and fire behavior of renewable vehicle propulsion options compared to conventional fuels (petrol/diesel)

	Heat release rate	Fire behavior
Battery Electric	Similar	Possibly characterized by multiple peaks, thermal runaway
Liquid bio-fuels	Lower	Similar
Liquefied gases	Similar	Probability of flare fire and BLEVE, possibly multiple spikes
Compressed gases	Similar	Probability of flare fire and BLEVE, possibly multiple spikes

With the exception of battery-electric, the fire scenarios (heat release rate and fire progression) are reasonably similar to those of fossil fuels. So in the future, we will continue to see fires similar to current petrol and diesel fires.
The risk of explosions will also remain, as we know today for LPG vehicles. However, vehicle fires in electric vehicles, when the battery goes into thermal runaway, may cause a different fire behavior. The most effective way to attack battery fires is to concentrate water flow onto the battery pack to reduce temperature of the cells and avoid thermal runaway and reignition [6]. However gaining access to the battery pack can be problematic. In addition, firefighting in tunnels of electrically powered trucks and buses will lead to specific issues: after all, you do not easily submerge them in a tunnel in an immersion container like electric passenger vehicles [6].

During an expert session at our institute, it was also noted that an additional danger of increasing fuel diversity lies in a lack of information on the types of fuels present during a fire. When it is unclear which fuels are involved in a tunnel fire, it is also unclear which (combination of) risks the fire brigade has to take into account. This increasing uncertainty may lead to firefighters becoming more cautious in their actions in fire situations.

Previous chapters have already described that firefighting in a road tunnel, even when all tunnel facilities are functioning properly, is complex and not without risk. Current and upcoming changes in the fuel mix of the vehicle fleet mean that firefighting in road tunnels will become even more complex because of new uncertainties and risks.

4. FIRE SUPPRESSION TECHNOLOGIES

It could be that technology developments (hardware and software, including organizational and human behavior)) might be helpful in future tunnel firefighting.

Information

Good information about the nature and extent of the fire is essential for proper and safe firefighting. Based on legal requirements, the necessary information is shared from the road traffic control center with the central emergency services control center. It is technically possible to transfer images of the

incident scene to the arriving fire engines. This is by no means always used.
It is also technically possible to use cameras with number plate recognition to retrieve data on (among other things) the fuel type of a vehicle. Possibly, based on this data, information on the cargo can also be obtained in case of transportation of hazardous materials. This information could increase the chances of effective firefighting.

Specialisation within the fire service
Firefighters are trained for all kinds of interventions, but always on a more general level. This means that they have knowledge of common dangers and how to combat them in their service area. However, society is becoming increasingly complex, and so are incidents. To deal with this safely and effectively, there is a tendency in The Netherlands towards more specialization within the fire brigade. This means that the fire brigade is developing so-called specialisms for special incident categories. Several regional and national structures, for instance, have been set up to fight complex or (very) large fires. The development of regional teams that are additionally trained and educated for fire fighting in road tunnels, and have access to specialist firefighting equipment, can have a significant impact on firefighting and fire behavior in road tunnels

Reconnaissance using technical devices such as drones
A drone is an unmanned flying object, often remotely controlled by a drone pilot/team. A drone team consists of a captain or pilot in command and sensor operation specialists. This team of specialists can be called in case of fire to use drones equipped with (thermal imaging) cameras to get a good overview of the situation on incident scene. Moreover, they can zoom in (from above), and also assess details. The added value of drones currently lies mainly in fire reconnaissance and imaging. However, using the CCTV camera images present in the road tunnel, a good picture of the fire on the incident scene can currently already be formed. Yet, drones currently play no role in firefighting itself.

Low pressure systems/O-bundles
In many cases, Dutch firefighters have access to 90-metre high pressure hoses that are present on a reel in the fire engine. These hoses are quick to roll out, but have a limited flow rate and provide limited cooling capacity. In addition, the fire brigade has access to low pressure hoses. These are hoses with a length of 20 meters, which are connected by Storz couplings. The flow rate (of 450 l/min) and cooling capacity (up to 10 MW) of such hoses is much higher than high pressure hoses. Getting these traditional low pressure hoses ready for deployment takes a relatively long time. However, more and more fire brigades are using improved low-pressure systems, or O-bundles.

Figure 1 O-bundles (photo: Hans Hazebroek)

An O-bundle is a bundle-folded (double-walled) low pressure hose with a length of 20 meters. This hose has the same capacity and cooling capacity as a normal low pressure hose and the working pressure of 6-10 bar is also similar. However, the fact that the hoses are double-walled makes them easier to handle. Moreover, the hoses are stored in bundles on the fire engine. When dispensing, bundles are connected slightly unfolded to the manifold piece (see Figure 1). When the manifold is opened, the hoses 'pop', after which they can be easily deployed. These hoses are ready for deployment much faster than regular low pressure hoses. However, a slightly higher pressure of around 8 bar is needed to 'pop' the O-bundles. In addition, too low a pressure can lead to kinking of hoses.

Firefighting robots

A firefighting robot is a remote-controlled or autonomously operating firefighting system with a large cooling capacity. There are several makes and types in circulation, each with a far differing size and capabilities. Several types also have the option of adding a compressed air foam systems (CAFS), or even moving vehicles. However, towing and removing vehicles is usually the job of the salvage company, which has specialized equipment for this.

Depending on the implementation type, the added value of a firefighting robot is considerable. An extinguishing robot can be used in (large) tunnel fires that have already developed under conditions that are too dangerous for humans. These include high temperatures, concrete spalling, collapse of structural parts and the risk of pressure tanks blowing off or exploding. The storage location of the extinguishing robot also determines the time in which it can be ready for deployment. A (autonomously operating) fire-fighting robot directly near the tunnel means it can, in theory, be deployed relatively quick. More research is needed to deploy robots in practice.

Figure 2 LUF 60 firefighting robot (photo: Haaglanden Safety Region)

Fixed fire control systems

The Dutch legally prescribed standard equipment of facilities in a road tunnel provides for the safe escape of road users present and increases the likelihood of safe and effective firefighting by the fire service. However, this standard tunnel equipment does not prevent for a fire developing to a fire size where firefighting within the incident tube is no longer obvious. Fixed fire control systems, also known as sprinkler systems, are designed to control a fire at an early stage to stop fire spread and growth, reduce heat release rate..

A fire detection system detects a fire, after which the extinguishing agent, usually water, is applied to the seat of the fire from multiple sprinkler heads in an area of 35 meters long and the entire with of the tunnel tube.

This leads to early suppression of the fire and, depending on the fire location, possibly also to extinguishing it. Water flow from sprinklers might not always be adequate to cool a tank effectively. Additionally it cools surrounding vehicles preventing fire spread. A controlled fire leads to better space conditions in the incident tube which ensures a:

> improvement of atmospheric conditions downwind [19]
> limiting the probability of fire spread between vehicles [20]
> risk mitigation for a tanker truck carrying a flammable liquid or gas [19]
> greater likelihood of safe and effective firefighting [21].

Various fire control systems exist [21] :

> water mist systems
> (compressed air) fire-fighting foam systems
> sprinkler systems
> fire-fighting robots (see above).

Depending on the type of vehicle fire, each fire control system has specific applications and limitations. These are shown in the table 4 below. In practice, a water mist system, often appears to be the preferred choice of engineers and road tunnel operators. The limited water consumption of water mist systems compared to regular sprinkler systems is the deciding factor in this [22]. Because of absent data for the effectiveness of water mist systems, in the US, water mist systems are not applied regularly in US road tunnels.

Table 4 Applications of fire control systems [22].

	Truck cargo fire	Flammable liquid	Passenger car/bus battery	Passenger car/bus combustion engine
Water mist	Applicable	Applicable	Applicable	Applicable
Extinguishing foam*	Applicable	Applicable	Depending on implementation	Depending on implementation
Sprinkler	Applicable	Not recommended	Applicable	Applicable

* in particular useful to reduces the heat release rate of haz.mat. fires and pool fires.

Fixed firefighting systems are not the common in Dutch road tunnels. In the Netherlands, fixed firefighting systems are not mandatory. In contrast, only one Dutch road tunnel is equipped with a fixed firefighting system. However, we do see more applications of fixed firefighting systems in other countries such as Norway, the Alpine countries and the United States. We also see an increase in fixed firefighting systems in industry, the healthcare sector, schools and even at home [23].

Firefighting systems in vehicles

Better than deploying fire fighters to suppress fires in tunnels, the vehicles itself reduces the fire. Motor management related to a fire suppression system in a vehicle is capable of detecting defects and/or temperature build-up in a vehicle's engine compartment early and, if necessary, taking mitigating measures. A fire can then potentially be prevented, or if necessary fought within the engine/battery compartment itself. The fire is then still very limited in size. This system is mandatory for new M2 /M3 ICE vehicles (fossile fueled buses). However, it is unlikely that all vehicles, including M1 (passenger cars), will also be equipped with such a system. The added value of this solution is therefore limited.

Special firefighting equipment for battery electric vehicles

For the battery electric vehicles, we came along a variety of techniques to help firefighters [24]:

- Fire blankets and fire-resistant blankets: to cover the vehicles and smother the flames
- Ultra high pressure cut and suppress systems (cold cutter systems): to penetrate the battery pack and apply water in the battery pack. This a manually controlled system.
- Stingray-like penetration systems: hydraulic apparatus is slide under a car, after which a piercing nozzle is punched into the battery pack from below.
- Mobile sprinklers: A mobile sprinkler system is a (movable) system that can be placed above, between or under passenger vehicles. The system can prevent fire spread by placing it above or between vehicles like a water curtain.
- Immersion containers: The immersion container is a liquid-tight container in which a passenger vehicle or other object can be placed. The container must be brought on site, for example on the loading platform of a tow truck or using a vehicle with a hook arm chassis.

We compared the techniques in 2020 and 2023. The immersion containers score pretty well because of its cooling capacity and relatively safe deployment. Relatively safe because firefighters and salvage personnel are at a distance from the battery electric vehicle. However, the container cannot be deployed in a tunnel or parking garage because of the restricted height. Our recent fire tests [25] in which fire crews from Dutch safety regions deployed the cold cutter systems to two battery electric car fires, showed that these systems could be deployed save and in an effective way.

5. DUTCH FIRE FIGHTERS PERSPECTIVE ON FUTURE TUNNEL FIRE SUPPRESSION

The findings in the sections above, show, partly due to the introduction of new energy carriers in the vehicle population, an increasing complexity in tunnel firefighting. These developments may, earlier than was previously the case, lead to uncontrolled tunnel fires. In the most extreme case (trucks loaded with enormous flammable cargo (wooden pallets, fossile fuels, …), this might lead to tunnel failures. These developments partly led the fire service to review the firefighting principles (SoP's) used so far. The new starting point for the fire service is no longer that that firefighting is offensively focused on the fire area itself. There are considerations that may lead to alternative firefighting tactics outside (defensive) at and around the incident scene. These (defensive) suppression tactics are more focused on preventing further fire spread beyond the incident scene [26] and [27].

In the event of a fire in a road tunnel, the officer-in-charge on site, in consultation with the Duty Officer, will make a decision on the firefighting tactics to be followed. If a fire is 'small' (< ~50 MW), then usually (offensive) fire suppression will be chosen within the incident tube, focusing on the fire scene. The effects of such a 'controlled' fire, for example in terms of damage appearance, will usually be limited.

A fire that has already been able to develop into a 'large' fire (> ~50 MW) when the fire brigade arrives, may impede safe and/or effective firefighting in the incident tube. Moreover, within a road tunnel, specific fire risks may play a significant role. These include:

> The presence of hazardous materials, including tanker(s) carrying a flammable liquid or gas.
> The presence of pressurized cylinders, including the fuel tank of CNG, LNG and hydrogen vehicles.
> The (localized) collapse of tunnel segments caused by the (large-scale) spalling of concrete.
> The presence of li-Ion batteries, in electric vehicles and the challenges associated with this.

In situations with high fire risks, nowadays and in the future, the fire brigade is more likely to opt for firefighting from the supporting tunnel tube or from the tunnel entrances, aimed at preventing further escalation of the fire. The fire in the incident tube is thus uncontrolled and has great influence on:

> **Fire service deployment:** An uncontrolled tunnel fire can lead to a disproportionate, and lengthy, deployment of the emergency services. Such a complex incident also poses risks to emergency workers.
> **Damage limitation:** An uncontrolled fire can lead to significant damage to the tunnel structure and to the installations, like ventilation, present in the tunnel.
> **Social and administrative detriment risk:** An uncontrolled fire may lead to indirect damage due to long-term restrictions on traffic flow and social disruption due to limited accessibility of areas. This consequence constitutes a social and administrative detriment risk for the local competent authority.
> **Environment and sustainability:** An uncontrolled fire is highly undesirable from an environmental and sustainability perspective. This concerns both the ecological consequences of the fire itself due to smoke dispersion and the discharge of contaminated fire-fighting water into the surrounding water and the ecological burden of repair or replacement works.

Below is a schematic overview of the risks resulting from the sustainability trend of the vehicle population and developments that contribute to the likelihood of effective firefighting in road tunnels.

Table 5 Risks due to new energy carriers car developments and measures for fire fighting [4]

Additional risks	Measures
Uncertain fire conditions due to	> Standardize information provision from the control room. > Transfer CCTV images to approaching vehicles.

unknown combination(s) of fuel types of vehicles involved in accidents in the road tunnel	> License plate registration of vehicles present in the tunnel and involved in fire. > Deployment of nationwide or regional tunnel firefighter specialists. > Use of rapidly deployable O-bundles with high cooling capacity. > Use of fixed extinguishing system in the form of sprinkler, water mist system or controlled fire monitors to control or extinguish the fire early. > Use of autonomously operating or controlled fire-fighting robots in situations where a fire service deployment is too risky, such as large fires.
Specific challenges new fuel types Blowing off pressure tanks Firefighting battery packs	> Deployment of nationwide or regional tunnel firefighter specialists. > Use of rapidly deployable O-bundles with high cooling capacity. > Use of fixed extinguishing system in the form of sprinkler, water mist system or controlled fire monitors to control or extinguish the fire early. > Use of autonomously operating or controlled firefighting robots in situations where a firefighter deployment is too risky, such as the likelihood of a tank blowing off or exploding. > Use of cold cutter systems to penetrate the battery pack and battery cell. > Use of an immersion container near the tunnel for battery-electric passenger vehicles.

6. CONCLUSION

The tunnel safety landscape is changing. New energy carriers and bigger vehicles cause bigger and more complex fires. Meanwhile, fire suppression techniques evolve as well and the firefighters become more defensive in their tactics. We think that the Dutch SoP for tunnel fire fighting should therefore be reconsidered by the tunnel providers and fire fighters together, taking into account the three above described developments. Despite the fact that we studied tunnel fire suppression from the Dutch perspective (Dutch road tunnels, Dutch SoP's and the car population), the arguments that we formulated for seriously (re) considering daily practise in tunnel fire suppression could be of great value for other countries and their tunnel providers and firefighters as well.

REFERENCES

[1] Ministerie van Infrastructuur en Waterstaat, Wet Aanvullende Regels Veiligheid Wegtunnels (WARVW), https://wetten.overheid.nl/BWBR0019516/2024-01-01, 2006.
[2] NIPV, Brandveiligheid van parkeergarages met elektrisch aangedreven voertuigen, https://nipv.nl/wp-content/uploads/2022/03/20210715-IFV-Brandveiligheid-parkeergarages-met-elektrisch-aangedreven-voertuigen-v2021.pdf, 2021.

[3] NIPV, Toekomstverkenning Brandweer 2022-2030, https://nipv.nl/wp-content/uploads/2022/10/20221012-NIPV-Toekomstverkenning-Brandweer-2022-2030.pdf, 2022.
[4] NIPV, Toekomstverkenning brandbestrijding in wegtunnels, 2024.
[5] NIPV, Handvatten voor de bevelvoerder bij brandbestrijding in wegtunnels direct na melding, https://archief.nipv.nl/wp-content/uploads/sites/2/2022/03/20200630-IFV-Handvatten-

bevelvoerder-brandbestrijding-wegtunnels.pdf, 2020.
[6] NFPA 502, Standard for road tunnels, bridges, and other limited access highways. https://www.nfpa.org/codes-and-standards/nfpa-502-standard-development/502
[7] Oosterveld, R., (2013). Slachtofferberekening bij een tunnelbrand. Een verkenning naar een kwantitatieve risico analyse voor het berekenen van gewonden bij een tunnelbrand. Master thesis, Universiteit van Twente.
[8] Rosmuller (2017), Betonperikelen en de consequenties voor tunnelbrandbestrijding. Presentation, at knowledge meeting orgized by the knowledge platform tunnel safety 16 November 2017.
[9] Piarc (2022). Impact of new propulsion technologies on road tunnel operations and safety Piarc, 2022R05EN.
[10] Cheong, M. K., Spearpoint M. J., Fleischmann C. M. (2008) Design fires for vehicles in road tunnels. Proc. 7th International Conference on Performance-Base
[11] IFV (2016a) Handreiking voorbereiding tunnelincidentbestrijding.
[12] wetten.nl - Regeling - Regeling aanvullende regels veiligheid wegtunnels - BWBR0019806
[13] IFV. (2020a). Handvatten voor de bevelvoerder bij brandbestrijding in wegtunnels direct na melding.
[14] Boehmer, H., Klassen, M., Olenick, S.(2020). Modern Vehicle Hazards in Parking Structures and Vehicle Carriers, FPRF.
[15] https://navigator.emis.vito.be/detail?woId=76083&woLang=nl (retreived7 November 2023).
[16] Reinders, J., Brans H., (2023). Veiligheid alternatief aangedreven voertuigen op chemische sites (Issue fase 2), NIPV.
[17] Spoelstra, M.B., (2023). Waterstofincidenten in besloten ruimtes, NIPV.
[18] TNO (2013). Consequenties voor QRA-tunnels van het vervoer van nieuwe stoffen.
[19] Lemaire, A.D. & Meeussen, V.J.A (2008). Effects of water mist on real large tunnel fires: Experimental determination of BLEVE-risk and tenability during growth and suppression, 2008-Efectis-R0425.
[20] Huijben, J.W. (2002). Tests on fire detection systems and sprinkler in a tunnel. Bouwdienst RWS.
[21] Meijer, G.J., Molenaar, D.J., Meeussen V (2008). Evaluatie vaste brandbestrijdingssystemen voor toepassing in wegtunnels, TNO: 2007-D-R0594/A.
[22] Liu, Y. Cassady, S. Jones, E. & Pospisil P. (2023). Review of design fire heat release rate for tunnels with fire suppression systems. HNTB Corporation
[23] https://www.fortunebusinessinsights.com/u-s-fire-sprinklers-market-109827
[24] NIPV, 2023, Onderzoek dompelcontainers, Een beoordeling van de dompelcontainer en mogelijke alternatieven. https://nipv.nl/nieuws/actualisatie-onderzoeksrapport-dompelcontainer/
[25] NIPV, 2024, Fire experiment to examine the use of ultra high pressure extinguishing systems for fires in batteries of electric vehicles https://nipv.nl/wp-content/uploads/2024/11/20241126-NIPV-Fire-experiment-to-examine-use-of-UHD-extinguishing-systems-for-fires-in-batteries-electric-vehicles.pdf
[26] IFV (2020b) Basisprincipes van brandbestrijding.
[27] Werkgroep brandweervisie Tunnelveiligheid, Visie en uitganspunten van Brandweer Nederland op tunnelveiligheid, 2024.

What fire modelling resolution is needed in AI training data for smart firefighting in tunnels?

José A. Morales Mere, Nils Johansson & Enrico Ronchi
Division of Fire Safety Engineering, Lund University
P O Box 118, SE-221 00 Lund, Sweden
E-mail: jose_antonio.morales_mere@brand.lth.se

ABSTRACT

The adoption of smart firefighting in tunnels – intended here as fire modelling coupled with sensor data - requires a broad discussion into the suitability of different tools and approaches for decision support in case of emergency. In particular, Artificial Intelligence (AI) tools have shown great potential to support real-time emergency management, given their ability to simulate and predict the evolution of fire scenarios with low computational cost. AI tools for fire modelling predictions generally rely on a given simulation database for their training. Such databases can be developed through a variety of fire modelling approaches with different resolutions, e.g. hand-calculations, (multi-)zone modelling and computational fluid dynamics (CFD). This study proposes an approach to investigate the suitability of different modelling resolutions for generating AI training datasets for tunnel fire scenarios, considering heat release rate as the key variable to predict. Regression modelling allows estimating this key variable. Testing has been performed through a set of fire scenarios within and outside the training dataset fire intensity intervals. An experimental dataset from real-world repeated experiments was used to understand the prediction performance based on different modelling resolutions. The prediction performance was assessed through the error evaluation for the testing and experimental datasets. The error of the testing data shows how strongly the regression model correlates to the assumptions taken in the training scenarios. Here, the regression model based on CFD shows the best fit when predicting fire intensity within the range used for training. The regression model based on multi-zone modelling shows a better fit for larger fires. Finally, the comparison to experimental data shows that hand-calculations are not suitable for this type of applications while multi-zone and CFD modelling approaches can provide sufficient resolution to predict fire intensity when adopting them to train a regression model and using temperature sensor data.

KEYWORD: smart firefighting, tunnel fire modelling, modelling resolution, training database

NOMENCLATURE

Symbols

c_p	Specific heat of air at constant pressure (kJ/kgK)
ρ	Density (kg/m^3)
ΔT	Temperature difference (K)
e	Error (%)
g	Gravity constant (m/s^2)
H	Tunnel height (m)
h_t	Total heat transfer coefficient (kW/m^{2}K)
k	Ventilation ratio (-)
l_f	Fire characteristic length (m)
$\dot{m}_0$	Mass flow rate (kg/s)
$\dot{Q}$	Heat release rate (kW)

$\dot{Q}''$	Heat release rate per unit area (kW/m^2)
$\dot{Q}^*$	Dimensionless heat release rate (-)
RMSPE	Root mean square percentage error (%)
T	Temperature (K)
t	Time (s)
T_0	Ambient temperature (K)
u_0	Longitudinal ventilation flow (m/s)
V_c	Critical velocity (m/s)
V_c*	Dimensionless critical velocity (-)
w_p	Perimeter of the tunnel cross-section (m)
x	Fire position (m)

Subscripts

i	Training scenario
j	Testing scenario
m	Fire modelling approach
e	Experiment

INTRODUCTION

Emergency procedures in tunnels are critical for ensuring the safety of individuals during fire incidents. In these events, smart firefighting can help ensure decisions are taken promptly so that evacuation and rescue service operations are safely executed. First responders such as rescue services and tunnel operators are expected to control the traffic, facilitate the evacuation, monitor the fire development and road obstructions, and perform fire and rescue operations [1]. All these activities are associated with a key set of decisions which rely on information available and a dynamic risk assessment which identify their consequences. However, available technology (such as camera systems, fire detection systems, and supervisory control and data acquisition ventilation controllers) most often only provide information on current status rather than predicted consequences [2].

In tunnel fires, after the arrival of the rescue service outside the tunnel, it is required to determine the location of the fire to define the closest safety access to the fire, especially if it is not known in advance, such as when being notified by tunnel operators who perform surveillance of the tunnel. In that location, it might be assumed that the ventilation flow is as much as required to suppress the back layering upstream of the fire. Depending on the facility's emergency procedures, ventilation flow may be minimized to maintain smoke stratification during self-evacuation. However, without immediate guidance on the situation or expected ventilation changes, occupants may independently choose an evacuation route with the highest smoke concentration caused by longitudinal ventilation, potentially the least safe direction. These procedures present a high degree of complexity as they involve the tunnel controller, the incident commander, and the firefighters on-site evaluating the heat release rate and determining the requirement for higher ventilation flows to prevent backlayering in case of longitudinal ventilation. [3]

For this reason, smart firefighting concepts such as fire modelling coupled with sensor data can be a useful tool to inform decisions and optimise the emergency response, resources, and defining strategies. Smart firefighting, intended here as guided emergency response through sensor data, can offer enhanced situational awareness and critical decision-support information. This approach can enable a more efficient and safer emergency response by providing deeper insights into the dynamics of the situation. This includes the assessment of current and future conditions that can be estimated through the integration of sensor data with fire models.

The scientific literature includes different fire modelling approaches of varying resolution, reliability,

precision, and computational cost for tunnel fire safety design and assessment, such as one-dimensional hand calculations [4], multi-zone modelling [5], and computational fluid dynamics (CFD) [6], [7]. Regardless of the model in use, the goal is to predict the fire and smoke development (and associated tenability conditions) in relation to different scenarios. In this context, the trade-offs between computational costs of each modelling approach and accuracy is an open question. This is particularly important for data-driven modelling approaches which rely on sensor data, i.e. those attempting integrating real-time measurements into fire models to perform predictions [8]. In fact, recent research has used machine learning models for tunnel fire development predictions. For instance, these models have been used to predict temperature distributions in tunnel and compartment fires concluding that higher accuracy results require deep learning models including hidden layers to process massive amounts of data [9], [10].

The purpose of the study is to investigate the resolution in training databases required to perform data-driven prediction for emergency response in tunnel fire scenarios. By determining whether a model that is faster or more efficient to run can generate a training dataset of sufficient quality, the study aims to assess its potential as a valuable resource for further development of predictive models for tunnels. Such advancements could enhance the capability of smart firefighting systems, supporting more effective and informed emergency response strategies. This will be demonstrated through a case study of a 60 meters tunnel fire experimental facility located in Revinge, Sweden for which mass loss rates and temperature sensor data have been collected in a range of repeated experiments [11]. The case study assumes the fire intensity as the key variable to be predicted by models using available sensor data.

METHODOLOGY

Figure 1 presents the overall methodology of this work. For the given case study, a set of 27 training design scenarios are defined varying the fire intensity (Q_i), fire position (x_i), and longitudinal ventilation flow (u_i). The training dataset is used to develop a prediction model based on a linear regression analysis. This method analyses the simulated temperature values (T) at certain positions in the tunnel. The temperature values are estimated through 3 different approaches: hand calculations [4], multi-zone modelling [5], and CFD through the Fire Dynamics Simulator (FDS) [7]. Then, the prediction model is tested by a set of 5 scenarios that are within and outside the range of fire intensity in the training scenarios. Finally, the performance of the prediction model is evaluated through a set of experimental heat release rate ($\dot{Q}_e$) and temperature (T_e) values.

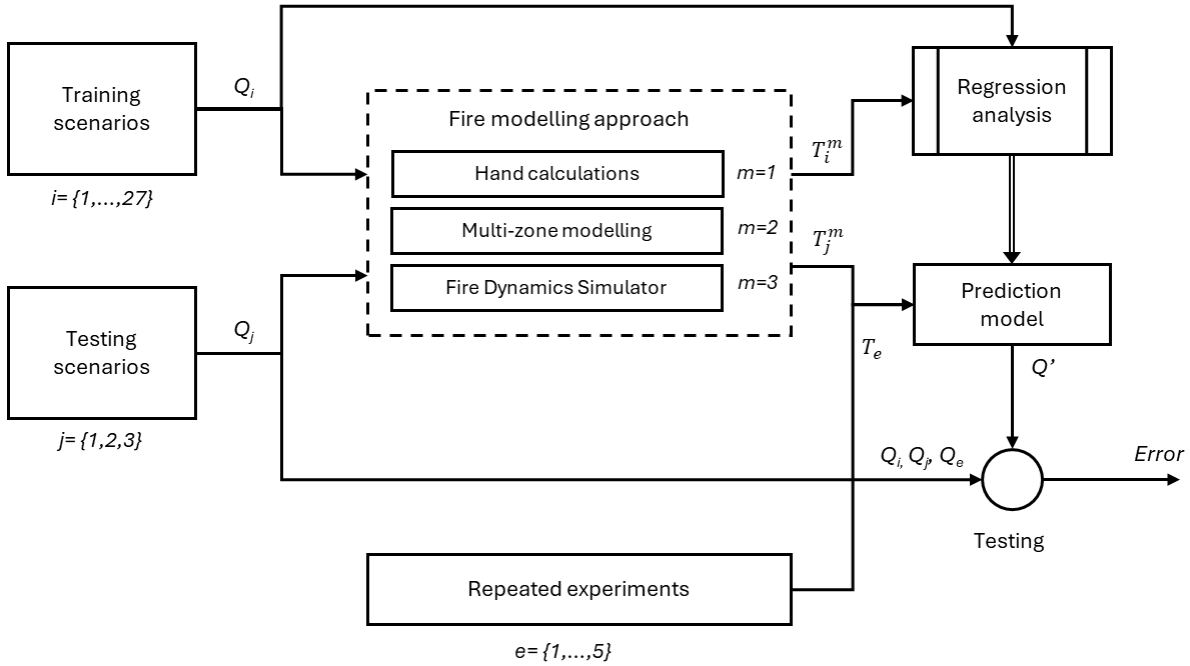

Figure 1 Research methodology flowchart for a 'blind' prediction method over three fire modelling

approaches (m) including testing and experimental benchmarking for a number of (j) scenarios. Q= heat release rate, T= temperature.

Regression analysis

The method used to determine the correlation between the heat release rate (HRR) and other variables (e.g., temperature) is the same for all fire modelling techniques adopted here. To ensure transparency and explainability, a simple and established statistical approach, specifically multiple linear regression analysis, is applied. It should be noted that more sophisticated approaches (e.g., based on artificial intelligence, AI) could have been used as an alternative to the simple method used here. Linear regression is indeed often used as baseline against AI approaches.

Linear regression is a statistical method used to model the relationship between a dependent variable such as HRR (Q) and one or more independent variables such as the longitudinal velocity (u_0) and temperature (T). The linear regression is used to predict the value of $\dot{Q}$ based on the values of u_0 and T to understand the relationship between them [12], [13]. A statistical package can be used to perform the linear regression, and it provides various statistics that can be used to analyze the result of the regression analysis. The coefficient of determination (R^2) gives a measure of the proportion of the variance in the dependent variable that is explained by the independent variables in the regression expression. The overall significance gives a *p*-value for that at least one of the variable coefficients is not equal to zero, i.e., there is at least one useful linear relationship. The significance of the individual coefficients is presented with the so-called *p*-value of coefficients, which indicated if the associated coefficient is significantly different form zero [12]. In this work the Microsoft Excel Analysis ToolPak is used to perform the regression analysis and to calculate the associated statistical parameters.

Error Analysis

As shown in *Figure* , an error analysis is performed to evaluate the performance of the regression analysis through the prediction ($\dot{Q}$) of the testing ($\dot{Q}_t$), and experimental cases ($\dot{Q}_e$). This is done through the Root Mean Square Percentage Error (equation 1) for a population of scenarios such as the training dataset, and through the Percentage Error (equation 2) to evaluate the error between expected and real values such as testing dataset or experimental data. The lower the score, the better the predictive performance of the model.

$$RMSPE = \sqrt{\frac{1}{n}\sum_{i=1}^{n}(e_i)^2} \quad (1)$$

$$e = \frac{Q\prime - Q_{i,j,e}}{Q_{i,j,e}}\ x100\% \quad (2)$$

TUNNEL FIRE SCENARIOS

The design of the scenarios under consideration is meant to represent a simplified version of a tunnel fire. As shown in *Figure 2*, this design setup represents a real-world tunnel facility in Revinge, Sweden, where repeated experiments were conducted as detailed in [11]. The tunnel case study assumes a rectangular cross-section, constant longitudinal flow, and unobstructed fire on a fixed position.

Figure 2 *Experimental tunnel located at the Swedish Contingency Agency training facility in Revinge, Sweden.*

A schematic representation of the tunnel layout is shown in *Figure 3*, including the dimensions of the tunnel cross-section, the position of the thermocouples and the fire source (x_i), the fire characteristic length (l_i), and the longitudinal ventilation flow (u_i).

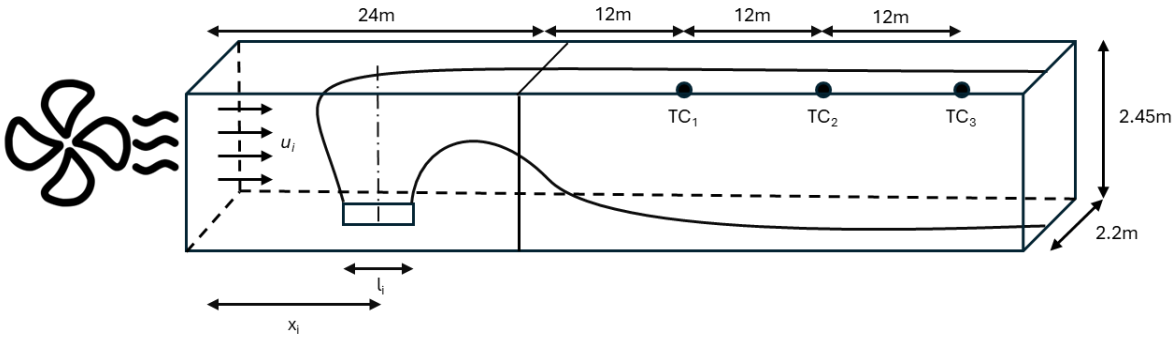

Figure 3 *Schematic representation of the tunnel case study. The tunnel layout is not in scale. TC=thermocouples, u= longitudinal ventilation flow, x= fire position, l= fire characteristic length.*

The fuel in the fire scenarios is represented with a heptane pool. The general assumptions taken for the case study are steady ventilation flow and no wind effect on the tunnel portals. Assuming well-ventilated fires where there is no significant heat feedback to the fuel and there is no increment of oxygen concentrations, the designed fires were simplified by decoupling the combustion process, setting up a constant value of heat release rate per unit area (HRRPUA) of 2000 kW/m^2.

The resulting fire scenarios are characterized by as per the document [14] for small, medium, and large pool fires, where the fire size is expressed in terms of the ratio between the length of the fire in the direction of the airflow, and the tunnel width.

The training data consists of 27 tunnel fire scenarios intended to represent a range of fire intensity, flow velocity, and fire position. For the testing a set of HRR values were defined, namely 80 kW, 1100 kW, 1500 kW, and 2200 kW. Those values are deliberately chosen outside and inside (650 kW) the HRR interval adopted in the training data. The fire characterisation for the training and testing sets is presented in Table 1. The fire of the training set was placed at three different fire positions (x_i): 5 m, 10 m, and 15 m relative to the ventilation inlet at the tunnel portal (see *Figure 3*).

Table 1 Characteristics of the prescribed HRR or the training and testing datasets.

Dataset	HRR (kW)	Fire width (m)	Fire characteristic length (m)	Fire ratio	Fire size	Q*
Training	320	0.4	0.4	0.18	small	0.03
	500	0.5	0.5	0.23	small	0.05
	980	0.7	0.7	0.32	small	0.09
Testing	80	0.2	0.2	0.09	small	0.01
	650	0.5	0.65	0.30	small	0.06
	1100	0.5	1.1	0.50	medium	0.11
	1500	0.5	1.5	0.68	medium	0.14
	2200	0.5	2.20	1.00	large	0.21

The training and testing sets can be characterised through the dimensionless critical velocity (V_c*) and the dimensionless heat release rate ($\dot{Q}^*$). Li et al. [15] developed an experimental and theoretical analysis to define the V_c* for a tunnel without blockage as shown in Equation (3). Where the dimensionless variables of heat release rate and critical velocity are defined by Equation (4) and (5), respectively.

$$V_c^* = \begin{cases} 0.81Q^*, \dot{Q}^* \leq 0.15 \\ 0.43, \quad \dot{Q}^* > 0.15 \end{cases} \tag{3}$$

where

$$Q^* = \frac{Q}{\rho_0 C_p T_0 g^{1/2} H^{5/2}} \tag{4}$$

$$V_c^* = \frac{V_c}{\sqrt{gH}} \tag{5}$$

The prescribed ventilation rates are 1.1 m/s, 2 m/s, and 4 m/s, which are intended to significantly impact the temperature values. Each scenario has been evaluated through the ratio of the design ventilation rate (u_0) and the respective critical velocity (V_c) leading to scenarios of longitudinal flows under and over the respective critical velocity. The characteristics of the ventilation flow for the training and testing sets are shown in *Table 2*.

Table 2 Characteristics of the prescribed ventilation for the training and testing datasets.

Dataset	$\dot{Q}^*$	V_c*	V_c (m/s)	u_0 (m/s)	V_c/u_0	Ventilation type
Training	0.03	0.25	1.24	1.1	0.88	Under critical velocity
	0.05	0.29	1.44	1.1	0.76	Under critical velocity
	0.09	0.37	1.81	1.1	0.61	Under critical velocity
	0.03	0.25	1.24	2.0	1.61	Above critical velocity
	0.05	0.29	1.44	2.0	1.38	Above critical velocity
	0.09	0.37	1.81	2.0	1.11	Above critical velocity
	0.03	0.25	1.24	4.0	3.21	Above critical velocity
	0.05	0.29	1.44	4.0	2.77	Above critical velocity
	0.09	0.37	1.81	4.0	2.21	Above critical velocity
Testing	0.01	0.16	0.78	2.0	2.55	Above critical velocity
	0.06	0.32	1.58	2.0	1.27	Above critical velocity
	0.11	0.38	1.88	2.0	1.06	Above critical velocity
	0.14	0.42	2.08	2.0	0.96	Under critical velocity
	0.21	0.48	2.37	2.0	0.84	Under critical velocity

The arrangement of HRR, ventilation rates and positions result in a total training set of 27 scenarios. In contrast, the testing set was limited to one outbound position of 20 m from the inlet portal to evaluate the dependency of the position in the regression models. All scenarios were simulated with different fire modelling approaches estimating data points of temperature values. The data points are used to train the regression model. The temperature values taken for the training sets are consistently taken after 900 seconds of simulation. This choice was because corresponding experimental measurements from the real-world tunnel are available.

Hand calculation method

The analytical model used in this paper has been presented by Ingason [4]. The models are valid for tunnel fires with longitudinal ventilation, that is such that the flow can be assumed one-dimensional. The methods are based on simple mass and energy balance. The average gas temperature at x (m) downstream of the fire source at time t (s) can be estimated with equation 6.

$$\Delta T_{avg}(x,t) = \Delta T_{avg}(0,\tau) e^{-\frac{h_t w_p}{\dot{m}_0 c_p} x} \tag{6}$$

Where ΔT_{avg} is the average temperature increase over the whole cross-section, h_t is the total heat transfer coefficient (kW/m^{2}K), w_p is the perimeter of the whole tunnel cross-section, and $\dot{m}_0$is the mass flow rate in the tunnel (kg/s). The time τ accounts for the transport time of the heat from the fire to the position x. For short distances $\tau = t - x/u_0$, where u_0 is the gas velocity, can be used. The average temperature increase at the fire source can be estimated with equation 7. It can be noted that the first term in equation 7 is a constant value, whereas the second term is a variable value depending on the fire scenario characteristics.

$$\Delta T_{avg}(0,\tau) = \frac{2}{3c_p} \frac{\dot{Q}(\tau)}{\dot{m}_0} \tag{7}$$

Ingason [4] points out that the method can describe the average gas temperature downstream of the fire reasonably well for one-dimensional flows, however when the velocity is to low the one-dimensional model will not be applicable.

Multi-zone modelling

The general multi-zone (MZ) concept has been described in previous work [16]. In a multi-zone model the enclosure is divided into several regions (horizontal) and zones (vertical). This means that the entire enclosure is made up of several smaller computational volumes. The conservation mass and energy are applied for each volume. The calculated properties (like temperature or soot concentration) are uniform in each zone, and the model extends into a three-dimensional volume. An empirical plume model is used to calculate the plume entrainment. The MZ fire model used in this paper has been adapted to tunnel fires and it has been tested against experimental data on large-scale tunnel fires [5].

Computational fluid dynamics model

The CFD model used is the Fire Dynamics Simulator (FDS). It is an established tool for fire safety analysis. FDS is developed by the National Institute of Standards and Technology [17], and it is a large-eddy simulation (LES) code for low-speed flows. The software solves the Navier–Stokes equations numerically, emphasising heat and smoke transport. The FDS validation guide [18] includes a large amount of validation and testing examples and independent research teams have done significant validation work of the model. FDS is tested and frequently used for tunnel fire scenarios [19].

The pressure considerations for the tunnel scenarios with medium and large fire size (see *Table*) were varied from default values to avoid numerical instabilities. These scenarios were configured to have a maximum of 30 pressure iterations and a reduced pressure tolerance of up to half the default value.

Experimental data

Experimental data were retrieved from repeated experiments of an experimental campaign conducted at the tunnel facility in Revinge (see *Figure 2*) and are summarised in *Table 3*. Thermocouple trees were positioned at different distances from the fire along the tunnel; however, in this study, information from only three thermocouples - assumed to represent temperature sensors underneath the ceiling - are used (see *Figure 3*). The fire source was a heptane pool fire with an area of 0.25 m^2 and the mass of the fuel was measured during the experimental tests. A longitudinal ventilation velocity was generated with a positive pressure fan; the ventilation flow velocity was measured with an anemometer prior to all tests. A full description of the experimental setup has been presented in a previous publication [11].

The HRR and temperature values in *Table 3* are estimated during the main burning period, approximately for a period of 600s, when the mass loss was stable. The HRR is calculated based on the load cell data, effective heat of combustion of 41.2 kJ/g for heptane (C_7H_{16}), as suggested in Table A.40 in [20] .

Table 3 Experimental data collected in the tunnel facility

Experiment	Q (kW)	u_o (m/s)	x (m)	ΔT_{24m}	ΔT_{36m}	ΔT_{48m}
1	659	2	6	88.0	74.7	64.1
2	667	2	6	116.9	96.0	82.1
3	663	2	6	106.6	88.1	77.2
4	737	2	6	66.4	57.7	51.0
5	651	2	6	65.0	55.9	49.4

RESULTS

This section presents the results of this study. First, it describes the temperature estimations obtained through the three fire modelling techniques adopted and an overview of the predicted HRR for the training scenarios. Then, the result of the multiple linear regression is presented for each fire model correlating the prescribed (in training) and predicted HRR. Finally, it presents the error evaluation for the testing and experimental datasets against the prediction method for the three fire modelling resolutions.

Training modelling results

The 27 training scenarios were simulated through Hand calculations (HC), Multi-Zone (MZ), and FDS. Each fire model estimated the temperature values for 900s at the three relative positions of 24m, 36m, and 48m from the tunnel portal. The temperature increment (ΔT) and HRR ($\dot{Q}$) values were averaged over the last 30s of the simulation time.

As described in Equation 7, the second term is the ratio between the HRR ($\dot{Q}$) and the mass flow rate (m_0). Therefore, when correlating ΔT with $\dot{Q}/\dot{m}_0$ it is expected to have a linear slope, as *Figure 7* shows the temperature increments (ΔT) at 24 meters. This figure shows that each fire model presents a different temperature trendline. As expected, the results from the hand calculations matches the trendline since it is based on Equation 7. In contrast, FDS and MZ present higher distributions at higher ratios.

Results of regression analysis

Figure 7 presents an overview of the predicted heat release rates. As the figure shows, the predicted values follow the prescribed HRR trendlines for each modelling approach. The following sub-sections present the linear regression equations shown in *Figure 7* for the different fire modelling resolutions.

Hand calculation method

The training dataset generated from the hand-calculation method results in the following regression expression:

$$\widehat{HRR} = 22.03 + 1174.03 \cdot \Delta T_{24m} - 2861.27 \cdot \Delta T_{36m} + 1763.40 \cdot \Delta T_{48m} - 5.52 \cdot u_0 \quad (8)$$

The R^2 values is 0.98 and the overall significance is much less than 0.05. The individual p-values of the coefficients are less than 0.05 for ΔT_{24m}, ΔT_{36m} and ΔT_{48m} while it is > 0.05 for the constant and u_0. Even though the p-values for the temperature measurements are < 0.05, an additional regression analysis is performed where ΔT_{36m} is excluded, and that analysis results in the following expression:

$$\widehat{HRR} = -149.71 - 24.56 \cdot \Delta T_{24m} + 62.28 \cdot \Delta T_{48m} + 77.08 \cdot u_0 \quad (9)$$

For this second expression the R^2 value decreased to 0.95 and the overall significance level is well below 0.05. The individual p-values for all the coefficients are below 0.05. *Figure 4* illustrates the correspondence between the training set data and the model predictions. Additionally, it includes the test data and its corresponding predictions.

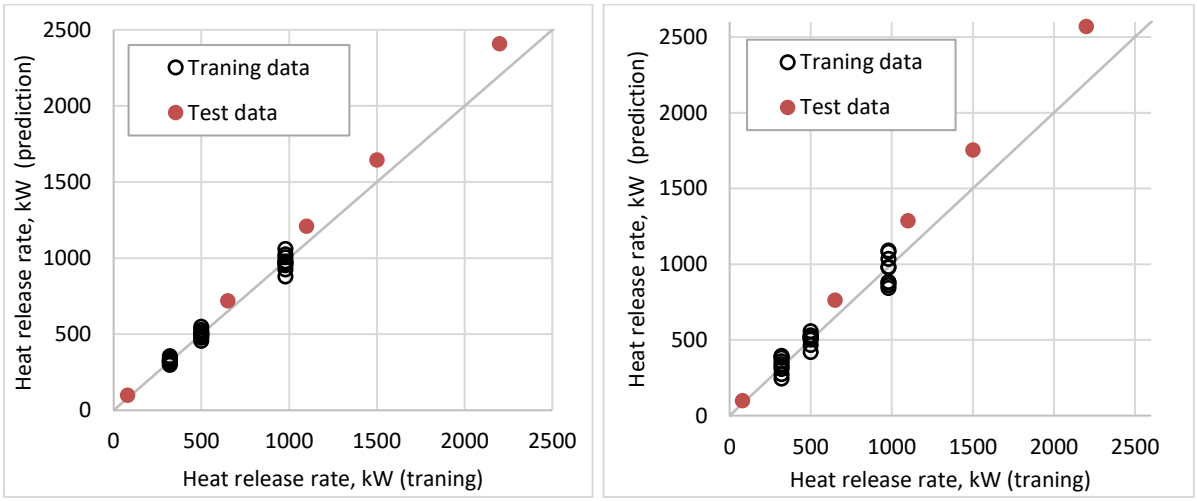

Figure 4 *Prediction vs. training dataset of HRR for the hand-calculation method. To the left is the four-variable model and to the right the three-variable model.*

Multi-zone modelling

The training dataset generated from the multi-zone model results in the following regression expression:

$$\widehat{HRR} = -276.26 - 9.07 \cdot \Delta T_{24m} + 23.17 \cdot \Delta T_{36m} - 4.11 \cdot \Delta T_{48m} + 72.99 \cdot u_0 \quad (10)$$

The R^2 value is 0.97, indicating a strong fit of the model to the data, and the overall significance level is well below 0.05. The individual p-values for the coefficients β_0 and u_0 are also below 0.05, suggesting they are statistically significant. However, the p-values for ΔT_{24m}, ΔT_{36m} and ΔT_{48m} are 0.08, 0.14, and 0.73, respectively, indicating that these coefficients are not significantly different from zero. To explore this further, a new regression analysis will be conducted, omitting ΔT_{36m}. This analysis results in the following expression:

$$\widehat{HRR} = -197.05 - 1.82 \cdot \Delta T_{24m} + 13.46 \cdot \Delta T_{48m} + 58.8 \cdot u_0 \quad (11)$$

The coefficient of determination decreased slightly to 0.94, which still indicates a strong fit of the model to the data, and the overall significance level is still well below 0.05. The individual p-values for the coefficients β_0, ΔT_{48m} and u_0 are below 0.05; however, the p-value of ΔT_{24m}, is now 0.10. If the

ΔT_{24m} as a variable in the regression analysis as a variable, the R^2 value is reduced to 0.93. In *Figure 5* it is shown how the prediction corresponds to the training set and test data for the four and three variable cases.

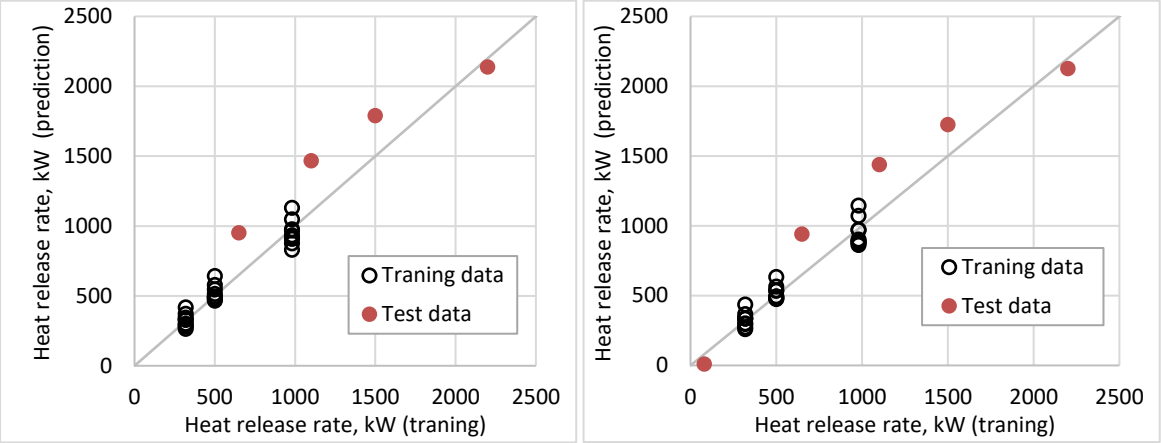

Figure 5 *Prediction vs. training dataset of HRR for the zone modelling. To the left is the four variable model and to the right the three-variable model.*

FDS modelling

The training dataset generated from the FDS model results in the following regression expression:

$$\widehat{HRR} = -252.0 + 60.63 \cdot \Delta T_{24m} - 67.78 \cdot \Delta T_{36m} + 45.70 \cdot \Delta T_{48m} + 144.03 \cdot u_0 \quad (12)$$

The coefficient of determination is 0.86, and the overall significance level is less than 10^{-8}. The individual p-values for the constant and coefficients for ΔT_{24m} and u_0 are also below 0.05, suggesting they are statistically significant. However, the p-values for ΔT_{36m} and ΔT_{48m} are 0.10 and 0.16 respectively, indicating that these coefficients are not significantly different from zero. To explore this further, a new regression analysis was conducted, omitting ΔT_{36m}. This analysis results in the following expression:

$$\widehat{HRR} = -311.40 + 13.24 \cdot \Delta T_{24m} - 5.98 \cdot \Delta T_{48m} + 163.73 \cdot u_0 \quad (13)$$

The R^2 value is 0.85, and the overall significance level is still well below 0.05. The individual p-values for the constant and the coefficients for ΔT_{24m} and u_0 are below 0.05; however, the p-value of ΔT_{48m}, is now 0.44. If the number of variables is further reduced, e.g., by removing ΔT_{48m} as a variable the coefficient of determination is reduced to 0.84. *Figure 6* shows the correspondence between training data and prediction for the four and three-variable regression expression. It should be noted that the four-variable prediction fails to represent the fire phenomena in test five leading to a negative HRR prediction value which does not have a physical meaning.

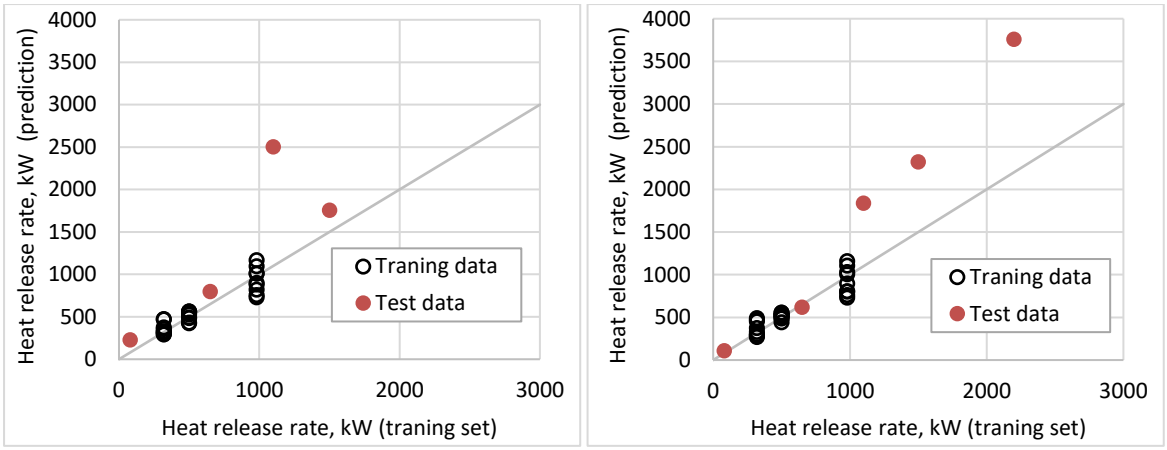

Figure 6 *Prediction vs. training data set of HRR for the FDS modelling. To the left is the four variable model and to the right the three-variable model.*

Prediction errors in testing

This comparison has been done considering the Root Mean Squared Percentage Error (RMSPE) of the testing data against the predicted HRR with the three-variable regression models (Equations 9, 11 and 13). Table 5 shows that the hand calculations have a strong dependence on the temperature values to estimate the heat release rate, and from *Figure 7* it is clear that the error increases linearly with increasing HRR.

In contrast, the FDS simulations show the best fit when predicting the second test case (HRR= 650 kW). The multi-zone model shows a better fit for larger fires. It should be noted that those results consider a position of the fire of 20 m which is outside the range of fire position that was used in the training data. This means that those results should not be considered as providing a definitive assessment of the errors for the testing datasets, but rather providing approximate estimates of errors.

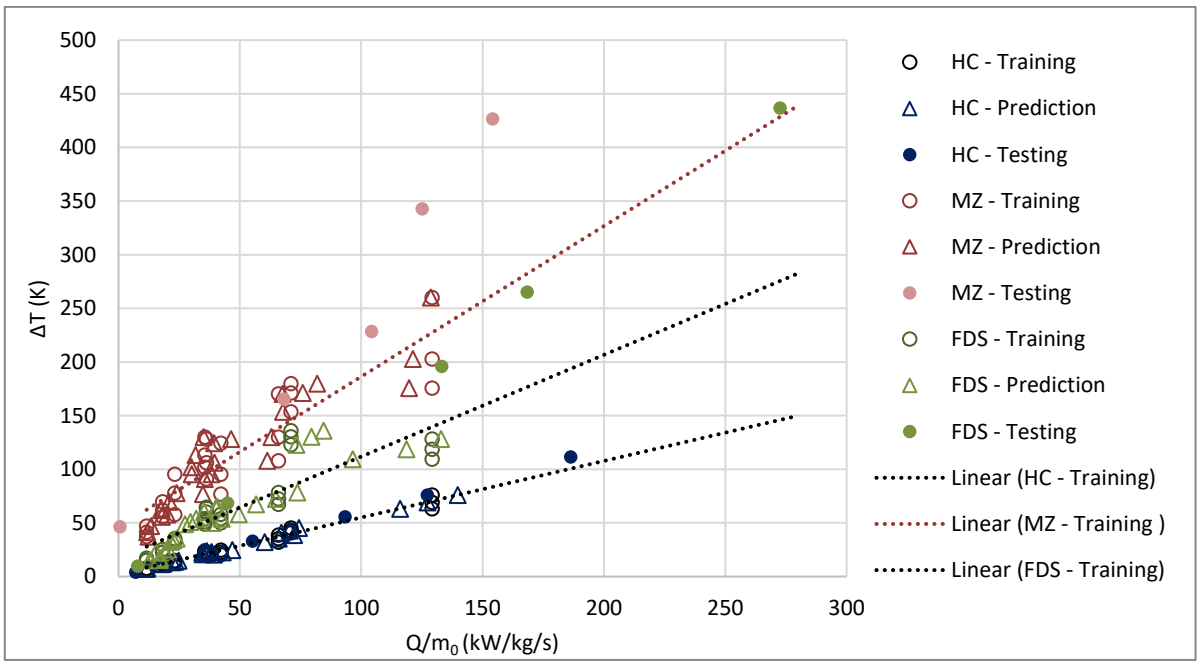

Figure 7 *Temperature increment of the 27 scenarios modelled through hand calculations (HC), multi-zone modelling (MZ), and the Fire Dynamics Simulator (FDS) at training, predicted, and testing HRR values.*

Table 4 Percentage errors of the testing datasets

Test	Q (kW)	Fire size	HC (%e)	MZ (%e)	FDS (%e)
1	80	small	22%	89%	36%
2	650	small	17%	45%	**5%**
3	1100	medium	17%	31%	67%
4	1500	medium	17%	15%	55%
5	2200	large	17%	**3%**	71%

Prediction errors in real experiments

The three-variable regression models (Equations 9, 11 and 13) together with experimental temperature measurements at 24 and 48 meters from the inlet tunnel portal are used to predict the experimental HRRs. As shown in *Figure 8*, the multi-zone and the FDS regression models provide predictions that are closer to the experimental HRRs. This is confirmed by the percentage error presented in *Table 5* for the five repeated tests. It is observed that the average HRR value of the training dataset (650 kW) is in the range of the experimental HRR values. This is the error between the predicted and expected values from the three fire modelling resolutions. On average, the multi-zone approach presents a lower percentage error (21%) than FDS (32%) and the hand calculations (177%) regression model predictions.

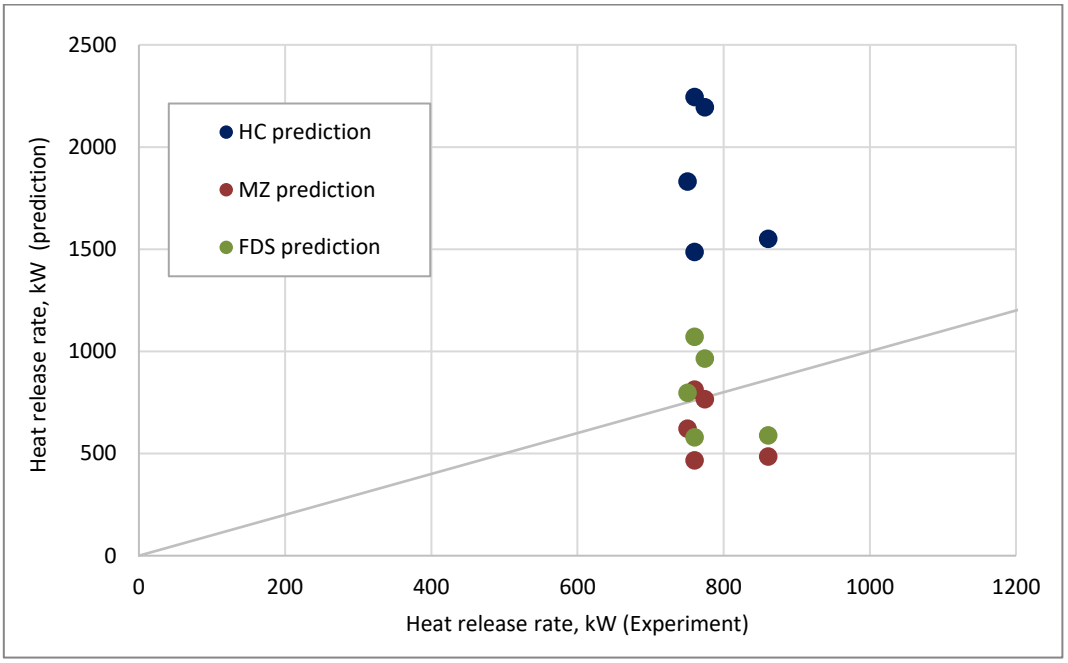

Figure 8 Prediction with the three models (three- variable) vs. data of HRR from five real experiments in a 60 m tunnel

Table 5 Percentage error of the predicted HRR for the repeated experiments

Experiment	Q (kW)	HC (%e)	MZ (%e)	FDS (%e)
1	659	178%	6%	21%
2	667	236%	22%	61%
3	663	231%	16%	46%
4	737	110%	34%	20%
5	651	128%	28%	11%
Mean	676	177%	21%	32%
Standard deviation	35	58%	11%	21%

DISCUSSION

The regression analysis results for the case study under consideration show a sufficient performance with a linear model, as the training dataset shows in Figure 4 - 6. The regression modelling shows an overfitting performance when correlating 4 variables. When considering 3 variables, including 2 temperature measurements and the ventilation velocity, it gives a more model that is sufficiently acceptable. It should however be stressed that multiple linear regression analysis assumes that the independent variables are uncorrelated. However, the temperature measurements are correlated with each other (mutual correlation). Additionally, temperature and velocity are correlated asymmetrically that is, temperature correlates with velocity but not vice versa.

As the analysis of testing data shows in Table 5, the regression model remains valid when the assumptions made in the training scenarios (such as the combustion process) are consistent with the specific scenario setup and its boundary conditions. Future research should investigate the suitability of different modelling resolutions in case of different scenarios and assumptions.

As mentioned in Section 3, the HRRPUA simplifies the combustion process. Therefore, the effect of ventilation on the heat release rate might not be accurately represented in the fire models, as the literature suggests in [14], [21], [22]. This issue should be considered when analysing the regression models.

Additionally, the predictions made for the repeated experiments are temperature sensor-dependent, where ventilation flow velocity was measured with an anemometer adding uncertainty to the estimated velocity value. The error analysis shows significant mean percentage errors on both models, multi-zone (21%) and FDS (32%), as shown in Table 5 and Table 6.

The results from the regression model based on hand-calculations (Equation 9) deviates from the experimental data. This is because the hand-calculation model gives the average cross section temperature and not the temperature underneath the ceiling. So, hand-calculations are not suitable if point sensor data should be used.

In Section 3, it was also mentioned that the characterization of the pool fire sizes is based on the ratio of the fire characteristic length and the tunnel width. Furthermore, the prediction errors in testing the FDS prediction model show higher errors at fuel geometries that are out of the training scenarios. However, since also the fire position was changed in the training dataset it is hard to separate which one of the two variables that had largest influence on the error. This highlights the importance that this type of predictive models needs to be based on a training dataset that covers all relevant scenario that can occur. It should not be expected that predictions can be done outside the boundaries of the training dataset.

Results demonstrate that CFD and MZ are promising approaches to use for the training of tools for smart firefighting. Nevertheless, more research is needed to explore other types of statistical and machine learning techniques that could be trained with those approaches. In addition, future work could focus on using other types of sensor data (i.e. not only temperature) to train this type of models, e.g. data from cameras [23], [24], [25]. However, temperature sensors are simple and robust and could together with a well-developed AI-based fire modelling tool be very efficient. In practice, smart firefighting requires a network to communicate real-world measurements to the model adopted, meaning that several practical issues need to be solved to ensure a functional and reliable smart firefighting approach which relies on coupling fire simulations with sensor data.

Furthermore, recent studies [24], [25] suggest that fire models should consider the position of obstructions in the airflow, as it reduces the longitudinal ventilation flow. This consideration should be included in a smart firefighting application.

Finally, multi-zone modelling [5] has shown to be promising in order to train a prediction model. This is an important finding since multi-zone modelling allows large computational savings compared to Computational Fluid Dynamics.

CONCLUSIONS

The present study demonstrates that multi-zone modelling and FDS are promising tools for the training of models for smart firefighting that rely on temperature sensor data and fire modelling. This implies that hand-calculations are not deemed suitable if point sensor data should be used. Multi-zone modelling has proven to be effective for training prediction models, and given its computational cost, it represents a valid option for this type of applications.

To avoid overfitting regression models, independent variables shall be included aiming to represent the assumptions (such as obstructions features and characteristic fuel length) and boundary conditions (such as tunnel geometry, obstructions, wall lining, and wind characteristics at the portals) for the training set of scenarios.

In this study, a simple linear regression approach was used. This simple statistical tool is a useful starting point for the analysis of needed modelling resolutions. Further studies can then explore the use of more complex machine learning approaches and test their ability to approximate physical fire phenomena. It is also important to highlight that regardless of the modelling approach in use, this study demonstrated how important it is to carefully select range of values in training datasets, so that they can allow representative predictions across all credible fire scenarios.

Finally, it is important to emphasize that further research is needed to translate the findings and concepts presented in this paper into practical methods applicable to real facilities. Efforts should also be made to ensure that the results from this type of smart-firefighting tools are accessible and usable for fire services, enabling them to improve decision-making in emergency situations.

ACKNOWLEDGEMENTS

This work is performed within the framework of a collaboration project funded by Cantene Srl called “Multi-scale modelling as a tool for fire risk assessment”. The authors thank Rugiada Scozzari and Michele Fronterrè for the fruitful discussion on the topic of tunnel fire safety. Furthermore, Alva Larsson, Johanna Gondinger, Dan Madsen, and Jonathan Wahlqvist are gratefully acknowledged for their assistance during the performed fire tests.

REFERENCES

[1] R. Carvel and A. Beard, *The Handbook of Tunnel Fire Safety*. 2005.
[2] W. Jahn, “Sensor and Modelling Driven Real-Time Fire Forecast,” in *Intelligent Building Fire Safety and Smart Firefighting*, X. Huang and W. C. Tam, Eds., Cham: Springer Nature Switzerland, 2024, pp. 281–303. doi: 10.1007/978-3-031-48161-1_12.
[3] “Fire and rescue operations oin tunnel fires: a discussion of some practical issues,” in *The Handbook of Tunnel Fire Safety*, 2005.
[4] H. Ingason, Y. Z. Li, and A. Lönnermark, *Tunnel Fire Dynamics*. New York, NY: Springer New York, 2015. doi: 10.1007/978-1-4939-2199-7.
[5] N. Johansson, E. Ronchi, R. Scozzari, and M. Fronterrè, “The use of multi-zone modelling for tunnel fires,” *Tunn. Undergr. Space Technol.*, vol. 134, p. 104996, Apr. 2023, doi: 10.1016/j.tust.2023.104996.
[6] H. K. Versteeg and W. Malalasekera, *An Introduction to Computational Fluid Dynamics: The Finite Volume Method*. Pearson Education Limited, 2007. [Online]. Available: https://books.google.se/books?id=RvBZ-UMpGzIC

[7] K. B. McGrattan and G. P. Forney, “Fire dynamics simulator (version 4) : user’s guide,” National Institute of Standards and Technology, Gaithersburg, MD, NIST SP 1019, 2004. doi: 10.6028/NIST.SP.1019.
[8] S.-H. Koo, J. Fraser-Mitchell, and S. Welch, “Sensor-steered fire simulation,” *Fire Saf. J.*, vol. 45, no. 3, pp. 193–205, Apr. 2010, doi: 10.1016/j.firesaf.2010.02.003.
[9] X. Zhang *et al.*, “Perspectives of big experimental database and artificial intelligence in tunnel fire research,” *Tunn. Undergr. Space Technol.*, vol. 108, p. 103691, Feb. 2021, doi: 10.1016/j.tust.2020.103691.
[10] X. Wu, X. Zhang, X. Huang, F. Xiao, and A. Usmani, “A real-time forecast of tunnel fire based on numerical database and artificial intelligence,” *Build. Simul.*, vol. 15, no. 4, pp. 511–524, Apr. 2022, doi: 10.1007/s12273-021-0775-x.
[11] J. A. Morales Mere, D. Madsen, N. Johansson, and E. Ronchi, “Repeatability Assessment in Tunnel Fire Experiments”.
[12] “Real World Research, 3rd Edition | Wiley,” Wiley.com. Accessed: Dec. 04, 2024. [Online]. Available: https://www.wiley.com/en-gb/Real+World+Research%2C+3rd+Edition-p-9781119959205
[13] J. O. Rawlings, S. G. Pantula, and D. A. Dickey, Eds., *Applied Regression Analysis*. in Springer Texts in Statistics. New York: Springer-Verlag, 1998. doi: 10.1007/b98890.
[14] “The influence of tunnel ventilation on fire behaviour,” in *The Handbook of Tunnel Fire Safety*, 2005, pp. 217–234.
[15] Y. Z. Li, B. Lei, and H. Ingason, “Study of critical velocity and backlayering length in longitudinally ventilated tunnel fires,” *Fire Saf. J.*, vol. 45, no. 6, pp. 361–370, Nov. 2010, doi: 10.1016/j.firesaf.2010.07.003.
[16] N. Johansson, “Evaluation of a zone model for fire safety engineering in large spaces,” *Fire Saf. J.*, vol. 120, p. 103122, Mar. 2021, doi: 10.1016/j.firesaf.2020.103122.
[17] K. McGrattan, R. McDermott, M. Vanella, S. Hostikka, and J. Floyd, “Fire Dynamics Simulator User’s Guide,” National Institute of Standards and Technology, Gaithersburg, Maryland, USA, NIST Special Publication 1019 revision FDS6.7.9, 2022.
[18] Kevin McGrattan, Randall McDermott, Marcos Vanella, and Eric Mueller, “Fire Dynamics Simulator Technical Reference Guide Volume 3: Validation,” National Institute of Standards and Technology, Gaithersburg, MD, NIST SP 1018, 2024. doi: 10.6028/NIST.SP.1018.
[19] K. McGrattan and M. Bilson, “Modeling longitudinal ventilation in tunnels using fire dynamics simulator,” *Fire Saf. J.*, vol. 141, p. 103982, Dec. 2023, doi: 10.1016/j.firesaf.2023.103982.
[20] M. J. Hurley *et al.*, Eds., *SFPE Handbook of Fire Protection Engineering*. in SpringerLink Bücher. New York, NY: Springer, 2016. doi: 10.1007/978-1-4939-2565-0.
[21] R. O. Carvel, A. N. Beard, P. W. Jowitt, and D. D. Drysdale, “Variation of heat release rate with forced longitudinal ventilation for vehicle fires in tunnels,” *Fire Saf. J.*, vol. 36, no. 6, pp. 569–596, Sep. 2001, doi: 10.1016/S0379-7112(01)00010-8.
[22] Y. Z. Li and H. Ingason, “The maximum ceiling gas temperature in a large tunnel fire,” *Fire Saf. J.*, vol. 48, pp. 38–48, Feb. 2012, doi: 10.1016/j.firesaf.2011.12.011.
[23] “Performance assessment of video-based fire detection system in tunnel environment - ScienceDirect.” Accessed: Dec. 13, 2024. [Online]. Available: https://www.sciencedirect.com/science/article/pii/S0886779813001314
[24] W. U. Rojas Alva, G. Jomaas, and A. S. Dederichs, “The influence of vehicular obstacles on longitudinal ventilation control in tunnel fires,” *Fire Saf. J.*, vol. 87, pp. 25–36, Jan. 2017, doi: 10.1016/j.firesaf.2016.11.001.
[25] Y. Z. Li, B. Lei, and H. Ingason, “Study of critical velocity and backlayering length in longitudinally ventilated tunnel fires,” *Fire Saf. J.*, vol. 45, no. 6–8, pp. 361–370, 2010, doi: 10.1016/j.firesaf.2010.07.003.

Review of emergency egress and rescue challenges in rail tunnels from emergency responder's perspective

Gary English, CEO (Seattle Fire Deputy Chief, ret.)
Underground Command and Safety
Vashon, Washington, USA

Abstract

NFPA 130 Standard for Fixed Guideway Transit and Passenger Rail Systems (130) provides 'life safety from fire and fire protection requirements for fixed guideway and passenger rail systems'. These requirements directly impact emergency egress and emergency responder ability to perform rescues and to mitigate fire and limit passenger harm. As 130 had received official proposals to modify the standard's egress sections, the technical committee asked Fire Protection Research Foundation (FPRF) to evaluate the 'consequences on available egress times and emergency response capabilities based on potential updated egress criteria in the enclosed trainways (tunnels)', The possible changes are critical to informing Rail Authorities (RA) and responders of current edition challenges and future change opportunities.

Specifically, the research request from 130 included "*Current (NFPA 130) language lacks technical substantiation for distances to point of safety, additionally, the minimum 610 mm (24 in.) emergency walkway widths in NFPA 130 are based upon outdated research, which does not accurately reflect current anthropometric data and limits evacuation to a single file. These conditions present greater challenges to safe evacuation compared to the experience in other public structures*." **(1)** This comparison to public structures is important as this provides safety comparison to well established people in structures..

Responders include, but not limited to firefighters, emergency medical, technical rescue, utilities, and RA personnel who have specific responsibilities in emergencies. Also note NFPA 130 only provides 'minimum requirements' and RA can impose their own safety improvements.

The product of this research is the 'Review of Emergency Egress and Rescue Challenges in Rail Tunnels (REERCRT) **(2)** which can be used to inform RA, tunnel designers, 130 users, and responders in advance of the NFPA 130 next (2029) edition. However, although 130 added a new Annex J for REERCRT, 130 had not completed the essential 'in depth' review of REERCRT in time for using this information in 2026 edition, thus the technical committee provides the following caution, "**REERCRT does not provide recommendations for implementation. Suggestions of REERCRT should not be construed as requirements by NFPA 130."** This will likely be modified for the 2029 edition. To make changes to 130, users are urged to read the full REERCRT and provide comment via Public Input process or contact the author.

Keywords: Tunnel, Trains, Fire, Emergency, Firefighters, Egress, Underground, Evacuation

PAPER APPROACH

This paper follows this research project's '**Five Tasks'** organization: with Task 1- Intensive literature review, Task 2- Tunnel fire case studies, Task 3- Anthropometric changes in US population physical and health characteristics and possible impacts on evacuation, Task 4- Comparative Analysis and Task 5- Identifying possible additional research needs.

This paper covers ONLY a small portion of the information identified in the 224 page REERCRT and

attempts to identify topics which could have a significant impact from a responder perspective with possible mitigation strategies. A second information source, a companion webinar of the same name **(3)** could also be reviewed as it provides visual and audible summations not available in print version.

NFPA 130 Technical Committee research request identified *"The aim of the overall research project is to evaluate the consequences on available egress time and emergency response capabilities of new criteria for both distances between exits and means of egress widths in rail tunnels"* **(4)**, i.e. before 130 makes standard changes, they prefer to be informed of the consequences.

NFPA 130 technical committee served as this research expert panel. NFPA technical committees develop and revise standards, promote fire and life safety and create consensus codes and standards.

INTRODUCTION - SCALE AND SCOPE

Although many envision an incident in a rail tunnel affecting only a handful of people who might need assistance, thus necessitating a 'few firefighters' to assist them, this significantly underestimates the possible reality. For emergency planning purposes, we must understand the possible, realistic scale (how big) and scope (how complex) for effective preparation and updates to NFPA 130 language. We must also understand key limits, e.g., "*Ability of emergency responders to perform rescues in smoke at the 762 m (2500 ft) spacing could be severely challenging, if not impossible, as their air supply is inadequate.*" **(5)**

In fact, trains can carry over 2000 people, a derailment and/or mid train fire could result in well over one hundred passengers needing responders assistance, i.e. well beyond the responder staffing levels is smaller communities. To clarify, a single person with significant injuries might need four responders to carry them to safety. This is time consuming. If responders are working in smoke they will be wearing their self-contained breathing apparatus (SCBA), with very limited air supply, so at best, if they must come from the downwind portal, they may only be able to assist only a few people before they must exit for air bottle refills.

Responders who live and work in cities with rail tunnel systems are keenly aware of rail tunnel challenges and anticipate the results of REERCRT and additional research to expand their knowledge on known and future challenges and more importantly, to improve passenger and responder safety.

One modeling egress scenario analysis assumes 762 m (2,500 ft) exit spacing and a counterflow on the egress walkway created by the first responders. The calculated emergency **egress time is approximately 2 hours and 40 minutes**. Although the ventilation should be able to maintain tenable conditions upstream of the fire, since the emergency power systems are only required to operate for one hour, longitudinal ventilation might simply cease before egress is complete, allowing smoke to fill the tunnel and exposing many passengers to heat, smoke and toxic gases..

REERCRT - FIVE RESEARCH TASKS

TASK 1 - EXTENSIVE LITERATURE REVIEW TO IDENTIFY SYSTEMS, EMERGENCY OPERATIONS, AND INTERFACES WITH EMERGENCY RESPONDERS

In REERCRT, trains are categorized as either 'Transit,' with passenger loads of less than 1000, or 'Intercity', with passenger loads of approximately 2000 (although higher/lower volumes occur for both types.) REERCRT included no discussion of self-powered trains (diesel, battery electric), that pose a different fire hazard due to fuels whose possible impacts should be investigated in future research.

Although the intercity passenger load may be MORE than double transit passenger loads, 130 does not distinguish between the two, thus the emergency egress paths, exits, cross passage spacing and distances per NFPA 130 which might be effective for transit, might be less effective for passenger rail. This is a fundamental and significant difference from recognized building codes which modify number of exits,

spacing and exit widths based on occupant load (number of people). The impact can be very significant. For instance, since a tunnel emergency walkway width is unchanged, the higher volumes of intercity train passengers who might need to exit in an emergency could take double the time to reach safety compared to transit systems to safely exit. This leaves passengers in a queue underground possibly exposed to more heat, toxic gases, and smoke induced loss of visibility. (See Worst Case Fire under Task 4)

Population Characteristics The proportion of elderly and obese within U.S. population has increased over time. Results show that for the defined fire scenarios, changes in population characteristics affect the egress time for large train occupant loads (2,000 persons) by up to 17%. **(6)**

Uni-directional Egress happens when an exit or the emergency walkway is blocked. Egress modeling indicates that the egress time can be doubled under this scenario. **The limitations of the egress walkway and exit capacity impact the flow of occupants who may come to a complete stop when the incident train carries large occupant loads." (7)** This could be monumental as the expected evacuation might cease necessitating responder go to the bottleneck of evacuees and create an orderly evacuation.

Illegal Acts (Terrorism) arson, bombing, gas attacks, nuisance fires, etc., are not specifically addressed in 130, NOR in most building/fire codes. Thus, planners and responders recognize the applicable fire and life safety codes/regulations and guidance documents such as 130 DO NOT NORMALLY REQUIRE the built environment i.e., structures, safety systems and related vehicles to prevent or mitigate acts of terrorism. However, the 'Emergency Operations Plans' (EOP) and requisite training' MUST account for these illegal acts to provide reasonable outcomes for passengers, responders, RA, and infrastructure. Some RA may voluntarily add or improve system components beyond what is minimally required by 130 for fires to mitigate these events, and close coordination of these tunnel components for incidents can optimize safety.

National Incident Management System (NIMS) is a US federal government mandated system for public and private organizations for managing incidents ensuring all responding agencies across all disciplines use commonly agreed terms, and organizational structure. This was not discussed in REERCRT but provides a platform for optimizing emergency responses, via the use of **Unified Command** where responder agencies work together (Fire, RA, Police, utilities e.g., traction power source). Some RAs have purpose built spaces for Unified Command 'in person' functions which can be more efficient than relying on radios to exchange information. This, along with the placement of a fire liaison in the Operations Control Center (OCC), streamlines emergency communications. For rail tunnels, use of pre-incident planning, tunnel/train systems monitoring, cameras, train operator reports and Operations Control Center information can be melded together in a NIMS compliant, Unified Command for optimal efficiency and safety..

Firefighter Air Supply firefighters use Self Contained Breathing Apparatus (SCBA) when in smoke/toxic atmosphere and are limited by SCBA air supply they wear on their backs. 'Walking 2,000 ft (610 m) to the incident and back, in a standard 45-Minute Self-SCBA with full personal protective equipment may deplete the "working" capacity of the SCBA **without having completed any rescue or firefighting operations at the scene**.' (7) 610 mm ((2000 ft) is the approximate possible evacuation distance with portal spacing at 762 (2500 feet). Firefighters must leave the smoke to replace the spent air bottle, OR Firefighter Air Replenishment System (FARS) could be installed allowing air bottle refilling while in the smoke. This dramatically improves their efficiency by allowing more time in smoke. FARS is recognized by NFPA and regulated by Fire Code and will be allowed in next NFPA 130 edition.

Emergency Walkway Width Genesis Some believe the NFPA 130, 610 mm (24 inch) minimum walkway width comes from NFPA 101, Life Safety Code, however, REERCRT research identified only one citation there to possibly validate that walkway width from NFPA. I.e. only NFPA 101 7.2.1.2.3.2 **(2)**, specifically 'https://link.nfpa.org/publications/101/2024/annexes/A/groups/7 - ID001010013207

i.e. 'Exit access door assemblies serving a room not exceeding 70 sq ft (6.5 m^2) and not required to be accessible to persons with severe mobility impairments and shall be not less than 24 in. (610 mm) in door leaf width.' Clearly the rail tunnels bear little resemblance to a 70 sq ft (6.5 m^2) room making the assertion of 24 in.(610 mm), which comes from 101, is incorrect**,** unless another code source is available.

Reconnaissance -REERCRT reported a widespread practice of responder use of 'reconnaissance team(s)' (Recon) by firefighters (and trained RA personnel,). Lacking tunnel and/or train cameras this Recon can be time consuming and delay necessary personnel dispatch and arrivals. However, real time view by cameras on trains and in tunnels, viewable by the Operations Control Center (and on site Fire Command Centers), could provide accurate conditions to Emergency Responders allowing resource assignments faster. In practice, fire responders arriving at a train with fire must identify the location, assess the situation, make decisions on resource needs, triage passengers for injuries, and inform fire dispatch of status. For trains with 2000 passengers in many rail cars, the assessment could be time consuming especially in a derailment. Live cameras from on board trains could be more effective.

Injured Transport Especially important to understand that even minor injuries can result in passengers needing assistance, e.g., a sprained ankle, which limits the ability to walk unaided, might need responder resources to assist. Moving injured patients long distances, i.e., to a station or out of a portal is both time consuming and exhausting. Alternate transportation modes are identified such as 'rail carts' to bring equipment, personnel into tunnel and carry injured out passengers, if passengers use wheelchairs, or need other mobility aids, the current walkway minimum width might simply be too narrow, necessitating relocating passengers with skeds, or collapsible wheeled extrication chairs.

Rescue Trains (RT) provide multiple functions which may need clarification. RT can be used to relocate uninjured passengers from a remote stopped train, bring maintenance/ operators to a nonfunctional train, push a disabled train, and in worst case scenarios, bring emergency responders (firefighters with rescue, medical and fire suppression equipment) to a remote train with derailment and fire and transport injured to more accessible location. This may occur when injured passengers need to be relocated out of a tunnel (i.e. beyond timely reach from surface) to waiting surface transport outside, this can be very complex, and use of Unified Command might be essential.

Initial reports from train operator (if available) can provide critically essential information using OCC checklist to identify scope and scale clarifying responder expectations. Once responder (including trained RA personnel) arrives on scene they can provide Initial Recon (cameras if available) and further clarify the scope/scale of rescue train's needs, i.e. fire suppression, how many passengers need assistance and categorized medical urgency. Code Red (advanced life support) are prioritized for stabilization and earliest removal via RT. Less injured (Code Yellow), to minor and uninjured (Code Green) can be sent out as soon as possible.

Use of predetermined joint EOP identifies exterior staging and patient drop off areas for massing resources for train movement into tunnels as well as medical transports to hospitals. This area is often at a larger intersection to accommodate responder vehicle access/parking and unloading equipment, as well as the many medical transports. Unified Command is in charge for larger incidents.

Tunnel Emergency Components

Emergency components include Egress Walkways, Emergency exits and Cross Passageways, Fire Resistant Rated Construction, Portals (also used as exits), Emergency Ventilation, Firefighting Water Supply, Fire Protection Doors, Emergency Lighting and Signage, Emergency Communication Systems, Fire Detection System, and Traction Power systems. (Note some systems use diesel trains and are therefore not reliant on traction power but have the additional challenges of diesel exhaust to control and potentially a fuel fire). Not all components are discussed in the following given space limits.

"The tunnels emergency components need to be designed to be maintain tenable conditions along the path of egress for the duration needed for safe evacuation of all passengers and train/railway crew in the event of a fire. These components need to be carefully integrated with each other to achieve a level of safety necessary to allow the safe evacuation of all passengers and train/railway crew while at the same time supporting effective access for emergency responders." **(8)**

Fire Detection is required in modern building systems and provide the nexus of automatic occupant and responder notifications, including specific room numbers/floor. However, these and related systems are oddly not as common in rail systems even though rapid detection could enhance safety and help overcome extraordinary challenges in safe tunnel exiting. Using multifunctional detection, i.e., not only early fire signs (smoke, heat, gases) as well as the exact train model, direction, passenger load, with an overlay of access/egress paths (cross passages, portals and other trains), can improve passenger safety. Camera based systems have been effective by proving fire detection but also camera views of fire, status of tunnel users and vehicles. Modern technology now allows reports/images from moving trains to occur in real time to OCC, as well as capture images of what was occurring before smoke obscured vision. These captured 'pre-alarm' images, when transferred to responder dispatch, fire command center, and first arriving responders, can expedite resource allocations.

Detection systems can also be used to identify 'overheat conditions' on train components such as wheels, cables, etc. Quality detection allows reporting agencies to provide an accurate 'scene picture' to response agencies, thus optimizing a positive outcome.

Many rail systems rely on a single train operator at the front of a train to perform multiple functions beyond train operations, such as confirming a reported fire and exact location, passenger conditions, and train movements. Expecting a lone operator to identify problems, notify OCC and direct passengers exiting (via unintelligible public address) of the direction to evacuate, as well as assisting passengers with limited ability to safety evacuate, may be too much to expect. Utilization of a building approach of displaying detected fires, ventilation activation, status of traction power, notifying passengers, and providing both audible and visual evacuation directions, might improve passenger safety.

Emergency Ventilation "Emergency evacuation during a fire event depends on the intricate and timely integration of all emergency components from the appropriate sizing of the egress path to the ability to guarantee tenable conditions along this egress path for the duration of the evacuation." **(9)** This can be a significant challenge given the **walkway widths can be too narrow for larger passengers to pass on the walkway**, limiting the evacuation speed to slowest person(s).

Many tunnels use longitudinal ventilation (pushing heat and smoke away from most passengers) thus providing a smoke protected egress route upwind i.e., not exposing these evacuating passengers to heat, smoke and reduced visibility. However, passengers without instructions on which direction to evacuate, can seek safety moving away from the fire but downstream in the smoke/ heat. They can be exposed to toxic smoke, significant heat and their vision obscured by smoke, all can reduce/prevent their self-rescue ability. Even evacuating to a cross passage at 800 feet spacing could exceed 60 minutes if ventilation fails or exit path is blocked by other passengers, debris from derailment, etc.

Also, many presume fires always 'burn hot', with smoke/gases stratifying near the ceiling for the duration of evacuation. In those specific conditions, not using mechanical ventilating effectively prevents destratification of smoke for short distances, however, not ventilating allows smoke to move in both tunnel directions. Possibly in the direction of emergency exiting due to piston effect. And, as smoke mixes with cooler air away from the fire, smoke/gases descend, and evacuating passengers can be enveloped in smoke with resultant loss of visibility and toxic gas exposure. This can occur a short distance.

Tunnels with hybrid ventilation or single point extraction which removes heat and smoke at or near the fire can significantly enhance evacuation as only the area proximate to the fire may be untenable. With this ventilation system, once passengers move away from the train, they will not be exposed to heat, smoke. Retrofitting point extraction into a tunnel may be feasible, however, as space is necessary to install ceiling smoke exhaust plenums, and/or midpoint ventilation shaft(s), although technically feasible, locating a vertical shaft in concentrated urban settings may be challenging and costly. For new rail systems, point extraction may prove viable and significantly improve fire safety.

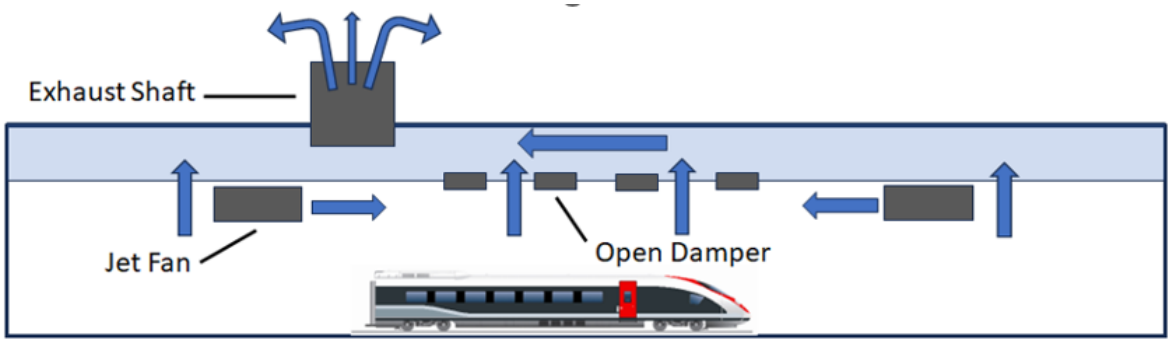

Figure 1 Single Point/Hybrid Extraction System (not representative of all point extraction)

Each of the case studies evaluated have referenced ventilation systems in whatever format is employed by the various railroads as being instrumental in meeting the required tunnel tenability. Keeping these fans operational is always a major concern. Fans that have been removed from service for maintenance are a key concern to operations, especially where their fans are necessary to ensure minimum critical velocities, and an extra fan can be included in design in case of a fan failure. However, to ensure critical velocities are met additional fans up and downstream of the incident location might also be used to compensate fan out of service until fans are restored. Some agencies plan their fan tests to take place on Fridays after rush hours. Thus, when a fan needs repair, this could occur over the weekend before Monday peak hours.

REERCRT identified NFPA 130 lacks necessary requirements for testing and maintenance of ventilation critical system components. Nor is tunnel ventilation addressed by other standards; therefore, this topic was specifically recommended to be addressed by 130 in REERCRT.

Firefighter Water Supply / Suppression Fires occur on trains in tunnels and without fire suppression (sprinklers or mist) and/or ability for firefighters to lay fire hose lines from water standpipes in/near tunnels to directly suppress the fire, fires have burned throughout a train. Additional water flow might also be needed for high fire heat release rates which have occurred due to the **'carried on' fire load (baggage, strollers, etc.) whose fires can contribute as much as one-half the fire load.** This occurs as many of these materials are hydrocarbons which burn rapidly with high heat release rates and can produce black, toxic smoke. To alleviate the risk of fires on board, compact mist fire suppression systems have been installed in some rail systems. (130 Annex G - Onboard Fire Suppression).

Fire Size "Table 11 provides information on the fuel load, ignition source, ventilation characteristics, measured Heat Release Rate (HRR) from various fire test data conducted in the last thirty years. The heat release rate measurements from the reviewed testing highlight two general types of fire behavior, influenced by the ignition source, fuel load, and ventilation.

1. Non-Arson Fires: Fires tests with wooden sticks as the ignition source show a linear fire growth rate of approximately 0.5 MW per minute until a peak HRR is reached. During these tests, the peak HRR varies between 13 MW and 19 MW with an average peak HRR of 16 MW.
2. Arson-Type Fires: Fires initiated with an ignitable liquid such as gasoline generally follow a two-step process: The first step constitutes the incipient phase of the fire and can generally be

characterized by a rapid linear fire growth (0.5 to 1 MW per minute) for approximately 260 seconds after ignition, although the factors governing the incipient phase duration are not well established. The second step of the fire (development phase) is characterized by a very rapid and linear fire growth rate (approx. 16 MW per minute) with a peak HRR achieved in a few minutes. The peak HRR measured during the large-scale fire testing varies from 31 MW to 77 MW with an average peak HRR of 55 MW." **(10)**

(Note 77 MW HRR mentioned in this paragraph were obtained in 'THE METRO PROJECT' i.e., full scale tunnel fire test which also showed the 'Impact of the Carried Fire Load in Mass Transport System' fires can be very significant http://www.metroproject.se/Pubs/METRO_report.pdf)

TASK 2 - REVIEW OF FIVE RAIL TUNNEL INCIDENTS

Reviewing these greatly abbreviated 'after action' reports, as well as RA documents and federal investigations, several common challenges were identified:

- High Heat challenges firefighters i.e., rail tunnel fires differ substantially than surface structure fires as the heat is 'contained' and 'reflected' within the tunnel and the structure absorbs and reradiates heat, making fire conditions more intense than occurs in most other structure fires where heat escapes to atmosphere.
- Difficult or inadequate firefighter water supply - tunnel water supply systems can be unfamiliar and differ from more commonly used surface water supply systems. Practicing on actual equipment and or building training props with the same equipment would improve water access.
- Limited ventilation - Ventilation is critical to move smoke, toxic gases, and convective heat away as much as possible. To determine what ventilation capacity is needed, the design fire is used which is based on the fire load, available oxygen, and other factors. After commissioning, periodic testing to ensure reliability and ventilation meets performance specifications are necessary. However, 130 lacks language which requires ventilation periodic testing, maintenance, and performance.
- Many rail tunnels ventilation systems were built before the potential fire size was understood and ventilation might be undersized, allowing heat, smoke, gases to back layer over escaping passengers.
- Firefighter communications - fire radio repeater systems were not functional (and had not been repaired when previously requested by fire command) at more than one incident. This severely negatively impacted at least one incident with ability for firefighters to coordinate emergency response and left them using time consuming 'firefighter runners' to relay orders.
- FTA, in at least one document, incorrectly identifies the minimum egress path as 914 mm (36"), which is the width at the chest, not the more restrictive 610 mm (24") width of the footpath which defines egress.
- Lack of Emergency Operating Procedures – although rail authority staff have written procedures and practices, these have not always been periodically practiced as required. The Homeland Security Exercise and Evaluation Program in 130 annex offers clear guidance on various levels and types of training.
- Lack of safe refuge for firefighters - tunnel fire geometry severely limits the ability for firefighters to seek safety in a shelter if needed especially where cross passages are not available.

TASK 3 - FIRE AND EGRESS MODELING ANALYSIS

The following are a few important examples of modeling results and case studies.

"Analysis of the 2,500 ft Exit Spacing Impact on Egress Time. The egress study has focused on the spacing of cross-passageways when used for egress in lieu of exits. NFPA 130 requires exits to be spaced no more than 762 m (2,500 ft) apart. Using inputs from the fire model with 2000 people, mid train 55 MW fire, several egress scenarios with exit spacings of 762 m (2,500 ft) and 381 m (1,250 ft) were analyzed to evaluate egress times. Results are presented in Table 36." **(11)**

Notably 2023 NFPA 130 7.3.2 requires the ventilation system to operate for 60 minutes, i.e., less than the modeled expected egress time, therefore even section of the tunnel upwind of the fire could be overwhelmed by smoke when longitudinal ventilation stops working and evacuation exceeds one hour.

There are options. Frankfurt, Germany uses, large 'mobile ventilation units' moved to exterior of a rail tunnel to add ventilation to rail tunnels via very large diameter air hoses fitted for access holes, or via portals.

REERCRT notes First Responders will need to adapt their personnel rotation strategy as air supply and fatigue will be an issue for NFPA compliant tunnels. However, Firefighter Air Replenishment Systems (FARS) can improve their air supply, which improves efficiency of responders.

"For large occupant loads, results show that the counterflow created by emergency responders can double the duration of egress for current NFPA 130 compliant systems" **(12)** Egress time is reduced when the egress walkway width is increased to 914 mm (36 in.) but conditions downstream of the fire may be untenable before egress is completed. (Note there was no modeling of 1220 mm (48") walkways.

NFPA 130 minimum requirement for egress walkway width does not allow for double file movement which is necessary to significantly reduce the egress times.

REERCRT did not consider responder access through interconnecting rail cars, over top of cars in derailments, or along non walkway side of trains which need to be researched for viability.
During the initial incident, firefighters will move through a train triaging passenger injuries, fire and damage to create a status report to command and resource requests.

"Analysis of the 2,500 ft Exit Spacing Impact on Egress Time. The egress study has focused on the spacing of cross-passageways when used for egress in lieu of exits. NFPA 130 requires exits to be spaced no more than 762 m (2,500 ft) apart. Using inputs from the fire model with 2000 people, mid train 55 MW fire, several egress scenarios with exit spacings of 762 m (2,500 ft) and 381 m (1,250 ft) were analyzed to evaluate egress times. Results are presented in Table 36." **(13)**

Also not modeled was the impact of 'automatic closing' fire resistant doors between train cars, which would isolate a fire to a single car, thus limiting fire byproducts in other cars and protecting passengers at least for a short time from heat, smoke, gases. Some RA have opted to eliminate doors to improve convenience of passenger movement which may allow fire spread. (Correctly designed doors would not block normal activities as doors could be opened to allow escape/ access if needed.)

TASK 4 - COMPARATIVE ANALYSIS

Comparing Building Fire Safety to Rail Tunnels - We have decades of experience with building fires in buildings with populations exceeding 10,000 people, i.e., well beyond maximum numbers of people in a rail tunnel. The building safety is optimized through regulations, design, fire systems and we can reasonably expect a 'worst case' fire in a building' to allow an orderly and relatively quick evacuation to safety, and prevention of a fire from spreading beyond initial areas. Code requirements increase exit capacities based on population changes and generally limit exit distance to 200 feet to exterior or fire hardened exit way. Also, fire sprinklers prevent fire from growing or spreading and are mandated in almost all new US structures. Retroactively installing sprinklers in some structures such as parking garages are now required. Note there has not been a US fire with more than two fatalities in a building with full sprinkler coverage, other than illegal acts (e.g. 9 1 1 attack). However, NFPA 130 does not require fire sprinklers in all public underground areas.

Comparing building safety vs 130 "Rail tunnels offer unique fire safety challenges. Their location and geometry limit the amount of egress paths resulting in greater escape distances than what is required for buildings. While egress requirements in buildings vary with occupant load, egress requirements in rail tunnels are independent of the number of occupants on the train. In the event there is a fire within a rail tunnel, standard emergency operating procedures typically recommend moving the train either to the nearest accessible station or out of the tunnel entirely. This allows passengers and crew to evacuate more efficiently and provides better access for emergency response teams. When the consequences of a

fire incident (poor visibility, extreme heat, system failure, etc.) are such that they require or cause the train to stop inside a rail tunnel, a protected route offering tenable conditions needs to be available to evacuate passengers, train railway crew and to provide access to emergency responders." **(14)**

Fire Scenario - Worst Case i.e. Mid Train Fire
Although NFPA 130 discusses a 'mid train fire', (usually defined as 'a fire that separates the passengers/train crew population into two different evacuation groups)', any fire located between the two end-cars constitutes a mid-train fire.' Mid-train fires are not necessarily the worst case scenario for NFPA 130 in compliant rail tunnels depending on the distances to cross passages or portals. However, adopting a 'possible worst case scenario is essential for emergency rail operations and emergency responders to develop emergency plans to mitigate.

'The worst-case scenario is a concept in risk management wherein the designer/operator/responders when planning for potential fire incidents, considers the most severe possible outcome that can reasonably be projected to occur in a given situation.' Experienced fire command officers often initially presume a 'worst case' until proven otherwise, this ensures possible essential resources are moving towards the incident and prevents major surprises at the incident or in incident planning. Canceling 'too many' resources is preferable to lengthy delays waiting for essential resources to arrive.

Worst case can be a stopped train mostly out of tunnel and longitudinal ventilation which pushes heat/smoke away from the 'most' passengers at nearest portal. This ventilation pushes smoke over passengers who decided to self-rescue towards farthest portal exit which could be 2000 feet to safety at distant portal, as shown in Figure 2.

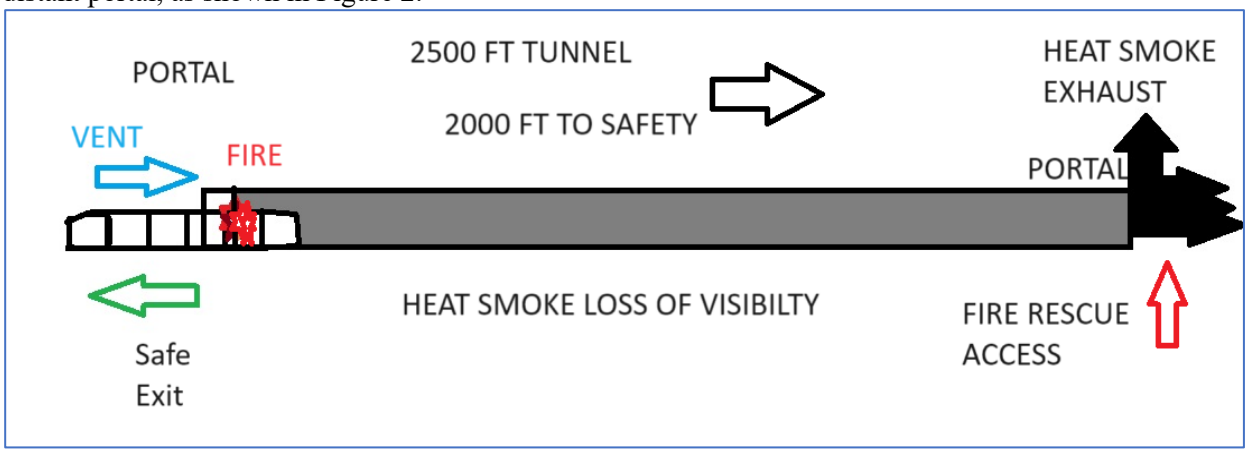

Figure 2. 'Worst Case' Train Fire in 2500 Foot Long Tunnel Section, Train partially out of tunnel, fire near portal. Passenger safety at 500 ft in no smoke or 2000 feet to downwind portal in heat and smoke

In this worst case scenario, once firefighters arrive at the train extending beyond the portal, they will start both passenger rescue and fire suppression. Depending on fire, they might be able to stop fire growth fast enough to allow passenger to evacuate past the fire toward nearby, upwind exit (portal), i.e. past fire location. Regardless of firefighter arrival, many passengers (lacking guidance) may have already chosen to self-rescue downwind in smoke i.e., towards the distant entry portal as they do not understand risks, nor have the risks been explained to them. Although firefighters might attempt to catch passengers walking away from them, the relative speeds might make this difficult.

NFPA 130 does not require ventilation in enclosed trainways (tunnels) less than 305 m (1000 ft). This may be due to presuming the fire will be at mid-point in a tunnel, and therefore the longest evacuations distance would be 152 m (500 feet). But, as shown in Mid Train Worst Case above, a similar phenomenon could occur in tunnels less than 305 m (1000 ft) (7.1.2.2).

Fire Sprinklers/ Mist Some trains now have 'mist' (fine droplet) fire suppression on board, i.e., inside/under the cars, which should reduce/stop fire growth and minimize fire spread depending on what is burning. Mist systems are preferred inside trains over common sprinklers as the volume of water (size

and weight) needed to suppress a fire is significantly less than required for typical sprinkler systems with larger droplet sizes.

Comparing Distances Between Exits to Surface and Cross Passages with Other Country Regulation

"Among the various standards and codes reviewed, the provisions for maximum distance between emergency exits vary between 760 m (2493 ft) from the Singapore Code of Practice for Fire Precautions on Rapid Transit Systems to 1,000 m (3,281 ft) from the European standards TSI-SRT 2014 and UIC 779-9 with an average maximum spacing of 848 m (2,780 ft) ± 120 m (392 ft)." **(16)**

The provisions for maximum distance between **cross-passageways** listed in **Table 3**, vary between 240 m (787 ft) from AS 4825:2011 to 800 m (2,625 ft) in the French standard ITI – 98 m (300ft) with an average value of 410 m (1,354 ft) ± 203 m (664 ft)." **(17)**

"The distance between emergency exits/cross-passageways needs to be contingent upon the estimated potential occupancy during a fire incident, the dimensions of the egress walkways, and a representative egress speed of the persons evacuating, taking into account Persons with Restricted Mobility (PRM)." **(18)**

REERCRT Table 3 SPACING BETWEEN EMERGENCY EXITS AND BETWEEN CROSS PASSAGEWAYS

Standard/Guideline	Region	Maximum Distance between Emergency Exits	Maximum Distance between Cross-passageways
NFPA 130[48]	USA	762 m (2500 ft) [6.3.1.4]	244 m (800 ft) [6.3.1.6]
TSI-SRT 2014[49]	EU	1000m (3281 ft) [4.2.1.5.2 (b) (1)]	500 m (1640 ft) [4.2.1.5.2 (b) (2)]
ITI – 98 300[50]	France	800 m (2625 ft) [4.1.2]	800 m (2625 ft) [4.1.3]
BS 9992:2020[51]	UK	N/A	500 m (1640 ft) [28.5]
AS 4825:2011[52]	Australia	N/A	240 m (787 ft)
Code of Practice for Fire Precautions in Rapid Transit Systems[53]	Singapore	760 m (2493 ft) [9.3.2 (b)]	250 m (820 ft) [9.3.3 (b)]
Guidelines on Formulation of Fire Safety Requirements for New Railway Infrastructures[54]	HK	762 m (2500 ft) [2.4.2 (i)]	244 m (800 ft) [2.4.2 (iii)]
UIC 779-9[55]	EU	1000 m (3281 ft) [I-43]	500 m (1640 ft) [I-43]
DECRETO 28 ottobre 2005. Sicurezza nelle gallerie ferroviarie.[56]	Italy	Single bore tunnel: 4000 m (13,123 ft), 2000 m (6,562 ft) in cities [1.3.5]	500 m (1640 ft) for [1.3.5]

None of the international distances between exits are significantly less than NFPA 130.

NFPA 130 allows using 'cross-passages' (passages between rail tunnels) as a point of safety in lieu of emergency exits to surface.

EMERGENCY WALKWAY WIDTHS and COMPARING OTHER COUNTRY REGULATIONS.

"Obstruction free walkways allow passengers, employees, and emergency responders to egress or access the area of a tunnel in which there is an incident. The design of the egress walkway should be

commensurate with the layout of the tunnel infrastructure and the rail system. Access to a walkway is usually expected from each track of a rail tunnel. Different configurations exist and are often constructed:

- on at least one side in a single track tunnel tube,
- on both sides of the tunnel,
- in between each track for multiple track tunnel tubes." **(19)**

"Irrespective of the location of egress walkways, additional walkways can be provided and reserved for emergency responders' access"**(20)** Although this could improve egress and emergency access and operations, this would add a significant cost to the tunnel construction. "In addition to the number of egress walkways, the other crucial design parameters governing the flow rate of rate of evacuating passengers and crew are clear width, clear height, continuity of path, presences of constrictions, accessibility for PRM." **(21)**

REERCRT Table 1

MINIMUM WIDTH AND HEIGHT STANDARDS REQUIREMENTS FOR EGRESS WALKWAYS.

Standard/Guideline	Region	Min. Width of Egress Walkway	Min. Height of Escape Walkway (m)
NFPA 130[23]	USA	*Height above walkway* / *Min. Width* 0 mm (0 in.) / 610 mm (24 in.) 1575 mm (62 in.) / 760 mm (30 in.) 2025 mm (80 in.) / 430 mm (17 in.) [6.3.2.1]	2025 mm (80 in.) [6.3.2.1]
TSI-SRT 2014[24]	EU	800 mm (31 in.) [4.2.1.6]	2250 mm (89 in.) [4.2.1.6]
SIA 197/1 2019[25]	CH	1000 mm (39 in.) [8.8.3.5]	2250 mm (89 in.) [8.8.3.5]
ITI – 98 300[26]	France	700 mm (28 in.) [3.1.2]	2000 mm (79 in.) [3.1.2]
BS 9992:2020[27]	UK	1000 mm (39 in) [28.2]	2250 mm (89 in.) [28.2]
AS 4825:2011[28]	Australia	850 mm (33 in.)	
Code of Practice for Fire Precautions in Rapid Transit Systems[29]	Singapore	800 mm (31 in.) [9.3.5]	N/A
Guidelines on Formulation of Fire Safety Requirements for New Railway Infrastructures[30]	HK	850 mm (33 in.) [2.4.2 (vii)]	2200 mm (87 in.) [2.4.2 (vii)]
UIC 779-9[31]	EU	700 mm (28 in.), optimally 1200 mm (47 in.) [I-40]	N/A
DECRETO 28 ottobre 2005. Sicurezza nelle gallerie ferroviarie.[32]	Italy	900 mm (35 in.) if tunnel ≥ 2000 m (6,562 ft) 500 mm otherwise [1.3.1]	N/A

"The size of the escape route in the emergency exits and cross-passageways are essential components of the egress and emergency responders access strategies. It should be harmonized with the expected train occupant load and the capacity of the egress walkways. The dimensions of emergency exits/cross passageways depend on factors such as the expected number of escaping persons in case of a fire incident, the planned sequence of evacuation, including area needed for emergency responders and

technical components installed. Geological conditions and cost also need to be considered when developing the egress components of a rail tunnel." **(22)**

"The width of the emergency walkway has been under discussion in 130 since 1982 when a suggestion was made to increase the emergency walkway width to 1118 mm (44 inches). This width would match NFPA 101 and International Building Code widths and allow two way movement on walkway, i.e., allowing evacuees and responders to move in opposite directions thus expediting evacuation and emergency response., However, increasing the walkway widths can increase the cost to construct a tunnel 508 mm (20 inches) wider for the length of the tunnel." **(23)** However, the **Seattle Link Light Rail tunnel bores provide enough width for 813 mm (32 inch) emergency walkways as required by the Seattle Fire Code. This allows use of emergency stretchers with wheels spread 584 mm (23 inch) wide vs. 130 walkway widths of 610 mm (24 in.) which presents a dangerous combination where stretcher wheels could fall off the walkway. LA Metro has 36" minimum walkway widths for newer tunnels.**

For comparison, "the egress walkway minimum clear widths compiled in Table 1 vary from 610 mm (24 in.) in NFPA 130 to 1000 mm (39 in.) in BS 9992:2020 and SIA 197/1:2019. The average egress walkway minimum clear width from the values listed in the different standards reviewed is 812 mm (32 in.) ± 132 mm (5 in.). The egress walkway minimum clear heights vary from 2025 mm (80 in.) in NFPA 130 to 2250 mm (89 in.) in TSI-SRT 2014, BS 9992:2020 and SIA 197/1:2019. The average egress walkway minimum clear height is 2162 mm (85 in.) ± 118 mm (5 in.)." **(24)**
(Note, NFPA 130 minimum walkway width is 102 mm (4 inches) narrower than any other regulation.)

As mentioned, these narrow walkways limit emergency exiting to single file, thus passenger evacuation speed is limited by the slowest evacuee as passing is difficult. This is made more severe as the passenger physical size is increasing over time per the anthropometric data research.

Since the 610 mm (24 in.) walkway width was adopted by NFPA 130 in 2003 edition, the physical passenger size dimensions have increased by 17%, further slowing or blocking the emergency egress path. "**Comparing intercity rail and rapid transit rail systems showed the higher passenger loads of intercity rail tend to create 7% to 17% longer egress times were estimated when using occupants' characteristics based on 2018 population data compared to occupants' characteristics based on the 2000 population data**." **(25)**

TASK 5- REERCRT KNOWLEDGE GAPS - Identified Research Needs

"Over the span of the project, three (3) general areas where additional research needs have been identified:
1) Models Limitations – Additional research is needed to adequately characterize current tunnel geometries, train characteristics, and occupant loads. In addition, developing representative physical and heath for train occupants characteristics, including occupants with impaired mobility, is a topic that remains to be addressed.

2) Egress Gaps - The origin of the current NFPA 130 exit spacing requirements and their substantiations are unknown (although some suggest these are based on the early Atlanta Marta dimensions.. Their limits are highlighted by egress scenarios where access to the egress walkway needs to be shared by train occupants and first responders as well as occupants with restricted mobility are present. A holistic approach needs to be developed to provide guidance on the appropriate design of egress walkway widths and exit spacing by considering tunnels, rail systems, and occupants characteristics as well as emergency ventilation strategies. Additional research needs to be conducted to assess the impact from each of these inputs to the overall egress design. To address the challenges of egress for occupants with restricted mobility, the inclusion of ADA requirements should be evaluated. Finally, occupant's survivability profiles should be developed for fire in rail tunnels to better define tenability criteria.

3) Fire Department Response Gaps - *"*Although fire services have developed standard operating procedures and guidelines for fire events in rail tunnels, there is a lack of emergency responders experience with NFPA 130 compliant tunnels due to the age of most rail tunnels in the U.S. (i.e., built before promulgation of 130 in 1975). A critical challenge faced by emergency responders is related to the limitations of current breathing and protective equipment to allow for extended work time during a fire event. Furthermore, each firefighter is unique with their own physiology, complicating the ability to reliably estimate how long the air supply may last during operations. Firefighters' capabilities are dependent on the environmental conditions inside the rail tunnels. Tenability inside a rail tunnel can be extended with adequate ventilation equipment and strategies, and or developing procedures and 'reversing longitudinal ventilation' when safe, thus providing fresh air to evacuees and firefighters." **(26)** Understanding this by the broader NFPA 130 audience should be a priority.

OTHER RESEARCH SUGGESTIONS

REERCRT provides excellent information and initial modeling analysis, which can be used to inform the rail tunnel community and specifically the NFPA 130 committee and others on the '**consequences on available egress times and emergency response capabilities based on potential updated egress criteria for future standard changes.'**

Several possible future research areas are identified:

1) Complete additional modeling needed as determined by NFPA 130 technical committee
2) Dimensions - Research widths needed to allow passing on walkway or potential of wider walkway niches to allow slower evacuees to move out of way and responders to pass. Determine stretcher wheel width and design to accommodate them.
3) Exits–Presuming physical passenger dimensions will continue to increase at the same pace (34% increase by 2044), project emergency walkway and doorway exit widths needed to maintain current egress capacities to 2050.
4) Research impacts of adopting ADA exit and notification processes in rail tunnel.
5) Identify impacts on fire smoke spread by intervening fire doors between train cars. Identify what fire impacts to oxygen level would occur if free burning train cars(s) with baggage occurs in a single track and twin track tunnel.
6) Determine safety impacts of adopting building type fire alarm systems on trains in tunnels. Fire/smoke detection, in trains, NFPA 72 compliant visual/audible alarms (ability challenged) ensure announcements meet intelligibility and audibility, including PA from Operator. Adding automated emergency notification systems in cars, with evacuation directional arrows, alarms, traction power status, signs for distances to exits
7) Clarify worst case emergency evacuation distances with current and projected distances to exits/cross passages and impacts to responders
8) Research impacts of using Firefighter Air Replenishment Systems (FARS) to improve firefighter air supply systems and enhance firefighter and rescue efficiency. Distance between FARS cabinets
9) Identify SOPs for Rescue trains, Rail carts. Identify equipment used in caches at stations or other locations (fire hoses, extrication equipment, backboards, SKEDs (low friction person sliding mat), evacuation chairs, prepackaged emergency medical equipment, collapsible search sticks, etc.)
10) Research needed for: optimal evacuation strategies – walkway vs 'though interior car' to invert, Use of train interior doors to isolate fire to reduce interior smoke/heat movement, sequential car evacuation to allow those at higher risk to escape before walkway is overwhelmed.. Battery powered trains, fuel powered trains
11) Identify changes necessary to provide same exiting capacity/times between intercity and transit systems.
12) Ventilation: Identify feasibility of adding point extraction to existing tunnels or including in design. Ensure 130 ventilation remains functional for duration of evacuation.
13) Identify impacts of trains with other fuels, diesel, battery, other?
14) Research feasibility of passengers self- rescue breathing devices

REFERENCES

1) Review of Emergency Egress and Rescue Challenges in Rail Tunnels, Fire Protection Research Foundation, 2024 Code Red Consultants, Herbert Biteau, et.al., January 2024, p2
2) Review of Emergency Egress and Rescue Challenges in Rail Tunnels, NFPA, Fire Protection Research Foundation, Code Red Consultants, Herbert Biteau, et.al., January 2024
3) Webinar, 'Review of Emergency Egress and Rescue Challenges in Rail Tunnels' https://www.nfpa.org/videos/review-of-emergency-egress-and-rescue-challenges-in-rail-tunnels , NFPA, Fire Protection Research Foundation, Code Red Consultants, Herbert Biteau, et.al., January 2024

4) BITEAU, p 2
5) BITEAU, p iii
6) BITEAU, p 2
7) BITEAU, p 27
8) BITEAU, p 7
9) BITEAU, p 113
10) BITEAU, p 33
11) BITEAU, p 113
12) BITEAU, p 123
13) BITEAU, p28
14) BITEAU, p28
15) BITEAU, p28
16) BITEAU, p28
17) BITEAU, p28
18) BITEAU, p28
19) BITEAU, p9
20) BITEAU, p8
21) BITEAU, p8
22) BITEAU, p9
23) BITEAU, p9
24) BITEAU, p20
25) BITEAU, p98
26) BITEAU, p3

Figures

1) Single Point/ Hybrid Extraction System, REERCRT, p 14
2) Diagram Worst Reasonable Case Tunnel Train Fire, Author
3) Table 3. Spacing Between Emergency Exits and Between Cross-Passageways, BITEAU, 2024, p 29
4) Table 1. Min Width and Height Standard Requirement for Egress Walkways, BITEAU, 2024, p 19

Learning from Disasters

Iain Bowman
Mott MacDonald
Renaissance House, 9-16 Dingwall Road, Croydon, United Kingdom
E-mail: iain.bowman@mottmac.com

ABSTRACT

Fire safety in underground infrastructure engineering largely focuses on ensuring the design and construction of the infrastructure is as safe as reasonably possible. To this end much design effort is expended on improving the understanding of the physics of fires, the optimal means of reducing the risk of fire, and of minimising the effects of fire should it occur. This design process follows the standard hazard control practices of elimination, substitution, engineering controls, administrative controls, and personal protective equipment (PPE). However these processes cannot fully eliminate the probability of fire from the operational infrastructure. Consequently, underground infrastructure owners, operators and first responders must have robust processes both (i) for the conduct of operations and maintenance and (ii) emergency response and recovery for when a fire does occur. To successfully develop and implement emergency responses, it is vital that owners and operators properly understand how human behaviours (HB) both prior to and during an incident can influence the outcome of an incident. Planning can be significantly strengthened by studying major incidents, both in tunnels and elsewhere, from the past to examine how they came to occur and how they escalated into disaster. The extent to which non-sector-specific human behaviours influence the outcome of an incident is examined and assessed. A set of relevant case histories, from multiple sectors, drawing on available sources such as public inquiries and previously published papers, is examined to determine the extent to which common cause human behaviours influence the occurrence and severity of a disaster.

KEYWORDS: Human behaviour, human behaviours, safety culture, emergency planning, emergency response, hazard control

INTRODUCTION

This paper attempts to assess the role of human behaviour in the escalation of emergency incidents into disasters that result in significant loss of life, other casualties, and large-scale damage to physical assets. Specifically, it attempts to determine whether there is any correlation between human behaviours, both organisational and individual, that contribute to disaster across different asset types. A set of case studies of well-known incidents from multiple sectors is examined to look for common cause human behaviours that occur when a disaster occurs. Types of assets involved include road and rail tunnels, surface railways, nuclear power generation facilities, offshore oil & gas drilling rigs, residential buildings, missile early-warning systems, and space vehicles. The primary focus was on incidents (twelve) that resulted in fatalities, with some incidents (four) where no fatalities occurred included for context. Available data for these incidents is analysed to assess the type and quantity of human behaviours that were determined by the relevant inquiries, or other published sources, to have been contributors to the escalation of the incident. The data is further assessed to analyse the extent of common human behaviours contributions to the development of each of the incidents.

ASSET SAFETY AND SAFETY CULTURE

Safety of an operational asset starts with design. Projects follow hazard control processes to minimise the risk of fire or other potentially catastrophic incidents, which can vary with the type of asset. These hazard control processes typically use a layered approach of elimination, substitution, engineering controls, administrative controls, and PPE to mitigate operational risks to an acceptable level. However these processes do not normally completely eliminate the risk of hazard occurrence. Faults in complex assets can arise from many causes. Reliability and safety assurance processes can assist in reducing the probability of fault occurrence but cannot eliminate them.

Assets are owned, managed, operated and maintained by humans. Safe use of an asset is fundamentally dependent on the behaviour of humans [1]. This includes management, planning, and implementation of procedures and processes to support safety. Consequently, the owners and operators of assets, along with the emergency services, need to develop, implement, enforce, and periodically review and revise policies and processes that will facilitate emergency response and recovery that minimises the consequences of any incident that may occur.

Safety culture is a key concept and is defined by the United Kingdom Health and Safety Executive [2] thus: “Safety culture is a combination of the attitudes, values and perceptions that influence how something is actually done in the workplace, rather than how it should be done.”

ACCIDENT MODELS

Accident models attempt to describe the interactions of various behaviours in a system that can lead to occurrence of an accident. Examples of accident models are linear models such as the domino model, the bowtie model, the “swiss cheese” model, and non-linear models such as the “drift into failure” model. Such models have value in incident analysis however caution needs to be used to when assessing an incident, particularly for complex cases such as major incidents and disasters. This paper includes some discussion of potentially appropriate accident model(s) for the incidents studied, drawing on the evidence extracted from the data sets used for the analysis.

INCIDENTS: PROXIMATE AND ROOT CAUSES, AND CONTRIBUTORY BEHAVIOURS

In reviewing incidents, especially disastrous incidents, it is important to distinguish between root cause and proximate cause. Proximate cause is the initiating event, the thing that goes wrong. Root cause is the reason why the initiating event occurred and can also be the reason why the incident was able to escalate to a disaster. The proximate cause may not be the root cause of the disaster. A simple example illustrates this: A person is driving a car with worn-out tires, and they crash because a tire blows out. The proximate cause of the crash is the blow out of the tire, however the root cause is the driver’s failure to monitor the condition of the tires and their failure to replace them before they become unsafe, i.e. the driver has a poor safety culture.

Not all incidents escalate. Only a small number of incidents become catastrophic. Such incidents, with rare exceptions, do not typically initiate as catastrophic, but develop from a potentially manageable initial incident due to a variety of escalating behaviours. While design sometimes contains such behaviours, it is common that human behavioural behaviours are found to have been contributors to the disaster. These behaviours can be categorised as summarised in Table 1. These categorisations are qualitative and there is a degree of overlap between some of them, however the intent is to capture different types of human behaviour related to different aspects of asset operation. Their temporal relationship with the occurrence of an incident is particularly important. This is captured in Table 1. It is also important to be aware that there is a cyclic aspect to such human behaviours. Following an incident, if appropriate lessons are not learned, the conditions for another incident may be present even after the first incident has been reviewed and mitigations apparently implemented. The approach taken in this paper was to utilise the findings in the data sources regarding applicable human behaviours and not to revisit those findings. Thus the behaviours listed in *Table* are derived directly

from the text in the data sources.

Table 1. List of contributory human behaviours

Behaviour No.	Behaviour description	Individual or organisational[1]	Stage of Incident
1	Poor planning	Organisational	Prior to incident
2	Poor maintenance	Organisational	Prior to incident
3	Failure to operate within safe parameters	Organisational	Prior to incident
4	Failure to learn from past near misses	Organisational	Prior to incident
5	Incorrect response	Individual	During incident
6	Inadequate communication	Individual	During incident
7	Complacency[2]	Organisational	At all times
8	Failure to prioritise life safety	Organisational	At all times
9	Poor safety culture[2]	Organisational	At all times

1 - Human behaviours can be differentiated by whether they are predominantly associated with individual human error, e.g. incorrect response during an incident, or more predominantly associated with organisational shortcomings, e.g. poor planning. This differentiation is not absolute, it is more nuanced.
2 - Safety culture is used as defined by the UK HSE as noted above. Complacency is used as defined by the Merriam-Webster Dictionary: "Self-satisfaction especially when accompanied by unawareness of actual dangers or deficiencies." [3]

Organisational issues are as much a human behaviour as individual human error since organisations are managed and operated by humans. *Table* captures nine different human behaviours, of which seven are predominantly organisational behaviours, with only two that are predominantly individual behaviours. Note that the two individual behaviours are primarily related to human response in emergency, while the organisational behaviours are primarily related to operations before and after an incident.

CASE STUDIES

In this paper, the selected data set consists of fifteen incident case histories and one near miss case history. The case histories were selected to represent a mixture of (i) catastrophic incidents with significant loss of life, (ii) major incidents with few casualties, (iii) one significant near miss, (iv) global locations, and (v) incidents from a variety of different types of operational assets. The list is shown alphabetically in *Table 2*. Nine occurred on underground transportation, and seven were related to other types of asset i.e. surface rail, nuclear power generation facility, offshore oil & gas drilling rig, residential building, missile early warning system, and space vehicles. Twelve of the case histories resulted in fatalities, while four case histories did not. The data varies somewhat in quality depending on the available sources. In *Table 2*, data quality is classified as follows:

Class A: Official inquiry reports are the highest quality sources.
Class B: Published research is second to the official inquiry sources.
Class C: News media and internet sources lacking higher quality corroboration are third level.

In cases where Class C sources have had to be relied upon, corroboration via use of multiple sources was used where possible.

Table 2. List of incident case histories

No	Date	Incident	Location	Operator	Type of asset	Type of incident	Data Class
1	1995-10-28	Baku [4,5,6]	Kazakhstan	Baku Metro	Underground rail	Fire	C
2	1986-01-28	Challenger [7]	United States	NASA	Space vehicle	Explosion & disintegration	A

3	1996-11-18	Channel Tunnel [8]	United Kingdom / France	Eurotunnel	Underground rail	Fire	A
4	2008-09-11	Channel Tunnel [9]	United Kingdom / France	Eurotunnel	Underground rail	Fire	A
5	1986-04-25	Chernobyl [10]	USSR	USSR Ministry of Power	Nuclear energy plant	Explosion, fire, radiation exposure	A
6	1988-12-12	Clapham Junction [11]	United Kingdom	British Rail	Surface rail	Collision	A
7	2003-02-01	Columbia [12]	United States	NASA	Space vehicle	Structural failure due to overheating	A
8	2003-02-19	Daegu [13]	South Korea	Daegu Metro	Underground rail	Fire	B
9	2017-06-14	Grenfell Tower [14,15]	United Kingdom	Kensington and Chelsea London Borough Council	High-rise residential building	Fire	A
10	2004-01-05	Hong Kong MTR [16]	Hong Kong	MTRCL	Underground rail	Fire	A
11	2000-11-11	Kaprun [17]	Austria	Gletscherbahnen Kaprun AG	Underground rail	Fire	B
12	1987-11-18	King's Cross [18]	United Kingdom	London Underground / London Regional Transport	Underground rail	Fire	A
13	1999-03-24	Mont Blanc [19,20]	France / Italy	ATMB / SITMB	Underground road	Fire	A, B
14	1988-07-06	Piper Alpha [21]	United Kingdom	Occidental Petroleum	Oil & gas offshore platform	Explosion & fire	A
15	1983-09-26	Soviet nuclear false alarm [22]	USSR	Soviet Air Defence Forces	Nuclear attack early warning facility	Near miss - nuclear war	C
16	2015-01-15	WMATA Lac L'Enfant Plaza [23]	United States	WMATA	Underground rail	Fire	A

The casualties associated with each incident are listed in *Table 3*. Casualties ranged from zero to 559. The fatality rate varied from 0% to 100%.

Table 3 Incident Casualties

		Casualties			
Date	**Incident**	**Non-fatal**	**Fatal**	**Total**	**% fatalities**
1995-10-28	Baku	270	289	559	52%
1986-01-28	Challenger	0	7	7	100%
1996-11-18	Channel Tunnel	2	0	2	0%
2008-09-11	Channel Tunnel	14	0	14	0%
1986-04-25	Chernobyl (Note 1)	Not available	30	30	-
1988-12-12	Clapham Junction	484	35	519	7%
2003-02-01	Columbia	0	7	7	100%
2003-02-19	Daegu	151	192	343	56%
2017-06-14	Grenfell Tower	74	72	146	49%

2004-01-05	Hong Kong MTR	17	0	17	0%
2000-11-11	Kaprun (Note 2)	12	155	167	93%
1987-11-18	King's Cross	100	31	131	24%
1999-03-24	Mont Blanc	14	39	53	74%
1988-07-06	Piper Alpha (Note 3)	61	167	228	73%
1983-09-26	Soviet nuclear false alarm	0	0	0	0%
2015-01-15	WMATA Lac L'Enfant Plaza	91	1	92	1%

1. Fatalities for incident only. Chernobyl total casualty figures are debated due to uncertainty over long-term effects on the global population. Estimates have ranged from 4000 to as high as 60000. 4000 is the current estimate for the eventual fatalities. Non-fatal casualty data is not available. [24, 25]
2. Kaprun non-fatal injuries not reported; figure listed is total number of survivors. [17]
3. Piper Alpha non-fatal injuries not reported, other than a number of survivors were burned; figure listed is total number of survivors. [21]

INCIDENT SUMMARIES

Brief summaries of each incident are listed here. For detailed assessments of each incident refer to the sources cited in the References section. Following each incident, inquiries were held, safety reviews were executed, and revisions to safety systems and/or procedures were implemented. Despite this, reoccurrences have been observed, most notably with the 2003 Columbia incident following the 1986 Challenger incident, and the 2008 Channel Tunnel fire following the 1996 Channel Tunnel fire.

Case History 1: Baku Metro tunnel fire [4, 5, 6]
The Baku Metro fire in 1995 remains one of the worst rail tunnel incidents to date. The proximate cause was an electrical fault on the incident train. Baku Metro had been constructed in 1967 and the rolling stock in use at the time was not constructed to current fire resistance standards. Due to the age of the vehicles the train materials readily ignited and produced significant quantities of toxic smoke and combustion products. The train stopped in a tunnel 200m after departing Ulduz Station. The tunnel ventilation did not appear to have been operated correctly. There were issues with passengers being unable to open train doors and many of the victims were found on board the train with crush-related injuries. There is no evidence of whether passengers received any emergency communications, however this cannot be determined definitively from the available evidence. In addition to the age of the train vehicles, there was evidence that the trains were poorly maintained, with faults being a common occurrence. Reports of prior safety incidents and near misses were recorded at the time. Overall there was strong evidence of a poor safety culture within the operator organisation.

Case Histories 2 and 7: STS-51 Challenger [7] & STS-107 Columbia [12] vehicle disintegration
The 1986 Challenger incident and the 2003 Columbia incident were separated by 17 years however they shared many common elements. Both occurred when a known flaw in the vehicle design led to a catastrophic structural failure of the orbiter. In Challenger's case the proximate cause was the Solid Rocket Booster (SRB) O-ring design; in Columbia it was damage to the thermal protection tiles on launch. In both incidents, the flaws were well known by NASA and had resulted in numerous near misses prior to each incident, however in neither case was any effort made to eliminate the flaws from the vehicles. In the case of Columbia, the thermal tiles were known to have suffered damage in 65 of the previous 79 launches of the space shuttle. In Challenger's case, the risk could have been mitigated by waiting for warmer weather, but NASA chose to proceed despite knowing the risks. In both cases, the inquiry reports assessed that there was a poor safety culture within both NASA and within the relevant suppliers. The Columbia incident shared numerous contributing human behaviours with the Challenger incident, which suggested that the lessons from Challenger had not been sufficiently learned and adopted.

Case Histories 3 and 4: Channel Tunnel rail tunnel fires [8, 9]
Both the 1996 and 2008 Channel tunnel fires were serious incidents, arising from a decision during project planning to transport Heavy Goods Vehicles (HGVs) in open sided rail cars. The proximate

cause in each case was an HGV with a fire in the vehicle when the train entered the tunnel. The open sided railcar design provided a strong airflow over the incident HGV in both cases, and this was assessed to have accelerated the growth of the HGV fire. In the 1996 incident the fire was serious enough to cause major structural damage to the tunnel. However both resulted in only minor casualties due to safety-related equipment having been maintained to a good standard and an overall appropriate response by staff and the emergency services, suggesting a good safety culture within the operator organisation.

Case History 5: Chernobyl nuclear power plant explosion and fire [10]
The 1986 Chernobyl incident remains the most catastrophic nuclear power incident to date. The proximate cause was the reactor being operated in an unsafe manner not consistent with the approved operational procedures, which was made possible due to the reactor design. Earlier incidents and near misses involving the same type of reactor at other plants demonstrated the limitations of the design however poor communication within the operator organisation meant these lessons were not shared with other plants such as that at Chernobyl. Poor safety culture within the Soviet nuclear power sector was explicitly identified as the root cause in the inquiry report.

Case History 6: Clapham Junction rail collision [11]
The 1988 Clapham Junction incident proximate cause was a signalling fault that was due to poor work executed as part of a program to replace end of life signalling cabling. An old wire was incorrectly left in place and left unsecured in such a way that it was left live and able to turn a signal that should have been red into green. The inquiry into the incident identified previous incidents and near misses related to similar prior work, poor planning, and complacency, and identified a poor safety culture in the operator.

Case History 8: Daegu metro tunnel fire [13]
The 2003 Daegu metro fire was an arson attack. The proximate cause was thus the arsonist. Like in Baku, the train vehicles were not constructed to current fire resistance standards and produced significant quantities of toxic smoke and combustion products once they had ignited. Errors in emergency communications and response by operator staff led to a non-incident train entering the station and stopping next to the incident train and then to occupants being locked in this non-incident train. Overall there was strong evidence of a poor safety culture within the operator organisation.

Case History 9: Grenfell Tower fire [14, 15]
The 2017 Grenfell Tower fire proximate cause was an electrical fault in one of the flats in the tower. This spread externally to the building cladding which was not fire-rated correctly for the usage. Other behaviours identified included poor building maintenance, poor safety advice to the occupants, poor performance by the fire service at the scene, failings in ensuring that the building refurbishment adhered to proper fire safety practices, failings in the testing and rating of cladding products, the owner-operator's failure to heed notifications of issues and a failure to act following similar prior incidents involving the cladding. The inquiry identified a poor safety culture within all organisations involved.

Case History 10: Hong Kong MTR metro tunnel fire [16]
The 2004 Hong Kong MTR fire was, like Daegu, an arson attack. In this incident however, there were no fatalities and only a small number of minor casualties. Emergency response and communications were effective and emergency systems were operational, available, and used correctly by staff, which suggested a good safety culture within the operator organisation.

Case History 11: Kaprun funicular tunnel fire [17]
The 2000 Kaprun funicular tunnel fire proximate cause was an unauthorised heater in the driver's cab, at the low elevation end of the train, that malfunctioned and ignited. The train vehicles were not constructed to current fire resistance standards, and there were no smoke detectors or fire extinguishers present. The train ignited and due to the gradient of the funicular tunnel, a chimney effect caused the fire to spread rapidly upwards through the entire train. Train systems, including

hydraulics, communications, electric power, and lighting, failed and doors could not be opened. Staff at the alpine centre at the top end of the tunnel evacuated but failed to close doors behind them, increasing the chimney effect. The only survivors were the few persons who evacuated downhill to the lower portal. The inquiry identified a poor safety culture as the root cause.

Case History 12: Kings Cross metro tunnel fire [18]
The 1987 Kings Cross fire proximate cause was a cigarette discarded on a wooden escalator that found its way under the escalator where it ignited a buildup of trash mixed with lubricating grease. The fire spread rapidly up the escalator and flashed over into the ticket hall. The inquiry found that there had been numerous prior near misses involving discarded cigarettes, despite a 1985 ban on smoking on the underground. The inquiry also found shortcomings in the maintenance processes and emergency response planning, and overall identified a poor safety culture in the operator organisation.

Case History 13: Mont Blanc road tunnel fire [19, 20]
The 1999 Mont Blanc incident proximate cause was an HGV that caught fire within the tunnel. The tunnel was completed in 1965 and by 1999 it was carrying a significantly higher vehicle load, particularly HGVs, than originally anticipated. Some safety measures reportedly failed to function on demand, while others were overwhelmed by conditions beyond their design capacity. There were issues with response coordination and communication, particularly for tunnel ventilation and fire-fighting services, between the two separate entities responsible for tunnel operations and emergency response. Prior to the incident, there were known concerns related to tunnel operations, which had not yet been addressed at the time of the incident. Overall there was evidence of a poor safety culture in the responsible organisations. Reference [26] was a direct consequence of this incident.

Case History 14: Piper Alpha offshore platform fire [21]
The 1988 Piper Alpha fire proximate cause was a failure of a temporary unrated blanking plate ("blind flange") in one of the two gas condensate pipelines on the platform. This resulted in a massive explosion and subsequent fire. The failure resulted from poor shift-change communication of the status of unfinished maintenance work, combined with a subsequent failure in the second of the two condensate pipelines. With incomplete knowledge of the safety status of the first pipeline, the new shift crew switched the condensate flow back to the first pipeline. This caused the unrated blind flange to fail and the resulting gas breach ignited and exploded, destroying the platform's command centre. The fire spread rapidly and consumed the platform in three hours. The peak heat release rate was estimated to be 100GW. The inquiry found numerous pre-existing operational human behaviours contributed to the disaster, ranging from poor planning, poor maintenance, poor communication to an insufficient consideration for safety. Overall there was strong evidence of a poor safety culture.

Case History 16: WMATA LRT tunnel fire [23]
The 2015 WMATA tunnel incident proximate cause was a cabling short circuit fault in the tunnel that caused an electrical fire in the tunnel that generated significant quantities of toxic smoke. Smoke detectors either did not function or were not responded to correctly. A train was engulfed with smoke and could not be moved as the traction power was shut off. Passengers were required to evacuate through the heavy smoke which could not be controlled due to the age of the tunnel ventilation system, which had not been designed for emergency smoke control, only for heat removal and temperature control. The inquiry identified multiple contributory human behaviours and explicitly highlighted the "lack of a safety culture" at the operator as the root cause.

NEAR MISSES

Case History 15: Soviet nuclear missile detection near miss [22]
A single near miss case history was included, due to its global significance. The 1983 Soviet Union nuclear missile early warning incident was likely the most significant near miss recorded. On 26 September, 1983, during a time of heightened tension between the Soviet Union and the USA, a Soviet early warning system detected the launch of six American ICBMs, for which the prescribed response under the Soviet Mutually Assured Destruction (MAD) policy was an automatic massive

nuclear retaliation. The officer in charge of the early warning facility, Stanislav Yevgrafovich Petrov, was required to immediately report this to his superiors, so they could initiate the automated response. However Petrov did not report the incident. He reasoned that (i) a US first strike would be massive, not a mere six missiles, (ii) the satellite-based computer system was new and had experienced issues previously, and (iii) there were no correlating reports from ground-based radar. Petrov's response, using logic, knowledge, experience and correlating data, likely averted a large-scale nuclear conflict between the Soviet Union and the West.

It was later concluded that the proximate cause of the false alarm was the satellite's sensors mistaking reflections of the sun off high altitude clouds due to the satellite's extreme elliptical Molniya orbit. This was rectified by cross-referencing against a geostationary satellite. Petrov's alert reasoning nullified the organisational planning issues of (i) the Soviet MAD policy, and (ii) reliance on the new computer-based monitoring system. This incident highlighted the criticality of good human behaviour in emergency.

HUMAN BEHAVIOURS ASSESSED TO BE CONTRIBUTORS TO THE INCIDENTS

Table 4 summarises the human behaviours from *Table* that were assessed by the references to have contributed to each incident. A behaviour is assessed as one of: (i) confirmed contributor, (ii) confirmed non-contributor, (iii) not applicable, or (iv) not assessed due to a lack of data.

Table 4 Assessed human behaviours contributing to the incident

		Human behaviours contributing to incident									
Incident	Proximate Cause	Incorrect response	Inadequate communication	Failure to prioritise life safety	Poor planning	Poor maintenance	Failure to learn from past near misses	Complacency	Failure to operate within safe parameters	Poor safety culture	**Human behaviours causes count**
Baku	Electrical fault	Y	?	Y	Y	Y	Y	Y	Y	Y	**8**
Challenger	O-ring seal failure	n/a	N	Y	Y	N	Y	Y	Y	Y	**6**
Channel Tunnel	HGV fire	N	N	N	Y	N	N	N	N	N	**1**
Channel Tunnel	HGV fire	N	N	N	Y	N	N	N	N	N	**1**
Chernobyl	Unsafe operation	Y	Y	Y	Y	Y	Y	Y	Y	Y	**9**
Clapham Junction	Signalling fault	N	Y	Y	Y	Y	Y	Y	Y	Y	**8**
Columbia	Damage to exterior tiles	n/a	N	Y	Y	N	Y	Y	?	Y	**5**
Daegu	Arson attack	Y	Y	Y	Y	N	N	Y	Y	Y	**7**
Grenfell Tower	Electrical fault	Y	Y	Y	Y	Y	Y	Y	Y	Y	**9**
Hong Kong MTR	Arson attack	N	N	N	N	N	?	N	N	N	**0**

Kaprun	Heater fault	Y	Y	Y	Y	Y	Y	Y	Y	Y	**9**
King's Cross	Discarded cigarette	?	N	Y	Y	Y	Y	Y	?	Y	**6**
Mont Blanc	HGV fire	Y	Y	Y	Y	Y	Y	Y	Y	Y	**9**
Piper Alpha	Blind flange failure	?	Y	Y	Y	?	Y	Y	Y	Y	**7**
Soviet nuclear false alarm	False monitoring signal	N	N	N	Y	N	N	N	N	N	**1**
WMATA	Cabling fault	Y	Y	Y	Y	Y	Y	Y	Y	Y	**9**

Legend:
Y = confirmed contributor; N = confirmed non-contributor; n/a = not applicable; ? = not assessed (lack of data)

INCIDENT DATA ANALYSIS

The data from the set of incidents was analysed to search for potential common cause human behaviours which were assessed to have contributed to the incidents. Casualty figures were compared with the number and type of assessed contributory human behaviours in Table 1.

Casualty rates were analysed to assess the comparative severity of each incident. Three parameters were used to assess incident severity (i) total casualty numbers, (ii) total fatality numbers, and (iii) fatality rates. The latter parameter is useful for classifying incidents that may not have resulted in large numbers of casualties but had a high rate of fatality. The Challenger and Columbia incidents are examples of this type of incident.

Figure 1 shows the numbers of casualties for each incident. *Figure 2* shows the fatality rates for each incident. The fatality rate for Chernobyl is skewed due to the lack of reliable non-fatal casualty data, i.e. the actual rate is unknown but lower than 100% however it was not deemed appropriate to present the fatality rate as a null value since there were significant fatalities and it was a severe incident. The fatality rate is significantly higher for incidents where escape was either critically restricted or effectively impossible: (i) Challenger and Columbia, (ii) Kaprun, (iii) Mont Blanc, and (iv) Piper Alpha.

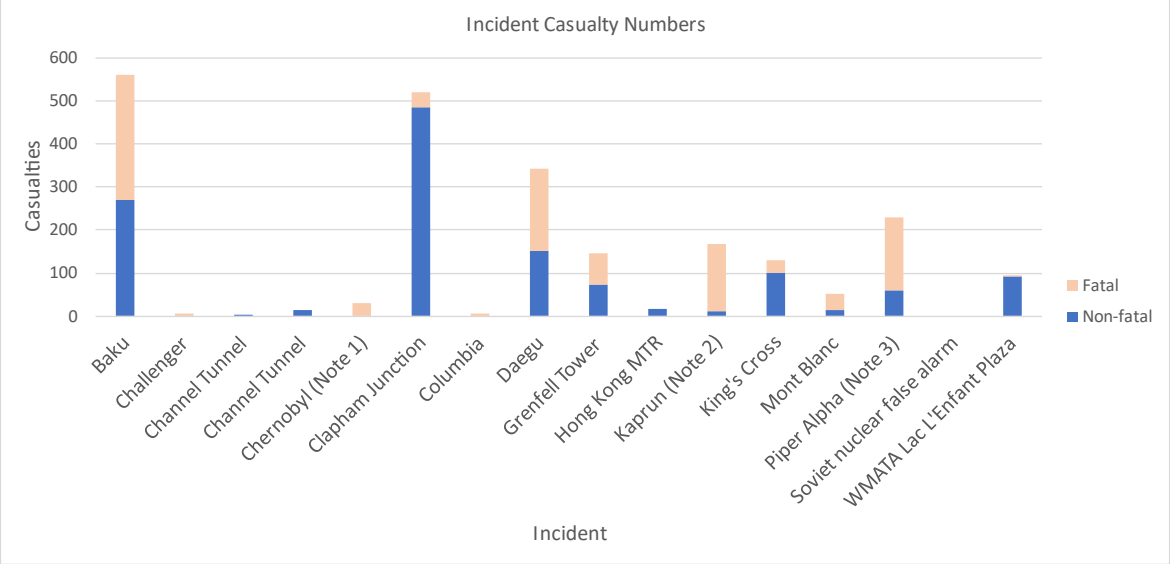

Figure 1. Incident casualty (fatal and non-fatal) numbers

Refer to Table 3 for notes explanations.

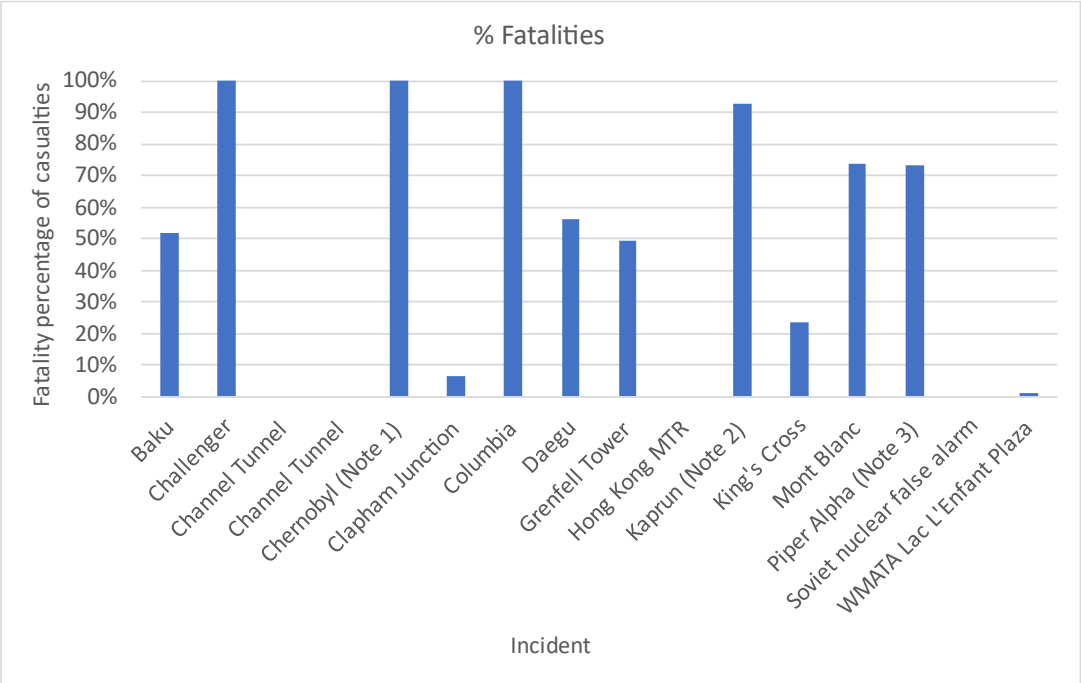

Figure 2. Fatality percentages vs Incident (incidents with fatalities only)
Refer to Table 3 for notes explanations.

Figure 3 shows the number of contributory human behaviours for each incident as assessed by the references.

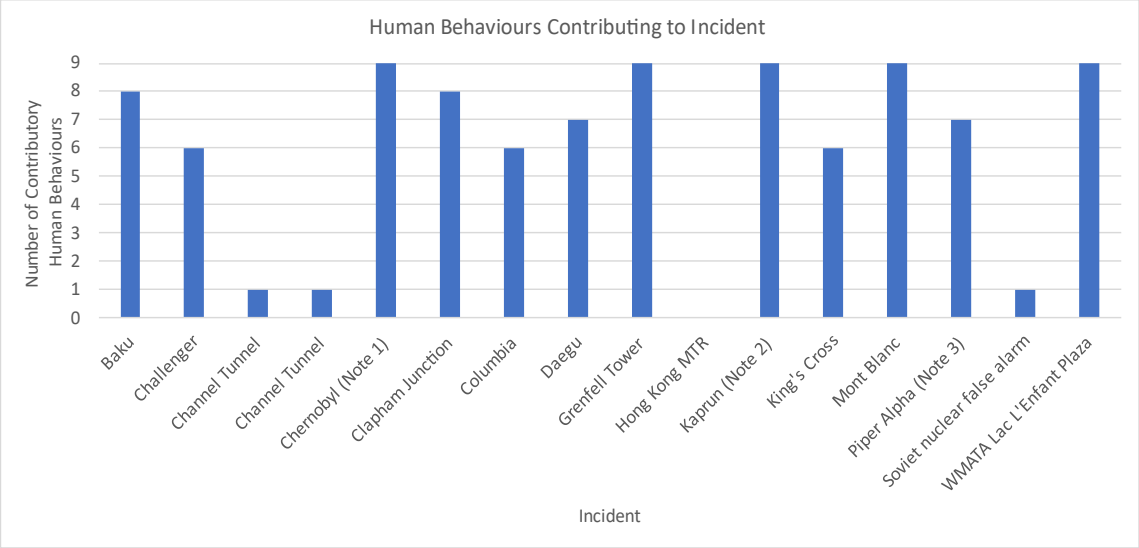

Figure 3. Number of human behaviours contributing to incident
Refer to Table 3 for notes explanations.

Figure 4 and *Figure 5* plot fatality percentages and casualties for all incidents in the data set as a function of the number of contributing human behaviours. These show that fatalities and significant numbers of casualties occurred only when an incident contained six or more of the nine human behaviours listed in Table 1.

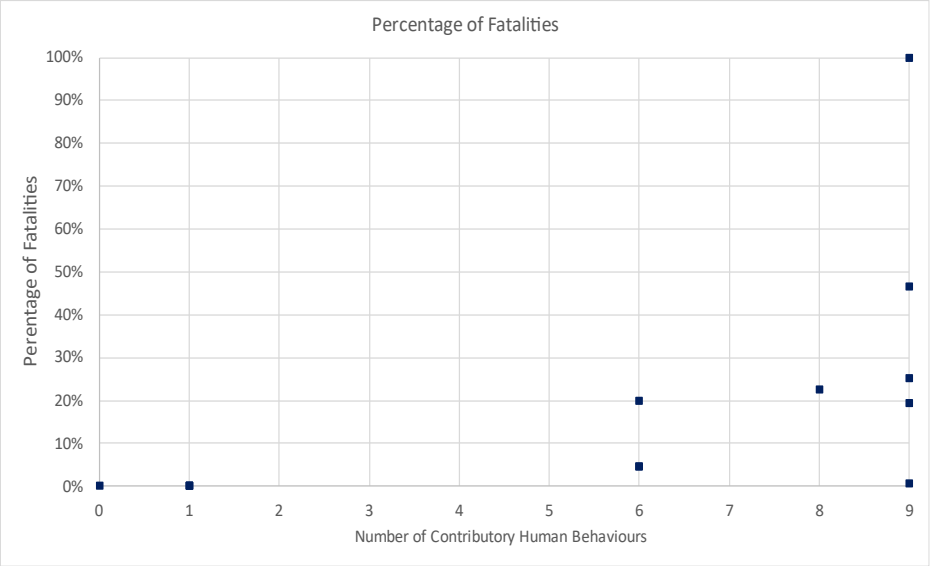

Figure 4. Percentage of fatalities vs number of contributory human behaviours

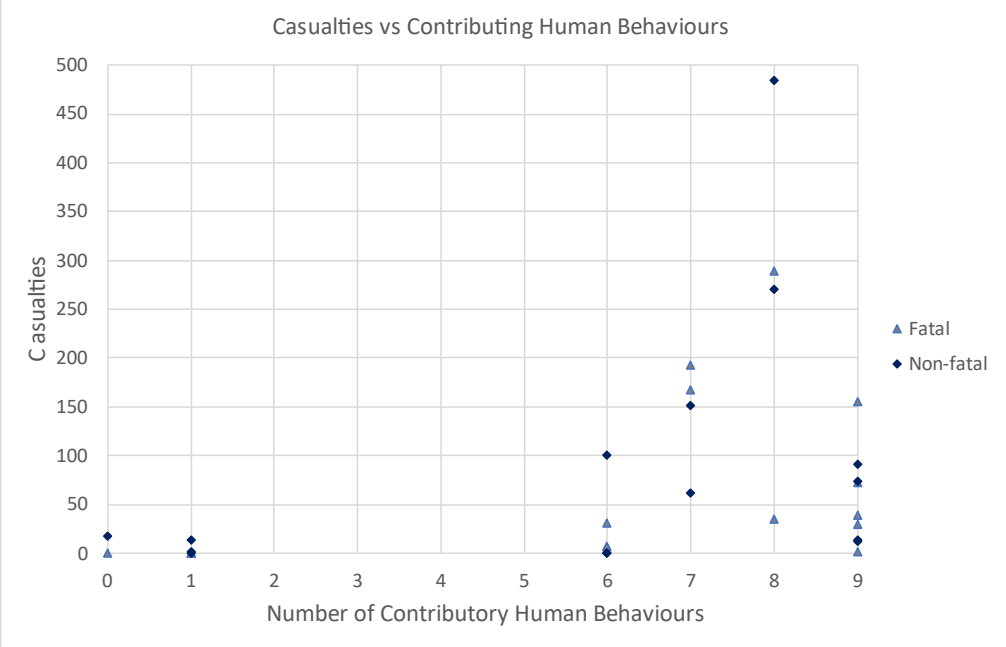

Figure 5. Casualty figures vs number of contributory human behaviours

Figure 6 plots the number of incidents resulting in fatalities for each of the specific contributing human behaviours attributed to each of the incidents. *Figure 7* plots the same data for the non-fatal incidents in the selected incidents set. This shows that the most common behaviours in catastrophic fatal incidents are predominantly organisational behaviours, while 'human error' behaviours such as incorrect responses and inadequate communication are not as widespread, though still common. Four organizational behaviours were assessed to be common to all the fatal incidents in the study.

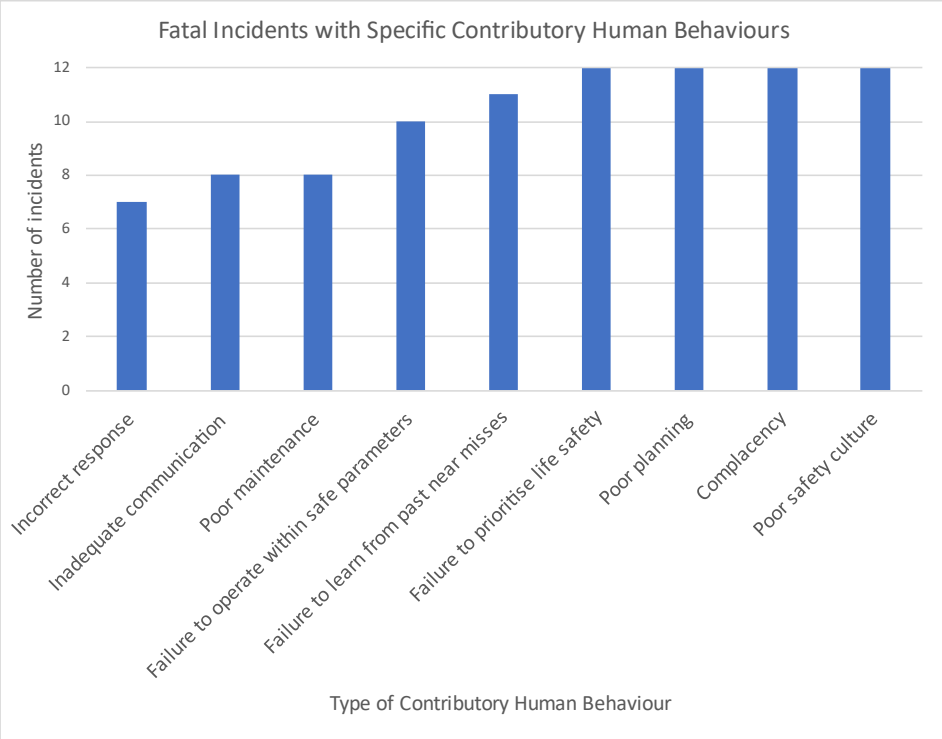

Figure 6. Fatal incidents vs type of contributory human behaviour

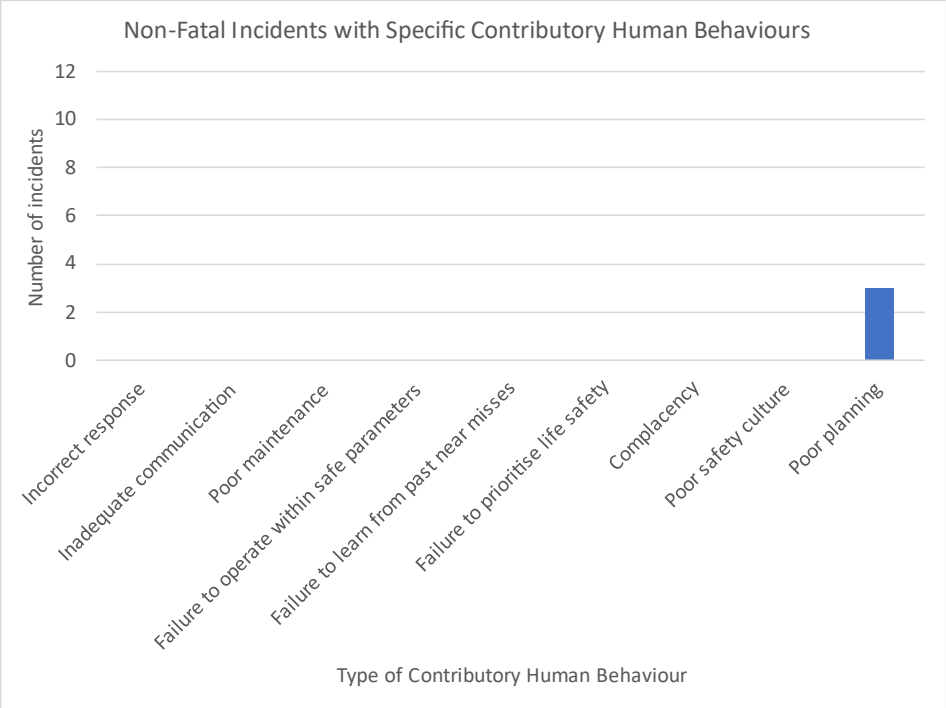

Figure 7. Non-fatal incidents vs type of contributory human behaviour

COMMON CAUSE HUMAN BEHAVIOURS IN INCIDENT ESCALATION

The raw data in *Figure - Figure 3* appear to show little evidence of contributory human behaviours which were assessed to be common causes across various types of incident, however when the data is analysed in *Figure 4 - Figure 7* there is evidence of a significant relationship between contributing human behaviours and catastrophic incidents. In particular, *Figure 6* shows that the human behaviours in *Table* were found to be contributors in all the fatal incidents. All nine behaviours were present in seven of the twelve incidents, eight were present in eight of the incidents, six were present in ten of

the incidents, five were present in eleven of the incidents, and four were present in all twelve of the incidents. In addition, the most common behaviours were the organisational behaviours, with human error behaviours being slightly less common. These behaviours presented in incidents across all the types of assets reviewed, with no evidence that any of the human behaviours were specific to any particular asset type.

Figure 7 shows that the non-fatal incidents possessed at most one of the contributory human behaviours, which was poor planning. This was likely linked to the conditions where the proximate cause could occur and initiate the incident. However, in these cases, the incident did not escalate, likely due to the absence of other common cause human behaviours.

As noted above, incident severity is a function of three behaviours: (i) numbers of casualties, (ii) number of fatalities and (iii) percentage of casualties that are fatalities, i.e. fatality rate. *Figure 8* summarises the normalised data for each incident, specifically (i) the human behaviours (HB) cause count, (ii) the casualties, (iii) fatalities and (iv) the fatality rate for each incident. Incidents are sorted by the number of assessed contributory HF causes.

The Baku incident was used to normalise the casualty and fatality numbers since it was the most severe incident in the data set. Only the incidents with multiple HF causes resulted in any fatalities and significant casualties. In each such case study, the initial incident escalated into disaster. Escalation was not observed in the cases with one or fewer human behaviours cause.

N.B. As noted, the normalised fatality rate for Chernobyl is skewed due to the lack of reliable non-fatal casualty data, i.e. the actual rate is unknown but lower than 100% however it was not deemed appropriate to present the fatality rate as a null value since there were significant fatalities and it was a severe incident.

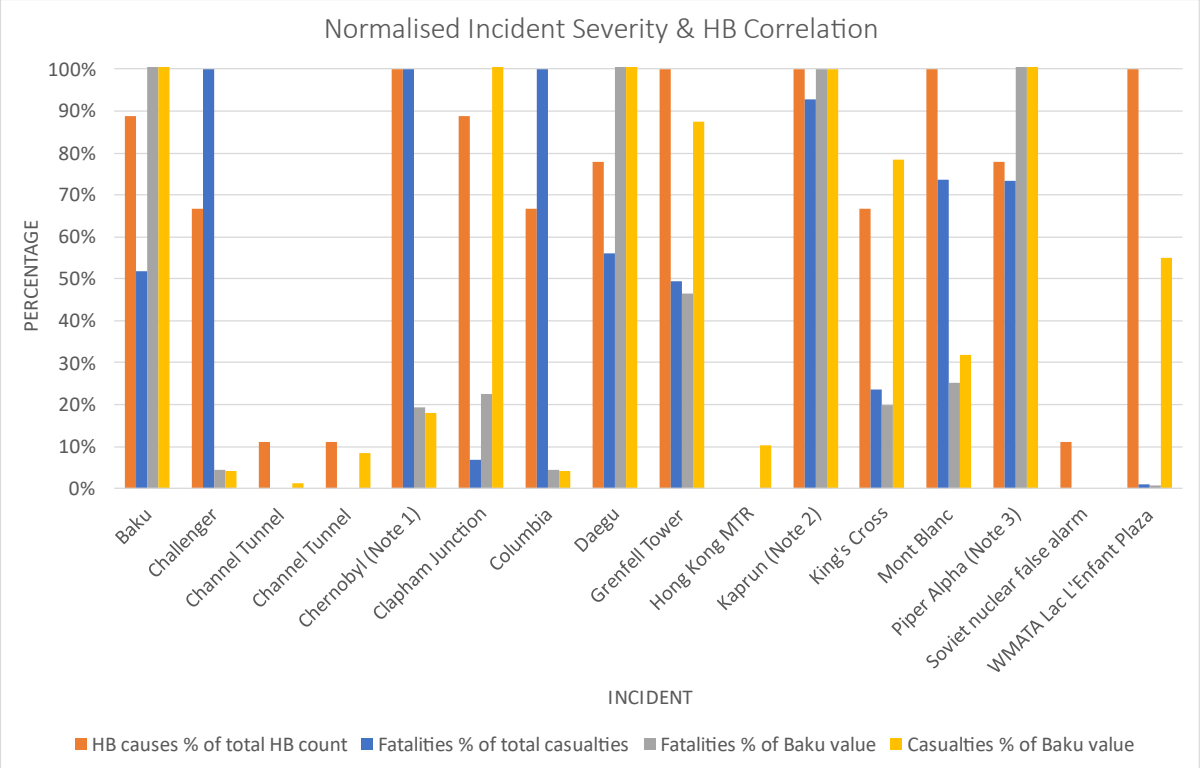

Figure 8. Normalised incident severity and Human Behaviours (HB) correlation
Refer to Table 3 for notes explanations.

Analysis of the data strongly suggests a relationship between the presence of common contributory human behaviours and the escalation of an incident into a disaster, irrespective of the type of asset

that is being operated. The analysis furthermore suggests that the common behaviours that most contribute to occurrence of disaster are organisational human behaviours, starting with poor planning. If other behaviours are not present, the data suggests that the incident may still be major, depending on the specifics of the initiating event, but likely will not escalate to disaster. However if there are other behaviours present, then there appears to be a reasonable likelihood of the incident becoming a disaster.

In each disaster case history, the conditions for disaster, i.e. the organisational human behaviours, were present in advance of the event and waiting only for the proximate cause to initiate the disastrous event. This in turn suggests that such disasters are not inevitable but in fact can be avoidable if the organisation responsible recognises the issues and acts to rectify them and to adopt, follow and enforce a good safety culture.

ACCIDENT MODEL DISCUSSION

Reviewing the circumstances of each of the case histories, it is difficult to confidently assign each incident firmly into any specific accident model. However some observations may be made.

First, in each of the incidents that escalated into disaster, there is a reasonable correlation with a non-linear model such as Rasmussen's [27] 'drift into failure' model, in that various contributory human behaviours occurred over time. This allowed the system to drift to an unresilient state of safety where, while apparently operating within a safe set of parameters, the system had become dangerously sensitive to safety stressors. Hence the proximate cause was sufficient to initiate the disaster. In these cases, existing mitigations such as emergency response, even if well implemented, were generally unable to arrest the escalation.

In contrast, the incidents that did not escalate appear to more closely resemble a linear model such as a bow-tie model, where the system was, prior to the incident, in a generally resilient safe state. A single behaviour contributed to the incident. The existing mitigations, e.g. emergency response, were thus able to fulfil their intended function and, following the proximate cause, were generally sufficient to prevent escalation to disaster.

OPPORTUNITIES FOR IMPROVEMENT / FURTHER RESEARCH

This preliminary study selected a limited number of case histories. Conclusions must therefore be limited, considering the sparseness of the data. This study should be considered as a starting point. There are many more case histories, for both fatal and non-fatal incidents, that could be added to extend the data set that would improve the confidence in the findings of this exercise. A larger data set could also permit more detailed findings, such as potentially yielding more insight into which specific human behaviours, if any, are most commonly associated with incident escalation. The accident model discussion could also be developed further, with the objective of improving the understanding of how disasters can be prevented.

Such insights could be beneficial to tunnel infrastructure operator organisations for future safety planning. Operators could review their current system and assess whether it contains behaviours that resemble the precursors to the system disasters discussed in this paper, or whether it more closely resembles the systems where an incident was managed without escalation. Findings of such an exercise could be used, where deemed necessary, to implement changes to improve their overall safety position and emergency preparedness.

CONCLUSIONS

A set of sixteen events which occurred on several types of operational asset was analysed to determine whether there are common cause human behaviours that can contribute to a safety incident's development into a disaster with loss of life and significant casualties. Incidents that were

prevented from escalation appear to be adequately represented by linear accident model theory, however disasters appear to be better represented by non-linear accident model theory that better captures the complexities of disaster occurrence. Analysis of the data in this study strongly suggests that incidents do not escalate into fatal incidents involving significant casualties without the presence of several contributory human behaviours. The analysis suggests that this conclusion is valid regardless of the asset type involved in the incident. The contributory human behaviours may be concluded to be asset-independent common causes for incident escalation to disaster.

REFERENCES

1. Fraser-Mitchell, J. and Charters, D., "Human Behaviour in Tunnel Fire Incidents," Proceedings of the 8th International Symposium for Fire Safety Science, International Association for Fire Safety Science, 2005.
2. https://www.hsl.gov.uk/what-we-do/safety-culture#:~:text=Safety%20culture%20is%20a%20combination,how%20it%20should%20be%20done, retrieved 30 October, 2024
3. https://www.merriam-webster.com/dictionary/complacency, retrieved 4 February, 2025
4. https://en.wikipedia.org/wiki/1995_Baku_Metro_fire, retrieved 13 August, 2024
5. https://railsystem.net/baku-metro-fire-1995/, retrieved 9 December, 2024
6. https://www.azer.com/aiweb/categories/magazine/34_folder/34_articles/34_metro.html, retrieved 9 December, 2024
7. "Report to the President by the Presidential Commission on the Space Shuttle Challenger Accident," June 6th, 1986, Washington, DC, USA, 1986
8. "Inquiry into the fire on Heavy Goods Vehicle shuttle 7539 on 18 November 1996," Channel Tunnel Safety Authority, Department of Transport, United Kingdom, 1997
9. "Report 37/2007: Rail Accident Report: Fire on HGV shuttle in the Channel Tunnel 21 August 2006," Rail Accident Investigation Branch, Department of Transport, October, 2007
10. "INSAG-7 The Chernobyl Accident: Updating of INSAG-1," Safety Series No. 75-INSAG-7, IAEA, Vienna, 1992
11. Hidden, A., "Investigation into the Clapham Junction Railway Accident," HMSO, November, 1989
12. "Columbia Accident Investigation Board, Report Volume 1," CAIB, NASA and the Government Printing Office, Washington, DC, USA, August, 2003
13. Won hwa, Hong, "The Progress and Controlling Situation of Daegu Subway Fire Disaster," Proceedings of the Asia-Oceania Symposium on Fire Science and Technology, International Association for Fire Safety Science, 2004.
14. "Grenfell Tower Inquiry: Phase 1 Report, HC 49-I," Chairman: The Rt Hon Sir Martin Moore-Bick, October, 2019
15. "Grenfell Tower Inquiry: Phase 2 Report, HC 19-I," Chairman: The Rt Hon Sir Martin Moore-Bick, September 2024
16. "Preventive and Response Measures for Emergency Incidents," LegCo Panel on Transport, subcommittee on matters relating to railways, LC Paper No. CB(1)1168/03-04(02), March, 2004
17. Asquini, A., "The Kaprun Funicular Network and its Demise," STS Research Paper, School of Engineering and Applied Science, University of Virginia, March, 2021
18. Fennell, D., "Investigation into the King's Cross Underground Fire, HMSO, November, 1988
19. Duffé, P. and Mare, M., "Report of the Task Force for Technical Investigation of the 24 March 1999 Fire in the Mont Blanc Vehicular Tunnel," Report of 30 June 1999, Minister of the Interior, Ministry of Equipment, Transport and Housing, Inspector General of the Administration, Board of Bridges and Highways, Government of France, June, 1999.
20. Catmur, J., King, K., Parsons, M., and Tarada, F., "A Service Analysis of the Mont Blanc Tunnel Fire," Proceedings of the 31st Safety Critical Systems Symposium SSS'23, York, February, 2023
21. The Lord Hon Cullen, "The Public Inquiry into the Piper Alpha Disaster," HMSO, London, November, 1990

22. https://en.wikipedia.org/wiki/1983_Soviet_nuclear_false_alarm_incident, retrieved 13 August, 2024
23. "WMATA L'Enfant Plaza Station Electrical Arcing and Smoke Accident," Washington, DC, January 12, 2015, NTSB Accident Report NTSB/RAR-16/01 PB2016-103217, National Transportation Safety Board, USA, 2016
24. https://world-nuclear.org/information-library/safety-and-security/safety-of-plants/chernobyl-accident, retrieved 31 October, 2024
25. https://press.un.org/en/2005/dev2539.doc.htm, retrieved 31 October, 2024
26. Directive 2004/54/EC of the European Parliament and of the Council of 29 April 2004 on minimum safety requirements for tunnels in the Trans-European Road Network, 2004
27. Rasmussen, J., "Risk Management in a Dynamic Society: A Modelling Problem," Safety Science Vol.27, No.2/3, pp.183-213, 1997

Evolution of a risk indexing method for evaluating safety in Swedish railway tunnels

Håkan Frantzich[1] & Karl Fridolf[2]
[1]Lund University, Lund, Sweden
[2]The Swedish Transport Administration, Malmö, Sweden

ABSTRACT

A risk indexing method for evaluating safety in railway tunnels has been developed. Firstly, a hierarchical structure with one objective, three sub-objectives, four strategies and ten attributes were defined. Secondly, attributes were elaborated and developed by means of assessable parameters related to tunnel safety. Thirdly, the relative importance of the attributes was analysed and assessed by means of expert judgement including using a focus group assessment and a Delphi process assessment. Fourth and finally, the index method was tested for a total of five railway tunnels, however, results are presented for two of these. In this paper, the adopted research method is elaborated, together with the results of the work.

KEYWORDS: risk indexing, tunnel safety, railway risks, prevention, mitigation, evacuation, rescue, safety in railway tunnels, condition-based maintenance

INTRODUCTION

Managers of railway infrastructure, such as railway tunnels, must have an established safety management system [1]. This means that the organisation shall have established methods to identify, analyse and evaluate all operational, organisational and technical risks relevant to the character and extent of operations carried out by the organisation. In addition, the organisation shall have methods to secure that safety measures are developed and put in place to mitigate these risks.

In Europe, measures to reduce specific tunnel risks are prescribed in Commission Regulation (EU) No 1303/2014 concerning the technical specification for interoperability relating to 'safety in railway tunnels' (TSI SRT) [2]. The TSI, which applies to new, renewed and upgraded tunnels which are located on the network of the Union rail system, are in Sweden complemented by the Swedish Transport Administration's infrastructure regulation TRVINFRA-00233 [3]. Both regulations do, however, lack specifications regarding how infrastructure managers shall monitor tunnel specific risks as well as safety measures that have been put in place to mitigate the risks.

There are a number of risk assessment approaches that may be considered for the risk monitoring such as a quantitative risk assessment, different checklist protocols and more semi-quantitative approaches as index or grading schemes. All have advantages and disadvantages considering the degree of details in the prediction of risk and in terms of time and recourses needed to perform the risk assessment. During the latest decades, risk indexing has evolved as a method to evaluate safety and there are several applications related to fire safety [4, 5 and 6]. Fire risk indexing has, for example, been suggested to provide a cost-effective means of risk evaluation that is both useful and valid. Hence, risk indexing may be applied where continuous risk screening is necessary. The index methods are also useful when the aspects of importance in the assessment are a combination of quantitative and qualitative nature [7].

A risk index method is a compromise between how detailed the outcome is and the time and competence needed to perform the assessment. Most index methods or grading schemes are relatively simple to use but they will in most cases only result in a relative measure of risk, which enables the assessor to put an assessment in relation to similar objects being investigated. In the context of railway tunnel safety, the relative measure of risk for one railway tunnel can be obtained and compared with the risk measure for other tunnels. Therefore, the Swedish Transport Administration funded research work to investigate if an indexing method may be appropriate for evaluating railway tunnel specific risks.

A HIERARCHICAL APPROACH TO TUNNEL SAFETY EVALUATION

The index method takes the form of a semi-quantitative method, which is based on the fact that the risk (or safety) in a railway tunnel can be described in a hierarchical system in which various attributes (e.g., properties of importance for safety) with varying degree of importance are allowed to be included. The hierarchical system eventually developed is described in Figure 1, and as can be seen, it is based on dividing safety in a hierarchy with an overall objective (top), sub objectives, strategies and attributes (bottom), for example, related to evacuation. The main reason for applying the hierarchical approach is to provide a transparent description of the relations of all components included in the hierarchical tree, i.e., how they relate to each other from a safety perspective. The components on the lowest level (attributes) were defined and included because they were judged to be the most important aspects contributing to the overall safety for, in this case, a railway tunnel.

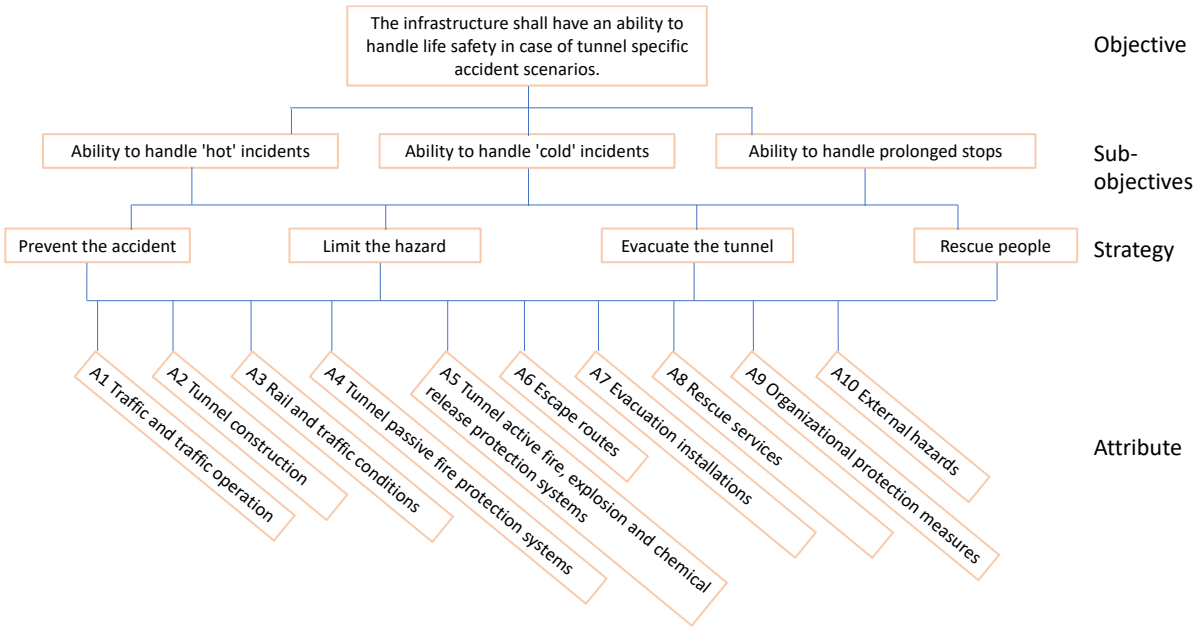

Figure 1. Hierarchal structure for the developed risk index method.

Developing a risk index assessment method comprise four different steps:

1. Establish the hierarchy structure with items on the different levels.
2. Define the grading structure for the attributes on the lowest level.
3. Derive the relative importance for the attributes on the lowest level with respect to components higher up in the hierarchical tree.
4. Verify that the assessment results are rational compared with other strategies for assessing safety.

ESTABLISH THE HIERARCHICAL STRUCTURE

The first step is obviously the most important as it will dictate the outcome of the later stages. When

assessing safety with indexing methods, it is common to define and use four to six levels in the hierarchical structure [4], having the overall safety objective on the top level. The next level is the sub-objective level, defining aspects that are important for reaching the overall objective. On the third level different strategies are defined which, to a varying degree, can be used to fulfil the sub-objectives. The attributes used to meet the strategies are defined on the next level below. In most cases, attributes need to be further sub-divided in an even finer level of detail: these are here termed parameters. During an actual assessment (i.e., application of the index method) each parameter is graded based on the design specifications for the assessed rail tunnel. The grading shall ideally be based on the typical range of how the parameter can be designed when considering all tunnels.

The hierarchical structure was developed in several steps during the continuation of the project and revised several times. The levels and the items comprising each level was determined based on various sources, e.g., past as well as current regulations and recommendations regarding safety in railway tunnels, interviews with national and international tunnel managers and expert judgement. During the structure revisions, external experts provided guidance and suggestions. The items on each level shall reflect the conditions which are relevant for the system to be analysed, in this case a rail tunnel.

Objective

The main objective, i.e. the top in the hierarchal tree, must reflect what the method is supposed to evaluate. As the current method focuses on safety in rail tunnels it is obvious that the objective has a safety related focus. But it is not evident how the objective should be formulated. To some degree a delimitation is inevitable introduced in the objective definition and the rest of the tree structure will relate to this. The delimitations are to some degree coinciding with the risks not being treated in the technical specification for interoperability relating to ‘safety in railway tunnels’ (TSI SRT) [2]. In the current method several suggested formulations were discussed, and the following was selected:

- The infrastructure shall have an ability to handle life safety in case of tunnel specific accident scenarios.

The objective has a limitation in terms of the type of scenarios indicating that only scenarios related to the tunnel environment are included, and that the focus is on safety for people being in the tunnel. The safety of the infrastructure and the continuation of tunnel operation is therefore not included. These objectives are considered by other means and must, therefore, not be included. It also means that not only accidents related to the regulations in the TSI SRT [2] are included leaving a wider interpretation of the meaning of "tunnel specific accident scenarios". One risk that is partly meant to be included is the safety of staff involved in maintenance work in the tunnel. Hence, they are not excluded from being considered when deriving the tunnel risk index. It is also worth mentioning that some risks are disregarded like hazards related to terrorist attacks and the risk that a collapsed tunnel will have an effect on infrastructures outside the tunnel.

In general, the idea is to embrace accident scenarios that could be relevant for a railway tunnel. Similarly, also mitigation measures that can be relevant are part of the method, even if they are not regulated in national or international regulations, but are still considered important for achieving a safe infrastructure. The risk index derived using the method will then indicate to what degree the objective is achieved.

Sub-objectives

It can be useful to divide the objective in a few sub-objectives to further clarify what is to be achieved. Commonly, sub-objectives for a safety related index method focus on life safety, property protection and other, e.g., cultural heritage and continuation of operation or facility resilience. In the current structure another strategy was selected, partly to establish a link to the current regulations in the TSI SRT [2]. Three sub-objectives were, therefore, selected:

- Ability to manage hot incidents: fire, explosion followed by fire, emission of toxic smoke or

gases.
- Ability to manage cold incidents: collision, derailment.
- Ability to handle prolonged stops: unplanned stop in the tunnel, for longer than 10 minutes.

The last sub-objective is intended to cover risks associated with a spontaneous evacuation during prolonged stops in a tunnel, not necessarily due to, for example, an accident.

Strategies
There are different ways to achieve good safety and the concept of safety in railway tunnels probably consists of a combination of different protective measures or barriers, both technical and administrative. The TSI SRT [2] describes the overall principle for handling accidents divided in four strategies which comes in a priority order:

- Prevention
- Mitigation
- Evacuation
- Rescue

The most desirable thing is to prevent accidents from happening, and an active rescue is the last link in the safety chain. The starting point for the development of the railway tunnel safety assessment method is to use these strategies.

Attributes
The assessable and grade-able characteristics for the safety of a railway tunnel are found in the lower levels of the hierarchy. Hence, the attributes are the characteristics that the user of the risk index method selects based on a set scale. The attributes are assessed by selecting the properties that define the attribute (the parameters) during practical application of the method, i.e., during a safety assessment. They are related to the physical infrastructure, the external environment and to society's resources for managing an event. Considerations by train operators are, though, not included as all operators can use a specific tunnel, therefore, not needed to be considered specifically.

Each attribute consists of one or more parameters, and it is the parameters that are graded and combined to an attribute grade. Together with other attribute grades, these then form the safety based naturally on a) the grading, and b) the relative importance of the attribute (see below).

In the development of a risk index method, there are consequently two steps to be carried during the development and definition of the attributes:

- Determine which characteristics are worth being assessed in an assessment, and to decide how these characteristics should be valued (graded) against each other.
- Evaluate the relative importance between the attributes in relation to the strategies, sub-objectives and the objective.

The selection of items in the tree structure was finally selected after a review process where tunnel safety experts were involved in expressing their opinion and the structure was subsequently updated.

SAFETY ASSESSMENT

The hierarchical tree described above defines the structure of the safety assessment method, i.e., to derive the risk index for the tunnel. The next step is to put numbers to the structure. As indicated in the previous section there are two important components that need to be defined: the attribute grade and the attribute weight (relative importance). Each attribute is characterised by a prescribed set of potential design outcomes which is used to select the attribute grade during a safety assessment or inspection. But the attributes are also differently important in relation to each other. The risk index,

RI, will be a combination of the joint attribute grades and the attributes importance using the following expression:

$$RI = \sum_{i=1}^{n} w_i * G_i$$

where w_i is the weight (or importance measure) for attribute i and G_i is the grade for the same attribute given during a safety assessment. The implication of this is that the weight information is a property of the method, and the scores are a property of the tunnel being assessed.

ESTABLISHING THE ATTRIBUTES

The selection of attributes to eventually be included in the hierarchical structure was based on expert assessment and through analysis of relevant regulations, design descriptions and the like. This was an ongoing activity during the entire development process. Following the selection of the most important attributes to be included was the task to define how each of them should be graded.

Each attribute must first be defined in terms of which parameters that should be used to describe the attribute. Furthermore, each parameter needs to have several options depending on the potential alternatives for that specific parameter. As an example, consider the parameter maximum train speed in the tunnel. The parameter options typically are train speed intervals commonly used in the railway infrastructure in the country. Each parameter option is associated with a grade indicating how "good" the option is in relation to other options. In the current method parameter options are grades between 0 and 5 but any range can be used and a grading 0–10 can be used to provide a more diversified distribution of the option grades.

I the current method a "0" indicate absence or poor performance while a "5" indicates a good performance. This will have an implication of the interpretation of the risk index (RI). A high value indicates a good performance as higher attribute gradings indicate a better performance. As a result, the term risk index would be appropriate, but for consistency the term risk index is kept even if a high value is not associated with high risk.

In general, the parameter grades for the parameters associated to the attribute are combined into a single attribute grade. This is usually done using a weighted average as all parameters usually are not equally important to describe the performance of a single attribute. Table 1 presents the attributes with their respective parameters. In a first stage, a proposal for attributes, their descriptions and parameter gradings were produced. These were then reviewed by railway infrastructure experts and refined before being finally determined.

Table 1. Attributes in the risk index method with parameters.

Attribute number	Attribute with parameters	Parameters
1	Railway traffic and operation	Highest allowed speed Number of train passages per day Rolling stock distribution (passenger/freight) Means for communication
2	Tunnel construction	Unwanted objects on the rail tracks Tunnel length Access to tunnel portals Ice occurring in the tunnel
3	Rail and traffic conditions	Number of tracks Derail protection Switches in or close to the tunnel Traffic signal system
4	Passive fire protection systems	Tunnel lining Cable protection Fire compartmentation
5	Active protection systems for fire, releases and explosion	Tunnel ventilation and water sprinkler system Train position system Railway heat detection system Management of contaminated water
6	Escape routes	Distance between exits Walking path along the track Exit door performance Escape route design (after the door)
7	Evacuation installations	Walking path illumination Escape illumination (emergency light) Way guiding signs
8	Local rescue services	First response team Evacuation and rescue points Rescue services communication Water access
9	Organisational protection measures	Train operation central capability Planning for emergencies Training conditions Operation and maintenance
10	External hazards	Unwanted person on the railway Risk for flooding Risk for landslide

As an example, attribute number 3 regarding rail and traffic conditions, is graded accordingly:

- Number of tracks (NOT)
  - 1: Single track tube (only one track in the tunnel)
  - 5: Two or more track tube (more than one track in the tunnel)
- Derailment protection (DP)
  - 0: No derailment protection
  - 3: Guard rail inside tunnel, but with gaps/interruptions (for example where balises are installed)
  - 5: Guard rail inside tunnel without gaps/interruptions
- Switches near and/or in tunnel (X [m] = (Highest allowed speed)^2/80; S)
  - 1: Switches inside tunnel
  - 2: Switches within X m of any of the tunnel openings
  - 5: No switches within X m of any of the tunnel openings or inside tunnel
- Traffic signal system (TSS)
  - 0: None
  - 3: Automatic train controlling system (ATC)
  - 4: ERTMS, level 1
  - 5: ERTMS, level 2

Thereafter, the value of the attribute is calculated accordingly: 0,2*NOT + 0,1*DP + 0,4*S + 0,3*TSS.

What may be seen odd is that having multiple tracks in the tunnel is better compared to having just a single track. Having two tracks in the tunnel could potentially result in a collision between two trains in the tunnel. The reason for the grading is that more tracks result in a larger tunnel cross section, which is favourable from a fire hazard perspective. The risk of having a derailment is covered in attribute 1.

ATTRIBUTE IMPORTANCE

It is evident that all attributes are not equally important for the tunnel safety objective or the sub-objectives. The advantage of using the hierarchy tree is the possibility to deduct the importance measures for attributes in relation to the objectives. The task is to estimate the importance of each attribute to the fulfilment of each objective, i.e.: how important is attribute 1 to fulfil the objective, how important is attribute 2 to fulfil the objective, and so forth. In this task lies also an estimation of the importance relations between attributes.

There are several ways to define the weights to be used in the assessment. In simple engineering problems one can use calculations to determine the importance measures such as sensitivity parameters if a statistical approach is selected. However, the current problem is not a simple engineering problem, but it consists of a variety of factors contribution to the tunnel safety. Some are qualitative, whereas others are of a quantitative nature. Therefore, approaches using expert judgements are preferred as there are no feasible alternatives that can produce the needed information in a reasonable time frame.

In developing the risk index method, it was initially decided to use the Analytical Hierarchy Process (AHP) approach described by Saaty [8] as it provides a consistent result. It was also decided to use an alternative method using focus group estimations for the weights. However, the participants in the focus groups and the Delphi process were not the same. Regardless of the technique used to determine the weights, it should be done step by step using the hierarchical tree-like structure. The participants who provided expert knowledge were all familiar with tunnel safety and they represented tunnel fire safety consultants, incident commanders from the rescue services and employees at the Swedish Transport Administration specifically working with tunnel safety.

Focus group importance estimation
To determine the weights between all the components in the tree structure, two independent focus groups were used. They were given the same task and the reason for having two groups was to identify any inconsistencies between them. In total eight people participated, divided in two groups. The entire focus group work took one day.

The task was mainly to, on a five graded Likert scale, decide the strength between each attribute in relation to each of the strategies. This means that each group had to agree on 40 expert judgements expressing the relation between attributes and strategies. The strength can be expressed as "how important is attribute x (e.g., 1) to fulfil strategy y (e.g., 2)". After this, the procedure was repeated in the same way, up through the structure tree, between strategies and sub-objectives and finally the relations between sub-objectives and the objective. The focus group judgements resulted in two matrices with importance data from the 10 attributes to the four strategies, from the four strategies to the three sub-objectives and finally a single vector with weights data from sub-objective to the objective.

Importance estimation using AHP
The other method to derive the data needed to express the importance weights used the technique behind the Analytical Hierarchy Process (AHP) presented by Saaty [8]. Twelve experts were asked about their opinion regarding the importance of the components in the structure tree. The task given to them was to perform a pairwise comparison of the aspects on each level in the hierarchy tree with respect to the next higher-level aspects. As an example, all ten attributes were compared to each other with respect to each of the four strategies. This means that there were in total almost 190 pairwise comparisons performed by the experts.

The AHP procedure used a Delphi process [9], a formal procedure for expert elicitation, to collect the information and communicate with the experts, who all were anonymous to each other. All communication was done by e-mail. The Delphi process was only used for two rounds asking the experts about their opinion. The process started by asking the experts about their opinion on the pairwise comparisons. After all experts had submitted their data, it was converted to mean values of all the comparisons. The experts were then given the opportunity, in the second round, to revise their first estimations, now having the aggregated information including all respondents' estimations. Formally the Delphi process shall continue until all experts have reached a consensus result, however, that can take long to reach. Therefore, a consensus was not achieved as only two rounds were performed.

After two rounds, all data was again aggregated, and the arithmetic mean values of all estimations were calculated. This resulted in a set of matrices with all pairwise comparisons. The information was used to calculate the weight for all components on each level with respect to all components on the next upper level. These weights are expressed in terms of the geometrical mean values [7] and can as an example be the vector of importance weights from the attributes to the first strategy. The result is presented in the same way as the data from the focus groups, i.e., as two matrices with importance data from the 10 attributes to the four strategies and from the four strategies to the three sub-objectives and finally as a single vector with weights data from sub-objective to the objective.

Deriving the importance weights
Having the data matrices and the vector, it is rather easy to derive the importance weights of the attributes against the objective, i.e. to see the relation from the lowest component directly to the top component. The importance values for attribute to objective is obtained by a matrix multiplication using the three matrixes as in Figure 2. Normally the importance values are normalized so values are between 0 and 1 and that the sum of the importance values are 1,0.

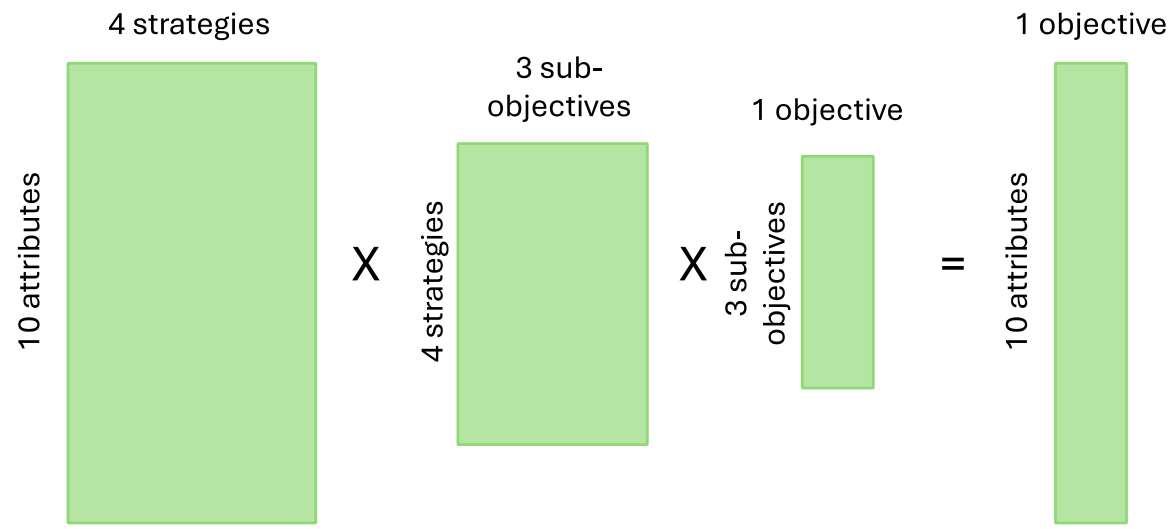

Figure 2. Steps to develop the weight vector from attributes to objective.

As there were two data sets, from the focus groups and from the Delphi process, a decision had to be made regarding which to use for the final index method. Prior to the decision, the calculation of the final vector was done with both sets of data. Figure 3 shows the normalized importance weights for the attributes using the two data collections techniques. In other words, Figure 3 illustrates the importance of each attribute as assessed by the individuals participating in the focus groups or in the Delphi procedure. As can be seen, there are both coherent values between the focus groups' results and the Delphi process assessment, as there are clear deviations. It is not obvious which of the two data sets to be selected for the future safety assessment, still one has to be selected, and both should not be used.

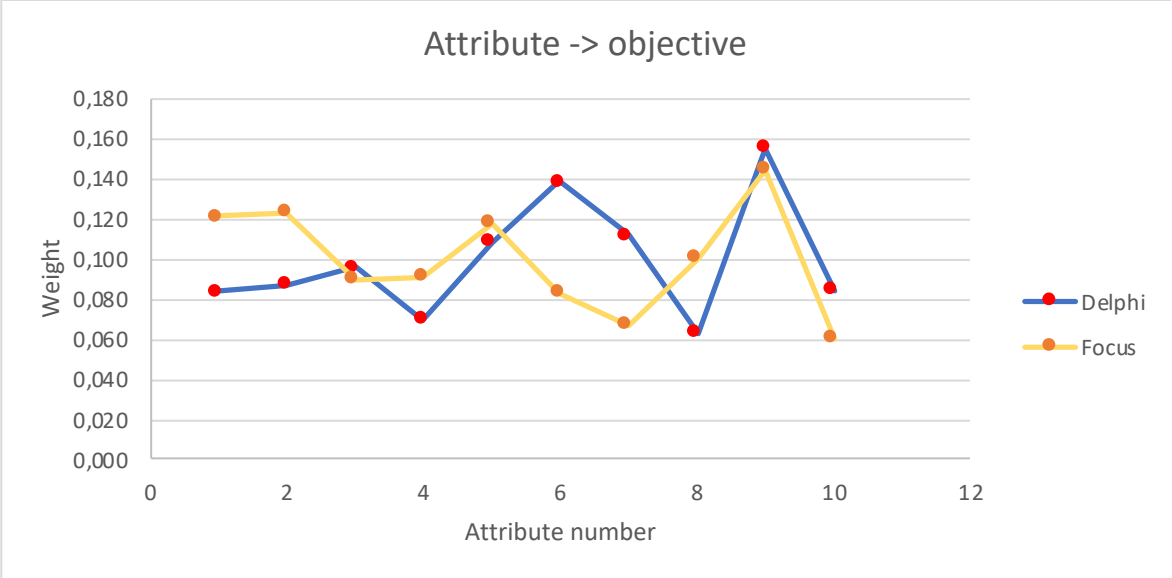

Figure 3. Importance weights using focus group data and Delphi process data.

In the final version of the risk index method, it was decided to use the data from the Delphi process. The reason for this is that the technique is well established and that it eliminates some drawbacks of the focus group method, e.g., that the results can be affected by influential persons in the group (during discussions and group assessment).

The main result is the one presented above considering the overall safety level for the railway tunnel. However, so called sub-indices could also be derived using part of the data material. Three so called

sub-indices were developed considering

- to prevent the accident from happening,
- to limit the consequences and
- to limit injuries to people.

By facilitating these sub-indices, a tunnel manager can for example assess how improved measures in a specific tunnel will affect certain desired goals for safety related work.

VERIFICATION ANALYSIS

In the development of the risk index method, it was deemed important to verify that derived results are coherent with the risk associated to the tunnel. However, as the main reason for selecting the risk index method in the first place is because tunnel safety features typically are of different nature, it is rather difficult and furthermore time consuming to use traditional quantitative approaches. Instead, one way of finding indications of validity of the results is to do safety assessments of some tunnels and have tunnel safety experts expressing their personal subjective judgement of the tunnel being on the acceptable side of some limit or if the tunnel needs to be improved with respect to safety.

Visits were therefore made to five different tunnels (A–E), see Table 1, of which two have been analysed so far. The tunnels differ in design characteristics and the intention was to select different types of tunnels considering length, number of tracks, type of evacuation routes, number of trains per day etc.

Table 1. Characteristics of the assessed tunnels.

Tunnel	Length (approx.)	No tracks	Escape routes	Max speed	Trains/day	Constr.
A	2 km	2	Yes	200	80	rock
B	3 km	1	Yes	250	29	rock
C	1 km	1	No	200	30	rock
D	0,5 km	2	No	200	138	concrete
E	0,5 km	1	No	110	34	rock

Each tunnel was assessed by three persons, two were the authors of the paper and the third was a person having experience of tunnel safety assessments and inspections. The assessors did their collection of tunnel conditions and interpretation of how to grade the parameters independently. They also did a subjective evaluation of the tunnel safety status, having sufficient safety level or not. The final assessment grades and the subjective assessment are presented in Table 2.

Table 2. Assessment results for the five tunnels.

Tunnel	Risk index, total safety	Risk index, prevent people injuries only	Subjective assessment
B	3,1	3,2	Sufficient safety
D	3,3	3,2	Sufficient safety

CONCLUSION

The paper presents the development technique for risk index approaches for safety assessments, in this case for a railway tunnel. The grading of attributes important for a safety assessment have been reviewed by other railway tunnel experts and can, therefore, be considered as valid even if no formal validation was performed at the time of this paper.

The attribute importance values were developed using two independent methods, focus group elicitation and a Delphi assessment using independent and anonymous participants. Both participants

in the focus groups and in the Delphi panel were all familiar with tunnel safety. As the two methods mostly indicated similar results, with some exceptions, it can also be assumed the values can be seen as relevant for a safety assessment of railway tunnels.

A comparison of the safety level in five tunnels were also conducted to verify that the formal safety index results were in line with a subjective judgement of the safety level in the tunnels. The results of this exercise indicated that the method have a capability to be used as a risk screening assessment method for safety in railway tunnels.

REFERENCES

1. COMMISSION DELEGATED REGULATION (EU) 2018/762 of 8 March 2018 establishing common safety methods on safety management system requirements pursuant to Directive (EU) 2016/798 of the European Parliament and of the Council.
2. Commission Regulation (EU) No 1303/2014 of 18 November 2014 concerning the technical specification for interoperability relating to safety in railway tunnels of the rail system of the European Union.
3. KRAV med RÅDSTEXT: TRVINFRA-00233 – Tunnel: Tunnelbyggande, (2021). Trafikverket, Stockholm.
4. Watts, J. M. (2008). Fire Risk Indexing. In the SFPE Handbook of Fire Protection Engineering (fourth edition). NFPA, Quincy, MA.
5. Shields T.,J. (1991). A Fire Safety Evaluation Points Scheme for Dwellings. Vol. 1 (2), Faculty of Sciences and Technology, University of Ulster at Jordanstown.
6. Frantzich H., McNamee M., Kimblad E., and Meacham, B. (2024). Decision Support Framework for Sustainable and Fire Resilient Buildings (SAFR-B). Fire Technology, DOI:10.1007/s10694-024-01678-7
7. Yoon K.P., Hwang C. (1995). Multiple Attribute Decision Making, An Introduction. Sage University Paper. Series: Quantitative Applications in the Societal Sciences 07-104. Ed. Lewis-Beck M., S. Sage Publications.
8. Saaty T.L. (1980). The Analytic Hierarchy Process. Planning, Priority Setting, Resource Allocation. McGraw Hill Higher Education, New York, NY.
9. Linstone H. and Turoff M. (1975). The Delphi method: techniques and applications. Addison–Wesley.

Rehabilitation of Fire Life Safety Systems for Existing Tunnels

Robert Faddoul, E.I.T; Yuan Li, P.E; Igor Maevski, PhD, P.E.; James Fiscella, E.I.T;
& Sharanya Nair, PhD
Jacobs, New York, USA

ABSTRACT

As existing tunnels age, rehabilitation projects to improve the fire life safety of these tunnels are becoming more prevalent. During rehabilitation design, an evaluation of the existing system is performed, which typically indicates that the current fire life safety system is insufficient to control potential fire hazards. This is mainly due to the tunnel systems being originally designed for normal operation rather than for emergency scenarios. To improve the safety of the tunnel, upgrades to prevent, mitigate, and manage the potential fire hazard should be explored during rehabilitation. This paper covers the upgrades considered during the rehabilitation of Big Walker Mountain Tunnel (BWMT) to handle a potential flammable liquid fire.

At this facility, no one upgrade alone could be done to meet the tunnel safety criteria, and a systematic approach was required to incrementally improve the system. To tackle the deficiencies with the existing ventilation system such that it is capable of controlling a flammable liquid fire (300 MW), the following upgrades were identified:

1. Providing a fixed fire suppression system to stop or reverse the fire growth rate during a fire incident, improving tenability for tunnel occupants, and providing a standpipe system to enhance the ability of first responders to engage in manual fire-fighting activities. This paper focuses on the parameters of the fixed fire suppression system for CFD modelling and the synergy between the ventilation system and sprinkler system to fight shielded fires.
2. Transforming the existing transverse ventilation system to a longitudinal ventilation system with the implementation of a Saccardo nozzle. The paper describes the optimization of the nozzle opening for this facility.
3. Replacing undersized supply fans originally designed for pollutant control with larger fans more appropriate for fire smoke control to improve the capability of the new longitudinal ventilation system. This paper describes the field tests conducted to obtain existing performance data of the fans and covers a CFD analysis to determine if the current arrangement of the fans has any impact on performance.

KEYWORD: rehabilitation, Saccardo nozzle, fire suppression, fire detection, fan replacement.

INTRODUCTION

Many existing tunnels built in the early- and mid-20th century were designed with a focus on normal operation, preceding current standards which include requirements for fire life safety systems under fire emergency conditions. As these tunnels age, rehabilitation projects are becoming more prevalent to maintain the integrity of the tunnel facility and to improve the existing fire life safety systems.

During rehabilitation design, the existing tunnel should be evaluated using a combination of fire life safety strategies including prevention, mitigation, and management strategies to limit the impact of a fire hazard in the tunnel. This paper describes the strategies used and systems designed during a

tunnel rehabilitation project for Big Walker Mountain Tunnel to improve the fire life safety of the tunnel.

EXISTING CONDITIONS

The Big Walker Mountain Tunnel (BWMT) is a 1,289 m long, two-tube, road tunnel on route I-77 in Virginia (USA) originally opened in 1972 [1]. Each tube of the tunnel includes two unidirectional traffic lanes, one dedicated to southbound traffic and the other to northbound traffic, with the road sloping upward at 3.5% toward the north. The tunnel currently does not have vehicle type restrictions, allowing for tanker vehicles, which have a potential fire size of 300 MW [2], to pass through the tunnel.

Like many tunnels built during this era, BWMT is equipped with a fully transverse ventilation system designed for normal operation. Each tube is divided into four ventilating sections located above the ceiling of the roadway. The sections are created by dividing the airspace above the roadway vertically, to create a side-by-side supply and exhaust air duct and a bulkhead wall to create separate sections for the north and south sides of the tube. Each supply section is served by three (3) blowers (supply fans) and each exhaust section is served by three (3) exhaust fans located in the ventilation buildings near the portals.

Since the system was designed for normal conditions, the fans that serve the uphill tube were designed for higher airflow capacity than those that serve the downhill tube. Although this is ideal for diluting vehicle emissions along the tunnel since vehicles emit less emissions moving downhill than uphill, it is not ideal for smoke control as the downhill slope makes smoke control more challenging because buoyant forces drive hot smoke uphill in the direction of egress.

As the basis for rehabilitation, the capability of the existing transverse ventilation system to control smoke for a potential flammable liquid fire was evaluated for both tubes using CFD. Through the analysis it was concluded that the current ventilation system is incapable of controlling smoke for this fire hazard in both directions. In the uphill tube (northbound), the system was capable of managing a 100 MW fire due to the buoyant forces driving smoke in the desired direction. While in the downhill tube (southbound), the system was not capable of managing a 5 MW fire (car fire) due to the buoyant forces driving smoke against ventilation and the ventilation fans being originally undersized.

METHODOLOGY

Initially, measures to prevent or mitigate the size of the fire in the tunnel were explored, as flammable liquid fires are nearly impossible to handle with the current transverse ventilation system, due to the amount of heat and smoke generated and to protect the tunnel structure from catastrophic damage that can be caused by a fire event of this magnitude. These methods are focused on limiting the size of the potential fire hazard and reducing the ventilation required for smoke control.

Prevention of this type of fire would require restricting flammable liquid cargo from travelling through the tunnel. At BWMT, restricting traffic to less hazardous vehicle types is not a viable option, as this is a major interstate route for trucks to transport goods between Virginia and West Virginia with no available by-pass road.

Mitigation includes the implementation of an automatic fire detection system and automatic fire suppression system to limit the size and impact of a rapidly growing liquid fuel fire. The automatic detection system reduces the time to detect fires, allowing first responders to arrive on site sooner and attack the fire at a more manageable size. Fast detection also allows for faster closing of the tunnel which can reduce the number of motorists exposed to the hazard. Also, the quick activation of a fire suppression system can stop the growth of a fire or extinguish it completely. In cases with flammable liquid tankers, like at BWMT, additives can be included with the fire suppression system to help stop

the growth of a flammable liquid fire by creating a film on top of the fuel surface to prevent oxygen from reaching flammable vapours.

With the activation of the suppression system to mitigate fire growth, the smoke generated from the fire will cool and de-stratify smoke layers below the tunnel ceiling, making exhausting smoke with the existing transverse ventilation system through the tunnel ceiling less effective. Since this phenomenon was expected, alternative ventilation options to manage smoke with the suppression system were explored. The conversion of the existing transverse ventilation system into a longitudinal system to push smoke away from the path of egress instead of extracting it was proposed. Due to the lack of clearance in the tunnel, the use of jet fans to induce longitudinal flow in the tunnel was not feasible. As a result, the existing system was converted into a longitudinal system using a Saccardo nozzle. To further improve the ventilation system, the undersized downhill supply fans serving the Saccardo nozzle were considered for replacement to increase the capacity of the fans and improve smoke control.

The following sections cover the specific upgrades designed for BWMT, including the fixed fire suppression system, Saccardo nozzle, and fan replacement which were all required to improve the safety of the tunnel.

FIXED FIRE SUPPRESSION SYSTEM

The fixed fire suppression system provides a means for fire mitigation prior to the arrival of first responders, which can reduce damage to the tunnel structure and maintain the fire at a more manageable size. At BWMT, it is estimated that first responders will arrive 15 to 20 minutes after detection, which allows a flammable liquid fire to reach its peak heat release rate (HRR) of 300 MW [2]. This is based on an assumed linear hydrocarbon pool fire growth rate of 20 MW/min as developed within the UPTUN program for European tunnel design criteria, meaning the fire will reach its peak heat release rate at 15 minutes. The expected pool size with the existing drainage system was analysed to determine if the design fire size can be reduced, but it was determined that due to the large spacing between drainage inlets, the pool size will become large enough to facilitate a 300 MW fire. However, the conveyance piping capacity based on its size and slope was determined to be sufficient to support drainage of the water supplied from the proposed deluge system.

The introduction of a fixed fire suppression system has two main benefits; 1) it limits the spread/growth of a liquid fuel fire resulting in an overall smaller fire and 2) it cools the smoke and surrounding environment to reduce the natural drive of smoke due to buoyant forces. The fire growth curve with the fixed fire suppression system activated, shown in *Figure 9*, is based on the following assumptions.

1. The fire is detected after 1 minute of fire ignition, at which time the fire has reached 20 MW. At 20 MW, the fire will be touching the ceiling and the temperature at the linear detection system will likely have already exceeded the alarm threshold. This assumption is based on NFPA 502 Annex A, which indicates that the automatic fire detection system shall be able to detect a 5 MW fire within 90 seconds. Due to the significantly larger fire size present it is expected that the fire will be detected 30 seconds sooner, since the temperatures at the ceiling will be much higher than those produced by a 5 MW fire after 90 seconds.
2. The fixed fire suppression system reaches full discharge at 2.5 minutes, at which time the fire has reached 50 MW. To achieve this discharge time, the main piping of the sprinkler system is filled with water up to the deluge valves located above each fire zone, limiting the fill time to short runs of dry sprinkler piping downstream of the fire zone deluge valve. Since the system is wet and ambient temperatures can drop below freezing, both heat tracing with insulation and a boiler system were implemented to prevent the water from freezing.
3. At full discharge, fire spread is mitigated, and the fire size is expected to stop growing. This does not include the potential for the sprinkler system to suppress the fire but assumes the sprinkler system prevents the unburned liquid fuel from igniting.

Under these assumptions, a liquid tanker fire reaches a maximum fire size of 45 - 50 MW after 2.5 minutes when the fixed fire suppression system reaches full discharge. More aggressive detection and activation of the sprinkler system will result in a smaller fire size. For instance, if full discharge is achieved after 2 minutes, the fire size can be limited to a maximum size of 40 MW. Without fire suppression, the fire can grow to a fire size of 300 MW, expected to occur after 15 minutes of ignition. To improve the detection times for quick activation of the suppression system, a linear heat detection (LHD) system was included in the design for automatic fire detection.

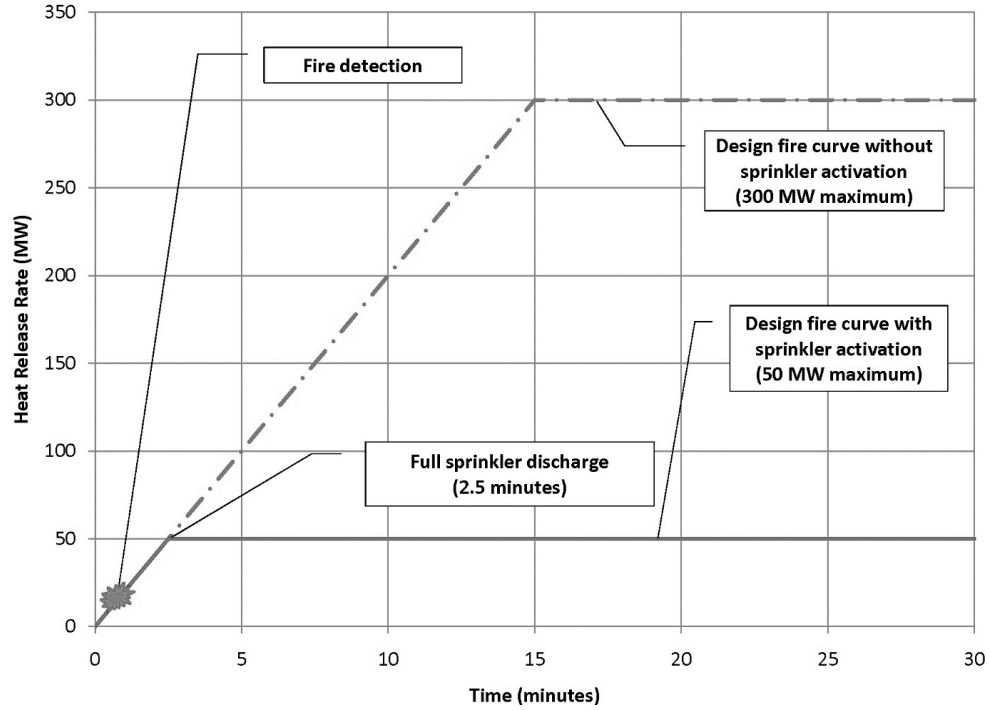

Figure 9 Fire Growth Curve with Fire Suppression System

The effectiveness of the ventilation system with the fire suppression system was analysed using Ansys Fluent, where the discharge from individual sprinklers was modelled. The water droplets and spray patterns from the sprinklers were implemented using discrete phase modelling (DPM) to obtain the cooling effects from the water supplied. The effect the droplets have on the fire growth rate was not modelled in CFD but provided as an input parameter which is represented by the curve in *Figure 9*. The effects of the additives cannot be modelled using CFD and were assumed to enhance the effectiveness of the fire suppression system to stop the growth of a flammable liquid fire.

The sprinkler density in each fire zone was determined by the number of sprinkler heads available in each zone. The existing openings from the abandoned exhaust and supply duct were utilized for the sprinkler heads which determined the number of heads available. In the majority of the tunnel, the fire zones were designed to be 22.9 m, such that the length of two adjacent zones exceed the maximum vehicle length and the zones correspond with a group of existing openings. As per the density/area curves in NFPA 13, the targeted sprinkler density is based on the requirement for ordinary hazard group 2, which corresponds to a density of 8 LPM/M^2. Included in NFPA are reductions to the density requirement when additives are used to 6.4 LPM/M^2, though the system was designed to achieve the 8 LPM/M^2.

The activation of the sprinklers of two adjacent fire zones were modelled in CFD as shown in *Figure 10*. The locations of the sprinkler heads align with the existing exhaust/supply openings, and the discharge pattern used was based on manufacturer data. Data on the recommended water droplet size for different fire applications is not provided in NFPA, thus the water droplet size was based on the sprinkler model used and pressure provided. For the sidewall sprinklers, a droplet size of 1,200

microns was used, and for the ceiling sprinklers, 2.2 microns was used. The displacement of the water droplets due to the ventilation system was captured in the model. In general, a slight displacement can help water droplets penetrate available vehicle openings to directly contact fires shielded by the burning vehicle.

The introduction of the suppression system with an automatic fire detection system for timely activation can limit the growth of a potential 300 MW fire to 50 MW, protecting the tunnel structure. However, this will reduce the effectiveness of smoke management using the existing transverse ventilation system due to smoke de-stratification. To manage the de-stratified smoke to protect evacuating occupants, the existing transverse system shall be converted to a longitudinal system using a Saccardo nozzle.

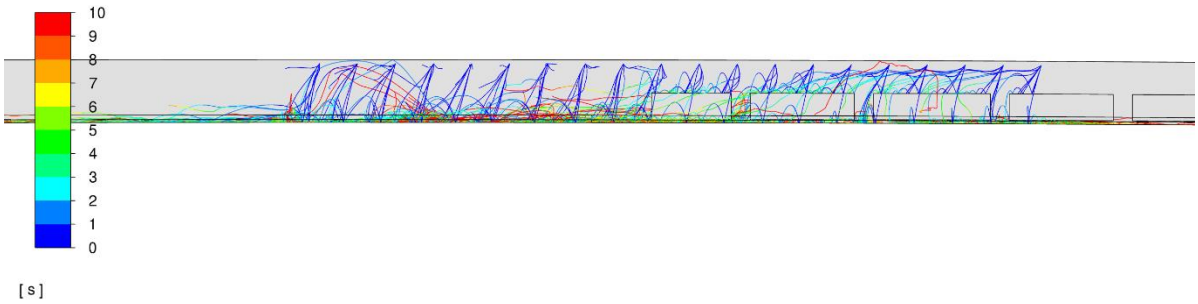

Figure 10 Section View of Droplet Tracks Colored by Particle Residence Time (sec)

SACCARDO NOZZLE

To improve the emergency ventilation capability of the tunnel, the existing transverse ventilation system was transformed into a longitudinal system using a nozzle constructed in the supply air duct above the roadbed. This transformation was considered for this facility since the tunnel only permits unidirectional traffic.

The nozzle was created near the entrance portal of each tube by making an opening in the supply duct and providing a deflecting plate (nozzle) to direct air at approximately 20° in the direction of traffic discharging air at a high velocity into the tunnel from the ceiling. The expected velocity through the nozzle using the existing fans was around 32.9 m/s for the uphill tube and 22.4 m/s for the downhill tube. Near the exit portal, four (4) large openings were created in the exhaust duct to remove smoke and to create negative pressure at the exit portal encouraging more flow to pass through the tunnel. The general layout for the Saccardo nozzle and the exhaust openings is shown in *Figure 11*.

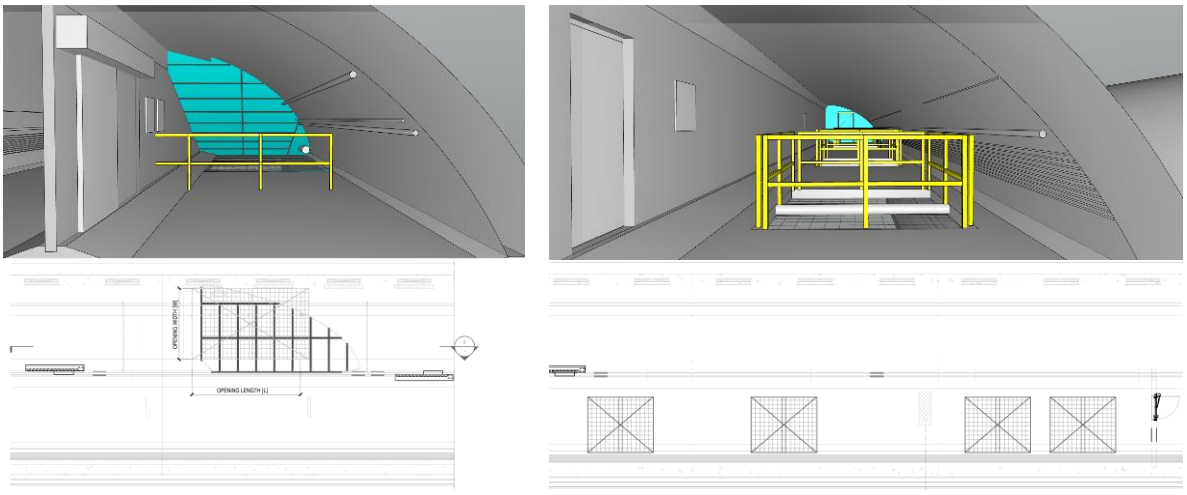

Figure 11 Saccardo Nozzle (Left) and Exhaust Openings (Right).

During design, to maximize the effectiveness of the nozzle for smoke control, the sizes of the nozzle .openings were optimized to maximize the thrust generated through the nozzle with the existing fans. The imparted thrust from the air jet to the tunnel is described by Equation (6) [3]. Assuming the installation efficiency and angle are constant, the thrust can be optimized by maximizing the product of the mass flow rate and ejection velocity [$\dot{m}V_j$] through the nozzle. This can be rewritten in terms of the total fan flow rate, *Q*, the effective area of the nozzle, *A*, and the density of the air, ρ, as $\rho Q^2/A$.

$$T = \dot{m}V_j\eta_j \cos(\theta) \quad (6)$$

Where

$T =$ Thrust imparted from the air jet to the tunnel air [N]
$\dot{m} =$ Mass flow of air jet [kg/s]
$V_j = Velo$city of air jet [m/s]
$\eta_j =$ Installation efficiency [−]
$\theta =$ Angle between the jet and the tunnel axis [radians]

It is known that the flow rate produced by the fans is based on the system resistance, which is a function of the effective nozzle opening area. As the nozzle gets smaller, the system resistance increases and the flow produced by the fans decreases, and vice versa. At this facility, the widths of the nozzle openings were selected to be the maximum available width of the supply duct to reduce the production of vortices adjacent to the opening. Given the width of the opening was fixed by the duct geometrical constraints, the opening area is now only a function of the opening length, *L*, in the longitudinal direction. Also, since the effective area of the nozzle, A, is the flow area perpendicular to the deflecting plate, it can be calculated from the geometry as a function of the opening length. In this scenario, the thrust can be defined as a function of the opening length as described in Equation (7). A drawing of this scenario is shown in *Figure 12*.

$$\max(T) = \mathrm{K}\max\left(\frac{Q\left(A(L)\right)^2}{A(L)}\right) \qquad (7)$$

Where

T = Thrust imparted from the air jet to the tunnel air [N]
Q = Flow rate through the nozzle[m^3/s]
A = Effective area of the nozzle [m^2]
L = Length of the opening [m]
K = Constants [kg/m^3]

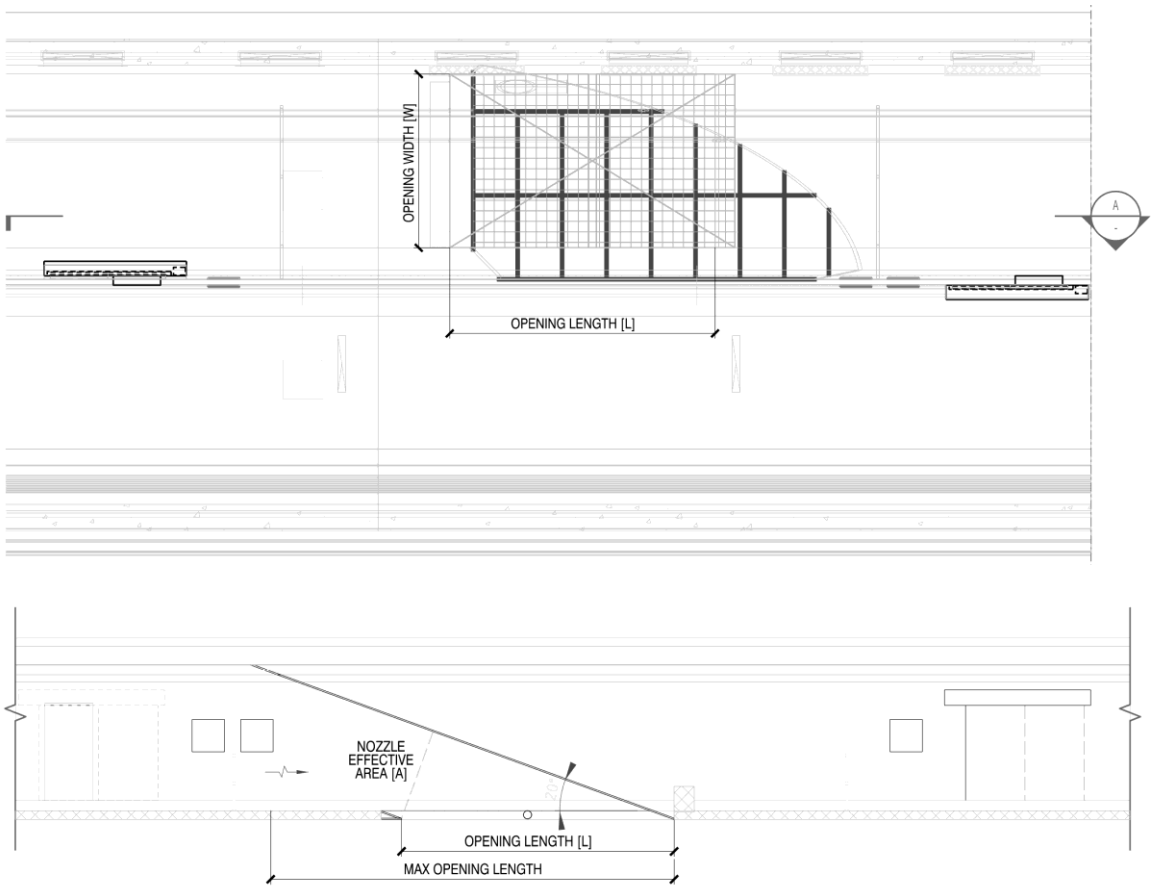

Figure 12 Nozzle Parameters.

To determine the flow rate of the fans for different opening lengths, the system resistance was approximated up to the nozzle discharge and used in conjunction with the existing fan curve to find the operating point of the fans. For the different opening lengths (nozzle sizes), the loss coefficient of the nozzle and the discharge loss will vary. To account for these effects, the loss coefficient of the nozzle was approximated using a duct transition fitting and the discharge loss was based on the effective area of the nozzle. For this 1-D analysis, all the loss coefficients were determined from Idelchik's Handbook of Hydraulic Resistance [4] and ASHRAE Duct Fitting Database [5] and it was assumed that all the air will be directed at the angle of the nozzle.

The optimal size of the nozzle was found by evaluating the approximate thrust for a range of opening sizes from 35% to 90% of the full opening, with a constant increment of 2.54 cm between lengths. A plot of the thrust as a function of the opening length is shown in *Figure 13*. From the figure, in this scenario, an opening length that is 66% of the full opening is the ideal size for the nozzle.

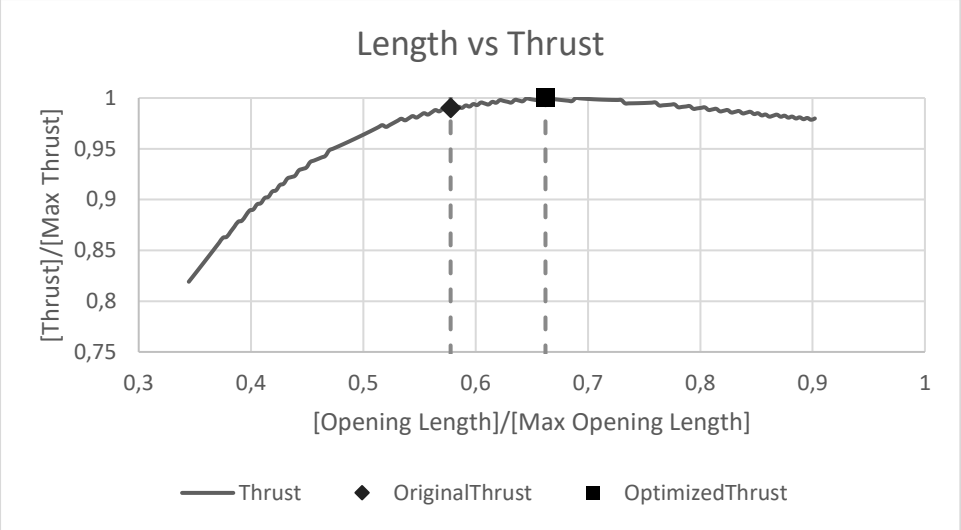

Figure 13 Thrust as a Function of Opening Length.

To verify the optimal size of the nozzle, a range of lengths between 47% and 66% of the maximum opening length were modeled in CFD to determine the effectiveness of the ventilation system during a fire. At the worst fire location, without the use of the sprinkler system, the optimized opening length was most effective at managing backlayering upstream of the fire. With the suppression system and the Saccardo nozzle the ventilation system can manage a 50 MW fire in the downhill tube. To further improve the effectiveness of the longitudinal system in the downhill tube, the undersized supply fans serving the nozzle are to be replaced with higher capacity fans.

REPLACING VENTILATION FANS

Replacement of the supply fans serving the downhill tube was considered to improve the effectiveness of the longitudinal ventilation system, as the fans were originally designed for normal operation. During replacement design, field tests were conducted to verify the fan curves and to set a baseline for fan replacement. Also, during the design, given the close proximity (about 1 impeller diameter) of the inlets of adjacent fans, a CFD study was conducted to quantify the system effects when two adjacent fans are operating in parallel using the current arrangement.

Field Tests - General

The in-field ventilation tests were performed to obtain sufficient data to generate the existing fan performance curves and system curves as the baseline for fan replacement. To obtain the data required to generate the curves, two test setups were used:

1. System Curve Setup – To obtain data points on the existing system curve, the operating points of the supply fans were measured operating in parallel (2-fan) at low, medium, and high speed.
2. Fan Performance Curve Setup – To obtain points on the fan curve besides the fan's current operating point, the system resistance was increased by adding a blockage in the airstream, forcing the fan to operate at a higher pressure. Each test blocked more area, raising the system resistance and providing a new operating point on the fan curve. A total of six (6) additional points on the fan curve were obtained using this method.

The operating point of the fan is determined by the total pressure across the fan and the airflow produced by the fan during operation at a certain air density and fan speed. Due to measurement limitations, the total pressure and airflow produced could not be measured directly and instead, measurable quantities including air velocity, area, static pressure, dry bulb temperature, and relative humidity were used to calculate the desired values.

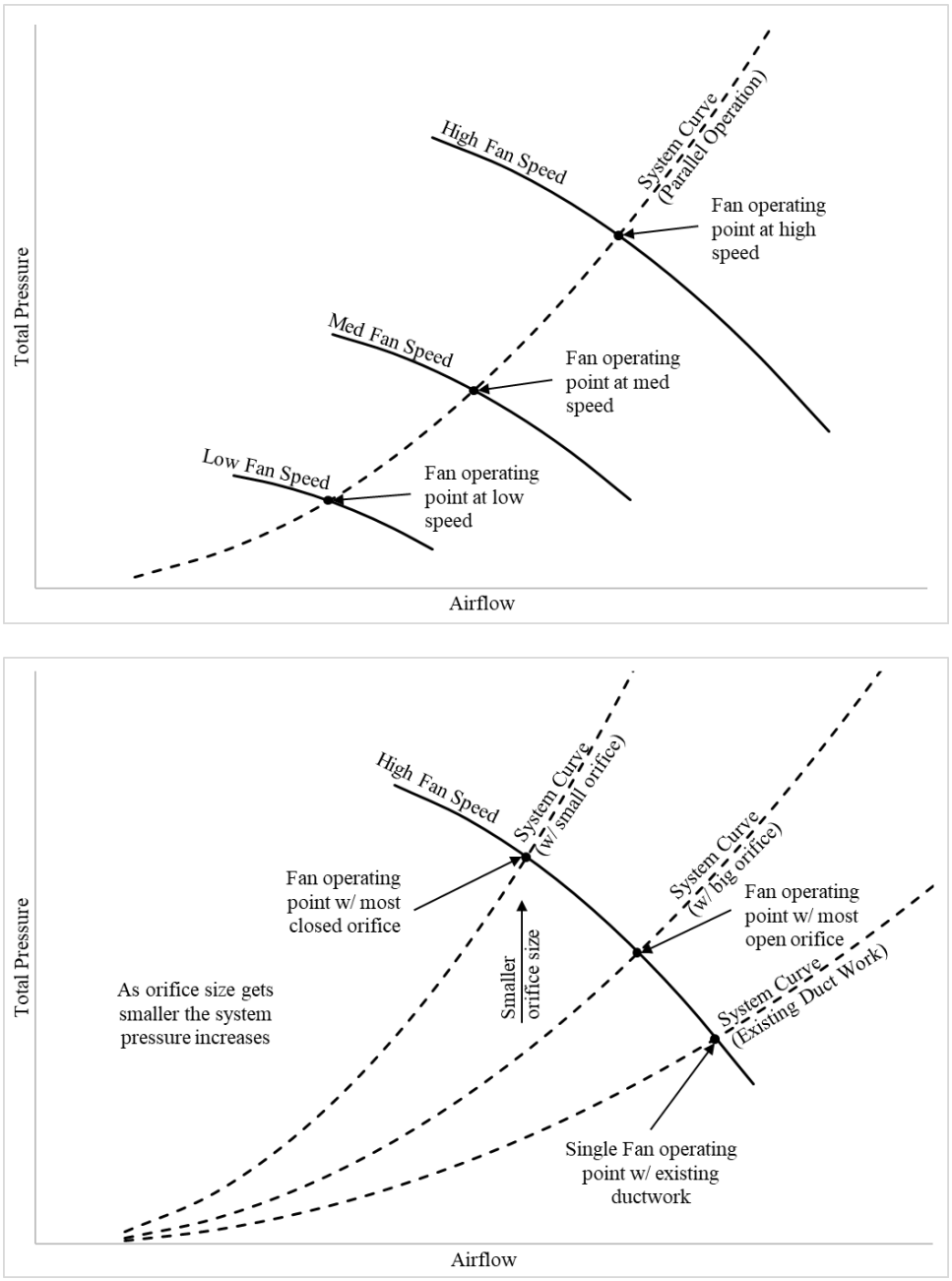

Figure 14 System Curve Tests Example (Top); Fan Performance Curve Tests (Bottom).

Field Tests – Airflow Measurements

The airflow was determined at two locations; the main measurement was located near the fan discharge before the flows converge, and a secondary measurement for verification was located further downstream in the tunnel duct after the flows have converged and fully developed. The locations for the main and secondary measurements are shown in *Figure 15*. In the rectangular section, the velocity was measured at multiple points along the plane as shown in *Figure 16*. The airflow for this section was determined from the velocity measurements and area using Equation (8). For the irregular section, a time average traverse using a vane anemometer was performed to determine the average air velocity within the plane. A sample path used for the time average traverse is shown in *Figure 16*. Using the average velocity and area of the section, the airflow was estimated.

Figure 15 Main – Fan Discharge (Left); Secondary – Flows Converged (Right).

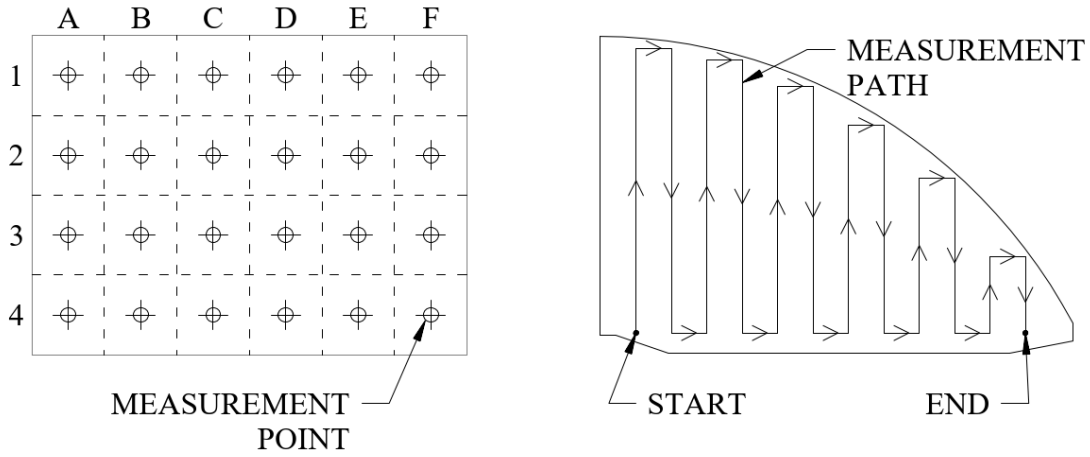

Figure 16 Rectangular Section Measurement Points (Left); Irregular Section Path (Right).

$$Q = \sum_{i=1}^{N} v_i A_i \qquad (8)$$

Where

$Q =$ Airflow $[\mathrm{m}^3/\mathrm{s}]$
$N =$ Number of measurement areas $[-]$
$v_i =$ Average velocity of measurement points within the i^{th} area $[\mathrm{m}/\mathrm{s}]$
$\mathrm{A_i} =$ Area $[\mathrm{m}^2]$

Field Tests – Total Pressure Measurements

The total pressure across the fan was determined using static pressure measurements upstream and downstream of the fan, in conjunction with the velocity pressures at the measurement planes. The static pressures were measured at the locations indicated in *Figure 17*. The static probe for the inlet side of the fan was placed in the fan plenum where the air movement is negligible. Since there is not significant pressure drop between the plenum and the fan inlet, the static pressure in the plenum and the total pressure at the fan inlet are similar. The static pressure probes at the fan discharge were placed around the perimeter and connected in a piezometer ring manifold to measure an average pressure at the outlet. The velocity pressures used to determine the total pressure were estimated using the average velocity at the static pressure measurement plane. Equation (9) was used to determine the total pressure across the fan.

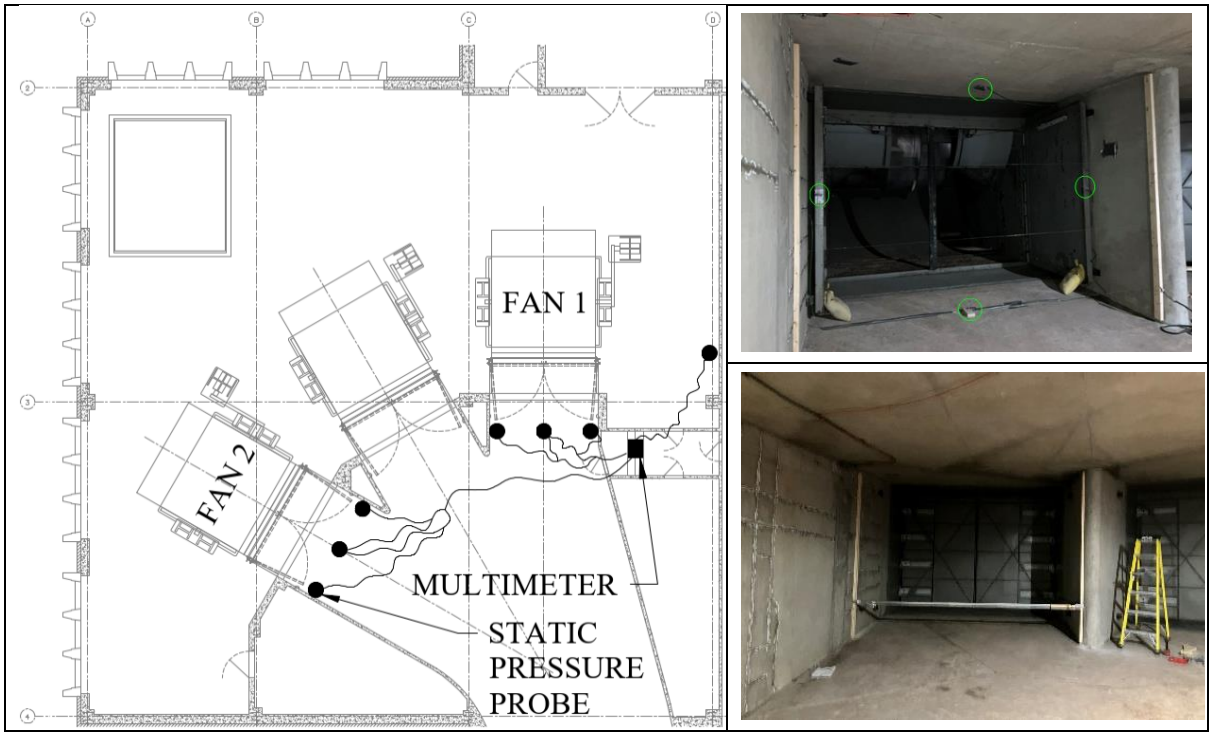

Figure 17 Static Pressure Measurements.

$$\begin{aligned}\Delta TP &= TP_{D/S} - TP_{U/S} \\ &= \left(SP_{D/S} + VP_{D/S}\right) - \left(SP_{U/S} + VP_{U/S}\right) \\ &= \left(SP_{D/S} + \frac{1}{2}\rho_{local}\left(\frac{Q}{A_{D/S}}\right)^2\right) - \left(SP_{U/S} + \frac{1}{2}\rho_{local}\left(\frac{Q}{A_{U/S}}\right)^2\right)\end{aligned} \quad (9)$$

Where

ΔTP = Total pressure difference across fan [Pa]
TP = Total pressure at measurement location [Pa]
SP = Static pressure at measurement location [Pa]
VP = Velocity pressure at measurement location [Pa]
Q = Airflow [m^3/s]
A = Area at measurement location [m^2]
ρ_{local} = Density of local air [kg/m^3]
D/S = Measurement location downstream of fan
U/S = Measurement location upstream of fan

Field Tests – Fan Curve Test Blockages

To perform the variable flow test, a wall was built downstream of the fan to modify the system curve and obtain the new fan operating points. A total of six (6) test scenarios with the wall blockage were performed, with each consecutive test decreasing the size of the orifice and in turn increasing the system pressure. After each test, a board was placed on the bottom and top of the wall to increase the pressure drop experienced by the fan. *Figure 18* shows the six (6) test scenarios conducted with the wall. A seventh test was conducted after the wall was deconstructed (totally open) to determine the current operating point of a single fan at high speed.

Test Scenario 1 (0 Planks)

Test Scenario 2 (2 Planks)

Test Scenario 3 (4 Planks)

Test Scenario 4 (6 Planks)

Test Scenario 5 (8 Planks)

Test Scenario 6 (10 Planks)

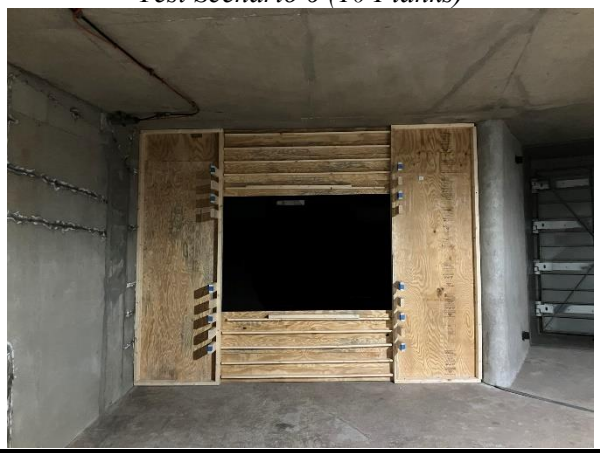

Figure 18 Test Blockage.

Field Tests – Results

Figure 19 shows the system curve generated for the supply duct ventilation system which was used to evaluate how the system differs from the original 1972 design. These curves were used to determine the temporary operating points of the new fans if they were to be installed prior to the conversion to the Saccardo Nozzle.

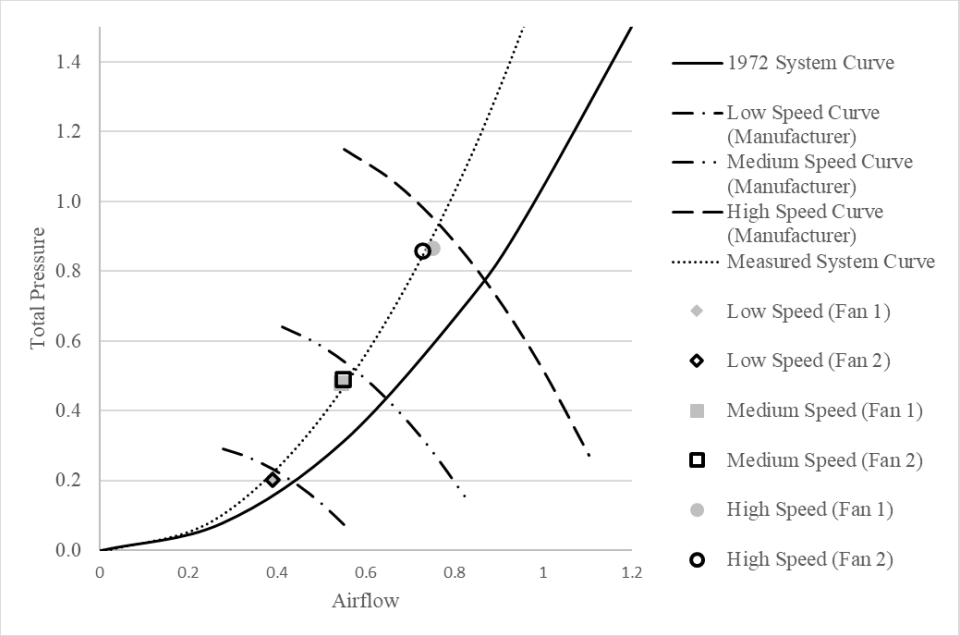

Figure 19 System Curve Test Results.

The fan curve generated for the tested fan is shown in Figure 20. This fan curve was used to obtain the expected operating point of the fans after the Saccardo Nozzle implementation and to set a baseline for fan replacement.

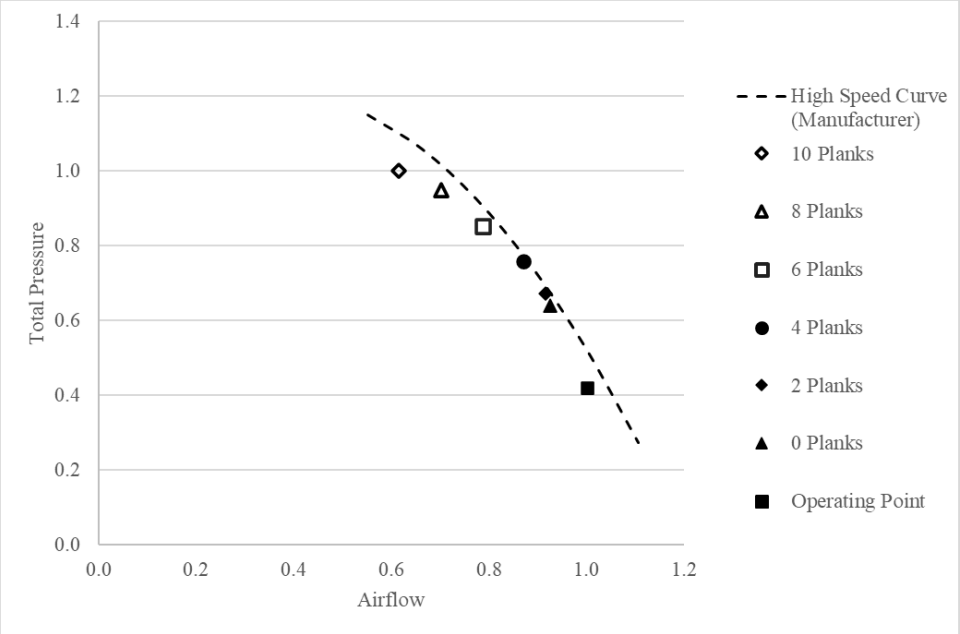

Figure 20 Fan Curve Test Results

The Figures shown are based on the relative performance of the fan as a percentage of the measured maximum pressure delivered by the fan with the greatest obstruction and the measured maximum flow delivered by the fan when there are no obstructions.

Fan Interaction Analysis

The three (3) centrifugal supply fans that serve a single supply section pull air from a common plenum and are in close proximity to each other, with about 1 impeller diameter between adjacent fan inlets as shown in Figure 21. For fan replacement, the existing layout was intended to be reused, but there were concerns that performance of the fans may degrade when adjacent fans are operating in parallel due to the closeness of the inlets which allows for fan interaction.

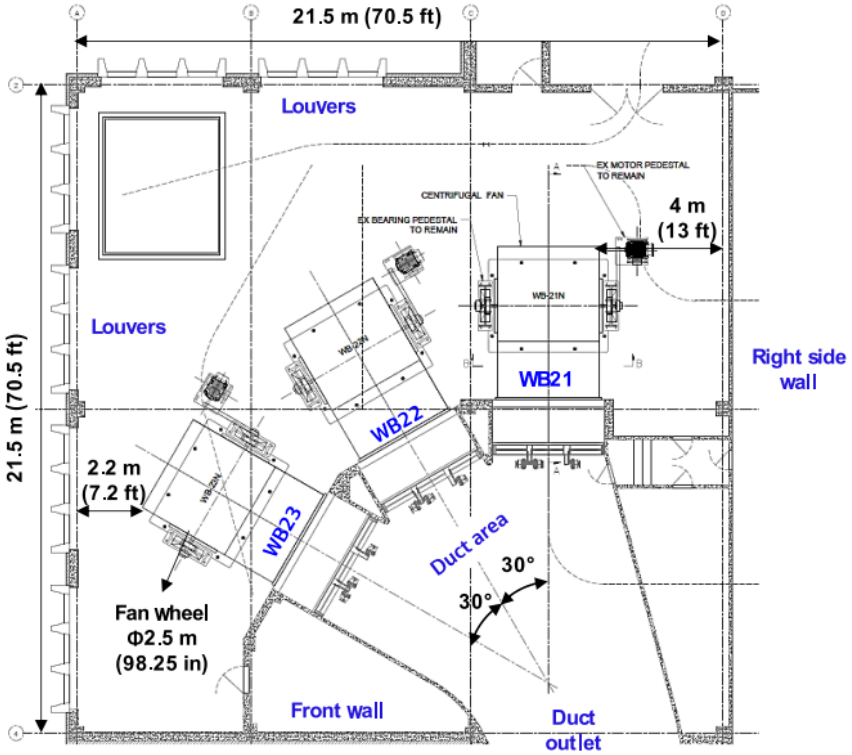

Figure 21 Fan Room Layout

To determine if the proximity of the inlets has an impact on fan performance when adjacent fans are operating in parallel, fan operation was modelled in CFD under two scenarios.

1. Parallel operation of two adjacent fans in close proximity to one another.
2. Parallel operation of the two furthest fans, which are sufficiently separated.

The pressure contour plots for the two cases are shown in Figure 22 for performance comparison. The pressure contours show that the negative pressure region between the blowers has a higher area and some overlap when adjacent fans are running in parallel as compared to the two furthest fans operating in parallel. However, on quantification of the pressure values, the differences are minimal. It is also noted that the volume flow rate out of the duct is approximately the same for both fan operation scenarios. This indicates that the interaction between adjacent fans when operating in parallel has some impact but is not significant and could be considered negligible in this case. This justifies the reuse of the existing fan layout for the new fans without modification.

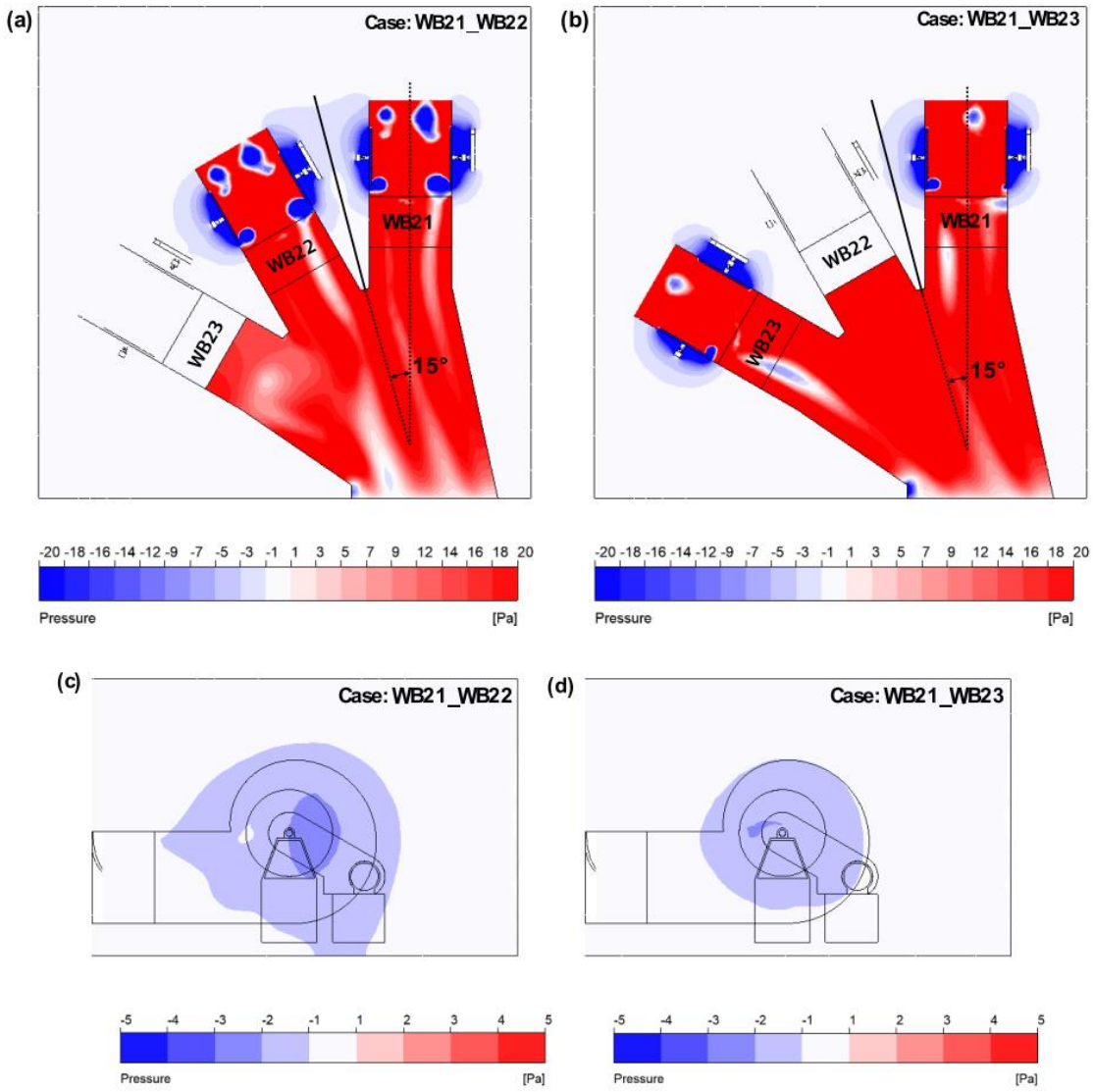

Figure 22 Fan Interaction CFD Results

Fan Replacement Impact

As discussed in previous sections, the performance of the longitudinal system can be improved by increasing thrust through the nozzle. One of the ways to achieve this is by replacing the fans with higher performance fans that will generate more flow through the nozzle. The maximum increase in fan capacity is limited by a variety of factors including:

1. Existing electrical system capacity– Increasing the flow produced by the fans will increase the power required to operate the fans.
2. Size constraints – If the existing structure and arrangement are to be reused, there are limits to the size of the new fans
3. Noise and velocity along the path of egress – Higher velocities through the nozzle increase the noise produced through the nozzle and the air velocities experienced by those evacuating along the roadway

Based on these considerations, the performance requirements for these new fans were based on a design velocity through the nozzle of 33 m/s. The increase in ventilation capacity from 22.4 m/s to 33 m/s through the nozzle increases the smoke control capability of the ventilation system. Although increasing the velocity through the nozzle further will make the system capable of controlling larger

fires, velocities that exceed 33 m/s will start to produce excessive noise and potentially knock over pedestrians evacuating the area and the authors would not recommend exceeding this velocity.

CONCLUSIONS

A systematic approach should be taken during tunnel rehabilitation projects to provide the tunnel facility with the systems it requires to meet current fire life safety needs. In many cases, such as at BWMT, a single upgrade alone may not be sufficient to meet tunnel safety criteria, and a series of modifications may be required, each incrementally improving tunnel safety. The impact of each modification on the facility's capability to control a potential fire hazard shall be considered in combination with one another during design.

Providing a reliable fire detection system can create a timely alarm and quick activation of other fire life safety systems. Early activation of the fixed fire suppression system can stop a fire from further growth and spread, and in the case of a flammable liquid fire, additives can enhance firefighting effectiveness. Using alternative ventilation schemes with the suppression system, such as a longitudinal ventilation system based on a Saccardo nozzle, can effectively manage the hot smoke from the residual fire. With these upgrades, the systems at BWMT which were originally capable of partially managing a 5 MW fire, are now capable of safely controlling flammable liquid tanker fires. The performance of the ventilation system was modelled in Ansys Fluent at the worst fire locations and it was confirmed from the results that no smoke backlayering is present.

ACKNOWLEDGEMENTS

Authors would like to thank Mr. David Gibbings, Mr. Casey Funk and other Jacobs staff for help during site visits and the Virginia Department of Transportation for support with the project and allowance to publish this paper. Authors would also like to acknowledge Mr. Sean Murphy for his development of the 3D models of the Saccardo nozzle.

REFERENCES

[1] "THE HISTORY AND HERITAGE OF CIVIL ENGINEERING IN VIRGINIA," 25 09 1998. [Online]. Available: http://www.roadstothefuture.com/VASCE-History/VASCE-Big-Walker.htm.

[2] National Fire Protection Association, NFPA 502: Standard for Road Tunnels, Bridges, and Other Limited Access Highways, Quincy: NFPA, 2023.

[3] F. Tarada and R. Brandt, "Impulse Ventilation for Tunnels - A State of the Art Review," in *13th International Symposium on Aerodynamics and Ventilation of Vehicle Tunnels*, New Brunswick, 2009.

[4] I. Idelchik, Handbook of Hydraulic Resistance, Delhi: Jaico Publishing House, 2003.

[5] American Society of Heating, Refrigerating, and Air-Conditioning Engineers, "ASHRAE Duct Firring Database v6.0.1," ASHRAE, Chicago, 201.

[6] AMCA, AMCA Standard 803-02, Industrial Process Power Generation Fans: Site Performace Test Standard, Arlington Heights, 2008.

CFD Modeling Of The Memorial Tunnel Fire Tests Using An Autonomous Meshing Approach And Adaptive Mesh Refinement

Mathias Vångö[1], Sarah Feher[1], Suresh Nambully[1], Matteo D'Elia[1] and Rainer Rothbauer[1]
[1]Convergent Science GmbH, Linz, Austria

ABSTRACT

Being able to predict smoke propagation in tunnels during fire incidents is critical to ensuring safe operation and essential in the ventilation systems design process. To that end, numerical tools such as Computational Fluid Dynamics (CFD) are often used because they are relatively inexpensive, quick, and provide a deeper understanding of the flow dynamics within the tunnel, as compared to fire tests.

In this work, we present a CFD model to simulate fire incidents in a tunnel, with the intent of being a valuable engineering tool. Hence, an autonomous meshing strategy with Adaptive Mesh Refinement (AMR) is employed, in which the mesh is dynamically updated during the simulation based on local flow conditions.

However, numerical models need to be validated against test data to be used with confidence. In this work, we have assessed the proposed model by comparing it to measurement data from the Memorial tunnel fire tests. Three different fire intensities were simulated, and sensitivity studies were conducted with regard to obstruction blockage ratio and grid size. Overall, a good agreement was observed with respect to the measurements, in regard to temperature stratification, smoke back layering, and bulk temperature distribution.

KEYWORDS: Computational Fluid Dynamics, CFD, autonomous mesh, adaptive mesh refinement, smoke propagation

INTRODUCTION

Computational Fluid Dynamics (CFD) is a valuable tool for safety and risk-scenario evaluation of fire incidents in road and railway tunnels, as several scenarios can be easily studied within a numerical framework at a relatively low cost. To ensure its ability to accurately reproduce the real-world scenario, a CFD model must be validated against experimental data.

CFD simulations have already been used extensively for fire safety related topics, such as compartment fire [1], fire extinguishing [2], venting of toxic battery gases [3], and tunnel ventilation [4, 5, 6, 7, 8]. Regarding CFD usage in tunnels, a major focus is the ability to predict the smoke propagation, especially upstream, which is commonly referred to as back layering. Accurately predicting the back layering is important to determine the critical velocity, required for the design of ventilation systems.

In our previous work, we introduced a numerical model and showed that it was able to satisfactorily predict the smoke propagation from the Koralm tunnel fire tests conducted by the Institute of Thermodynamics and Sustainable Propulsion Systems (ITnA) at the Graz University of Technology [8, 9]. In this work, we extend the validation efforts to the well-known Memorial tunnel fire tests [10]. We evaluate the performance of the model for various fire sizes, by comparing the simulation results to the extensive temperature measurements.

Accurately modeling fire incidents poses several challenges due to the complex physics involved, e.g., turbulence, combustion, radiation, buoyancy, and heat transfer. Furthermore, these phenomena are taking place over a wide range of length and time scales, from the complex small-scale fire dynamics to large-scale tunnels, often with domain lengths of several hundred meters. Thus, accurately modeling the physical phenomena is often not feasible due to computational limitations. Therefore, well-chosen simplifications must be made to achieve a balance of accuracy and computational cost, in order to be effectively used as an engineering tool.

TEST CASE DESCRIPTION

The data from the Memorial tunnel fire tests are often used for validating CFD models, as the tests are very comprehensive and cover a wide range of fire and ventilation conditions. In total, 98 tests were conducted with fire intensities varying between 10 and 100 MW, as well as various ventilation strategies such as fully transverse, natural, and forced longitudinal. In the tests, several sensors measured certain critical quantities, such as temperature, velocity, CO, and CO_2 concentrations at various locations distributed throughout the tunnel [11, 12].

The Memorial tunnel is 853 m long with a 3.2% inclination from the south to the north portal. The present work focuses on the longitudinal ventilation tests, where the false ceiling was removed and jet fans had been installed. The tunnel cross-section is depicted in Figure 1, and the total tunnel cross-sectional area is approximately 60 m^2.

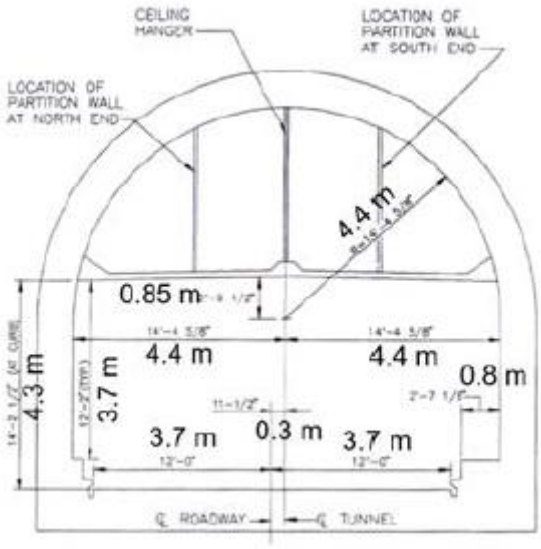

Figure 1: Illustration of the Memorial tunnel cross-section [11].

To control the ventilation, 24 jet fans were installed in groups of three at various locations in the tunnel, as shown in Figure 2. The fans were operating with a discharge velocity of 34.2 m/s and a volumetric flow rate of 42.95 m^3/s, and each test had its own configuration of active fans.

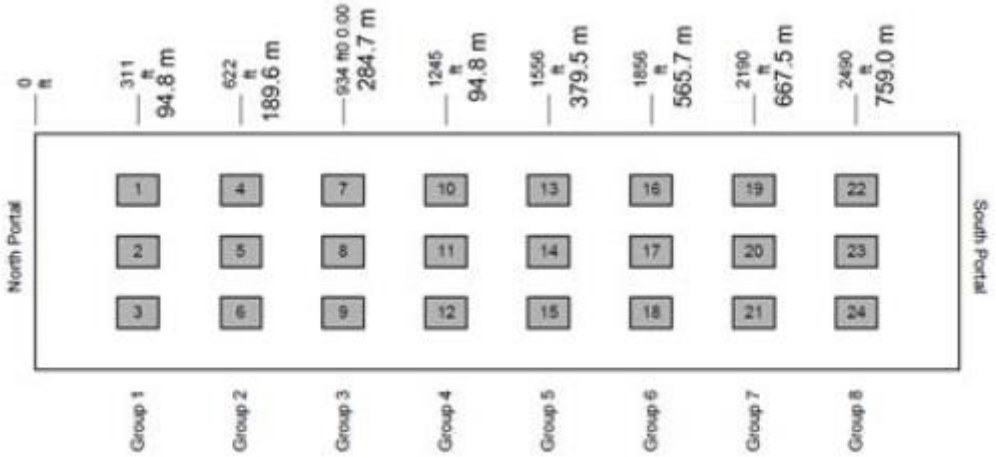

Figure 2: Schematic of the fan layout within the tunnel. Depending on the test, different fans were activated [11].

Within the tunnel, several measurement "loops" were constructed with instrumentation to collect temperature, velocity, and CO/CO_2 concentration data. Hence, a detailed description of the temporal evolution and the spatial distributions could be measured. The locations of the loops are illustrated in Figure 3. However, the blockage area of these loops is not negligible compared to the overall cross-section of the tunnel and must therefore be assumed to impact the tunnel flow. Furthermore, the exact blockage area appears to be uncertain, as values ranging from 10.2 m^2 to 15.82 m^2 have been reported in literature [11, 13]. Consequently, we decided to investigate the impact of the blockage area by performing a sensitivity analysis study.

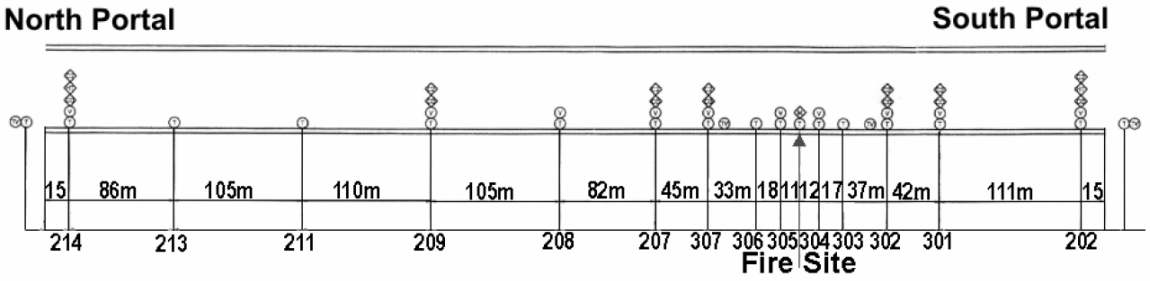

Figure 3: Illustration of the loops and fire site location within the tunnel [14].

As seen from Figure 3, the fire site was situated between loop 304 and 305, at roughly 615 m from the north portal. To facilitate the fire tests ranging from 10 MW to 100 MW, four fire pans were set up as shown in Figure 4.

Although there were extensive testing and data collection from these tests, there are still several questions and challenges regarding the suitability of this data as validation data for CFD simulations. Firstly, there appears to be some uncertainty as to the actual blockage ratio from the measurement loops; some sources report a blockage ratio of 17%, whereas others report values as high as 26% [11, 13]. Secondly, the tests were performed over an extended period, with dynamic activation and deactivation of the fans to control the back layering. Simulations of such long amounts of physical time might prove unfeasible without significantly sacrificing accuracy. To that end, Beyer & Stacey [11] averaged the measured temperatures for test numbers 606A, 610, and 615B (corresponding to heat release rates (HRR) of 10, 50, and 100 MW, respectively) over a period when the flow and smoke propagation were reasonably constant, so that they could perform steady-state simulations.

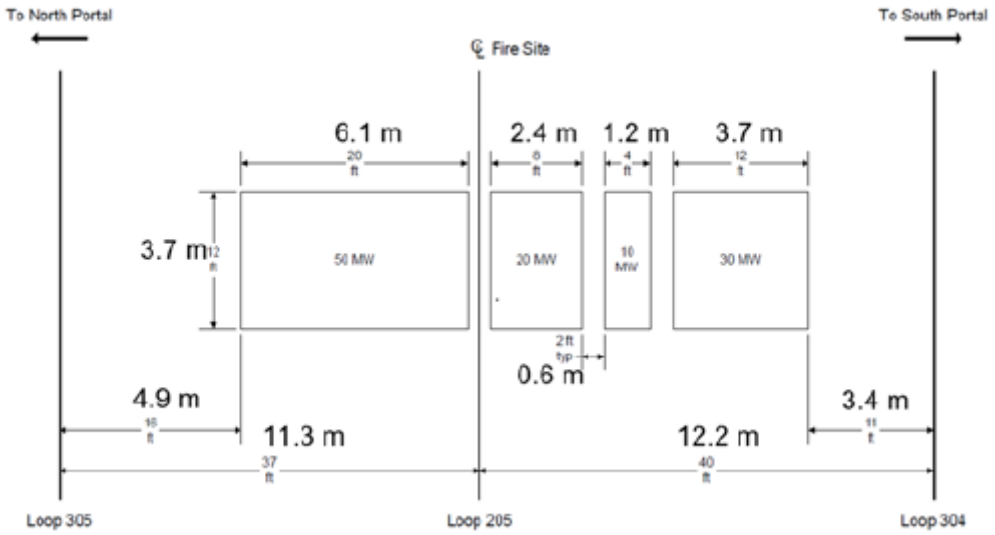

Figure 4: Schematic of the fire pans arrangement at the fire site [11].

Although not perfect, we do believe that comparisons to the quasi-steady averaged values from Beyer & Stacey [11] are a reasonable approach to give an indication of the CFD model's predictability. Hence, we have decided to run the 10, 50, and 100 MW cases (tests 606A, 610, and 615B, respectively) using steady boundary conditions to be able to compare to the averaged measured temperatures. To evaluate the uncertainties regarding the loop blockage ratios, we also ran a variation from the 17% to the 26% reported in the FDS validation input files. Furthermore, we also carried out a grid sensitivity study to evaluate grid convergence.

COMPUTATIONAL MODEL

The model we used for this work is based on a fully compressible unsteady Reynolds-Averaged Navier-Stokes (URANS) framework within the CONVERGE version 4.1.1 software [15]. CONVERGE is a finite-volume density-based solver that uses a collocated grid with Rhie-Chow interpolation. For the simulations in this work, we used a modified version of the Pressure Implicit with Splitting of Operators (PISO) algorithm for the pressure-velocity coupling and a second-order central difference discretization scheme for all transport equations, except for turbulence, for which a first-order upwind scheme was employed. Furthermore, the gas compressibility was considered using the ideal gas law as the equation of state, and the realizable k-ε turbulence model was used. For a detailed description of the numerics, we refer the reader to Richards et al. [16].

To model the fire, there are several approaches of varying complexity and computational cost available. The most common ones used for these types of simulations are a volumetric heat source and the Eddy Dissipation Model (EDM) [17]. For this work, we chose the latter as we believe the volumetric heat source approach to be oversimplified. EDM assumes a one-step chemical reaction to govern the species conversion, while using the turbulent mixing time scale to determine the rate of combustion. While we could have utilized the detailed chemistry solver in CONVERGE to model the combustion, at the large length scales involved here, EDM generally provides a good compromise in terms of accuracy and computational cost.

Although radiation is important for large-scale fire simulations, we did not directly model it in this work, because the flame temperature tends to not be properly resolved with the relatively large computational cells used. Instead, to account for radiation, we assume that a certain amount of the fuel energy does not contribute to heating the gas, which is determined by the radiative fraction [18]. In the simulations, this is accounted for by reducing the heat of combustion (LHV) in accordance with the specified radiative fraction. Hence, in this simplified approach, the heat release rate is artificially reduced and might have an impact on the resulting temperature distribution. Although, we consider

this approach to be in line with the other model simplifications and assumptions, as well as with the uncertainties to the geometry.

The autonomous meshing in CONVERGE is done via a modified Cartesian cut-cell approach, meaning that all the geometry details are preserved. Because the process is done automatically, the mesh is dynamically regenerated as required during the simulation, which allows easy modeling of moving and deforming boundaries. Additionally, this allows the mesh to be automatically refined during runtime using Adaptive Mesh Refinement (AMR). AMR evaluates the magnitude of the sub-grid field ϕ' of user-specified variables (e.g., temperature and velocity) to assess if mesh refinement should be applied, which eliminates the need for *a priori* knowledge of the local flow features to construct an adequate mesh. ϕ' is defined as $\phi' = \phi - \bar{\phi}$, where ϕ and $\bar{\phi}$ are the actual and resolved fields, respectively. The sub-grid field is approximated as the second order derivative:

$$\phi' = -\alpha_{[k]} \frac{\partial^2 \bar{\phi}}{\partial x_k \partial x_k}, \tag{1}$$

arising from an infinite series expression of ϕ', where, α_k is $(\Delta x_k)^2/24$ for rectangular shaped cell.

SIMULATION SETUP

The entire tunnel was included in the computational domain, along with all fans and loops previously described. The obstructions were set up based on the FDS validation input files [13]; thus, the blockage ratio of the base case was 26% instead of the 17% commonly used otherwise. All of the simulations were run for 600 seconds to ensure that a quasi-steady state was reached, and the average temperature over the last 100 seconds was used to compare to the averaged measurement data. Furthermore, steady-state simulations were run for the cold flow of each test case, to be used as initialization for the full case. This was done to ensure that the combustion started from a developed flow field.

Mesh

Although the meshing is autonomous in CONVERGE, the grid is controlled by a few parameters. In this case, the base case is set up with the base grid size $\Delta x_{base} = 0.6\ m$, which represents the largest cell size in the domain. A fixed embedding of scale one is set up on the wall boundaries, and an embedding of scale two is used in the active jet fans as well as around the fire pans. The fixed embeddings add local mesh refinements with the relation $\Delta x = \Delta x_{base}/2^n$, where n is the embedding scale. To ensure adequate mesh resolution at the fire location, temperature-based AMR was applied with scale three. Therefore, the smallest cells for the base case were $\Delta x = 0.075\ m$, located in the vicinity of the fire, which corresponds to $D^*/\Delta x \sim 25$ for the 50 MW case, where D^* denotes the characteristic fire diameter [19] defined as

$$D^* = \left(\frac{\dot{Q}}{\rho c_p T \sqrt{g}} \right)^{\frac{2}{5}}. \tag{2}$$

Here, $\dot{Q}$ and g refer to the fire heat release rate and gravity, whereas ρ, c_p, and T denote the ambient density, specific heat, and temperature, respectively. A snapshot of the mesh at the fire location is depicted in Figure 5.

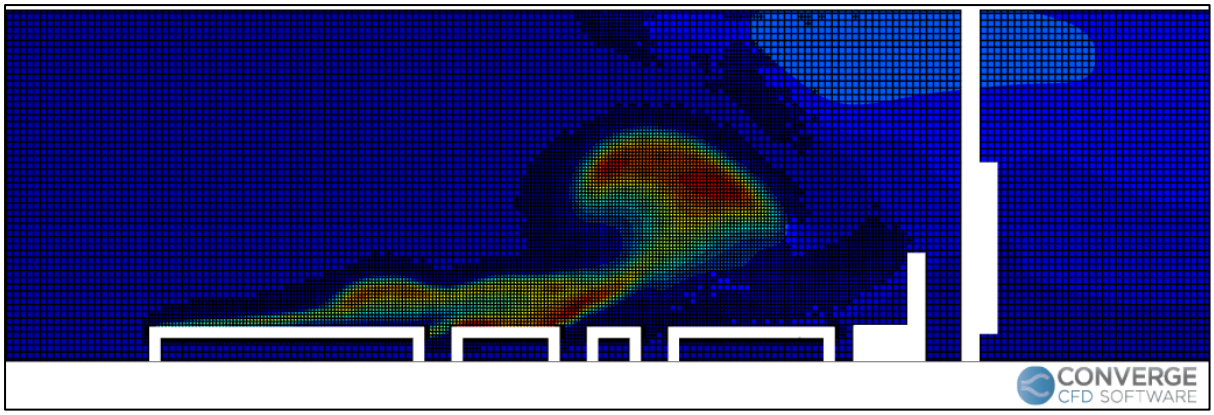

Figure 5: A cut plane of the domain at the fire location, highlighting a snapshot of the mesh and the flame.

Boundary conditions

Both the north and south portals were treated as open boundaries with an ambient pressure of one atmosphere. The inclination of the tunnel was accounted for by modifying the gravity vector, such that the tunnel domain could be aligned with the x-axis. As no ventilation velocity was imposed, it was a consequence of the jet fans which were set to deliver a discharge velocity of 34.2 m/s, as given by the test description. Furthermore, all wall boundaries used standard wall functions with a surface roughness of 1.5 mm and a fixed temperature equal to ambient.

The fire intensity was controlled by imposing a mass flow rate of n-heptane at the fire pans, which were ramped from zero to full intensity from t = 0 s to t = 100 s. Additionally, as previously mentioned, the fuel LHV was modified based on the radiative fraction to indirectly account for radiative heat losses.

A summary of the boundary conditions and case relevant parameters is listed below in Table 1.

Test	*606A*	*610*	*615B*
HRR (MW)	10	50	100
Ambient temperature (°C)	8.5	4.0	12.0
Radiative fraction (-)	0.21	0.24	0.17
LHV (MJ/kg)	35.55	34.2	37.35
Blockage ratio (-)	0.26	0.26	0.26

Table 1: Case relevant parameters and boundary conditions of the three simulated test conditions.

Sensitivity analysis setup

The 50 MW case serves as the baseline for the sensitivity analyses. For the blockage ratio variation, in addition to the base value of 0.26, two simulations with the ratios 0.17 and 0.20 were performed, by scaling the size of certain blocks of the obstructions. Similarly, for the grid size study, in addition to the base case with a base grid of 0.6 m (baseline), two additional simulations with base grids of 0.4 m (fine) and 0.8 m (coarse) were run.

RESULTS

Figure 6 shows a cut-plane of the fire site through the center of the tunnel for the 10, 50, and 100 MW cases, respectively. We can observe how the fire shape increases with increasing intensity, but also that there is generally only a minor back layering occurring, as expected from the tests.

A quantitative comparison of the temperature distribution at the various loops, as well as the bulk temperature distribution throughout the tunnel for the baseline 50 MW case is depicted in Figures 7

and 8. The temperature distribution downstream of the fire site is generally well reproduced, while overall slightly underpredicting the bulk temperature, especially close to the fire. Upstream from the fire, the test data suggests some back layering reaching loop 305, which is not captured in the simulations. However, the back layering length is relatively short, and with the assumptions and simplifications in both the simulation setup and the test data, we do consider this level of accuracy to be reasonable.

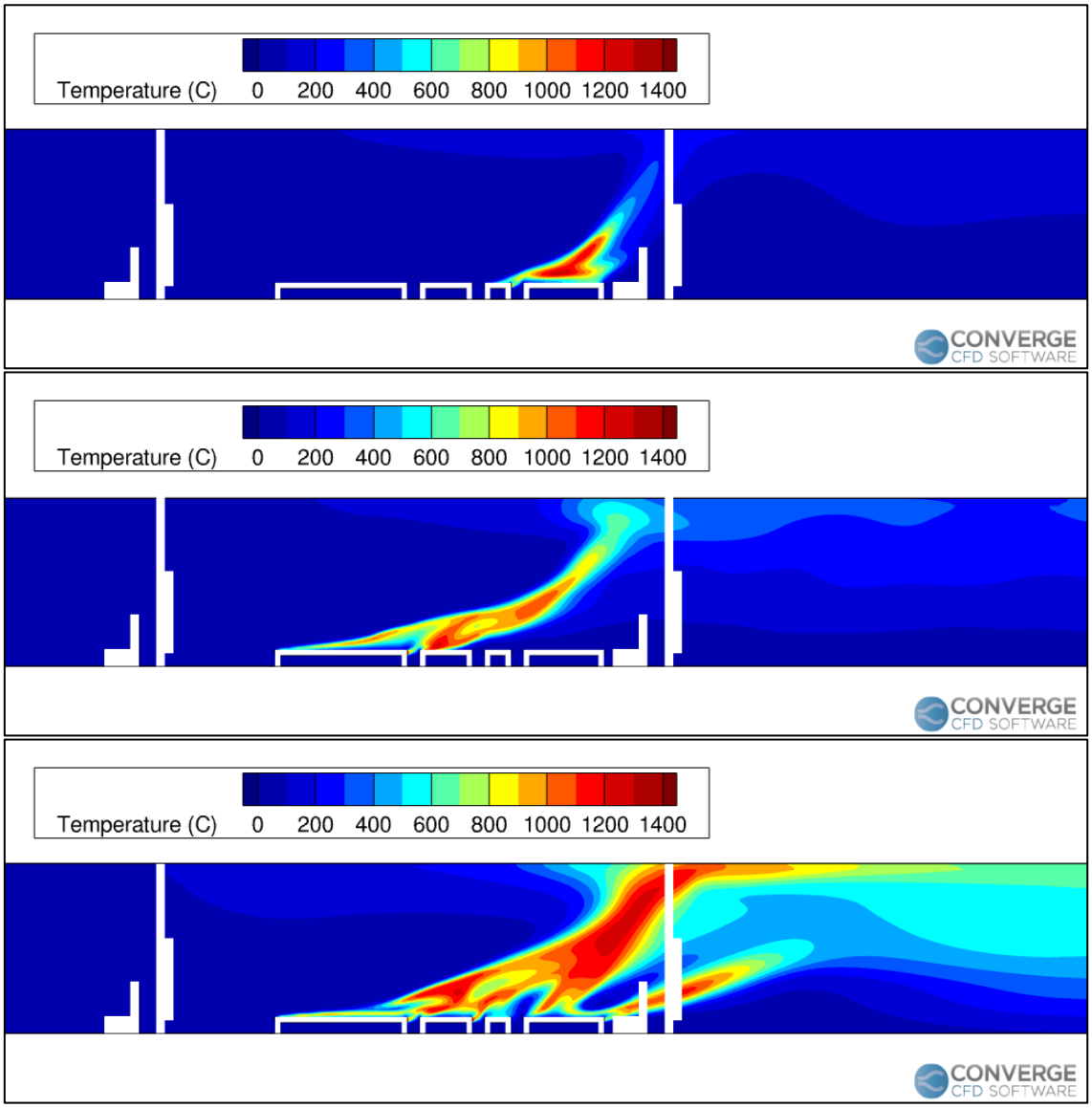

Figure 6: Centerline cut-plane visualizing the time-averaged temperature at the fire site for the 10 MW (upper), 50 MW (middle), and 100 MW (lower) fire intensities.

Likewise, Figures 9 – 12 show the vertical temperature profiles and bulk temperature distribution for the 10 and 100 MW cases. The 100 MW case shows trends very similar to the 50 MW case, where overall the temperature distribution is well represented, albeit an underprediction of the bulk temperature. The largest differences are found close to the fire here as well. Interestingly, the trend in the 10 MW case has shifted to instead slightly overpredict the bulk temperature. Again, the largest difference compared to the test data is in the direct vicinity of the fire. Note that the differences in the graphs are exaggerated due to the difference in scale of the temperature axis. We do, however, observe a better back layering length prediction, where small increases in temperature were observed at loops 305 and 306 in the test as well as in the simulation.

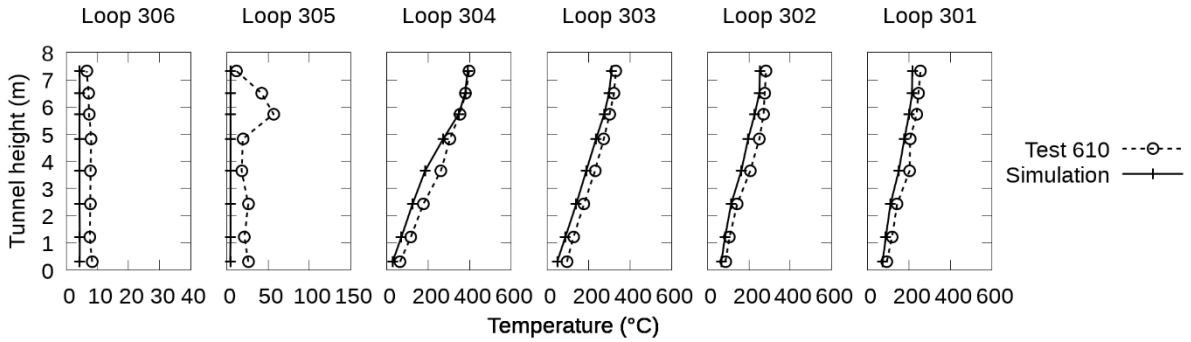

Figure 7: Comparison of vertical temperature profiles at the various measuring loops between simulation and test data for the 50 MW case.

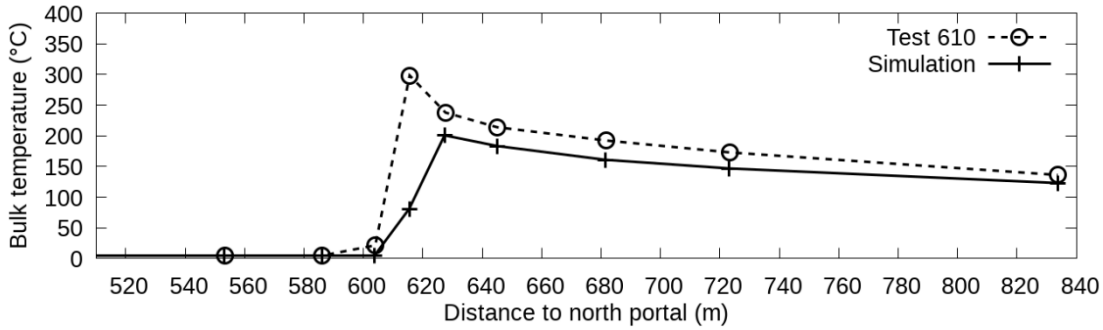

Figure 8: Comparison of the bulk temperature distribution throughout the tunnel for the 50 MW case.

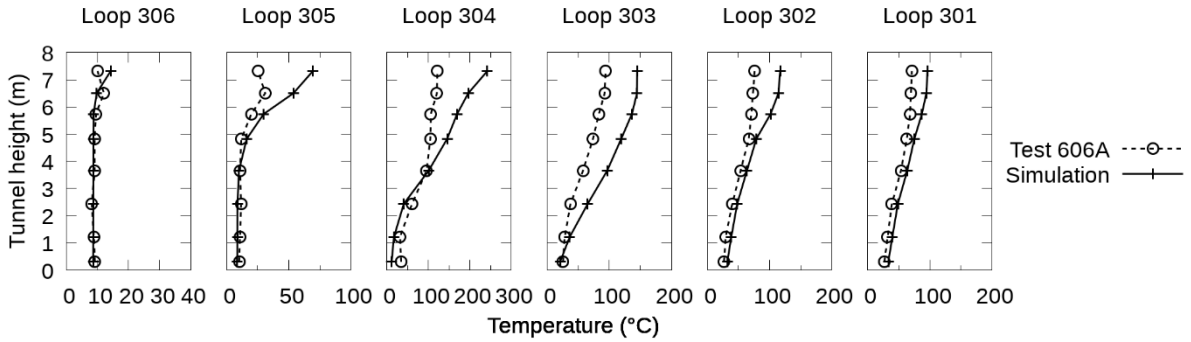

Figure 9: Comparison of vertical temperature profiles at the various measuring loops between simulation and test data for the 10 MW case.

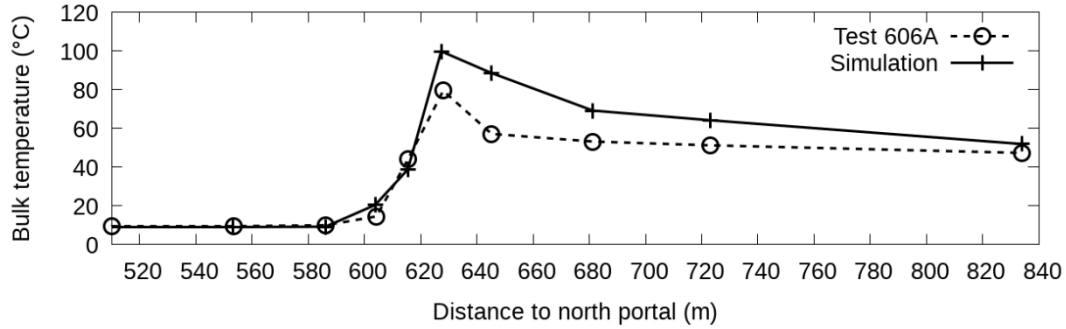

Figure 10: Comparison of the bulk temperature distribution throughout the tunnel for the 10 MW case.

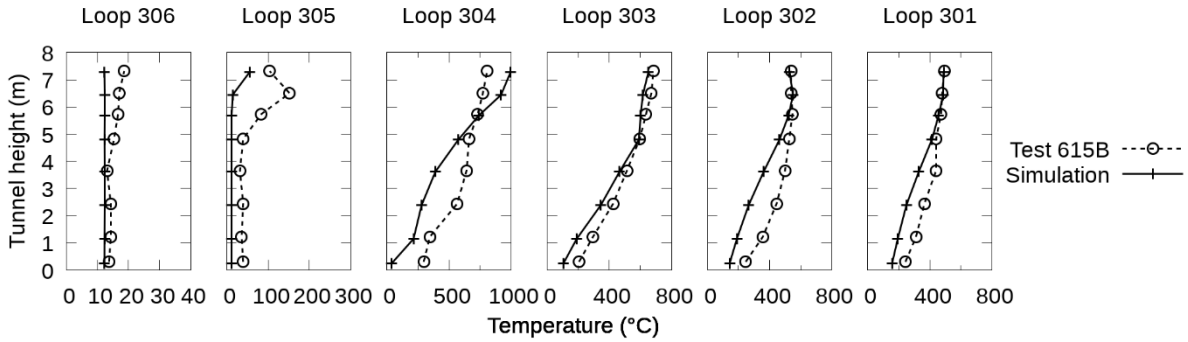

Figure 11: Comparison of vertical temperature profiles at the various measuring loops between simulation and test data for the 100 MW case.

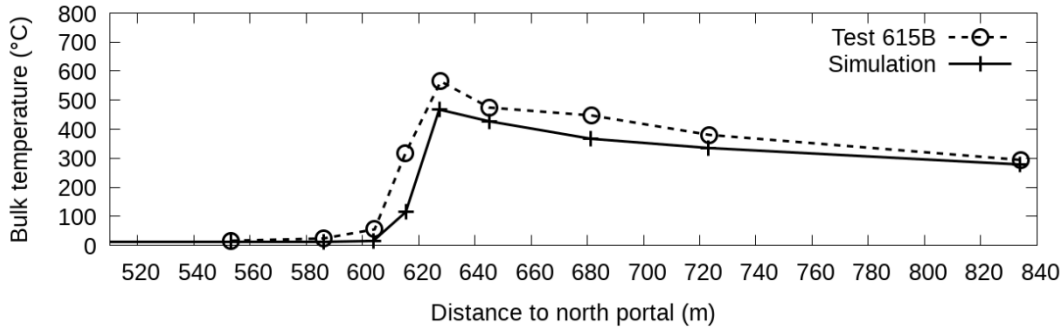

Figure 12: Comparison of the bulk temperature distribution throughout the tunnel for the 100 MW case.

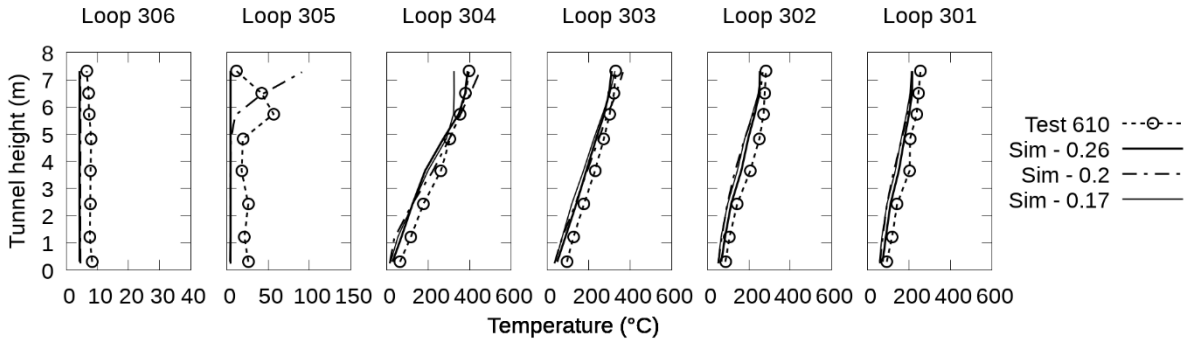

Figure 13: Comparison of vertical temperature profiles at the various measuring loops between simulation and test data for the various blockage ratios.

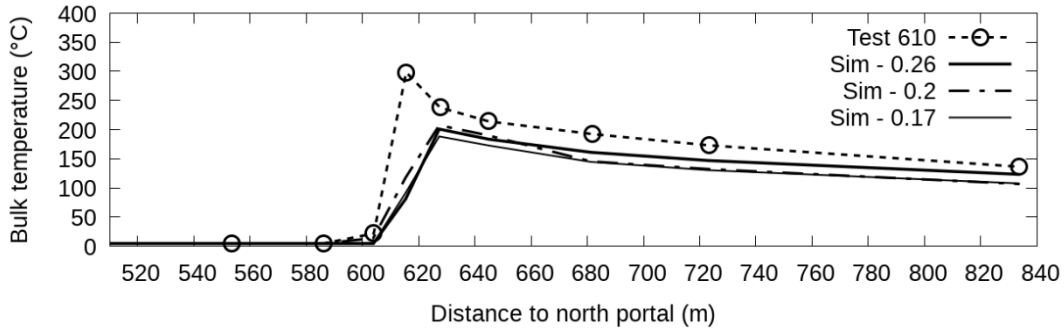

Figure 14: Comparison of the bulk temperature distribution throughout the tunnel for the various blockage ratios.

Figures 13 and 14 depict the results of the sensitivity analysis of the blockage ratio. Broadly speaking, the differences are quite small for the various blockage ratios. The one outlier is the 0.2 blockage ratio case, which predicts back layering at loop 305, whereas the others do not. The reason for that should be further investigated, but the changes to the shape of the obstructions influence not only the bulk behavior due to the changed blockage ratio, but also the local flow around the obstructions and, subsequently, the incoming flow to the fire.

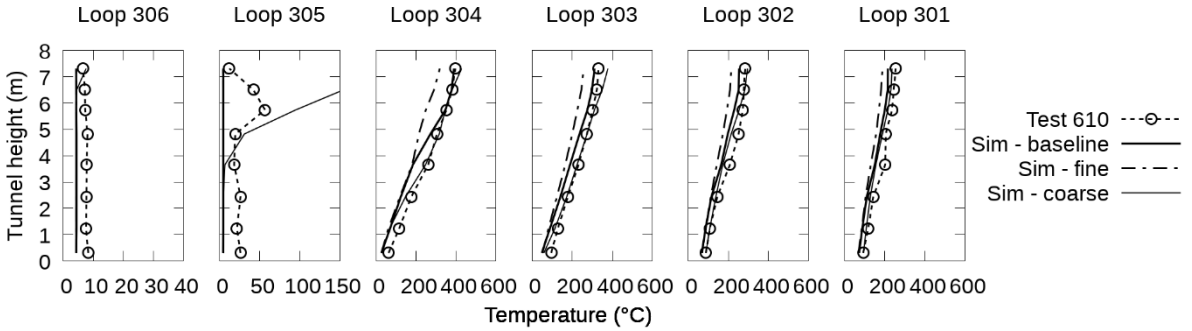

Figure 15: Comparison of vertical temperature profiles at the various measuring loops between simulation and test data for the various grid sizes.

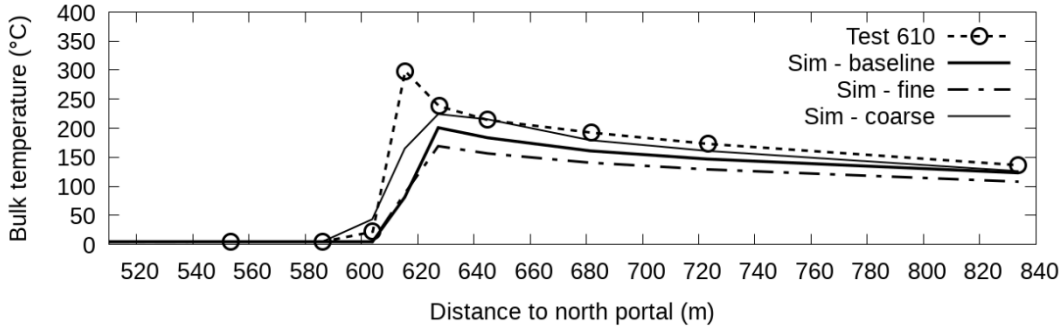

Figure 16: Comparison of the bulk temperature distribution throughout the tunnel for the various grid sizes.

Similarly, Figures 15 and 16 show the temperature profiles for the various grid sizes. Generally, we observe a difficulty in achieving grid convergence, which is not unusual for these types of simulations. Overall, the coarse mesh predicts the highest temperatures, whereas the fine mesh predicts the lowest. This could possibly be explained by less numerical viscosity being present as the grid is refined, which reduces the mixing of fuel and oxidizer, resulting in a slower combustion rate.

CONCLUSION

In this work, we have presented a CFD model to simulate fire scenarios in tunnels, to predict smoke propagation and evaluate ventilation strategies. The intent of the model is to serve as a useful engineering tool, which is achieved through the use of an autonomous meshing strategy with Adaptive Mesh Refinement to simplify the workflow and maintain a reasonable balance between computational cost and accuracy.

To evaluate the performance of the model, we compared temperature stratification, back layering, and bulk temperature distribution to the test data from the Memorial tunnel fire tests. More specifically, the results were compared to the time-averaged data presented by Beyer & Stacey [11]. The comparisons were carried out for three different fire intensities: 10, 50, and 100 MW. Furthermore, investigations into the sensitivity of the blockage ratio of the obstructions as well as grid size were performed.

Generally, the simulations showed a good agreement with the test data. Except for the 10 MW case, the results trended towards slightly underpredicting the bulk temperature as well as the back layering length. The 10 MW case trended in the opposite direction in this regard, although the differences were exaggerated due the overall lower temperatures. The variation of the blockage ratio showed only minor differences in the results, whereas the grid convergence study highlighted the difficulties of reaching grid convergence with these cases. A possible explanation for the observed behavior is that the induced differences to the numerical viscosity from altering the grid size, affect the fuel and oxidizer mixing rate, which directly influences the rate of combustion.

We believe that the model generally managed to predict the temperature distribution within the tunnel well for all fire intensities given the uncertainties in the geometry of the obstructions, the averaging of the test data, and the required simplifications to the physical models.

REFERENCES

1. He, Y., Jamieson, C., Jeary, A., & Wang, J. (2008). Effect of computation domain on simulation of small compartment fires. *Fire safety science*, *9*, 1365-1376.
2. Riess, I., & Steck, M. (2018). On the aerodynamics of water mist from a ventilation designer's perspective, 9. In *International Conference Tunnel Safety and Ventilation, Graz*.
3. Truchot, B., Leroy, G., & Marlair, G. (2016). CFD and engineering method coupling for evaluating the fire relative to battery transportation. In *8. International Conference on Tunnel Safety and Ventilation* (pp. 132-140).
4. Fleming, & C., Rhodes, N. (2018). A validation of the fire dynamics simulator for smoke dispersion from metro stations. In *International Conference Tunnel Safety and Ventilation, Graz*.
5. Sturm, P., Beyer, M., & Rafiei, M. (2017). On the problem of ventilation control in case of a tunnel fire event. *Case Studies in Fire Safety*, *7*, 36-43.
6. Khattri, S. K., Log, T., & Kraaijeveld, A. (2019). Tunnel fire dynamics as a function of longitudinal ventilation air oxygen content. *Sustainability*, *11*(1), 203.
7. Fruhwirt, D., Sturm, P., Bacher, M., & Schwingenschlögl, H. (2020). Smoke propagation in tunnels-comparison of in-situ measurements, simulation and literature. In *10th International Conference Tunnel Safety and Ventilation*.
8. Vångö, M., Scienza, P., Fößleitner, P., & Fruhwirt, D., (2022). Numerical Investigation of the Koralm Tunnel Fire Tests Using an Autonomous Meshing Approach with Adaptive Mesh Refinement. In Tunnel Safety and Ventilation, Graz, Austria.
9. Sturm, P., Rodler, J., Thaller, T., Fruhwirt, D., & Fößleitner, P. (2019). Hot smoke tests for smoke propagation investigations in long rail tunnels. Fire safety journal, 105, 196-203.
10. MTFVTP, "Memorial Tunnel Fire Ventilation Test Program - Comprehensive Test Report," Bechtel/Parsons Brinckerhoff, Boston, 1995a.
11. Beyer, M., & Stacey, C. (2022). CFD Validation for Tunnel Smoke Control Design. In *Proceedings of the Eleventh Tunnel Safety and Ventilation Conference*. Institute of Thermodynamics and Sustainable Propulsion Systems, Graz Technical University, Austria.
12. Chalasani, N. R., Greiner, M., & Suo-Anttila, A. (2012). Benchmarking of Container Analysis Fire Environment simulation using the memorial tunnel fire ventilation tests. *Journal of Fire Protection Engineering*, *22*(1), 45-70.
13. McGrattan, K., McDermott, R., Vanella, M., Mueller, E., Hostikka, S., Floyd, J., (2014). Fire dynamics simulator technical reference guide volume 3: validation. NIST special publication, 1018, 3.
14. Vega, M. G., Díaz, K. M. A., Oro, J. M. F., Tajadura, R. B., & Morros, C. S. (2008). Numerical 3D simulation of a longitudinal ventilation system: memorial tunnel case. *Tunnelling and Underground Space Technology*, *23*(5), 539-551.
15. Richards, K. J., Senecal, P. K., and Pomraning, E., CONVERGE 4.1, Convergent Science, Madison, WI (2024)
16. Richards, K. J., Senecal, P. K., and Pomraning, E., CONVERGE 4.1 Manual, Convergent Science, Madison, WI (2024)
17. Magnussen, B. F., & Hjertager, B. H. (1977). On mathematical modeling of turbulent combustion

with special emphasis on soot formation and combustion. In *Symposium (international) on Combustion* (Vol. 16, No. 1, pp. 719-729). Elsevier.
18. Karki, K. C., Patankar, S. V., Rosenbluth, E., & Levy, S. (2000, November). CFD model for jet fan ventilation systems. In *BHR group conference series publication* (Vol. 43, pp. 355-380). Bury St. Edmunds; Professional Engineering Publishing; 1998.
19. McGrattan, K., Hostikka, S., McDermott, R., Floyd, J., Weinschenk, C., & Overholt, K. (2013). Fire dynamics simulator user's guide. *NIST special publication*, *1019*(6), 1-339.

Examining tunnel safety features in sustainability-led design

Sigurjon Ingolfsson[1], Peter Woodburn[3], Sven Valdemar Sørensen[1], Fabiano Scarbi[1], Bryan Tamakloe[2], Simone Curletto[2]
[1]COWI Arup Joint Venture, [2]Metroselskabet
[3]Now Jacobs
Copenhagen, Denmark

ABSTRACT

Large construction projects contribute significantly to global carbon emissions and are as such increasingly scrutinised for their carbon footprints. This presents designers with the opportunity to critically review how all aspects of these projects are designed and delivered, including identifying alternative ways of designing for fire safety. In this paper, the authors have used Copenhagen's M5 metro line as a case study to showcase several tunnel fire safety features that have been significantly re-designed as part of sustainability-led design. Additionally, several other features have been highlighted as essential and irreplaceable, regardless of their carbon footprint.

The goal of this paper it to highlight how a discipline which is typically believed to have small contribution to the project's carbon footprint, such as fire safety engineering, can have a significant contribution to carbon reduction efforts, while at the same time sufficiently addressing fire safety objectives.

KEYWORDS:

Sustainability, carbon, tunnel fire safety, design fires, tunnel ventilation systems

INTRODUCTION

The M5 scheme is the fifth phase of the Copenhagen Metro and will significantly increase the city's metro network connectivity, serve new development areas, and provide additional links across the harbour.

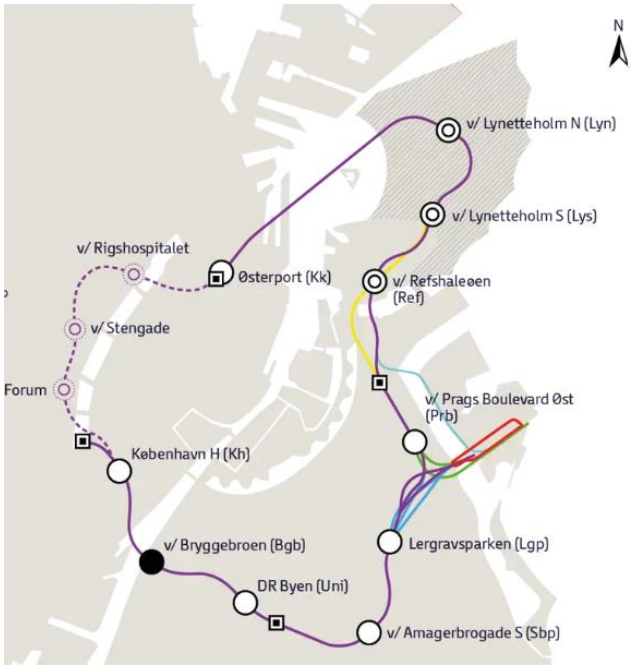

Figure 1: M5 scheme map

Metroselskabet (MS) have a target to reduce the carbon footprint associated with construction by 50% compared to metro lines constructed in Copenhagen previously. This is also aligned with the sustainability goals of Cowi Arup Joint Venture (CAJV) who are the civil works designers for the project. This scale of reduction in carbon footprint can only be achieved through a review of the function, form and benefits of each element within the system.

As a result, the design team has looked to challenge the provision of elements considered to be 'business as usual' and to truly understand the importance of each when applied to the M5 system specifically. This paper discusses specific studies undertaken by CAJV relating to systems for underground fire safety, the challenges faced and the benefits to the overall design that have been identified.

The focus of this paper is the carbon footprint of construction, rather than during operation as per the particular target set for the project, so the operational carbon footprint has generally not been quantified for the project or this paper. Nonetheless, none of the resulting changes to mechanical or electrical systems which were a consequence of this work resulted in an increase in capacity or energy usage.

REDUCING CARBON FOOTPRINT

Globally, construction currently accounts for around 37% of annual global carbon emissions according to data set out by the UN Environment Program [1]. The World Economic Forum [2] states that 50-60% of the carbon emissions from infrastructure are derived from the production of materials. The UNEP identifies that decarbonizing of the buildings and construction sector is critical to delivering on the UN climate change goals.

All construction projects should now consider the carbon impact of their activities, and 'business as usual' in terms of design is no longer appropriate if the world is to achieve its carbon-reduction aims. It is our view that this sustainability view should be applied to all systems, including safety systems, with the aim of eliminating low safety benefit / high carbon cost measures, and promoting low carbon cost / high safety benefit measures. As well as the measures themselves, reduced construction associated with safety systems can yield significant sustainability gains, such as reductions in the size

of underground plant rooms for ventilation plant.

Fortunately, our need to determine the effectiveness and benefits of safety systems is supported by improved analysis techniques which allow designers to understand the performance of all aspects of the design, the benefits they achieve, and the carbon cost of providing them. Computational Fluid Dynamics (CFD), Quantitative Risk Assessment (QRA), fire modelling of structures and similar techniques allow us to understand better than ever the performance of our designs in fires, and the effectiveness of the measures intended to support safety.

The carbon footprint of a rail system can be achieved through a number of routes, which include:

- Eliminating the need for construction of one or more elements
- Reduced use of materials by design, including reduced excavation and materials for smaller stations
- Use of more sustainable alternatives

The order above generally represents the scale of the carbon reduction which can be achieved by each route. All of the above should be considered, focusing on the most carbon-intensive elements of the system.

This paper now goes on to look at how the project objectives of reducing the carbon cost of the M5 system drove detailed analysis.

The measures subject to analysis included:

- Fire heat release rate and design fires
- Quantitative risk assessment for the replacement of intermediate shafts with cross-passages
- Tunnel ventilation system optimization

These yielded savings in carbon emissions through:

- Shallower stations requiring less excavation and concrete for construction.
- Elimination of a number of intermediate shafts
- Optimised tunnel ventilation systems

FIRE HEAT RELEASE RATE

Rolling stock design fires have typically considered a worst-case scenario, which was then applied to all fire scenarios for the design of the tunnel ventilation system. This has previously been identified as potentially overly onerous [3]. Train fires occur with a range of sizes, and larger fires are less frequent than smaller fires, as per fires generally within the built environment. Modern rolling stock designed to standards such as EN 45545 are resilient to fire spread beyond the initial ignition source, as demonstrated by recent e-bike fires in Madrid, Toronto and Barcelona. Progression of a fire to full flashover within a tunnel as envisaged by worst case scenarios is operationally very low likelihood [4]. Particularly for open-gangway trains as reported in [5] The analysis particularly considered the separation between groups of seats in the rolling stock proposed for M5.

To more closely examine the risks of rolling stock fires, a scenario-based approach which considers several fire sizes is proposed, in line with approaches adopted in some jurisdictions, including Australia [6]:

- Design fire scenarios
- High challenge fire scenarios
- Extreme events – Beyond design

It was identified that reducing the peak heat release rate (HRR) would have a significant impact on fan and plantroom sizes and therefore save capital cost and carbon. Adopting fire sizes which are informed by the risks involved enables the system to be designed accounting for credible scenarios in a manner appropriate for each, rather than all cases being dealt with by a worst of the worst scenario. This enabled stations to be made shallower.

Further, the physics of back-layering indicates that the pass/fail norms of tunnel ventilation design are overconservative as the consequences of minor failures are limited lengths of backlayering as demonstrated by Li et al [6]. In these cases, achieving confinement of smoke to a short backlayer can be acceptable where it can be shown that the risks to passengers and firefighters are not significantly increased.

The sustainability burden of increasing the capacity of the TVS to mitigate the risks of a limited length of backlayer occurring in limited scenarios may be considered in the selection of the fire scenarios.

The analysis particularly considered the separation between groups of seats in the rolling stock proposed for M5. Considering the layout of the passenger compartment in the rolling stock, the groups of seats and separation between them suggested a number of design fires. The gap between the seated areas is likely to slow if not prevent fire spreading down the train cars [8], as the only continuous fuel source is the ceiling, floors and walls. The space between the seats is 2.3 m within the car or 7.8 m to the seats in the next car.

- One group of seats and adjacent train fabric materials
- One carriage
- Two carriages

Figure 2 Seating layout in M5 rolling stock, showing separation between groups of seating.

The rolling stock has been designed to EN 45545-2 Hazard Level 2 [8] which imposes a Maximum Average Rate of Heat Emission (MARHE) requirement on the materials present in the train. The maximum permissible MAHRE values for HL2 were adopted for the analysis. Note that flooring materials are not required to meet a MAHRE maximum, but the design fires were then related to the size of ignition source responsible for the initial ignition (small-medium or large for the design, high-challenge & extreme fires respectively). Noting that (a) flooring materials are unlikely to become significantly involved in a fire which does not reach flashover [5], and that flashover involves full involvement of the materials within the space, the contribution of the flooring was not generally included.
Using MAHRE values, the design fires adopted for the three scenarios were:

Location	Factor	Design fire	High challenge fire	Extreme fire
Station	Fire HRR	3.7 MW t^2 medium growth rate	10 MW t^2 medium growth rate	20.1 MW t^2 medium growth rate
	Acceptance criteria	Tenability with margin for safety	Tenability without margin for safety	Mitigate and confirm outcomes
Tunnels	Fire HRR	3.7 MW t^2 medium growth rate	10 MW t^2 medium growth rate	20.1 MW t^2 medium growth rate
	Acceptance	Tenability with	Tenability without	Mitigate and

	criteria	margin for safety	margin for safety	confirm outcomes

Adopting fire sizes which are informed by the risks involved enables the systems to be designed accounting for credible scenarios in a manner appropriate for each, rather than all cases being dealt with by a worst of the worst scenario. This allowed the Over Track Exhaust to be removed from underground stations, with smoke control being achieved using a single point of extraction above the train, allowing the station depth to be reduced by 1m.

TUNNEL VENTILATION DESIGN APPROACH

The carbon cost of the tunnel ventilation system includes the carbon associated with:

- The tunnel ventilation system, including power supplies
- The underground space required to accommodate the TVS
- The operation of the system

Typically, TVS have been designed to achieve critical velocity for a conservatively large design fire, located at the worst location for the worst flow direction (down-grade). The worst location is generally a short extent of track (often near portals) which forms a very small percentage of the overall length of tunnels. In these sections the optimum response for the ventilation system is to allow smoke to vent uphill via the short distance to the portal, irrespective of the direction of travel. With fire frequencies in the tunnels as a whole of one per thousands of years, the likelihood of a train stopped with a fire on board and needing to vent smoke downhill in this section is vanishingly small.

Further, the physics of back-layering indicates that the pass/fail norms of tunnel ventilation design are overconservative as the consequences of minor failures are limited lengths of backlayering, rather than catastrophic filling of long sections of tunnel, impact on stations etc. This was demonstrated by Li et al [3], in which a longitudinal velocity of 95% of the critical velocity is associated with a backlayering length of approximately 1 tunnel height. This is not a catastrophic failure, and was considered alongside the safety margins in the design to optimise the TVS.

The sustainability burden of increasing the capacity of the TVS to mitigate the risks of a limited length of backlayer in an extremely low likelihood event can be considered in the selection of the fire scenarios.

The design scenarios considered included the following:

10 MW design fire [without additional margin]

Uphill venting of smoke on ramps adjacent to portals

Utilising these methodologies two clear gains were made in optimising the TVS:

Power requirements were able to be significantly optimised with a lower requirement for peak flow rates as estimated within Figure 3.

It was feasible to show that jet fans used for assistance within ramps/portals were not needed for the system to function effectively.

						Base Case	
Volumetric Flow (m3/s)	**50**	**60**	**70**	**80**	**90**	**100**	**110**
Power (kW)	30.8	53.2	84.4	126	179.4	246.2	327.6
% Power Req Change	-87%	-79%	-66%	-49%	-27%	-	+33%

Assumed system efficiency: 65%

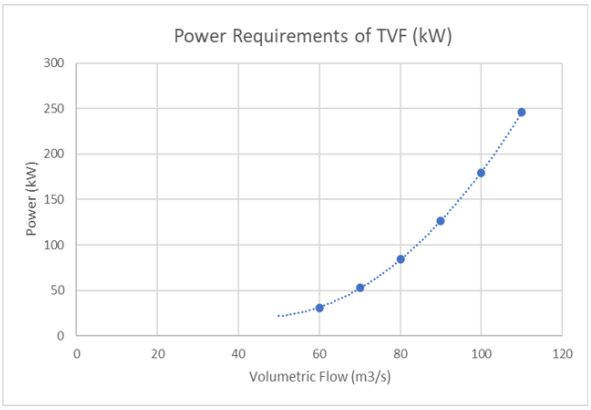

Figure 3: Estimated power requirement reduction based on required flow rates

SHALLOW STATIONS

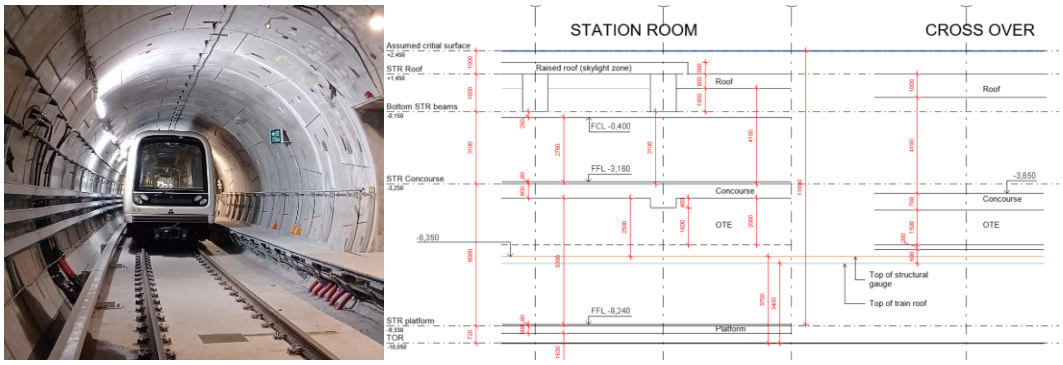

Figure 4 – Illustration of drivers for station & tunnel depth

The fire strategy for the stations is that tenable conditions must be maintained during evacuation of a train on fire which is located at a station. A smoke control system (in the form of over-track exhaust (OTE)) is to be provided at all stations of M5 project within the concept design, designed to minimise smoke spread from a train on fire at the station platform into the station.

The principles of the credible worst case train fire scenario are illustrated in Figure 5 and the location & indicative size of the OTE are shown in Figure 6.

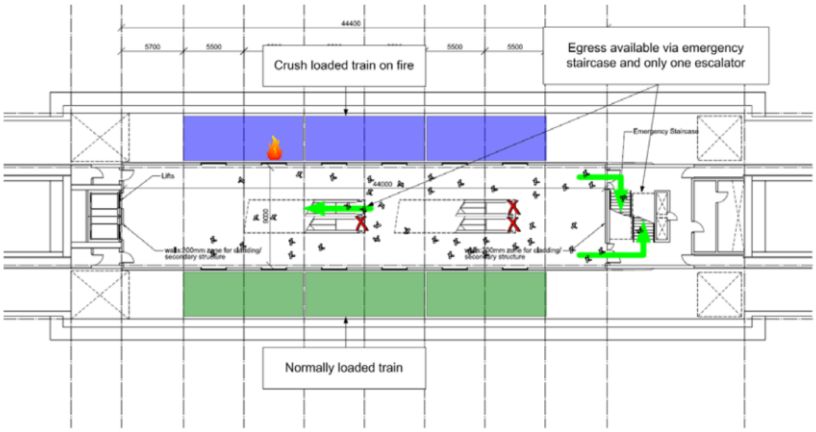

Figure 5 – Train fire scenario – platform level

Figure 6 – OTE indicative location 3D view and a typical Cityringen station track view

A typical, known within Copenhagen, approach to OTE is to implement it as an approximately 2-3 m deep, smoke exhaust duct that contains extraction points in multiple locations for each track on the stations. This enables the exhaust of smoke to be regulated with a more uniform extract airflow along the train and mitigates the risk of 'plug holing' and localised deepening of the smoke layer in any area.

This approach was adopted for below ground stations on Copenhagen Metro's lines M1-M4, with the performance verified using CFD.

However, the overall volume of the stations could be reduced by moving the platform levels upwards closer to ground level. This is not just good for carbon reduction (as the construction of the station requires less excavation, and reduced concrete in the station structures), but it also means there is a shorter distance from surface to platform which provides an improved passenger experience. However, with a reduced depth comes a design challenge for the whole design team where the required equipment and structural support has to be provided within a shallower depth and be readily maintainable, safe and reliable for the ultimate operator.

In terms of safety, elements which significantly influence the depth of the stations include:

Overtrack exhaust within stations and tunnel crossovers
Size and number of tunnel ventilation fans
Accommodation for M&E equipment supporting smoke control, including power systems.

Methodology and analysis

As part of the OTE and tunnel ventilation system (TVS) review, there are 3 major aspects which were investigated:

1. Can the OTE have a single exhaust point per track rather than multiple exhaust points?
2. Is a smoke exhaust duct required or can the smoke layer be contained by a combined arrangement of platform screen doors and downstands?
3. Can we reduce the depth required for the smoke layer/OTE which might allow rail level to be raised?

Through CFD analysis the design was evaluated and verified that a single exhaust point without a specific extract point was shown to be effective at a 1.5 m deep smoke reservoir (a reduction of about 1.5 m from the existing design).

This was particularly driven by two main factors:

- The detailed heat release rate studies undertaken as part of the project enabled a more nuanced view on the required exhaust capabilities.
- The relatively short full train length of the CPH metro (~45 m) makes a single exhaust point more readily viable than in other systems where the train lengths are greater.

QUANTITATIVE RISK MODEL

Tunnel firefighting provisions were reviewed through the lens of a quantitative risk model (described in a separate paper at this conference [10]). The primary purpose of this exercise was to understand the overall benefits of particular safety measures when applied to the M5 scheme, to identify those measures with high benefits, and those with low benefits and high sustainability cost: The principal outcomes from this analysis were:

- Intervention shafts when compared with cross passages. The analysis demonstrated that replacing shafts with cross-passages was associated with a negligible reduction in passenger safety.
- Passenger decision-making. The consequences of an incident were strongly dependent on the number of passengers who might evacuate in the wrong (downstream) direction. The importance of signage and PA announcements which give passengers clear instructions which way to move was identified and will be developed in later stages of the project
- Resilience of rolling stock. The risk model highlighted that the resilience of rolling stock to being disabled by a fire was an important contributor to passenger safety. This was not surprising – measures to improve the rolling stock fire resilience to avoid the train becoming stranded in the tunnel with a fire on board have been identified previously as cost-effective compared to measures to mitigate the effects of the train on fire in the tunnel. [11]
- Ventilation system reliability. The model highlighted the benefits to passenger safety of a more reliable ventilation system to provide a tenable route for egress over the period of evacuation.

The removal of one of the shafts originally in the scheme and replacement with a cross-passage resulted in a saving of 3.4 k tonnes of CO_2e. There were other significant benefits to the neighbourhood and city through reduced construction impacts including temporary loss of facilities, noise, lorry movements, and similar.

A total of four shafts which would have been required for M5 by the M3 fire strategy were removed from the scheme, replaced by cross-passages. Therefore, the overall net saving in carbon from undertaking this exercise was significant.

FIRE SAFETY MEASURES RETAINED

A number of other fire safety systems were also considered, as requiring considerable carbon cost to provide. However, following investigation these were decided to be retained as summarised in Table 5

Table 5 – Fire safety measures investigated and retained

Item	Reason for investigation	Summary of findings
Elevated side walkways	Elevated side walkways require an increase in tunnel diameter to accommodate	Elevated side walkways were retained primarily to enable the fire brigade to utilise fire-fighting trolleys within the tunnels without clashing with occupants egressing at the rail level. In short, an egress strategy without elevated side walkways was incompatible with the

Item	Reason for investigation	Summary of findings
		intended fire-fighting strategy.
Tunnel ventilation fan redundancy	In existing designs, 2 TVS fans are provided at each station	Due to maintenance, design simplicity and system reliability needs, which were highlighted by the QRA study, two fans were retained in each station.
OTE duct within crossovers	Having optimized the station OTE, the crossovers adjacent to the stations became the limiting factor on station depth due to the need to install OTE ductwork within the crossovers.	Due to the need to maintain a clear layer height for occupant egress and the ability of the TVS system to ventilate the tunnels effectively, a single point extract was analysed using CFD and did not provide the required tenability within the crossover section.

OVERALL OPTIMISATION OF THE DESIGN

The optimisations set out above were integrated into the overall design optimisation including structures, MEP and architecture to generate the following updates to the design of M5:

Stations depth generally reduced by 1m

4 Shafts replaced by cross-passages

Optimisation of the tunnel ventilation system

This has contributed to currently approximately 36% saving in carbon in construction over the project as a whole with further reductions expected as the design progresses.

At this point in the scheme design, the project is on track to achieve its 50% carbon footprint target.

CONCLUSIONS

To meet the ambitious aims of the M5 project to reduce the emitted carbon of the construction by 50% compared to previous lines, it has been necessary for all disciplines to consider whether it is possible to maintain the required performance of their systems, whilst reducing the emitted carbon required to construct them. By adopting a sustainability-driven design process, the Fire Life Safety team were able to identify a number of design optimisations which have significant carbon reduction benefits while not impacting upon the safe operation of the system.

These optimisations were achieved using more detailed analysis techniques including CFD and QRA in a scenario and risk-based analysis to quantify the benefits and costs of elements, and to optimise the design to reduce areas of over-conservatism.

Following review of the fire load on the rolling stock, a single worst-case design fire was replaced by three design fires representing different ignition scenarios to better represent the range of fire scenarios expected. The tunnel ventilation system was optimised based on the range of design fires, as well as using a risk-based approach to reduce the conservatisms associated with some low-likelihood scenarios. These optimisations allowed significant reduction in the depths of stations. QRA was used to support replacement of four intermediate shafts by cross-passages, resulting in savings in emitted carbon, but also reduced impacts on the city during construction and operation.

Overall carbon savings of 36% have been achieved to date for the project as whole, without an increase in the risks to passengers or staff.

REFERENCES

1. United Nations Environment Programme, & Yale Center for Ecosystems + Architecture (2023). Building Materials and the Climate: Constructing a New Future. https://wedocs.unep.org/20.500.11822/43293.
2. World Economic Forum 'Scaling Low-Carbon Design and Construction with Concrete: Enabling the Path to Net-Zero for Buildings and Infrastructure', WHITE PAPER MARCH 2023
3. Stacy C, Agnew N – 'Recommendations from the METRO project – Don't Panic!'. ISTSS, March 2014.
4. Johnson, P., Woodburn, P., Henderson, L., 'Evacuation of Modern Rail Tunnels – Emergency Ventilation and Large Fires or Not? ISTSS, Montreal, Canada, March 2016.
5. Ting Y.S, Eckford D.C, Dinsdale-Young O.R, Liang H., Bowman I.N., Crossrail Fire Safety Designs, Sixth International Conference 'Tunnel Safety and Ventilation' 2012, Graz
6. AS 4825 Tunnel Fire Safety 2011
7. Li, Y., Z., Lei, B., Ingason, H 'Study of critical velocity and backlayering length in longitudinally ventilated tunnel fires', Fire Safety Journal 45 p 361-370, 2010.
8. Chiam, B.H, Numberical Simulation of a Metro Train Fire, Masters Thesis, University of Canterbury, 2005
9. EN 45545-2 – Railway applications – fire protection on railway vehicles - Requirements for fire behaviour of materials and components.
10. Ingolfsson, S., Woodburn, P., Moller Paulsen, F., Turrnbull, R., , Use of a Risk Model to Evaluate Tunnel Safety Features' ISTSS, Reykjavik, Iceland 2025,.
11. A. Ross and P. Woodburn, "Copenhagen Metro - Alternative Strategies for Tunnel Ventilation," 2022

Implications of Peak Heat Release Rate to Optimize Metro Tunnel Ventilation Systems

Robert Till PE PHD, John Jay College of Criminal Justice (CUNY), New York, USA
E-mail: rtill@jjay.cuny.edu
Argun Bagis CPE, Arup, Australia
Bruce Dandie CPE, RRT Pty Ltd, Australia

ABSTRACT

Underground rail system designers often develop fire scenarios for tunnel and underground stations using the same size design fire sizes for both incidents. The requirements of a train fire event generally determine the tunnel ventilation system design capacity for new metro tunnel designs, particularly for shorter tunnels where tunnel temperature control (during scheduled or unscheduled train operation) is not the dominant constraint. Usually, these fires are based on a fire's peak heat release rate (HRR) involving the contents of the passenger compartment of a typical metro rail car in the system or from a full conflagration of a metro car. An under-car fire is the most likely fire scenario that will force a train experiencing a fire incident to stop in a tunnel. Under-car fires only involve burning equipment below the rail car floor, and they generally have a significantly lower HRR than passenger compartment fires. This paper reviews the implications of this disparity and the effects on the holistic system emergency egress and ventilation design.

KEYWORD: Tunnel Ventilation, Design Fire Optimization, Emergency Fan Plant Operation, Metro, Subway

INTRODUCTION

In the event of a fire in an underground metro system, passengers must be evacuated from the fire zone as soon as practicable. In a rail car fire in a station, passengers can evacuate directly to a platform and out of the station. This can usually be done without direct operator or emergency services assistance to passengers, and the time required is in the order of minutes. Supporting this, the NFPA 130 Standard base requirement is that the egress capacity of a station allows passengers to evacuate the platform in four minutes and be in an area of safety in six minutes. Passenger safety during this time is generally evaluated using a CFD model that establishes the effectiveness of any smoke control available in the station, using an established fire size and duration for the design of the metro car. Smoke control systems in stations are generally designed to manage the smoke flow and density by removing smoke from the environment in sufficient quantities to keep the smoke above the heads of evacuating passengers during station egress.

However, in the event of a rail car fire inside a tunnel, the evacuation of passengers from the dangers of smoke and fire becomes more complex. Passengers generally require rail or emergency personnel assistance to egress from trains through the tunnel system. In this case, passengers must leave a familiar location and enter an unfamiliar environment containing an unknown exit route to safety. Most passengers have never encountered this scenario, which adds complexity and confusion. Passengers will likely be forced to wait in a smoky environment until 3rd rail power is cut for the process to begin.

Should a train stop inside the tunnel, coordinating the required assistance takes some time, allowing

the fire to grow. Tunnel smoke control systems in tunnels usually use Push-Pull ventilation systems for both general tunnel ventilation and emergency ventilation. Fire events are generally the dominant design criterion; therefore, the system capacity is based on the critical velocity of the design fire event. As they are push-pull systems, they do not provide tenable air for passengers in the tunnel downstream of a fire and do not provide any protection for passengers in the event of a fire in the passenger compartment. Consequently, if the coordination time is lengthy, passengers may accidentally evacuate into an area of the tunnel that will ultimately be filled with smoke due to the operation of the tunnel ventilation system.

The procedures for evacuating a train in a tunnel recognize these limitations. The prime goal of all modern metro systems when a train is on fire is to get the train to the nearest station. Evacuation from a station can occur rapidly as all doors are accessed, and the passengers are in a known environment and do not become disoriented.

Designers of tunnel ventilation systems do not appear to recognize the benefits of this mismatch. This paper discusses the benefits of recognizing that rail tunnels and their design should operate holistically.

SIGNIFICANT METRO FIRES IN RAIL TUNNELS

BART – San Francisco – 1979

The Bay Area Rapid Transit (BART) Transbay Tube fire in San Francisco occurred on January 17, 1979. An electrical malfunction ignited a fire beneath a BART train traveling through the Transbay Tube, a 3.6-mile underwater tunnel connecting San Francisco and Oakland. The fire started beneath a train carrying approximately 1,000 passengers, producing dense smoke that rapidly filled the tunnel and train cars.

The train's location within the tunnel and the use of tunnel vent fans significantly impacted the evacuation process. The train's location complicated evacuation efforts because the incident occurred about halfway through the Transbay Tube. The tunnel’s length and underwater location limited access for emergency responders. Passengers had to be evacuated on foot through the smoke-filled tunnel, which extended evacuation times and increased exposure to hazardous conditions.

Early BART rail cars, such as the ones involved in this incident, were not fire-hardened as there were no requirements at the time. It has been documented that “Both the roof and floor were made of outer and inner 0.60-inch aluminum sheets separated at intervals by structural reinforcement. The void between the aluminum sheets was filled with a 2-inch core of polyurethane foam for rigidity and insulation.” (Bay Area Rapid Transit District Fire On Train No.117 And Evacuation Of Passengers While In The Transbay Tube, 1979) This resulted in a combustible design that has since been prohibited. As stated previously, typical requirements for modern car floors specify that they pass a test that measures their ability to withstand exposure to fire for a specified period. NFPA 130 requires that floors withstand fire until the entire vehicle is evacuated.

The combustibility of plastics and the volume of toxic smoke they can produce were not as well understood as they are today. Although the BART system was equipped with ventilation systems designed to clear smoke, the sheer volume of smoke and the confined space within the tube hindered their operation. The fans were eventually turned on, but the delay in venting allowed smoke to accumulate, further complicating the evacuation and increasing the risk for passengers and rescuers.

Clark St., New York City – 1990

The Clark Street subway fire in New York City occurred on June 5, 1990, within the Clark Street Tunnel, part of the Number 2 and 3 train lines. Large volumes of smoke were produced due to an overheated cable beneath a train in the tunnel, filling the subway cars and tunnel with smoke. This incident became a critical example of subway system emergency response and evacuation strategies. Hundreds of passengers were trapped within smoke-filled subway cars, leading to a challenging and

prolonged evacuation process. The train's location within the tunnel significantly influenced the evacuation. The fire occurred mid-tunnel, restricting the number of access points for firefighters and emergency responders to reach the train and assist passengers. The position also limited the exit routes for passengers, with many forced to evacuate on foot along the narrow subway tracks.

In summary, the train's mid-tunnel position and the delayed response of the tunnel vent fans were significant factors in the time and difficulty of passenger evacuation during the Clark Street fire. This incident underscored the need for efficient smoke control systems and streamlined evacuation procedures, especially in tunnel environments with limited access points and smoke management. It should be noted that the need to improve the capacity of the smoke control system so it could handle this cable fire was not in question, only its operation.

Baku Metro Fire – Azerbaijan 1995

The Baku Metro fire in Azerbaijan, then part of the Soviet Union, occurred on October 28, 1995, and remains one of the deadliest subway disasters. The fire broke out on an overcrowded metro train traveling between the Ulduz and Nariman Narimanov stations. The blaze, believed to have started in a traction motor (Baku Metro fire, 337 Killed, n.d.), spread rapidly through the train, filling both cars and the tunnel with thick, toxic smoke. Tragically, the fire resulted in the deaths of 289 people and injured over 270 others, with many victims succumbing to smoke inhalation.

The train's location within the tunnel severely impacted the outcome of the fire. Caught mid-tunnel, it was positioned at a considerable distance from either station, complicating evacuation efforts. The tunnel's confined structure exacerbated the smoke accumulation, creating low visibility and hazardous breathing conditions. Due to the distance from station exits and the lack of adequate emergency evacuation routes, many passengers were forced to attempt an escape on foot along the tracks, making them vulnerable to toxic smoke.

The construction of the cars was again one of the critical factors in the production of smoke and the spread of this fire through the floor of the train cars to the passenger compartments. "The coaches were of Russian E-type with chassis of steel, strengthened glass windows and doors of aluminum. The floor material was partly wood with a surface of linoleum, foam seats, and laminated plastic as surface on walls and roof. The coaches had approximately 1500 kg of combustible material, which is approximately three times as much as modern coaches." (Kumm, 2011) The pneumatic doors also played a significant role in this fire. Modern rail cars are not constructed this way.

The limited ventilation within the tunnel also played a critical role in the disaster. Although the Baku Metro was equipped with vent fans, they were inadequate in clearing the smoke rapidly enough to facilitate a safe evacuation. This disaster highlighted the potential risks of inadequate tunnel evacuation strategies and the need for modern metro car construction.

It is worth noting that all these fires occurred without the benefit of modern smoke management system design or modern rolling stock.

CHARACTERISTICS OF METRO (SUBWAY) SYSTEMS AND ROLLING STOCK

The characteristics of Metro/Subway systems make them a distinct subset of all passenger rail systems. This distinction influences the scenarios that may endanger passengers.

Subway systems are generally fully electrified and do not share tracks with freight systems, so a collision with diesel-driven freight trains is improbable or even impossible. In general, heavy goods are not transported on these trains. They also don't generally have crossings, so interaction with heavy goods vehicles and large quantities of flammable goods such as gasoline is also improbable.

Many parameters could affect the development of a fire in a train carriage. These include the body material (steel, aluminum, etc.), the quality and material of the windows, the geometry of openings,

the amount and type of combustible interiors along with their initial moisture content, the construction of wagon joints, the air velocity within the tunnel, and the geometry of the tunnel cross-section. All these parameters should be considered in the design process of a rail or metro tunnel.
Modern subway systems generally have relatively spartan rail car interiors and minimize the use of materials that may result in severe, rapidly growing fires both inside the passenger compartment and beneath the rail cars. The short distance between stops, with passengers entering and leaving these trains very frequently, means that the durability of the interior and its finishes are essential. Many systems use hard seating versus the cushioned seating that is seen on inter-city commuter lines. All modern rail cars usually comply with fire tests specified in standards such as NFPA 130. This may not be the case for cars that predate modern standards.

Typical requirements for modern car floors include passing a test that measures their ability to withstand exposure to fire for a specified period. NFPA 130 requires that floors withstand fire until the entire vehicle is evacuated.

Fire Tests
Testing modern metro cars to determine an accurate HRR is generally considered financially prohibitive. Consequently, modern fire-hardened trains have not undergone thorough full-scale testing. Research has focused on older train models, where the extent of fire hardening is not well defined. Initiating fires to ignite even these older, unhardened subway cars often involved very large, sustained heat sources, considering the typical ignition sources found on a subway and has been purposefully placed in the worst-case scenario for combustion.

However, when the cost of such a test is compared to the potential increase in the cost of mining in a particular system, such a test could be valuable. Determining an energy source with a realistic potential to ignite a fire in a modern rail car could increase confidence in passenger safety.

The EUREKA 499 – FIRETUN project, conducted between 1990 and 1992, was a comprehensive series of full-scale fire tests in tunnels, aiming to investigate fire behavior in various vehicles, including passenger cars, train wagons, subway cars, and heavy goods vehicle (HGV) trailers. The tests were primarily conducted in the disused Repparfjord Tunnel in Norway. A metro train car that was tested measured 18 m in length, 2.8 m in width, and 3 m in height, and it was made of aluminum. It had a total of 40 seats, which were made from polyurethane foam and covered with textiles. The total fire load for the seats was calculated to be 6000 MJ, while the total fire load for the metro train car was determined to be 41300 MJ. The heat release rate (HRR) reached 35 MW during the experiment in about five minutes.

The METRO project, initiated by Stockholm Public Transport (Storstockholms Lokaltrafik or SL), was an extensive research project to improve fire safety and emergency management strategies within underground transportation systems. The project was conducted primarily from 2009 to 2012. It involved comprehensive full-scale fire tests, including controlled burning of real train carriages, to closely examine how fires develop and spread in underground metro environments. Retired X1 commuter trains, provided by Stockholm Public Transport for the METRO project, were tested. Built between 1967 and 1975, each train included a motor carriage and a control carriage. Only the control carriage, about 24 meters long, was used in the fire tests, featuring a driver's compartment and a 21.7-meter passenger area. With a width of 3 meters and a height of 2.32 meters at the center and 2.06 meters at the walls, the carriage had a ceiling approximately 1.1 meters wide. It included six double doors (three on each side), 22 double seats, and 18 triple seats, accommodating up to 98 passengers. Three fire tests were conducted in commuter train carriages within a tunnel. In the first test, original seats and linings ignited, achieving a maximum heat release rate (HRR) of 76.7 MW at 12.7 minutes post-ignition.

In contrast, the refurbished carriage with modern, non-combustible materials reached an HRR of approximately 77.4 MW after nearly 118 minutes. Although both tests recorded similar maximum HRR values, the time to achieve these rates varied significantly due to the combustible materials in

the original carriage. In the third test, the highest gas temperature near the tunnel ceiling was used for HRR calculations, determining about 75 MW. This underscores the importance of lining materials, as high-performance options can provide extended evacuation times.

Both fire tests discussed here reinforce the importance of material selection in the construction of railcars and justify the increased regulation of materials used in codes and standards. (Lönnermark, et al., 2012)

Undercar Fires Used for Floor Testing

Kapahi et al. explored the calibration of scaled fire tests with fire modeling to determine the performance of metro car floors in the event of an undercar fire (Kapahi, et al., 2018). To develop typical fires, they attempted to obtain data on undercar fire incidents in Intra-City vehicles and found data was difficult to obtain because these fires are uncommon. They ultimately chose to explore three design fires: a trash fire, a gasoline fire, and a diesel fuel fire. Trash fires are relatively common in some systems, which is why this fire was introduced. However, they are usually 400 kW or less (Kapahi, et al., 2018) and do not pose a significant subway car hazard. The other two fires are more substantial but unlikely for most metro systems, as they are isolated from freight and road systems.

Design Fire/Under Car Fire Heat Release Rates

Liu et al. summarize Metro/Subway car design fires for systems from many cities and countries (Liu, Cassady, Casey, Zlatanic, & Munfah, 2014). These fires range from 5 – 15 MW for individual cars, with higher heat release rates for systems that assume multiple cars are alight simultaneously. Kennedy et al. (Kennedy, Ray, & Quinan, 1998) include a table providing a breakdown of the mass of combustible material for a typical car in the areas above the floor, the floor itself, and below the floor. For this typical car, on a percentage basis, 45% of the combustible mass was above the floor, the floor itself contained 17%, and below the floor was 38 percent of the combustible mass. Using these figures to provide a sense of proportion of the heat release rate below the car, the range would be 2 – 6 MW.

TYPICAL TUNNEL VENTILATION SYSTEM DESIGN

The selected design fire has significant implications for the cost of subway systems. The NYU Marron School of Urban Management has published a recent study (Goldwyn, Levy, Ensari, & Chitti, 2024) criticizing the overall cost of deep subway projects, particularly the cost of ventilation systems. This study states that mining one cubic meter of material can cost over 5000 USD per cubic meter. Where the capacity of the tunnel ventilation system is determined by a train fire event that occurs in the tunnel sections between stations, calculations determining the required tunnel ventilation capacity include allowances for tunnel cross-sectional diameter, tunnel gradient, design heat release rate, and fire growth rate.

Once the tunnel ventilation system capacity is determined by the design fire size, system operations to satisfy the tunnel ventilation system's other functions are generally configured within this defining parameter. Fan capacities for emergency operation are determined based on achieving a minimum air velocity within the train annular area sufficient to stop backlayering of smoke. This minimum velocity is called the critical velocity and is a direct function of the design fire size and tunnel grade. The smaller the design fire size, the lower the airflow required to achieve critical velocity. The airflow volume necessary to maintain critical velocity in the tunnel generally differs from that needed for extracting smoke overhead in the station. The fan sizing will depend on both scenarios, but the most likely driver of fan size will be the maintenance of critical velocity for a given fire in the subway tunnel.

Due to the improved time it takes to evacuate people from a train, the preferred mode of operation is for the train to proceed to the next station. So, even if a train is stopped in the tunnel because the drive system is incapacitated by fire, a lower heat release rate would be adequate as a design fire size. In contrast, the size of the fire at a station would be designed for full conflagration. As obtaining critical

velocity in the tunnel is the driving (Li & Ingason, 2016) characteristic in most designs, the smaller design fire for the tunnel could result in cost savings.

Using 3-dimensional CFD analysis, instead of the critical velocity formula in NFPA 130/502, the critical velocity for a typical metro train with a design fire size of 15 MW (on the high end of the range determined previously) is approximately 2.6 m/s based on a 3% grade (this can also be seen in Figure 1 below [5]). This velocity is applied within the annular area between the train and the surrounding tunnel. The graphic (Hong & Fu, 2022) below presents the relationship between critical velocity and design fire size.

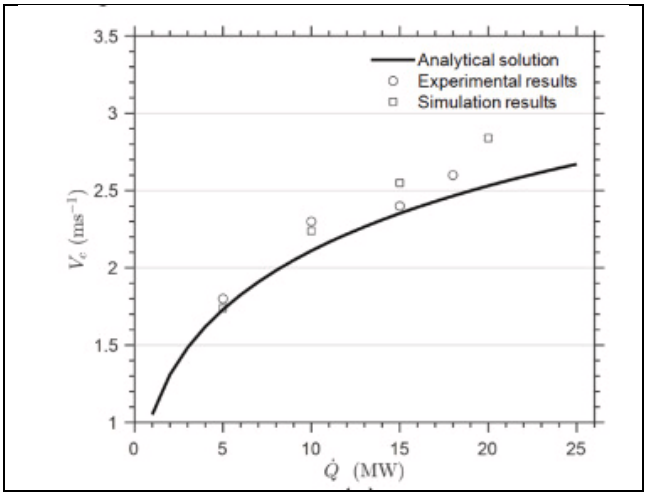

Figure 1- Smoke Condition with and Without Fan Operation

The graphic shows that reducing the design fire size below 15 MW significantly reduces the critical velocity needed to prevent smoke backlayering. For example, a reduced design fire size of 5 MW results in a lower critical velocity of approximately 1.8 m/s, with a corresponding lower airflow rate across the annular area to achieve this velocity.

The reduced critical velocity and associated flow rate corresponding to a reduction in the fan plant room footprint and associated ancillary systems, such as dampers, attenuators, electrical and cabling systems, primary and secondary structures, and a substantial reduction in motor power requirements, access provisions, and maintenance requirements.

The implications for the tunnel ventilation system plant sizing at the stations are equally dramatic. This can be demonstrated using a representative plant room layout, as in Figure 2 below. The figure reflects the reduction in plant room size that could be achievable should the design fire size be reduced from 15 MW to 5 MW, corresponding to an annular critical velocity of approximately 2.6 m/s and 1.8 m/s, respectively.

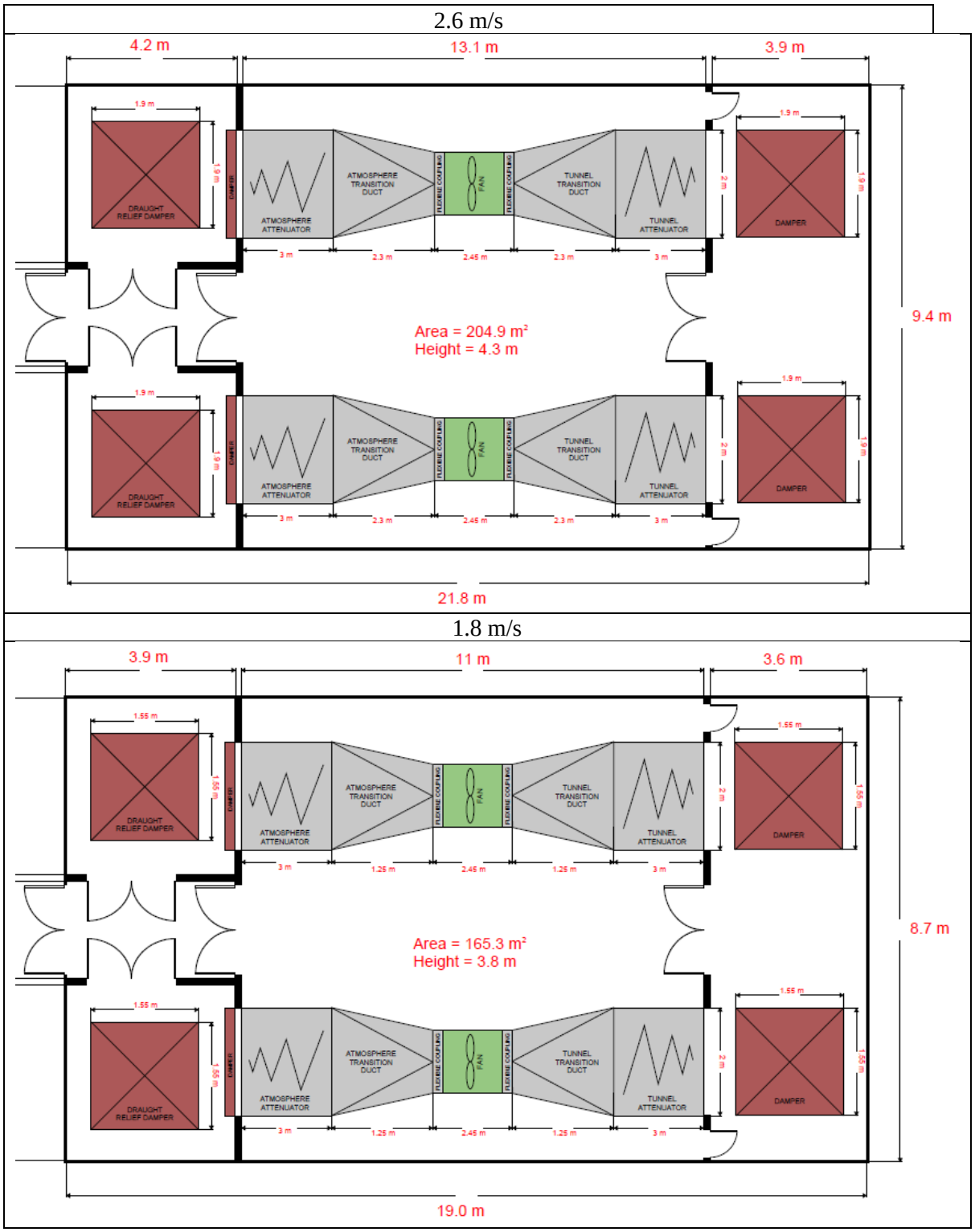

Figure 2- Comparison of plantroom size with a reduction in critical velocity

The main physical difference between the two plantrooms is the length reduction by 3 m and width by approximately 1 m. It is acknowledged that there is an opportunity to optimize the fan plant sizes. However, as this is a comparative assessment, the difference between the two sizes is of interest rather than the layout itself.

Nonetheless, as plantroom space within stations is often at a premium, where any reduction in

plantroom sizes, whether directly due to the decrease in the size of the fan plantrooms or in conjunction with the plantrooms of associated ancillary systems, will be of benefit to station planning, station height, services reticulation, and in aggregate result in the minimization of the overall station box (or cavern) size.

Based on the reduction in area in the example provided above, the total area saving could be 100 m^2 (~1100 ft^2), considering there are usually two such plantrooms per station.

Further, a reduction in the fan capacity benefits the access provisions required for installing and replacing the fans and associated elements (transitions, attenuators, and dampers) due to their smaller size. The smaller tunnel ventilation equipment and ancillary systems would also require less clearance through the station's back-of-house areas and corridors to move them in and out of the station.

However, in addition to the spatial and station planning benefits, other benefits become evident when the tunnel ventilation system is viewed as a holistic arrangement encompassing the broader electrical, structural, and architectural disciplines.

The effort required to push air at a lower velocity through a tunnel is much easier than to move air at a higher velocity through the same tunnel. The difference in the electrical power required would vary with the cube of the velocity, with the latter (in this case) being in the order of three times that of the former. This directly translates to a significantly smaller electrical system, from transformers to switchgear/rooms to panels, motor control cabinets, and variable speed drives – not to mention the cabling size in between. Although significant operational benefits are also evident, these can vary from country to country and metro system to metro system, so a unifying operational cost is difficult to develop and could be misleading, which is why it has not been considered in this paper.

The step change in reducing the fan size also means a lighter fan, positively affecting the main support structure (support columns, beams, and flooring) and the secondary structure (steel frame supporting the fan assembly itself).

While the above sets out the permanent installation benefits that could directly be capitalized on due to a reduction in the design fire size, there are also benefits during the procurement and construction phases that should not be overlooked. The smaller equipment sizes could facilitate ease of transportation from supplier to site (e.g., the difference in equipment sizes can result in the difference between a simple shipping container and bespoke transportation arrangements). Storage, on-site cranage, and equipment maneuverability to their respective places would also be improved.

TYPICAL PROCEDURES - TUNNEL EVACUATION AND INTERVENTION

It should be remembered that a fire can occur at the head of a train, at the tail, or anywhere in between. Therefore, for a fire within a train compartment, should the passengers need to evacuate. However, the train, it is probable that some passengers may have to negotiate a course around the fire site due to the fire location. As previously noted, for a train fire, the prime goal of all modern metro systems is to get the train to the nearest station. At a station, evacuation can occur through all available doors, enhancing all evacuating passengers' safety. The only reasons a train would not proceed to the next station would be if it were unable to due to its being disabled, and a train would only be disabled in a fire event if the fire occurs in the drive train, located under the floor area.

The typical design scenario for a train fire between stations assumes the train is stopped and the ventilation system commences operation. As a default, the ventilation system typically operates in the direction of train travel. Fans upwind and downwind of the fire operate collaboratively in a push-pull arrangement to create airflow through the tunnel and over the train. Reasons for this include the fact that the system inertia doesn't need to be overcome by operating the fans in the opposite direction and the associated quicker response time to achieve the required airflow. Furthermore, this reduces delays or coordination issues in getting emergency personnel on-site. Most procedures for emergency

personnel prohibit them from entering the track area until they are confident that traction power is not active. Once emergency services personnel arrive at the site, the fan operation mode can be reversed if required.

However, the primary reason a train would not be able to proceed to the next station during a fire event would be if it was disabled due to a fire occurring in the drive train, located under the floor area. As the floor of a modern rail car is fire-rated, rapid ventilation system operation allows passengers to evacuate over the fire inside the train in the upwind direction, as shown in Figure 1. This mode of operation exposes passengers to the least amount of smoke, as they can then move on to a walkway adjacent to the train after they are upstream of the smoke.

Of course, an issue that might stop a train mid-tunnel is the application of an emergency brake. The only appropriate emergency for brake application in an underground system occurs when the train is in the station. For example, a passenger is in danger of falling from a platform to tracks in front of the train, or if a passenger is stuck in a closing door and the train starts moving. A fire in a moving train does not constitute an emergency where stopping a train mid-tunnel is desirable. Passenger illness or an armed passenger are also situations where stopping a train mid-tunnel is likely unwanted. In all these cases, stopping the train in a tunnel is likely problematic and could result in extended evacuation times for passengers in underground systems, putting them in danger.

The ventilation system may also be used to pressurize the non-incident tunnel to minimize smoke ingress through the cross passages while the passengers are evacuating. A similar strategy is used for fire brigade intervention, where firefighters could approach the fire site along the non-incident tunnel, through the cross passage, and enter the incident tunnel from the upwind direction.

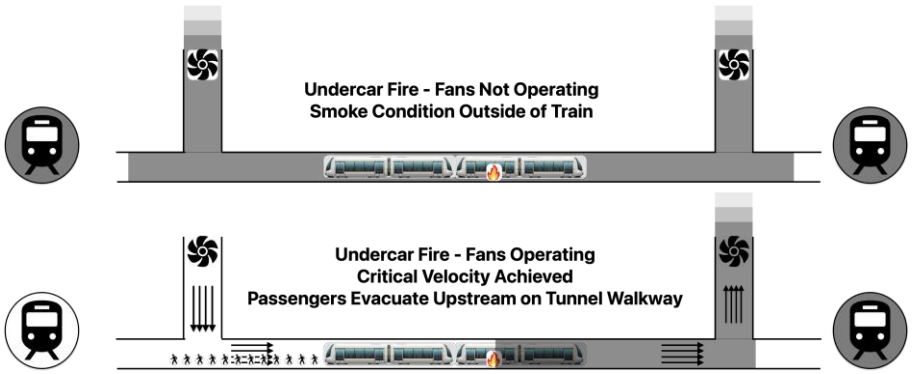

Figure 3- Smoke Condition with and Without Fan Operation

CONCLUSION

Designing a tunnel ventilation system based on the assumption that only an undercar fire will occur is a rational approach, given that modern metro cars are built with fire-rated floors that significantly delay fire penetration into the passenger compartment. Historical fire incidents show that passenger compartment fires are rare in modern systems. When they do occur, they typically result from external ignition sources rather than spontaneous fire growth from within the vehicle. In a well-maintained system with fire-rated materials, even if an undercar fire occurs, the likelihood of it burning through the floor is minimal.

Furthermore, designing ventilation systems around a larger fire scenario—such as a fully developed over car fire—assumes a failure of multiple fire protection layers, including fire-resistant flooring, any early fire detection, and the ability to move a train to a station for rapid passenger evacuation.

Since modern rolling stock prioritizes materials with low combustibility and compliance with NFPA 130 fire standards, the probability of a fire escalating into a full-car fire is low. By designing for the

most likely scenario rather than an extreme, unlikely event, tunnel ventilation can be optimized to balance life safety with cost efficiency, ensuring adequate smoke control without excessive system sizing.

Designing a tunnel ventilation system with excessive capacity presents financial risks that could strain transit budgets and lead to unnecessary operational costs. Oversizing fans to handle an unrealistic worst-case fire scenario, such as a multi-car fully developed fire, significantly increases capital costs associated with larger fan plants, extended ducting infrastructure, and increased power supply requirements. The cost of acquiring and installing oversized fans, along with the required ancillary systems (e.g., dampers, attenuators, switchgear, and power transformers), can substantially elevate project expenses. According to studies on transit infrastructure costs, tunnel ventilation systems are among the most expensive components of underground metro projects. An overly conservative fire design approach may result in financial inefficiencies without providing meaningful safety improvements, especially if historical data and fire dynamics modeling suggest that such extreme fire scenarios are highly improbable.

Beyond initial capital expenditures, oversized ventilation systems also impose long-term financial burdens related to maintenance and energy consumption. High-capacity fans require more frequent servicing due to increased wear and tear, and their higher power demands contribute to elevated electricity costs during routine tunnel ventilation and emergency operations. The increased airflow velocities associated with oversized systems may also cause unnecessary stress on tunnel structures, leading to accelerated degradation of tunnel linings and ancillary equipment. In addition, oversized fans may require more extensive space allocations within underground stations, affecting overall station design and potentially leading to increased excavation and construction costs. Therefore, while ensuring adequate ventilation is essential for fire safety, an overly conservative approach with a significantly oversized system may lead to diminishing safety and financial sustainability returns. A balance must be struck between safety margins and cost-effectiveness to ensure an optimized and practical tunnel ventilation design.

REFERENCES

1. “Bay Area Rapid Transit District Fire On Train No.117 And Evacuation Of Passengers While In The Transbay Tube,” National Transportation Safety Board, Washington DC, 1979.
2. “Baku Metro fire, 337 Killed,” [Online]. Available: https://mercortecresa.com/en/blog/baku-metro-fire-337-killed.
3. M. Kumm, “Carried Fire Load In Mass Transport Systems,” Mälardalen University, Västerås, Sweden, 2011.
4. A. Lönnermark, A. Claesson, J. Lindström, Y. Z. Li, M. Kumm and H. Ingason, “Full-scale fire tests with a commuter train in a tunnel,” SP Technical Research Institute of Sweden, Borås, 2012.
5. A. Kapahi, M. McKinnon, C. Rippe, M. DiDomizio, C. Luo, S. Yazdani and B. Lattimer, “Evaluation of Rail Car Floor Fire Resistance Exposure and Test Article Scaling,” DOT/FRA/ORD-18/38, Washington, DC, 2018.
6. Y. Liu, S. Cassady, J. Casey, S. Zlatanic and N. Munfah, “Smoke Management in Subway Stations Due to Train Arson Fire Scenario,” in *Sixth International Symposium on Tunnel Safety and Security*, Marseille, 2014.
7. N. White, J. Barnett and I. Bennetts, “Fully Developed Passenger Train Fire Experiment,” in *Proceedings of the International Conference on Fire Safety – Sea, Road, Rail*, Melbourne Australia, November 2005.
8. W. D. Kennedy, R. E. Ray and J. W. Quinan, “A Short History of Train Heat Release Calculations,” in *ASHRAE Proceedings* , Toronto, 1998.
9. E. Goldwyn, A. Levy, E. Ensari and M. Chitti, “Transit Costs Project: Understanding Transit Infrastructure Costs in American Cities,” NYU Marron School of Urban Management, New

York, 2024.

10. Y. Z. Li and H. Ingason, "A New Methodology of Design Fires for Train Carriages Based on Exponential Curve Method," *Fire Technology,* vol. 52, p. 1449–1464, 2016.
11. Y. Hong and C. Fu, "A full-range analytical solution of the critical velocity for smoke control in tunnel fires," *Case Studies in Thermal Engineering,* vol. 40, 2022.
12. "NFPA 130 - Standard for Fixed Guideway Transit and Passenger Rail Systems," National Fire Protection Association, 2023.
13. B. H. Chiam, "Numerical Simulation of a Metro Train Fire," University of Canterbury, Christchurch, New Zealand, 2004.
14. "Standard Test Methods for Fire Tests of Building Construction and Materials (ASTM E119)," ASTM, 2020.

Influence of tunnel portal geometry on wind-driven airflow in naturally ventilated tunnels

Jakub Bielawski[1,2], Dia Luan[2,3], Xinyan Huang[3], Aleksander Król[4], Małgorzata Król[4], Wojciech Węgrzyński[1]
[1]Building Research Institute, Filtrowa 1 St., 00-611 Warsaw, Poland
[2]Hong Kong Polytechnic University, 11 Yuk Choi Rd, Hung Hom, Hong Kong, China
[3]Central South University, 932 Lushan S Rd, Changsha, China
[4]Silesian University of Technology, Akademicka 2A, 44-100 Gliwice

KEYWORDS: longitudinal ventilation, deluge system, pressure drop

INTRODUCTION

Airflow in tunnels is constantly susceptible to atmospheric influences. External weather effects, such as winds of a certain angle of attack, can induce dynamic pressure at the tunnel portal [1]. However, determining this value is difficult to achieve and current design approaches are based on conservatively assumed efficiency factors [2]. This can be referred to as the classic problem of flow through the opening depending on the discharge coefficient. This is a direct result of the geometry of the tunnel portal, and additional obstacles present can affect the precipitation of wind momentum. This can have an adverse effect on the performance of the sanitary or smoke ventilation system when the wind flows in a direction opposite to the nominal longitudinal ventilation direction. On the other hand, wind-driven flow could support in diluting the concentration of exhaust gases [3], [4], [5], exceeding the critical ventilation velocity [6], [7], [8] or change flame behavior [9], [10] in the windward side.

INVESTIGATION METHODOLOGY

The main objective of this study is to quantify the airflow characteristics in the tunnel caused by the wind. A series of CFD analyses using code ANSYS Fluent were carried out for selected typical tunnel portal shapes. Rectangular shapes (with different height-to-width ratios) and horseshoe shape, which is characteristic of TBM tunnels, were selected as representative. For each geometry, the wind flow was simulated over a specific range of reference velocities and angles of attack. A logarithmic wind profile was selected for representative locations such as urbanized, rural, and mountainous areas to compare the effect of the roughness of the tunnel portal surroundings. In addition, an analysis of the occurrence of an 'entry chamber', understood as a transfer between a rectangular shape and a horseshoe shape, was carried out when a TBM tunnel is present in the central part. Figure 1 shows examples of boundary conditions in CFD simulations and a bunch of investigated geometries.

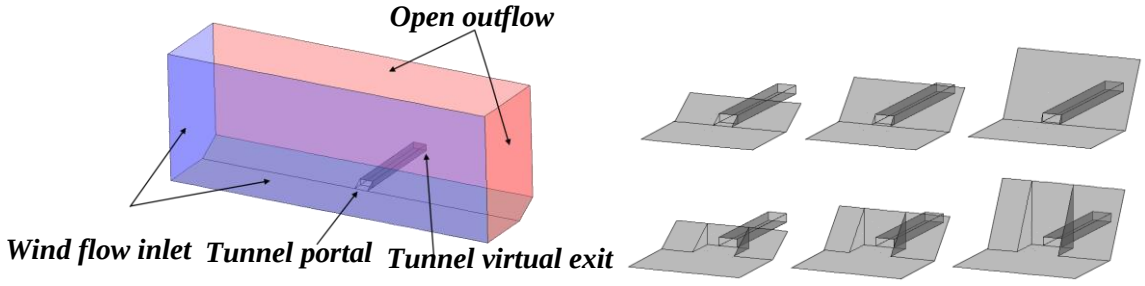

Fig. 1. Scheme of the numerical domain used in CFD simulations and examples of portal geometries.

WIND TUNNEL VALIDATION

Validation of wind flow modelling was performed in wind tunnel tests using selected mock-ups in scale 1:100. There was measured pressure differences and average velocity inside model tunnel. Figure 2 shows example of mock-up and CFD model of wind tunnel test.

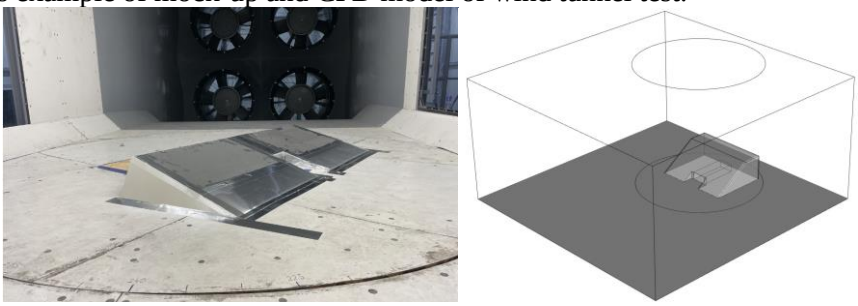

Fig. 2. Wind tunnel experimental setup and numerical domain.

DISCUSSION

The final paper will present the results of a parametric study of the portal effect on wind-induced airflow. The variables will be portal types and geometries, tunnel cross-sections, and wind parameters. The authors then envisage implementing the obtained wind flow data to simulate the interaction of tunnel fire and smoke spread with at different wind conditions.

REFERENCES

[1] T. Kubwimana, P. Salizzoni, E. Bergamini, A. Mos, P. Méjean, and L. Soulhac, "Wind-induced pressure at a tunnel portal," *Environmental Fluid Mechanics*, vol. 18, no. 3, pp. 769–786, Jun. 2018, doi: 10.1007/S10652-018-9589-5/FIGURES/12.

[2] NCHRP Research Report 836, "Guidelines for Emergency Ventilation Smoke Control in Roadway Tunnels," 2017, *National Cooperative Highway Research Program*.

[3] I. Kanda, Y. Yamao, K. Uehara, and T. Ohara, "A wind-tunnel study on diffusion from urban major roads," *Journal of Wind Engineering and Industrial Aerodynamics*, vol. 99, no. 12, pp. 1227–1242, Dec. 2011, doi: 10.1016/J.JWEIA.2011.10.009.

[4] G. Sztarbała, T. Lipecki, and J. Bęc, "Wind influence on air flow inside road tunnels," in *6th European and African conference on wind engineering*, 2013, pp. 1–9.

[5] M. Wang, Y. Tian, L. Yu, X. Wang, Z. Zhang, and G. Yan, "Research on the wind pressure coefficient in natural wind calculations for extra-long highway tunnels with shafts," *Journal of Wind Engineering and Industrial Aerodynamics*, vol. 195, p. 104020, Dec. 2019, doi: 10.1016/J.JWEIA.2019.104020.

[6] W. Zhao *et al.*, "An experimental study on smoke back-layering and critical velocity in tunnel fires with canyon cross wind," *Journal of Wind Engineering and Industrial Aerodynamics*, vol. 209, p. 104477, Feb. 2021, doi: 10.1016/J.JWEIA.2020.104477.

[7] W. Zhong, C. G. Fan, J. Ji, and J. P. Yang, "Influence of longitudinal wind on natural ventilation with vertical shaft in a road tunnel fire," *Int J Heat Mass Transf*, vol. 57, no. 2, pp. 671–678, Feb. 2013, doi: 10.1016/J.IJHEATMASSTRANSFER.2012.10.063.

[8] L. Yang *et al.*, "Experimental study on thermal stratification characteristics in tunnel fires under the effect of canyon cross wind," *Journal of Wind Engineering and Industrial Aerodynamics*, vol. 218, p. 104756, Nov. 2021, doi: 10.1016/J.JWEIA.2021.104756.

[9] R. Ouyang, W. Zhao, L. Yang, A. Jiao, Z. Xu, and C. Fan, "An experimental investigation of burning rate and flame geometric parameters of tunnel fires under canyon cross wind and longitudinal ventilation," *Fire Saf J*, vol. 126, Dec. 2021, doi: 10.1016/j.firesaf.2021.103474.

[10] F. Guo, L. Ding, J. Ji, and F. Ge, "Influence of longitudinal wind and sidewall restriction on burning rates and thermal feedback of pool fires in a tunnel," *International Journal of Thermal Sciences*, vol. 193, p. 108500, Nov. 2023, doi: 10.1016/J.IJTHERMALSCI.2023.108500.

A PID sensor, for initial fire phase detection, with ppb capabilities

Madeleine Martinsen & Erik Dahlquist
Mälardalen University, MDU
Box 883, 721 23 Västerås, Sweden
E-mail: madeleine.martinsen@mdu.se

KEYWORDS: Gas detection, Initial fire phase, Underground Mining

INTRODUCTION

Fire in underground mines is one of the primary safety concerns, as it can originate from various sources, including pool fires caused by leaks in hoses or pipes, vehicle fires, and fires in tires or conveyor belts [1]. Additionally, the storage of flammable materials such as gasoline, diesel, and explosives poses a significant fire risk. When a fire occurs in an underground mine, it releases heat, smoke, and toxic gases, including carbon monoxide and methane, which can create life-threatening conditions for miners. Moreover, smoke severely impairs visibility, complicating evacuation efforts. To minimize miners' exposure to hazardous gas concentrations, they are equipped with personal monitoring devices, or "tags," that record gas levels and trigger alarms when necessary. The data collected from these devices is also used to ensure compliance with national occupational safety regulations, including short-term exposure limits (KGV, 15-minute average) and long-term exposure limits (NGV, 8-hour average), which define permissible exposure durations for specific gases.

METHODS

Interviews revealed that most fires in underground mines are currently detected by miners and machine operators who visually observe smoke, smell burning materials, and notify the appropriate personnel. Some fixed fire detection systems, such as smoke and heat detectors, are installed in locations like offices, workshops, and hydraulic or electrical rooms. Additionally, FLIR cameras may be positioned at certain levels in some mines. However, fire detection is often absent in the production environment itself. This is understandable, as the production area is not static; it continuously evolves as mining operations progress deeper underground, making it difficult to strategically place smoke and heat detectors. A recent study [2] comparing fire incidents in electric vehicles (EVs) and internal combustion engine vehicles (ICEVs) highlights that statistical data on EV fires in enclosed spaces (such as tunnels and parking garages) remains limited. This finding is equally relevant to mining vehicles. The study emphasizes the importance of early fire detection through fixed detection systems and/or the integration of intelligent fire detection technologies directly into vehicles.

Some mining companies envision a future in which no human workers are required underground, marking the transition to fully autonomous mining operations. This vision includes a fully automated mine where processes are continuously monitored and optimized to enhance productivity and safety. In a fully autonomous mining environment, where no personnel are present to see, hear, or smell early signs of fire, there would be no immediate human response to initiate fire suppression before emergency services arrive. This underscores the urgent need to replace human sensory perception with advanced detection systems. Sensors have been evaluated based on their sensitivity, robustness, and resistance to moisture and dust [3]. Furthermore, a foundational framework has been developed for establishing a fire detection system using a Bayesian Network (BN) approach. In this system, data from gas sensors will serve as input signals to the BN, enabling predictive fire detection and improving overall mine safety [4].

RESULT

In the initial phase of this thesis, various gas sensors were tested to evaluate their effectiveness in

detecting fire-related gases. Among these, photoionization detector (PID) sensors demonstrated promising potential for timely gas detection [3]. The high-intensity lamp in the PID sensor allowed for the identification of low gas concentrations. However, a key limitation was its insufficient sensitivity to detect very low concentrations of hydrocarbons—substances commonly found in vaporized gases associated with fire hazards. To address this limitation, a new type of PID sensor from Falco, featuring enhanced sensitivity in the parts-per-billion (ppb) range, was identified for hydrocarbon detection. Laboratory tests conducted at Mälardalen University (MDU) in the spring of 2024 confirmed its exceptional sensitivity, detecting concentrations as low as approximately 10 ppb, compared to the standard PID sensors' detection range of 2 to 5 ppm. Since October 2024, on-site testing of the sensor has been ongoing at KUJ (LKAB), an underground mine. The sensor has been installed on a diesel-powered drilling rig, with a sampling interval set at five minutes. Initial results have revealed peaks reaching approximately 9 ppm. To better understand the cause of these peaks, correlations between sensor readings and machine operation data were analyzed. Additionally, LKAB provided information on the machine's location at different times. Based on this data, several potential sources for the detected hydrocarbons were identified, including:

- Workshop visits where surfactants were used to dissolve grease, releasing solvent particles into the air.
- Refueling operations that emitted fuel vapors.
- The presence of gasoline fumes in the surrounding environment.

Furthermore, frequent sensor spikes were observed when the machine was operating with the power cable, suggesting that the sensor successfully detected airborne hydrocarbons during equipment operation.

DISCUSSION

Based on the results of extensive on-site and off-site experiments, various sensors—particularly gas sensors—have been proposed for installation on mining machines to enable early gas detection. Among the tested technologies, the photoionization detector (PID) technique emerged as particularly effective. Mounting gas sensors on mining machines offers several advantages, including:

- **Proximity to Fire Sources**: Most fires in underground mines originate from mining machines, making onboard sensors well-positioned for early detection.
- **Adaptability to Changing Mining Environments**: Unlike fixed sensors, mobile sensors move with the machines, ensuring continuous monitoring as mining operations expand to new depths.
- **Simplified Maintenance and Calibration**: Sensors can be inspected and recalibrated as part of routine machine maintenance, maintaining long-term accuracy.
- **Integrated Data Logging**: Sensor data can be seamlessly correlated with machine operation data, providing valuable insights into gas emissions and fire risk factors.

Increasing awareness of elevated gas concentrations and temperature levels enhances rescue efforts and significantly improves the likelihood of preventing hazardous situations from escalating. Beyond safety improvements, this approach could also optimize air-quality management in underground mining environments by providing deeper insights into ventilation needs and efficiency.

REFERENCES

1. Salami, O., Xu, G. (2022) "Experimental investigation of fire and product combustion (POC) spread in underground mines: A case study" SME Annual Conference and Expo 2022, pp. 470-473.
2. Hynynen, J., Quant, M., Pramanik. R., Olofsson, A., Li, Y., Arvidson, M., Andersson, P. (2023). Electric Vehicle Fire Safety in Enclosed Spaces. Research Institutes of Sweden AB, RISE Report 2023:42, ISBN: 978-91-89757-90-5.
3. Martinsen, M., Dahlqvist, E., Lönnermark, A., Säker, Ö. (2020) "Energy and Safety Diagnostic in Underground Facilities" in Ninth International Symposium on Tunnel Safety and Security. Proceedings ISTSS 2020. ISBN 978-91-89049-89-5.
4. Martinsen, M., Desalegn, A., Dahlqvist, E., Zhou, Y. (2023) "Holistic approach promotes failure prevention of smart mining machines based on Bayesian Networks". Journal Machines 2023, 11 940. https://doi.org/10.3390/machines11100940.

Statistical Analysis of Highway Tunnel Fire Incidents in Zhejiang Province, China from 2020 to 2024

Qian Zhou[1], Kai Zhu[1,*], Haitao Mao[2], Qixin He[1], Wenwen Hua[1], Dong Ye[1], Qiang Wang[1]
1. College of Energy Environment and Safety Engineering, China Jiliang University, Hangzhou, China
2. Quzhou Fire and Rescue Detachment, Quzhou, China
E-mail: zhukai@cjlu.edu.cn

KEYWORDS: Highway tunnel, fire incidents, incident characteristics

INTRODUCTION

With an increase in traffic volume, the number of tunnel fire incidents is rising faster relative to the length of tunnels, which leads to an increasing risk of fire. Zhejiang Province just ranks fifth in total tunnel length in China, whereas the fire incidents are prone to occurring in Zhejiang [1]. As a consequence, severe casualties and economic losses are easily caused. For example, a tunnel fire occurring in Maoliling Tunnel (located in Zhejiang Province) caused 5 fatalities and 31 injuries in 2019.

To mitigate fire-related casualties and losses, characterizing tunnel fire incidents is crucial to inform preventive strategies for management authorities. However, partial scholars [1-3] conducted an analysis on the fire characteristics of Chinese highway tunnels. But the data obtained in the aforementioned studies were largely based on public report. This may introduce a certain sampling bias, casting doubt on the representativeness of the incident characteristic analysis results and thus lacking analysis of short-term fire incidents due to the lack of refined data granularity.

For these reasons, Zhejiang Province, a high-incidence area for tunnel fire incidents, was selected as the research object. Through the data on 390 tunnel fire incidents from January 2020 to August 2024 were collected from the Fire and Rescue Brigade (FRB), Zhejiang Communications Investment Group Co., Ltd. (CICO) and news reports, the characteristics and disparities of tunnel fire incidents could be clarified. With elucidating the impact of statistical methods on the characteristics of tunnel fire incidents, insights into the prevention and control of such fires would be rationally offered.

STATISTIC ANALYSIS OF TUNNEL FIRE INCIDENTS

1. Spatiotemporal Distribution Characteristics

The proportion of tunnel fires occurring on holidays (34%) slightly exceeds the share of holidays in years. In spring and summer, tunnel fires show the most frequent occurrence. In terms of hourly distribution, influenced by tunnel vehicle flow, 71.1% of fires occur during the daytime, significantly higher than the nighttime occurrences. This pattern contrasts with the trend of general vehicle fires, which are more prevalent at night.

2. Analysis of Ignition Causes

Vehicles are the primary source of tunnel fires (83.6%). Among tunnel vehicle fire incidents, trucks have the highest fire rate (59.8%) (Fig. 1), which aligns with the existing research findings but significantly differ from general vehicle fires, where cars account for 58.8%. Additionally, spontaneous combustion is identified as the primary cause of tunnel fires in Zhejiang Province (86.2%), with engine failures being the leading cause of spontaneous combustion (27.6%). Notably, two-wheeled vehicles, as essential means of short-distance transportation, account for up to 8% of fire incidents (Fig. 2).

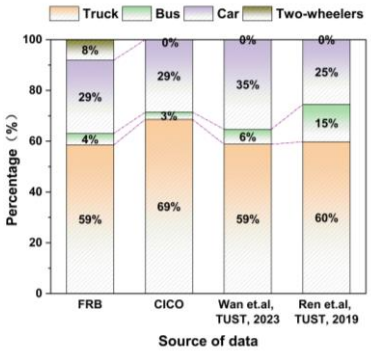

Fig. 1 Comparative analysis of vehicle types in tunnel fires

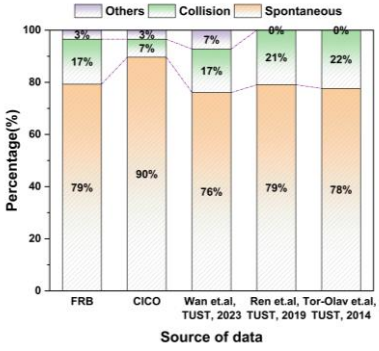

Fig. 2 Comparative analysis of causes in tunnel fires

3. Analysis of Influencing Factors of Tunnel Fire Frequency

The study reveals a high correlation between tunnel length and the number of tunnel fires. And influenced by the proportion of tunnel entrances and exits, the average number of fires increases linearly before plateauing for the tunnels with the length of <3.5 km (Fig. 3). However, for tunnels with the length of >3.5 km, the impact of the tunnel environment becomes more intensified, leading to a significant rise in average number of tunnel fires.

The average fire frequency among different tunnels is 1.20 incidents per 100 million vehicle-kilometers. In addition to factors such as the number of tunnels, tunnel length and traffic volume, tunnel type also plays a crucial role in tunnel fire occurrences (Fig. 4). Notably, the fire frequency in highway tunnels is significantly higher than that in urban tunnels, which falls below the average level. Future research will incorporate tunnel fire incident data from a national scope, systematically explore the influencing factors tunnel fire incidents.

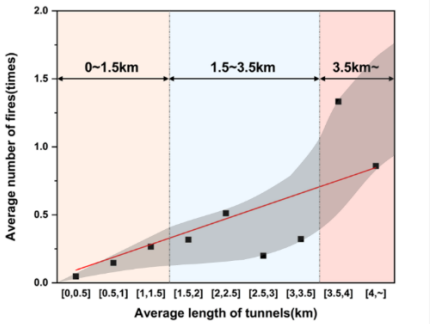

Fig. 3 Correlation analysis between tunnel length and tunnel fire incidents

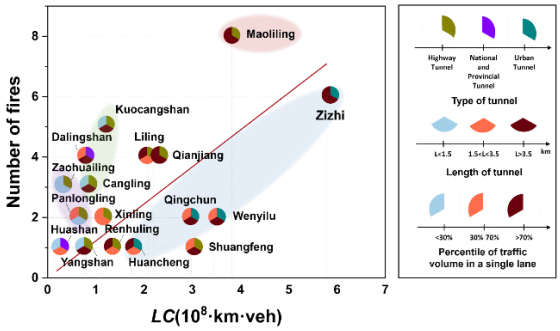

Fig. 4 The characteristic of tunnel fires in a typical tunnel over a 5-year period

REFERENCES

[1] Wan H, Jiang Y, Jiang J. A survey of fire accidents during the process of highway tunnel operation in China from 2010 to 2021: characteristics and countermeasures. Tunnelling and Underground Space Technology, 2023, 139: 105237.

[2] Ren R, Zhou H, Hu Z, et al. Statistical analysis of fire accidents in Chinese highway tunnels 2000-2016. Tunnelling and Underground Space Technology, 2019, 83: 452-460.

[3] Nævestad T O, Meyer S. A survey of vehicle fires in Norwegian road tunnels 2008-2011. Tunnelling and Underground Space Technology, 2014, 41: 104-112.

Impact of Emergency Exit Separation on Passenger Safe Egress in Longitudinally Ventilated Intercity Train Tunnels

Manuel Barros-Daza & Jonathan Hodges & Nishant Nayan
Jensen Hughes
2020 Kraft Drive, Suite 3020, Blacksburg, VA 24060, US
E-mail: mdaza@jensenhughes.com

KEYWORDS: Tunnel ventilation, railway tunnel, numerical simulation, coupled CFD-evacuation, tenability analysis, ventilation requirements, performance based-design

INTRODUCTION

The 2023 edition of NFPA 130, the Standard for Fixed Guideway Transit and Passenger Rail Systems, stipulates that the distance between cross-passageways, when used as alternatives to exits, should not exceed 244 meters, and that the distance between exits should not exceed 762 meters. However, the rationale behind these distances lacks comprehensive scientific validation, raising concerns about their effectiveness in ensuring safe passenger evacuation across all rail tunnel fire scenarios. A previous study [1] evaluating the impact of different exit distances and walkway widths on egress time found limitations in the current NFPA 130 requirements. In particular, conditions downstream of the fire became untenable before egress was completed. While this analysis focused on a limited range of fire sizes, fire growth rates, and generic train designs, the authors recommended further investigation to provide more robust guidance on the optimal spacing of exits and walkway widths in rail tunnel design.

The distance between exits can significantly impact passengers' ability to safely evacuate in an emergency. Distances which are too far apart may lead to passengers being forced to evacuate through smoke-filled environments for a significant duration. Prolonged exposure to smoke can severely hinder their ability to escape, potentially trapping them within the tunnel. Although increasing the longitudinal ventilation speed can help confine smoke and restrict its spread to upwind evacuation paths, there are scenarios where passengers must evacuate downwind. In such cases, this ventilation approach could compromise smoke stratification downstream of the fire, creating hazardous conditions for downwind evacuees. The impact of critical parameters such as train capacity, train design, egress walkway width, fire size, and fire growth on the maximum safe distance between emergency exits remains underexplored.

Previous studies have examined factors such as ventilation system activation, fire position on the train, train location within the tunnel, and evacuation timing to identify the worst-case fire scenarios for different fire sizes in metro and rail tunnels [2], [3]. This study builds upon this prior work, evaluating the life safety risks of occupants based on NFPA 130's exit separation distances, and considering various fire characteristics, passenger load, and egress parameters (including walkway width and passenger behaviour profiles). The findings provide a solid foundation for establishing emergency exit spacing and egress walkway width for integration into existing guidance, codes, and standards.

METHODOLOGY

This research employed a coupled analysis of smoke spread and passenger evacuation to assess the impact of smoke exposure during the evacuation process in railway car fires, with peak heat release rates up to 55 MW. Fires with different growth rates—slow, medium, and fast—were considered. The progression of smoke spread, tenability along the evacuation route, and conditions inside and outside the train were assessed using computational fluid dynamics (CFD), with the Fire Dynamics Simulator (FDS) version 6.9.1 [4]. Visibility, toxic products concentration, and temperature were predicted at a height of 1.5 to 2 meters above the walking surface in each scenario. These parameters were used in evaluating the tenability and walking speeds of each passenger. Toxicity was quantified through the Fractional Effective Dose (FED) method for each passenger.

The evacuation process was modelled using Pathfinder (2024) [5], incorporating passenger walking speed distributions, tracking occupant positions over time, and lowering walking speed due to reduced visibility. Key parameters such as the passenger load of the rail car, distribution of able bodied and disabled passengers and egress aisle width, were investigated.

Fire and egress simulations were conducted using the Amtrak Intercity Trainsets designs with capacity up to 500 passengers, corresponding to the Siemens Configuration B2 -Dual Power. The simulations were conducted in an NFPA 130-compliant tunnel, with emergency exits placed between 244 m and 762 meters. The worst-case train fire location was modelled, positioning the fire near the centre of the train and the train situated midway between the exits. This configuration required at least 50 percentage of the passengers to evacuate downstream of the fire.

RESULTS AND DISCUSSION

The key findings of this study are:

- For the Siemens Amtrak Trainset, with a maximum capacity of 500 passengers (Configuration B2), using exits spaced at 244 meters and 762 meters, simulation results indicate that approximately 5% and 35% of passengers are at risk of being trapped downstream of the fire due to untenable conditions in fires with a fast growth rate. However, when the walkway width was increased to 0.85 meters (0.24 meters above the minimum required width), with exits spaced at 244 meters, no passengers were predicted to be trapped downstream of the fire.
- For fires with fast growth rates, increased walkway width to 0.85 meters, and with Amtrak trainsets up to 300-passenger capacity, simulation results predict no passengers being trapped if tunnel exits are spaced no more than 275 meters apart.
- For fires with slow and medium growth rates, simulation results predict no passengers being trapped in an NFPA 130-compliant tunnel (with exits spaced at 244 meters or 762 meters) for any of the simulated designs of the Siemens Amtrak trainsets under the assumed conditions.

This study aimed to evaluate the impact of following NFPA 130 requirements on the life safety risks faced by Amtrak Intercity Trainset passengers under varying key operational and design parameters. The findings are expected to significantly contribute to fire life safety criteria in railway tunnels, particularly in determining the optimal tunnel design parameters to minimize passenger risk. The findings of this study highlight that simply adhering to current regulations may not ensure a high probability of safe passenger evacuation. This study provides a more holistic and robust foundation for establishing emergency exit spacing guidelines that enhance the likelihood of safe evacuation in rail tunnel fire scenarios.

REFERENCES

[1] H. Biteau, J. Donovan, A. Went, A. Biery, A. Smith, and N. Birmingham, "Review of Emergency Egress and Rescue Challenges in Rail Tunnels ," 2024. Accessed: Aug. 29, 2024. [Online]. Available: https://www.nfpa.org/education-and-research/research/fire-protection-research-foundation/projects-and-reports/review-of-emergency-egress-and-rescue-challenges-in-rail-tunnels

[2] Y. Z. Li, A. Lönnermark, and J. Gehandler, "Numerical study on the influence of the ventilation strategy on life safety in a metro tunnel," in *Tenth International Symposium on Tunnel Safety and Security*, Stavanger, Norway, Apr. 2023, pp. 526–541. [Online]. Available: www.ri.se/en/istss/

[3] T. Zisis, K. Vasilopoulos, and I. Sarris, "Numerical Simulation of a Fire Accident in a Longitudinally Ventilated Railway Tunnel and Tenability Analysis," *Applied Sciences (Switzerland)*, vol. 12, no. 11, Jun. 2022, doi: 10.3390/app12115667.

[4] K. B. McGrattan, S. Hostikka, J. Floyd, R. McDermott, M. Vanella, and E. Mueller, "Fire Dynamics Simulator User's Guide (Revision: FDS-6.9.1-0-g889da6a)," Apr. 08, 2024, *Gaithersburg, MD*. doi: 10.6028/NIST.SP.1019.

[5] C. Thornton, R. O'Konski, B. Hardeman, and D. Swenson, "Pathfinder: An Agent-Based Egress Simulator," in *Pedestrian and Evacuation Dynamics*, Boston, MA: Springer US, 2011, pp. 889–892. doi: 10.1007/978-1-4419-9725-8_94.

Automate the important stuff of fire safety

Ben Wolf & Wolfgang Lahner
Honeywell life safety Austria GmbH
Technologiestr. 5, 1120 Vienna, Austria
E-Mail: wolfgang.lahner@honeywell.com

KEYWORDS: automation, fire detection, self-test detector, digitization, Honeywell Connected Life Safety Services (CLSS), digitized documentation with storage in a secure cloud environment

INSTALLING AND MAINTAINING LIFE SAFETY SYSTEMS IN COMPLIANCE WITH A BUILDING'S OCCUPANCY TYPE IS REQUIRED BY FIRE CODES AND FOLLOWS LEGAL REQUIREMENTS GLOBALLY

Once a building owner installs a new life safety system, proof must be filed with the local fire authority that the system has been designed to the local code of practice and that it is working as intended. At prescribed intervals during the lifecycle of the installed fire system, it will require testing, inspection, and maintenance to confirm that it continues to work well for the building and those who occupy it. For example, smoke detectors are generally required to be functionally tested and inspected annually.
Historically, processes relating to the provision of life safety Test and Inspection have been manual. Digitising these processes can help service providers and building owners in many ways, including saving time on site, reducing building disruption, providing real-time updates on Test and Inspect progress, and improving life safety performance by validating that the entire system works as intended and has been tested to code.

WHAT HAS CHANGED IN THE LIFE SAFETY SYSTEM INDUSTRY?

As the world around us has become increasingly connected and automated using new Internet of Things (IoT) technologies, using connected devices and apps in fields ranging from banking to home appliances has become second nature, life safety is no different. The expectation to manage and control building systems, including the fire system, using a mobile device is growing. Fire code enforcement authorities have also benefited from 'going digital' and some regions have implemented electronic compliance reports. Many life safety system manufacturers and Test and Inspect app providers have introduced connected features enabling remote status updates, and in some applications, controlling and even automating processes anytime or anywhere using connected software. In the context of the last few years, COVID-19 prevention efforts accelerated the pre-pandemic trend of automating Test and Inspect processes to ensure engineers on site are there for a shorter amount of time, with the added intent of being less invasive and manage occupancy levels in sensitive areas of the hospital. Furthermore, as service providers are finding it difficult to hire and retain skilled labour, there is even more focus on ways to speed up and improve the Test and Inspect compliance process.

IMPROVINGLIFE SAFETY

So why is proper maintenance fire and life safety systems so important?
According to a Fire Safe Europe report[1], every day in Europe alone there are on average 5,000 fires, 11 lives lost, and 190 hospitalisations due to building fires. Total GDP impacted is ~1% from building fires and, in the UK alone, 5,000 full-time jobs are lost each year due to warehouse fires. There is an environmental impact, too. A Swedish study[2] showed that Carbon Monoxide (CO) created by unburned particles from building fires was greater than the CO emissions from commercial transport. More advanced digitised maintenance such as automation can help to uncover hidden issues that are

often missed with manual processes, such as covered detectors. Some detectors can remain covered for years, especially if they are placed in ceiling in voids and hard to reach areas. These issues can lead to tragic events such as a real case in the UK, where a fire occurred in a community housing association[3] property leading to the death of an elderly resident. The coroner confirmed that this fire was not detected quickly enough as the dust covers were still in place. All app-based Test and Inspect processes help to support the effective and provable maintenance of fire alarm system. Thorough maintenance processes help to uncover issues that might prevent fires being detected and located, which can lead to property damage, work disruption, environmental impact and, most importantly, loss of life.

SAVING YOU TIME

Manual inspection processes are time consuming and cause disruption to building occupants whilst testing is underway. Testing smoke detectors manually represents about 70%-80%[4] of the time needed to inspect an average fire detection system. All appbased process are designed to improve engineer efficiency and accuracy. The least intrusive automated processes can mean that maintenance inspection can now be done during normal working hours, as opposed to being supported on evenings or weekends. Manual test report creation can take days to complete yet, as app-based testing is stored digitally, consequently report generation to specific to code compliant templates can now be done in seconds.

PROVING COMPLIANCE

Professional life safety Test and Inspect service providers strive to do a thorough and accurate inspection; however, evidence demonstrates the limitations of relying on manual Test and Inspect processes, ‘the word’ of a poor service provider or the negligence of a building owner.

- Approximately 70% of automatic fire alarm systems in Danish companies and public institutions are faulty when they are inspected[5]
- A restaurant director was sent to prison because the fire alarm system had been turned off which led to a huge fire going undetected[6]
- An “indecipherable message” on the fire alarm control panel leading to the wrong part of the Notre Dame cathedral being inspected after a fire[7]

We are no longer required to blindly trust that life safety systems were inspected, tested, and maintained accurately. With digital Test and Inspect compliance reports, now you can prove it.

CLSS CASE STUDY USING THE EXAMPLE OF THE ZAB TUNNEL FACILITY

In 2024, the Zentrum am Berg (Underground research, development, training and education at 1:1 scale[8]) was the first tunnel project to use self-test detectors to increase safety. This simplifies maintenance planning and execution. All activities are logged through the CLSS gateway, with maintenance reports generated automatically. The owner's self-checks are documented, and fire alarm system operators receive immediate live notifications via the CLSS.

FACTS FOR INCREASING SAFETY IN TUNNELS

- Automatic self test detectors are only out of operation for a few minutes for maintenance. This increases safety with the availability of detectors that can detect fires, compared to traditional automatic fire detector maintenance, where the time can be up to hours.
- Depending on the local regulation, the maintenance personnel only have to carry out the visual inspection of the automatic self test detectors during maintenance, which means that the personnel spend less time in the tunnel for maintenance and thus reduce the safety risk.
- The transparency of the status of the Fire alarm system and the safety checks carried out, gives both the operator and the maintenance engineer the certainty that everything is in order.

REFERENCES

1. Fire Safe Europe firesafeeurope.eu/facts-figures/
2. Raddningsverket, Karlstad, Risk- och miljöavdelningen. “Emissions from fires to the environment”, SP Brandteknik, 2002.
3. fia.uk.com/news/the-impact-of-covid-on-fire-safety-risk-management.html
4. Validated by Honeywell time and motion study
5. cfpa-e.eu/many-fire-protection-systems-are-faulty/
6. birminghammail.co.uk/news/midlands-news/sparkhill-pranzo-restaurant-director-qaissar-23932840
7. archpaper.com/2019/07/notre-dame-fire-mismanagement/
8. zab.at/en/

The Effectiveness of a Smoke Barrier Wall in Controlling Portal to Portal Smoke Recirculation: A Case Study

Göran Nygren, Raheleh Omranimanesh, Sofia Lundegårdh and Erik Lundström
WSP Sverige AB
121 88 Stockholm-Globen, Sweden
E-mail: goran.nygren@wsp.com

KEYWORDS: Tunnels, Smoke spread, Smoke recirculation, Tunnel portals, Smoke barrier wall, Tenable conditions, Longitudinal ventilation, Safe location.

INTRODUCTION

The standard approach to enable safe egress from twin tube road tunnels is to have fire and smoke separated tunnel tubes interconnected by cross passages at fixed intervals. Typically, longitudinal ventilation using jet fans is also provided to control the spread of smoke. When using this approach, where the non-incident tunnel tube serves as a place of safety, it is essential to prevent the spread of smoke between the tunnel tubes. If smoke spread occurs, it can expose evacuees to untenable conditions or result in undesirable behaviors, such as evacuees returning to the incident tunnel or being struck by traffic.

Measures to limit the spread of smoke through open cross passage doors has been studied extensively and design methods are widely available. However, smoke spread between the tunnel tubes is also possible at the tunnel portals e.g. due to unfavorable wind conditions, poor ventilation design or incorrect operation. It is also a phenomenon that cannot be studied using 1D or 2D analysis methods. This case study was developed as part of a project to investigate the effect of introducing a smoke barrier wall, as a risk reducing measure, to prevent portal to portal smoke recirculation.

BACKGROUND

The Swedish Transport Agency's regulations and general advice on safety in road tunnels, etc., TSFS 2019:93 [1] states that:

> 18 § If two adjacent tunnel tubes serve as each other's place of safety, measures shall be taken to prevent fire gases from entering the opposite tunnel tube via the portals.

The Swedish transport administration has in their infrastructure regulations on the design of tunnel TRVINFRA-00233, has similar requirements [2]:

> K43622
> If parallel tunnel tubes constitute each other's escape route and place of safety, fire gases from the incident tunnel tube must be prevented from entering the non-incident tunnel tube. This also applies at the tunnel portals.
> *Recommendation*
> At the tunnel portals, fire gases can be prevented from reaching the tunnel tube that is escape route and places of safety by reversing fans.

In various other countries, e.g. in Switzerland, the regulations for road tunnels prescribes passive methods to minimize tunnel portal smoke recirculation. For example, the Swiss standard ASTRA (2008) [3] requires a 30 m long screen (smoke barrier) outside of the portals if the tunnel has two tubes.

In accordance with deemed to satisfy provisions measures must be taken to prevent smoke from entering the adjacent tunnel tube through the openings. In tunnels with longitudinal ventilation and escape routes through cross-passages to the non-incident tunnel tube, it is common to follow the

strategy recommended by TRVINFR-00233, which involves reversing the air flow in the opposite tunnel tube, the non-incident tunnel tube. When a fire is detected, the ventilation in the non-incident tunnel is adjusted to match the air flow direction in the incident tunnel to prevent smoke from spreading to the non-incident tunnel tube. However, this adjustment can only happen after the fire is detected, and it may take some time to achieve the desired air flow direction and speed, especially if the air flow caused by traffic also needs to be overcome. Additionally, some shorter tunnels lack means for mechanical ventilation altogether. Therefore, designs relying solely on tunnel ventilation are not sufficient to prevent smoke spread due to smoke recirculation at the portals, and passive measures are thus also required. The latter measures can consist of e.g. staggered tunnel portals, a smoke screen or smoke barrier outside the tunnel portals.

In previous Swedish road tunnel projects, the design of smoke screens has rarely been verified using performance based methods. Instead, the projects have reused ad hoc designs from previous projects or adopted conservative prescriptive solutions from international standards, often resulting in barriers up to 25-30 meters long. However, such designs offer limited flexibility, impacts architectural design and can lead to unjustified costs. The sector has therefore seen a need to develop a method to verify the design of such barriers.

TUNNEL DESCRIPTION

The road tunnel under study is a concrete structure consisting of two main parallel tubes. The tunnel's length is approximately 450 meters. The tunnel is equipped with jet fans that provide longitudinal ventilation in the direction of traffic.

METHOD

Smoke movement calculations have been performed using the simulation software FDS (Fire Dynamics Simulator). It has been studied whether smoke from the incident tunnel tube can recirculate into the non-incident tunnel tube via the tunnel portals. In this study, smoke spread to the non-incident tunnel tube is considered to occur if smoke spreads to such an extent that it affects visibility in the tunnel.
In fire simulations, the dynamic pressure at openings have been adjusted to achieve the desired air velocity for environmental ventilation, 8-10 m/s (for a queue situation). When a fire is detected, the tunnel's fire ventilation system is activated, resulting in an air velocity of approximately 2.5–3.0 m/s. In the fire simulations, the dynamic pressures are adjusted to ensure that the air velocity falls within the desired range. In the non-incident tunnel tube, jet fans create an airflow in the traffic direction.

The influence of wind is represented in the model by applying a dynamic constant pressure against the tunnel portals. Various scenarios were evaluated to understand how the length of the smoke barrier, ranging from 0 to 25 meters beyond the tunnel entrances, affects the outcome. Additionally, the smoke barrier was studied at two different heights: one matching the tunnel entrance height and another one meter higher.

DESIGN FIRE

The design fire is selected based on the types of vehicles traveling through the tunnel. In this analysis, an HGV fire scenario with an HRR of 100 MW is studied [4].

DISCUSSION

The poster will present the method used to verify the design of a smoke barrier wall for preventing smoke spread between tunnel tubes via the tunnel portals. Results from the fire simulations will be presented as well as a discussion of the factors influencing the risk of smoke spread.

REFERENCES

1. Transportstyrelsen, TSFS 2019:93 - Transportstyrelsens föreskrifter och allmänna råd om säkerhet i

vägtunnlar m.m. Transportstyrelsens författningssamling, 2019.
2. Trafikverket, TRVINFRA-00233 - Krav tunnelbyggande. Version 1.0. Trafikverket, 2021.
3. ASTRA, 13001, Richtlinie, Ausgabe 2008 V2.02, Lüftung der Strassentunnel, Systemwahl, Dimensionierung und Ausstattung, Schweiz, 2008.
4. RISE, Beräkning brandeffektkurvor för personbilar, bussar och lastbilar. Borås: RISE Research Institute of Sweden AB, 2017.

Study on the mechanism of bidirectional flow in the natural ventilation shaft of urban tunnel

Xiaofeng Chen[1,2,3], Ke Wu[1,2,3], Yachao Li[4], Xin Zhang[5], Fanghong Zhao[4], Tianhang Zhang[1,2,3]
1, Research Center for Urban Fire Safety Engineering, Zhejiang University., Hangzhou, China
2, Center of Balance Architecture, Zhejiang University., Hangzhou, China
3, Key Laboratory of Offshore Geotechnics and Material of Zhejiang Province, Zhejiang University., Hangzhou, China
4, China Railway Tunnel Stock CO., LTD. Zhengzhou, China
5, College of Electronic Engineering, Xi'an Shiyou University., Xi'an, China
E-mail: thz@zju.edu.cn

KEYWORDS: Urban tunnel fire, natural smoke exhaust, natural ventilation shaft, bidirectional flow

INTRODUCTION

Natural ventilation shaft is a new method for exhausting fire smoke with zero energy consumption, maintenance-free, and high reliability. The cross-section of the shafts in the previous studies is generally small (as shown in Table 1), and there are two typical flow phenomena: "Boundary layer separation" and "Smoke pull-holing" (bottom air in tunnel invades the shaft) [1,2], which are unidirectional flow. In order to eliminate as many pollutants or smoke as possible, the cross-sectional dimension of natural ventilation shafts has gradually become larger, such as the shaft with an area of 40 m^2 in Shanghai Beidi Road Tunnel and the shaft with an area of 55.8 m^2 in Nanjing Shuiximen Tunnel. Although the larger shafts can improve the smoke exhaust ability, the large cross-section will also induce the ambient air into tunnel, forming a "Bidirectional flow" [3-5]. The "Bidirectional flow" may destroy the smoke layer, which not only reduces the smoke exhaust efficiency but also affects the evacuation. It should be noted that the formation mechanism of the "Bidirectional flow" phenomenon in the shaft has not yet been revealed, and the triggering conditions are not yet clear.

Table 1 Geometric characteristics of natural ventilation shafts in urban tunnels

Authors	L_s/m	W_s/m	H_s/m	A_s/m^2
Ji, 2012	1.8	1.8	0~6	3.24
Fan, 2014	2~4	1~3	5	2~12
Zhang, 2018	2	3	1.5~6	6
Jiang, 2020	2	3~6	3	6~12
Xie, 2018	4	4	5	16

In this work, the influence of shaft area and shaft aspect ratio on the flow state in the shaft was investigated through the CFD method, and the formation mechanism and triggering conditions of the "Bidirectional flow" were clarified. The research results provide a new perspective for the design of natural smoke exhaust in urban tunnels.

NUMERICAL METHOD

Fire dynamics simulator (FDS) software is adopted to simulate the tunnel fire scenarios in this work. An urban tunnel model with two natural ventilation shafts was constructed. The tunnel length, width, and height are 300 m, 12 m, and 5 m respectively. The fire HRR is 5 MW, simulating a car fire (Trucks or bus are not allowed to enter urban tunnels), which is located between the two shafts. To

improve the calculation efficiency, this paper adopts symmetric boundaries, as shown in Fig. 1. Thermocouples with a spacing of 1.0 m are arranged 0.2 m below the tunnel ceiling (Fig. 1a). To capture the smoke temperature characteristics and flow characteristics, some slices are set in the middle of the tunnel section (Fig. 1b). In order to explore the influence of the shaft cross-section size on the gas flow in shaft, multiple cross-sectional sizes were set regarding Table 1 and recent tunnel projects [3-5]: 16 ~ 144 m^2, corresponding to shaft area ratio α (shaft area/tunnel section area) of 0.32~2.88. In addition, multiple aspect ratios β of the shaft are considered as 0.36~10.67. The shaft height was set to 4 m, which was a common value in practical projects. And the grid-independent test has been conducted in other works of our team.

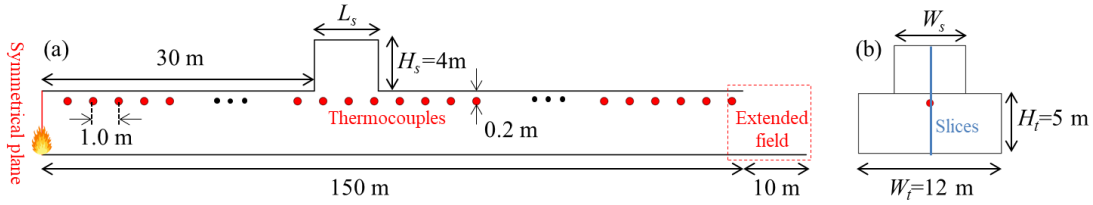

Figure 1 Numerical model tunnel and measurement point layout

RESULTS AND DISCUSSION

There will be “Bidirectional flow” in natural ventilation shafts with excessive cross-section and deteriorating evacuation conditions. The effect of shaft area ratio α and aspect ratio β on the gas flow pattern was investigated numerically. The results show that the increasing area ratio α will decrease the static pressure difference, resulting in the shaft flow pattern being changed from “Unidirectional flow” to “Bidirectional flow”. Its critical α_c is about 1.1~2.0 (Fig. 2), which is significantly smaller than 5.76 of the compartment fires. The increasing shaft aspect ratio β weakens the exhaust capacity of the shaft upstream but strengthens the shaft side. The “Bidirectional flow” occurs in the wide-short (small β) and narrow-long (great β) shafts with a certain area ratio. The mechanism of “Bidirectional flow” and the critical conditions were revealed, which improves the design theory of natural ventilation and smoke exhaust in urban tunnels.

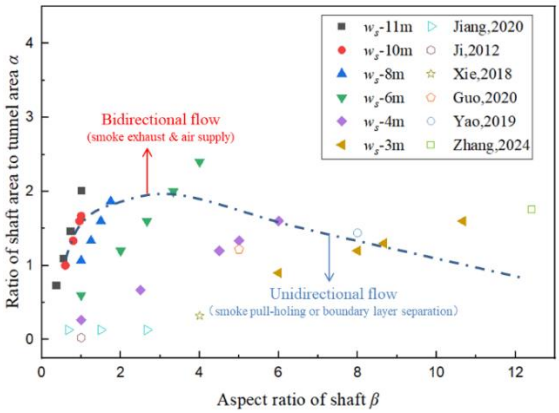

Figure 2 Classification of flow patterns in natural ventilation shafts from this work and previous studies

REFERENCES

[1] Ji J., Gao Z., Fan C., Zhong W., and Sun J., "A study of the effect of plug-holing and boundary layer separation on natural ventilation with vertical shaft in urban road tunnel fires", *International Journal of Heat and Mass Transfer*, **55**, 6032-6041,2012.

[2] Jiang X., Xiang Y., Wang Z., Mao Y., and Park H., "A numerical study on the effect of the shaft group arrangement on the natural ventilation performance in tunnel fires". *Tunnelling and Underground Space Technology*, **103**, 103464, 2020.

[3] Zhang G., Peng T., Tong Y., Gong Y., Chen Z., Huang W., and Dai B., "Full-scale experiments on the fire smoke extraction from naturally ventilated shafts for shallow-buried urban road tunnels in hot summer". *Tunnelling and Underground Space Technology*, **143**, 105441, 2024.

[4] Yao Y., Li Y., Ingason H., and Chen X., "Numerical study on overall smoke control using naturally ventilated shafts during fires in a road tunnel". *International Journal of Thermal Sciences*, **140**, 491-504, 2019.

[5] Guo Q., Zhu H., Zhang Y., Shen Y., Zhang Y., and Yan Z., "Smoke flow in full-scale urban road tunnel fires with large cross-sectional vertical shafts". *Tunnelling and Underground Space Technology*, **104**,103536, 2020.

Life-safety targets in underground stations, continued

Erik Hall Midholm[1], Johan Lundin[1], Bo Wahlström[1], Oskar Jansson[2]
[1] Brandskyddslaget AB; [2] RiskTec Projektledning AB
Långholmsgatan 27 10 tr, SE-117 33 Stockholm, Sweden
E-mail: erik.midholm@bsl.se

KEYWORDS: underground station, submerged platform station, safety target, risk analysis, life-safety, severe accident, dangerous goods, fire.

INTRODUCTION

The Swedish Transport Agency and the Swedish Transport Administration have carried out two pivotal research and development projects titled "Life-safety targets in underground stations." The first report assessed the feasibility of formulating a harmonized life-safety target for platform areas, while the follow-up report in 2023 further developed and validated these initial conclusions. The goal was to lay the foundation for national legislation and improve regulatory risk control in underground stations.

Current regulations set safety design requirements for underground platforms but lack standardized life-safety targets, leading to variability in safety levels and approval processes across projects and transport modes. This research tackles both frequent, low-consequence incidents (such as suicides and falls) and rare, high-consequence events (including large fires and dangerous goods accidents).

METHODOLOGY

This study introduces a comprehensive, risk-based methodology to develop and assess safety targets for underground stations, focusing on the complexity of station design, potential accident scenarios, and passenger volume. A new risk framework is proposed that challenges traditional safety approaches for Swedish underground stations by integrating societal and individual risk metrics with assessment tools.

The methodology is structured around six key investigations, which are meant to cooperate, achieving a equivalent safety level in both ordinary underground stations and more complex facilities:

A. **Defining acceptable societal and individual risk levels**, with a unified approach to underground station safety.
B. **Developing a regulatory framework (basic standard)** aligned with proposed safety standards and assessing their applicability.
C. **Evaluating the adequacy of the basic standard** for simple platform areas, determining when it requires adaptation.
D. **Assessing catastrophic accident scenarios** (e.g., incidents involving >1,000 casualties) using quantitative methods.
E. **Cost-benefit analysis** within the ALARP (As Low As Reasonably Practicable) framework to determine the need for additional safety measures.
F. **Contextualizing safety objectives** within broader risk management systems and regulatory practices.

RESULTS AND DISCUSSION

The proposed methodology offers a new perspective on safety target formulation, emphasizing the need for a tiered approach based on station complexity. For simpler platform areas, the basic safety standard, aligns with existing safety requirements under the Swedish Planning and Building Act.

For more complex environments, the methodology employs quantitative analysis to assess potential risks and determine the need for additional measures. While traditional ALARP principles guide this analysis, the proposed methodology enhances its application by offering more robust decision-making criteria for complex underground environments.

Quantitative safety targets: The research also introduces a safety target system: with an upper limit reflecting "Safety targets in tunnels" that sets a baseline acceptable risk level for underground stations. The safety target, however, lacks a lower limit. This ensures a generally lower risk level in platform areas compared to adjacent tunnels, due to better risk management possibilities. This approach bridges the gap between tunnel and platform safety, ensuring that underground stations are not only safe but are held to a consistently high standard across diverse risk scenarios. A major innovation of the study is its focus on accidents with catastrophic potential, an area typically underexplored in current safety frameworks.

Cost benefit analysis: An advanced cost/benefit analysis methodology is incorporated to optimize safety measures against their associated costs, providing a more scientifically rigorous approach to ALARP. By assessing additional safety measures required in non-standard scenarios, this analysis ensures that resources are allocated efficiently, addressing the most pressing risks while minimizing unnecessary expenditures.

CONCLUSION

The proposed framework offers several key contributions to the field of underground station safety:

- **Scientific Innovation**: The integration of individual and societal risk measures into a unified safety target system challenges traditional risk management for Swedish underground stations by offering a more precise, scientifically grounded approach to safety assessment.
- **Targeted Safety Measures**: A more granular, quantitative safety target system provides better differentiation between varying levels of station complexity and accident risk.
- **Efficient and Cost-Effective Regulation**: The framework aligns with existing regulatory structures, ensuring its integration into current safety protocols without significant cost increases.
- **Global Relevance**: The research provides a universal approach to safety target formulation that could be adapted to other countries and transport systems, driving international harmonization in underground station safety standards.

By advancing risk assessment methodologies, challenging traditional safety frameworks, and presenting scientifically derived life-safety targets, this research paves the way for a more standardized, evidence-based approach to safety in Swedish underground stations and similar infrastructure projects.

REFERENCES

1. Lundin, Wahlström, Hall Midholm, Jansson, “Life-safety objectives for underground platform areas” (in Swedish), Transportstyrelsen, 2021.
2. Lundin, Wahlström, Hall Midholm, Jansson, “Life-safety objectives for underground platform areas – part 2” (in Swedish), Transportstyrelsen, 2023.

Research on the Ceiling Maximum Temperature in Inclined Tunnel Fires Based on a Non-Orthogonal Ventilation Plume Model

Lei Liu[1,2,3], Ke Wu[1,2,3]& Tianhang Zhang[1,2,3]
[1]Key Laboratory of Offshore Geotechnics and Material of Zhejiang Province, Zhejiang University, Hangzhou 310058, China
[2]Center for Balance Architecture, Zhejiang University, Hangzhou 310058, China
[3]Research Center for Urban Fire Safety Engineering, Zhejiang University, Hangzhou 310058, China
E-mail: wuke@zju.edu.cn

KEYWORDS: Inclined Tunnel fire, Non-orthogonal ventilation, Maximum ceiling temperature

INTRODUCTION

Tunnel fire safety research identifies maximum ceiling temperature as a critical risk indicator. Key classical models – Alpert's ceiling jet theory [1], AGA correlation [2],, and Li's plume model [3]– were developed under horizontal tunnel assumptions where ventilation airflow is perpendicular to the vertical fire plume(Fig. 1a). For inclined tunnels, many scholars established empirical formulas for the maximum ceiling temperature via scaled experiments or simulations[4–7]. It is worth noting that most previous prediction models are based on dimensional analysis and data fitting methods. They do not consider the plume model from the perspective of ventilation and plume interaction. In other words, the models proposed by previous researchers are data fittings of physical quantities, whose extensibility is limited by the data itself. Actrually, in inclined tunnels, the ventilation direction should be parallel to the tunnel line (inclined) whereas the buoyancy (gravity) still keeps vertical (Fig. 1b). This leads to the non-orthogonal interactions between the airflow's inertial forces and the plume's buoyancy, resulting in different dynamic effects from existing plume models. In response to a deeper understanding of the tunnel fire scenario in the inclind tunnel, the current study proposes a novel correlation for the ceiling temperature rise. This model is grounded in the dynamics of plume behavior under non-orthogonal ventilation and aims to provide robust theoretical guidance for fire protection design, smoke detection, and firefighting strategies in inclined tunnel environments.

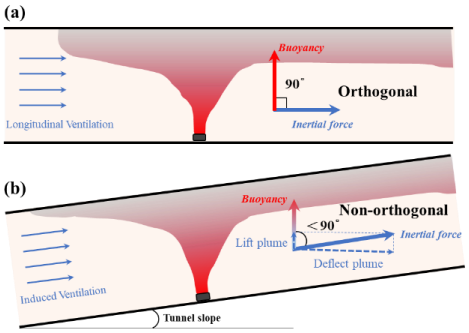

Fig. 1. Diagram of ventilation and plume interaction in (a) horizontal longitudinal ventilation tunnel (b) natural ventilation inclined tunnel

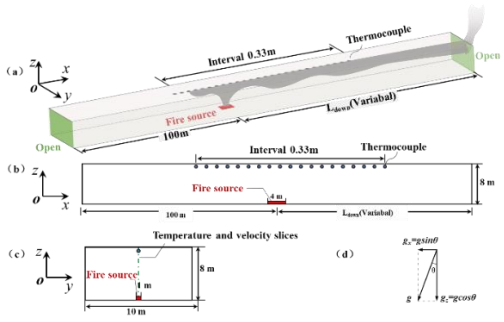

(a) 3-D view (b) Side view (c) Cross-section view (d) Effective gravitational acceleration
Fig. 2. Numerical model of the tunnel.

METHODOLOGY

A comprehensive series of numerical simulations is conducted using the Fire Dynamics Simulator (FDS) to explore the behavior of fire plumes and ceiling temperatures in inclined tunnels. The tunnel model, with dimensions of 10 m in width, 8 m in height, and the length of the downstream of fire source ranges from 50 m to 1000 m (Fig. 2a-c), is subjected to different heat release rates (HRR) of 5 MW, 10 MW, and 20 MW, representing typical fire scenarios for vehicles in urban tunnels. The range of inclination angles studied is from 1% to 10%, simulated by adjusting the gravitational acceleration to

reflect the common slopes in actual tunnels (Fig. 2d). Detailed temperature data are collected from multiple measurement points beneath the tunnel ceiling to analyze the impact of slope and induced airflow on plume behavior. The selection of grid sizes for the simulations is rigorously based on sensitivity analyses to ensure the precision and stability of the results. The model's predictions are validated against experimental data from prior research to establish its reliability and applicability

RESULTS AND DISCUSSION

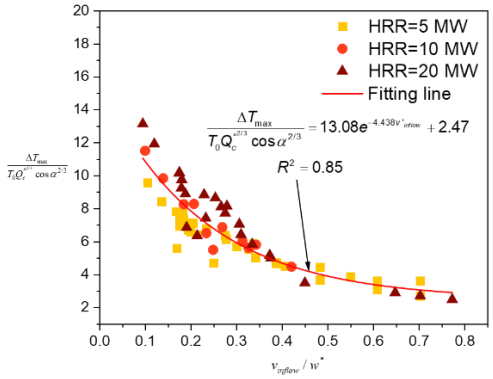

Fig. 3. Establishment of the Ceiling Maximum Temperature Prediction model

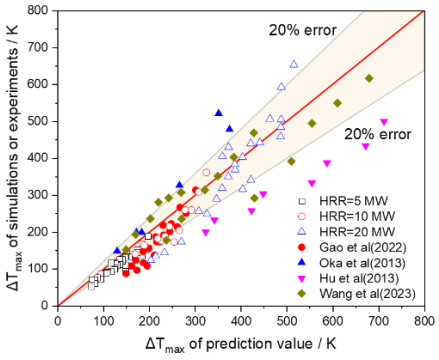

Fig. 4. Validation of the Ceiling Maximum Temperature Prediction model

The results indicate that as the tunnel slope increases and the downstream length of the fire source grows, the chimney effect within the inclined tunnel intensifies. This leads to a stronger induced airflow on the lower slope side, which consequently results in a reduction in the maximum ceiling temperature. An analysis of the forces acting on the fire plume during its rise in the inclined tunnel reveals that the induced airflow interacts with the fire plume at a non-orthogonal angle, decomposing into horizontal and vertical components (see Fig. 1b). The horizontal component, perpendicular to the buoyancy, causes the plume to deflect, similar to the behavior observed in horizontal tunnels. Meanwhile, the vertical component, aligned with the buoyancy, drives the plume upward. The combined effects of these interactions lead to a reduction in the maximum ceiling temperature and a downstream shift of the plume's impact point.

Based on this force analysis, a modified dimensionless wind speed, V', is proposed. This wind speed characterizes the coupling effect between the vertical buoyancy force and the horizontal deflection inertia acting on the plume within the inclined tunnel. Additionally, by examining the relationship between the gas mass flow rate under ventilated conditions and in an open, windless environment, $m_{ventilation}/m_{open} = KV'$, and incorporating the empirical formula relating fire source power to the maximum temperature, $Q = \lambda c_p m \Delta T_{max}$, an empirical equation for the maximum ceiling temperature rise in a inclined tunnel is derived. Finally, by fitting the equation to numerical simulation data, a predictive equation for the maximum ceiling temperature rise in inclined tunnels is obtained (see Fig.3). The model provides a more accurate prediction for fire behavior in inclined tunnels, and is verified with previous experimental data, confirming the accuracy and applicability of the model (see Fig.4).

REFERENCES

[1] R.L. Alpert, Calculation of Response Time of Ceiling-Mounted Fire Detectors, n.d.
[2] P.P.K. Raj, A.N. Moussa, K. Aravamudan, Experiments involving pool and vapor fires from spills of liquefied natural gas on water, 1979.
[3] Y.Z. Li, B. Lei, H. Ingason, The maximum temperature of buoyancy-driven smoke flow beneath the ceiling in tunnel fires, Fire Saf. J. 46 (2011) 204–210.
[4] L.H. Hu, L.F. Chen, L. Wu, Y.F. Li, J.Y. Zhang, N. Meng, An experimental investigation and correlation on buoyant gas temperature below ceiling in a slopping tunnel fire, Appl. Therm. Eng. 51 (2013) 246–254.
[5] Z. Gao, L. Li, C. Sun, W. Zhong, C. Yan, Effect of longitudinal slope on the smoke propagation and ceiling temperature characterization in sloping tunnel fires under natural ventilation, Tunn. Undergr. Sp. Technol. 123 (2022) 104396.
[6] J. Ji, H. Wan, K. Li, J. Han, J. Sun, A numerical study on upstream maximum temperature in inclined urban road tunnel fires, Int. J. Heat Mass Transf. 88 (2015) 516–526.
[7] X. Zhang, Y. Lin, C. Shi, J. Zhang, Numerical simulation on the maximum temperature and smoke back-layering length in a tilted tunnel under natural ventilation, Tunn. Undergr. Sp. Technol. 107 (2021) 103661.

Multidirectional Pedestrian Flow Dynamics: Impact of Cultural Differences on Individual and Group Movement

Nashiru Mumuni Daniel Bilintoh (PhD), Jun Zhang, (Professor) & Rehmat Karim, (PhD)
State Key Laboratory of Fire Science, University of Science and Technology of China, Hefei 230027, China E-mail: bilnash@mail.ustc.edu.cn

***Keywords**: Multidirectional* pedestrian flow, Cultural influence on movement, social group dynamics, Pedestrian behavior analysis, Crowd movement efficiency.

Introduction

The study of pedestrian group dynamics highlights how cultural influences shape collective behavior. Navigation involves complex group interactions, with cultural backgrounds, impacting priorities and coordination. Collectivist cultures may stress group cohesion, while individualist cultures often allow more independent movement. [1][2]

Several studies [3]were conducted at various densities of pedestrians while considering social groupings to understand better how one gets to their destination in a crowd with multidirectional mobility [4][5]. There was noticeable difference in the experiment between the velocities of individuals and social groups. Individuals' walk paths, in contrast, were 3.1% longer than those of social groups. The experiment showed various methods for getting pedestrians to their destinations. 55.4% of pedestrians with behaviors associated with acceleration walked directly to their goals. 3% -10% of pedestrians used detour behavior to shorten their distance traveled during the multidirectional restricted movement stage, notably for individuals. In the behaviors of waiting and following, 44.6% of pedestrians preferred their initial approach, whereas 5% modified it to take other behaviors, which might shorten their movement time.

Materials and conditions

The experiment was conducted at Wa Senior High School, Ghana, in June 2021. It involved 72 participants, consisting of high school students and teachers between the ages of 17 and 50. Recognizing that gender can influences pedestrian dynamics such as walking speed [6], The ratio of males to females is only considered if it is close to 1:1. They were all in good physical and mental health.

Each participant positioned themselves equally around a circular perimeter with a radius of 5m. Participants were instructed to walk toward the opposing side of the circle to create a multidirectional flow. Each one moved in a different direction. In each experiment, the number of flows equals the number of pedestrians. All participants began moving simultaneously after giving the start instruction. pedestrian trajectories were extracted from the video recording with Blender and PeTrack software. The entire experiment's trajectory data was also manually corrected. The trajectory data were collected at 25 frames per second and calculated using a global density: $\rho_{global} = {}^{N}/_{L}$, where the number of person's N, setup participants in our experiments is 13, 24, 36, 48, 60, and 72. The circumference of a circle ($2\pi r$) is L. The pedestrian number in experiment index 1 is 13, and the global density equals the number of participants ${}^{(13)}/_{(31.4)} = 0.41 ped/m$. Analysis with OriginPro.

Characteristics of pedestrians' behavior and trajectories

Experiment conducted investigated the influence of cultural on pedestrians in social groups and individuals navigating multidirectional flows,[7][8] using a detailed data analysis procedure described. Four behaviors associated with pedestrians were identified during the movement[5];

These four behaviors were examined; behaviors associated with acceleration (BAA), behaviors of wait

and follow (BWF), detour behaviors (DB), and other behaviors (OB). Based on our analysis,[8][5] the Ghanaian pedestrian's average speed was 1.34m/s, with behavior associated with acceleration (BAA) of 9:22s at a low density and 13.22s at a high density with a speed of 0.34m/s. The Chinese time was 7:89s, while the average speed was 1.22m/s and 15:25s with an average speed of 0.15m/s. Concerning detour behavior (DB), the Ghanaians had 10:00s with a velocity of 1.08m/s and 12.44s with a velocity of 0.44m/s, while the Chinese had 9:00s with an average speed of 1.08m/s, and 11:68s with an average velocity of 0.76m/s. During the experiment, the analysis revealed differences in behaviors, body weight, and highness between all pedestrians, possibly due to cultural differences.

Discussion and findings

The research conducted examined pedestrian behavior when people moved in multidirectional flows, paying attention to how culture and social cliques affected things[5]. Four significant behaviors emerged: acceleration, waiting and following, detours, and other behaviors. As it turned out, lone individuals proved quite nimble at sidestepping bottlenecks[9], whereas packs proceeded ponderously since they had to stick together. Cultural differences played a significant role, with collectivist cultures emphasizing group cohesion and individualist cultures promoting faster, independent movement [8].

The findings highlighted how cultural contexts shape pedestrian trajectories, with individuals often exhibiting greater flexibility and adaptability compared to groups. Detour behavior proved effective in optimizing movement and reducing congestion, while waiting and following strategies emphasized collision avoidance. The experiments also demonstrated that group dynamics could slow overall movement efficiency, particularly in high-density conditions.

Conclusion

Pedestrian behavior revealed valuable insights into the influence of cultural factors on group and individual movement dynamics in multidirectional flows.

By linking cultural influences on pedestrian movement strategies, this research offers a framework for improving crowd management systems and evacuation protocols. The results can inform urban planning, event management, and safety strategies in culturally diverse settings, ensuring smoother pedestrian flows and enhanced public safety. Future studies should explore the role of demographic factors, such as age and gender, and refine behavioral models for broader applications.

References

[1] R. Brislin, “Encouraging Depth Rather than Surface Processing about Cultural Differences Through Critical Incidents and Role Plays,” p. p 7, 2002.

[2] N. M. D. Bilintoh, J. Zhang, R. Karim, and W. Rafaqat, “Experimental study of the effects of culture and location on single-file fundamental diagrams,” *Heliyon*, vol. 9, no. 9, p. e19378, 2023, doi: 10.1016/j.heliyon.2023.e19378.

[3] F. Zanlungo, L. Crociani, and Y. Zeynep, “The effect of social groups on the dynamics of bi-directional pedestrian flow : a numerical study,” pp. 1–18, 2019.

[4] J. J. Faria, S. Krause, and J. Krause, “Collective behavior in road crossing pedestrians: The role of social information,” *Behav. Ecol.*, vol. 21, no. 6, pp. 1236–1242, 2010, doi: 10.1093/beheco/arq141.

[5] Y. Hu *et al.*, “Experimental study and analysis on behaviours and strategies of social groups and individuals,” *Saf. Sci.*, vol. 127, no. March, p. 104736, 2020, doi: 10.1016/j.ssci.2020.104736.

[6] et al. A. Willis, “Human movement behaviour in urban spaces: Implications for the design and modelling of effective pedestrian environments,” *Environ. Plan. B Plann. Des.*, pp. 31 (6) (2004) 805–828., 2004.

[7] M. Moussaïd, N. Perozo, S. Garnier, D. Helbing, and G. Theraulaz, “The walking behaviour of pedestrian social groups and its impact on crowd dynamics,” *PLoS One*, vol. 5, no. 4, pp. 1–18, 2010, doi: 10.1371/journal.pone.0010047.

[8] M. K. Biswal, “Comparison of Pedestrian Fundamental Diagram : a Cultural and Gender Aspect Comparison of Pedestrian Fundamental Diagram : a Cultural and Gender Aspect,” vol. 6, no. 7, pp. 246–254, 2014.

Integrating Risk-Based Design into a Decision Support System for Enhancing Fire Resilience in Road Tunnels

Marta Galuppi, Davide Berardi & Mara Lombardi
Sapienza University of Rome
Via Eudossiana, 18 Rome
E-mail: marta.galuppi@uniroma1.it

KEYWORDS: tunnel fire; decision support system; risk based design; road tunnel safety; sustainability; tunnel resilience indicator.

INTRODUCTION

The proposed research aims to develop an integrated risk-based monitoring and verification system to improve safety and sustainability conditions for road tunnels, specifically those classified as bidirectional and longer than 1000 meters, which require a ventilation system in compliance with Directive 2004/54 [1] on minimum safety requirements for tunnels in the Trans-European Road Network. This framework is implemented through the development of a Decision Support System (DSS) to enhance fire resilience.

MATERIAL AND METHOD

The proposed innovation in the infrastructure resilience management enables the definition of an integrated risk-based monitoring and verification system, " aimed at improving safety and sustainability conditions for road tunnels. This conceptualized Decision Support System (DSS) integrates the concepts of safety and sustainability, both of which contribute to enhancing the resilience of road infrastructure. The system architecture is illustrated in figure 1.

Critical initiating events serve as precursors for modelling representative scenarios for risk assessment. Once these scenarios are defined, a quantitative probabilistic risk analysis model is adopted to verify the safety conditions of the tunnel. This model combines Event Tree Analysis with exposure and damage estimation, allowing for the quantification of the Individual Risk Indicator (annual probability of death for an exposed individual) due to hazards arising from the evolution of initiating events and their expected impact on road tunnel users [2].

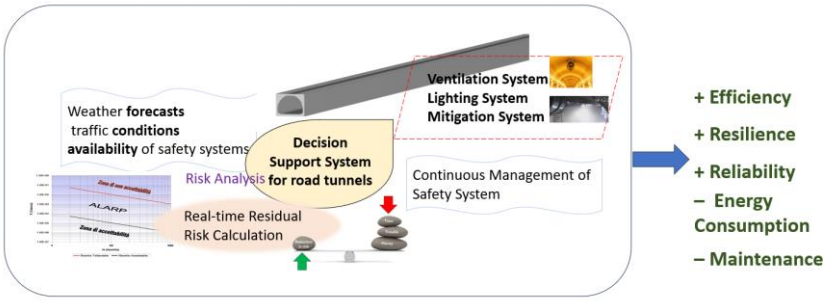

Figure 1 DS4T: Design overview

The model's output consists of quantitative risk indicators over time, particularly estimating risks to human life based on the Expected Damage Value, which defines the Individual Risk and introduces the concept of real-time risk analysis. Specifically, the Individual Risk Indicator is evaluated by considering the exposure level of the analyzed area as a normalization factor. This logically structured representation of the sequence of events is explained by critical initiating event, which serve as connection points between causes and consequences. The coherence and stability of the final risk indicators depend on the number of simulations conducted for the Event Tree Analysis. The representativeness of the indicators developed through the risk analysis process is based on the synthesis of a comprehensive set of scenarios fitting the initial event, supported by the computational capacity of the simulator such us

the Fire Dynamic Simulator (FDS) [3], particularly for fire events, and in accordance with the boundary conditions.

RESULTS

A specific application of the Decision Support System (DSS), currently in the refinement phase, concerns a critical event in road tunnel safety design: fire. In recent years, fire safety management in tunnels has become closely linked to artificial intelligence. To enhance the DSS's ability to detect different types of fires and promptly activate emergency procedures, a reference database has been integrated with fire test data, thereby improving its response capabilities.

The process illustrates the entire cycle of tunnel safety systems management during a fire scenario, highlighting how real-time data collection, transmission, and processing are essential to ensuring the effectiveness of the safety measures implemented. The use of full-scale fire tests provides valuable insights into the functionality and resilience of tunnel safety systems, ensuring reliable operation in real emergency situations.

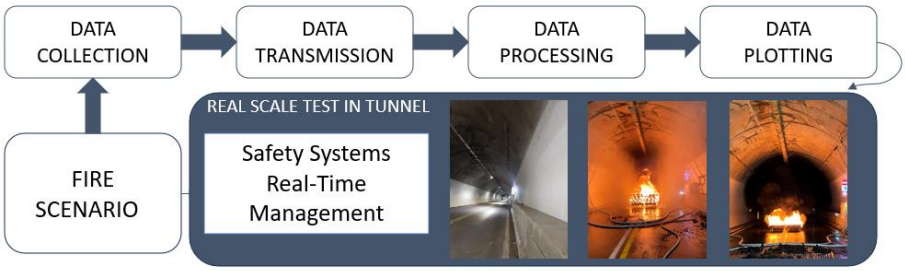

Figure 2 DS4T: Application to fire road tunnel management

DISCUSSION

The proposed application is innovative in its objective of connecting the operation of different safety systems within the tunnel through an integrated approach. In common practice, these systems are typically managed independently, such as ventilation and fire suppression algorithms. Proper coordination of these systems is essential for their effective operation, and the DSS can support the entire system during emergencies. In line with this premise, the innovation of DS4T is particularly effective in enhancing the reliability of tunnel systems where structural deficiencies cannot be address (e.g., the absence of intermediate emergency exits). Additionally, it is highly effective for new tunnels, optimizing, for instance, the design of smoke extraction systems without increasing construction costs while simultaneously reducing operational and maintenance expenses. This can be achieved through the integration of safety systems, such as the water mist system and longitudinal ventilation, by designing for lower ventilation power while ensuring tunnel structure protection through the compensatory effect of the water mist system.The management of infrastructure resilience is therefore based on continuous monitoring during operation and modulation of the integrated functionality of system elements, both under normal and emergency conditions, ensuring user safety.

ACKNOWLEDGMENTS

This study was carried out within the RETURN Extended Partnership and received funding from the European Union Next-GenerationEU (National Recovery and Resilience Plan—NRRP, Mission 4, Component 2, Investment 1.3—D.D. 1243 2/8/2022, PE0000005).

REFERENCES

1. European Parliament and Council. Directive 2004/54/EC. Official Journal of the European Union. L.167, Bruxelles. Availableonline: https://eur-lex.europa.eu/legalcontent/EN/TXT/?uri=celex%3A32004L0054.
2. M. Guarascio, M. Lombardi, G. Rossi & G. Sciarra,Risk Analysis And Acceptability, WIT Transactions on The Built Environment,2007,94,8, doi: 10.2495/SAFE070131
3. McGrattan, K. , McDermott, R. , Weinschenk, C. and Forney, G. (2013), Fire Dynamics Simulator, Technical Reference Guide, Sixth Edition, Special Publication (NIST SP), National Institute of Standards and Technology, Gaithersburg, MD.

Safety Aspects of the Technical Galleries Consolidation Program

Iga Krautsztrung & Sebastien Evrard & Olivier Prouteau
CERN European Organization for Nuclear Research
Esplanade des Particules 1, Meyrin, Switzerland
E-mail: iga.maria.krautsztrung@cern.ch

KEYWORDS: Emergency preparedness, personnel safety, environmental protection, infrastructure consolidation, infrastructure optimization

INTRODUCTION

The distribution of services throughout a large scientific facility like CERN relies on a 14-km network of technical galleries. They provide essential utilities to CERN's office buildings and technical facilities, including hot water, drinking water, compressed air, gas, and electrical supply. The ongoing Technical Galleries Consolidation Project aims to address existing issues and refurbish the conditions of the galleries and their related infrastructure to the extent reasonably possible. [1]

At the core of the Project, alongside the renovation of services hosted in technical galleries, is the improvement of safety to ensure the protection of the personnel and the environment, property preservation, and business continuity at CERN. In 2021, comprehensive studies were conducted to evaluate multiple safety aspects. As a result, the official rules and procedures were established to address the most important safety questions that had not been previously considered within the context of technical galleries. Unlike other projects at CERN, the Technical Galleries Consolidation Project addresses the existing systems which were built in the late fifties. Since then, the safety rules have changed significantly. This is why TG-CONS is a unique opportunity to conduct detailed and holistic studies on many safety aspects that had not previously been considered.

COMPLETED STUDIES

To identify the risks, an extensive inventory was done, resulting in a survey report. To respond to all the recognized hazards, several studies were conducted regarding fire safety and emergency preparedness, Oxygen Deficiency Hazard, environmental pollutants, ventilation, access, and access control. A preliminary risk register was developed to ensure risk control and appropriate responses. Each issue was analyzed with the corresponding expert Group, documented in reports, and reviewed with the HSE – Health and Safety Engineering Unit at CERN. Some of the studies are transversal, making them suitable for application in other facilities.

One of the crucial studies, with significant potential for transferability, concerns alert and alert-triggering technology. As a result, the Emergency Call Point System is currently under development to address the identified need for a reliable two-way communication system between the galleries and the CERN Fire and Rescue Service. [2] This system is designed to meet a wide range of functional requirements such as providing unambiguous geolocation, uninterrupted operation in case of power failure, and adaptability to different environmental conditions (e.g., underground). Approximately 35 call points will be installed in the technical galleries of the West Area at the Meyrin CERN site by the end of 2026. As a future step, the Emergency Call System will serve as a dependable means of communication for hotels, cold rooms, areas designated for reduced mobility, and kindergarten facilities located within CERN.

To further enhance emergency preparedness, all the access points were reviewed, and certain upgrades were planned. All entrances will be refurbished to meet the current safety standards and will be equipped with an access control system, preventing unauthorized visits.

INDIVIDUAL SAFETY MEASURES

One of the aspects provided by the Project is the individual safety measures to be applied when visiting the galleries. In addition to collective measures – safety systems described above – the following rules should be respected. As in all technical buildings, at a strict minimum, Personal Protective Equipment must be worn (safety shoes, a helmet with a headlamp). Due to the detected risk of oxygen deficiency in the galleries, a portable ODH detector is mandatory. Solitary visits must be avoided due to limited mobile phone signal coverage and the low occupancy of the premises. When moving through the corridors, personnel should respect local signs, keep the fire doors closed, and avoid touching unknown equipment. Adhering to these simple rules, in alignment with the Pareto principle, can prevent the most common personnel accidents.

EMERGENCY SIGNS, LIGHTS, AND ESCAPE ROUTES

To enhance safety in the technical galleries in case of emergencies, a general evacuation plan has been developed for all the galleries located in the Meyrin West Area (in accordance with the established consolidation sequence). [3] Along with the escape routes plan, emergency signs and lights will be deployed on-site. The equipment will be installed in a coordinated manner to ensure the most effective cooperation between the systems and provide maximum safety for personnel.

SYNERGIES OF EFFORTS AND BENEFITS

The TG-CONS Project strives to think globally, seeking synergies that would allow mutual benefits and greater progress. In collaboration with the North Area Consolidation Project, a large joint study regarding the consolidation of fire-retardant partitions in the North Area was carried out. As a result, 63 fire doors compliant with the latest safety standards will be upgraded by 2027, limiting the spread of fire and smoke in case of an accident. The Project not only aims to fulfill its mandate but also to create added value for the entirety of CERN. To better analyze, plan, and optimize the existing equipment layout in the galleries, 3D integration models are developed. Thanks to them, the Project can provide CERN with reliable, up-to-date information on the gallery-housed equipment.

ENVIRONMENTAL PROTECTION

Like any consolidation project, TG-CONS must handle legacy issues by removing obsolete equipment, resulting in substantial waste production. In the first two years of consolidation, more than 337 tons of old piping and material have already been removed – 6.1 kilometers of old piping have been dismantled and replaced by 4.7 kilometers of new piping. In addition, as a result of several decabling campaigns, a total of 397 kilometers of cables were removed. To make the best usage of the obsolete equipment deemed for disposal, unpolluted materials such as pipes or cables are sold to external companies for recycling. This approach enables the Project to recover capital from reusable resources and minimize waste to the unavoidable minimum. One of the challenges to overcome is the diagnostics, removal, and disposal of polluting and hazardous materials such as asbestos, lead, polycyclic aromatic hydrocarbons (PAH), or polychlorinated biphenyls (PCB), found in items like cable trays, paints, pipes insulation, and glue.

CONCLUSIONS

With the recognition of the Project's importance, it is imperative to make every necessary effort to ensure the refurbishment of the galleries to a level that guarantees the services' safety, reliability, and optimal expansion in line with CERN's future facility development. Undoubtedly, a profound commitment from multiple Groups will be crucial to reach this goal, but its achievement will establish a solid foundation for all CERN operations.

REFERENCES

1. CERN (2021) Technical Galleries Consolidation. Available at: https://tg-cons.web.cern.ch/ (Accessed: 27 February 2025)
2. "Emergency Call System for Technical Galleries Progress Report - Presentation to HSE (5th April 2023)" by E. Sanchez-Corral, J. Ramos, H. Nissen, EDMS 2823833
3. "General Evacuation Plan For CERN's Technical Galleries: Meyrin West Area" by J. P. R. Grandvillemin, EDMS 2921024

Optimization of passive fire protection in cut-and-cover concrete tunnels through numerical structural analysis

Thomas Thienpont & Ruben Van Coile
Department of Structural Engineering and Building Materials, Ghent University
Ghent, B-9000, Belgium
E-mail: Thomas.Thienpont@UGent.be

KEYWORDS: Structural Fire Engineering, Optimized passive fire protection, Concrete Spalling, Finite element modelling,

Introduction

Tunnel fires are catastrophic events that can compromise structural integrity, causing significant economic and safety risks. In reinforced concrete tunnels, spalling – the explosive detachment of the concrete surfaces – can exacerbate fire damage by reducing the structural cross-sections and by directly exposing the reinforcing steel to high temperatures [1]. Although prior research has thoroughly explored spalling in tunnels with circular cross-sections [2], there is limited research on its effect in shallow cut-and-cover rectangular tunnels, common in urban settings. This study investigates the influence of spalling location on the structural fire response of a cut-and-cover rectangular tunnel, and explores the optimal application of passive fire protection to prevent structural collapse. Numerical analyses, using the SAFIR finite element software and a custom Python script, were conducted to simulate fire exposure under the Rijkswaterstaat (RWS) fire curve. Six localized spalling scenarios were analyzed to evaluate how spalling in specific regions (roof slab, outer wall, and inner wall) impacts the tunnel's structural response. Based on the results of these analyses, an optimized passive fire protection design can be derived.

Methodology

The present study utilizes a numerical finite element approach to investigate the effect of localized spalling on the structural fire response of a shallow rectangular tunnel. A 2D model of the tunnel cross-section is developed using the SAFIR finite element software, supplemented by a custom Python script to account for concrete spalling. The details of this approach are outlined in [3].
The reinforced concrete tunnel examined in the study consists of two four-lane traffic tubes and a central evacuation shaft, see the Figure below. Spalling was modelled as the progressive removal of concrete cover layers at a constant rate of 5 mm/min. The spalling is assumed to stop once the first layer of rebars is reached. This approach adheres to the recommendations for performance-based fire design as outlined in the state-of-the-art recommendations in [4]. In the analyses, the left tube of the tunnel is exposed to a two-hour RWS (Rijkswaterstaat) fire curve followed by an exponential cooling phase, representing an intense fire event such as a fuel truck fire. Six cases of localized spalling were analysed to assess the sensitivity of structural behaviour to the location of spalling. For each case, spalling was applied only to specified regions of the tunnel, while other sections were assumed to retain full concrete cover.

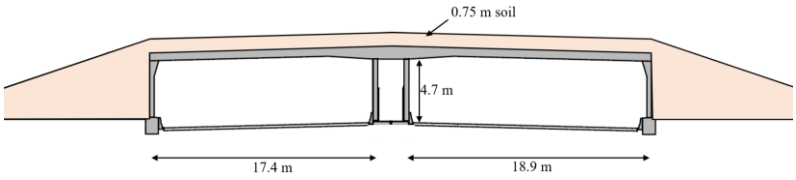

Results and discussion

The results in the Table show that the tunnel's fire performance is highly dependent on the location of spalling. The tunnel is prone to collapse in cases where spalling occurs in the roof slab near the middle of the span or near the outer wall (cases 1 and 3). In these cases, the structure is unable to redistribute the applied loads to the parts of the structure that are not experiencing spalling.

When spalling occurs only in the outer wall (cases 2 and 4) or near the inner wall (cases 5 and 6), the results indicate that the tunnel is able to survive the entire fire scenario including the cooling phase. Although the tunnel withstands the full duration of the fire in these cases, significant structural damage still occurs beyond that caused by spalling alone. In all cases, the structure remains permanently deformed and suffers from cracking at the unexposed side of the outer wall and the roof slab. These cold side cracks are caused by the high internal forces and stresses that occur inside the concrete structure due to the severe heating.

Overall, these results illustrate that the damage to the tunnel in case of fire highly depends on the parts of the tunnel where the concrete suffers from spalling, as some cases lead to rapid loss of stability, while others are able to survive hours of RWS fire.

Using these findings, a cost-effective refurbishment of the tunnel could be considered, in which only the most vulnerable areas are protected by means of passive protection, while other areas (e.g. the inner and outer walls) can remain unprotected. By applying passive protection only in the areas which are found to lead to premature collapse, the overall cost and installation time for such a refurbishment can be significantly reduced.

Case 1 **Central roof** 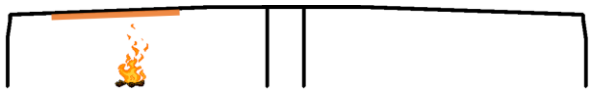 Collapse after 17 minutes.	**Case 4** **Outer wall** 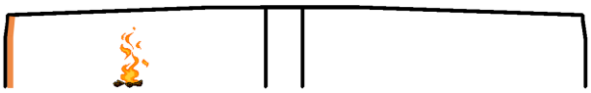 Tunnel survives full fire scenario, incl. cooling phase
Case 2 **Top side outer wall** 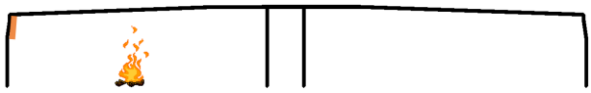 Tunnel survives full fire scenario, incl. cooling phase	**Case 5** **Roof near inner wall** Tunnel survives full fire scenario, incl. cooling phase
Case 3 **Roof near outer wall + top side outer wall** Collapse after 85 minutes.	**Case 6** **Roof near inner wall + inner wall** Tunnel survives full fire scenario, incl. cooling phase

Conclusion

This study highlights the significant impact of spalling location on the structural fire performance of cut-and-cover rectangular tunnels. Spalling in critical areas, such as the central roof slab or roof-wall junctions, can result in premature collapse. In contrast, when the spalling is confined to the walls or less critical areas in the roof, the tunnel is able to withstand a full two-hour RWS fire. These results highlight the potential for a targeted application of passive fire protection to enhance the fire resistance of the most vulnerable regions while optimizing costs and installation efforts.

References

1. Lo Monte, F., Bamonte, P., Beltrami, C., 2023, Study on the effects of cooling phase and construction technology on the fire performance of R/C tunnels. Tunnelling and Underground Space Technology. 132, 104838.
2. Hua, N., Tessari, A.F., Elhami-Khorasani, N., 2020, Damage assessment framework for tunnel structures subjected to fire. In Proceedings of the 11th International Conference on Structures in Fire (SiF2020).
3. Thienpont, T., Put, F., Jovanović, B., Chaudhary, R. K. & Van Coile, R. (2024). Numerical investigation of the structural fire response of tunnel structures with rectangular cross-sections. In Proceedings of the 13th International Conference on Structures in Fire, 915–925.
4. Gernay, T., et al., 2023, Performance-based fire design of concrete structures: state of the art-report. Fédération internationale du béton (fib), Lausanne, Switzerland

Use of Procedural Content Generation and pixel streaming in VR training of Firefighters

Jo Skjermo & Gunnar Deinboll Jennsen
SINTEF Community
Høgskoleringen 7B, Pb 4760 Sluppen, 7465 Trondheim
E-mail: jo.skjermo@sintef.no

KEYWORDS: Fire figting, tactical training, VR, undergound parking garage.

INTRODUCTION

This paper explains ongoing work in development of next-gen Virtual Reality (VR) training applications for tactical training of firefighters in (underground) parking garages. Using approaches such as Procedural Content Generation (PCG) enables non-static worlds, reducing repetition of training environments and tasks, while technologies such as pixel streaming enables training to involve more than just the user of a VR application itself by easily plugin into existing infrastructure.

FIRE IN PARKING GARAGES

Fire in (underground) parking garages are frequently becoming a more common and costly problem. Some main causes for such fires are the increased use of electronics and flammable materials in modern vehicles, increasing the number of potential ignition sources. In the evaluation report after the fire at the parking garage at Sola airport [1], where several hundred cars was damaged and the parking garage partially collapsed, is was pointed out that learning points included needs for exercise and training, collaboration and common situational understanding, as well as communication and collaboration. As such, one should consider how to improve tactical training and decision making. In this work we consider this in the context of Virtual Reality (VR). An early application has been developed to explore use of VR for tactical decision making during the approach toward a fire object (Figure 1) in a parking garage setting. During development, discussions were held with Trøndelag Brann og Redningstjeneste (TBR) to uncover requirements. Two main feature requests were uncovered in these discussions; the need for training material that is not static (reducing recognition effect), and the need to possibly encompass multiple levels of the firefighting chain of command. We consider two methods from game development to enable these features.

Figure 1. From VR application: Left - Critical objects, Right - Car on fire (with smoke)

CONTROLLED VARIATIONS USING PCG GRAMMAR

To avoid building a static VR training application where the user recognizes the scene and task after a few uses, (controllable) randomness in both the scenes appearance and placement of critical objects needs to be introduced. However, such randomness needs to be controlled. One approach for such controlled randomness is using PCG: «Procedural Content Generation (PCG) in games is the automatic or computer-assisted generation of content such as levels, landscapes, items, rules, and quests.» [2]. We consider shape Grammar based PCG to generate the variations in the world's appearance, including placement of objects a firefighter should pay attention to. PCG Grammar uses a specific syntax to combine symbol modules [3]. For instance given module A and B, string [A,B] combines module A and B, meaning they are placed together once, while [A,B]* means place A and B together as many times as possible. To randomly choose between two or more set of modules, one can use "{}". Examples of the approach used to define (semirandom) walls along a spline can be seen in Figure 2-4. In [4] this concept was extended to generate a space station hallway, with object placement. This approach can be utilized to generate (controlled randomized) parking garage scenes.

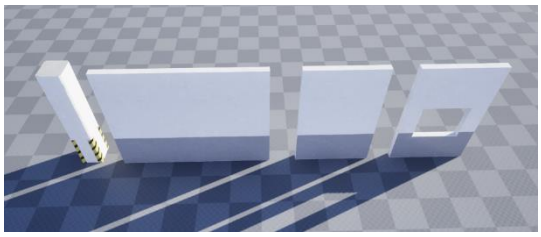

Figure 2. Wall element shapes defined as A, B, C and D (left to right).

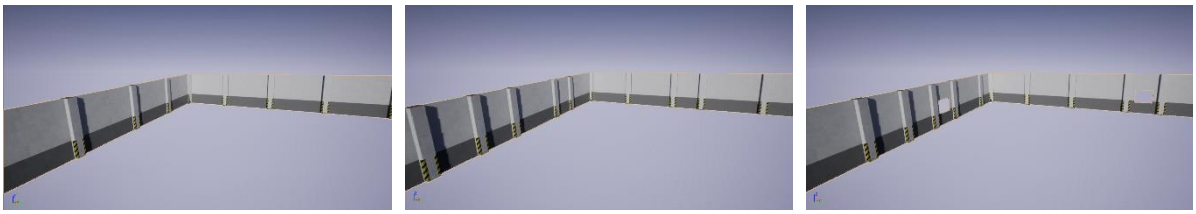

Figure 3. From left: results of string [A,B], {[A,B]:2,[C,B]:1}* and {[A,B]:4,[C,B]:2,[D,B]:1}**

INCLUDE MORE STAKEHOLDER IN CHAIN OF COMMAND

To enable tactical training with several stakeholders, such as a task force leader or even fire station control room observers, the stakeholders should be able to look at camera feeds from a VR users (virtual) helmet camera. To show the scene as the user moves through the world, we use Pixel Streaming over WebRTC (as implemented in Unreal Engine 5.5). This enables us to plug the camera feeds directly into existing infrastructure (to anything that can run a WebRTC compatible web browser, ranging from Pad/phone to fire station control rooms) and thereby into existing control hierarchy. This enables further increase in training potential. One should note that this approach can also be used to simulate (potential) access to on-site monitoring/security cameras. Finally, Unreal Engine 5.5 has experimental support for use of microphone (simulate communication), and more importantly pixel streaming for VR itself. This allows future VR training experiences for fire fighter to be implemented as cloud services not requiring other PC infrastructure than an HMD. This will simplify administration and usage to a large degree, with easier support for multiple types of HMDs.

DISCUSSION AND FUTURE WORK

We present ongoing work on exploring methods for development of VR application targeted toward firefighter training. The use of PCG and definition of Grammar rules, as well as streaming of multiple views are considered. In the future we wish to explore other tools, such as use of thermal cameras in VR setting, and other settings such as office or residential buildings by PCG for room partitioning [5].
.

REFERENCES

1. Karolina Storsund, Christian Sesseng, Ragna F. Mikalsen and Ole A. Holmvaag. Evaluation of fire in Stavanger airport car park 7 January 2020. Report number: RISE-report 2020:91. DOI:10.13140/RG.2.2.24520.14080
2. Noor Shaker, Julian Togelius , Mark J. Nelson. Procedural Content Generation in games. 26 October 2016, Springer Cham. Computational Synthesis and Creative Systems, ISSN 2509-6575, ISBN 978-3-319-42714-0, 26 October 2016, DOI: 10.1007/978-3-319-42716-4.
3. Unreal Engine 5.5 Shape Grammar documentation, https://dev.epicgames.com/documentation/en-us/unreal-engine/using-shape-grammar-with-pcg-in-unreal-engine, accessed 12/12/2024.
4. Julien L'Heureux and Jaen-Sebastien Guay, PCG Advanced topics & New Features in 5.5. Unreal Fest Seatle 2024 Presentation. Youtube: https://youtu.be/j3ke6MmcaeY?si=LDENhZ5qaRV5RSPt.
5. Daniel Bengtsson and John W. Melin, Constrained procedural floor plan generation for game environments. 2016, https://api.semanticscholar.org/CorpusID:116416317

Adaptive Control System for Tunnel Ventilation in the LIAISON Project

Jorge González Norniella
ZITRÓN
Autovía AS-II nº2386, 33211 Gijón, Spain
E-mail: jnorniella@zitron.com

KEYWORDS: sustainability, tunnel safety, jet fan, energy optimization, vibration, noise, maintenance, speed control, monitoring

INTRODUCTION

The LIAISON project, funded by the European Union, addresses emissions across the entire life cycle of transport infrastructure (TI), including construction, maintenance, operation, and decommissioning. Developing innovative technical solutions, LIAISON includes a governance framework to promote the adoption of sustainable and circular TI lifespan. LIAISON developments are being demonstrated in different TI (roads and railways) and in different European countries (Spain, Poland, Slovenia and Italy). Particularly, ZITRÓN is responsible of improving the traditional ventilation systems of the road tunnels for the LIAISON project. The innovation presented in this application significantly enhance tunnel safety by ensuring reliable air quality management and optimal emergency response capabilities.

OBJECTIVE

An effective ventilation system is crucial for tunnel safety, ensuring air quality in normal conditions and appropriate performance in the event of fire. Fans are designed to control extreme conditions but are often used inefficiently, leading to high energy consumption. Current ventilation systems operate on a simple on-off basis without regulating fan speed, resulting in limited performance. The development of an adaptive control system using Variable Frequency Drives (VFDs) together with sine wave filters optimizes the efficiency of the ventilation system. The implementation of this technology aims for up to 40% energy savings, significantly reducing operational costs while maintaining system effectiveness.

By regulating the speed of tunnel fans, the system not only adapts to varying scenarios without wasting energy but also increases the service life of the fans. Reduced mechanical stress and smoother operation decrease wear and tear, translating into lower maintenance needs. Operating the fans at lower speeds inherently reduces vibration levels, further protecting the mechanical components and improving overall reliability. Lower speeds also results in lower acoustic noise levels, contributing to a quieter environment both inside and outside the tunnel. This improvement is particularly valuable in urban areas or tunnels near residential zones, where noise reduction is a critical factor for community acceptance. Reduced noise levels are also essential in case of fire, as they allow tunnel users and emergency personnel to clearly hear audible emergency signals. Moreover, it is highly recommended to monitor fan signals and perform periodic diagnostics to ensure that the system remains in optimal condition, allowing for early detection of potential issues.

The described system directly improves tunnel safety by ensuring optimal airflow management in both normal and emergency conditions. Fan speed regulation, together with the monitoring of different parameters, extends service life, reduces the risk of mechanical failures and acoustic noise levels, and provides a more reliable ventilation system and safer environment for all tunnel users.

INSTRUMENTATION

To implement the system proposed by ZITRÓN for the LIAISON project, it is essential to incorporate VFDs with sine wave filters, along with the electronic cards (ZJET) developed by ZITRÓN. These

cards are installed in the fans and centralize signals from them, such as accelerometers, temperature sensors, and heaters, while also providing connectivity within the tunnel. ZJET incorporates vibration spectrum measurement, which enables precise monitoring of fan performance. This tool allows the system to detect any anomalies and identify their root causes, facilitating maintenance and preventing unexpected failures. In addition to this, when the ZJET cards are integrated during factory assembly, the fans are delivered fully wired, eliminating potential connection errors during final installation and significantly simplifying the process.

The new system is monitored using ZITRÓN's ventilation-specific control software, ZVM, which collects operational data and sends it to the cloud platform. This data is subsequently analyzed with the ZCARE tool, designed to assess the health of the fans and enable proactive maintenance. Additionally, ZCARE integrates all tunnel signals, including readings from anemometers and environmental sensors. This comprehensive monitoring capability optimizes fan performance and supports the development of algorithms that ensure consistent air quality while achieving energy savings under the various scenarios that may occur in the tunnel. It is also remarkable the potential to develop different strategies for controlling the fumes in case of fire.

TESTS

The validation of the system has been carried out in the Mamariga Tunnel in Spain. The tunnel comprises two separate tubes, one for each traffic direction, and is equipped with ZITRÓN model JZR 14-30/4 fans. These fans have a diameter of 1.4 meter, a power output of 30 kW, and a nominal speed of 1500 rpm. One tube is equipped with two fans, while the other has four. As part of the validation process, the electrical cabinets in the control room were upgraded to enable variable speed control, and ZJET electronic cards were integrated into the fans. This integration provided enhanced connectivity and streamlined the monitoring and control processes. Utilizing ZVM for real-time monitoring and ZCARE for advanced data analysis, the system's performance has been optimized to align with modern operational and energy efficiency standards. Before implementing the control upgrade, the original control algorithm is retained and tested to establish a baseline for performance comparison. This allowed for an accurate assessment of the improvements achieved after the enhancements.The system will continue to be monitored throughout 2025 and 2026 to validate its performance over time. This long-term monitoring will provide concrete evidence of the energy savings, tunnel safety improvement, sustainability, and contribution to the circular economy achieved within the framework of the LIAISON project. The Mamariga Tunnel thus serves as a real-world demonstration of how innovative ventilation solutions can enhance infrastructure performance and security while reducing environmental impact.

CONCLUSION

The system provided for the LIAISON project delivers a highly efficient, safe, and sustainable solution for tunnel ventilation, meeting the demands of modern infrastructure with advanced technology and intelligent control systems. The first conclusions, based on initial measurements taken in late 2024 and early 2025, confirm up to 40% energy savings, directly linked to optimized airspeed control and measured power consumption. The extended fan service life is supported by lower recorded motor temperatures due to reduced speeds, as well as a decrease in vibrations, which consequently also contributes to noise reduction. The system further ensures simplified installation, extended remote commissioning, proactive maintenance, and improved safety, particularly in fire scenarios.

ACKNOWLEDGMENTS

This work has received funding from the Horizon Europe research and innovation program under the grant agreement 101103698 (LIAISON project). This paper reflects only the author's views. The European Commission and INEA are not responsible for any use that may be made of the information contained therein.

Influence of sensor data on fire service operations in road tunnels

Nils Johansson
Division of Fire Safety Engineering, Lund University
E-mail: nils.johansson@brand.lth.se

KEYWORDS: fire service operations, smart firefighting, sensor data.

INTRODUCTION

"Smart firefighting" has become an established concept in fire engineering research in recent years. There is no established definition of the term, but in its simplest form, smart firefighting can be seen as a framework [1] for (1) gathering and integrating large amounts of information from various sources; (2) processing, analyzing, and predicting events and developments using this information; and (3) delivering the data to provide a basis for decision-making for the fire department, the community, or others (see Figure 1).

NIST [1] provides a comprehensive overview of several areas where research and development are needed in the context of Smart Firefighting. These areas include standardization, databases, analysis, sensors, simulations, data transfer, system compatibility, practical solutions, and more. It is, however, evident that there are various areas to study and a wealth of data that could be made available to the fire service. However, it also appears that unless data is processed and presented intelligently, it can quickly become an overload of data that may not necessarily improve the ability to make informed decisions, especially for an incident commander. Therefore, once valuable data has been identified, it is important to process it effectively to provide interpretable results.

The overarching research question in this study has been: *How can data from a smart tunnel be packaged and communicated to the fire service to improve fire service operations?*

METHOD

A scenario-based interview study involving 24 Swedish fire officers was conducted to examine their responses to various types of data during a fire incident in a road tunnel. The scenario presented in the study was an 820-meter-long road tunnel with parallel tubes and connecting access doors for evacuation and fire service operations. Participants were initially provided with general information about the tunnel and the basic details of the incident. Subsequently, they were introduced to three levels of data (see *Figure*):

1. Level 1: Basic pre-planning information (Swedish: *insatsplan*).
2. Level 2: Real-time information from sensors within the tunnel.
3. Level 3: Processed sensor data that provided predictive insights into the situation at intervals of 0, 5, and 10 minutes into the future.

After each level, the participants were asked to share their impressions of the incident and describe the actions and decisions they would consider taking. Following the presentation of Level 2 and Level 3 information, they were also asked whether they wished to revise any of the decisions or actions they had chosen at the previous level.

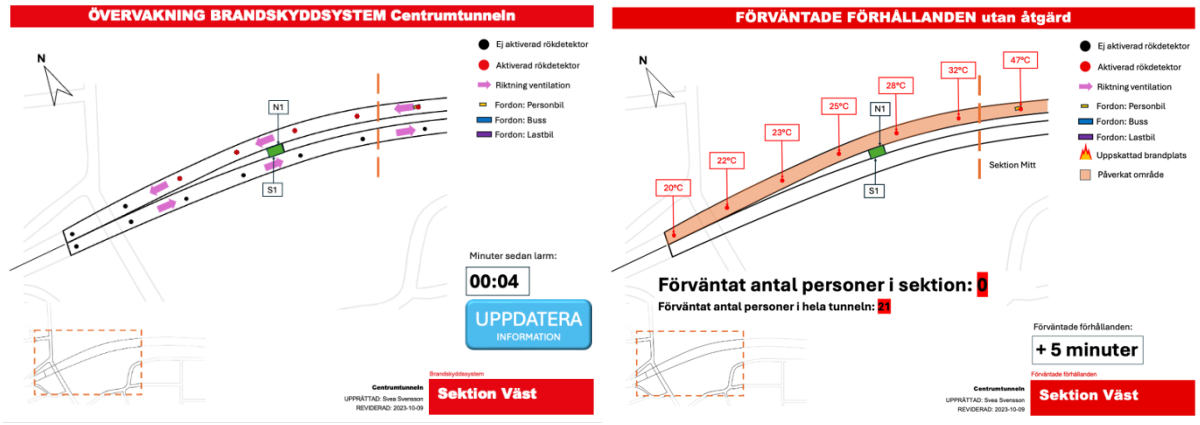

Figure 1: Example of information at level 2 (left) and level 3 (right)

RESULTS

The participants valued the information provided at higher levels, particularly the sensor data presented at Level 2. They responded significantly more positively to this data, finding it especially useful for supporting decisions and considering it beneficial for most incident commanders (see *Figure 2*). However, a majority of participants expressed difficulty in fully trusting the Level 3 information, especially regarding the predicted number of people in the tunnel.

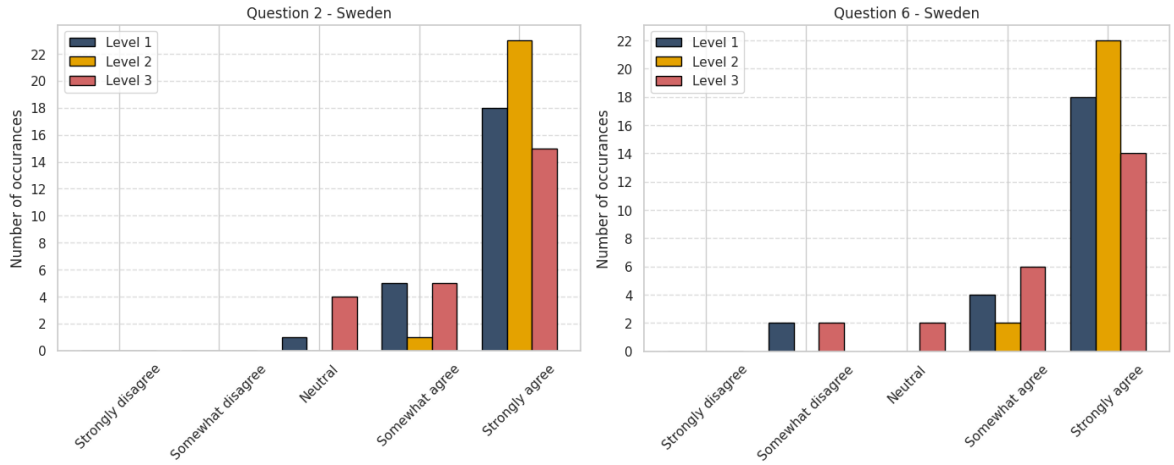

Figure 2: Answers to the questions: "The information material presented provided me with support for decision making" (left) and "The information material presented would be useful for most incident commanders" (right).

This study should be regarded as a case study, and the results are challenging to generalize to all possible situations. The specific scenario and the different levels of information used in the study significantly influence the outcomes. Nevertheless, the scenario and the design of the information at Level 1 (which also served as a template for Levels 2 and 3) are considered to align well with actual conditions in Sweden.

REFERENCES

1. A. P. Hamins, C. Grant, N. P. Bryner, A. W. Jones, and G. H. Koepke, 'Research Roadmap for Smart Fire Fighting', NIST, Jun. 2015.

Enhancing Safety in a Long Bidirectional Road Tunnel: A Risk-Based Approach to Ventilation Design

Juan Carlos de Rueda, Sorosuh Dabiri & Reinhard Gertl
ILF Consulting Engineers Austria GmbH
Feldkreuzstrasse 3, 6063 Rum/Innsbruck, Austria
E-mail: juan-carlos.rueda@ilf.com

KEYWORDS: Tunnel safety, risk assessment, transversal and longitudinal ventilation system, road tunnel, decision-making tool

INTRODUCTION

The Guillermo Gaviria Echeverri Tunnel (TGGE), with a length of 9,73 km, which will be Latin America's longest road tunnel, is currently under construction in Colombia's Antioquia Department with a single bidirectional tube connected to a parallel rescue tube through multiple cross-passages. The study addresses the challenges in implementing the prescriptive semitransversal ventilation system due to design restrictions which affected negatively its safety. Different ventilation concepts were explored to find the most suitable system for regular operation and fire scenarios. A quantitative risk assessment evaluated each alternative system and identified the longitudinal ventilation system, accompanied by risk mitigation measures, as the safest choice, since it surpasses the prescribed semitransversal ventilation concept.

METHODOLOGY

The TGGE is located in Colombia's Antioquia Department and is designed for bidirectional traffic. The tunnel's ventilation design is aligned with its length and longitudinal inclination. Two ventilation systems are compared: semitransversal and longitudinal.

The semitransversal system uses an exhaust duct and fans to remove smoke, while the longitudinal system relies on jet fans to transport smoke out of the tunnel portals. In the semitransversal system, smoke is exhausted via an exhaust duct connected to the traffic tube through controllable exhaust air dampers at regular intervals. The longitudinal system uses jet fans to transport smoke longitudinally in the traffic tube, directing it towards the tunnel portals.

The TGGE spans 9,730 meters and is planned for bidirectional traffic operation. The tunnel has a longitudinal inclination ranging from -0.5% to 0.9%, with portals at varying elevations. The standard cross-sectional area of the traffic tube is 83.3 m², and its height is 9.2 m. The traffic tube can be ventilated through the piston effect created by moving vehicles, inducing airflow along the main driving direction. When self-ventilation is insufficient, an external tunnel ventilation system is required. The tunnel's wall temperature is assumed to be constantly 15°C. To estimate the fresh air demand conservatively, the international guideline PIARC 2019 edition [1] is employed. Fresh air demand for high traffic volume is calculated at around 172 m³/54 m² (3.2 m/s flow velocity). The semitransversal system must guarantee a minimum air flow rate of 120 m³/s per exhaust fan, increasing during fire incidents due to hot air expansion. In bidirectional tunnels, the ventilation system must ensure an equal air velocity of 1.5 m/s from both sides of the fire. Approximately 162 m³/s of cold air, or roughly 300-400 m³/s of hot air, needs to be extracted. If one exhaust fan is inactive, the remaining exhaust fan must handle 70% of the required flow rate, in accordance with EABT-80/100 R2 [2]. The air velocity through the exhaust damper is limited to 25 m/s.

QUANTITATIVE RISK ANALYSIS

A quantitative risk analysis is conducted using the Austrian Tunnel Risk Model TuRisMo [4]. The principles are also defined following the PIARC [3] which evaluates the safety of each ventilation system. TuRisMo calculates an expected risk value for tunnel users, representing the long-term average number of statistically expected fatalities per year. The risk shares originating from mechanical damage effects, fire effects, and dangerous goods effects are calculated separately.

The frequency analysis involves calculating the frequency of various predefined damage scenarios using event tree analysis. These scenarios are developed step by step, branching out from an initial event with known frequency and differing in scenario type, vehicle involvement, and damage effects.

The consequence analysis employs a two-part simulation model within the TuRisMo system. The first part simulates smoke propagation, considering factors like fire size, location, and airflow conditions. The second part focuses on simulating the evacuation of tunnel users, taking into account the presence of noxious substances and visibility. Both simulation modules generate representative scenarios and combinations, which are then interpolated to create a continuous consequence function.

The fire consequence analysis consists of a large number of simulation scenarios, limited to 162 case combinations due to computational demand. These scenarios include variations in traffic volume, fire size, fire location, and delay time. The same number of smoke propagation scenarios and simulation cases is carried out for each tunnel design option.

RESULTS

The risk assessment demonstrates that the longitudinal ventilation system results in a higher fire risk compared to the semitransversal system. However, additional safety measures, such as installing 24 extra emergency exits or a fixed firefighting system (FFFS), can reduce the risk to acceptable levels, as the efficacy of water-based fire supression systems has been substantiated through various test series conducted in real fire tests [5]. In this case, water-based fire supression systems are effective in mitigating fire risk, reducing it by approximately 64%.

CONCLUSION

The study highlights the importance of implementing additional safety measures to ensure the acceptability of the longitudinal ventilation system. A quantitative risk assessment demonstrates that, with appropriate risk mitigation measures, the system can be safely implemented in the TGGE. The FFFS, with its proven track record in European tunnel projects, offers significant safety benefits by reducing smoke propagation and improving evacuation conditions, while the installation of additional emergency exits further enhances safety by shortening evacuation distances. In conclusion, the study recommends either installing additional emergency exits or a FFFS to achieve a fire risk level below the reference profile set by the semitransversal system.

REFERENCES

1. PIARC, W. R. (2016). Experience with significant incidents in road tunnels. World Road Association (PIARC), Technical Committee 3.3 Road Tunnel Operations.
2. ILF. (2022). Tunnel Guillermo Gaviria Echeverri – Detailed Ventilation Study. Austria: ILF Consulting Engineers Austria.
3. PIARC. (2013). Current Practice for Risk Evaluation for Road Tunnels. World Road Association (PIARC), Technical Committee 3.3 Road Tunnel Operations.
4. RVS, P. K.-K. (2011). Österreichische Forschungsgesellschaft Straße-Schiene-Verkehr, 3: 14. Austria: RVS.
5. Tarada. (2013). The Energy Budget in Suppressed Tunnel Fires. Barcelona: BHR